

NON-PROPRIETARY VERSION

**SAFETY ANALYSIS REPORT**  
**on**  
**THE HI-STAR 100 CASK SYSTEM**  
(Holtec International Storage, Transport, And Repository Cask System)

(Revision 16)

by

Holtec International  
Holtec Center  
One Holtec Drive  
Marlton, NJ 08053  
(holtecinternational.com)

USNRC Docket No. : 71-9261  
Holtec Report No. : HI-951251  
Quality Designation : Safety Significant\*

NON-PROPRIETARY VERSION

**Copyright Notice and Notice of Proprietary Information**

This document is a copyrighted intellectual property of Holtec International. All rights reserved. Excerpting any part of this document, except for public domain citations included herein, by any person or entity except for the USNRC, a Holtec User Group (HUG) member company, or a foreign regulatory authority with jurisdiction over a HUG member's nuclear facility without written consent of Holtec International is unlawful.

---

\* The safety designation is pursuant to Holtec International's Quality Assurance Program.

## TABLE OF CONTENTS

---

### CHAPTER 1: GENERAL INFORMATION

1.0	GENERAL INFORMATION .....	1.0-1
1.0.1	Engineering Change Orders .....	1.0-3
1.1	INTRODUCTION .....	1.1-1
1.2	PACKAGE DESCRIPTION .....	1.2-1
1.2.1	Packaging .....	1.2-1
1.2.1.1	Gross Weight .....	1.2-2
1.2.1.2	Materials of Construction, Dimensions, and Fabrication .....	1.2-2
1.2.1.3	Impact Limiters .....	1.2-9
1.2.1.4	Shielding .....	1.2-9
1.2.1.5	Lifting and Tie-Down Devices .....	1.2-16
1.2.1.6	Heat Dissipation .....	1.2-17
1.2.1.7	Coolants .....	1.2-17
1.2.1.8	Pressure Relief Systems .....	1.2-18
1.2.1.9	Security Seal .....	1.2-18
1.2.1.10	Design Life .....	1.2-18
1.2.2	Operational Features .....	1.2-19
1.2.2.1	Applicability of Operating Procedures for the Dual-Purpose HI-STAR 100 System .....	1.2-20
1.2.3	Contents of Package .....	1.2-22
1.2.3.1	Determination of Design Basis Fuel .....	1.2-22
1.2.3.2	Design Payload for Intact Fuel .....	1.2-23
1.2.3.3	Design Payload for Damaged Fuel and Fuel Debris .....	1.2-24
1.2.3.4	Structural Payload Parameters .....	1.2-26
1.2.3.5	Thermal Payload Parameters .....	1.2-26
1.2.3.6	Radiological Payload Parameters .....	1.2-27
1.2.3.7	Criticality Payload Parameters .....	1.2-28
1.2.3.8	Non-Fuel Hardware and Neutron Sources .....	1.2-31
1.2.3.9	Summary of Authorized Contents .....	1.2-32
1.2.3.10	Summary of Authorized Contents .....	1.2-32
1.3	DESIGN CODE APPLICABILITY .....	1.3-1

## TABLE OF CONTENTS (continued)

1.4	DRAWINGS .....	1.4-1
1.5	COMPLIANCE WITH 10CFR71 .....	1.5-1
1.6	REFERENCES .....	1.6-1
Appendix 1.A:	Alloy X Description	
Appendix 1.B:	Holtite™ Material Data	
Appendix 1.C:	Miscellaneous Material Data	
Supplement 1.I:	General Description of the HI-STAR HB Package with MPC-HB	
Supplement 1.II:	General Description of the HI-STAR HB GTCC Package with GWC-HB	
Supplement 1.III:	General Description of the HI-STAR 100 Package with Diablo Canyon MPC-32	
 <b>CHAPTER 2: STRUCTURAL EVALUATION</b>		
2.0	STRUCTURAL EVALUATION .....	2.0-1
2.1	STRUCTURAL DESIGN. ....	2.1-1
2.1.1	Discussion .....	2.1-1
2.1.2	Design Criteria .....	2.1-5
2.1.2.1	Loading and Load Combinations .....	2.1-6
2.1.2.2	Allowables .....	2.1-11
2.1.2.3	Brittle Fracture Failure .....	2.1-14
2.1.2.4	Impact Limiter .....	2.1-16
2.1.2.5	Buckling .....	2.1-16
2.1.2.6	Partially Loaded MPC's .....	2.1-16
2.2	WEIGHTS AND CENTERS OF GRAVITY .....	2.2-1
2.3	MECHANICAL PROPERTIES OF MATERIALS .....	2.3-1
2.3.1	Structural Materials .....	2.3-1
2.3.1.1	Alloy X .....	2.3-1
2.3.1.2	Carbon Steel, Low-Alloy, and Nickel Alloy Steel .....	2.3-2
2.3.1.3	Bolting Materials .....	2.3-2

## TABLE OF CONTENTS (continued)

2.3.1.4	Weld Material .....	2.3-2
2.3.1.5	Impact Limiter .....	2.3-2
2.3.2	Nonstructural Materials .....	2.3-5
2.3.2.1	Neutron Shield .....	2.3-5
2.3.2.2	Solid Neutron Absorber .....	2.3-5
2.3.2.3	Aluminum Heat Conduction Elements .....	2.3-5
2.4	GENERAL STANDARDS FOR ALL PACKAGES .....	2.4-1
2.4.1	Minimum Package Size .....	2.4-1
2.4.2	Tamperproof Feature .....	2.4-1
2.4.3	Positive Closure .....	2.4-1
2.4.4	Chemical and Galvanic Reactions .....	2.4-1
2.5	LIFTING AND TIE-DOWN STANDARDS .....	2.5-1
2.5.1	Lifting Devices .....	2.5-1
2.5.1.1	Overpack Trunnion Analysis .....	2.5-3
2.5.1.2	Stresses in the Overpack Closure Plate, Main Flange, and Baseplate During Lifting .....	2.5-4
2.5.1.3	MPC Lifting Analyses .....	2.5-6
2.5.2	Tie-Down Devices .....	2.5-7
2.5.2.1	Discussion .....	2.5-7
2.5.2.2	<i>Intentionally Deleted</i>	
2.5.2.3	<i>Intentionally Deleted</i>	
2.5.2.4	<i>Intentionally Deleted</i>	
2.5.2.5	<i>Intentionally Deleted</i>	
2.5.2.6	<i>Intentionally Deleted</i>	
2.5.2.7	Structural Integrity of Pocket Trunnions on Applicable HI-STAR 100 Systems .....	2.5-8
2.5.3	Failure of Lifting and Tie-Down Devices .....	2.5-9
2.5.4	Conclusion .....	2.5-10
2.6	NORMAL CONDITIONS OF TRANSPORT .....	2.6-1



**TABLE OF CONTENTS (continued)**

2.6.1	Heat .....	2.6-1
2.6.1.1	Summary of Pressures and Temperatures .....	2.6-1
2.6.1.2	Differential Thermal Expansion .....	2.6-1
2.6.1.3	Stress Calculations .....	2.6-3
2.6.1.4	Comparison with Allowable Stresses .....	2.6-32
2.6.2	Cold .....	2.6-39
2.6.2.1	Differential Thermal Expansion .....	2.6-40
2.6.2.2	MPC Stress Analysis .....	2.6-41
2.6.2.3	Overpack Stress Analysis .....	2.6-41
2.6.3	Reduced External Pressure .....	2.6-45
2.6.4	Increased External Pressure .....	2.6-46
2.6.5	Vibration .....	2.6-46
2.6.6	Water Spray .....	2.6-47
2.6.7	Free Drop .....	2.6-47
2.6.8	Corner Drop .....	2.6-47
2.6.9	Compression .....	2.6-47
2.6.10	Penetration .....	2.6-47
2.7	HYPOTHETICAL ACCIDENT CONDITIONS.....	2.7-1
2.7.1	Free Drop .....	2.7-1
2.7.1.1	End Drop .....	2.7-7
2.7.1.2	Side Drop (Load Cases F3 (Table 2.1.6), E3 (Table 2.1.7), and 3 and 11 (Table 2.1.9)) .....	2.7-13
2.7.1.3	Corner Drop .....	2.7-15
2.7.1.4	Oblique Drops .....	2.7-21
2.7.1.5	Comparison with Allowable Stresses .....	2.7-24
2.7.2	Puncture .....	2.7-25
2.7.3	Thermal .....	2.7-27
2.7.3.1	Summary of Pressures and Temperatures .....	2.7-27
2.7.3.2	Differential Thermal Expansion .....	2.7-29
2.7.3.3	Stress Calculations .....	2.7-30

## TABLE OF CONTENTS (continued)

2.7.3.4	Comparison of Fire Accident Results with Allowable Stresses ...	2.7-35
2.7.4	Immersion - Fissile Material .....	2.7-35
2.7.5	Immersion - All Packages .....	2.7-36
2.7.6	Summary of Damage .....	2.7-37
2.8	SPECIAL FORM .....	2.8-1
2.9	FUEL RODS .....	2.9-1
2.10	MISCELLANEOUS ITEMS .....	2.10-1
2.10.1	Appendices.....	2.10-1
2.10.2	Summary of NUREG-1617/10CFR71 Compliance.....	2.10-1
2.11	REFERENCES .....	2.11-1
Appendix 2.A:	Design, Testing, and Computer Simulation of the AL-STAR™ Impact Limiter	
Appendix 2.B:	Summary of Results for Structural Integrity of Damaged Fuel Canisters	
Appendix 2.C:	Evaluation of an Improved HI-STAR 100 Impact Limiter Design Based on LS-DYNA Drop Simulations	
Supplement 2.I:	Structural Evaluation of the HI-STAR HB Package with MPC-HB	
Supplement 2.II:	Structural Evaluation of the HI-STAR HB GTCC Package with GWC-HB	
Supplement 2.III:	Structural Evaluation of the HI-STAR 100 Package with Diablo Canyon MPC-32	

## CHAPTER 3: THERMAL EVALUATION

3.0	INTRODUCTION .....	3.0-1
3.1	DISCUSSION .....	3.1-1
3.2	SUMMARY OF THERMAL PROPERTIES OF MATERIALS .....	3.2-1
3.3	TECHNICAL SPECIFICATIONS FOR COMPONENTS .....	3.3-1
3.3.1	Evaluation of Moderate Burnup Fuel .....	3.3-1

## TABLE OF CONTENTS (continued)

3.4	THERMAL EVALUATION FOR NORMAL CONDITIONS OF TRANSPORT .....	3.4-1
3.4.1	Thermal Model.....	3.4-1
3.4.1.1	Analytical Model - General Remarks .....	3.4-1
3.4.1.2	Test Model .....	3.4-29
3.4.2	Maximum Temperatures Under Normal Transport Conditions.....	3.4-29
3.4.2.1	Maximum Accessible Surface Temperatures .....	3.4-32
3.4.3	Minimum Temperatures.....	3.4-32
3.4.3.1	Post Rapid Ambient Temperature Drop Overpack Cooldown Event.....	3.4-32
3.4.4	Maximum Internal Pressures .....	3.4-34
3.4.5	Maximum Thermal Stresses .....	3.4-34
3.4.6	Evaluation of System Performance for Normal Conditions of Transport .....	3.4-34
3.5	HYPOTHETICAL ACCIDENT THERMAL EVALUATION.....	3.5-1
3.5.1	Thermal Model.....	3.5-2
3.5.1.1	Analytical Model .....	3.5-2
3.5.1.2	Test Model .....	3.5-4
3.5.2	System Conditions and Environment.....	3.5-4
3.5.3	System Temperatures.....	3.5-4
3.5.4	Maximum Internal Pressure.....	3.5-6
3.5.5	Maximum Thermal Stresses .....	3.5-6
3.5.6	Evaluation of System Performance for the Hypothetical Accident Thermal Conditions .....	3.5-6
3.6	REGULATORY COMPLIANCE.....	3.6-1
3.7	REFERENCES .....	3.7-1
Appendix 3.A: Conservatism in the Thermal Analysis of the HI-STAR System		

## TABLE OF CONTENTS (continued)

Appendix 3.B:	The Forced Helium Dehydration (FHD) System	
Supplement 3.I:	Thermal Evaluation of the HI-STAR HB Package with MPC-HB	
Supplement 3.II:	Thermal Evaluation of the HI-STAR HB GTCC Package with GWC-HB	
Supplement 3.III:	Thermal Evaluation of the HI-STAR 100 Package with Diablo Canyon MPC-32	

### CHAPTER 4: CONTAINMENT

4.0	INTRODUCTION .....	4.0-1
4.1	CONTAINMENT BOUNDARIES.....	4.1-1
4.1.1	Containment Vessel .....	4.1-1
4.1.2	Containment Penetrations .....	4.1-1
4.1.3	Seals and Welds .....	4.1-1
4.1.3.1	Containment Seals .....	4.1-2
4.1.3.2	Containment Welds.....	4.1-2
4.1.4	Closure .....	4.1-2
4.1.5	Damaged Fuel Container .....	4.1-3
4.2	REQUIREMENTS FOR NORMAL AND HYPOTHETICAL ACCIDENT CONDITIONS OF TRANSPORT .....	4.2-1
4.2.1	Containment Criteria.....	4.2-1
4.2.2	Containment of Radioactive Material.....	4.2-1
4.2.3	Pressurization of Containment Vessel .....	4.2-1
4.2.4	Assumptions.....	4.2-2
4.2.5	Analysis and Results .....	4.2-4
4.2.5.1	Volume in the Containment Vessel .....	4.2-4
4.2.5.2	Source Terms for Spent Nuclear Fuel Assemblies .....	4.2-5
4.2.5.3	Effective $A_2$ of Individual Contributors (Crud, Fines, Gases, and Volatiles).....	4.2-9
4.2.5.4	Releasable Activity .....	4.2-10
4.2.5.5	Effective $A_2$ for the Total Source Term.....	4.2-10

## TABLE OF CONTENTS (continued)

4.2.5.6	Allowable Radionuclide Release Rates .....	4.2-10
4.2.5.7	Allowable Leakage Rates at Operating Conditions .....	4.2-11
4.2.5.8	Leakage Rate Acceptance Criteria for Test Conditions.....	4.2-12
4.2.5.9	Leak Test Sensitivity .....	4.2-13
4.3	REGULATORY COMPLIANCE.....	4.3-1
4.4	REFERENCES .....	4.4-1
Appendix 4.A:	Bolt and Plug Torques	
Appendix 4.B:	Manufacturer Seal Information	
Supplement 4.I:	Containment Evaluation of the HI-STAR HB Package with MPC-HB	
Supplement 4.II:	Containment Evaluation of the HI-STAR HB GTCC with GWC-HB	
Supplement 4.III:	Containment Evaluation of the HI-STAR 100 Package with Diablo Canyon MPC-32	

## CHAPTER 5: SHIELDING EVALUATION

5.0	INTRODUCTION .....	5.0-1
5.1	DISCUSSION AND RESULTS .....	5.1-1
5.1.1	Normal Operations.....	5.1-2
5.1.2	Hypothetical Accident Conditions.....	5.1-5
5.2	SOURCE SPECIFICATION .....	5.2-1
5.2.1	Gamma Source.....	5.2-2
5.2.2	Neutron Source .....	5.2-4
5.2.3	Stainless Steel Clad Fuel Source .....	5.2-4
5.2.4	Non-fuel Hardware .....	5.2-5
5.2.4.1	BPRAs and TPDs.....	5.2-5
5.2.4.2	RCCAs .....	5.2-7
5.2.5	Choice of Design Basis Assembly.....	5.2-9
5.2.5.1	PWR Design Basis Assembly .....	5.2-9
5.2.5.2	BWR Design Basis Assembly .....	5.2-10

## TABLE OF CONTENTS (continued)

5.2.5.3	Decay Heat Loads .....	5.2-11
5.2.6	Thoria Rod Canister .....	5.2-11
5.2.7	Fuel Assembly Neutron Sources .....	5.2-12
5.2.7.1	Dresden Unit 1 Neutron Source Assemblies .....	5.2-12
5.2.7.2	Trojan Nuclear Plant Neutron Source Assemblies .....	5.2-12
5.2.7.3	MPC-32 Design Basis Neutron Source Assemblies .....	5.2-13
5.2.8	Trojan Non-Fuel Bearing Components, Damaged Fuel and Fuel Debris .....	5.2-14
5.3	MODEL SPECIFICATIONS .....	5.3-1
5.3.1	Description of the Radial and Axial Shielding Configuration .....	5.3-1
5.3.1.1	Fuel Configuration .....	5.3-3
5.3.1.2	Streaming Considerations .....	5.3-4
5.3.2	Regional Densities .....	5.3-5
5.4	SHIELDING EVALUATION .....	5.4-1
5.4.1	Streaming Through Radial Steel Fins and Pocket Trunnions .....	5.4-2
5.4.2	Damaged Fuel Post-Accident Shielding Evaluation .....	5.4-4
5.4.3	Mixed Oxide Fuel Evaluation .....	5.4-5
5.4.4	Stainless Steel Clad Fuel Evaluation .....	5.4-5
5.4.5	Dresden Unit 1 Antimony-Beryllium Neutron Sources .....	5.4-6
5.4.6	Thoria Rod Canister .....	5.4-7
5.4.7	Trojan Fuel Contents .....	5.4-8
5.4.8	Trojan Antimony-Beryllium Neutron Sources .....	5.4-8
5.4.9	MPC-32 with Non-Fuel Hardware .....	5.4-10
5.5	REGULATORY COMPLIANCE .....	5.5-1

## TABLE OF CONTENTS (continued)

5.6	REFERENCES .....	5.6-1
Appendix 5.A:	Sample Input File for SAS2H	
Appendix 5.B:	Sample Input File for ORIGEN-S	
Appendix 5.C:	Sample Input File for MCNP	
Supplement 5.I:	Shielding Evaluation of the HI-STAR HB Package with MPC-HB	
Supplement 5.II:	Shielding Evaluation of the HI-STAR HB GTCC Package with GWC-HB	
Supplement 5.III:	Shielding Evaluation of the HI-STAR 100 Package with Diablo Canyon MPC-32	
 <b>CHAPTER 6: CRITICALITY EVALUATION</b>		
6.1	DISCUSSION AND RESULTS .....	6.1-2
6.2	SPENT FUEL LOADING .....	6.2-1
6.2.1	Definition of Assembly Classes.....	6.2-1
6.2.2	PWR Fuel Assemblies in the MPC-24.....	6.2-2
6.2.3	BWR Fuel Assemblies in the MPC-68 .....	6.2-3
6.2.4	Damaged BWR Fuel Assemblies and BWR Fuel Debris.....	6.2-5
6.2.5	Thoria Rod Canister.....	6.2-6
6.2.6	PWR Assemblies in the MPC-24E and MPC-24EF .....	6.2-6
6.2.7	PWR Intact Fuel, Damaged Fuel And Fuel Debris in the Trojan MPC-24E/EF .....	6.2-6
6.2.8	PWR Assemblies in the MPC-32.....	6.2-6
6.3	MODEL SPECIFICATION.....	6.3-1
6.3.1	Description of Calculational Model.....	6.3-1
6.3.2	Cask Regional Densities .....	6.3-3
6.3.3	Eccentric Positioning of Assemblies in Fuel Storage Cells.....	6.3-4
6.4	CRITICALITY CALCULATIONS.....	6.4-1

## TABLE OF CONTENTS (continued)

6.4.1	Calculational or Experimental Method.....	6.4-1
6.4.2	Fuel Loading or Other Contents Loading Optimization .....	6.4-2
6.4.2.1	Internal and External Moderation .....	6.4-2
6.4.2.2	Partial Flooding.....	6.4-5
6.4.2.3	Clad Gap Flooding.....	6.4-5
6.4.2.4	Preferential Flooding .....	6.4-6
6.4.2.5	Hypothetical Accident Conditions of Transport.....	6.4-7
6.4.3	Criticality Results .....	6.4-7
6.4.4	Damaged Fuel Container for BWR Fuel .....	6.4-9
6.4.5	Fuel Assemblies with Missing Rods.....	6.4-11
6.4.6	Thoria Rod Canister.....	6.4-11
6.4.7	Sealed Rods Replacing BWR Water Rods .....	6.4-11
6.4.8	Neutron Sources in Fuel Assemblies .....	6.4-11
6.4.9	PWR Damaged Fuel and Fuel Debris.....	6.4-12
6.4.9.1	Bounding Intact Assemblies .....	6.4-13
6.4.9.2	Bare Fuel Rod Arrays .....	6.4-13
6.4.9.3	Results for MPC-24E and MPC-24EF.....	6.4-15
6.4.9.4	Results for Trojan MPC-24E and MPC-24EF .....	6.4-15
6.4.10	Non-fuel Hardware in PWR Fuel Assemblies .....	6.4-15
6.4.11	Reactivity Effect of Potential Fixed Neutron Absorber Damage .....	6.4-16
6.4.12	Fixed Neutron Absorber Material.....	6.4-16
6.4.13	Reactivity Effect of Manufacturing Variations .....	6.4-17
6.5	CRITICALITY BENCHMARK EXPERIMENTS .....	6.5-1
6.6	REGULATORY COMPLIANCE.....	6.6-1
6.7	REFERENCES .....	6.7-1



## TABLE OF CONTENTS (continued)

Appendix 6.A:	Benchmark Calculations	
Appendix 6.B:	Distributed Enrichments in BWR Fuel	
Appendix 6.C:	Burnup Credit in the MPC-32 Based on ISG-8 Revision 3	
Appendix 6.D:	Sample Input Files	
Appendix 6.E:	Burnup Credit in the MPC-32	
Supplement 6.I:	Criticality Evaluation of the HI-STAR HB Package with MPC-HB	
Supplement 6.II:	Criticality Evaluation of the HI-STAR HB GTCC Package with GWC-HB	
Supplement 6.III:	Criticality Evaluation of the HI-STAR 100 Package with Diablo Canyon MPC-32 and Burnup Credit	

## CHAPTER 7: OPERATING PROCEDURES

7.0	INTRODUCTION .....	7.0-1
7.1	PROCEDURE FOR LOADING AND PREPARATION FOR TRANSPORT OF THE HI-STAR 100 SYSTEM .....	7.1-1
7.1.1	Overview of HI-STAR Loading Operations .....	7.1-1
7.1.2	Preparation of HI-STAR for Loading .....	7.1-1
7.1.3	Loading of Contents into HI-STAR .....	7.1-2
7.1.4	Closure of HI-STAR .....	7.1-5
7.1.5	Preparation of HI-STAR for Transport .....	7.1-6
7.2	PROCEDURE FOR UNLOADING THE HI-STAR 100 SYSTEM .....	7.2-1
7.2.1	Receipt of Package from Carrier .....	7.2-1
7.2.2	Removal of Contents .....	7.2-2
7.3	PREPARATION OF AN EMPTY PACKAGE FOR TRANSPORT .....	7.3-1
7.4	PROCEDURE FOR PREPARING THE HI-STAR 100 OVERPACK FOR TRANSPORT FOLLOWING A PERIOD OF STORAGE .....	7.4-1
7.5	REFERENCES .....	7.5-1

## TABLE OF CONTENTS (continued)

Supplement 7.I: Operating Procedures of the HI-STAR HB Package with MPC-HB  
 Supplement 7.II: Operating Procedures of the HI-STAR HB GTCC Package with GWC-HB  
 Supplement 7.III: Operating Procedures of the HI-STAR 100 Package with Diablo Canyon  
 MPC-32 and Burnup Credit

### CHAPTER 8: ACCEPTANCE TESTS AND MAINTENANCE PROGRAM

8.0	INTRODUCTION .....	8.1-1
8.1	ACCEPTANCE TESTS.....	8.1-1
8.1.1	Visual Inspections and Measurements.....	8.1-1
8.1.2	Weld Examinations .....	8.1-2
8.1.3	Structural and Pressure Tests.....	8.1-2
8.1.3.1	Lifting Trunnions.....	8.1-2
8.1.3.2	Pressure Testing.....	8.1-3
8.1.3.3	Pneumatic Testing of the Neutron Shield Enclosure Vessel .....	8.1-4
8.1.4	Leakage Tests .....	8.1-4
8.1.5	Component and Material Tests .....	8.1-4
8.1.5.1	Seals .....	8.1-4
8.1.5.2	Impact Testing .....	8.1-5
8.1.5.3	Impact Limiter Crush Material Testing .....	8.1-5
8.1.5.4	Neutron Shielding Material .....	8.1-5
8.1.5.5	Neutron Absorber Material.....	8.1-5
8.1.6	Gamma Shielding.....	8.1-7
8.1.7	Thermal Tests.....	8.1-7
8.2	MAINTENANCE PROGRAM .....	8.2-1
8.2.1	Structural and Pressure Tests.....	8.2-1
8.2.2	Leakage Tests .....	8.2-1
8.2.3	Component and Material Tests .....	8.2-2
8.2.3.1	Relief Devices.....	8.2-2
8.2.3.2	Shielding Materials .....	8.2-2

---

**TABLE OF CONTENTS (continued)**


---

8.2.3.3	Packaging Surfaces .....	8.2-2
8.2.3.4	Packaging Fasteners.....	8.2-2
8.2.3.5	Cask Trunnions .....	8.2-3
8.2.3.6	Closure Seals.....	8.2-3
8.2.4	Thermal Tests.....	8.2-3
8.2.5	Miscellaneous Tests .....	8.2-3
8.3	REFERENCES .....	8.3-1
Supplement 8.I:	Acceptance Tests and Maintenance Program of the HI-STAR HB Package with MPC-HB	
Supplement 8.II:	Acceptance Tests and Maintenance Program of the HI-STAR HB GTCC Package with GWC-HB	
Supplement 8.III:	Acceptance Tests and Maintenance Program of the HI-STAR 100 Package with Diablo Canyon MPC-32	

## CHAPTER 1: GENERAL INFORMATION

### 1.0 OVERVIEW

This Safety Analysis Report (SAR) for Holtec International's HI-STAR 100 packaging is a compilation of information and analyses to support a United States Nuclear Regulatory Commission (NRC) licensing review as a spent nuclear fuel transportation package **and as a reactor-related non-fuel waste transportation package** (Docket No. 71-9261) under requirements specified in 10CFR71 [1.0.1] and 49CFR173 [1.0.2]. This SAR supports NRC approval and issuance of Certificate of Compliance No. 9261, issued under the provisions and definitions in 10CFR71, Subpart D, for the design Model: HI-STAR 100 as an acceptable Type B(U)F-96 packaging for transport by exclusive use shipment (10CFR71.47).

The HI-STAR 100 packaging complies with the requirements of 10CFR71 for a Type B(U)F-96 package. The HI-STAR 100 packaging does not have a maximum normal operating pressure (MNOP) greater than 700 kPa (100 lb/in<sup>2</sup>). The HI-STAR 100 internal design pressure is specified in Table 2.1.1 as 100 psig to calculate bounding stress values. Section 3.4 calculates the MNOP (reported in Table 3.4.15) and demonstrates that the value remains below the design value specified in Table 2.1.1. No pressure relief device is provided on the HI-STAR 100 containment boundary, as discussed in Subsection 1.2.1.8. Therefore, there is no pressure relief device that would allow the release of radioactive material under the tests specified in 10CFR71.73. Analyses that demonstrate that the HI-STAR 100 packaging complies with the requirements of Subparts E and F of 10CFR71 are provided in this SAR. Specific reference to each section of the SAR that is used to specifically address compliance to 10CFR71 is provided in Table 1.0.2. Therefore, the HI-STAR 100 packaging to transport spent nuclear fuel should be designated B(U)F-96.

The HI-STAR 100 Criticality Safety Index (CSI) is zero, as an unlimited number of packages is subcritical under the procedures specified in 10CFR71.59(a). Section 6.1 provides the determination of the CSI. The Transport Index (TI) based on radiation is in excess of 10 for the HI-STAR 100 Packaging with design basis fuel contents. Therefore, the HI-STAR 100 Packaging must be transported by exclusive use shipment (10CFR71.47).

The HI-STAR 100 packaging design, fabrication, assembly, and testing shall be performed in accordance with Holtec International's quality assurance program. Holtec International's quality assurance program was originally developed to meet NRC requirements delineated in 10CFR50, Appendix B, and was expanded to include provisions of 10CFR71, Subpart H, and 10CFR72, Subpart G, for structures, systems, and components designated as important to safety. NRC approval of Holtec International's quality assurance program is documented by the Quality Assurance Program Approval for Radioactive material Packages (NRC Form 311), Approval Number 0784, Docket No. 71-0784.

This SAR has been prepared in the format and content suggested in NRC Regulatory Guide 7.9 [1.0.3]. The purpose of this chapter is to provide a general description of the design features and transport capabilities of the HI-STAR 100 packaging including its intended use. This chapter provides a summary description of the packaging, operational features, and contents, and provides

reasonable assurance that the package will meet the regulations and operating objectives. Table 1.0.1 contains a listing of the terminology and notation used in preparing this SAR.

This SAR was initially prepared prior to the issuance of the draft version of NUREG-1617 [1.0.5]. To aid NRC review, additional tables and references have been added to facilitate the location of information needed to demonstrate compliance with 10CFR71 as outlined by NUREG-1617.

The HI-STAR 100 System is a dual purpose system, certified under 10 CFR 71 and 10 CFR 72. The HI-STAR 100 Final Safety Analysis Report (FSAR) [1.0.6] supports Certificate of Compliance No. 1008 for HI-STAR 100 to store spent nuclear fuel at an Independent Spent Fuel Storage Installation (ISFSI) facility under requirements of 10CFR72, Subpart L [1.0.4] (Docket Number 72-1008).

Within this report, all figures, tables and references cited are identified by the double decimal system m.n.i, where m is the chapter number, n is the section number, and i is the sequential number. Thus, for example, Figure 1.1.1 is the first figure in Section 1.1 of Chapter 1 (which is the next section in this chapter).

Revision of this document was made on a section level. Therefore, if any change occurs on a page, the entire section was updated to the current revision. The locations of specific text changes are indicated by revision bars in the margin of the page. Figures are controlled individually at the latest SAR revision level for that particular figure. Sections and figures unchanged in the latest SAR revision indicate the revision level corresponding to the last changes made in the section/figure. Drawings are also controlled individually within the Holtec International drawing control system.

Information pertaining to the safety analysis on the HI-STAR 100 transportation package containing contents from Host Sites other than the contents specified in Section 1.2.3 and/or based on customized “version(s)” of the HI-STAR 100 packaging, is generally contained in supplements to each chapter identified by a Roman numeral “I” (i.e., Chapter 1 and Supplement 1.I). Certain sections of the main SAR are also affected and are appropriately modified for continuity with the “I” supplements. Unless superseded or specifically modified by information in the “I” supplements, the information in the main SAR chapters remains applicable.

Through revision 11 of this SAR, discussions were presented that described MPC designs called the MPC-24EF, and MPC-68F. These designs contain features required to classify them as secondary containments, which was necessary for transportation of fuel debris under an earlier version of 10 CFR 71, and were the only MPC designs allowed to be loaded with fuel debris. The F-canister designs have been retained in this SAR; however, any requirements regarding the secondary containment function of these canisters have been removed **since the function is no longer required by 10CFR71.**

**Package Design Control:** The design information presented in this SAR is subject to validation, safety compliance and configuration control in accordance with Holtec's NRC approved quality assurance (QA) program which comports with the provisions of 10CFR71.107. Chapters 7 and 8 and the licensing drawing package contain conditions to the CoC, and as such, they can be modified only through an NRC licensing action. The other chapters contain substantiating information to support

the safety case and unless otherwise noted (e.g. referenced COC conditions or by licensing drawing package), the information can be amended subject to the stipulations of 71.107(c).

Quality Assurance Program: The HI-STAR 100 Package design, material acquisition, fabrication, assembly, and testing shall be performed in accordance with Holtec International's QA program. Holtec International's QA program was originally developed to meet NRC requirements delineated in 10CFR50, Appendix B, and was expanded in the early 90s to include provisions of 10CFR71, Subpart H, and 10CFR72, Subpart G, for structures, systems, and components (SSCs) designated as important-to-safety. NRC approval of Holtec International's QA program is documented by the Quality Assurance Program Approval for Radioactive Material Packages (NRC Form 311), Approval Number 0784, Docket No. 71-0784.

### 1.0.1 Engineering Change Orders

The changes authorized by Holtec Engineering Change Orders (ECOs) for the following licensed components are reflected in this revision of this SAR (see Supplement(s) to this chapter for listing of additional ECOs for respective applicable licensed components).

MPC-68/68F Basket: 1021-108R0, 111R0, 119R0, 125R0

MPC-24 Basket: 1022-87R0, 91R0

MPC-24E/24EF Basket: None.

MPC-32 Basket: None.

HI-STAR 100 overpack: 5014-239R0

MPC Enclosure Vessel:

- 1021-106R0, 107R0, 109R0, 111R0, 112R0, 115R0, 126R0
- 1022-84R0, 85R0, 86R0, 87R0, 88R0, 90R0, 92R0
- 1023-63R0, 64R0, 65R0, 66R0, 67R0, 68R0, 69R0

HI-STAR 100 Assembly for Transport: None.

Ancillary Equipment:

- AL-STAR Impact Limiters - 5014-185R1, 237R0,
- MPC Spacer: New Drawing

Trojan Equipment: None.

Table 1.0.1

## TERMINOLOGY AND NOTATION

**ALARA** is an acronym for As Low As Reasonably Achievable.

**AL-STAR™** is the trademark name of the HI-STAR 100 impact limiter.

**Boral** is a generic term to denote an aluminum-boron carbide cermet manufactured in accordance with U.S. Patent No. 4027377. The individual material supplier may use another trade name to refer to the same product.

**Boral™** means Boral manufactured by AAR Advanced Structures.

**BWR** is an acronym for boiling water reactor.

**C.G.** is an acronym for center of gravity.

**Commercial Spent Fuel or CSF** refers to nuclear fuel used to produce energy in a commercial nuclear power plant.

**Containment System** means the HI-STAR 100 overpack that forms the containment boundary of the packaging intended to contain the radioactive material during transport.

**Containment System Boundary** means the enclosure formed by the overpack inner shell welded to a bottom plate and top flange plus the bolted closure plate with dual seals and the vent and drain port plugs with seals.

**Cooling Time (or post-irradiation cooling time/ PCDT)** for a spent fuel assembly is the time between reactor shutdown and the time the spent fuel assembly is loaded into the MPC.

**Critical Characteristic** means a feature of a component or assembly that is necessary for the proper safety function of the component or assembly. Critical characteristics of a material are those attributes that have been identified, in the associated material specification, as necessary to render the material's intended function.

**Criticality Safety Index (CSI)** is the dimensionless number (rounded up to the next tenth) assigned to and placed on the label of a fissile material package, to designate the degree of control of accumulation of packages containing fissile material during transportation.

**Damaged Fuel Assembly** is a fuel assembly with known or suspected cladding defects, as determined by a review of records, greater than pinhole leaks or hairline cracks, empty fuel rod locations that are not filled with dummy fuel rods, missing structural components such as grid spacers, whose structural integrity has been impaired such that geometric rearrangement of fuel or

gross failure of the cladding is expected based on engineering evaluations, or that cannot be handled by normal means. Fuel assemblies that cannot be handled by normal means due to fuel cladding damage are considered FUEL DEBRIS.

**Damaged Fuel Container (or Canister)** means a specially designed enclosure for damaged fuel assemblies or fuel debris which permits gaseous and liquid media to escape while minimizing dispersal of gross solid particulates.

**Enclosure Vessel (or MPC Enclosure Vessel)** means the pressure vessel defined by the cylindrical shell, baseplate, port cover plates, lid, closure ring, and associated welds that provides confinement for the helium gas contained within the MPC. The Enclosure Vessel (EV) and the fuel basket together constitute the multi-purpose canister.

**Exclusive use** means the sole use by a single consignor of a conveyance for which all initial, intermediate, and final loading and unloading are carried out in accordance with the direction of the consignor or consignee. The consignor and the carrier must ensure that loading or unloading is performed by personnel having radiological training and resources appropriate for safe handling of the consignment. The consignor must issue specific instructions, in writing, for maintenance of exclusive use shipment controls, and include them with the shipping paper information provided to the carrier by the consignor.

**Fracture Toughness** is a property, which is a measure of the ability of a material to limit crack propagation under a suddenly applied load.

**FSAR** is an acronym for Final Safety Analysis Report (10CFR72).

**Fuel Basket** means a honeycomb structural weldment with square openings which can accept a fuel assembly of the type for which it is designed.

**Fuel Debris** is ruptured fuel rods, severed fuel rods, loose fuel pellets, or fuel assemblies with known or suspected defects which cannot be handled by normal means due to fuel cladding damage, including containers and structures supporting these parts. Fuel debris also includes certain Trojan plant-specific fuel material contained in Trojan Failed Fuel Cans.

**Greater-than-Class C radioactive waste (GTCC Waste)** means low-level radioactive waste that exceeds the concentration limits of radionuclides established for Class C waste in § 61.55 of 10CFR Chapter 1. GTCC waste is a subset of low level radioactive waste (LLRW). Also see reactor-related GTCC waste.

**GTCC Waste Canister (GWC)** means the sealed canister consisting of a basket for GTCC waste housed in an all welded cylindrical enclosure (the GWC Enclosure Vessel). With the exception of its internal basket and qualified contents, the GWC is nearly identical to its MPC counterpart.

**GWC Enclosure Vessel** means the pressure vessel defined by the cylindrical shell, baseplate, port cover plates, lid, and associated welds that provides confinement for the helium gas contained within



the GWC. The Enclosure Vessel (EV) and its waste basket together constitute the Greater-Than-Class C Waste canister.

**High Burnup Fuel (HBF)** is a commercial spent fuel assembly with an average burnup greater than 45000 MWd/MtU.

**High-Level Radioactive Waste (HLW)** means (1) the highly radioactive material resulting from the reprocessing of spent nuclear fuel, including liquid waste produced directly in reprocessing and any solid material derived from such liquid waste that contains fission products in sufficient concentrations; and (2) other highly radioactive material such as spent (used) fuel that the NRC (or other competent authority), consistent with existing law, determines by rule (or other legal method) requires permanent isolation.

**HI-STAR 100 overpack or overpack** means the cask that receives and contains the sealed multi-purpose canisters containing spent nuclear fuel **or containing the sealed Greater-Than-Class C radioactive waste canisters**. It provides the containment boundary for radioactive materials, gamma and neutron shielding, and a set of lifting trunnions for handling. Certain overpack models also include optional pocket trunnions for upending and downending.

**HI-STAR 100 System or HI-STAR 100 Package** consists of the MPC **or GWC** sealed (with licensed radioactive contents) loaded within the HI-STAR 100 overpack with impact limiters installed.

**Holtite™** is the trade name for all present and future neutron shielding materials formulated under Holtec International's R&D program dedicated to developing shielding materials for application in dry storage and transport systems. The Holtite development program is an ongoing experimentation effort to identify neutron shielding materials with enhanced shielding and temperature tolerance characteristics. Holtite-A™ is the first shielding material qualified under the Holtite R&D program. The terms Holtite and Holtite-A may be used interchangeably throughout this SAR.

**Holtite™-A** is a trademarked Holtec International neutron shield material.

**Host Site** is a generic term used in this SAR to mean the Commercial Nuclear Power Plant Sites (each which may be comprised of various units) from which fuel assemblies and/or other fuel related contents may be selected for loading and transport in accordance with the requirements in this SAR. This SAR may address specific technical matters related to specific Host Sites as necessary to ensure a complete safety evaluation.

**Humboldt Bay Damaged Fuel Container (or Canister)** is a Holtec damaged fuel container custom-designed for Humboldt Bay plant damaged fuel and fuel debris.

**Hypothetical Accident Conditions** are postulated events that for the purposes of this SAR are considered to occur infrequently, if ever during the use of a transportation package. These events may or may not be credible but set a transportation package design standard to provide reasonable

assurance that the packaging has adequate structural integrity to satisfy the subcriticality, containment, shielding, and temperature requirements of 10CFR71.

**ILP** is an acronym for Interfacing Lift Points. Types of ILPs include the lifting trunnions on the overpack and threaded anchor locations (TALs) on the MPC. Interfacing Lift Point is a term used in NUREG-0612 Subsection 5.1.6, item (3).

**Impact Limiter** means a set of fully-enclosed energy absorbers that are attached to the top and bottom of the overpack during transport. The impact limiters are used to absorb kinetic energy resulting from normal and hypothetical accident drop conditions. The HI-STAR impact limiters are called AL-STAR.

**Important to Safety (ITS)** means a function or condition required to transport spent nuclear fuel safely; to prevent damage to spent nuclear fuel, and to provide reasonable assurance that spent nuclear fuel can be received, handled, packaged, transported, and retrieved without undue risk to the health and safety of the public.

**Insolation** means incident solar radiation.

**Intact Fuel Assembly** is defined as a fuel assembly without known or suspected cladding defects greater than pinhole leaks and hairline cracks, and which can be handled by normal means. Fuel assemblies without fuel rods in fuel rod locations shall not be classified as Intact Fuel Assemblies unless dummy fuel rods are used to displace an amount of water greater than or equal to that displaced by the original fuel rod(s).

**Load-and-Go** is a term used in this SAR that means the practice of loading spent fuel (or GTCC waste) into the HI-STAR 100 System packaging and placing the packaging into transportation service under 10 CFR 71, without first deploying the system at an Independent Spent Fuel Storage Installation (ISFSI) under 10 CFR 72.

**Low Level Radioactive Waste (LLRW)** consists of a wide range of wastes having various physical and chemical characteristics and concentrations of radioactive isotopes. LLRW is classified as Class A, B, C and waste that is not generally acceptable for near-surface disposal (i.e., GTCC LLRW). LLRW is radioactive waste that is not high-level radioactive waste, transuranic waste, spent nuclear fuel, or byproduct material (uranium and thorium mill tailings and wastes).

**Lowest Service Temperature (LST)** is the minimum metal temperature of a part for the specified service condition.

**Maximum Normal Operating Pressure (MNOP)** means the maximum gauge pressure that would develop in the containment system in a period of 1 year under the heat condition specified in 10CFR71.71(c)(1), in the absence of venting, external cooling by an ancillary system, or operational controls during transport.

**Maximum Reactivity** means the highest possible k-effective including bias, uncertainties, and calculational statistics evaluated for the worst-case combination of fuel basket manufacturing tolerances.

**METAMIC<sup>®</sup>** is a trade name for an aluminum/boron carbide composite neutron absorber material qualified for use in the MPCs.

**Minimum Enrichment** is the minimum assembly average enrichment (unless otherwise specified in this SAR). Axial blankets are not considered in determining minimum enrichment.

**MGDS** is an acronym for Mined Geological Depository System.

**MPC Fuel Basket** means the honeycombed composite cell structure utilized to maintain subcriticality of the spent nuclear fuel. The number and size of the storage cells depends on the type of spent nuclear fuel to be transported. Each MPC fuel basket has sheathing welded to the storage cell walls for retaining the neutron absorber. The neutron absorber is a commercially-available thermal neutron poison material composed of boron carbide and aluminum.

**Multi-Purpose Canister (MPC)** means the sealed canister consisting of a honeycombed fuel basket for spent nuclear fuel storage, contained in a cylindrical canister shell (the MPC Enclosure Vessel). There are different MPCs with different fuel basket geometries for storing PWR or BWR fuel. All MPCs except the Trojan and Humboldt Bay plant MPCs have identical exterior dimensions. The Trojan plant MPCs have the same outside diameter, but are approximately nine inches shorter than the generic MPC design. The Humboldt Bay plant MPCs have the same outside diameter, but are approximately 6.3 feet shorter. MPC is an acronym for multi-purpose canister. Many of the MPCs used as part of the HI-STAR 100 Packaging are identical to the MPCs authorized for use in the HI-STAR 100 Storage (Docket No. 72-1008) and HI-STORM 100 Storage (72-1014) [1.0.7] CoCs to the extent that many of the particular MPC models are authorized for use under both CoCs.

**NDTT** is an acronym for Nil Ductility Transition Temperature, which is defined as the temperature at which the fracture stress in a material with a small flaw is equal to the yield stress in the same material if it had no flaws.

**Neutron Absorber Material** is a generic term used in this SAR to indicate any neutron absorber material qualified for use in the HI-STAR 100 System MPCs.

**Neutron Shielding** means Holtite, a material used in the overpack to thermalize and capture neutrons emanating from the radioactive spent nuclear fuel.

**Neutron Sources** means specially designed inserts for fuel assemblies that produce neutrons for startup of the reactor. The specific types of neutron sources authorized for transportation in the HI-STAR 100 System are discussed in **Subsection 1.2.3**.

**Non-fuel Hardware (NFH)** means Burnable Poison Rod Assemblies (BPRAs), Thimble Plug Devices (TPDs), Control Rod Assemblies (CRAs), Axial Power Shaping Rods (APSRs), Wet

Annular Burnable Absorbers (WABAs), Rod Cluster Control Assemblies (RCCAs), Control Element Assemblies (CEAs), water displacement guide tube plugs, orifice rod assemblies, and vibration suppressor inserts. The specific types of NFH authorized for transportation in the HI-STAR 100 System are discussed in Section 1.2 of this SAR.

**Nondestructive Examination (NDE)** is testing, examination and/or inspection of a component which does not affect the use of the component. NDE can be broadly divided into three categories: visual, surface and volumetric examinations. Additional information may be found in the ASME B&PV Code, Section V, Nondestructive Examination, Appendix A.

**Normal Condition** means the maximum level of an event or condition expected to routinely occur.

**Packaging** means the HI-STAR 100 System consisting of a single HI-STAR 100 overpack, a set of impact limiters, and a multi-purpose canister (MPC). It excludes all lifting devices, rigging, transporters, saddle blocks, welding machines, and auxiliary equipment (such as the drying and helium backfill system) used during fuel loading operations and preparation for off-site transportation.

**Package** means the HI-STAR 100 System plus the licensed radioactive contents loaded for transport.

**Planar-Average Initial Enrichment** is the average of the distributed fuel rod initial enrichments within a given axial plane of the assembly lattice.

**Post-Core Decay Time (PCDT)** is synonymous with cooling time.

**PWR** is an acronym for pressurized water reactor.

**Radwaste** means waste which is hazardous as a result of its containing nuclear materials; may be high or low-level waste.

**Reactivity** is used synonymously with effective multiplication factor or k-effective.

**Reactor-Related GTCC Waste** is a subset for GTCC Waste and generally consists of segmented solid radiation activated and surface contaminated reactor related hardware, cutting debris (chips) generated by mechanical cutting, metallic filter media and other operational/process waste arising from reactor decommissioning.

**SAR** is an acronym for Safety Analysis Report (10CFR71).

**Single Failure Proof** means that the handling system is designed so that a single failure will not result in the loss of the capability of the system to safely retain the load.

**SNF** is an acronym for spent nuclear fuel.

**Special Nuclear Material (SNM)** is defined by Title I of the Atomic Energy Act of 1954 as plutonium, uranium-233, or uranium enriched in the isotopes uranium-233 or uranium-235. The definition includes any other material that the Commission determines to be special nuclear material, but does not include source material. As of this writing, the NRC has not declared any other material as SNM.

**STP** is Standard Temperature (298°K) and Pressure (1 atm) conditions.

**TAL** is an acronym for the Threaded Anchor Location. TALs are used in the MPC closure lid for lifting the loaded MPC.

**Transport Index (TI)** means the dimensionless number (rounded up to the next tenth) placed on the label of a package, to designate the degree of control to be exercised by the carrier during transportation. The transport index is the number determined by multiplying the maximum radiation level in mSv/hr at one meter (3.3 ft) from the external surface of the package by 100 (equivalent to the maximum radiation level in mrem/hr at one meter (3.3 ft)).

**Trojan Damaged Fuel Container (or Canister)** is a Holtec damaged fuel container custom-designed for Trojan plant damaged fuel and fuel debris. Trojan plant damaged fuel and fuel debris not loaded into a Trojan Failed Fuel Can must be loaded into a Trojan Damaged Fuel Container.

**Trojan Failed Fuel Can (FFC)** is a non-Holtec designed Trojan plant-specific damaged fuel container that may be loaded with Trojan plant damaged fuel assemblies, Trojan fuel assembly metal fragments (e.g., portions of fuel rods, grid assemblies, bottom nozzles, etc.), a Trojan fuel rod storage container, a Trojan Fuel Debris Process Can Capsule, or a Trojan Fuel Debris Process Can.

**Trojan Failed Fuel Can Spacer** is a square, structural steel tube with a baseplate designed to be placed inside one Trojan Failed Fuel Can to occupy any space between the top of the contents and the top of the FFC in order to minimize movement of the FFC contents during transportation.

**Trojan Fuel Debris Process Can** is a Trojan plant-specific canister containing fuel debris (metal fragments) and was used to process organic media removed from the Trojan plant spent fuel pool during cleanup operations in preparation for spent fuel pool decommissioning. Trojan Fuel Debris Process Cans are loaded into Trojan Fuel Debris Process Can Capsules or directly into Trojan Failed Fuel Cans.

**Trojan Fuel Debris Process Can Capsule** is a Trojan plant-specific canister that contains up to five Trojan Fuel Debris Process Cans and is vacuumed, purged, backfilled with helium, and then seal-welded closed.

**Undamaged fuel assemblies** are fuel assemblies where all the exterior rods in the assembly are visually inspected and shown to be intact. The interior rods of the assembly are in place; however the cladding of these rods is of unknown condition. This definition only applies to Humboldt Bay fuel assembly array/class 6x6D and 7x7C.

**Water Tight** is defined as a degree of leaktightness that in a practical sense precludes any significant intrusion of water through all water exclusion barriers. This degree of leaktightness ranges from  $1 \times 10^{-2}$  std cm<sup>3</sup>/s air to  $1 \times 10^{-4}$  std cm<sup>3</sup>/s air in accordance with ASTM E1003-05 “Standard Test Method for Hydrostatic Leak Testing.”

**ZR** means any zirconium-based fuel cladding material authorized for use in a commercial nuclear power plant reactor. Any reference to Zircaloy fuel cladding in this SAR applies to any zirconium-based fuel cladding material.

Table 1.0.2

INTENTIONALLY DELETED

## 1.1 INTRODUCTION TO THE HI-STAR 100 PACKAGE

HI-STAR 100 (acronym for Holtec International Storage, Transport and Repository) is a spent nuclear fuel (SNF) packaging designed to be in general compliance with the U.S. Department of Energy's (DOE) original design procurement specifications for multi-purpose canisters and large transportation casks [1.1.1], [1.1.2]. **HI-STAR 100 also serves to transport reactor-related non-fuel waste as discussed in Supplement 1.II of this SAR.**

The HI-STAR 100 System consists of a sealed, metal multi-purpose canister, herein abbreviated as the "MPC", contained within an overpack with impact limiters. Figure 1.1.1 provides a pictorial view of the HI-STAR 100 System. The HI-STAR 100 System is designed to accommodate a wide variety of spent fuel assemblies in a single overpack design by utilizing different MPC basket designs. The exterior dimensions of all MPCs (except the custom-designed Trojan, **Diablo Canyon** and Humboldt Bay MPCs) are identical to allow the use of a single overpack design. The Trojan and **Diablo Canyon** plant MPCs are approximately nine inches shorter than the generic Holtec MPC design and have the same outer diameter. The Humboldt Bay MPCs/**GWCs** are approximately 6.3 feet shorter than the generic Holtec MPC design and have the same outer diameter. Each of the MPCs has different design features (e.g., fuel baskets) to accommodate distinct fuel characteristics. Each MPC is identified by the maximum quantity of fuel assemblies it is capable of receiving. The MPC-24, -24E, and -24EF each can contain a maximum of 24 PWR assemblies; the MPC-32 can contain up to 32 PWR assemblies; the MPC-68 and -68F each can contain a maximum of 68 BWR fuel assemblies; and the MPC-HB for Humboldt Bay can contain up to 80 fuel assemblies. Figure 1.1.2 depicts the HI-STAR 100 with two of its major constituents, the MPC and the overpack, in a cutaway view. This view does not include depiction of the **MPC** spacer required for the Trojan version of the MPC-24E/EF design **or of the MPC spacer required for the Diablo Canyon version of the MPC-32**. The **MPC** spacer is required for shorter MPCs to ensure the design characteristics of the HI-STAR 100 System (e.g., center-of-gravity, MPC lid-to-overpack closure plate gap, etc.) remain bounded by the supporting analyses. See Figure 1.1.5 for a depiction of the Trojan MPC spacer. A drawing of the Trojan MPC spacer is also included in Section 1.4. A summary of the qualification of the spacer for performing its design function is provided in Section 2.7.1.1. **A generic (i.e. standard) MPC spacer design is provided in Section 1.4. This standard MPC spacer is pre-qualified (See Supplement 2.III) for use with the Diablo Canyon version of the MPC-32 with the required length of the standard MPC spacer specified in the drawing package in Section 1.4.**

Figure 1.1.2 also indicates that the overpack pocket trunnions are optional appurtenances. Overpack serial numbers 1020-001 through 1020-007 include the pocket trunnions, while later serial number overpacks do not. The impact of this design change on vehicle tie down methods and qualification analyses are discussed in Section 2.5 of this SAR. The pocket trunnions are not part of the qualified vehicle tie-down system for the package. Figure 1.1.3 provides an elevation cross sectional view of an MPC, and Figure 1.1.4 contains an elevation cross sectional view of the HI-STAR 100 overpack.

The HI-STAR 100 System is designed for both storage and transport. The HI-STAR 100 System's multi-purpose design reduces SNF handling operations and thereby enhances radiological protection. Once SNF is loaded and the MPC and overpack are sealed, the HI-STAR 100 System can be



positioned on site for temporary or long-term storage or transported directly off-site. The HI-STAR 100 System's ability to both store and transport SNF eliminates repackaging.

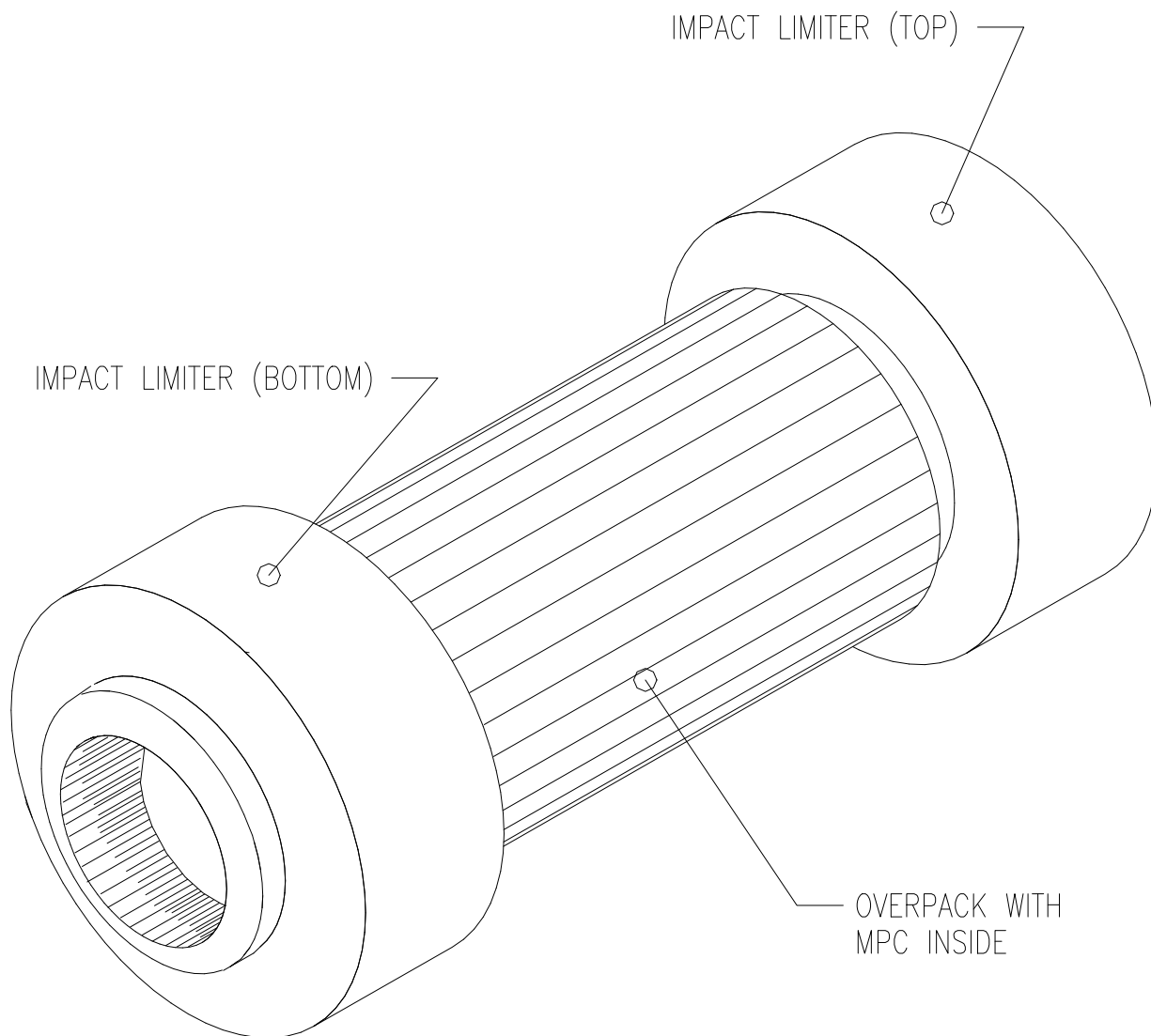


FIGURE 1.1.1; PICTORIAL VIEW OF  
HI-STAR 100 PACKAGE

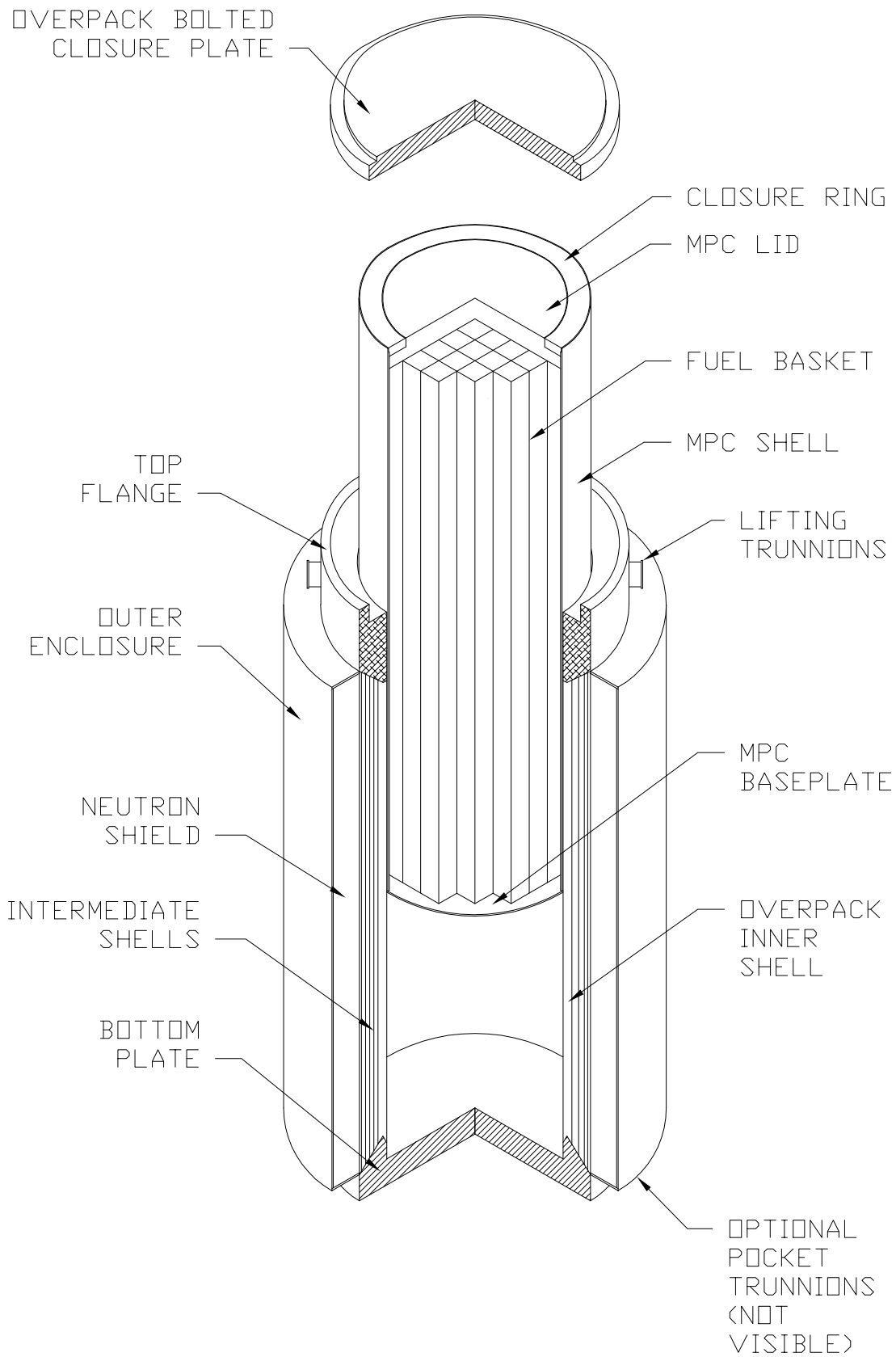


FIGURE 1.1.2; HI-STAR 100 OVERPACK WITH MPC PARTIALLY INSERTED

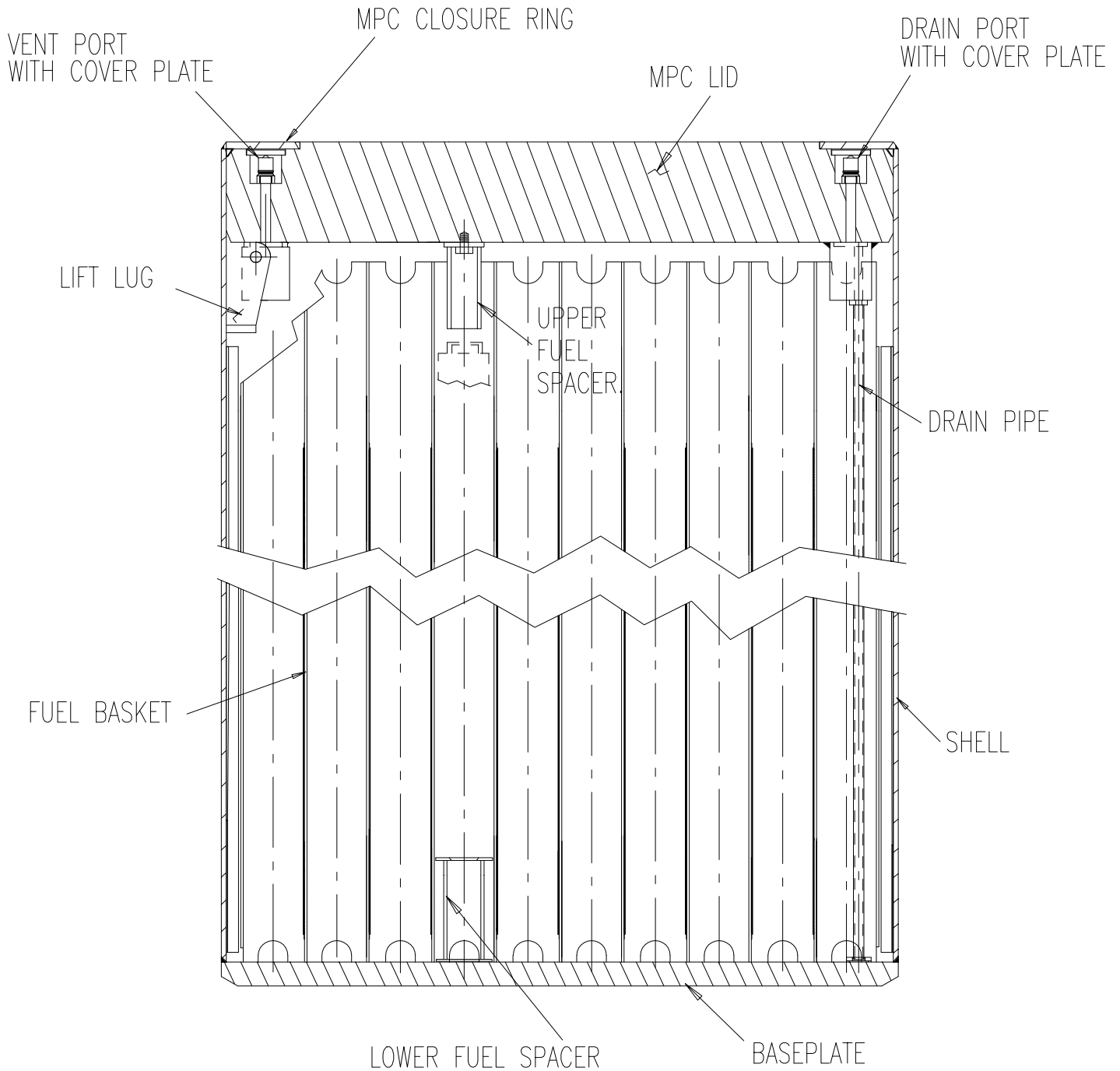


FIGURE 1.1.3; CROSS SECTION ELEVATION VIEW OF MPC

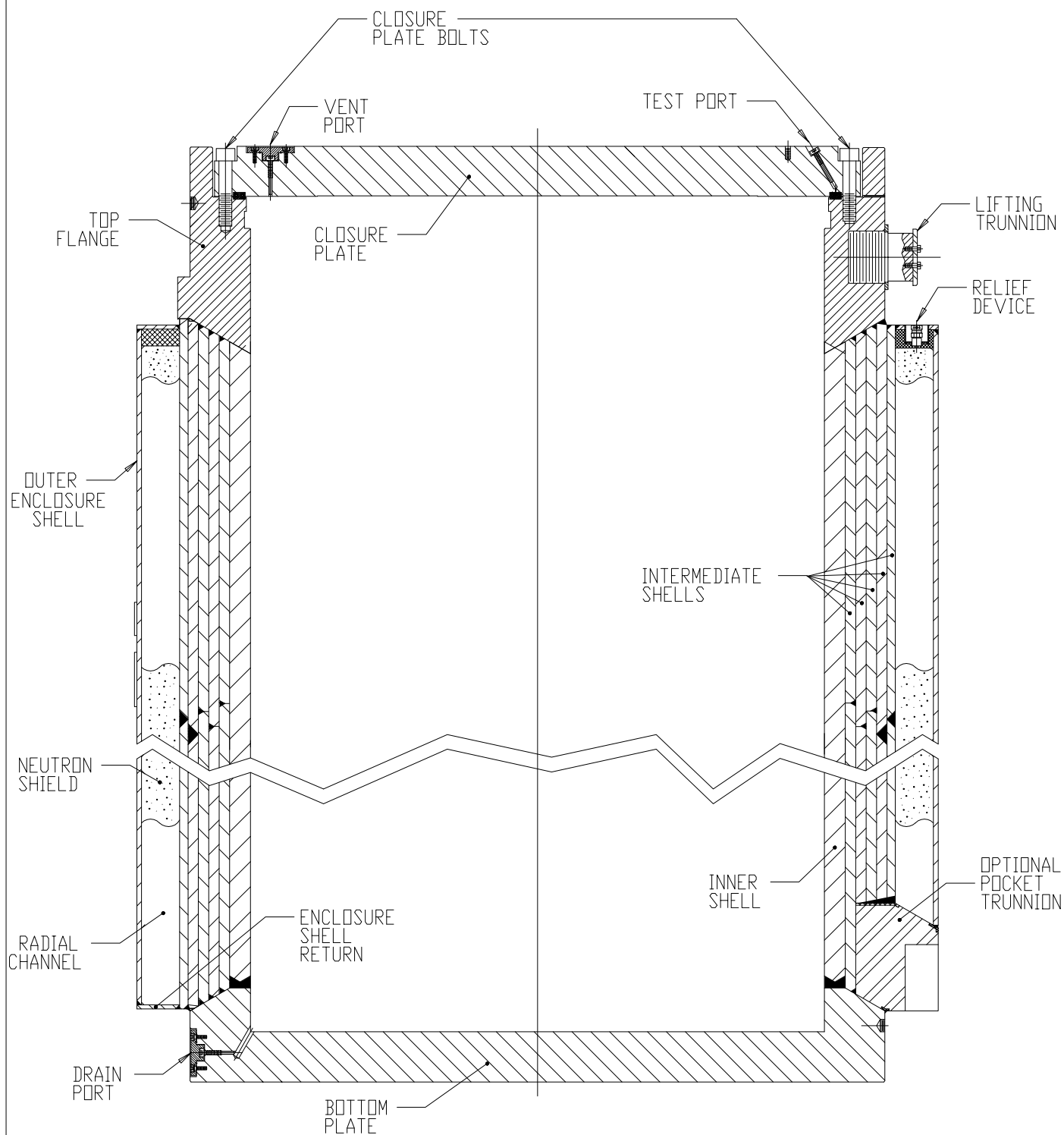


FIGURE 1.1.4; CROSS SECTION ELEVATION VIEW OF OVERPACK



FIGURE 1.1.5; TROJAN MPC SPACER

REPORT HI-951251

REV. 10

G:\SAR DOCUMENTS\HI-STAR SAR\Figures\SAR Revision 10\Chapter 01\Fig 1\_1\_5.doc

## 1.2 DESCRIPTION OF PACKAGING COMPONENTS AND THEIR DESIGN OPERATIONAL FEATURES

### 1.2.1 Packaging

The HI-STAR 100 System consists of an MPC designed for BWR or PWR spent nuclear fuel, an overpack that provides the containment boundary and a set of impact limiters that provide energy absorption capability for the normal and hypothetical accident conditions of transport. Each of these components is described below, including information with respect to component fabrication techniques and designed safety features. This discussion is supplemented by a set of drawings in Section 1.4. Section 1.3 provides the HI-STAR 100 design code applicability and details any alternatives to the ASME Code.

Before proceeding to present detailed physical data on HI-STAR 100, it is contextual to summarize the design attributes that set it apart from the prior generation of spent fuel transportation packages.

There are several features in the HI-STAR 100 System design that increase its effectiveness with respect to the safe transport of spent nuclear fuel (SNF). Some of the principal features of the HI-STAR 100 System that enhance its effectiveness are:

- the honeycomb design of the MPC fuel basket
- the effective distribution of neutron and gamma shielding materials within the system
- the high heat rejection capability
- the structural robustness of the multi-shell overpack construction

The honeycomb design of the MPC fuel baskets renders the basket into a multi-flanged plate weldment where all structural elements (box walls) are arrayed in two orthogonal sets of plates. Consequently, the walls of the cells are either completely coplanar (no offset) or orthogonal with each other. There is complete edge-to-edge continuity between contiguous cells.

Among the many benefits of the honeycomb construction is the uniform distribution of the metal mass over the body of the basket (in contrast to the “box and spacer disk” construction where the support plates are localized mass points). Physical reasoning suggests that a uniformly distributed mass provides a more effective shielding barrier than can be obtained from a non-uniform (box and spacer disk) basket. In other words, the honeycomb basket is a more effective radiation attenuation device.

The complete cell-to-cell connectivity inherent in the honeycomb basket structure provides an uninterrupted heat transmission path, making the HI-STAR 100 MPC an effective heat rejection device.

The multi-layer shell construction in the overpack provides a natural barrier against crack propagation in the radial direction across the overpack structure. If, during a hypothetical accident (impact) event, a crack was initiated in one layer, the crack could not propagate to the adjacent layer. Additionally, it is highly unlikely that a crack would initiate as the thinner layers are more ductile than a thicker plate.

In this Safety Analysis Report the HI-STAR 100 System design is demonstrated to have predicted responses to accident conditions that are clearly acceptable with respect to certification requirements for post-accident containment system integrity, maintenance of subcriticality margin, dose rates, and adequate heat rejection capability. Table 1.2.18 presents a summary of the HI-STAR 100 System performance against these aspects of post-accident performance at two levels. At the first level, the integrity of the MPC boundary prevents release of radioactive material or helium from the MPC, and ingress of moderator. The integrity of the MPC is demonstrated by the analysis of the response of this high quality, ASME Code, Section III, Subsection NB-designed, pressure vessel to the accident loads while in the overpack. With this demonstration of MPC integrity, the excellent performance results listed in the second column of Table 1.2.18 constitute an acceptable basis for certification of the HI-STAR 100 System for the safe transport of spent nuclear fuel. However, no credit is taken for MPC integrity for certification of the HI-STAR 100 System for the transport of intact or damaged fuel assemblies.

The HI-STAR 100 System provides a large margin of safety. The third column in Table 1.2.18 summarizes the performance if the MPC is postulated to suffer gross failure in the post-accident analysis. Even with this postulated failure, the performance of the HI-STAR 100 System is acceptable for the transport of intact and damaged fuel assemblies, showing the defense-in-depth methodology incorporated into the HI-STAR 100 System.

The containment boundary of the HI-STAR 100 System is shown to satisfy the special requirements of 10CFR71.61 for irradiated nuclear fuel shipments.

#### 1.2.1.1 Gross Weight

The gross weight of the HI-STAR 100 System depends on which of the MPCs is loaded into the HI-STAR 100 overpack for shipment. Table 2.2.1 summarizes the maximum calculated component weights for the HI-STAR 100 overpack, impact limiters, and each MPC loaded to maximum capacity with design basis SNF. The maximum gross transport weight of the HI-STAR 100 System is to be marked on the packaging nameplate.

#### 1.2.1.2 Materials of Construction, Dimensions, and Fabrication

All materials used to construct the HI-STAR 100 System are ASME Code materials, except the neutron shield, neutron poison, optional aluminum heat conduction elements, thermal expansion foam, seals, pressure relief devices, aluminum honeycomb, pipe couplings, and other material classified as Not Important to Safety. The specified materials of construction along with outline dimensions for important-to-safety items are provided in the drawings in Section 1.4.



The materials of construction and method of fabrication are further detailed in the subsections that follow. Section 1.3 provides the codes applicable to the HI-STAR 100 packaging for materials, design, fabrication, and inspection, including NRC-approved alternatives to the ASME Code.

#### 1.2.1.2.1 HI-STAR 100 Overpack

The **standard** HI-STAR 100 overpack is a heavy-walled steel cylindrical vessel. The inner diameter of the overpack is approximately 68-3/4 inches, **the outer diameter is approximately 96 inches**, the height of the internal cavity is usually 191-1/8 inches **and the overall height is approximately [PROPRIETARY INFORMATION WITHHELD PER 10CFR2.390]**. Shorter overpacks are available to meet site-specific requirements. The overpack inner cavity is sized to accommodate the MPCs **(MPC spacer(s) may be applicable)**.

Figure 1.2.1 provides a cross sectional elevation view of the overpack containment boundary. The overpack containment boundary is formed by a steel inner shell welded at the bottom to a bottom plate and, at the top, to a heavy top flange with a bolted closure plate. Two concentric grooves are machined into the closure plate for the seals. The closure plate is recessed into the top flange and the bolted joint is configured to protect the closure bolts and seals in the event of a drop accident. The closure plate has test and vent ports that are closed by a threaded port plug with a seal. The bottom plate has a drain port that is also closed by a threaded port plug with a seal. The containment boundary forms an internal cylindrical cavity for housing the MPC.

The outer surface of the overpack inner shell is buttressed with intermediate shells of gamma shielding that are installed in a manner to ensure a permanent state of contact between adjacent layers. Besides serving as an effective gamma shield, these layers provide additional strength to the overpack to resist puncture or penetration. Except in the HI-STAR HB (refer to Supplement 1.I), radial channels are vertically welded to the outside surface of the outermost intermediate shell at equal intervals around the circumference. These radial channels act as fins for improved heat conduction to the overpack outer enclosure shell surface and as cavities for retaining and protecting the neutron shielding. The enclosure shell is formed by welding enclosure shell panels between each of the channels to form additional cavities. Neutron shielding material is placed into each of the radial cavity segments formed by the radial channels, the outermost intermediate shell, and the enclosure shell panels. The exterior flats of the radial channels and enclosure shell panels form the overpack outer enclosure shell (Figure 1.2.2). Atop the outer enclosure shell, pressure relief devices (e.g., rupture disks) are positioned in a recessed area. The relief devices relieve internal pressure that may develop as a result of the fire accident and subsequent off-gassing of the neutron shield material. Within each radial channel, a layer of silicone sponge is positioned to act as a thermal expansion foam to compress as the neutron shield expands in the axial direction. Appendix 1.C provides material information on the thermal expansion foam. Figure 1.2.2 provides a mid-plane cross section view of the overpack, depicting the inner shell, intermediate shells, radial channels, outer enclosure shell, and neutron shield. Refer to drawings in Supplement 1.I for HI-STAR HB.

The exposed steel surfaces (except seal seating surfaces) of the overpack and the intermediate shell layers are coated to prevent corrosion. Coating materials are chosen based on the expected service conditions, considering the dual purpose certification status of the HI-STAR 100 System under 10

CFR 72 for spent fuel storage as well as transportation. The coatings applied to the overpack exposed exterior and interior surfaces are specified on the drawings in Section 1.4. The material data on the coatings is provided in Appendix 1.C. The inner cavity of the overpack is coated with a material appropriate to its high temperatures and the exterior of the overpack is coated with a material appropriate for fuel pool operations and environmental exposure. The coating applied to the intermediate shells acts as a surface preservative and is not exposed to the fuel pool or ambient environment.

Lifting trunnions are attached to the overpack top flange for lifting and rotating the cask body between vertical and horizontal positions. The lifting trunnions are located 180° apart in the sides of the top flange. On overpack serial numbers 1020-001 through 1020-007, pocket trunnions are welded to the lower side of the overpack 180° apart to provide a pivoting axis for rotation. The pocket trunnions are slightly off-center to ensure proper rotation direction of the overpack. As shown in Figure 1.1.4, the trunnions do not protrude beyond the cylindrical envelope of the overpack outer enclosure shell. This feature reduces the potential for direct impact on a trunnion in the event of an overpack side impact. After fabrication of HI-STAR overpack serial number 1020-007, the pocket trunnions were deleted from the overpack design.

#### 1.2.1.2.2 Multi-Purpose Canisters

##### 1.2.1.2.2.1 General Description

In this subsection, discussion of those attributes applicable to all of the MPC models is provided. Differences among the models are discussed in subsequent subsections. Specifications for the authorized contents of each MPC model, including non-fuel hardware and neutron sources are provided in Section 1.2.3.

The HI-STAR 100 MPCs are welded cylindrical structures with flat ends. Each MPC is an assembly consisting of a honeycombed fuel basket, a baseplate, a canister shell, a lid with vent and drain ports and cover plates, and a closure ring. The outer diameter of all MPCs and cylindrical height of each generic design MPC is fixed (**custom length MPCs are also qualified** in Subsection 1.2.1 regarding Trojan plant-specific MPCs and **in SAR Supplements** for **additional** plant-specific MPCs). The number of spent nuclear fuel storage locations in each of the MPCs depends on the fuel assembly characteristics. As the generic MPCs are interchangeable, they correspondingly have identical exterior dimensions. The outer dimension of the **generic MPCs** is nominally 68-3/8 inches and the length is nominally 190-1/4 inches. Figures 1.2.3-1.2.5 depict the cross sectional views of the different MPCs. Drawings of the MPCs are provided in Section 1.4. Key system data for the HI-STAR 100 System are outlined in Tables 1.2.2 and 1.2.3.

The generic MPC-24/24E/24EF and Trojan plant MPC-24E/EF differ in construction from the MPC-32 and MPC-68/68F in one important aspect: the fuel cells are physically separated from one another by a flux trap between each cell for criticality control (Figures 1.2.3 and 1.2.4). All MPC baskets are formed from an array of plates welded to each other, such that a honeycomb structure is created that resembles a multi-flanged, closed-section beam in its structural characteristics.

The MPC fuel basket is positioned and supported within the MPC shell by a series of basket supports welded to the inside of the MPC shell. In the peripheral area created by the basket, the MPC shell, and the basket supports, optional aluminum heat conduction elements are installed in some early production MPC-68 and MPC-68F models (see Figure 1.2.3). These heat conduction elements are fabricated from thin aluminum alloy 1100 in shapes and a design that allows a snug fit in the confined spaces and ease of installation. The heat conduction elements are along the full length of the MPC basket, except at the drain pipe location, to create a nonstructural thermal connection that facilitates heat transfer from the basket to the shell. In their operating condition, the heat conduction elements conform to, and contact the MPC shell and basket walls. In SAR Revision 10, a refined thermal analysis, described in Chapter 3, has allowed the elimination of these heat conduction elements from the MPC design, thus giving this design feature “optional” status.

Lifting lugs attached to the inside surface of the MPC canister shell serve to permit placement of the empty MPC into the overpack, and are considered non-structural, non-pressure retaining attachments to the MPC pressure boundary. The lifting lugs also serve to axially locate the MPC lid prior to welding. These internal lifting lugs are not used to handle a loaded MPC, since the MPC lid blocks access to the lifting lugs.

The top of the HI-STAR 100 MPC incorporates a redundant closure system. Figure 1.2.6 provides a sketch of the MPC closure details. The MPC lid is a circular plate (fabricated from one piece, or two pieces - split top and bottom) that is edge-welded to the MPC shell. If the two-piece lid design is employed, only the top piece is analyzed as part of the enclosure vessel pressure boundary. The bottom piece acts primarily as a radiation shield and is attached to the top piece with a non-structural, non-pressure retaining weld, as depicted on the MPC enclosure vessel drawing in Section 1.4. The MPC lid is equipped with vent and drain ports that are used to remove moisture and gas from the MPC and backfill the MPC with a specified pressure of inert gas (helium). The vent and drain ports are sealed closed by cover plates welded to the MPC lid before the closure ring is installed. The closure ring is a circular ring edge-welded to the MPC shell and MPC lid. The MPC lid provides sufficient rigidity to allow the entire MPC loaded with SNF to be lifted by the threaded holes in the MPC lid during transfer from the storage-only HI-STORM 100 System to the HI-STAR 100 overpack for transportation. Threaded insert plugs are installed to provide shielding when the threaded holes are not in use.

Unless otherwise noted, all MPCs are designed to handle intact fuel assemblies, damaged fuel assemblies, and fuel classified as fuel debris. Damaged fuel and fuel debris must be transported in damaged fuel containers or other approved damaged/failed fuel canister. At this time, BWR damaged fuel and fuel debris from Dresden Unit 1 is certified for transportation in the MPC-68 and the MPC-68F. Humboldt Bay damaged fuel and fuel debris will be transported in the MPC-HB (refer to Supplement 1.I). Similarly, only PWR damaged fuel and fuel debris from the Trojan plant is certified for transportation in the Trojan plant-specific MPC-24E and the MPC-24EF. **Diablo Canyon MPC-32 (See Supplement 1.III) is not qualified to transport damaged fuel containers; therefore Diablo Canyon damaged fuel and fuel debris are not qualified for transport in a Diablo Canyon MPC-32.** The definitions, and applicable specifications for all authorized contents, including the requirements for canning certain fuel, are provided in Subsection 1.2.3.

Intact SNF can be placed directly into the MPC. Damaged SNF and fuel debris must be placed into a Holtec damaged fuel container or other authorized canister for transportation inside the MPC and the HI-STAR 100 overpack. Figures 1.2.10 through 1.2.11 provide sketches of the containers authorized for transportation of damaged fuel and fuel debris in the HI-STAR 100 System. One Dresden Unit 1 Thoria rod canister, shown in Figure 1.2.11A, is also authorized for transportation in HI-STAR 100.

The MPC-68 and MPC-24E enclosure vessels have been slightly modified to further strengthen the lid-to-shell joint area. These MPCs are given the “F” suffix (hence, MPC-68F and MPC-24EF)<sup>†</sup>. The differences between the standard and “F-model” MPC lid-to-shell joints are shown on Figure 1.2.17, and include a thickened upper shell, a larger lid-to-shell weld size, and a correspondingly smaller lid diameter. The design of the rest of the enclosure vessel is identical between the standard MPC and the “F-model” MPC.

#### 1.2.1.2.2.2 MPC-24/24E/24EF

The MPC-24 is designed to transport up to 24 PWR intact fuel assemblies meeting the limits specified in Subsection 1.2.3. The MPC 24E is designed to transport up to 24 PWR intact and up to four PWR damaged fuel assemblies in damaged fuel containers. The MPC-24EF is designed to transport up to 24 PWR intact fuel assemblies and up to four PWR damaged fuel assemblies or fuel assemblies classified as fuel debris. At this time, however, generic PWR damaged fuel and fuel debris are not authorized for transportation in the MPC-24E/EF.

All MPC-24-series fuel baskets employ the flux trap design for criticality control, as shown in the drawings in Section 1.4. The fuel basket design for the MPC-24E is an enhanced MPC-24 basket layout designed to improve the fuel storage geometry for criticality control. The fuel basket design of the MPC-24EF is identical to the MPC-24E. The MPC-24E/EF basket designs also employ a higher <sup>10</sup>B loading than the MPC-24, as shown in Table 1.2.3. The differences between the MPC-24EF enclosure vessel design and the MPC-24/24E enclosure vessel are discussed in Subsection 1.2.1.2.2.1.

#### 1.2.1.2.2.3 Trojan Plant MPC-24E/EF

The Trojan plant MPC-24E and -24EF models are designs that have been customized for that plant’s fuel and the concrete storage cask being used at the Trojan plant Independent Spent Fuel Storage Installation (ISFSI) (Docket 72-0017). The design features that are unique to the Trojan plant MPCs are specifically noted on the MPC enclosure vessel and MPC-24E/EF fuel basket drawings in Section 1.4. These differences include:

- a shorter MPC fuel basket and cavity length to match the shorter Trojan fuel assembly length
- shorter corner fuel storage cell lengths to accommodate the Trojan Failed Fuel Cans

<sup>†</sup> The drawing in Section 1.4 also denotes an MPC-68FF canister design. However, the MPC-68FF is not authorized for use in transportation under the HI-STAR 100 10 CFR 71 CoC.

- a different fuel storage cell and flux trap dimension in the corner cells to accommodate the Trojan Failed Fuel Cans
- a different configuration of the flow holes at the bottom of the fuel basket (rectangular vs. semi-circular)

All other design features in the Trojan MPCs are identical to the generic MPC-24E/EF design. The HI-STAR 100 overpack design has not been modified for the Trojan MPC design.

The technical analyses described in this SAR were verified in most cases to bound the Trojan-specific design features. Where necessary, Trojan plant-specific evaluations were performed and are summarized in the appropriate SAR section. To accommodate the shorter Trojan plant MPC length in a standard-length HI-STAR 100 overpack, a spacer was designed for installation into the overpack above the Trojan MPC (see Figure 1.1.5 and the drawing in Section 1.4) for transportation in the standard-length HI-STAR 100 overpack. This spacer prevents the MPC from moving more than the MPC was analyzed to move in the axial direction and serves to transfer the axial loads from the MPC lid to the overpack top closure plate within the limits of the supporting analyses. See Section 2.7.1.1 for additional discussion of the spacer used with the Trojan MPC design. Hereafter in this SAR, the Trojan plant-specific MPC design is only distinguished from the generic MPC-24E/EF design when necessary to describe unique evaluations performed for those MPCs.

#### 1.2.1.2.2.4 MPC-32

The MPC-32 is designed to transport up to 32 PWR intact fuel assemblies, **non-fuel hardware and neutron sources** meeting the specifications in Subsection 1.2.3. Damaged fuel and fuel debris are not permitted to be transported in the MPC-32. The MPC-32 enclosure vessel design is identical to the MPC-24/24E enclosure vessel design as shown on the drawings in Section 1.4. The MPC-32 fuel basket does not employ flux traps for criticality control. Credit for burnup of the fuel is taken in the criticality analyses for accident conditions and to meet the requirements of 10 CFR 71.55(b). Because the MPC is designed to preclude the intrusion of moderator under all normal and credible accident conditions of transport, the moderator intrusion condition analyzed as required by 10 CFR 71.55(b) is a non-mechanistic event for the HI-STAR 100 System.

#### 1.2.1.2.2.5 MPC-68/68F

The MPC-68 is designed to transport up to 68 BWR intact fuel assemblies and damaged fuel assemblies meeting the specifications in Subsection 1.2.3. Zircaloy channels are permitted. At this time, only damaged fuel from the Dresden Unit 1 plant is authorized for transportation in the MPC-68. The MPC-68F is designed to transport only fuel and other authorized material from the Dresden Unit 1 plant meeting the specifications in Subsection 1.2.3. The sole difference between the MPC-68 and MPC-68F fuel basket design is a reduction in the required  $^{10}\text{B}$  areal density in the neutron absorber. A reduction in the required  $^{10}\text{B}$  areal density of the neutron absorber is possible for the MPC-68F due to limited types of fuel and low enrichments permitted to be transported in this MPC model. The differences between the MPC-68F enclosure vessel design and the MPC-68 enclosure vessel are discussed in Subsection 1.0.

#### 1.2.1.2.2.6 Alloy X

The HI-STAR MPC is constructed entirely from stainless steel alloy materials (except for the neutron absorber and aluminum vent and drain cap seal washers in all MPCs, and the aluminum heat conduction elements in the first several production units of MPC-68 and MPC-68F). No carbon steel parts are used in the design of the HI-STAR 100 MPC. Concerns regarding interaction of coated carbon steel materials and various MPC operating environments [1.2.1] are not applicable to the HI-STAR MPCs. All structural components in a HI-STAR MPC will be fabricated of Alloy X, a designation that warrants further explanation.

Alloy X is a fictitious material that should be acceptable as a Mined Geological Depository System (MGDS) waste package and that meets the thermophysical properties set forth in this document.

At this time, there is considerable uncertainty with respect to the material of construction for an MPC that would be acceptable as a waste package for the MGDS. Candidate materials being considered for acceptability by the DOE include:

- Type 316
- Type 316LN
- Type 304
- Type 304LN

The DOE material selection process is primarily driven by corrosion resistance in the potential environment of the MGDS. As the decision regarding a suitable material to meet disposal requirements is not imminent, this application requests approval for use of any one of the four Alloy X materials.

For the MPC design and analysis, Alloy X (as defined in this SAR) may be one of the following materials. Any steel part in an MPC may be fabricated from any of the acceptable Alloy X materials listed below, except that all steel pieces comprising the MPC shell (i.e., the 1/2" thick cylinder) must be fabricated from the same Alloy X stainless steel type:

- Type 316
- Type 316LN
- Type 304
- Type 304LN

The Alloy X approach is accomplished by qualifying the MPC for all mechanical, structural, neutronic, radiological, and thermal conditions using material thermophysical properties that are the least favorable for the entire group for the analysis in question. For example, when calculating the rate of heat rejection to the outside environment, the value of thermal conductivity used is the lowest for the candidate material group. Similarly, the stress analysis calculations use the lowest value of the ASME Code allowable stress intensity for the entire group. Stated differently, we have defined a

material, which is referred to as Alloy X, whose thermophysical properties, from the MPC design perspective, are the least favorable of the candidate materials group. The evaluation of the Alloy X constituents to determine the least favorable properties is provided in Appendix 1.A.

The Alloy X approach is conservative because no matter which material is ultimately utilized, the Alloy X approach guarantees that the performance of the MPC will exceed the analytical predictions contained in this document.

#### 1.2.1.3 Impact Limiters

The HI-STAR 100 overpack is fitted with aluminum honeycomb impact limiters, termed AL-STAR™, one at each end, once the overpack is positioned and secured in the transport frame. The impact limiters ensure the inertia loadings during the normal and hypothetical accident conditions of transport are maintained below design levels. The impact limiter design is discussed further in Chapter 2 and drawings are provided in Section 1.4. **A slightly customized version of the AL-STAR™ impact limiter is qualified in SAR Supplements I and II for use with HI-STAR HB and HI-STAR HB GTCC.**

#### 1.2.1.4 Shielding

The HI-STAR 100 System is provided with shielding to minimize personnel exposure. The HI-STAR 100 System will be transported by exclusive use shipment to ensure the external radiation requirements of 10CFR71.47 are met. During transport, a personnel barrier is installed to restrict access to the overpack to protect personnel from the HI-STAR 100 exterior surface temperature in accordance with 10CFR71.43(g). The personnel barrier provides a stand-off equal to the exterior radial dimension of the impact limiters. Figure 1.2.8 provides a sketch of the personnel barrier being installed.

The initial attenuation of gamma and neutron radiation emitted by the radioactive spent fuel is provided by the MPC fuel basket structure built from inter-welded plates and Boral neutron poison panels with sheathing attached to the fuel cell walls. The MPC canister shell, baseplate, and lid provide additional thicknesses of steel to further reduce gamma radiation and, to a smaller extent, neutron radiation at the outer MPC surfaces. No shielding credit is taken for the aluminum heat conduction elements installed in some of the early production MPC-68 and MPC-68F units.

The primary HI-STAR 100 shielding is located in the overpack and consists of neutron shielding and additional layers of steel for gamma shielding. Neutron shielding is provided around the outside circumferential surface of the overpack. Gamma shielding is provided by the overpack inner, intermediate and enclosure shells with additional axial shielding provided by the bottom plate and the top closure plate. During transport, the impact limiters will provide incremental gamma shielding and provide additional distance from the radiation source at the ends of the package. An additional circular segment of neutron shielding is contained within each impact limiter to provide neutron attenuation.



#### 1.2.1.4.1 Neutron Absorber Materials

Both Boral and Metamic are neutron absorber materials made of B<sub>4</sub>C and Aluminum. Boral is used in the MPC-24/24E/24EF, MPC-32, MPC-68/68F, and Trojan MPC-24E/24EF. Metamic is used in MPC-24/24E/24EF, MPC-68, and MPC-32 Models. Metamic is the only neutron absorber used in the MPC-HB (See drawing package in Supplement 1.I).

##### 1.2.1.4.1.1 Boral Neutron Absorber

Boral is a thermal neutron poison material composed of boron carbide and aluminum alloy 1100. Boron carbide is a compound having a high boron content in a physically stable and chemically inert form. The boron carbide contained in Boral is a fine granulated powder that conforms to ASTM C-750-80 nuclear grade Type III. The aluminum alloy 1100 is a lightweight metal with high tensile strength that is protected from corrosion by a highly resistant oxide film. The two materials, boron carbide and aluminum, are chemically compatible and ideally suited for long-term use in the radiation, thermal, and chemical environment of a nuclear reactor, spent fuel pool, or dry cask.

The documented historical applications of Boral, in environments comparable to those in spent fuel pools and fuel storage casks, dates to the early 1950s (the U.S. Atomic Energy Commission's AE-6 Water-Boiler Reactor [1.2.2]). Technical data on the material was first printed in 1949, when the report "Boral: A New Thermal Neutron Shield" was published [1.2.3]. In 1956, the first edition of the "Reactor Shielding Design Manual" [1.2.4], contains a section on Boral and its properties.

In the research and test reactors built during the 1950s and 1960s, Boral was frequently the material of choice for control blades, thermal-column shutters, and other items requiring very good thermal-neutron absorption properties. It is in these reactors that Boral has seen its longest service in environments comparable to today's applications.

Boral found other uses in the 1960s, one of which was a neutron poison material in baskets used in the shipment of irradiated, enriched fuel rods from Canada's Chalk River laboratories to Savannah River. Use of Boral in shipping containers continues, with Boral serving as the poison in many cask designs.

Boral has been licensed by the NRC for use in numerous BWR and PWR spent fuel storage racks and has been extensively used in international nuclear installations.

Boral has been exclusively used in fuel storage applications in recent years. Its use in spent fuel pools as the neutron absorbing material can be attributed to its proven performance and several unique characteristics, such as:

- The content and placement of boron carbide provides a very high removal cross section for thermal neutrons.
- Boron carbide, in the form of fine particles, is homogeneously dispersed throughout the central layer of the Boral panels.



- The boron carbide and aluminum materials in Boral do not degrade as a result of long-term exposure to radiation.
- The neutron absorbing central layer of Boral is clad with permanently bonded surfaces of aluminum.
- Boral is stable, strong, durable, and corrosion resistant.

Boral absorbs thermal neutrons without physical change or degradation of any sort from the anticipated exposure to gamma radiation and heat. The material does not suffer loss of neutron attenuation capability when exposed to high levels of radiation dose.

Holtec International's QA Program ensures that Boral is manufactured under the control and surveillance of a Quality Assurance/Quality Control Program that conforms to the requirements of 10CFR71, Subpart H and 10CFR72, Subpart G. Holtec International has procured over 200,000 panels of Boral from AAR Advanced Structures for over 20 projects. Boral has always been purchased with a minimum  $^{10}\text{B}$  loading requirement. Coupons extracted from production runs were tested using the "wet chemistry" procedure. The actual  $^{10}\text{B}$  loading, out of thousands of coupons tested, has never been found to fall below the design specification. The size of this coupon database is sufficient to provide confidence that all future procurements will continue to yield Boral with full compliance with the stipulated minimum loading. Furthermore, the surveillance, coupon testing, and material tracking processes that have so effectively controlled the quality of Boral are expected to continue to yield Boral of similar quality in the future. Nevertheless, to add another layer of insurance, only 75%  $^{10}\text{B}$  credit of the fixed neutron absorber is assumed in the criticality analysis.

Operating experience in nuclear plants with fuel loading of Boral equipped MPCs as well as laboratory test data indicate that the aluminum used in the manufacture of the Boral may react with water, resulting in the generation of hydrogen. The numerous variables (i.e., aluminum particle size, pool temperature, pool chemistry, etc.) that influence the extent of the hydrogen produced make it impossible to predict the amount of hydrogen that may be generated during MPC loading or unloading at a particular plant. Therefore, due to the variability in hydrogen generation from the Boral-water reaction, the operating procedures in Chapter 7 describe steps to monitor and mitigate combustible gas accumulation beneath the MPC lid during loading and unloading operations when an ignition event could occur (i.e., when the space beneath the MPC lid is open to the welding or cutting operation).

#### 1.2.1.4.1.2 METAMIC<sup>®</sup>

METAMIC<sup>®</sup> is a neutron absorber material developed by the Reynolds Aluminum Company in the mid-1990s for spent fuel reactivity control in dry and wet storage applications. Metallurgically, METAMIC<sup>®</sup> is a metal matrix composite (MMC) consisting of a matrix of 6061 aluminum alloy reinforced with Type 1 ASTM C-750 boron carbide. METAMIC<sup>®</sup> is characterized by extremely fine aluminum (325 mesh or better) and boron carbide powder. Typically, the average  $\text{B}_4\text{C}$  particle size is

between 10 and 25 microns. As described in the U.S. patents held by Holtec International<sup>1,2</sup>, the high performance and reliability of METAMIC<sup>®</sup> derives from the particle size distribution of its constituents, rendered into a metal matrix composite by the powder metallurgy process. This yields excellent and uniform homogeneity.

The powders are carefully blended without binders or other additives that could potentially adversely influence performance. The maximum percentage of B<sub>4</sub>C that can be dispersed in the aluminum alloy 6061 matrix is approximately 40 wt.%, although extensive manufacturing and testing experience is limited to approximately 31 wt.%. The blend of powders is isostatically compacted into a green billet under high pressure and vacuum sintered to near theoretical density.

According to the manufacturer, billets of any size can be produced using this technology. The billet is subsequently extruded into one of a number of product forms, ranging from sheet and plate to angle, channel, round and square tube, and other profiles. For the METAMIC<sup>®</sup> sheets used in the MPCs, the extruded form is rolled down into the required thickness.

METAMIC<sup>®</sup> has been subjected to an extensive array of tests sponsored by the Electric Power Research Institute (EPRI) that evaluated the functional performance of the material at elevated temperatures (up to 900°F) and radiation levels (1E+11 rads gamma). The results of the tests documented in an EPRI report (Ref. [1.2.17]) indicate that METAMIC<sup>®</sup> maintains its physical and neutron absorption properties with little variation in its properties from the unirradiated state. The main conclusions provided in the above-referenced EPRI report are summarized below:

- The metal matrix configuration produced by the powder metallurgy process with a complete absence of open porosity in METAMIC<sup>®</sup> ensures that its density is essentially equal to the theoretical density.
- The physical and neutronic properties of METAMIC<sup>®</sup> are essentially unaltered under exposure to elevated temperatures (750° F - 900° F).
- No detectable change in the neutron attenuation characteristics under accelerated corrosion test conditions has been observed.

In addition, independent measurements of boron carbide particle distribution show extremely small particle-to-particle distance<sup>†</sup> and near-perfect homogeneity.

An evaluation of the manufacturing technology underlying METAMIC<sup>®</sup> as disclosed in the above-referenced patents and of the extensive third-party tests carried out under the auspices of EPRI makes

---

1 U.S. Patent No. 5,965,829, “Radiation Absorbing Refractory Composition”.

2 U.S. Patent No. 6,042,779, “Extrusion Fabrication Process for Discontinuous Carbide Particulate Metal Matrix Composites and Super, Hypereutectic Al/Si.”

† Medium measured neighbor-to-neighbor distance is 10.08 microns according to the article, “METAMIC Neutron Shielding”, by K. Anderson, T. Haynes, and R. Kazmier, EPRI Boraflex Conference, November 19-20, 1998.

METAMIC<sup>®</sup> an acceptable neutron absorber material for use in the MPCs. Holtec's technical position on METAMIC<sup>®</sup> is also supported by the evaluation carried out by other organizations.

Consistent with its role in reactivity control, all METAMIC<sup>®</sup> material procured for use in the Holtec MPCs will be qualified as important-to-safety (ITS) Category A item. ITS category A manufactured items, as required by Holtec's NRC-approved Quality Assurance program, must be produced to essentially preclude the potential of an error in the procurement of constituent materials and the manufacturing processes. Accordingly, material and manufacturing control processes must be established to eliminate the incidence of errors, and inspection steps must be implemented to serve as an independent set of barriers to ensure that all critical characteristics defined for the material by the cask designer are met in the manufactured product.

All manufacturing and in-process steps in the production of METAMIC<sup>®</sup> shall be carried out using written procedures. As required by the company's quality program, the material manufacturer's QA program and its implementation shall be subject to review and ongoing assessment, including audits and surveillances as set forth in the applicable Holtec QA procedures to ensure that all METAMIC<sup>®</sup> panels procured meet with the requirements appropriate for the quality genre of the MPCs. Additional details pertaining to the qualification and production tests for METAMIC<sup>®</sup> are summarized in Subsection 8.1.5.5.2.

Because of the absence of interconnected porosities, the time required to dehydrate a METAMIC<sup>®</sup>-equipped MPC is expected to be less compared to an MPC containing Boral.

NUREG/CR-5661 (Ref. [1.2.20]) recommends limiting poison material credit to 75% of the minimum <sup>10</sup>B loading because of concerns for potential "streaming" of neutrons, and allows for greater percentage credit in criticality analysis "if comprehensive acceptance tests, capable of verifying the presence and uniformity of the neutron absorber, are implemented". The value of 75% is characterized in NUREG/CR-5661 as a very conservative value, based on experiments with neutron poison containing relatively large B<sub>4</sub>C particles, such as BORAL with an average particle size in excess of 100 microns. METAMIC<sup>®</sup>, however, has a much smaller particle size of typically between 10 and 25 microns on average. Any streaming concerns would therefore be drastically reduced.

Analyses performed by Holtec International show that the streaming due to particle size is practically non-existent in METAMIC<sup>®</sup>. Further, EPRI's neutron attenuation measurements on 31 and 15 B<sub>4</sub>C weight percent METAMIC<sup>®</sup> showed that METAMIC<sup>®</sup> exhibits very uniform <sup>10</sup>B areal density. This makes it easy to reliably establish and verify the presence and microscopic and macroscopic uniformity of the <sup>10</sup>B in the material. Therefore, 90% credit can be applied to the minimum <sup>10</sup>B areal density in the criticality calculations, i.e. a 10% penalty can be applied. This 10% penalty is considered conservative since there are no significant remaining uncertainties in the <sup>10</sup>B areal density. In Chapter 8 the qualification and production tests for METAMIC<sup>®</sup> to support 90% <sup>10</sup>B credit are specified. With 90% credit, the target weight percent of boron carbide in METAMIC<sup>®</sup> is 31, consistent with the test coupons used in the EPRI evaluations [1.2.17]. The maximum permitted value is 33.0 wt% to allow for necessary fabrication flexibility.

Because METAMIC<sup>®</sup> is a solid material, there is no capillary path through which spent fuel pool water can penetrate METAMIC<sup>®</sup> panels and chemically react with aluminum in the interior of the material to generate hydrogen. Any chemical reaction of the outer surfaces of the METAMIC<sup>®</sup> neutron absorber panels with water to produce hydrogen occurs rapidly and reduces to an insignificant amount in a short period of time. Nevertheless, operating procedures in Chapter 7 describe steps to monitor and mitigate combustible gas accumulation beneath the MPC lid during loading and unloading operations when an ignition event could occur (i.e., when the space beneath the MPC lid is open to the welding or cutting operation).

Mechanical properties of 31 wt.% METAMIC<sup>®</sup>, based on coupon tests of the material in the as-fabricated condition and after 48 hours of an elevated temperature state at 900°F, are summarized below from the EPRI report [1.2.17].

Mechanical Properties of 31wt.% B <sub>4</sub> C METAMIC		
Property	As-Fabricated	After 48 hours of 900°F Temperature Soak
Yield Strength (psi)	32937 ± 3132	28744 ± 3246
Ultimate Strength (psi)	40141 ± 1860	34608 ± 1513
Elongation (%)	1.8 ± 0.8	5.7 ± 3.1

The required flexural strain of the neutron absorber to ensure that it will not fracture when the supporting basket wall flexes, due to the worst case lateral inertial loading is 0.2%, which is the flexural strain of the Alloy X basket panel material. The 1% minimum elongation of 31wt.% B<sub>4</sub>C METAMIC<sup>®</sup> indicated by the above table means that a large margin of safety against cracking exists, so there is no need to perform testing of the METAMIC<sup>®</sup> for mechanical properties.

EPRI's extensive characterization effort [1.2.17], which was focused on 15 and 31 wt.% B<sub>4</sub>C METAMIC<sup>®</sup> served as the principal basis for a recent USNRC SER for 31wt.% B<sub>4</sub>C METAMIC for used in wet storage [1.2.18]. Additional studies on METAMIC<sup>®</sup> [1.2.19], EPRI's and others work provide the confidence that 31wt.% B<sub>4</sub>C METAMIC<sup>®</sup> will perform its intended function in the MPCs. Finally to further substantiate the performance of Metamic (with maximum B<sub>4</sub>C of up to 33%), Holtec has performed robust independent qualification testing as documented in Holtec Proprietary Report [1.2.21].

#### 1.2.1.4.2 Holtite<sup>TM</sup> Neutron Shielding Material

##### (a) Qualification of the Holtite<sup>TM</sup> Neutron Shielding Material

The shielding against neutron radiation in HI-STAR 100 Packaging is provided by Holtite-A. Holtite<sup>TM</sup> is a hydrogen rich, radiation resistant, polymeric material impregnated with boron carbide. Holtite-A was developed by Holtec International in the early 90s as a part of the company's HI-STAR 100 design development program.

Holtite-A was subjected to extensive studies of its critical characteristics (viz., radiation resistance, physical stability at service temperature and homogeneity) during its evaluation and validation program, which led to its regulatory approval in the HI-STAR 100 Docket (71-9261) and subsequent use in manufactured HI-STAR 100 overpacks.

Holtite-A is a relatively poor conductor of heat and possesses limited gamma attenuation capability. Its main function is to provide neutron shielding which is enabled by a hydrogen rich polymeric matrix and a spatially distributed particles of Boron Carbide. Holtite-A has been subjected to a battery of tests to establish its radiation resistance, physical stability at service temperature and homogeneity. Holtite-A is qualified to operate under 149°C (300°F) temperature in sustained use without a significant weight loss.

Additional information on Holtite-A is provided in Appendix 1.B of this SAR.

In this SAR, the terms Holtite-A and Holtite are used interchangeably.

## (b) Critical Characteristics of the Holtite Neutron Shielding Material

### (i) Critical Characteristics for Shielding Function

The bulk density, hydrogen concentration and weight fraction of Boron Carbide are specified as critical properties since the properties are used in the shielding analysis in Chapter 3. The required values for hydrogen concentration bulk density, and Boron Carbide are provided in Table 1.B.1.

### (ii) Critical Characteristics for Thermal Function

The thermal conductivity of Holtite-A is a critical characteristic if utilized in the thermal analysis of the package in Chapter 3. Table 1.B.1 provides the minimum acceptable effective conductivity of Holtite-A including the contribution of conductivity enhancers and for information on its use.

#### 1.2.1.4.3 Gamma Shielding Material

For gamma shielding, HI-STAR 100 utilizes carbon steel in plate stock form. Instead of utilizing a thick forging, the gamma shield design in the HI-STAR 100 overpack borrows from the concept of layered vessels from the field of ultra-high pressure vessel technology. The shielding is made from successive layers of plate stock. The fabrication of the shell begins by rolling the inner shell plate and making the longitudinal weld seam. Each layer of the intermediate shells is constructed from two halves. The two halves of the shell are precision sheared, beveled, and rolled to the required radii. The two halves of the second layer are wrapped around the first shell. Each shell half is positioned in its location and while applying pressure using a specially engineered fixture, the halves are tack welded. The beveled edges to be joined are positioned to make contact or have a slight gap. The second layer is made by joining the two halves using two longitudinal welds. Successive layers are assembled in a like manner. Thus, the welding of every successive shell provides a certain inter-layer contact (Figure 1.2.7).

A thick structural component radiation barrier is thus constructed with four key features, namely:

- The number of layers can be increased as necessary to realize the required design objectives.
- The layered construction is ideal to stop propagation of flaws.
- The thinner plate stock is much more ductile than heavy forgings used in other designs.
- Post-weld heat treatment is not required by the ASME Code, simplifying fabrication.

#### 1.2.1.5 Lifting and Tie-Down Devices

The HI-STAR 100 overpack is equipped with two lifting trunnions located in the top flange. The lifting trunnions are designed in accordance with 10CFR71.45, NUREG-0612 [1.2.11], and **Regulatory Guide 3.61** [1.3.4], manufactured from a high strength alloy, and are installed in threaded openings. The lifting trunnions may be secured in position by optional locking pads, shaped to make conformal contact with the curved overpack. Once the locking pad is bolted in position, the inner diameter is sized to restrain the trunnion from backing out. The two off-center pockets located near the overpack bottom plate on overpack serial numbers 1020-001 through 1020-007 are pocket trunnions. The pocket trunnions were eliminated from the design after serial number 1020-007 was fabricated and are no longer considered qualified tie-down devices. However, the pocket trunnions on these overpacks may still be used for normal handling activities such as upending and downending.

The lifting, upending, and downending of the HI-STAR 100 System requires the use of external handling devices. A lifting yoke is utilized when the cask is to be lifted or set in a vertical orientation. For those overpacks that have been fabricated with the pocket trunnions, transport and rotation cradles may include rotation trunnions that interface with the pocket trunnions to provide a pivot axis. A lift yoke may be connected to the lifting trunnions and the crane hook used for upending or downending the HI-STAR 100 System by rotating on the pocket trunnions for these overpacks. For those overpacks fabricated without pocket trunnions, the overpack must be transferred into the transport saddle with appropriate lift rigging. If an overpack having pocket trunnions is secured to the transport vehicle without engaging the pocket trunnions, plugs are required to be installed in the pocket to provide radiation shielding (see the overpack drawing in Section 1.4).

For transportation, the HI-STAR 100 System is engineered to be mounted on a transport frame secured to the transporter bed. Figure 1.2.8 provides a sketch of the HI-STAR 100 System secured for transport and the drawing in Section 1.4 provides additional details. The transport frame has a lower saddle with attachment points for belly slings around the cask body designed to prevent excessive vertical or lateral movement of the cask during normal transportation. The impact limiters affixed to both ends of the cask are designed to transmit the design basis axial loads into the cradle structure. See Section 2.5 for discussion of the qualification of tie-down devices.



The top of the MPC lid is equipped with four threaded holes that allow lifting of the loaded MPC. These holes allow the loaded MPC to be raised and/or lowered from the HI-STAR overpack. For users of the HI-STORM 100 Dry Storage System, MPC handling operations are performed using a HI-TRAC transfer cask of the HI-STORM 100 System (Docket No. 72-1014). The HI-TRAC transfer cask allows the sealed MPC loaded with spent fuel to be transferred from the HI-STORM 100 overpack (storage-only) to the HI-STAR 100 overpack, or vice versa. The threaded holes in the MPC lid are designed in accordance with NUREG-0612 and [Regulatory Guide 3.61](#) and are plugged during transportation to prevent radiation streaming.

#### 1.2.1.6 Heat Dissipation

The HI-STAR 100 System can safely transport SNF by maintaining the fuel cladding temperature below the limits specified in Table 1.2.3 for normal and accident conditions. These limits have been established consistent with the guidance in NRC Interim Staff Guidance (ISG) document No. 11, Revision 3 (Ref. [1.2.14]). The temperature of the fuel cladding is dependent on the decay heat and the heat dissipation capabilities of the cask. The total heat load per BWR and PWR MPC is identified in Table 1.2.3. The SNF decay heat is passively dissipated without any mechanical or forced cooling.

The HI-STAR 100 System must meet the requirements of 10 CFR 71.43(g) for the accessible surface temperature limit. To meet this requirement the HI-STAR 100 System is shipped as an exclusive use shipment and includes an engineered personnel barrier during transport.

The primary heat transfer mechanisms in the HI-STAR 100 System are conduction and surface radiation.

The free volume of the MPC and the annulus between the external surface of the MPC and the inside surface of the overpack containment boundary are filled with 99.995% pure helium gas during fuel loading operations. Table 1.2.3 specifies the acceptance criteria for helium fill pressure in the MPC internal cavity. Besides providing an inert dry atmosphere for the fuel cladding, the helium also provides conductive heat transfer across any gaps between the metal surfaces inside the MPC and in the annulus between the MPC and overpack containment boundary. Metal conduction transfers the heat throughout the MPC fuel basket, through the MPC aluminum heat conduction elements (if installed) and shell, through the overpack inner shell, intermediate shells, steel radial connectors and finally, to the outer neutron shield enclosure shell. The most adverse temperature profiles and thermal gradients for the HI-STAR 100 System with each of the MPCs are discussed in detail in Chapter 3. The thermal analysis in Chapter 3 no longer takes credit for the aluminum heat conduction elements and they have been designated as optional equipment.

#### 1.2.1.7 Coolants

There are no coolants utilized in the HI-STAR 100 System. As discussed in Subsection 1.2.1.6 above, helium is sealed within the MPC internal cavity. The annulus between the MPC outer surface and overpack containment boundary is also purged and filled with helium gas.

#### 1.2.1.8 Pressure Relief Systems

No pressure relief system is provided on the HI-STAR 100 packaging containment boundary.

The sole pressure relief devices are provided in the overpack outer enclosure (Figure 1.1.4). The overpack outer enclosure contains the neutron shield material. Normal loadings will not cause the rupture disks to open. The rupture disks are installed to relieve internal pressure in the neutron shield cavities caused by the fire accident. The overpack outer enclosure is not designed as a pressure vessel. Correspondingly, the rupture disks are designed to open at relatively low pressures as stated below.

Relief Device location	Set pressure, psig
Overpack outer enclosure	30, +/- 5

#### 1.2.1.9 Security Seal

The HI-STAR 100 packaging provides a security seal that while intact, provides evidence that the package has not been opened by unauthorized persons. When installed, the impact limiters cover all penetrations into the HI-STAR 100 packaging containment boundary. Therefore, the security seal is placed to ensure that the impact limiters are not removed which thereby ensures that the package has not been opened. As shown on the HI-STAR transport assembly drawing in Section 1.4, security seals are provided on one impact limiter attachment bolt on the top impact limiter and through two adjacent bolts on the bottom impact limiter. A hole is provided in the head of the bolt and the impact limiter. Lock wire shall be threaded through the hole and joined with a security seal.

#### 1.2.1.10 Design Life

The design life of the HI-STAR 100 System is 40 years. This is accomplished by using materials of construction with a long proven history in the nuclear industry and specifying materials known to withstand their operating environments with little to no degradation. A maintenance program, as specified in Chapter 8, is also implemented to ensure the HI-STAR 100 System will exceed its design life of 40 years. The design considerations that assure the HI-STAR 100 System performs as designed throughout the service life include the following:

##### HI-STAR Overpack

- Exposure to Environmental Effects
- Material Degradation
- Maintenance and Inspection Provisions

##### MPC

- Corrosion



- Structural Fatigue Effects
- Maintenance of Helium Atmosphere
- Allowable Fuel Cladding Temperatures
- Neutron Absorber Boron Depletion

### 1.2.2 Operational Features

Table 1.2.7 provides the sequence of basic operations necessary to load fuel and prepare the HI-STAR 100 System for transport. More detailed guidance for transportation-related loading, unloading, and handling operations is provided in Chapter 7 and is supported by the drawings in Section 1.4. A summary of the loading and unloading operations is provided below. Figures 1.2.9 and 1.2.16 provide a pictorial view of the loading and unloading operations, respectively.

#### 1.2.2.1 Applicability of Operating Procedures for the Dual-Purpose HI-STAR 100 System

The HI-STAR 100 System is a dual-purpose system certified for use as a dry storage cask under 10 CFR 72 and as a transportation package under 10 CFR 71. In addition, the MPC is certified for use under 10 CFR 72 in the storage-only HI-STORM 100 System (a ventilated concrete cask system). Therefore, it is possible that the HI-STAR 100 overpack and/or the MPC may be loaded, prepared, and sealed under the operating procedures for storage, delineated in the HI-STAR 100 storage FSAR (Docket 72-1008) or the HI-STORM 100 storage FSAR (Docket 72-1014) or under a site specific storage license. In those cases, the operating procedures governing MPC and overpack preparation for storage would apply. The MPC and HI-STAR 100 overpack, as applicable, must be confirmed to meet all requirements of the Part 71 Certificate of Compliance before being released for shipment.

For those instances where the MPC is being loaded and shipped off-site in a HI-STAR 100 overpack under 10 CFR 71 without first being deployed at an ISFSI (known as “load-and-go” operations), the operating procedures in Chapter 7 (and summarized below) apply for preparation of the MPC and HI-STAR overpack. For those cases where the MPC is transferred from storage in a HI-STORM overpack to a HI-STAR overpack for shipment, the operating procedures in Chapter 7 (and summarized below) govern the preparation activities for the HI-STAR overpack.

#### Loading Operations

At the start of loading operations, the overpack is configured with the closure plate removed. The lift yoke is used to position the overpack in the designated preparation area or setdown area for overpack inspection and MPC insertion. The annulus is filled with plant demineralized water and an annulus seal is installed. The seal prevents contact between spent fuel pool water and the MPC shell reducing the possibility of contaminating the outer surfaces of the MPC. The MPC is then filled with spent fuel pool water or plant demineralized water. The overpack and MPC are lowered into the spent fuel pool for fuel loading using the lift yoke. Pre-selected assemblies are loaded into the MPC and a visual verification of the assembly identification is performed.

While still underwater, a thick shielding lid (the MPC lid) is installed. The lift yoke is remotely engaged to the overpack lifting trunnions and is used to lift the overpack close to the spent fuel pool

surface. The MPC lift bolts (securing the MPC lid to the lift yoke) are removed. As the overpack is removed from the spent fuel pool, the lift yoke and overpack are sprayed with demineralized water to help remove contamination.

The overpack is removed from the pool and placed in the designated preparation area. The top surfaces of the MPC lid and the top flange of the overpack are decontaminated. The annulus seal is removed, and an annulus shield is installed. The annulus shield provides additional personnel shielding at the top of the annulus and also prevents small items from being dropped into the annulus (foreign material exclusion). If used, the Automated Welding System (AWS) is installed. The MPC water level is lowered slightly (See Chapter 7 for steps describing monitoring and mitigation of combustible gas accumulation). The MPC lid is seal-welded using the AWS. Liquid penetrant examinations are performed on the root and final passes and ultrasonic examination is also performed on the MPC lid-to-shell weld or, in place of the ultrasonic examination, the weld may be inspected by multiple-pass liquid penetrant examination at approximately every 3/8 inch of weld depth. At the appropriate time in the sequence of activities, based on the type of test performed (hydrostatic or pneumatic), a pressure test of the MPC enclosure vessel is performed.

The Forced Helium Dehydration (FHD) System is connected to the MPC and is used to remove residual water from the MPC and reduce the level of moisture in the MPC to acceptable levels. This is accomplished by recirculating dry, heated helium through the MPC cavity to absorb the moisture. When the helium exiting the MPC is determined to meet the required moisture limit, the MPC is considered sufficiently dried for transportation (see Section 3.4.1.1.16 for a description of the FHD System).

Following MPC drying operations, the MPC is backfilled with a predetermined amount of helium gas. The helium backfill ensures adequate heat transfer and provides an inert atmosphere for fuel cladding integrity.

The MPC closure ring is then placed on the MPC, aligned, tacked in place, and seal welded, providing redundant closure of the MPC enclosure vessel closure welds. Tack welds are visually examined, and the root and/or final welds (depending on the number of weld passes required) are inspected using the liquid penetrant examination technique to ensure weld integrity. The annulus shield is removed and the remaining water in the annulus is drained. The AWS is removed. The overpack closure plate is installed and the bolts are torqued. The overpack annulus is dried using the vacuum drying system (VDS).

The overpack annulus is backfilled with helium gas for heat transfer and seal testing. Concentric metallic seals in the overpack closure plate prevent the leakage of the helium gas from the annulus and provide the containment boundary to the release of radioactive materials. The seals on the overpack vent and drain port plugs are leak tested along with the overpack closure plate inner seal. Cover plates with metallic seals are installed over the overpack vent and drain ports to provide redundant closure of the overpack penetrations. A port plug with a metallic seal is installed in the overpack closure plate test port to provide fully redundant closure of all overpack penetrations.

The overpack is surveyed for removable contamination and secured on the transport vehicle with impact limiters installed, the security seals are attached, and the personnel barrier is installed. The HI-STAR 100 packaging is then ready for transport.

### Unloading Operations

The HI-STAR 100 System unloading procedures describe the general actions necessary to prepare the MPC for unloading, cool the stored fuel assemblies in the MPC (if necessary), flood the MPC cavity, remove the lid welds, unload the spent fuel assemblies, and recover the overpack and empty MPC. Special precautions are outlined to ensure personnel safety during the unloading operations, and to prevent the risk of MPC overpressurization and thermal shock to the stored spent fuel assemblies.

After removing the impact limiters, the overpack and MPC are positioned in the designated preparation area. At the site's discretion, a gas sample is drawn from the overpack annulus and analyzed. The gas sample provides an indication of MPC enclosure vessel performance. The annulus is depressurized, the overpack closure plate is removed, and the annulus is filled with plant demineralized water. The annulus shield is installed to protect the annulus from debris produced from the lid removal process. Similarly, overpack top surfaces are covered with a protective fire-retarding blanket.

The Weld Removal System (WRS) is positioned on the MPC lid. The MPC closure ring is core drilled over the locations of the vent and drain port cover plates. The MPC closure ring and vent and drain port cover plates are core drilled to the extent necessary to allow access by the Remote Valve Operating Assemblies (RVOAs). Local ventilation is established around the vent and drain ports. The RVOAs are connected to allow access to the MPC cavity for re-flooding operations.

The MPC cavity gas is verified to be below an appropriate temperature (approximately 200°F) to allow water flooding. Depending on the time since initial fuel loading and the age and burnup of the contained fuel, mechanical cooling of the MPC cavity gas may or may not be required to ensure the cavity gas temperature meets the acceptance criterion. A thermal evaluation should be performed to determine the MPC bulk cavity gas temperature at the time of unloading. Based on that thermal evaluation, if the MPC cavity gas temperature does not already meet the acceptance limit, any appropriate means to cool the cavity gas may be employed to reduce the gas temperature to the acceptance criterion. Typically, this may involve intrusive means, such as recirculation cooling of the MPC cavity helium, or non-intrusive means, such as cooling of the exterior surface of the MPC enclosure vessel with water or air. The thermal evaluation should include an evaluation of the cooling process, if required, to determine the appropriate criteria for the cooling process, such as fluid flow rate(s), fluid temperature(s), and the cooling duration required to meet the acceptance criterion. Following fuel cool-down (if required), the MPC is flooded with water. The WRS is positioned for MPC lid-to-shell weld removal. The WRS is then removed with the MPC lid left in place.

The annulus shield is removed and the annulus seal is installed and pressurized. The MPC lid is rigged to the lift yoke and the lift yoke is engaged to overpack lifting trunnions. The overpack is

placed in the spent fuel pool and the MPC lid is removed. All fuel assemblies are returned to the spent fuel storage racks. The overpack and MPC are returned to the designated preparation area. The annulus water is drained and the MPC and overpack are dispositioned for re-use or waste.

### 1.2.3 Contents of Package

The HI-STAR 100 packaging is classified as a Type B package under 10CFR71. As the HI-STAR 100 System is designed to transport spent nuclear fuel, the maximum activity of the contents requires that the HI-STAR 100 packaging be classified as Category I in accordance with Regulatory Guide 7.11 [1.2.10]. This section delineates the authorized contents permitted for shipment in the HI-STAR 100 System, including fuel assembly types; non-fuel hardware; neutron sources; physical parameter limits for fuel assemblies and sub-components; enrichment, burnup, cooling time, decay heat limits, and core operating parameters as applicable; location requirements; and requirements for canning the material. See **SAR Supplements** for the contents of **additional packages**.

#### 1.2.3.1 Determination of Design Basis Fuel

The HI-STAR 100 package is designed to transport most types of fuel assemblies generated in the commercial U.S. nuclear industry. Boiling-water reactor (BWR) fuel assemblies have been supplied by General Electric (GE), Siemens (SPC), Exxon Nuclear, ANF, UNC, ABB Combustion Engineering, Allis-Chalmers (AC) and Gulf Atomic. Pressurized-water reactor (PWR) fuel assemblies are generally supplied by Westinghouse, Babcock & Wilcox, ANF, and ABB Combustion Engineering. ANF, Exxon, and Siemens are historically the same manufacturing company under different ownership. Within this report, SPC is used to designate fuel manufactured by ANF, Exxon, or Siemens. Publications such as Refs. [1.2.6], [1.2.7], and [1.2.15] provide a comprehensive description of fuel discharged from U.S. reactors. A central object in the design of the HI-STAR 100 System is to ensure that a majority of SNF discharged from the U.S. reactors can be transported in one of the MPCs.

The cell openings in the fuel basket have been sized to accommodate all BWR and PWR assemblies listed in Refs. [1.2.6], [1.2.7], and [1.2.15], except as noted below. Similarly, the cavity length of the MPC has been set at a dimension that permits transportation of most types of PWR fuel assemblies and BWR fuel assemblies with or without fuel channels. The one exception is as follows:

- The South Texas Units 1 & 2 SNF, and CE 16x16 System 80<sup>TM</sup> SNF are too long to be accommodated in the available MPC cavity length.

In addition to satisfying the cross sectional and length compatibility, the active fuel region of the SNF must be enveloped in the axial direction by the neutron absorber located in the MPC fuel basket. Alignment of the neutron absorber with the active fuel region is ensured by the use of upper and lower fuel spacers suitably designed to support the bottom and restrain the top of the fuel assembly. The spacers axially position the SNF assembly such that its active fuel region is properly aligned with the neutron absorber in the fuel basket. Figure 1.2.15 provides a pictorial representation of the fuel spacers positioning the fuel assembly active fuel region. Both the upper and lower fuel spacers are designed to perform their function under normal and hypothetical accident conditions of

transport. Due to the shorter, custom MPC design for Trojan plant fuel, only lower fuel spacers are needed for certain fuel assemblies that do not contain integral control rod assemblies. This creates the potential for a slight misalignment between the active fuel region of a fuel assembly and the neutron absorber panels affixed to the cell walls of the Trojan MPCs. This condition is addressed in the criticality evaluations described in Chapter 6.

In summary, the geometric compatibility of the SNF with the MPC designs does not require the definition of a design basis fuel assembly. This, however, is not the case for structural, containment, shielding, thermal-hydraulic, and criticality criteria. In fact, the same fuel type in a category (PWR or BWR) may not control the cask design in all of the above-mentioned criteria. To ensure that no SNF listed in Refs. [1.2.6], [1.2.7], and [1.2.15] that is geometrically admissible in the HI-STAR MPC is precluded from loading, it is necessary to determine the governing fuel specification for each analysis criteria. To make the necessary determinations, potential candidate fuel assemblies for each qualification criteria were considered. Table 1.2.8 lists the PWR fuel assemblies evaluated. These fuel assemblies were evaluated to define the governing design criteria for PWR fuel. The BWR fuel assembly designs evaluated are listed in Table 1.2.9. Tables 1.2.10 and 1.2.11 provide the fuel characteristics determined to be acceptable for transport in the HI-STAR 100 System. Each “array/class” listed in these tables represents a bounding set of parameters for one or more fuel assembly types. The array/classes are defined in SAR Section 6.2. Table 1.2.12 lists the BWR and PWR fuel assembly designs that are found to govern for the qualification criteria, namely reactivity, shielding, and thermal. Thermal is broken down into three criteria, namely: 1) fuel assembly effective planar conductivity, 2) fuel basket effective axial conductivity, and 3) MPC density and heat capacity. Substantiating results of analyses for the governing assembly types are presented in the respective chapters dealing with the specific qualification topic. Tables 1.2.10, 1.2.11, and 1.2.21 through 1.2.36 provide the specific limits for all material authorized to be transported in the HI-STAR 100 System. Additional information on the design basis fuel definition is presented in the following subsections.

#### 1.2.3.2 Design Payload for Intact Fuel

Intact fuel assemblies are defined as fuel assemblies without known or suspected cladding defects greater than pinhole leaks and hairline cracks, and which can be handled by normal means. The design payload for intact fuel to be transported in the HI-STAR 100 System is provided in Tables 1.2.10, 1.2.11, and 1.2.22 through 1.2.36. The placement of a single stainless steel clad fuel assembly in an MPC necessitates that all fuel assemblies (stainless steel clad or Zircaloy clad) stored in that MPC meet the maximum heat generation requirements for stainless steel clad fuel. Stainless steel clad fuel assemblies are not authorized for transportation in the MPC-68F or MPC-32.

Fuel assemblies without fuel rods in fuel rod locations cannot be classified as intact fuel unless dummy fuel rods, which occupy a volume equal to or greater than the original fuel rods, replace the missing rods prior to loading. Any intact fuel assembly that falls within the geometric, thermal, and nuclear limits established for the design basis intact fuel assembly can be safely transported in the HI-STAR 100 System.

Some Trojan fuel assemblies not loaded into DFCs or FFCs show conditions of minor impairments on some grid straps [1.2.16]. These conditions, as determined by visual inspection of the assemblies, consist of small portions of grid straps that are missing or bent. The worst condition is the exposure of a single fuel rod on the periphery of one grid strap. These conditions do not meet the definition of damaged fuel in the CoC, since the impairment is minor, no grid spacers are missing, and the overall structural integrity of the assembly is not affected. Such assemblies are therefore classified as intact assemblies.

The fuel characteristics specified in Tables 1.2.10, 1.2.11, and 1.2.21 have been evaluated in this SAR and are acceptable for transport in the HI-STAR 100 System.

### 1.2.3.3 Design Payload for Damaged Fuel and Fuel Debris

Damaged fuel and fuel debris are defined in Table 1.0.1. The only PWR damaged fuel and fuel debris authorized for transportation in the HI-STAR 100 System is that from the Trojan plant. The only BWR damaged fuel and fuel debris authorized for transportation in the HI-STAR 100 System is that from the Dresden Unit 1 and Humboldt Bay plants.

Damaged fuel may only be transported in the MPC-24E, MPC-24EF, MPC-68, or MPC-68F as shown in Tables 1.2.23 through 1.2.26. Fuel debris may only be transported in the MPC-24EF and the MPC-68F as shown in Tables 1.2.24 and 1.2.26. Damaged fuel and fuel debris must be transported in stainless steel Holtec damaged fuel containers (DFCs) or other approved stainless steel damaged/failed fuel canister in the HI-STAR 100 System. The list of approved damaged/failed fuel canisters and associated SAR figures are provided below:

- Holtec-designed Dresden Unit 1 Damaged Fuel Container (Figure 1.2.10)
- Sierra Nuclear-designed Trojan Failed Fuel Can (Figure 1.2.10A) containing Trojan damaged fuel, fuel debris, or Trojan Fuel debris process cans; or containing Trojan Fuel Debris Process Can Capsules (Figure 1.2.10C), which themselves contain Trojan Fuel Debris Process Cans (Figure 1.2.10B).
- Holtec-designed Damaged Fuel Container for Trojan plant fuel (Figure 1.2.10D)
- Dresden Unit 1's TN Damaged Fuel Container (Figure 1.2.11)
- Dresden Unit 1's Thoria Rod Canister (Figure 1.2.11A)
- Holtec-designed Humboldt Bay Damaged Fuel Container (refer to Supplement 1.I)

#### 1.2.3.3.1 BWR Damaged Fuel and Fuel Debris

Dresden Unit 1 (UO<sub>2</sub> fuel rods and MOX fuel rods) fuel arrays (Assembly Classes 6x6A, 6x6B, 6x6C, 7x7A, and 8x8A) are authorized for transportation as damaged fuel in the MPC-68 and

damaged fuel or fuel debris in the MPC-68F. No other BWR damaged fuel or fuel debris is authorized for transportation.

The limits for transporting Dresden Unit 1 damaged fuel and fuel debris are given in Table 1.2.23 and 1.2.24. The placement of a single damaged fuel assembly in an MPC-68 or MPC-68F, or a single fuel debris damaged fuel container in an MPC-68F necessitates that all fuel assemblies (intact, damaged, or debris) placed in that MPC meet the maximum heat generation requirements specified in Tables 1.2.23 and 1.2.24.

The fuel characteristics specified in Tables 1.2.11, 1.2.23 and 1.2.24 for Dresden Unit 1 fuel arrays have been evaluated in this SAR and are acceptable for transport as damaged fuel or fuel debris in the HI-STAR 100 System. Because of the long cooling time, small size, and low weight of spent fuel assemblies qualified as damaged fuel or fuel debris, the DFC and its contents are bounded by the structural, thermal, and shielding analyses performed for the intact BWR design basis fuel. Separate criticality analysis of the bounding fuel assembly for the damaged fuel and fuel debris has been performed in Chapter 6.

The fuel characteristics specified in Table 1.2.11 for the Dresden Unit 1 fuel arrays (Assembly Classes 6x6A, 6x6B, 6x6C, 7x7A, and 8x8A) have been evaluated in this SAR and are acceptable for transport as damaged fuel or fuel debris in the HI-STAR 100 System after being placed in a damaged fuel container.

Refer to Supplement 1.I for information regarding Humboldt Bay damaged fuel and fuel debris.

#### 1.2.3.3.2 PWR Damaged Fuel and Fuel Debris

The PWR damaged fuel and fuel debris authorized for transportation in the HI-STAR 100 System is limited to that from the Trojan plant. The limits for transporting Trojan plant damaged fuel and fuel debris in the Trojan MPC-24E/EF are given in Tables 1.2.10, 1.2.25 and 1.2.26. All Trojan plant damaged fuel, and fuel debris listed below is authorized for transportation in the HI-STAR 100 System [1.2.12]:

- Damaged fuel assemblies in Trojan failed fuel cans
- Damaged fuel assemblies in Holtec's Trojan plant PWR damaged fuel container
- Fuel assemblies classified as fuel debris in Trojan failed fuel cans
- Trojan fuel assemblies classified as fuel debris in Holtec's Trojan damaged fuel container
- Fuel debris consisting of loose fuel pellets, fuel pellet fragments, and fuel assembly metal fragments (portions of fuel rods, portions of grid assemblies, bottom nozzles, etc.) in Trojan failed fuel cans

- Trojan fuel debris process cans loaded into Trojan fuel debris process can capsules and then into Trojan failed fuel cans. The fuel debris process cans contain fuel debris (metal fragments) and were used to process organic media removed from the Trojan spent fuel pool during cleanup operations in preparation for decommissioning the pool. The fuel debris process cans have metallic filters in the can bottom and lid that allowed removal of water and organic media using high temperature steam, while retaining the solid residue from the processed media and fuel debris inside the process can<sup>†</sup>. Up to five process cans can be loaded into a process can capsule, which is vacuumed, purged, backfilled with helium, and seal-welded closed to provide a sealed containment for the fuel debris.

One Trojan Failed Fuel Can is not completely filled with fuel debris. Therefore, a stainless steel failed fuel can spacer is installed in this FFC to minimize movement of the fuel debris during normal transportation and hypothetical accident conditions. The spacer is a long, square tube with a baseplate that rests atop the fuel debris inside the Trojan FFC. A drawing of the Trojan failed fuel can spacer is provided in Section 1.4. A summary of the structural analysis of the FFC spacer is provided in Section 2.6.1.3.1.3.

#### 1.2.3.4 Structural Payload Parameters

The main physical parameters of an SNF assembly applicable to the structural evaluation are the fuel assembly length, envelope (cross sectional dimensions), and weight. These parameters, which define the mechanical and structural design, are listed in Tables 1.2.22 through 1.2.27 for the various MPC models. The centers of gravity reported in Chapter 2 are based on the maximum fuel assembly weight. Upper and lower fuel spacers (as appropriate) maintain the axial position of the fuel assembly within the MPC basket and, therefore, the location of the center of gravity. The upper and lower spacers are designed to withstand normal and accident conditions of transport. An axial clearance of approximately 2 inches is provided to account for the irradiation and thermal growth of the fuel assemblies. The suggested upper and lower fuel spacer lengths are listed in Tables 1.2.16 and 1.2.17. Due to the custom design of the Trojan MPCs, only lower fuel spacers are required with Trojan plant fuel assemblies not containing non-fuel hardware or neutron sources. In order to qualify for transport in the HI-STAR 100 MPC, the SNF must satisfy the physical parameters listed in Tables 1.2.21 through 1.2.36, as applicable.

#### 1.2.3.5 Thermal Payload Parameters

The principal thermal design parameter for the fuel is the peak fuel cladding temperature, which is a function of the maximum heat generation rate per assembly and the decay heat removal capabilities of the HI-STAR 100 System. The maximum heat generation rate per assembly for the design basis fuel assembly is based on the fuel assembly type with the lowest thermal performance characteristics. The parameters that define this decay heat design basis fuel are listed in Table 1.2.12. The governing thermal parameters to ensure that the range of SNF discussed previously are bounded by the thermal analysis discussed in detail and specified in Chapter 3. By utilizing these bounding thermal

<sup>†</sup> The Trojan Fuel Debris Process Cans were used in the spent fuel pool cleanup effort conducted as part of plant decommissioning. This project is complete and not associated with certification of Trojan fuel debris for transportation in the HI-STAR 100 System under 10 CFR 71.



parameters, the calculated peak fuel rod cladding temperatures are conservative for the actual spent fuel assemblies, which are apt to have a higher thermal conductivity.

The peak fuel cladding temperature limit for normal conditions of transport is 400°C (752°F), which is consistent with the guidance in ISG-11, Revision 3 [1.2.14]. Tables 1.2.21 through 1.2.27 provide the maximum heat generation for all fuel assemblies authorized for transportation in the HI-STAR 100 System. The basis for these limits is discussed in Chapter 3.

Finally, the axial variation in the heat emission rate in the design basis fuel is defined based on the axial burnup distribution. For this purpose, the data provided in Refs. [1.2.8], [1.2.9], and [1.2.12] are utilized and summarized in Table 1.2.15 and Figures 1.2.13, 1.2.13A, and 1.2.14, for reference. These distributions are representative of fuel assemblies with the design burnup levels considered. These distributions are used for analysis only, and do not provide a criteria for fuel assembly acceptability for transport in the HI-STAR 100 System.

#### 1.2.3.6 Radiological Payload Parameters

The principal radiological design criteria are the 10CFR71.47 and 10CFR71.51 radiation dose rate and release requirements for the HI-STAR 100 System. The radiation dose rate is directly affected by the gamma and neutron source terms of the SNF assembly.

The gamma and neutron sources are separate and are affected differently by enrichment, burnup, and cool time. It is recognized that, at a given burnup, the radiological source terms increase monotonically as the initial enrichment is reduced. The shielding design basis fuel assembly is, therefore, evaluated for different combinations of maximum burnup, minimum cooling time, and minimum enrichment. The shielding design basis intact fuel assembly thus bounds all other intact fuel assemblies.

The design basis dose rates can be met by a variety of burnup levels, cooling times, and minimum enrichments. Tables 1.2.21 through 1.2.36 include the burnup and cooling time values that meet the radiological dose rate requirements for all authorized contents to be transported in each MPC model. The allowable maximum burnup, minimum cooling time, and minimum enrichment limits were chosen strictly based on the dose rate requirements. All allowable burnup, cooling time, and minimum enrichment combinations result in calculated dose rates less than the regulatory dose rate limits.

Table 1.2.15 and Figures 1.2.13, 1.2.13A, and 1.2.14 provide the axial distribution for the radiological source term for PWR and BWR fuel assemblies, and for Trojan plant-specific fuel, based on the actual burnup distribution. The axial burnup distributions are representative of fuel assemblies with the design basis burnup levels considered. These distributions are used for analysis only, and do not provide criteria for fuel assembly acceptability for transport in the HI-STAR 100 System.

Thoria rods placed in Dresden Unit 1 Thoria Rod Canisters meeting the requirements of Table 1.2.21 and Dresden Unit 1 fuel assemblies with one Antimony-Beryllium neutron source have been

qualified for transport. Up to one Dresden Unit 1 Thoria Rod Canister plus any combination of damaged fuel assemblies in damaged fuel containers and intact fuel, up to a total of 68 may be transported.

#### 1.2.3.7 Criticality Payload Parameters

As discussed earlier, the MPC-68/68F and MPC-32 feature a basket without flux traps. In these fuel baskets, there is one panel of neutron absorber between adjacent fuel assemblies. The MPC-24/24E/24EF employs a construction wherein two neighboring fuel assemblies are separated by two panels of neutron absorber with a water gap between them (flux trap construction). The MPC-24 flux trap basket can accept a much higher enrichment fuel than a non-flux trap basket without taking credit for fuel assembly burnup in the criticality analysis. The maximum initial  $^{235}\text{U}$  enrichment for PWR and BWR fuel authorized for transport is specified by fuel array/class in Tables 1.2.10 and 1.2.11, respectively, **except for MPC-32 which is specified in Table 1.2.27 for authorized array/classes**. Trojan plant fuel is limited to a lower maximum initial enrichment of 3.7 wt.%  $^{235}\text{U}$  compared to other fuel in its array/class, based on the specific analysis performed for the custom-designed Trojan MPCs containing only Trojan plant fuel.

The minimum  $^{10}\text{B}$  areal density in the neutron absorber panels for each MPC model is shown in Table 1.2.3. Values for MPC-HB are found in Supplement 1.I.

For all MPCs, the  $^{10}\text{B}$  loading areal density used for analysis is conservatively established below the minimum values shown in Table 1.2.3. For Boral, the value used in the analysis is 75% of the minimum  $^{10}\text{B}$  areal density, while for METAMIC, 90% of the minimum value can be used to demonstrate that the reactivity under the most adverse accumulation of tolerances and biases is less than 0.95. The reduction in  $^{10}\text{B}$  areal density credit meets NUREG-1617 [1.0.5], which requires up to a 25% reduction in  $^{10}\text{B}$  areal density credit. A large body of sampling data accumulated by Holtec from thousands of manufactured Boral panels indicates the average  $^{10}\text{B}$  areal densities to be approximately 15% greater than the specified minimum.

Credit for burnup of the fuel, in accordance with the intent of the guidance in Interim Staff Guidance Document 8 (ISG-8) [1.2.13], is taken in the criticality analysis to allow the transportation of certain PWR fuel assemblies in MPC-32. Burnup credit is a required input to qualify PWR fuel for transportation in the MPC-32, considering the inleakage of moderator (i.e., unborated water) under accident conditions. This hypothetical event is non-credible given the double barrier design engineered into the HI-STAR 100 System with the fully welded MPC enclosure vessel (designed for 60 g's) surrounded by the sealed overpack, which is designed for deep submersion under water (greater than 650 feet submersion) without breach. The details of the burnup credit analyses are provided in Chapter 6, including detailed discussion of how the recommendations of ISG-8 were implemented.

### 1.2.3.7.1 Core Operating Parameters<sup>†</sup>

For burnup credit in the MPC-32, assemblies must meet certain operating limits during their in-core depletion. These limits are listed in Table 1.2.27 **for the standard MPC-32**. For each assembly, the parameters Soluble Boron Concentration (SBC), Specific Power (SP), and Moderator Temperature (MT) must be calculated using the following equations. In these equations, and the symbols used therein, the subscript i denotes the cycle. The summation ( $\sum$ ) in these equation is to be performed over all cycles i that the assembly was in the core.

Given

$B_i$  Assembly-average burnup for cycle i  
 $BC_i$  Core-average burnup for cycle i  
 $SB_i$  Average In-Core Soluble Boron Concentration for cycle i  
 $T_i$  Length of Cycle  
 $CIT_i$  Core Inlet Temperature  
 $COT_i$  Core Outlet temperature

the values to compared to the limits in Table 1.2.27 are to be calculated as follows:

Soluble Boron:

$$SB = \sum (SB_i * B_i) / \sum B_i$$

Assembly Average Specific Power:

$$SP = \sum B_i / \sum T_i$$

Assembly Average Moderator Temperature:

$$CFC_i = B_i / BC_i \quad \text{Correction Factor; if } CFC_i < 1 \text{ then set } CFC_i = 1$$

$$MT = \sum (B_i * (CIT_i + CFC_i * (COT_i - CIT_i))) / \sum B_i$$

### 1.2.3.7.2 Burnup Verification<sup>††</sup>

**For those spent fuel assemblies that need to meet the burnup requirements specified in Table 1.2.34, a burnup verification shall be performed in accordance with either Method A or Method B described below.**

<sup>†</sup> This subsection is included by reference into Appendix A of the CoC.

<sup>††</sup> This subsection is included by reference into Appendix A of the CoC.

### Method A: Burnup Verification Through Quantitative Burnup Measurement

For each assembly in MPC-32, the minimum burnup is determined from the burnup requirement applicable to the configuration chosen for the cask (see Table 1.2.34). A measurement is then performed that confirms that the fuel assembly burnup exceeds this minimum burnup using one of the following three approaches:

- Burnup measurements of every assembly to be loaded without correlation to reactor records on burnup. In this case, the measured burnup value is used for comparison with the limit, but shall be reduced by the uncertainty of the burnup measurement.
- Burnup measurements of every assembly based on correlation to reactor records on burnup. In this case, the reactor record burnup value is used for the comparison with the limit, but shall be reduced by the uncertainty of the reactor record burnup value compared to the measured burnup, combined with the uncertainty of the burnup measurement. The uncertainty of the reactor burnup value shall be determined at a 95 percent confidence level. Burnup measurements for another plant may be used if it is shown that they are applicable to the fuel to be qualified. This applicability review shall include a comparison of the fuel type, general core design and operation, and method for calculating burnup, and shall be supplemented by confirmatory burnup measurements.
- Burnup measurements of a sampling of the fuel assemblies. In this case a database of measured burnup, either based on correlation to reactor records on burnup or independent of reactor records must be provided to justify the adequacy of the sampling approach. The assigned burnup value shall be adjusted by the applicable method described above.

### Method B: Burnup Verification Through an Administrative Procedure and Qualitative Measurements

The assembly burnup value to be compared with the minimum required burnup should be the reactor record burnup value as adjusted by reducing the value by the uncertainties in the reactor record value. An administrative procedure shall be established that prescribes the following steps, which shall be performed for each cask loading:

- Based on a review of the reactor records, all assemblies in the spent fuel pool that have a burnup that is below the minimum required burnup of the loading curve for the cask to be loaded are identified.
- After the cask loading, but before the release for shipment of the cask, the presence and location of all those identified assemblies is verified.
- In-pool minimum soluble boron during loading and unloading as specified in Table 1.2.27.

Additionally, for all assemblies to be loaded that are required to meet a minimum burnup, a measurement shall be performed that verifies that the assembly is not a fresh assembly.

### 1.2.3.7.3 Combined Burnup and Enrichment Curves

In addition to the minimum burnup requirements for the MPC-32 for burnup credit (Table 1.2.34), there are also maximum burnup limits based on the dose rate requirements (Tables 1.2.32 and 1.2.33). As a result, there is an acceptable burnup range for each enrichment.

### 1.2.3.8 Non-Fuel Hardware and Neutron Sources

#### 1.2.3.8.1 MPC-68

BWR fuel is permitted to be stored with or without Zircaloy channels. **BWR control** blades and stainless steel channels are not authorized for transportation in the HI-STAR 100 System. Dresden Unit 1 (D-1) neutron sources are authorized for transportation as shown in Tables 1.2.23 and 1.2.24. The D-1 neutron sources are single, long rods containing Sb-Be source material that fits into a water rod location in a D-1 fuel assembly.

#### 1.2.3.8.2 MPC-24

**Only** Trojan non-fuel hardware **and** neutron sources are authorized for transportation in the HI-STAR 100 System **with MPC-24**. For Trojan plant fuel only, the following non-fuel hardware and neutron sources are permitted for transportation in specific quantities as shown in Tables 1.2.25 and 1.2.26:

- Rod Cluster Control Assemblies (RCCAs) with cladding made of Type 304 stainless steel and Ag-In-Cd neutron absorber material.
- Burnable Poison Rod Assemblies (BPRAs) with cladding made of Type 304 stainless steel and borosilicate glass tube neutron poison material.
- Thimble Plug Devices made of Type 304 stainless steel.
- Neutron source assemblies with cladding made of Type 304 stainless steel - two (2) californium primary source assemblies and four (4) antimony-beryllium secondary source assemblies.

These devices are designed with thin rods of varying length and materials as discussed above, that fit into the fuel assembly guide tubes within the fuel rod lattice. The upper fittings for each device can vary to accommodate the handling tool (grapple) design. During reactor operation, the positions of the RCCAs are controlled by the operator using the control rod drive system, while the BPRAs, TPDs, and neutron sources stay fully inserted.

A complete list of the authorized non-fuel hardware and neutron sources, including appropriate limits on the characteristics of this material, is provided in Tables 1.2.23 through 1.2.36, as applicable.

#### 1.2.3.8.3 MPC-32

Some PWR non-fuel hardware and neutron sources are authorized for transportation in HI-STAR 100 System with MPC-32. Table 1.2.27 lists the authorized types and quantity of non-fuel hardware devices that are authorized for transportation in MPC-32. The allowable combinations of non-fuel hardware burnup and post-irradiation cooling time are provided in Table 1.2.38.

#### 1.2.3.9 Summary of Authorized Contents

The criticality safety index for the HI-STAR 100 Package is zero. A fuel assembly is acceptable for transport in a HI-STAR 100 System if it fulfills the following criteria.

- a. It satisfies the physical parameter characteristics listed in Tables 1.2.10 or 1.2.11, as applicable.
- b. It satisfies the cooling time, decay heat, burnup, enrichment, and other limits specified in Tables 1.2.21 through 1.2.36, as applicable.

A damaged fuel assembly shall be transported in a damaged fuel container or other authorized damaged/failed fuel canister, and shall meet the characteristics specified in Tables 1.2.22 through 1.2.27 as applicable. Fuel classified as fuel debris shall be placed in a damaged fuel container or other authorized damaged/failed fuel canister and shall meet the characteristics specified in Tables 1.2.22 through 1.2.27 as applicable.

Stainless steel clad fuel assemblies shall meet the characteristics specified in Tables 1.2.22 through 1.2.33 as applicable.

MOX BWR fuel assemblies shall meet the requirements of Tables 1.2.23 or 1.2.24 for intact and damaged fuel/fuel debris.

Thoria rods placed in Dresden Unit 1 Thoria Rod Canisters meeting the requirements of Table 1.2.21 and Dresden Unit 1 fuel assemblies with one Antimony-Beryllium neutron source have been qualified for transport. Up to one Dresden Unit 1 Thoria Rod Canister plus any combination of damaged fuel assemblies in damaged fuel containers and intact fuel, up to a total of 68 may be transported.

Dresden Unit 1 fuel assemblies with one Antimony-Beryllium neutron source are authorized for loading in the MPC-68 or MPC-68F.

Table 1.2.2 summarizes the key system data for the HI-STAR 100 System. Table 1.2.3 summarizes the key parameters and limits for the HI-STAR 100 MPCs. Tables 1.2.10, 1.2.11, and 1.2.21 through

1.2.36 and other tables referenced from these tables provide the limiting conditions for all material to be transported in the HI-STAR 100 System. Refer to Supplement 1.I for HI-STAR HB.

#### 1.2.3.10 Partially Loaded MPCs

MPC's shall be loaded to at least 50% of their capacity. Thus for example, MPC-24, MPC-32, and MPC-68 must have at least 12, 16 and 34 fuel assemblies loaded respectively. Additionally, the contents of the MPC should be symmetrical or evenly distributed to the extent practical. Complete requirements and/or recommendations from an operations perspective are provided in Chapter 7 of this SAR to ensure that the HI-STAR 100 package remains in an "analyzed" condition from a structural perspective.

Table 1.2.1

TABLE INTENTIONALLY DELETED



Table 1.2.2

## SUMMARY OF KEY SYSTEM DATA FOR HI-STAR 100

PARAMETER	VALUE (Nominal)	
Types of MPCs in this SAR	6 <sup>†</sup>	4 for PWR 2 for BWR
Types of GWCs in this SAR	1	Reactor-Related Waste in Solid Form (see Supplement 1.II)
Canister capacity	MPC-24	Up to 24 intact ZR or stainless steel clad PWR fuel assemblies
	MPC-24E	Up to 24 intact ZR or stainless steel clad PWR fuel assemblies. Up to four (4) Trojan plant fuel assemblies classified as damaged fuel, each in a Trojan Failed Fuel Can or a Holtec damaged fuel container, and the complement intact fuel assemblies.
	MPC-24EF	Up to 24 intact ZR or stainless steel clad PWR fuel assemblies. Up to four (4) Trojan plant fuel assemblies classified as damaged fuel or fuel debris, each in a Trojan Failed Fuel Can or a Holtec damaged fuel container; or other Trojan fuel debris stored in Trojan Process Cans either placed directly into a Trojan Failed Fuel Can or placed inside Trojan Process Can Capsules and then in Trojan Failed Fuel Cans; and the complement intact fuel assemblies.
	MPC-32	Up to 32 intact ZR clad PWR fuel assemblies.
	MPC-68	Up to 68 intact ZR or stainless steel clad BWR fuel assemblies or damaged ZR clad fuel assemblies* in damaged fuel containers within an MPC-68
	MPC-68F	Up to 4 damaged fuel containers with ZR clad BWR fuel debris* and the complement intact or damaged* ZR clad BWR fuel assemblies within an MPC-68F.  *Only damaged fuel and fuel debris from Dresden Unit 1 is authorized for transportation in the MPC-68 and MPC-68F.
	GWC-HB	see Supplement 1.II

<sup>†</sup> - excluding MPC-HB (see Supplement 1.I) and Diablo Canyon MPC-32 (see Supplement 1.III).

Table 1.2.3  
KEY PARAMETERS FOR HI-STAR 100 MULTI-PURPOSE CANISTERS

PARAMETER	PWR	BWR
Unloaded MPC weight (lb)	See Table 2.2.1	See Table 2.2.1
Minimum Boral neutron absorber $^{10}\text{B}$ loading ( $\text{g}/\text{cm}^2$ )	See SAR Table 8.1.3	See SAR Table 8.1.3
Minimum Metamic neutron absorber $^{10}\text{B}$ loading ( $\text{g}/\text{cm}^2$ )	See SAR Table 8.1.3	See SAR Table 8.1.3
Pre-disposal service life (years)	40	40
Design temperature, max./min. ( $^{\circ}\text{F}$ )	$725^{\circ\ddagger}/-40^{\circ\ddagger\ddagger}$	$725^{\circ\ddagger}/-40^{\circ\ddagger\ddagger}$
Design Internal pressure (psig)		
Normal Conditions	100	100
Off-normal Conditions	100	100
Accident Conditions	225	225
Total heat load, max. (kW)	20.0	18.5
Maximum permissible peak fuel cladding temperature ( $^{\circ}\text{F}$ )	$752^{\circ}$ (normal conditions) $1058^{\circ}$ (accident conditions)	$752^{\circ}$ (normal conditions) $1058^{\circ}$ (accident conditions)
MPC internal environment Helium filled (psig)	$\geq 0$ and $\leq 44.8$ psig $^{\ddagger\ddagger\ddagger}$ at a reference temperature of $70^{\circ}\text{F}$	$\geq 0$ and $\leq 44.8$ psig $^{\ddagger\ddagger\ddagger}$ at a reference temperature of $70^{\circ}\text{F}$
MPC external environment/overpack internal environment Helium filled initial pressure (psig, at STP)	$\geq 10$ and $\leq 14$	$\geq 10$ and $\leq 14$
Maximum permissible reactivity including all uncertainty and biases	$<0.95$	$<0.95$
End closure(s)	Welded	Welded
Fuel handling	Opening compatible with standard grapples	Opening compatible with standard grapples
Heat dissipation	Passive	Passive

$\ddagger$  Maximum normal condition design temperature for the MPC fuel basket. A complete listing of design temperatures for all components is provided in Table 2.1.2

$\ddagger^{\ddagger}$  Temperature based on minimum ambient temperature (10CFR71.71(c)(2)) and no fuel decay heat load.

$\ddagger^{\ddagger\ddagger}$  This value represents the nominal backfill value used in the thermal analysis, plus 2 psig operating tolerance. Based on the MPC pressure results in Table 3.4.15 and the pressure limits specified in Table 2.1.1, there is sufficient analysis margin to accommodate this operating tolerance.

Tables 1.2.4 through 1.2.6

INTENTIONALLY DELETED

Table 1.2.7

## HI-STAR 100 LOADING OPERATIONS DESCRIPTION

Site-specific handling and operating procedures will be prepared, reviewed, and approved by each owner/user.	
1	Overpack and MPC lowered into the fuel pool without closure plate and MPC lid
2	Fuel assemblies transferred to the MPC fuel basket
3	MPC lid lowered onto the MPC
4	Overpack/MPC assembly moved to the decon pit and MPC lid welded in place, examined, and pressure tested
5	MPC dewatered, dried, backfilled with helium, and the vent/drain port cover plates and closure ring welded
6	Overpack drained and external surfaces decontaminated
7	Overpack seals and closure plate installed and bolts pre-tensioned
8	Overpack cavity dried, backfilled with helium, and helium leak tested
9	HI-STAR 100 System transferred to transport bay
10	HI-STAR 100 placed onto transport saddles, tied down, impact limiters and personnel barrier installed, and package surveyed for release for transport.

Table 1.2.8

## PWR FUEL ASSEMBLIES EVALUATED TO DETERMINE DESIGN BASIS SNF

<b>Assembly Class</b>	<b>Array Type</b>
B&W 15x15	All
B&W 17x17	All
CE 14x14	All
CE 16x16	All except System 80™
WE 14x14	All
WE 15x15	All
WE 17x17	All
St. Lucie	All
Ft. Calhoun	All
Haddam Neck (Stainless Steel Clad)	All
San Onofre 1 (Stainless Steel Clad, except MOX)	All
Indian Point 1	All

Table 1.2.9

## BWR FUEL ASSEMBLIES EVALUATED TO DETERMINE DESIGN BASIS SNF

Assembly Class	Array Type			
GE BWR/2-3	All 7x7	All 8x8	All 9x9	All 10x10
GE BWR/4-6	All 7x7	All 8x8	All 9x9	All 10x10
Humboldt Bay	All 6x6	All 7x7 (Zircaloy Clad)		
Dresden-1	All 6x6	All 8x8		
LaCrosse (Stainless Steel Clad)	All			

Table 1.2.10  
PWR FUEL ASSEMBLY CHARACTERISTICS (Note 1)

<b>Fuel Assembly Array/Class</b>	<b>14x14A</b>	<b>14x14B</b>	<b>14x14C</b>	<b>14x14D</b>	<b>14x14E</b>
Clad Material (Note 2)	ZR	ZR	ZR	SS	ZR
Design Initial U (kg/assy.) (Note 3)	$\leq 407$	$\leq 407$	$\leq 425$	$\leq 400$	$\leq 206$
Initial Enrichment (MPC-24, 24E, and 24EF) (wt % $^{235}\text{U}$ )	$\leq 4.6$ (24) $\leq 5.0$ (24E/24EF)	$\leq 4.6$ (24) $\leq 5.0$ (24E/24EF)	$\leq 4.6$ (24) $\leq 5.0$ (24E/24EF)	$\leq 4.0$ (24) $\leq 5.0$ (24E/24EF)	$\leq 5.0$
Initial Enrichment (MPC-32) (wt % $^{235}\text{U}$ ) (Note 5)	N/A	N/A	N/A	N/A	N/A
No. of Fuel Rod Locations	179	179	176	180	173
Fuel Clad O.D. (in.)	$\geq 0.400$	$\geq 0.417$	$\geq 0.440$	$\geq 0.422$	$\geq 0.3415$
Fuel Clad I.D. (in.)	$\leq 0.3514$	$\leq 0.3734$	$\leq 0.3880$	$\leq 0.3890$	$\leq 0.3175$
Fuel Pellet Dia. (in.)	$\leq 0.3444$	$\leq 0.3659$	$\leq 0.3805$	$\leq 0.3835$	$\leq 0.3130$
Fuel Rod Pitch (in.)	$\leq 0.556$	$\leq 0.556$	$\leq 0.580$	$\leq 0.556$	Note 6
Active Fuel Length (in.)	$\leq 150$	$\leq 150$	$\leq 150$	$\leq 144$	$\leq 102$
No. of Guide and/or Instrument Tubes	17	17	5 (Note 4)	16	0
Guide/Instrument Tube Thickness (in.)	$\geq 0.017$	$\geq 0.017$	$\geq 0.038$	$\geq 0.0145$	N/A

Table 1.2.10 (continued)  
PWR FUEL ASSEMBLY CHARACTERISTICS (Note 1)

Fuel Assembly Array/Class	15x15A	15x15B	15x15C	15x15D	15x15E	15x15F
Clad Material (Note 2)	ZR	ZR	ZR	ZR	ZR	ZR
Design Initial U (kg/assy.) (Note 3)	$\leq 464$	$\leq 464$	$\leq 464$	$\leq 475$	$\leq 475$	$\leq 475$
Initial Enrichment (MPC-24, 24E, and 24EF (wt % $^{235}\text{U}$ ))	$\leq 4.1$ (24) $\leq 4.5$ (24E/24EF)	$\leq 4.1$ (24) $\leq 4.5$ (24E/24EF)	$\leq 4.1$ (24) $\leq 4.5$ (24E/24EF)	$\leq 4.1$ (24) $\leq 4.5$ (24E/24EF)	$\leq 4.1$ (24) $\leq 4.5$ (24E/24EF)	$\leq 4.1$ (24) $\leq 4.5$ (24E/24EF)
Initial Enrichment (MPC-32) (wt % $^{235}\text{U}$ ) (Note 5)	N/A	(Note5)	N/A	(Note5)	(Note5)	(Note5)
No. of Fuel Rod Locations	204	204	204	208	208	208
Fuel Clad O.D. (in.)	$\geq 0.418$	$\geq 0.420$	$\geq 0.417$	$\geq 0.430$	$\geq 0.428$	$\geq 0.428$
Fuel Clad I.D. (in.)	$\leq 0.3660$	$\leq 0.3736$	$\leq 0.3640$	$\leq 0.3800$	$\leq 0.3790$	$\leq 0.3820$
Fuel Pellet Dia. (in.)	$\leq 0.3580$	$\leq 0.3671$	$\leq 0.3570$	$\leq 0.3735$	$\leq 0.3707$	$\leq 0.3742$
Fuel Rod Pitch (in.)	$\leq 0.550$	$\leq 0.563$	$\leq 0.563$	$\leq 0.568$	$\leq 0.568$	$\leq 0.568$
Active Fuel Length (in.)	$\leq 150$	$\leq 150$	$\leq 150$	$\leq 150$	$\leq 150$	$\leq 150$
No. of Guide and/or Instrument Tubes	21	21	21	17	17	17
Guide/Instrument Tube Thickness (in.)	$\geq 0.0165$	$\geq 0.015$	$\geq 0.0165$	$\geq 0.0150$	$\geq 0.0140$	$\geq 0.0140$



Table 1.2.10 (continued)  
PWR FUEL ASSEMBLY CHARACTERISTICS (Note 1)

<b>Fuel Assembly Array/Class</b>	<b>15x15G</b>	<b>15x15H</b>	<b>16x16A</b>	<b>17x17A</b>	<b>17x17B</b>	<b>17x17C</b>
Clad Material (Note 2)	SS	ZR	ZR	ZR	ZR	ZR
Design Initial U (kg/assy.) (Note 3)	$\leq 420$	$\leq 475$	$\leq 443$	$\leq 467$	$\leq 467$	$\leq 474$
Initial Enrichment (MPC-24, 24E, and 24EF) (wt % <sup>235</sup> U)	$\leq 4.0$ (24) $\leq 4.5$ (24E/24EF)	$\leq 3.8$ (24) $\leq 4.2$ (24E/24EF)	$\leq 4.6$ (24) $\leq 5.0$ (24E/24EF)	$\leq 4.0$ (24) $\leq 4.4$ (24E/24EF)	$\leq 4.0$ (24) $\leq 4.4$ (24E/24EF) (Note 7)	$\leq 4.0$ (24) $\leq 4.4$ (24E/24EF)
Initial Enrichment (MPC-32) (wt % <sup>235</sup> U) (Note 5)	N/A	(Note5)	N/A	(Note5)	(Note5)	(Note5)
No. of Fuel Rod Locations	204	208	236	264	264	264
Fuel Clad O.D. (in.)	$\geq 0.422$	$\geq 0.414$	$\geq 0.382$	$\geq 0.360$	$\geq 0.372$	$\geq 0.377$
Fuel Clad I.D. (in.)	$\leq 0.3890$	$\leq 0.3700$	$\leq 0.3320$	$\leq 0.3150$	$\leq 0.3310$	$\leq 0.3330$
Fuel Pellet Dia. (in.)	$\leq 0.3825$	$\leq 0.3622$	$\leq 0.3255$	$\leq 0.3088$	$\leq 0.3232$	$\leq 0.3252$
Fuel Rod Pitch (in.)	$\geq 0.563$	$\geq 0.568$	$\geq 0.506$	$\geq 0.496$	$\geq 0.496$	$\geq 0.502$
Active Fuel Length (in.)	$\leq 144$	$\leq 150$	$\leq 150$	$\leq 150$	$\leq 150$	$\leq 150$
No. of Guide and/or Instrument Tubes	21	17	5 (Note 4)	25	25	25
Guide/Instrument Tube Thickness (in.)	$\geq 0.0145$	$\geq 0.0140$	$\geq 0.0400$	$\geq 0.016$	$\geq 0.014$	$\geq 0.020$

Table 1.2.10 (continued)  
PWR FUEL ASSEMBLY CHARACTERISTICS

## Notes:

1. All dimensions are design nominal values. Maximum and minimum dimensions are specified to bound variations in design nominal values among fuel assemblies within a given array/class.
2. ZR designates any zirconium-based fuel cladding material authorized for use in a commercial power reactor.
3. Design initial uranium weight is the nominal uranium weight specified for each assembly by the fuel manufacturer or reactor user. For each PWR fuel assembly, the total uranium weight limit specified in this table may be increased up to 2.0 percent for comparison with users' fuel records to account for manufacturer's tolerances.
4. Each guide tube replaces four fuel rods.
5. "NA" means that this array/class is not authorized for transportation in the MPC-32. For authorized array/classes, maximum initial enrichment is specified in Table 1.2.27.
6. This fuel assembly array/class includes only the Indian Point Unit 1 fuel assembly. This fuel assembly has two pitches in different sectors of the assembly. These pitches are 0.441 inches and 0.453 inches.
7. Trojan plant-specific fuel is governed by the limits specified for array/class 17x17B and will be transported in the custom-designed Trojan MPC-24E/EF canisters. The Trojan MPC-24E/EF design is authorized to transport only Trojan plant fuel with a maximum initial enrichment of 3.7 wt.%  $^{235}\text{U}$ .

Table 1.2.11  
BWR FUEL ASSEMBLY CHARACTERISTICS (Note 1)

Fuel Assembly Array/Class	6x6A	6x6B	6x6C	7x7A	7x7B	8x8A
Clad Material (Note 2)	ZR	ZR	ZR	ZR	ZR	ZR
Design Initial U (kg/assy.) (Note 3)	$\leq 110$	$\leq 110$	$\leq 110$	$\leq 100$	$\leq 195$	$\leq 120$
Maximum Planar-Average Initial Enrichment (wt % $^{235}\text{U}$ )	$\leq 2.7$	$\leq 2.7$ for the $\text{UO}_2$ rods. See Note 4 for MOX rods.	$\leq 2.7$	$\leq 2.7$	$\leq 4.2$	$\leq 2.7$
Initial Maximum Rod Enrichment (wt % $^{235}\text{U}$ )	$\leq 4.0$	$\leq 4.0$	$\leq 4.0$	$\leq 5.5$	$\leq 5.0$	$\leq 4.0$
No. of Fuel Rod Locations	35 or 36	35 or 36 (up to 9 MOX rods)	36	49	49	63 or 64
Fuel Clad O.D. (in.)	$\geq 0.5550$	$\geq 0.5625$	$\geq 0.5630$	$\geq 0.4860$	$\geq 0.5630$	$\geq 0.4120$
Fuel Clad I.D. (in.)	$\leq 0.5105$	$\leq 0.4945$	$\leq 0.4990$	$\leq 0.4204$	$\leq 0.4990$	$\leq 0.3620$
Fuel Pellet Dia. (in.)	$\leq 0.4980$	$\leq 0.4820$	$\leq 0.4880$	$\leq 0.4110$	$\leq 0.4910$	$\leq 0.3580$
Fuel Rod Pitch (in.)	$\leq 0.710$	$\leq 0.710$	$\leq 0.740$	$\leq 0.631$	$\leq 0.738$	$\leq 0.523$
Active Fuel Length (in.)	$\leq 120$	$\leq 120$	$\leq 77.5$	$\leq 80$	$\leq 150$	$\leq 120$
No. of Water Rods (Note 11)	1 or 0	1 or 0	0	0	0	1 or 0
Water Rod Thickness (in.)	$> 0$	$> 0$	N/A	N/A	N/A	$\geq 0$
Channel Thickness (in.)	$\leq 0.060$	$\leq 0.060$	$\leq 0.060$	$\leq 0.060$	$\leq 0.120$	$\leq 0.100$

Table 1.2.11 (continued)  
BWR FUEL ASSEMBLY CHARACTERISTICS (Note 1)

Fuel Assembly Array/Class	8x8B	8x8C	8x8D	8x8E	8x8F	9x9A
Clad Material (Note 2)	ZR	ZR	ZR	ZR	ZR	ZR
Design Initial U (kg/assy) (Note 3)	$\leq 185$	$\leq 185$	$\leq 185$	$\leq 185$	$\leq 185$	$\leq 177$
Maximum Planar-Average Initial Enrichment (wt % $^{235}\text{U}$ )	$\leq 4.2$	$\leq 4.2$	$\leq 4.2$	$\leq 4.2$	$\leq 4.0$	$\leq 4.2$
Initial Maximum Rod Enrichment (wt % $^{235}\text{U}$ )	$\leq 5.0$	$\leq 5.0$	$\leq 5.0$	$\leq 5.0$	$\leq 5.0$	$\leq 5.0$
No. of Fuel Rod Locations	63 or 64	62	60 or 61	59	64	74/66 (Note 5)
Fuel Clad O.D. (in.)	$\geq 0.4840$	$\geq 0.4830$	$\geq 0.4830$	$\geq 0.4930$	$\geq 0.4576$	$\geq 0.4400$
Fuel Clad I.D. (in.)	$\leq 0.4295$	$\leq 0.4250$	$\leq 0.4230$	$\leq 0.4250$	$\leq 0.3996$	$\leq 0.3840$
Fuel Pellet Dia. (in.)	$\leq 0.4195$	$\leq 0.4160$	$\leq 0.4140$	$\leq 0.4160$	$\leq 0.3913$	$\leq 0.3760$
Fuel Rod Pitch (in.)	$\leq 0.642$	$\leq 0.641$	$\leq 0.640$	$\leq 0.640$	$\leq 0.609$	$\leq 0.566$
Design Active Fuel Length (in.)	$\leq 150$	$\leq 150$	$\leq 150$	$\leq 150$	$\leq 150$	$\leq 150$
No. of Water Rods (Note 11)	1 or 0	2	1 - 4 (Note 7)	5	N/A (Note 12)	2
Water Rod Thickness (in.)	$\geq 0.034$	$> 0.00$	$> 0.00$	$\geq 0.034$	$\geq 0.0315$	$> 0.00$
Channel Thickness (in.)	$\leq 0.120$	$\leq 0.120$	$\leq 0.120$	$\leq 0.100$	$\leq 0.055$	$\leq 0.120$

Table 1.2.11 (continued)  
BWR FUEL ASSEMBLY CHARACTERISTICS (Note 1)

Fuel Assembly Array/Class	9x9 B	9x9 C	9x9 D	9x9 E (Note 13)	9x9 F (Note 13)	9x9 G
Clad Material (Note 2)	ZR	ZR	ZR	ZR	ZR	ZR
Design Initial U (kg/assy.) (Note 3)	$\leq 177$	$\leq 177$	$\leq 177$	$\leq 177$	$\leq 177$	$\leq 177$
Maximum Planar-Average Initial Enrichment (wt % $^{235}\text{U}$ )	$\leq 4.2$	$\leq 4.2$	$\leq 4.2$	$\leq 4.0$	$\leq 4.0$	$\leq 4.2$
Initial Maximum Rod Enrichment (wt % $^{235}\text{U}$ )	$\leq 5.0$	$\leq 5.0$	$\leq 5.0$	$\leq 5.0$	$\leq 5.0$	$\leq 5.0$
No. of Fuel Rod Locations	72	80	79	76	76	72
Fuel Clad O.D. (in.)	$\geq 0.4330$	$\geq 0.4230$	$\geq 0.4240$	$\geq 0.4170$	$\geq 0.4430$	$\geq 0.4240$
Fuel Clad I.D. (in.)	$\leq 0.3810$	$\leq 0.3640$	$\leq 0.3640$	$\leq 0.3640$	$\leq 0.3860$	$\leq 0.3640$
Fuel Pellet Dia. (in.)	$\leq 0.3740$	$\leq 0.3565$	$\leq 0.3565$	$\leq 0.3530$	$\leq 0.3745$	$\leq 0.3565$
Fuel Rod Pitch (in.)	$\leq 0.572$	$\leq 0.572$	$\leq 0.572$	$\leq 0.572$	$\leq 0.572$	$\leq 0.572$
Design Active Fuel Length (in.)	$\leq 150$	$\leq 150$	$\leq 150$	$\leq 150$	$\leq 150$	$\leq 150$
No. of Water Rods (Note 11)	1 (Note 6)	1	2	5	5	1 (Note 6)
Water Rod Thickness (in.)	$> 0.00$	$\geq 0.020$	$\geq 0.0300$	$\geq 0.0120$	$\geq 0.0120$	$\geq 0.0320$
Channel Thickness (in.)	$\leq 0.120$	$\leq 0.100$	$\leq 0.100$	$\leq 0.120$	$\leq 0.120$	$\leq 0.120$

Table 1.2.11 (continued)  
BWR FUEL ASSEMBLY CHARACTERISTICS (Note 1)

<b>Fuel Assembly Array/Class</b>	<b>10x10 A</b>	<b>10x10 B</b>	<b>10x10 C</b>	<b>10x10 D</b>	<b>10x10 E</b>
Clad Material (Note 2)	ZR	ZR	ZR	SS	SS
Design Initial U (kg/assy.) (Note 3)	$\leq 186$	$\leq 186$	$\leq 186$	$\leq 125$	$\leq 125$
Maximum Planar-Average Initial Enrichment (wt % $^{235}\text{U}$ )	$\leq 4.2$	$\leq 4.2$	$\leq 4.2$	$\leq 4.0$	$\leq 4.0$
Initial Maximum Rod Enrichment (wt % $^{235}\text{U}$ )	$\leq 5.0$	$\leq 5.0$	$\leq 5.0$	$\leq 5.0$	$\leq 5.0$
No. of Fuel Rod Locations	92/78 (Note 8)	91/83 (Note 9)	96	100	96
Fuel Clad O.D. (in.)	$\geq 0.4040$	$\geq 0.3957$	$\geq 0.3780$	$\geq 0.3960$	$\geq 0.3940$
Fuel Clad I.D. (in.)	$\leq 0.3520$	$\leq 0.3480$	$\leq 0.3294$	$\leq 0.3560$	$\leq 0.3500$
Fuel Pellet Dia. (in.)	$\leq 0.3455$	$\leq 0.3420$	$\leq 0.3224$	$\leq 0.3500$	$\leq 0.3430$
Fuel Rod Pitch (in.)	$\leq 0.510$	$\leq 0.510$	$\leq 0.488$	$\leq 0.565$	$\leq 0.557$
Design Active Fuel Length (in.)	$\leq 150$	$\leq 150$	$\leq 150$	$\leq 83$	$\leq 83$
No. of Water Rods (Note 11)	2	1 (Note 6)	5 (Note 10)	0	4
Water Rod Thickness (in.)	$\geq 0.030$	$> 0.00$	$\geq 0.031$	N/A	$\geq 0.022$
Channel Thickness (in.)	$\leq 0.120$	$\leq 0.120$	$\leq 0.055$	$\leq 0.080$	$\leq 0.080$

Table 1.2.11 (continued)  
BWR FUEL ASSEMBLY CHARACTERISTICS

## NOTES:

1. All dimensions are design nominal values. Maximum and minimum dimensions are specified to bound variations in design nominal values among fuel assemblies within a given array/class.
2. ZR designates any zirconium-based fuel cladding material authorized for use in a commercial power reactor.
3. Design initial uranium weight is the nominal uranium weight specified for each assembly by the fuel manufacturer or reactor user. For each BWR fuel assembly, the total uranium weight limit specified in this table may be increased up to 1.5 percent for comparison with users' fuel records to account for manufacturer tolerances.
4.  $\leq 0.635$  wt. %  $^{235}\text{U}$  and  $\leq 1.578$  wt. % total fissile plutonium ( $^{239}\text{Pu}$  and  $^{241}\text{Pu}$ ), (wt. % of total fuel weight, i.e.,  $\text{UO}_2$  plus  $\text{PuO}_2$ ).
5. This assembly class contains 74 total rods; 66 full length rods and 8 partial length rods.
6. Square, replacing nine fuel rods.
7. Variable.
8. This assembly contains 92 total fuel rods; 78 full length rods and 14 partial length rods.
9. This assembly class contains 91 total fuel rods; 83 full length rods and 8 partial length rods.
10. One diamond-shaped water rod replacing the four center fuel rods and four rectangular water rods dividing the assembly into four quadrants.
11. These rods may also be sealed at both ends and contain ZR material in lieu of water.
12. This assembly is known as "QUAD+." It has four rectangular water cross segments dividing the assembly into four quadrants.
13. For the SPC 9x9-5 fuel assembly, each fuel rod must meet either the 9x9E or the 9x9F set of limits or clad O.D., clad I.D., and pellet diameter.

Table 1.2.12

## DESIGN BASIS FUEL ASSEMBLY FOR EACH DESIGN CRITERION

<b>Criterion</b>	<b>MPC-68/68F</b>	<b>MPC-24/24E/24EF/32</b>
Reactivity	SPC 9x9-5 (Array/Class 9x9E/F)	B&W 15x15 (Array/Class 15x15F)
Shielding (Source Term)	GE 7x7	B&W 15x15
Fuel Assembly Effective Planar Thermal Conductivity	GE 11 9x9	<u>W</u> 17x17 OFA
Fuel Basket Effective Axial Thermal Conductivity	GE 7x7	<u>W</u> 14x14 OFA
MPC Density and heat Capacity	Dresden 6x6	<u>W</u> 14x14 OFA



Tables 1.2.13 and 1.2.14

INTENTIONALLY DELETED

Table 1.2.15

## NORMALIZED DISTRIBUTION BASED ON BURNUP PROFILE

<b>GENERIC FUEL DISTRIBUTION<sup>†</sup></b>			
<b>Interval</b>	<b>Axial Distance From Bottom of Active Fuel (% of Active Fuel Length)</b>	<b>PWR Fuel Normalized Distribution</b>	<b>BWR Fuel Normalized Distribution</b>
1	0% to 4-1/6%	0.5485	0.2200
2	4-1/6% to 8-1/3%	0.8477	0.7600
3	8-1/3% to 16-2/3%	1.0770	1.0350
4	16-2/3% to 33-1/3%	1.1050	1.1675
5	33-1/3% to 50%	1.0980	1.1950
6	50% to 66-2/3%	1.0790	1.1625
7	66-2/3% to 83-1/3%	1.0501	1.0725
8	83-1/3% to 91-2/3%	0.9604	0.8650
9	91-2/3% to 95-5/6%	0.7338	0.6200
10	95-5/6% to 100%	0.4670	0.2200
<b>TROJAN PLANT FUEL DISTRIBUTION<sup>††</sup></b>			
<b>Interval</b>	<b>Axial Distance From Bottom of Active Fuel (% of Active Fuel Length)</b>	<b>Normalized Distribution</b>	
1	0% to 5%	0.59	
2	5% to 10%	0.89	
3	10% to 15%	1.03	
4	15% to 20%	1.07	
5	20% to 25%	1.09	
6	25% to 45%	1.10	
7	45% to 70%	1.09	
8	70% to 75%	1.07	
9	75% to 80%	1.05	
10	80% to 85%	1.02	
11	85% to 90%	0.96	
12	90% to 95 %	0.82	
13	95% to 100%	0.56	

<sup>†</sup> References [1.2.8] and [1.2.9]

<sup>††</sup> Reference [1.2.12]

Table 1.2.16

## SUGGESTED PWR UPPER AND LOWER FUEL SPACER LENGTHS (Note 1)

<b>Fuel Assembly Type</b>	<b>Assembly Length w/o NFH<sup>†</sup> (in.)</b>	<b>Location of Active Fuel from Bottom (in.)</b>	<b>Max. Active Fuel Length (in.)</b>	<b>Upper Fuel Spacer Length (in.)</b>	<b>Lower Fuel Spacer Length (in.)</b>
CE 14x14	157	4.1	137	9.5	10
CE 16x16	176.8	4.7	150	0	0
BW 15x15	165.7	8.4	141.8	6.7	4.1
W 17x17 OFA	159.8	3.7	144	8.2	8.5
W 17x17S	159.8	3.7	144	8.2	8.5
W 17x17V5H	160.1	3.7	144	7.9	8.5
W 15x15	159.8	3.7	144	8.2	8.5
W 14x14S	159.8	3.7	145.2	9.2	7.5
W 14x14 OFA	159.8	3.7	144	8.2	8.5
Ft. Calhoun	146	6.6	128	10.25	20.25
St. Lucie 2	158.2	5.2	136.7	10.25	8.05
B&W 15x15 SS	137.1	3.873	120.5	19.25	19.25
W 15x15 SS	137.1	3.7	122	19.25	19.25
W 14x14 SS	137.1	3.7	120	19.25	19.25
Indian Point 1	137.2	17.705	101.5	18.75	20.0

Notes: 1. These fuel spacer lengths are not applicable to Trojan plant fuel. Trojan plant fuel spacer lengths are determined uniquely for the custom-designed Trojan MPC-24E/EF, as necessary, based on the presence of non-fuel hardware. They are sized to maintain the active fuel within the envelope of the neutron absorber affixed to the cell walls and allow for an approximate 2-inch gap between the fuel and the MPC lid. See Chapter 6 for discussion of potential misalignments between the active fuel and the neutron absorber.

<sup>†</sup> NFH is an abbreviation for non-fuel hardware, including control components. Fuel assemblies with control components may require shorter fuel spacers.

Table 1.2.17

## SUGGESTED BWR UPPER AND LOWER FUEL SPACER LENGTHS (Note 1)

<b>Fuel Assembly Type</b>	<b>Assembly Length (in.)</b>	<b>Location of Active Fuel from Bottom (in.)</b>	<b>Max. Active Fuel Length (in.)</b>	<b>Upper Fuel Spacer Length (in.)</b>	<b>Lower Fuel Spacer Length (in.)</b>
GE/2-3	171.2	7.3	150	4.8	0
GE/4-6	176.2	7.3	150	0	0
Dresden 1	134.4	11.2	110	18	28.0
Dresden 1 Damaged Fuel or Fuel Debris	142.1 <sup>†</sup>	11.2	110	17	16.9
LaCrosse	102.5	10.5	83	37	37.5

Notes: 1. Each user shall specify the fuel spacer lengths based on their fuel length and allowing an approximate 2-inch gap between the fuel and the MPC lid. See Chapter 6 for discussion of potential misalignments between the active fuel and the neutron absorber.

---

<sup>†</sup> Fuel length includes the damaged fuel container.

Table 1.2.18

## SUMMARY OF HI-STAR 100 SYSTEM POST-ACCIDENT PERFORMANCE

Aspect of Post-Accident Performance	Results with Demonstrated Integrity of MPC Enclosure Vessel	Results with Postulated Gross Failure of MPC Enclosure Vessel
Containment Boundary Integrity	The overpack containment boundary is standard air leak tested to $4.3 \times 10^{-6}$ atm cm <sup>3</sup> /s (helium). Boundary is shown to withstand all hypothetical accident conditions. Therefore, there will be no detectable release of radioactive materials.	The overpack containment boundary is leak tested to $4.3 \times 10^{-6}$ atm cm <sup>3</sup> /s (helium). The overpack containment boundary is shown to withstand all hypothetical accident conditions. Therefore, the overpack containment boundary meets the accident condition leakage rates.
Maintenance of Subcritical Margins (Maximum $k_{\text{eff}}$ )	The MPC enclosure vessel is seal welded and there is no breach of the MPC. The bolted closure overpack containment boundary has been shown to prevent water immersion. Therefore, the maximum reactivity of the fuel in a dry MPC is less than 0.5.	The bolted closure overpack containment boundary has been shown to prevent water immersion. Therefore, the maximum reactivity of the fuel in a dry MPC is less than 0.5. Assuming the MPC is fully flooded with water, the reactivity is shown to be below the regulatory requirement of 0.95 including uncertainties and bias.
Adequate Shielding	The MPC enclosure vessel boundary has no effect on the dose rates of the HI-STAR 100 System.	Failure of the MPC enclosure vessel to maintain a release boundary has no effect on the dose rates of the HI-STAR 100 System.
Adequate Heat Rejection (Peak Fuel Cladding Temperature)	The MPC enclosure vessel maintains the helium and the peak fuel cladding temperature is demonstrated to remain below 800°F in the post-fire hypothetical accident condition.	Assuming the MPC internal helium fill pressure is released into the overpack containment, the pressure within the small annulus would rise to equalize with the MPC internal pressure. There would be a corresponding slight pressure decrease in the MPC enclosure vessel. The comparatively small volume of the annulus and pressure differential results in the slight pressure change. This will have a negligibly small effect on the peak fuel cladding temperature.  The overpack containment boundary is demonstrated to withstand all hypothetical accident conditions. Therefore, there is no credible mechanism for the release of the helium.

Tables 1.2.19 and 1.2.20

INTENTIONALLY DELETED

Table 1.2.21

## DESIGN CHARACTERISTICS FOR THORIA RODS IN D-1 THORIA ROD CANISTERS

PARAMETER	MPC-68 or MPC-68F
Cladding Type	ZR
Composition	98.5 wt.% ThO <sub>2</sub> , 1.5 wt.% UO <sub>2</sub> with an enrichment of 93.5 wt. % <sup>235</sup> U
Number of Rods Per Thoria Canister	≤ 18
Decay Heat Per Thoria Canister	≤ 115 watts
Post-Irradiation Fuel Cooling Time and Average Burnup Per Thoria Canister	Cooling time ≥ 18 years and average burnup ≤ 16,000 MWD/MTIHM
Initial Heavy Metal Weight	≤ 27 kg/canister
Fuel Cladding O.D.	≥ 0.412 inches
Fuel Cladding I.D.	≤ 0.362 inches
Fuel Pellet O.D.	≤ 0.358 inches
Active Fuel Length	≤ 111 inches
Canister Weight	≤ 550 lbs., including Thoria Rods
Canister Material	Type 304 SS

Table 1.2.22

## LIMITS FOR MATERIAL TO BE TRANSPORTED IN MPC-24

PARAMETER	VALUE
Fuel Type	Uranium oxide, PWR intact fuel assemblies meeting the limits in Table 1.2.10 for the applicable array/class
Cladding Type	ZR or Stainless Steel (SS) as specified in Table 1.2.10 for the applicable array/class
Maximum Initial Enrichment	As specified in Table 1.2.10 for the applicable array/class
Post-irradiation Cooling Time, Average Burnup, and Minimum Initial Enrichment per Assembly	ZR clad: As specified in Table 1.2.28 or Table 1.2.29, as applicable SS clad: As specified in Table 1.2.30
Decay Heat Per Assembly	ZR clad: $\leq 833$ Watts SS clad: $\leq 488$ Watts
Fuel Assembly Length	$\leq 176.8$ in. (nominal design)
Fuel Assembly Width	$\leq 8.54$ in. (nominal design)
Fuel Assembly Weight	$\leq 1,680$ lbs
Other Limitations	<ul style="list-style-type: none"> <li>▪ Quantity is limited to up to 24 PWR intact fuel assemblies.</li> <li>▪ Non-fuel hardware and neutron sources not permitted.</li> <li>▪ Damaged fuel assemblies and fuel debris not permitted.</li> <li>▪ Trojan plant fuel not permitted.</li> </ul>



Table 1.2.23

## LIMITS FOR MATERIAL TO BE TRANSPORTED IN MPC-68

PARAMETER	VALUE (Note 1)			
Fuel Type(s)	Uranium oxide, BWR intact fuel assemblies meeting the limits in Table 1.2.11 for the applicable array/class, with or without Zircaloy channels	Uranium oxide, BWR damaged fuel assemblies meeting the limits in Table 1.2.11 for array/class 6x6A, 6x6C, 7x7A, or 8x8A, with or without Zircaloy channels, placed in Damaged Fuel Containers (DFCs)	Mixed Oxide (MOX) BWR intact fuel assemblies meeting the limits in Table 1.2.11 for array/class 6x6B, with or without Zircaloy channels	Mixed Oxide (MOX) BWR damaged fuel assemblies meeting the limits in Table 1.2.11 for array/class 6x6B, with or without Zircaloy channels, placed in Damaged Fuel Containers (DFCs)
Cladding Type	ZR or Stainless Steel (SS) as specified in Table 1.2.11 for the applicable array/class	ZR	ZR	ZR
Maximum Initial Planar-Average and Rod Enrichment	As specified in Table 1.2.11 for the applicable array/class	As specified in Table 1.2.11 for the applicable array/class	As specified in Table 1.2.11 for array/class 6x6B	As specified in Table 1.2.11 for array/class 6x6B
Post-irradiation Cooling Time, Average Burnup, and Minimum Initial Enrichment per Assembly	ZR clad: As specified in Table 1.2.31 except as provided in Notes 2 and 3 SS clad: Note 4	Cooling time $\geq 18$ years, average burnup $\leq 30,000$ MWD/MTU, and minimum initial enrichment $\geq 1.45$ wt. % $^{235}\text{U}$ .	Cooling time $\geq 18$ years, average burnup $\leq 30,000$ MWD/MTIH M, and minimum initial enrichment $\geq 1.8$ wt. % $^{235}\text{U}$ .	Cooling time $\geq 18$ years, average burnup $\leq 30,000$ MWD/MTIHM, and minimum initial enrichment $\geq 1.8$ wt. % $^{235}\text{U}$ .
Decay Heat Per Assembly	ZR clad: $\leq 272$ Watts (Note 5) SS clad: $\leq 83$ Watts	$\leq 115$ Watts	$\leq 115$ Watts	$\leq 115$ Watts

Table 1.2.23 (cont'd)

## LIMITS FOR MATERIAL TO BE TRANSPORTED IN MPC-68

PARAMETER	VALUE (Note 1)			
Fuel Assembly Length	$\leq 176.2$ in. (nominal design)	$\leq 135.0$ in. (nominal design)	$\leq 135.0$ in. (nominal design)	$\leq 135.0$ in. (nominal design)
Fuel Assembly Width	$\leq 5.85$ in. (nominal design)	$\leq 4.70$ in. (nominal design)	$\leq 4.70$ in. (nominal design)	$\leq 4.70$ in. (nominal design)
Fuel Assembly Weight	$\leq 700$ lbs (including channels)	$\leq 550$ lbs, (including channels and DFC)	$\leq 400$ lbs, (including channels)	$\leq 550$ lbs, (including channels and DFC)
Quantity per MPC	Up to 68 BWR intact fuel assemblies	Up to 68 BWR damaged and/or intact fuel assemblies	Up to 68 BWR intact fuel assemblies	Up to 68 BWR damaged and/or intact fuel assemblies
Other Limitations	<ul style="list-style-type: none"> <li>Quantity is limited to up to one (1) Dresden Unit 1 thoria rod canister meeting the specifications listed in Table 1.2.21 plus any combination of Dresden Unit 1 damaged fuel assemblies in DFCs and intact fuel assemblies up to a total of 68.</li> <li>Stainless steel channels are not permitted.</li> <li>Fuel debris is not permitted.</li> <li>Dresden Unit 1 fuel assemblies with one antimony-beryllium neutron source are permitted. The antimony-beryllium neutron source material shall be in a water rod location.</li> </ul>			

## Notes:

1. A fuel assembly must meet the requirements of any one column and the other limitations to be authorized for transportation.
2. Array/class 6x6A, 6x6C, 7x7A, and 8x8A fuel assemblies shall have a cooling time  $\geq 18$  years, an average burnup  $\leq 30,000$  MWD/MTU, and a minimum initial enrichment  $\geq 1.45$  wt. %  $^{235}\text{U}$ .
3. Array/class 8x8F fuel assemblies shall have a cooling time  $\geq 10$  years, an average burnup  $\leq 27,500$  MWD/MTU, and a minimum initial enrichment  $\geq 2.4$  wt. %  $^{235}\text{U}$ .
4. SS-clad fuel assemblies shall have a cooling time  $\geq 16$  years, an average burnup  $\leq 22,500$  MWD/MTU, and a minimum initial enrichment  $\geq 3.5$  wt. %  $^{235}\text{U}$ .
5. Array/class 8x8F fuel assemblies shall have a decay heat  $\leq 183.5$  Watts.

Table 1.2.24

## LIMITS FOR MATERIAL TO BE TRANSPORTED IN MPC-68F

PARAMETER	VALUE (Notes 1 and 2)			
Fuel Type(s)	Uranium oxide, BWR intact fuel assemblies meeting the limits in Table 1.2.11 for array/class 6x6A, 6x6C, 7x7A, or 8x8A, with or without Zircaloy channels	Uranium oxide, BWR damaged fuel assemblies or fuel debris meeting the limits in Table 1.2.11 for array/class 6x6A, 6x6C, 7x7A, or 8x8A, with or without Zircaloy channels, placed in Damaged Fuel Containers(DFCs)	Mixed Oxide (MOX) BWR intact fuel assemblies meeting the limits in Table 1.2.11 for array/class 6x6B, with or without Zircaloy channels	Mixed Oxide (MOX) BWR damaged fuel assemblies or fuel debris meeting the limits in Table 1.2.11 for array/class 6x6B, with or without Zircaloy channels, placed in Damaged Fuel Containers (DFCs))
Cladding Type	ZR	ZR	ZR	ZR
Maximum Initial Planar-Average and Rod Enrichment	As specified in Table 1.2.11 for the applicable array/class	As specified in Table 1.2.11 for the applicable array/class	As specified in Table 1.2.11 for array/class 6x6B	As specified in Table 1.2.11 for array/class 6x6B
Post-irradiation Cooling Time, Average Burnup, and Minimum Initial Enrichment per Assembly	Cooling time $\geq 18$ years, average burnup $\leq 30,000$ MWD/MTU, and minimum initial enrichment $\geq 1.45$ wt. % $^{235}\text{U}$ .	Cooling time $\geq 18$ years, average burnup $\leq 30,000$ MWD/MTU, and minimum initial enrichment $\geq 1.45$ wt. % $^{235}\text{U}$ .	Cooling time $\geq 18$ years, average burnup $\leq 30,000$ MWD/MTIH M, and minimum initial enrichment $\geq 1.8$ wt. % $^{235}\text{U}$ .	Cooling time $\geq 18$ years, average burnup $\leq 30,000$ MWD/MTIHM, and minimum initial enrichment $\geq 1.8$ wt. % $^{235}\text{U}$ .
Decay Heat Per Assembly	$\leq 115$ Watts	$\leq 115$ Watts	$\leq 115$ Watts	$\leq 115$ Watts

Table 1.2.24 (cont'd)

## LIMITS FOR MATERIAL TO BE TRANSPORTED IN MPC-68F

PARAMETER	VALUE (Note 1)			
Fuel Assembly Length	$\leq 135.0$ in. (nominal design)	$\leq 135.0$ in. (nominal design)	$\leq 135.0$ in. (nominal design)	$\leq 135.0$ in. (nominal design)
Fuel Assembly Width	$\leq 4.70$ in. (nominal design)	$\leq 4.70$ in. (nominal design)	$\leq 4.70$ in. (nominal design)	$\leq 4.70$ in. (nominal design)
Fuel Assembly Weight	$\leq 400$ lbs (including channels)	$\leq 550$ lbs (including channels and DFC)	$\leq 400$ lbs (including channels)	$\leq 550$ lbs (including channels and DFC)
Other Limitations	<ul style="list-style-type: none"> <li>▪ Quantity is limited to up to four (4) DFCs containing Dresden Unit 1 uranium oxide or MOX fuel debris. The remaining fuel storage locations may be filled with array/class 6x6A, 6x6B, 6x6C, 7x7A, and 8x8A fuel assemblies of the following type, as applicable: <ul style="list-style-type: none"> <li>- uranium oxide BWR intact fuel assemblies</li> <li>- MOX BWR intact fuel assemblies</li> <li>- uranium oxide BWR damaged fuel assemblies in DFCs</li> <li>- MOX BWR damaged fuel assemblies in DFCs</li> <li>- up to one (1) Dresden Unit 1 thoria rod canister meeting the specifications listed in Table 1.2.21</li> </ul> </li> <li>▪ Stainless steel channels are not permitted.</li> <li>▪ Dresden Unit 1 fuel assemblies with one antimony-beryllium neutron source are permitted. The antimony-beryllium neutron source material shall be in a water rod location.</li> </ul>			

## Notes:

1. A fuel assembly must meet the requirements of any one column and the other limitations to be authorized for transportation.
2. Only fuel from Dresden Unit 1 is permitted for transportation in the MPC-68F.

Table 1.2.25

## LIMITS FOR MATERIAL TO BE TRANSPORTED IN MPC-24E

PARAMETER	VALUE (Note 1)	
Fuel Type	Uranium oxide PWR intact fuel assemblies meeting the limits in Table 1.2.10 for the applicable array/class	Trojan plant damaged fuel meeting the limits in Table 1.2.10 for array/class 17x17B, placed in a Holtec Damaged Fuel Container (DFC) designed for Trojan plant fuel or a Trojan Failed Fuel Can (FFC)
Cladding Type	ZR or Stainless Steel (SS) assemblies as specified in Table 1.2.10 for the applicable array/class	ZR
Maximum Initial Enrichment	As specified in Table 1.2.10 for the applicable array/class	3.7 wt. % <sup>235</sup> U
Post-irradiation Cooling Time, Average Burnup, and Minimum Initial Enrichment per Assembly (except Trojan plant fuel and non-fuel hardware)	ZR clad: As specified in Table 1.2.28 or 1.2.29, as applicable SS clad: As specified in Table 1.2.30	Not applicable
Post-irradiation Cooling Time, Average Burnup, and Minimum Initial Enrichment per Assembly for Trojan plant fuel	As specified in Table 1.2.35	As specified in Table 1.2.35
Post-irradiation Cooling Time and Burnup for Trojan plant Non-fuel Hardware and Neutron Sources	As specified in Table 1.2.36	Not applicable
Decay Heat Per Assembly (except for Trojan plant fuel)	ZR clad: $\leq 833$ Watts SS clad: $\leq 488$ Watts	Not applicable
Decay heat per Assembly for Trojan plant fuel	$\leq 725$ Watts	$\leq 725$ Watts

Table 1.2.25 (cont'd)

## LIMITS FOR MATERIAL TO BE TRANSPORTED IN MPC-24E

PARAMETER	VALUE (Note 1)	
Fuel Assembly Length	$\leq 176.8$ in. (nominal design)	$\leq 169.3$ in. (nominal design)
Fuel Assembly Width	$\leq 8.54$ in. (nominal design)	$\leq 8.43$ in. (nominal design)
Fuel Assembly Weight	$\leq 1680$ lbs (including non-fuel hardware)	$\leq 1680$ lbs (including DFC or Failed Fuel Can)
Other Limitations	<ul style="list-style-type: none"> <li>▪ Quantity per MPC: up to 24 PWR intact fuel assemblies. For Trojan plant fuel only, up to four (4) damaged fuel assemblies may be stored in fuel storage locations 3, 6, 19, and/or 22. The remaining fuel storage locations may be filled with Trojan plant intact fuel assemblies.</li> <li>▪ Trojan plant fuel must be transported in the custom-designed Trojan MPCs with the MPC spacer installed (see Figure 1.1.5). Fuel from other plants is not permitted to be transported in the Trojan MPCs.</li> <li>▪ Except for Trojan plant fuel, the fuel assemblies shall not contain non-fuel hardware. Trojan intact fuel assemblies containing non-fuel hardware may be transported in any fuel storage location.</li> <li>▪ Trojan plant damaged fuel assemblies must be transported in a Holtec DFC for Trojan plant fuel or a Trojan plant FFC.</li> <li>▪ One (1) Trojan plant Sb-Be and/or two (2) Cf neutron sources, each in a Trojan plant intact fuel assembly may be transported in any one MPC. Each neutron source may be transported in any fuel storage location.</li> <li>▪ Fuel debris is not authorized for transportation in the MPC-24E.</li> <li>▪ Trojan plant non-fuel hardware and neutron sources may not be transported in the same fuel storage location with damaged fuel assemblies.</li> </ul>	

## Notes:

1. A fuel assembly must meet the requirements of any one column and the other limitations to be authorized for transportation.

Table 1.2.26

## LIMITS FOR MATERIAL TO BE TRANSPORTED IN MPC-24EF

PARAMETER	VALUE (Note 1)		
Fuel Type	Uranium oxide PWR intact fuel assemblies meeting the limits in Table 1.2.10 for the applicable array/class	Trojan plant damaged fuel meeting the limits in Table 1.2.10 for array/class 17x17B, placed in a Holtec Damaged Fuel Container (DFC) designed for Trojan plant fuel or a Trojan Failed Fuel Can (FFC)	Trojan plant Fuel Debris Process Can Capsules and/or Trojan plant fuel assemblies classified as fuel debris, for which the original fuel assemblies meet the applicable criteria in Table 1.2.10 for array/class 17x17B, placed in a Holtec Damaged Fuel Container (DFC) designed for Trojan plant fuel or a Trojan Failed Fuel Can (FFC)
Cladding Type	ZR or Stainless Steel (SS) assemblies as specified in Table 1.2.10 for the applicable array/class	ZR	ZR
Maximum Initial Enrichment	As specified in Table 1.2.10 for the applicable array/class	$\leq 3.7 \text{ wt. } \% {}^{235}\text{U}$	$\leq 3.7 \text{ wt. } \% {}^{235}\text{U}$
Post-irradiation Cooling Time, Average Burnup, and Minimum Initial Enrichment per Assembly (except Trojan plant fuel and non-fuel hardware)	ZR clad: As specified in Table 1.2.28 or 1.2.29, as applicable  SS clad: As specified in Table 1.2.30	Not applicable	Not applicable
Post-irradiation Cooling Time, Average Burnup, and Minimum Initial Enrichment per Assembly for Trojan plant fuel	As specified in Table 1.2.35	As specified in Table 1.2.35	As specified in Table 1.2.35

Table 1.2.26 (cont'd)

## LIMITS FOR MATERIAL TO BE TRANSPORTED IN MPC-24EF

PARAMETER	VALUE (Note 1)		
Post-irradiation Cooling Time and Burnup for Trojan plant Non-fuel Hardware and Neutron Sources	As specified in Table 1.2.36	As specified in Table 1.2.36	As specified in Table 1.2.36
Decay Heat Per Assembly (except for Trojan plant fuel)	ZR clad: $\leq 833$ Watts SS clad: $\leq 488$ Watts	Not applicable	Not applicable
Decay heat per Assembly for Trojan plant fuel	$\leq 725$ Watts	$\leq 725$ Watts	$\leq 725$ Watts
Fuel Assembly Length	$\leq 176.8$ in. (nominal design)	$\leq 169.3$ in. (nominal design)	$\leq 169.3$ in. (nominal design)
Fuel Assembly Width	$\leq 8.54$ in. (nominal design)	$\leq 8.43$ in. (nominal design)	$\leq 8.43$ in. (nominal design)
Fuel Assembly Weight	$\leq 1680$ lbs (including non-fuel hardware)	$\leq 1680$ lbs (including DFC or Failed Fuel Can)	$\leq 1680$ lbs (including DFC or Failed Fuel Can)



Table 1.2.26 (cont'd)

## LIMITS FOR MATERIAL TO BE TRANSPORTED IN MPC-24EF

Other Limitations	<ul style="list-style-type: none"> <li>▪ Quantity per MPC: Up to 24 PWR intact fuel assemblies. For Trojan plant fuel only, up to four (4) damaged fuel assemblies, fuel assemblies classified as fuel debris, and/or Trojan Fuel Debris Process Can Capsules may be stored in fuel storage locations 3, 6, 19, and/or 22. The remaining fuel storage locations may be filled with Trojan plant intact fuel assemblies.</li> <li>▪ Trojan plant fuel must be transported in the custom-designed Trojan MPCs with the MPC spacer installed (see Figure 1.1.5). Fuel from other plants is not permitted to be transported in the Trojan MPCs.</li> <li>▪ Except for Trojan plant fuel, the fuel assemblies shall not contain non-fuel hardware or neutron sources. Trojan intact fuel assemblies containing non-fuel hardware may be transported in any fuel storage location.</li> <li>▪ Trojan plant damaged fuel assemblies, fuel assemblies classified as fuel debris, and Fuel Debris Process Can Capsules must be transported in a Trojan Failed Fuel Can or a Holtec DFC for Trojan plant fuel.</li> <li>▪ One (1) Trojan plant Sb-Be and/or two (2) Cf neutron sources, each in a Trojan plant intact fuel assembly may be transported in any one MPC. Each neutron source may be transported in any fuel storage location.</li> </ul>
-------------------	--

## Notes:

1. A fuel assembly must meet the requirements of any one column and the other limitations to be authorized for transportation.

Table 1.2.27 (Sheet 1 of 2)

## LIMITS FOR MATERIAL TO BE TRANSPORTED IN MPC-32

PARAMETER	VALUE
Fuel Type	Uranium oxide, PWR intact fuel assemblies meeting the limits in Table 1.2.10 for array/classes 15x15D, E, F, and H and 17x17A, B, and C
Cladding Type	ZR
Maximum Initial Enrichment	5.0 wt% <sup>235</sup> U
Post-irradiation Cooling Time, Average Burnup, and Minimum Initial Enrichment per Assembly	As specified in Table 1.2.32 or Table 1.2.33, as applicable
Decay Heat Per Assembly	≤ 625 Watts
Minimum Burnup per Assembly	As specified in Table 1.2.34 for the applicable array/class
Fuel Assembly Length	≤ 176.8 in. (nominal design)
Fuel Assembly Width	≤ 8.54 in. (nominal design)
Fuel Assembly Weight	≤ 1,680 lbs including non-fuel hardware and neutron sources
Operating Parameters During Irradiation of the Assembly (See Subsection 1.2.3.7.1)	
Average in-core soluble boron concentration	≤ 1000 ppmb
Average Moderator Temperature	≤ 601 K for array/classes 15x15D, E, F and H ≤ 610 K for array/classes 17x17A, B and C
Average Specific Power	≤ 47.36 kW/kg-U for array/classes 15x15D, E, F and H ≤ 61.61 kW/kg-U for array/classes 17x17A, B and C

Table 1.2.27 (Sheet 2 of 2)

## LIMITS FOR MATERIAL TO BE TRANSPORTED IN MPC-32

PARAMETER	VALUE
In-Pool Minimum Soluble Boron Required by Burnup Verification Method B During Loading and Unloading (See Subparagraph 1.2.3.7.2)	800 ppmb
Other Limitations	<ul style="list-style-type: none"> <li>▪ Quantity is limited to up to 32 PWR intact fuel assemblies in the above-specified array/classes only.</li> <li>▪ Damaged fuel assemblies and fuel debris not permitted.</li> <li>▪ Trojan plant fuel not permitted.</li> <li>▪ One NSA is permitted for loading with a fuel assembly in fuel storage locations 13, 14, 19, or 20 (the fuel storage location numbers are provided in Figure 1.2.4). The allowable combinations of burnup and post-irradiation cooling time are provided in Table 1.2.38.</li> <li>▪ BPRAs, TPDs, WABAs, water displacement guide tube plugs, orifice rod assemblies, and/or vibration suppressor inserts may be stored with fuel assemblies in any fuel cell location. The allowable combinations of burnup and post-irradiation cooling time are provided in Table 1.2.38.</li> <li>▪ RCCAs, CRAs, and CEAs may be stored with fuel in fuel cell locations 7, 8, 12-15, 18-21, 25 and/or 26 (the fuel storage location numbers are provided in Figure 1.2.4). The allowable combinations of burnup and post-irradiation cooling time are provided in Table 1.2.38.</li> <li>▪ ITTRs may be present in the fuel assembly along with other types of non-fuel hardware or neutron sources.</li> <li>▪ APSRs not permitted.</li> </ul>

Table 1.2.28

FUEL ASSEMBLY COOLING, AVERAGE BURNUP, AND MINIMUM ENRICHMENT  
LIMITS FOR TRANSPORTATION IN MPC-24/24E/24EF; PWR FUEL WITH ZR  
CLADDING AND WITH NON-ZIRCALOY IN-CORE GRID SPACERS

<b>ASSEMBLY POST-IRRADIATION COOLING TIME (years)</b>	<b>ASSEMBLY BURNUP (MWD/MTU)</b>	<b>ASSEMBLY ENRICHMENT (wt. % <sup>235</sup>U)</b>
$\geq 9$	$\leq 24,500$	$\geq 2.3$
$\geq 11$	$\leq 29,500$	$\geq 2.6$
$\geq 13$	$\leq 34,500$	$\geq 2.9$
$\geq 15$	$\leq 39,500$	$\geq 3.2$
$\geq 18$	$\leq 44,500$	$\geq 3.4$

Table 1.2.29

FUEL ASSEMBLY COOLING, AVERAGE BURNUP, AND MINIMUM ENRICHMENT  
LIMITS FOR TRANSPORTATION IN MPC-24/24E/24EF; PWR FUEL WITH ZR  
CLADDING AND WITH ZIRCALOY IN-CORE GRID SPACERS

<b>ASSEMBLY POST-IRRADIATION COOLING TIME (years)</b>	<b>ASSEMBLY BURNUP (MWD/MTU)</b>	<b>ASSEMBLY ENRICHMENT (wt. % <sup>235</sup>U)</b>
$\geq 6$	$\leq 24,500$	$\geq 2.3$
$\geq 7$	$\leq 29,500$	$\geq 2.6$
$\geq 9$	$\leq 34,500$	$\geq 2.9$
$\geq 11$	$\leq 39,500$	$\geq 3.2$
$\geq 14$	$\leq 44,500$	$\geq 3.4$

Table 1.2.30

FUEL ASSEMBLY COOLING, AVERAGE BURNUP, AND MINIMUM ENRICHMENT  
LIMITS FOR TRANSPORTATION IN MPC-24/24E/24EF; PWR FUEL WITH  
STAINLESS STEEL CLADDING

<b>ASSEMBLY POST-IRRADIATION COOLING TIME (years)</b>	<b>ASSEMBLY BURNUP (MWD/MTU)</b>	<b>ASSEMBLY ENRICHMENT (wt. % <sup>235</sup>U)</b>
$\geq 19$	$\leq 30,000$	$\geq 3.1$
$\geq 24$	$\leq 40,000$	$\geq 3.1$

Table 1.2.31

FUEL ASSEMBLY COOLING, AVERAGE BURNUP, AND MINIMUM ENRICHMENT  
LIMITS FOR TRANSPORTATION IN MPC-68

<b>ASSEMBLY POST-IRRADIATION COOLING TIME (years)</b>	<b>ASSEMBLY BURNUP (MWD/MTU)</b>	<b>ASSEMBLY ENRICHMENT (wt. % <sup>235</sup>U)</b>
$\geq 5$	$\leq 10,000$	$\geq 0.7$
$\geq 7$	$\leq 20,000$	$\geq 1.35$
$\geq 8$	$\leq 24,500$	$\geq 2.1$
$\geq 9$	$\leq 29,500$	$\geq 2.4$
$\geq 11$	$\leq 34,500$	$\geq 2.6$
$\geq 14$	$\leq 39,500$	$\geq 2.9$
$\geq 19$	$\leq 44,500$	$\geq 3.0$

Table 1.2.32

FUEL ASSEMBLY COOLING, AVERAGE BURNUP, AND MINIMUM ENRICHMENT  
LIMITS FOR TRANSPORTATION IN MPC-32; PWR FUEL WITH ZR CLADDING  
AND WITH NON-ZIRCALOY IN-CORE GRID SPACERS

ASSEMBLY POST-IRRADIATION COOLING TIME (years)	ASSEMBLY BURNUP (MWD/MTU)	ASSEMBLY ENRICHMENT (wt. % <sup>235</sup> U)
WITHOUT NON-FUEL HARDWARE		
≥ 12	≤ 24,500	≥ 2.3
≥ 14	≤ 29,500	≥ 2.6
≥ 16	≤ 34,500	≥ 2.9
≥ 19	≤ 39,500	≥ 3.2
≥ 20	≤ 42,500	≥ 3.4
≥ 24	≤ 45,000	≥ 3.6
WITH NON-FUEL HARDWARE		
≥ 13	≤ 24,500	≥ 2.3
≥ 16	≤ 29,500	≥ 2.6
≥ 18	≤ 34,500	≥ 2.9
≥ 21	≤ 39,500	≥ 3.2
≥ 23	≤ 42,500	≥ 3.4
≥ 25	≤ 45,000	≥ 3.6



Table 1.2.33

FUEL ASSEMBLY COOLING, AVERAGE BURNUP, AND MINIMUM ENRICHMENT  
LIMITS FOR TRANSPORTATION IN MPC-32; PWR FUEL WITH ZR CLADDING  
AND WITH ZIRCALOY IN-CORE GRID SPACERS

ASSEMBLY POST-IRRADIATION COOLING TIME (years)	ASSEMBLY BURNUP (MWD/MTU)	ASSEMBLY ENRICHMENT (wt. % <sup>235</sup> U)
WITHOUT NON-FUEL HARDWARE		
≥ 8	≤ 24,500	≥ 2.3
≥ 9	≤ 29,500	≥ 2.6
≥ 12	≤ 34,500	≥ 2.9
≥ 14	≤ 39,500	≥ 3.2
≥ 19	≤ 44,500	≥ 3.4
≥ 20	≤ 45,000	≥ 3.6
WITH NON-FUEL HARDWARE		
≥ 13	≤ 24,500	≥ 2.3
≥ 16	≤ 29,500	≥ 2.6
≥ 18	≤ 34,500	≥ 2.9
≥ 21	≤ 39,500	≥ 3.2
≥ 23	≤ 42,500	≥ 3.4
≥ 25	≤ 45,000	≥ 3.6

Table 1.2.34

**FUEL ASSEMBLY MAXIMUM ENRICHMENT AND MINIMUM BURNUP  
REQUIREMENTS FOR TRANSPORTATION IN MPC-32**

<b>FUEL ASSEMBLY ARRAY/CLASS</b>	<b>CONFIGURATION  (Note 2)</b>	<b>MINIMUM BURNUP (B) AS A FUNCTION OF INITIAL ENRICHMENT (E) (Note 1)  (GWD/MTU)</b>
15x15D, E, F, H	A	$B = +(1.2222) * E^3 - (14.9530) * E^2 + (70.1230) * E - 81.1400$
	B	$B = +(1.6446) * E^3 - (19.1690) * E^2 + (84.1940) * E - 94.3490$
17x17A, B, C	A	$B = +(0.6704) * E^3 - (8.7858) * E^2 + (49.6000) * E - 62.7720$
	B	$B = +(1.2284) * E^3 - (14.5450) * E^2 + (69.7780) * E - 82.1460$

## Notes:

1. E = Initial enrichment, i.e., for 4.05wt. %, E = 4.05. **Maximum initial enrichment as specified in Table 1.2.27.**
2. See Table 1.2.37

Table 1.2.35

TROJAN PLANT FUEL ASSEMBLY COOLING, AVERAGE BURNUP, AND MINIMUM  
ENRICHMENT LIMITS (Note 1)

<b>Post-irradiation Cooling Time (years)</b>	<b>Assembly Burnup (MWD/MTU)</b>	<b>Assembly Minimum Enrichment (wt. % <sup>235</sup>U)</b>
$\geq 16$	$\leq 42,000$	$\geq 3.09$
$\geq 16$	$\leq 37,500$	$\geq 2.6$
$\geq 16$	$\leq 30,000$	$\geq 2.1$

Notes:

1. Each fuel assembly must only meet one set of limits (i.e., one row).

Table 1.2.36

TROJAN PLANT NON-FUEL HARDWARE AND NEUTRON SOURCE COOLING AND  
BURNUP LIMITS

<b>Type Of Hardware or Neutron Source</b>	<b>Burnup (MWD/MTU)</b>	<b>Post-irradiation Cooling Time (years)</b>
BPRAs	$\leq 15,998$	$\geq 24$
TPDs	$\leq 118,674$	$\geq 11$
RCCAs	$\leq 125,515$	$\geq 9$
Cf neutron source	$\leq 15,998$	$\geq 24$
Sb-Be neutron source with 4 source rods, 16 burnable poison rods, and 4 thimble plug rods	$\leq 45,361$	$\geq 19$
Sb-Be neutron source with 4 source rods and 20 thimble plug rods	$\leq 88,547$	$\geq 9$

Table 1.2.37

## LOADING CONFIGURATIONS FOR THE MPC-32

Configuration	Assembly Specifications
A	<ul style="list-style-type: none"> <li>○ Assemblies that have not been located in any cycle under a control rod bank that was permitted to be inserted during full power operation (per plant operating procedures); or</li> <li>○ Assemblies that have been located under a control rod bank that was permitted to be inserted during full power operation (per plant operating procedures), but where it can be demonstrated, based on operating records, that the insertion never exceeded 8 inches from the top of the active length during full power operation.</li> </ul>
B	<ul style="list-style-type: none"> <li>○ Of the 32 assemblies in a basket, up to 8 assemblies can be from core locations where they were located under a control rod bank, that was permitted to be inserted more than 8 inches during full power operation. There is no limit on the duration (in terms of burnup) under this bank.</li> <li>○ The remaining assemblies in the basket must satisfy the same conditions as specified for configuration A.</li> </ul>

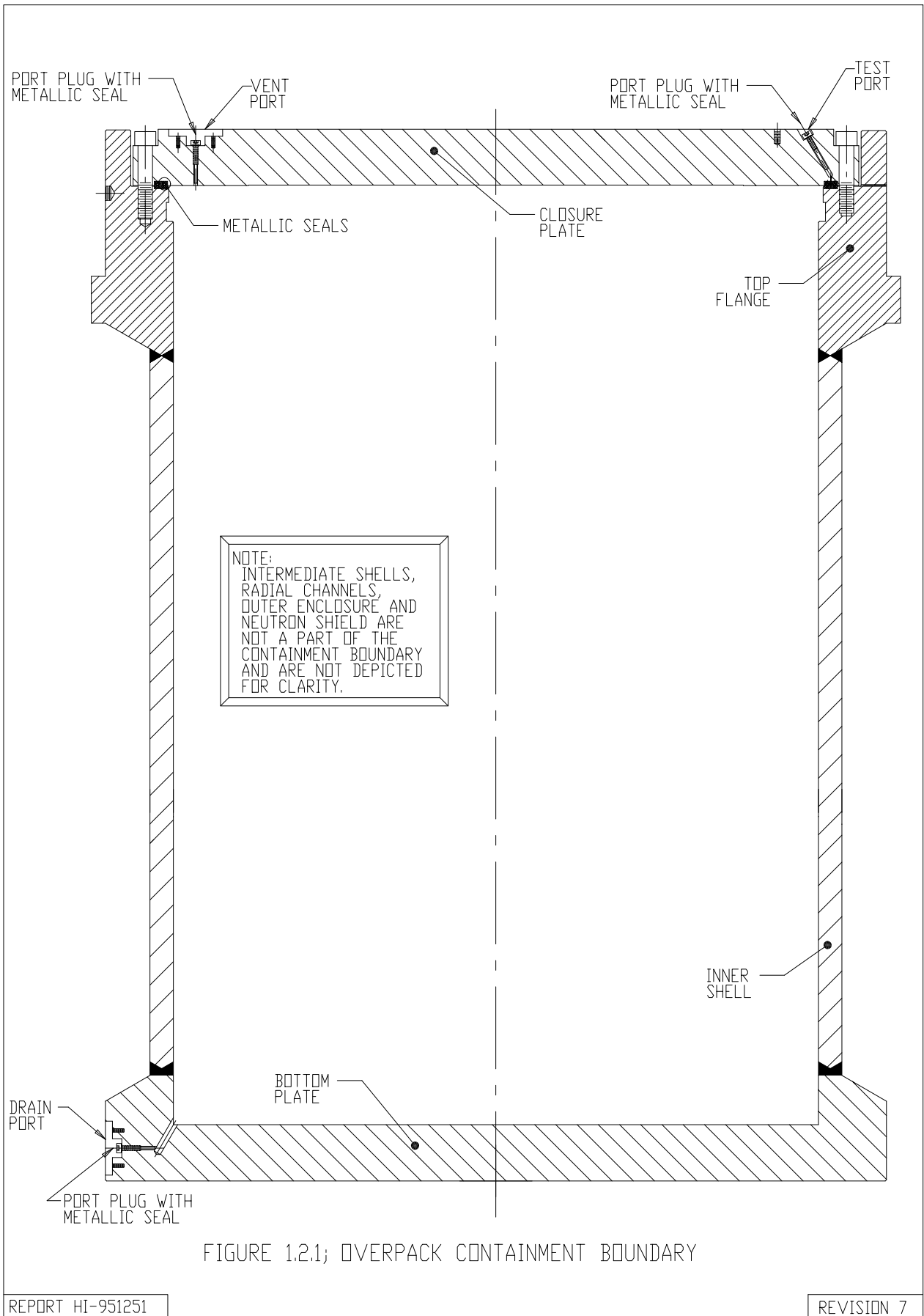
Table 1.2.38

**NON-FUEL HARDWARE AND NEUTRON SOURCES BURNUP  
AND COOLING TIME LIMITS (Notes 1, 2, and 8)**

<b>Post-irradiation Cooling Time (yrs)</b>	<b>Inserts (Note 4) Maximum Burnup (MWD/MTU)</b>	<b>NSA or Guide Tube Hardware (Notes 5 and 9) Maximum Burnup (MWD/MTU)</b>	<b>Control Component (Note 6) Maximum Burnup (MWD/MTU)</b>
$\geq 15$	$\leq 24,635$	N/A (Note 7)	N/A
$\geq 16$	$\leq 30,000$	$\leq 20,000$	N/A
$\geq 17$	$\leq 36,748$	$\leq 25,000$	$\leq 630,000$
$\geq 18$	$\leq 44,102$	$\leq 30,000$	-
$\geq 19$	$\leq 52,900$	$\leq 40,000$	-
$\geq 20$	$\leq 60,000$	$\leq 45,000$	-
$\geq 21$	-	$\leq 50,000$	-
$\geq 22$	-	$\leq 60,000$	-
$\geq 23$	-	$\leq 75,000$	-
$\geq 24$	-	$\leq 90,000$	-
$\geq 25$	-	$\leq 180,000$	-
$\geq 26$	-	$\leq 630,000$	-

**NOTES:**

1. Burnups for non-fuel hardware are to be determined based on the burnup and uranium mass of the fuel assemblies in which the component was inserted during reactor operation.
2. Linear interpolation between points is permitted, except that NSA or Guide Tube Hardware burnups  $> 180,000$  MWD/MTU and  $\leq 630,000$  MWD/MTU must be cooled  $\geq 26$  years.
3. Not used.
4. Includes Burnable Poison Rod Assemblies (BPRAs), Wet Annular Burnable Absorbers (WABAs), and vibration suppressor inserts. For TPDs with absorber rodlets refer to Note 9.
5. Includes Thimble Plug Devices (TPDs), water displacement guide tube plugs, and orifice rod assemblies.
6. Includes Control Rod Assemblies (CRAs), Control Element Assemblies (CEAs), and Rod Cluster Control Assemblies (RCCAs).
7. N/A means not authorized for loading at this cooling time.
8. Non-fuel hardware burnup and cooling time limits are not applicable to Instrument Tube Tie Rods (ITTRs), since they are installed post-irradiation.
9. Maximum burnup for TPDs with absorber rodlets is limited to 60,000 MWD/MTU.



G:\SAR DOCUMENTS\HI-STAR SAR\FIGURES\REVISION 7\CHAPTER 1\FIG 1\_2\_1

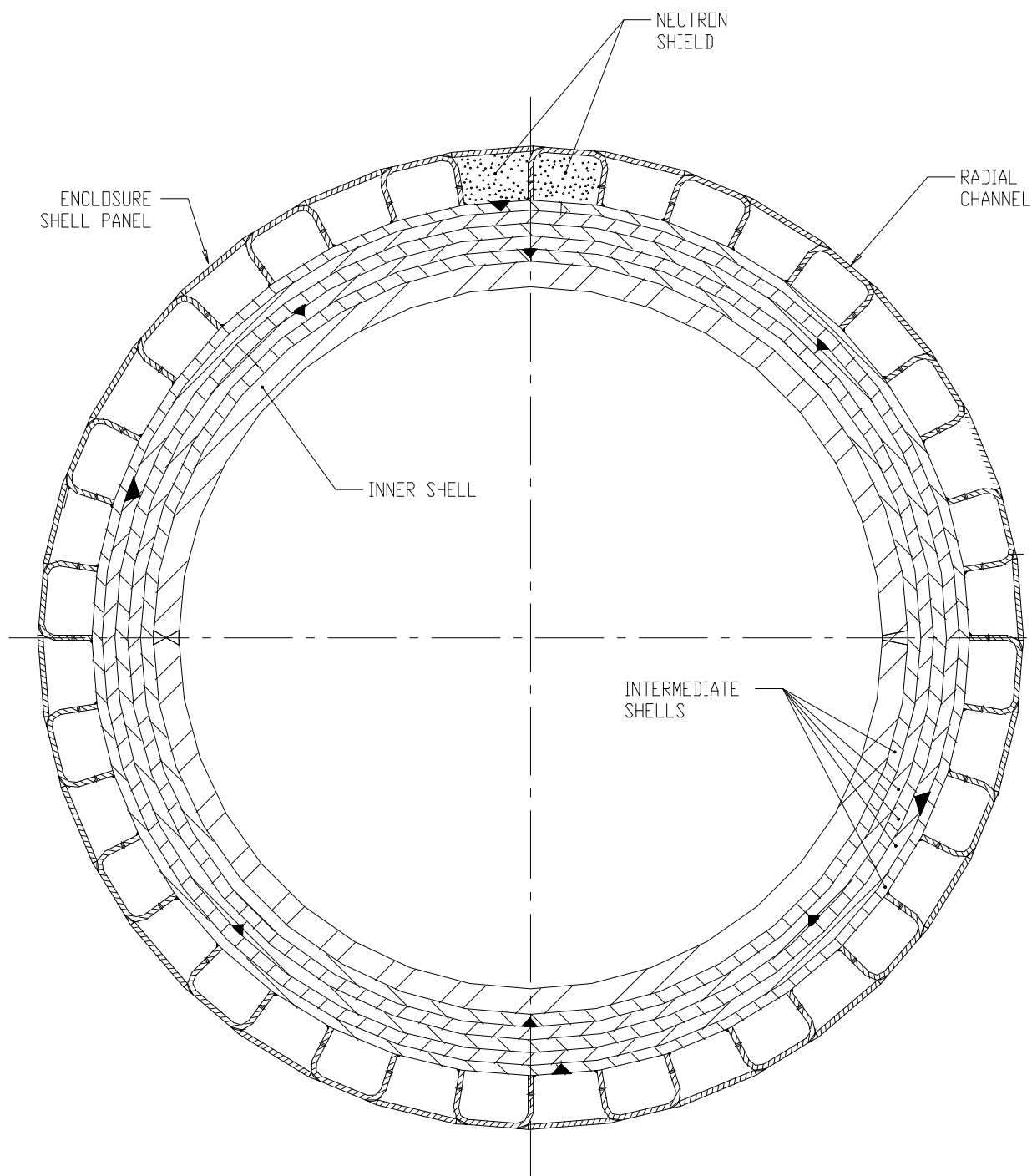


FIGURE 1.2.2; OVERPACK MID-PLANE CROSS SECTION



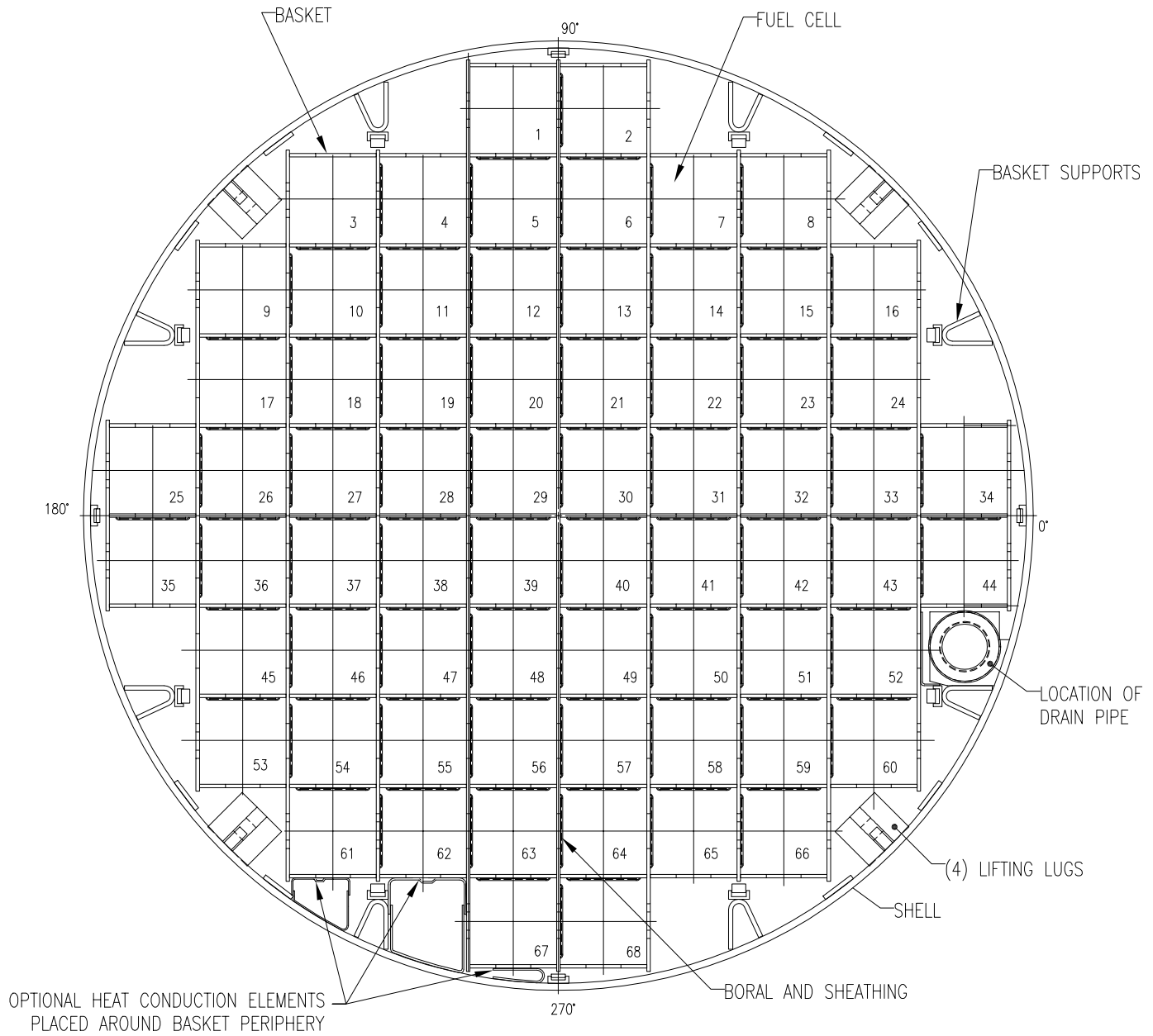


FIGURE 1.2.3; MPC-68/68F CROSS SECTION VIEW

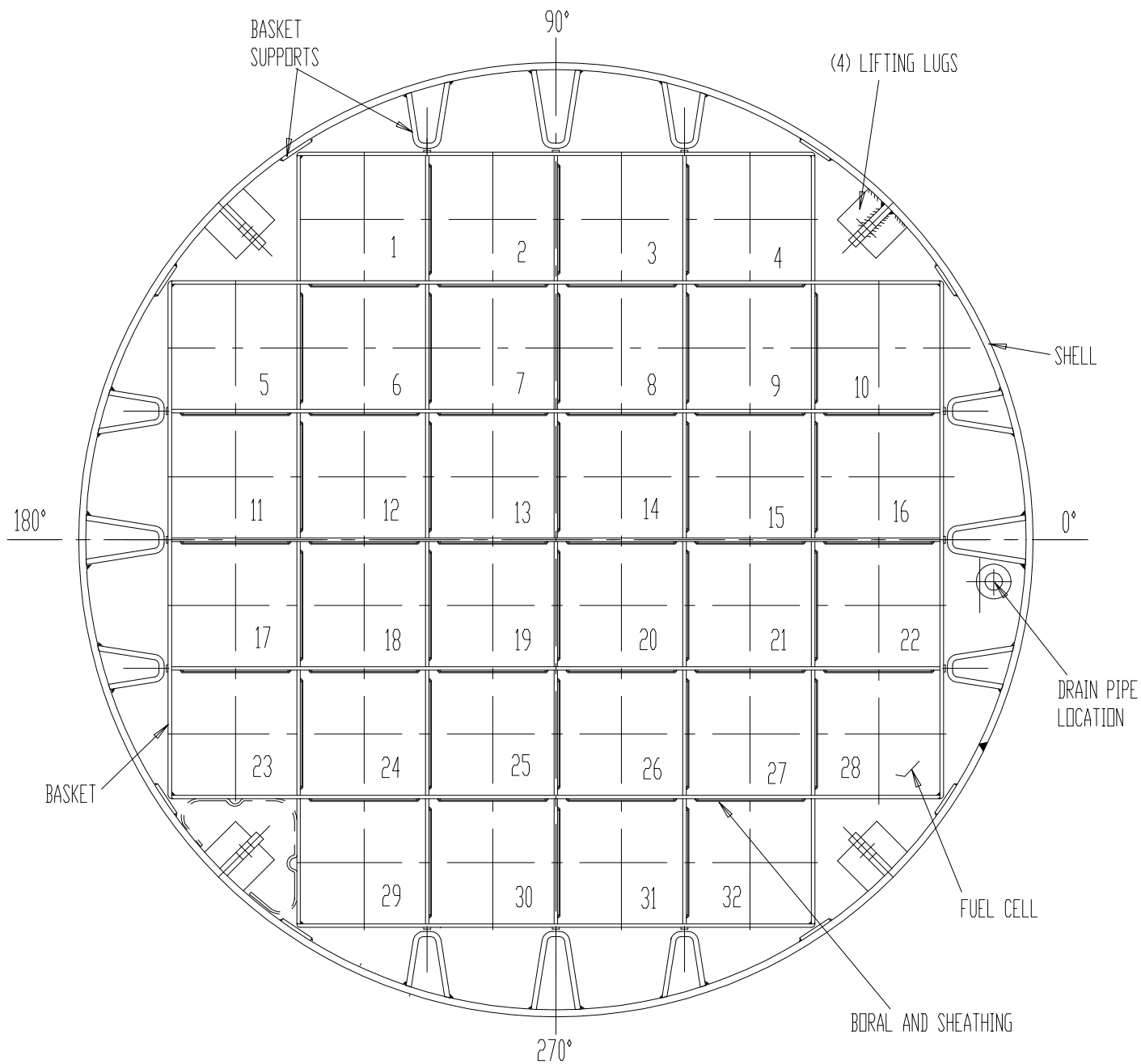


FIGURE 1.2.4; MPC-32 CROSS SECTION VIEW

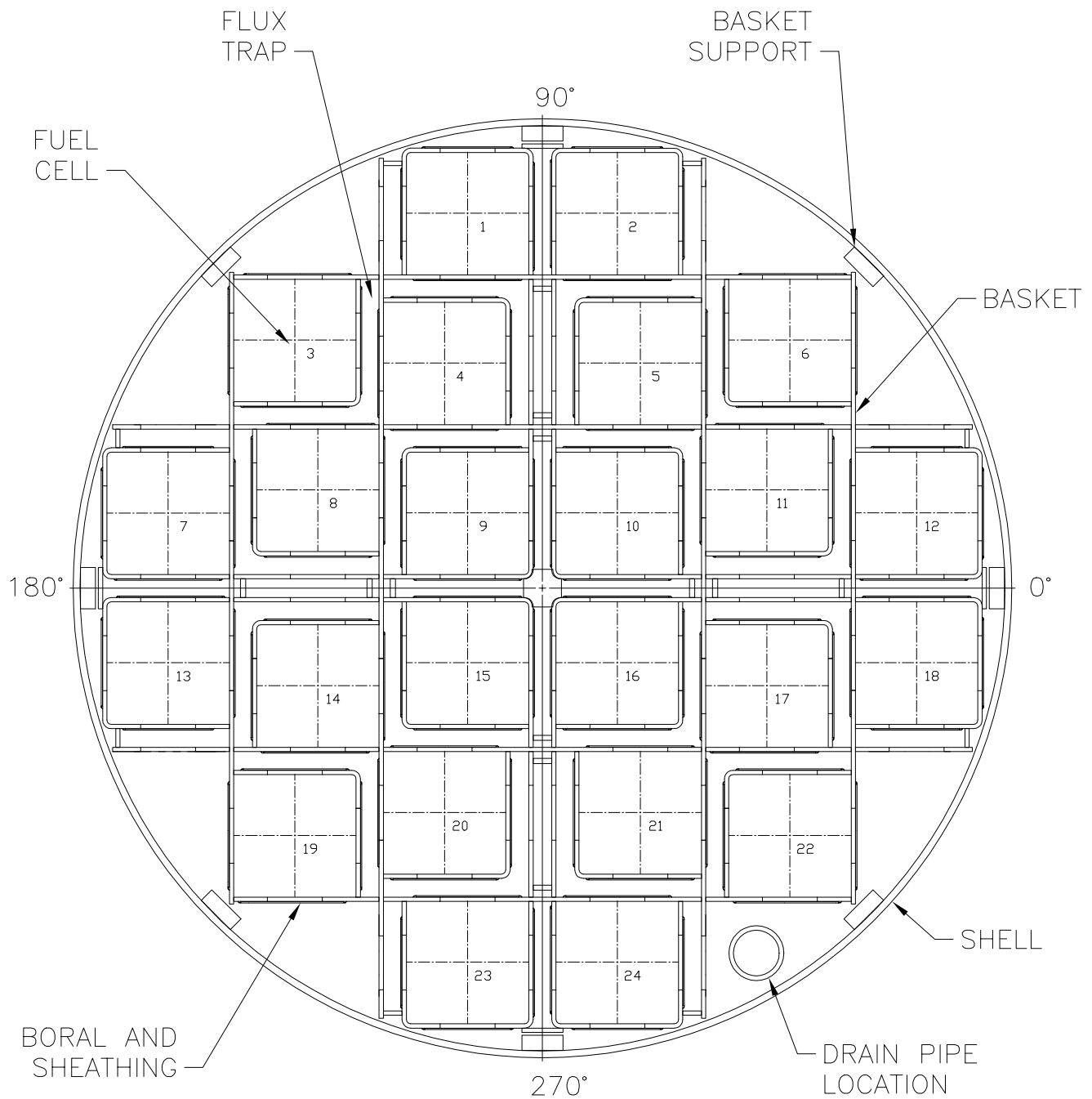


FIGURE 1.2.5; MPC-24/E/EF CROSS SECTION VIEW

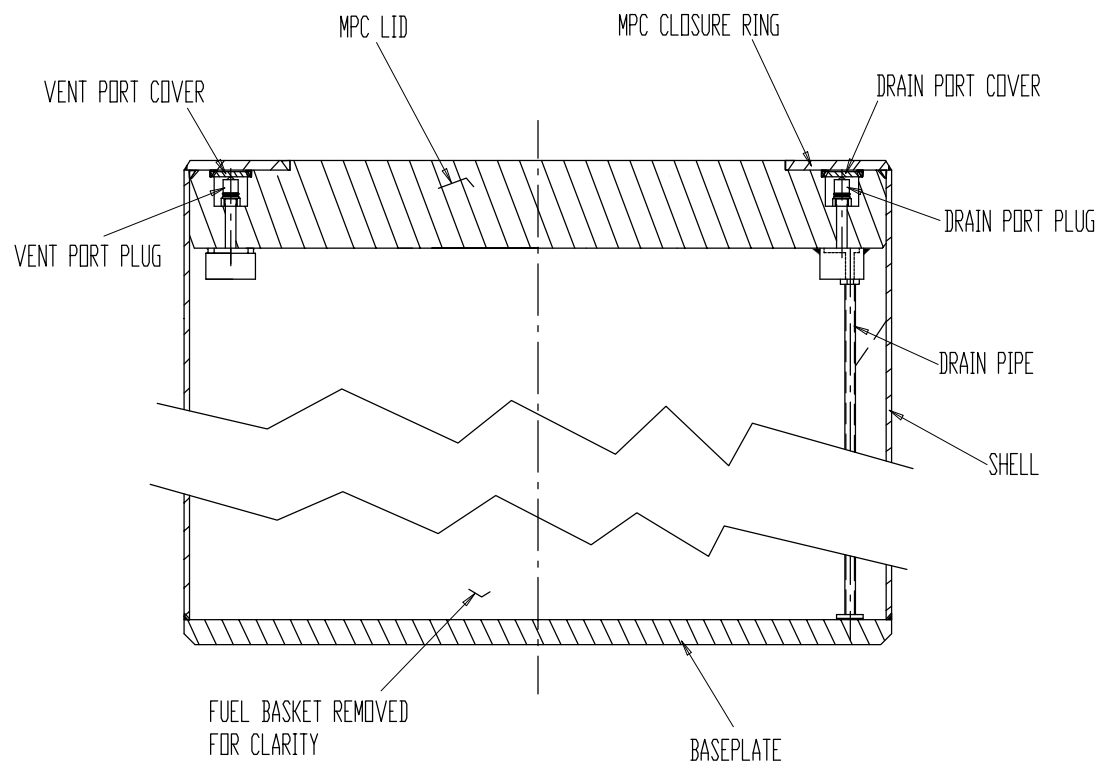
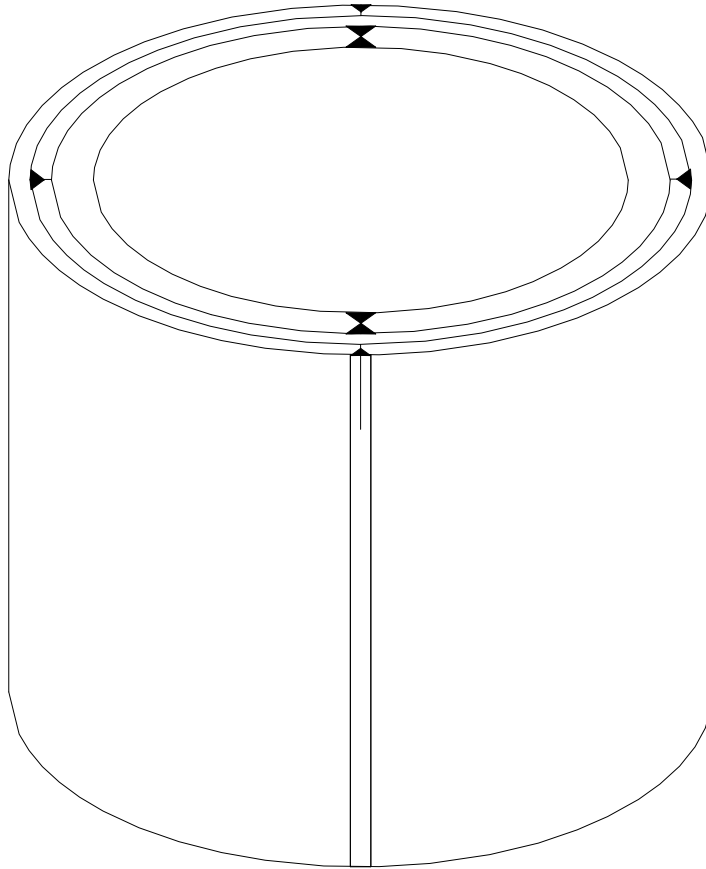


FIGURE 1.2.6; MPC LID AND PORT DETAILS

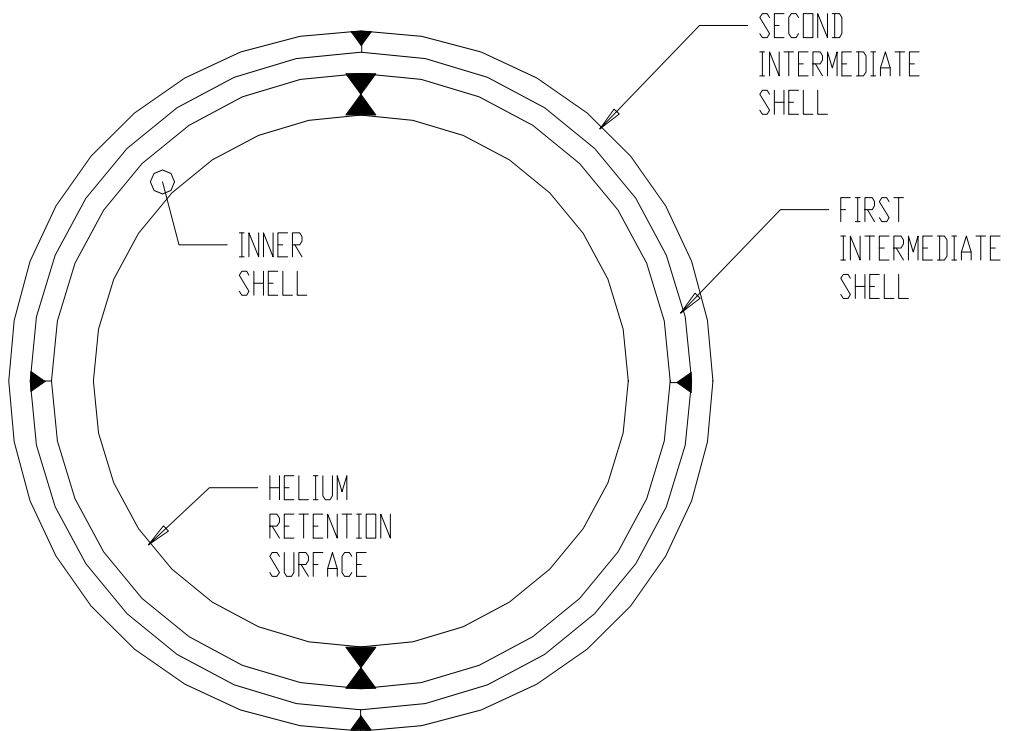
REPORT HI-951251

REV. 7

G:\SAR DOCUMENTS\HI-STAR SAR\FIGURES\REVISION 7\CHAPTER 1\FIG1\_2\_6



ISOMETRIC VIEW OF CENTRAL REGION OF THE OVERPACK



CROSS SECTION AT MID-HEIGHT

FIGURE 1.2.7; HI-STAR 100 OVERPACK SHELL LAYERING

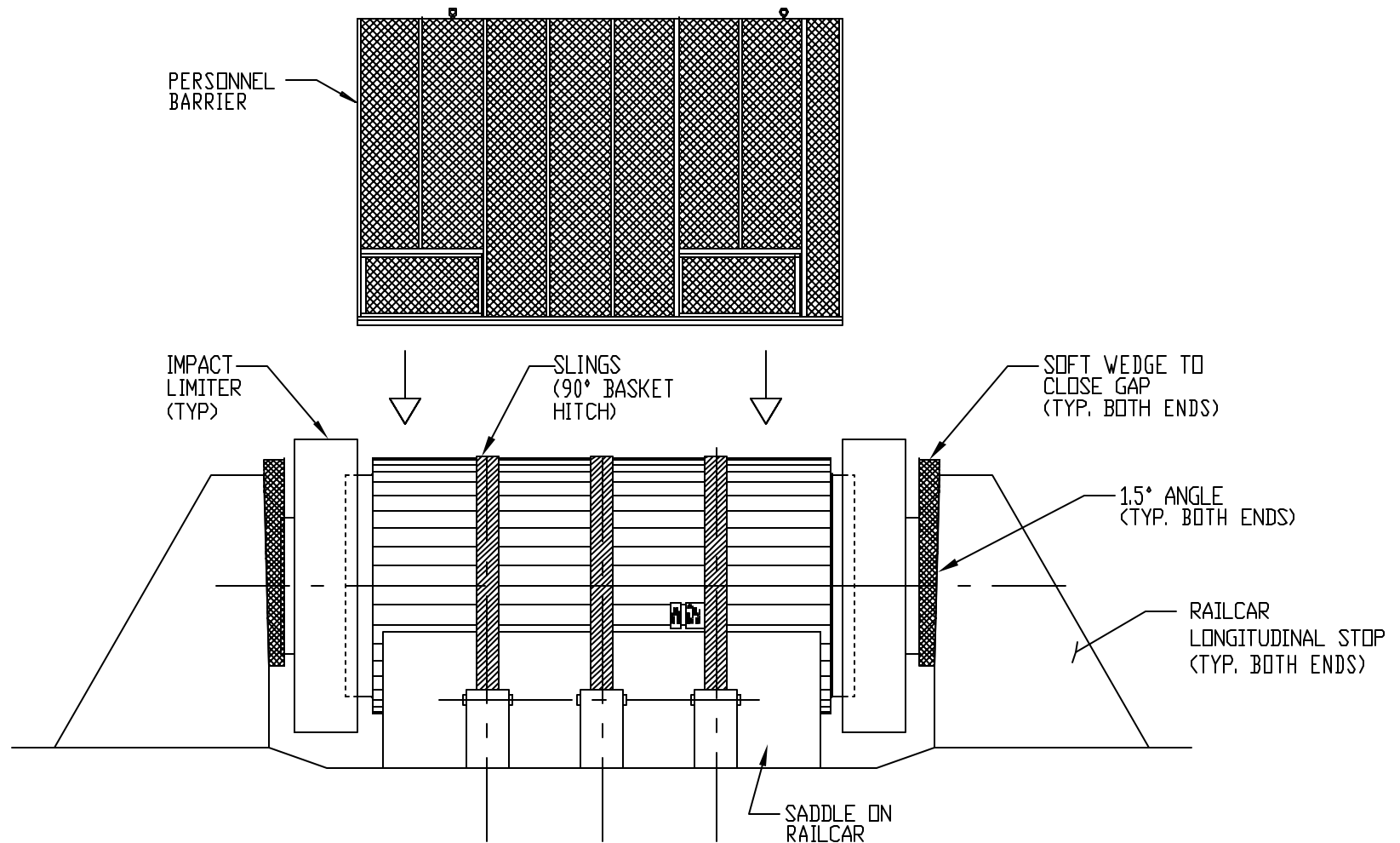
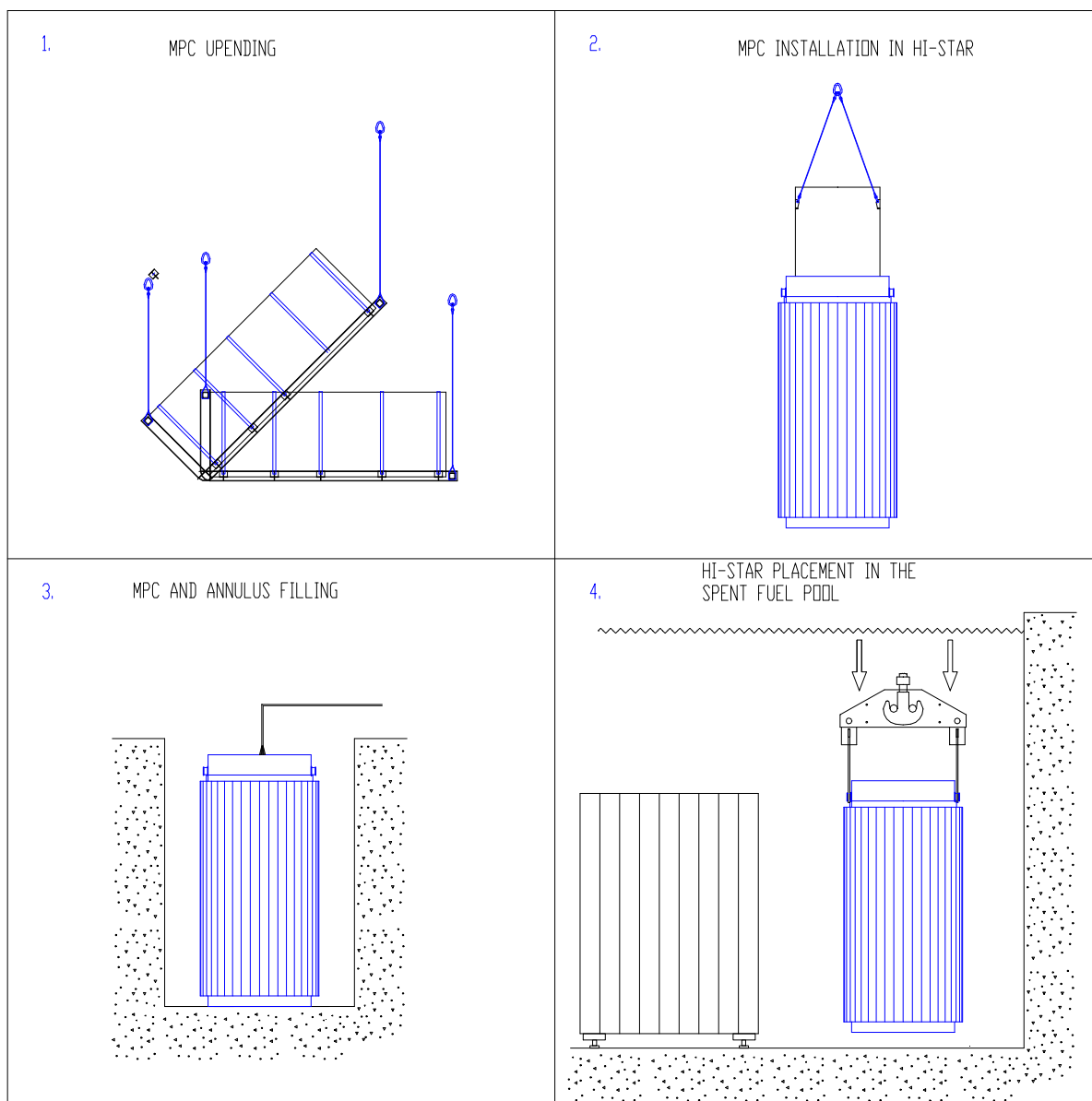
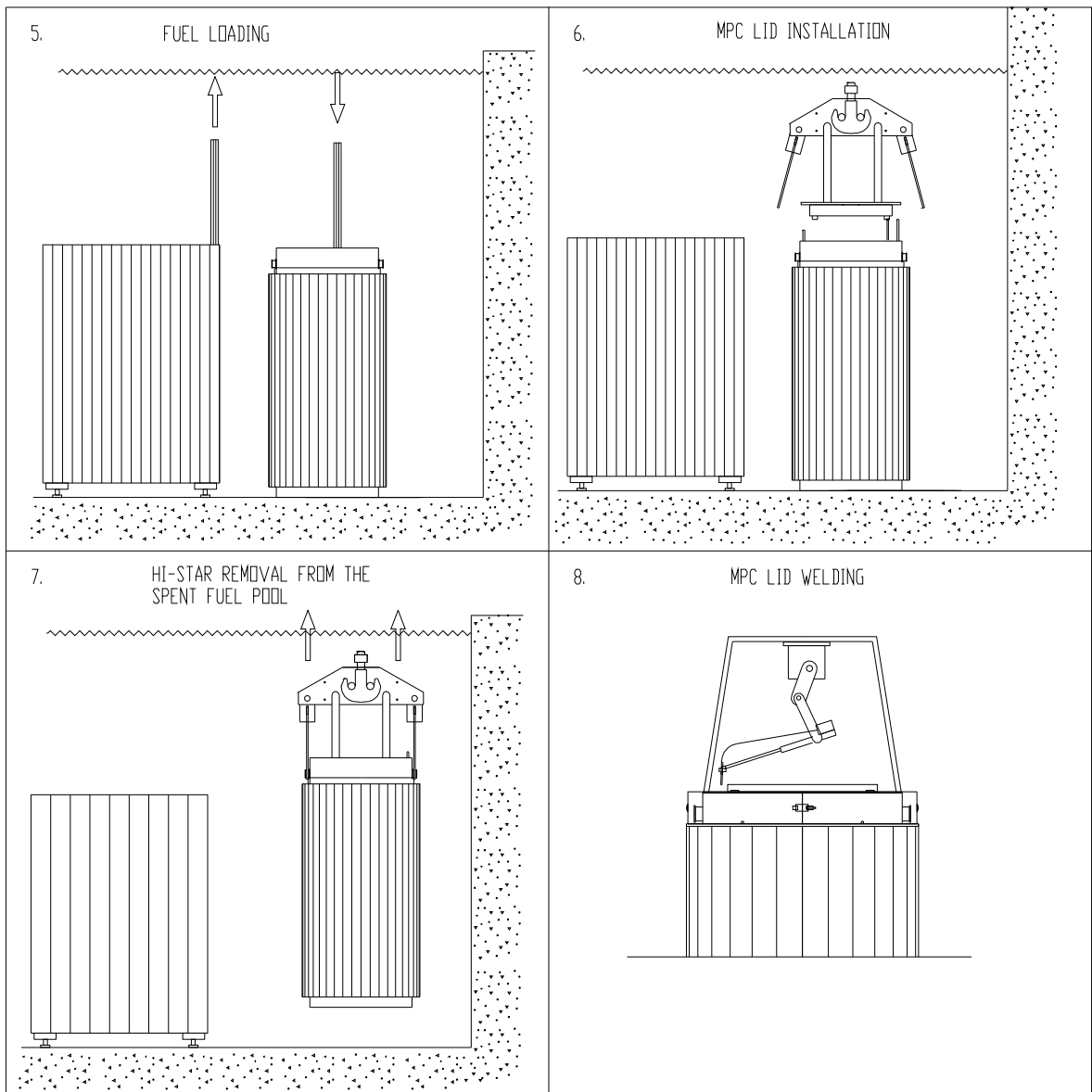


FIGURE 1.2.8; HI-STAR 100 TRANSPORT CONFIGURATION



**Figure 1.2.9; Major HI-STAR 100 Loading Operations (Sheet 1 of 3)**



**Figure 1.2.9; Major HI-STAR 100 Loading Operations (Sheet 2 of 3)**



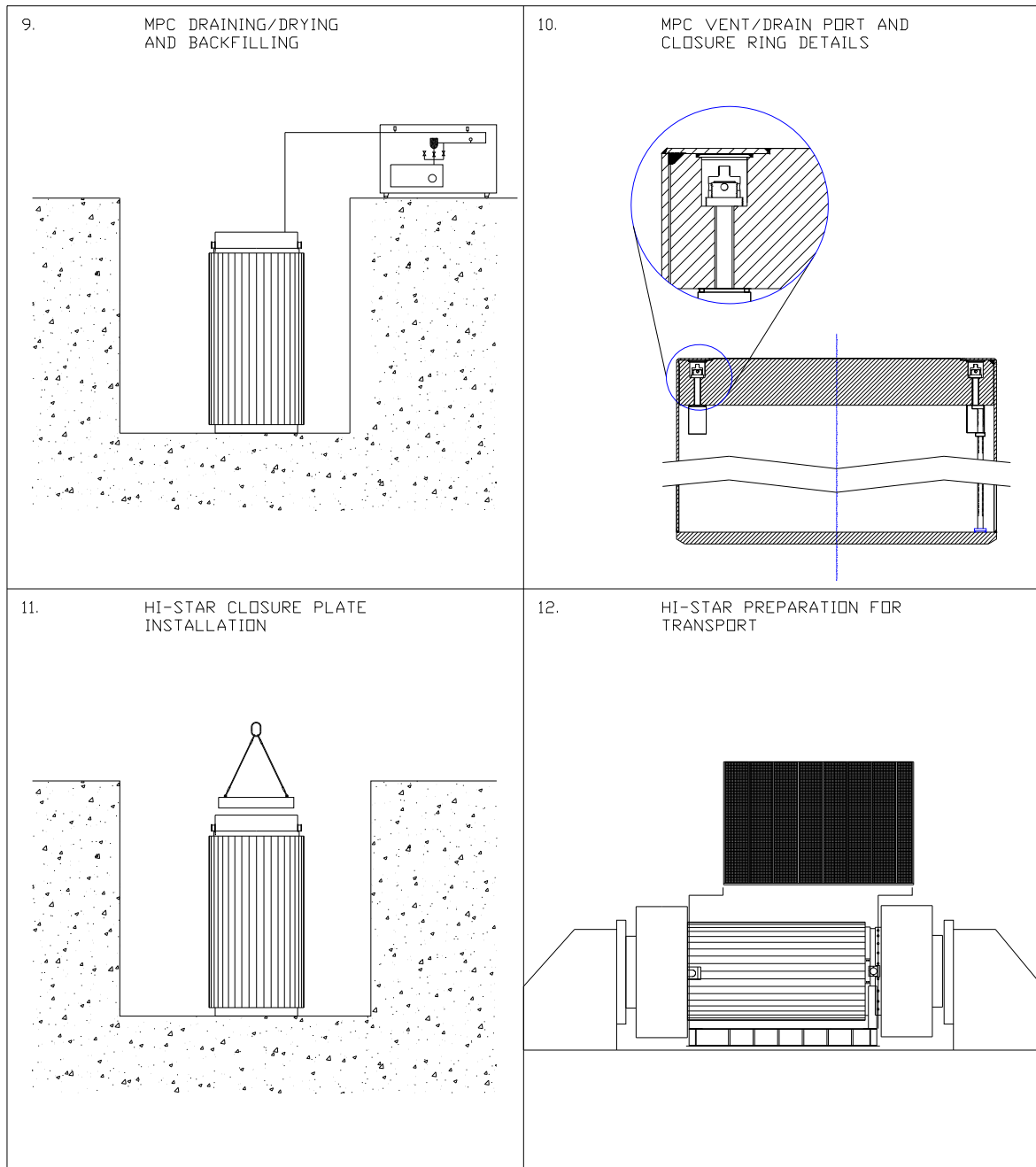


**Figure 1.2.9; Major HI-STAR 100 Loading Operations (Sheet 3 of 3)**

# Security-Related Information Figure Withheld Under 10 CFR 2.390.

REPORT HI-951251

G:\SAR DOCUMENTS\HI-STAR SAR\FIGURES\REVISION 10\CHAPTER1\FIG1\_2\_10R10

REV. 13

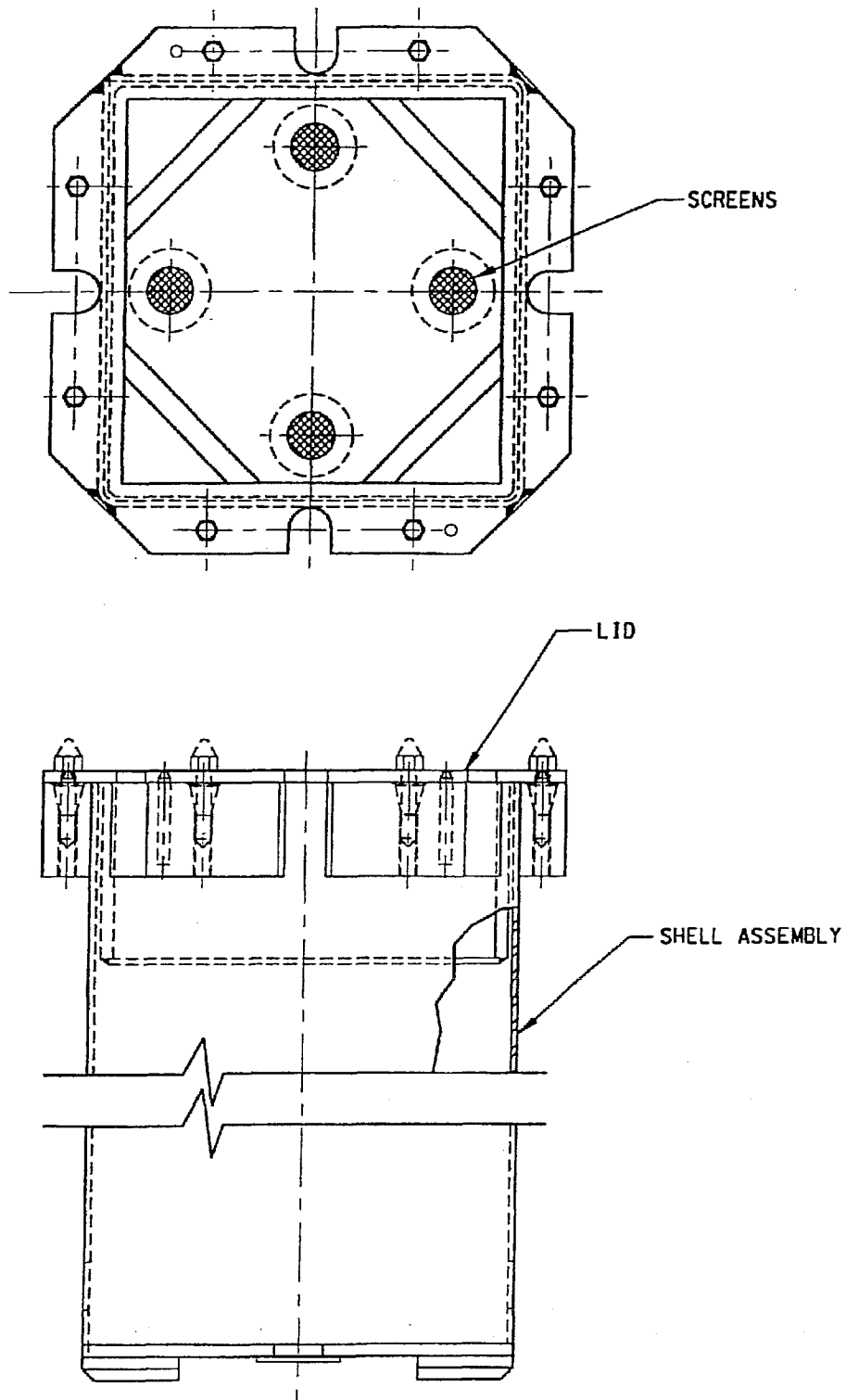


FIGURE 1.2.10A; TROJAN FAILED FUEL CAN

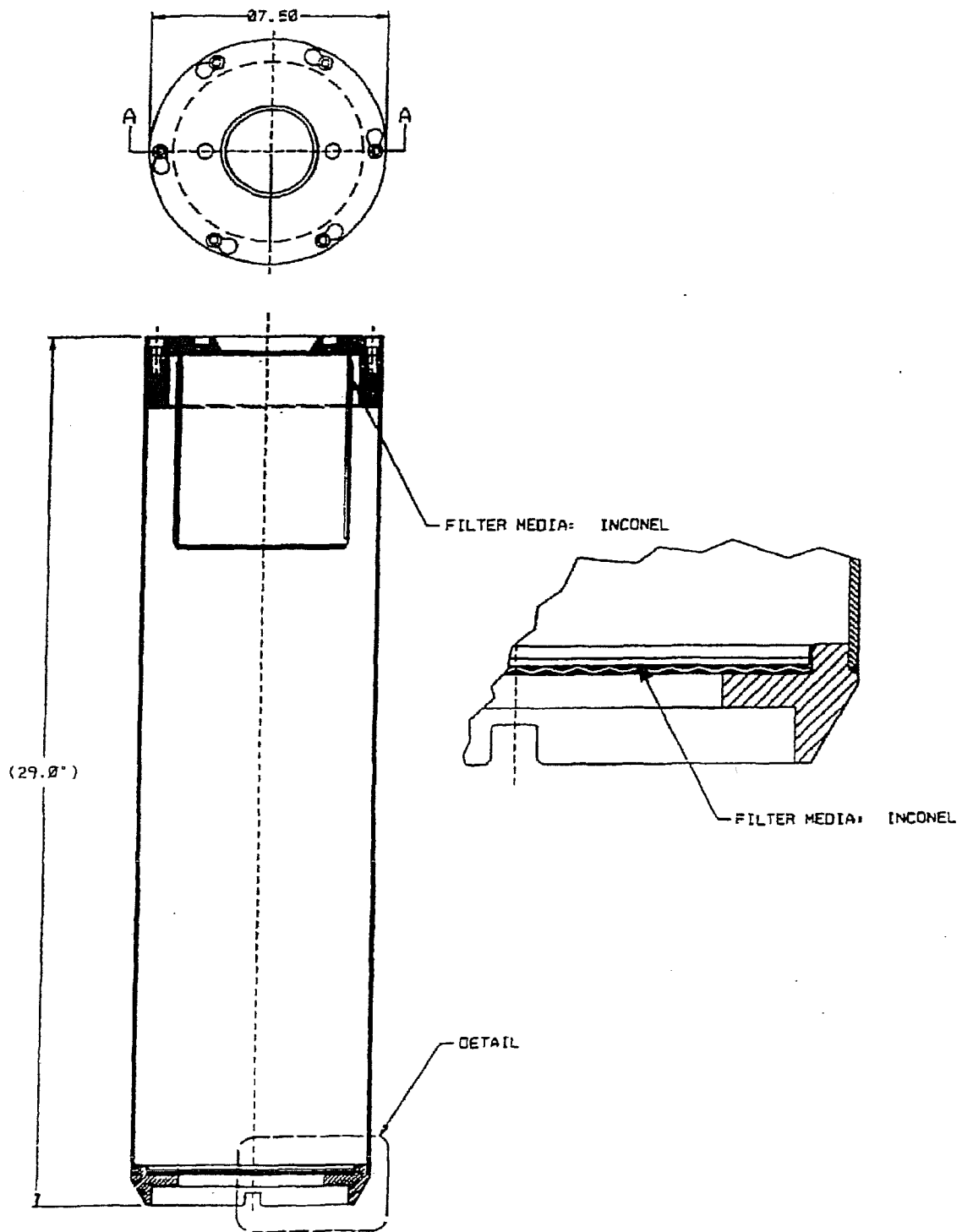


FIGURE 1.2.10B; TROJAN FUEL DEBRIS PROCESS CAN

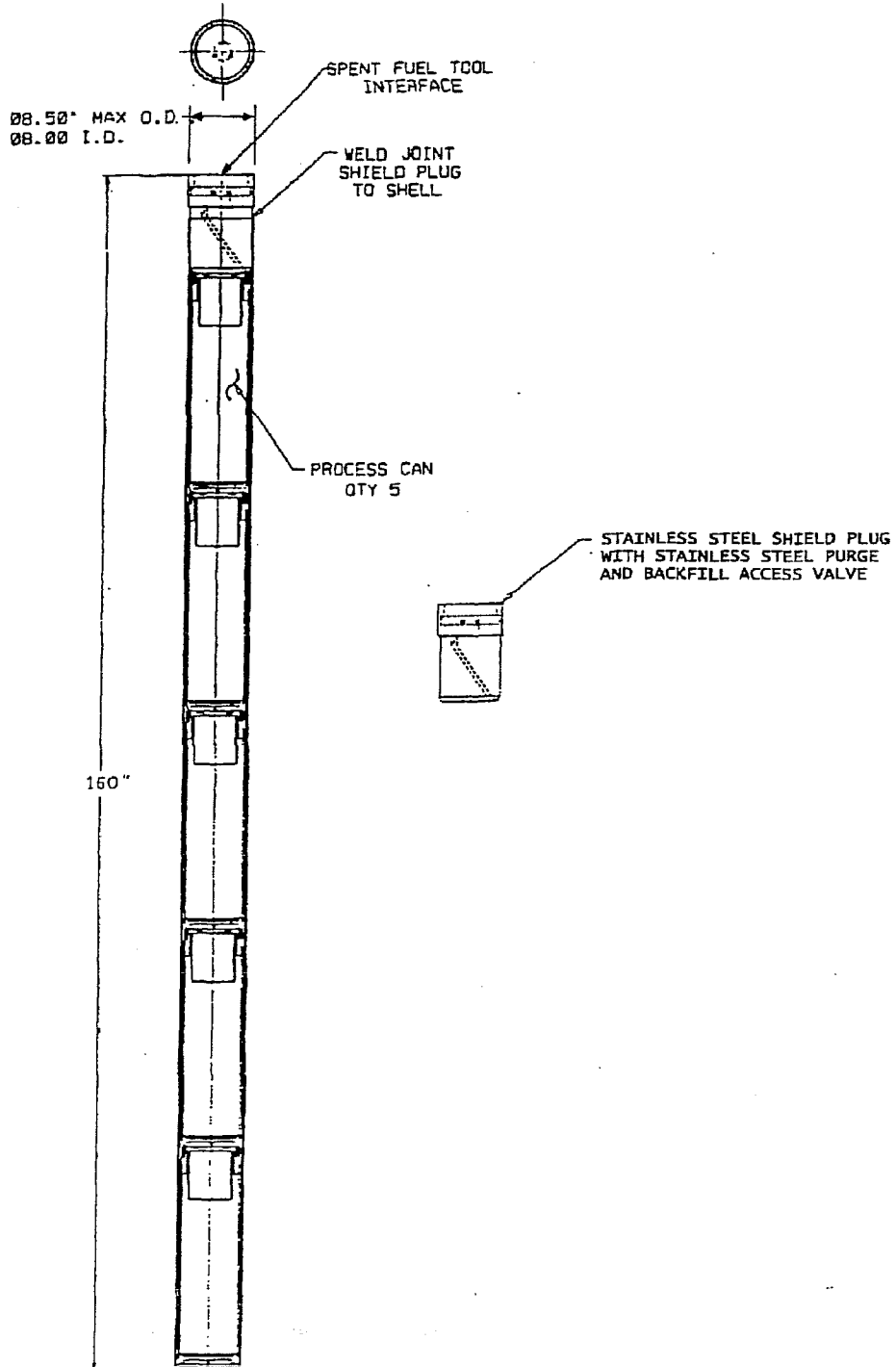


FIGURE 1.2.10C; TROJAN FUEL DEBRIS PROCESS CAN CAPSULE

REPORT HI-951251

G:\SAR DOCUMENT\HI STAR SAR\FIGURES\AMENDMENT REQUEST\9261-2\CHAPTER1\1\_2\_10C

REV.10

# Security-Related Information Figure Withheld Under 10 CFR 2.390.

FIGURE 1.2.10D; HOLTEC DAMAGED FUEL CONTAINER  
FOR TROJAN PLANT SNF IN MPC-24E/24EF

# Security-Related Information Figure Withheld Under 10 CFR 2.390.

FIGURE 1.2.11: TN DAMAGED FUEL CANISTER FOR DRESDEN UNIT-1

REVISION 16

REVISION 16

REVISION 16: TN DAMAGED FUEL CANISTER FOR DRESDEN UNIT-1

# Security-Related Information Figure Withheld Under 10 CFR 2.390.



FIGURE 1.2.12  
INTENTIONALLY DELETED

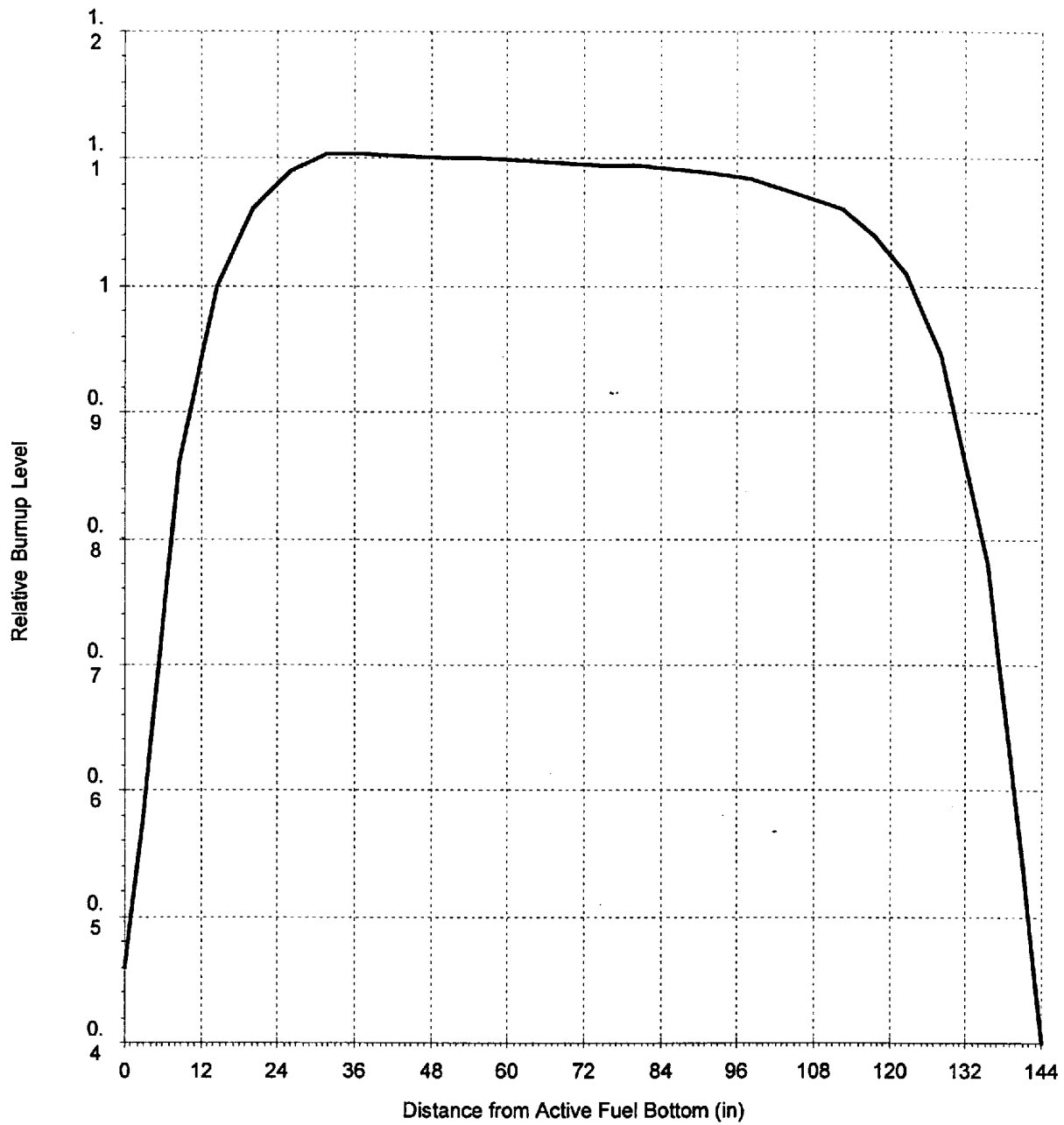


Figure 1.2.13A; Trojan Plant Fuel Axial Burnup Distribution Profile

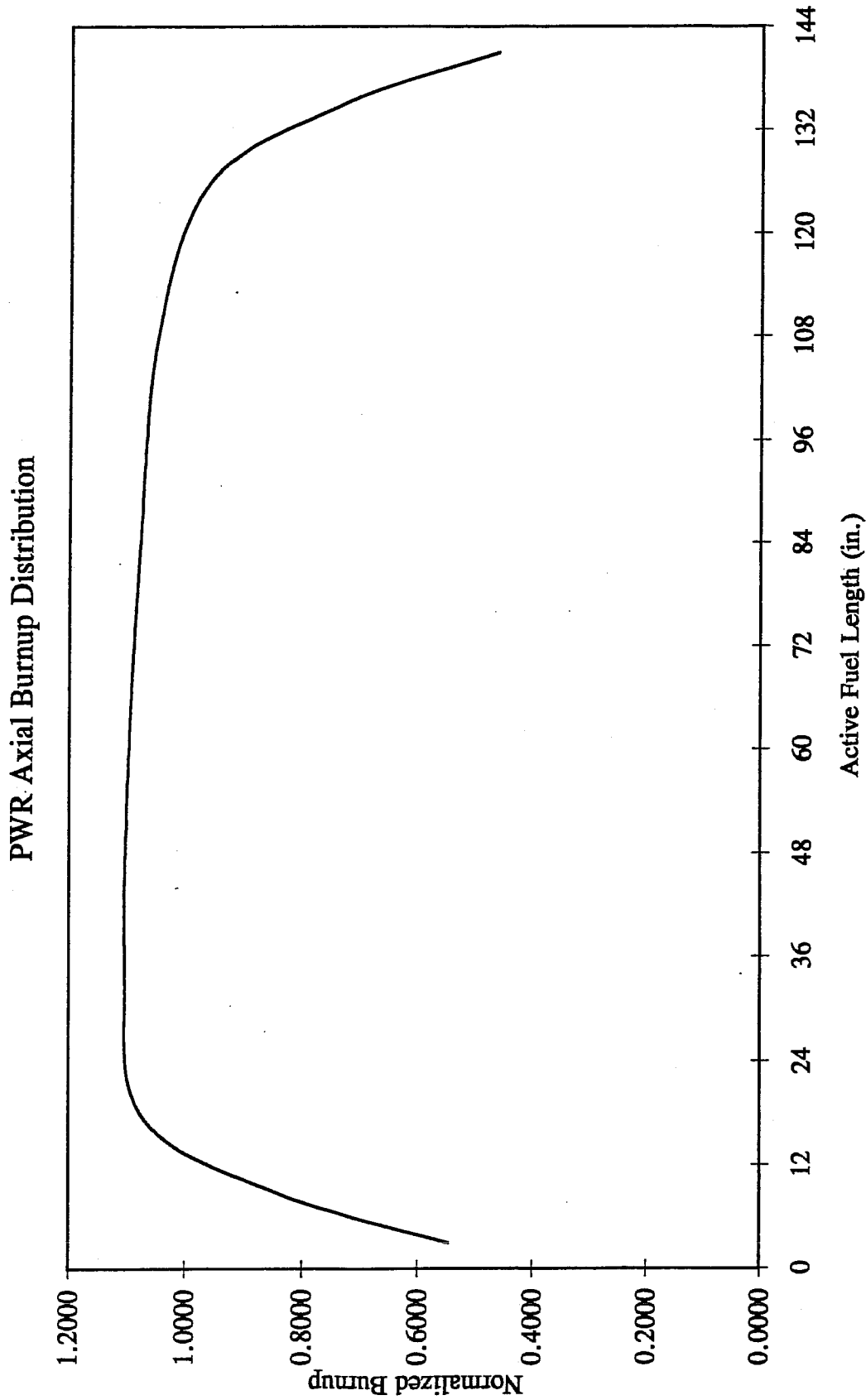


Figure 1.2.13; PWR Axial Burnup Profile with Normalized Distribution

BWR Axial Burnup Distribution

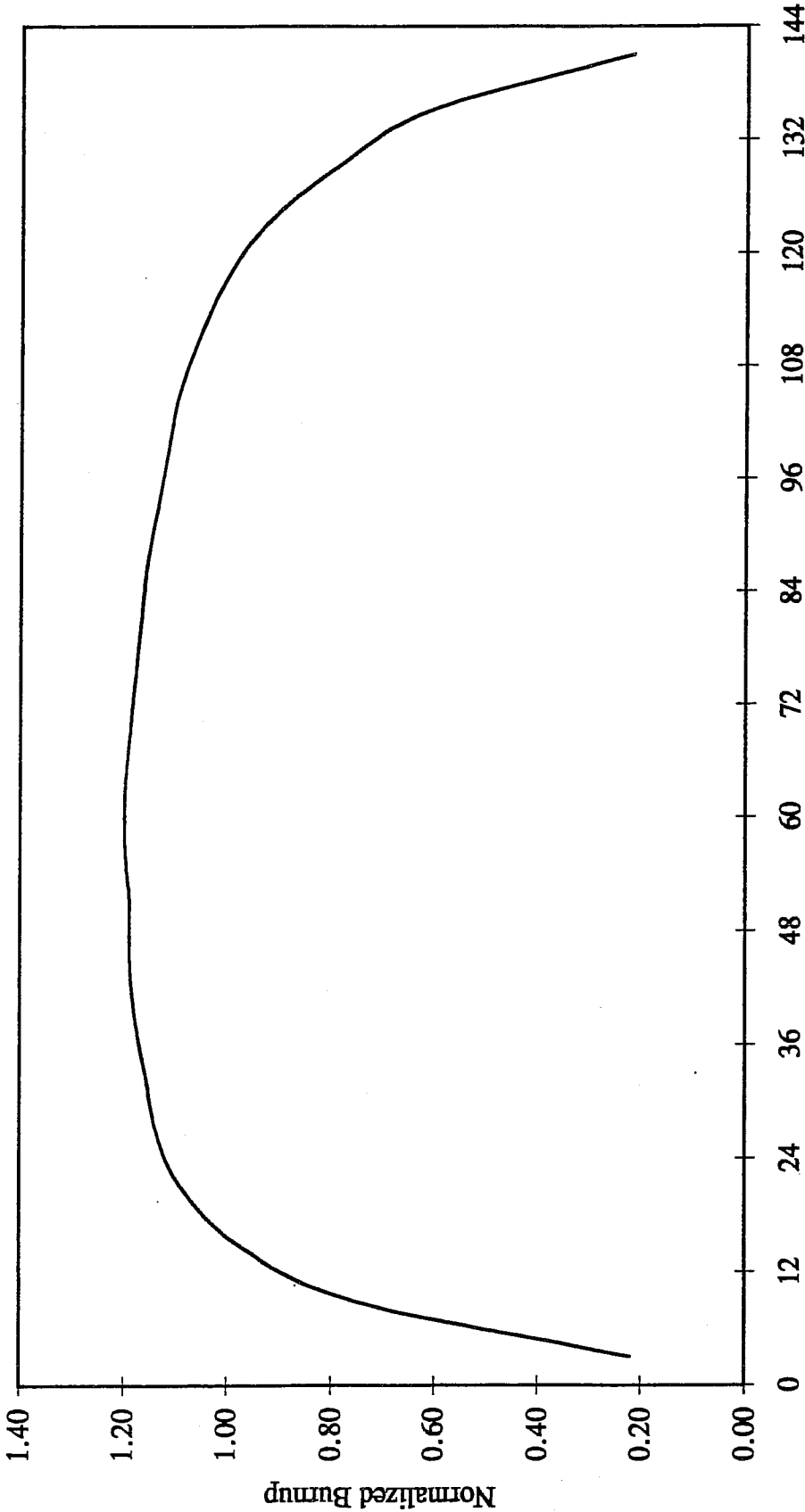


Figure 1.2.14; BWR Axial Burnup Profile with Normalized Distribution

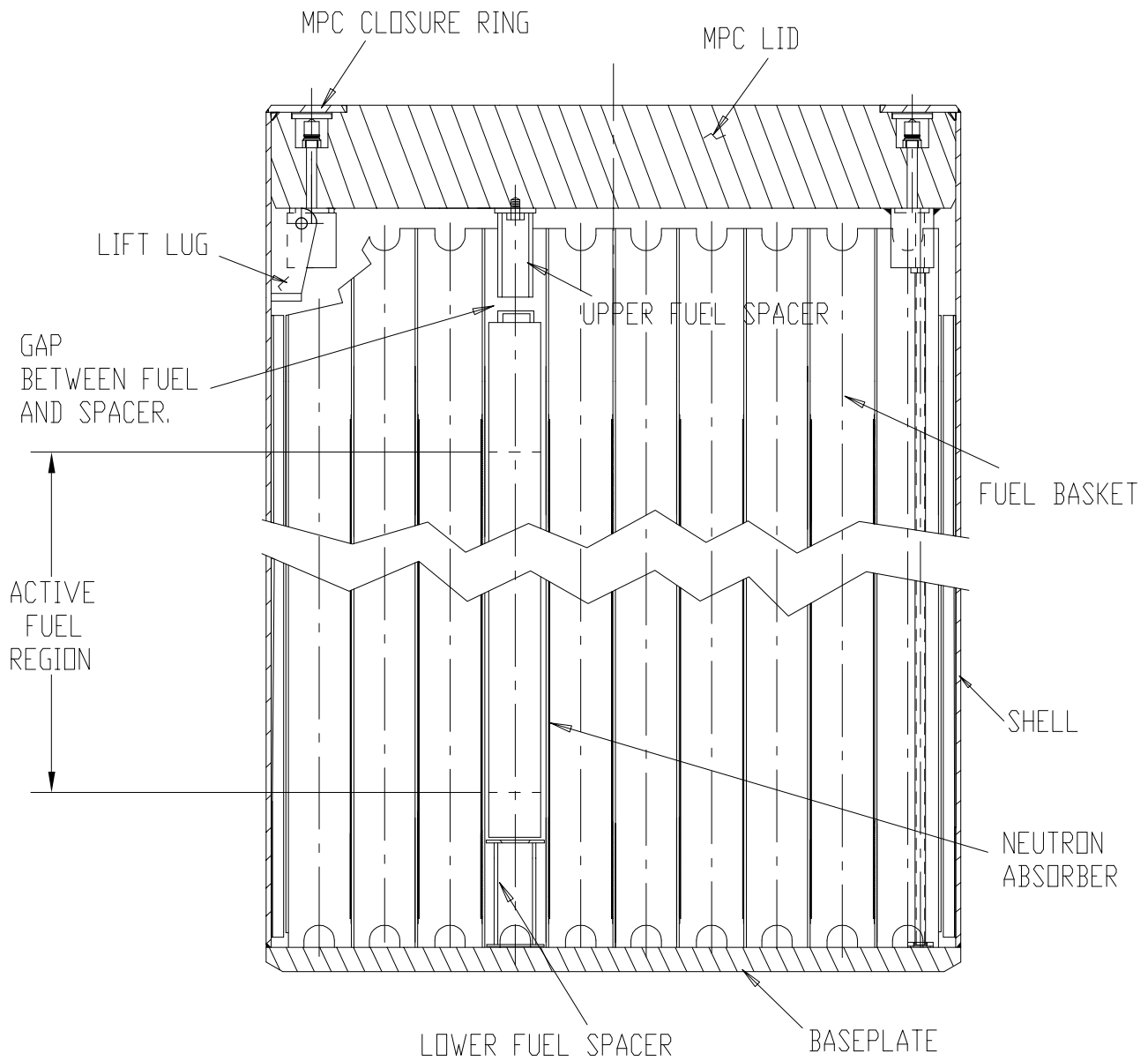
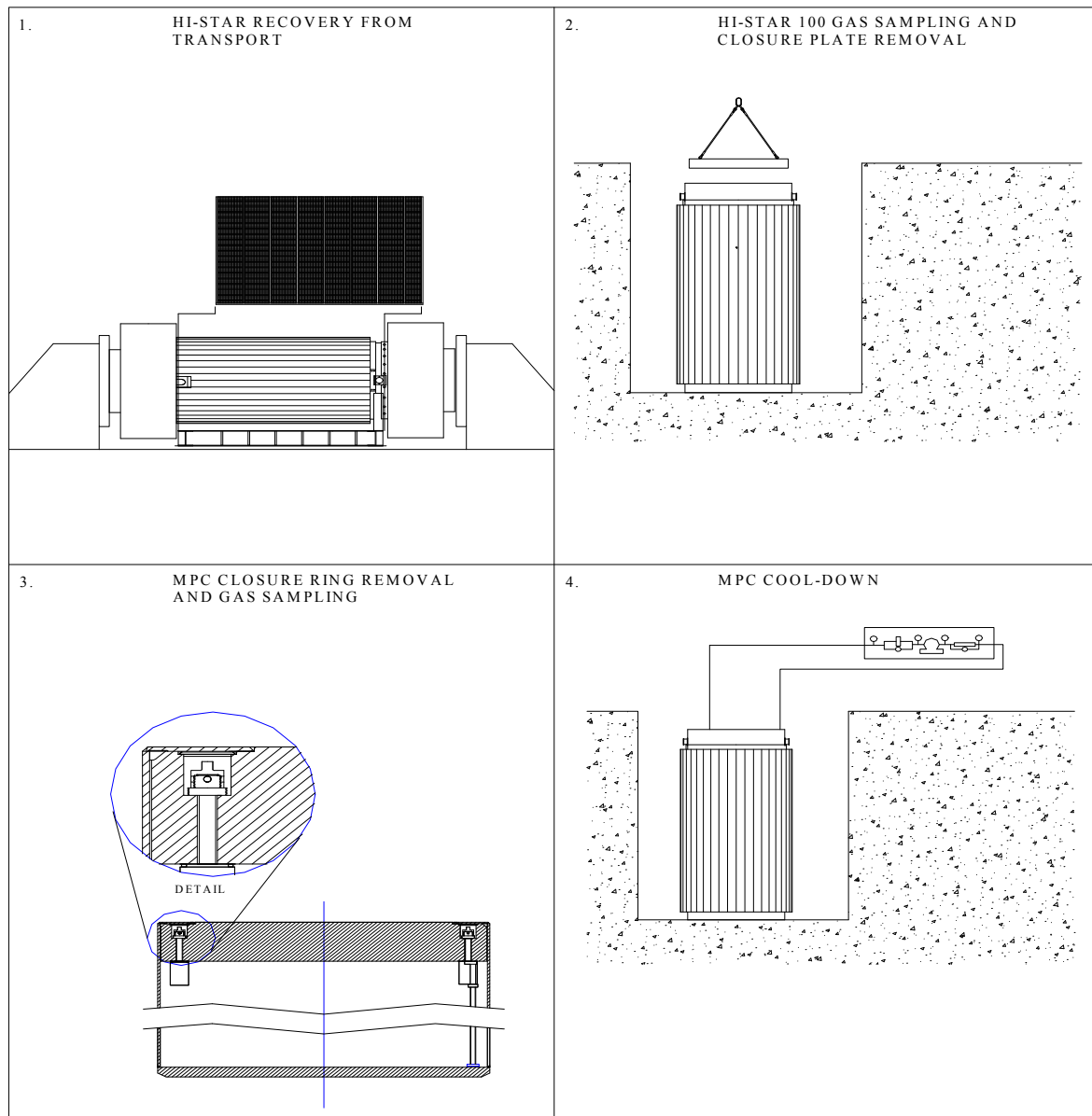
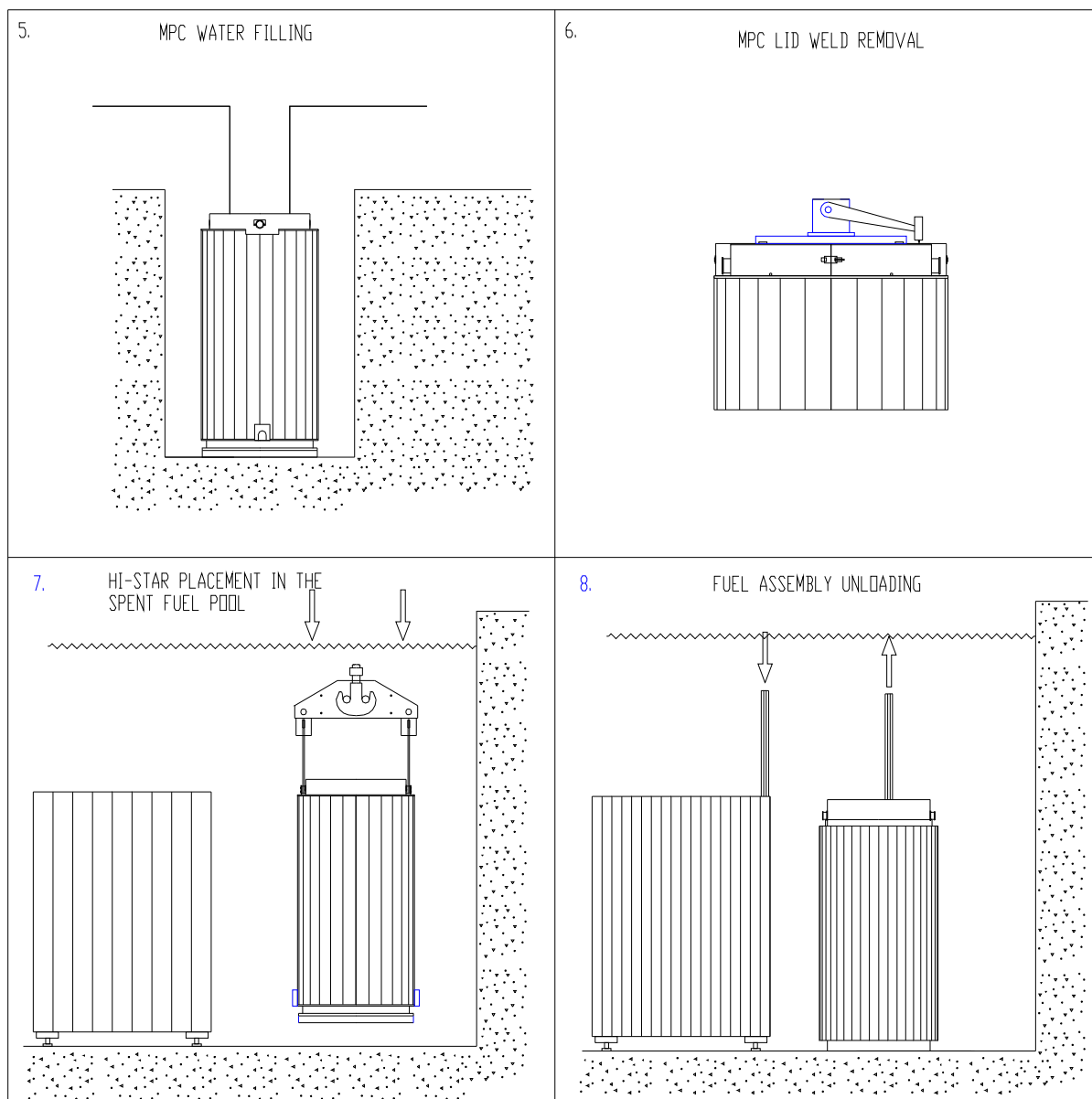


FIGURE 1.2.15; HI-STAR 100 MPC WITH UPPER AND LOWER FUEL SPACERS



**Figure 1.2.16; Major HI-STAR 100 Unloading Operations (Sheet 1 of 3)**



**Figure 1.2.16; Major HI-STAR 100 Unloading Operations (Sheet 2 of 3)**

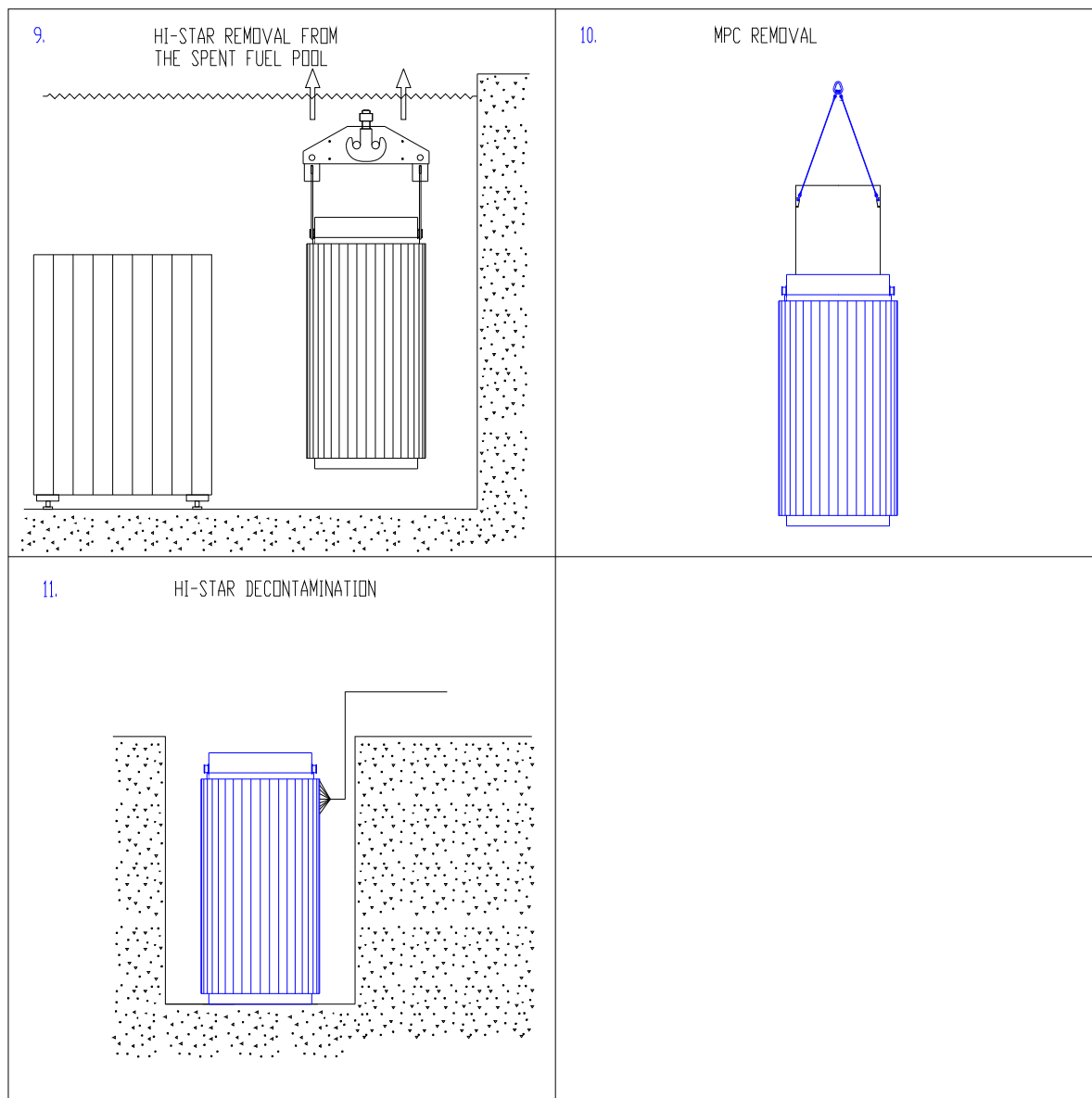
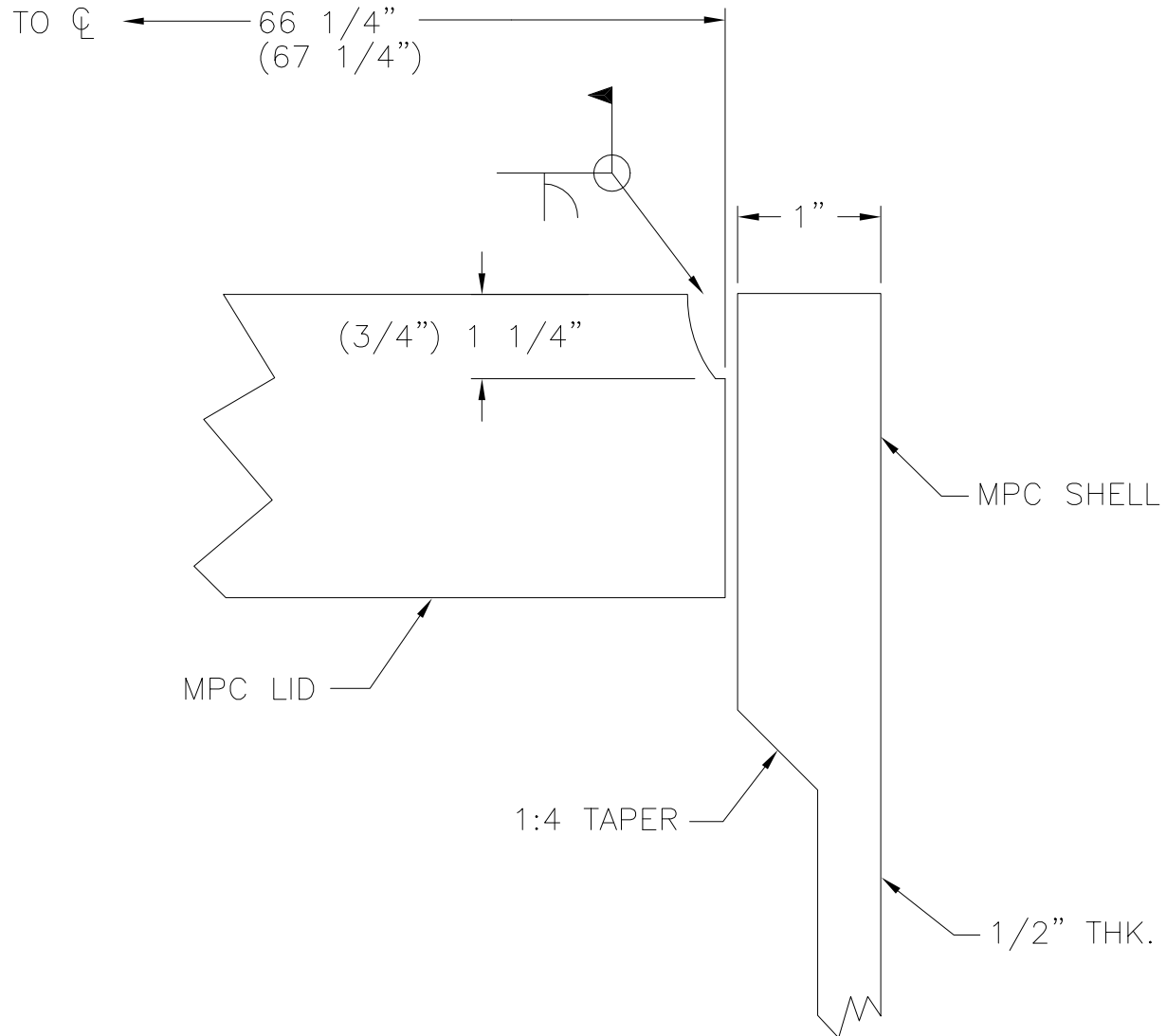


**Figure 1.2.16; Major HI-STAR 100 Unloading Operations (Sheet 3 of 3)**





- NOTES:
1. Standard MPC dimensions in parentheses.
  2. Standard MPC shell thickness is 1/2" along its entire length.
  3. Figure is not to scale.
  4. All dimensions are nominal.

Figure 1.2.17; Fuel Debris MPC ("F" Model)

Figure 1.2.18

INTENTIONALLY DELETED

### 1.3 DESIGN CODE APPLICABILITY

The ASME Boiler and Pressure Vessel Code (ASME Code), 1995 Edition with Addenda through 1997 [1.3.1], is the governing code for the construction of the HI-STAR 100 System, as clarified in Table 8.1.5. The ASME Code is applied to each component consistent with the function of the component. Table 1.3.3 lists each structure, system and component (SSC) of the HI-STAR 100 System that are labeled Important to Safety (ITS), along with its function and governing Code. Some components perform multiple functions and in those cases, the most restrictive Code is applied. In accordance with NUREG/CR-6407, "Classification of Transportation Packaging and Dry Spent Fuel Storage System Components" [1.3.2] and according to importance to safety, the components of the HI-STAR 100 System shall be classified as A, B, C, or NITS (not important to safety). Table 1.3.3 of this SAR lists the component classification as ITS or NITS. The detailed classification according to NUREG/CR-6407 is documented in a lower tier document. Table 1.3.3 may not include all NITS items associated with the HI-STAR 100 Package.

Table 8.1.4 lists the applicable ASME Code and other standards for material procurement, design, fabrication and inspection of the components of the HI-STAR 100 System that are governed by the ASME Code. The ASME Code section listed in the design column is the section used to define allowable stresses for structural analyses.

Table 8.1.5 lists the alternatives to the ASME Code for the HI-STAR 100 System and the justification for those alternatives.

The MPC is classified as important to safety. The MPC structural components include the internal fuel basket and the enclosure vessel. The fuel basket is designed and fabricated as a core support structure, in accordance with the applicable requirements of Section III, Subsection NG of the ASME Code, with certain NRC-approved alternatives, as discussed in Table 8.1.5. The enclosure vessel is designed and fabricated as a Class 1 component pressure vessel in accordance with Section III, Subsection NB of the ASME Code, with certain NRC-approved alternatives, as discussed in Table 8.1.5. The principal exceptions are the MPC lid, vent and drain cover plates, and closure ring welds to the MPC lid and shell, as discussed in Table 8.1.5. In addition, the threaded holes in the MPC lid are designed in accordance with the requirements of NUREG-0612 and Regulatory Guide 3.61 to facilitate vertical MPC transfer.

The MPC closure welds are partial penetration welds that are structurally qualified by analysis, as presented in Chapter 2. The MPC closure ring welds are inspected by performing a liquid penetrant examination of the root pass (if more than one weld pass is required) and final weld surface, in accordance with the requirements contained in Section 8.1. The MPC lid weld may be examined by either volumetric or multi-layer liquid penetrant examination. If volumetric examination is used, it shall be the ultrasonic method and shall include a liquid penetrant examination of the root and final weld layers. If multi-layer liquid penetrant examination is used alone, at a minimum, it must include the root and final weld layers and each approximately 3/8 inch of weld to detect critical weld flaws. The integrity of the MPC lid weld is further verified by performing a pressure test (hydrostatic or pneumatic) in accordance with the requirements contained in Section 8.1.

The structural analysis of the MPC, in conjunction with the redundant closures and nondestructive examination, and pressure testing performed during MPC fabrication and MPC closure, provides assurance of canister closure integrity in lieu of the specific weld joint requirements of the ASME Code, Section III, Subsection NB.

The HI-STAR overpack is classified as important to safety. The HI-STAR overpack top flange, closure plate, inner shell, and bottom plate are designed and fabricated in accordance with the requirements of ASME Code, Section III, Subsection NB, to the maximum extent practical (see Table 8.1.5). The remainder of the HI-STAR overpack steel structure is designed and fabricated in accordance with the requirements of ASME Code, Section III, Subsection NF, to the maximum extent practical (see Table 8.1.5).

Table 1.3.1

HI-STAR 100 ASME BOILER AND PRESSURE VESSEL CODE APPLICABILITY

Note: This table has been superseded by Table 8.1.4

Table 1.3.2

LIST OF ASME CODE ALTERNATIVES FOR HI-STAR 100 SYSTEM

Note: This table has been superseded by Table 8.1.5

Table 1.3.3

## MATERIALS AND COMPONENTS OF THE HI-STAR 100 SYSTEM

OVERPACK <sup>(1, 2)</sup>

Primary Function	Component <sup>(3)</sup>	Safety Class <sup>(4)</sup>	Codes/Standards (as applicable to component)	Material	Strength (ksi)	Special Surface Finish/Coating	Contact Matl. (if dissimilar)
Containment	Inner Shell	ITS	ASME Section III; Subsection NB	SA203-E or SA350-LF3	Table 2.3.4	Paint inside surface with Thermaline 450 (Note 5). External surface to be coated with a surface preservative.	NA
Containment	Bottom Plate	ITS	ASME Section III; Subsection NB	SA350-LF3	Table 2.3.4	Paint inside surface with Thermaline 450 (Note 5).	NA
Containment	Top Flange	ITS	ASME Section III; Subsection NB	SA350-LF3	Table 2.3.4	Paint inside surface with Thermaline 450. Paint outside surface with Carboline 890 (Note 5).	NA
Containment	Closure Plate	ITS	ASME Section III; Subsection NB	SA350-LF3	Table 2.3.4	Paint inside surface with Thermaline 450. Paint outside surface with Carboline 890 (Note 5).	NA
Containment	Closure Plate Bolts	ITS	ASME Section III; Subsection NB	SB637-N07718	Table 2.3.5	NA	NA
Containment	Port Plug	ITS	Non-code	SA193-B8	Not required	NA	NA
Containment	Port Plug Seal	ITS	Non-code	Alloy X750	Not required	NA	NA
Containment	Closure Plate Seal	ITS	Non-code	Alloy X750	Not required	NA	NA
Containment	Port Cover Seal	ITS	Non-code	Alloy X750	Not required	NA	NA

Notes: 1) There are no known residuals on finished component surfaces.

2) All welding processes used in welding the components shall be qualified in accordance with the requirements of ASME Section IX. All welds shall be made using welders qualified in accordance with ASME Section IX. Weld material shall meet the requirements of ASME Section II and the applicable Subsection of ASME Section III. For parts beyond the purview of ASME Section III, compliance with Section IX and Section II of the Code shall be observed to the extent practicable.

3) Component nomenclature taken from drawings in Chapter 1.

4) A, B and C safety classifications as described in NUREG/CR-6407 are provided in written procedures. NITS stands for Not Important To Safety.

5) Thermaline 450 and Carboline 890 were the product names at the time of initial licensing. Chemically identical products with different names are permitted. For example, Carboline 890 was re-named Carboguard 890 in 2000, with no change to the coating material and is, therefore, acceptable for use where Carboline 890 is specified.

TABLE 1.3.3 (continued)

## MATERIALS AND COMPONENTS OF THE HI-STAR 100 SYSTEM

OVERPACK <sup>(1,2)</sup>

Primary Function	Component <sup>(3)</sup>	Safety Class <sup>(4)</sup>	Codes/Standards (as applicable to component)	Material	Strength (ksi)	Special Surface Finish/Coating	Contact Matl. (if dissimilar)
Shielding	Intermediate Shells	ITS	ASME Section III; Subsection NF per Table 8.1.4	SA516-70	Table 2.3.2	Internal surfaces to be coated with a silicone encapsulant (Dow-Corning SYLGARD 567 or equivalent) for surface preservation, except for HI-STAR HB. Exposed areas of fifth intermediate shell to be painted with Carboline 890 (Note 5).	NA
Shielding	Neutron Shield	ITS	Non-code per Table 8.1.4	Holtite-A	Not required	NA	Holtite/CS
Shielding	Plugs for Drilled Holes	NITS	Non-code	SA193-B7	Not required	NA	NA
Shielding	Removable Shear Ring	ITS	ASME Section III; Subsection NF	Carbon Steel	Not required	Paint external surface with Carboline 890 (Note 5).	NA
Shielding	Pocket Trunnion Plug Plate	ITS	Non-code	SA240-304	Not required	NA	NA
Heat Transfer	Radial Channels (not used on the HI-STAR HB)	ITS	ASME Section III; Subsection NF per Table 8.1.4	SA515-70 or SA516-70	Table 2.3.3	Paint outside surface with Carboline 890 (Note 5).	NA

Notes: 1) There are no known residuals on finished component surfaces.

2) All welding processes used in welding the components shall be qualified in accordance with the requirements of ASME Section IX. All welds shall be made using welders qualified in accordance with ASME Section IX. Weld material shall meet the requirements of ASME Section II and the applicable Subsection of ASME Section III. For parts beyond the purview of ASME Section III, compliance with Section IX and Section II of the Code shall be observed to the extent practicable.

3) Component nomenclature taken from drawings in Chapter 1.

4) A, B and C safety classifications as described in NUREG/CR-6407 are provided in written procedures. NITS stands for Not Important To Safety.

5) Thermaline 450 and Carboline 890 were the product names at the time of initial licensing. Chemically identical products with different names are permitted. For example, Carboline 890 was re-named Carboguard 890 in 2000, with no change to the coating material and is, therefore, acceptable for use where Carboline 890 is specified.



TABLE 1.3.3 (continued)

## MATERIALS AND COMPONENTS OF THE HI-STAR 100 SYSTEM

OVERPACK <sup>(1,2)</sup>

Primary Function	Component <sup>(3)</sup>	Safety Class <sup>(4)</sup>	Codes/Standards (as applicable to component)	Material	Strength (ksi)	Special Surface Finish/Coating	Contact Matl. (if dissimilar)
Rotation Pivot and Shielding	Pocket Trunnion	ITS	Non-Code	SA705-630 17-4 PH or SA564-630 17-4 PH	Table 2.3.5	NA	NA
Structural Integrity	Lifting Trunnion	ITS	NUREG 0612 and RG 3.61 per Table 8.1.4	SB637- N07718	Table 2.3.5	NA	NA
Structural Integrity	Relief Device	ITS	Non-code	Commercial	Not required	NA	Brass-C/S
Structural Integrity	Relief Device Plate	ITS	Non-code	SA 516 Grade 70 or A569	Not required	NA	NA
Structural Integrity	Removable Shear Ring Bolt	ITS	Non-code	SA193-B7	Not required	NA	NA
Structural Integrity	Thermal Expansion Foam	NITS	Non-code	Silicone Foam	Not required	NA	Silicone with CS, brass, and Holtite
Structural Integrity	Closure Bolt Washer	NITS	Non-code	ASTM A564, 17-7 PH	Not required	NA	NA

Notes: 1) There are no known residuals on finished component surfaces.

2) All welding processes used in welding the components shall be qualified in accordance with the requirements of ASME Section IX. All welds shall be made using welders qualified in accordance with ASME Section IX. Weld material shall meet the requirements of ASME Section II and the applicable Subsection of ASME Section III. For parts beyond the purview of ASME Section III, compliance with Section IX and Section II of the Code shall be observed to the extent practicable.

3) Component nomenclature taken from drawings in Chapter 1.

4) A, B and C safety classifications as described in NUREG/CR-6407 are provided in written procedures. NITS stands for Not Important To Safety.

5) Thermaline 450 and Carboline 890 were the product names at the time of initial licensing. Chemically identical products with different names are permitted. For example, Carboline 890 was re-named Carboguard 890 in 2000, with no change to the coating material and is, therefore, acceptable for use where Carboline 890 is specified.

TABLE 1.3.3 (continued)

## MATERIALS AND COMPONENTS OF THE HI-STAR 100 SYSTEM

OVERPACK <sup>(1,2)</sup>

Primary Function	Component <sup>(3)</sup>	Safety Class <sup>(4)</sup>	Codes/Standards (as applicable to component)	Material	Strength (ksi)	Special Surface Finish/Coating	Contact Matl. (if dissimilar)
Structural Integrity	Enclosure Shell Panels	ITS	ASME Section III; Subsection NF per Table 8.1.4	SA515-70 or SA516-70	Table 2.3.3	Paint outside surface with Carboline 890 (Note 5).	NA
Structural Integrity	Enclosure Shell Return	ITS	ASME Section III; Subsection NF per Table 8.1.4	SA515-70 or SA516-70	Table 2.3.3	Paint outside surface with Carboline 890 (Note 5).	NA
Structural Integrity	Port Cover	ITS	ASME Section III; Subsection NF	SA203E or SA350-LF3	Table 2.3.4	Paint outside surface with Carboline 890 (Note 5).	NA
Structural Integrity	Port Cover Bolt	ITS	Non-code	SA193-B7	Not required	NA	NA
Operations	Trunnion Locking Pad and End Cap Bolt	ITS	Non-code	SA193-B7	Not required	NA	NA
Operations	Lifting Trunnion End Cap	ITS	Non-code	SA516-70 or SA515 Gr. 70	Table 2.3.2	Paint exposed surfaces with Carboline 890 (Note 5).	NA
Operations	Lifting Trunnion Locking Pad	ITS	Non-code	SA516-70	Table 2.3.2	Paint exposed surfaces with Carboline 890 (Note 5).	NA
Operations	Nameplate	NITS	Non-code	S/S	Not required	NA	NA

Notes: 1) There are no known residuals on finished component surfaces.

2) All welding processes used in welding the components shall be qualified in accordance with the requirements of ASME Section IX. All welds shall be made using welders qualified in accordance with ASME Section IX. Weld material shall meet the requirements of ASME Section II and the applicable Subsection of ASME Section III. For parts beyond the purview of ASME Section III, compliance with Section IX and Section II of the Code shall be observed to the extent practicable.

3) Component nomenclature taken from drawings in Chapter 1.

4) A, B and C safety classifications as described in NUREG/CR-6407 are provided in written procedures. NITS stands for Not Important To Safety.

5) Thermaline 450 and Carboline 890 were the product names at the time of initial licensing. Chemically identical products with different names are permitted. For example, Carboline 890 was re-named Carboguard 890 in 2000, with no change to the coating material and is, therefore, acceptable for use where Carboline 890 is specified.

Table 1.3.3 (cont'd)

## MATERIALS AND COMPONENTS OF THE HI-STAR 100 SYSTEM

MPC <sup>(1, 2)</sup>

Primary Function	Component <sup>(3)</sup>	Safety Class <sup>(4)</sup>	Codes/Standards (as applicable to component)	Material	Strength (ksi)	Special Surface Finish/Coating	Contact Matl. (if dissimilar)
Helium Retention	Shell	ITS	ASME Section III; Subsection NB	Alloy X <sup>(5)</sup>	See Appendix 1.A	NA	NA
Helium Retention	Baseplate	ITS	ASME Section III; Subsection NB	Alloy X	See Appendix 1.A	NA	NA
Helium Retention	Lid (One-piece design and top portion of optional two-piece design)	ITS	ASME Section III; Subsection NB	Alloy X	See Appendix 1.A	NA	NA
Helium Retention	Closure Ring	ITS	ASME Section III; Subsection NB	Alloy X	See Appendix 1.A	NA	NA
Helium Retention	Port Cover Plates	ITS	ASME Section III; Subsection NB	Alloy X	See Appendix 1.A	NA	NA
Criticality Control	Basket Cell Plates	ITS	ASME Section III; Subsection NG; core support structures (NG-1121)	Alloy X	See Appendix 1.A	NA	NA
Criticality Control	Boral	ITS	Non-code	NA	NA	NA	Aluminum/SS
Shielding	Drain and Vent Shield Block	ITS	Non-code	Alloy X	See Appendix 1.A	NA	NA
Shielding	Plugs for Drilled Holes	NITS	Non-code	Alloy X	See Appendix 1.A	NA	NA
Shielding	Bottom portion of optional two-piece MPC lid design	ITS	Non-code	Alloy X	See Appendix 1.A	NA	NA
Heat Transfer	Optional Heat Conduction Elements	ITS	Non-code	Aluminum; Alloy 1100	NA	Sandblast Specified	Aluminum/SS

Notes: 1) There are no known residuals on finished component surfaces.

2) All welding processes used in welding the components shall be qualified in accordance with the requirements of ASME Section IX. All welds shall be made using welders qualified in accordance with ASME Section IX. Weld material shall meet the requirements of ASME Section II and the applicable Subsection of ASME Section III. For parts beyond the purview of ASME Section III, compliance with Section IX and Section II of the Code shall be observed to the extent practicable.

3) Component nomenclature taken from Bill of Materials in Chapter 1.

4) A, B and C **safety** classifications as described in NUREG/CR-6407 **are provided in written procedures**. NITS stands for Not Important To Safety.

5) For details on Alloy X material, see Appendix 1.A.

Table 1.3.3 (cont'd)

## MATERIALS AND COMPONENTS OF THE HI-STAR 100 SYSTEM

MPC <sup>(1, 2)</sup>

Primary Function	Component <sup>(3)</sup>	Safety Class <sup>(4)</sup>	Codes/Standards (as applicable to component)	Material	Strength (ksi)	Special Surface Finish/Coating	Contact Matl. (if dissimilar)
						Surfaces	
Structural Integrity	Upper Fuel Spacer Column	ITS	ASME Section III; Subsection NG (only for stress analysis)	Alloy X	See Appendix 1.A	NA	NA
Structural Integrity	Sheathing	ITS	Non-code	Alloy X	See Appendix 1.A	Aluminum/SS	NA
Structural Integrity	Shims	NITS	Non-code	Alloy X	See Appendix 1.A	NA	NA
Structural Integrity	Basket Supports (Angled Plates)	ITS	ASME Section III; Subsection NG; internal structures (NG-1122) per Table 8.1.4	Alloy X	See Appendix 1.A	NA	NA
Structural Form	Basket Supports (Flat Plates)	NITS	Non-code	Alloy X	See Appendix 1.A	NA	NA
Structural Integrity	Upper Fuel Spacer Bolt	NITS	Non-code	A193-B8	Per ASME Section II	NA	NA
Structural Integrity	Upper Fuel Spacer End Plate	ITS	Non-code	Alloy X	See Appendix 1.A	NA	NA
Structural Integrity	Lower Fuel Spacer Column	ITS	ASME Section III; Subsection NG (only for stress analysis)	S/S	See Appendix 1.A	NA	NA
Structural Integrity	Lower Fuel Spacer End Plate	ITS	Non-code	Alloy X	See Appendix 1.A	NA	NA

Notes: 1) There are no known residuals on finished component surfaces.

2) All welding processes used in welding the components shall be qualified in accordance with the requirements of ASME Section IX. All welds shall be made using welders qualified in accordance with ASME Section IX. Weld material shall meet the requirements of ASME Section II and the applicable Subsection of ASME Section III. For parts beyond the purview of ASME Section III, compliance with Section IX and Section II of the Code shall be observed to the extent practicable.

3) Component nomenclature taken from Bill of Materials in Chapter 1.

4) A, B and C safety classifications as described in NUREG/CR-6407 are provided in written procedures. NITS stands for Not Important To Safety.

5) For details on Alloy X material, see Appendix 1.A.

Table 1.3.3 (cont'd)

## MATERIALS AND COMPONENTS OF THE HI-STAR 100 SYSTEM

MPC <sup>(1, 2)</sup>

Primary Function	Component <sup>(3)</sup>	Safety Class <sup>(4)</sup>	Codes/Standards (as applicable to component)	Material	Strength (ksi)	Special Surface Finish/Coating	Contact Matl. (if dissimilar)
Structural Integrity	Vent Shield Block Spacer	ITS	Non-code	Alloy X	See Appendix 1.A	NA	NA
Structural Integrity	Trojan MPC Spacer	ITS	Non-code	304 S/S	Per ASME Section II	NA	NA
Structural Integrity	Trojan Failed Fuel Can Spacer	ITS	ASME Section III, Subsection NF	304 or 304LN S/S	Per ASME Section II	NA	NA
Operations	Vent and Drain Tube	ITS	Non-code	S/S	Per ASME Section II	Thread area surface hardened	NA
Operations	Vent & Drain Cap	ITS	Non-code	S/S	Per ASME Section II	NA	NA
Operations	Vent & Drain Cap Seal Washer	NITS	Non-code	Aluminum	NA	NA	Aluminum/SS
Operations	Vent & Drain Cap Seal Washer Bolt	NITS	Non-code	Aluminum	NA	NA	NA
Operations	Reducer	NITS	Non-code	Alloy X	See Appendix 1.A	NA	NA
Operations	Drain Line	NITS	Non-code	Alloy X	See Appendix 1.A	NA	NA
Operations	Damaged Fuel Container	ITS	ASME Section III; Subsection NG	Primarily 304 S/S	See Appendix 1.A	NA	NA
Operations	Trojan Failed Fuel Can	ITS	ASME Section III; Subsection NG	304 S/S	Per ASME Section II	NA	NA
Operations	Drain Line Guide Tube	NITS	Non-code	S/S	NA	NA	NA

Notes: 1) There are no known residuals on finished component surfaces.

2) All welding processes used in welding the components shall be qualified in accordance with the requirements of ASME Section IX. All welds shall be made using welders qualified in accordance with ASME Section IX. Weld material shall meet the requirements of ASME Section II and the applicable Subsection of ASME Section III. For parts beyond the purview of ASME Section III, compliance with Section IX and Section II of the Code shall be observed to the extent practicable.

3) Component nomenclature taken from Bill of Materials in Chapter 1.

4) A, B and C **safety** classifications as described in NUREG/CR-6407 **are provided in written procedures**. NITS stands for Not Important To Safety.

5) For details on Alloy X material, see Appendix 1.A.

## 1.4 ENGINEERING DRAWINGS

The following drawings provide sufficient detail to describe the HI-STAR 100 packaging. Refer to Supplement 1.I for drawings related to the HI-STAR HB.

The classification of all components important to safety in accordance with Regulatory Guide 7.10 and NUREG/CR-6407 is provided in Table 1.3.3. Operational information, such as bolt torque and pressure-relief specifications are provided in Chapters 7 and 8. The maximum weight of the package and the maximum weight of the contents is provided in Table 2.2.1.

The following HI-STAR 100 System design drawings are provided in this section.

Drawing Number/Sheet	Description	Rev.
3913	Licensing Drawing for HI-STAR 100 Overpack Assembly	11
3923	Licensing Drawing for MPC Enclosure Vessel	31
3925	Licensing Drawing for MPC-24E/EF Fuel Basket Assembly	9
3926	Licensing Drawing for MPC-24 Fuel Basket Assembly	13
3927	Licensing Drawing for MPC-32 Fuel Basket Assembly	16
3928	Licensing Drawing for MPC-68/68F/68FF Fuel Basket Assembly	18
5014-C1765 Sht 1/7 <sup>†</sup>	HI-STAR 100 Impact Limiter	6
5014-C1765 Sht 2/7 <sup>†</sup>	HI-STAR 100 Bottom Impact Limiter	5
5014-C1765 Sht 3/7 <sup>†</sup>	HI-STAR 100 Top Impact Limiter	5
5014-C1765 Sht 4/7 <sup>†</sup>	HI-STAR 100 Top Impact Limiter	5
5014-C1765 Sht 5/7 <sup>†</sup>	HI-STAR 100 Top Impact Limiter Detail of Item #6	2
5014-C1765 Sht 6/7 <sup>†</sup>	HI-STAR 100 Impact Limiter Honeycomb Details	6
5014-C1765 Sht 7/7 <sup>†</sup>	HI-STAR 100 Bottom Impact Limiter	1
3930	HI-STAR 100 Assembly For Transport	2
10341	Licensing Drawing for MPC Spacer Ring	0
4111	Licensing Drawing for Trojan MPC Spacer Ring	0

<sup>†</sup>□ These drawing titles include the term “CoC No. 9261, Appendix B.” Rather than appending the drawings directly to the CoC, they are incorporated into the CoC by reference. The “Appendix B” will be removed from each drawing as part of its next normal revision.

<b>Drawing Number/Sheet</b>	<b>Description</b>	<b>Rev.</b>
4119	Licensing Drawing for Holtec Damaged Fuel Container for Trojan Plant Fuel	1
4122	Licensing Drawing for Trojan FFC Spacer	0
PFFC-001	Failed Fuel Can Assembly	8
PFFC-002	Failed Fuel Can Shell and Lid Assembly	7

[DRAWINGS ARE PROPRIETARY INFORMATION WITHHELD PER 10CFR2.390]

## 1.5 Compliance with 10CFR71

The HI-STAR 100 packaging complies with the requirements of 10CFR71 for a Type B(U)F-96 package. Analyses which demonstrate that the HI-STAR 100 packaging complies with the requirements of Subparts E and F of 10CFR71 are provided in this SAR. Specific reference to each section of the SAR that is used to specifically address compliance is provided in Table 1.0.2. The HI-STAR 100 packaging complies with the general standards for all packages, 10CFR71.43, as demonstrated in Section 2.4. Under the tests specified in 10CFR71.71 (normal conditions of transport) the HI-STAR 100 packaging is demonstrated to sustain no degradation in its safety function allowing the HI-STAR 100 packaging to meet the requirements of 10CFR71, Paragraphs 71.45, 71.51, and 71.55. Under the tests specified in 10CFR71.73 (hypothetical accident conditions) and 10CFR71.61 (special requirement for irradiated nuclear fuel shipments), the degradation sustained by the HI-STAR 100 packaging is shown not to cause the HI-STAR 100 packaging to exceed the requirements of 10CFR71, Paragraphs 71.51, 71.55, and 71.63.

The HI-STAR 100 packaging meets the structural, thermal, containment, shielding and criticality requirements of 10CFR71, as described in Chapters 2 through 6. The operational procedures and acceptance tests and maintenance program provided in Chapters 7 and 8 ensure compliance with the requirements of 10CFR71.

The following is a summary of the information provided in Chapter 1 that is directly applicable to verifying compliance with 10CFR71:

- The HI-STAR 100 packaging has been described in sufficient detail to provide an adequate basis for its evaluation.
- Drawings provided in Section 1.4 contain information that provides an adequate basis for evaluation of the HI-STAR 100 packaging against the 10CFR71 requirements. Each drawing is identified, consistent with the text of the SAR, and contains keys or annotation to explain and clarify information on the drawing.
- Section 1.0 includes a reference to the NRC-approved Holtec International quality assurance program for the HI-STAR 100 packaging.
- Section 1.3 identifies the applicable codes and standards for the HI-STAR 100 packaging design, fabrication, assembly, and testing.
- The HI-STAR 100 packaging meets the general requirements of 10CFR71.43(a) and 10CFR71.43(b), as demonstrated by the drawings provided in Section 1.4 and the discussion provided in Subsection 1.2.1.9, respectively.
- The drawings provided in Section 1.4 provide a detailed packaging description that can be evaluated for compliance with 10CFR71 for each technical discipline.



- Any restrictions on the use of the HI-STAR 100 packaging are specified in Subsection 1.2.3 and Chapter 7.

## 1.6 REFERENCES

- [1.0.1] 10CFR Part 71, "Packaging and Transportation of Radioactive Materials", Title 10 of the Code of Federal Regulations, Office of the Federal Register, Washington, D.C.
- [1.0.2] 49CFR173, "Shippers - General Requirements For Shipments and Packagings", Title 49 of the Code of Federal Regulations, Office of the Federal Register, Washington, D.C.
- [1.0.3] Regulatory Guide 7.9, "Standard Format and Content of Part 71 Applications for Approval of Packaging for Radioactive Material", Proposed Revision 2, USNRC, May 1986.
- [1.0.4] 10CFR Part 72, "Licensing Requirements for the Storage of Spent Fuel in an Independent Spent Fuel Storage Installation", Title 10 of the Code of Federal Regulations, Office of the Federal Register, Washington, D.C.
- [1.0.5] NUREG-1617, "Standard Review Plan for Transportation Packages for Spent Nuclear Fuel", U.S. Nuclear Regulatory Commission, March 2000.
- [1.0.6] HI-STAR 100 Final Safety Analysis Report, Holtec Report No. HI-2012610, Revision 1, Docket No. 72-1008.
- [1.0.7] HI-STORM 100 Final Safety Analysis Report, Holtec Report No. HI-2002444, Revision 1, Docket No. 72-1014.
- [1.0.8] Pacific Gas & Electric Company HIL-06-001, "Humboldt Bay ISFSI Final Safety Analysis Report", Revision 0, January 2006, USNRC Docket 72-27 (License No. SNM-2514).
- [1.0.9] Pacific Gas & Electric Company HIL-06-001, "Diablo Canyon ISFSI Final Safety Analysis Report", Revision 5 (Living – June 24, 2015, USNRC Docket 72-26 (License No. SNM-2511)).
- [1.1.1] U.S. Department of Energy, "Multi-Purpose Canister (MPC) Subsystem Design Procurement Specification", Document No. DBG000000-01717-6300-00001, Rev. 5, January 11, 1996.
- [1.1.2] U.S. Department of Energy, "MPC Transportation Cask Subsystem Design Procurement Specification", Document No. DBF 000000-01717-6300-00001, Rev. 5, January 11, 1996.
- [1.2.1] U.S. NRC Information Notice 96-34, "Hydrogen Gas Ignition During Closure Welding of a VSC-24 Multi-Assembly Scale Basket".

- [1.2.2] Directory of Nuclear Reactors, Vol. II, Research, Test & Experimental Reactors, International Atomic Energy Agency, Vienna, 1959.
- [1.2.3] V.L. McKinney and T. Rockwell III, Boral: A New Thermal-Neutron Shield, USAEC Report AECD-3625, August 29, 1949.
- [1.2.4] Reactor Shielding Design Manual, USAEC Report TID-7004, March 1956.
- [1.2.5] Deleted.
- [1.2.6] ORNL/TM-10902, "Physical Characteristics of GE BWR Fuel Assemblies", by R.S. Moore and K.J. Notz, Martin Marietta (1989).
- [1.2.7] U.S. DOE SRC/CNEAF/95-01, Spent Nuclear Fuel Discharges from U.S. Reactors 1993, Feb. 1995.
- [1.2.8] S.E. Turner, "Uncertainty Analysis - Axial Burnup Distribution Effects," presented in "Proceedings of a Workshop on the Use of Burnup Credit in Spent Fuel Transport Casks", SAND-89-0018, Sandia National Laboratory, Oct., 1989.
- [1.2.9] Commonwealth Edison Company, Report No. NFS-BND-95-083, Chicago, Illinois.
- [1.2.10] Regulatory Guide 7.11, "Fracture Toughness Criteria of Base Material for Ferritic Steel Shipping Cask Containment Vessels with a Maximum Wall Thickness of 4 Inches (0.1m)", U.S. Nuclear Regulatory Commission, Washington, D.C., June 1991.
- [1.2.11] NUREG-0612, "Control of Heavy Loads at Nuclear Power Plants", U.S. Nuclear Regulatory Commission, Washington, D.C., July 1980.
- [1.2.12] Trojan ISFSI Safety Analysis Report, Revision 3, USNRC Docket 72-0017.
- [1.2.13] **"Burnup Credit in the Criticality Safety Analyses of PWR Spent Fuel in Transport and Storage Casks", ISG-8 Rev. 3, USNRC, Washington, D.C., 2012.**
- [1.2.14] NRC Interim Staff Guidance Document No. 11, "Cladding Considerations for the Transportation and Storage of Spent Fuel", Revision 3.
- [1.2.15] DOE/RW-0184, Volume 3, "Characteristics of Spent Fuel, High Level Waste, and Other Radioactive Wastes Which May Require Long-Term Isolation," Appendix 2.A, "Physical Descriptions of LWR Fuel Assemblies," U.S. Department of Energy, Office of Civilian Radioactive Waste Management, December 1987.
- [1.2.16] PGE Letter ISFSI-004-04L, dated June 17, 2004, "Change to the Definition of Damaged Fuel – Detailed Trojan Fuel Assembly Damage", from S. B. Nichols (PGE) to Eric G. Lewis (Holtec)

- [1.2.17] “Qualification of METAMIC® for Spent Fuel Storage Application,” EPRI, 1003137, Final Report, October 2001.
- [1.2.18] “Safety Evaluation by the Office of Nuclear Reactor Regulation Related to Holtec International Report HI-2022871 Regarding Use of Metamic in Fuel Pool Applications,” Facility Operating License Nos. DPR-51 and NPF-6, Entergy Operations, Inc., Docket No. 50-313 and 50-368, USNRC, June 2003.
- [1.2.19] “Metamic 6061+40% Boron Carbide Metal Matrix Composite Test”, California Consolidated Tech. Inc. Report dated August 21, 2001 to NAC International.
- [1.2.20] “Recommendations for Preparing the Criticality Safety Evaluation for Transportation Packages”, NUREG/CR-5661, USNRC, Dyer and Parks, ORNL.
- [1.2.21] Holtec Proprietary Report HI-2043215, “Sourcebook for Metamic Performance Assessment”, Revision 2.
- [1.2.22] Holtite A: Development History and Thermal Performance Data”, Holtec Report HI-2002396, Latest Revision, Holtec Proprietary.
- [1.2.23] “Holtite-A: Results of Pre-and-Post-Irradiation Tests and Measurements”, Holtec Report HI-2002420, Latest Revision.
- [1.3.1] American Society of Mechanical Engineers, "Boiler and Pressure Vessel Code", 1995 with Addenda through 1997.
- [1.3.2] NUREG/CR-6407, "Classification of Transportation Packaging and Dry Spent Fuel Storage System Components According to Importance to Safety", U.S. Nuclear Regulatory Commission, Washington D.C., February 1996.
- [1.3.3] ANSI N14.6-1993, "Special Lifting Devices for Shipping Containers Weighing 10,000 Pounds (4500 Kg) or More", June 1993.
- [1.3.4] Regulatory Guide 3.61 (Task CE306-4) “Standard Format for a Topical Safety Analysis Report for a Spent Fuel Storage Cask”, USNRC, February 1989.

**No table of contents entries found.**

## **APPENDIX 1.A: ALLOY X DESCRIPTION**

### **1.A ALLOY X DESCRIPTION**

#### **1.A.1 Alloy X Introduction**

Alloy X is used within this licensing application to designate a group of stainless steel alloys. Alloy X can be any one of the following alloys:

- Type 316
- Type 316LN
- Type 304
- Type 304LN

Qualification of structures made of Alloy X is accomplished by using the least favorable mechanical and thermal properties of the entire group for all MPC mechanical, structural, neutronic, radiological, and thermal conditions. The Alloy X approach is conservative because no matter which material is ultimately utilized, the Alloy X approach guarantees that the performance of the MPC will meet or exceed the analytical predictions.

This appendix defines the least favorable material properties of Alloy X.

#### **1.A.2 Alloy X Common Material Properties**

Several material properties do not vary significantly from one Alloy X constituent to the next. These common material properties are as follows:

- density
- specific heat
- Young's Modulus (Modulus of Elasticity)
- Poisson's Ratio

The values utilized for this licensing application are provided in their appropriate chapters.

#### **1.A.3 Alloy X Least Favorable Material Properties**

The following material properties vary between the Alloy X constituents:

- Design Stress Intensity ( $S_m$ )
- Tensile (Ultimate) Strength ( $S_u$ )
- Yield Strength ( $S_y$ )
- Coefficient of Thermal Expansion (  $\alpha$  )
- Coefficient of Thermal Conductivity ( $k$ )

Each of these material properties are provided in the ASME Code Section II [1.A.1]. Tables 1.A.1 through 1.A.5 provide the ASME Code values for each constituent of Alloy X along with the least favorable value utilized in this licensing application. The ASME Code only provides values to -20°F. The design temperature of the MPC is -40°F to 725°F as stated in Table 1.2.3. Most of the above-mentioned properties become increasingly favorable as the temperature drops. Conservatively, the values at the lowest design temperature for the HI-STAR 100 System have been assumed to be equal to the lowest value stated in the ASME Code. The lone exception is the thermal conductivity. The thermal conductivity decreases with the decreasing temperature. The thermal conductivity value for -40°F is linearly extrapolated from the 70°F value using the difference from 70°F to 100°F.

The Alloy X material properties are the minimum values of the group for the design stress intensity, tensile strength, yield strength, and coefficient of thermal conductivity. Using minimum values of design stress intensity is conservative because lower design stress intensities lead to lower allowables that are based on design stress intensity. Similarly, using minimum values of tensile strength and yield strength is conservative because lower values of tensile strength and yield strength lead to lower allowables that are based on tensile strength and yield strength. When compared to calculated values, these lower allowables result in factors of safety that are conservative for any of the constituent materials of Alloy X. Further discussion of the justification for using the minimum values of coefficient of thermal conductivity is given in Chapter 3. The maximum and minimum values are used for the coefficient of thermal expansion of Alloy X. The maximum and minimum coefficients of thermal expansion are used as appropriate in this submittal. Figures 1.A.1-1.A.5 provide a graphical representation of the varying material properties with temperature for the Alloy X materials.

#### 1.A.4 References

[1.A.1] ASME Boiler & Pressure Vessel Code Section II, 1995 ed. with Addenda through 1997.

Table 1.A.1

ALLOY X AND CONSTITUENT DESIGN STRESS INTENSITY ( $S_m$ ) vs. TEMPERATURE

Temp. ( $^{\circ}$ F)	Type 304	Type 304LN	Type 316	Type 316LN	Alloy X (minimum of constituent values)
-40	20.0	20.0	20.0	20.0	20.0
100	20.0	20.0	20.0	20.0	20.0
200	20.0	20.0	20.0	20.0	20.0
300	20.0	20.0	20.0	20.0	20.0
400	18.7	18.7	19.3	18.9	18.7
500	17.5	17.5	18.0	17.5	17.5
600	16.4	16.4	17.0	16.5	16.4
650	16.2	16.2	16.7	16.0	16.0
700	16.0	16.0	16.3	15.6	15.6
750	15.6	15.6	16.1	15.2	15.2
800	15.2	15.2	15.9	14.9	14.9

Notes:

1. Source: Table 2A on pages 314, 318, 326, and 330 of [1.A.1].
2. Units of design stress intensity values are ksi.

Table 1.A.2

ALLOY X AND CONSTITUENT TENSILE STRENGTH ( $S_u$ ) vs. TEMPERATURE

Temp. ( $^{\circ}$ F)	Type 304	Type 304LN	Type 316	Type 316LN	Alloy X (minimum of constituent values)
-40	75.0 (70.0)	75.0 (70.0)	75.0 (70.0)	75.0 (70.0)	75.0 (70.0)
100	75.0 (70.0)	75.0 (70.0)	75.0 (70.0)	75.0 (70.0)	75.0 (70.0)
200	71.0 (66.2)	71.0 (66.2)	75.0 (70.0)	75.0 (70.0)	71.0 (66.2)
300	66.0 (61.5)	66.0 (61.5)	73.4 (68.5)	70.9 (66.0)	66.0 (61.5)
400	64.4 (60.0)	64.4 (60.0)	71.8 (67.0)	67.1 (62.6)	64.4 (60.0)
500	63.5 (59.3)	63.5 (59.3)	71.8 (67.0)	64.6 (60.3)	63.5 (59.3)
600	63.5 (59.3)	63.5 (59.3)	71.8 (67.0)	63.1 (58.9)	63.1 (58.9)
650	63.5 (59.3)	63.5 (59.3)	71.8 (67.0)	62.8 (58.6)	62.8 (58.6)
700	63.5 (59.3)	63.5 (59.3)	71.8 (67.0)	62.5 (58.4)	62.5 (58.4)
750	63.1 (58.9)	63.1 (58.9)	71.4 (66.5)	62.2 (58.1)	62.2 (58.1)
800	62.7 (58.5)	62.7 (58.5)	70.9 (66.2)	61.7 (57.6)	61.7 (57.6)

## Notes:

1. Source: Table U on pages 437, 439, 441, and 443 of [1.A.1].
2. Units of tensile strength are ksi.
3. Values in parentheses are for SA-336 forging material (Types F304, F304LN, F316, and F316LN) that are used solely for the one-piece MPC lids. Other values correspond to SA-240 plate material.



Table 1.A.3

ALLOY X AND CONSTITUENT YIELD STRESSES ( $S_y$ ) vs. TEMPERATURE

Temp. (°F)	Type 304	Type 304LN	Type 316	Type 316LN	Alloy X (minimum of constituent values)
-40	30.0	30.0	30.0	30.0	30.0
100	30.0	30.0	30.0	30.0	30.0
200	25.0	25.0	25.8	25.5	25.0
300	22.5	22.5	23.3	22.9	22.5
400	20.7	20.7	21.4	21.0	20.7
500	19.4	19.4	19.9	19.4	19.4
600	18.2	18.2	18.8	18.3	18.2
650	17.9	17.9	18.5	17.8	17.8
700	17.7	17.7	18.1	17.3	17.3
750	17.3	17.3	17.8	16.9	16.9
800	16.8	16.8	17.6	16.6	16.6

## Notes:

1. Source: Table Y-1 on pages 518, 519, 522, 523, 530, 531, 534, and 535 of [1.A.1].
2. Units of yield stress are ksi.

Table 1.A.4

**ALLOY X AND CONSTITUENT COEFFICIENT OF THERMAL EXPANSION  
vs. TEMPERATURE**

Temp. (°F)	Type 304 and Type 304LN	Type 316 and Type 316LN	Alloy X Maximum	Alloy X Minimum
-40	8.55	8.54	8.55	8.54
100	8.55	8.54	8.55	8.54
150	8.67	8.64	8.67	8.64
200	8.79	8.76	8.79	8.76
250	8.90	8.88	8.90	8.88
300	9.00	8.97	9.00	8.97
350	9.10	9.11	9.11	9.10
400	9.19	9.21	9.21	9.19
450	9.28	9.32	9.32	9.28
500	9.37	9.42	9.42	9.37
550	9.45	9.50	9.50	9.45
600	9.53	9.60	9.60	9.53
650	9.61	9.69	9.69	9.61
700	9.69	9.76	9.76	9.69
750	9.76	9.81	9.81	9.76
800	9.82	9.90	9.90	9.82

## Notes:

1. Source: Table TE-1 on pages 590 and 591 of [1.A.1].
2. Units of coefficient of thermal expansion are in./in.-°F x 10<sup>-6</sup>.

Table 1.A.5

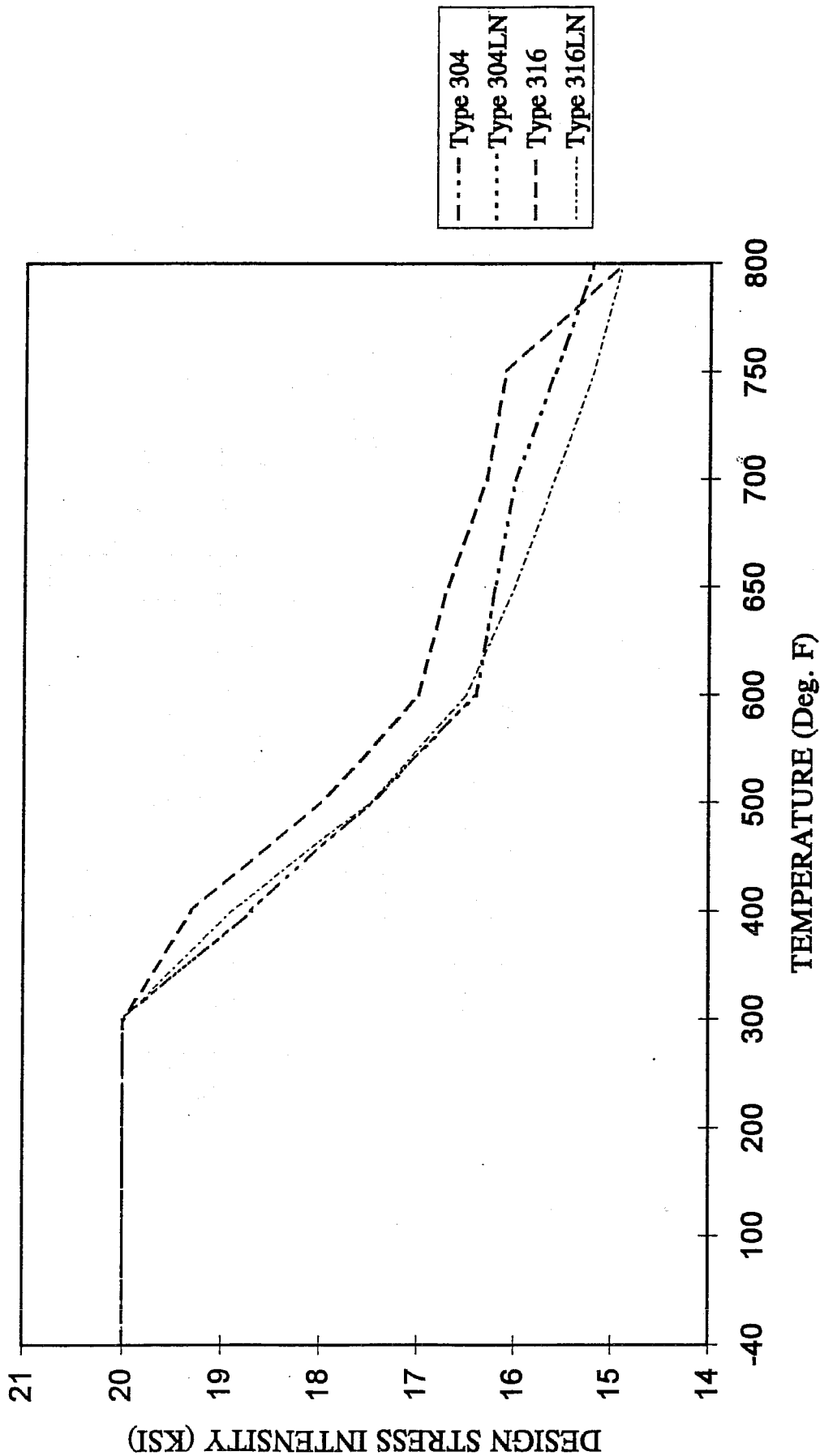
## ALLOY X AND CONSTITUENT THERMAL CONDUCTIVITY vs. TEMPERATURE

Temp. (°F)	Type 304 and Type 304LN	Type 316 and Type 316LN	Alloy X (minimum of constituent values)
-40	8.23	6.96	6.96
70	8.6	7.7	7.7
100	8.7	7.9	7.9
150	9.0	8.2	8.2
200	9.3	8.4	8.4
250	9.6	8.7	8.7
300	9.8	9.0	9.0
350	10.1	9.2	9.2
400	10.4	9.5	9.5
450	10.6	9.8	9.8
500	10.9	10.0	10.0
550	11.1	10.3	10.3
600	11.3	10.5	10.5
650	11.6	10.7	10.7
700	11.8	11.0	11.0
750	12.0	11.2	11.2
800	12.2	11.5	11.5

Notes:

1. Source: Table TCD on page 606 of [1.A.1].
2. Units of thermal conductivity are Btu/hr-ft-°F.

DESIGN STRESS INTENSITY VS. TEMPERATURE



SOURCE: TABLE 1.A.1      FIGURE 1.A.1; DESIGN STRESS INTENSITY VS. TEMPERATURE

# TENSILE STRENGTH VS. TEMPERATURE

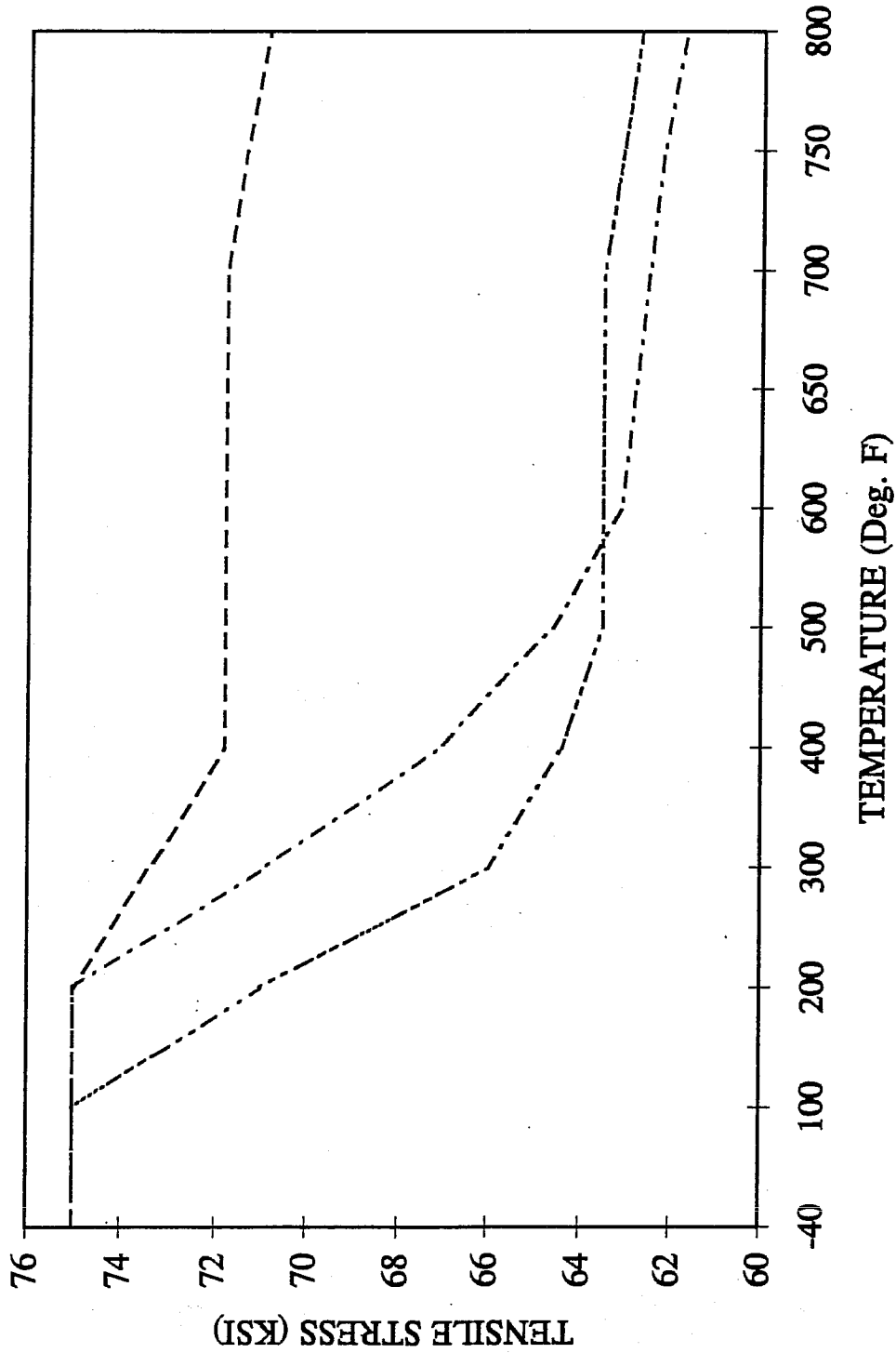


FIGURE 1.A.2; TENSILE STRENGTH VS. TEMPERATURE

SOURCE: TABLE 1.A.2

HI-STAR SAR  
REPORT HI-951251

Rev. 4

YIELD STRESS VS. TEMPERATURE

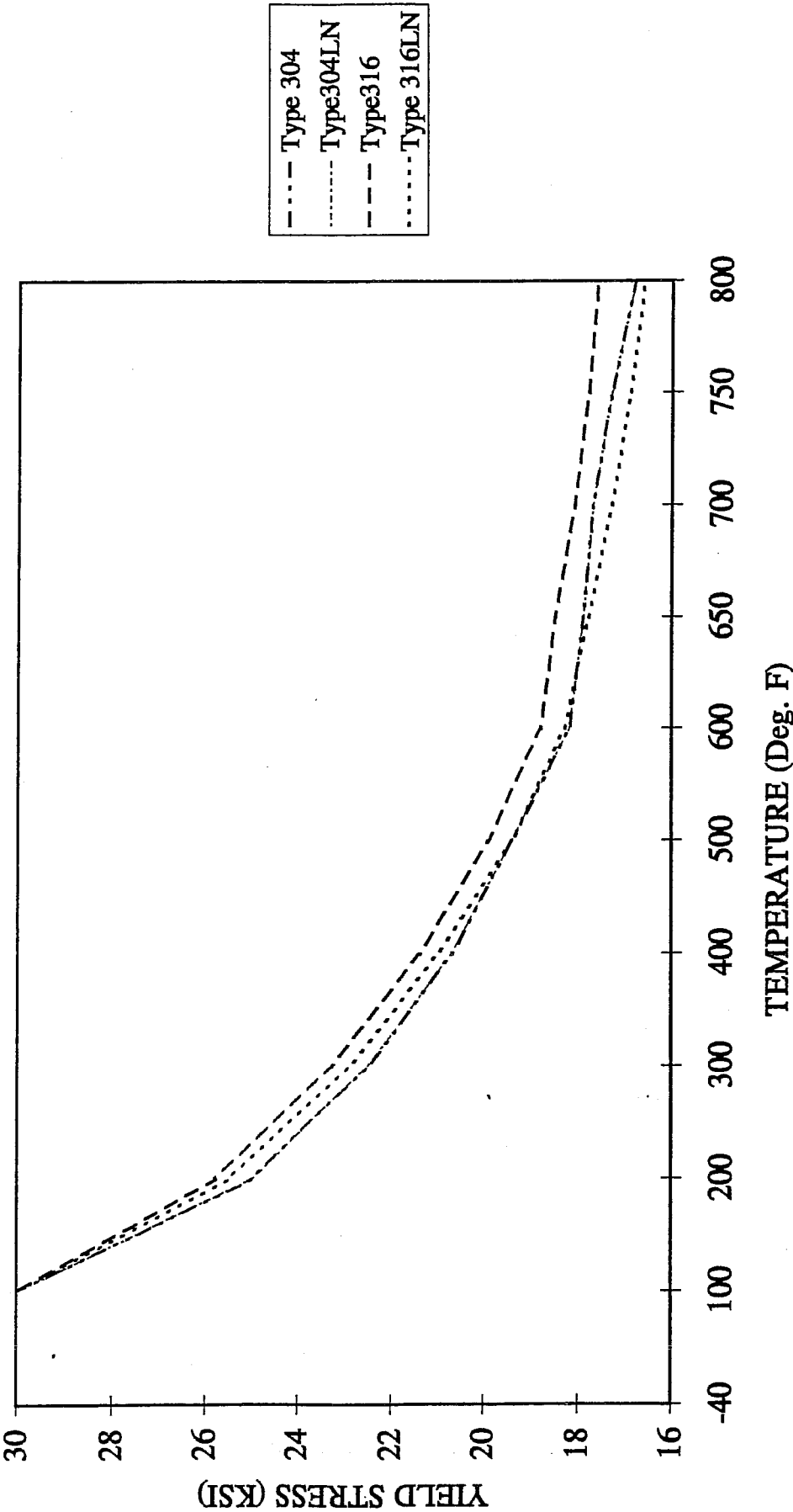
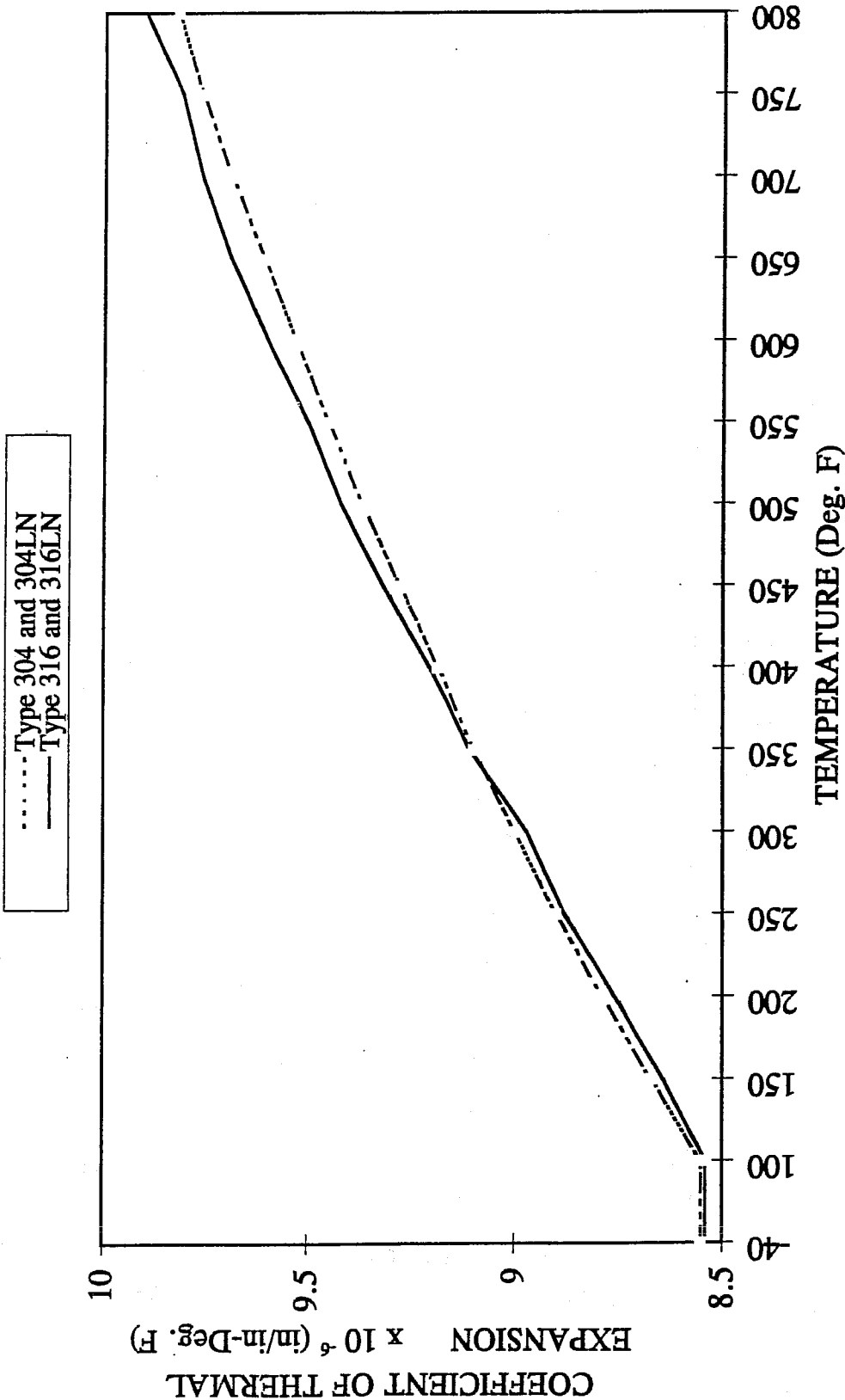


FIGURE 1.A.3; YIELD STRESS VS. TEMPERATURE

SOURCE: TABLE 1.A.3

COEFFICIENT OF THERMAL EXPANSION VS. TEMPERATURE



SOURCE: TABLE 1.A.4      FIGURE 1.A.4; COEFFICIENT OF THERMAL EXPANSION VS. TEMPERATURE

# THERMAL CONDUCTIVITY VS. TEMPERATURE

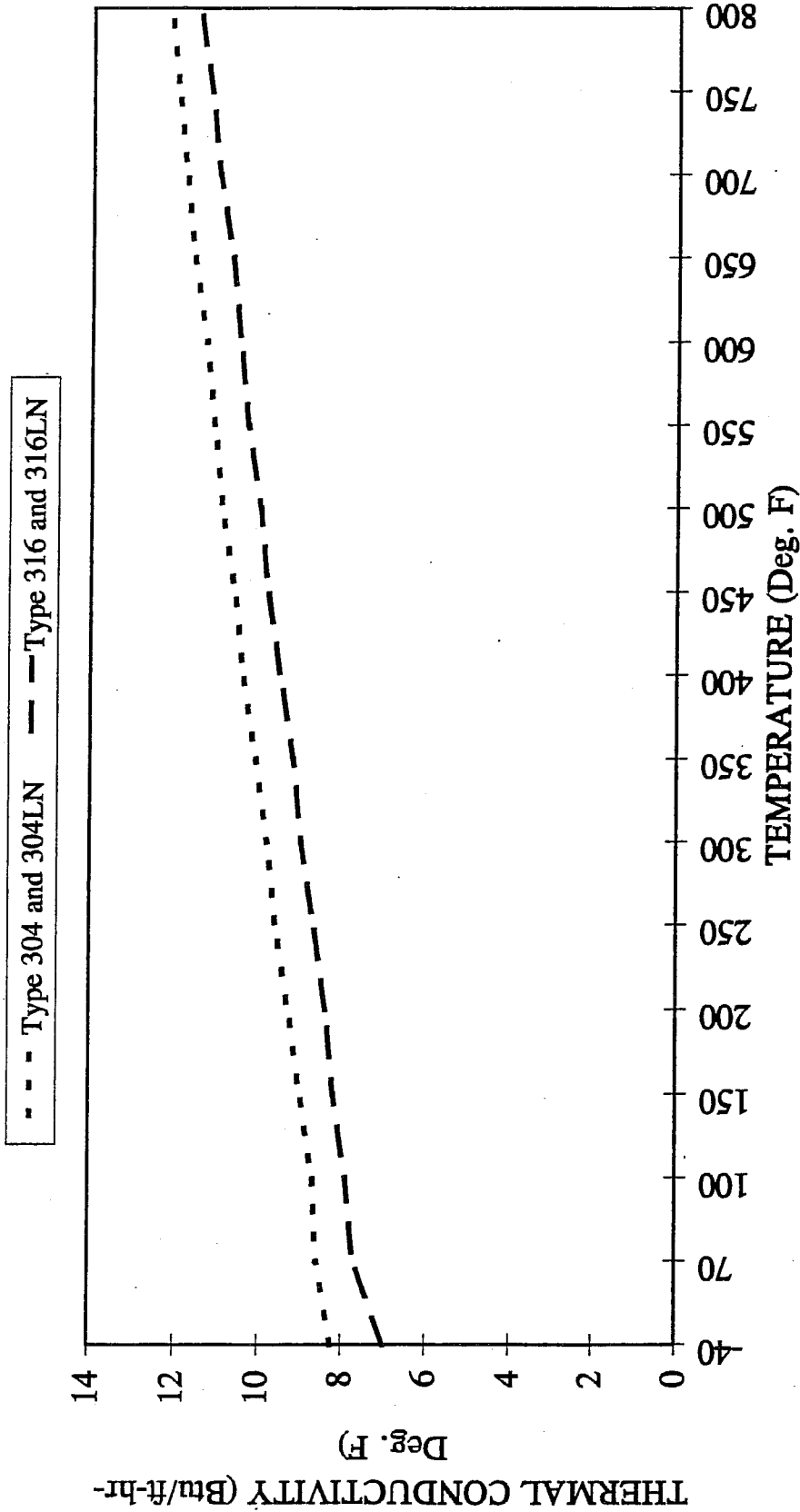


FIGURE 1.A.5; THERMAL CONDUCTIVITY VS. TEMPERATURE

SOURCE: TABLE 1.A.5



## APPENDIX 1.B: HOLTITE™ MATERIAL DATA

The information provided in this appendix describes the neutron absorber material, Holtite-A for the purpose of confirming its suitability for use as a neutron shield material in spent fuel storage casks. Holtite-A is one of a family of Holtite neutron shield materials denoted by the generic name Holtite™. It is currently the only neutron shield material approved for installation in the HI-STAR 100 cask. It is chemically identical to NS-4-FR which was originally developed by Bisco, Inc. and used for many years as a shield material with B<sub>4</sub>C or Pb added.

Holtite-A contains aluminum hydroxide (Al(OH)<sub>3</sub>) in an epoxy resin binder. Aluminum hydroxide is also known by the industrial trade name of aluminum tri-hydrate or ATH. ATH is often used commercially as a fire-retardant. Holtite-A contains ATH supported in a typical 2-part epoxy resin as a binder. Holtite-A B<sub>4</sub>C, a chemically inert material added to enhance the neutron absorption property. Pertinent properties of Holtite-A are listed in Table 1.B.1.

The essential properties of Holtite-A are:

1. the hydrogen density (needed to thermalize neutrons),
2. thermal stability of the hydrogen density, and
3. the uniformity in distribution of B<sub>4</sub>C needed to absorb the thermalized neutrons.

ATH and the resin binder contain nearly the same hydrogen density so that the hydrogen density of the mixture is not sensitive to the proportion of ATH and resin in the Holtite-A mixture. B<sub>4</sub>C is added as a finely divided powder and does not settle out during the resin curing process. Once the resin is cured (polymerized), the ATH and B<sub>4</sub>C are physically retained in the hardened resin. Qualification testing for B<sub>4</sub>C throughout a column of Holtite-A has confirmed that the B<sub>4</sub>C is uniformly distributed with no evidence of settling or non-uniformity. Furthermore, an excess of B<sub>4</sub>C is specified in the Holtite-A mixing and pouring procedure as a precaution to assure that the B<sub>4</sub>C concentration is always adequate throughout the mixture.

The specific gravity specified in Table 1.B.1 does not include an allowance for weight loss. The specific gravity assumed in the shielding analysis includes a 4% reduction to conservatively account for potential weight loss at the design temperature or an inability to reach theoretical density. Tests on the stability of Holtite-A were performed by Holtec International. The results of the tests are summarized in Holtec Proprietary Reports HI-2002396, "Holtite-A Development History and Thermal Performance Data" [1.2.22] and HI-2002420, "Results of Pre- and Post-irradiation Test Measurements." [1.2.23]. The information provided in these reports demonstrates that Holtite-A possesses the necessary thermal and radiation stability characteristics to function as a reliable shielding material in the HI-STAR 100 overpack.

The Holtite-A is encapsulated in the HI-STAR 100 overpack and therefore should experience a very small weight reduction during the design life of the HI-STAR 100 System.

The data and test results confirm that Holtite-A remains stable under design thermal and radiation conditions, the material properties meet or exceed that assumed in the shielding analysis, and the B<sub>4</sub>C remains uniformly distributed with no evidence of settling or non-uniformity.

Based on the information described above, Holtite-A meets all of the requirements for an acceptable neutron shield material.

Table 1.B.1

## REFERENCE PROPERTIES OF HOLTITE-A NEUTRON SHIELD MATERIAL

<b>PHYSICAL PROPERTIES</b>	
% ATH	62 (nominal)
Bulk Density	See Table 8.1.8
Max. Continuous Operating Temperature (Design Temperature)	300°F
Hydrogen Density	See Table 8.1.8
Radiation Resistance	Excellent
Minimum Effective Thermal Conductivity (including contribution from conductivity enhancers)	See Table 3.2.2
<b>CHEMICAL PROPERTIES (Nominal)</b>	
wt% Aluminum	21.5
wt% Hydrogen	6.0 (nominal)
wt% Carbon	27.7
wt% Oxygen	42.8
wt% Nitrogen	2.0
wt% B <sub>4</sub> C	See Table 8.1.8

## APPENDIX 1.C: MISCELLANEOUS MATERIAL DATA

The information provided in this appendix specifies the thermal expansion foam (silicone sponge), paint, and anti-seize lubricant properties and demonstrates their suitability for use in spent nuclear fuel storage casks. The following is a listing of the information provided.

- HT-800 Series, Silicone Sponge, Bisco Products Technical Data Sheet
- Thermaline 450, Carboline, Product Data Sheet and Application Instructions
- Carboline 890, Carboline, Product Data Sheet and Application Instructions
- FEL-PRO Technical Bulletin, N-5000 Nickel Based-Nuclear Grade Anti-Seize Lubricant

HT-870 silicone sponge is specified as a thermal expansion foam to be placed in the overpack outer enclosure with the neutron shield. Due to differing thermal expansion of the neutron shield and outer enclosure carbon steel, the silicone sponge is provided to compress and allow the neutron shield material to expand. The compression-deflection physical properties are provided for the silicone sponge.

Silicone has a long and proven history in the nuclear industry. Silicone is highly resistant to degradation as a result of radiation at the levels required for the HI-STAR 100 System. Silicone is inherently inert and stable and will not react with the metal surfaces or neutron shield material. Additionally, typical operating temperatures for silicone sponges range from -50° F to 400° F.

Thermaline 450 is specified to coat the inner cavity of the overpack and Carboline 890 is specified to coat the external surfaces of the overpack. As can be seen from the product data sheets, the paints are suitable for the design temperatures (see Table 2.2.3) and chemical environment. Chemically identical substitutes are permitted (i.e., Carboguard 890 in lieu of Carboline 890).

Nuclear grade anti-seize lubricant, N-5000, from FEL-PRO is specified as the lubricant for the overpack closure bolts. The lubricant is formulated to have the lowest practical levels of halogens, sulfur, and heavy metals. NEVER-SEEZ NGBT provides equivalent properties to FEL-PRO N-5000 and is also acceptable for use on the HI-STAR 100 System.

**Bisco Products**  
A Dow Corning Subsidiary

# Technical Data

## HT-800 SERIES

Specification Grade  
Silicone Sponge

### PHYSICAL PROPERTIES

PROPERTY	SPECIFICATION			TEST METHOD
	HT-870 (Soft)	HT-800 (Medium)	HT-820 (Firm)	
Density	12 - 24 pcf	16 - 28 pcf	20 - 32 pcf	ASTM D-3574
Compression Force @ 25% Deflection	2 - 7 psi	6 - 14 psi	12 - 20 psi	ASTM D-1056
Compression Set (Maximum)	10%	10%	10%	ASTM D-1056 (Compressed 50% for 22 hrs. @ 100°C)
Water Absorption (Maximum)	10%	5%	5%	ASTM D-1056

Available Industry Specifications:

AMS-3195 (HT-800)

AMS-3196 (HT-820)

UL-94 (Limited to specific classes, densities, thicknesses and colors)

Data is based on laboratory tests and should not be used for writing specifications. Each user should run independent tests to confirm material suitability for each specific application.

Bisco Products and Dow Corning neither represent nor use this material for medical device applications or for pharmaceutical end-use.

**carboline**®

# THERMALINE 450



## SELECTION DATA

**GENERIC TYPE:** A glass flake filled, phenolic modified, amine cured epoxy novalac.

**GENERAL PROPERTIES:** A dense cross-linked polymer which exhibits outstanding barrier protection against a variety of chemical exposures. Excellent resistance to wet/dry cycling conditions at elevated temperatures. Designed to coat the exterior of insulated piping. It is also suitable for coating non-insulated piping and equipment exposed to chemical attack. The glass flakes help provide excellent abrasion resistance, permeation resistance and internal reinforcement.

- Temperature resistance to 450°F
- Excellent abrasion resistance
- Excellent overall chemical resistance
- Excellent thermal shock resistance

**RECOMMENDED USES:** Typically used as a one coat system to coat pipes and tanks that will be insulated. May also be used to coat non-insulated pipe, structural steel, equipment or concrete that may be subjected to severe chemical attack, abrasion or other abuse typical of a chemical plant environment.

### TYPICAL CHEMICAL RESISTANCE:

<u>Exposure</u>	<u>Splash &amp; Spillage</u>	<u>Fumes</u>
Acids	Excellent	Excellent
Alkalies	Excellent	Excellent
Solvents	Excellent	Excellent
Salt	Excellent	Excellent
Water	Excellent	Excellent

### TEMPERATURE RESISTANCE (Under insulation):

Continuous: 425°F (218°C)  
Excursions to: 450°F (232°C)

At 200°F (93°C) coating discoloration may be observed without loss of film integrity.

**SUBSTRATES:** Apply over properly prepared steel.

**COMPATIBLE COATINGS:** Normally applied directly to substrate. May be applied over epoxies and phenolics as recommended. May be topcoated with epoxies, polyurethanes or other finish coats as recommended.

July 96 Replaces September 95

## SPECIFICATION DATA

### THEORETICAL SOLIDS CONTENT OF MIXED MATERIAL:

THERMALINE 450

By Volume  
70 ± 2%

### VOLATILE ORGANIC CONTENT (VOC):

The following are nominal values:

As supplied: 2.13 lbs./gal. (255 gm./liter).

<u>Thinner</u>	<u>Fluid Ounces/Gal.</u>	<u>Pounds/Gallon</u>	<u>Grams/Liter</u>
213	13	2.56	307

### RECOMMENDED DRY FILM THICKNESS:

8-10 mils (200-250 microns) to be achieved in 1 or 2 coats.

### THEORETICAL COVERAGE PER MIXED GALLON:\*

1,117 mil sq. ft. (27.9 sq.m/l at 25 microns)  
139 sq. ft at 8 mils (3.5 sq. m/l at 200 microns)  
111 sq. ft at 10 mils (2.8 sq.m/l at 250 microns)

\*Mixing and application losses will vary and must be taken into consideration when estimating job requirements.

### STORAGE CONDITIONS:

Store indoors.  
Temperature: 40-110°F (4-43°C) Humidity: 0-90%

**SHELF LIFE:** 24 months when stored indoors at 75°F (24°C)

**COLOR:** Red (0500) and Gray (5742)

**GLOSS:** Low (Epoxies lose gloss, discolor and eventually chalk in sunlight exposure.)

## ORDERING INFORMATION

Prices may be obtained from your Carboline Sales Representative or Carboline Customer Service Department.

### APPROXIMATE SHIPPING WEIGHT:

	<u>1's</u>	<u>5's</u>
THERMALINE 450	12 lbs. (5.5 kg)	58 lbs. (26.3 kg)
Thinner 213	8.4 lbs. (3.8 kg)	41 lbs. (18.6 kg)

### FLASH POINT: (Setaflash)

THERMALINE 450 Part A:	53°F	( 12°C)
THERMALINE 450 Part B:	>200°F	(>93°C)
Thinner 213	22°F	( -6°C)

To the best of our knowledge the technical data contained herein are true and accurate at the date of issuance and are subject to change without prior notice. User must contact Carboline Company to verify correctness before specifying or ordering. No guarantee of accuracy is given or implied. We guarantee our products to conform to Carboline quality control. We assume no responsibility for coverage, performance or injuries resulting from use. Liability, if any, is limited to replacement of products. Prices and cost data, if shown, are subject to change without prior notice. NO OTHER WARRANTY OR GUARANTEE OF ANY KIND IS MADE BY CARBOLINE, EXPRESS OR IMPLIED, STATUTORY, BY OPERATION OF LAW, OR OTHERWISE, INCLUDING MERCHANTABILITY AND FITNESS FOR A PARTICULAR PURPOSE.

# APPLICATION INSTRUCTIONS

Holtec Non-Proprietary SAR. Copyrighted Material

## THERMALINE 450

These instructions are not intended to show product recommendations for specific service. They are issued as an aid in determining correct surface preparation, mixing instructions and application procedure. It is assumed that the proper product recommendations have been made. These instructions should be followed closely to obtain the maximum service from the materials.

**SURFACE PREPARATION:** Remove all oil or grease from surface to be coated with Thinner 2 or Surface Cleaner 3 (refer to Surface Cleaner 3 instructions) in accordance with SSPC-SP 1.

### STEEL:

**Not Insulated:** Abrasive blast to a Commercial Finish in accordance with SSPC-SP 6 and obtain a 2-3 mil (50-75 micron) blast profile.

**Under Insulation:** Abrasive blast to a Near White Finish in accordance with SSPC-SP 10 and obtain a 2-3 (50-75 micron) blast profile.

**MIXING:** Power mix each component separately, then combine and power mix in the following proportions.

**Allow 30 minutes induction time at 75°F (24°C) prior to use.**

	<u>1 Gal. Kit</u>	<u>5 Gal. Kit</u>
THERMALINE 450 Part A:	0.8 gals.	4.0 gals.
THERMALINE 450 Part B:	0.2 gals.	1.0 gals.

**THINNING:** May be thinned up to 13 oz/gal with Thinner 213.

Use of thinners other than those supplied or approved by Carboline may adversely affect product performance and void product warranty, whether express or implied.

**POT LIFE:** Three hours at 75°F (24°C) and less at higher temperatures. Pot life ends when coating loses body and begins to sag.

### APPLICATION CONDITIONS:

	<u>Material</u>	<u>Surfaces</u>	<u>Ambient</u>	<u>Humidity</u>
Normal	65-85°F (18-29°C)	65-85°F (18-29°C)	65-85°F (18-29°C)	30-60%
Minimum	55°F (13°C)	50°F (10°C)	50°F (10°C)	0%
Maximum	90°F (32°C)	110°F (43°C)	100°F (38°C)	85%

Do not apply when the surface temperature is less than 5°F or 3°C above the dew point.

Special thinning and application techniques may be required above or below normal conditions.

**SPRAY:** The following spray equipment has been found suitable and is available from manufacturers such as Binks, DeVilbiss and Graco.

**Conventional:** Pressure pot equipped with dual regulators, 1/2" I.D. minimum material hose, .110" I.D. fluid tip and appropriate air cap.

July 96 Replaces September 95

**CAUTION:** CONTAINS FLAMMABLE SOLVENTS. KEEP AWAY FROM SPARKS AND OPEN FLAMES. WORKMEN IN CONFINED AREAS MUST WEAR FRESH AIRLINE RESPIRATORS. HYPERSENSITIVE PERSONS SHOULD WEAR GLOVES OR USE PROTECTIVE CREAM. ALL ELECTRICAL EQUIPMENT AND INSTALLATIONS SHOULD BE MADE IN ACCORDANCE WITH THE NATIONAL ELECTRICAL CODE. IN AREAS WHERE EXPLOSION HAZARDS EXIST, WORKMEN SHOULD BE REQUIRED TO USE NONFERROUS TOOLS AND TO WEAR CONDUCTIVE AND NONSPARKING SHOES.

### Airless:

<b>Pump Ratio:</b>	30:1 (min)*
<b>GPM Output:</b>	3.0 (min)
<b>Material Hose:</b>	1/2" I.D. (min)
<b>Tip Size:</b>	.035"-.041"
<b>Output psi:</b>	2200-2500

\*Teflon packings are recommended and are available from the pump manufacturer.

**BRUSH:** For striping of welds, touch-up of small areas only. Use a natural bristle brush, applying full strokes. Avoid rebrushing.

**ROLLER:** Not recommended.

**DRYING TIMES:** These times are based on a dry film thickness of 10 mils (250 microns). Higher film thickness, insufficient ventilation or cooler temperatures will require longer cure times and could result in solvent entrapment and premature failure.

<u>Surface Temperature</u>	<u>Dry To Handle</u>	<u>Dry to Topcoat</u>	<u>Final Cure</u>
50°F (10°C)	18 hours	48 hours	21 days
60°F (16°C)	12 hours	32 hours	14 days
75°F (24°C)	6 hours	16 hours	7 days
90°F (32°C)	3 hours	8 hours	4 days

If the final cure time has been exceeded, the surface must be abraded by sweep blasting prior to the application of any additional coats.

**EXCESSIVE HUMIDITY OR CONDENSATION ON THE SURFACE DURING CURING MAY RESULT IN A SURFACE HAZE OR BLUSH; ANY HAZE OR BLUSH MUST BE REMOVED BY WATER WASHING BEFORE RE-COATING.**

**VENTILATION & SAFETY: WARNING: VAPORS MAY CAUSE EXPLOSION.** When used in enclosed areas, thorough air circulation must be used during and after application until the coating is cured. The ventilation system should be capable of preventing the solvent vapor concentration from reaching the lower explosion limit for the solvents used. In addition to insuring proper ventilation, fresh air respirators or fresh air hoods must be used by all application personnel. Where flammable solvents exist, explosion-proof lighting must be used. Hypersensitive persons should wear clean, protective clothing, gloves and/or protective cream on face, hands and all exposed areas.

**CLEANUP:** Use Thinner 2.

**CAUTION: READ AND FOLLOW ALL CAUTION STATEMENTS ON THIS PRODUCT DATA SHEET AND ON THE MATERIAL SAFETY DATA SHEET FOR THIS PRODUCT.**

**carboline**



### SELECTION DATA

**GENERIC TYPE:** Cross-linked epoxy.

**GENERAL PROPERTIES:** CARBOLINE 890 is a self priming, high solids, high gloss, high build epoxy mastic. It can be applied by spray, brush, or roller over hand or power tool cleaned steel and is compatible with most existing coatings and tightly adhered rust. The cured film provides a tough, cleanable surface and is available in a wide variety of colors.

- Single coat corrosion protection.
- Excellent chemical resistance.
- Good flexibility and lower stress upon curing than most epoxy coatings.
- Excellent tolerance of damp (not wet) substrates.
- Very good abrasion resistance.
- Suitable replacement for Carbomastic 801.

**RECOMMENDED USES:** Recommended where a high performance, chemically resistant epoxy coating is desired. Offers outstanding protection for interior floors, walls, piping, equipment and structural steel or as an exterior coating for railcars, structural steel and equipment in various corrosive environments. Industrial environments include Chemical Processing, Offshore Oil and Gas, Food Processing, Pharmaceutical, Water and Waste Water Treatment, Pulp and Paper and Power Generation among others. May be used as a two coat system direct to metal or concrete for Water and Municipal Waste Water immersion. Acceptable for use in incidental food contact areas and as a lining for hopper cars carrying food grade plastic pellets when processed according to FDA criteria (ref: FDA 21 CFR 175.300). Consult Carboline Technical Service Department for other specific uses.

**NOT RECOMMENDED FOR:** Strong acid or solvent exposures, immersion service other than water, exterior weathering where color retention is desired, such as a finish for tank exteriors or over chlorinated rubber and latex coatings.

#### TYPICAL CHEMICAL RESISTANCE:

Exposure	Immersion	Splash & Spillage	Fumes
Acids	NR	Very Good	Very Good
Alkalies	NR	Excellent	Excellent
Solvents	NR	Very Good	Excellent
Salt Solutions	Excellent	Excellent	Excellent
Water	Excellent	Excellent	Excellent

#### TEMPERATURE RESISTANCE: (Non-Immersion)

Continuous: 250°F (121°C)  
Non-continuous: 300°F (149°C)

At temperatures above 225°F, coating discoloration and loss of gloss can be observed, without loss of film integrity.

**SUBSTRATES:** Apply over suitably prepared metal, concrete, or other surfaces as recommended.

**COMPATIBLE COATINGS:** May be applied directly over inorganic zincs, weathered galvanizing, epoxies, phenolics or other coatings as recommended. A test patch is recommended before use over existing coatings. A mist coat of CARBOLINE 890 is required when applied over inorganic zincs to minimize bubbling. May be topcoated with polyurethanes or acrylics to upgrade weathering resistance. Not recommended over chlorinated rubber or latex coatings. Consult Carboline Technical Service Department for specific recommendations.

### SPECIFICATION DATA

#### THEORETICAL SOLIDS CONTENT OF MIXED MATERIAL:\*

By Volume  
75% ± 2%

CARBOLINE 890

#### VOLATILE ORGANIC CONTENT:\*

As Supplied: 1.78 lbs./gal. (214 grams/liter)

Thinned:

Thinner	Fluid Ounces/Gal.	Pounds/Gallon	Grams/Liter
2	8	2.08	250
2	13	2.26	271
33	16	2.38	285

\*Varies with color

#### RECOMMENDED DRY FILM THICKNESS PER COAT:

4-6 mils (100-150 microns).

6-8 mils (150-200 microns) DFT for a more uniform gloss over inorganic zincs, or for use over light rust.

In more severe environments a second coat of 4-6 mils (100-150 microns) is recommended.

Dry film thickness in excess of 10 mils (250 microns) per coat is not recommended. Excessive film thickness over inorganic zinc may increase damage during shipping or erection.

#### THEORETICAL COVERAGE PER MIXED GALLON:

1203 mil sq. ft. (30 sq. m/l at 25 microns)

241 sq. ft. at 5 mils (6.0 sq. m/l at 125 microns)

Mixing and application losses will vary and must be taken into consideration when estimating job requirements.

#### STORAGE CONDITIONS: Store Indoors

Temperature: 40-110°F (4-43°C)

Humidity: 0-100%

**SHELF LIFE:** 36 months when stored at 75°F (24°C).

**COLORS:** Available in Carboline Color Chart colors. Some colors may require two coats for adequate hiding.

**GLOSS:** High gloss (Epoxies lose gloss, discolor and eventually chalk in sunlight exposure).

### ORDERING INFORMATION

Prices may be obtained from your Carboline Sales Representative or Carboline Customer Service Department.

#### APPROXIMATE SHIPPING WEIGHT:

	2 Gal. Kit	10 Gal. Kit
CARBOLINE 890	29 lbs. (13 kg)	145 lbs. (66 kg)
	1's	5's
THINNER #2	8 lbs. (4 kg)	39 lbs. (18 kg)
THINNER #33	9 lbs. (4 kg)	45 lbs. (20 kg)

#### FLASH POINT: (Setaflash)

CARBOLINE 890 Part A	89°F (32°C)
CARBOLINE 890 Part B	71°F (22°C)
THINNER #2	24°F (-5°C)
THINNER #33	89°F (32°C)

June 96 Replaces December 95

To the best of our knowledge the technical data contained herein are true and accurate at the date of issuance and are subject to change without prior notice. User must contact Carboline Company to verify correctness before specifying or ordering. No guarantee of accuracy is given or implied. We guarantee our products to conform to Carboline quality control. We assume no responsibility for coverage, performance or injuries resulting from use. Liability, if any, is limited to replacement of products. Prices and cost data, if shown, are subject to change without prior notice. NO OTHER WARRANTY OR GUARANTEE OF ANY KIND IS MADE BY CARBOLINE, EXPRESS OR IMPLIED, STATUTORY, BY OPERATION OF LAW, OR OTHERWISE, INCLUDING MERCHANTABILITY AND FITNESS FOR A PARTICULAR PURPOSE.

HI-STAR 100 SAR Revision 16 (January 27, 2016)

Holtec Non-Proprietary SAR. Copyrighted Material



These instructions are not intended to show product recommendations for specific service. They are issued as an aid in determining correct surface preparation, mixing instructions and application procedure. It is assumed that the proper product recommendations have been made. These instructions should be followed closely to obtain the maximum service from the materials.

**SURFACE PREPARATION:** Remove all oil or grease from surface to be coated with Thinner #2 or Surface Cleaner #3 (refer to Surface Cleaner #3 instructions) in accordance with SSPC-SP 1.

**Steel:** For mild environments Hand Tool or Power Tool Clean in accordance with SSPC-SP 2, SSPC-SP 3 or SSPC-SP 11 to produce a rust-scale free surface.

For more severe environments, abrasive blast to a Commercial Finish in accordance with SSPC-SP 6 and obtain a 1 1/2 - 3 mil (40-75 micron) blast profile.

For immersion service, abrasive blast to a Near White Metal Finish in accordance with SSPC-SP10 and obtain a 1 1/2 - 3 mil (40-75 micron) blast profile.

**Concrete:** Must be cured at least 28 days at 70°F (21°C) and 50% R.H. or equivalent time. Remove fins and other protrusions by stoning, sanding or grinding. Abrasive blast to open all surface voids and remove all form oils, incompatible curing agents, hardeners, laitance and other foreign matter and produce a surface texture similar to that of a medium grit sandpaper. Voids in the concrete may require surfacing. Blow or vacuum off sand and dust.

**MIXING:** Power mix separately, then combine and power mix in the following proportions:

	<u>2 Gal. Kit</u>	<u>10 Gal. Kit</u>
CARBOLINE 890 Part A	1 gallon	5 gallons
CARBOLINE 890 Part B	1 gallon	5 gallons

**THINNING:** For spray applications, may be thinned up to 13 oz./gal. with Thinner #2. For hot and windy conditions, or for brush and roller application, may be thinned up to 16 oz./gal. with Thinner #33.

Use of thinners other than those supplied or approved by Carboline may adversely affect product performance and void product warranty, whether express or implied.

**POT LIFE:** Three hours at 75°F (24°C) and less at higher temperatures. Pot life ends when material loses film build.

#### APPLICATION CONDITIONS:

	<u>Material</u>	<u>Surfaces</u>	<u>Ambient</u>	<u>Humidity</u>
Normal	60-85°F (16-29°C)	60-85°F (16-29°C)	60-90°F (16-32°C)	0-80%
Minimum	50°F (10°C)	50°F (10°C)	50°F (10°C)	0%
Maximum	90°F (32°C)	125°F (52°C)	110°F (43°C)	90%

Do not apply or cure the material when the surface temperature is less than 5°F or 3°C above the dew point.

Special thinning and application techniques may be required above or below normal conditions.

**SPRAY:** This is a high solids coating and may require slight adjustments in spray techniques. Wet film thicknesses are easily and quickly achieved. The following spray equipment has been found suitable and is available from manufacturers such as Binks, DeVilbiss and Graco.

**Conventional:** Pressure pot equipped with dual regulators, 3/8" I.D. minimum material hose, .070" I.D. fluid tip and appropriate air cap.

June 96 Replaces December 95

<b>Airless:</b>	
<i>Pump Ratio:</i>	30:1 (min.)*
<i>GPM Output:</i>	3.0 (min.)
<i>Material Hose:</i>	3/8" I.D. (min.)
<i>Tip Size:</i>	.017-.021"
<i>Output psi:</i>	2100-2300
<i>Filter Size:</i>	60 mesh

\*Teflon packings are recommended and are available from the pump manufacturer.

**BRUSH OR ROLLER:** Use medium bristle brush, or good quality short nap roller. Avoid excessive rebrushing and rerolling. Two coats may be required to obtain desired appearance, hiding and recommended DFT. For best results, tie-in within 10 minutes at 75°F (24°C).

**DRYING TIMES:** These times are based on a 5 mils (125 microns) dry film thickness. Higher film thicknesses, insufficient ventilation or cooler temperatures will require longer cure times and could result in solvent entrapment and premature failure.

Dry to Touch 2 1/2 hours at 75°F (24°C)  
Dry to Handle 6 1/2 hours at 75°F (24°C)

<u>Surface Temperature</u>	<u>Recoatng With Itself</u>	<u>Dry to Topcoat</u>	<u>Final Cure</u>
50°F (10°C)	12 hours	24 hours	3 days
60°F (16°C)	8 hours	16 hours	2 days
75°F (24°C)	4 hours	8 hours	1 day
90°F (32°C)	2 hours	4 hours	16 hours

Excessive humidity or condensation on the surface during curing can interfere with the cure, can cause discoloration and may result in a surface haze or blush. Any haze or blush must be removed by water washing before recoating. During high humidity conditions, it is recommended that the application be done while temperatures are increasing. For best results over "damp" surfaces, apply by brush or roller.

#### Maximum Recoat or Topcoat Times at 75°F (24°C):

With Epoxies - 30 days  
With Polyurethanes - 90 days

If the maximum recoat time has been exceeded, surface must be abraded by sweep blasting prior to the application of any additional coats.

Minimum cure time before immersion service is 5 days at 75°F (24°C) surface temperature. Cure at temperatures below 60°F (16°C) is not recommended for immersion service.

**VENTILATION & SAFETY: WARNING: VAPORS MAY CAUSE EXPLOSION.** When used as a tank lining or in enclosed areas, thorough air circulation must be used during and after application until the coating is cured. The ventilation system should be capable of preventing the solvent vapor concentration from reaching the lower explosion limit for the solvents used. In addition to ensuring proper ventilation, fresh air respirators or fresh air hoods must be used by all application personnel. Where flammable solvents exist, explosion-proof lighting must be used. Hypersensitive persons should wear clean, protective clothing, gloves and/or protective cream on face, hands and all exposed areas.

**CLEANUP:** Use Thinner # 2.

**CAUTION: READ AND FOLLOW ALL CAUTION STATEMENTS ON THIS PRODUCT DATA SHEET AND ON THE MATERIAL SAFETY DATA SHEET FOR THIS PRODUCT.**

**CAUTION: CONTAINS FLAMMABLE SOLVENTS. KEEP AWAY FROM SPARKS AND OPEN FLAMES. IN CONFINED AREAS, WORKMEN MUST WEAR FRESH AIRLINE RESPIRATORS. HYPERSENSITIVE PERSONS SHOULD WEAR GLOVES OR USE PROTECTIVE CREAM. ALL ELECTRIC EQUIPMENT AND INSTALLATIONS SHOULD BE MADE AND GROUNDED IN ACCORDANCE WITH THE NATIONAL ELECTRICAL CODE. IN AREAS WHERE EXPLOSION HAZARDS EXIST, WORKMEN SHOULD BE REQUIRED TO USE NONFERROUS TOOLS AND TO WEAR CONDUCTIVE AND NONSPARKING SHOES.**



# FELPRO®

## Technical Bulletin

### N-5000 NICKEL BASED - NUCLEAR GRADE ANTI-SEIZE LUBRICANT

N-5000 is a nickel based nuclear grade anti-seize lubricant produced under 100% controlled conditions for highest purity and traceability. It is formulated to have the lowest practical levels of halogens, sulfur, and heavy metals, including copper. N-5000 has a general composition of nickel and graphite flake in petroleum carrier. All ingredients are selected for extreme purity. It meets or exceeds the following specifications, appendix A of NEDE-31295P, "BWR Operator's Manual for Materials and Processes", Westinghouse Material Specification 53701WQ, and 10CFR Ch1, Part 21, and Part 50, appendix B.

#### Special Features:

- High purity- made from highest purity ingredients.
- Traceability- each can marked.
- Free from copper- less than 50 ppm copper.
- Testing- each batch tested before packaging.
- Certifications- 3 copies with each case.

#### Recommended applications:

- Bolts, studs, valves, pipe fittings, slip fits and press fits in electric power generating plants, chemical plants, pharmaceutical plants, paper mills, and other locations where stainless steel fasteners are used.

#### Operational Benefits:

- Before assembly - certifications and traceability.
- During assembly - prevents high friction, galling, and seizing. Promotes uniform and predictable clamping.
- During operation - high purity prevents stress corrosion.
- Disassembly - prevents seizing, galling, destruction of threads.

#### Typical Physical Properties:

Composition	Nickel and Graphite in Petroleum Oil
Appearance	Silver-Gray paste
Specific gravity	1.0
Flash point (ASTM D 92-85)	424°F/218°C
Torque coefficient, K (Steel nuts and Bolts) (Type 304 Stainless)	0.15 0.18
Maximum use temperature	1800°F/982°C

#### Quality Control Physical Properties:

Weight per gallon (ASTM D 1475-85)	Range 9.5 - 10.4
Penetration (ASTM D 217-88 unworked)	300 - 380

#### Purity:

Impurities - Elemental and Combined	Test Method Type	References ASTM OR (SM16)	Controlled Maximum	Average Values
Halogens, Chlorine, Bromine, Iodine	Parr Bomb, Turbidimetric	D808-87, C69979	50 ppm	18 ppm
Fluorine	Parr Bomb, Specific ION Electrode	D3761-84	200 ppm	7 ppm
Sulfur	Parr Bomb, Turbidimetric	D129-64, D1266-87	100 ppm	9 ppm
Lead	Wet Digestion, AAS	(302D), D3559-84	25 ppm	1 ppm
Cadmium	Wet Digestion, AAS	(302D), D3557-84	2 ppm	0.2 ppm
Tin	Wet Digestion, AAS	(302D), E37-76	25 ppm	9 ppm
Zinc	Wet Digestion, AAS	(302D), D1691-84	25 ppm	1 ppm
Copper	Wet Digestion, AAS	(302D), D1688-84	50 ppm	12 ppm
Mercury	Wet Digestion, Cold Vapor AAS	(302D), D3223-80	2 ppm	0.04 ppm

**Directions for use:**

- Before or during assembly, wipe brush onto threads and other joint surfaces needing protection.
- Do not overuse, as excess will be pushed off.
- Use full strength, do not thin.

**Packaging:**

Part Number	Net Contents	Type Container	Units/Case	Shipping Wt./Case
51243	8 oz. (227 g)	Can-brush top	12	9 lb. (4. Kg.)
51245	8 lb. (3.6 kg)	Can	2	18 lb. (8. Kg.)
51246	2 lb. (908 g)	Can	12	29 lb. (13. Kg.)
51269	1 lb. (454 g)	Can-brush top	12	16 lb. (7. Kg.)
51346	1 oz. (28 g)	Tube	48	6 lb. (2.7 Kg.)

N-5000 has an unlimited shelf life when stored at room temperature in the original unopened container.

**FOR INDUSTRIAL USE ONLY.**

**WASH THOROUGHLY AFTER HANDLING.**

**KEEP OUT OF REACH OF CHILDREN.**

**SEE MATERIAL SAFETY DATA** For immediate answers to your technical questions, in the United States or Canada call the **Technical Support Line at 1-800-992-9799.**

International customers call (303) 289-5651, or fax (303) 289-5283

For a Material Safety Data Sheet or Technical Bulletin on this or any Fel-Pro product call our toll-free **FAX FOR THE INFO** line 24 hours a day, 7 days a week, in the United States or Canada call **800-583-3069**. International customers call (303) 289-5651, or fax (303) 289-5283.

Except as expressly stipulated, Fel-Pro's liability, expressed or implied, is limited to the stated selling price of any defective goods.

N-5000 8/97

**FEL-PRO CHEMICAL PRODUCTS, L.P.**

Fel-Pro  
3412 W. Touhy Ave.  
Lincolnwood, IL  
60465 U.S.A.  
847-568-2820  
Fax 847-674-0019

Fel-Pro  
6120 E. 58th Ave  
Commerce City, CO  
80022 U.S.A.  
800-992-9799  
Fax 303-289-5283

Fel-Pro of Canada, Ltd  
6105 Kestrel Road  
Mississauga, Ontario  
L5T 1Y8 Canada  
905-564-1530  
Fax 905-564-1534

Fel-Pro Ltd.  
4 Arkwright Way  
North Newmoor, Irvine  
KA11 4JU Scotland  
44-1294-216094  
Fax 44-1294-218157

Fel-Pro Chemical Products Latin America L.P.  
Bodega No. 12, Zona Franca Palmaseca  
Aeropuerto Internacional Bonilla Aragon  
Cali, Colombia  
57-2-651-1168  
Fax 57-2-651-1179

Fel-Pro Chemical Products, Chile S.A.  
Av. Pdt. Eduardo Frei M. 9231 Quilicura  
Casilla (P.O. Box) 14325  
Santiago, Chile  
56-2-623-9216  
Fax 56-2-623-2569

## SUPPLEMENT 1.I

### GENERAL DESCRIPTION OF THE HI-STAR HB PACKAGE WITH MPC-HB

#### 1.I.0 GENERAL INFORMATION

The HI-STAR 100 System has been expanded to include options specific for use at PG&E's Humboldt Bay (HB) plant for dry storage and future transportation of spent nuclear fuel (SNF)[1.0.8]. HB fuel assemblies are considerably shorter in length than the typical BWR fuel assemblies. As a result, the HI-STAR 100 system now includes an overpack assembly and MPC for use at HB; the HI-STAR 100 Version HB (also called HI-STAR HB) and the MPC-HB. Note that the HB fuel has a cooling time of more than 25 years and relatively low burnup. The heat load and nuclear source terms of this fuel are therefore substantially lower than the design basis fuel described in the main part of this chapter. Consequently, peak cladding temperatures and dose rates are below the regulatory limits with a substantial margin. Nevertheless, all major dimensions and features, such as diameter, wall thickness, flange design, top and bottom thicknesses, are maintained identical to the standard design. Therefore, from a structural perspective, the HI-STAR HB will be even more robust than the standard overpack, due to its shorter length. Information pertaining to the HI-STAR HB System is generally contained in the "I" supplements to each chapter of this SAR. Certain sections of the main SAR are also affected and are appropriately modified for continuity with the "I" supplements. Unless superseded or specifically modified by information in the "I" supplements, the information in the main SAR is applicable to the HI-STAR System for use at HB host site. Supplement I may make certain references to Supplement II when appropriate, for example, both Supplements share the same impact limiter drawing.

##### 1.I.0.1 Engineering Change Orders

The changes authorized by Holtec Engineering Change Orders (ECOs) for the following licensed components are reflected in this revision of this SAR.

HI-STAR HB overpack: 1125-30R0

MPC-HB Basket: None.

MPC-HB Enclosure Vessel: None.

Ancillary Equipment:

- HB Impact Limiter: new drawing
- Damaged Fuel Container HB: None.

#### 1.I.1 INTRODUCTION

The HI-STAR 100 System as deployed at Humboldt Bay will consist of a HI-STAR HB overpack, an MPC-HB that includes a fuel basket assembly and enclosure vessel specific to HB, and custom AL-STAR impact limiters. The HB specific components are described below and

key parameters for HI-STAR HB are presented in Table 1.I.1. Section 1.I.3 provides the HI-STAR HB design code applicability and details any alternatives to the ASME Code if different than HI-STAR 100. All discussion is supplemented by a set of drawings in Section 1.I.4.

## 1.I.2 PACKAGE DESCRIPTION

### 1.I.2.1 Packaging

#### 1.I.2.1.1 Gross Weight

Table 2.I.2.1 summarizes the maximum calculated weights for the HI-STAR HB overpack, impact limiters, and each MPC loaded to maximum capacity with design basis SNF. Table 2.I.2.1 also provides the location of the center of gravity of the fully loaded package.

#### 1.I.2.1.2 Materials of Construction, Dimensions, and Fabrication

Humboldt Bay specific materials of construction along with outline dimensions for important-to-safety items are provided in the drawings in Section 1.I.4.

##### 1.I.2.1.2.1 HI-STAR HB Overpack

The HI-STAR HB overpack is a heavy-walled, steel cylindrical vessel identical to the standard HI-STAR, except that the outer and inner heights are approximately 128 and 115 inches, respectively. Unlike the HI-STAR 100, the HI-STAR HB overpack does not contain radial channels vertically welded to the outside surface of the outermost intermediate shell.

##### 1.I.2.1.2.2 MPC-HB

MPC-HB is similar to the MPC-68F except it is approximately 114 inches high. Key parameters of the MPC-HB are given in Table 1.I.2. The MPC-HB is designed to transport up to 80 Humboldt Bay BWR spent nuclear fuel assemblies meeting the specifications in Table 1.I.4. Damaged SNF and fuel debris must be placed into a Holtec damaged fuel container or other authorized canister for transportation inside the MPC-HB and the HI-STAR HB overpack. Figure 1.I.1 provides a sketch of the container authorized for transportation of damaged fuel and fuel debris in the HI-STAR HB System.

##### 1.I.2.1.3 Impact Limiters

The impact limiter evaluated is the HI-STAR 100 Impact Limiter Version HB (also referred to as HB Impact Limiter) provided in the drawing package in Section 1.I.4. HB Impact Limiter (a customized version of the standard HI-STAR 100 impact limiter) is qualified for the HI-STAR HB Package (SAR Supplement I) and the HI-STAR HB GTCC Package (SAR Supplement II). HB Impact Limiter features a longer “outer donut”, the crush zone furthest away from the cask (identified in the standard impact limiter drawing in Section 1.4 as Section Type 4) and does not feature Holtite shielding material. There are no other significant differences compared to the

standard impact limiter. The evaluation of HB Impact Limiters are documented in Supplement 2.II.

### 1.I.2.2 Operational Features

The sequence of basic operations necessary to load fuel and prepare the HI-STAR HB system for transport is identical to that of HI-STAR 100. The supporting drawings for HB can be found in Section 1.I.4.

### 1.I.2.3 Contents of Package

This section delineates the authorized contents permitted for shipment in the HI-STAR HB System, including fuel assembly types; non-fuel hardware; neutron sources; physical parameter limits for fuel assemblies and sub-components; enrichment, burnup, cooling time, and decay heat limits; location requirements; and requirements for canning the material, as applicable.

#### 1.I.2.3.1 Determination of Design Basis Fuel

The HI-STAR HB package is designed to transport Humboldt Bay fuel assemblies. The HB fuel assembly designs evaluated are listed in Table 1.I.3. Table 1.I.4 provides the fuel characteristics determined to be acceptable for transport in the HI-STAR HB System. Each “array/class” listed in this table represents a bounding set of parameters for one or more fuel assembly types. The array/classes are defined for HB in Section 6.I.2. Table 1.I.5 lists the fuel assembly designs that are found to govern for the qualification criteria. Tables 1.I.4 and 1.I.7 provide the specific limits for all material authorized to be transported in the HI-STAR HB System.

#### 1.I.2.3.2 Design Payload for Intact and/or Undamaged Fuel

The fuel characteristics specified in Table 1.I.4 have been evaluated in this SAR and are acceptable for transport in the HI-STAR HB System. Holtec considers that almost all of the Humboldt Bay fuel assemblies not classified as damaged are intact, however the inspection records of the Humboldt Bay fuel assemblies precludes classifying the assemblies as intact fuel since the interior rods of the assembly are in an unknown condition. This fuel is therefore classified as undamaged and can still perform all fuel specific and system related functions, even with possible breaches or defects. Except where specifically noted, throughout this document references to Humboldt Bay fuel as intact or undamaged are equivalent.

#### 1.I.2.3.3 Design Payload for Damaged Fuel and Fuel Debris

Limits for transporting HB damaged fuel and fuel debris are given in Table 1.I.7. Damaged HB fuel and fuel debris must be transported in the Holtec designed Humboldt Bay Damaged Fuel Container (DFC) as shown in Figure 1.I.1.

#### 1.I.2.3.4 Structural Payload Parameters

The main physical parameters of an SNF assembly applicable to the structural evaluation are the fuel assembly length, envelope (cross sectional dimensions), and weight. In order to qualify for transport in the HI-STAR HB MPC, the SNF must satisfy the physical parameters listed in Table 1.I.7. The center of gravity for HB, reported in Chapter 2.I, is based on the maximum fuel assembly weight. Upper fuel spacers (as appropriate) in the form of welded I-beams, approximately 4 inches high, maintain the axial position of the fuel assembly within the MPC basket and, therefore, the location of the center of gravity. The upper spacers are designed to withstand normal and accident conditions of transport. An axial clearance of approximately 2 inches is provided to account for the irradiation and thermal growth of the fuel assemblies.

#### 1.I.2.3.5 Thermal Payload Parameters

Table 1.I.7 provides the maximum heat generation for all fuel assemblies authorized for transportation in the HI-STAR HB System.

#### 1.I.2.3.6 Radiological Payload Parameters

The design basis dose rates are met by the burnup level, cooling time, and minimum enrichment presented in Table 1.I.6 for HI-STAR HB.

#### 1.I.2.3.7 Criticality Payload Parameters

The neutron absorber's minimum  $^{10}\text{B}$  areal density loading for MPC-HB is specified in Table 1.I.2.

#### 1.I.2.3.8 Non-Fuel Hardware and Neutron Sources

None.

#### 1.I.2.3.9 Summary of Authorized Contents

Table 1.I.1 summarizes the key system data for the HI-STAR HB. Table 1.I.2 summarizes the key parameters and limits for the MPC-HB. Tables 1.I.4 and 1.I.7 and other tables referenced from these tables provide the limiting conditions for all material to be transported in the HI-STAR HB.

### 1.I.3 DESIGN CODE APPLICABILITY

Design code applicability for the HI-STAR HB is identical to HI-STAR 100 as presented in Section 1.3, except that the internal surfaces of the intermediate shells will not be coated with a silicone encapsulant due to its lower heat loads.

1.I.4 DRAWINGS

<b>Drawing Number/Sheet</b>	<b>Description</b>	<b>Rev.</b>
4082	Licensing Drawing for HI-STAR HB Overpack Assembly	8
4102	Licensing Drawing for MPC HB Enclosure Vessel	1
4103	Licensing Drawing for MPC HB Fuel Basket Assembly	6
4113	Licensing Drawing for Damaged Fuel Container	2
10447	HB Impact Limiter	0

[DRAWINGS ARE PROPRIETARY INFORMATION WITHHELD PER 10CFR2.390]

1.I.5 COMPLIANCE WITH 10CFR71

Same as in Section 1.5.

1.I.6 REFERENCES

Same as in Section 1.6.



Table 1.I.1

## SUMMARY OF KEY SYSTEM DATA FOR HI-STAR HB

PARAMETER	VALUE (Nominal)	
Types of MPCs in this Supplement	1	MPC HB
MPC capacity	MPC HB	<ul style="list-style-type: none"> <li>- Up to 80 intact and/or undamaged ZR Humboldt Bay fuel assemblies.</li> <li>- Up to 28 Damaged Fuel Assemblies/Fuel Debris in DFCs located in the peripheral basket cells, remaining cells loaded with intact and/or undamaged ZR Humboldt Bay fuel assemblies; or,</li> <li>- Up to 40 Damaged Fuel Assemblies/Fuel Debris in DFCs arranged in a checkerboard pattern with 40 intact and/or undamaged ZR Humboldt Bay fuel assemblies</li> </ul>

Table 1.I.2  
KEY PARAMETERS FOR MPC-HB

PARAMETER	VALUE (Nominal)
Unloaded MPC weight (lb)	See Table 2.I.2.1
Fixed neutron absorber (Metamic) $^{10}\text{B}$ loading density ( $\text{g}/\text{cm}^3$ )	0.01
Pre-disposal service life (years)	40
Design temperature, max. /min. ( $^{\circ}\text{F}$ )	725 $^{\circ}$ /-40 $^{\circ}$
Design Internal pressure (psig)	
Normal Conditions	100
Off-normal Conditions	100
Accident Conditions	200
Total heat load, max. (kW)	2
Maximum permissible peak fuel cladding temperature ( $^{\circ}\text{F}$ )	752 (Normal conditions) 1058 (Accident conditions)
MPC internal environment Helium filled (psig)	$\geq 0$ and $\leq 48.8$ psig at a reference temperature of 70 $^{\circ}\text{F}$
MPC external environment/overpack internal environment Helium filled initial pressure (psig, at STP)	$\geq 10$ and $\leq 14$
Maximum permissible reactivity including all uncertainty and biases	$<0.95$
End closure(s)	Welded
Fuel handling	Opening compatible with standard grapples
Heat dissipation	Passive

Table 1.I.3

HUMBOLDT BAY FUEL ASSEMBLIES EVALUATED TO DETERMINE DESIGN BASIS  
SNF

Assembly Class	Array Type	
Humboldt Bay	All 6x6	All 7x7

Table 1.I.4

HUMBOLDT BAY FUEL ASSEMBLY CHARACTERISTICS

Fuel Assembly Array/Class	6x6D	7x7C
Clad Material	ZR	ZR
Design Initial U (kg/assy.)	$\leq 78$	$\leq 78$
Initial Maximum Rod Enrichment (wt.% $^{235}\text{U}$ )	$\leq 4.0$ (see Note 1)	$\leq 4.0$
Maximum planar- average initial enrichment (wt.% $^{235}\text{U}$ )	$\leq 2.6$	$\leq 2.6$
No. of Fuel Rod Locations	36	49
Fuel Clad O.D. (in.)	$\geq 0.5585$	$\geq 0.4860$
Fuel Clad I.D. (in.)	$\leq 0.5050$	$\leq 0.426$
Fuel Pellet Dia. (in.)	$\leq 0.4880$	$\leq 0.4110$
Fuel Rod Pitch (in.)	$\leq 0.740$	$\leq 0.631$
Active Fuel Length (in.)	$\leq 80$	$\leq 80$
No. of Water Rods	0	0
Channel Thickness (in.)	$\leq 0.060$	$\leq 0.060$

Note 1: Two 6x6D assemblies contain one high power test rod with an initial enrichment of 5.5%.

Table 1.I.5

## DESIGN BASIS FUEL ASSEMBLY FOR EACH DESIGN CRITERION

<b>Criterion</b>	<b>MPC-HB</b>
Reactivity	6x6D and 7x7C
Shielding (Source Term)	6x6D
Fuel Assembly Effective Planar Thermal Conductivity	7x7C
Fuel Basket Effective Axial Thermal Conductivity	6x6D

Table 1.I.6

## HUMBOLDT BAY FUEL ASSEMBLY COOLING, AVERAGE BURNUP, AND MINIMUM ENRICHMENT LIMITS

<b>Post-irradiation Cooling Time (years)</b>	<b>Assembly Burnup (MWD/MTU)</b>	<b>Assembly Minimum Enrichment (wt. % <sup>235</sup>U)</b>
≥ 29	≤ 23,000	≥ 2.08

Table 1.I.7  
LIMITS FOR MATERIAL TO BE TRANSPORTED IN MPC-HB

PARAMETER	VALUE (Note 1)	
Fuel Type (Note 2)	Uranium oxide, HB BWR intact and/or undamaged fuel assemblies meeting the limits in Table 1.I.4 for the applicable array/class, with or without Zircaloy channels	Uranium oxide, HB BWR damaged fuel assemblies or fuel debris meeting the limits in Table 1.I.4 for array/class 6x6D or 7x7C with or without Zircaloy channels, placed in HB Damaged Fuel Containers (DFCs)
Cladding Type	ZR	ZR
Maximum Initial Enrichment	As specified in Table 1.I.4 for the applicable array/class	As specified in Table 1.I.4 for the applicable array/class
Post-irradiation Cooling Time, Average Burnup, and Minimum Initial Enrichment per Assembly	As specified in Table 1.I.6.	As specified in Table 1.I.6.
Decay Heat Per Assembly	$\leq 50$ Watts	Fuel debris up to a maximum of one equivalent fuel assembly is allowed (Note 4)
Fuel Assembly Length	$\leq 96.91$ in. (nominal design)	$\leq 96.91$ in. (nominal design)
Fuel Assembly Width	$\leq 4.70$ in. (nominal design)	$\leq 4.70$ in. (nominal design)
Fuel Assembly Weight	$\leq 400$ lbs (including channels)	$\leq 400$ lbs, (including channels and DFC)(Note 3)
Quantity per MPC	Up to 80 HB BWR intact and/or undamaged fuel assemblies	Up to 28 DFCs loaded in the peripheral cells of the basket with 52 intact and/or undamaged assemblies in the remainder (figure 6.I.3) <b>or</b> Up to 40 DFCs with 40 intact and/or undamaged assemblies loaded in a checkerboard pattern (figure 6.I.4)
Other Limitations	Stainless steel channels are not permitted.	

Table 1.I.7 (cont.)  
LIMITS FOR MATERIAL TO BE TRANSPORTED IN MPC-HB

Notes:

1. A fuel assembly must meet the requirements of any one column and the other limitations to be authorized for transportation.
2. Fuel assemblies with channels may be stored in any fuel cell location.
3. The total quantity of damaged fuel permitted in a single DAMAGED FUEL CONTAINER is limited to the equivalent weight and special nuclear material quantity of one intact or undamaged assembly.
4. Fuel debris in the form of loose debris consisting of zirconium clad pellets, stainless steel clad pellets, unclad pellets or rod segments up to a maximum of one equivalent fuel assembly is allowed. A maximum of 1.5 kg of stainless steel clad is allowed per cask.

# Security-Related Information Figure Withheld Under 10 CFR 2.390.

FIGURE 1.1.1

HOLTEC DAMAGED FUEL CONTAINER FOR HUMBOLDT BAY SNF IN MPC-HB

## SUPPLEMENT 1.II

### GENERAL DESCRIPTION OF THE HI-STAR HB GTCC PACKAGE WITH GWC-HB

#### 1.II.0 GENERAL INFORMATION

The HI-STAR 100 System has been expanded to include options specific for use at PG&E's Humboldt Bay (HB) plant for dry storage and future transportation of reactor-related non-fuel waste (NFW) which may be referred to as Greater-Than-Class C (GTCC) waste [1.0.8]<sup>1</sup>. However, any host site with radioactive waste that meets the specified allowable contents may also use the system. The HI-STAR 100 system now includes the HI-STAR 100 Version HB GTCC overpack (also called HI-STAR HB GTCC) and the GWC-HB multi-purpose canister. The HI-STAR HB GTCC packaging and its allowable contents comply with the requirements of 10CFR71 for a Type B(U)-96, fissile exempt, package. HI-STAR HB GTCC is fissile exempt per 10 CFR 71.15 (c)(1).

GWC-HB does not have a criticality function, heat load is negligible, and radiological source terms are substantially lower than the design basis fuel described in the main part of this chapter. However the GWC-HB enclosure vessel is credited as the sole containment boundary. The HI-STAR HB GTCC overpack provides structural protection and the majority of shielding for the system.

Unless otherwise indicated, the information pertaining to the HI-STAR HB GTCC System is generally contained in the "II" supplements to each chapter of this SAR. Certain sections of the main SAR are also affected and are appropriately modified for continuity with the "II" supplements. Unless superseded or specifically modified by information in the "II" supplements, the information in the main SAR is applicable to the HI-STAR HB GTCC System for use at HB host site. Supplement II may make certain references to Supplement I when appropriate, for example, both Supplements share the same impact limiter drawing.

#### 1.II.0.1 Engineering Change Orders

The changes authorized by Holtec Engineering Change Orders (ECOs) for the following licensed components are reflected in this revision of this SAR.

HI-STAR HB GTCC overpack: New drawing.

GWC-HB: New drawing.

Ancillary Equipment:

- HB Impact Limiter: See Section 1.I.4

---

<sup>1</sup> See Glossary for the definition of GTCC Waste. For the purposes of this transport SAR supplement, the term GTCC Waste is loosely used as a convenient way to describe the waste contents and should not to be interpreted as an official characterization or specification of the waste contents.



## 1.II.1 INTRODUCTION

The HI-STAR 100 System as deployed at Humboldt Bay consists of a HI-STAR HB GTCC overpack, a GWC-HB multi-purpose canister, and custom AL-STAR impact limiters. The GWC-HB consists of an enclosure vessel with built-in primary and secondary waste baskets. The packaging is described below with key parameters presented in Table 1.II.1. The NFW specifications are discussed Subsection 1.II.2.3 and approved contents are summarized in Table 1.II.1. Section 1.II.3 provides the design code applicability and details any alternatives to the ASME Code if different than HI-STAR 100 or HI-STAR 100 Version HB. All discussions are supplemented by a set of drawings in Section 1.II.4.

## 1.II.2 PACKAGE DESCRIPTION

### 1.II.2.1 Packaging

The HI-STAR HB GTCC package is designed to maintain loadings from hypothetical 30 foot (9 meter) to 60gs or less. The structural integrity safety cases for GWC enclosure vessel to serve as a containment vessel and for the HI-STAR HB GTCC overpack to serve as shielding and structural protection to the GWC, have been independently qualified in Supplement 2.II. The AL-STAR impact limiters qualified for HI-STAR HB GTCC with GWC-HB are the same impact limiters qualified for HI-STAR HB with MPC-HB (see Supplement I).

GWC-HB is vacuum dried, backfilled with helium and leak tested by hydrostatic pressure test while the HI-STAR HB GTCC overpack is not vacuum dried, helium backfilled or pressure tested. Instead the overpack closure lid is placed with ambient air in the overpack and the closure lid features no containment seal(s).

A personnel barrier is not required for the HI-STAR HB GTCC Package.

#### 1.II.2.1.1 Gross Weight

Table 2.II.2.1 summarizes the maximum calculated weights for the HI-STAR HB GTCC overpack, impact limiters, and GWC-HB loaded to maximum capacity with approved contents. Table 2.II.2.1 also provides the location of the center of gravity of the fully loaded package.

#### 1.II.2.1.2 Materials of Construction, Dimensions, and Fabrication

Specific materials of construction along with outline dimensions for important-to safety items are provided in the drawings in Section 1.II.4.

##### 1.II.2.1.2.1 HI-STAR HB GTCC Overpack

The HI-STAR HB GTCC overpack is a heavy-walled, steel cylindrical vessel identical to the standard HI-STAR 100 overpack, except that the outer overpack and inner cavity heights are approximately 128 and 115 inches, respectively, the monolithic neutron shield (and associated

steel support structure) surrounding the cask body has been removed, the closure lid does not feature a containment seal or other type of seal, and the only penetration is the drain port.

All major HI-STAR HB GTCC overpack dimensions and features, such as cask inside diameter, major component thicknesses, closure lid design, top flange design, inner shell design, bottom baseplate design and lifting trunnion design are identical or nearly identical to the standard HI-STAR 100. Furthermore, all major materials of construction of important to safety components are the same as the standard HI-STAR 100. The design of the overpack lifting features, lifting trunnions (also referred to as ILPs), are identical to the HI-STAR HB and standard HI-STAR 100 for operational compatibility and ALARA.

#### 1.II.2.1.2.2 GWC-HB

GWC-HB is a welded cylindrical structure with flat ends in the same manner as the standard MPC. The outer diameter of the GWC HB is identical to the standard MPCs and MPC-HB. At approximately 114 inches high, GWC-HB is shorter than the standard MPC but approximately the same height as MPC-HB. The GWC lid and closure ring are the same thickness, material (Alloy X enclosure vessel), design and weldment configuration as the standard MPC. GWC-HB baseplate is significantly thicker than the standard MPC. Thus from a structural perspective, the GWC-HB is equivalent to or more robust than the standard MPC. The design of the GWC lifting features, TALs (also referred to as ILPs), are identical to the MPC-HB and standard MPC for operational compatibility and ALARA.

GWC-HB is a multi-purpose canister customized to accommodate Humboldt Bay NFW, more specifically, reactor-related GTCC waste in solid form. The GWC-HB features a primary waste basket (referred to as the Inner Shell in the drawing package in Section 1.II.4) consisting of a cylindrical shell weldment that is affixed to the GWC baseplate by an all-around weld. The primary waste basket is conservatively classified as important-to-safety; however, the waste basket serves no direct safety function and the package complies with regulatory radiation level limits even if the primary waste basket was assumed to not be present (See Supplement 5.II for further discussion). Lastly, GWC-HB does not employ criticality control features due to limited quantities of fissile material per 10 CFR 71.15 (a); therefore the primary function of the GWC-HB is containment, a function that is provided by the enclosure vessel.

GWC-HB also features a secondary waste basket (referred to as the Waste Pipe in the drawing package in Section 1.II.4). The secondary waste basket features a baseplate and closure lid and is designed to house a process waste container (PWC), a secondary container. The secondary waste basket is not-important-to-safety. The process waste container (PWC) is described in Table 1.II.1. Process waste specifications are discussed in Subsection 1.II.2.3.

#### 1.II.2.1.3 Impact Limiters

The impact limiter evaluated is the HI-STAR 100 Impact Limiter Version HB (also called HB Impact Limiter) provided in the drawing package in Section 1.I.4. HB impact limiter (a customized version of the standard HI-STAR 100 impact limiter) is qualified for the HI-STAR HB Package (Supplement I) and the HI-STAR HB GTCC Package (Supplement II). HB Impact

Limiter features a longer outer crush section (shown in the standard impact limiter as Section Type 4) and does not require Holtite; otherwise the impact limiters are the same design. The evaluation of HB Impact Limiter is documented in Supplement 2.II.

#### 1.II.2.1.4 Heat Dissipation

The HI-STAR HB GTCC Package can safely transport NFW waste by maintaining NFW waste component temperatures at least 50% below their melting point (See Table 1.II.1), although the package payload heat load, specified in Table 1.II.1, is negligible. Safety evaluations assume conservative temperatures and pressures (structural and containment safety evaluations may use conservative values with respect to temperature and pressure such as those for reported for standard MPCs as deemed appropriate). The total decay heat of the GTCC waste is conservatively overstated in Table 1.II.1. The HI-STAR HB GTCC Package does not require an engineered personnel barrier to comply with the temperature limits of 10CFR71.43(g) under exclusive use shipment.

#### 1.II.2.1.5 Pressure Relief Systems

No pressure relief system is provided on the HI-STAR HB GTCC overpack for pressure relief of its cavity space. The overpack does not provide a containment function and does not feature containment seals but is nevertheless evaluated as a pressure vessel in Supplement 2.II. No pressure relief system is provided on the GWC containment boundary. Therefore, there is no pressure relief device that would allow the release of radioactive material under the tests specified in 10CFR71.73. Analyses that demonstrate that the HI-STAR 100 packaging complies with the requirements of Subparts E and F of 10CFR71 are provided in this SAR.

#### 1.II.2.2 Operational Features

The sequence of essential operations necessary to load fuel and prepare the HI-STAR HB GTCC system for transport is provided in Supplement 7.II. As a brief summary, the overpack and the GWC are placed in a pool for loading NFW. A process waste container, containing process waste material, is placed in the GWC secondary waste basket, the reactor-related NFW is placed in the GWC. The lid is placed on the GWC. The overpack is removed from the pool, the GWC closure lid is welded and the GWC is pressure tested per ASME Code. The GWC is vacuum dried, backfilled with helium and the GWC closure ring is welded. The overpack is drained of water and the closure lid is bolted. Impact limiters are attached to each end of the cask to complete the assembly of the transport package.

#### 1.II.2.3 Contents of Package

The HI-STAR HB GTCC Package is classified as a Type B package under 10CFR71. The maximum activity of the GWC requires that the package be classified as Category II package in accordance with Regulatory Guide 7.9 [1.0.3]. Nevertheless codes and standards for package design are conservatively established consistent with Category I packages, namely HI-STAR HB and HI-STAR 100.

This section delineates the authorized contents permitted for shipment in the HI-STAR HB GTCC, including the general waste type, typical waste descriptions, radioactive material limits, heat load, weight limitations and other applicable requirements, as summarized in Table 1.II.1.

The general waste type and typical components are provided in Table 1.II.1. The NFW consists of segmented solid radiation-activated and surface-contaminated reactor related hardware and canisterized process waste. The large majority of the NFW mass is stainless steel (typically type 304) and a small portion of the contents may include process waste with limited Special Nuclear Material (SNM) as specified in Table 1.II.1. The reactor-related components are typically cut and segmented with the objective to provide good packing density of the GWC and is typically in the form of neutron activated metals and metal oxides in solid form. Surface contamination is expected and may include contaminants from pool water exposure, crud from reactor operations and fine chips from cutting operations.

Process waste is stored in a separate stainless steel container, a secondary container referred to as a Process Waste Container (PWC). Additional “inner containers” may be stored in the PWC. These “inner containers” may be made from steel and/or aluminum. The PWC (and other “inner containers” if used) is a not-important-to-safety mechanically-sealed, vacuum dried, helium-backfilled and leak-tested separate canister that provides no safety function for transportation. The process waste is thermally processed (e.g. by dry-ashing) to remove organics and other hydrogen bearing components to produce a dry concentrated residue. The PWC maintains a hydrogen concentration of less than 5 percent by volume of the PWC void space (the void space of the GWC enclosure vessel is significantly larger).

The allowable contents do not contain or produce gaseous products and will be dried within the GWC according to the operating procedures in SAR Supplement 7.II; therefore without the presence of significant moisture, the potential for production of significant quantity of combustible gases by radiolysis or the possibility of significant chemical or galvanic reactions with the stainless steel canister is expected to be insignificant. Consequently there is no pressure increase due to gas generation.

The packaging contents and dunnage (if used) are configured to ensure or conservatively improve packaging effectiveness and ALARA using the following methods.

- Components with high specific activity are generally placed near the center of the canister, when practical.
- Each canister is essentially filled to volumetric capacity to the extent practical to mitigate significant shifting of the contents during transport. If the canister is not filled to capacity with GTCC waste then appropriate dunnage may be used to prevent significant movement of the contents. The dunnage shall be made from stainless steel. The weight of dunnage and allowable contents shall not exceed the maximum permissible weight in Table 1.II.1.

### 1.II.3 DESIGN CODE APPLICABILITY

The ASME Boiler and Pressure Vessel Code (ASME Code), 1995 Edition with Addenda through 1997 [1.3.1], is the governing code for the construction of the HI-STAR HB GTCC System. The

list of ASME Code Alternatives per Table 1.3.2 provides clarification as applicable (e.g. the ASME code exceptions for the MPC apply to the GWC where appropriate equivalency exists between Subsection NB and Subsection ND). The ASME Code is applied to each component consistent with the function of the component. Each structure, system and component (SSC) of the HI-STAR 100 GTCC Package labeled Important to Safety (ITS) is provided in the drawing package in Section 1.II.4.

Table 8.II.1 lists the applicable ASME Code section and paragraph for material procurement, design, fabrication and inspection of the components of HI-STAR HB GTCC and GWC HB that are governed by the ASME Code. The ASME Code section listed in the design column is the section used to define allowable stresses for structural analyses.

The GWC is classified as important to safety. The GWC structural components only includes the enclosure vessel. The primary and secondary waste baskets do not perform important to safety functions.

The threaded holes in the GWC lid are designed in accordance with the requirements of NUREG-0612 and Regulatory Guide 3.61 to facilitate vertical GWC transfer.

The GWC closure welds are partial penetration welds that are structurally qualified by analysis, as presented in Chapter 2. The GWC closure ring welds are inspected by performing a liquid penetrant examination of the root pass (if more than one weld pass is required) and final weld surface, in accordance with the requirements contained in Section 8.1. The GWC lid weld may be examined by either volumetric or multi-layer liquid penetrant examination. If volumetric examination is used, it shall be the ultrasonic method and shall include a liquid penetrant examination of the root and final weld layers. If multi-layer liquid penetrant examination is used alone, at a minimum, it must include the root and final weld layers and each approximately 3/8 inch of weld to detect critical weld flaws. The integrity of the GWC lid weld is further verified by performing a pressure test (hydrostatic) in accordance with the requirements contained in Section 8.1.

The structural analysis of the GWC, in conjunction with the redundant closures and nondestructive examination, and pressure testing performed during GWC fabrication and GWC closure, provides assurance of canister closure integrity in lieu of the specific weld joint requirements of the ASME Code, Section III, Subsection ND.

The HI-STAR overpack is classified as important to safety. The HI-STAR overpack top flange, closure plate, inner shell, and bottom plate are designed and fabricated in accordance with the requirements of ASME Code, Section III, Subsection NB, to the maximum extent practical (see Table 1.3.2). The overpack closure bolts are also ASME Code Subsection NB components. The remainder of the HI-STAR overpack steel structure is non-code; however, the design follows the requirements of ASME Code, Section III, Subsection NF, as clarified in Chapter 2, Supplement 2.II, to the maximum extent practical (see Table 1.3.2).

1.II.4 DRAWINGS

<b>Drawing Number/Sheet</b>	<b>Description</b>	<b>Rev.</b>
10315	Licensing Drawing for HI-STAR HB GTCC Overpack Assembly	0
10316	Licensing Drawing for GWC HB	0
10447 See Section 1.I.4	HB Impact Limiters	See Section 1.I.4

[DRAWINGS ARE PROPRIETARY INFORMATION WITHHELD PER 10CFR2.390]

1.II.5 COMPLIANCE WITH 10CFR71

Same as in Section 1.5.

1.II.6 REFERENCES

Same as in Section 1.6.

Table 1.II.1 (Sheet 1 of 2)

## KEY CHARACTERISTICS FOR HI-STAR HB GTCC PACKAGE CONTENTS

Parameter	Data
General Description of Non-Fuel Waste (NFW)	Fissile-exempt reactor-related waste in solid form irradiated in a commercial light water reactor.
Typical Waste Components (see Note 1)	<u>Activated Metals</u> <ul style="list-style-type: none"> <li>- Reactor Vessel Internals</li> <li>- Upper Core Shroud</li> <li>- Lower Chimney (aka Upper Core Guide)</li> <li>- Lower Chimney Hangars</li> </ul> <p>Crud from long-term reactor operations will be present on certain component surfaces, other components may be contaminated due to spent fuel pool water exposure and cross-contamination.</p>
	<u>Process Waste:</u> <ul style="list-style-type: none"> <li>- Special Nuclear Material (SNM)</li> <li>- Resins</li> <li>- Metallic Oxides</li> <li>- Stellite particles</li> <li>- Fuel debris fines</li> </ul>
	(See Note 2)
Maximum permissible quantity of fissile material (including SNM)	19 grams (See Note 3)
Co-60 Activity Limit (Package Payload)	381 curies ( $1.41 \times 10^{13}$ Bq)
Co-60 Type A Quantity (Package Payload)	$A_2 \leq 35.3$
Co-60 Specific Activity Limit (Package Payload)	$6 \times 10^{-4}$ curies/gram
Process Waste Specific Activity Limit (Process Waste Container Payload)	$1 \times 10^{-3}$ curies/gram
Minimum Cooling Time (Package Payload)	1 yr (See Note 4)
Maximum Heat Load (Package Payload)	Negligible (0.01 kW) (See Note 5)
Maximum Permissible Weight of GWC Content (including stainless steel dunnage if used)	4000 lb (1815 kg)
Maximum permissible GTCC Waste temperature	Below 50% of melting point of steel (See Note 5)

TABLE 1.II.1 (Sheet 2 of 2)

## KEY CHARACTERISTICS FOR HI-STAR HB GTCC PACKAGE CONTENTS

## Notes:

1. The reactor-related GTCC waste contents, although mostly activated metals, fall under two general categories (Activated metals and Process wastes). The term GTCC is a waste classification defined in 10CFR60 and used in this SAR only as a convenient means to describe the waste in a general manner. The contents may include fissile materials provided the mass limits of 10CFR71.15(c)(1) are not exceeded (maximum permissible quantity of fissile material and Note 3).
2. The process waste is debris material representative of typical material collected from spent fuel pool cleanup including material generated as a result of cladding failures. SNM is defined in the glossary of this SAR. The process waste consists of waste pieces typically less than ¼ inch in size and may include fines; therefore, for conservatism, the process waste is conservatively characterized as dispersible solids (i.e. particles with diameters less than about 100 µm per NUREG/CR-6487 [4.03]) for containment evaluation purposes.
3. Fissile material and SNM are defined in the glossary of this SAR. For simplicity, all SNM is assumed to be fissile material. For full compliance with 10CFR71.15(c)(1), each gram of fissile material shall be distributed within 2,000 grams of contiguous solid non-fissile material.
4. The minimum cooling time cited is a requirement independent of other waste characteristics (i.e. activity and heat load).
5. The heat load is negligible relative to the mass, size of the package and package materials of construction. For general safety evaluations of hot conditions, normal operating temperature and pressure of reported in Table 1.II.2 may be assumed for the GWC per NUREG 6487, Section 4.2. For hypothetical fire event evaluations purposes nominal component temperatures reported in Supplement I (for the HI-STAR HB package) may be assumed for the GWC. Higher or lower temperatures and pressures may be used with appropriate justification (see safety evaluations contained in Supplement II).



Table 1.II.2  
KEY PARAMETERS FOR HI-STAR HB GTCC PACKAGE with GWC-HB

Parameter	Data
Category Designation for Type B Package	Category II (Based on Table 2-1 of RG 7.9 [1.0.3])
Design life	40 years
Design (Normal) Ambient Temperatures, max. /min.	+38°C (+100°F)  -40°C (-40°F) for extreme cold temperatures
Maximum Normal Operating Pressure (MNOP) and Temperature of the GWC	17.94 psig 150°F (65.5°C) (Note 1)
Design Internal Pressure of HI-STAR Overpack  Normal Conditions Accident Condition	  17.94 psig 25 psig (Note 2)
Design Internal Pressure of GWC Enclosure Vessel  Normal Conditions Accident Conditions	  100 psig 200 psig (Note 3)
Total heat load, max.	See Table 1.II.1
GWC internal environment 99% helium purity fill pressure (Pressure range is at a reference temperature of 21,1°C or 70°F):  Minimum Pressure Maximum Pressure	  10 psig 15 psig
GWC external environment/HI-STAR overpack internal ambient air environment	Ambient 0 kPa gauge (0 psig)
End Closure(s)	Welded
GTCC Waste Handling	Opening compatible with waste handling equipment/grapples
Heat Dissipation	Passive

## Notes:

1. NUREG 6487, Section 4.2 recommends a pressure of 1.2 atmospheres and a temperature of 150 F for radioactive contents that provide no appreciable heat load for packages loaded at 1 atmosphere. The pressure reported has been adjusted to account for the initial GWC backfill pressure.
2. The HI-STAR overpack does not provide a containment or pressure boundary function (it is not sealed by a closure lid containment seal); nevertheless a design internal pressure equal to the GWC MNOP is specified for conservative structural analysis purposes.
3. The design pressures are set significantly higher than the MNOP for conservatism. The hydrostatic test pressure of 125% of the GWC design pressure is significantly higher than a test pressure of 150% of the MNOP and therefore results in a conservative leakage rate test of the GWC lid-to-shell weld.

FIGURE 1.II.1  
[PROPRIETARY INFORMATION WITHHELD PER 10CFR2.390]

## SUPPLEMENT 1.III

### GENERAL DESCRIPTION OF THE HI-STAR 100 PACKAGE WITH DIABLO CANYON MPC-32

#### 1.III.0 GENERAL INFORMATION

The HI-STAR 100 System has been expanded to include options specific for use with Diablo Canyon nuclear plant (DCNPP) spent nuclear fuel for dry storage and future transportation [1.0.9]. DCNPP fuel assemblies are shorter in length than typical PWR fuel assemblies. As a result, the HI-STAR 100 system now includes an MPC for use with DCNPP contents referred to as Diablo Canyon MPC-32. The DCNPP contents (fuel and non-fuel hardware) are qualified generically for loading in both the standard length MPC-32 as well as the Diablo Canyon MPC-32. Information pertaining to the Diablo Canyon MPC-32 is generally contained in the “III” supplements to each chapter of this SAR (approved contents are provided in the main SAR). Certain sections of the main SAR are also affected and are appropriately modified for continuity with the “III” supplements. Unless superseded or specifically modified by information in the “III” supplements, the information in the main SAR is applicable to the HI-STAR System for use with Diablo Canyon MPC-32.

##### 1.III.0.1 Engineering Change Orders

The changes authorized by Holtec Engineering Change Orders (ECOs) for the following licensed components are reflected in this revision of this SAR.

HI-STAR 100 overpack: See SAR Section 1.4

Diablo Canyon MPC-32 Fuel Basket: New drawing

Diablo Canyon Enclosure Vessel: New drawing

Ancillary Equipment:

- AL-STAR Impact Limiters: See SAR Section 1.4
- MPC Spacer: See SAR Section 1.4

#### 1.III.1 INTRODUCTION

The HI-STAR 100 System for transporting DCNPP fuel consists of a HI-STAR 100 overpack with Diablo Canyon MPC-32, a Diablo Canyon MPC-32 that includes a compatible fuel basket assembly and HI-STAR 100 AL-STAR impact limiters. The Diablo Canyon MPC-32 specific components are described below and all other packaging components are described in the main SAR. Section 1.III.3 provides the packaging code applicability and details any alternatives to the ASME Code if different than HI-STAR 100 in the main SAR. All discussion is supplemented by a set of drawings in Section 1.III.4.

## 1.III.2 PACKAGE DESCRIPTION

### 1.III.2.1 Packaging

#### 1.III.2.1.1 Gross Weight

Table 2.III.2.1 summarizes the maximum calculated weights for the HI-STAR 100 overpack, impact limiters, and Diablo Canyon MPC-32 loaded to maximum capacity with design basis SNF and with the MPC Spacer located over the MPC lid. Table 2.III.2.1 also provides the location of the center of gravity of the fully loaded package.

#### 1.III.2.1.2 Materials of Construction, Dimensions, and Fabrication

The specific materials of construction, along with outline dimensions for important-to safety items, of the Diablo Canyon MPC-32 are provided in the drawing package in Section 1.III.4.

##### 1.III.2.1.2.1 HI-STAR 100 Overpack

The transport overpack model evaluated is the HI-STAR 100 Overpack. The HI-STAR 100 accommodates the Diablo Canyon MPC-32 and an MPC Spacer customized for the Diablo Canyon MPC-32. The HI-STAR 100 Overpack description in Section 1.2 is applicable to this supplement. A drawing package for the HI-STAR 100 Overpack is provided in Section 1.4.

##### 1.III.2.1.2.2 Diablo Canyon MPC-32

The MPC model evaluated is Diablo Canyon MPC-32. Diablo Canyon MPC-32 is identical to the generic MPC-32 except it is shorter. Furthermore the fuel spacer design is different as discussed later in this Subparagraph. All other major dimensions and features, such as diameter, wall thickness, closure design, closure lid and baseplate thicknesses, basket panel thicknesses, etc. are maintained identical to the standard design. Therefore, from a structural perspective, the MPC-32 will be equivalent or due to its shorter length even more robust than the generic MPC-32.

The MPC-32 is designed to accommodate up to thirty-two (32) PWR undamaged fuel assemblies with or without non-fuel hardware and/or neutron sources meeting the specifications in Subsection 1.III.2.3. Key parameters for the Diablo Canyon MPC-32 are outlined in Table 1.III.1.

To accommodate the shorter MPC-32 in a standard-length HI-STAR 100 overpack a generic MPC Spacer Ring is designed for installation inside the overpack and above MPC closure lid (see drawing package in Section 1.III.4). The MPC Spacer Ring is a non-code component. Its shim style design eliminates all critical structure failure modes that could challenge its structural function (e.g. the MPC spacer ring is not prone to buckling or weldment failure or failure by compression). Compression performance of the MPC Spacer Ring under normal and hypothetical accident conditions is evaluated in Section 2.III.7 and the results show significant

safety margins. Due to its immunity to structural failure and its non-critical role in other safety evaluations the MPC Spacer Ring is classified as Not Important to Safety.

The center four fuel basket cell locations are provided with removable/adjustable fuel spacers attached to the bottom of the MPC closure lid to accommodate either different length fuel assemblies or assemblies with certain non-fuel hardware that requires the extra length. All other cell locations are provided with fixed length fuel spacers permanently affixed to the bottom of the MPC closure lid. Consistent with Paragraph 1.2.3.4 in the main chapter, an axial clearance of approximately two inches is provided to account for the irradiation and thermal growth of the fuel assemblies for all fuel basket cell locations. See the drawing package in Section 1.III.4.

#### 1.III.2.1.3 Impact Limiters

The Impact Limiter model evaluated is the AL-STAR Impact Limiter. The AL-STAR Impact Limiter description in Section 1.2 is applicable to this supplement. A drawing package for the AL-STAR Impact Limiter is provided in Section 1.4.

#### 1.III.2.2 Operational Features

The discussion on operational features in Section 1.2 is applicable to this supplement.

#### 1.III.2.3 Contents of Package

SAR Subsection 1.2.3 delineates the authorized contents permitted for shipment in the HI-STAR 100 with Diablo Canyon MPC-32, including fuel assembly types; non-fuel hardware; neutron sources; physical parameter limits for fuel assemblies and sub-components; enrichment, burnup, cooling time, and decay heat limits; location requirements; and requirements for canning the material, as applicable. The content authorized for Diablo Canyon MPC-32 is set in Table 1.III.2 with many requirements set in Table 1.2.27.

##### 1.III.2.3.1 Determination of Design Basis Fuel

The discussion in SAR Paragraph 1.2.3.1 is applicable to this supplement.

##### 1.III.2.3.2 Design Payload for Intact and/or Undamaged Fuel

The discussion in SAR Paragraph 1.2.3.2 is applicable to this supplement.

##### 1.III.2.3.3 Design Payload for Damaged Fuel and Fuel Debris

The discussion in SAR Paragraph 1.2.3.1 is applicable to this supplement.

##### 1.III.2.3.4 Structural Payload Parameters

The discussion in SAR Paragraph 1.2.3.4 is applicable to this supplement.

#### 1.III.2.3.5 Thermal Payload Parameters

Table 1.III.1 provides the maximum heat generation for all fuel assemblies authorized for transportation in the HI-STAR 100 with Diablo Canyon MPC-32.

#### 1.III.2.3.6 Radiological Payload Parameters

The discussion in SAR Paragraph 1.2.3.6 is applicable to this supplement.

#### 1.III.2.3.7 Criticality Payload Parameters

The neutron absorber's minimum  $^{10}\text{B}$  areal density loading for Diablo Canyon MPC-32 is specified in Table 1.III.1.

#### 1.III.2.3.8 Non-Fuel Hardware and Neutron Sources

Allowable non-fuel hardware and neutron sources are specified in Table 1.2.27 and Table 1.III.2.

#### 1.III.2.3.9 Summary of Authorized Contents

Table 1.III.1 summarizes key package parameters and Table 1.III.2 summarizes the limits for material to be transported.

### 1.III.3 DESIGN CODE APPLICABILITY

Same as in Section 1.3.

### 1.III.4 DRAWINGS

<b>Drawing Number/Sheet</b>	<b>Description</b>	<b>Rev.</b>
3913 See Section 1.4	Licensing Drawing for HI-STAR 100 Overpack Assembly	See Section 1.4
4459	Licensing Drawing for MPC-32 Diablo Canyon Enclosure Vessel	14
4458	Licensing Drawing for MPC-32 Diablo Canyon Fuel Basket Assembly	11
10341 See Section 1.4	Licensing Drawing for MPC Spacer Ring	See Section 1.4

[DRAWINGS ARE PROPRIETARY INFORMATION WITHHELD PER 10CFR2.390]

1.III.5        COMPLIANCE WITH 10CFR71

Same as in Section 1.5.

1.III.6        REFERENCES

Same as in Section 1.6.

Table 1.III.1  
KEY PARAMETERS FOR HI-STAR 100 WITH DIABLO CANYON MPC-32

PARAMETER	HI-STAR 100 WITH DIABLO CANYON MPC-32
Unloaded MPC weight (lb)	See Table 1.2.3
Minimum Boral neutron absorber $^{10}\text{B}$ loading ( $\text{g}/\text{cm}^2$ )	See Table 1.2.3 (same as standard MPC-32)
Minimum Metamic neutron absorber $^{10}\text{B}$ loading ( $\text{g}/\text{cm}^2$ )	See Table 1.2.3 (same as standard MPC-32)
Pre-disposal service life (years)	See Table 1.2.3
Design temperature, max./min. ( $^{\circ}\text{F}$ )	See Table 1.2.3
Design Internal pressure (psig)  Normal Conditions Off-normal Conditions Accident Conditions	See Table 1.2.3
Total heat load, max. (kW)	18
Maximum permissible peak fuel cladding temperature ( $^{\circ}\text{F}$ )	See Table 1.2.3
MPC internal environment Helium filled (psig)	$\geq 0$ and $\leq 40$ psig at a reference temperature of $70^{\circ}\text{F}$
MPC external environment/overpack internal environment Helium filled initial pressure (psig, at STP)	See Table 1.2.3
Maximum permissible reactivity including all uncertainty and biases	See Table 1.2.3
End closure(s)	See Table 1.2.3
Fuel handling	See Table 1.2.3
Heat dissipation	See Table 1.2.3



Table 1.III.2 (Sheet 1 of 2)  
LIMITS FOR MATERIAL TO BE TRANSPORTED IN DIABLO CANYON MPC-32

PARAMETER	VALUE
Fuel Type	Uranium oxide, PWR intact fuel assemblies meeting the limits in Table 1.2.10 for array/class 17x17A and array/class 17x17B (subclasses 17x17B01 and 17x17B06 as modified by SAR Table 6.III.1)
Cladding Type	See Table 1.2.27
Maximum Initial Enrichment	See Table 1.2.27
Post-irradiation Cooling Time, Average Burnup, and Minimum Initial Enrichment per Assembly	See Table 1.2.27
Decay Heat Per Assembly	$\leq 562.5$ Watts
Minimum Burnup per Assembly	As specified in Table 1.II.3
Fuel Assembly Length	$\leq 166.9$ in. (nominal design)
Fuel Assembly Width	See Table 1.2.27
Fuel Assembly Weight	$\leq 1,621$ lbs including non-fuel hardware and neutron sources
Operating Parameters During Irradiation of the Assembly (See Subsection 6.III.2.3)	
Average in-core soluble boron concentration	See Table 6.III.2
Average Moderator Temperature	See Table 6.III.2
Average Specific Power	See Table 6.III.2
In-Pool Minimum Soluble Boron Required by Burnup Verification Method B During Loading and Unloading (See Subparagraph 1.2.3.7.2)	See Table 1.2.27

Table 1.III.2 (Sheet 2 of 2)  
LIMITS FOR MATERIAL TO BE TRANSPORTED IN DIABLO CANYON MPC-32

PARAMETER	VALUE
Other Limitations	<p style="text-align: center;">See Table 1.2.27</p> <p>The following additional limitations also apply:</p> <ul style="list-style-type: none"> <li>▪ The total number of BPRA's, TPDs and RCCAs is limited to 25.</li> <li>▪ Fuel assemblies with or without ITTRs, containing RCCAs or NSAs must be loaded in fuel storage locations 13, 14, 19 and/or 20 (the fuel storage location numbers are provided in Figure 1.2.4).</li> </ul>

Table 1.III.3

**FUEL ASSEMBLY MAXIMUM ENRICHMENT AND MINIMUM BURNUP  
REQUIREMENTS FOR TRANSPORTATION IN DIABLO CANYON MPC-32**

<b>FUEL ASSEMBLY ARRAY/CLASS</b>	<b>CONFIGURATION (Note 2)</b>	<b>MINIMUM BURNUP (B) AS A FUNCTION OF INITIAL ENRICHMENT (E) (Note 1)  (GWD/MTU)</b>
17X17A (Note 3)	A	See SAR Table 6.III.4
17x17B (subclasses 17X17B01 and 17X17B06)  (Note 4)	A	See SAR Table 6.III.4.

## Notes:

1. E = Initial enrichment, i.e., for 4.05wt. %, E = 4.05. Maximum initial enrichment as specified in Table 1.III.2.
2. See Table 1.2.37
3. Array/classes 17x17A characteristics per SAR Table 1.2.10.
4. Array/Subclasses 17x17B01 and 17x17B06 characteristics are defined by Array/classes 17x17B characteristics per Table 1.2.10 with certain parameters modified per SAR Table 6.III.1.

## CHAPTER 2: STRUCTURAL EVALUATION

This chapter presents a synopsis of the evaluations carried out to establish the mechanical and structural characteristics of the HI-STAR 100 package as they pertain to demonstrating compliance with the provisions of 10CFR71. All required structural design analyses of the packaging, components, and systems Important to Safety (ITS) pursuant to the provisions of 10CFR71 are documented in this chapter. The objectives of this chapter are twofold:

- a. To demonstrate that the structural performance of the HI-STAR 100 package has been adequately evaluated for the conditions specified under normal conditions of transport and hypothetical accident conditions.
- b. To demonstrate that the HI-STAR 100 package design has adequate structural integrity to meet the regulatory requirements of 10CFR71 [2.1.1].

To facilitate regulatory review, the assumptions and conservatism inherent in the analyses are identified along with a complete description of the analytical methods, models, and acceptance criteria. A summary of other considerations germane to satisfactory structural performance, such as corrosion and material fracture toughness is also provided.

This SAR is written to conform to the requirements of NUREG-1617 and 10CFR71 and follows the format of Regulatory Guide 7.9 [1.0.3]. It is noted that the areas of NRC staff technical inquiries with respect to 10CFR71 structural compliance span a wide array of technical topics within and beyond the material in this chapter. To facilitate the staff's review, Table 2.0.1 "Matrix of NUREG-1617/10CFR71 Compliance - Structural Review", is included in this chapter. A comprehensive cross-reference of the topical areas set forth in Section 2.3.2 (Regulatory Requirements) of the draft Regulatory Guide 1617, along with the sponsoring paragraphs in 10CFR71, and the location of the required compliance information, within this SAR, is contained in Table 2.0.1.

Section 2.10.2 contains a summary of the evaluation findings derived from the technical information presented in this chapter.

TABLE 2.0.1- MATRIX OF NUREG-1617/10CFR71 COMPLIANCE – STRUCTURAL REVIEW<sup>†</sup>

SECTION IN NUREG-1617 AND APPLICABLE 10CFR71/REG.GUIDE (R.G.) SECTIONS	NUREG-1617/10CFR71 COMPLIANCE ITEM	LOCATION IN SAR CHAPTER 2	LOCATION OUTSIDE OF SAR CHAPTER
<b>2.3.1 Description of Structural Design</b>			
10CFR71.31(a)(1); 10CFR71.33	Description of Structural Design	2.1	1.2.3
10CFR71.33	Drawings		1.4
10CFR71.33	Weights and Center of Gravity	2.2	
10CFR71.31(c)	Applicable Codes/Standards		1.3
<b>2.3.2 Material Properties</b>			
10CFR71.33	Materials and Material Specifications	2.3	
10CFR71.33	Prevention of Chemical, Galvanic, or Other Reactions	2.4	
10CFR71.43(d)	Effects of Radiation on Materials	2.4.4	

TABLE 2.0.1- MATRIX OF NUREG-1617/10CFR71 COMPLIANCE – STRUCTURAL REVIEW (Continued)

SECTION IN NUREG-1617 AND APPLICABLE 10CFR71/REG.GUIDE (R.G.) SECTIONS	NUREG-1617/10CFR71 COMPLIANCE ITEM	LOCATION IN SAR CHAPTER 2	LOCATION OUTSIDE OF SAR CHAPTER
R.G 7.11, 7.12	Brittle Fracture	2.1.2.3	
<b>2.3.3 Lifting and Tie Down Standards for All Packages</b>			
10CFR71.45(a)	Lifting Devices	2.5	1.4
10CFR71.45(b)	Tie-Down Devices	2.5	1.4
<b>2.3.4 General Considerations for Structural Evaluation of Packaging</b>			
10CFR71, Subpart E,F	Evaluation by Analysis		
10CFR71.35(a), 71.41(a)	• Models, Methods, and Results	2.6, 2.7.1, 2.7.2	
10CFR71, Subpart E,F	• Material Properties	2.3	
“	• Boundary Conditions	2.6	
“	• Dynamic Amplifiers	2.6, 2.7	
“	• Load Combinations	2.1	
“	• Margins of Safety	2.5, 2.6, 2.7	

TABLE 2.0.1- MATRIX OF NUREG-1617/10CFR71 COMPLIANCE – STRUCTURAL REVIEW (Continued)

SECTION IN NUREG-1617 AND APPLICABLE 10CFR71/REG.GUIDE (R.G.) SECTIONS	NUREG-1617/10CFR71 COMPLIANCE ITEM	LOCATION IN SAR CHAPTER 2	LOCATION OUTSIDE OF SAR CHAPTER
10CFR71, Subparts E,F	Evaluation by Test		
10CFR71.73(a)	• Procedures for Impact Testing	2.7.1 2.A	
“	• Test Specimens	2.7.1 2.A	
10CFR71.73(c)(1)	• Drop Orientations	2.7.1 2.A	
“	• Conclusions	2.7.1 2.A	
<b>2.3.5 Normal Conditions of Transport</b>			
10CFR71.71 with reference to 10CFR71 sections 71.35(a), 71.43(f), 71.51(a)(1), 71.55(d)(4)	Heat	2.6.1	
“	Cold	2.6.2	
“	Reduced External Pressure	2.6.3	
“	Increased External Pressure	2.6.4	
“	Vibration	2.6.5	
“	Water Spray	2.6.6	
“	Free Drop	2.6.1; 2.6.2; 2.6.7	
“	Corner Drop	NA	NA
“	Compression	NA	NA
“	Penetration	NA	NA

TABLE 2.0.1- MATRIX OF 10CFR71 COMPLIANCE – STRUCTURAL REVIEW (Continued)

SECTION IN NUREG-1617 AND APPLICABLE 10CFR71/REG.GUIDE (R.G.) SECTIONS	NUREG-1617/10CFR71 COMPLIANCE ITEM	LOCATION IN SAR CHAPTER 2	LOCATION OUTSIDE OF SAR CHAPTER
<b>2.3.6 Hypothetical Accident Conditions</b>			
10CFR71.73(c)(1)	Free Drop	2.7.1, 2.A	
10CFR71.73(c)(2)	Crush	NA	NA
10CFR71.73(c)(3)	Puncture	2.7.2	
10CFR71.73(c)(4)	Thermal	2.7.3	
10CFR71.73(c)(5)	Immersion-Fissile Material	2.7.4	NA
10CFR71.73(c)(6)	Immersion – All Material	2.7.5	
<b>2.3.7 Special Requirements for Irradiated Nuclear Fuel Shipments</b>			
10CFR71.61	Elastic Stability of Containment	2.7.5	
“	Closure Seal Region Below Yield Stress	2.7.1	
<b>2.3.8 Internal Pressure Test</b>			
10CFR71.85(b)	Internal Pressure Test – All stresses below yield	2.6.1.4.3	8.1



TABLE 2.0.1- MATRIX OF 10CFR71 COMPLIANCE – STRUCTURAL REVIEW (Continued)

SECTION IN 10CFR71	10CFR71 COMPLIANCE ITEM	LOCATION IN SAR CHAPTER 2	LOCATION OUTSIDE OF SAR CHAPTER
<b>Appendices</b>			
	Supplemental Information	2.10	

† Legend for Table 2.0.1

Per the nomenclature defined in Chapter 1, the first digit refers to the chapter number, the second digit is the section number within the chapter; an alphabetic character in the second place means it is an appendix to the chapter.

NA Not Applicable for this item

## 2.1 STRUCTURAL DESIGN

### 2.1.1 Discussion

The HI-STAR 100 System (also designated as the HI-STAR 100 Package) consists of three principal components: the multi-purpose canister (MPC), the overpack assembly, and a set of impact limiters. The overpack confines the MPC and provides the containment boundary for transport conditions. The MPC is a hermetically sealed, welded structure of cylindrical profile with flat ends and an internal honeycomb fuel basket for SNF. A complete description of the HI-STAR MPC is provided in Section 1.2.1.2.2 wherein its design and fabrication details are presented with the aid of figures. A discussion of the HI-STAR 100 overpack is presented in Subsection 1.2.1.2.1. Drawings for the HI-STAR 100 System are provided in Section 1.4. In this section, the discussion is directed to characterizing and establishing the structural features of the MPC and the transport overpack.

The design of the HI-STAR 100 MPC seeks to attain three objectives that are central to its functional adequacy, namely;

- **Ability to Dissipate Heat:** The thermal energy produced by the spent fuel must be transported to the outside surface of the MPC such that the prescribed temperature limits for the fuel cladding and the fuel basket metal walls are not exceeded.
- **Ability to Withstand Large Impact Loads:** The MPC with its payload of nuclear fuel must be sufficiently robust to withstand large impact loads associated with the hypothetical accident conditions during transportation of the system. Furthermore, the strength of the MPC must be sufficiently isotropic to assure structural qualification under a wide variety of drop orientations.
- **Restraint of Free End Expansion:** The membrane and bending stresses produced by restraint of free end expansion of the fuel basket are conservatively categorized as primary stresses. In view of the concentration of heat generation in the fuel basket, it is necessary to ensure that structural constraints to its external expansion do not exist.

Where the first two criteria call for extensive inter-cell connections, the last criterion requires the opposite. The design of the HI-STAR 100 MPC seeks to realize all of the above three criteria in an optimal manner.

As the description presented in Chapter 1 indicates, the MPC enclosure vessel is a spent nuclear fuel (SNF) pressure vessel designed to meet ASME Code, Section III, Subsection NB stress limits. The enveloping canister shell, the MPC baseplate, and the closure lid system form a complete closed pressure vessel referred to as the "enclosure vessel". This enclosure vessel serves as the helium retention boundary when the HI-STAR 100 is within the purview of 10CFR71. Within this cylindrical vessel is an integrally welded assemblage of cells of square cross sectional openings, referred to herein as the "fuel basket". The fuel basket is analyzed under the provisions of Subsection NG of Section III of the ASME Code. There are different multi-purpose canisters that are exactly alike in their external dimensions. The essential difference between the MPCs lies in the fuel

baskets. Each fuel storage MPC is designed to house fuel assemblies with different characteristics. Although all HI-STAR 100 MPC fuel baskets are configured to maximize structural ruggedness through extensive inter-cell connectivity, they are sufficiently dissimilar in structural details to warrant separate evaluations. Therefore, analyses for the different MPC types are presented, as appropriate, throughout this chapter.

The HI-STAR 100 overpack provides the containment function for the stored SNF. There is an undivided reliance on the structural integrity of this containment vessel to maintain complete isolation of its contained radioactive contents from the environment under all postulated accident scenarios, even though the MPC is a completely autonomous, ASME Section III Class 1 pressure vessel which provides an unbreachable enclosure for the fuel. The containment boundary is made up of the inner shell, the bottom plate, the top flange, and the closure plate.

Components of the HI-STAR 100 System that are important to safety and their applicable design codes are defined in Chapter 1.

The structural function of the MPC in the transport mode is:

1. To maintain position of the fuel in a sub-critical configuration.
2. To maintain a helium confinement boundary.

The structural function of the overpack in the transport mode is:

1. To serve as a penetration and puncture barrier for the MPC.
2. To provide a containment boundary.
3. To provide a structurally robust support for the radiation shielding.

The structural function of the impact limiters in the transport mode is:

1. To cushion the HI-STAR 100 overpack and the contained MPC with fuel during normal transport handling and in the event of a hypothetical drop accident during transport.

Some structural features of the MPCs that allow the system to perform their structural functions are summarized below:

- There are no external or gasketed ports or openings in the MPC. The MPC does not rely on any sealing arrangement except welding. The absence of any gasketed or flanged joints precludes joint leaks. The MPC enclosure vessel contains no valves or other pressure relief devices.

- The closure system for the MPCs consists of two components, namely, the MPC lid and the closure ring. The MPC lid is a thick circular plate continuously welded to the MPC shell along its circumference. The MPC closure system is shown in the drawings in Section 1.4. The MPC lid-to-MPC shell weld is a J-groove weld that is subject to root and final pass liquid penetrant examinations and finally, a volumetric examination to ensure the absence of unacceptable flaws and indications. The MPC lid is equipped with vent and drain ports which are utilized for evacuating moisture and air from the MPC following fuel loading and subsequent backfilling with an inert gas (helium) in a specified quantity. The vent and drain ports are covered by a cover plate and welded before the closure ring is installed. The closure ring is a thin circular annular plate edge-welded to the MPC shell and to the MPC lid. Lift points for the MPC are provided in the MPC lid.
- The MPC fuel basket consists of an array of interconnecting plates. The number of storage cells formed by this interconnection process varies depending on the type of fuel being transported. Basket designs for different PWR and BWR cell configurations have been designed and are explained in detail in Subsection 1.2. All baskets are designed to fit into the same MPC shell. Welding the plates along their edges essentially renders the fuel basket into a multi-flange beam. For example, Figure 2.1.1 provides an isometric illustration of a fuel basket for the MPC-68 design.
- The MPC basket is separated from the longitudinal supports installed in the enclosure vessel by a small gap. The gap size decreases as a result of thermal expansion (depending on the magnitude of internal heat generation from the stored spent fuel). The provision of a small gap between the basket and the basket support structure is consistent with the natural thermal characteristics of the MPC. The planar temperature distribution across the basket, as shown in Chapter 3, approximates a shallow parabolic profile. This profile will create high thermal stresses unless structural constraints at the interface between the basket and the basket support structure are removed.

The MPCs will be loaded with fuel assemblies with widely varying heat generation rates. The basket/basket support structure gap tends to be reduced for higher heat generation rates due to increased thermal expansion rates. The basket/basket support structure gap tends to be reduced due to thermal expansion from decay heat generation. Gaps between the fuel basket and the basket support structure are specified to be sufficiently large such that a gap exists around the periphery under all normal or accident conditions of transport.

A small number of optional flexible thermal conduction elements (thin aluminum tubes) may be interposed between the basket and the MPC shell. The elements are designed to be resilient. They do not provide structural support for the basket, and thus their resistance to thermal growth is negligible.

Structural features of the overpack that allow the HI-STAR 100 package to perform its safety function are summarized below:

- The overpack features a thick inner shell welded to a bottom plate which forms a load bearing surface for the HI-STAR 100 System. A solid metal top flange welded at the top of the inner shell provides the attachment location for the lifting trunnions. The top flange is designed to provide a recessed ledge for the closure plate to protect the bolts from direct shear loading resulting from an impulsive load at the top edge of the overpack (Figure 2.1.2). In the transport mode the overpack inner shell, bottom plate, top flange, and closure plate with metallic seals constitute the containment boundary for the HI-STAR 100 System. The HI-STAR 100 overpack is subject to the stress limits of the ASME Code, Section III, Subsection NB [2.1.5].
- The inner shell (containment boundary) is reinforced by multi-layered intermediate shells. The multi-layer approach eliminates the potential for a crack in any one layer, developed by any postulated mechanical loading or material flaw, to travel uninterrupted through the vessel wall. The intermediate shells also buttress the overpack inner shell against buckling. The intermediate shells of the HI-STAR 100 overpack are **conservatively evaluated using** the stress limits of the ASME Code, Section III, Subsection NF, Class 3 [2.1.7].
- To facilitate handling of the loaded package, the HI-STAR 100 overpack is equipped with two lifting trunnions at the top of the overpack. The initial seven HI-STAR 100 overpacks are also equipped with pocket trunnions, embedded in the overpack intermediate shells, just above the bottom plate. HI-STAR 100 overpacks fabricated after the initial seven do not have pocket trunnions (see Subsection 2.5 for further discussion). Lifting trunnions are conservatively designed to meet the design safety factor requirements of NUREG-0612 [2.1.9], ANSI N14.6-1993 [2.1.10] **and Regulatory Guide 3.61 [2.1.19]** for single failure proof lifting equipment.
- A circular recess is incorporated on the inner surface of the overpack closure plate. The purpose of this recess is to reduce the moment applied to the flanged joint from MPC impact during a hypothetical top end drop accident. During a hypothetical drop accident where the top end of the overpack impacts first, the MPC contacts the inner surface of the overpack closure plate. Because of the recess, the MPC will only contact an annular region of the inner surface of the overpack closure plate. Thus, the load on the overpack closure plate from the MPC is located closer to the bolt circle, and the moment on the flanged joint is reduced.
- A small circular gap between the MPC external surface and the inside surface of the overpack is provided to allow insertion and removal of the MPC. This gap diminishes monotonically with the increase in the heat generation rate in the MPC, but is sized to avoid metal-to-metal contact between the MPC and the overpack cylindrical surface as a result of thermal expansion under the most adverse thermal conditions.
- There are no valves in the HI-STAR 100 overpack containment boundary. The vent and drain ports used during HI-STAR 100 overpack loading and unloading operations are closed with port plugs and metallic seals. The port plugs are recessed and are suitably protected with a cover plate with seal. These small penetrations equipped with dual seals are not deemed to be

particularly vulnerable locations in the HI-STAR 100 System.

The HI-STAR 100 System is equipped with a set of impact limiters (AL-STAR) attached to the top and bottom ends of the overpack. The structural function of the impact limiters is to cushion the HI-STAR 100 overpack and the contained MPC with fuel in the event of a hypothetical drop accident during transport, and to provide the necessary resistance to the longitudinal decelerations experienced during normal rail transport. The design of the impact limiter is independent of the design of the MPC and overpack. This is achieved by establishing design basis deceleration limits for normal transport and for the hypothetical 30-foot drop accident and demonstrating that impact limiter performance limits the deceleration levels imposed on the cask.

Table 1.3.3 provides a listing of the applicable design codes for all structures, systems, and components that are designated as Important to Safety (ITS).

### 2.1.2 Design Criteria

Regulatory Guide 7.6 provides design criteria for the structural analysis of shipping casks [2.1.4]. Loading conditions and load combinations that must be considered for transport are defined in 10CFR71 [2.1.1] and in USNRC Regulatory Guide 7.8 [2.1.2]. Consistent with the provisions of these documents, the central objective of the structural analysis presented in this chapter is to ensure that the HI-STAR 100 System possesses sufficient structural capability to meet the demands of normal conditions and hypothetical accident conditions of transport.

The following table provides a synoptic matrix to demonstrate our explicit compliance with the seven regulatory positions stated in Regulatory Guide 7.6.

<b>REGULATORY GUIDE 7.6 COMPLIANCE</b>	
<b>Regulatory Position</b>	<b>Compliance in HI-STAR 100 SAR</b>
1. Material properties, design stress intensities, and fatigue curves are obtained from the ASME Code	Tables 2.1.12-2.1.20 for allowable stresses/stress intensities and Tables 2.3.1-2.3.5 for material properties are obtained from the ASME Code (the 1995 Code tables are used). Section 2.6.1.3.3 uses the appropriate fatigue data from the Code.
2. Under normal conditions of transport, the limits on stress intensity are those limits defined by the ASME Code for primary membrane and for primary membrane plus bending for Level A conditions.	Tables 2.1.3-2.1.5 define the correct stress intensity limits for normal conditions of transport as stated in the ASME Code for Level A conditions.
3. Perform fatigue analysis for normal conditions of transport using ASME Code Section III methodology (NB) and appropriate fatigue curves.	Section 2.6.1.3.3 considers the potential for fatigue using accepted ASME Code methodology and fatigue data from the ASME Code.
4. The stress intensity $S_n$ associated with the range of primary plus secondary stresses under normal conditions should be less than $3S_m$ where $S_m$ is the primary membrane stress intensity from the Code.	Section 2.6.1.3.3 considers the fatigue potential of the HI-STAR 100 Package based on the $3S_m$ limit.

<b>REGULATORY GUIDE 7.6 COMPLIANCE</b>	
<b>Regulatory Position</b>	<b>Compliance in HI-STAR 100 SAR</b>
5. Buckling of the containment vessel should not occur under normal or accident conditions.	The methodology used is Code Case N-284; this has been accepted by the NRC as an appropriate vehicle to evaluate buckling of the containment.
6. Under accident conditions, the values of primary membrane stress intensity should not exceed the lesser of $2.4S_m$ and $0.7S_u$ (ultimate strength), and primary membrane plus bending stress intensity should not exceed the lesser of $3.6S_m$ and $S_u$ .	Tables 2.1.3-2.1.5 of the SAR state these requirements.
7. The extreme total stress intensity range should be less than $S_a$ at 10 cycles as given by the appropriate fatigue curves.	Subsection 2.6.1.3.3 demonstrates compliance by conservatively bounding the total stress intensity range and demonstrating that the bounding value is less than $S_a$ at 10 cycles as given by the appropriate fatigue curves.

Note that Regulatory Guide 7.6 references ASME Code Sections in the 1977 code year. This SAR has been prepared using the identical information on allowable stress intensities and fatigue data as listed in the 1995 ASME Code.

Table 8.1.4 in Chapter 8 summarizes the ASME pressure vessel code applicability to HI-STAR 100 components. Table 8.1.5 in Chapter 8 provides a statement of exceptions taken to the ASME Code requirements.

Stresses arise in the components of the HI-STAR 100 System due to various loads that originate under normal and hypothetical accident conditions of transport. These individual loads are combined to form load combinations. Stresses and stress intensities resulting from the load combinations are compared to allowable stresses and stress intensities. The following subsections present loads, load combinations, and allowable strengths for use in the structural analyses of the MPC and the HI-STAR 100 overpack.

#### 2.1.2.1 Loading and Load Combinations

10CFR71 and Regulatory Guide 7.6 define two conditions that must be considered for qualification of a transport package. These are defined as "Normal Conditions of Transport" and "Hypothetical Accident Conditions", which are related herein to the ASME Code Service Levels for the purposes of quantifying allowable stress limits. In terms of the ASME terminology, the following parallels are applicable.

Normal Conditions of Transport = ASME Design Condition and ASME Level A or B Service Condition

Hypothetical Accident Condition = ASME Level D Service Condition

[ PROPRIETARY INFORMATION WITHHELD PER 10CFR 2.390 ]

[

PROPRIETARY INFORMATION WITHHELD PER 10CFR2.390

]



[

PROPRIETARY INFORMATION WITHHELD PER 10 CFR 2.390

]

[

PROPRIETARY INFORMATION WITHHELD PER 10CFR2.390

]

[

PROPRIETARY INFORMATION WITHHELD PER 10CFR2.390

]

[

PROPRIETARY INFORMATION WITHHELD PER 10CFR2.390

]

[

PROPRIETARY INFORMATION WITHHELD PER 10CFR2.390

]

[

PROPRIETARY INFORMATION WITHHELD PER 10CFR2.390

]

[

PROPRIETARY INFORMATION WITHHELD PER 10CFR2.390

]

[

PROPRIETARY INFORMATION WITHHELD PER 10CFR2.390

]



[

PROPRIETARY INFORMATION WITHHELD PER 10CFR2.390

]

#### 2.1.2.4 Impact Limiter

The impact limiters are designed as energy absorbers to ensure that the maximum impact deceleration applied to the package is limited to values less than the design basis deceleration, as applicable.

#### 2.1.2.5 Buckling

Certain load combinations subject structural sections with relatively large slenderness ratios (such as the MPC enclosure vessel shell) to compressive stresses that may actuate buckling instability before the allowable stress is reached. Tables 2.1.7 and 2.1.9 list load combinations for the MPC enclosure vessel and the HI-STAR 100 overpack structure; the cases that warrant stability (buckling) check are listed therein.

#### 2.1.2.6 Partially Loaded MPC's

All MPC's (including Trojan MPC-24E/EF) shall be loaded to at least 50% of their capacity. Thus for example, MPC-24, MPC-32, and MPC-68 must have at least 12, 16 and 34 fuel assemblies, respectively, loaded. Additionally, the loading of the MPC should be symmetrical as described in Table 7.1.1. These requirements ensure that the HI-STAR 100 package remains in an "analyzed" condition, i.e., the handling of MPC's and overpack is not affected, and the bounding deceleration

limits for normal and hypothetical drop events in Table 2.1.10 are satisfied. The detailed evaluations, which are based on the relation that the impact deceleration is inversely proportional to the square root of the weight [2.5.1], are documented in [2.6.6].

Table 2.1.1

[PROPRIETARY INFORMATION WITHHELD PER 10CFR2.390]

Table 2.1.2

NORMAL REFERENCE TEMPERATURES AND ACCIDENT BULK METAL  
TEMPERATURE LIMITS

<b>HI-STAR 100 Component</b>	<b>Normal Operating Condition Reference Temp. Limits<sup>†</sup> (Deg.F)</b>	<b>Hypothetical Accident Condition Metal Bulk Temp. Limits<sup>††</sup> (Deg.F)</b>
MPC shell	450	550
MPC basket	725	950
MPC lid	550	775
MPC closure ring	400	775
MPC baseplate	400	775
MPC neutron absorber	800	950
MPC heat conduction elements	725	950
Overpack inner shell	400	500
Overpack bottom plate	350	700
Overpack closure plate	400	700
Overpack top flange	400	700
Overpack closure plate seals	400	1200
Overpack closure plate bolts	350	600
Port plug seals (vent and drain)	400	1600
Port cover seals (vent and drain)	400	932
Neutron shielding	300	†††
Overpack Intermediate Shells	350	700
Overpack Outer Enclosure Shell	350	1350
Optional Pocket Trunnion	200	700
Impact Limiter	150	1105

<sup>†</sup> These temperatures are maximum possible temperatures for the normal operating condition. They bound the actual calculated temperatures.

<sup>††</sup> These temperatures are maximum possible temperatures for the postulated fire accident. They must bound the actual calculated temperatures.

<sup>†††</sup> For shielding analysis, the neutron shield is conservatively assumed to be lost during the fire accident.

Table 2.1.3

**OVERPACK CONTAINMENT STRUCTURE AND MPC ENCLOSURE VESSEL STRESS INTENSITY LIMITS  
FOR DIFFERENT LOADING CONDITIONS (ELASTIC ANALYSIS PER NB-3220)<sup>†</sup>**

<b>STRESS CATEGORY</b>	<b>NORMAL CONDITIONS OF TRANSPORT</b>	<b>HYPOTHETICAL ACCIDENT<sup>††</sup></b>
Primary Membrane, $P_m$	$S_m$	AMIN ( $2.4S_m$ , $.7S_u$ )
Local Membrane, $P_L$	$1.5S_m$	150% of $P_m$ Limit
Membrane plus Primary Bending	$1.5S_m$	150% of $P_m$ Limit
Primary Membrane plus Primary Bending	$1.5S_m$	150% of $P_m$ Limit
Membrane plus Primary Bending plus Secondary	$3S_m$	N/A
Average <sup>†††</sup> Primary Shear (Section in Pure Shear)	$0.6S_m$	$0.42S_u$

<sup>†</sup> Stress combinations including F (peak stress) apply to fatigue evaluations only.

<sup>††</sup> Governed by Appendix F, Paragraph F-1331 of the ASME Code, Section III. Stress limited to  $S_u$

<sup>†††</sup> Governed by NB-3227.2 or F-1331.1(d) of the ASME Code, Section III (NB or Appendix F)

Table 2.1.4

**MPC BASKET STRESS INTENSITY LIMITS  
FOR DIFFERENT LOADING CONDITIONS (ELASTIC ANALYSIS PER NG-3220)**

<b>STRESS CATEGORY</b>	<b>NORMAL CONDITIONS OF TRANSPORT</b>	<b>HYPOTHETICAL ACCIDENT<sup>†</sup></b>
Primary Membrane, $P_m$	$S_m$	$AMIN(2.4S_m, .7S_u)^{††}$
Primary Membrane plus Primary Bending	$1.5S_m$	150% of $P_m$ Limit (Limited to $S_u$ )
Primary Membrane plus Primary Bending plus Secondary	$3S_m$	N/A

---

<sup>†</sup> Governed by Appendix F, Paragraph F-1331 of the ASME Code, Section III.

<sup>††</sup> Average primary shear stress across a section loaded in pure shear shall not exceed  $0.42S_u$ .

Table 2.1.5

STRESS INTENSITY LIMITS FOR DIFFERENT  
LOADING CONDITIONS FOR THE EXTERNAL STRUCTURALS IN THE HI-STAR OVERPACK  
(ELASTIC ANALYSIS PER NF-3260 - CLASS 3)  
(ELASTIC ANALYSIS PER NF-3220 - CLASS 1)

<b>STRESS CATEGORY</b>	<b>NORMAL CONDITION OF TRANSPORT<sup>†</sup></b>	<b>HYPOTHETICAL ACCIDENT<sup>††</sup></b>
Primary Membrane, $P_m$	$S$ (Class 3) $S_m$ (Class 1)	AMAX ( $1.2S_y$ , $1.5S_m$ ) but $< .7S_u$
Primary Membrane, $P_m$ , plus Primary Bending, $P_b$	$1.5S$ (Class 3) $1.5S_m$ (Class 1)	150% of $P_m$ (Limited to $S_u$ )
Shear Stress	N/A (Class 3) $.6S_m$ (Class 1)	$< 0.42S_u$

## Definitions:

$S$  = Allowable Stress Value for Table 1A, ASME Section II, Part D

$S_m$  = Allowable Stress Intensity Value from Table 2A, ASME Section II, Part D

$S_u$  = Ultimate Strength

<sup>†</sup> Limits for Normal Condition of Transport are on stress for Class 3 and on stress intensity for Class 1, upper value in column is for Class 3; lower value in column is for Class 1.

<sup>††</sup> Governed by Appendix F, Paragraph F-1332 of the ASME Code, Section III. Class 1 and Class 3 use same stress intensity limits.

Table 2.1.6

## LOADING CASES FOR THE MPC FUEL BASKET

Case Number	Load Combination <sup>†</sup>	Notes
F1	T or T'	Demonstrate that the most adverse of the temperature distributions in the basket will not cause fuel basket to expand and contact the enclosure vessel wall. Compute the stress intensity and show that it is less than allowable.
F2		
F2.a	D+H	1 ft. side drop, 0 degrees circumferential orientation (Figure 2.1.3)
F2.b	D+H	1 ft. side drop, 45 degrees circumferential orientation (Figure 2.1.4)
F3		
F3.a	D + H'	30 ft. vertical axis drop
F3.b	D + H'	30 ft. side Drop, 0 degrees circumferential orientation (Figure 2.1.3)
F3.c	D + H'	30 ft. side Drop, 45 degrees circumferential orientation (Figure 2.1.4)

<sup>†</sup> The symbols used for loads are defined in Subsection 2.1.2.1.



Table 2.1.7

## LOADING CASES FOR THE MPC ENCLOSURE VESSEL

Case Number	Load Combination <sup>†</sup>	Notes
E1		
E1.a	Design internal pressure, $P_i$	Primary Stress intensity
E1.b	Design external pressure, $P_o$	Primary stress intensity limits, buckling stability
E1.c	Design internal pressure plus Temperature, $P_i + T$	Primary plus secondary stress intensity under Level A condition
E2		
E2.a	$(P_i, P_o) + D + H$	1 ft. side drop, 0° circumferential orientation (Figure 2.1.3)
E2.b	$(P_i, P_o) + D + H$	1 ft. side drop, 45° circumferential orientation (Figure 2.1.4)

<sup>†</sup> The symbols used for loads are defined in Subsection 2.1.2.1. Note that in the analyses, the bounding pressure ( $P_i, P_o$ ) is applied, e.g., in stability calculations  $P_o$  is bounding, whereas in stress calculations both  $P_o$  and  $P_i$  are appropriate.

Table 2.1.7 (continued)

Case Number	Load Combination <sup>†</sup>	Notes
E3		
E3.a	$D + H' + P_o$ (Stability of the shell considers internal pressure plus drop deceleration)	30 ft. vertical axis drop
E3.b	$D + H' + P_i$	30 ft. side drop, 0° circumferential orientation (Figure 2.1.3)
E3.c	$D + H' + P_i$	30 ft. side drop, 45° circumferential orientation (Figure 2.1.4)
E4	T or T'	Demonstrate that interference with the overpack will not develop for T
E5	$(P_i^*, P_o^*) + D + T'$	Demonstrate compliance with level D stress limits - buckling stability

<sup>†</sup> The symbols used for loads are defined in Subsection 2.1.2.1. Note that in the analyses, the bounding pressure ( $P_i$ ,  $P_o$ ) is applied, e.g., in stability calculations  $P_o$  is bounding, whereas in stress calculations both  $P_o$  and  $P_i$  are appropriate.

Table 2.1.8

## OVERPACK LOAD CASES FOR NORMAL CONDITION OF TRANSPORT

Case Number	Load Combination <sup>†</sup>	Notes
1	$T_h + P_i + F + W_s$	Hot Environment
2	$T_s + P_o + F + W_s$	Super-Cold Environment
3	$T_h + D_{sn} + P_i + F + W_s$	Free One Foot Side Drop - Hot Environment
4	$T_c + D_{sn} + P_o + F + W_s$	Free One Foot Side Drop - Cold Environment
5	$T_c$ and $T_h + P_i + V$	Rapid Ambient Temperature Change

Note that load case 5 is outside of the load combinations of Reg. Guide 7.8

<sup>†</sup> The symbols used here are defined in Subsection 2.1.2.1.

Table 2.1.9

## OVERPACK LOAD CASES FOR HYPOTHETICAL ACCIDENT CONDITIONS OF TRANSPORT

Case Number	Load Combination <sup>†</sup>	Notes
1	$T_h + D_{ba} + P_i + F + W_s$	Bottom End 30 ft. Drop - Hot
2	$T_h + D_{ta} + P_i + F + W_s$	Top End 30 ft Drop - Hot
3	$T_h + D_{sa} + P_i + F + W_s$	Side 30 ft Drop - Hot
4	$T_h + D_{ea} + P_i + F + W_s$	30 ft C.G. Over-the-Bottom-Corner Drop - Hot
5	$T_h + D_{ga} + P_i + F + W_s$	30 ft C.G. Over-the-Top-Corner Drop Hot
6	$T_h + P_s + P_i + F + W_s$	Side Puncture - Hot
7	$T_h + P_t + P_i + F + W_s$	Top End Puncture - Hot
8	$T_h + P_b + P_i + F + W_s$	Bottom End Puncture - Hot
9	$T_c + D_{ba} + P_o + F + W_s$	Case 1 - Cold
10	$T_c + D_{ta} + P_o + F + W_s$	Case 2 - Cold
11	$T_c + D_{sa} + P_o + F + W_s$	Case 3 - Cold
12	$T_c + D_{ea} + P_o + F + W_s$	Case 4 - Cold
13	$T_c + D_{ga} + P_o + F + W_s$	Case 5 - Cold
14	$T_c + P_s + P_o + F + W_s$	Case 6 - Cold
15	$T_c + P_t + P_o + F + W_s$	Case 7 - Cold
16	$T_c + P_b + P_o + F + W_s$	Case 8 - Cold
17	$T_f + P_i + F + W_s$	Fire Event (Bolt unloading)
18	$P_o^*$	Containment Stability - Hot Deep Submergence
19	$P_i^* + T_f + F + W_s$	Fire Accident Internal Pressure - Hot
20	$T_h + D_{ga} + P_i + F + W_s$	30 ft C.G. Oblique Drop (30 Degree) on Top Forging - Hot
21	$T_c + D_{ga} + P_i + F + W_s$	30 ft C.G. Oblique Drop (30 Degree) on Top Forging - Cold
22	$T_c + D_{ga} + P_i + F + W_s$	30 ft Drop -Slapdown Secondary Impact Limiter at Top Forging - Hot

<sup>†</sup> The symbols used here are defined in Subsection 2.1.2.1.

Table 2.1.10  
BOUNDING DECELERATIONS FOR DROP EVENTS

<b>Event</b>	<b>Deceleration Value (in multiples of acceleration due to gravity)</b>
Normal conditions of transport, drop from 1 ft. height (any circumferential orientations)	17
Transport hypothetical accident conditions; drop from 30 ft. height (any axial and circumferential orientations)	60

Table 2.1.11

## DESIGN, LEVELS A AND B: STRESS INTENSITY

Code: ASME NB  
 Material: SA203-E  
 Service Conditions: Normal Conditions of Transport  
 Item: Stress Intensity

Temp. (degree F)	Classification and Value (ksi)					
	$S_m$	$P_m^\dagger$	$P_L^\dagger$	$P_L + P_b^\dagger$	$P_L + P_b + Q$	$P_e^{\dagger\dagger}$
-20 to 100	23.3	23.3	35.0	35.0	69.9	69.9
200	23.3	23.3	35.0	35.0	69.9	69.9
300	23.3	23.3	35.0	35.0	69.9	69.9
400	22.9	22.9	34.4	34.4	68.7	68.7
500	21.6	21.6	32.4	32.4	64.8	64.8

## Definitions:

$S_m$  = Stress intensity values per ASME Code  
 $P_m$  = Primary membrane stress intensity  
 $P_L$  = Local membrane stress intensity  
 $P_b$  = Primary bending stress intensity  
 $P_e$  = Expansion stress  
 $Q$  = Secondary stress  
 $P_L + P_b$  = Either primary or local membrane plus primary bending

Definitions for Table 2.1.11 apply to all following tables unless modified.

---

<sup>†</sup> Evaluation required for Design condition only.

<sup>††</sup>  $P_e$  not applicable to vessels.

Table 2.1.12

## LEVEL D: STRESS INTENSITY

Code: ASME NB  
 Material: SA203-E  
 Service Condition: Hypothetical Accident  
 Item: Stress Intensity

Temp. (degree F)	Classification and Value (ksi)		
	$P_m$	$P_L$	$P_L + P_b$
-20 to 100	49.0	70.0	70.0
200	49.0	70.0	70.0
300	49.0	70.0	70.0
400	48.2	68.8	68.8
500	45.4	64.9	64.9

## Notes:

1. Level D allowables per NB-3225 and Appendix F, Paragraph F-1331.
2. Average primary shear stress across a section loaded in pure shear may not exceed  $0.42 S_u$ .
3. Limits on values are presented in Table 2.1.3.

Table 2.1.13

## DESIGN, LEVELS A AND B: STRESS INTENSITY

Code: ASME NB  
 Material: SA350-LF3  
 Service Conditions: Normal Conditions of Transport  
 Item: Stress Intensity

Temp. (degree F)	Classification and Value (ksi)					
	$S_m$	$P_m^\dagger$	$P_L^\dagger$	$P_L + P_b^\dagger$	$P_L + P_b + Q$	$P_e^{\dagger\dagger}$
-20 to 100	23.3	23.3	35.0	35.0	69.9	69.9
200	22.8	22.8	34.2	34.2	68.4	68.4
300	22.2	22.2	33.3	33.3	66.6	66.6
400	21.5	21.5	32.3	32.3	64.5	64.5
500	20.2	20.2	30.3	30.3	60.6	60.6
600	18.5	18.5	27.75	27.75	55.5	55.5
700	16.8	16.8	25.2	25.2	50.4	50.4

Notes:

1. Source for  $S_m$  is ASME Code.
2. Limits on values are presented in Table 2.1.3.

---

<sup>†</sup> Evaluation required for Design condition only.

<sup>††</sup>  $P_e$  not applicable to vessels.



Table 2.1.14

## LEVEL D, STRESS INTENSITY

Code: ASME NB  
 Material: SA350-LF3  
 Service Conditions: Hypothetical Accident  
 Item: Stress Intensity

Temp. (degree F)	Classification and Value (ksi)		
	$P_m$	$P_L$	$P_L + P_b$
-20 to 100	49.0	70.0	70.0
200	48.0	68.5	68.5
300	46.7	66.7	66.7
400	45.2	64.6	64.6
500	42.5	60.7	60.7
600	38.9	58.4	58.4
700	35.3	53.1	53.1

## Notes:

1. Level D allowables per NB-3225 and Appendix F, Paragraph F-1331.
2. Average primary shear stress across a section loaded in pure shear may not exceed  $0.42 S_u$ .
3. Limits on values are presented in Table 2.1.3.

Table 2.1.15

## DESIGN AND LEVEL A: STRESS AND STRESS INTENSITY

Code:	ASME NF (Class 3)	ASME NF (Class 1)
Material:	SA515, Grade 70	SA515, Grade 70
	SA516, Grade 70	SA516, Grade 70
Service Conditions:	Normal Conditions of Transport	Normal Conditions of Transport
Item:	Stress	Stress Intensity

Temp. (degree F)	Classification and Value (ksi)					
	S (Class 3)	S <sub>m</sub> (Class 1)	Membrane Stress (Class 3)	P <sub>m</sub> (Class 1)	Membrane plus Bending Stress (Class 3)	P <sub>m</sub> +P <sub>b</sub> (Class 1)
-20 to 100	17.5	23.3	17.5	23.3	26.3	34.95
200	17.5	23.1	17.5	23.1	26.3	34.65
300	17.5	22.5	17.5	22.5	26.3	33.75
400	17.5	21.7	17.5	21.7	26.3	32.55
500	17.5	20.5	17.5	20.5	26.3	30.75
600	17.5	18.7	17.5	18.7	26.3	28.05
650	17.5	18.4	17.5	18.4	26.3	27.6
700	16.6	18.3	16.6	18.3	24.9	27.45

## Notes:

1. S = Maximum allowable stress values from Table 1A of ASME Code, Section II, Part D.
2. Stress classification per Paragraph NF-3260.
3. Limits on values are presented in Table 2.1.5.
4. Level A allowable stress intensities per NF.3221.1.
5. S<sub>m</sub> = Stress intensity values per Table 2A of ASME, Section II, Part D.

Table 2.1.16

## LEVEL D: STRESS INTENSITY

Code: ASME NF  
 Material: SA515, Grade 70  
 SA516, Grade 70  
 Service Conditions: Hypothetical Accident  
 Item: Stress Intensity

Temp. (degree F)	Classification and Value (ksi)		
	$S_m$	$P_m$	$P_m + P_b$
-20 to 100	23.3	45.6	68.4
200	23.1	41.5	62.3
300	22.5	40.4	60.6
400	21.7	39.1	58.7
500	20.5	36.8	55.3
600	18.7	33.7	50.6
650	18.4	33.1	49.7
700	18.3	32.9	49.3

## Notes:

1. Level D allowable stress intensities per Appendix F, Paragraph F-1332.
2.  $S_m$  = Stress intensity values per Table 2A of ASME, Section II, Part D.
3. Limits on values are presented in Table 2.1.5.

Table 2.1.17

## DESIGN, LEVELS A AND B: STRESS INTENSITY

Code: ASME NB  
 Material: Alloy X  
 Service Conditions: Normal Conditions of Transport  
 Item: Stress Intensity

Temp. (degree F)	Classification and Numerical Value					
	$S_m$	$P_m^\dagger$	$P_L^\dagger$	$P_L + P_b^\dagger$	$P_L + P_b + Q$	$P_e^{\dagger\dagger}$
-20 to 100	20.0	20.0	30.0	30.0	60.0	60.0
200	20.0	20.0	30.0	30.0	60.0	60.0
300	20.0	20.0	30.0	30.0	60.0	60.0
400	18.7	18.7	28.1	28.1	56.1	56.1
500	17.5	17.5	26.3	26.3	52.5	52.5
600	16.4	16.4	24.6	24.6	49.2	49.2
650	16.0	16.0	24.0	24.0	48.0	48.0
700	15.6	15.6	23.4	23.4	46.8	46.8
750	15.2	15.2	22.8	22.8	45.6	45.6
800	14.9	14.9	22.4	22.4	44.7	44.7

Notes:

1.  $S_m$  = Stress intensity values per Table 2A of ASME II, Part D.
2. Alloy X  $S_m$  values are the lowest values for each of the candidate materials at temperature.
3. Stress classification per NB-3220.
4. Limits on values are presented in Table 2.1.3.

<sup>†</sup> Evaluation required for Design condition only.

<sup>††</sup>  $P_e$  not applicable to vessels.

Table 2.1.18

## LEVEL D: STRESS INTENSITY

Code: ASME NB  
 Material: Alloy X  
 Service Conditions: Hypothetical Accident  
 Item: Stress Intensity

Temp. (degree F)	Classification and Value (ksi) <sup>†</sup>		
	P <sub>m</sub>	P <sub>L</sub>	P <sub>L</sub> + P <sub>b</sub>
-20 to 100	48.0 (48.0)	72.0 (72.0)	72.0 (72.0)
200	48.0 (46.3)	72.0 (69.5)	72.0 (69.5)
300	46.2 (43.1)	69.3 (64.7)	69.3 (64.7)
400	44.9 (42.0)	67.4 (63.0)	67.4 (63.0)
500	42.0 (41.5)	63.0 (62.3)	63.0 (62.3)
600	39.4 (39.4)	59.1 (59.1)	59.1 (59.1)
650	38.4 (38.4)	57.6 (57.6)	57.6 (57.6)
700	37.4 (37.4)	56.1 (56.1)	56.1 (56.1)
750	36.5 (36.5)	54.8 (54.8)	54.8 (54.8)
800	35.8 (35.8)	53.7 (53.7)	53.7 (53.7)

## Notes:

1. Level D stress intensities per ASME NB-3225 and Appendix F, Paragraph F-1331.
2. The average primary shear strength across a section loaded in pure shear may not exceed 0.42 S<sub>u</sub>.
3. Limits on values are presented in Table 2.1.3.

<sup>†</sup> Values in parentheses apply strictly to the one-piece construction MPC lids, which are made from SA-336 forging material rather than SA-240 plate material.

Table 2.1.19

## DESIGN, LEVELS A AND B: STRESS INTENSITY

Code: ASME NG  
 Material: Alloy X  
 Service Conditions: Normal Conditions of Transport  
 Item: Stress Intensity

Temp. (degree F)	Classification and Value (ksi)				
	$S_m$	$P_m$	$P_m+P_B$	$P_m+P_b+Q$	$P_e$
-20 to 100	20.0	20.0	30.0	60.0	60.0
200	20.0	20.0	30.0	60.0	60.0
300	20.0	20.0	30.0	60.0	60.0
400	18.7	18.7	28.1	56.1	56.1
500	17.5	17.5	26.3	52.5	52.5
600	16.4	16.4	24.6	49.2	49.2
650	16.0	16.0	24.0	48.0	48.0
700	15.6	15.6	23.4	46.8	46.8
750	15.2	15.2	22.8	45.6	45.6
800	14.9	14.9	22.4	44.7	44.7

## Notes:

1.  $S_m$  = Stress intensity values per Table 2A of ASME, Section II, Part D.
2. Alloy X  $S_m$  values are the lowest values for each of the candidate materials at temperature.
3. Classifications per NG-3220.
4. Limits on values are presented in Table 2.1.4.

Table 2.1.20

## LEVEL D: STRESS INTENSITY

Code: ASME NG  
 Material: Alloy X  
 Service Conditions: Hypothetical Accident  
 Item: Stress Intensity

Temp. (degrees F)	Classification and Value (ksi)		
	$P_m$	$P_L$	$P_L + P_b$
-20 to 100	48.0	72.0	72.0
200	48.0	72.0	72.0
300	46.2	69.3	69.3
400	44.9	67.4	67.4
500	42.0	63.0	63.0
600	39.4	59.1	59.1
650	38.4	57.6	57.6
700	37.4	56.1	56.1
750	36.5	54.8	54.8
800	35.8	53.7	53.7

## Notes:

1. Level D stress intensities per ASME NG-3225 and Appendix F, Paragraph F-1331.
2. The average primary shear strength across a section loaded in pure shear may not exceed 0.42  $S_u$ .
3. Limits on values are presented in Table 2.1.4.

Table 2.1.21

REFERENCE TEMPERATURES AND STRESS LIMITS  
FOR THE VARIOUS LOAD CASES

Load Case Number	Material	Reference Temperature <sup>†</sup> , (°F)	Stress Intensity Allowables, ksi		
			P <sub>m</sub>	P <sub>L</sub> + P <sub>b</sub>	P <sub>L</sub> + P <sub>b</sub> + Q
F1	Alloy X	725	15.4	23.1	46.2
F2	Alloy X	725	15.4	23.1	46.2
F3	Alloy X	725	36.9	55.4	NL <sup>††</sup>
E1	Alloy X	450 <sup>†††</sup>	18.1	27.2	NL
E2	Alloy X	450 <sup>†††</sup>	18.1	27.2	54.3
E3	Alloy X	450 <sup>†††</sup>	43.4	65.2	NL
E4	Alloy X	450 <sup>†††</sup>	18.1	27.2	54.3
E5	Alloy X	775 <sup>†††</sup>	36.15	54.25	NL

<sup>†</sup> Values for reference temperatures are taken as the design temperatures (Table 2.1.2).

<sup>††</sup> NL: No specific limit in the Code.

<sup>†††</sup> Levels used for enclosure vessel top closure and baseplate only.



Table 2.1.21 (continued)

REFERENCE TEMPERATURES AND STRESS LIMITS  
FOR THE VARIOUS LOAD CASES

Condition	Material	Reference Temperature, (°F)	Stress Intensity Allowables, ksi		
			P <sub>m</sub>	P <sub>L</sub> + P <sub>b</sub>	P <sub>L</sub> + P <sub>b</sub> + Q
Normal	SA203-E	400 <sup>†</sup>	22.9	34.4	68.7
	SA350-LF3	400 <sup>†</sup>	21.5	32.3	64.5
	SA516 Gr. 70 SA515 Gr. 70	400 <sup>†</sup>	17.5	26.3	52.5
	SA203-E	-20	23.3	35.0	69.9
	SA350-LF3	-20	23.3	35.0	69.9
	SA516 Gr. 70 SA515 Gr. 70	-20	17.5	26.3	52.5
Hypothetical Accident - Mechanical Loads	SA203-E	400 <sup>†</sup>	48.2	68.8	NL <sup>††</sup>
	SA350-LF3	400 <sup>†</sup>	45.2	64.6	NL
	SA516 Gr. 70 SA515 Gr. 70	400 <sup>†</sup>	39.1	58.7	NL
	SA203-E	-20	49.0	70.0	NL
	SA350-LF3	-20	49.0	70.0	NL
	SA516 Gr. 70 SA515 Gr. 70	-20	45.6	68.4	NL
Fire	SA203-E	500	45.4	64.9	NL
	SA350-LF3	700	35.3	53.1	NL
	SA516 Gr. 70	700	32.9	49.3	NL

<sup>†</sup> Values for reference temperatures are taken as the design temperatures (Table 2.1.2).

<sup>††</sup> NL: No limit specified in the Code.

Table 2.1.22

INTENTIONALLY DELETED

Table 2.1.23

INTENTIONALLY DELETED

Table 2.1.24

## ALLOWABLE STRESS CRITERIA FROM OTHER SOURCES

OVERPACK CLOSURE BOLTS<sup>†</sup>:

STRESS CATEGORY	NORMAL CONDITIONS OF TRANSPORT	HYPOTHETICAL ACCIDENT
Average Tensile Stress	$2/3 S_y$	$\text{AMIN}(S_y, 0.7 S_u)$
Average Shear Stress	$0.6 (2/3 S_y)$	$\text{AMIN}(0.6 S_y, 0.42 S_u)$
Combined Tensile and Shear Stress <sup>††</sup>	$R_t^2 + R_s^2 < 1.0$	$R_t^2 + R_s^2 < 1.0$

## IMPACT LIMITER ATTACHMENT BOLTS:

STRESS CATEGORY	NORMAL CONDITIONS OF TRANSPORT	HYPOTHETICAL ACCIDENT
Average Tensile Stress	$2/3 S_y$	$S_u$
Average Shear Stress	$0.6 (2/3 S_y)$	$S_u$
Combined Tensile and Shear Stress	$R_t^2 + R_s^2 < 1.0$	$R_t^2 + R_s^2 < 1.0$

LIFTING TRUNNIONS AND **THREADED ANCHOR LOCATIONS**:

The lifting trunnions and the **TALs** for the overpack closure plate and the MPC lid are designed in accordance with NUREG-0612 and **Regulatory Guide 3.61**. Specifically, the design must meet factors of safety of **three** based on the material yield stress and ten based on the material ultimate stress.

**SPECIAL LIFTING DEVICES**:

The special lifting devices that are used to handle the overpack and the MPC are designed in accordance with NUREG-0612 and ANSI-N14.6. Specifically, the design must meet factors of safety of six based on the material yield stress and ten based on the material ultimate stress for non-redundant lifting devices.

<sup>†</sup> The overpack closure bolts are designed in accordance with NUREG/CR-6007, "Stress Analysis of Closure Bolts for Shipping Casks".

<sup>††</sup>  $R_t$  and  $R_s$  are the ratios of actual stress to shear stress, respectively.

**FIGURES 2.1.1 THROUGH 2.1.14: PROPRIETARY INFORMATION PER 10CFR2.390**

## 2.2 WEIGHTS AND CENTERS OF GRAVITY

Table 2.2.1 provides the weights of the individual HI-STAR 100 components as well as the total system weights. The weight of the impact limiter is also provided.

The locations of the calculated centers of gravity (CGs) are presented in Table 2.2.2 per the locations described in Figure 2.2.1. All centers of gravity are located on the cask centerline since the non-axisymmetry effects of the cask system plus contents are negligible.

Table 2.2.3 provides the lift weight for the HI-STAR 100 System when the heaviest fully loaded MPC is lifted from the fuel pool. The effect of buoyancy is neglected, and the weight of rigging is set at a conservative value.

Table 2.2.4 provides a table of bounding weights that may be used in calculations where additional conservatism is introduced by increasing the weight.

Table 2.2.1  
[PROPRIETARY INFORMATION WITHHELD PER 10CFR2.390]

Table 2.2.2

[PROPRIETARY INFORMATION WITHHELD PER 10CFR2.390]



Table 2.2.3

[PROPRIETARY INFORMATION WITHHELD PER 10CFR2.390]

Table 2.2.4

[PROPRIETARY INFORMATION WITHHELD PER 10CFR2.390]

**FIGURE 2.2.1: PROPRIETARY INFORMATION WITHHELD PER 10CFR2.390**

## 2.3 MECHANICAL PROPERTIES OF MATERIALS

This section provides the mechanical properties used in the structural evaluation. The properties include yield stress, ultimate stress, modulus of elasticity, Poisson's ratio, weight density, and coefficient of thermal expansion. The property values are presented for a range of temperatures for which structural calculations are performed.

The materials selected for use in the HI-STAR 100 MPC and overpack are presented in the Bills-of-Materials in Chapter 1, Section 1.4. In this chapter, the materials are divided into two categories, structural and nonstructural. Structural materials are those that serve a load bearing function. Materials that do not support mechanical loads are considered nonstructural. For example, the overpack inner shell is a structural material, while Holtite-A (neutron shield) is a nonstructural material.

### 2.3.1 Structural Materials

#### 2.3.1.1 Alloy X

A hypothetical material termed Alloy X is defined for all MPC structural components. The material properties of Alloy X are the least favorable values from the set of candidate stainless alloys. The purpose of a "least favorable" material definition is to ensure that all structural analyses are conservative, regardless of the actual MPC material. For example, when evaluating the stresses in the MPC, it is conservative to work with the minimum values for yield strength and ultimate strength. This guarantees that the material used for fabrication of the MPC is of equal or greater strength than the hypothetical material used in the analysis. In the structural evaluation, the only property for which it is not always conservative to use the minimum values is the coefficient of thermal expansion. Two sets of values for the coefficient of thermal expansion are specified, a minimum set and a maximum set. For each analysis, the set of coefficients, minimum or maximum that causes the more severe load on the cask system is used. Table 2.3.1 lists the numerical values for the material properties of Alloy X versus temperature. These values, taken from the ASME Code, Section II, Part D [2.1.11], are used to complete all structural analyses. The maximum temperatures in MPC components may exceed the allowable limits of temperature during short time duration events. However, under no scenario does the maximum temperature of Alloy X material used in the helium confinement boundary exceed 1000°F. As shown in ASME Code Case N-47-33 (Class 1 Components in Elevated Temperature Service, 1995 Code Cases, Nuclear Components), the strength properties of austenitic stainless steels do not change due to exposure to 1000 °F temperature for up to 10,000 hours. Therefore, there is no significant effect on mechanical properties of the helium confinement boundary or fuel basket material during the short time duration loading. Further description of Alloy X, including the materials from which it is derived, is provided in Appendix 1.A.

Two properties of Alloy X which are not included in Table 2.3.1 are weight density and Poisson's ratio. These properties are assumed constant for all structural analyses, regardless of the temperature. The values used are shown in the table below.

PROPERTY	VALUE
Weight Density (lb./in <sup>3</sup> )	0.290
Poisson's Ratio	0.30

#### 2.3.1.2 Carbon Steel, Low-Alloy, and Nickel Alloy Steel

The carbon steels used in the HI-STAR 100 System are SA516 Grade 70, SA515 Grade 70. These steels are not constituents of Alloy X. The material properties of SA516 Grade 70 and SA515 Grade 70 are shown in Tables 2.3.2 and 2.3.3, respectively. The nickel alloy and low-alloy steels are SA203-E and SA350-LF3, respectively. The material properties of SA203-E and SA350-LF3 are given in Table 2.3.4.

Two properties of these steels which are not included in Tables 2.3.2 through 2.3.4 are weight density and Poisson's ratio. These properties are assumed constant for all structural analyses. The values used are shown in the table below.

PROPERTY	VALUE
Weight Density (lb./in <sup>3</sup> )	0.283
Poisson's Ratio	0.30

#### 2.3.1.3 Bolting Materials

Material properties of the bolting materials used in the HI-STAR System are given in Table 2.3.5.

#### 2.3.1.4 Weld Material

All weld filler materials utilized in the welding of the Code components will comply with the provisions of the appropriate ASME subsection (e.g., Subsection NB for the overpack and enclosure vessel) and Section IX. All non-Code welds shall also be made using weld procedures that meet Section IX of the ASME Code. All non-code welds shall also be made using weld procedures that meet Section IX of the ASME Code. The minimum tensile strength of the weld wire and filler material (where applicable) will be equal to or greater than the tensile strength of the base metal listed in the ASME Code.

#### 2.3.1.5 Impact Limiter

The Impact Limiter for the HI-STAR 100 System has been named AL-STAR™. The original design of AL-STAR for the HI-STAR 100 package is composed of cross core (i.e., bi-directional) and uni-directional aluminum honeycomb made by layering corrugated sheets of aluminum (Alloy 5052). With appropriately adjusted crush strengths of aluminum honeycomb, AL-STAR is also used for HI-STAR HB (see Supplement 2.I), which is a shorter and lighter

version of HI-STAR 100. An improved design of AL-STAR, which is evaluated in Appendix 2.C for use with the HI-STAR 100 cask only, uses just one type of cross core aluminum honeycomb material and no uni-directional material. For the cross core material, alternate layers of corrugated aluminum sheets are laid in orthogonal direction to each other (Figure 2.3.1). The layers are bonded together by a high-temperature epoxy. The Holtec drawing in Section 1.4 illustrates the arrangement of the cross core and uni-directional honeycomb sectors in AL-STAR to realize adequate crush moduli in all potential impact modes. The external surface of AL-STAR consists of a stainless steel skin to provide long-term protection against weather and environmental conditions.

Rail transport considerations limit the maximum diameter of the impact limiter to 128 inches. The axial dimension of AL-STAR is limited by the considerations of maximum permissible packaging weight for rail transport. Within the limitations of space and weight, AL-STAR must possess sufficient energy absorption capacity so as to meet the design basis rigid body deceleration limits (Table 2.1.10) under all postulated drop orientations. The sizing of the AL-STAR internal structure is principally guided by the above considerations. For example, in order to ensure that a sufficient portion of the honeycomb structure participates in lateral impacts, a thick carbon steel shell buttressed with gussets provides a hard backing surface for the aluminum honeycomb to crush against.

Two properties of the cross core honeycomb germane to its function are the crush strength and the nominal density. The crush strength of AL-STAR is the more important of the two properties; the density is significant in establishing the total weight of the package. The crush strength increases monotonically with density. For example, the cross core honeycomb of 2500 psi crush strength has a nominal density of 27 lb. per cubic foot. At 2,000 psi crush strength, the change in aluminum honeycomb parameters lowers the density to approximately 22 lb. per cubic foot. The crush strength of the honeycomb can be varied within a rather wide range by adjusting the aluminum foil thickness and corrugation size. Table 2.3.7 lists the required crush strengths of the honeycomb section types (see drawings in Section 1.4) in the various regions of AL-STAR for use with the HI-STAR 100 and HI-STAR HB transport casks.

Like all manufactured materials, the crush strength and density of the honeycomb material are subject to slight variation within a manufactured lot. For all aluminum honeycomb materials used in AL-STAR, the crush strength will be held to the tolerance specified in Table 2.3.7.

Hexcel Corporation's publication TSB 120, "Mechanical Properties of Hexcel Honeycomb Materials", [2.3.1] provides detailed information on the mechanical characteristics of aluminum honeycomb materials. Hexcel's experimental data shows that the load-deflection curve of aluminum honeycomb simulates the shape of elastic-perfectly plastic materials. The honeycomb crushes at a nearly uniform load (slowly applied) until solidity in the range of 30 to 40% is reached. It is the crushing at constant load characteristic of aluminum honeycomb along with its excellent crush strength-to-weight ratio that makes it an ideal energy absorption material. The cross layered honeycomb (cross-core) has an identical crush strength in two orthogonal directions. In other words, from a load-deflection standpoint, the cross-layered honeycomb is a transversely isotropic material.

A typical honeycomb pressure-strain curve is illustrated in Figure 2.A.2.1 in Appendix 2.A wherein additional discussion on the crush properties of the honeycomb material is provided.

However, three key properties of the honeycomb material which are central to its function as a near-ideal impact limiter crush material are summarized below.

- i. The honeycomb material can be used in the "un-crushed" or "pre-crushed" condition. The difference is in the initial "bump" in the pressure-strain curve shown in Figure 2.A.2.1. By pre-crushing the honeycomb, its pressure-strain relationship simulates that of an ideal elastic-perfectly-plastic material, which is most desirable in limiting abrupt peaks in the deceleration of the package under drop events.
- ii. Irrespective of the crush strength, under quasi-static loading, all honeycomb materials begin to strain harden at about 60% strain and lock up at about 70%. Thus, a 10-inch thick honeycomb column will crush down to a thickness of 4 inches at near constant force; crushing further will require progressively greater compression force. The six inches of available crush distance is referred to as the available "stroke" in the lexicon of impact limiter design technology.
- iii. Because the crush material is made entirely out of one of the most cryogenically competent industrial metals available, aluminum, the pressure-crush behavior of the AL-STAR honeycomb material is insensitive to the environmental temperature range germane to Part 71 transport (-20 degrees F to 100 degrees F). Table Y-1 of the ASME Code [2.1.11] lists the yield strength of the material (Alloy 5052) to be constant in the range -20 degrees F to 350 degrees F.

Independent confirmation of the invariance of the ALSTAR's crush properties with temperature in the range of temperatures applicable to the HI-STAR 100 packaging was provided by experiments conducted by Holtec International in June 1998 [2.3.2] using sample material obtained from Hexcell. The test objective was to evaluate the temperature sensitivity, if any, of the static compression strength of the honeycomb material. To that end, test specimens were cut from the sample material and were subject to static compression testing using a Q.A. validated procedure.

A series of specimens of two different strengths were tested at three different temperatures. The specimens were tested at -29 degrees C, 23 degrees C and 80 degrees C which represent "Cold", "Ambient", and "Heat" environmental conditions. Ten specimens were prepared for each crush strength, to allow for multiple data points at each test temperature. The specimens were not pre-crushed so the static compression-crush curves exhibited an initial peak. After discounting the initial peaks in the static force-crush curve, the constant force range for each specimen could be identified from the test data and a crush pressure for the specimen defined by dividing this constant force by the measured specimen loaded area.

The computed crush pressures showed no significant trending that could be ascribed to environmental effects. Figure 2.3.2 is a plot of the test results and plots the average of the calculated test crush pressures from the series of specimens at each of the three temperatures.

The results for individual test samples at any given temperature were within manufacturing tolerance. It is clear from the plotted results that the effect of temperature is well within the data scatter due to manufacturing tolerance. Therefore, within the temperature range germane to the ALSTAR impact limiter, the force-crush characteristic is expected to be essentially unaffected by the coincident honeycomb metal temperature. This leads to the conclusion that environmental temperature effects will not influence impact limiter performance predictions.

Appendix 2.A contains further information on the AL-STAR honeycomb and its performance characteristics. The sensitivity of the package performance to variations in compression strength of the aluminum honeycomb is evaluated in Appendix 2.C for the latest HI-STAR 100 impact limiter design and in Supplement 2.I for the HI-STAR HB impact limiter design, respectively.

In summary, the AL-STAR impact limiter is composed of a carbon steel inner shell structure, an assemblage of cross core and uni-directional aluminum honeycombs and a stainless steel external sheathing.

None of the structural materials has a low melting point or is flammable. A Holtite-A layer is situated deep in the honeycomb in such a manner that it does not participate in the crushing process, but provides neutron shielding in the axial direction.

### 2.3.2 Nonstructural Materials

#### 2.3.2.1 Neutron Shield

The neutron shield in the overpack is not considered as a structural member of the HI-STAR 100 System. Its load carrying capacity is neglected in all structural analyses except where such omission would be nonconservative. The only material property of the neutron shield which is important to the structural evaluation is weight density ( $1.63 \text{ g/cm}^2$ ).

#### 2.3.2.2 Solid Neutron Absorber

The fuel basket solid neutron absorber is not a structural member of the HI-STAR 100 System. Its load carrying capacity is neglected in all structural analyses. The only material property of solid neutron absorber that is important to the structural evaluation is weight density. As the MPC fuel baskets can be constructed with neutron absorber panels of variable areal density, the weight that produces the most severe cask load is assumed in each analysis. (Density  $2.644 \text{ g/cm}^3$ ).

#### 2.3.2.3 Aluminum Heat Conduction Elements

The aluminum heat conduction elements are located between the fuel basket and MPC vessel in several of the early vintage MPC-68s and MPC-68Fs. They have since been removed from the MPC design and none were installed in the PWR MPCs. They are thin, flexible elements whose sole function is to transmit heat from the basket. They are not credited with any structural load capacity and are shaped to provide negligible resistance to basket thermal expansion. The total weight of the aluminum heat conduction elements is less than 1,000 lb. per MPC.



Table 2.3.1

## ALLOY X MATERIAL PROPERTIES

Temp. (°F)	Alloy X				
	$S_y$	$S_u^\dagger$	$\alpha_{\min}$	$\alpha_{\max}$	E
-40	30.0	75.0 (70.0)	8.54	8.55	28.82
100	30.0	75.0 (70.0)	8.54	8.55	28.14
150	27.5	73.0 (68.1)	8.64	8.67	27.87
200	25.0	71.0 (66.2)	8.76	8.79	27.6
250	23.75	68.5 (63.85)	8.88	8.9	27.3
300	22.5	66.0 (61.5)	8.97	9.0	27.0
350	21.6	65.2 (60.75)	9.10	9.11	26.75
400	20.7	64.4 (60.0)	9.19	9.21	26.5
450	20.05	64.0 (59.65)	9.28	9.32	26.15
500	19.4	63.5 (59.3)	9.37	9.42	25.8
550	18.8	63.3 (59.1)	9.45	9.50	25.55
600	18.2	63.1 (58.9)	9.53	9.6	25.3
650	17.8	62.8 (58.6)	9.61	9.69	25.05
700	17.3	62.5 (58.4)	9.69	9.76	24.8
750	16.9	62.2 (58.1)	9.76	9.81	24.45
800	16.6	61.7 (57.6)	9.82	9.90	24.1

## Definitions:

 $S_y$  = Yield Stress (ksi) $\alpha$  = Mean Coefficient of thermal expansion (in./in. per degree F x  $10^{-6}$ ) $S_u$  = Ultimate Stress (ksi)E = Young's Modulus (psi x  $10^6$ )

## Notes:

1. Source for  $S_y$  values is Table Y-1 of [2.1.11].
2. Source for  $S_u$  values is Table U of [2.1.11].
3. Source for  $\alpha_{\min}$  and  $\alpha_{\max}$  values is Table TE-1 of [2.1.11].
4. Source for E values is material group G in Table TM-1 of [2.1.11].

<sup>†</sup> The ultimate stress of Alloy X is dependent on the product form of the material (i.e., forgings vs. plate). Values in parentheses are based on SA-336 forging materials (Type F304, F304LN, F316, and F316LN), which are used solely for the one-piece construction MPC lids. All other values correspond to SA-240 plate material.

Table 2.3.2

## SA516, GRADE 70 MATERIAL PROPERTIES

Temp. (°F)	SA516, Grade 70			
	S <sub>y</sub>	S <sub>u</sub>	$\alpha$	E
-40	38.0	70.0	5.53	29.34
100	38.0	70.0	5.53	29.34
150	36.3	70.0	5.71	29.1
200	34.6	70.0	5.89	28.8
250	34.15	70.0	6.09	28.6
300	33.7	70.0	6.26	28.3
350	33.15	70.0	6.43	28.0
400	32.6	70.0	6.61	27.7
450	31.65	70.0	6.77	27.5
500	30.7	70.0	6.91	27.3
550	29.4	70.0	7.06	27.0
600	28.1	70.0	7.17	26.7
650	27.6	70.0	7.30	26.1
700	27.4	70.0	7.41	25.5
750	26.5	69.3	7.50	24.85

## Definitions:

S<sub>y</sub> = Yield Stress (ksi) $\alpha$  = Mean Coefficient of thermal expansion (in./in. per degree F x 10<sup>-6</sup>)S<sub>u</sub> = Ultimate Stress (ksi)E = Young's Modulus (psi x 10<sup>6</sup>)

## Notes:

1. Source for S<sub>y</sub> values is Table Y-1 of [2.1.11].
2. Source for S<sub>u</sub> values is Table U of [2.1.11].
3. Source for  $\alpha$  values is material group C in Table TE-1 of [2.1.11].
4. Source for E values is "Carbon steels with C ≤ 0.30%" in Table TM-1 of [2.1.11].

Table 2.3.3

## SA515, GRADE 70 MATERIAL PROPERTIES

Temp. (°F)	SA515, Grade 70			
	S <sub>y</sub>	S <sub>u</sub>	α	E
-40	38.0	70.0	5.53	29.34
100	38.0	70.0	5.53	29.34
150	36.3	70.0	5.71	29.1
200	34.6	70.0	5.89	28.8
250	34.15	70.0	6.09	28.6
300	33.7	70.0	6.26	28.3
350	33.15	70.0	6.43	28.0
400	32.6	70.0	6.61	27.7
450	31.65	70.0	6.77	27.5
500	30.7	70.0	6.91	27.3
550	29.4	70.0	7.06	27.0
600	28.1	70.0	7.17	26.7
650	27.6	70.0	7.30	26.1
700	27.4	70.0	7.41	25.5
750	26.5	69.3	7.50	24.85

## Definitions:

S<sub>y</sub> = Yield Stress (ksi)α = Mean Coefficient of thermal expansion (in./in. per degree F x 10<sup>-6</sup>)S<sub>u</sub> = Ultimate Stress (ksi)E = Young's Modulus (psi x 10<sup>6</sup>)

## Notes:

1. Source for S<sub>y</sub> values is Table Y-1 of [2.1.11].
2. Source for S<sub>u</sub> values is Table U of [2.1.11].
3. Source for α values is material group C in Table TE-1 of [2.1.11].
4. Source for E values is "Carbon steels with C ≤ 0.30%" in Table TM-1 of [2.1.11].

Table 2.3.4

## SA350-LF3 AND SA203-E MATERIAL PROPERTIES

Temp. (°F)	SA350-LF3			SA350-LF3/SA203-E		SA203-E		
	S <sub>m</sub>	S <sub>y</sub>	S <sub>u</sub>	E	$\alpha$	S <sub>m</sub>	S <sub>y</sub>	S <sub>u</sub>
-100	23.3	37.5	70.0	28.5	6.20	23.3	40.0	70.0
100	23.3	37.5	70.0	27.6	6.27	23.3	40.0	70.0
200	22.8	34.2	68.5	27.1	6.54	23.3	36.5	70.0
300	22.2	33.2	66.7	26.7	6.78	23.3	35.4	70.0
400	21.5	32.2	64.6	26.1	6.98	22.9	34.3	68.8
500	20.2	30.3	60.7	25.7	7.16	21.6	32.4	64.9
600	18.5	-	-	-	-	-	-	-
700	16.8	-	-	-	-	-	-	-

## Definitions:

- S<sub>m</sub> = Design Stress Intensity (ksi)  
 S<sub>y</sub> = Yield Stress (ksi)  
 S<sub>u</sub> = Ultimate Stress (ksi)  
 $\alpha$  = Coefficient of Thermal Expansion (in./in. per degree F x 10<sup>-6</sup>)  
 E = Young's Modulus (psi x 10<sup>6</sup>)

## Notes:

1. Source for S<sub>m</sub> values is Table 2A of [2.1.11].
2. Source for S<sub>y</sub> values is Table Y-1 of [2.1.11].
3. Source for S<sub>u</sub> values is ratioing S<sub>m</sub> values.
4. Source for  $\alpha$  values is material group E in Table TE-1 of [2.1.11].
5. Source for E values is material group B in Table TM-1 of [2.1.11].

Table 2.3.5

## SB637-N07718, SA564-630, AND SA705-630 MATERIAL PROPERTIES

Temp. (°F)	SB637-N07718				
	S <sub>y</sub>	S <sub>u</sub>	E	α	S <sub>m</sub>
-100	150.0	185.0	29.9	---	50.0
-20	150.0	185.0	---	---	50.0
70	150.0	185.0	29.0	7.05	50.0
100	150.0	185.0	---	7.08	50.0
200	144.0	177.6	28.3	7.22	48.0
300	140.7	173.5	27.8	7.33	46.9
400	138.3	170.6	27.6	7.45	46.1
500	136.8	168.7	27.1	7.57	45.6
600	135.3	166.9	26.8	7.67	45.1
SA705-630/SA564-630 (Age Hardened at 1075°F)					
Temp. (°F)	S <sub>y</sub>	S <sub>u</sub>	E	α	-
200	115.6	145.0	28.5	5.9	-
300	110.7	145.0	27.9	5.9	-
400	106.7	141	-	-	-
500	103.5	140	-	-	-
SA705-630/SA564-630 (Age Hardened at 1150°F)					
200	97.1	135.0	28.5	5.9	-
300	93.0	135.0	27.9	5.9	-
400	89.8	131.4	-	-	-
500	87	128.5	-	-	-

## Definitions:

S<sub>m</sub> = Design Stress Intensity (ksi)S<sub>y</sub> = Yield Stress (ksi)α = Mean Coefficient of thermal expansion (in./in. per degree F x 10<sup>-6</sup>)S<sub>u</sub> = Ultimate Stress (ksi)E = Young's Modulus (psi x 10<sup>6</sup>)

## Notes:

1. Source for S<sub>m</sub> values is Table 4 of [2.1.11].
2. Source for S<sub>y</sub>, S<sub>u</sub> values is ratioing design stress intensity values.
3. Source for α values is Tables TE-1 and TE-4 of [2.1.11], as applicable.
4. Source for E values is Table TM-1 of [2.1.11].

Table 2.3.6

## YIELD STRENGTH OF SA-193-B8S IMPACT LIMITER ATTACHMENT BOLTS

Yield Stress for Attachment Bolt Calculations <sup>†</sup>	
Item	Yield Stress (psi)
Yield Stress	50,000

---

<sup>†</sup> Source for stress is Table 3 of [2.1.11].

Table 2.3.7

**CRUSH STRENGTHS OF AL-STAR IMPACT LIMITER ALUMINUM HONEYCOMB MATERIALS**

Honeycomb Section Type <sup>(1)</sup>	Allowable Crush Strength (psi)	
	HI-STAR 100	HI-STAR HB
Type 1	[PROPRIETARY INFORMATION WITHHELD PER 10CFR2.390]	[PROPRIETARY INFORMATION WITHHELD PER 10CFR2.390]
Type 2	[PROPRIETARY INFORMATION WITHHELD PER 10CFR2.390]	[PROPRIETARY INFORMATION WITHHELD PER 10CFR2.390]
Type 3	[PROPRIETARY INFORMATION WITHHELD PER 10CFR2.390]	[PROPRIETARY INFORMATION WITHHELD PER 10CFR2.390]
Type 4	[PROPRIETARY INFORMATION WITHHELD PER 10CFR2.390]	[PROPRIETARY INFORMATION WITHHELD PER 10CFR2.390]
Notes: (1) Honeycomb block types for HI-STAR 100 and HI-STAR HB are defined on impact limiter drawings (listed in Sections 1.4 and 1.I.4); (2) Bi-directional core with the crush strength specified in primary impact directions T1 and T2 as shown on the impact limiter drawings (listed in Sections 1.4 and 1.I.4)		

**FIGURES 2.3.1 THROUGH 2.3.2: PROPRIETARY INFORMATION WITHHELD PER  
10CFR2.390**



## 2.4 GENERAL STANDARDS FOR ALL PACKAGES

The compliance of the HI-STAR 100 System to the general standards for all packaging, specified in 10CFR71.43, is demonstrated in the following paragraphs.

### 2.4.1 Minimum Package Size

The HI-STAR 100 package meets the requirements of 10CFR71.43(a); the outer diameter of the overpack is approximately 96" and its length is approximately 203".

### 2.4.2 Tamperproof Feature

During transport operations, a wire tamper seal with a stamped identifier will be attached between the lower base of the upper impact limiter shell and the head of one of the impact limiter attachment bolts for the purpose of indicating possible tampering. In order to access the radioactive contents of the overpack, the upper impact limiter is required to be removed to access the closure plate bolting. This tamper seal satisfies the requirements of 10CFR71.43(b). A second wire tamper seal will be attached between the lower impact limiter and an attachment bolt head to indicate tampering. This seal will prevent access to the drain port. The assembly drawing in Section 1.4 depicts the security seals.

### 2.4.3 Positive Closure

There are no quick-connect/disconnect valves in the containment boundary of the HI-STAR 100 packaging. [

PROPRIETARY INFORMATION WITHHELD PER 10CFR2.390

]

### 2.4.4 Chemical and Galvanic Reactions

There is no credible mechanism for significant chemical or galvanic reactions in the HI-STAR 100 System during loading operations.

The MPC, which is filled with helium, provides a nonaqueous and inert environment. Insofar as corrosion is a long-term time-dependent phenomenon, the inert gas environment in the MPC precludes the incidence of corrosion during transport. Furthermore, the only dissimilar material groups in the MPC are: (1) the neutron absorber material and stainless steel and (2) aluminum

and stainless steel. Neutron absorber materials and stainless steel have been used in close proximity in wet storage for over 30 years. Many spent fuel pools at nuclear plants contain fuel racks, which are fabricated from neutron absorber materials and stainless steel materials, with geometries similar to the HI-STAR 100 MPC. Not one case of chemical or galvanic degradation has been found in fuel racks built by Holtec. This experience provides a sound basis to conclude that corrosion will not occur in these materials. Additionally, the aluminum heat conduction elements and stainless steel basket are very close on the galvanic series chart. Aluminum, like other metals of its genre (e.g., titanium and magnesium) rapidly passivates in an aqueous environment, leading to a thin ceramic ( $\text{Al}_2\text{O}_3$ ) barrier, which renders the material essentially inert and corrosion-free over long periods of application. The physical properties of the material, e.g., thermal expansion coefficient, diffusivity, and thermal conductivity, are essentially unaltered by the exposure of the aluminum metal stock to an aqueous environment.

The aluminum in the optional heat conduction elements will quickly passivate in air and in water to form a protective oxide layer that prevents any significant hydrogen production during MPC cask loading and unloading operations. The aluminum in neutron absorber material may also react with water to generate hydrogen gas. The exact rate of generation and total amount of hydrogen generated is a function of a number of variables (see Section 1.2.1.4.1) and cannot be predicted with any certainty. Therefore, to preclude the potential for hydrogen ignition during lid welding or cutting, the operating procedures in Chapter 7 describe steps to monitor and mitigate combustible gas accumulation space beneath the MPC lid. Once the MPC cavity is drained, dried, and backfilled with helium, the source of hydrogen gas (the aluminum-water reaction) is eliminated.

The HI-STAR 100 overpack combines low-alloy and nickel alloy steels, carbon steels, neutron and gamma shielding, thermal expansion foam, and bolting materials. All of these materials have a long history of nongalvanic behavior within close proximity of each other. The internal and external carbon steel surfaces of the overpack and closure plates are sandblasted and coated to preclude surface oxidation. The coating does not chemically react with borated water. Therefore, chemical or galvanic reactions involving the overpack materials are highly unlikely and are not expected.

The interfacing seating surfaces of the closure plate metallic seals are clad with stainless steel to assure long-term sealing performance and to eliminate the potential for localized corrosion of the seal seating surfaces.

In accordance with NRC Bulletin 96-04, a review of the potential for chemical, galvanic, or other reactions among the materials of the HI-STAR 100 System, its contents and the operating environment, which may produce adverse reactions, has been performed. Table 2.4.1 provides a listing of the materials of fabrication for the HI-STAR 100 System and evaluates the performance of the material in the expected operating environments during short-term loading/unloading operations and transport operations. As a result of this review, no operations were identified which could produce adverse reactions beyond those conditions already analyzed in this SAR.

The HI-STAR 100 System is composed of materials with a long proven history of use in the nuclear industry. The materials are not affected by the radiation levels caused by the spent nuclear fuel. Gamma radiation damage to metals (e.g., aluminum, stainless steel, and carbon steel) does not occur until the dose reaches  $10^{18}$  rads or more. The gamma dose from the spent nuclear fuel transported in the HI-STAR 100 System is on the order of  $10^{10}$  rads. Moreover, significant radiation damage due to neutron exposure does not occur for neutron fluences below approximately  $10^{19}$  n/cm<sup>2</sup> [2.4.1, 2.4.2], which is far greater than the neutron fluence for which components of the HI-STAR 100 System will be exposed.

Table 2.4.1

HI-STAR 100 SYSTEM MATERIAL COMPATIBILITY  
WITH OPERATING ENVIRONMENTS

Material/Component	Fuel Pool (Borated and Unborated Water) <sup>1</sup>	Transport (Open to Environment)
Alloy X:  -MPC Fuel Basket -MPC Baseplate -MPC Shell -MPC Lid -MPC Fuel Spacers	Stainless steels have been extensively used in spent fuel storage pools with both borated and unborated water with no adverse reactions or interactions with spent fuel.	The MPC internal and external environment will be inert (helium) atmosphere. No adverse interactions identified.
Aluminum  -Conduction Inserts	Aluminum and stainless steels form a galvanic couple. However, they are very close on the galvanic series chart and aluminum rapidly passivates in an aqueous environment forming a thin ceramic (Al <sub>2</sub> O <sub>3</sub> ) barrier. The aluminum will be installed in a passivated condition. Therefore, during the short time they are exposed to fuel pool water, corrosion is not expected.	In a non-aqueous atmosphere galvanic corrosion is not expected.
Neutron Absorber Material:	Extensive in-pool experience on spent fuel racks with no adverse reactions. See Chapter 7 for additional requirements for combustible gas monitoring and required actions for control of combustible gas accumulation under the MPC lid.	No adverse reactions identified.

<sup>1</sup> HI-STAR 100 System short-term operating environment during loading and unloading.

Table 2.4.1 (continued)

HI-STAR 100 SYSTEM MATERIAL COMPATIBILITY  
WITH OPERATING ENVIRONMENTS

Material/Component	Fuel Pool (Borated and Unborated Water) <sup>2</sup>	Transport (Open to Environment)
<p>Steels:</p> <ul style="list-style-type: none"> <li>-SA350-LF3</li> <li>-SA203-E</li> <li>-SA515 Grade 70</li> <li>-SA516 Grade 70</li> <li>-SA750 630 17-4 PH</li> <li>-SA564 630 17-4 PH</li> <li>-SA106</li> <li>-SA193-B7</li> </ul> <p>Overpack Body</p>	<p>All exposed steel surfaces (except seal areas, pocket trunnions, and bolt locations) will be coated with paint specifically selected for performance in the operating environments. Even without coating, no adverse reactions (other than nominal corrosion) have been identified.</p>	<p>Internal surfaces of the overpack will be painted and maintained in an inert atmosphere. Exposed external surfaces (except those listed in fuel pool column) will be painted and will be maintained with a fully painted surface. No adverse reactions identified.</p>
<p>Stainless Steels:</p> <ul style="list-style-type: none"> <li>-SA240 304</li> <li>-SA193 Grade B8</li> <li>-18-8 S/S</li> </ul> <p>Miscellaneous Components</p>	<p>Stainless steels have been extensively used in spent fuel storage pools with both borated and unborated water with no adverse reactions.</p>	<p>Stainless steel has a long proven history of corrosion resistance when exposed to the atmosphere. These materials are used for bolts and threaded inserts. No adverse reactions with steel have been identified. No impact on performance.</p>

<sup>2</sup> HI-STAR 100 System short-term operating environment during loading and unloading.

Table 2.4.1 (continued)

HI-STAR 100 SYSTEM MATERIAL COMPATIBILITY  
WITH OPERATING ENVIRONMENTS

Material/Component	Fuel Pool (Borated and Unborated Water) <sup>3</sup>	Transport (Open to Environment)
Nickel Alloy: -SB637-NO7718 Bolting	Bolts are not used in pool.	Exposed to weathering effects. No adverse reactions with overpack closure plate. No impact on performance.
Brass: -Rupture Disk	Small surface of rupture disk will be exposed. No significant adverse impact identified.	Exposed to external weathering. No loss of function expected. Disks inspected prior to transport.
Holtite-A: -Neutron Shield	The neutron shield is fully enclosed by the outer enclosure. No adverse reaction identified. No adverse reactions with thermal expansion foam or steel.	The neutron shield is fully enclosed in the outer enclosure. No adverse reaction identified. No adverse reactions with thermal expansion foam or steel.
Silicone Foam: -Thermal Expansion Foam	Fully enclosed in the outer enclosure. No adverse reaction identified. No adverse reactions with neutron shield or steel.	Foam is fully enclosed in outer enclosure. No adverse reaction identified. No adverse reactions with neutron shield or steel.

---

<sup>3</sup> HI-STAR 100 System short-term operating environment during loading and unloading.

Table 2.4.1 (continued)

HI-STAR 100 SYSTEM MATERIAL COMPATIBILITY  
WITH OPERATING ENVIRONMENTS

Material/Component	Fuel Pool (Borated and Unborated Water) <sup>4</sup>	Transport (Open to Environment)
<u>Paint:</u>  - Carboline 890 - Thermaline 450	<p>Carboline 890 used for exterior surfaces. Acceptable performance for short-term exposure in mild borated pool water.</p> <p>Thermaline 450 selected for excellent high temperature resistance properties. Will only be exposed to demineralized water during in-pool operations as annulus is filled prior to placement in the spent fuel pool and the inflatable seal prevents fuel pool water in-leakage. No adverse interaction identified which could affect MPC/fuel assembly performance.</p>	<p>Good performance on exterior surfaces. Discoloration is not a concern.</p> <p>During transport, internal overpack surfaces will operate in an inert (helium) atmosphere. No adverse reaction identified.</p>
<u>Metallic Seals:</u>  - Alloy X750 - 304 S/S	Not installed or exposed during in-pool handling.	<p>Seals enclosed by closure plate or port cover plates.</p> <p>Closure plate seals seat against stainless steel overlay surfaces. No degradation of seal integrity due to corrosion is expected.</p>

<sup>4</sup> HI-STAR 100 System short-term operating environment during loading and unloading.

## 2.5 LIFTING AND TIE-DOWN STANDARDS

### 2.5.1 Lifting Devices

As required by Reg. Guide 7.9, in this subsection, analyses for all lifting operations applicable to the transport of a HI-STAR 100 package are presented to demonstrate compliance with the requirements of paragraph 71.45(a) of 10CFR71.

The HI-STAR 100 System has the following types of lifting devices: lifting trunnions located on the overpack top flange and threaded holes for eye bolts to lift the overpack closure plate. Lifting devices associated with movement of the MPC are not considered here; MPC lifting is addressed in a companion HI-STORM 100 document (FSAR, Docket 72-1014), and summarized in Subsection 2.5.1.3.

The evaluation of the adequacy of the lifting devices entails careful consideration of the applied loading and associated stress limits. The load combination  $D+H$ , where  $H$  is the "handling load", is the generic case for all lifting adequacy assessments. The term  $D$  denotes the dead load. Quite obviously,  $D$  must be taken as the bounding value of the dead load of the component being lifted. Table 2.2.4 gives bounding weights. In all lifting analyses considered in this document, the handling load  $H$  is assumed to be equal to  $0.15D$ . In other words, the inertia amplifier during the lifting operation is assumed to be equal to  $0.15g$ . This value is consistent with the guidelines of the Crane Manufacturer's Association of America (CMAA), Specification No. 70, 1988, Section 3.3, which stipulates a dynamic factor equal to  $0.15$  for slowly executed lifts. Thus, the "apparent dead load" of the component for stress analysis purposes is  $D^* = 1.15D$ . Unless otherwise stated, all lifting analyses in this section use the "apparent dead load",  $D^*$ , in the lifting analysis.

Analysis methodology to evaluate the adequacy of the lifting device may be analytical or numerical. For the analysis of the trunnion, an accepted conservative technique for computing the bending stress is to assume that the lifting force is applied at the tip of the trunnion "cantilever" and that the stress state is fully developed at the base of the cantilever. This conservative technique, recommended in NUREG-1536 for use in a storage FSAR, is applied to the trunnion analyses presented in this SAR.

The lifting trunnions are designed to meet the requirements of 10CFR71.45(a). The lifting attachments that are part of the HI-STAR 100 package also meet the design requirements of NUREG-0612 [2.1.9] and Regulatory Guide 3.61 [2.1.19], which define specific additional safety margins to ensure safe handling of heavy loads in critical regions of nuclear power plants. Satisfying the more conservative design requirements of NUREG-0612 and Regulatory Guide 3.61 ensures that the design requirements of 10CFR71.45(a) are met.

In general, the stress analysis to establish safety in lifting, pursuant to NUREG-0612 and Regulatory Guide 3.61, 10CFR71.45(a), and the ASME Code, requires evaluation of three discrete zones which may be referred to as (i) the ILPs, (ii) the trunnion/component interface, hereinafter referred to as Region A, and (iii) the rest of the component, specifically the stressed metal zone adjacent to Region A, herein referred to as Region B.



Stress limits germane to each of the above three areas are discussed below:

- i. **Interfacing Lift Points:** Under the “apparent dead load”,  $D^*$ , the maximum primary stress in the ILPs (trunnions and TALs) must be less than  $1/10^{\text{th}}$  of the material ultimate strength per NUREG-0612 and less than  $1/3^{\text{rd}}$  of the material yield strength per Regulatory Guide 3.61. For example, the maximum moment and shear forces developed in the trunnion cantilever must be less than  $1/3^{\text{rd}}$  of the moment and shear forces corresponding to incipient plasticity, and less than  $1/10^{\text{th}}$  of the flexural collapse moment or the ultimate shear force for the section.
- ii. **Region A: Trunnion/Component Interface:** Stresses in Region A must meet ASME Code Level A limits under applied load  $D^*$ . Additionally, paragraph 71.45(a) of 10CFR71 requires that the maximum primary stress under  $3D^*$  be less than the yield strength of the weaker of the two materials at the trunnion/component interface. In cases involving section bending, the developed section moment must be compared against the plastic moment at yield. Typically, the stresses in the component in the vicinity of the trunnion/component interface are higher than elsewhere. However, exceptional situations exist. For example, when lifting a loaded MPC, the overpack baseplate, which supports the entire weight of the loaded MPC, is a candidate location for high stress even though it is far removed from the lifting location (which is located in the top lid).
- iii. **Region B:** This region constitutes the remainder of the component where the stress limits under the concurrent action of the apparent dead load  $D^*$  and other mechanical loads that may be present during handling (e.g. internal pressure) are required to meet Level A Service Limits under normal conditions of transport.

In summary, both Region A and Region B are required to meet the stress limits corresponding to ASME Level A under the load  $D^*$ . Additionally, portions of the component that may experience high stress during the lift are subject to the stress criterion of paragraph 71.45(a) of 10CFR71, which requires satisfaction of yield strength as the limit when the sole applied load is  $3D^*$ . In general, all locations of high stress in the component under  $D^*$  must also be checked for compliance with ASME Code Level A stress limits.

Unless explicitly stated otherwise, all analyses of lifting operations presented in this report follow the load definition and allowable stress provisions of the foregoing. Consistent with the practice adopted throughout this chapter, results are presented in dimensionless form, as safety factors, defined as SF, where

$SF = (\text{Allowable Stress in the Region Considered})/(\text{Computed Maximum Stress in the Region})$

It should be emphasized that the safety factor, SF, defined in the foregoing, represents the additional margin that is over and beyond the margin built into NUREG 0612 (e.g. a factor of 10 on ultimate strength) **and Regulatory Guide 3.61 (e.g. a factor of 3 on yield strength)**.

In the following subsections, each of the lifting analyses performed to demonstrate compliance with regulations is described. Summary results are presented for each of the analyses.

It is recognized from the discussion in the foregoing that stresses in Region A are subject to two distinct criteria, namely Level A stress limits under D\* and any other loading that may be present (such as pressure) and yield strength at 3D\*. The “3D\*” identifier is used whenever the paragraph 71.45(a) load case (the stresses must be bounded by the yield point at 3D\*) is the applied loading.

The HI-STAR 100 System has two types of lifting devices that are used during handling and loading operations. Two lifting trunnions are located on the overpack top flange for vertical package handling operations. There are also four lifting eyeholes for handling of the overpack closure plate. Four lifting eyes are installed in the holes for connection to lifting slings.

The two lifting trunnions on the overpack top flange are spaced at 180-degree intervals. Trunnion analysis results are presented in Subsection 2.5.1.1.

The four threaded holes of the overpack closure plate accommodate lifting eyes that are used only for installation or removal of the overpack closure plate.

#### 2.5.1.1 Overpack Trunnion Analysis

The lifting trunnion for the HI-STAR 100 overpack is presented in the Holtec Drawings (Section 1.4). The two lifting trunnions for HI-STAR 100 are circumferentially spaced at 180 degrees. The trunnions are designed for a two-point lift and are sized to satisfy the aforementioned NUREG-0612 **and Regulatory Guide 3.61** criteria. The trunnion material is SB-637-N07718 bolt material, which is the same high strength material used for the closure plate bolts.

Each trunnion is initially threaded into the outer wall of the overpack top flange and is held in place by a locking pad. During a lifting operation, the moment and shear force are resisted by bearing and shearing stresses in the threaded connection.

The embedded trunnion is analyzed as a cantilever beam subjected to a uniformly distributed load applied over a short span of surface at the outer edge of the trunnion. Calculations demonstrate that the stresses in the trunnions, computed in the manner of the foregoing, comply with NUREG-0612 **and Regulatory Guide 3.61 criteria**.

Specifically, the following results are obtained:

Safety Factors from HI-STAR 100 Lifting Trunnion Stress Analysis <sup>†</sup>			
Item	Value (ksi) or (lb) or (lb-in)	Allowable (ksi) or (lb) or (lb-in)	Safety Factor
Bending stress (Comparison with Yield Stress/ <b>3</b> )	17.3	<b>49.0</b>	<b>2.83</b>
Shear stress (Comparison with Yield Stress/ <b>3</b> )	7.4	<b>29.4</b>	<b>3.98</b>
Bending Moment (Comparison with Ultimate Moment/10)	323,000	574,600	1.78
Shear Force (Comparison with Ultimate Force/10)	144,000	282,000	1.97

<sup>†</sup> The bounding lifted load is 250,000 lb. (per Table 2.2.4).

We note from the above that all safety factors are greater than 1.0. A factor of safety of exactly 1.0 means that the maximum stress, under apparent lift load D\*, is equal to the yield stress in tension or shear divided by **3**, or that the section moment or shear force is equal to the ultimate section moment capacity or section force capacity divided by 10.

It is also important to note that **the** safety factors associated with 10CFR71.45(a) are **inherently satisfied**.

#### 2.5.1.2 Stresses in the Overpack Closure Plate, Main Flange, and Baseplate During Lifting

##### 2.5.1.2.1 Analysis of Closure Plate Lifting Holes and Eyes

The closure plate of the HI-STAR 100 overpack is lifted using four wire rope slings. The slings are attached to the closure plate using clevis eyebolts threaded into four holes in the closure plate.

10CFR71.45(a) requires a safety factor of 3 (based on yield strength) for the stress qualification of the clevis eyebolts. Lid lifting will normally be carried out with a lift angle of 90 degrees. However, to be conservative, the analysis assumes a minimum lift angle of 45 degrees.

The eyebolts are sized for a bounding weight of 9,200 lbs. (a value that includes a 15% dynamic amplifier). The working capacity of standard eyebolts is specified with a safety factor of four. Accordingly, its bolt size is selected such that it has a working capacity of approximately 17,000 lb (vertical). This results in a safety factor of greater than 7.0 calculated against the clevis ultimate load capacity. The tapped holes and the specified bolts in the closure plate are analyzed and it is demonstrated that adequate thread strength and engagement length exists using allowable stresses in accordance with NUREG-0612 **and Regulatory Guide 3.61** requirements (which are more severe than 10CFR71.45(a) requirements)

Minimum safety factors are summarized in the table below where we note that a safety factor of 1.0 means that the stress is the **lesser** of yield stress/6 or ultimate stress/10.

Overpack Top Closure Bolts Minimum Safety Factors			
Item	Value (lb.)	Capacity (lb.)	Minimum Safety Factor
Overpack Top Closure Lifting Bolt <b>Thread</b> Shear	9,200	<b>48,850</b>	<b>5.31</b>
Overpack Top Closure Lifting Bolt Tension	9,200	<b>30,490</b>	<b>3.31</b>

#### 2.5.1.2.2 Top Flange

- ASME Service Condition (Region B)

During lifting of a loaded HI-STAR 100, the top flange of the overpack (in which the lift trunnions are located) is identified as a potential location for high stress levels.

The top flange interface with the trunnion under the lifted load D\* is analyzed using simplified strength of materials models that focus on the local stress state in the immediate vicinity of the connection that develops to react the applied trunnion load. The bending moment that is transferred from the trunnion to the top forging is reacted by a shear stress distribution on the threads. Figure 2.5.1 shows a schematic of the distribution used to react the applied moment by thread shear. The top flange is considered a NB component subject to the lifted load and internal pressure. The membrane stress intensity due to both components of load is computed at the interface and compared to the allowable local membrane stress intensity. The interface region is subject to the provisions of **Regulatory Guide (RG) 3.61**, and the thread shear stress and bearing stress are compared to 1/3<sup>rd</sup> of the top forging yield stress in shear or compression. The following table summarizes the results.

Top Flange Minimum Safety Factors (Interface with Trunnion)			
Item	Value (ksi)	Allowable (ksi)	Safety Factor
Bearing Stress ( <b>RG 3.61</b> Comparison)	3.808	<b>11.95</b>	<b>3.14</b>
Thread Shear Stress ( <b>RG 3.61</b> Comparison)	3.376	<b>7.17</b>	<b>2.12</b>
Stress Intensity ( <b>ASME</b> NB Comparison)	7.857	34.6	4.4

It is noted from the above that all safety factors are greater than 1.0 and that the safety factors for bearing stress and thread shear stress represent the *additional* margin over the factor of safety inherent in the member by virtue of the load multiplier mandated in **RG 3.61**.

- Overpack Top Flange and Baseplate Under 3D\*

Analyses are performed for the components of the HI-STAR 100 structure that are considered as Region A (namely, the top flange region and baseplate) and evaluated for safety under three times the apparent lifted load (3D\*). A one-quarter symmetry finite element model of the top section of the HI-STAR, without the lid has been constructed. The model is assumed constrained at 36" below the top of the top flange. Contact elements are used to model the interface between the trunnion and the top flange and the material behavior is assumed to be elastic-plastic in nature (i.e. a bi-linear stress strain curve is input into the finite element analysis model). The analysis seeks to demonstrate that under 3 times the lifted load, the maximum primary membrane stress across any section in the immediate vicinity of the trunnion is below the material yield strength and the primary membrane plus primary bending stress across any section does not exceed 1.5 times yield. The overpack baseplate is also analyzed using formulas from classical plate theory, conservatively assuming that the allowable strengths are determined at the component design temperature rather than at the lower normal operating conditions.

The results are summarized in the table below.

Overpack Top Flange and Baseplate Minimum Safety Factors (10CFR71.45(a) Loading)			
Item	Value (ksi)	Allowable (ksi)	Safety Factor
Top Flange Membrane Stress Intensity (3D*)	27.44	32.2	1.17
Top Flange Membrane plus Bending Stress Intensity (3D*)	30.0	48.3	1.61
Baseplate Membrane plus Bending Stress Intensity (3D*)	1.452	32.2	22.2

The safety factors are all greater than 1.0 indicating that the requirements of 10CFR71.45(a) are satisfied in the top flange and baseplate of the HI-STAR 100 overpack.

#### 2.5.1.3 MPC Lifting Analyses

The MPC can be inserted or removed from an overpack by lifting bolts that are designed for installation into threaded holes in the MPC top lid. In the HI-STORM 100 FSAR (Docket 72-1014) [2.5.1], the MPC top closure is examined considering the top lid as "Region B", where satisfaction of ASME Code Level A requirements is demonstrated. The analysis also considers highly stressed regions of the top closure as "Region A" where applied load is "3D\*". The MPC baseplate is analyzed under normal handling and subject to the allowable strengths appropriate to a component considered in "Region B". Finally, the baseplate region is further analyzed where loading is "3D\*" consistent with the MPC baseplate being considered as "Region A". The definitions of "Region A", "Region B", and "3D\*" as they apply to lifting analyses have been introduced at the beginning of this Subsection.

The lifting analysis of the MPC considers both the one-piece and the two-piece MPC lid

constructions, which are shown on the licensing drawings in Section 1.4. In addition, for the two-piece lid construction the analysis assumes that the bottom piece is fabricated from Alloy X material, since it is the weaker of the two material options (i.e., Alloy X or carbon steel covered/coated with stainless steel). The results of the MPC lifting analyses are summarized in Subsection 3.4.3 of the HI-STORM 100 FSAR [2.5.1], which show that all factors of safety are greater than 1.0 as required. It is important to note that conservative acceptance criteria are used in [1.0.7] in the evaluation of the TALs in the MPC lid. Specifically, the lesser of  $1/10^{\text{th}}$  of material ultimate strength and  $1/6^{\text{th}}$  of material yield strength is used which is applicable to special lifting devices per NUREG-0612 instead of the lesser of  $1/10^{\text{th}}$  of material ultimate strength (per NUREG-0612) and  $1/3^{\text{rd}}$  of material yield strength (per RG 3.61) for ILPs. The results from the updated analysis [2.6.5] for TALs using the stress limits for ILPs from Section 2.5.1 above are tabulated below.

Minimum Safety Factor for Internal Threads in MPC Lid from MPC Lifting Analysis			
Item	Value (ksi)	Allowable (ksi)	Safety Factor
MPC Lid	3.56	5.95	1.67

#### 2.5.1.4.1 Lifting of Damaged Fuel Canisters

All damaged fuel canisters suitable for deployment in the HI-STAR 100 Package are analyzed for structural integrity during a lifting operation. Appendix 2.B describes the analyses undertaken and summarizes the results obtained.

In conclusion, the synopses of lifting device, device/component interface, and component stresses, under all contemplated lifting operations for the HI-STAR 100 overpack and MPC have been presented in the foregoing, and show that all factors of safety are greater than 1.0.

### 2.5.2 Tie-Down Devices

#### 2.5.2.1 Discussion

The initial design of the HI-STAR 100 Systems envisioned a shear ring located on the top flange and pocket trunnions located near the bottom of the outer enclosure shell to serve as locations for tie-down. Accordingly, previous issues of the SAR included analyses to qualify the shear ring/pocket trunnion components as tie-down devices complying with the requirements of 10CFR71.45(b).

The pair of semi-obround recesses referred to as pocket trunnions were originally incorporated into the HI-STAR design to permit the cask to be upended (or downended) by using circular shafts inserted in the “pockets” to serve as rotation pivots. Recent handling experience with the seven HI-STAR 100 overpacks manufactured thus far (ca. April 2002) and the HI-TRAC transfer casks (which are similar in overall dimensions and weight) has shown that utilizing an L-shaped cradle, designed as an ancillary under Part 72 regulations for the upending and downending operations, is a more robust method of cask handling. The cradle method of handling Holtec’s overpacks and MPCs has garnered considerable experience through ISFSI implementation operations at several sites. Because the cradle method of upending and downending does not require the pocket trunnions, and because the recesses to incorporate the pocket trunnions lead to increased local dose, the pocket trunnions are

being henceforth eliminated from the HI-STAR design. All HI-STAR 100 overpacks (except the first seven units already manufactured) shall be fabricated without the twin pocket trunnions; even in the first seven units that have the shear ring and pocket trunnions, these locations are no longer designated as tie-down locations.

In lieu of relying on the pocket trunnions for tie-down, the revised tie-down arrangement for HI-STAR 100 secures the overpack to the transport vehicles in such a manner that the longitudinal inertia forces (the most frequent mode of motion-induced loading the package during transport) do not exert an overturning moment on the cask (as is the case with a pocket trunnion-based fastening means). In fact, the revised tie-down device seeks to eliminate or minimize all localized loadings on the body of the overpack, thus incorporating an additional element of safety in the transport package.

The new tie-down configuration, pictorially illustrated in Figure 1.2.8, essentially consists of a near-full-length saddle integral to the bed of the transport vehicle to react the lateral and vertical loads, and a pair of End-Restraints, also integral to the transport vehicle, that save for a small calibrated axial clearance to provide for differential thermal expansion, provide a complete axial confinement to the overpack.

*The revised tie-down arrangement is not a structural part of the HI-STAR 100 Package. Therefore, 10CFR71.45(b) is not applicable.*

*The saddle supports under the cask, the straps, and the front and rear end structures that resist longitudinal load are not part of the HI-STAR 100 package. The loads used to design these components are determined using the load amplifiers given by the American Association of Railroads (AAR) Field Manual, Rule 88 [2.5.2].*

*Subsections 2.5.2.2 to 2.5.2.6 are intentionally deleted.*

#### 2.5.2.7 Structural Integrity of Pocket Trunnions on Applicable HI-STAR 100 Systems

The summary of results provided in tabular form, herein, is applicable only to the units that have been previously manufactured and, therefore, have pocket trunnions. The structural function of the pocket trunnions on applicable HI-STAR 100 Systems is limited to supporting the HI-STAR overpack during upending /downending operations if a separate downending cradle is not employed. If the pocket trunnion recess is utilized as a loaded pivot point during downending, the applied load for this operation is conservatively considered as the loaded weight of the package without impact limiters (250,000 lb.), amplified by a 15% inertia load factor. This load can be applied in any direction as the package is rotated 90 degrees. Results of structural integrity analyses, performed to qualify the rotation trunnion recess on the affected units, are summarized below.

Analyses are performed to evaluate the structural performance of various portions of the pocket trunnion under the stated total load, divided equally between the two trunnions. Since the trunnions are not utilized as tie-down devices, they are not considered as ASME Code items; nevertheless,



their performance is evaluated by comparing calculated stresses against yield strengths (to conform to the methodology employed in the HI-STAR 100 FSAR). Analyses for bearing stress levels, primary stress levels in the trunnion recess body, and weld stress in the weld group that attaches the recess forging to the intermediate shells. The methods of analysis include both simple strength of materials evaluation and finite element analysis of the pocket trunnion body. For the bearing stress analysis, the average bearing stress is computed based on the diameter of the male trunnion that would fit the trunnion pocket. For the general primary stress state in the trunnion forging, a finite element model of the trunnion recess is developed. Finally, for the analysis of the weld stress distribution, simple strength of materials equilibrium analysis is used with weld sizes appropriate to the minimum weld configuration in-place on the affected HI-STARs. The maximum weld stress is computed accounting for the weld material between the trunnion recess and the intermediate shells and between the pocket trunnion and the outer enclosure shell.

The results of the pocket trunnion recess analyses for an upending/downending load equal to 125,000 lb. x 1.15, are summarized in the following table:

Structural Integrity Results for HI-STAR Systems Equipped with Pocket Trunnions			
Item	Calculated Stress (ksi)	Allowable Stress (ksi)	Safety Factor = $\frac{\text{Allowable Value}}{\text{Calculated Value}}$
Bearing Stress	6.183	97.1	15.71(based on material yield strength)
Pocket Recess Primary Membrane + Primary Bending Stress	14.17	32.33	2.282 (based on 1/3 of trunnion material yield strength)
Maximum Weld Stress	2.399	14.533	4.802 (based on 1/3 of base metal yield strength)

### 2.5.3 Failure of Lifting and Tie-Down Devices

10CFR71.45 establishes criteria for minimum safety factors for lifting attachments, and provides input design loads for tie-down devices. 10CFR71.45 also requires that the lifting attachments and tie-down devices permanently attached to the cask, be designed in a manner such that a structural failure during lifting or transport will not impair the ability of the transportation package to meet other requirements of Part 10CFR71. In this section of the SAR, the issues concerning a structural failure during lifting or tie-down during transport are addressed. Specifically, the following issues are considered and resolved below:

#### a. Lifting Attachments:

Analyses are performed, using simple strength of materials concepts and evaluations to demonstrate that the ultimate load carrying capacity of the lifting trunnions is governed by the cross section of the trunnion external to the overpack top forging rather than by any section within the top forging. Detailed calculations that compare the ultimate load capacity of the shank of the lifting trunnion (the external cylindrical portion extending outside of the overpack top forging) to the ultimate load



capacity of the top forging are performed. The ultimate load carrying capacity of the trunnion shank is based on an examination of the ultimate capacity of the section in both shear and bending. The ultimate load capacity of the top forging is determined by its capacity to resist moment by thread shear at the trunnion/forging threaded interface and to equilibrate the lifting load by bearing action at the trunnion forging bearing surface interface. It is concluded that the trunnion shank reaches ultimate load capacity limit prior to the top forging reaches its corresponding ultimate load capacity limit. Loss of the external shank of the lifting trunnion will not cause loss of any other structural or shielding function of the HI-STAR 100 overpack; therefore, the requirement imposed by 10CFR71.45(a) is satisfied.

The following **ratios** are established:

$$\frac{(\text{Ultimate Bearing Capacity at Trunnion/Top Forging Interface})}{(\text{Ultimate Trunnion Shear Capacity})} = 1.16$$

$$\frac{(\text{Ultimate Moment Capacity at Trunnion/Top Forging Thread Interface})}{(\text{Ultimate Trunnion Moment Capacity})} = 1.57$$

b. Tie-Down Devices

There are no tie-down devices that are permanently attached to the cask; therefore, no analyses are required to demonstrate that the requirements of 10CFR71.45(b)(3) are satisfied.

#### 2.5.4 Conclusions

Lifting devices have been considered in Subsection 2.5.1 and Tie-Down devices have been considered in Subsection 2.5.2. It is shown that requirements of 10CFR71.45(a) (lifting devices) and 10CFR71.45(b) (tie-down devices) are satisfied. All safety factors exceed 1.0.

No tie-down device is a permanent part of the cask. All tie-down devices (saddle, tie-down straps, and fore and aft impact limiter targets), are part of the rail car and accordingly are not designed in this SAR. The maximum loads imposed on these items are recorded for subsequent design efforts.

**Tables 2.5.1 and 2.5.2**  
**INTENTIONALLY DELETED**

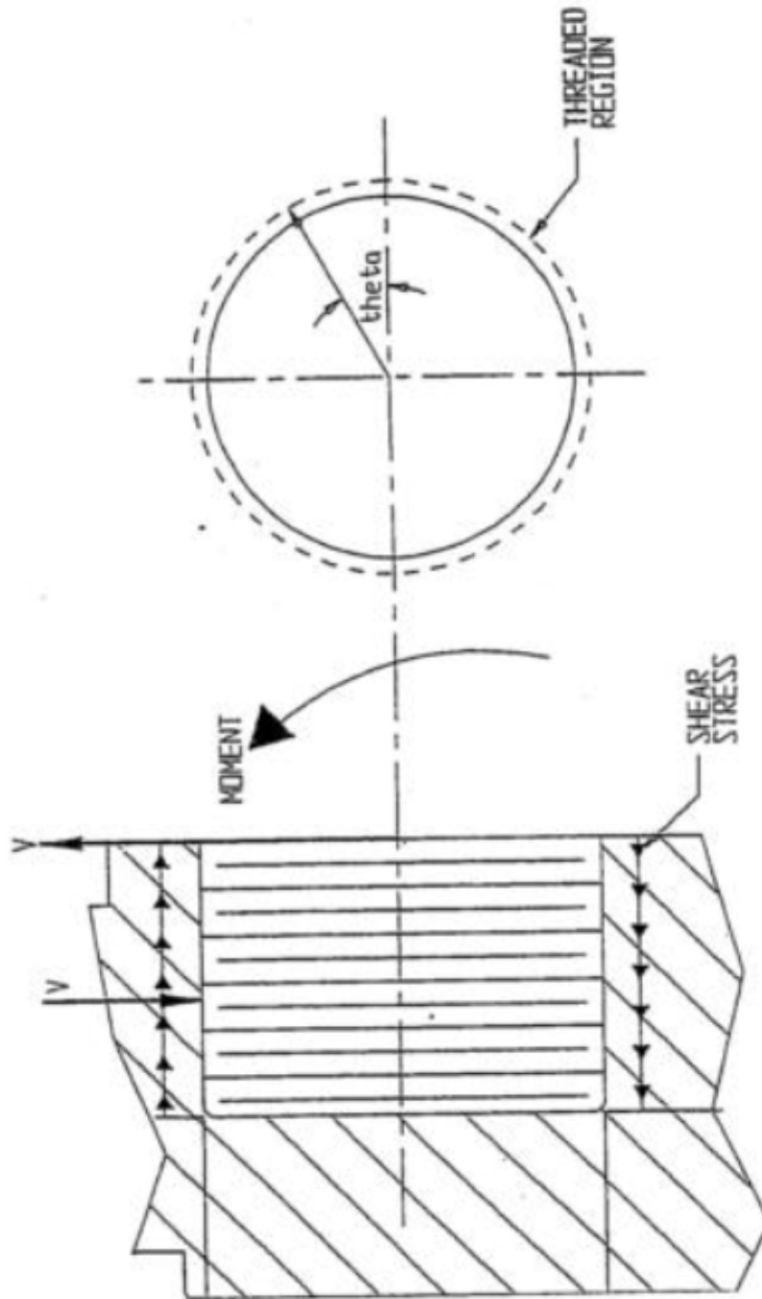


FIGURE 2.5.1; FREE BODY SKETCH OF LIFTING TRUNNION THREADED REGION SHOWING MOMENT BALANCE BY SHEAR STRESS

**Figures 2.5.2**

**INTENTIONALLY DELETED**

**Figures 2.5.3 through 2.5.11**

**INTENTIONALLY DELETED**

**Figures 2.5.12 and 2.5.13**

**INTENTIONALLY DELETED**

## 2.6 NORMAL CONDITIONS OF TRANSPORT

The HI-STAR 100 package, when subjected to the normal conditions of transport specified in 10CFR71.71, meets the design criteria in Subsection 2.1.2 (derived from the stipulations in 10CFR71.43 and 10CFR71.51) as demonstrated in the following section.

### 2.6.1 Heat

Subsection 2.6.1, labeled “Heat” in Regulatory Guide 7.9, is required to contain information on all structural (including thermoelastic) analyses performed on the cask to demonstrate positive safety margins, except for lifting operations that are covered in the preceding Section 2.5. Accordingly, this subsection contains all necessary information on the applied loadings, differential thermal expansion considerations, stress analysis models, and results for all normal conditions of transport. Assessment of potential malfunction under “Cold” conditions is required to be presented in Subsection 2.6.2.

Consistent with Regulatory Guide 7.9, the thermal evaluation of the HI-STAR 100 Package is reported in Chapter 3. The thermal evaluation also establishes the material temperatures, which are used in the structural evaluations discussed in this section and in Section 2.7.

#### 2.6.1.1 Summary of Pressures and Temperatures

Design pressures and design temperatures for all conditions of transport are listed in Tables 2.1.1 and 2.1.2, respectively.

Load cases F1 (Table 2.1.6) and E4 (Table 2.1.7) are defined to study the effect of differential thermal expansion among the constituent components in the HI-STAR 100 Package. Figures 2.6.1 and 2.6.2 provide the defining bounding temperature distributions used for the MPC and overpack finite element thermal stress calculations to maximize stresses that develop due to temperature gradients. The distribution T is applied conservatively to analyze its effect on the fuel basket, the enclosure vessel (helium retention boundary), and the overpack.

#### 2.6.1.2 Differential Thermal Expansion

In addition to the finite element solutions for free expansion stress (due to temperature gradients), simplified closed form calculations are independently performed to demonstrate that a physical interference will not develop between the overpack and the MPC canister, and between the MPC canister and the fuel basket due to unconstrained thermal expansion of each component during normal conditions of transport. To assess this in the most conservative manner, the thermal solutions computed in Chapter 3 are surveyed for the following information.

- The radial temperature distribution in each of the fuel baskets at the location of peak center metal temperature.
- The highest and lowest mean temperatures of the canister shell for the hot environment condition.

- The inner and outer surface temperature of the overpack shell (inner shell, intermediate shells, neutron shield, and outer closure) at the location of highest and lowest surface temperature (which will produce the lowest mean temperature).

The thermal evaluation is performed in Chapter 3. Tables 3.4.17 and 3.4.18 present the resulting temperatures used in the deflection evaluation.

Using the temperature information in the above-mentioned tables, simplified thermoelastic solutions of equivalent axisymmetric problems are used to obtain conservative estimates of gap closures. The following procedure, which conservatively neglects axial variations in temperature distribution, is utilized.

1. Use the surface temperature information for the fuel basket to define a parabolic distribution in the fuel basket that bounds (from above) the actual temperature distribution. Using this result, generate a conservatively high estimate of the radial and axial growth of the different fuel baskets using classical closed form solutions for thermoelastic deformation in cylindrical bodies.
2. Use the temperatures obtained for the canister to predict an estimate of the radial and axial growth of the canister to check the canister-to-basket gaps.
3. Use the temperatures obtained for the canister to predict an estimate of the radial and axial growth of the canister to check the canister-to-overpack gaps.
4. Use the overpack surface temperatures to construct a logarithmic temperature distribution (characteristic of a thick walled cylinder) at the location used for canister thermal growth calculations; and use this distribution to predict an estimate of overpack radial and axial growth.
5. For given initial clearances, compute the operating clearances.



The results are summarized in the tables given below for normal conditions of transport.

THERMOELASTIC DISPLACEMENTS IN THE MPC AND OVERPACK UNDER HOT TEMPERATURE ENVIRONMENT CONDITION				
<b>CANISTER - FUEL BASKET</b>				
	Radial Direction (in.)		Axial Direction (in.)	
Unit	Initial Clearance	Final Gap	Initial Clearance	Final Gap
All PWR MPCs	0.1875	0.101	2.0	1.57
MPC-68	0.1875	0.104	2.0 (min)	1.586 (min)
<b>CANISTER – OVERPACK</b>				
	Radial Direction (in.)		Axial Direction (in.)	
Unit	Initial Clearance	Final Gap	Initial Clearance	Final Gap
All PWR MPCs	0.09375	0.058	0.625	0.422
MPC-68	0.09375	0.059	0.625	0.429

It can be verified by referring to the Design Drawings provided in Section 1.4 of this report, and the foregoing table, that the clearances between the MPC basket and canister structure, as well as those between the MPC shell and overpack inside surface, are sufficient to preclude a temperature induced interference from the thermal expansions listed above.

It is concluded that the HI-STAR 100 package meets the requirement that there be no restraint of free thermal expansion in any of the constituent components (i.e, the fuel basket, the enclosure vessel, and the overpack structure).

#### 2.6.1.3 Stress Calculations

In this subsection, the normal conditions of transport associated with the thermal environment designated as “Heat” are considered. The stresses due to the combined effect of pressure, mechanical loads, and thermal gradient are evaluated. Within this subsection, the effects of fatigue and structure elastic/plastic stability under compression and lateral loading are also considered. Included in the subsection is a complete description of the finite element models developed to assess package performance under various loads. A two-dimensional finite element model of the fuel basket and the MPC enclosure shell is developed to evaluate the effect of pressure, radial temperature gradients and lateral deceleration induced inertia loads. A three-dimensional model of the overpack is also developed in this section to assess performance of the overpack under all load cases. Since both of

these finite element models are used again in Section 2.7, where hypothetical accident conditions of transport are examined, the explanation of the features of the model is presented herein in a general manner. Included in this description of the features of the model is a discussion of the loads applied, how they are chosen, and the methodology used to insure satisfaction of equilibrium. Where the loads, assumptions, geometry, etc. are common to both normal conditions of transport analyses and to hypothetical accident conditions of transport, the detailed description is presented in this section. Where the descriptions and discussions are relevant only for the hypothetical accident condition of transport, the detailed descriptions required for full understanding of the analysis are presented in Section 2.7.

This subsection presents the methodology for calculation of the stresses in the different components of the HI-STAR 100 Package from the load cases assembled in Section 2.1. Where the results are finite element based the methodology and the model is described in detail in this section. Results of finite element stress analyses are used for the comparison with allowable stresses performed in Subsection 2.6.1.4. Loading cases for the MPC fuel basket, the MPC enclosure vessel, and the HI-STAR 100 storage overpack are listed in Tables 2.1.6 through 2.1.8, respectively, for normal conditions of transport. An abbreviated description of each of the analyses is presented in the body of the chapter.

In general, as required by Regulatory Guide 7.9, the comparison of the calculated stresses with their corresponding allowables is presented in Subsection 2.6.1.4. However, for clarity in the narrative in this subsection (2.6.1.3), unnumbered summary tables are presented within the text. The key stress comparisons are subsequently reproduced in numbered tables in Subsection 2.6.1.4 to provide strict compliance with Regulatory Guide 7.9.

For all stress evaluations, the allowable stresses and stress intensities for the various HI-STAR 100 System components are based on bounding high metal temperatures to provide additional conservatism (Table 2.1.21 for the MPC basket and shell, for example). Elastic behavior is assumed for all stress analyses. Elastic analysis is based on the assumption of a linear relationship between stress and strain.

In Section 2.7, the same analytical models described here for normal conditions of transport are used to assess package performance under the hypothetical accident conditions. Therefore, the description of the models provided below is also applicable to the analysis performed in Section 2.7 except as previously noted.

In addition to the loading cases germane to stress evaluations mentioned above, cases pertaining to the elastic stability of the overpack are also considered.

The specific finite element models and component calculations described and reported in this subsection are:

1. MPC stress and stability calculations
2. HI-STAR 100 overpack stress and stability calculations

MPC stress and elastic stability analyses are considered in Subsection 2.6.1.3.1 wherein load cases from Tables 2.1.6 and 2.1.7 appropriate to normal conditions of transport are considered. The following analyses for the MPC are performed:

- a. Finite element analysis of the MPC fuel basket and MPC helium retention shell under lateral loads from handling loads during normal transport.
- b. Finite element and analytical analysis of the helium retention vessel (enclosure vessel) as an ASME Code pressure vessel.
- c. Analysis of the fuel support spacers under longitudinal inertia compression load appropriate to normal conditions of transport.
- d. Elastic stability and yielding of the MPC enclosure shell under axial and lateral loads arising from normal handling and external pressure.

Overpack stress and elastic stability analyses are considered in Subsection 2.6.1.3.2. Load cases from Table 2.1.8 are considered. The following analyses are performed to establish the structural adequacy of the overpack:

- a. Three-dimensional finite element analysis of the overpack subjected to load cases listed in Table 2.1.8 for normal conditions of transport.
- b. Consideration of fabrication stresses.
- c. Structural analysis of the closure bolting for normal condition of transport.
- d. Stress Analysis of overpack enclosure shell and return.

#### 2.6.1.3.1 MPC Stress Calculations

The structural function of the MPC in the transport mode is stated in Section 2.1. The calculations presented here demonstrate the ability of the MPC to perform its structural function. Analyses are performed for each of the MPC designs. The following subsections describe the model, individual loads, load combinations, and analysis procedures applicable to the MPC.

##### 2.6.1.3.1.1 Analysis of Load Cases F2 (Table 2.1.6) and E2, and E4 (Table 2.1.7)

The load cases considered herein pertain to lateral loading on the MPC components, namely the fuel basket and the enclosure vessel. For this purpose, a finite element model of the MPC is necessary. During normal conditions of transport, a bounding handling load is simulated by applying a deceleration induced inertia load from a 1' drop with impact limiters installed. During hypothetical accident conditions (see Section 2.7), the MPC is subject to the design basis decelerations from a 30' drop. The finite element model used to simulate both load cases is described here and is used for analyses for normal conditions of transport and later in Section 2.7 is used for the hypothetical accident analyses.

- Description of Finite Element Models of the MPCs under Lateral Loading

A finite element model of each MPC is used to assess the effects of normal and accident conditions of transport. The models are constructed using ANSYS [2.6.4], and they are identical to the models

used in HI-STAR's 10CFR72 submittal under Docket Number 72-1008. The following model description is common to all MPCs.

The MPC structural model is two-dimensional. It represents a one-inch long cross section of the fuel basket and the MPC canister.

The MPC model includes the fuel basket, the basket support structures, and the MPC shell. A basket support is defined as any structural member that is welded to the inside surface of the MPC shell. A portion of the overpack inner surface is modeled to provide the correct boundary conditions for the MPC. Figures 2.6.3 through 2.6.11 show the MPC models.

The fuel basket support structure shown in the figures here, and in the design drawings in Section 1.4, is a multi-plate structure consisting of solid shims or support members having two separate compressive load supporting members. For conservatism in the finite element model some dual path compression members are simulated as single columns. Therefore, the calculated stress intensities in the fuel basket supports from the finite element solution are conservatively overestimated in some locations. Independent strength of materials calculations for the fuel basket supports (including the standard and optional constructions for the MPC-32 and MPC-68) have also been performed in [2.6.5] to demonstrate that their load bearing members and their attachment welds meet the applicable ASME code stress limits.

The ANSYS model is not intended to resolve the detailed stress distributions in weld areas. Individual welds are not included in the finite element model.

No credit is taken for any load support offered by the neutron absorber panels, sheathing, and the optional aluminum heat conduction elements. Therefore, these so-called non-structural members are not represented in the model. The bounding MPC weight used, however, does include the mass contributions of these non-structural components.

The model is built using five ANSYS element types: BEAM3, PLANE82, CONTAC12, CONTAC26, and COMBIN14. The fuel basket and MPC shell are modeled entirely with two-dimensional beam elements (BEAM3). Plate-type basket supports are also modeled with BEAM3 elements. Eight-noded plane elements (PLANE82) are used for the solid-type basket supports. The gaps between the fuel basket and the basket supports are represented by two-dimensional point-to-point contact elements (CONTAC12). Contact between the MPC shell and the overpack is modeled using two-dimensional point-to-ground contact elements (CONTAC26) with an appropriate clearance gap.

For each MPC type, three variations of the finite element model were prepared. The basic model includes only the fuel basket and the enclosure shell (Figures 2.6.3 through 2.6.5 show representative configurations) and is used only to study the free thermal expansion due to the temperature field developed in the system. The other two models include a representation of the overpack and are used for the two drop cases considered. Two orientations of the deceleration vector are considered. The 0-degree drop model includes the overpack-MPC interface in the basket orientation illustrated in Figures 2.6.6 through 2.6.8. The 45-degree drop model represents the overpack interface with the

basket oriented in the manner shown in Figures 2.6.9 through 2.6.11. Table 2.6.1 lists the element types and number of elements for all three models for all fuel storage MPC types.

A contact surface is provided in the models used for drop analyses to represent the overpack inner shell. As the MPC makes contact with the overpack, the MPC shell deforms to mate with the inside surface of the inner shell. The nodes that define the elements representing the fuel basket and the MPC shell are located along the centerline of the plate material. As a result, the line of nodes that forms the perimeter of the MPC shell is inset from the real boundary by a distance that is equal to half of the shell thickness. In order to maintain the specified MPC shell/overpack gap dimension, the radius of the overpack inner shell is decreased by an equal amount in the model.

Contact is simulated using two-dimensional point-to-ground elements (CONTAC26). The surface is tangent to the MPC shell at the initial point of impact and extends approximately 135 degrees on both sides. This is sufficient to capture the full extent of contact between the MPC and the overpack.

The three discrete components of the HI-STAR System, namely the fuel basket, the MPC shell, and the overpack, are engineered with small diametral clearances that are large enough to permit unconstrained thermal expansion of the three components under the rated (maximum) heat duty condition. A small diametral gap under ambient conditions is also necessary to assemble the system without physical interference between the contiguous surfaces of the three components. The required gap to ensure unrestricted thermal expansion between the basket and the MPC shell is less than 0.1 inch. This gap, too, will decrease under maximum heat load conditions, but will introduce a physical nonlinearity in the structural events involving lateral loadings (such as side drop of the system) under ambient conditions. It is evident from the system design drawings that the fuel basket, which is non-radially symmetric, is in proximate contact with the MPC shell at a discrete number of locations along the circumferences. At these locations, the MPC shell, backed by the massive overpack weldment, provides a virtually rigid support line to the fuel basket during lateral drop events. Because the fuel basket, the MPC shell, and the overpack are all three-dimensional structural weldments, their inter-body clearances may be somewhat uneven at different azimuthal locations. As the lateral loading is increased, clearances close at the support locations, resulting in the activation of the support from the overpack.

The bending stresses in the basket and the MPC shell at low lateral loading levels, which are too small to close the support location clearances, are secondary stresses since further increase in the loading will activate the overpack's support action, mitigating further increase in the stress. Therefore, to compute primary stresses in the basket and the MPC shell under lateral drop events, the gaps should be assumed to be closed. However, for conservatism, it is assumed that an initial gap of 0.1875" exists, in the direction of the applied deceleration, at all support locations between the basket and the shell, and the diametral gap between the shell and the overpack at the support locations is 3/32". All stresses produced by the applied loading on this configuration are compared with primary stress levels even though the self-limiting stresses should be considered secondary in the strict definition of the ASME Code. Therefore, many of the reported safety factors for conditions of normal transport are conservative in that secondary stress allowables are ignored in the computation of safety factors. Similarly, in Section 2.7, the safety factors reported for the hypothetical accident conditions will also be conservative since the secondary stress is contained in the result.

- Description of Individual Loads and Boundary Conditions Applied to the MPCs

The method of applying each individual load to the MPC model is described in this subsection. The individual loads and the load combinations are shown in Tables 2.1.6 and 2.1.7. As an example, a free-body diagram of the MPC-68 corresponding to each individual load is given in Figures 2.6.12 through 2.6.14. In the following discussion, reference to vertical and horizontal orientations is made. Vertical refers to the direction along the cask axis, and horizontal refers to a radial direction.

Quasi-static structural analysis methods are used. The effect of any dynamic load factors (DLFs) is included in the final evaluation of safety factors. All analyses are carried out using the design basis decelerations in Table 2.1.10.

The MPC models used for side drop evaluations are shown in Figures 2.6.6 through 2.6.11. In each model, the fuel basket and the enclosure vessel are constrained to move only in the direction that is parallel to the acceleration vector. The overpack inner shell, which is defined by three nodes needed to represent the contact surface, is fixed in all degrees of freedom. The fuel basket, enclosure vessel, and overpack inner shell are all connected at one location by linear springs (see Figure 2.6.6, for example).

(a) Accelerations (Load Case F2 (Table 2.1.6) and E2 (Table 2.1.7))

During a side impact event, the stored fuel is directly supported by the cell walls in the fuel basket. Depending on the orientation of the drop, 0 or 45 degrees (see Figures 2.1.3 and 2.1.4), either one or two walls support the fuel. The effect of deceleration on the fuel basket and canister metal structure is accounted for by amplifying the gravity field in the appropriate direction. In the finite element model this load is introduced by applying a uniformly distributed pressure over the full span of the supporting walls. Figure 2.6.15 shows the pressure load on a typical cell for both the 0 degree and the 45 degree drop cases. The magnitude of the pressure is determined by the weight of the fuel assembly (Table 1.2.13), the axial length of the fuel basket support structure, the width of the cell wall, and the impact acceleration. It is assumed that the load is evenly distributed along an axial length of basket equal to the fuel basket support structure. For example, the pressure applied to an impacted cell wall during a 0-degree side drop event is calculated as follows:

$$p = \frac{a_v W}{L \ell}$$

where:

$p$  = pressure

$a_v$  = ratio of the impact acceleration to the gravitational acceleration

$W$  = weight of a stored fuel assembly

$L$  = axial length of the fuel basket support structure

$\ell$  = width of a cell wall

For the case of a 45-degree side drop the pressure on any cell wall equals  $p$  (defined above) divided by the square root of two. Figures 2.6.13, 2.6.14, and 2.6.15 show the details of the fuel assembly pressure load on the fuel basket.

(b) Internal/External Pressure (Load Case E1 (Table 2.1.7))

Design internal pressure in the MPC model is applied by specifying pressure on the inside surface of the enclosure vessel. The magnitude of the internal pressure applied to the model is taken from Table 2.1.1.

For this load condition, the center of the fuel basket is fixed in all degrees of freedom.

(c) Temperature (Load Cases F1 (Table 2.1.6) and E4 (Table 2.1.7))

Temperature distributions are developed in Chapter 3 and applied as nodal temperatures to the finite element model of the MPC enclosure vessel (confinement boundary). Maximum design heat load has been used to develop the temperature distribution used to demonstrate compliance with ASME Code stress intensity levels. A plot of the applied temperature distribution as a function of radius is shown in Figure 2.6.1. Figure 2.6.12 shows the MPC-68 with the typical boundary conditions for all thermal and pressure load cases.

- Analysis Procedure

The analysis procedure for this set of load cases is as follows:

1. The stress intensity and deformation field due to the combined loads is determined by the finite element solution. Results are then subject to post-processing.
2. The results for each load combination are compared to allowables. The comparison with allowable values is made in Subsection 2.6.1.4.

2.6.1.3.1.2 Analysis of Load Cases E1.a and E1.c (Table 2.1.7)

Load Cases E1.a and E1.c pertain to the performance of the helium retention boundary structure (enclosure vessel) considered as an ASME Section III, Subsection NB pressure vessel.

Since the MPC shell is a pressure vessel, the classical Lamé's calculations should be performed to demonstrate the shell's performance as a pressure vessel. Note that dead load has an insignificant effect on this stress state. Calculations for the shell under internal pressure are performed initially. Subsequently, a finite element analysis on the entire helium retention boundary as a pressure vessel subject to both internal pressure and temperature gradients is performed. Finally, confirmatory hand calculations are performed to gain confidence in the finite element predictions,

- **Lame's Solution for the MPC Shell**

The stress from internal pressure is found using classical formulas:

Define the following quantities:

P = pressure, r = MPC radius, and t = shell thickness.

Using classical thin shell theory, the circumferential stress,  $\sigma_1 = Pr/t$ , the axial stress  $\sigma_2 = Pr/2t$ , and the radial stress  $\sigma_3 = -P$  are computed for both normal and accident internal pressures. The results are given in the following table:

Classical Shell Theory Results for Normal and Accident Internal Pressures				
Item	$\sigma_1$ (psi)	$\sigma_2$ (psi)	$\sigma_3$ (psi)	$\sigma_1 - \sigma_3$ (psi)
P= 100 psi	6,850	3,425	-100	6,950
P= 225 psi	15,413	7,706	-225	15,638

Table 2.1.21 provides the allowable membrane stress for Load Case E1 for Alloy X under normal conditions of transport. It is seen that a safety factor greater than 1.0 exists

$$FS = \frac{18.1 \text{ ksi}}{6.95 \text{ ksi}} = 2.60$$

Subsection 2.7.3.3.1 develops the corresponding safety factor for the case of accident pressure.

- **Finite Element Analysis (Load Case E1.a and E1.c of Table 2.1.7)**

Having performed the classical “thin shell under pressure” evaluation, a finite element analysis is performed where the interaction between the end closures and the MPC shell is rigorously modeled.

The MPC shell, the top lid, and the baseplate together form the helium retention boundary (enclosure vessel) for storage of spent nuclear fuel. In this section, the operating condition consisting of dead weight, internal pressure, and thermal effects for the normal heat condition of transport is evaluated. The top and bottom plates of the MPC enclosure vessel (EV) are modeled using plane axisymmetric elements, while the shell is modeled using the axisymmetric thin shell element. The thickness of the top lid varies in the MPC types and can be either a single thick lid, or two lids, welded around their common periphery; the minimum thickness top lid is modeled in the finite element analysis. As applicable, the results for the MPC top lid are modified to account for the fact that in the dual lid configuration, the two lids act independently under mechanical loading. The temperature distributions for all MPC constructions are nearly identical in magnitude and gradient. Temperature differences across the thickness of both the baseplate and the top lid exist during HI-STAR 100's operations. There is also a thermal gradient from the center of the top lid and baseplate out to the



shell wall. The metal temperature profile is essentially parabolic from the centerline of the MPC out to the MPC shell. There is also a parabolic temperature profile along the length of the MPC canister. Figure 2.6.20 shows a sketch of the confinement boundary structure with identifiers A-I (also called locating points) where temperature input data is used to represent a continuous temperature distribution for analysis purposes. The overall dimensions of the confinement boundary are also shown in the figure.

Section 3.4 provides the desired temperatures for thermal stress analysis of the helium retention boundary. From the tables (3.4.22 and 3.4.23), it is seen that the distribution from PWRs provides the largest temperature gradients in the baseplate (from centerline to outer edge) and in the shell (from the joint at the baseplate to the half-height of the cask). It will be shown later that stress intensities are greatest in these components of the vessel. Because of the intimate contact between the two lid plates when the MPC lid is a two-piece unit, there is no significant thermal discontinuity through the thickness; thermal stresses arising in the MPC top lid will be bounding when there is only a single lid. Therefore, for thermal stresses, results from the analysis that considers the lid as a one-piece unit are used and are amplified to reflect the increase in stress in the dual lid configuration

Figure 2.6.21 shows details of the finite element model of the top lid (considered as a single piece), canister shell, and baseplate. The top lid is modeled with 40 axisymmetric quadrilateral elements; the weld connecting the lid to the shell is modeled by a single element solely to capture the effect of the top lid attachment to the canister offset from the middle surface of the top lid. The MPC canister is modeled by 50 axisymmetric shell elements, with 20 elements concentrated in a short length of shell appropriate to capture the so-called "bending boundary layer" at both the top and bottom ends of the canister. The remaining 10 shell elements model the MPC canister structure away from the shell ends in the region where stress gradients are lower (from the physics of the problem). The baseplate is modeled by 20 axisymmetric quadrilateral elements. Deformation compatibility at the connections is enforced at the top by the single weld element, and deformation and rotation compatibility at the bottom by additional shell elements between nodes 106-107 and 107-108.

The geometry of the model is listed below (terms are defined in Figure 2.6.21):

$H_t =$	9.5" (the minimum total thickness lid is assumed)
$R_L =$	0.5 x 67.25" (Nominal dimension used for calculation)
$L_{MPC} =$	190.5" (Nominal dimension used for calculation)
$t_s =$	0.5" (MPC drawing in Section 1.4)
$R_s =$	0.5 x 68.375" (Nominal radius)
$t_{BP} =$	2.5" (MPC drawing in Section 1.4)
$\beta L =$	$2\sqrt{R_s t_s} \approx 12"$ (The bending boundary layer)

Stress analyses are carried out for two cases as follows:

- a. internal pressure = 100 psi
- b. internal pressure = 100 psi, plus applied temperature field

The dead weight of the top lid reduces the stresses due to pressure. For example, the equivalent pressure simulating the effect of the weight of the top lid is an external pressure of 3 psi, which reduces the pressure difference across the top lid to 97 psi. Thus, for conservatism, dead weight of the top lid is neglected to provide additional conservatism in the results. The dead weight of the baseplate, however, adds approximately 0.73 psi to the effective internal pressure acting on the base. The effect of dead weight is still insignificant compared to the 100 psi design pressure, and is therefore neglected. The thermal loading in the confinement vessel is obtained by developing a parabolic temperature profile to the entire length of the MPC canister and to the top lid and baseplate. The temperature data provided at locations A-I in Figures 2.6.20 and 2.6.21 are sufficient to establish the profiles. Through-thickness temperatures are assumed linearly interpolated between top and bottom surfaces of the top lid and baseplate. All material properties and expansion coefficients are considered to be temperature-dependent in the model.

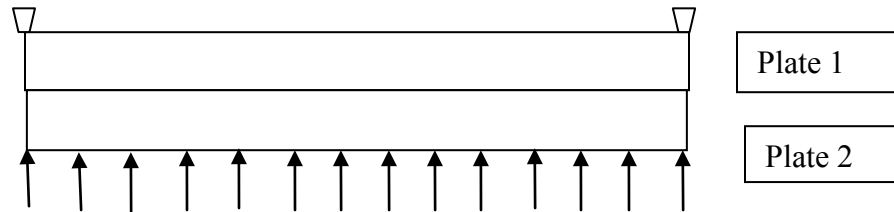
Results for stress intensity are reported for the case of internal pressure alone and for the combined loading of pressure plus temperature (Load Case E1.c in Table 2.1.7). Tables 2.6.6 and 2.6.7 report results at the inside and outside surfaces of the top lid and baseplate at the centerline and at the extreme radius. Canister results are reported in the "bending boundary layer" and at a location near mid-length of the MPC canister. In the tables, the calculated value is the value from the finite element analysis, the categories are  $P_m$  = primary membrane;  $P_L + P_b$  = local membrane plus primary bending; and  $P_L + P_b + Q$  = primary plus secondary stress intensity. The allowable stress intensity value is obtained from the appropriate table in Section 2.1 for Level A conditions, and the safety factor SF is defined as the allowable strength divided by the calculated value. Allowable stresses for Alloy X are taken at 300° F, which bounds the normal heat condition of transport temperatures everywhere except at the mid-length position of the MPC shell (Location I in Figure 2.6.20) during the normal operation. At Location I, the allowable strength is taken at 400°F. The results given in Tables 2.6.6 and 2.6.7 demonstrate the ruggedness of the MPC as a confinement boundary. Since mechanically induced stresses in the top lid are increased when a dual lid configuration is considered, the stress results obtained from an analysis of a single top lid must be corrected to reflect the maximum stress state when a dual lid configuration is considered. The modifications required are based on the following logic:

Consider the case of a simply supported circular plate of thickness  $h$  under uniform lateral pressure " $q$ ". Classical strength of materials provides the solution for the maximum stress, which occurs at the center of the plate, in the form:

$$\sigma_s = 1.225q(a/h)^2 \quad \text{where } a \text{ is the radius of the plate and } h \text{ is the plate thickness.}$$

Now consider the MPC simply supported top lid as fabricated from two plates "1" and "2", of thickness  $h_1$  and  $h_2$ , respectively, where the lower surface of plate 2 is subjected to the internal

pressure “q”, the upper surface of plate 1 is the outer surface of the helium retention boundary, and the lower surface of plate 1 and the upper surface of plate 2 are in contact. The following sketch shows the dual lid configuration for the purposes of this discussion:



From classical plate theory, if it is assumed that the interface pressure between the two plates is uniform and that both plates deform to the same central deflection, then if

$$h_1 + h_2 = h, \text{ and if } h_2/h_1 = r$$

the following relations exist between the maximum stress in the two individual plates,  $\sigma_1$ ,  $\sigma_2$  and the maximum stress  $\sigma_s$  in the single plate of thickness “h”:

$$\frac{\sigma_1}{\sigma_s} = \frac{(1+r)^2}{(1+r^3)} \qquad \frac{\sigma_2}{\sigma_s} = \frac{(1+r)^2}{(1+r^3)} r$$

Since the two lid thicknesses are the same in the dual lid configuration,  $r = 1.0$  so that the stresses in plates 1 and 2 are both two times larger than the maximum stress computed for the single plate lid having the same total thickness. In Tables 2.6.6 and 2.6.7, bounding results for the dual lid configuration are reported by using these ratios at all locations in the top lid.

The preceding analysis for the dual lid configuration assumes that both lids are made from the same material (i.e., Alloy X). Per the licensing drawings in Section 1.4, there is an option for the bottom lid to be fabricated from carbon steel (covered or coated with stainless steel) in lieu of Alloy X. However, since carbon steel has a higher yield strength and Young’s modulus than Alloy X, all stress calculations for the MPC split lid conservatively assume that the bottom lid is made from the weaker of the two material options (i.e., Alloy X).

- Confirmatory Closed Form Solution

The results in Table 2.6.6 and 2.6.7 also show that the baseplate and the shell connection to the baseplate are the most highly stressed regions under the action of internal pressure. To confirm the finite element results, an alternate closed form solution is performed using classical plate and shell theory equations that are listed in or developed from the reference Timoshenko and Woinowsky-Krieger, Theory of Plate and Shells, McGraw Hill, Third Edition.

Assuming that the thick baseplate receives little support against rotation from the thin shell, the bending stress at the centerline is evaluated by considering a simply supported plate of radius  $a$ , and thickness  $h$ , subjected to lateral pressure  $p$ . The maximum bending stress is given by

$$\sigma = \frac{3(3 + \nu)}{8} p \left( \frac{a}{h} \right)^2$$

where:

$$a = 0.5 \times 68.375''$$

$$h = 2.5''$$

$$\nu = 0.3 \text{ (Poisson's Ratio)}$$

$$p = 100 \text{ psi}$$

Calculating the stress in the plate gives  $\sigma = 23,142$  psi.

Now consider the thin MPC shell ( $t = 0.5''$ ) and first assume that the baseplate provides a clamped support to the shell. Under this condition, the bending stress in the thin shell at the connection to the plate is given as:

$$\sigma_{Bp} = 3p \frac{a}{t} \frac{(1 - \nu/2)}{\sqrt{3(1 - \nu^2)}^{1/2}} = 10,553 \text{ psi}$$

In addition to this stress, there is a component of stress in the shell due to the baseplate rotation that causes the shell to rotate. The joint rotation is essentially driven by the behavior of the baseplate as a simply supported plate; the shell offers little resistance because of the disparity in thickness and will essentially follow the rotation of the thick plate.

Using formulas from thin shell theory, the additional axial bending stress in the shell due to this rotation  $\theta$  can be written in the form

$$\sigma_{B\theta} = 12 \beta D_s \frac{\theta}{t^2}$$

where

$$\theta = pa^3 / 8D(1 + \nu) * \left( \frac{1}{1 + \alpha} \right)$$

and

$$D = \frac{E h^3}{12(1-\nu^2)} \quad E = \text{plate Young's Modulus}$$

and

$$\alpha = \frac{2\beta a t^3}{h^3(1+\nu)}$$

$$\beta^2 = \sqrt{3(1-\nu^2)} / at$$

$$D_s = \frac{E t^3}{12(1-\nu^2)}$$

Substituting the numerical values gives

$$\sigma_{B_-} = 40,563 \text{ psi}$$

Note that the approximate solution is independent of the value chosen for Young's Modulus as long as the material properties for the plate and shell are the same.

Combining the two contributions to the shell bending stress gives the total extreme fiber stress in the longitudinal direction as 51,116 psi. Note that the same confirmatory solution can be obtained from Roark's Formulas for Stress and Strain, McGraw-Hill, 4th Edition, Table XIII. Case 30 in that text contains the solution for the bending moment at the intersection of a long cylinder and a flat plate due to internal pressures. Using the handbook formula, 53,090 psi is obtained.

The baseplate stress value, 23,142 psi, compares well with the finite element result 20,528 psi (Table 2.6.6). The shell joint stress, 51,116 psi, is greater than the finite element result (43,986 psi in Table 2.6.6). This is due to the local effects of the shell-to-baseplate connection offset. That is, the connection between shell and baseplate in the finite element model is at the surface of the baseplate, not at the middle surface of the baseplate. This offset will cause an additional bending moment that will reduce the rotation of the plate and hence, reduce the stress in the shell due to the rotation of the baseplate.

In summary, the approximate closed form solution confirms the accuracy of the finite element analysis in the MPC baseplate region.

### 2.6.1.3.1.3 Supplementary MPC Calculations

The MPC has been subject to extensive analysis in the companion HI-STAR 100 FSAR (storage) submittal (Docket Number 72-1008). For completeness, certain information from the FSAR has been repeated here and in Section 2.7 where the results are germane to normal conditions of transport and to hypothetical accident conditions of transport, respectively. Because of the different requirements for storage and transport submittals, some of the results presented here may not be directly associated with a load case defined in Tables 2.1.6 and 2.1.7. Nevertheless, their inclusion here is warranted for completeness. In this subsection, results are summarized from these analyses that pertain to normal conditions of transport. In Section 2.7, additional results pertaining to the hypothetical accident conditions of transport are reported.

- **Structural Analysis of the Fuel Support Spacers (Load Case F2)**

Upper and lower fuel support spacers are utilized to position the active fuel region of the spent nuclear fuel within the poisoned region of the fuel basket. It is necessary to ensure that the spacers will continue to maintain their structural integrity during normal conditions of transport. Ensuring structural integrity implies that the spacer will not buckle under the maximum compressive load, and that the maximum compressive stress will not exceed the compressive strength of the spacer material (Alloy X). Detailed calculations demonstrate that large structural margins in the fuel spacers are available for the entire range of spacer lengths that may be used in HI-STAR 100 applications (for the various acceptable fuel types). The fuel spacers are shown to meet ASME Code Subsection NG stress limits (the spacers are not, however, required to be designed to any ASME Code, however). Standard Code design formulas are used to evaluate elastic stability limits. For normal conditions of transport (Level A Service Condition), a 10g deceleration load is applied and stress and stability issues are considered. The results are summarized below:

Fuel Spacers - Minimum Safety Factors (Load Cases F2)			
Item	Load (lb.)	Capacity (lb.)	Safety Factor
PWR Fuel Spacer - 10 g Axial Load	16,800	46,200	2.75
BWR Fuel Spacer – 10g Axial Load	7,000	19,250	2.75

The safety factor is greater than 1.0, which demonstrates that the fuel spacers meet the requirements of Level A Service Conditions for the normal condition of transport.

The above results are determined based on the original design of the fuel spacers, which consists of a length of square tubing welded between top and bottom end plates. Per the licensing drawing, the lower fuel spacers may also be fabricated using I-beams instead of square tubing. Since the cross-sectional area and moment of inertia of the specified I-beam are greater than the section properties of the square tubing, the above analysis bounds both options.

The above result also represents a conservative minimum safety factor for the Trojan failed fuel can (FFC) spacer under normal conditions of transport. The reasons are (i) the FFC spacer has

the same cross sectional area as the PWR lower fuel spacer and (ii) the FFC spacer supports less weight than the PWR lower fuel spacer. Whereas the PWR lower fuel spacer is designed and licensed to support the design fuel assembly weight of 1680 lb, the maximum weight that the FFC spacer supports is somewhat less than 1680 lb since the total weight of the Trojan FFC plus its contents, which includes the FFC spacer, is restricted to 1680 lb.

- MPC Shell Stability

The MPC shell is examined for elastic/plastic instability due to external pressure or compressive loads introduced as part of the load cases (design external pressure, normal transport). Each load component is examined separately. Design external pressure is applied to the outer surface of the enclosure vessel shell in the MPC model. The magnitude of the external pressure applied to the model is taken from Table 2.1.1. Analysis of the MPC under external pressure is performed using the methodology of ASME Code Case N-284 [2.1.8]. The following stability evaluations are performed for the MPC shell for normal transport conditions:

- Normal Transport Deceleration Load from 10CFR71.45(b).
- Design external pressure plus a 1g compressive dead load.

The following table summarizes the limiting result from the calculations:

MPC Shell - Elastic/Plastic Stability (ASME Code Case N-284) - Minimum Safety Factors			
Item	Value	Allowable	Safety Factor
Load Case 10CFR71.45(b) (Yield)	0.193	2.0	10.36
Load Case E1.b - Table 2.1.7 (Stability Interaction Curve)	0.832	1.0	1.20

Note that for the load case associated with the 10CFR71.45(b) requirement, the yield strength criteria in the Code Case N-284 method governs the “allowable” value. In this event, the safety factor 2.0, built into the Code Case, is included in the tabular result in order to obtain the actual safety factor with respect to the yield strength of the material.

The results demonstrate that the MPC shell meets the requirements of Code Case N-284. Note that the stability results presented above are very conservative. The stability analyses carried out for the MPC shell assumed no axial stiffening from the fuel basket supports that run the full length of the shell. An analysis that included the effect of the stiffening (and therefore, recognized the fact that instability will most likely occur between stiffeners) will give increased safety factors for Load Case E1.b.

### 2.6.1.3.2 Overpack Stress Calculations

The structural functions of the overpack are stated in Section 2.1. The analyses documented here demonstrate the ability of components of the HI-STAR 100 overpack to perform their structural functions under normal conditions of transport. Load cases applicable to the structural evaluation of the HI-STAR 100 overpack under these conditions are compiled in Table 2.1.8.

In this subsection, stresses and stress intensities in the HI-STAR 100 overpack due to the combined effects of thermal gradients, pressure, and mechanical loads are presented. The results are obtained from a series of finite element analyses on the complete overpack and separate analyses on overpack components.

#### 2.6.1.3.2.1 Finite Element Analysis - Load Cases 1 to 4 in Table 2.1.8

Load Case 1 pertains to a demonstration of the containment boundary as an ASME “NB component under Design Pressure and Level A Service Condition thermal loading. Other cases pertain to handling inertia loads imposed during normal conditions of transport and an extreme environmental condition. To analyze these load cases, a suitable finite element model of the complete overpack is required. As noted earlier, since the identical finite element model is used in Section 2.7 to analyze the hypothetical accident conditions of transport, the following discussion refers to both sets of analyses to avoid textual repetition.

- Description of Finite Element Model (Normal Conditions and Hypothetical Accident)

The purpose of the HI-STAR 100 overpack model is to calculate stresses and stress intensities resulting from the loadings defined in Subsection 2.1 and compiled into load cases in Table 2.1.8.

A three-dimensional finite element model of the HI-STAR 100 overpack is used to assess the effects of loads associated with normal conditions of transport. The same finite element model is used in Section 2.7 to evaluate the effects of loading due to hypothetical accident scenarios. The overpack is a large structure subject to a variety of complex loads and boundary conditions. The finite element model developed for this analysis allows efficient determination of the stresses in this complex structure.

The finite element model of the overpack is constructed using ANSYS [2.6.4]. This model is duplicated in the HI-STAR 100 FSAR (10CFR72) submittal for storage.

For structural analysis purposes, the overpack is assumed to be symmetric about a diametral mid-plane. This assumption is reasonable because the purpose of the model is to investigate global stresses in the model. The model is not intended to resolve effects due to small penetrations that produce peak stresses (which are significant only in cyclic fatigue conditions).

Element plots of the model are shown in a series of figures (Figures 2.6.16 through 2.6.19C). Figure 2.6.16 shows an overall view of half of the overpack subject to detailed finite element analysis. The view is directed toward the internal cavity and shows the surface of symmetry. To enforce symmetry,



displacements normal to the plane of symmetry at all nodes on the plane of symmetry are not permitted. Out-of-plane rotations at the nodes on the plane of symmetry are also set to zero. The basic building blocks of the finite element model are 20-node brick (SOLID95), 8-node brick (SOLID45), and 6-node tetrahedron elements (SOLID45). These are 3-D solid elements with 3 degrees of freedom at each node (three linear displacement degrees of freedom). Element densities are increased towards the top and bottom of the model in order to provide increased resolution of the stress fields in those regions.

The top flange/closure plate interface is modeled using linear spring elements (COMBIN14). The concentric seals are not modeled explicitly. The model is not intended to resolve the stress field around the grooves for the seals. The status of joint seal is ascertained by “compression springs” that simulate the O-ring gaskets. Contact between the overpack top flange and closure plate is verified by checking the status of these spring elements. If contact between the closure plate and top flange is maintained under an applied loading (indicated by a compressive load in the “compression springs”), then the integrity of the seal is determined to have been maintained under that load.

The overpack closure bolts are modeled with beam elements (BEAM4). The top of the beam elements represent the bolt head and are connected to the overpack closure plate. The bottom of the elements represents the threaded region of the bolt and is connected to nodes of elements representing the top flange. Torsional displacements of the bolts are suppressed to conform to the degrees of freedom permitted at the nodes of the connecting solid elements.

The inner shell of the overpack is modeled with two solid element layers through the thickness of the shell.

Each of the lifting trunnions is modeled as three rigid beam elements (BEAM4) connected to the top forging. The beams extend from the forging and meet at a single node location. Trunnion stress analysis is documented in Subsection 2.5; the inclusion of the trunnion herein is solely to provide the appropriate offset for handling loads. The beam elements representing the trunnions are not shown on any of the figures describing the finite element model.

The neutron shield material is not a load bearing or supporting component in the finite element model. However, the weight of the neutron shield material must be included in the model in order to obtain the proper inertia loads. The neutron shield material is modeled with SOLID45 elements having a weight density that is specified in Subsection 2.3.2.1. In the model herein, the neutron shield material is included as an element set to ensure that proper accounting of total weight (and accompanying deceleration loads) occurs. Therefore, the neutron shield material must be assigned a Young's Modulus in the model. A value approximately equal to 1% of the Modulus of the steel load carrying components is assigned to the neutron shield material to insure that the neutron shield material serves as a load rather than a structural member in the model.

Figure 2.6.17 shows the finite element grid used for the bottom plate.

Figure 2.6.18 provides the details of the solid element grid for the top forging. Also shown in the figure are the line elements that represent the lid bolts. Since the lid is not shown in this figure, the

upper part of the line elements is not attached to any node point.

Figure 2.6.19 shows a view from above of the overpack lid and details the element grid around the 180-degree periphery modeled.

Figure 2.6.19A shows the finite element grid for the inner shell and the five intermediate shells. The inner shell is modeled with two layers of solid elements; each of the five intermediate shells is modeled by a single layer of solid elements to capture a linear stress distribution through the thickness.

Figure 2.6.19B presents the solid element distribution modeling the Holtite-A material. As noted previously, the structural effect of this material is neglected; the elements are included in the model to insure a proper mass distribution for the different analyses.

Finally, Figure 2.6.19C shows the shell element grid used to model the enclosure shell. Thin shell elements are used to simulate all components of the enclosure shell.

It is recognized that the layered shells of the overpack (shown in Figures 2.6.16 and 2.6.19A) are connected to each other and to the inner shell only at their top and bottom extremities. The finite element model must allow for separation between the intermediate shells in the non-connected regions under certain loading. Likewise, the intermediate shells cannot interpenetrate each other or the inner shell structure. To simulate these competing effects without making the model non-linear because of the introduction of contact elements, radial coupling of adjacent intermediate shell nodes is used in appropriate locations of the model. It is necessary to utilize physical reasoning to establish the regions where a nodal coupling is warranted because the shells cannot separate from each other. For example, radial coupling over two 60-degree spans serves to prevent interpenetration where it may occur during an impact simulation. Similarly, where physical reasoning indicates that a separation between the shell layers may occur, the nodes are left uncoupled. For example, when ovalization of the shells may occur under a specified loading, no coupling between shells is assumed. Figure 2.6.22 illustrates the nodal coupling pattern. The intermediate shell nodes that lie in the 60-degree sector between the top and bottom portions of the model remain uncoupled. The intermediate shells, in the uncoupled region, are free to separate from one another as the overpack cross section ovalizes during side impact. This modeling approach ensures that load transfer in a drop with significant lateral deceleration loads is modeled correctly. With respect to the overpack model, "bottom portion" refers to the 60-degree segment of the model closest to the point of impact. Conversely, "top portion" refers to the 60-degree sector farthest from the point of impact. This nodal coupling arrangement conservatively represents the structural behavior of the intermediate shells. In addition, no axial or circumferential nodal coupling has been used between adjacent intermediate shells. Thus, axial bending stiffness of the composite shell structure is conservatively underestimated. This underestimation of stiffness provides additional conservatism to the predicted values for safety factors.

The rotation trunnions present in the first seven HI-STAR 100 units (see Subsection 2.5) are conservatively neglected in the finite element models. Separate calculations, where applicable, are summarized later.

Elements at locations of welds in the modeled components are assumed to have complete connectivity in all directions. Material in the model located at positions where welds exist is assumed to have material properties identical to the base material.

To summarize, the total number of nodes and elements in the overpack model are 11265 and 8642, respectively. The elements used are SOLID45, SOLID95, BEAM4, SHELL63, and COMBIN14.

For all structural analyses, material properties are obtained from the appropriate tables in Section 2.3. Property data for temperatures that are not listed in the material property tables are obtained by linear interpolation. Property values are not extrapolated beyond the limits of the code for any structural analysis.

- Description of Individual Loads and Boundary Conditions

The method of applying each individual load to the overpack model is described in this subsection. The individual loads are defined in Subsection 2.1.2.1 and are listed in Table 2.1.8 for normal conditions of transport. A free-body diagram of the overpack corresponding to each individual load is given in Figures 2.1.5 through 2.1.14. The figures presented in Section 2.1 present a general description of the loading but are lacking in specific details concerning the extent of the area exposed to the load. Therefore, in this subsection, each of the applied loadings for the various cases considered is further discussed and additional details on the specific application of the loads are provided. In the following discussion, reference to vertical and horizontal orientations is made. Vertical refers to the longitudinal direction along the cask axis, and horizontal refers to a lateral direction.

Quasi-static methods of structural analysis are used. The effects of any dynamic load factors (DLF) are discussed in the final evaluation of safety factors. The load combinations are formed from the solution of individual load cases

(a) Accelerations (Used to Form Load Cases 3 and 4 in Table 2.1.8)

Table 2.1.10 provides the bounding values of the accelerations used for design basis structural evaluation. The loading is imposed by amplifying the gravity vector by the design basis deceleration. The proper distribution of the body forces induced by the accelerations is internally consistent based on the mass distribution associated with the different components of the finite element model. How these acceleration induced loadings are put in equilibrium with reaction loads from the impact limiters is discussed in detail in a later section.

In the following, appropriate boundary conditions for analyses for load cases associated with normal conditions of transport (Table 2.1.8) are discussed. However, since the same finite element model is used to evaluate hypothetical accident conditions of transport (Table 2.1.9) in Section 2.7, boundary conditions for Section 2.7 analyses are discussed here, as well, in the ongoing interest of conciseness of the presentation.

Boundary conditions for the model are as follows:

- i. End drop - In an end drop, displacement fixities are applied to the model on a cross-section through the top flange that is normal to the drop direction. Figures 2.1.7 and 2.1.8 show the free-body diagram for these load events. No reactions or internal body forces are shown. Further discussion is provided in Section 2.7.
- ii. Side drop - In a side drop, the inertia loads are reacted by the impact limiters. The overpack is in equilibrium with essentially end pinned supports. Figure 2.1.9 shows the configuration for this case. Further elaboration is provided in Section 2.7.

(b) Loads on the Overpack from the MPC

Pressures are applied on the inner surfaces of the overpack model to represent loads from the MPC for the drop loads.

- i. End drop - For a bottom end drop (Load Case1, Hypothetical Accident, Table 2.1.9), the pressure load on the inside surface of the overpack bottom plate is assumed to be uniform and represents the load from the heaviest MPC (Figure 2.1.7). Note that this analysis conservatively assumes that the drop angle is not exactly  $90^\circ$  from the horizontal; attention is focussed on the overpack baseplate subject to the deceleration load from the heaviest MPC (applied as a uniform pressure) without the ameliorating effect of opposing distributed reaction from the impacted surface.

The magnitude of the pressure is the weight of the heaviest fully loaded MPC divided by the area of the faces of the elements over which the pressure is applied. The weight of the heaviest fully loaded MPC is taken from the tables in Section 2.2, and is amplified by the design basis deceleration. Amplified loads from the MPC (weight times 60g acceleration) are applied as a pressure load to the entire inner surface of the bottom plate or the lid depending on the drop orientation. Note that for a top end drop, the MPC inertia loads act only on an outer annulus of the lid due to the raised surface deliberately introduced to act as a “landing” area for the MPC and reduce lid stress and deformation. By neglecting this raised annular area on the lid and applying the MPC load as a uniform pressure, stresses in the lid and the bolts are maximized. Further discussion is provided in Section 2.7.

- ii. Side drop - The shape and extent of the pressure distribution is determined from the results of the structural analysis of the MPC under similar orientations. In the MPC structural analysis, the extent of the support conditions of the MPC shell is determined with contact elements. In the analysis of the MPC under amplified inertia loads, the overpack is represented as a rigid circular surface. Based on results from the MPC evaluations, the loaded region is taken as 72 degrees (measured from the vertical). The MPC load on the overpack model is applied uniformly along the

axial length of the inner surface of the model. Further discussion is provided in Section 2.7.

- iii. Oblique drop - Figures 2.1.10 and 2.1.11 show the balance loading applied for the oblique drop. A fixed node is defined away from the assumed impact point to insure that the package is in equilibrium under the applied loads. This drop orientation is only considered for the hypothetical accident evaluation. Therefore, a detailed discussion as to the methodology used to apply the loads and insure overall equilibrium is provided in Section 2.7 (specifically 2.7.1.3 and 2.7.1.4).

(c) Temperature (Used to Form Load Case 05 in Table 3.1.5)

Based on the results of the thermal evaluation for the normal hot environment presented in Chapter 3, a temperature distribution with a bounding gradient is applied to the overpack model. The purpose is to determine the stress intensities that develop in the overpack under the applied thermal load. A plot of the applied temperature distribution as a function of radius is shown in Figure 2.6.2.

The temperature distribution is applied to the ANSYS finite element model at discrete nodes using a parabolic curve fit of the computed distribution.

(d) Internal Pressure (Used to Form Load Cases 1 in Table 2.1.8)

Design internal pressure is applied to the overpack model. All interior overpack surfaces, including the inner shell, the bottom of the closure plate, and the top of the bottom plate are loaded with pressure. The magnitude of the internal pressure applied to the model is taken from Table 2.1.1. Figure 2.1.5 shows the displacement constraints for this load case. Figure 2.6.23 is a finite element grid plot showing the surfaces where internal pressure is applied.

(e) External Pressure (Used to Form Load Case 2 in Table 2.1.8)

Design external pressure is applied to the overpack model. External pressure is applied to the model as a uniform pressure on the outer surface of the model. The magnitude of the external pressure applied to the model is taken from Table 2.1.1. Figure 2.1.6 shows the displacement constraints for this load case. External pressures are imposed in the same manner as shown in Figure 2.6.23 except that the surfaces and magnitude are different.

(f) Bolt Pre-load (Used in all load cases in Tables 2.1.8 and 2.1.9)

The overpack closure bolts are torqued to values predicted to preclude separation. This torque generates a pre-load in the bolts and stresses in the closure plate and top flange in the region adjacent to the bolts. The finite element representation of the bolt elements is shown in Figure 2.6.18. The initial preload of the bolts is applied to the overpack model by applying an initial strain to the beam elements representing the bolts. This induces a tensile stress in each of the bolts and a corresponding compression in the seals (represented by spring elements). This load case is present in every load combination.

## (g) Fabrication stresses

Fabrication stresses are conservatively computed for the inner shell and all of the intermediate shells. Fabrication effects are not easily introduced into the finite element model unless compression-only contact elements are used. Since the fabrication stresses are circumferential secondary stresses in the shells, the incorporation of this load case is best accomplished outside of the finite element analysis. Therefore, there is no fabrication load case associated with the finite element analyses.

- Finite Element Analysis Solution Procedure

The analysis procedure is as follows:

1. The stress and deformation field due to each individual load is determined.
2. The results from each individual load case are combined in a postprocessor to create each load case. The load cases analyzed are listed in Table 2.1.8 for normal conditions of transport and in Table 2.1.9 for hypothetical accident conditions of transport.
3. The results for each load case are compared to allowables. The calculated values are compared with allowable values in Subsection 2.6.1.4 for normal conditions of transport and in an appropriate subsection of Section 2.7 for hypothetical accident conditions.

#### 2.6.1.3.2.2 Fabrication Stress

The fabrication stresses originate from welding operations to affix the intermediate shells in position. As the molten weld metal solidifies, it shrinks pulling the two parts of the shells together. Adjacent points at the weld location will close together after welding by an amount " $\delta$ " which is a complex function of the root opening, shape of the bevel, type of weld process, etc. The residual stresses generated by the welding process are largely confined to the weld metal and the "heat affected zone". The ASME Code recognizes the presence of residual stresses in the welds, but does not require their calculation. The Code also seeks to minimize fabrication stresses in the welds through controlled weld procedures. Nevertheless, fabrication stresses cannot be eliminated completely.

The computation of fabrication stresses is carried out to comply with the provisions of Regulatory Guide 7.8, Article C-1.5. The Regulatory Guide requires that "Fabrication and installation stresses in evaluating transportation loadings should be consistent with the joining, forming, fitting, and aligning processes employed during the construction of casks...the phrase fabrication stresses includes the stresses caused by interference fits and the shrinkage of bonded lead shielding during solidification but does not include the residual stresses due to plate formation, welding, etc.".

A literal interpretation of the above-cited Regulatory Guide text exempts the HI-STAR 100 designer from computing the stresses in the containment and intermediate shells due to welding. However, in the interest of conservatism, an upper bound, on the stresses induced in the containment shell and in the intermediate shells, is computed for the fabrication process.

To calculate the so-called fabrication stresses, it is recalled that in affixing the intermediate shells to the cask body, the design objective does not call for a definite radial surface pressure between the layers. Rather, the objective is to ensure that the shells are not loosely installed. Fortunately, extensive experience in fabricating multi-layer shells has been acquired by the industry over the past half-century. The technology that was developed and has matured for fabrication in older industries (such as oil and chemical) is used in HI-STAR 100 fabrication of the multi-layered shells. Mock-up tests on carbon steel coupons indicate that the total shrinkage after welding can range from 0.010" to 0.0625" for the bevel and fit-up geometry in the HI-STAR 100 design drawings. Therefore, the evaluations are carried out using the upper bound gap of 0.0625". To bound the computed stresses even further, the inter-layer friction coefficient is set equal to zero. It is intuitively apparent that increasing the friction increases the localized stresses near the "point of pull" (i.e., the weld) while mitigating the stresses elsewhere. Since the object is to maximize the distributed (membrane) stress, the friction coefficient is set equal to zero in the analysis.

A two-dimensional finite element analysis of the inner confinement shell and the five intermediate shells is performed to establish the level of fabrication circumferential stress developing during the assembly process. A 180-degree section through the overpack, consisting of six layers of metal, is modeled. The ANSYS finite element code is used to model the fabrication process; each layer is modeled using PLANE42 four node quadrilateral elements. Contact (or lack of contact) is modeled by CONTAC48 point-to-surface elements. Symmetry boundary conditions apply at 90 degrees, and radial movement of the inner node point of the confinement layer is restrained. At -90 degrees, the inner confinement layer is restrained while the remaining layers are subject to a prescribed circumferential displacement  $d$  to stretch the layer and to simulate the shrinkage caused by the weld process. Although the actual fabrication process locates the longitudinal weld in each layer at different circumferential orientation, in the analytical simulations all layer welds are located together. This is acceptable for analysis since the stress of interest is the primary membrane component. Figure 2.6.24 shows a partial free body of a small section of one of the layers. Normal pressures  $p$  develop between each layer due to the welding process; shear stresses due to friction between the layers also develop since there is relative circumferential movement between the layers. Figure 2.6.25 shows a free body of the forces that develop on each layer.

The fabrication stress distribution is a function of the coefficient-of-friction between the layers. For a large enough coefficient-of-friction the effects of the assembly process are localized near the weld. Localized stresses are not considered as primary stresses. For a coefficient-of-friction = 0.0, the membrane hoop stress in the component shells is non-local in nature. Therefore, the fabrication stress computation conservatively considers only the case coefficient of friction (COF) = 0.0 since this will develop the largest in-plane primary membrane stress in each layer. The simulation is nonlinear in that each of the contact elements is checked for closure during increments of applied loading (the weld displacement).

The results from the analyses are summarized in the table below.

Fabrication Stresses in Overpack Shells - Minimum Safety Factors (Level A Service Condition at Assembly Temperature)			
Item	Value (ksi)	Allowable (ksi) (Note 3)	Safety Factor
First Intermediate Shell (Note 1)	11.22	52.5	4.68
Fourth Intermediate Shell (Note 1)	7.79	52.5	6.74
Inner Shell Mid Plane (Note 2)	10.6	69.9	6.59
Inner Shell Outer Surface (Note 2)	16.27	69.9	4.30

Notes:

1. The fabrication stress is a tensile circumferential stress.
2. The fabrication stress is a compressive circumferential stress
3. Fabrication stresses are self-limiting and are therefore classified as “secondary” and are compared to 3 times the allowable membrane stress or stress intensity.

The above table leads to the conclusion that the maximum possible values for stresses resulting from HI-STAR 100 fabrication process are only a fraction of the relevant ASME Code limit. **It is noted that Subsection NF allowable limits are used for conservatism.**

#### 2.6.1.3.2.3 Structural Analysis of Overpack Closure Bolting (Load Case1 - Table 2.1.8)

Stresses are developed in the closure bolts due to pre-load, pressure loads, temperature loads, and accident loads. Closure bolts are explored in detail in Reference [2.6.3] prepared for analysis of shipping casks. The analysis herein of the overpack closure bolts under normal conditions of transport and for the hypothetical accident conditions uses the methodology and the procedures defined and explained in [2.6.3]; the sole exception is that some of the formulas in the reference are modified to account for the annulus on the inner surface of the overpack closure lid; this annulus exists for the sole purpose of ensuring that the interface area between the MPC lid and the overpack top closure is a peripheral ring area rather than the entire surface area of the MPC lid. This feature ensures a reduction in the computed bolt stress.

The following combined load case is analyzed for normal conditions of transport.

Normal: Pressure, temperature, and pre-load loads are included (Load Case 1 in Table 2.1.8).

Reference [2.6.3] reports safety factors defined as the calculated stress combination divided by the allowable stress for the load combination. This definition of safety factor is the inverse of the definition consistently used in this SAR. In summarizing the closure bolt analyses performed, results



are reported using the safety factor definition of allowable stress divided by calculated stress. The following result for closure lid bolting for normal conditions of transport are obtained:

Overpack Closure Bolt - Safety Factor (Load Case 1 in Table 2.1.8)	
Combined Load Case	Safety Factor
Average Tensile Stress	1.42
Combined Tension, Shear, Bending, and Torsion	1.09

It is seen from the above table that the safety factor is greater than 1.0 as required. Note that the magnitude of the safety factors reflect the large preload required for successful performance of the bolts under a hypothetical accident drop event where the demand is more severe.

#### 2.6.1.3.2.4 Stress Analysis of Overpack Enclosure Shell

The overpack enclosure shell and the overpack enclosure return are examined for structural integrity under a bounding internal pressure. Flat beam strips of unit width are employed to simulate the performance of the flat panels and the flat plate return section (see drawings in Subsection 1.4). It is shown that large safety factors exist against overstress due to an internal pressure developing from off-gassing of the neutron absorber material. The minimum safety factors are summarized below:

Location	Calculated Stress (ksi)	Allowable Stress (ksi)	Safety Factor
Enclosure Shell Return (bottom)	2.56	26.3	10.2
Enclosure Shell Return (top)	3.42	26.3	7.68
Enclosure Shell Flat Panels	5.58	26.3	4.71
Weld Shear	0.63	10.52	16.7

#### 2.6.1.3.2.5 Design Changes in HI-STAR 100 Overpack

The latest revision of HI-STAR 100 Overpack Assembly Drawing (listed in Section 1.4) provides few design changes that are evaluated in [2.6.6] for a bounding internal pressure of 45 psi to account for pressure developing from off-gassing of the neutron shield material combined with a reduced external pressure. This pressure value exceeds the design enclosure shell internal pressure of 30 psi per Table 2.1.1 for normal and accident conditions. Specifically, the enclosure shell welds and the channel to gamma shell welds are evaluated. The results are summarized in the table below.

Safety Factors for Overpack Design Changes Under Internal Pressure			
Item	Calculated Stress (psi)	Allowable Stress (psi)	Safety Factor
Enclosure Shell Welds	1,845	13,260	7.19
Channel to Gamma Shell Welds	2,716	13,260	4.88

### 2.6.1.3.3 Fatigue Considerations

Regulatory Guide 2.9 requires consideration of fatigue due to cyclic loading during normal conditions of transport. Considerations of fatigue associated with long-term exposure to vibratory motions associated with normal conditions of transport are considered below where individual components of the package are assessed for the potential for fatigue.

- Overpack and MPC Fatigue Considerations

The temperature and pressure cycles within the MPC and the inner shell of the overpack are entirely governed by the mechanical and thermal-hydraulic conditions presented by the fuel. The external surfaces of the overpack, however, are in direct contact with the ambient environment. The considerations of cyclic fatigue due to temperature and pressure cycling of the HI-STAR 100 System, therefore, must focus on different locations depending on the source of the cyclic stress.

As shown in the following, the overpack and the MPCs in the HI-STAR 100 System do not require a detailed fatigue analysis because all applicable loadings are well within the range that permits exemption from fatigue analysis per the provisions of Section III of the ASME Code. Paragraph NB-3222.4 (d) of Section III of the ASME Code provides five criteria that are strictly material and design condition dependent to determine whether a component can be exempted from a detailed fatigue analysis. The sixth criterion is applicable only when dissimilar materials are involved, which is not the case in the HI-STAR 100 System.

The Design Fatigue curves for the overpack and MPC materials are given in Appendix I of Section III of the ASME Code. Each of the five criteria is considered in the following:

- i. Atmospheric to Service Pressure Cycle

The number of permissible cycles,  $n$ , is bounded by  $f(3S_m)$ , where  $f(x)$  means the number of cycles from the appropriate fatigue curve at stress amplitude of  $x$  psi. In other words

$$n < f(3S_m)$$

From Tables 2.1.11 through 2.1.20 for normal conditions, and the fatigue curves, the number of permissible cycles is

$$\begin{aligned} n(\text{overpack}) &\leq 1600 \quad (3S_m = 68,700 \text{ psi}) \text{ (Figure I.9-1 of ASME Appendix I)} \\ n(\text{MPC}) &\leq 40,000 \quad (3S_m = 46,200 \text{ psi}) \text{ (Figure I.9-2 of ASME Appendix I)} \end{aligned}$$

The MPC, which is an all-welded component, is unlikely to undergo more than one cycle, indicating that a huge margin of safety with respect to this criterion exists. The overpack, however, is potentially subject to multiple uses. However, 1000 pressurizations in the 40-year life of the overpack is an upper bound estimate. In conclusion, the projected pressurizations of the HI-STAR components do not warrant a usage factor evaluation.

ii. Normal Service Pressure Fluctuation

Fluctuations in the service pressure during normal operation of a component are considered if the total pressure excursion  $\delta_p$  exceeds  $\Delta_p$ .

where

$$\Delta_p = \text{Design pressure} * S / (3S_m)$$

$$S = \text{Value of } S_a \text{ for one million cycles}$$

Using the above mentioned tables and appropriate fatigue curves,

$$(\Delta p)_{\text{overpack}} = \frac{(100)(13000)}{(3)(22,900)} = 18.9 \text{ psi}$$

$$(\Delta p)_{\text{MPC}} = \frac{(100)(26000)}{(3)(16000)} = 54.2 \text{ psi}$$

During normal operation the pressure fields in the MPC and the overpack are steady state. Therefore, normal pressure fluctuations are negligibly small. Normal service pressure oscillations do not warrant a fatigue usage factor evaluation.

iii. Temperature Difference - Startup and Shutdown

Fatigue analysis is not required if the temperature difference  $\Delta T$  between any two adjacent points on the component during normal service does not exceed  $S_a / 2E\alpha$ , where  $S_a$  is the cyclic stress amplitude for the specified number of startup and shutdown cycles.  $E$  and  $\alpha$  are the Young's Modulus and instantaneous coefficients of thermal expansion (at the service temperature). Assuming 1000 startup and shutdown cycles, Tables 2.3.1 and 2.3.4 and the appropriate ASME fatigue curves in Appendix I or Section III of the ASME Code give:

$$(\Delta T)_{\text{overpack}} = \frac{90,000}{(2)(26.1)(6.98)} = 247^\circ \text{F}$$

$$(\Delta T)_{\text{MPC}} = \frac{130,000}{(2)(25)(9.69)} = 268^\circ \text{F}$$

There are no locations on either the overpack or MPC where  $\Delta T$  between any two adjacent points approach these calculated temperatures. As reported in Tables 3.4.16-18, the maximum  $\Delta T$  that occurs between two components, the MPC shell and the basket periphery, is only 115 degrees F. Therefore, it is evident this temperature criterion is satisfied for 1,000 startup and shutdown cycles.

iv. Temperature Difference - Normal Service

Significant temperature fluctuations that require consideration in this criterion are those in which the range of temperature difference between any two adjacent points under normal service conditions is less than  $S/2E\alpha$  where S corresponds to  $10^6$  cycles. Substituting, gives

$$(\Delta T)_{MPC} = \frac{26,000}{(2)(25)(9.69)} = 53.7^\circ F$$

$$(\Delta T)_{overpack} = \frac{13,000}{(2)(26.1)(6.98)} = 35.7^\circ F$$

During normal operation, the temperature fields in the MPC and the overpack are steady state. Therefore, normal temperature fluctuations are negligibly small. Normal temperature fluctuations do not warrant a fatigue usage factor evaluation.

v. Mechanical Loads

Mechanical loadings of appreciable cycling occur in the HI-STAR 100 System only during transportation. The stress cycling under transportation conditions is considered significant if the stress amplitude is greater than  $S_a$  corresponding to  $10^6$  cycles. It, therefore, follows that the stress limits that exempt the overpack and MPC are 13,000 psi and 26,000 psi, respectively.

From Subsection 2.5.2.1, g-loads typically associated with rail transport will produce stress levels in the MPC and overpack which are a small fraction of the above limits. Therefore, no potential for fatigue expenditure in the MPC and overpack materials is found to exist under transportation conditions.

In conclusion, the overpack and the MPC do not require fatigue evaluation under the exemption criteria of the ASME Code.

- Fatigue Analysis of Closure Bolts:

The maximum tensile stress developed in the overpack closure bolts during normal operating conditions is shown by analyses not to exceed 114 ksi. The alternating stress in the bolt is equal to

1/2 of the maximum stress due to normal conditions, or 57 ksi. The design service temperature for the bolts per Table 2.1.2 is 350 degrees F. Per Table 2.3.5, the Young's Modulus at 350 degrees F is 27,700 ksi. The effective stress intensity amplitude is used to calculate the maximum number of cycles for the closure bolts using Figure I-9.4 of [2.1.12] (ASME Code, Section III, Appendices [2.1.12]). Figure I-9.4 contains design fatigue curves for high strength steel bolting for temperatures not exceeding 700 °F, assuming a Young's modulus of 30E6 psi. The maximum number of cycles for the overpack closure bolts is calculated by scaling the alternating stress intensity by the ratio of design curve modulus to the actual closure bolt modulus. The resulting stress intensity is used to find an appropriate maximum number of loading cycles from the design curves. Note that a stress concentration factor of 4 is conservatively applied to the calculation.

$$S_a = \frac{(57.0)(4)(30 \times 10^6)}{27.7 \times 10^6} \\ = 246.9 \text{ ksi}$$

Using Figure I-9.4 and the corresponding table [2.1.12], the permissible number of cycles is 166.

This result indicates the main closure bolts should *not be torqued and untorqued more than 166 times. After 166 loading cycles, they must be replaced.*

The maximum shear stress developed in the top overpack closure bolt threads is 14.13 ksi [2.6.6] during normal conditions.

The shear stress developed in the threads of the overpack closure bolts is significantly less than the tensile stress developed in the bolt. Therefore, fatigue of the overpack closure bolts is not controlled by shear stress in the bolt threads.

- Fatigue Considerations for Top Flange Closure Bolt Threads:

The maximum shear stress developed in the top flange closure bolt threads (internal threads) is 11.00 ksi [2.6.6] during normal conditions.

The primary membrane stress in the main flange threads is equal to twice the maximum shear stress, or 22.0 ksi. The alternating stress in the threads,  $S_a$ , is equal to 1/2 of the total stress range, or 11.0 ksi. At 400 degrees F design temperature (per Table 2.1.2) the Young's Modulus (Table 2.3.4) is  $26.1 \times 10^6$  psi.

The effective stress amplitude accounting for the fatigue strength reduction and Young's Modulus effects is given by

$$S_a = \frac{(11.0)(4)(30)}{26.1} = 50.6 \text{ ksi}$$

Using Figure I-9.1 and the corresponding table [2.1.12], the allowable number of cycles is equal to

3,950.

Therefore, the *maximum service life of the main flange threads is 3,950 cycles of torquing and untorquing of the overpack closure system.*

- MPC Fatigue Analysis

The maximum primary and secondary alternating stress range for normal transport conditions is conservatively assumed to be equal to the allowable alternating stress range of  $0.5 \times 40,000$  psi. Conservatively using a Young's Modulus of  $25 \times 10^6$  psi for the fatigue evaluation, yields

$$S = 20,000 \text{ psi} \times \frac{28.3 \times 10^6 \text{ psi}}{25 \times 10^6 \text{ psi}} = 22,640 \text{ psi}$$

Cyclic life is in excess of  $1 \times 10^6$  cycles per Figure I-9.2.1 of Appendix I of the ASME Code.

- Satisfaction of Regulatory Guide 7.6 Commitment

The minimum alternating stress range,  $S_a$ , at 10 cycles from all appropriate fatigue curves is 600 ksi. All primary stresses under any of the analyses performed in this SAR under the required load combinations are shown to lead to stress intensities that are less than the ultimate strength of the containment vessel material (70 ksi). Fabrication stresses are conservatively evaluated and are summarized in Subsection 2.6.1.3.2.2. Maximum fabrication stress intensities are less than 17 ksi. Conservatively assuming a stress concentration of 4 regardless of specific location produces a stress intensity range below  $4 \times (70 + 17) = 348$  ksi ( $< 600$  ksi). Therefore, satisfaction of the Regulatory Guide 7.6 commitment is assured.

#### 2.6.1.4 Comparison with Allowable Stresses

Consistent with the formatting guidelines of Regulatory Guide 7.9, calculated stresses and stress intensities from the finite element analyses are compared with the allowable stresses and stress intensities defined in Subsection 2.1 (Tables 2.1.11 through 2.1.21) as applicable for conditions of normal transport. The results of these comparisons are presented in the form of factors of safety (SF) defined as:

$$SF = \frac{\text{Allowable Stress}}{\text{Calculated Stress}}$$

Safety factors associated components identified as lifting devices have been presented in Section 2.5 as required by Regulatory Guide 7.9.

Major conservatisms are inherent in the finite element models for both the MPC fuel basket and the enclosure vessel, and for the HI-STAR 100 overpack. These conservatisms are elucidated here with additional discussion as needed later in the text associated with each particular issue.

### Conservative Assumptions in Finite Element Analyses and Evaluation of Safety Factors

1. Comparison with allowable stresses or stress intensities is made using the design temperature of the component rather than the actual operating temperature existing in the metal at that location. As an example, all comparisons with allowables for the Alloy X fuel basket material uses the allowable strength at 725 degrees F (Table 2.1.21). Under the normal heat conditions of transport, temperatures near the periphery of the fuel basket are below 450 degrees F. High stresses in the fuel basket generally occur at the basket periphery. From Table 2.1.19, the allowable stresses for primary membrane plus bending at the two temperatures are compared to evolve the additional margin in the computed safety factor as  $27.2/23.1 = 1.18$ . Therefore, the reported safety factors from the analysis have at least an additional 18% hidden component from this effect. Similar hidden margins from this kind of simplification arise in the various components of the overpack. Depending on the material, these hidden margins, which increase the reported safety factor, may be large or small. From Figures 3.4.17 and 3.4.18 in Chapter 3, it is concluded that the normal heat condition of transport maximum inner shell temperature is less than 300 degrees F. The allowable stresses are uniformly assumed at 400 degrees F per Table 2.1.21. From Table 2.1.11, the additional hidden safety factor multiplier is computed as  $35/34.4 = 1.02$ . In the inner shell of the overpack, the increase in the reported safety factor from this effect is only 2% for normal conditions of transport.
2. Comparisons with primary stress allowables are made with secondary stresses included. This has an adverse effect on the reported safety factor, especially in areas near discontinuities.
3. In the modeling of the HI-STAR 100 overpack, the full structural connectivity of the intermediate shells and the inner containment shell is not included in the finite element model in order to maintain the linear elastic analysis methodology. The neglect of such interaction means that the overall bending stiffness of the overpack is underestimated; this leads to over-prediction of stresses and consequent adverse effects on reported safety factors.
4. In the modeling of the MPC fuel basket, the local reinforcement of the fuel basket panel from the fillet welds is neglected. The increase in the section modulus at the weld location is ignored leading to a decrease in stiffness of the basket panel. Consequently, under mechanical loading, the stress state is overestimated at the basket panel connection.

#### 2.6.1.4.1 MPC Fuel Basket and Enclosure Vessel

It is recalled that the stress analyses have been performed for the load cases applicable to normal conditions of transport as assembled in Tables 2.1.6 and 2.1.7 for the fuel basket and the enclosure vessel, respectively. Detailed analyses, including finite element model details and the necessary explanations to collate and interpret the voluminous numerical results have been archived. A compendium of finite element results for the fuel basket and enclosure vessel for each load case associated with normal conditions of transport has been developed. Tables 2.6.6 and 2.6.7 summarize results obtained from the analyses (for all baskets) of Load Cases E1.a and E1.c defined in Table 2.1.7. Table 2.6.8 contains a synopsis of all safety factors obtained from the results. To further facilitate perusal of results, another level of summarization is performed in Tables 2.6.2 and 2.6.3 where the global minima of safety factor for each load case are presented. Finally,

miscellaneous safety factors associated with the fuel basket and the MPC enclosure vessel are reported in Table 2.6.10.

The following element of information is relevant in ascertaining the safety factors under the various load cases presented in the tables.

- In the interest of simplification of presentation and conservatism, the total stress intensities under mechanical loading are considered to be of the primary genre' even though, strictly speaking, a portion can be categorized as secondary (that have much higher stress limits).

A perusal of the results for Tables 2.6.2 and 2.6.3 under different load combinations for the fuel basket and the enclosure vessel reveals that all factors of safety are above 1.0. The relatively modest factor of safety for the fuel basket under side drop events (Load Case F2.a and F2.b) in Table 2.6.2 warrants further explanation.

The wall thickness of the storage cells, which is by far the most significant variable in the fuel basket's structural strength, is significantly greater in the HI-STAR 100 MPCs than in comparable fuel baskets licensed in the past. For example, the cell wall thickness in the TN-32 basket (Docket No. 72-1021, M-56), is 0.1 inch and that in the NAC-STC basket (Docket No. 71-7235) is 0.048 inch. In contrast, the cell wall thickness in the MPC-68 is 0.25 inch. In spite of their relatively high flexural rigidities, computed margins in the HI-STAR 100 fuel baskets are rather modest. This is because of some conservative assumptions in the analysis that lead to an overstatement of the state of stress in the fuel basket. For example:

- i. The section properties of longitudinal fillet welds that attach contiguous cell walls to each other are completely neglected in the finite element model (Figure 2.6.15). The fillet welds strengthen the cell wall section modulus at the very locations where maximum stresses develop.
- ii. The radial gaps at the fuel basket-MPC shell and at the MPC shell-overpack interface are explicitly modeled. As the applied loading is incrementally increased, the MPC shell and fuel basket deform until a "rigid" backing surface of the overpack is contacted, making further unlimited deformation under lateral loading impossible. Therefore, some portion of the fuel basket and enclosure vessel (EV) stress has the characteristics of secondary stresses (which by definition, are self-limited by deformation in the structure to achieve compatibility). For conservativeness in the incremental analysis, no distinction between deformation controlled (secondary) stress and load controlled (primary) stress in the stress categorization is made. All stresses, regardless of their origin, are considered as primary stresses. Such a conservative interpretation of the Code has a direct (adverse) effect on the computed safety factors.

The above remarks can be illustrated simply by a simple closed-form bounding calculation. If all deformation necessary to close the gaps is eliminated from consideration, then the capacity of the fuel basket cell wall under loads which induce



primary bending stress can be ascertained by considering a clamped beam (cell wall) subject to a lateral pressure representing the amplified weight of fuel assembly plus self-weight of the cell wall (e.g., see Figure 2.6.15).

Using the cell wall thickness and an appropriate unsupported length for the MPC-68, for example, the fixed edge bending stress is computed as 238.22 psi (using the actual fuel weights, cell wall weights, cell wall thickness and unsupported length). This implies a safety factor of 5.704 for a Level A event (for a 17g deceleration,  $SF = 23,100/(238.22 \times 17) = 5.704$ ) where the allowable bending stress intensity for Alloy X at 725 degrees F (Table 2.1.21) has been used. The above simple calculation demonstrates that the inherent safety margin under accident loading is considerably greater than is implied by the result in Table 2.6.8 ( $SF=2.42$ ) for the MPC-68 and 0-degree drop orientation. Similar conclusions can be reached for other MPCs by performing scoping calculations in a similar manner.

- iii. The SNF inertia loading on the cell panels is simulated by a uniform pressure, which is a most conservative approach for incorporating the SNF/cell wall structure interaction.

The above assumptions all act to depress the computed values of factors of safety in the fuel basket finite element analysis and render conservative results.

The reported values do not include the effect of dynamic load amplification. Calculations show that, for the duration of impact and the predominant natural frequency of the basket panels under lateral hypothetical accident conditions, the dynamic load factors (DLF) are bounded by 1.05. It is expected that for the normal condition of transport 1' drop, the amplification would be reduced further.

Table 2.6.8 does not report the safety factors associated with Load Case F1 in Table 2.1.6 where it is shown that secondary stresses due to the thermal gradients are below the allowable secondary stress intensity limits. A representative stress intensity level arising from fuel basket thermal gradients is 15.07 ksi. Using the allowable stress intensity limit for primary plus secondary components per Table 2.1.21, the following representative fuel basket safety factor appropriate to Load Case F1 is obtained as "SF", where:

$$SF = 46.2 \text{ ksi} / 15.07 \text{ ksi} = 3.06 \quad (\text{Load Case F1 from Table 2.1.6})$$

It is concluded that since all reported factors of safety for the fuel basket panels (based on stress analysis) are greater than the DLF, the MPC fuel basket is structurally adequate for its intended functions during and after a postulated lateral drop event associated with the normal conditions of transport.

Tables 2.6.6 and 2.6.7 report stress intensities and safety factors for the helium retention boundary (enclosure vessel) subject to internal pressure alone and to internal pressure plus the normal operating condition temperature with the most severe thermal gradient (Load Cases E1.a and E1.c in Table 2.1.7). Table 2.6.8 reports safety factors from the finite element analyses of the 1' free drop

simulating a normal handling condition of transport. The final values for safety factors in the various locations of the helium retention boundary provide assurance that the MPC enclosure vessel is a robust pressure vessel.

#### 2.6.1.4.2 Overpack

##### 2.6.1.4.2.1 Discussion

The overpack is subject to the load cases listed in Table 2.1.8 for normal conditions of transport. Results from the series of finite element analyses are tabulated for normal heat and cold conditions of transport. The tabular results include contributions from mechanical and thermal loading and are needed to insure satisfaction of primary plus secondary stress limits for normal conditions of transport. Results are also tabulated from analyses that neglect thermal stresses. These tables are used to check primary stress limits.

The following text is a brief description of how the results are presented for evaluation and how the evaluation is organized in final form:

- The stress intensity results are sorted by safety factor in ascending order for each component making up the overpack. In particular, results are sorted separately for locations in the lid, the inner shell, and the bottom plate that together make up the containment boundary.
- The extensive body of results is initially summarized in Table 2.6.9 wherein the minimum safety factor for different components of the overpack for each of the load cases is presented. This table lists minimum safety factors for the load cases associated with the normal heat conditions of transport. All safety factors are conservatively computed using allowable stresses based on the maximum normal operating temperatures (see Tables 2.1.2 and 2.1.21 for temperatures and for allowable stresses).
- The finite element analyses include the stress state induced by bolt preload but do not include the effect of secondary fabrication stresses. Table 2.6.5 presents results of re-calculation of the safety factors for the inner containment shell and for the intermediate shells to include the “fabrication stresses” reported in Subsection 2.6.1.3.2.2. Table 2.6.5 summarizes these recomputed safety factors, based on limits for primary plus secondary stresses, and reports the limiting safety factors for the overpack shells for events subject to normal conditions of transport (Level A Service Conditions). The incorporation of the fabrication stress and the computation of revised safety factors begin with the individual principal stress components for the shells, conservatively adds the circumferential fabrication stress in the inner and intermediate shells to the principal stress having the same sign as the fabrication stress, and then re-computes the stress intensity and the safety factor. For the inner shell, the safety factors including fabrication stress are computed from principal stress data including mechanical and thermal loading. For the intermediate shell, however, the recomputed safety factors are based on principal stresses that only include mechanical loading (no thermal stresses need be evaluated for a component designed in accordance with ASME Code Section III, Subsection NF regardless of Class 1 or Class 3 designation (see paragraph NF-3121.11)). **It is noted that Subsection NF allowable limits are used for conservatism.**

- Finally, Table 2.6.4 summarizes the minimum values of safety factors (global minima) for the overpack components for the normal conditions of transport.

The modifications summarized in Table 2.6.5 are briefly discussed below for the normal heat conditions of transport. The same series of modifications are also performed for the normal cold conditions of transport.

Case 1 (Pressure) - Safety factors are summarized in Table 2.6.9 prior to inclusion of fabrication stress. Table 2.6.5 shows the modified safety factor resulting from "adding" the fabrication stress for the inner containment shell to the appropriate principal stress that includes the combination of mechanical plus thermal loads. The same conservative methodology is applied to modify the safety factor for the intermediate shell to include fabrication stress. However, since the intermediate shells are **conservatively** designed to ASME Code Section III, Subsection NF, no thermal stresses need be included in the strength evaluation.

Case 3 (1 foot drop): Results are tabulated including both thermal and mechanical loading. Safety factors for the inner containment shell are summarized in Table 2.6.9 prior to inclusion of fabrication stress. Table 2.6.5 shows modified safety factors that are computed in the same manner as reported for Case 1. For the intermediate shell, principal stress results that do not include thermal stress effects are conservatively modified to include fabrication effects.

#### 2.6.1.4.3 Result Summary for the Normal Heat Condition of Transport

- Stress Results from Overall Finite Element Models of the MPC and Overpack

Tables 2.6.6 through 2.6.9 summarize minimum safety factors from load cases analyzed using the finite element models of the MPC fuel basket plus canister and the overpack described in Subsections 2.6.1.3.1 and 2.6.1.3.2. All safety factors are greater than 1.0 and are greater than any credible dynamic amplifier for the location. Table 2.6.5 provides a summary table that includes the effect of fabrication stress on safety factors for the intermediate and inner shells of the overpack. Table 2.6.5 reports safety factors based on primary plus secondary allowable strengths.

- Status of Lid Bolts and Seals on the Overpack

The finite element analysis for the overpack provides results at the lid-to-top flange interface. In particular, tabulated results for seals and lid bolts are examined. The output results for each load combination indicate that all seal springs remain closed (i.e. the loading in the elements representing the seal remains compressive) indicating that the sealworthiness of the bolted joint will not be breached during normal heat conditions of transport.

Each load combination results in a report of the total compressive force on the closure plate-overpack interface as well as the total tangential force ("friction force"). If the ratio "total friction force/total compressive force" is formed for each set of results, the maximum value of the ratio is 0.219. There will be no slip of the closure plate relative to the overpack if the interface coefficient of friction is greater than the value given above. Mark's Handbook for Mechanical Engineers [3.4.9] in

Table 3.2.1 shows  $\mu = 0.74\text{--}0.79$  for clean and dry steel on steel surfaces. Therefore, it is concluded that there is no propensity for relative movement.

Based on the results of the finite element analysis for normal heat conditions of transport, the following conclusions are reached.

No bolt overstress is indicated under any loading event associated with normal conditions of transport. This confirms the results of alternate closure bolt analyses, performed in accordance with NUREG/CR-6007 UCRL-ID-110637, "Stress Analysis of Closure Bolts for Shipping Casks", by Mok, Fischer, and Hsu, LLL, 1993.

The closure plate seals do not unload under any load combination; therefore, the seals continue to perform their function.

- Stress and Stability Results from Miscellaneous Component Analyses in Subsection 2.6.1.3

Tables 2.6.10 and 2.6.11 repeat summary results from additional analyses described and reported on in Subsection 2.6.1.3 for components of the MPC and the overpack. The safety factors are summarized in this subsection in accordance with the requirements of Regulatory Guide 7.9. The tables report comparisons of calculated values with allowable values for both stress and stability and represent a compilation of miscellaneous analyses.

- Overpack Internal Pressure Test

The overpack is considered as an ASME pressure vessel. A hydrostatic test of the overpack under 1.5 times internal pressure must result in no stresses in excess of the material yield strength at room temperature to meet the requirement of 10CFR71.85(b). In the following, the necessary results to support the conclusion that the HI-STAR 100 transport containment boundary meets the requirement are presented. Table 2.3.4 gives the material yield strengths of SA350 LF3 and SA 203-E as 37.5 ksi and 40.0 ksi, respectively, at 100 degrees F. A survey of the safety factors for the containment boundary reported in Table 2.6.9 gives the following minimum safety factors.

CONTAINMENT BOUNDARY SAFETY FACTORS - Internal Pressure	
Item	Safety Factor
Lid	2.87
Inner Shell	12.1
Baseplate	11.2

These safety factors are determined using allowable stress intensities at the reference temperatures listed in Table 2.1.21 that are less than the yield stress for the corresponding material at room temperature. From the large safety factors in the above table, it is concluded, without further analysis, that an increase in the internal pressure by 50% will not cause stresses in the containment

boundary to exceed the material yield stress.

- Summary of Minimum Safety Factors for Normal Heat Conditions of Transport

Tables 2.6.2 through 2.6.4 present a concise summary of safety factors for the fuel basket, the enclosure vessel, and the overpack, respectively. Locations within this SAR from which the summary results are culled are also indicated in the above tables.

Based on the results of all analyses, with results presented or summarized in the text and in tables, it is concluded that:

- i. All safety factors reported in the text and in the summary tables are greater than 1.0.
- ii. There is no restraint of free thermal expansion between component parts of the HI-STAR 100 System.

Therefore, the HI-STAR 100 System, under the normal heat conditions of transport, has adequate structural integrity to satisfy the subcriticality, containment, shielding, and temperature requirements of 10CFR71.

## 2.6.2 Cold

Per Reg. Guide 7.8 [2.1.2], the Normal Cold Condition of Transport assumes an ambient environmental temperature of -20 degrees Fahrenheit and maximum decay heat. A special condition of extreme cold is also defined where the system and environmental temperature is at -40 degrees F and the system is exposed to increased external pressure with minimum internal pressure. A discussion of the resistance to failure due to brittle fracture is provided in Subsection 2.1.2.3 for the LST options of -20 °F and -40 °F.

The value of the ambient temperature has two principal effects on the HI-STAR 100 storage system, namely:

- i. The steady-state temperature of all material points in the cask system will go up or down by the amount of change in the ambient temperature.
- ii. As the ambient temperature drops, the absolute temperature of the contained helium will drop accordingly, producing a proportional reduction in the internal pressure in accordance with the Ideal Gas Law.

In other words, the temperature gradients in the cask system under steady-state conditions, will remain the same regardless of the value of the ambient temperature. The internal pressure, on the other hand, will decline with the lowering of the ambient temperature. Since the stresses under normal transport condition arise principally from pressure and thermal gradients, it follows that the stress field in the MPC under a bounding "cold" ambient would be smaller than the "heat" condition of normal transport, treated in the preceding subsection. Therefore, the stress margins computed in

Section 2.6.1 can be conservatively assumed to apply to the "cold" condition as well. Calculations using the methodology outlined in NUREG/CR-6007 UCRL-ID-110637, "Stress Analysis of Closure Bolts for Shipping Casks", by Mok, Fischer, and Hsu, LLL, 1993 demonstrate that the overpack closure bolts will retain the helium seal under the cold ambient conditions.

In addition, allowable stresses generally increase with decreasing temperatures. Safety factors, therefore, will be greater for an analysis at cold temperatures than at hot temperatures. Therefore, the safety factors reported for the hot conditions in Subsection 2.6.1 provide the limiting margins. The overpack, however, is analyzed under cold conditions to ensure that the integrity of the seals is maintained.

As no liquids are included in the HI-STAR 100 System design, loads due to expansion of freezing liquids are not considered.

#### 2.6.2.1 Differential Thermal Expansion

The methodology for determination of the effects of differential thermal expansion in the normal heat condition of transport has been presented in Subsection 2.6.1.2. The same methodology is applied to evaluate the normal cold condition of transport. The results are summarized in the tables given below for normal cold condition of transport.

THERMOELASTIC DISPLACEMENTS IN THE MPC AND OVERPACK UNDER COLD TEMPERATURE ENVIRONMENT CONDITION				
CANISTER - FUEL BASKET				
	Radial Direction (in.)		Axial Direction (in.)	
Unit	Initial Clearance	Final Gap	Initial Clearance	Final Gap
All PWRs	0.1875	0.095	2.0	1.524
BWR	0.1875	0.101	2.0(min)	1.554 (min)
CANISTER - OVERPACK				
	Radial Direction (in.)		Axial Direction (in.)	
Unit	Initial Clearance	Final Gap	Initial Clearance	Final Gap
All PWRs	0.09375	0.069	0.625	0.487
BWR	0.09375	0.071	0.625	0.497

It can be verified by referring to the Design Drawings, and the foregoing table, that the clearances between the MPC basket and canister structure, as well as those between the MPC shell and overpack inside surface, are sufficient to preclude a temperature induced interference from the

thermal expansions listed above.

It is concluded that the HI-STAR 100 package meets the requirement that there be no restraint of free thermal expansion that would lead to development of primary stresses under normal cold conditions of transport.

#### 2.6.2.2 MPC Stress Analysis

The only significant load on the MPCs under cold conditions arises from the postulated 1-foot side drop. Since the allowable stress intensities are higher under the extreme cold condition, results for the MPCs are bounded by the analysis for heat; no additional solutions need to be considered. Since the MPCs are constructed of austenitic stainless steel, there is no possibility of a brittle fracture occurring in any of the MPCs

#### 2.6.2.3 Overpack Stress Analysis

Table 1 of NRC Regulatory Guide 7.8 [2.1.2] mandates load cases at the extreme cold temperature. The overpack may not be bounded by the results of the heat condition load cases for these following conditions:

- increased external pressure with minimum internal pressure, and extreme cold at - 40 degrees F.
- minimal internal pressure plus 1 foot drop with extreme cold condition at - 20 degrees F.
- rapid ambient temperature change during normal condition of transport (note that this case is not explicitly listed as a load case in Regulatory Guide 7.8).

The first two bulleted items are presented in Table 2.1.8; the results of those analyses are presented here. Structural evaluation for the last bulleted item is performed in this subsection. The structural evaluation uses inputs from thermal transient analyses performed and reported in Chapter 3 subsection 3.4.3.1.

#### Results of finite element analyses for increased external pressure with minimum internal pressure, and for minimum internal pressure plus 1 foot drop (Load Cases 2 and 4 in Table 2.1.8)

Safety factors for Load Cases 2 and 4 in Table 2.1.8 are computed from the results tabulated from the archived finite element analyses Table 2.6.12 summarizes the safety factors obtained. The finite element analysis does not clearly elucidate the effect of temperature on bolt preload. Separate calculations, using the methodology outlined in NUREG/CR-6007 UCRL-ID-110637, “Stress Analysis of Closure Bolts for Shipping Casks”, by Mok, Fischer, and Hsu, LLL, 1993 analyze the closure bolts under extreme cold ambient condition plus pressure and provides the appropriate change in bolt preload expected from operation at the extreme low temperature. A small decrease from the initial preload stress in the bolt results from this operating condition.

The computed change in stress due to the assumption of a severe local low temperature condition is insignificant compared to the initial bolt stress and to the change in the allowable bolt stress because of the lowered temperature. It is concluded that the small change in bolt preload stress has no effect on structural calculations and safety factors.

The overpack load cases for normal conditions of transport described for the hot condition are re-analyzed for the cold condition in accordance with the requirements of Regulatory Guide 7.9. Since higher allowable stresses apply to the overpack components, it is not expected that the re-analyses will result in lower safety factors than have been already reported for the heat condition. The purpose of the analyses is to demonstrate that the overpack seals remain intact under the cold condition. The results of the analyses for normal cold conditions of transport are summarized in Tables 2.6.12 and 2.6.13.

#### Stress Analysis for Rapid Lowering of Ambient Temperature from 100 degrees F to -40 degrees F (Load Case 5 in Table 2.1.8)

During transportation, the HI-STAR 100 packaging may experience changes in the ambient temperature. Since the HI-STAR 100 packaging is a passive heat rejection device, a change in the ambient temperature has a direct influence on the temperature of its metal parts. In the preceding sub-sections, all structural integrity evaluations have focused on the steady state thermal conditions using 100°F and -40°F as the limiting upper and lower ambient steady state values. In this sub-section, the structural consequences of a rapid change from the hot (100°F) to cold (-40°F) ambient condition is considered. This scenario is labelled as ASME Code Service Condition A, which requires that the range of primary plus secondary stress intensity must be less than  $3 S_m$  ( $S_m$  = allowable stress intensity at the mean metal temperature). The loadings assumed to exist coincidentally with the thermal stresses from the transient event are: (i) overpack internal design pressure,  $P_i$  and (ii) the inertial deceleration load during transport (10g's). The primary plus secondary stress intensity range from the simultaneous action of internal pressure, axial g-load (10 g's), and thermal transient must be shown to be less than  $3S_m$ .

It should be noted that the reverse transient (i.e. rapid change from cold to hot will produce a less severe thermal stress gradient. Therefore, the magnitudes of the results of a "rapid cooldown" event bound the corresponding results for the "rapid heat up" event.

To perform a bounding evaluation, it is necessary to identify the material locations on the overpack where the thermal stresses are apt to be most adverse. The thick top forging, which is directly exposed to the ambient air during transport is clearly a candidate location. The other location is the planar cross section of the overpack at approximately mid-height where the heat emission rate from the SNF is at its maximum. These locations are identified in Figure 3.4.24 and further explained in sub-section 3.4.3.

To evolve thermal gradient results for the postulated rapid ambient temperature change, a transient temperature problem is formulated and solved in Chapter 3. The thermal problem and finite element model are fully articulated in Chapter 3 (Subsection 3.4.3.1) where a three-dimensional thermal transient analysis of the HI-STAR 100 Package is performed under a postulated rapid drop in



ambient temperature (100 degree F to –40 degree F in one hour). The design basis decay heat load is imposed throughout the time span of the transient solution. The temperature profiles through the wall of the overpack and the top forging are determined as functions of time and the change in thermal gradient through the wall of the sections are documented in Chapter 3, Figures 3.4.25-3.4.27. These locations are limiting since there is direct exposure to the ambient temperature on the outer surface of these components. It is shown in the figures that the top forging experiences a change in through-wall thermal gradient of less than 2.5 degrees K (4.5 degrees F) and that other sections of the overpack experience an even weaker change in thermal gradient. The finite element analyses for normal conditions of transport report results and safety factors for all locations for the normal heat and cold conditions of storage (under assumed steady state thermal conditions). The following additional calculation provides the stress state due to the maximum through-wall thermal gradient in the top forging. This stress state is then combined with the stresses from other load cases and stress intensities formed.

Based on the results from the thermal solutions, the material properties for this calculation are obtained for a metal temperature of 150 degrees F. For the top forging material, the Young's Modulus,  $E$ , and the coefficient of linear thermal expansion,  $\alpha$ , are (at 150 degrees F):

$$E = 27,400,000 \text{ psi}$$

$$\alpha = 6.405 \times 10^{-6} \text{ inch/inch-degree F}$$

As reported in sub-section 3.4.3.1, the maximum change in temperature difference in the top forging material is bounded by 4.5°F. The ASME Code, (paragraph NB-3222.4(a)(4)) defines a significant temperature change  $\Delta T_s$  as

$$\Delta T_s = S/2E\alpha$$

Where  $S$  is the value of  $S_a$  from the applicable design fatigue curve for 1 million cycles. For the forging material,  $S = 18,900$  psi, which yields

$$\Delta T_s = 18,900 / (2 \times 27,400,000 \times 0.00000641) = 53.9 \text{ } ^\circ\text{F}$$

It therefore follows that the metal temperature gradient change produced by the rapid cooldown (or heat up event) does not lead to a significant stress adder. Nevertheless, the factor of safety under this loading condition is quantified.

The linear temperature profile gives a linear stress distribution through the wall thickness with compressive stresses at the inside surface of the top forging. The magnitude of the stress due to the maximum thermal gradient is:

$$\Delta \sigma = E\alpha(\Delta T)/(2(1-\nu))$$

For  $\Delta T = (4.5 \text{ degrees F (change)} + 1.5 \text{ degrees F (initial)})$  and  $\nu = 0.3$ , the stress intensity is computed as:

$$\Delta\sigma = 752 \text{ psi}$$

This stress is now combined with transport longitudinal stress from a 10g deceleration plus longitudinal stress from the normal condition internal pressure. These stresses are computed below:

Pressure stress:

$$\begin{aligned} p &= 100 \text{ psi (internal pressure per Table 2.1.1)} \\ \text{inside radius of top forging} &= a = 34.375'' \\ \text{outside radius of top forging} &= b = 41.625'' \end{aligned}$$

The magnitude of the longitudinal and circumferential stresses at the inside surface is

$$\sigma_x = (a^2/(b^2 - a^2))p = 2.14 \times p = 214 \text{ psi}$$

$$\sigma_h = ((a^2 + b^2)/(b^2 - a^2))p = 5.289 \times p = 529 \text{ psi}$$

Axial stress from deceleration:

The package weight = 282,000 lb. (Table 2.2.4)

The direct stress due to the axial deceleration is

$$\sigma_d = 10g \times 282,000 \text{ lb/Area} \quad \text{where the cross-section area is Area} = 1731 \text{ sq. inch}$$

Therefore,

$$\sigma_d = 1,629 \text{ psi}$$

Adding the absolute values of the stresses (for conservatism), the maximum surface stress intensity is

$$SI = (\sigma_d + \sigma_x + \Delta\sigma) + p = 2,695 \text{ psi}$$

This value is compared against 3 x the allowable stress intensity since it involves a secondary thermal stress. From Table 2.1.13, the allowable primary plus secondary stress intensity is

$$SI(\text{allowable}) = 3 \times \text{allowable membrane stress intensity} = 69,100 \text{ psi}$$

$$\text{The safety factor is } 69,100/2,695 = 25.64$$

Therefore, the HI-STAR 100 overpack is shown to meet the Level A stress intensity limits under the rapid ambient temperature change event with a large margin of safety.

### Conclusions

Based on the results of the finite element analysis and the calculations carried out within this subsection, the following conclusions are reached for normal cold conditions of transport:

- No bolt yielding is indicated under any loading event.
- The closure plate seal springs do not unload under any load combination; therefore, the seals continue to perform their function.
- The postulated rapid drop in the ambient temperature from hot (100 degrees F) to cold (-40 degrees F) conditions of transport has no appreciable effect on the stress intensities in the transport overpack. The top forging will experience a small increase in through-wall thermal gradient. Calculations show that the change in thermal stress induced by this through-wall thermal gradient is small; large safety factors are calculated when the secondary thermal stress is combined with the pressure stress and the longitudinal transport stress.

Relative movement between the top flange and the top closure lid has been examined for the normal cold condition of transport. Each load combination reported provides the total compressive force on the lands as well as the total tangential force on the lands ("friction force"). If the ratio "total friction force/total compressive force" is formed for each set of results appropriate to the cold condition of normal transport, the maximum value of the ratio is 0.138. There will be no slip of the closure plate relative to the overpack if the coefficient of friction is greater than the value given above. Mark's Handbook for Mechanical Engineers [2.6.2] shows  $\mu = 0.74-0.79$  for clean and dry steel on steel surfaces. Therefore, it is concluded that there is no propensity for relative movement.

Since the results show that all safety factors are greater than 1.0, it is concluded that the HI-STAR 100 System under the normal cold conditions of transport has adequate structural integrity to satisfy the subcriticality, containment, shielding, and temperature requirements of 10CFR71.

### 2.6.3 Reduced External Pressure

The effects of a reduced external pressure equal to 3.5 psia, which is required by USNRC Regulatory Guide 7.8 [2.1.2], are bounded by the effects of the accident internal pressure for the overpack (Table 2.1.1). This is considered in Subsection 2.7 for the overpack inner shell. This case does not provide any bounding loads for other components of the overpack containment boundary. Therefore, the only additional analysis performed here to demonstrate package performance for this condition is an analysis of the outer enclosure shell panels.

Under this load condition, the outer enclosure shell panels (see Section 1.4, Drawing) deform as long plates under the 3.5 psi pressure that tends to deform the panels away from the neutron absorber material. The stress developed in this situation can be determined by considering the panel as a clamped beam subject to lateral pressure. The appropriate dimensions are:

$L = \text{unsupported width of panel} = 7.875''$

$t = \text{panel thickness} = 0.5''$

$p$  = differential pressure = 3.5 psi

The stress is computed from classical strength of materials beam theory as:

$$\sigma = 0.5p\left(\frac{L}{t}\right)^2$$

Substituting the numerical values gives the stress as 434 psi. From Table 2.1.15, the allowable stress is 26.3 ksi for this condition. Therefore, the safety factor is

$$SF = 60.6$$

Clearly, this event is not a safety concern for package performance.

#### 2.6.4 Increased External Pressure

The effects of an external pressure equal to 20 psia on the package, which is required by USNRC Regulatory Guide 7.8 [2.1.2], are bounded by the effects of the large value for the design external pressure specified for the hypothetical accident (Table 2.1.1). Instability of the overpack shells is examined in Section 2.7. Therefore, no additional analyses need be performed here to demonstrate package performance.

#### 2.6.5 Vibration

During transport, vibratory motions occur which could cause low-level stress cycles in the system due to beam-like deformations. If any of the package components have natural frequencies in the flexible range (i.e., below 33 Hz), or near the flexible range, then resonance may amplify the low level input into a significant stress response.

As discussed in Section 2.1, there are no "flexible" beam-like members in the HI-STAR 100 MPC. The MPC is a fully welded, braced construction over its entire length and it is fully supported by the overpack during transport. Since the MPC is supported by the overpack, and is itself a rigid structure, any vibration problems would manifest themselves in the fuel basket walls.

It is shown below that the lowest frequency of the fuel basket walls and the overpack, acting as a beam, are well above 33 Hz. Therefore, additional stresses from vibration are not expected.

The lowest frequency of vibration during normal transport conditions will occur due to vibrations of a fuel basket cell wall. It is demonstrated that the lowest frequency of the component, computed based on the assumption that there is support sufficient to limit vibration to that representative of a clamped beam, is 658 Hz for a PWR basket and 1,200 Hz for a BWR basket.

These frequencies are significantly higher than the 33 Hz transition frequency for rigidity.

When in a horizontal position, the overpack is supported over a considerable length of the enclosure shell. Conservatively considering the HI-STAR as a supported beam at only the two ends of the enclosure shell, and assuming the total mass of the MPC moves with the overpack, an estimate of the lowest material frequency of the structure during transport is in excess of 469 Hz

Based on these frequency calculations, it is concluded that vibration effects are minimal and no new calculations are required.

#### 2.6.6 Water Spray

The condition is not applicable to the HI-STAR 100 System per Reg. Guide 7.8 [2.1.2].

#### 2.6.7 Free Drop

The structural analysis of a 1-foot side drop under heat and cold conditions has been performed in Subsections 2.6.1 and 2.6.2 for heat and cold conditions of normal transport. As demonstrated in Subsections 2.6.1 and 2.6.2, safety factors are well over 1.0.

#### 2.6.8 Corner Drop

This condition is not applicable to the HI-STAR 100 System per [2.1.2].

#### 2.6.9 Compression

The condition is not applicable to the HI-STAR 100 System per [2.1.2].

#### 2.6.10 Penetration

The condition is not applicable to the HI-STAR 100 System per [2.1.2].

Table 2.6.1

## FINITE ELEMENTS IN THE MPC STRUCTURAL MODELS

MPC Type Element Type	Model Type		
	Basic	0 Degree Drop	45 Degree Drop
<b>MPC-24</b>	1068	1179	1178
BEAM3	1028	1028	1028
CONTAC12	40	38	38
CONTAC26	0	110	110
COMBIN14	0	3	2
<b>MPC-32</b>	766	873	872
BEAM3	738	738	738
CONTAC12	28	27	24
CONTAC26	0	106	105
COMBIN14	0	2	5
<b>MPC-68</b>	1234	1347	1344
BEAM3	1174	1174	1174
PLANE82	16	16	16
CONTAC12	44	43	40
CONTAC26	0	112	111
COMBIN14	0	2	3

Table 2.6.1 Continued

## FINITE ELEMENTS IN THE MPC STRUCTURAL MODELS

MPC Type Element Type	Model Type		
	Basic	0 Degree Drop	45 Degree Drop
<b>MPC-24E/24EF</b>	1070	1183	1182
BEAM3	1030	1030	1030
CONTAC12	40	38	38
CONTAC26	0	112	112
COMBIN14	0	3	2

Table 2.6.2

## MINIMUM SAFETY FACTORS FOR THE MPC FUEL BASKET - NORMAL CONDITIONS OF TRANSPORT

<b>Case Number</b>	<b>Load<sup>1</sup> Combination</b>	<b>Safety Factor</b>	<b>Location in SAR where Details are Provided</b>
F1	T or T'	3.06	2.6.1.4.1
F2			
F2.a	D+H, 1 ft side drop 0°	1.57	Table 2.6.8
F2.b	D+H, 1 ft side drop 45°	1.29	Table 2.6.8

---

1 The symbols used for loads are defined in Subsection 2.1.2.1.



Table 2.6.3

## MINIMUM SAFETY FACTORS FOR THE MPC ENCLOSURE VESSEL - NORMAL CONDITIONS OF TRANSPORT

Case Number	Load Combination <sup>1</sup>	Safety Factor	Location in SAR where Details are Provided or Safety Factors Extracted
E1			
E1.a	Design internal pressure, $P_i$	5.06 1.5 1.36	Lid Table 2.6.6 Baseplate Table 2.6.6 Shell Table 2.6.6
E1.b	Design external pressure, $P_o$	NA NA 1.2	Lid $P_i$ bounds Baseplate $P_i$ bounds Shell Table 2.6.10
E1.c	Design internal pressure plus temperature	8.50 2.67 1.5	Lid Table 2.6.7 Base Table 2.6.7 Shell Table 2.6.7
E2			
E2.a	$(P_i, P_o) + D + H$ , 1 ft side drop, 0 deg.	1.41	Table 2.6.8
E2.b	$(P_i, P_o) + D + H$ , 1 ft. side drop, 45 deg.	1.63	Table 2.6.8
E4	T or T'	Sections show expansion does not result in restraint of free thermal expansion	2.6.1.2

<sup>1</sup> The symbols used for loads are defined in Subsection 2.1.2.1.

Table 2.6.4

## MINIMUM SAFETY FACTORS FOR OVERPACK FOR NORMAL CONDITION OF TRANSPORT

Case Number	Load Combination <sup>1</sup>	Safety Factor	Location in SAR where Details are Provided
1	$T_h + P_i + F + W_s$	1.09	Table 2.6.11
2	$T_s + P_o + F + W_s$	3.38	Table 2.6.13
3	$T_h + D_{sn} + P_i + F + W_s$	1.68	Table 2.6.9
4	$T_c + D_{sn} + P_o + F + W_s$	2.41	Table 2.6.13

---

1 The symbols used here are defined in Subsection 2.1.2.1.

Table 2.6.5

MINIMUM SAFETY FACTORS INCLUDING FABRICATION STRESSES –  
PRIMARY PLUS SECONDARY STRESS INTENSITY, NORMAL HEAT CONDITIONS OF TRANSPORT

<b>Case</b>	<b>Inner Shell Exterior Surface</b>	<b>Intermediate Shell</b>
1 - Internal pressure	1.65*	4.12
3 - 1 ft. Side Drop	1.70*	2.42

\* Applicable to inner shell fabricated from SA203-E material. Safety factor must be multiplied by 0.93 if inner shell is fabricated from optional SA350-LF3 material.

Note: Thermal stresses are included for inner containment shell per ASME Section III, Subsection NB, but excluded in intermediate shell per ASME Code, Section III, Subsection NF.

Table 2.6.6

STRESS INTENSITY RESULTS FOR CONFINEMENT BOUNDARY -  
INTERNAL PRESSURE ONLY (Load Case E1.a in Table 2.1.7)

Component Locations (Per Fig. 2.6.20)	Calculated Value of Stress Intensity (psi)	Category	Table 2.1.19 Allowable Value (psi) <sup>†</sup>	Safety Factor (Allowable/Calculated)
<u>Top Lid</u> <sup>††</sup>				
A	3,282	$P_L + P_b$	30,000	9.14
Neutral Axis	40.4	$P_m$	20,000	495
B	3,210	$P_L + P_b$	30,000	9.34
C	1,374	$P_L + P_b$	30,000	21.8
Neutral Axis	1,462	$P_m$	20,000	13.6
D	5,920	$P_L + P_b$	30,000	5.06
<u>Baseplate</u>				
E	19,683	$P_L + P_b$	30,000	1.5
Neutral Axis	412	$P_m$	20,000	48.5
F	20,528	$P_L + P_b$	30,000	1.5
G	9,695	$P_L + P_b$	30,000	3.1
Neutral Axis	2,278	$P_m$	20,000	8.8
H	8,340	$P_L + P_b$	30,000	3.5

<sup>†</sup> Stress intensity taken at 300 degrees F in this comparison.

<sup>††</sup> The stresses in the top lid are reported for the dual lid configuration. The stresses for the single lid configuration are 50% less (see Subsection 2.6.1.3.1.2 for further details).

Table 2.6.6 Continued

STRESS INTENSITY RESULTS FOR CONFINEMENT BOUNDARY -  
INTERNAL PRESSURE ONLY (Load Case E1.a in Table 2.1.7)

Component Locations (Per Fig.2.6.20)	Calculated Value of Stress Intensity (psi)	Category	Table 2.1.19 Allowable Value (psi) <sup>†</sup>	Safety Factor (Allowable/Calculated)
<u>Canister</u>				
I	6,860	P <sub>m</sub>	18,700	2.72
Upper Bending Boundary Layer Region	7,189	P <sub>L</sub> + P <sub>b</sub> + Q	30,000	4.2
	7,044	P <sub>L</sub> + P <sub>b</sub>	20,000	2.8
Lower Bending Boundary Layer Region	43,986	P <sub>L</sub> + P <sub>b</sub> + Q	60,000	1.36
	10,621	P <sub>L</sub> + P <sub>b</sub>	30,000	2.82

<sup>†</sup> Allowable stress intensity based at 300 degrees F except for Location I where allowable stress intensity values are based on 400 degree F.

Table 2.6.7

PRIMARY AND SECONDARY STRESS INTENSITY RESULTS FOR  
HELIUM RETENTION BOUNDARY - PRESSURE PLUS THERMAL LOADING (Load Case E1.c in Table 2.1.7)

Component Locations (Per Fig. 2.6.20)	Calculated Value of Stress Intensity (psi)	Category	Table 2.1.19 Allowable Value (psi) <sup>†</sup>	Safety Factor (Allowable/Calculated)
<u>Top Lid</u> <sup>††</sup>				
A	4,634	$P_L + P_b + Q$	60,000	12.9
Neutral Axis	1,464	$P_L$	30,000	20.4
B	2,140	$P_L + P_b + Q$	60,000	28.0
C	1,942	$P_L + P_b + Q$	60,000	30.8
Neutral Axis	3,528	$P_L$	30,000	8.50
D	7,048	$P_L + P_b + Q$	60,000	8.51
<u>Baseplate</u>				
E	22,434	$P_L + P_b + Q$	60,000	2.67
Neutral Axis	1,743	$P_L$	30,000	17.2
F	18,988	$P_L + P_b + Q$	60,000	3.16
G	5,621	$P_m + P_L$	60,000	10.7
Neutral Axis	5,410	$P_L$	30,000	5.55
H	12,128	$P_L + P_b + Q$	60,000	4.95

<sup>†</sup> Allowable stresses based on temperature of 300 degrees F.

<sup>††</sup> The stresses in the top lid are reported for the dual lid configuration. The stresses for the single lid configuration are 50% less (see Subsection 2.6.1.3.1.2 for further details).

Table 2.6.7 Continued

PRIMARY AND SECONDARY STRESS INTENSITY RESULTS FOR  
HELIUM RETENTION BOUNDARY - PRESSURE PLUS THERMAL LOADING (Load Case E1.c in Table 2.1.7)

Component Locations (Per Fig.2.6.20)	Calculated Value of Stress Intensity (psi)	Category	Table 2.1.19 Allowable Value (psi) <sup>1</sup>	Safety Factor (Allowable/Calculated)
<u>Canister</u>				
I	6,897	P <sub>L</sub>	28,100	4.07
Upper Bending Boundary Layer Region	6,525 3,351	P <sub>L</sub> + P <sub>b</sub> + Q P <sub>L</sub>	60,000 30,000	9.2 8.95
Lower Bending Boundary Layer Region	40,070 6,665	P <sub>L</sub> + P <sub>b</sub> + Q P <sub>L</sub>	60,000 30,000	1.5 4.5

<sup>1</sup> Allowable stresses based on temperature of 300 degree F except at Location I where the temperatures are based on 400 degrees F.

Table 2.6.8 - FINITE ELEMENT ANALYSIS RESULTS  
MINIMUM SAFETY FACTORS FOR MPC COMPONENTS UNDER NORMAL CONDITIONS

Component - Stress Result	MPC-24		MPC-68	
	1 Ft. Side Drop, 0 deg Orientation  Load Case F2.a or E2.a	1 Ft. Side Drop, 45 deg Orientation  Load Case F2.b or E2.b	1 Ft. Side Drop, 0 deg Orientation  Load Case F2.a or E2.a	1 Ft. Side Drop, 45 deg Orientation  Load Case F2.b or E2.b
Fuel Basket – Primary Membrane ( $P_m$ )	4.12	5.64	4.42	6.15
Fuel Basket - Local Membrane Plus Primary Bending ( $P_L + P_b$ )	1.73	1.87	2.42	1.50
Enclosure Vessel - Primary Membrane ( $P_m$ )	2.71	2.71	2.67	2.72
Enclosure Vessel - Local Membrane Plus Primary Bending ( $P_L + P_b$ )	3.30	3.29	2.17	1.80
Basket Supports - Primary Membrane ( $P_m$ )	N/A	N/A	5.32	5.33
Basket Supports - Local Membrane Plus Primary Bending ( $P_L + P_b$ )	N/A	N/A	1.67	2.16



Table 2.6.8 (Continued) - FINITE ELEMENT ANALYSIS RESULTS  
 MINIMUM SAFETY FACTORS FOR MPC COMPONENTS UNDER NORMAL CONDITIONS

Component - Stress Result	MPC-32		MPC-24E/EF	
	1 Ft. Side Drop, 0 deg Orientation  Load Case F2.a or E2.a	1 Ft. Side Drop, 45 deg Orientation  Load Case F2.b or E2.b	1 Ft. Side Drop, 0 deg Orientation  Load Case F2.a or E2.a	1 Ft. Side Drop, 45 deg Orientation  Load Case F2.b or E2.b
Fuel Basket - Primary Membrane ( $P_m$ )	4.05	5.65	4.04	5.55
Fuel Basket - Local Membrane Plus Primary Bending ( $P_L + P_b$ )	1.57	1.29	1.69	1.83
Enclosure Vessel - Primary Membrane ( $P_m$ )	2.55	2.69	2.70	2.70
Enclosure Vessel - Local Membrane Plus Primary Bending ( $P_L + P_b$ )	1.41	1.63	3.04	3.13
Basket Supports - Primary Membrane ( $P_m$ )	3.96	5.33	N/A	N/A
Basket Supports - Local Membrane Plus Primary Bending ( $P_L + P_b$ )	3.49	3.12	N/A	N/A

Table 2.6.9 - FINITE ELEMENT ANALYSIS RESULTS  
 MINIMUM SAFETY FACTORS FOR OVERPACK COMPONENTS UNDER NORMAL CONDITIONS (Hot Environment)

Component – Stress Result	Hot Environment Load Case 1	1 Ft. Side Drop Load Case 3
Lid - Local Membrane Plus Primary Bending ( $P_L + P_b$ )	2.87	2.14
Inner Shell - Local Membrane Plus Primary Bending ( $P_L + P_b$ )	12.1*	3.24*
Inner Shell - Primary Membrane ( $P_m$ )	13.7*	3.53*
Intermediate Shells - Local Membrane Plus Primary Bending ( $P_L + P_b$ )	17.3	2.51
Baseplate - Local Membrane Plus Primary Bending ( $P_L + P_b$ )	11.2	6.28
Enclosure Shell - Primary Membrane ( $P_m$ )	35.2	3.24

\* Applicable to inner shell fabricated from SA203-E material. Safety factor must be multiplied by 0.93 if inner shell is fabricated from optional SA350-LF3 material.

Table 2.6.9 (Continued) - FINITE ELEMENT ANALYSIS RESULTS

## MINIMUM SAFETY FACTORS FOR OVERPACK COMPONENTS UNDER NORMAL CONDITIONS (Hot Environment)

Component - Stress Result	Hot Environment Load Case 1	1 Ft. Side Drop Load Case 3
Lid - Local Membrane Plus Primary Bending Plus Secondary ( $P_L + P_b + Q$ )	2.14	1.90
Inner Shell - Local Membrane Plus Primary Bending Plus Secondary ( $P_L + P_b + Q$ )	2.69*	2.84*
Intermediate Shells - Local Membrane Plus Primary Bending Plus Secondary ( $P_L + P_b + Q$ excluding thermal stress)	34.5	5.01
Baseplate - Local Membrane Plus Primary Bending Plus Secondary ( $P_L + P_b + Q$ )	1.81	1.68
Enclosure Shell - Local Membrane Plus Primary Bending Plus Secondary ( $P_L + P_b + Q$ )	1.97	1.88

\* Applicable to inner shell fabricated from SA203-E material. Safety factor must be multiplied by 0.93 if inner shell is fabricated from optional SA350-LF3 material.

Table 2.6.10

SAFETY FACTORS FROM MISCELLANEOUS MPC CALCULATIONS -  
NORMAL CONDITIONS OF TRANSPORT - HOT ENVIRONMENT

Item	Loading	Safety Factor	Location in SAR Where Details are Provided
Fuel Support Spacers	1' Drop (Load Case F2 in Table 2.1.6)	2.75	Subsection 2.6.1.3.1.3
MPC Stability	Code Case N-284 (Load Case E1.b in Table 2.1.7)	1.2	Subsection 2.6.1.3.1.3

Table 2.6.11

MINIMUM SAFETY FACTORS FROM MISCELLANEOUS OVERPACK CALCULATIONS  
NORMAL HOT CONDITIONS OF TRANSPORT

Item	Loading	Safety Factor	Location in SAR where Details are Provided
Fabrication Stress in Inner Shell	Fabrication	4.30	Subsection 2.6.1.3.2.2
Closure Bolt	Combined Tension, Shear, Bending and Torsion (Including Pre-Load)	1.09	Subsection 2.6.1.3.2.3

Table 2.6.12 - FINITE ELEMENT ANALYSIS RESULTS  
 MINIMUM SAFETY FACTORS FOR OVERPACK COMPONENTS UNDER NORMAL CONDITIONS (Cold Environment)

Component - Stress Result	Super-Cold Environment Load Case 2	1 Ft. Side Drop Load Case 4
Lid - Local Membrane Plus Primary Bending ( $P_L + P_b$ )	4.55	2.97
Inner Shell - Local Membrane Plus Primary Bending ( $P_L + P_b$ )	14.4	3.37
Inner Shell - Primary Membrane ( $P_m$ )	16.5	3.53
Intermediate Shells - Local Membrane Plus Primary Bending ( $P_L + P_b$ )	21.7	2.48
Baseplate - Local Membrane Plus Primary Bending ( $P_L + P_b$ )	722.8	7.84
Enclosure Shell - Primary Membrane ( $P_m$ )	50.2	3.21

Table 2.6.12 (Continued)

FINITE ELEMENT ANALYSIS RESULTS  
MINIMUM SAFETY FACTORS FOR OVERPACK COMPONENTS UNDER NORMAL CONDITIONS (Cold Environment)

Component - Stress Result	Super-Cold Environment Load Case 2	1 Ft. Side Drop Load Case 4
Lid - Local Membrane Plus Primary Bending Plus Secondary ( $P_L + P_b + Q$ )	8.79	5.79
Inner Shell - Local Membrane Plus Primary Bending Plus Secondary ( $P_L + P_b + Q$ )	15.5	6.36
Intermediate Shells - Local Membrane Plus Primary Bending Plus Secondary ( $P_L + P_b + Q$ excluding thermal stress)	43.24	4.95
Baseplate - Local Membrane Plus Primary Bending Plus Secondary ( $P_L + P_b + Q$ )	83.8	15.1
Enclosure Shell - Local Membrane Plus Primary Bending Plus Secondary ( $P_L + P_b + Q$ )	21.4	7.67

Table 2.6.13

MINIMUM SAFETY FACTORS INCLUDING FABRICATION STRESS - PRIMARY PLUS SECONDARY  
STRESS INTENSITY, NORMAL COLD CONDITIONS OF TRANSPORT

Case	Inner Shell Exterior Surface	Intermediate Shell
2 Pressure (Secondary Stress)	3.38	4.22
4 1 ft. Side Drop (Secondary Stress)	2.58	2.41

Note: Thermal stresses are included for inner containment shell per ASME Section III, Subsection NB, but excluded in intermediate shell per ASME Code, Section III, Subsection NF.



Table 2.6.14

MISCELLANEOUS SAFETY FACTOR FOR OVERPACK			
Item	Loading	Safety Factor	Location in SAR Where Details are Provided
Outer Enclosure Panels	Reduced External Pressure	60.6	Subsection 2.6.3

**FIGURES 2.6.1 THROUGH 2.6.25: PROPRIETARY INFORMATION WITHHELD PER  
10CFR2.390**

## 2.7 HYPOTHETICAL ACCIDENT CONDITIONS

It was shown in the preceding section that the load combinations for normal conditions of transport do not induce stresses or stress intensities in excess of allowables. Therefore, it is concluded that the effectiveness of the HI-STAR 100 System is not reduced under normal conditions of transport.

The hypothetical accident conditions, as defined in 10CFR71.73 and Regulatory Guide 7.9, are applied to the HI-STAR 100 System in the required sequence. The system is first subjected to a 9 meter (30 foot) drop in the most damaging orientation, then subject to a 1 meter (40 inch) drop onto a 6 inch diameter mild steel pin (of length sufficient to cause damage to the steel structure), followed by a 1475°F temperature fire environment for 30 minutes, and finally to a water immersion test.

The overpack containment boundary is also subjected to deep immersion in accordance with 10CFR71.61.

It is shown in the following subsections that the HI-STAR 100 System meets the standards set forth in 10CFR71, when it is subjected to the hypothetical accident conditions specified in 10CFR71.73. In particular, sufficient analytical and experimental evidence is presented herein to support the conclusion that HI-STAR 100 packaging, when subjected to hypothetical accident conditions, has adequate structural integrity to satisfy the subcriticality, containment, shielding, and temperature requirements of 10CFR71.

### 2.7.1 Free Drop

In this section the performance and structural integrity of the HI-STAR 100 System is evaluated for the most severe drop events. The drop events that are potentially most damaging are the end drops (top or bottom), the side drop, the orientation for which the center of gravity is directly over the point of impact, an oblique drop where the angle of impact is somewhere between center of gravity over corner and a near side drop, and an orientation where package rotation after an impact at one end induces a larger impact deceleration when the other end impacts the target (e.g., slapdown).

The structural assessment of the package is performed in two parts. In the first part, a numerical model to simulate the drop events is prepared and benchmarked against 1/8 scale static tests of the HI-STAR 100 impact limiters, and 1/4-scale dynamic drop tests of the HI-STAR 100 Package. This numerical/experimental effort is carried out to confirm that the maximum rigid body decelerations experienced by the package are less than the design basis values set forth in Table 2.1.10. This Classic Dynamics Method (CDM) is discussed in detail in this section and in Appendix 2.A. Note that the scale model test data is also used to benchmark the finite element code LS-DYNA for predicting the dynamic response of the AL-STAR™ impact limiter in a drop event [2.7.4]. The state of the art LS-DYNA analysis method has been employed to perform drop analyses for both HI-STAR 60 [2.7.5] and HI-STAR 180 [2.7.6] transport packages. Appendix 2.C documents the LS-DYNA drop simulations performed to evaluate the improved HI-STAR 100 impact limiter design (Drawing listed in Section 1.4), which consists of only one type of aluminum honeycomb material, as opposed to four types in the original design. In the second part, the structural integrity of components under the inertia loads due to design basis deceleration levels is evaluated. The

deceleration sustained by the internals, such as the fuel basket, are further amplified in recognition of the elasticity of the internal structures. The dynamic amplifier is considered as an added multiplier on the rigid body deceleration in the structural assessments. Dynamic amplifiers applicable to components of the package have been developed from evaluating the behavior of simplified models.

### Part One: Maximum Rigid Body Deceleration Under 10CFR71.73 Free Drop Event

The determination of the AL-STAR impact limiter performance under postulated 10CFR71.73 free drop events was carried out in six phases as summarized below and further elaborated in Appendix 2.A.

- i. Characterize honeycomb material crush behavior: Coupons of both unidirectional and cross-core honeycomb materials at different nominal crush strength values were prepared and tested. A typical pressure vs. deflection curve is shown in Figure 2.A.2.1 in Appendix 2.A. The pressure in the flat portion of the curve denotes the crush pressure.

Mathematical correlation of the data from the population of coupons tested showed that the pressure/crush curve for a honeycomb stock can be represented by one equation wherein the crush pressure,  $p_c$ , is the sole variable. This commonality in the deformation characteristic of the AL-STAR honeycomb materials of different crush strength is extremely helpful in simplifying the dynamic model for the impact limiter.

- ii. AL-STAR Force-Crush Relationship: The AL-STAR impact limiter is a radially symmetric structure whose external and internal diameters are fixed: the I.D. is set by the overpack diameter at its extremities and the O.D. is limited by rail transport considerations to 128". Within this annular space, the arrangement of the aluminum honeycomb material is specified so that the impact limiter can absorb the kinetic energy from a 30' drop event in *any* orientation. The axial dimension of the impact limiter is also limited by considerations of the overall weight of the packaging. To design the impact limiter within the above-mentioned constraints called for a method to predict the force required to crush the impact limiter by a given amount in any given orientation. The mathematical model to define the force-crush (F-d) curve is described in Appendix 2.A. The F-d model was used to establish the nominal crush strengths of the honeycomb sectors used in the various locations of the AL-STAR honeycomb volume to obtain the desired energy absorption characteristics in the equipment.
- iii. Static Scale Model Tests: The static 1/8 scale model tests consisted of preparing 1/8 scale models of the AL-STAR impact limiter and subjecting them to static crush tests in various orientations under normal and abnormal temperature conditions. One object of these tests was to confirm the validity of the theoretical F-d model. Confirming the structural adequacy of the AL-STAR backing structure (which is a thick carbon steel weldment) and the external skin were also objectives of the scale model test. The 1/8 scale static tests, as described in Appendix 2.A, met all project goals: a weakness in the AL-STAR backing structure was identified and corrected in a redesign of the backing structure. The test data also showed that Holtec's F-d model provided a reasonably accurate analytical tool to predict the static crushing behavior of AL-STAR in the various potential crushing orientations. The adequacy

of the F-d model to predict static crush behavior was an essential prerequisite for the dynamic test correlation effort that followed.

- iv. Dynamic Scale Model Tests: A 1/4 scale model of the HI-STAR 100 Package, including AL-STAR impact limiters, was used for drop testing. Appendix 2.A herein provides a complete synopsis of the AL-STAR impact limiter design development program, including the 1/4 scale model drop tests which demonstrated the performance of the package. The objectives of the drop tests may be stated as follows:
- i. Select a sufficient number of drop orientations to ensure that under the worst-case orientations, the structural adequacy of the package is demonstrated by testing.
  - ii. Prove that the peak rigid body decelerations experienced by the package in any of the tests is below the Table 2.1.10 design basis value.
  - iii. Demonstrate that the impact limiters prevent the cask from direct contact with the unyielding surface and remain attached through the end of the drop event.

Four drop configurations, namely, vertical (top end), horizontal (side), center-of-gravity-over-corner (CGOC), and slap-down (fully described in Appendix 2.A) were identified as a complete set capable of realizing the aforementioned objectives. The tests were performed in two distinct series as described below.

The first test series, conducted in August 1997, indicated the need to modify the honeycomb material crush strength utilized. The first dynamic test series also helped quantify the dynamic multiplier applicable to the statically determined honeycomb crush strength under impact conditions.

The second test series showed that the peak deceleration in all four drop orientations tested met the Table 2.1.10 limits. Despite meeting deceleration limits, the attachment bolts between the bottom impact limiter and the overpack failed in the side drop test. This required an additional design improvement to the bottom impact limiter-to-overpack attachment design, and re-performance of the side drop test. For the final four tests used for evaluation in Appendix 2.A, no attachment bolts sustained a failure.

- v. AL-STAR Dynamic Response Model: The 1/4 scale tests provided valuable information on the package response which was used to confirm the veracity of Holtec's dynamic simulation model developed for predicting the package response under the other drop conditions. Like all orthotropic materials, the crushing of the honeycomb requires greater force under an impact load than the load necessary to achieve the same extent of crush under static conditions. The conversion of the static "force (F) - crush (d)" model to dynamic conditions simply means applying a dynamic factor to the formula. In other words, under dynamic conditions, the relation between crush force "F" and crush "d" is given as:

$$F = Z f(d)$$

where  $f(d)$  is the crush force corresponding to the compression “d” under static conditions and  $Z$  is the dynamic multiplier function. The value of  $Z$  was quantified by the first series of 1/4 scale dynamic scale model test, such that a dynamic response simulation model could be developed that satisfied all equilibrium expectations.

In addition to comparing the predicted peak decelerations with the measured value, the duration of crushing and crush depth predicted by the dynamic model were also compared with the measured test data. The comparisons, presented in Appendix 2.A, confirm the ability of the dynamic model to simulate the behavior of the package under a drop event.

- vi. Sensitivity Studies: A significant result from the 1/4 scale model dynamic tests was a complete validation of the dynamic model. For every test performed, the AL-STAR dynamic model was able to simulate the peak accelerations, total crush, *and* crush duration with reasonable agreement. The experimentally benchmarked mathematical model could now be used to simulate drop events for a variety of HI-STAR 100 package weights and honeycomb crush strengths. Results of the simulations to determine the effects of variations in aluminum honeycomb crush strengths and package weights are presented in Appendix 2.A.

The results summarized in Table 2.A.5 of Appendix 2.A, as well as in Appendix 2.C, demonstrates that the maximum rigid body deceleration experienced by the HI-STAR 100 package equipped with the AL-STAR impact limiter will be less than 60g's regardless of the orientation of impact. Therefore, in the balance of analyses performed to evaluate the consequences of "free drop" under the provisions of 10CFR71.73, the package will be assumed to be subject to a rigid body deceleration equal to 60 g's. It is clear from inspection of the geometry of the package that the most vulnerable direction of inertia loading for the HI-STAR fuel basket is the transverse direction wherein the flat panels of the basket are subjected to lateral inertia loading from the contained SNF. As mentioned earlier, the flexibility of basket panel acts to further amplify the package deceleration, which must be considered in the evaluation of results from the stress analysis model. In summary, the net result of the work effort described in the foregoing and further elaborated in Appendix 2.A was to confirm the validity of 60g as the *design basis* rigid body deceleration for the 10CFR71.73 drop event.

In Appendix 2.A, additional supporting technical information requested in Paragraph 2.7 of Reg. Guide 7.9 is provided. Information provided includes free-body diagrams, sketches, governing equations, test method for model testing, scaling factors, discussion of the law of similitude, measurements of crush, impact duration, deceleration histograms, effect of tolerances on package response, and demonstration that the model test will give conservative results for peak g-force and maximum deformation.

Additionally, Reg. Guide 7.9 calls for evaluation of the response of the package in terms of stress and strain to components and structural members, including investigation of structural stability as well as the consequences of the combined effects of temperature gradients, pressure, and other loads. Part Two of the work effort, described in the following, fulfills the above Reg. Guide 7.9 stipulations.

## Part Two: Stress Analysis

The second part of the analysis is performed using the ANSYS finite element software [2.6.4]. The MPC and overpack models used here are identical to those presented in Section 2.6. The loads are applied to the models in accordance with the load combinations defined in Table 2.1.6 (Load Cases F3), Table 2.1.7 (Load Cases E3), and Table 2.1.9 (Load Cases 1-16) for hypothetical accident conditions of transport. The detailed application of each load case is described in the subsections that follow. The presentation and content follows the formatting requirements of Regulatory Guide 7.9. The results from conditions of “Heat” and “Cold” are considered together in the following presentation.

The analysis of the different hypothetical accident conditions of transport are carried out using general finite element models of the MPC and the overpack as well as calculations based on simplified models amenable to strength of materials solutions. The analyses using strength of materials solutions focus on specific loading conditions applied to component parts of the MPC and/or the overpack. The finite element analysis of the overpack involves a complex 3-D model of the overpack to which a series of loads are applied. The results from the solutions are then combined in a post-processing phase to make up the different accident load combination. Given the complexity of the overpack finite element analysis model, some discussion of the stress report is presented to facilitate an understanding of the conclusions. For each of the load combinations, the following components are identified for reporting purposes:

1. Seal
2. Bolts
3. Lid
4. Inner Shell (including the top flange)
5. Intermediate Shells
6. Baseplate
7. Enclosure

The postprocessor collects the nodal stresses from the finite element solution, for each of the components in turn, and reports the principal stresses and the stress intensity at selected locations where physical reasoning suggests that high stresses may occur under the different postulated load combinations. In order to identify the minimum safety factor for each of the above components after the load cases are combined, the collection of nodes is sorted by stress intensity magnitude in descending order. Therefore, since the hypothetical accident condition load combinations involve a comparison of primary stress intensities, a minimum safety factor for each of the defined components in the model may be identified as occurring at the node point with the largest calculated stress intensity. Safety factors are computed using the allowable stress intensities for the material at the reference temperature identified for the component and reported under one of the seven groups identified above. The post-processor collects, sorts, and reports the necessary information to enable documentation of the satisfaction of the applicable requirements. The following items are collected and evaluated for each load combination:

**Seals:** The normal force in each of the springs representing the seal is reported and shown to remain in compression under the load. Maintaining a compressive load in the seal springs assures that there is no separation at the component interfaces.

**Bolts:** The bolts are initially preloaded by applying an initial strain sufficient to result in the desired pre-stress. Subsequent to the application of the different loads to form a specified load combination, the bolts are shown not to unload.

**Lid:** For each load combination, the lid primary membrane plus primary bending stress intensities are compared to the allowable values at the designated reference temperature.

**Inner Shell:** Primary membrane and primary membrane plus bending stress intensity distributions are examined and compared to allowable stress intensity values

**Intermediate Shells:** The five intermediate shells are examined at stress location points and compared to allowable stress intensities at the appropriate reference temperature. Since accident conditions of transport represent a Level D condition (where the comparison of calculated value vs. allowable value is always based on stress intensity), there is no differentiation between intermediate shells considered as Class 1 or Class 3 components.

**Baseplate:** Primary membrane plus bending stress intensities are compared to allowable values at the component reference temperature.

**Enclosure:** The plate and shell elements making up the enclosure for the Holtite-A material are compared to primary membrane stress intensity allowable values.

In the finite element analysis of all load combinations associated with hypothetical accident events, the initial preload case of the bolts and the internal pressure case are included in the final combination. Since no secondary stresses need be evaluated per the ASME Code requirements for an accident level event, the thermal stress load case for the “Heat” condition is not included as a specific load case. However, the allowable stress intensities used for the safety factor evaluation are obtained at the appropriate “Heat” condition reference temperature. In the reporting of safety factors, the variation in allowable stress intensity with temperature is ignored; this introduces an additional measure of conservatism in the reported safety factors since the reference temperatures (Table 2.1.21) are higher than the actual calculated temperatures. For the “Cold” condition, there are no temperature gradients developed. The interaction stresses developed to maintain compatibility under the uniform ambient temperature change are included in the analysis and are treated as primary stresses in the evaluation of the safety factor.



### 2.7.1.1 End Drop

- Overpack Stress (Load Cases 1,2,9, and 10 in Table 2.1.9)

The overpack is evaluated under both a top end drop and a bottom end drop. In both cases, the impact limiter reaction is assumed to act over the entire area that is backed by structural metal. Given that the total dropped weight is  $W$  and that the maximum acceleration is  $A$ , the impact

$$|R| = \frac{WA}{g}$$

limiter total reaction load follows from force equilibrium.

This reaction load  $R$  is imposed on the appropriate region of the overpack (either lid outer surface or bottom plate outer surface as a uniform pressure load to maximize the bending of the lid or bottom plate.

Since the same finite element model described and used in Section 2.6 for evaluation of loading associated with normal conditions of transport is used here with different applied loads, no further discussion of the model or the analysis methodology is required. Figures 2.1.7 and 2.1.8 show the loading on the overpack in the bottom down and the top down configurations, respectively. The results of the analyses for the top end and bottom end drops are collected and safety factors from the limiting locations in the model are reported in Tables 2.7.5 and 2.7.6 for both heat and cold environments. Table 2.7.5 presents the minimum safety factors for each of the components identified above for the “Heat” condition and Table 2.7.6 presents the safety factors for the “Cold” condition. Within each table, the component is identified, and the minimum safety factor reported.

- Overpack Stability

Structural stability of the overpack containment inner shell under the end drop is assessed. The case of the accident end drop is evaluated for elastic and plastic stability in accordance with the methodology of ASME Code Case N-284 [2.1.8]. All required interaction equation requirements set by [2.1.8] are met. For this event, yield strength limits rather than instability limits govern the minimum safety factor. The minimum safety factor for this case is summarized below:

Code Case N-284 Minimum Safety Factors - (Load Case 1 and 2 in Table 2.1.9)			
Item	Calculated Interaction Value	Allowable Interaction Value <sup>†</sup>	Safety Factor against Yield <sup>†</sup>
Load Case 1 and 2 in Table 2.1.9	0.62*	1.34	2.16*

\* Applicable to inner shell fabricated from SA203-E material. Safety factor must be multiplied by 0.93 if inner shell is fabricated from optional SA350-LF3 material.

<sup>†</sup> Note that in computing the safety factor against yield for this table, the safety factor implicit in the Code Case N-284 allowable interaction equation is included. Note also that the safety factors given

above from the Code Case analysis are all safety factors against the circumferential or longitudinal stresses reaching the material yield stress. The actual safety factors against instability are larger than the factors reported in the table. In other words, yield strength rather than stability is the limiting condition. Finally, note that fabrication stresses have been included in the stability calculations even though these stresses are self-limiting. Therefore, all results corresponding to the calculated stability interaction equations are very conservative.

The result for the heat environment bound the similar result for the cold environment since yield strengths and elastic modulus are higher. Therefore, no analysis is performed for stability under cold conditions.

- Closure Bolt Analysis

Stresses are developed in the closure bolts due to pre-load, pressure loads, temperature loads, and accident loads. Closure bolts are explored in detail in Reference [2.6.3], which deals with the analysis of shipping casks. The analysis of the overpack closure bolts under normal conditions of transport has been reported in Section 2.6. This subsection presents the results for the analysis for the hypothetical accident end drop. The analysis follows the procedures defined in Reference [2.6.3]. The allowable stresses used for the closure bolts follows that reference. Note that the analyses provide alternative confirmation of the results from the finite element analysis; namely, under any of the identified load combinations, the bolts do not unload.

The following combined load case is for the hypothetical top end drop accident condition of transport. This drop conservatively assumes a nearly vertical orientation with the impact limiter reaction load applied at the outermost location of the lid. This results in the closure bolts resisting the inertial load from the MPC plus contents in addition to the inertia load from the closure lid itself. In reality, the load from the MPC would not load the bolts.

Top End Drop: Pressure, temperature, and pre-load loads are included.

Reference [2.6.3] reports safety factors defined as the calculated stress divided by the allowable stress for the load combination. This definition of safety factor is the inverse of the definition consistently used in this SAR. In summarizing the closure bolt analyses, results are reported using the safety factor definition of allowable stress divided by calculated stress. The following result for closure lid bolting for the top end drop hypothetical accident condition of transport is obtained.

Overpack Closure Bolt - Safety Factor (Load Case 2 in Table 2.1.9)	
Combined Load Case	Safety Factor
Average Tensile Stress	1.30
Combined Tension, Shear, Bending and Torsion	1.02

It is seen from the above table that the safety factors **are** greater than 1.0 as required. Note that the **stress conditions** reflect the preload stress required for successful performance of the bolts as well as the applied load from the hypothetical accident drop event.

- MPC Fuel Basket Stability and Stress (Load Case F3.a in Table 2.1.6)

Under top or bottom end drop in a hypothetical accident condition of transport, the MPC is subject to its own amplified self-weight, causing compressive longitudinal stress in the fuel basket cell walls. The following analysis demonstrates that stability or yield is not a credible safety concern in the fuel basket walls under a hypothetical end drop accident condition of transport.

- MPC Fuel Basket Stability

Stability of the basket panels, under longitudinal deceleration loading (Load Cases F3.a in Table 2.1.6), is demonstrated in the following manner. Table 2.2.1 provides the weight of each fuel basket (including sheathing and neutron absorber panels). The corresponding metal areas of the basket bearing on the MPC baseplate or top lid can be computed for each MPC basket by direct calculation from the appropriate drawings. Dividing weight by bearing area and multiplying by the design basis deceleration for the hypothetical accident from Table 2.1.10 gives the axial stress in the load bearing walls. The results for each basket are compared and the bounding result (maximum weight/area) reported below:

Fuel Basket Compressive Stress For End Drop (Load Case F3.a)			
Item	Weight (lb.)	Bearing Area (sq. inch)	Stress (psi)
Bounding Basket (at 60g's deceleration)	23,535	346.61	4,074

To demonstrate that elastic instability in the basket panels is not credible, the flat panel buckling stress,  $\sigma_{cr}$ , (critical stress level at which elastic buckling may occur) is computed using the formula in reference [2.6.1].

For conservatism, the MPC fuel basket is modeled as a rectangular plate simply supported along two sides and uniformly compressed in the parallel direction. The width of the plate is equal to the maximum unsupported width of a panel from all fuel basket types. Reference [2.6.1] provides the critical stress formula for these conditions as

$$\sigma_{cr} = \frac{2.3 \pi^2 E}{12(1-\nu^2)} \left( \frac{T}{W} \right)^2$$

where T is the panel thickness and W is the width of the panel, E is the Young's Modulus at the metal temperature and  $\nu$  is the metal Poisson's Ratio. The following table summarizes the calculation for the critical buckling stress using the formula given above:

Elastic Stability Result for a Flat Panel	
Reference Temperature	725 degrees F
T (bounding thickness)	9/32 inch
W (bounding width)	11.0 inch
E	24,600,000 psi
Critical Axial Stress	33,430 psi

It is noted that the critical axial stress is an order of magnitude greater than the computed basket axial stress reported in the foregoing. Therefore, it is demonstrated that elastic stability under hypothetical accident condition of transport longitudinal deceleration inertia load is not a concern.

- MPC Fuel Basket Stress

The safety factor against yielding of the basket under longitudinal compressive stress from a design basis inertial loading is given by

$$SF = 17,100/4,074 = 4.198$$

where the yield stress of Alloy X has been taken from Table 2.3.1 at 725 degrees F.

Therefore, plastic deformation of the fuel basket under design basis deceleration is not credible.

Analyses of the Damaged Fuel canisters to be transported in the HI-STAR 100 Package are performed to demonstrate structural integrity under an end drop condition. A summary of the methodology and the results for all canisters is provided in Appendix 2.B.

- MPC Enclosure Shell Stability

Structural stability of the MPC enclosure shell under the end drop is evaluated for elastic and plastic/stability in accordance with the ASME Code Case N-284 [2.1.8]. All required interaction equation requirements set by [2.1.8] are met. It is shown that yield strength limits rather than instability limits govern the minimum safety factor. The minimum safety factor for this case is summarized below:

MPC Shell Elastic/Plastic Stability (Load Case E3.a Table 2.1.7)			
Item	Value	Allowable*	Safety Factor
Yield	0.698	1.34	1.92

\* For Load Case E3.a, the yield strength criteria in the Code Case N-284 method govern. In this event, the safety factor 1.34, built into the Code Case, is included in the tabular result in order to obtain the actual safety factor with respect to the yield strength of the material.

- MPC Closure Lid Stress (Load Case E3.a)

The closure lid, the closure lid peripheral weld, and the closure ring are examined for maximum stresses developed during the hypothetical end drop accident event.

The closure lid is modeled as a single simply supported plate and is subject to deceleration from an end drop plus appropriate design pressures. Results are presented for both the single and dual lid configurations (in parentheses) for top end and bottom end drops. For the dual lid configuration, the two plates each support their own amplified weight as simply supported plates under a bottom end drop. The inner lid transfers the total load to the outer plate through the peripheral weld between the two lids. Under a top end drop scenario, the inner lid is partially supported by the outer lid and the amplified load is transmitted by a combination of peripheral support and interface contact pressure. The results for minimum safety factor are reported in the table below:

MPC Top Closure Lid - Minimum Safety Factors - Load Case E3.a in Table 2.1.7			
Item	Stress(ksi) or Load(lb.)	Allowable Stress (ksi) or Load Capacity (lb.)	Safety Factor
Lid Bending Stress - Load Case E3.a (bottom end drop)	3.35/(7.94)	60.7	18.1/(7.65)
Lid Bending Stress* - Load Case E3.a (top end drop)	21.9/(43.8)	60.7	2.77/(1.39)
Lid-to-Shell Peripheral Weld Load - Load Case E3.a	624,000	1,477,000**	2.37
Lid-to-Lid Peripheral Weld Load - Load Case E3.a (bottom end drop)	312,000	443,200***	1.42

\* Stress computation is conservatively based on peripheral support at the outer diameter of the MPC lid. For a top end drop, the actual support diameter is .77 of the outer diameter. Therefore, an analysis based on an overhung plate would provide stresses reduced by a multiplier of 0.59. Consequently, the safety factors would be amplified by the factor 1.69.

\*\* Based on a 0.625" single groove weld and conservatively includes a quality factor of 0.45.

\*\*\* This is a non-Code weld; limit is based on a 0.1875 groove weld and includes a quality factor of 0.45 for additional conservatism

Safety factors are greater than 1.0 as required. The limiting condition for the lid bending evaluation is a top end hypothetical accident end drop because the lid supports the amplified fuel weight as well as the lid amplified self-weight.

- MPC Baseplate and Canister Stress (Load Case E3.a)

Load Case E3.a provides the limiting accident loading on the baseplate wherein the combined effect of a 60g deceleration plus external pressure is considered. The top end hypothetical accident condition is limiting in transport, and here it is conservatively assumed that accident external pressure acts simultaneously, which exceeds the requirements of Table 2.1.7. The results are summarized below.

MPC Baseplate Minimum Safety Factors – Load Cases E3, Table 2.1.7			
Item	Value (ksi)	Allowable (ksi)	Safety Factor
Center of Baseplate - Primary Bending (Load Case E3)	22.12	67.32	3.04
Shell Bending Stress at Connection to Baseplate	31.47	67.32	2.14

Note that all safety factors are greater than 1.0. Also, note that the calculated stress conservatively includes both primary and secondary self-limiting stress components. For the hypothetical transport drop accident, the safety factor computed for the shell bending stress intensity need only consider the effect of primary membrane plus bending stresses that are to be compared against the ultimate stress at temperature for this ASME Code Service Level D event. Since secondary stresses have been included in the evaluation, the reported result for safety factor is conservatively low.

- Generic MPC Spacer Ring

For MPC's that are shorter in length than the generic MPC's, an MPC spacer is positioned on top of the MPC lid in order to prevent the shorter MPC from thrusting forward and impacting the MPC lid during a top-end drop or a tip-over event (i.e., slapdown). The conservatively bounding generic MPC spacer ring design (drawing is listed in Section 1.4) is evaluated in [2.6.5] for compressive stress under a bounding deceleration of 60g's (Table 2.1.10). The results from the evaluation are summarized in the table below.

Bounding Generic MPC Spacer Ring Minimum Safety Factor			
Item	Value (ksi)	Allowable (ksi)	Safety Factor
Compressive Stress	12.95	28.45	2.20

- Trojan MPC Spacer

The Trojan MPC-24E/EF enclosure vessel is 9 inches shorter in length than the generic MPC-24E/EF enclosure vessel. Thus, when the Trojan MPC-24E/EF is transported inside the HI-STAR 100, the axial clearance between the MPC lid and the HI-STAR 100 closure plate is greater than 10 inches. In order to prevent the Trojan MPC from thrusting forward and impacting the closure plate during a top-end drop or a tip-over event (i.e., slapdown), a spacer device is positioned on top of the MPC lid. The Trojan MPC spacer, depicted in Figure 1.1.5, is fabricated from SA240-304 stainless steel in the shape of a circular I-beam. The web of the spacer measures 1-inch thick and has a mean

diameter of 60 inches. The total height of the MPC spacer is 9 inches.

During a top end drop, the MPC spacer must support the amplified weight of a fully loaded Trojan MPC-24E/EF. Based on a bounding MPC weight of 90,000 lb (Table 2.2.4) and a bounding deceleration of 60g (Table 2.1.10), the maximum compressive stress in the web is computed as follows.

$$\text{Cross-sectional area of web (A)} = \pi \times D \times t = \pi (60) (1) = 188.5 \text{ in}^2$$

$$\text{Amplified weight of MPC (P)} = G \times W = (60) (90,000) = 5.4 \times 10^6 \text{ lb}$$

$$\text{Compressive stress in web} = P/A = (5.4 \times 10^6) / 188.5 = 28,647 \text{ psi}$$

From Table 2.1.18, the primary membrane stress intensity limit for Alloy X (of which SA240-304 is a member) under Level D conditions is 44.9 ksi at 400°F. Therefore, the safety factor against compressive failure of the Trojan MPC spacer, per ASME Code Subsection NB stress limits, is

$$SF = 44,900 / 28,647 = 1.56$$

- Design Changes in HI-STAR 100 Overpack

The latest revision of HI-STAR 100 Overpack Assembly Drawing (listed in Section 1.4) provides few design changes that are evaluated in [2.6.6] for an end drop load of 60g's. Specifically, the welds connecting the bottom annular plate to the toe plate and the top annular plate to the outer gamma shell, and the combined shear capacity of the weld connecting the gamma shell to the top flange and the toe plate are evaluated. The results are summarized in the table below.

Governing Safety Factors for Overpack Design Changes Under 60g's End Drop			
Item	Calculated Force (lbf)	Allowable Capacity (lbf)	Safety Factor
Annular Plate Welds	$1.26 \times 10^6$	$1.98 \times 10^6$	1.57
Gamma Shell Weld and Toe Plate	$2.05 \times 10^6$	$5.71 \times 10^6$	2.79

#### 2.7.1.2 Side Drop (Load Cases F3 in Table 2.1.6, E3 in Table 2.1.7, and 3 and 11 in Table 2.1.9)

- MPC Fuel Basket and Canister Finite Element Analysis (Load Cases E3.b, E3.c in Table 2.1.7 and Load Cases F3.b, F3.c in Table 2.1.6)

The MPC configurations are assessed for a hypothetical accident condition of transport side drop. All fuel cells are loaded with design basis spent nuclear fuel (SNF). Evaluations are performed for the 0 degree and the 45 degree circumferential orientations of the fuel basket as defined in Figures 2.1.3 and 2.1.4 and are obtained using the finite element model described in Section 2.6.

The results for each MPC configuration for the two different drop orientations are evaluated for each appropriate load case listed in Tables 2.1.6 and 2.1.7. Analyses are performed only for the hot

ambient temperature condition since this is the bounding case for the MPC; as noted in Section 2.6, allowable stresses are lower for the “heat” environmental condition.

- Elastic/Plastic Stability of the MPC Fuel Basket

Following the provisions of Appendix F of the ASME Code [2.1.12] for stability analysis of Subsection NG structures, (F1331.5(a)(1)), a comprehensive buckling analysis is performed using ANSYS. For this analysis, ANSYS's large deformation capabilities are used. This feature allows ANSYS to account for large nodal rotations in the fuel basket, which are characteristic of column buckling. The large deflection option is “turned on” so that equilibrium equations for each load increment are computed based on the current deformed shape. The interaction between compressive and lateral loading, caused by the deformation, is included in a rigorous manner. Subsequent to the large deformation analysis, the basket panel that is most susceptible to buckling failure is identified by a review of the results. The lateral displacement of a node located at the mid-span of the panel is measured for the range of impact decelerations. The buckling or collapse load is defined as the impact deceleration for which a slight increase in its magnitude results in a disproportionate increase in the lateral displacement.

The stability requirement for the MPC fuel basket under lateral loading is satisfied if two-thirds of the collapse deceleration load is greater than the design basis horizontal acceleration (Table 2.1.10). Figures 2.7.1, through 2.7.6 are plots of lateral displacement versus impact deceleration for representative fuel baskets. It should be noted that the displacements in Figures 2.7.1, 2.7.2, 2.7.3, 2.7.4, and 2.7.5 are expressed in  $1 \times 10^{-1}$  inch and Figure 2.7.6 is expressed in  $1 \times 10^{-2}$  inch. The plots clearly show that the large deflection collapse load of the MPC fuel basket is greater than 1.5 times the inertia load corresponding to the design basis deceleration for all baskets in all orientations. Thus, the requirements of Appendix F are met for lateral deceleration loading under Subsection NG stress limits for faulted conditions. Therefore, it is concluded that stability of the spent fuel basket cell walls is assured under the hypothetical accident side drop (from 30') condition of transport.

An alternative solution for the stability of the fuel basket panel is obtained using the methodology espoused in NUREG/CR-6322 [2.7.3]. In particular, the fuel basket panels are considered as wide plates in accordance with Section 5 of NUREG/CR-6322. Eq.(19) in that section is utilized with the “K” factor set to the value appropriate to a clamped panel. Material properties are selected corresponding to a metal temperature of 500 degrees F which bounds computed metal temperatures at the periphery of the basket. The critical buckling stress is:

$$\sigma_{cr} = \left( \frac{\pi}{K} \right)^2 \frac{E}{12(1-\nu^2)} \left( \frac{h}{a} \right)^2$$

where h is the panel thickness, a is the unsupported panel length, E is the Young's Modulus of Alloy X at 500 degrees F (Table 2.3.1),  $\nu$  is Poisson's Ratio, and  $K=0.65$  (per Figure 6 of NUREG/CR-6322).

Parameters appropriate to a MPC-24E basket are used; the following table shows the results from the



finite element stress analysis and from the stability calculation.

Panel Buckling Results From NUREG/CR-6322			
Item	Finite Element Stress (ksi)	Critical Buckling Stress (ksi)	Factor of Safety
Stress	13.339	49.826	3.74

For a stainless steel member under an accident condition load, the recommended safety factor is 2.12. It is seen that the calculated safety factor exceeds this value; therefore, an independent confirmation of the stability predictions of the large deflection analysis is obtained based on classical plate stability analysis.

- Overpack Stress Analysis (Load Cases 3 and 11 in Table 2.1.9)

The overpack is assumed to be subject to a 60g side drop in the manner of the load combinations of Table 2.1.9 for both heat and cold environmental conditions as prescribed by Regulatory Guide 7.9. Reaction loads provided by the impact limiters are imposed as vertical pressures at each end of the overpack on areas of the structure that serve as backing. The applied mechanical loading is internal pressure, inertia load from the MPC and inertia load from the overpack self-weight. Figure 2.1.9 shows the assumed loading for this simulation. Figures 2.7.7, and Figures 2.7.11-2.7.13 are useful to aid in understanding the methodology used to apply the MPC loads and the balancing impact limiter reactions. Figure 2.7.7 shows a view of the overpack looking along the longitudinal axis for the general case of an oblique drop. While the intent of the figure is to describe the reaction loads from the impact limiter under a general oblique drop orientation, only the features necessary to elaborate on the side drop reaction load are discussed here. A region defined by the angle  $\theta$  supports the applied loading in a side drop.

This angle is 18 degrees for the side drop and is chosen based on two considerations. First, the predictions from the theoretical model at the time of maximum “g” loading are examined and a projected loaded area on the top forging and bottom plate estimated. Second, the post-drop evaluation of the tested impact limiters from the one-eighth scale static test and the one-quarter scale dynamic test were visually examined and provided insight into the extent of the loaded region of the overpack at the impact limiter-hard surface interface. From these two evaluations, a conservatively low angle estimate is made for the finite element analysis. Figure 2.7.12 shows the extent around the periphery of the loading imposed by the MPC. From Section 2.6, the angle over which the MPC load is applied to the inner shell of the overpack is 72 degrees from the vertical on each half of the overpack. This angle is determined from the detailed analysis of the MPC enclosure shell and the fuel basket under 60g loading. The inertia load from overpack self-weight is applied by imposing an amplified value for the gravitational constant. Details of the finite element model have been discussed in Section 2.6. The results of the finite element analyses for load cases 3 and 11 in Table 2.1.9, for the overpack, are post-processed as previously discussed; Tables 2.7.5 and 2.7.6 summarize the results for each overpack component and identify the minimum safety factors.

#### 2.7.1.3 Corner Drop

Figures 2.1.10 and 2.1.11 show the assumed loading for the bottom center of gravity over corner

(CGOC) drop and the top CGOC drop, respectively. The impact limiter reaction load is applied as a pressure loading acting on two surfaces. From the geometry of the cask, with impact limiters in place, the angle of impact is 67.5 degrees from the horizontal plane. Although the theoretical and tested deceleration levels are below 60g's, the design basis 60g-deceleration load is used as the input loading and applied vertically. Therefore, a 55g load is applied along the longitudinal axis of the cask, and a 23g load is applied perpendicular to the cask longitudinal axis.

The lateral inertia load from the MPC, amplified by the appropriate multiplier corresponding to 23g's, is applied in the manner shown in Figures 2.7.11 and 2.7.12. The longitudinal component of the load from the MPC, amplified by 55g, is applied as a pressure over the inside surface of the lid as shown in Figure 2.7.8. In reality, the load would be applied over a narrow annulus near the outside radius of the lid because of the raised "landing region". To maximize lid and bolt stress, however, the load is applied as a uniform pressure in the finite element model. The corresponding lateral and longitudinal loads from the overpack self-weight are applied by imposing amplified gravitational accelerations in the appropriate directions.

The loading from the impact limiter at the other end of the overpack, not involved in the impact, is applied as a uniform pressure over the surface of the backed area at the other impact limiter. Figure 2.7.10 shows the loading on the outside surface of the bottom plate that arises from the bottom end impact limiter during simulation of a top end drop. The total bottom impact limiter weight is amplified by 55g's and applied as a pressure load. At the top end, where the impact limiter provides the distributed crush force to balance the inertia forces, the balancing reaction loads from the impact limiter are applied as a distributed side pressure loading and a distributed end surface pressure. The extent of the loaded region for this drop orientation is defined by the angle  $\theta$  in Figure 2.7.7. For this case, the angle is approximately 68 degrees since a large "backed" area of the impact limiter is involved in resisting the crush. The angle is consistent with the predictions from the intersection geometry analysis used to develop the force-deformation data used in Appendix 2.A. That force-crush model has been successfully used to predict maximum decelerations and extent of crush. Static finite element models require setting a fixed origin to insure satisfaction of all equilibrium equations. The center of gravity-over-corner orientation, in theory, provides automatic satisfaction of moment equilibrium so that all forces and moments at such a fixed origin location should be zero.

In this analysis and in the general oblique drop analysis, the fixed point is assumed at a location at the end of the overpack not impacted. The results from the finite element simulation confirm that the computed reactions are negligibly small compared to the applied loads. The loads from internal pressure are self-balancing and do not alter the calculation of equilibrium reactions. Tables 2.7.5 and 2.7.6 summarize the results from these analyses.

Results for the MPC and its internals have been discussed in Subsections 2.7.1.1 and 2.7.1.2 for the end and side drops, respectively, under the action of 60g deceleration and appropriate pressure loading. Under an oblique drop at an angle  $\theta$  with respect to the target plane ( $\theta = 0$  degrees equals the side drop), the MPC and its internals experience deceleration loads parallel and perpendicular to the MPC longitudinal axis. Each of these deceleration components, however, is less than the 60g design basis deceleration used in the end and side drop analyses. For the pure end drop, all stresses in the fuel basket and in the MPC canister (enclosure vessel) are axial. For the pure side drop, the

conservative analysis of a 2-D section of the fuel basket and enclosure vessel gives rise to stresses in a plane perpendicular to the longitudinal axis of the MPC/fuel basket.

The results for any oblique drop can be obtained by a linear combination of the results for pure end drop and pure side drop. That is, the combined stress intensity is formed from the results of the two individual cases, after adjustment for the actual lateral and longitudinal “g” levels experienced by the components.

The MPC lid and baseplate are thick plate components; as such, the stress intensities experienced in the end drop orientation (which loads the lid and/or the baseplate in flexure) bound all other cases. Therefore, in what follows; only the enclosure vessel and the fuel basket need be considered. For each of these structures, the result “ $R_\theta$ ”, at a general oblique drop angle  $\theta$ , is expressed in terms of the result for an end drop “ $R_{90}$ ” and the result obtained for a pure side drop “ $R_0$ ” as:

$$R_\theta = R_{90} \left( \frac{g_E}{60} \right) + R_0 \left( \frac{g_S}{60} \right)$$

where  $g_E$  and  $g_S$  are the axial and lateral decelerations imposed on the MPC canister and fuel basket during the oblique drop at angle  $\theta$ .

Since  $g_E = 60 \sin \theta$ , and  $g_S = 60 \cos \theta$ ,

for a design basis oblique drop where the vertical deceleration is 60 g’s, the result for the oblique drop is always expressed in the form,

$$R_\theta = R_{90} \sin \theta + R_0 \cos \theta$$

The following results are obtained for the end drop and side drop analyses:

#### End Drop:

Fuel Basket – maximum longitudinal membrane stress = 4,074 psi

Enclosure Vessel – maximum longitudinal compressive stress = 11,260 psi

The enclosure vessel result is obtained from the Code Case N-284 evaluation for a bottom end drop and conservatively bounds the result for a top end drop. The longitudinal compressive stress in the enclosure vessel includes the effect of external pressure.

#### Side Drop:

Stress intensity results for the fuel basket and enclosure vessel are summarized in Table 2.7.4. From Table 2.7.4, for the pure side drop, the minimum safety factor for the fuel basket is 1.17 (primary membrane plus primary bending). The corresponding minimum safety factor for the enclosure vessel is 2.64 (again, for primary membrane plus primary bending). The preceding results are obtained by surveying the summary of minimum safety factors in Table 2.7.4 for all MPC’s and both fuel basket orientations within the MPC.

For the pure side drop orientation, the stress intensities (SI) associated with the minimum safety factors are:

Fuel Basket SI = 47,060 psi

Enclosure Vessel SI = 24,650 psi

The stress intensities at the most limiting location for the general oblique drop orientation are then computed as:

Fuel Basket SI =  $4,074 \sin \theta + 47,060 \cos \theta$

Enclosure Vessel SI =  $11,260 \sin \theta + 24,650 \cos \theta$

For the corner drop,  $\theta = 67.5^\circ$  leading to the following final results:

C.G. OVER CORNER DROP MPC SAFETY FACTORS			
Item	Calculated S.I.	Allowable S.I.	Safety Factor
Fuel Basket	21,773 psi	55,450 psi <sup>†</sup>	2.55
Enclosure Vessel	19,836 psi	65,200 psi <sup>††</sup>	3.29

<sup>†</sup> at 725°F

<sup>††</sup> at 450°F

As expected, the safety factors obtained for the corner drop are larger than the corresponding values obtained for the side drop.

Results for general oblique drop angles are now considered for the overpack. In particular, a 30-degree oblique drop is deemed to be most representative of a scenario where only a primary impact is involved. The general formula utilized in the preceding for the specific case of center-of-gravity-over-corner can also be used for a 30-degree drop angle. The following results are reported for the fuel basket and enclosure vessel.

30 DEGREE OBLIQUE DROP MPC SAFETY FACTORS			
Item	Calculated S.I. (psi)	Allowable S.I. (psi)	Safety Factor
Fuel Basket	42,792	55,450 <sup>†</sup>	1.30
Enclosure Vessel	26,978	65,200 <sup>††</sup>	2.42

<sup>†</sup> at 725°F

<sup>††</sup> at 450°F

#### 2.7.1.3.1 MPC “F Class” Enclosure Vessel Lid-to-Shell Weld

The Holtec MPCs labeled with the suffix “F” (designated as “F Class” in this subsection) are intended to store non-intact fuel (defined as damaged fuel in the latest revision of ISG-1 and “failed fuel and fuel debris” in this SAR).

To be certified to store loose fuel debris, the MPC must fulfill the function of the “secondary containment” required by 10CFR71.63(b). To qualify as a “secondary containment”, the MPC Enclosure Vessel must be able to withstand the accident condition loading without releasing its contents. The accident condition mechanical loading for the secondary containment is identical to those for the primary containment, namely the inertia forces produced by a 60g deceleration. From Table 2.1.7, the pressure loads applicable to the MPC Enclosure Vessel during a hypothetical vertical end drop (Load Case E3.a) are the normal condition pressures. Therefore, per Table 2.1.1, the maximum pressure differential that exists across the MPC shell when a drop occurs is 60 psig. For conservatism, however, the accident condition internal pressure, [defined in Table 2.1.1](#), is used to qualify the MPC Enclosure Vessel as a secondary containment. All candidate vulnerable locations in the MPC Enclosure Vessel must be analyzed to ensure that a thru-wall breach in the pressure-retaining boundary does not occur under the loading combination defined above. In the case of the primary containment (the HI-STAR 100 overpack), the location of containment vulnerability is the cask lid-to-body forging bolted joint; the evaluation of the lid-to-body closure bolt has been analyzed to demonstrate containment integrity and the results of the evaluation summarized in Subsection 2.7.1.1 of the SAR. For the MPC “F Class”, considered as secondary containment, the corresponding locations of vulnerability are the two extremities of the Enclosure Vessel where the vessel shell is joined to flat (plate-like) members.

The top lid-to-shell joint, a J-groove (partial penetration) joint made at the plant after fuel loading, is one candidate location, as this weld cannot be volumetrically examined even though the top lid is relatively thick. The MPC baseplate to the shell weld, on the other hand, is a shop-fabricated and volumetrically examined junction. However, because the baseplate is thinner than the top lid, it may experience greater flexural action under the accident condition mechanical loading, resulting in somewhat greater junction region stresses. Therefore, the weld joints at both extremities of the MPC Enclosure Vessel are denoted as candidate locations whose structural integrity under the load combination appropriate to the MPC’s secondary containment function must be demonstrated.

a. Top lid-to-shell joint

For MPCs with the “F” designation, this joint has been buttressed with a thick tapered shell and deeper J-groove weld than that utilized in the standard MPC Enclosure Vessel. A Holtec proprietary position paper, DS-213, “Acceptable Flaw Size in MPC Lid-to-Shell Welds”, submitted to the NRC in support of the original certification of HI-STAR 100 in 1999 demonstrates that the largest postulated flaw in the most adverse orientation in the lid-to-shell joint in the “F” canister will not propagate under the impulsive inertia loading arising from a 60g axial deceleration of the MPC’s contents.

An elastic stress analysis in the spirit of the ASME Code documented below likewise shows a large margin of safety against joint failure. For conservatism, the following assumptions are made.

- i. The closure ring (the structural member present to provide a second welded barrier against leakage of the contents) is assumed to be absent.
- ii. Even though a thru-wall failure of the joint is the appropriate failure criterion for the joint, non-exceedance of the ASME Code Section III Subsection NB stress intensity limits appropriate to

Level D limits, which will occur at a much lower loading level, is set down as the acceptance limit. However, no weld efficiency factor is applied to the lid-to-shell weld since it is not required by Subsection NB.

iii. The MPC model with the heaviest contents (MPC-32) is used in the analysis to bound the results for all “Type F” MPC models.

The MPC top lid may be fabricated as a single thick circular plate, or may be fabricated as a dual lid with the outer lid attached to the shell with the “J” groove weld, and the inner lid attached to the outer lid around the common periphery. The dual lid configuration has been analyzed for both Normal Conditions of Transport and Hypothetical Accident Conditions of Transport for MPC’s carrying intact fuel; the results are documented in Subsection 2.6.1.3.1.2, and 2.7.1.1, respectively. The evaluation for the “F Class” MPC to provide secondary containment capability utilizes the same analytical model but introduces additional assumptions into the analysis to direct load to the lid-to-shell weld. In particular, a top end drop is postulated with the dual lids subjected to a 60g deceleration loading from the fuel, fuel basket, and lid weight, together with the accident internal pressure of the MPC. During a top end drop, the MPC cannot rotate relative to the HI-STAR overpack because of close clearances between the vessel shell and the inner surface of the overpack cavity. Therefore, regardless of the angle of impact, the reaction load from the HI-STAR to equilibrate the applied loads on the lid is uniformly distributed around the circumference. A bounding condition for this analysis for secondary containment is presumed to be a top end drop where the Enclosure Vessel shell is assumed to contact the support (the HI-STAR lid) before the Enclosure Vessel lid; with this conservative assumption, the peripheral weld is subject to the entire applied load. The key results from the analyses (the case of dual lids bounds the analysis assuming a single thick lid) to support qualification of the MPC “F Class” as secondary containment are summarized in the table below.

KEY RESULTS FOR SECONDARY CONTAINMENT QUALIFICATION OF F CLASS MPC's – Load Case E3.a in Table 2.1.7 (Top End Drop)			
Item	Stress Intensity (ksi) or Load (lb)	Allowable Stress Intensity @ 550 Degrees F (ksi) or Load Capacity (lb)	Safety Factor
Structural Lid Bending Stress Intensity	46.83	60.7	1.30
Shield Plug Bending Stress Intensity	47.44	60.7	1.28
Lid-to-Shell Weld Load	5,358,000	6,627,000	1.24
Primary Local Axial Membrane Stress Intensity at Shell Contact Interface	24.94	40.45	1.62

b. Baseplate-to-Shell Joint

Because the baseplate-to-shell connection is a volumetrically examined, full penetration joint, flaw propagation under the accident condition inertia loads is not a concern for this location. As in the case of the top lid-to-shell junction, the baseplate-to-shell joint is established to be sufficiently robust if the stress intensity limits under the above load combination (appropriate for §71.63(b)) are below their corresponding limits for level D condition for Section III Class 1 (NB) components. Since the baseplate-to-shell joint in the MPC “F Class” units is identical to the joint in the MPC's used for intact fuel, no new analyses are required. The results of evaluation of this joint are reported in Subsection 2.7.1.1 and demonstrate substantial safety factors.

The above analyses demonstrate that the Enclosure Vessel for “Type F” MPCs is capable of serving as a “secondary containment” as required by §71.63(b).

2.7.1.4 Oblique Drops

Appendix 2.A contains results of analytical simulations for various orientations of the cask at impact. In Appendix 2.A, it is shown that lateral decelerations are large for the near side drop (slapdown) and decrease as the angle of orientation, with respect to the horizontal plane, increases. Therefore, it is likely that results presented in Subsections 2.7.1.1 through 2.7.1.3 are bounding for all orientations other than the near side drop (slapdown) in that at any other angle, the resulting g-loads in each direction (longitudinal and lateral) are smaller than the bounding deceleration loads applied in the end, side, and corner drops. Nevertheless, based on the results obtained in Appendix 2.A, the case of

an oblique drop with primary impact at 30 degrees from the horizontal is analyzed in detail. This case covers all orientations where the maximum deceleration load occurs and is reacted by the primary impact limiter. For this case, moment equilibrium includes inertia loads from overpack rotation as well as linear deceleration. For the 30-degree drop orientation at the primary impact location, the design basis deceleration load is applied with 52g lateral component and 30g longitudinal component. The loads are applied in the same manner as discussed in Subsection 2.7.1.3 with one additional complication. In contrast to the center of gravity over corner orientation where moment equilibrium is automatically satisfied when the loads are correctly applied, the applied loads and the reaction loads from the impact limiter are not initially in moment equilibrium. No inertial loading due to overpack rotational motion at the instant being considered is included. Without an additional inertial moment loading component, a large reaction force would develop at the far-removed arbitrary fixed reference point because the impact limiter reaction loads are offset from the overpack and MPC inertia loads from the linear decelerations. Figure 2.7.14 shows the overpack in a general oblique orientation. Appropriate arrows show the impact limiter reaction forces and the components of the applied linear decelerations. The loads from the MPC are not shown on the figure but they are applied as previously described for the corner drop. It is clear that moment equilibrium is not satisfied unless reaction loads develop at the arbitrarily chosen fixed support location far removed from the impact point. In the real drop scenario, since there is only a primary impact reaction, the cask must have angular accelerations imposed to insure moment equilibrium since the fixed point is an artifact to meet the requirements of the finite element analysis. To zero this reaction load at the point far-removed from the impact location, an additional load case with a unit angular velocity imposed at the mass center of the system and no other loads is developed. An angular acceleration is internally generated by ANSYS for this load case. The solution to this load case provides a reaction at the hypothetical fixed point assumed at the end of the overpack far removed from the impact location to balance the imposed inertial moment. The addition of this load case, with proper magnitude and sign ascribed to the input angular velocity, serves to eliminate all reactions at the far-removed fixed point. By adding this inertia moment load case, both force and moment equilibrium equations are satisfied for the oblique drop case where there is only a single impact limiter providing external forces to react the cask motion. With reference to Figure 2.7.7, the extent of the impact limiter loaded region on the overpack for this case is  $\theta = 63$  degrees. This angle is estimated from the projected geometry from the theoretical analysis in Appendix 2.A. Figure 2.7.9 shows a side view of the top forging with the end loading from the impact limiter applied as a pressure over the loaded region.

The finite element solution provides stress intensity results for the hot and cold conditions. The safety factors are summarized in Tables 2.7.5 and 2.7.6 (identified as Load Cases 20 and 21 corresponding to the “heat” and “cold” environmental conditions).

The near side drop with impact at the secondary impact limiter (slapdown) is a special case that also merits detailed analysis. For this case, the angle of the cask with the target is near zero degrees, similar to that used for the side drop analysis. The nature of the equilibrium equations is quite different, however. For the side drop, Figure 2.7.17 shows that equilibrium is satisfied by impact limiter reaction pressures at both impact locations. The reaction lateral pressure distribution at each impact limiter is distributed in the manner described by Figure 2.7.7. For the side drop evaluation, no introduction of a rotational component to the overpack is required to insure moment equilibrium. For



the analysis of the near side drop secondary impact case, all of the reaction force required to insure that force equilibrium is maintained under the inertia induced loads, is imposed at the location of the secondary impact limiter. Figure 2.7.18 shows a side view of the overpack with the reaction load applied over a specified arc in the same manner as described by Figure 2.7.7. At the time of peak secondary impact deceleration, the theoretical analysis predicted minimal axial deceleration. Therefore, to perform the stress analysis using the finite element model, no axial deceleration is imposed. Referring to Figure 2.7.7, the angle  $\theta$  for this evaluation is chosen on the basis of observed experimental results and theoretical prediction. The angle is related to the angle associated with the observed crush depth of the impact limiter itself. For a near side drop, the outer diameter of the impact limiter is known, and if the crush depth is observed, calculated, or measured, the angular extent of impact limiter crushed material is easily determined. The outer radius, “ $R_i$ ” of the impact limiter, and the observed and calculated crush depth (see results in Appendix 2.A for a full scale impact limiter), “ $d$ ”, are:

$$R_i = 64''; \quad d = 15''$$

Therefore, the angle “ $\phi$ ” (on either side of a vertical diameter through the impact limiter) that is associated with the extent of loaded crushed surface of the impact limiter is obtained from simple geometry as:

$$\cos(\phi) = 1 - d/R_i$$

The angle over which the load is applied at the crushed surface of the impact limiter is calculated to be:

$\phi = 40$  degrees (measured from the vertical, on both sides of the vertical centerline).

The angle of significant reaction loads on the interface surface of the top forging, is greater than this angle. However, it is conservative to perform the finite element analysis of the “slapdown” secondary impact event, using the load angle

$$\theta = \phi = 40 \text{ degrees.}$$

Note that this angle used for the “slapdown” evaluation is larger than the conservative value used to evaluate the side drop. This reflects the increased crush imparted to the impact limiter since the entire amplified load is reacted at the top end. The load from the MPC is imposed on the appropriate inside surface of the inner shell as a uniform load in the same manner as for the side drop analysis. Moment equilibrium is provided by imposing the additional pure rotation on the overpack sufficient to generate opposite reaction forces that zero out the combined reactions at the “balance point” from the applied inertia decelerations plus the pure rotation case. Because the MPC is constrained within the overpack, no departure from a uniform load transfer to the overpack is anticipated. Therefore, the enforcement of moment equilibrium for this condition is ensured solely by the determination of a proper balancing moment by determining an appropriate angular acceleration for the overpack. This assumption has little effect on the computation of the primary stress intensity distribution that results from the impact.

The results of the analysis are tabulated and combined with other load conditions, and the combined load case is designated as “Load Case 22”. Bolt preload, internal pressure, and the inertia loads are combined to form this “slapdown” simulation. The top-end secondary impact analysis reported herein bounds a similar analysis of the bottom end secondary impact case. Summary results for minimum safety factors are reported in Table 2.7.5 only for the “Heat” environmental condition as previous results have demonstrated that this case produces the minimum safety factors. Only primary stress intensities are surveyed and reported in accordance with ASME requirements. Also evaluated is the bolt stress, the net friction force, and the state of the seals and lands. From the post-processed results, it is concluded that no bolts are overstressed, no portion of the seals suffer unloading, and that there is sufficient frictional force to insure that the lid is maintained in position.

The preceding discussion focused on the transport overpack analyses. The minimum safety factors for the MPC fuel basket and enclosure vessel, for arbitrary drop orientation, are obtained from the general formulation in the preceding subsection 2.7.1.3. The angle that provides the maximum combined stress intensity (S.I.) can be determined by classical means, and the minimum safety factor established. The results are summarized in the table below.

GENERAL OBLIQUE DROP ORIENTATION MPC – SAFETY FACTORS				
Item	Drop Orientation Angle (Degrees)	Calculated S.I. (psi)	Allowable S.I. (psi)	Safety Factor
Fuel Basket	4.54	47,208	55,450	1.17
Enclosure Vessel	24.55	27,100	65,200	2.41

#### 2.7.1.5 Comparison with Allowable Stresses

Tables 2.7.4 through 2.7.8 summarize the limiting safety factor obtained for each hypothetical free drop accident condition of transport defined by the requirements of Regulatory Guide 7.9. In particular, Table 2.7.4 is a summary of safety factors from the analyses of the MPC fuel basket and enclosure vessel, and Tables 2.7.5 and 2.7.6 report safety factors from the overpack analyses. Finally, Tables 2.7.7 and 2.7.8 contain safety factor summary results from miscellaneous evaluations reported within the text. From these results, tables are constructed that summarize limiting safety factors for all of the hypothetical accident conditions of transport that are associated with drop events. Tables 2.7.1 through Tables 2.7.3 present the overall summary of the most limiting safety factor for each of the components of interest for all hypothetical accident conditions of transport. It is concluded from these tables that large factors of safety exist in the fuel basket, in the MPC shell, and in the various components of the overpack under all hypothetical accident conditions of transport associated with free drop events.

It is noted that the overpack finite element results are developed using a 3-D model of the overpack. Even though symmetry conditions reduce the size of the model, there are over 8000 elements and 11000 nodes.

The postulated accident conditions all tend to load localized regions of the overpack. As an illustration, consider Load Case 20, the 30-degree oblique top-end impact with the target. The limiting results for safety factors are reported in Table 2.7.5. Figures 2.7.15 and 2.7.16 show stress intensity distributions for the inner shell and for the assemblage of intermediate shells, respectively. As expected, the regions of highest stress intensity are naturally concentrated near the impacted region.

### 2.7.2 Puncture

- Overpack Structural Components

10CFR71 mandates that a puncture event be considered as a hypothetical accident condition. For this event, it is postulated that the package falls freely through a distance of 1 meter and impacts a 6 inch diameter mild steel bar. The effects of the puncture drop are most severe when the steel bar is perpendicular to the impact surface. Therefore, all puncture analyses assume that the bar is perpendicular to the impact surface. It is assumed that the steel bar has a flow stress equal to 48,000 psi, which is representative of mild steel. The maximum resisting force can then be calculated as

$$F_R = \frac{\pi D^2}{4} \times 48,000 \text{ psi} = 1.357 \times 10^6 \text{ lb}$$

where D equals the diameter of the steel bar.

$$|A_p| = \frac{F_R g}{W}$$

Since the maximum force applied to the cask is limited to the above value, the average deceleration of the cask can be computed assuming it to be rigid. The average deceleration of the cask (plus contents) (weight = W) is determined as:

For a bounding (low) weight of 230,000 lb. (Table 2.2.1), for example, the rigid body average deceleration over the time duration of impact, is 5.9g.

Candidate locations for impact that have the potential to cause the most severe damage are near the center of the closure plate (top-end puncture), the center of the bottom plate (bottom puncture), and the center height of the overpack shells (side puncture). In accordance with Regulatory Guide 7.9, local damage near the point of impact and the overall effect on the package must be assessed.

An estimate of local puncture resistance is obtained by using Nelms' equation [2.7.1] that is generally applicable only for lead backed shells. Nevertheless, it is useful to obtain an indication as to whether a potential problem exists in the HI-STAR 100 System. The equation is applied using an ultimate strength of 70,000 psi that is appropriate for the selected impact regions. Nelms' equation predicts a minimum thickness of material necessary to preclude significant puncture damage. For the HI-STAR 100 System,

$$t_m = \left( W / S_u \right)^{0.71} = 2.65 \quad inch$$

Inasmuch as the HI-STAR 100 overpack has substantially more material thickness in the baseplate, the closure plate, the top flange and the inner plus the initial intermediate shell, the overpack meets local puncture requirements as required by Nelms' equation.

The global effects of puncture are calculated using the overpack model described in Section 2.6, which is the same model that is used for the drop assessments. Figures 2.1.12 through 2.1.14 show free body diagrams of the overpack for the side, top, and bottom puncture events, respectively. In each case, the nodes on the surface of the overpack that directly impact the steel bar are fixed in all degrees of freedom. By then applying acceleration,  $A_p$ , a reaction force develops at those nodes equal in magnitude with  $F_R$ . Tables 2.7.5 and 2.7.6 summarize the safety factors for the overpack components obtained for the puncture acceleration computed above for both heat and cold environmental conditions. Note that for the stress intensities in the lid and baseplate, the highest stresses are exactly under the impact point. The results include the effect of the interface contact stress between the puncture pin and the plate surface. This local effect is not required to be included in the stress intensity comparison with allowable values for the hypothetical accident. Therefore, in the reporting of safety factors, the effect of local surface pressure is not included; rather, the radial and tangential stresses at the load point are used to form the stress intensity and set the lateral surface stress to zero. Tables 2.7.5 and 2.7.6 specifically identify this item by a note. Figure 2.7.17 shows the stress intensity distribution in the lid resulting from a top-end puncture analysis. The localized nature of the stress intensity distribution is clearly evident. The reported safety factors in the summary tables are adjusted to eliminate the effect of non-primary stress components.

- Closure Bolts

The methodology to analyze closure bolts is provided in reference [2.6.3] prepared for analysis of shipping casks. The analysis of the overpack closure bolts under normal conditions of transport, in accordance with the provisions of [2.6.3], has been reported in Section 2.6. In this subsection, the similar analysis for the hypothetical puncture accident is summarized. The analysis follows the procedures defined in Reference [2.6.3] and uses the allowable stresses for the closure bolts in that reference.

The following combined load case is analyzed for the hypothetical pin puncture accident condition of transport.

Puncture: Pressure, temperature, and pre-load loads are included.

Reference [2.6.3] reports safety factors defined as the calculated stress combination divided by the allowable stress for the load combination. This definition of safety factor is the inverse of the definition consistently used in this SAR. In summarizing the closure bolt analysis, results are reported using the SAR safety factor definition of allowable stress divided by calculated stress. The following result for closure lid bolting for the top end drop hypothetical accident condition of transport is obtained.

Overpack Closure Bolt - Safety Factor (Load Case 7 in Table 2.1.9)	
Item	Safety Factor
Average Tensile Stress	1.84
<b>Combined Tension, Shear, Bending and Torsion</b>	<b>1.55</b>

### 2.7.3 Thermal

In this subsection, the structural consequences of the thirty-minute fire event are evaluated using the metal temperature data from Section 3.5 where a detailed analysis of the fire and post-fire condition is presented. Specifically, it desired to establish that:

1. The metal temperature, averaged across any section of the containment boundary, remains below the maximum permissible temperature for the Level A condition in the ASME Code for NB components. Strictly speaking, the fire event is a Level D condition for which Subsection NB of the ASME Code, Section III does not prescribe a specific metal temperature limit. The Level A limit is imposed herein for convenience because it obviates the need for creep considerations to ascertain post-fire containment integrity.
2. The external skin of the overpack, directly exposed to the fire will not slump (i.e., suffer rapid primary creep). This condition is readily ruled out for steel components if the metal temperature remains below 50% of the metal melting point.
3. Internal interferences among the constituents of the HI-STAR 100 System do not develop due to their differential thermal expansion during and after the fire transient.
4. **The load in the overpack closure bolts remains above the minimum seal seating load at all times during a transport fire.**
5. The helium retention boundary and the containment boundary both continue to perform their function as ASME "NB" pressure vessels.

#### 2.7.3.1 Summary of Pressures and Temperatures

The following peak temperatures (per Tables 3.5.4 and 3.4.11) and pressures are used in Subsections 2.7.3.2, 2.7.3.3, and 2.7.3.4.

Overpack closure plate/bolts	514 degrees F (post-fire)
Overpack bottom plate	662 degrees F (post-fire)
Overpack outer closure	226 degrees F (initial pre-fire cold temperature); 1348 degrees F (maximum)
Overpack containment shell	395 degrees F (MPC –Shell post-fire temp. - increment of 24 degrees F (from data in Table 3.4.11))
MPC-Shell	419 degrees F (post-fire)

Basket (center)	751 degrees F (post-fire)
Basket (periphery)	478 degrees F (MPC-Shell post fire + 59 degrees F - (from data in Table 3.4.11))

It should be noted that the overpack containment shell, closure plate, and bottom plate temperatures are not specifically reported in Table 3.5.4. The temperatures listed above are based on the closest temperature report location. The overpack containment shell temperature is the lowest temperature that occurs prior to the fire accident and is used for the differential thermal expansion analysis. The overpack containment shell temperature falls (post-fire) below the outside basket temperature and subsequently lags the basket temperature by 24 degrees F. The 24 degree F lag is the same lag that occurs in the normal heat condition listed in Table 3.4.11 (i.e., 306 degrees F for the MPC outer shell surface - 282 degrees F for the overpack inner surface). This will maximize the potential for interference between the overpack and the MPC. Similarly, the temperature difference between the MPC shell and the fuel basket periphery will be essentially the same exists in the normal heat conditions of transport. Therefore, from Table 3.4.11, the basket peripheral temperature for the fire event analyses is set as the MPC shell temperature plus the maximum difference (365-306) degrees F from the table.

Subsection 3.5.3 contains a discussion of the peak bulk temperatures occurring during and after the fire transient. It is concluded in that section that:

1. The containment boundary protected by the intermediate shells remains below 500 degrees F (SA-203-E material).
2. The containment boundary that is within the confines of the impact limiters remains below 700 degrees F (SA-350 LF3 material).
3. The portion of the containment boundary directly exposed to the fire may have local outer surface temperatures in excess of 700 degrees F, but the bulk metal temperature of the material volume remains under 700 degrees F (SA-350 LF3 material).

The conclusions in Subsection 3.5.3 enable the statement that the containment boundary metal bulk temperatures remain at or below the upper limits permitted by the ASME Code. Therefore, stress evaluations that make comparisons to allowable stresses to demonstrate that the containment boundary continues to perform as a viable pressure vessel use allowable stresses that are given in the ASME Code (i.e., there is no extrapolation of allowable stresses beyond the recognized code limits). For the helium retention boundary stress calculations, however, allowable stresses for a conservatively high temperature (see Table 2.1.2 and 2.1.21) are used when pressure vessel code compliance is demonstrated.

From Table 3.5.4 in Subsection 3.5.4 of Chapter 3, it is concluded that:

The maximum temperature of the ferritic steel material in the body of the HI-STAR 100 overpack (the outer enclosure and the intermediate shells outside of the containment boundary is well below 50% of the material melting point. (The melting point of carbon and low alloy steels is approximately 2750 degrees F, per Mark's Standard Handbook, Ninth Edition, pp 6-11.)

The shielding experiences temperatures above its stated limit for effectiveness. This means that a limited loss of shielding effectiveness may occur. The shielding analysis in Chapter 5 (Subsection 5.1.2) recognizes this and conservatively assumes that all shielding is lost in post-fire shielding analyses.

Pressures during the fire transient are bounded by the internal and the external design pressures for accident conditions for the MPC shell as stated in Section 2.1. For internal pressure, Table 3.5.3 supports this conclusion. The following calculation is presented to support the conclusion for MPC external pressure.

The overpack annulus initial fill pressure is 14 psig (max.) per the specification in Chapter 7. The overpack annulus lower bound fill temperature is 70 degrees F. The fire condition MPC shell peak temperature is 419 degrees F per Table 3.5.4 and the use of this as the average gas temperature in the annulus is conservative.

Using the above data, the fire condition peak pressure in the annulus between the overpack and the MPC shell is calculated by using the ideal gas law with constant volume assumed in the gap as:

$$p_{\text{fire}} = (14 + 14.7) \times (419 + 460) / (70 + 460) = 47.6 \text{ psia} = 32.9 \text{ psig.}$$

### 2.7.3.2 Differential Thermal Expansion

The methodology for establishing that there will be no restraint of free thermal expansion has been presented in Subsection 2.6.1.2 for normal conditions of transport. The same methodology is applied in this subsection to evaluate the potential for component interference during and after the postulated hypothetical fire. For conservatism, use the temperatures in the overpack and the MPC temperatures that will maximize the potential for interference between the overpack and the MPC regardless of at what point in time the temperatures occurred. It is shown that there is no structural restraint of free-end expansion in the axial or radial directions under the most limiting temperature difference between the hot basket and the colder overpack/enclosure vessel. Thus, the ability to remove fuel by normal means is not inhibited by structural constraint of free-end expansion. The table below summarizes the results obtained for the limiting MPC temperature distributions assumed.

THERMOELASTIC DISPLACEMENTS IN THE MPC AND OVERPACK UNDER FIRE CONDITION				
CANISTER - FUEL BASKET				
	Radial Direction(in.)		Axial Direction (in.)	
Worst Case Unit	Initial Clearance	Final Gap	Initial Clearance	Final Gap
Bounding MPC	0.1875	0.117	2.0	1.672
CANISTER – OVERPACK				
	Radial Direction (in.)		Axial Direction (in.)	
Worst Case Unit	Initial Clearance	Final Gap	Initial Clearance	Final Gap
Bounding MPC	0.09375	0.004	0.625	0.291

Using the most conservative assumptions (i.e., do not consider a real “snapshot” in time during and after the fire, but rather assume the most detrimental temperature distribution occurs at the same instant in time) that maximize the potential for interference, it is demonstrated that no restraint of free thermal expansion in either the radial or axial directions occurs.

### 2.7.3.3 Stress Calculations

Under the fire accident, pressures in the MPC and overpack increase simultaneously, while the allowable strengths of the material may decrease from their values under normal conditions of transport. The MPC and overpack stresses are shown below (allowables are taken from Tables 2.1.21). It is required that both the helium retention boundary and the containment boundary meet Level D Service Limits of the ASME Code and continue to function as pressure vessels.

#### 2.7.3.3.1 MPC

- Top Closure

The MPC Top Closure analysis for the fire condition is Load Case E5 in Table 2.1.7. The top closure is conservatively modeled as a simply supported plate considered to be loaded by the accident internal pressure plus self-weight acting in the same direction. For determination of the safety factor, the value of allowable stress from Table 2.1.20 appropriate to the fire temperature is used. The table below summarizes the result (where a multiplier of 2.0 has been incorporated to reflect the bounding dual lid design):

MPC Top Closure Safety Factor for Load Case E5 in Table 2.1.7			
Item	Value (ksi)	Allowable (ksi)	Safety Factor
Bending Stress	3.547 x 2	54.23	7.64

- Baseplate

Under the fire accident condition, the baseplate is subject to accident internal pressure (per Table 2.1.1). If the HI-STAR 100 is assumed to be in the vertical position, then the baseplate also may support the weight of the fuel basket and the fuel loading. If the HI-STAR 100 is assumed to be oriented in the horizontal position, then the baseplate supports only internal pressure. For a conservative analysis, it is assumed that the internal pressure stress and the stress from basket weight and from fuel weight add. This Load Case E5 is summarized below. The second row is the result that is obtained if the basket and fuel weight is neglected.



MPC Baseplate Safety Factor under Hypothetical Fire Accident			
Item	Value (ksi)	Allowable (ksi)	Safety Factor
Baseplate Bending Stress (Including Basket and Fuel Weight)	51.60	54.23	1.05
Baseplate Bending Stress (Neglecting Basket, Fuel, and Self Weight)	47.57	54.23	1.14

• Shell

The MPC shell is examined for elastic/plastic stability under the fire accident external pressure using the ASME Code Case N-284 analysis method. The result from the stability analysis for Load Case E5 in Table 2.1.7 is summarized below:

MPC Canister Safety Factor - Stability under External Accident Pressure			
Item	Calculated Interaction Factor	Allowable Interaction Factor	Safety Factor
Elastic Stability	0.845	1.00	1.18

The shell is also analyzed for stress under the accident internal pressure by using the Lamé' solution previously used in Section 2.6. The stress due to the internal accident pressure is ( $P$  = pressure,  $r$  = MPC radius,  $t$  = shell thickness):

$$\sigma_1 = \frac{Pr}{t} = \frac{(225 \text{ psi})(68.5 \text{ in}/2)}{0.5 \text{ in}} = 15,413 \text{ psi}$$

$$\sigma_2 = \frac{Pr}{2t} = 7,706 \text{ psi}$$

$$\sigma_3 = -P = -225 \text{ psi}$$

The maximum stress intensity is  $\sigma_1 - \sigma_3 = 15,638 \text{ psi}$

The safety factor is,

$$SF = \frac{36.15 \text{ ksi}}{15.638 \text{ ksi}} = 2.31$$

#### 2.7.3.3.2 Overpack

The overpack stresses for normal heat conditions of transport are reported in Section 2.6. Since these stress solutions are based on linear elasticity, the stresses reported can be scaled up to account for the accident internal pressure and the safety factor computed based on the allowable stress for the fire temperature.

Generally, in the fire accident case, only primary stresses are of interest to demonstrate continued containment. Secondary stresses may be included in the evaluation, but they merely demonstrate additional levels of conservatism. Table 2.6.4 gives the minimum safety factor for the primary stress case of  $T_h + P_i + F + W_s$ .

The highest stress occurs in the inner shell, and has the value 2,832 psi.

The ratio of the accident pressure to normal pressure is (see Table 2.1.1)  $\frac{225}{100} = 2.25$ .

Using this factor, the safety factor is computed as follows:

For the inner shell at 500 degree F fire temperature, the allowable membrane stress intensity (per Table 2.1.14) under the fire condition is compared to the amplified mean stress and the safety factor computed as

$$SF = \frac{42.5 \text{ ksi}}{(2.832 \times 2.25 + 0.225) \text{ ksi}} = 6.44$$

#### 2.7.3.3.3 Closure Bolts

Under the fire transient, it is required to demonstrate that the stresses in the closure bolts do not exceed allowable limits and the bolted joint does not unload to the extent that the pressure boundary is breached. To that end, an analysis of the fire condition is carried out with the purpose of determining the bolt stresses under the applied loading. The methodology employed for this analysis is that presented in the report, "Stress Analysis for Closure Bolts for Shipping Casks" [2.6.3]. The loadings applied are fire temperature, bolt preload, and accident internal pressure. The following result for closure lid bolting for the hypothetical fire accident is obtained.

Overpack Closure Bolt - Safety Factor (Load Case 19 in Table 2.1.9)	
Combined Load Case	Safety Factor
Average Tensile Stress	1.98
Combined Tension, Shear, Bending and Torsion	1.18

The fire accident thermal gradient in the closure lid and closure bolts counteracts the additional tensile load due to the accident internal pressure. The average bolt tensile stress in the fire accident therefore decreases below the average tensile stress during the normal condition of transport. However, the bolt load is still over five times the seal sealing load. Therefore, it is concluded that there will be only minor unloading of the bolted joint and no breach of containment.

#### 2.7.3.3.4 Bounding Thermal Stresses During the Fire Transient

Regulatory Guide 7.6, Section C.7 states that the extreme total stress intensity range between the initial state and accident conditions should be less than twice the adjusted value of the alternating stress intensity at 10 cycles given by the appropriate fatigue curves. It is demonstrated here that under very conservative assumptions on the calculation of thermal stresses, this regulatory requirement is met by the HI-STAR 100 System.

Under the fire transient, thermal gradients can lead to secondary or peak stresses due to local constraint by adjacent material that is at a lower temperature. The ASME Code does not require that secondary stresses be held to any limit for Level D Service Conditions. Nevertheless, bounding calculations are performed here to estimate the magnitude of the thermal stress. The most limiting secondary stress intensity state arises by conservatively assuming complete restraint of material by surrounding cooler material and has the solution:

$$|\sigma| = E \alpha \Delta T$$

where

E = Young's Modulus at temperature  
 $\alpha$  = coefficient of linear thermal expansion  
 $\Delta T$  = temperature change from 70 degrees F, the assumed assembly temperature

For the fuel basket,  $\Delta T = 775 - 70 = 705$  degrees F. The use of 775 degrees F is justified as follows: The peak temperature of the fuel basket is 950 degrees F during the fire per Table 2.1.2. For a conservative estimate of the temperature between *two adjacent points* on the fuel basket, use the bounding hypothetical accident temperature limit for the enclosure vessel lid or baseplate from Table 2.1.2 as representative of the change between *two adjacent points* on the fuel basket. Therefore, no extrapolation of data is required for the calculations to follow.

From the material property table for Alloy X,

$$E = 24.282 \times 10^6 \text{ psi}$$

$$\alpha = 9.853 \times 10^{-6} \text{ inch/inch-degree F}$$

Therefore,

$$\sigma = 24.282 \times 9.853 \times 705 = 168,672 \text{ psi}$$

The conservative assumption is made that the maximum peak stress intensity due to mechanical loading plus thermal constraint occur at the same point at the same instant in time and reaches the value of  $S_u$  at room temperature. Thus, the total stress intensity range from assembly to this hypothetical conservative state is

$$S_R = 168,672 + 75,000 = 243,672 \text{ psi}$$

The alternating stress intensity range, after accounting for temperature effects of Young's Modulus, is

$$S_a = \frac{S_R}{2} \times \frac{\text{Young's Modulus (70° F)}}{\text{Young's Modulus (775° F)}}$$

$$= 121,836 \text{ psi} \times \frac{28.14}{24.282} = 141,194 \text{ psi}$$

For the overpack, the most severely constrained material is at the bottom plate. Material properties for this calculation are the values available at 700 degrees F and the peak temperature is conservatively set at 700 degrees F.

$$\text{Young's Modulus} = E = 24.9 \times 10^6 \text{ psi (at 700 degrees F)}$$

$$\text{Coefficient of linear thermal expansion} = \alpha = 7.52 \times 10^{-6} \text{ inch/inch-degrees F (Estimated)}$$

Therefore, the secondary stress intensity due to fully constrained thermal growth is

$$\sigma = 24.9 \times 7.52 \times (700-70) = 117,966 \text{ psi}$$

Conservatively, assuming that the membrane plus primary bending stress intensity achieves the ultimate strength at room temperature, at the same location in space and at the same instant in time, gives the total stress intensity range at this hypothetical location as

$$S_R = 117,966 + 75,000 = 192,966 \text{ psi}$$

The alternating stress intensity range, after accounting for temperature effects of Young's Modulus, is

$$S_a = \frac{192,966}{2} \times \frac{28.14}{24.9} = 109,037 \text{ psi}$$

These computed values for bounding alternating stress intensities are used in the next subsection for comparisons with allowable values.

#### 2.7.3.4 Comparison of Fire Accident Results with Allowable Stresses

##### Stress

The safety factors for the MPC and overpack during a fire are addressed in Section 2.7.3.3. The lowest safety factors are 1.18 and 7.74 for the MPC and overpack, respectively.

##### Bounding Fire Transient

In accordance with Regulatory Position C.7 of the Regulatory Guide 7.6, Figure I-9.2.1 of ASME, Section III, Appendix I, gives the 10-cycle alternating stress intensity range as

$$S_{ALT} (\text{Alloy X}) = 700,000 \text{ psi}$$

Using the calculated stress intensity range from Subsection 2.7.3.3, the safety factor for the MPC basket is

$$SF = \frac{700,000}{141,194} = 4.96$$

Figure I-9.1 of ASME Section III, Appendix I is used for the overpack even though the temperature is limited to below 700 degrees F. It is conservative to use this curve for this short time event since increased temperatures will improve the material ductility. From that table, the 10-cycle alternating stress intensity range is given as 400,000 psi. Therefore using the aforementioned calculated results for stress intensity range from Subsection 2.7.3.3, the safety factor is computed as:

$$SF = \frac{400,000}{109,037} = 3.67$$

An analysis of the threaded holes in the top closure has been performed to assess the length of engagement and stress requirements imposed on the connection by the transport loads. The methodology used to evaluate the connection is that set forth in Machinery's Handbook and uses the specific characteristics of the threaded joint. As part of the calculation, it is demonstrated that the bolt force required to maintain the seal (seal seating load plus pressure force) is only 27% of the total bolt preload force that must be applied to ensure bolt performance under the various drop scenarios. That is, there is 73% excess capacity. Therefore, the momentary joint decompression due to the hypothetical fire accident is not sufficient to unload the seal.

The above calculations demonstrate that the requirements of Paragraph C.7 of Regulatory Guide 7.6 are satisfied.

#### 2.7.4 Immersion - Fissile Material

In order for the spent nuclear fuel in the HI-STAR 100 System to become flooded with water, a leak

must develop in both the overpack containment structure and the MPC enclosure vessel. The analysis provided demonstrates that both the overpack containment boundary and the MPC enclosure vessel meet the applicable stress and stress intensity allowables for normal conditions of transport and hypothetical accident conditions. Therefore, no leak will develop.

10CFR71.73(c)(5) specifies that fissile material packages, in those cases where water inleakage has not been assumed for criticality analysis, must be evaluated for immersion under a head of water of at least 0.9 m (3 ft.) in the attitude for which maximum leakage is expected. The criticality analyses presented in Chapter 6 conservatively assumes flooding with water at optimum moderation. Therefore, this paragraph is not applicable. However, analysis is presented to demonstrate that there is no water inleakage and verify that the flooded assumption made in the criticality analysis is conservative.

A head of water at a depth of 0.9 m (3 ft.) is equal to 1.3 psi. This pressure is bounded by the MPC enclosure vessel normal condition of transport and hypothetical accident condition external pressures listed in Table 2.1.1. The head of water (1.3 psi) is also bounded by the hypothetical accident condition external pressure for the overpack. Analysis provided in this chapter demonstrates that both the overpack containment boundary and the MPC enclosure vessel meet the applicable stress and stress intensity allowables for normal conditions of transport and hypothetical accident conditions. Therefore, there is no in-leakage of water into the overpack or MPC under a head of water at a depth of 0.9 m (3 ft.).

#### 2.7.5 Immersion - All Packages

Deep submergence of the HI-STAR 100 System in 200 meters (656 ft.) of water creates an external pressure load equal to 284 psi, which is less than the external design pressure of 300 psi. This condition is established as Load Case 18 in Table 2.1.9. Since the containment boundary is not punctured, stability of the package can be evaluated considering an undamaged package. The results for an external pressure of 300 psi bound the results for 21.7 psi gauge pressure that is established in 10CFR71.73(c)(6) as the applicable external pressure for this evaluation. The elastic/plastic stability of the overpack has been examined using the methodology of ASME Code Case N-284. In the analysis, all structural resistance to the external pressure is conservatively concentrated in the inner containment shell. No credit is given to any structural support by the intermediate shells. The external pressure is assumed to act directly on the outer surface of the inner containment shell and the secondary fabrication stress is assumed to add to the stress due to the deep submergence pressure. The results for this case are summarized below:

Overpack Stability using ASME Code Case N-284 - Load Case 18 in Table 2.1.9			
Item	Value from Interaction Curve	Allowable Interaction Curve Value	Safety Factor
Yield Stress Limit	0.577*	1.34	2.32*
Elastic Stability	0.253	1.0	3.95

\* Applicable to inner shell fabricated from SA203-E material. Safety factor must be multiplied by 0.93 if inner shell is fabricated from optional SA350-LF3 material.

It is noted that Code Case N-284 imposes limits on both stress and stability and includes a built-in safety factor of 1.34 for the Level D Service Limit. Therefore, the first row in the table above reports the true safety factor existing against exceeding the yield stress in the inner containment shell; the second row in the table provides the safety factor against elastic instability of the inner shell. The large values for the safety factors that are obtained, even with the conservative assumptions, attests to the ruggedness of the inner containment shell.

The analysis performed above for a 300 psi external pressure also confirms that the package meets the requirements of 10CFR71.61 that a 290 psi external pressure can be supported without any instability.

#### 2.7.6 Summary of Damage

The results presented in Subsections 2.7.1 through 2.7.5 show that the HI-STAR 100 System meets the requirements of 10CFR71.61 and 10CFR71.73. All safety factors are greater than 1.0 for the hypothetical accident conditions of transport. Therefore, the HI-STAR 100 package, under the hypothetical accident conditions of transport, has adequate structural integrity to satisfy the subcriticality, containment, shielding, and temperature requirements of 10CFR71.

Table 2.7.1

MINIMUM SAFETY FACTORS FOR THE MPC FUEL BASKET UNDER HYPOTHETICAL ACCIDENT CONDITIONS OF  
TRANSPORT

Load Case Number	Load Combination <sup>†</sup>	Safety Factor	Location in SAR where Calculations or Results are Presented
F3			
F3.a	D + H', end drop	4.19	Subsection 2.7.1.1; Table 2.7.7
F3.b	D + H', 0° side drop	1.16	Table 2.7.4
F3.c	D + H', 45° side drop	1.28	Table 2.7.4

<sup>†</sup> The symbols used for loads are defined in Subsection 2.1.2.1.



Table 2.7.2

MINIMUM SAFETY FACTORS FOR THE MPC ENCLOSURE VESSEL  
FOR HYPOTHETICAL CONDITIONS OF TRANSPORT

Load Case Number	Load Combination <sup>†</sup>	Safety Factor	Location in SAR where Calculations or Results are Presented
E3			
E3.a	D + H' + P <sub>o</sub> , end drop	1.4 3.04 1.92	Lid Table 2.7.7 Baseplate Table 2.7.7 Shell <sup>††</sup> Table 2.7.7
E3.b	D + H' + P <sub>i</sub> , 0 deg. side drop	2.14 1.16	Shell Table 2.7.4 Supports Table 2.7.4
E3.c	D + H' + P <sub>i</sub> , 45 deg. side drop	2.74 1.51	Shell Table 2.7.4 Supports Table 2.7.4
E5	P <sub>i</sub> <sup>*</sup> or P <sub>o</sub> <sup>*</sup>	7.64 1.05 1.18 (buckling) 2.32 (mean stress)	Lid Table 2.7.7 Baseplate Table 2.7.7 Shell Table 2.7.7 Subsection 2.7.3.3.1

<sup>†</sup> The symbols used for loads are defined in Subsection 2.1.2.1.

<sup>††</sup> The minimum local thickness of MPC shell (Drawing listed in Section 1.4) due to grinding of excess weld material is evaluated in [2.6.5] and considered to be acceptable.

Table 2.7.3

**MINIMUM SAFETY FACTORS FOR THE OVERPACK  
FOR HYPOTHETICAL ACCIDENT CONDITIONS OF TRANSPORT**

<b>Load Case Number</b>	<b>Load Combination<sup>†</sup></b>	<b>Safety Factor</b>	<b>Location in SAR where Calculations or Results are Presented</b>
1	$T_h + D_{ba} + P_i + F + W_s$	2.16	Table 2.7.8
2	$T_h + D_{ta} + P_i + F + W_s$	1.02	Table 2.7.8
3	$T_h + D_{sa} + P_i + F + W_s$	2.19 (see note 2)	Table 2.7.5
4	$T_h + D_{ea} + P_i + F + W_s$	1.49	Table 2.7.5
5	$T_h + D_{ga} + P_i + F + W_s$	2.60 (see note 2)	Table 2.7.5
6	$T_h + P_s + P_i + F + W_s$	2.80 (see note 2)	Table 2.7.5
7	$T_h + P_t + P_i + F + W_s$	1.55 (see note 1)	Table 2.7.8
8	$T_h + P_b + P_i + F + W_s$	1.46	Table 2.7.5
9	$T_c + D_{ba} + P_o + F + W_s$	4.17	Table 2.7.6
10	$T_c + D_{ta} + P_o + F + W_s$	1.87	Table 2.7.6
11	$T_c + D_{sa} + P_o + F + W_s$	2.19	Table 2.7.6
12	$T_c + D_{ea} + P_o + F + W_s$	1.73	Table 2.7.6
13	$T_c + D_{ga} + P_o + F + W_s$	2.65	Table 2.7.6
14	$T_c + P_s + P_o + F + W_s$	3.05	Table 2.7.6
15	$T_c + P_t + P_o + F + W_s$	2.09 (see note 1)	Table 2.7.6
16	$T_c + P_b + P_o + F + W_s$	1.46	Table 2.7.6
17	$T_f + P_i + F + W_s$	pre-load maintained	Subsection 2.7.3.4
18	$P_o^*$	2.32	Table 2.7.8
19	$P_i^* + T_f + F + W_s$	1.18	Table 2.7.8
20	$T_h + D_{ga} + P_i + F + W_s$	1.77	Table 2.7.5
21	$T_c + D_{ga} + P_i + F + W_s$	1.84	Table 2.7.6
22	$T_c + D_{ga} + P_i + F + W_s$	2.14 (see note 2)	Table 2.7.5

- Note:
1. This reported stress is directly under the point of impact. Therefore, the calculated value does not represent a primary stress; however, primary stress levels are met by this peak stress intensity.
  2. Applicable to inner shell fabricated from SA203-E material. Safety factor must be multiplied by 0.93 if inner shell is fabricated from optional SA350-LF3 material.

<sup>†</sup> The symbols used here are defined in Subsection 2.1.2.1.

Table 2.7.4 - FINITE ELEMENT ANALYSIS RESULTS  
MINIMUM SAFETY FACTORS FOR MPC COMPONENTS UNDER ACCIDENT CONDITIONS

Component - Stress Result	MPC-24		MPC-32		MPC-68	
	30 Ft. Side Drop, 0° Orientation Load Case F3.b or E3.b	30 Ft. Side Drop, 45° Orientation Load Case F3.c or E3.c	30 Ft. Side Drop, 0° Orientation Load Case F3.b or E3.b	30 Ft. Side Drop, 45° Orientation Load Case F3.c or E3.c	30 Ft. Side Drop, 0° Orientation Load Case F3.b or E3.b	30 Ft. Side Drop, 45° Orientation Load Case F3.c or E3.c
Fuel Basket – Primary Membrane ( $P_m$ )	2.80	3.85	2.78	3.90	3.07	4.30
Fuel Basket - Local Membrane Plus Primary Bending ( $P_L + P_b$ )	1.19	1.29	1.19	1.28	2.64	1.56
Enclosure Vessel - Primary Membrane ( $P_m$ )	6.43	6.88	5.77	6.95	5.64	7.12
Enclosure Vessel - Local Membrane Plus Primary Bending ( $P_L + P_b$ )	4.24	4.28	2.14	3.56	3.07	2.74
Basket Supports - Primary Membrane ( $P_m$ )	N/A	N/A	2.72	3.83	6.67	8.67
Basket Supports - Local Membrane Plus Primary Bending ( $P_L + P_b$ )	N/A	N/A	3.89	4.75	1.16	1.51

Table 2.7.4 (Continued) - FINITE ELEMENT ANALYSIS RESULTS  
 MINIMUM SAFETY FACTORS FOR MPC COMPONENTS UNDER ACCIDENT CONDITIONS

Component - Stress Result	MPC-24E/EF	
	30 Ft. Side Drop, 0 deg Orientation Load Case F3.b or E3.b	30 Ft. Side Drop, 45 deg Orientation Load Case F3.c or E3.c
Fuel Basket – Primary Membrane ( $P_m$ )	2.74	3.79
Fuel Basket - Local Membrane Plus Primary Bending ( $P_L + P_b$ )	1.16	1.28
Enclosure Vessel - Primary Membrane ( $P_m$ )	6.39	6.86
Enclosure Vessel - Local Membrane Plus Primary Bending ( $P_L + P_b$ )	3.14	4.13

Table 2.7.5 - FINITE ELEMENT ANALYSIS RESULTS  
MINIMUM SAFETY FACTORS FOR OVERPACK COMPONENTS UNDER ACCIDENT CONDITIONS (Hot Environment)

Component – Stress Result	30 Ft. Bottom End Drop Load Case 1	30 Ft. Top End Drop Load Case 2	30 Ft. Side Drop Load Case 3	30 Ft. C.G. Over-the- Bottom-Corner Drop Load Case 4
Lid – Local Membrane Plus Primary Bending ( $P_L + P_b$ )	34.04	1.75	2.60	7.76
Inner Shell – Local Membrane Plus Primary Bending ( $P_L + P_b$ )	4.35 (Note 2)	10.02 (Note 2)	2.19 (Note 2)	2.93 (Note 2)
Inner Shell – Primary Membrane ( $P_m$ )	4.48 (Note 2)	7.39 (Note 2)	2.45 (Note 2)	2.33 (Note 2)
Intermediate Shells - Local Membrane Plus Primary Bending ( $P_L + P_b$ )	6.63	7.95	2.33	1.49
Baseplate - Local Membrane Plus Primary Bending ( $P_L + P_b$ )	7.05	21.6	4.71	2.78
Enclosure Shell - Primary Membrane ( $P_m$ )	16.44	12.23	2.19	5.48

- Notes:
1. Load cases are defined in Table 2.1.9.
  2. Applicable to inner shell fabricated from SA203-E material. Safety factor must be multiplied by 0.93 if inner shell is fabricated from optional SA350-LF3 material.

Table 2.7.5 (Continued) - FINITE ELEMENT ANALYSIS RESULTS  
 MINIMUM SAFETY FACTORS FOR OVERPACK COMPONENTS UNDER ACCIDENT CONDITIONS (Hot Environment)

Component - Stress Result	30 Ft. C.G. Over- the-Top-Corner Drop Load Case 5	Side Puncture Load Case 6	Top End Puncture Load Case 7	Bottom End Puncture Load Case 8	30 Ft. – 30 degree Drop Load Case 20	30 Ft. – Slapdown Load Case 22
Lid – Local Membrane Plus Primary Bending ( $P_L + P_b$ )	3.69	5.70	2.03 (See Note 2)	6.29	1.77	2.22
Inner Shell – Local Membrane Plus Primary Bending ( $P_L + P_b$ )	3.16 (Note 3)	2.80 (Note 3)	29.29 (Note 3)	9.52 (Note 3)	2.78 (Note 3)	2.73 (Note 3)
Inner Shell – Primary Membrane ( $P_m$ )	2.60 (Note 3)	5.95 (Note 3)	26.5 (Note 3)	10.61 (Note 3)	2.45 (Note 3)	2.14 (Note 3)
Intermediate Shells - Local Membrane Plus Primary Bending ( $P_L + P_b$ )	3.52	6.19	32.52	15.12	3.28	2.88
Baseplate - Local Membrane Plus Primary Bending ( $P_L + P_b$ )	6.95	21.62	28.62	1.46	27.32	17.9
Enclosure Shell - Primary Membrane ( $P_m$ )	3.56	4.53	51.32	29.9	8.02	2.40

- Notes:
1. Load cases are defined in Table 2.1.9.
  2. Stress Intensity computed just outboard of the loaded area since surface stress is not a primary stress component.
  3. Applicable to inner shell fabricated from SA203-E material. Safety factor must be multiplied by 0.93 if inner shell is fabricated from optional SA350-LF3 material.

Table 2.7.6 - FINITE ELEMENT ANALYSIS RESULTS  
 MINIMUM SAFETY FACTORS FOR OVERPACK COMPONENTS UNDER ACCIDENT CONDITIONS (Cold Environment)

Component – Stress Result	30 Ft. Bottom End Drop Load Case 9	30 Ft. Top End Drop Load Case 10	30 Ft. Side Drop Load Case 11	30 Ft. C.G. Over-the- Bottom-Corner Drop Load Case 12
Lid – Local Membrane Plus Primary Bending ( $P_L + P_b$ )	30.29	1.87	2.73	8.00
Inner Shell – Local Membrane Plus Primary Bending ( $P_L + P_b$ )	4.17	9.69	2.19	2.94
Inner Shell – Primary Membrane ( $P_m$ )	4.37	7.33	2.47	2.36
Intermediate Shells - Local Membrane Plus Primary Bending ( $P_L + P_b$ )	4.95	8.66	2.61	1.73
Baseplate - Local Membrane Plus Primary Bending ( $P_L + P_b$ )	7.73	17.07	4.80	2.73
Enclosure Shell - Primary Membrane ( $P_m$ )	20.08	18.4	2.45	5.71

Notes: 1. Load cases are defined in Table 2.1.9.

Table 2.7.6 (Continued) - FINITE ELEMENT ANALYSIS RESULTS  
 MINIMUM SAFETY FACTORS FOR OVERPACK COMPONENTS UNDER ACCIDENT CONDITIONS (Cold Environment)

Component – Stress Result	30 Ft. C.G. Over- the-Top-Corner Drop Load Case 13	Side Puncture Load Case 14	Top End Puncture Load Case 15	Bottom End Puncture Load Case 16	30 Ft.. – 30 degree Drop Load Case 21
Lid – Local Membrane Plus Primary Bending ( $P_L + P_b$ )	3.91	5.91	2.09 (See Note 2)	6.64	1.84
Inner Shell – Local Membrane Plus Primary Bending ( $P_L + P_b$ )	3.21	3.05	24.97	8.54	2.78
Inner Shell – Primary Membrane ( $P_m$ )	2.65	7.60	17.03	9.59	2.48
Intermediate Shells - Local Membrane Plus Primary Bending ( $P_L + P_b$ )	4.10	7.06	27.55	14.9	3.81
Baseplate - Local Membrane Plus Primary Bending ( $P_L + P_b$ )	7.08	29.69	47.25	1.46	21.91
Enclosure Shell - Primary Membrane ( $P_m$ )	4.13	5.17	57.21	76.5	9.64

- Notes: 1. Load cases are defined in Table 2.1.9.  
 2. Surface pressure not included in safety factor evaluation since it is not a primary stress.



Table 2.7.7

**MINIMUM SAFETY FACTORS FOR MISCELLANEOUS ITEMS - MPC FUEL BASKET/CANISTER - HYPOTHETICAL  
ACCIDENT CONDITIONS OF TRANSFER**

Item	Loading	Safety Factor	Location in SAR Where Calculations or Results are Presented
Fuel Basket Axial Stress	End Drop	4.19	Subsection 2.7.1.1
Fuel Basket Axial Stress	Fire Transient (Regulatory Position C.7 of Regulatory Guide 7.6)	4.96	Subsection 2.7.3.4
MPC Canister Stability	30' End Drop (Load Case E3.a, Table 2.1.7)	1.92	Subsection 2.7.1.1
MPC Top Closure Lid Bending Stress	30' End Drop (Load Case E3.a in Table 2.1.7)	2.8 (single lid) 1.4 (dual lid)	Subsection 2.7.1.1
MPC Top Closure Lid – Loading in Peripheral Weld	30' End Drop (Load Case E3.a in Table 2.1.7)	2.37	Subsection 2.7.1.1
MPC Baseplate Bending Stress	30' End Drop (Load Case E3.a in Table 2.1.7)	3.04	Subsection 2.7.1.1
MPC Canister at Connection to Baseplate	30' End Drop (Load Case E3.a in Table 2.1.7)	2.14	Subsection 2.7.1.1
MPC Top Closure Lid Bending Stress	Fire accident (Load Case E5 in Table 2.1.7)	7.64	Subsection 2.7.3.3.1
MPC Baseplate Bending Stress	Fire accident (Load Case E5 in Table 2.1.7)	1.05	Subsection 2.7.3.3.1
MPC Canister Stability	Fire accident (Load Case E5 in Table 2.1.7)	1.18	Subsection 2.7.3.3.1
MPC Shell Mean Stress	Fire accident (Load Case E5 in Table 2.1.7)	2.32	Subsection 2.7.3.3.1

Table 2.7.8

**MINIMUM SAFETY FACTORS FOR MISCELLANEOUS ITEMS - OVERPACK -  
HYPOTHETICAL ACCIDENT CONDITIONS OF TRANSPORT**

Item	Loading	Safety Factor	Location in SAR Where Calculations or Results are Presented
Overpack Stability	30' End Drop (Load Cases 1 and 2 in Table 2.1.9)	2.16*	Subsection 2.7.1.1
Closure Bolts	30' End Drop (Load Case 2 in Table 2.1.9)	1.02	Subsection 2.7.1.1
Closure Bolts	Top End Puncture	1.55	Subsection 2.7.2
Overpack Inner Shell Mean Stress	Fire Transient	6.44	Subsection 2.7.3.3.2
Closure Bolts	Fire Transient	1.18	Subsection 2.7.3.3.3
Overpack Stress	Fire Transient (Regulatory Position C.7 of Regulatory Guide 7.6)	3.67	Subsection 2.7.3.4
Overpack Stability (Yield Stress Criteria)	Immersion (Load Case 18 in Table 2.1.9)	2.32*	Subsection 2.7.5
Overpack Stability (Stability Criteria)	Immersion (Load Case 18 in Table 2.1.9)	3.95	Subsection 2.7.5

\* Applicable to inner shell fabricated from SA203-E material. Safety factor must be multiplied by 0.93 if inner shell is fabricated from optional SA350-LF3 material.

**FIGURES 2.7.1 THROUGH 2.7.21: PROPRIETARY INFORMATION WITHHELD PER  
10CFR2.390**

**Figures 2.7.19 through 2.7.22**  
**INTENTIONALLY DELETED**

## 2.8 SPECIAL FORM

This section is not applicable to the HI-STAR 100 System. This application does not seek approval for transport of special form radioactive material as defined in 10CFR71.4.

## 2.9 FUEL RODS

The cladding of the fuel rods is the initial confinement boundary in the HI-STAR 100 System. Analyses have been performed in Chapter 3 to ensure that the maximum temperature of the fuel cladding is below the Pacific Northwest Laboratory's threshold values for various cooling times. These temperature limits ensure that the fuel cladding will not degrade in an inert helium environment. Additional details on the fuel rod cladding temperature analyses for the spent fuel to be loaded into the HI-STAR 100 System are provided in Chapter 3.

The dimensions of the storage cell openings in the MPC are equal to or greater than those used in spent fuel racks supplied by Holtec International. Thousands of fuel assemblies have been shuffled in and out of these cells over the years without a single instance of cladding failure. The vast body of physical evidence from prior spent fuel handling operations provides confirmation that the fuel handling and loading operations with the HI-STAR 100 MPC will not endanger or compromise the integrity of the cladding or the structural integrity of the assembly.

The HI-STAR 100 System is designed and evaluated for a maximum deceleration of 60g's. Studies of the capability of spent fuel rods to resist impact loads [2.9.1] indicate that the most vulnerable fuel can withstand greater than 60 g's in the side impact orientation. Therefore, limiting the HI-STAR 100 System to a maximum deceleration of 60 g's (perpendicular to the longitudinal axis of the overpack during all normal and hypothetical accident conditions) ensures that fuel rod cladding integrity is maintained. In [2.9.1], it is assumed that the fuel rod cladding provides the only structural resistance to bending and buckling of the rod. For accidents where the predominate deceleration is directed along the longitudinal axis of the overpack, [2.9.1] also demonstrates that no elastic instability or yielding of the cladding will occur until the deceleration level is well above the HI-STAR 100 limit of 60g's. The solutions presented in [2.9.1], however, assume that the fuel pellets are not intimately attached to the cladding when subjected to an axial deceleration load that may cause an elastic instability of the fuel rod cladding.

The limit based on classical Euler buckling analyses performed by Lawrence Livermore National Laboratory in [2.9.1] is 82 g's. In the LLNL report, the limiting axial load to ensure fuel rod stability is obtained by modeling the fuel rod as a simply supported beam with unsupported length equal to the grid strap spacing. The limiting load under this condition is:

$$F = \pi^2 EI / L^2$$

In the preceding formula, E = Young's Modulus of the cladding, I = area moment of inertia of the cladding, and L = spacing of the grid straps.

Assuming that  $F = W \times A/g$  with W being the weight of a fuel rod, and A = the deceleration, the Euler buckling formula can be expressed as

$$A/g = \pi^2 (ER^3 / W_{fa} L^2) = \pi^2 \beta$$

In the preceding formula,  $g$  = gravity,  $n$  = number of fuel rods in the fuel assembly,  $W_{fa}$  = the total weight of the fuel assembly,  $t$  = cladding wall thickness, and  $R$  = cladding mean radius.

Using the preceding formula, a survey of a large variety of fuel assembly types in [2.9.1] concluded that a 17 x 17 PWR assembly resulted in the minimum value for deceleration and results in the lower bound limit of:

$$A/g = 82$$

The fuel pellet weight was omitted from the analysis in [2.9.1] by virtue of the assumption that under axial load, the cladding did not support the fuel pellet mass. Since the results may not be conservative because of the assumption concerning the behavior of the fuel pellet mass, a new analysis of the structural response of the fuel cladding is presented here... It is demonstrated that the maximum axially oriented deceleration that can be applied to the fuel cladding is in excess of the design basis deceleration specified in this SAR. Therefore, the initial confinement boundary remains intact during a hypothetical accident of transport where large axially directed decelerations are experienced by the HI-STAR 100 package.

The analysis reported here considers the most limiting fuel rod in the fuel assembly. Most limiting is defined as the fuel rod that may undergo the largest bending (lateral) deformations in the event of a loss of elastic stability. The fuel rod is modeled as a thin-walled elastic tube capable of undergoing large lateral displacements in the event that high axial loads cause a loss of stability (i.e., the non-linear interaction of axial and bending behavior of the elastic tube is included in the problem formulation). The fuel rod and the fuel pellet mass is included in the analysis with the fuel pellet mass assumed to contribute only its mass to the analysis. In the HI-STAR 100 spent fuel basket, continuous support to limit lateral movement is provided to the fuel assembly along its entire length. The extent of lateral movement of any fuel rod in a fuel assembly is limited to: (1) the clearance gap between the grid straps and the fuel basket cell wall at the grid strap locations; and, (2) the maximum available gap between the fuel basket cell wall and the fuel rod in the region between the grid straps. Note that the grid straps act as fuel rod spacers at the strap locations; away from the grid straps, however, there is no restraint against fuel rod –to-rod contact under a loading giving rise to large lateral motion of the individual rods. Under the incremental application of axial deceleration to the fuel rod, the fuel rod compresses and displaces from the axially oriented inertial loads experienced. The non-linear numerical analysis proceeds to track the behavior of the fuel rod up to and beyond contact with the rigid confining walls of the HI-STAR 100 fuel basket.

The analysis is carried out for the “most limiting” spent fuel assembly. The “most limiting” criteria used herein is based on the simple elastic stability formula assuming buckling occurs only between grid straps. This is identical to the methodology employed in [2.9.1] to identify the fuel assembly that limits design basis axial deceleration loading. Table 2.9.1 presents tabular data for a wide variety of fuel assemblies. Considerable data was obtained using the tables in [2.9.2]. The configuration with the lowest value of “Beta” is the most limiting for simple elastic Euler buckling between grid straps; the Westinghouse 14x14 Vantage, “W14V”, PWR configuration is used to obtain results.

The material properties used in the non-linear analysis are those for irradiated Zircalloy and are obtained from [2.9.1]. The Young's Modulus and the cladding dynamic yield stress are set as:

$$E = 10,400,000 \text{ psi}$$

$$\sigma_y = 80,500 \text{ psi}$$

The fuel cladding material is assumed to have no tensile or compressive stress capacity beyond the material yield strength.

Calculations are performed for two limiting assumptions on the magnitude of resisting moment at the grid straps. Figures 2.9.1 through 2.9.9 aid in understanding the calculation. It is shown in the detailed calculations that the maximum stress in the fuel rod cladding occurs subsequent to the cladding deflecting and contacting the fuel basket cell wall. Two limiting analyses are carried out. The initial analysis assumes that the large deflection of the cladding between two grid straps occurs without any resisting moment at the grid strap supports. This maximizes the stress in the free span of the cladding, but eliminates all cladding stress at the grid strap supports. It is shown that this analysis provides a conservative lower bound on the limiting deceleration. The second analysis assumes a reasonable level of moment resistance to develop at the grid straps; the level developed is based on an assumed deflection shape for the cladding spans adjacent to the span subject to detailed analysis. For this second analysis, the limiting decelerations are much larger with the limit stress level occurring in the free span and at the grid strap support locations.

It is concluded that the most conservative set of assumptions on structural response still lead to the conclusion that the fuel rod cladding remains intact under the design basis deceleration levels set for the HI-STAR 100.



Table 2.9.1 FUEL ASSEMBLY DIMENSIONAL DATA

Array ID	Array Name	Rod O.D. (in.)	Clad Thk. (in.)	R <sub>mean</sub> (in.)	# of Rods	Assy Wt. (lb.)	Rod Length (in.)	# of Spans	Average Span (in.)	Material Modulus	BETA
PWR											
14x14A01	W14OFA	0.4000	0.0243	0.20608	179	1177	151.85	6	25.30833	10400000	0.525127806
14x14A02	W14OFA	0.4000	0.0243	0.20608	179	1177	151.85	6	25.30833	10400000	0.525127806
14x14A03	W14V	0.4000	0.0243	0.20608	179	1177	151.85	6	25.30833	10400000	0.525127806
14x14B01	W14STD	0.4220	0.0243	0.21708	179	1302	152.4	6	25.4	10400000	0.550863067
14x14B02	XX14TR	0.4170	0.0295	0.21588	179	1215	152	6	25.33333	10400000	0.708523868
14x14B03	XX14STD	0.4240	0.0300	0.21950	179	1271.2	149.1	8	18.6375	10400000	1.337586884
14x14C01	CE14	0.4400	0.0280	0.22700	176	1270	147	8	18.375	10400000	1.398051576
14x14C02	CE14	0.4400	0.0280	0.22700	176	1220	137	8	17.125	10400000	1.67556245
14x14D01	W14SS	0.4220	0.0165	0.21513	180	1247	126.68	6	21.11333	24700000	1.31385062
15x15A01	CE15P	0.4180	0.0260	0.21550	204	1360	140	9	15.55556	10400000	1.677523904
15x15B01	W15OFA	0.4220	0.0245	0.21713	204	1459	151.85	6	25.30833	10400000	0.569346561
15x15B02	W15V5H	0.4220	0.0245	0.21713	204	1459	151.85	6	25.30833	10400000	0.569346561
15x15B03	W15	0.4220	0.0243	0.21708	204	1440	151.83	6	25.305	10400000	0.571905185
15x15B04	W15	0.4220	0.0243	0.21708	204	1443	151.83	6	25.305	10400000	0.570716193
15x15B05	15(2a-319)	0.4220	0.0242	0.21705	204	1472	151.88	6	25.31333	10400000	0.556610964
15x15C01	SPC15	0.4240	0.0300	0.21950	204	1425	152	6	25.33333	10400000	0.73601861
15x15C02	SPC15	0.4240	0.0300	0.21950	204	1425	152	6	25.33333	10400000	0.73601861
15x15C03	XX15	0.4240	0.0300	0.21950	204	1432.8	152.065	6	25.34417	10400000	0.731386148
15x15C04	XX15	0.4170	0.0300	0.21600	204	1338.6	139.423	9	15.49144	10400000	1.996693327
15x15D01	BW15	0.4300	0.0265	0.22163	208	1515	153.68	7	21.95429	10400000	0.854569793
15x15D02	BW15	0.4300	0.0265	0.22163	208	1515	153.68	7	21.95429	10400000	0.854569793
15x15D03	BW15	0.4300	0.0265	0.22163	208	1515	153.68	7	21.95429	10400000	0.854569793
15x15G01	HN15SS	0.4220	0.0165	0.21513	204	1421	126.72	6	21.12	24700000	1.305875606
16x16A01	CE16	0.3820	0.0250	0.19725	236	1430	161	10	16.1	10400000	1.270423729

Table 2.9.1 FUEL ASSEMBLY DIMENSIONAL DATA (continued)

Array ID	Array Name	Rod O.D. (in.)	Clad Thk. (in.)	R <sub>mean</sub> (in.)	# of Rods	Assy Wt. (lb)	Rod Length (in.)	# of Spans	Average Span (in.)	Material Modulus	BETA
16x16A02	CE16	0.3820	0.0250	0.19725	236	1300	146.499	9	16.27767	10400000	1.367126598
17x17A01	W17OFA	0.3600	0.0225	0.18563	264	1373	151.635	7	21.66214	10400000	0.613275783
17x17A02	W17OFA	0.3600	0.0225	0.18563	264	1365	152.3	7	21.75714	10400000	0.611494853
17x17B01	W17STD	0.3740	0.0225	0.19263	264	1482	151.635	7	21.66214	10400000	0.634902014
17x17B02	W17P+	0.3740	0.0225	0.19263	264	1482	151.635	7	21.66214	10400000	0.634902014
17x17C01	BW17	0.3790	0.0240	0.19550	264	1505	152.688	7	21.81257	10400000	0.687604262
BWR											
6x6A02	XX/ANF6	0.5645	0.0360	0.29125	36	328.4	116.65	4	29.1625	10400000	1.192294364
6x6C01	HB6	0.5630	0.0320	0.28950	36	270	83	3	20.75	10400000	2.500527046
7x7A01	HB7	0.4860	0.0330	0.25125	49	276	83.2	3	20.8	10400000	2.233705011
7x7B01	GE-7	0.5630	0.0320	0.28950	49	682.5	159	7	19.875	10400000	1.467601583
7x7B02	GE-7	0.5630	0.0370	0.29075	49	681	164	7	20.5	10400000	1.619330439
7x7B03	GE-7	0.5630	0.0370	0.29075	49	674.4	164	7	20.5	10400000	1.635177979
7x7B04	GE-7	0.5700	0.0355	0.29388	49	600	161.1	7	20.1375	10400000	1.887049713
7x7B05	GE-7	0.5630	0.0340	0.29000	49	600	161.1	7	20.1375	10400000	1.736760659
8x8B03	GE-8	0.4930	0.0340	0.25500	63	681	164	7	20.5	10400000	1.2906798
8x8C02	GE-8R	0.4830	0.0320	0.24950	62	600	159	7	19.875	10400000	1.352138354
8x8C03	GE-8R	0.4830	0.0320	0.24950	62	600	163.71	7	20.46375	10400000	1.27545448
9x9D01	XX/ANF9	0.4240	0.0300	0.21950	79	575.3	163.84	8	18.20444	10400000	1.367212516
10x10E01	XX10SS	0.3940	0.0220	0.20250	96	376.6	89.98	4	17.996	24700000	3.551678654

Array ID, Rod OD, Clad Thk and # of Rods from Tables 6.2.1 and 6.2.2.

R<sub>mean</sub>, Average Span and THETA are Calculated.

Zircaloy Modulus from LLNL Report [2.9.1].

Stainless Steel (348H) Modulus from ASME Code, Section III, Part D.

Table 2.9.1 FUEL ASSEMBLY DIMENSIONAL DATA (continued)

PWR Assy. Wt., Rod Len. and # of Spans (exc. as noted below) from DOE/RW-0184, Vol. 3, UC-70, -71 and -85, Dec. 1987.  
 Assy. Wt., Rod Len. and # of Spans for 15x15B03, 15x15B04, 15x15C01 and 15x15C02 from ORNL/TM-9591/V1-R1.  
 BWR Assy. Wt., Rod Len. and # of Spans (exc. as noted below) from ORNL/TM-10902.  
 Assy. Wt., Rod Len. and # of Spans for 6x6A02, 9x9D01 and 10x10E01 from DOE/RW-0184, Vol. 3, UC-70, -71 and -85, Dec. 1987.  
 Assy. Wt., Rod Len. and # of Spans for 7x7B04 and 7x7B05 from ORNL/TM-9591/V1-R1.  
 Assy. Wt. for 8x8C02 and 8x8C03 from ORNL/TM-9591/V1-R1.

In the following, a physical description of the structural instability problem is provided with the aid of Figures 2.9.1 to 2.9.9. A stored fuel assembly consists of a square grid of fuel rods. Each fuel rod consists of a thin-walled cylinder surrounding and containing the fuel pellets. The majority of the total weight of a fuel rod is in the fuel pellets; however, the entire structural resistance of the fuel rod to lateral and longitudinal loads is provided by the cladding. Hereinafter, the use of the words "fuel rod", "fuel rod cladding", or just "cladding" means the structural thin cylinder. The weight of the fuel pellets is conservatively assumed to be attached to the cladding for all discussions and evaluations.

Figure 2.9.1 shows a typical fuel rod in a fuel assembly. Also shown in Figure 2.9.1 are the grid straps and the surrounding walls of the spent fuel basket cell walls. The grid straps serve to maintain the fuel rods in a square array at a certain number of locations along the length of the fuel assembly. When the fuel rod is subject to a loading causing a lateral deformation, the grid strap locations are the first locations along the length of the rod where contact with the fuel basket cell walls occurs. The fuel basket cell walls are assumed to be rigid surfaces. The fuel rod is assumed to be subjected to some axial load and has some slightly initially deformed shape. For the purposes of the analysis, it is assumed that displacement under load occurs in a 2-D plane and that the ends of the fuel rod cladding have a specified boundary condition to restrain lateral deflection. The ends of the fuel rod cladding are assumed to be simply supported and the grid straps along the length of the fuel assembly are assumed to have gap " $g_1$ " relative to the cell walls of the fuel basket. The figure shows a typical fuel rod in the assembly that is located by gaps " $g_2$ " and " $g_3$ " with respect to the fuel basket walls. Because the individual fuel rod is long and slender and is not perfectly straight, it will deform under a small axial load into the position shown in Figure 2.9.2. The actual axial load is due to the distributed weight subject to a deceleration from a hypothetical accident of transport. For the purposes of this discussion, it is assumed that some equivalent axial load is applied to one end of the fuel rod cladding. Because of the distributed weight and the fact that a deceleration load is not likely to be exactly axially oriented, the predominately axial load will induce a lateral displacement of the fuel rod cladding between the two end supports. The displacement will not be symmetric but will be larger toward the end of the cladding where support against the axial deceleration is provided. Depending on the number of grid straps, either one or two grid straps will initially make contact with the fuel basket cell wall and the contact will not be exactly centered along the length of the cell. Figure 2.9.3 illustrates the position of the fuel rod after the axial load has increased beyond the value when initial contact occurred and additional grid straps are now in contact with the cell wall. The maximum stress in the fuel rod will occur at the location of maximum curvature and will be a function of the bending moment ( $F_2 \times (g_2 - g_1)$ ).

At some load  $F_3 > F_2$ , either the limiting stress in the fuel rod cladding is achieved or the rod begins to experience large lateral movements between grid plates because of the coupling between axial and lateral load and deformation. Figure 2.9.4 shows the deformation mode experienced by the fuel rod cladding caused by the onset of an instability between two grid straps that are in contact with the fuel basket cell wall.

Once the lateral displacement initiates, the rod displaces until contact with the cell wall occurs at the mid point "A" ( see Figure 2.9.5) or the cladding stress exceeds the cladding material yield strength.

Depending on the particular location of the fuel rod in the fuel assembly, the highest stressed portion of the fuel rod will occur in the segment with the larger of the two gaps " $g_2$ " and " $g_3$ ". For the discussion to follow, assume that  $g_2 > g_3$ . The boundary condition at the grid strap is conservatively assumed as simply-supported so that the analysis need not consider what happens in adjacent spans between grid straps. At this point in the loading process, the maximum bending moment occurs at the contact point and has the value  $F_4 \times (g_2 - g_1)$ . Figure 2.9.5 shows the displaced configuration at the load level where initial contact occurs with the fuel cell wall. If the maximum fuel rod stress (from the bending moment and from the axial load) equals the yield stress of the fuel rod cladding, it is assumed that  $F_3 = F_4$  is the maximum axial load that can be supported. The maximum stress in the fuel rod cladding occurs at point "A" in Figure 2.9.5 since that location has the maximum bending moment. If the cladding stress is still below yield, additional load can be supported. As the load is further increased, the bending moment is decreased and replaced by reaction loads, "V", at the grid strap and the contact point. These reaction loads V are shown in Figure 2.9.7 and are normal to the cell wall surface. Figure 2.9.6 shows the configuration after the load has been further increased from the value at initial contact. There are two distinct regions that need to be considered subsequent to initial contact with the fuel basket cell wall. During the additional loading phase, the point "A" becomes two "traveling" points, A, and A'. Since the bending moment at A' and A is zero, the moment  $F_5 \times (g_2 - g_1)$  is balanced by forces V at the grid strap and at point A or A'. This is shown in Figure 2.9.7 where the unsupported length current "a" is shown with the balancing load. At this point in the process, two "failure" modes are possible for the fuel rod cladding.

The axial load that develops in the unsupported region between the grid strap and point A' causes increased deformation and stress in that segment, or,

The straight region of the rod, between A and A', begins to experience a lateral deformation away from the cell wall.

Note that in this latter scenario, the slope at A or A' remains zero so this should never govern unless the flat region becomes large. The final limiting load occurs when the maximum stress in either portion of the rod exceeds the yield stress of the tube. In what follows, the most limiting fuel assembly from the array of fuel types considered is subject to detailed analysis and the limiting load established. This limit axial load is considered as the product of the fuel rod weight times the deceleration. Therefore, establishing the limiting load to reach cladding material yield establishes the limiting axial deceleration that can be imposed.

The preceding discussion has assumed end conditions of simple support for conservatism. The location of the fuel rod determines the actual free gap between grid straps. For example, a fuel rod furthest from the cell wall that resists lateral movement of the assembly moves to close up all of the clearances that exist between it and the resisting cell wall. The clearance between rods is the rod pitch minus the rod diameter. In a 14 x 14 assembly, there are 13 clearance gaps plus an additional clearance  $g_3$  between the nearest rod and the cell wall. Therefore, the gap  $g_2$  is given as

$$g_2 = 13(\text{pitch-diameter}) + g_3$$

Figure 2.9.9 provides an illustration of the fuel rod deformation for a case of 5 fuel rods in a column. Clearly for this case, the available lateral movement can be considerable for the "furthest" fuel rod. On the other hand, for this fuel rod, there will be considerable moment resistance at the grid strap from the adjacent section of the fuel rod. The situation is different when the rod being analyzed is assumed to be the closest to the cell wall. In this case, the clearance gap is much smaller, but the moment resistance provided by adjacent sections of the rod is reduced. For calculation purposes, we assume that a moment resistance is provided as  $M = f \times K$  for the fuel rod under analysis where

$K = 3EI/L$ ,  $L$  = span between grid straps, and " $f$ " is an assumed fraction of  $K$

The preceding result for the rotational spring constant assumes a simple support at each end of the span with an end moment " $M$ " applied. Classical strength of materials gives the result for the spring constant. The arbitrary assumption of a constant reduction in the spring constant is to account for undetermined interactions between axial force in the rod and the calculated spring constant. As the compressive force in the adjacent members increases, the spring constant will be reduced. On the other hand, as the adjacent span contacts its near cell wall, the spring constant increases. On balance, it should be conservative to assume a considerable reduction in the spring constant available to the span being analyzed in detail. As a further conservatism, the angle defined by the geometry is used without including any additional elastic displacement shape. This will further reduce the value of the resisting moment at any stage of the solution. In the detailed calculations, two limiting cases are examined. To limit the analysis to a single rod, it is assumed that after "stack-up" of the rods (see Figure 2.9.9), the lateral support provided by the cell wall supports all of the rods. That is, the rods are considered to have non-deforming cross-section.

Numerical Analysis - Based on the tabular results in Table 2.9.1, the fuel assembly with the smallest value for the deceleration based on the classical Euler buckling formula is analyzed in detail. The following input data is specified for the limiting 14 x 14 assembly [2.9.2]:

Inside dimension of a HI-STAR 100 fuel basket cell

$s := 8.75 \cdot \text{in}$

Outside envelope dimension of grid plate

$gp := 7.763 \cdot \text{in}$

Outer diameter of fuel rod cladding

$D := .4 \cdot \text{in}$

Wall thickness of cladding

$t := .0243 \cdot \text{in}$

Weight of fuel assembly (including end fittings)

$W := 1177 \cdot \text{lbf}$

Number of fuel rods + guide/instrument tubes in a column or row

$$n := 14$$

Overall length of fuel rod between assumed end support

$$L_t := 151 \cdot \text{in}$$

Length of fuel rod between grid straps

$$L_s := 25.3 \cdot \text{in}$$

Average clearance to cell wall at a grid strap location  
assuming a straight and centered fuel assembly

$$g_1 := .5 \cdot (s - gp)$$

$$g_1 = 0.494 \text{ in}$$

Rod pitch

$$\text{pitch} := 0.556 \cdot \text{in}$$

$$\text{Clearance} := (n - 1) \cdot (\text{pitch} - D)$$

$$\text{Clearance} = 2.028 \text{ in}$$

Minimum available clearance for lateral movement of a fuel  
rod between grid straps

$$g_3 := g_1 + .5 \cdot [gp - (n \cdot D + \text{Clearance})]$$

$$g_3 = 0.561 \text{ in}$$

Maximum available clearances for lateral movement of a  
fuel rod between grid straps

$$g_2 := g_3 + \text{Clearance}$$

$$g_2 = 2.589 \text{ in}$$

Young's Modulus of Zircalloy [2.9.1]

$$E := 10400000 \cdot \text{psi}$$

Dynamic Yield Strength of Zircalloy [2.9.1]

$$\sigma_y := 80500 \cdot \text{psi}$$

## Geometry Calculations:

Compute the metal cross section area  $A$ , the metal area moment of inertia  $I$ , and the total weight of a single fuel rod (conservatively assume that end fittings are only supported by fuel rods in the loading scenario of interest).

$$A := \frac{\pi}{4} \cdot [D^2 - (D - 2 \cdot t)^2]$$

$$I := \frac{\pi}{64} \cdot [D^4 - (D - 2 \cdot t)^4]$$

$$A = 0.029 \text{ in}^2$$

$$I = 5.082 \times 10^{-4} \text{ in}^4$$

$$W_r := \frac{W}{n^2}$$

$$W_r = 6.005 \text{ lbf}$$

As an initial lower bound calculation, assume no rotational support from adjacent spans and define a multiplying factor

$$f := 0.0$$

Compute the rotational spring constant available from adjacent sections of the rod.

$$K := 3 \cdot E \cdot \frac{I}{L_s} \cdot f$$

$$K = 0 \text{ lbf} \cdot \text{in}$$

Now compute the limiting load, if applied at one end of the fuel rod cladding, which causes an overall elastic instability and contact with the cell wall. Assume buckling in a symmetric mode for a conservatively low result. The purpose of this calculation is solely to demonstrate the flexibility of the single fuel rod. No resisting moment capacity is assumed to be present at the fittings.

$$P_0 := \pi^2 \cdot E \cdot \frac{I}{L_t^2}$$

$$P_0 = 2.288 \text{ lbf}$$

Note that this is less than the weight of the rod itself. This demonstrates that in the absence of any additional axial support, the fuel rod will bow and be supported by the cell walls under a very small axial load. In reality, however, there is additional axial support that would increase this initial buckling load. The stress induced in the rod by this overall deflected shape is small.



$$\text{Stress}_1 := \frac{P_0 \cdot g_1 \cdot D}{2 \cdot I}$$

$$\text{Stress}_1 = 444.32 \text{ psi}$$

$$\text{Stress}_d := \frac{P_0}{A}$$

$$\text{Stress}_d = 79.76 \text{ psi}$$

The conclusion of this initial calculation is that grid straps come in contact; consideration of what happens between a grid strap is the only region that requires further investigation. First calculate the classical Euler buckling load based on a pin-ended rod and assume conservatively that the entire weight of the rod is providing the axial driving force. This gives a conservatively low estimate of the limiting deceleration that can be resisted before a perfectly straight rod buckles.

$$a_{\text{lim}1} := \pi^2 \cdot E \cdot \frac{I}{L_s^2 \cdot W_r}$$

$$a_{\text{lim}1} = 13.57$$

The rigid body angle of rotation at the grid strap under this load that causes contact is:

$$\theta_1 := \text{atan} \left[ 2 \cdot \frac{(g_2 - g_1)}{L_s} \right]$$

$$\theta_1 = 9.406 \text{ deg}$$

Conservatively assume resisting moment at the grid is proportional to this "rigid body" angle:

$$M_r := K \cdot \theta_1$$

$$M_r = 0 \text{ in} \cdot \text{lbf}$$

(in this first analysis, no resisting moment is assumed)

The total stress at the grid strap due to the axial force and the resisting moment is

$$\sigma_{gs} := \frac{W_r \cdot a_{\text{lim}1}}{A} + \frac{M_r \cdot D}{2 \cdot I}$$

$$\sigma_{gs} = 2841.172 \text{ psi}$$

The total stress at the contact location is

$$\text{Stress}_2 := \frac{[W_r \cdot a_{\text{lim}1} \cdot (g_2 - g_1) - M_r] \cdot D}{2 \cdot I}$$

$$\text{Stress}_2 = 6.721 \times 10^4 \text{ psi}$$

$$\text{Stress}_{2d} := \frac{W_r \cdot a_{\text{lim}1}}{A}$$

$$\text{Stress}_{2d} = 2841.172 \text{ psi}$$

$$\text{Stress}_{2t} := \text{Stress}_2 + \text{Stress}_{2d}$$

$$\text{Stress}_{2t} = 7.005 \times 10^4 \text{ psi}$$

This is the maximum value of the stress at this location since, for further increase in axial load, the moment will decrease with consequent large decrease in the total stress.

The safety factor is

$$\frac{\sigma_y}{\text{Stress}_{2t}} = 1.149$$

The axial load in the unsupported portion of the beam at this instant is

$$P_{ax} := \frac{(W_r \cdot a_{\text{lim}1})}{\cos(\theta_1)}$$

$$P_{ax} = 82.599 \text{ lbf}$$

At this point in the load process, a certain axial load exists in the unsupported span on either side of the contact point. However, since the unsupported span is approximately 50% of the original span, the allowable deceleration limit is larger. As the axial load is incrementally increased, the moment at the contact point is reduced to zero with consequent increases in the lateral force V at the grid strap and at the contact points A and A'. Figure 2.9.8 provides the necessary information to determine the elastic deformation that occurs in the unsupported span as the axial load increases and the contact points separate (and, therefore, decreasing the free span).

From geometry, coupled with the assumption that the deflected shape is a half "sin" function with peak value  $\delta$ , the following relations are developed:

Assume "a" is a fraction of 50% of the span (the following calculations show only the final iterated assumption for the fraction

$$\varepsilon := .9$$

$$a := \varepsilon \cdot \left( \frac{L_s}{2} \right)$$

$$a = 11.385 \text{ in}$$

Calculate "b" in Figure 2.9.8

$$b := \left[ (a)^2 + (g_2 - g_1)^2 \right]^{.5}$$

$$b = 11.576 \text{ in}$$

An equation for  $\delta$  can be developed from the geometric relation

$$\frac{(g_2 - g_1)}{a} := \frac{b}{2(R - \delta)} \quad \blacksquare$$

(please note that the above equation is imported from the electronic spreadsheet program MathCad. The solid rectangle appearing after the equation is a MathCad symbol designating that no computations are performed on that line)

The inverse of the radius of curvature,  $R$ , at the point of peak elastic deflection of the free span, is computed as the second derivative of the assumed sin wave deflection shape. Based on the geometry in Figure 2.9.8, the peak deflection is:

$$\delta := .5 \cdot \left[ \left[ a \cdot \frac{b}{2 \cdot (g_2 - g_1)} \right]^2 + 4 \cdot \left( \frac{b}{\pi} \right)^2 \right]^{.5} - a \cdot \frac{b}{4 \cdot (g_2 - g_1)}$$

$$\delta = 0.426 \text{ in}$$

For the assumed "a", the limiting axial load capacity in the unsupported region is conservatively estimated as:

$$a_{\text{lim2}} := \pi^2 \cdot E \cdot \frac{I}{(b)^2 \cdot W_r}$$

$$a_{\text{lim2}} = 64.816$$

The corresponding rigid body angle is:

$$\theta_2 := \text{atan} \left[ 1 \cdot \frac{(g_2 - g_1)}{a} \right]$$

$$\theta_2 = 10.429 \text{ deg}$$

The axial load in the unsupported portion of the beam at this instant is

$$P_{\text{ax}} := \frac{(W_r \cdot a_{\text{lim2}})}{\cos(\theta_2)}$$

$$P_{\text{ax}} = 395.763 \text{ lbf}$$

The resisting moment is

$$M_r := K \cdot \theta_2$$

$$M_r = 0 \text{ in}\cdot\text{lbf}$$

The total stress in the middle of the unsupported section of free span "b" is

$$\text{stress}_3 := \frac{(P_{ax} \cdot \delta - M_r) \cdot D}{2 \cdot I}$$

$$\text{stress}_3 = 6.635 \times 10^4 \text{ psi}$$

$$\text{stress}_{3d} := \frac{P_{ax}}{A}$$

$$\text{stress}_{3d} = 1.38 \times 10^4 \text{ psi}$$

$$\text{stress}_{3t} := \text{stress}_3 + \text{stress}_{3d}$$

$$\text{stress}_{3t} = 8.015 \times 10^4 \text{ psi}$$

The safety factor is

$$\frac{\sigma_y}{\text{stress}_{3t}} = 1.004$$

The total stress at the grid strap due to the axial force and the resisting moment is

$$\sigma_{gs} := \frac{W_r \cdot a_{lim2}}{A} + \frac{M_r \cdot D}{2 \cdot I}$$

$$\sigma_{gs} = 1.357 \times 10^4 \text{ psi}$$

The safety factor is

$$\frac{\sigma_y}{\sigma_{gs}} = 5.932$$

For this set of assumptions, the stress capacity of the rod cladding has been achieved, so that the limiting deceleration is:

$$A_{limit} := a_{lim2}$$

$$A_{limit} = 64.816$$

This exceeds the design basis for the HI-STAR 100 package.

If there is any restraining moment from the adjacent span, there is a possibility of exceeding the rod structural limits at that location due to the induced stress. Therefore, the above calculations are repeated for an assumed moment capacity at the grid strap.

$$f := 1.$$

$$K := 3 \cdot E \cdot \frac{I}{L_s} \cdot f$$

The rigid body angle of rotation at the grid strap under this load that causes contact is:

$$\theta_1 := \text{atan} \left[ 2 \cdot \frac{(g_2 - g_1)}{L_s} \right]$$

$$\theta_1 = 9.406 \text{ deg}$$

Conservatively assume resisting moment at the grid is a function of this angle,

$$M_r := K \cdot \theta_1$$

$$M_r = 102.875 \text{ in}\cdot\text{lb}$$

The total stress at the grid strap due to the axial force and the resisting moment is

$$\sigma_{gs} := \frac{W_r \cdot a_{lim1}}{A} + \frac{M_r \cdot D}{2 \cdot I}$$

$$\sigma_{gs} = 4.333 \times 10^4 \text{ psi}$$

The total stress at the contact location is

$$\text{Stress}_2 := \frac{[W_r \cdot a_{lim1} \cdot (g_2 - g_1) - M_r] \cdot D}{2 \cdot I}$$

$$\text{Stress}_2 = 2.672 \times 10^4 \text{ psi}$$

$$\text{Stress}_{2d} := \frac{W_r \cdot a_{lim1}}{A}$$

$$\text{Stress}_{2d} = 2841.172 \text{ psi}$$

$$\text{Stress}_{2t} := \text{Stress}_2 + \text{Stress}_{2d}$$

$$\text{Stress}_{2t} = 2.956 \times 10^4 \text{ psi}$$

This is the maximum value of the stress at this location since, for further increase in axial load, the moment will decrease with consequent large decrease in the total stress.

The axial load in the unsupported portion of the beam at this instant is

$$P_{ax} := \frac{(W_r \cdot a_{lim1})}{\cos(\theta_1)}$$

$$P_{ax} = 82.599 \text{ lbf}$$

At this point in the load process, a certain axial load exists in the unsupported span on either side of the contact point. However, since the unsupported span is approximately 50% of the original span, the allowable deceleration limit is larger. As the axial load is incrementally increased, the moment at the contact point is reduced to zero with consequent increases in the lateral force V at the grid strap and at the contact points A and A'. Figure 2.9.8 provides the necessary information to determine the elastic deformation that occurs in the unsupported span as the axial load increases and the contact points separate (and, therefore, decreasing the free span).

From geometry, coupled with the assumption that the deflected shape is a half "sine" function with peak value " $\delta$ ", the following relations are developed:

Assume "a" is a fraction of 50% of the span (the following calculations show only the final iterated assumption for the fraction

$$\varepsilon := .7$$

$$a := \varepsilon \cdot \left( \frac{L_s}{2} \right)$$

$$a = 8.855 \text{ in}$$

Calculate "b" in Figure 2.9.8

$$b := \left[ (a)^2 + (g_2 - g_1)^2 \right]^{.5}$$

$$b = 9.1 \text{ in}$$

The inverse of the radius of curvature, R, at the point of peak elastic deflection of the free span, is computed as the second derivative of the assumed sin wave deflection shape. Based on the geometry in Figure 2.9.8, the peak deflection is:

$$\delta := .5 \cdot \left[ \left[ a \cdot \frac{b}{2 \cdot (g_2 - g_1)} \right]^2 + 4 \cdot \left( \frac{b}{\pi} \right)^2 \right]^{.5} - a \cdot \frac{b}{4 \cdot (g_2 - g_1)}$$

$$\delta = 0.427 \text{ in}$$

For the assumed "a", the limiting axial load capacity in the unsupported region is conservatively estimated as:

$$a_{lim2} := \pi^2 \cdot E \cdot \frac{I}{(b)^2 \cdot W_r}$$

$$a_{lim2} = 104.9$$

The corresponding rigid body angle is:

$$\theta_2 := \text{atan} \left[ 1 \cdot \frac{(g_2 - g_1)}{a} \right]$$

$$\theta_2 = 13.314 \text{ deg}$$

The axial load in the unsupported portion of the beam at this instant is

$$P_{ax} := \frac{(W_r \cdot a_{lim2})}{\cos(\theta_2)}$$

$$P_{ax} = 647.331 \text{ lbf}$$

The resisting moment is

$$M_r := K \cdot \theta_2$$

$$M_r = 145.619 \text{ in} \cdot \text{lbf}$$

The total stress in the middle of the unsupported section of free span "b" is

$$\text{stress}_3 := \frac{(P_{ax} \cdot \delta - M_r) \cdot D}{2 \cdot I}$$

$$\text{stress}_3 = 5.145 \times 10^4 \text{ psi}$$

$$\text{stress}_{3d} := \frac{P_{ax}}{A}$$

$$\text{stress}_{3d} = 2.257 \times 10^4 \text{ psi}$$

$$\text{stress}_{3t} := \text{stress}_3 + \text{stress}_{3d}$$

$$\text{stress}_{3t} = 7.402 \times 10^4 \text{ psi}$$

The safety factor is

$$\frac{\sigma_y}{\text{stress}_{3t}} = 1.088$$

The total stress at the grid strap due to the axial force and the resisting moment is

$$\sigma_{gs} := \frac{W_r \cdot a_{lim2}}{A} + \frac{M_r \cdot D}{2 \cdot I}$$

$$\sigma_{gs} = 7.928 \times 10^4 \text{ psi}$$

The safety factor is

$$\frac{\sigma_y}{\sigma_{gs}} = 1.015$$

For this set of assumptions, the stress capacity of the rod cladding has been achieved, so that the limit deceleration is:

$$A_{limit} := a_{lim2}$$

$$A_{limit} = 104.9$$

## Conclusions

An analysis has demonstrated that for the most limiting PWR fuel assembly stored in the HI-STAR 100 fuel basket, a conservative lower bound limit on acceptable axial decelerations exceeds the 60g design basis of the cask. For a reasonable assumption of moment resisting capacity at the grid straps, the axial deceleration limit exceeds the design basis by a large margin.

It is concluded that fuel rod integrity is maintained in the event of a hypothetical accident condition leading to a 60g design basis deceleration in the direction normal to the target.



A schematic diagram of a fuel rod assembly. A central horizontal line represents the 'FUEL ROD'. It is surrounded by a 'GRID STRAP' and a 'FUEL BASKET CELL WALL'. The assembly is shown within a larger structure, with a distance  $L_s$  indicated on the left. Various points and distances are labeled:  $g_1$  at the top,  $g_2$  and  $g_3$  at the bottom, and  $g_4$  at the very bottom. The diagram illustrates the mechanical arrangement and spacing of the fuel rod within the cell wall structure.

FIGURE 2.9.1:  $\mathfrak{g}_1 > 0$

FUEL ROD DEFORMATION PHASES

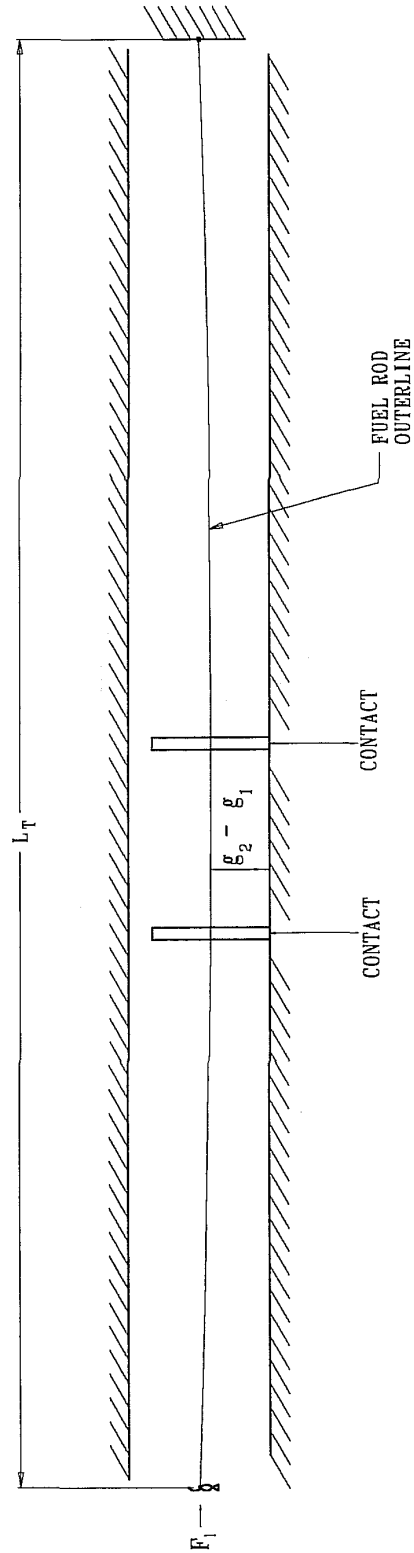
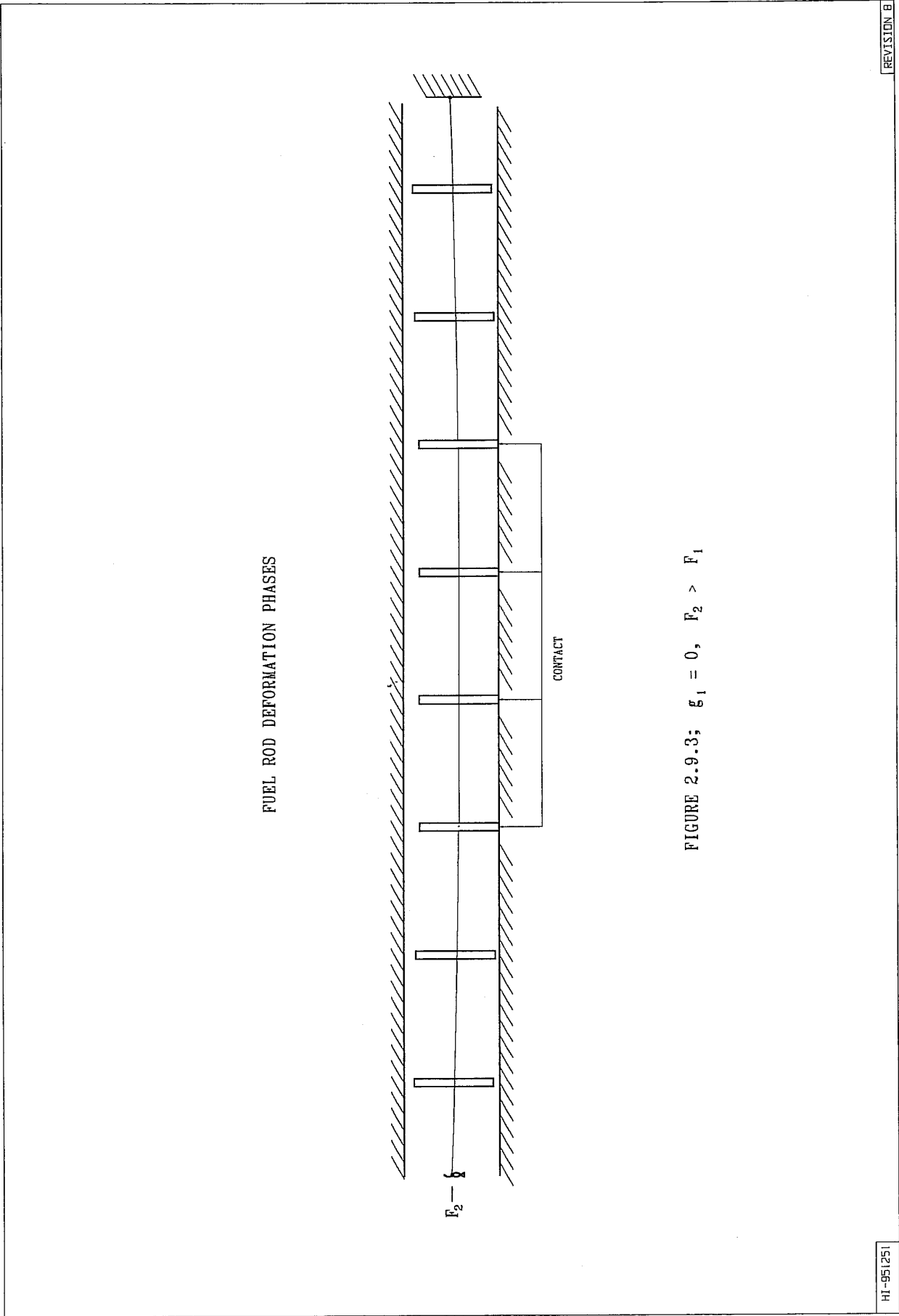


FIGURE 2.9.2;  $g_1 = 0$



FUEL ROD DEFORMATION PHASES

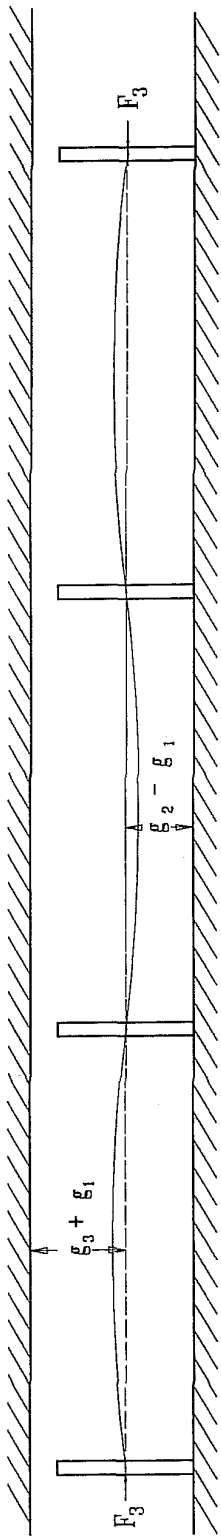


FIGURE 2.9.4; INTER-GRID STRAP DEFORMATION  $F_3 > F_2$

# FUEL ROD DEFORMATION PHASES

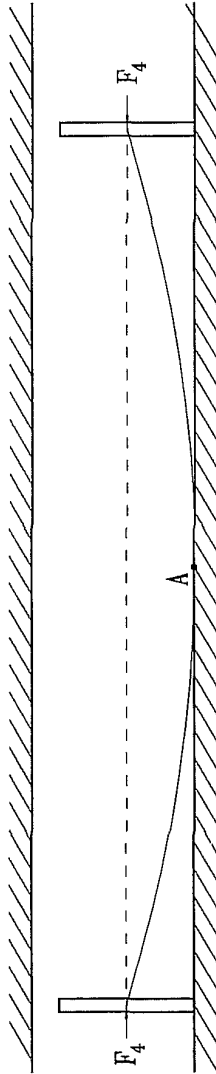


FIGURE 2.9.5; POINT CONTACT AT LOAD  $F_4$   
MAXIMUM BENDING MOMENT AT A

REVISION 8

HI-951251

# FUEL ROD DEFORMATION PHASES

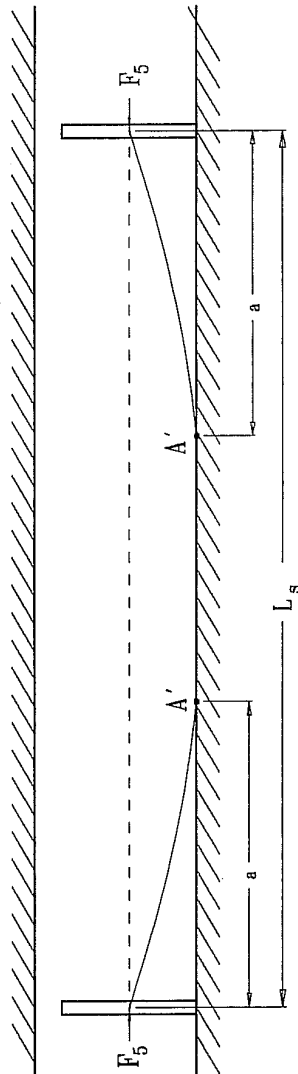


FIGURE 2.9.6; EXTENDED REGION OF CONTACT  
 $F_5 > F_4$ , ZERO BENDING MOMENT AT  $A'$

REVISION B

HI-951251

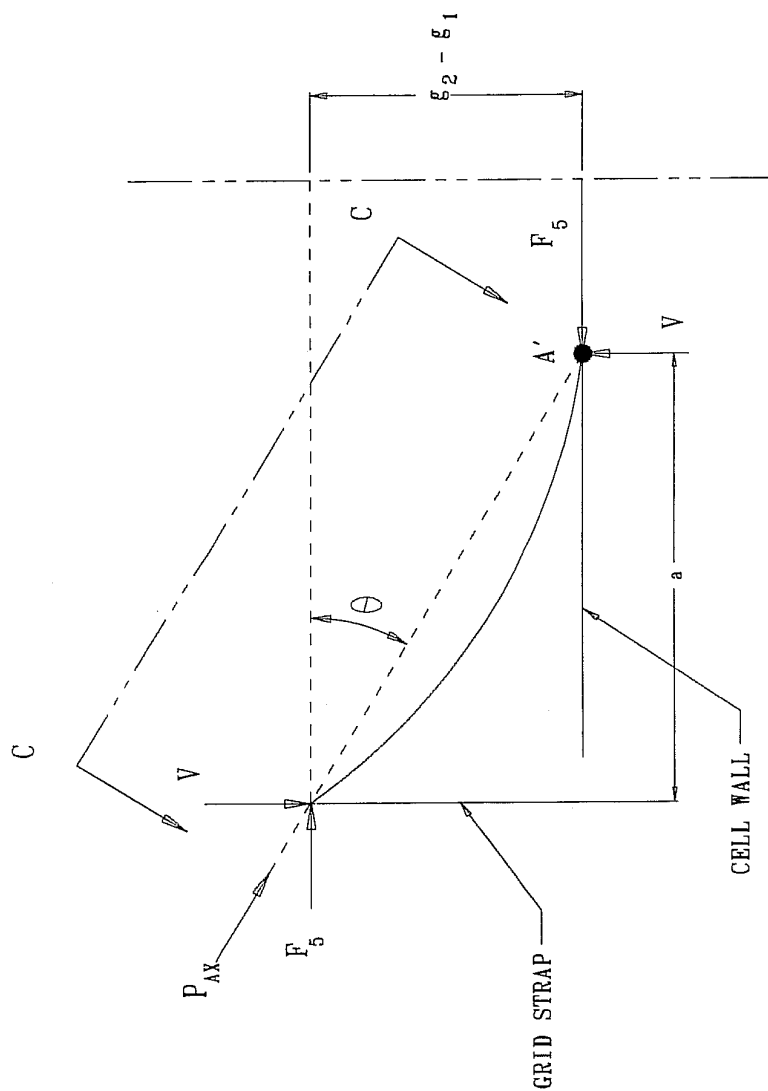
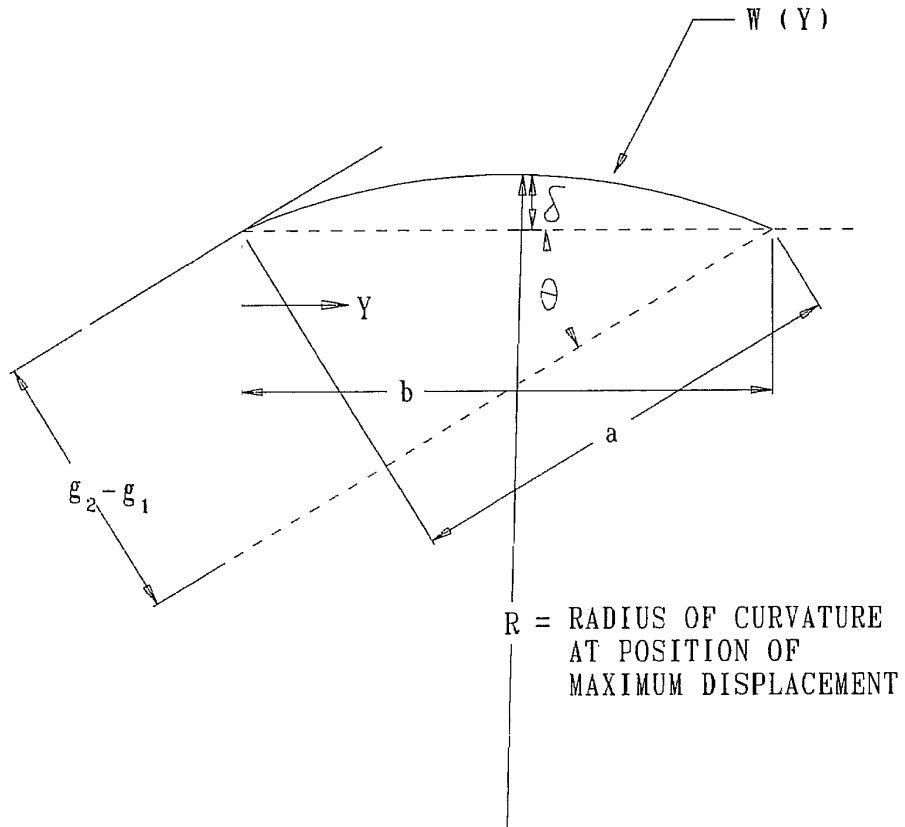


FIGURE 2.9.7; FREE BODY DIAGRAM WHEN MOMENT AT A' = 0  
 $P_{AX} = F_5 / \cos(\theta)$ . RESISTING MOMENT  $M_R$   
 AT GRID STRAP NOT SHOWN



$$Z = R - \delta$$

$$W(Y) = \delta \sin(\pi Y/b)$$

FIGURE 2.9.8; VIEW C - C

HI951251

REVISION 8



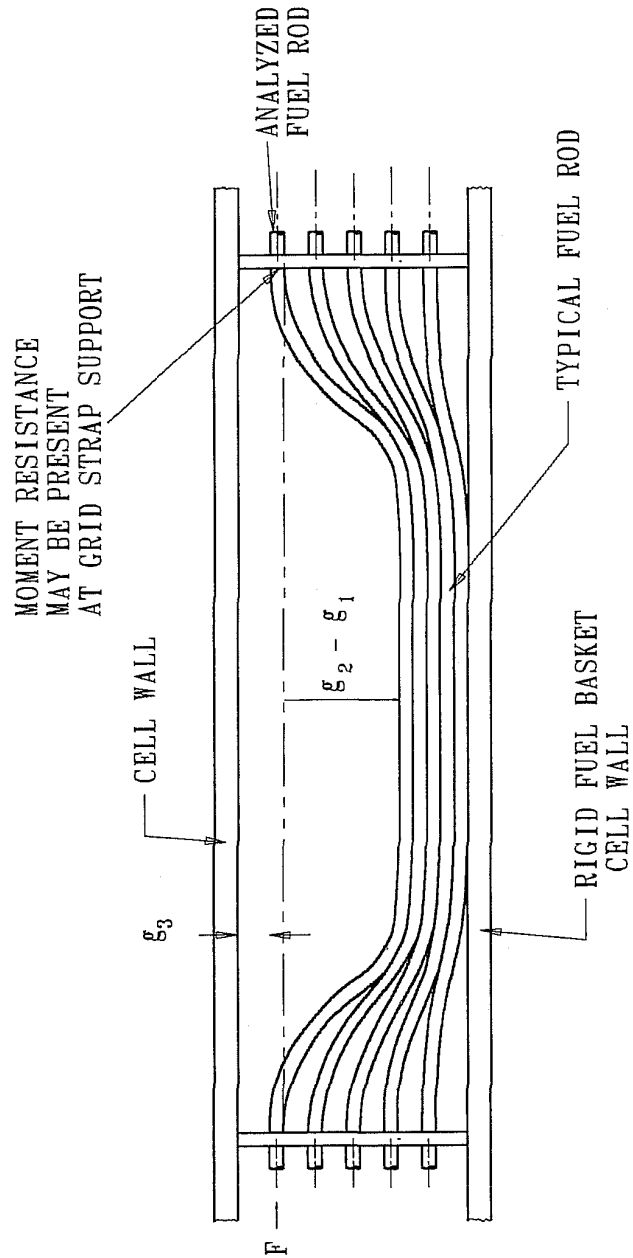


FIGURE 2.9.9; EXAGGERATED DETAIL SHOWING MULTIPLE FUEL RODS SUBJECT TO LATERAL DEFLECTION WITH FINAL STACKING OF ROD COLUMN

REVISION 8

HI-951251

## 2.10 MISCELLANEOUS ITEMS

### 2.10.1 Appendices

The following appendices are included as supplementary material for Chapter 2 of the SAR.

APPENDIX 2.A: IMPACT LIMITER CHARACTERISTICS, DYNAMIC SIMULATION OF  
HYPOTHETICAL ACCIDENT EVENT, AND SCALE MODEL TESTS

(This appendix was 2.H in previous SAR revisions; it has been renumbered reflecting the removal of other appendices from the SAR)

APPENDIX 2.B: SUMMARY OF RESULTS FOR STRUCTURAL INTEGRITY OF  
DAMAGED FUEL CANISTERS

APPENDIX 2.C: EVALUATION OF AN IMPROVED HI-STAR 100 IMPACT LIMITER  
DESIGN BASED ON LS-DYNA DROP SIMULATIONS

ALL OTHER APPENDICES (2.D through 2.AO) - DELETED

### 2.10.2 Summary of NUREG -1617/10CFR71 Compliance

This subsection provides a “road map” of technical information to demonstrate that the SAR in compliance with the provisions of NUREG-1617 and associated referenced sections of 10CFR71 necessary to certify the HI-STAR 100 package for transport.

#### **Description of Structural Design**

The package structural design description and the contents of the application meet the requirements of 10CFR 71.31 and Regulatory Guide 7.9. Applicable sections where this is demonstrated are 1.2.1; 1.3; 1.4; and 2.1.

The codes and standards used in the package design are listed in 1.3. The use of the ASME Boiler and Pressure Vessel Code is in compliance with NUREG/CR-6407, “Classification of Transportation Packaging and Dry Spent Fuel Storage Components”.

#### **Material Properties**

There are no significant chemical, galvanic or other reactions among the packaging components, among package contents, or between the packaging components and the contents in dry or wet environment conditions. The applicable subsection where this is demonstrated is 2.4.4.

The effects of radiation on materials are considered and package containment is constructed from materials that meet the requirements of Reg. Guides 7.11 and 7.12. Applicable subsections where this is demonstrated are: 1.2.1; 2.1.2; and, 2.4.4.

## **Lifting and Tie-Down Standards for All Packages**

Lifting systems meet 10CFR 71.45(a) standards. The applicable section where this is demonstrated is 2.5. The revised tie-down arrangement is not a structural part of the HI-STAR 100 Package. Therefore, 10CFR71.45(b) is not applicable.

## **General Considerations for Structural Evaluation of Packaging**

The packaging structural evaluation meets the requirements of 10CFR 71.35. Applicable chapters and/or sections where this is demonstrated are: 2.5; 2.6; 2.7

## **Normal Conditions of Transport**

The packaging structural performance under normal conditions of transport demonstrate that there will be no substantial reduction in the effectiveness of the packaging. The applicable section where this is demonstrated is 2.6.

## **Hypothetical Accident Conditions**

The packaging structural performance under the hypothetical accident conditions demonstrates that the packaging has adequate structural integrity to satisfy the subcriticality, containment, shielding, and temperature requirements of 10CFR Part 71. The applicable section where this is demonstrated is 2.7.

## **Special Requirement for Irradiated Nuclear Fuel Shipments**

The containment structure meets the 10CFR 71.61 requirements for irradiated nuclear fuel shipments. The applicable section where this is demonstrated is 2.7.

## **Internal Pressure Test**

The containment structure meets the 10CFR 71.85(b) requirements for pressure test without yielding. The applicable subsection where this is demonstrated is 2.6.1.4.3.

## 2.11 REFERENCES

- [2.1.1] 10CFR Part 71, "Packaging and Transportation of Radioactive Materials", Title 10 of the Code of Federal Regulations, Office of the Federal Register, Washington, D.C.
- [2.1.2] Regulatory Guide 7.8, "Load Combinations for the Structural Analysis of Shipping Casks for Radioactive Material", Revision 1, March, 1989, U.S. Nuclear Regulatory Commission.
- [2.1.3] 10CFR Part 72, "Licensing Requirements for the Storage of Spent Fuel in an Independent Spent Fuel Storage Installation", Title 10 of the Code of Federal Regulations, Office of the Federal Register, Washington, D.C.
- [2.1.4] Regulatory Guide 7.6, "Design Criteria for the Structural Analysis of Shipping Cask Containment Vessels", Revision 1, March, 1978, U.S. Nuclear Regulatory Commission.
- [2.1.5] ASME Boiler & Pressure Vessel Code, Section III, Subsection NB, American Society of Mechanical Engineers, 1995.
- [2.1.6] ASME Boiler & Pressure Vessel Code, Section III, Subsection NG, American Society of Mechanical Engineers, 1995.
- [2.1.7] ASME Boiler & Pressure Vessel Code, Section III, Subsection NF, American Society of Mechanical Engineers, 1995.
- [2.1.8] Code Case N-284, "Metal Containment Shell Buckling Design Methods", Section III, Division 1, Class MC, Approval Date 8/25/80.
- [2.1.9] NUREG-0612, "Control of Heavy Loads at Nuclear Power Plants", United States Nuclear Regulatory Commission, July, 1980.
- [2.1.10] ANSIN14.6-1993, "American National Standard for Special Lifting Devices for Shipping Containers Weighing 10,000 Pounds (4,500 kg) or More for Nuclear Materials", American National Standards Institute, Inc.
- [2.1.11] ASME Boiler & Pressure Vessel Code, Section II, Part D, American Society of Mechanical Engineers, 1995.
- [2.1.12] ASME Boiler & Pressure Vessel Code, Section III, Appendices, American Society of Mechanical Engineers, 1995.

- [2.1.13] Regulatory Guide 7.11, "Fracture Toughness Criteria of Base Material for Ferritic Steel Shipping Cask Containment Vessels with a Maximum Wall Thickness of 4 Inches", United States Nuclear Regulatory Commission, June, 1991.
- [2.1.14] Regulatory Guide 7.12, "Fracture Toughness Criteria of Base Material for Ferritic Steel Shipping Cask Containment Vessels with a Wall Thickness Greater Than 4 Inches But Not Exceeding 12 Inches", United States Regulatory Commission, June, 1991.
- [2.1.15] NUREG/CR-1815, "Recommendations for Protecting Against Failure by Brittle Fracture in Ferritic Steel Shipping Containers Up to Four Inches Thick".
- [2.1.16] Aerospace Structural Metals Handbook, Manson.
- [2.1.17] ARMCO Product Data Bulletin S-22.
- [2.1.18] NUREG-1617 Standard Review Plan for Transportation Packages for Spent Nuclear Fuel (Draft Report, March 1998).
- [2.1.19] **Regulatory Guide 3.61 (Task CE306-4) "Standard Format for a Topical Safety Analysis Report for a Spent Fuel Storage Cask", USNRC, February 1989.**
- [2.3.1] Hexcel Corporation Publication TSB 120, "Mechanical Properties of Hexcel Honeycomb Materials".
- [2.3.2] Test Report For Aluminum Honeycomb Static Compression Testing Under Different Temperatures, Holtec Proprietary Report HI-981979, June 1998.
- [2.4.1] NRC Bulletin 96-04: Chemical, Galvanic or Other Reactions in Spent Fuel Storage and Transportation Casks, July 5, 1996.
- [2.4.2] L.W. Ricketts, "Fundamentals of Nuclear Hardening of Electronic Equipment", Robert E. Krieger Publishing Company, Malabar, FL, 1986.
- [2.4.3] D.R. Olander, "Fundamental Aspects of Nuclear Reactor Fuel Elements", TID-26711-P1, 1976.
- [2.5.1] **HI-STORM 100 Final Safety Analysis Report, Holtec Report No. HI-2002444, Revision 12, Docket No. 72-1014.**

- [2.5.2] Field Manual of the A.A.R. Interchange Rules, Rule 88, American Association of Railroads, 1996.
- [2.6.1] Theory of Elastic Stability, S.P. Timoshenko and J. Gere, McGraw Hill.
- [2.6.2] Mark's Standard Handbook for Mechanical Engineering, 9<sup>th</sup> Edition.
- [2.6.3] Mok, Fischer, and Hsu, "Stress Analysis of Closure Bolts for Shipping Casks", (NUREG/CR-6007-UCRL-ID-110637), Lawrence Livermore National Laboratory/Kaiser Engineering, 1993.
- [2.6.4] ANSYS Finite Element Code, Version 5.2, ANSYS Inc., 1995.
- [2.6.5] "Structural Calculation Package for MPC", Holtec Proprietary Report HI-2012787, Revision 18.
- [2.6.6] "Structural Calculation Package for HI-STAR Overpack", Holtec Proprietary Report HI-2012786, Revision 4.
- [2.7.1] Shappert, L.B., "Cask Designer's Guide: A Guide for Design, Fabrication, and Operation of Shipping Casks for Nuclear Applications", ORNL-RSIC-68, Oak Ridge National Laboratories, Feb. 1970.
- [2.7.2] American Society of Civil Engineers, Structural Analysis and Design of Nuclear Power Plants, ASCE No. 58.
- [2.7.3] NUREG/CR-6322, "Buckling Analysis of Spent Fuel Basket", Lawrence Livermore National Laboratory, May, 1995.
- [2.7.4] "Benchmarking of the LS-DYNA Impact Response Prediction Model for the HI-STAR Transport Package Using the AL-STAR Impact Limiter Test Data", Holtec Proprietary Report HI-2073743, Revision 1.
- [2.7.5] HI-STAR 60 (Docket 71-9336) Safety Analysis Report, Holtec Report HI-2073710, Revision 2.
- [2.7.6] HI-STAR 180 (Docket 71-9325) Safety Analysis Report, Holtec Report HI-2073681, Revision 3.
- [2.7.7] *Intentionally deleted.*
- [2.9.1] Chun, Witte, Schwartz, "Dynamic Impact Effects on Spent Fuel Assemblies", UCID-21246, Lawrence Livermore National Laboratory, October 20, 1987.
- [2.9.2] Physical and Decay Characteristics of Commercial LWR Spent Fuel, Oak

Ridge National Laboratory Report, J. Roddy, H. Claiborne, R. Ashline, P. Johnson, and B. Rhyne, ORNL/TM-9591/V1-R1, 1/86.

## APPENDIX 2.A: DESIGN, TESTING, AND COMPUTER SIMULATION OF THE AL-STAR™ IMPACT LIMITER

### 2.A.1 INTRODUCTION

As stated in Subsection 2.7, the central purpose of the AL-STAR™ impact limiter is to limit the package maximum deceleration,  $\alpha_{\max}$ , under a postulated drop event to a specified design value. For the regulatory 9-meter hypothetical free drop event, the AL-STAR design is engineered to limit the maximum rigid body deceleration to 60 times the acceleration due to gravity (Table 2.1.10). The HI-STAR packaging, consisting of the loaded overpack and top and bottom impact limiters (illustrated in Figure 2.A.1.1) is essentially a cylindrical body with a rigid interior (namely, the overpack) surrounded by a pair of relatively soft crushable structures. The crushable structure (impact limiter) must deform and absorb the kinetic energy of impact without detaching itself from the overpack, disintegrating, or otherwise malfunctioning. A falling cylindrical body may theoretically impact the target surface in an infinite number of orientations; the impact limiter must limit the HI-STAR 100 decelerations to below 60g's and preserve the limiter-to-overpack connection regardless of the impact orientation. Figure 2.A.1.2 presents the side drop event. In general, a drop event orientation is defined by the angle of the HI-STAR 100 longitudinal axis,  $\theta$ , with the impact surface. In this notation,  $\theta = 0$  means a side drop and  $\theta = 90^\circ$  implies a vertical or end drop scenario. Inasmuch as the top and bottom impact limiter are made of identical crush material, the top or bottom vertical drop events are mathematically and physically equivalent as far as the impact limiter design is concerned. In any orientation, the drop height is measured from the lowest point on the package.

An intermediate value of  $\theta$ ,  $\theta = 67.5^\circ$ , warrants special mention. At  $\theta = 67.5$  degrees, the point of impact is directly below the center of gravity (C.G.) of the HI-STAR 100 package. This drop orientation is traditionally called the C.G.-over-corner (CGOC) configuration. The CGOC orientation is the demarcation line between single and dual impact events. At  $90^\circ > \theta > 67.5^\circ$ , the leading end of the packaging (denoted as the “primary” impact limiter) is the sole participant in absorbing the incident kinetic energy. At  $\theta < 67.5^\circ$  drop orientations, the initial impact and crush of the leading (primary) impact limiter is followed by the downward rotation of the system with the initial impact surface acting as the pivot, culminating in the impact of the opposite (secondary) impact limiter on the target surface. In the dual impact scenarios, the first and second impact limiter crush events are referred to as the “primary” and “secondary” impacts, respectively. It is reasonable to speculate that for certain values of  $\theta$ , the secondary impact may be the more severe of the two. As stated earlier, the design of AL-STAR must ensure that  $\alpha_{\max} \leq 60$ , regardless of the value of  $\theta$ .

The AL-STAR attachment design must ensure that both impact limiters remain attached to the cask during and after the impact event. The impact limiters are also required to prevent cask body-to-unyielding target contact.



Finally, the package design must satisfy all criteria in ambient temperature conditions ranging from -20° to 100°F, and with humidity ranging from 0 to 100%. Therefore, the impact limiter design must be functionally insensitive to temperature and environmental conditions.

An aluminum honeycomb-based impact limiter design was selected as the preferred material for development. The detailed design of the AL-STAR impact limiters is presented in Holtec Drawing C1765 located in Section 1.4. A pictorial view of AL-STAR is presented in Figure 2.A.1.3.

Figure 2.A.1.3 indicates that in addition to the crushable honeycomb, the AL-STAR contains two internal cylindrical shells (also denoted as “rings”), which are stiffened with radial gussets. These carbon steel shells are sized to behave as undeformable surfaces during impact events. They are essentially the “backbone” of the impact limiter, lending a predictability to the impact limiter crush behavior and forcing the energy absorption to occur in the honeycomb metal mass. The design of this backbone structure was a subject of in-depth computer and experimental 1/8 scale static testing, as documented in Holtec Report HI-962501 [2.A.4] and summarized in Section 2.A.4 herein.

Another noteworthy aspect of the AL-STAR impact limiter design is the arrangement of uniaxial and cross core (biaxial) honeycombs. Regions of the honeycomb space that experience impact loading in only one direction are equipped with unidirectional honeycomb sectors. The regions where the direction of the impact loads can vary have cross-core (bi-directional) honeycomb material, as detailed in Subsection 2.3.1.5.

To summarize, the design objectives of the AL-STAR impact limiter are set down as five discrete items, namely:

- i. Limit peak deceleration ( $\alpha_{\max}$ ) to 60g's under all potential drop orientations.
- ii. Impact limiter must not detach from the cask under a 9-meter drop event, under any impact orientation.
- iii. The impact limiters must bring the cask body to a complete stop, such that the overpack does not come in physical contact with the target surface.
- iv. Crush material must be equally effective at ambient temperature conditions ranging from -20° to 100°F, with humidity ranging from 0 to 100%.
- v. All external surfaces must be corrosion-resistant.

The last two objectives are realized by utilizing aluminum honeycomb (Type 5052) as crush material and stainless steel (Type 304), for the external skin enclosure. As shown in the ASME Code (Section II, Part D, Table Y-1), the essential property of the constituent material for the honeycomb and the external skin, namely the yield strength remains constant in the -20° F to

100° F range. The surface of the carbon steel impact limiter backbone is painted to limit corrosion.

The remaining design objectives, namely, limiting of the maximum rigid body deceleration,  $\alpha_{\max}$ , to 60 g's under a 9-meter drop event, maintaining positive attachment of the AL-STAR impact limiters to the overpack, and preventing contact of the overpack with the unyielding surface, are demonstrated by a combination of numerical simulations and scale model static and dynamic testing. This was accomplished through a research and development effort that is broadly subdivided into six phases, as follows:

- Phase 1: Characterize the honeycomb pressure-deflection relationship.
- Phase 2: Propose a force (static) vs. crush (F vs. d) model for AL-STAR.
- Phase 3: Perform 1/8 scale model static compression tests to validate the force-crush model and to establish the adequacy of the AL-STAR backbone structure.
- Phase 4: Conduct 9-meter quarter-scale model dynamic drop tests in selected limiting drop configurations and obtain test data.
- Phase 5: Simulate the experimental drop tests with a suitable “dynamic model” and establish that the dynamic model predictions of deceleration, crush and event time duration reasonably match the experimentally measured values. A reasonable prediction of the peak decelerations of each drop event is the minimum for the dynamic model to be acceptable.
- Phase 6: Utilize the experimentally confirmed dynamic model to evaluate the effects of tolerances on crush properties and on package weight, and to confirm the adequacy of the full-scale impact limiter design.

It is of crucial importance that the dynamic model benchmarked in Phase 5 be of high reliability, since it becomes the analytical model for the accident-event response prediction of the packaging when tolerances on material behavior and package mass are considered (Phase 6).

In this appendix, a description of the overall program and results for each of the six phases is presented.

### 2.A.2 Phase 1: Material Pressure-Crush Relationship

The extent of deflection,  $\Delta$ , sustained by a honeycomb material when subjected to a uniform pressure,  $p$ , is an essential element of information in the impact limiter design. Towards this end, coupon specimens of uniaxial and cross-core honeycomb of various nominal crush strengths and

densities were compression-tested by the material manufacturer. The results showed that all honeycomb coupons shared some common load-deflection characteristics, namely:

The initial pressure-deflection curve resembled an elastic material (pressure roughly proportional to deflection).

Upon reaching a limiting pressure, the material crushed at near constant pressure until the crush reached approximately 60-70 percent of the initial thickness. The required crush force had to increase rapidly to achieve small incremental crushing for strains beyond approximately 60-70 percent.

Figure 2.A.2.1 shows a typical static pressure-deflection curve for a 1”-thick honeycomb specimen. The curve with the initial peak is that of an un-precrushed honeycomb specimen; the curve without the peak (shown as a dashed line only where a difference occurs) corresponds to a pre-crushed specimen. Dynamic testing subsequently showed that removal of the initial peak by pre-crushing the material was a desired feature whenever a large flat area of honeycomb material experienced a crush force (such as in a 90 degree end drop).

Curve fitting of data from all tested coupons indicated that a single mathematical relationship between the applied pressure and compression strain could be developed. The mathematical relationship can provide a reasonable fit for coupons of all crush strengths (crush strength defined as the pressure corresponding to the flat portion of the curve in Figure 2.A.2.1; i.e., it is the constant pressure at which the honeycomb undergoes near-perfect plastic deformation). In other words, the pressure,  $p$ , for a given strain,  $\epsilon$ , is represented by a unique function of the crush pressure,  $p_c$ , i.e.

$$p = f(p_c, \epsilon)$$

The relationship between  $p$  and compression strain was used in the subsequent mathematical efforts to simulate AL-STAR crush behavior. The above mathematical relation was developed to simulate material behavior for a honeycomb material under both non-pre-crushed and pre-crushed conditions.

### 2.A.3 Phase 2: Static Force-Crush Prediction Model

An essential step towards the development of a reliable dynamic model to simulate the impact of a dropped HI-STAR 100 package is to develop a static force-crush model that can subsequently be validated by scale model tests. The force-crush model should reliably duplicate the resistance provided by an impact limiter for a range of crush orientations for the full range of crush depths.

The required force-crush model for AL-STAR is developed using the concept of interpenetration, which is explained using the case of the side drop ( $\theta = 0$ ) as an example (Figure 2.A.3.1(a)).

The condition existing in all impact limiter drop scenarios is that the relatively soft honeycomb material lies between two “hard” surfaces that are advancing towards each other during the impact. One of these two rigid surfaces is the essentially unyielding target (Rigid Body 1) and the other is the structural backbone of the impact limiter (Rigid Body 2). While the target surface is flat, the backbone structure is cylindrical in profile. When squeezed between the two surfaces, the honeycomb material (at each instant in time) will crush at one or both interface locations. To determine which interface surface will undergo crushing at a given point during the impact event, the concept of interpenetration area is utilized as explained below.

In this concept, two separate crush scenarios, one assuming that the crush occurs at the external interface (target-to-impact limiter), and the other assuming that the crushing is at the internal interface (structural backbone/overpack-to-impact limiter), are compared at each instant during a simulated compression of the impact limiter. A metal honeycomb impact limiter, in general, may have multiple honeycomb material sections crushing at each interface. For simplicity in explaining the concept of interpenetration, we assume that each of the interfaces is characterized by a uniform distribution of honeycomb having crush pressures  $p_1$  and  $p_2$ , respectively. To determine the resistive force developed to crush the impact limiter by a small amount,  $d$ , against the external target, the impact limiter is assumed to penetrate the target by the amount “ $d$ ” without deformation. The resulting area  $A_1$  for the case of side drop, illustrated in Figure 2.A.3.1(b), can be computed as an algebraic expression in the amount of approach,  $d$ . (For oblique drop events, ANSYS [2.A.1] or CADKEY [2.A.2] are used to compute interpenetration area as a function of incremental interpenetration.) The pressure-compression relationship for the honeycomb stock at the external interface provides the crush pressure  $p_1$  that develops due to deformation “ $d$ ”. The total force required for crush “ $d$ ”, at the external interface, is therefore equal to  $p_1 A_1$ .

In the second (independent) scenario, the impact limiter external surface is assumed to undergo no movement; rather, the backbone structure (along with the overpack) advances towards the target by an amount  $d$  (Figure 2.A.3.1(c)). Once again, assuming that the cylindrical rigid body moves through an amount “ $d$ ”, the resistance pressure developed in the honeycomb material lying in the path of penetration is available from the appropriate material pressure-compression curve. If the pressure corresponding to the deformation is  $p_2$  and the projected area at the internal interface is  $A_2$ , then the total resistive force encountered in realizing an approach equal to “ $d$ ” between the overpack-backbone assemblage and the target under this latter scenario is  $p_2 A_2$ . In an actual drop event, at each instant during the event, incremental crush occurs at one of the two interfaces. If  $p_1 A_1 < p_2 A_2$  at a given instant then crushing will occur at the external interface. Likewise,  $p_1 A_1 > p_2 A_2$  will imply that crushing will occur internal to the impact limiter. The smaller of  $p_1 A_1$  and  $p_2 A_2$  is the required crush force and the corresponding location of crush is where the honeycomb material will compress to realize the approach equal to  $d$ . This “inequality test” to determine where crushing occurs is performed at every increment of crush during the simulation of the event. The appropriate value of the crush force is used in the equilibrium equations at that instant. The concept of interpenetration at two interfaces has been confirmed during testing of the impact limiters; the total crush is observed to be a sum of compression at each of the two interfaces.

To construct a mathematical force-deformation relationship for AL-STAR in any given orientation, the above process is repeated as the crush “d” is increased in small increments starting with the beginning of compression ( $d = 0$ ). It is quite clear that the development of the force-deflection model (F-d model) for AL-STAR in any orientation is a straightforward analysis in 3-D geometry. The F-d curve for AL-STAR for any given value of  $\theta$  can be developed where, other than the geometry of the impact limiter, the crush strengths  $p$  of the honeycomb materials utilized in the impact limiter are the only other required inputs.

The force (F) vs. crush (d) relationship developed using the foregoing method is referred to as the F-d model that is subject to validation by appropriate 1/8 scale model compression tests described in the following section.

#### 2.A.4 Phase 3: One-Eighth Scale Model Static Compression Tests

The 1/8 scale model tests consist of subjecting scaled replicas of the full-size AL-STAR to static compression tests in an engineered fixture such that the force-compression curve for the scaled model can be obtained in various orientations of compression. The scale model is made by making the diameters and length of the model one-eighth of the full-size AL-STAR. The thicknesses of the backbone components (i.e., the inner and outer shells and gussets), and the external skin (see Figure 2.A.1.3) are also scaled to one-eighth times the corresponding dimensions (to the nearest sheet metal gage, where applicable) in the full-size AL-STAR. In the one-eighth model, the performance of the attachment system is not assessed nor is the cask body modeled. However, the interface between overpack and impact limiter where the compression load is resisted is properly simulated. The crush pressure is a material property of the energy absorbing material; therefore, the material (and its density) is not scaled. The 1/8 scale model, therefore, has approximately  $(1/8)^3$ , or 1/512 the volume and weight of the full-size unit. Holtec documents [2.A.3, 2.A.4] provide complete details on the 1/8 scale model geometry and fabrication. The static compression behavior of such a 1/8-scale model is correlated with that of a full-size unit using the geometric scaling information. For example, under an axial compression test the area under crush in the scale model will be 1/64 of the full-size AL-STAR (recall that the diameter is scaled down by a factor of 8). Therefore, the crush force (which is crush force pressure times the area under crush) will be 1/64 of the full-size unit. On the other hand, the crush stroke (extent of deformation before “lock up”) will be 1/8 of the full-size AL-STAR because the axial length of the scale model (which corresponds to the height of the crush column in axial compression) is one-eighth of the full-size hardware. Thus, the total energy absorbed (force times compression) will be  $(1/8)^3$  of the full-size unit. The same scaling factor can be shown to apply in all directions of crush.

In summary, the 1/8 scale model scales the geometric dimensions of AL-STAR. The previously discussed F-d model is required to translate the force-crush relationship from the 1/8 scale replica to the full-size unit. In order to use the analytical F-d model as a valid vehicle for predicting the force-crush of the full-size (or quarter-scale) AL-STAR, it is necessary to check its prediction ability against actual test data from 1/8-scale model static compression tests.

The objectives of static scale model tests are twofold:

- i. Determine whether the static force-crush relationship predicted by the F-d model appropriately simulates the actual relationship determined by test;
- ii. Determine whether the backbone structure of the AL-STAR impact limiter is sufficiently rigid to withstand and transmit the large loads associated with the postulated accident scenarios.

#### 2.A.4.1 Static Compression Tests on Initial Candidate Crush Material

To assess compression performance, a QA validated AL-STAR static test procedure was prepared [2.A.3] for the one-eighth scale model static compression tests and a series of cold and hot static compression tests performed on an impact limiter configuration with the initial candidate crush material. Holtec calculation package HI-961501 [2.A.4] contains a comprehensive documentation of the 1/8 scale static test program and results for the impact limiter configuration. A summary of the complete test program and test results is presented below.

Four 1/8-scale models were fabricated with details of the impact limiter carefully scaled, including the stiffening cylinders and the stainless steel skin. No impact limiter attachment bolts were incorporated in the model.

Aluminum honeycomb segments provided for the 1/8-scale models were manufactured utilizing the same procedures and processes as for the full-scale impact limiter. As stated earlier, the crush strengths were not scaled because they are considered as material properties.

An adjustable 1/8 scale static test fixture was designed, analyzed, and fabricated. The test fixture interfaced with the impact limiter and simulated the overpack hard surface. The test fixture could be adjusted to simulate any crush orientation. Figure 2.A.4.1 shows the test fixture and the 1/8 scale impact limiter being loaded in the heavy-load testing machine.

The following static one-eighth scale test series were carried out:

Test No.	Orientation, degrees	Temperature
1	0 (side)	+120°F
2	30 (oblique)	Ambient
3	60 (oblique)	Ambient
4	90 (end)	-30°F

For all tests except the end compression (where the orientation is immaterial), the circumferential orientation of the impact limiter was selected so that the initial point of contact between the impact limiter and the test machine was at the interface of two aluminum honeycomb sections. After each test, the impact limiters were cut open and examined.

### Observations Based on 1/8 Scale Model Testing

- Effect of Ambient Temperature:

The end compression test was performed with the impact limiter cold (-30°F), the side compression test was performed with the impact limiter hot (+120°F), and the two oblique tests performed at ambient temperature. The material behavior showed no influence of test temperature. This confirms the expected result since the aluminum honeycomb and stainless steel skin yield strengths are insensitive to temperature in the range of interest (-20° F to 100° F) as prescribed in Table Y-1 of the ASME Code.

- Side compression orientation - 0 degree:

The inner stiffening cylinder experienced considerable permanent deformation. The gussets which buttress the inner cylinder buckled. The outer stiffening cylinder performed elastically.

- Oblique compression orientation:

Two oblique orientation static tests were performed. The 30-degree oblique test again showed the need to thicken the inner stiffening cylinder and to rearrange the stiffening gussets.

The 60-degree oblique test was a complete success; no plastic deformation of the backbone structure was indicated.

As would be expected, in those cases where the hard region (backbone structure) of the impact limiter sustained deformations, the scale model exhibited greater flexibility in the physical testing than the analytical prediction (the flexibility of the backbone structure added to the crush of the honeycomb resulting in a greater total measured deflection).

- End compression orientation - 90 degree:

The end-compression orientation is, structurally speaking, the least complicated of the four test configurations. The loading of the AL-STAR scale model in this test is purely axisymmetric. The initial peak in the pressure/deformation curve seen in the coupon tests (Figure 2.A.2.1) was clearly evident in the axial (end) compression test (Figure 2.A.4.3). The backbone structure performed without sustaining plastic deformation.

- Comparison of experimental and analytical predictions

Out of the four static 1/8-scale model tests, two tests (side compression and 30-degree oblique) were unsatisfactory because the backbone structure of the impact limiter did not remain elastic. These tests served to identify the need to reinforce the AL-STAR backbone structure. The other tests, namely end-compression (90 degree) and 60-degree oblique, wherein the backbone structure performed as designed, showed close agreement with the numerical model. Figures 2.A.4.3 and 2.A.4.4, respectively, show the static test results for 90-degree (end-compression) and 60 degree (oblique) cases, along with the prediction of the F-d model. There is good agreement between the computer model and the test data.

In summary, the 1/8 scale model static test program identified the required design changes to the internal structure of the impact limiters. The 1/8 scale model tests showed that the load-compliance characteristics of AL-STAR are insensitive to the changes in the ambient environment. A comparison of the test results with the mathematical model predictions from the F-d model indicated that the mathematical model was in good agreement with 1/8-scale static crush tests whenever the backbone structure performed as required (i.e. remained elastic). Since the crush geometry of the scale model was *not altered* by the strengthening of the backbone, any subsequent reinforcing of the backbone did not alter the F-d relationship for the impact limiter. The two successful static tests that showed excellent agreement with the computer F-d model, therefore, continued to serve as a valid benchmark of the numerical model after the backbone is stiffened. The reinforced backbone structure is incorporated into the final design drawings for the AL-STAR, and was confirmed as acceptable during the dynamic (1/4-scale) model drop tests. Subsequent to the one-quarter scale dynamic tests and the analytical correlation (Phases 4-6), three additional 1/8<sup>th</sup> scale confirmatory static tests were performed on impact limiters that included the internal backbone structure and the final crush material orientations used in the quarter-scale drop tests and in the analytical correlation. These additional confirmatory static tests were performed at room temperature. The tests simulated the crush orientation corresponding to the side drop, the “center-of-gravity-over corner” drop, and the end drop, respectively. Force-deflection results from the static test are compared with the predictions from the theory for the 1/8<sup>th</sup>-scale impact limiters. Subsection 2.A.10 discusses the results obtained from these three additional static tests.

#### 2.A.5 Phase 4: 9 Meter Quarter-Scale Model Drop Tests

The one-quarter scale model dynamic tests provide physical confirmation of the HI-STAR impact limiter design and the performance of the attachment system.

In the 1/4 scale model drop test program, an instrumented scale model of the HI-STAR 100 dual-purpose cask was assembled with the top and bottom AL-STAR impact limiters, raised to a height of 9 meters (measured from the lowest point on the package), and then released to free fall onto an unyielding concrete and steel armor target (unyielding target). The impact limiter attachment system is reproduced in the model using the appropriate scale for bolt diameters, etc.



A detailed description of the quarter-scale model, instrumentation, data acquisition, and data processing is presented in a proprietary Holtec document [2.A.7]; a concise self-contained summary is provided in the following.

#### 2.A.5.1 Test Plan:

The drop test program was performed at the drop testing facilities at the Oak Ridge National Laboratory. The target at the ORNL facility complies with guidance of IAEA Safety Series 37, Article A-618.

The quarter-scale model testing of the package required the design and fabrication of scale models of AL-STAR, the HI-STAR overpack, and the multi-purpose canister. The quarter-scale replicas of AL-STAR were prepared using the scaling procedure described previously in the context of the 1/8 scale model. In the scale model for the MPC and the overpack, the emphasis is in scaling the weight and moment of inertia, because it is these properties (translational as well as rotational) which are key to the response in the drop event. A schematic of the MPC design used in the scale model is shown in Figure 2.A.5.1. The weight of the MPC replica was set at 1,380 lbs (to simulate an 88,320 lb loaded multi-purpose canister).

The overpack scale model likewise is a cylindrical body whose length and outside diameter are 1/4, whose weight is 1/64, and whose mass moment of inertia is 1/1024 of the respective design parameters in the full-size hardware, as summarized below:

Key Quarter Scale HI-STAR Overpack Model Data			
Length (inch)	O.D. (nominal) (inch)	Overpack Plus MPC Weight (lb.)	Mass Moment of Inertia About a Transverse Centroidal Axis (Overpack Plus MPC) (lb.-in <sup>2</sup> )
50.7813	21	3,733	1.351E+06

Figures 2.A.5.2 through 2.A.5.4 illustrate the principal geometric data of the quarter-scale overpack model. It is evident from the above description that the quarter-scale model is, from a geometrical and inertia standpoint, a quarter-scale emulation of a 84" diameter x 203.125" long, 238,900 lb. (approximate) HI-STAR system (overpack and loaded MPC). Finally, the attachment bolts which join the impact limiter to the overpack are also scaled down to 25% of their size in the full-size hardware (in both diameter and thread engagement length), as can be seen from Figures 2.A.5.3 and 2.A.5.4 or the applicable drawing in Section 1.4.

The one-quarter scale drop tests were performed with four discrete orientations of the cask longitudinal axis with respect to the impact surface, as defined below.

Test A – Vertical Drop (Top End): The cask is dropped such that the deceleration of the cask upon impact is essentially vertical.

Test B: Center of Gravity-Over-Corner (CGOC): For HI-STAR 100, C.G.-over-corner means an orientation wherein the axis of the cask is at  $67.5^\circ$  from the horizontal at the instant of release at the 9-meter height. This test seeks to establish the adequacy of the impact limiter under non-symmetric impact loading.

Test C – Side Drop: The cask is held horizontal with the lowest point on the package 9 meters above the target surface when released for free fall. In this test, both impact limiters participate, and the impact impulse is essentially equally divided between them.

Test D – Slapdown: In this test, the cask axis is held at  $15^\circ$  from the horizontal with the lowest point of the cask assembly at 9 meters from the impact surface. The orientation is such that the top end impact limiter impacts the surface first and the bottom end impact limiter experiences the secondary impact.

Each of the four tests has distinct impact characteristics. For example, in the “side drop” test both impact limiters will strike the target simultaneously; only one impact limiter sustains impact in the “end drop” test. The CGOC test involves a primary impact on one impact limiter at an angle such that the gravity vector is oriented with a line passing through the cask center of gravity and the lowest corner of the limiter. Finally, the slapdown test involves impact at both impact limiters with a very slight time separation. These four tests are deemed to adequately represent the limiting impact scenarios under the hypothetical accident conditions of 10CFR71.73.

The torque values used to secure the attachment bolts in the scale model package warrant special mention. The impact limiter attachment bolts serve two major functions during transportation:

1. During normal transport, the attachment bolts ensure that the impact limiters remain attached to the HI-STAR 100 overpack during a 10g axial deceleration as mandated by 10CFR71.45, and during exposure to normal vibratory loading that may reasonably be expected during the course of a normal transport operation. To ensure against loss of attachment due to vibratory loading during normal transport, an initial bolt pre-stress of 30,000 psi has been set, based on common engineering practice. For the bolt diameters specified for the HI-STAR 100 package, the pre-load torque is 245 ft-lb and 1,500 ft-lb for the top and bottom impact limiter attachment bolts, respectively.
2. During the hypothetical accident, the attachment bolts ensure that the impact limiters remain attached to the HI-STAR 100 overpack during and after the impact with the unyielding surface.

The bottom impact limiter is attached to the overpack by 16 bolts aligned with the longitudinal axis of the overpack and arranged in a circular pattern (Figure 2.A.5.4 shows the bottom view of the one-quarter scale replica). These bolts perform their function by developing tensile stress to resist loading during the hypothetical accident. Because of close clearances with the overpack shielding, the bottom impact limiter also has a set of eight circumferentially arranged alignment

pins that fit into mating holes in the overpack bottom plate. These mating holes are plugged when the impact limiter is not in place.

The top impact limiter is attached to the overpack using twenty radial bolts that are designed to resist relative motion and transfer loads by shear (Figure 2.A.5.3 shows the top view of the one-quarter scale replica).

Although the attachment analyses do not require pre-load (by application of an initial bolt torque) to demonstrate that the required performance during normal transport conditions is achieved, the presence of pre-load serves only to enhance the performance of bolting which resists loads by developing tensile bolt forces (bottom impact limiter attachment bolts). Pre-stress in the bottom impact limiter attachment bolts serves to develop an interfacial pressure between the two components being joined together. This interfacial pressure acts as a reserve against separation at the interface of the impact limiter and the overpack when the external force or moment act to separate them during the drop event. The actual tensile stress bolt will rise significantly over the initial pre-stress if and only if the external load acting to break apart the interface is large enough to cancel out the interfacial pressure.

The effect of pre-load on the performance of bolting that resists loads by shear (top impact limiter attachment bolts) is different. The presence of both tensile stress (due to bolt pre-load) and shear stress in the bolt (due to the impact loads in a drop event) will increase the maximum principal stress in the bolt, which will consequently reduce the shear capacity of the bolts. Applying a pre-load in excess of the required amount in the 1/4 scale HI-STAR 100 drop tests will therefore result in a conservative evaluation of the top impact limiter attachment bolts.

Based on the initial torque values set in the full-scale package, the appropriate bolt pre-load torque for the 1/4-scale impact limiter attachment bolts is (to the nearest foot-pound):

Top impact limiter (radial) bolts: 4 ft.-lb. (full scale equivalent = 245 ft.-lb.)  
 Bottom impact limiter (axial) bolts: 23 ft.-lb. (full scale equivalent = 1500 ft.-lb.)

Since a bolt pre-load will enhance the performance of bolts (located at the bottom impact limiter interface) that resist loading by developing tensile stress, the bolt torque was conservatively set at 20 ft.-lb. or below for the bottom impact limiter bolts. Since a bolt pre-load will degrade the performance of bolts (located at the top impact limiter interface) that resist loading by developing shear stress, the bolt torque was conservatively set at 4 ft.-lb. or above for the top impact limiter bolts.

The end drop onto the top impact limiter tests the resistance of the twenty radial attachment bolts against failure from shear. The use of an initial torque value (15 ft.-lb.), in excess of 4 ft.-lb., is conservative for evaluation of the performance of the bolts to resist shearing strains (i.e., as noted earlier, due to an interaction relation between tension and shear, the presence of any tensile strain will reduce the allowable shear strain prior to failure).

The C.G. over corner drop used an initial torque of 15 ft-lb., a value below the mandated value of 20 ft-lb. on the bottom impact limiter. This is again conservative for the evaluation of the performance of the bottom impact limiter attachment bolts, since the presence of additional prestress would enhance the ability of the bolts to retain the impact limiter in position.

The slapdown test was performed using low initial bolt torque values for both impact limiters that simulated "hand-tight" values. Thus, there is almost no contribution from pre-load on the bolts on either impact limiter. In the slapdown drop, the bottom impact limiter experienced the largest deceleration. This test demonstrated that the use of a lower pre-load on the most highly loaded attachment bolt does not affect the ability of the bolts to perform their required function.

Finally, the final side drop used the bolt pre-loads that correlate with the final bolt pre-loads specified (top impact limiter - 4 ft-lb.; bottom impact limiter - 20 ft-lb.) for the one-quarter scale tests.

A minimum of five calibrated unidirectional accelerometers was installed on the test package for each test. Schematics of the accelerometer locations and numbering system for all four tests are presented in Figures 2.A.5.5 and 2.A.5.6.

The accelerometers are placed at three axial locations along the height of the overpack model and at different circumferential locations at each axial location. The placement of the accelerometers axially reflects locations consistent with the detailed 2-D finite element analyses of the MPC that conservatively neglected the effect of stiffening provided to the MPC shell by the MPC baseplate. Figure 2.A.5.2 shows the three cutouts of the outer 5/8" thick cylinder that are machined flat to position the accelerometers. The following table provides the locations of the accelerometers.

ACCELEROMETER LOCATIONS FOR ONE-QUARTER SCALE DROP TESTS								
NUMBER	TOP END DROP		SIDE DROP		SLAPDOWN		CG-OVER-CORNER	
	Axial (inch)	Peripheral (degrees)	Axial (inch)	Peripheral (degrees)	Axial (inch)	Peripheral (degrees)	Axial (inch)	Peripheral (degrees)
1	44.781	0	5	0	44.781 25	0	5	0
2	25	0	25	0	25	0	5	+120
3	5	0	44.781	0	5	0	5	-120
4	44.781	+120	25	+90	44.781	+120	44.781	0
5	44.781	-120	25	-90	44.781	-120	44.781	+120
6	5	+120	--	--	5	+120	44.781	-120

## Notes:

1. All accelerometer axial distances measured from top end surface of overpack model (without impact limiters in place).
2. Peripheral locations measured from plane containing accelerometer #1; clockwise direction, viewed from Section A-A in Figures 2.A.5.5 and 2.A.5.6, is positive.

In addition to recording the deceleration during impact, a high-speed camera and a video camera were used to record the test events. The high-speed camera was used to confirm orientation angles just prior to impact and to aid in the evaluation of extent of crush subsequent to the test. The tests were conducted by attaching the ¼ scale package to a 15-ton mobile crane through appropriate rigging and lifting the package to the required height. An electronically activated guillotine-type cable cutter device was used for releasing the package for free fall. An array of photographs labelled Figures 2.A.5.7 through 2.A.5.13 provide pre-test and post-test visuals of the package. These photographs show quite clearly that the post-crush impact limiters maintained their own physical integrity and the attachments to the overpack scale model suffered no failures.

The following acceptance criteria for the scale model dynamic drop tests were identified in the Test Plan [2.A.11]:

- Filtered decelerations limited to a maximum of 60g's (after scaling to full-scale geometry) for all drop orientations.
- No impact of the cask body on the target surface.
- No separation of impact limiters from the cask body through the entire drop event.

#### 2.A.5.2 Results of First Series of Drop Tests

The first series of three one-quarter scale drop tests (types A, B, and C denoted above) were performed in August 1997 and produced significant information [2.A.5]. Table 2.A.1 shows the maximum filtered decelerations registered in the three one-quarter scale tests after the test results are scaled up to the full-scale AL-STAR (by dividing test results by four).

Table 2.A.1: Peak Decelerations from August 1997 Tests

Test I.D.	Orientation	Deceleration (g)
A.	End Drop	134
B.	C.G.-Over-Corner	37.84
C.	Side Drop	51.3

The peak filtered deceleration in the first end-drop test was clearly above the 60g-design limit established for the HI-STAR 100 design. The reasons for this discrepancy were determined to be the use of a low value of the dynamic multiplier assumed in designing the impact limiter, and the lack of pre-crush of the honeycomb material. Numerical analyses also indicated that the honeycomb compression modulus was dependent on the impact limiter velocity during the drops. This confirms laboratory data available in the historical literature [2.A.9]. The velocity and deceleration information obtained from the first round dynamic drop tests enabled development of a simple dynamic correlation multiplier to be applied to the honeycomb material's static F-d behavior. This multiplier is an additional "experimentally based" input term in the computer prediction model for simulation of dynamic drop events [2.A.6]. Data from the initial test series shows that this multiplier is independent of test orientation and is a function of the ratio of crush velocity during the crushing process divided by the impact velocity at the initiation of crush. Based on the numerical analysis of the August 1997 tests, the honeycomb material was appropriately revised with new crush strengths and new sets of ¼ scale model impact limiters were manufactured. The correlation of the August 1997 quarter-scale tests with the numerical results from the computer model is presented in section 2.A.6.

In summary, the chief contribution of the August tests, therefore, lay in providing the database to quantify the crushing characteristic of the honeycomb material under dynamic conditions [2.A.6]. Since none of these tests is ascribed to confirmation of the final performance of the AL-STAR impact limiters, no accelerometer raw or filtered results are included herein. The full set of acceleration data (both raw and filtered) is provided in [2.A.5].

### 2.A.5.3 Results of the Second Series of Drop Tests

The second round of one-quarter scale dynamic drop tests, conducted in December 1997 and February 1998, using the new (lower crush strength) impact limiter materials, occurred in three phases. The first phase consisted of the top end drop, CGOC drop, and side drop tests. While the decelerations in all cases were within the design limit, the attachment system for the bottom impact limiter did not survive the side drop test. The attachment system was redesigned prior to the remaining (slapdown) test. The slapdown test is considered to be the most definitive test of the cask/impact limiter attachment integrity. The slapdown test was successfully completed, with the bottom impact limiter remaining in place during and after the secondary impact, on December 29, 1997 in Phase 2 of the second test series. In order to confirm the adequacy of the attachment system under side drop conditions, the side drop test was repeated in February 1998 during Phase 3. This test reconfirmed the attachment system integrity.

The results from the second round test series demonstrates that the HI-STAR 100 package meets all test acceptance criteria, namely:

- Appropriately filtered decelerations of less than 60g's (after appropriate scaling to reflect the full-size mass and geometry) for all tested orientations;
- All attachment bolts remained intact, ensuring that the impact limiters do not separate from the cask body through and after the drop event;
- No impact of the cask body on the target surface.

Figures 2.A.5.14 through 2.A.5.21, drawn from reference 2.A.7, provide the raw (unfiltered) and filtered deceleration time-histories for each of the four drop scenarios for the key accelerometers used to assess package performance. The accelerometer station numbers indicated in these accelerograms are located by referring to Figures 2.A.5.5 or 2.A.5.6, as applicable. The test report [2.A.7] provides the necessary background to justify the use of this data to evaluate package performance. The following remarks are pertinent concerning the results presented in Figures 2.A.5.14 through 2.A.5.21.

#### End Drop Decelerations (Figures 2.A.5.14, 2.A.5.15, and 2.A.5.15a-c)

All accelerometers for this test recorded decelerations in the direction of crush. Two accelerometers were subsequently determined to be defective (documented in [2.A.7]). The figures show the raw, the filtered response at 450Hz cut-off frequency, and a combined plot of the raw and filtered data covering a reduced time period. All of these results are obtained from the records from the working accelerometers. All working accelerometers gave essentially identical response; the final evaluation of performance presented herein is the average of the response from the accelerometers deemed to be recording correctly. Figures 2.A.5.15b and 2.A.5.15c demonstrate that the sensitivity to cut-off filter frequency is small even up to 1250Hz.

#### Center of Gravity Over Corner Decelerations (Figures 2.A.5.16, 2.A.5.17, and 2.A.5.17a)

The CGOC test was performed immediately after the end drop using the same set of accelerometers. The evaluation of the data after this test clearly determined that the same two accelerometers deemed suspect in the end drop test was also providing erroneous data here. Subsequent independent plate impact tests that definitively showed that these accelerometers were indeed faulty are documented in [2.A.7]. The acceleration data in the figures represents the vertical acceleration obtained by appropriate combination of the raw time data from the longitudinal and lateral mounted accelerometers on the inclined scale model cask. The raw vertical accelerations were then subject to filtering to remove non-rigid body behavior. Raw, filtered, and combined raw and filtered data over the strong response time period are presented.

### Slap Down Decelerations (Figures 2.A.5.18, 2.A.5.19, and 2.A.5.19a)

Although the initial release of the package was at an angle of 15 degrees from the horizontal, the high-speed camera showed that impact occurred with the overpack longitudinal axis at an angle of 7.2 degrees from the horizontal. The numerical simulation of this test reflected the actual angle of impact rather than the initial setting at nine meters. The results for all accelerometers (raw data and filtered) are provided in [2.A.7]. The raw and filtered data presented in the figures here represent the deceleration at the bottom end of the package that experiences the larger magnitude secondary impact. Numerical analysis demonstrated that the peak deceleration from secondary impact is insensitive to impact angles between 5 and 12 degrees from the horizontal and decreases as the angle increases above 12 degrees. Raw, filtered, and combined raw and filtered data over the strong response time period are presented.

### Side Drop Decelerations (Figures 2.A.5.20, 2.A.5.21, and 2.A.5.21a)

Both impact limiters are supposed to impact the target simultaneously in this test. An evaluation of the individual accelerometer data and an examination of the high-speed camera film clearly indicated that there was a small angle existing between the overpack longitudinal axis and the target horizontal surface at the moment of impact. This caused the expected result that accelerometer readings at one end of the package were slightly higher than readings at the other end. The results for raw and filtered data represent results obtained by averaging the data from the accelerometers at the ends of the package. Raw, filtered, and combined raw and filtered data over the strong response time period are presented.

The filter frequency used for the End Drop and CGOC Drop is 450 Hz. The filter frequency used for the Slap Down and Side Drops was 350 Hz. These filter frequencies were established by examination of the power spectral density function for each raw data trace that clearly showed that the majority of the energy occurred at frequencies well below the cut-off frequency. Independent confirmation of the appropriateness of the cut-off frequencies was made by determining the lowest frequency of elastic vibration of the package acting as either a bar or a simply supported beam. As described above, the sensitivity to cut-off frequency was examined for the end drop case by re-analyzing the data for three cut-off frequencies.

Table 2.A.2 provides the peak deceleration data culled from the above-mentioned accelograms for the four drop scenarios after filtering to remove high frequency effects. The table contains the results from the actual 1/4-scale experiments scaled up to the full-size packaging. The test report [2.A.7] provides the detailed information on this final one-quarter scale dynamic drop test series with raw and filtered outputs from all accelerometers. The test report also includes details on the filtering methodology, on the data reduction, and on the evaluation of the performance of the various accelerometers used in each of the tests.



In all of the four final one-quarter scale dynamic drop tests, the impact limiter attachments successfully performed without a single attachment bolt failure (ensuring that the impact limiters did not separate from the overpack), rigid body decelerations were below 60 g's, and the cask body did not contact the unyielding target surface. Also, additional crush margin remained in the aluminum honeycomb material.

Table 2.A.2: Peak Decelerations from AL-STAR™ Drop Tests (Second Series)

Test Case	Orientation	Peak Decelerations (g)
A	End-Drop	53.9
B	C.G.-over-Corner	38.8
C	Side Drop	45.7
D	Slap-Down	59

## 2.A.6 Phase 5: Numerical Prediction Model for Dynamic Analysis

The numerical prediction model for dynamic drop events utilizes the previously discussed force-crush (F-d) model and incorporates the information into the dynamic equations of equilibrium. Using the procedure discussed previously, the static F-d curves for the AL-STAR impact limiter under the four drop scenarios are readily constructed. Figures 2.A.6.1 to 2.A.6.4, respectively, provide the static force vs. crush plots for the full scale impact limiter with test orientations for drop cases A, B, C, and D (primary impact). An appropriate analytical fit for each curve is developed using the commercial graphing package Deltagraph [2.A.8]. Figures 2.A.6.1 through 2.A.6.4 also provide curves for upper and lower bound material strengths.

We now discuss the application of the F-d model to the prediction of impact limiter performance in a dynamic drop environment. In symbolic form, we can write the static resistive (crush) force,  $F$ , as a function of the crush depth,  $\Delta$ , where a zero value for  $\Delta$  represents an uncrushed condition.

$$F = f(\Delta)$$

The above symbolic formula represents the data on Figures 2.A.6.1 to 2.A.6.4 in analytical form. We have previously explicitly discussed the mathematical concepts underlying the above formulation by referencing the particular case of a side drop. In general, the static F-d curve can be expressed as a sum of local crush pressures multiplied by interface areas where the interface areas may be a function of the current crush. That is, the mathematical relation for static compression (which is validated by comparison to static testing) is also expressible in the form

$$f(\Delta) = \sum_i p_i A_i$$

where  $p_i$  are the crush pressures of the materials participating in the crush and  $A_i$  are the interface areas associated with the different crush strengths. The determination of the areas  $A_i$  as a function of crush depth,  $\Delta$ , has previously been discussed within the context of interpenetration.

The dynamic model for simulating a packaging drop event consists of solving the classical Newtonian equations of motion. In the case of a unidirectional impact such as an end drop ( $\theta=90^\circ$ ), side drop ( $\theta=0$ ), or CGOC drop, the equation of motion simply reduces to:

$$M \frac{d^2 \Delta}{dt^2} = Force + Mg$$

where:  $M$  = mass of system undergoing deceleration

$d^2 \Delta / dt^2$  = second derivative of package movement (which is equal to the impact limiter crush because the target is immovable and rigid).

The resistive “Force” opposes the downward movement and is given by the static force-crush functional relationship (appropriate for the drop orientation) multiplied by a dynamic multiplier  $Z$ . As noted earlier, there is historical evidence that metal honeycomb crush pressure is a linear function of velocity [2.A.9]. The Holtec correlation of the August 1997 test data by numerical simulation [2.A.6] also confirmed that the best correlation is achieved if the dynamic multiplier is represented by a linear function of local crush velocity ( $d\Delta/dt$ ). Introducing the dynamic multiplier, the dynamic equation of force equilibrium for a case involving only primary impacts becomes

$$M \frac{d^2 \Delta}{dt^2} = ZF + Mg = Zf(\Delta) + Mg$$

The above equation is a second order non-linear differential equation in the time coordinate  $t$ , which can be solved for the post-contact event using any standard equation solver package. The initial condition is: @  $t = 0$ ,  $\Delta = 0$ ,  $d\Delta/dt = V_o$  (approach velocity at impact). We note that since the acceleration is an explicit function of both deformation and velocity, maximum acceleration will not, in general, occur at the instant when the velocity of the package is zero.

If the impact event involves both primary and secondary impacts, as is the case for the slapdown event (indeed any event wherein  $\theta < 67.5^\circ$ ), then both the mass  $M$  and rotational moment of inertia  $I$  are involved. The modeling of a dual impact event is only slightly more involved than

the single variable modeling of the single impact case discussed above. Figure 2.A.6.5 pictorially illustrates the sequence of events leading to an appropriate mathematical model. Figure 2.A.6.6 provides the appropriate free-body diagrams associated with each portion of the event.

In the first step, the inertia force of the falling package is resisted by the crush force developed at the primary impact location. While the downward momentum of the package is dissipated by the resistive force, the package also experiences the overturning couple produced by the non-collinearity of the inertia force (which acts at the centroid) and the resistive force which acts at the primary impact zone (Figure 2.A.6.5(a)). The dynamic equation of force equilibrium is given above in terms of the downward movement of the package centroid and the resistive force static compression curve, modified by the dynamic factor  $Z$ , appropriate to the initial orientation at primary impact. The package decelerates and then begins to overturn, in effect pivoting about the initial point of contact in the primary impact region, gathering angular momentum as the second impact limiter (mounted at the far end) approaches the target surface. Referring to Figure 2.A.6.5(b), the dynamic equation insuring moment equilibrium during the overturning (before the initiation of the secondary impact) phase can be written as

$$I_p \frac{d^2\phi}{dt^2} = -MgR \cos(\phi)$$

where  $I_p$ : moment of inertia of the package about the pivot point  
 $\phi$ : angular acceleration with respect to the horizontal plane  
 $R$ : radial distance of the package C.G. with respect to the pivot point.

The initial conditions for this phase are:  $t = 0$ ,  $\phi = \theta$ ,  $d\phi/dt = 0$  where  $t$  is now redefined at the initiation of rotational motion.

Finally, the secondary impact commences wherein the angular momentum of the package plus any linear momentum not dissipated by the primary impact is dissipated by the crushing of the second impact limiter. During the secondary impact phase, the equation of dynamic moment equilibrium can be written by inspection of Figure 2.A.6.5(c):

$$I_p \frac{d^2\phi}{dt^2} = -MgR \cos(\phi) + Zf(D\phi)D$$

where  $f(D\phi)$  is the static resistive force at the secondary impact location under compression  $D\phi$ ,  $Z$  is the current dynamic multiplier appropriate to the secondary impact location,  $D$  is the moment arm, and  $I_p$  is the moment of inertia of the package about the pivot point. During this phase of the motion, the equation of dynamic force equilibrium is modified to reflect dynamic resistive forces from both impact limiters since the entire package may continue to move toward

the target surface with both impact limiters providing a dynamic resistive force. Therefore, during the final phase of the impact event, the dynamic force equilibrium equation can be written as

$$M \frac{d^2 \Delta}{dt^2} = Z_1 F_1 + Z_2 F_2 + Mg$$

where  $Z_i$  and  $F_i$  ( $i=1,2$ ) represent the dynamic multiplier and static compression force appropriate to the primary and secondary impact limiter behavior during the final phase of the event. The dynamic multipliers  $Z_i$  ( $i=1,2$ ) reflect the current value of the local crush velocities at each of the limiters.

The above formulation assumes, for simplicity, that the pivot point does not slide during the overturning or secondary impact phases.

It is evident from the foregoing that the impact limiter is essentially simulated by a non-linear spring whose static force-deformation curve is known a priori (from the F-d model) as a function of the drop orientation. The solution of this rigid body dynamics problem featuring up to two non-linear springs can be determined using any one of several standard software packages available in the public domain. Holtec International utilizes the commercial package WORKING MODEL [2.A.10], which has been validated in the company's QA system for this purpose.

The dynamic simulation model, constructed in the manner of the foregoing, was utilized to simulate all seven one-quarter scale drop events (three in the first series, four in the second series). In order to develop a high level of confidence, it was decided that the model should be validated at all three levels, namely, a comparison of acceleration, crush, and duration of impact. In other words, to be acceptable, the numerical prediction model must predict  $\alpha_{\max}$ , maximum crush sustained  $d_{\max}$ , and the duration of impact, with reasonable accuracy. Since the actual crush  $d_{\max}$  could be measured, and the duration of impact and  $\alpha_{\max}$  were available from accelerometer data, comparison between theory and experiment with respect to all three key indicators was possible. Tables 2.A.3 and 2.A.4 provide the results in a concise form for all of the one-quarter scale dynamic drop tests for the first and second series, respectively.

Note that in the tables, the comparison is made after scaling up the model results to reflect a full-scale package.

Table 2.A.3: Comparison Between Test Data and Prediction Model Results (First Test Series)

Case I.D.	Deceleration (g's)		Total Crush Depth (inch)		Impact Duration (milli-seconds)	
	Predicted	Measured	Predicted	Measured	Predicted	Measured
A. End-Drop	134.2	134.0	2.42	2.42	3.5	Not measured
B. C.G.O.C.	37.8	37.84	16	16	13.25	16.6
C. Side Drop	50.5	51.3	9.1	9.51	8.25	10.74

Table 2.A.4: Comparison Between Test Data and Prediction Model Results (Second Test Series)

Case I.D.	Deceleration (g's)		Total Crush Depth (inch)			Impact Duration (milli-seconds)	
	Predicted	Measured	Predicted	Measured	Max. Available	Predicted	Measured
A. End Drop	53.0	53.9	11.3	10.6	17.659	38.8	37.2
B. C.G.-Over-Corner	38.7	38.8	12*	9.82*	25.06	51.0	61/45.2
C. Side Drop	43.5	45.7	10.9	12.5	16	38.5	53.1 (averaged value)
D. Slap-Down							
Primary	46.4	49.0	9.50	10.7	16	48.5	44.4
Secondary	59.9	59.0	12.8	13.5	16	35.8	41.2

\* For C.G.-Over-Corner, only crush at the external interface is measured.

It is evident from both Tables 2.A.3 and 2.A.4 that the numerical prediction model is robust in predicting all seven impact tests. Not only are peak values of  $\alpha_{\max}$  for each test predicted with good agreement, but also the crush depth and impact duration is also reliably simulated.

A perusal of the numerical results in Table 2.A.4 yields two additional insights into the behavior of AL-STAR which are most helpful in the “fine tuning” of the full-scale AL-STAR design:

- i. The maximum deceleration,  $\alpha_{\max}$ , predicted as well as measured, under the most limiting scenario (slapdown), is close to the permissible limit of 60g's.
- ii. The maximum crush, predicted as well as measured, in all drop scenarios, is well below the available limit (i.e., the value at which the crush material will “lock up”).

The state-of-the-art manufacturing technology for aluminum honeycombs permits the material to be manufactured within a total tolerance range of 12 to 13% (between the maximum and minimum values). The above observations suggest that the upper and lower bound range of crush pressures for the honeycomb material in the AL-STAR impact limiter should be set at 95% and 82% of the values of honeycomb material used in the second series quarter-scale tests.

Finally, the agreement between the predictions and measured data in the above correlation effort fosters a high level of confidence in the numerical model, which can now be used to conduct sensitivity studies.

#### 2.A.7 Phase 6: Simulation of the Effects of Material Crush Strength Variation, Package Mass Tolerances, and Oblique Drop Orientations

Having ensured the technical reliability of the numerical prediction model, it is now necessary to evaluate the system behavior under all “limiting conditions”. As noted earlier, the impact limiter materials are insensitive to environmental temperature changes within the limits of  $-20^{\circ}$  F and  $100^{\circ}$  F. Therefore, limiting conditions are broadly defined here as arising from two sources:

- i. Variation in the impact limiter honeycomb crush strength due to material manufacturing tolerance.
- ii. Variation in the package weight (due to different MPC types that may be transported in the HI-STAR 100 overpack, and manufacturing tolerances in fabrication of the overpack and impact limiters).
- iii. Variation in package angle of impact with the target.

To examine all limiting scenarios, additional simulations using the mathematical model were performed. The crush strength of the honeycomb material was varied within the range permitted in the Holtec Drawing 1765. The packaging weight was set at its upper bound and lower bound value (upper bound weight is 280,000 lb., and lower bound weight is 270,000 lb. based on values listed in Table 2.2.1). Three additional drop orientations (30 degree, 45 degree, and 60 degree orientation angle, measured from the horizontal) that were not the subject of tests were also analyzed numerically using input crush strength data that would maximize the decelerations with an average weight. The purpose of these additional simulations with varied drop angle is to ascertain which, if any, oblique drop orientation merits detailed finite element stress analysis to meet the requirements of the Regulatory Guide. Figures 2.A.7.1-2.A.7.3 provide the static crush force vs. crush depth information used in the dynamic simulation of these accident events. Table 2.A.5 provides key output data, peak decelerations and maximum crush, as obtained from these numerical simulations.

Table 2.A.5: Sensitivity of Package Response to Package Weight, Crush Material Strength Variations, and Package Orientation at Impact

Orientation	Case	Deceleration (g's)	Maximum Total Crush (2-interfaces) (inch)	Available Crush Stroke (inch)
End Drop	Max. Strength, Min. Weight	52.85	11.4	17.659
	Min. Strength, Max. Weight	46.3	12.8	17.659
C.G. Over Corner	Max. Strength, Min. Weight	38.25	17.0	25.06
	Min. Strength, Max. Weight	35.6	18.5	25.06
Side Drop	Max. Strength, Min. Weight	42.5	11.2	16
	Min. Strength, Max. Weight	37.5	12.7	16
Slap Down (secondary impact bounds)	Max. Strength, Min. Weight	58.5	13.2	16
	Min. Strength, Max. Weight	52.6	15.1	16
Oblique Drop – 30 degrees	Max. Strength, Min. Weight	36.44	19.57	24.1
Oblique Drop – 45 degrees	Max. Strength, Min. Weight	35.62	22.39	25.72
Oblique Drop – 60 degrees	Max. Strength, Min. Weight	38.01	19.2	25.65

The following conclusions are readily derived from Table 2.A.5 results:

- i. The maximum value of  $\alpha_{\max}$  is less than 60g's in all cases.
- ii. The total crush of the impact limiter is below the available “stroke”, i.e., the overpack body will not contact the unyielding target surface nor will any “lock-up” of the crush material occur.
- iii. The three oblique drop simulations considered all produce approximately the same vertical deceleration from the primary impact. The decelerations resulting from the subsequent secondary impact, after rotation of the HI-STAR 100, are all below the value obtained from the simulation of the “slapdown” at low angles of

impact. If the “limiting” oblique drop is considered as the simulation providing maximum deceleration perpendicular to the longitudinal axis of the cask, then the drop most likely to develop the largest bending of the overpack in the oblique orientation is at 30 degree orientation (from the horizontal axis). Therefore, this case is subjected to detailed stress analysis in Section 2.7 with the applied impact loading (along and perpendicular to the cask axis) balanced solely by the cask inertia forces and moments.

In conclusion, the above work provides full confidence that the HI-STAR 100 packaging will perform in the manner set forth in the NRC regulations (10CFR71.73) under all conceivable hypothetical accident conditions of transport.

#### 2.A.8 One-Foot Drop

Paragraph 2.6 of Reg. Guide 7.8 requires evaluation of the package response under a one-foot drop onto a flat unyielding surface in a position that is expected to inflict maximum damage.

Using the prediction model, the maximum deceleration sustained by the package under the one-foot end and side drop scenarios, the latter expected to produce maximum stress in the fuel basket, was computed. Table 2.A.6 provides summary results for the limiting case of minimum package weight and upper bound material crush strength (so as to maximize the decelerations).

Table 2.A.6: Peak Decelerations Under One-Foot Drop Event

Scenario	Max. Deceleration in g's	Crush (inch)	Duration of Impact (milli-seconds)
90° End Drop	17.25	0.85	20.0
0° Side Drop	11.45	1.33	26.0

#### 2.A.9 Equivalent Dynamic Factor (EDF)

It is instructive to compute an effective equivalent dynamic factor on the predicted static crush force corresponding to the instant of maximum deceleration during the drop event. Table 2.A.7 presents the pseudo-deceleration (obtained by dividing the static force by the mass of the package) and the predicted deceleration; the ratio of the two is the “equivalent dynamic factor” (EDF). The EDF is also equal to the peak dynamic crush force divided by the static resistance force at the coincident instance of crush when the dynamic crush force is maximized. Note that the differences in package weight used in the table below reflect the actual weight of the impact limiters used in each one-quarter scale drop test (after increasing to full-scale equivalent values).



Table 2.A.7: Equivalent Dynamic Factor (EDF) for Different Drop Scenarios

Scenario	Predicted Force (lbs) $\times 10^{-7}$		Participating Package Weight (lbs)	Predicted Max. Deceleration		EDF
	Static	Dynamic		Pseudo- Accn (static)	Dynamic (from Table 2.A.4)	
End Drop	1.0785	1.454	274,336	39.313	53	1.348
CGOC Drop	0.8	1.059	273,680	29.231	38.7	1.324
Side Drop	0.4	0.597	137,270*	29.14	43.5	1.493
Slapdown	0.345	0.6607	†	†	59.9	1.915

\* Only half of the total package weight participates at each impact limiter.

† Indeterminate for this drop configuration.

The last column of the above table demonstrates that the EDF, as defined above, is not a constant value independent of drop orientation.

#### 2.A.10 Additional 1/8<sup>th</sup> Scale Static Tests

Three additional static crush tests on 1/8<sup>th</sup> scale impact limiters have been performed subsequent to the completion of all quarter-scale dynamic testing and theoretical correlation. The F-d test results for each of three impact limiter orientations are compared with the analytical F-d predictions in Figures 2.A.10.1-2.A.10.3. Figure 2.A.10.1 compares test results with theoretical prediction for the crush orientation corresponding to a side impact, Figure 2.A.10.2 presents the results for the Center-of-Gravity-Over-Corner impact orientation, and Figure 2.A.10.3 presents results for the end impact orientation. In all tests, the crush material orientation and location duplicated the final configurations subjected to quarter-scale tests. The internal backbone structure was also faithfully reproduced. The welds were also scaled to the extent practical given the thin material gages used for the one-eighth-scale model. In the three figures, the solid line without symbols represents the predictions of the theory developed for the F-d curves, while filled circles represent test results. Within the range tested for each orientation, good agreement is observed between theory and test for the side and CGOC crush orientation. For the end drop orientation, however, the tested results suggest that inclusion of some elastic behavior at the cask-impact limiter interface into the theory might improve the static correlation. The dynamic test results presented in Table 2.A.4, however, demonstrate conclusively that the prediction of peak deceleration, extent of crush, and impact duration would not be affected by these elastic effects that “smooth” the abrupt “staircase” shape of the F-d curve.

### 2.A.11 Conclusions

The AL-STAR impact limiter design was subjected to a series of static and dynamic tests to validate its functional performance. The 1/8 model static tests conducted under cold and hot, as well as ambient conditions, confirmed that AL-STAR's functional characteristics are independent of the environmental temperature conditions in the range specified in 10CFR71.73. The successful static tests on the 1/8 scale model (namely, end test and 60° oblique test) also correlated well with the theoretical force-crush model developed by Holtec. Subsequent static tests, performed after the final successful one-quarter scale dynamic tests, provided additional confirmation of the validity of the fundamental F-d model.

The static compression tests were followed by quarter-scale drop tests. The first series, in August 1997, consisting of three tests, provided the necessary test data to determine the dynamic multiplier applicable to the honeycomb materials. The numerical model for simulating the dynamic crushing of AL-STAR showed good agreement with the first test series data when the correct dynamic factor was incorporated in the computer model (Table 2.A.3).

While the prediction model for simulating AL-STAR crushing under 9-meter drop conditions was extremely well correlated, the peak deceleration under the end- drop condition in the August 1997 tests exceeded the acceptance criteria.

The second series of tests wherein the crush strength of the honeycomb was lowered (as selected by the prediction model), performed as expected. The agreement between the test data and the prediction model is high (Table 2.A.4).

The prediction model for AL-STAR therefore stands correlated with seven (7) quarter-scale drop events. The first three tests used different honeycomb crush strength materials than the last four, proving the ability of the prediction model to predict the AL-STAR crush performance for a wide range of crush material properties. The backbone structure of AL-STAR, enhanced after the 1/8-model static compression tests, performed as designed in all seven quarter-scale drop tests.

Finally, the AL-STAR-to-overpack attachment system remained intact and the cask did not contact the unyielding target during all four final dynamic tests.

## 2.A.12 References

- [2.A.1] ANSYS 5.3 Ansys Inc., 1996.
- [2.A.2] CADKEY, Version 7, 1996.
- [2.A.3] Project Procedure No. HPP-5014-5, HI-STAR Aluminum Honeycomb 1/8 Scale Impact Limiter Static Test Procedure.
- [2.A.4] HI-STAR 1/8 Scale Impact Limiter Test Report, HI-961501, Holtec International, June 1996.
- [2.A.5] Holtec Report HI-971774, Revision 1, “Impact Limiter Test Results – 30’ Drop Tests” – August 1997
- [2.A.6] Holtec Report HI-971823, Revision 0, “Improved Correlation of ORNL 30’ Drop Tests” – August 1997
- [2.A.7] Holtec Report HI-981891, Revision 3, “Impact Limiter Test Report - Second Series”, 2007.
- [2.A.8] Deltagraph Pro 3.5, Deltapoint Software, 1995.
- [2.A.9] J.M. Lewallen and E.A. Ripperger, Energy Dissipating Characteristics of Trussgrid Aluminum Honeycomb, SMRL RM-5, University of Texas Structural Mechanics Research Laboratory, 1962.
- [2.A.10] Working Model 3.0, Knowledge Revolution, 1995.
- [2.A.11] HI-STAR 100 Impact Limiter Test Program, Holtec Report No. HI-951278.

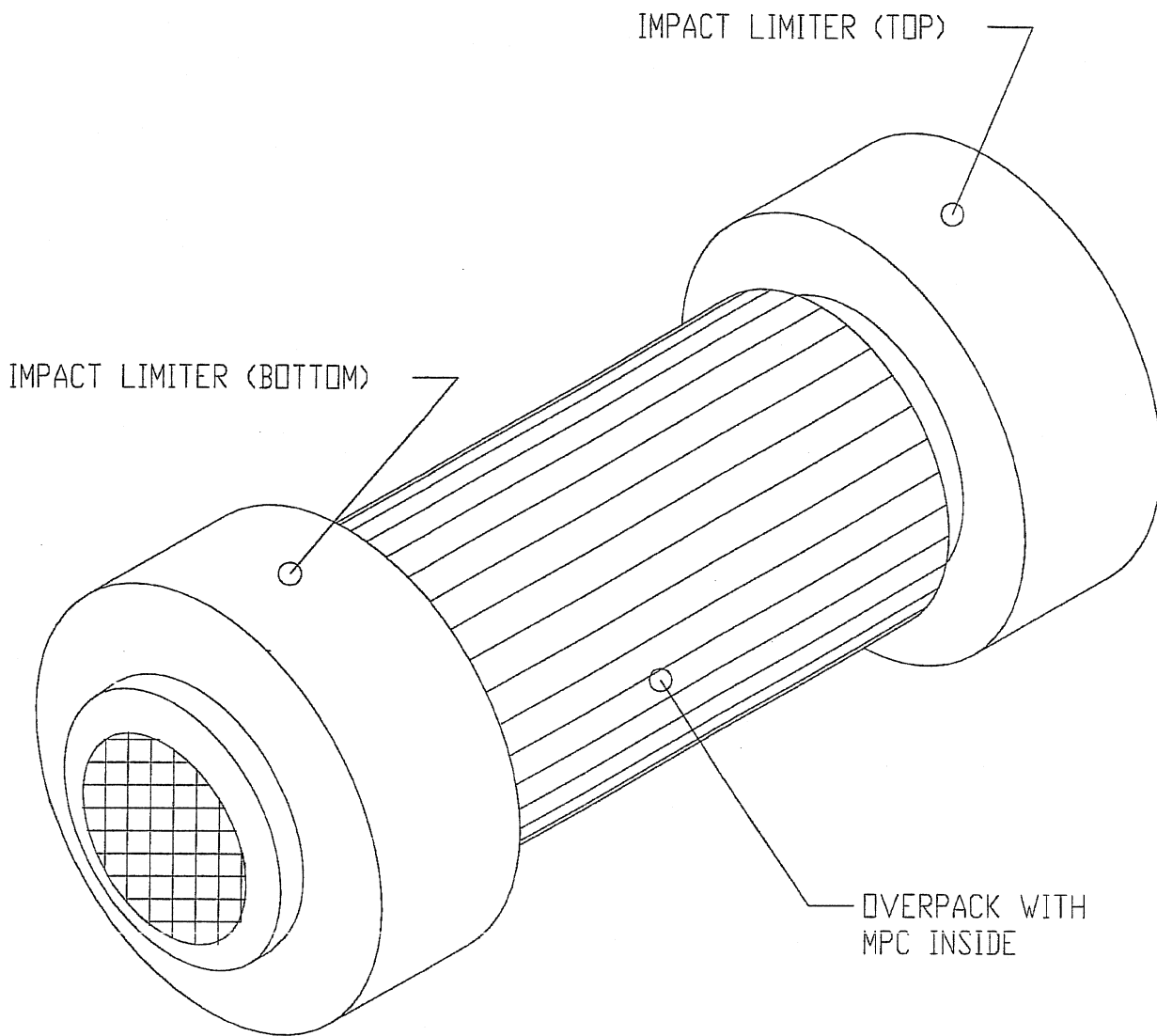


FIGURE 2.A.1.1; HI-STAR 100 PACKAGE WITH  
TOP AND BOTTOM IMPACT  
LIMITERS

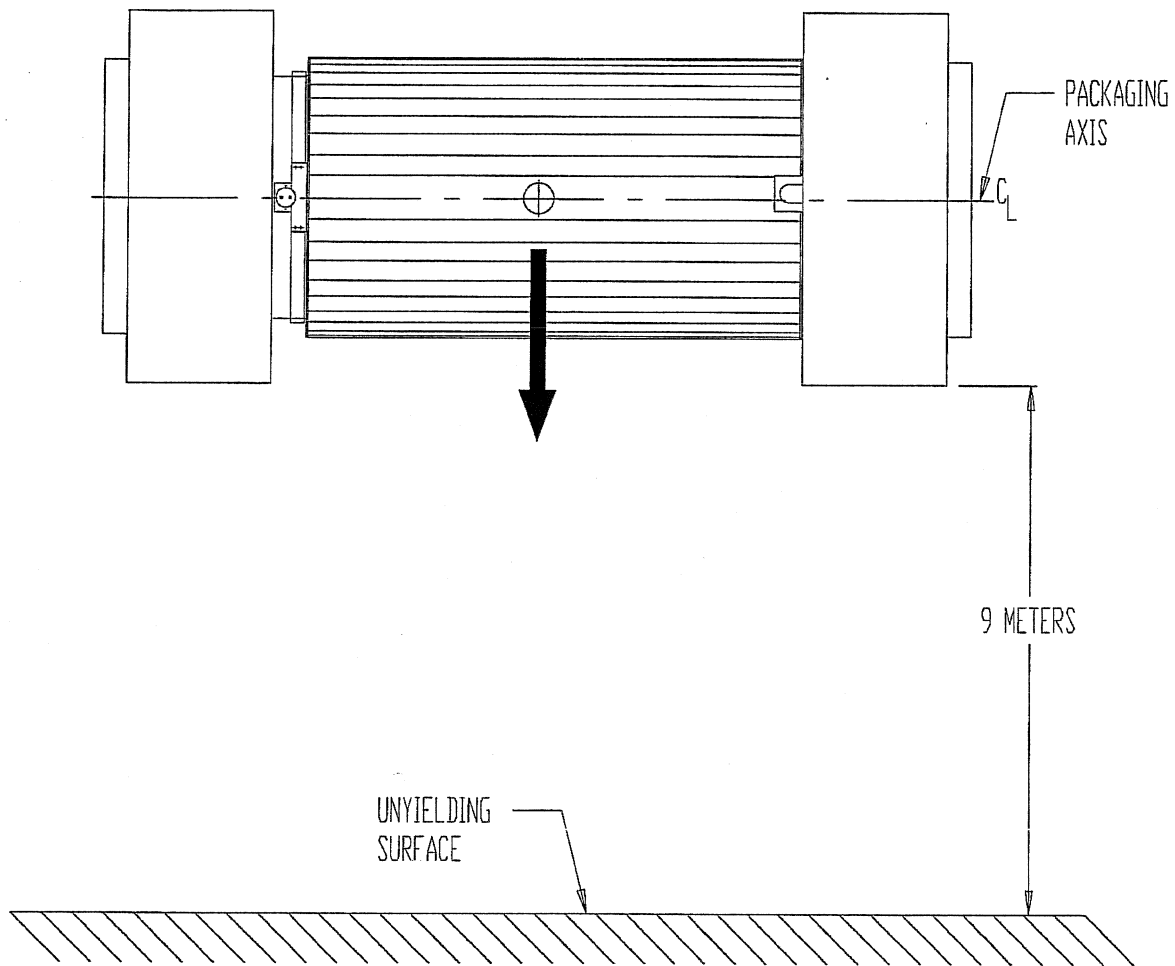


FIGURE 2.A.1.2; DROP FROM 9 METERS ON TO AN ESSENTIALLY UNYIELDING SURFACE (HYPOTHETICAL ACCIDENT CONDITION)

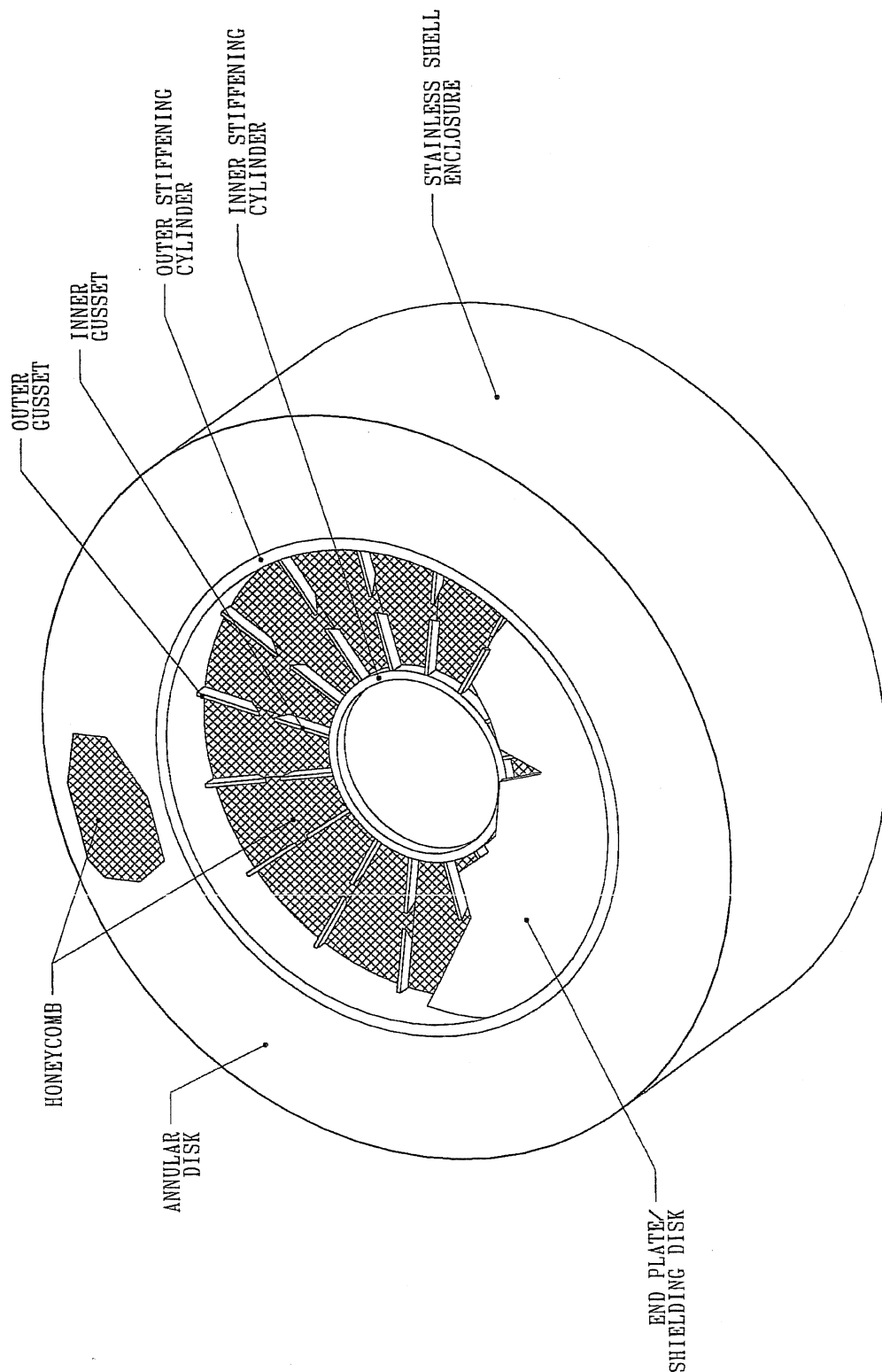


FIGURE 2.A.1.3; PICTORIAL VIEW OF AL-STAR  
(WITH A PORTION REMOVED)

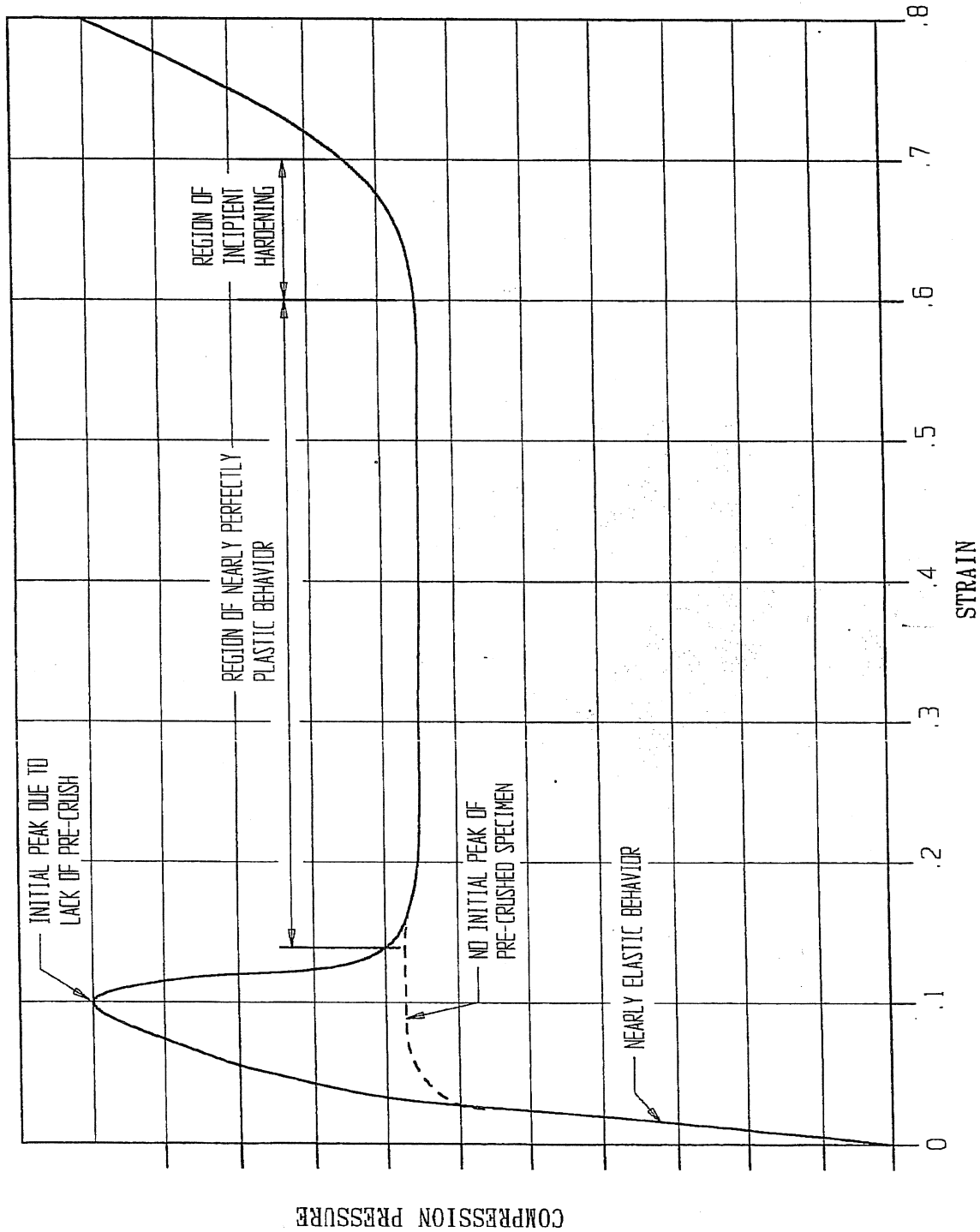
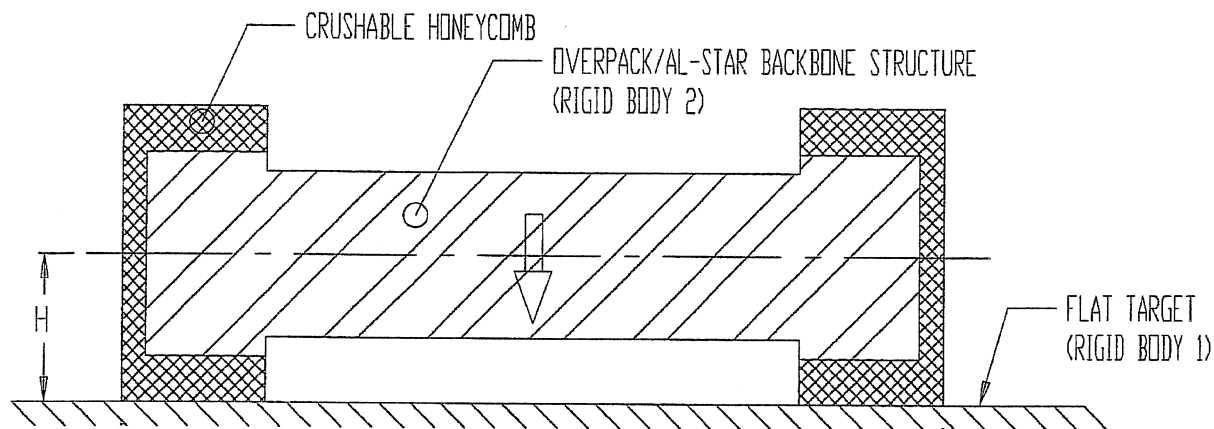


FIGURE 2.A.2.1; PRESSURE-CRUSH STRAIN CURVE (STATIC TESTING)

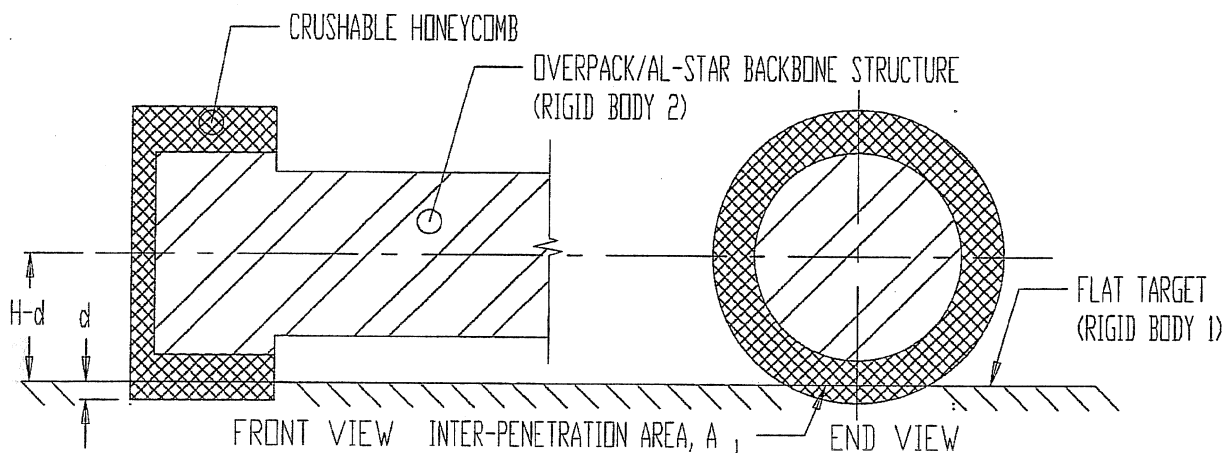
REPORT HI-951251

REVISION 10

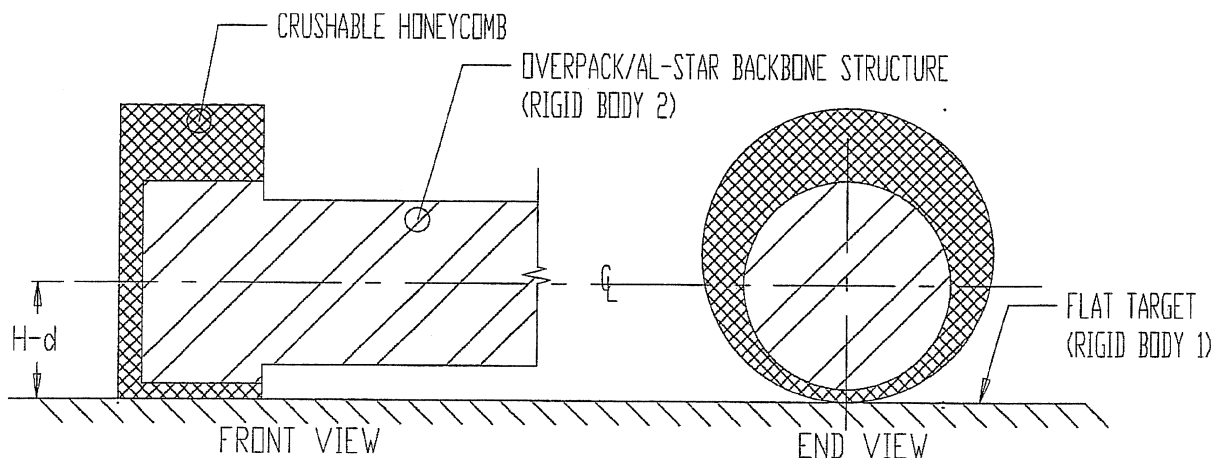
V5014/HI951251/2 H 2



(a) TWO RIGID BODIES APPROACH EACH OTHER WITH A SOFT CRUSHABLE METAL MASS BETWEEN THEM (INITIATION OF CRUSHING)



(b) SCENARIO ONE: CRUSHING OCCURS AT THE AL-STAR/TARGET INTERFACE; DEFORMATION =  $d$ ; NO CRUSH AT AL-STAR BACKBONE/HONEYCOMB INTERFACE



(c) SCENARIO TWO: CRUSHING OCCURS AT THE AL-STAR BACKBONE/HONEYCOMB INTERFACE; NO CRUSH AT THE AL-STAR/TARGET INTERFACE

FIGURE 2.A.3.1; ILLUSTRATION OF THE FORCE-CRUSH MODEL CONSTRUCTION USING THE EXAMPLE OF THE SIDE DROP EVENT.



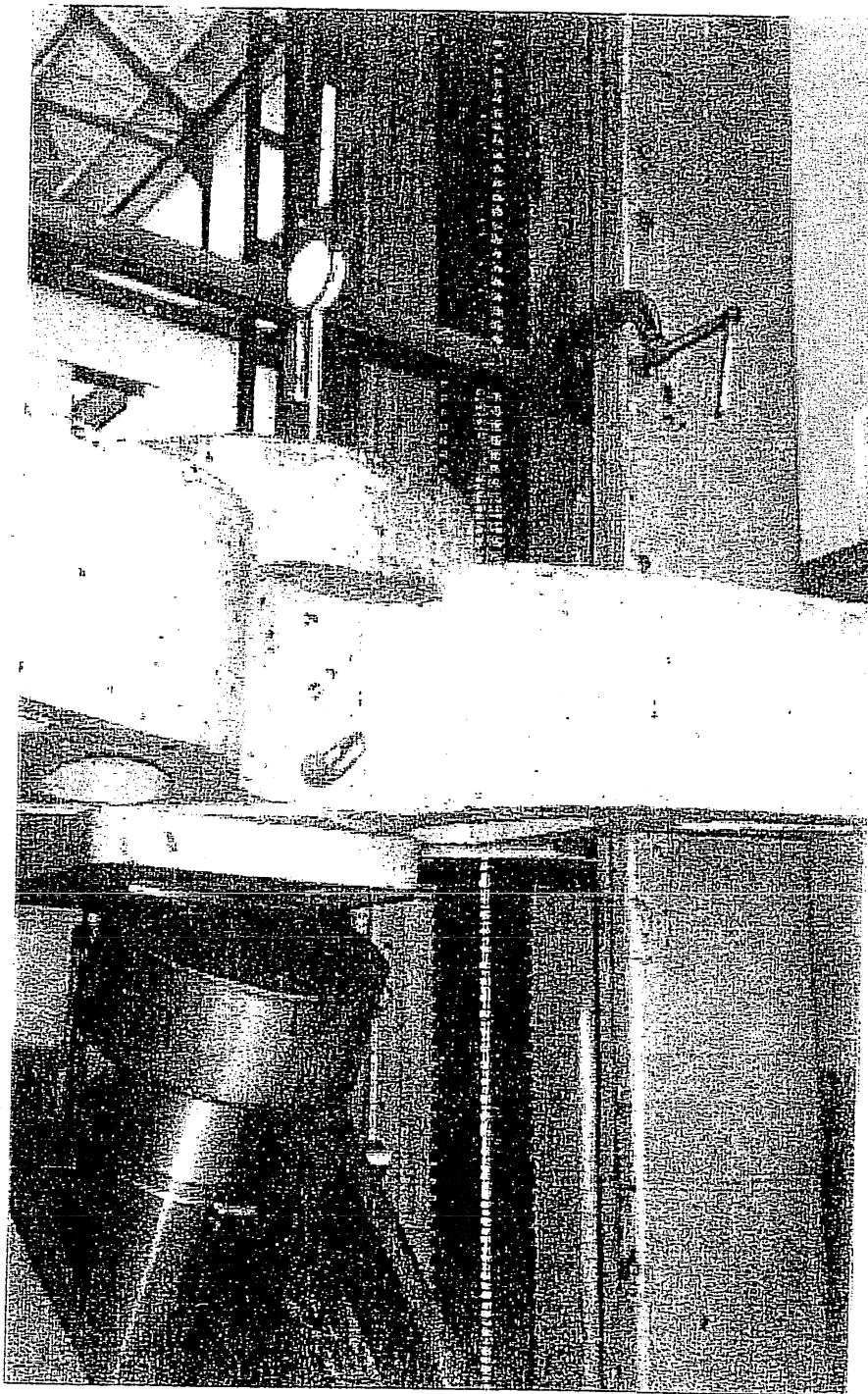


FIGURE 2.A.41; TEST FIXTURE

REPORT HI-951251

REVISION 10

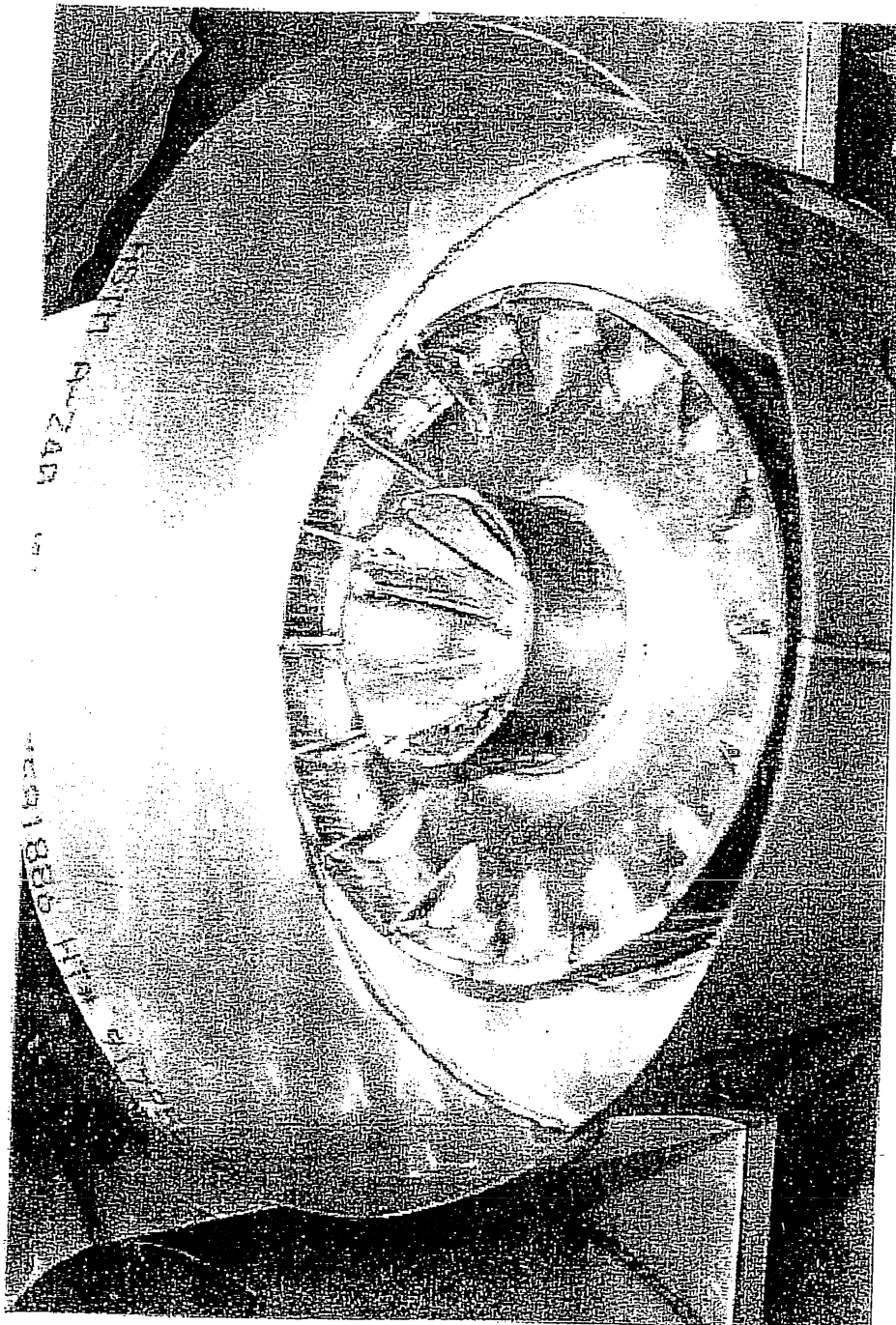


FIGURE 2.A.4.2; INTERNAL STIFFENING STRUCTURE IN 1/8 SCALE MODEL

REPORT HI-951251

REVISION 10

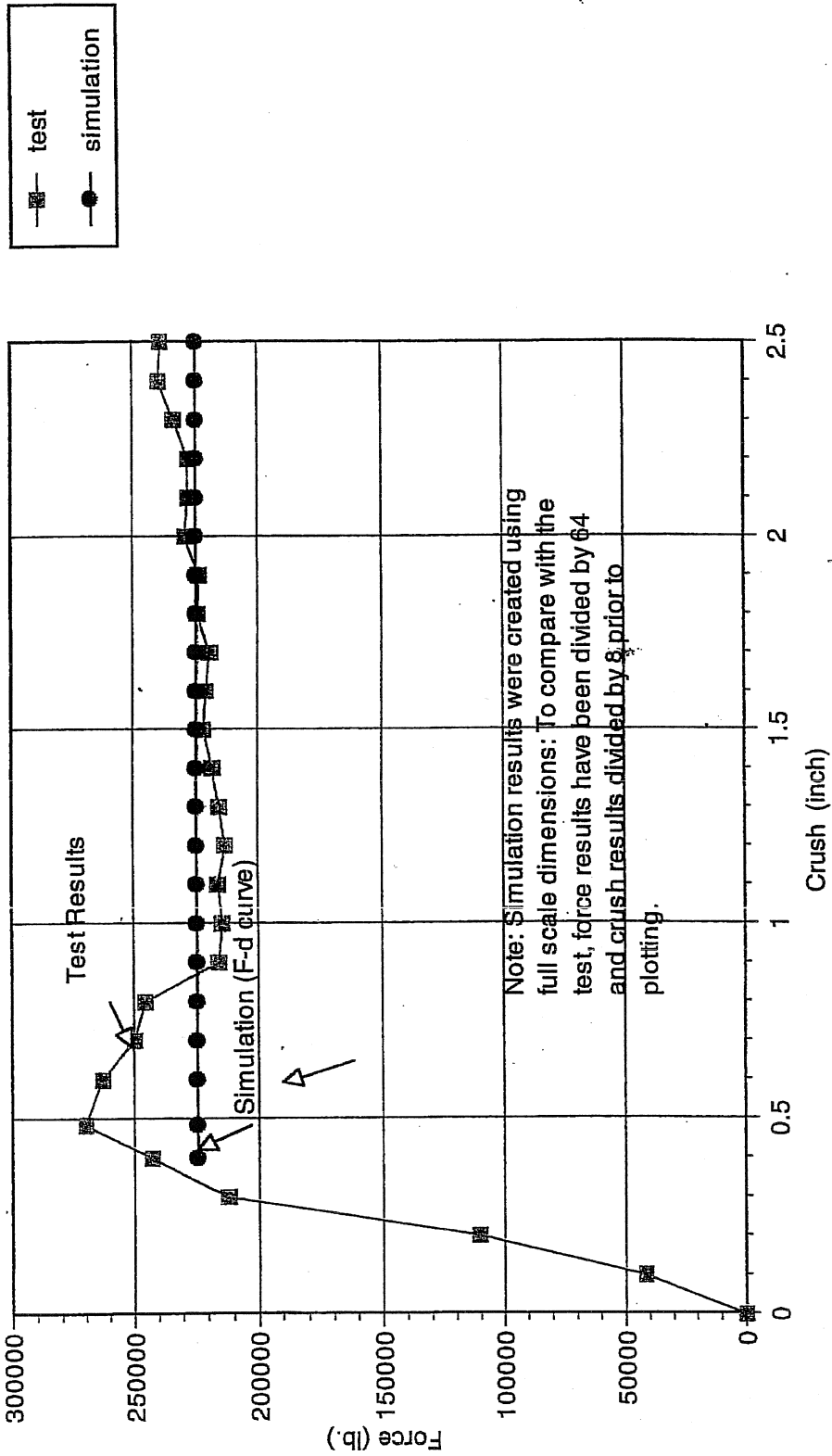


FIGURE 2.A.4.3, 1 - 1/8th Scale Initial Impact Limiter Configuration - Comparison of Static Force-Crush Data from Test and Simulation - END DROP

REV. 10

HI-951251

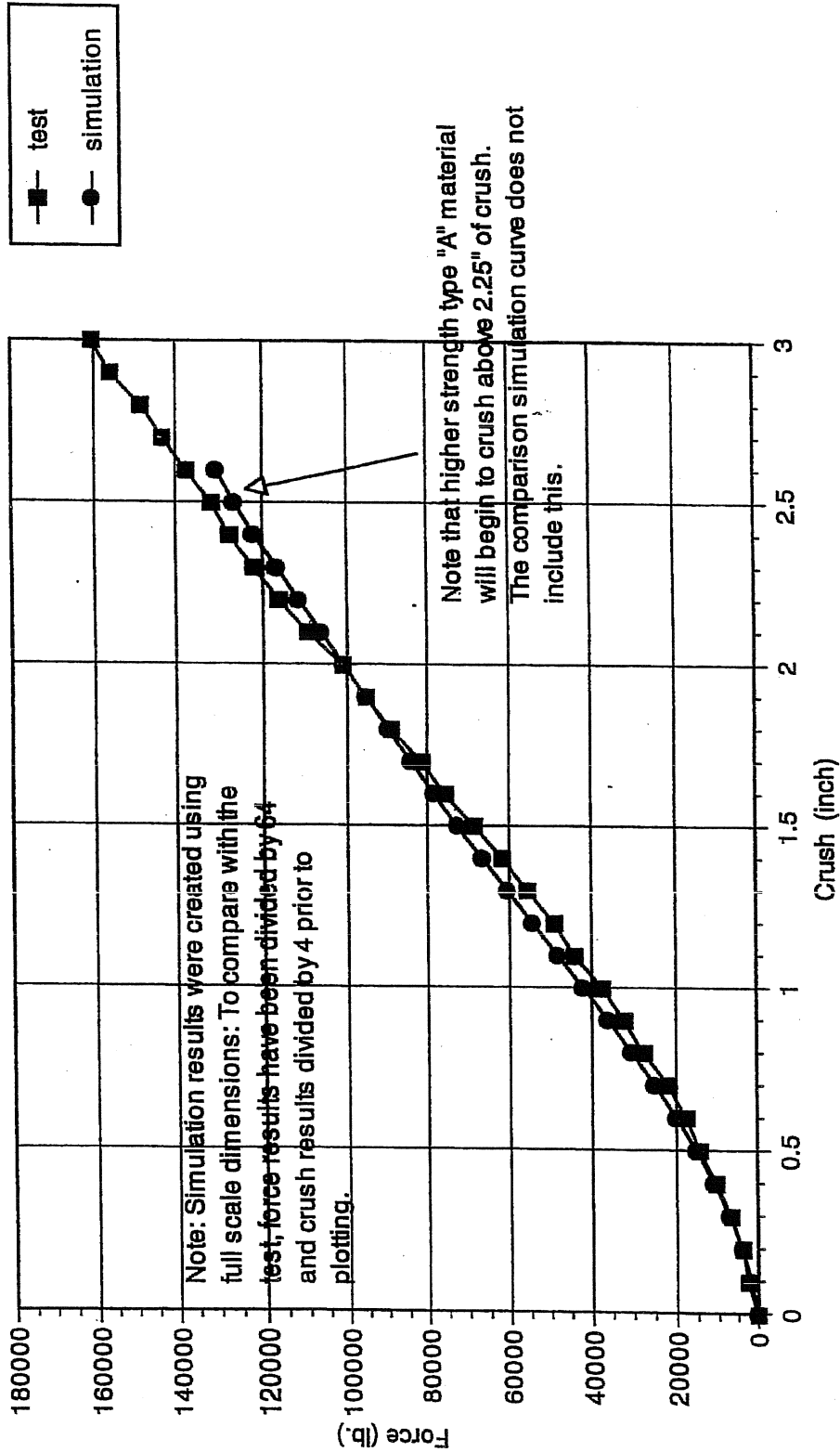


FIGURE 2A.4.4: 1/8th Scale Initial Impact Limiter Configuration - Comparison of Static Force-Crush Data from Test and Simulation - 60 DEGREE CRUSH

REVISION 10

HI-951251

# Security-Related Information Figure Withheld Under 10 CFR 2.390.

FIGURE 2.A.5.1: QUARTER SCALE MODEL OF LOADED MPC FOR  
QUARTER SCALE DROP TEST EXPERIMENT

# Security-Related Information Figure Withheld Under 10 CFR 2.390.

FIGURE 2.A.5.2; OVERPACK QUARTER SCALE MODEL (CROSS SECTION VIEW)

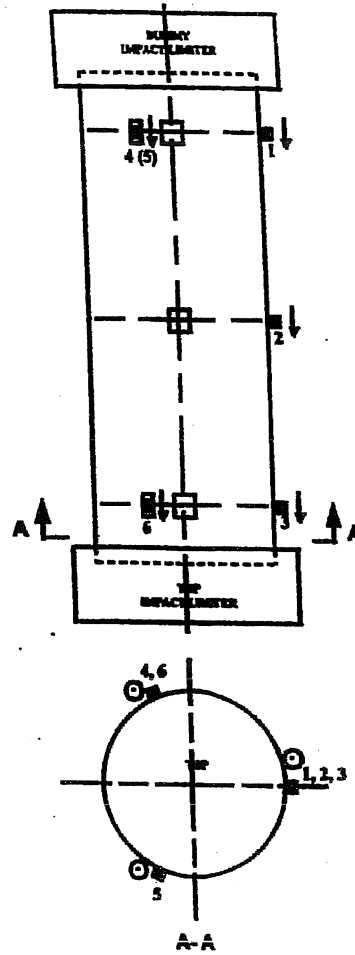
# Security-Related Information Figure Withheld Under 10 CFR 2.390.

FIGURE 2.A.5.3; OVERPACK QUARTER SCALE MODEL (TOP VIEW)

# Security-Related Information Figure Withheld Under 10 CFR 2.390.

FIGURE 2.A.5.4; OVERPACK QUARTER SCALE MODEL (BOTTOM VIEW)





(a) Accelerometer Location - Top End Drop

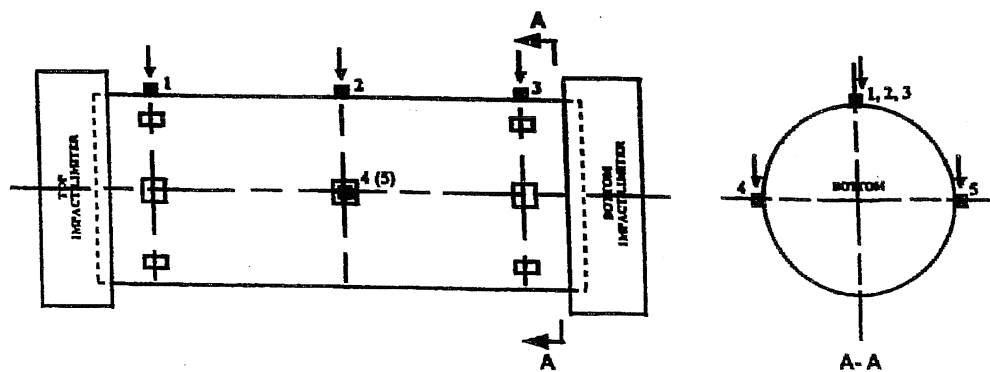
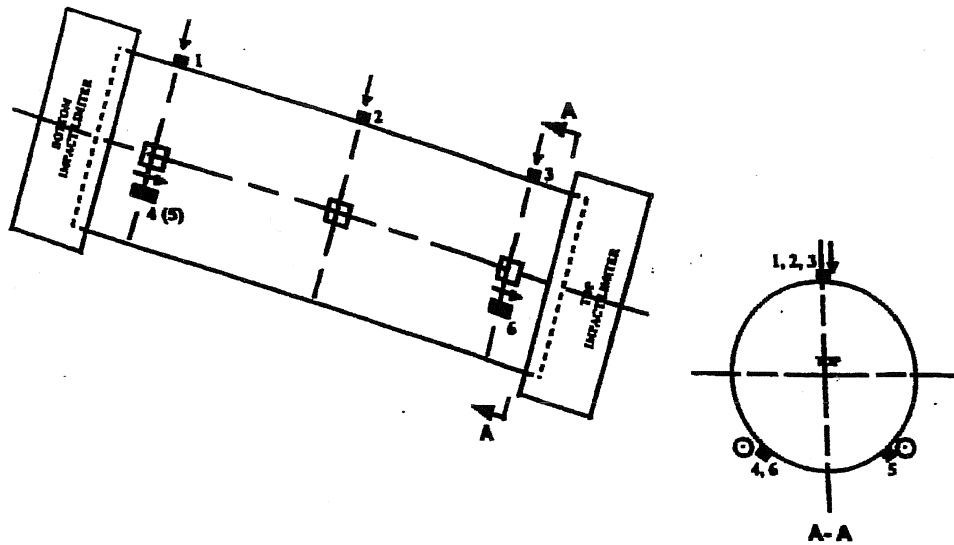
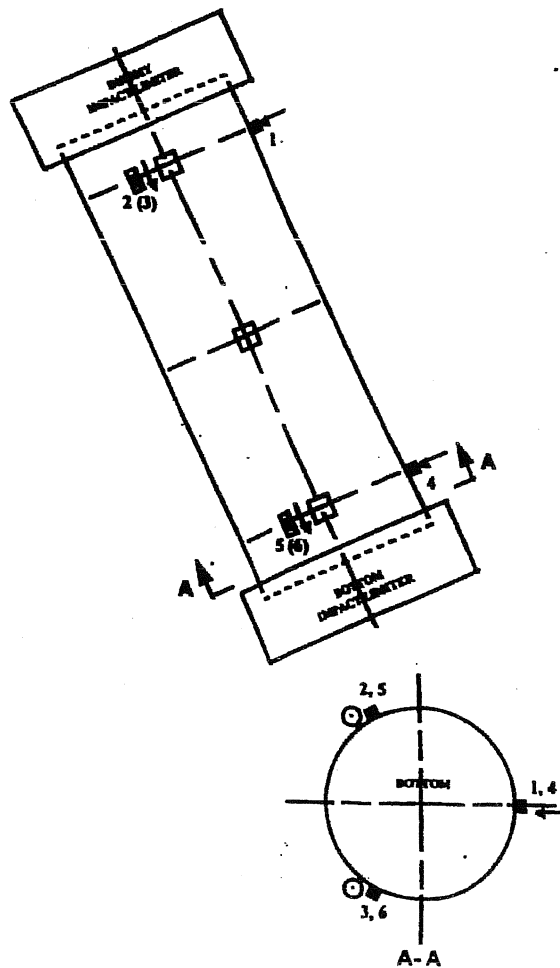


FIGURE 2A.5.5 ; ACCELEROMETER LOCATIONS FOR END AND SIDE DROPS



(c) Accelerometer Location - Slap Down Drop



HI-951251

REV. 10

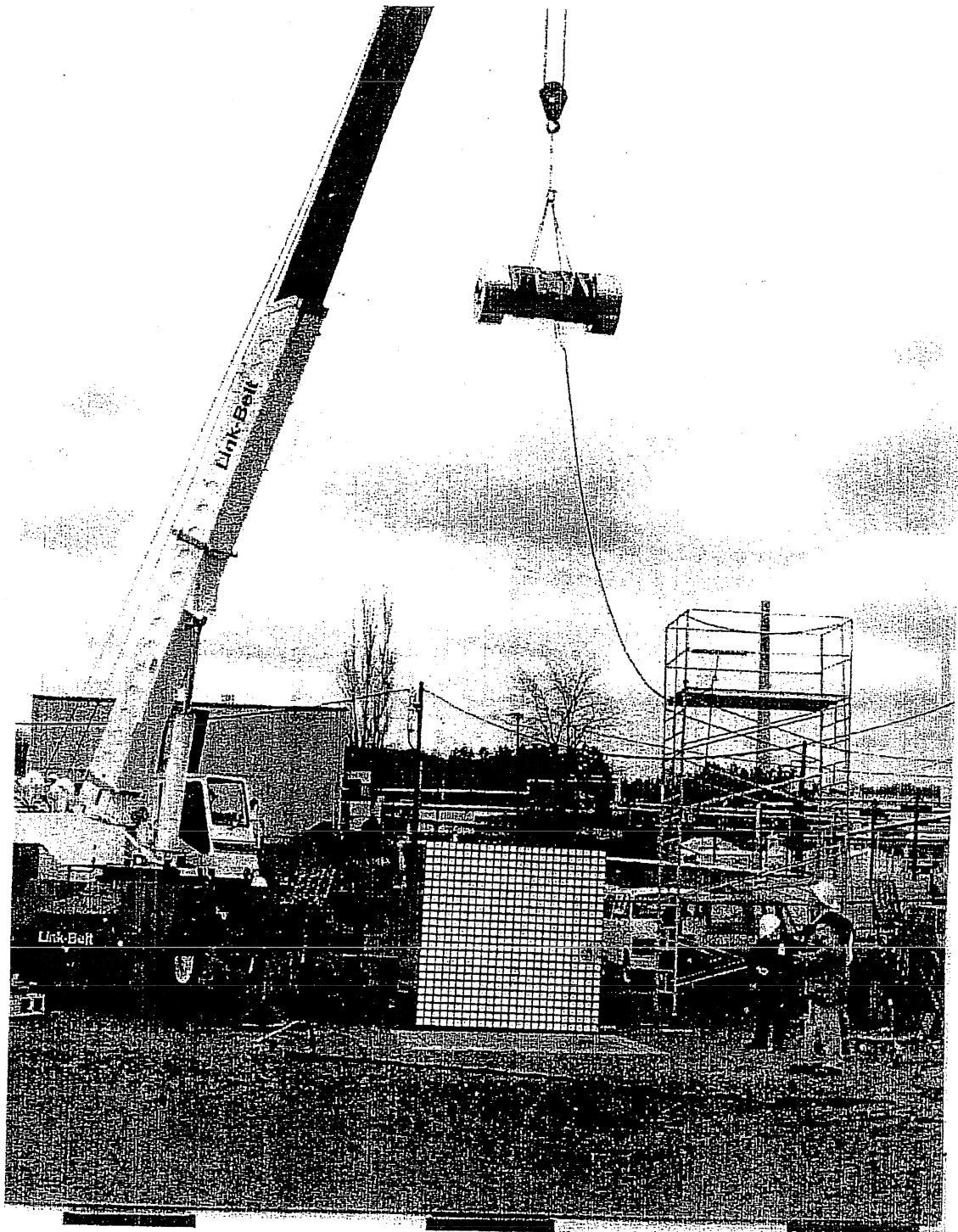


**FIGURE 2.A.5.7 : ¼ SCALE HI-STAR 100 PACKAGING  
AT 30 FT (9 M) PRIOR TO SIDE DROP**

HI-951251

REV. 10

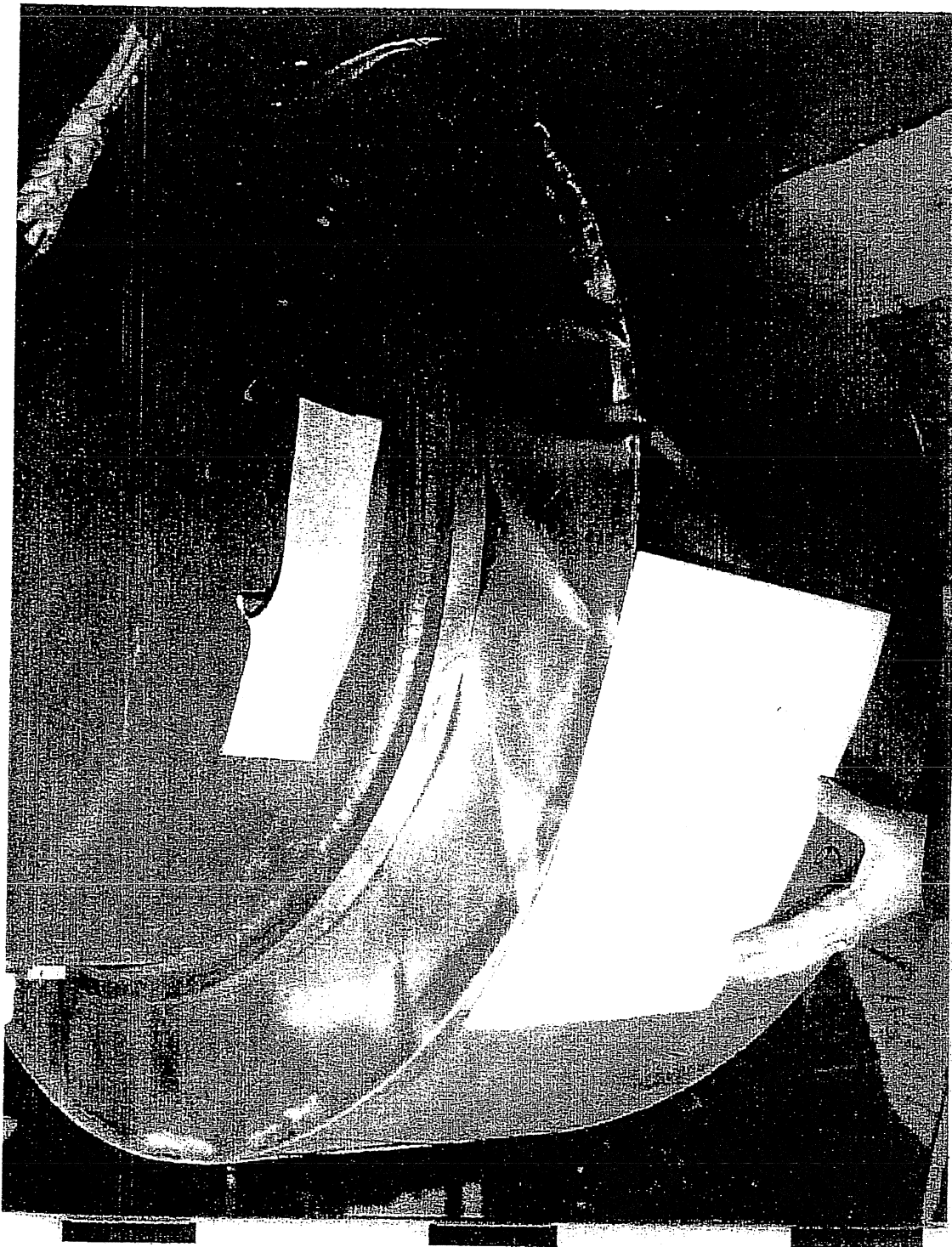


FIGURE 2A.5.8 ; 1/4 SCALE BOTTOM IMPACT LIMITER AFTER SIDE DROP

HI-951251

REV. 10

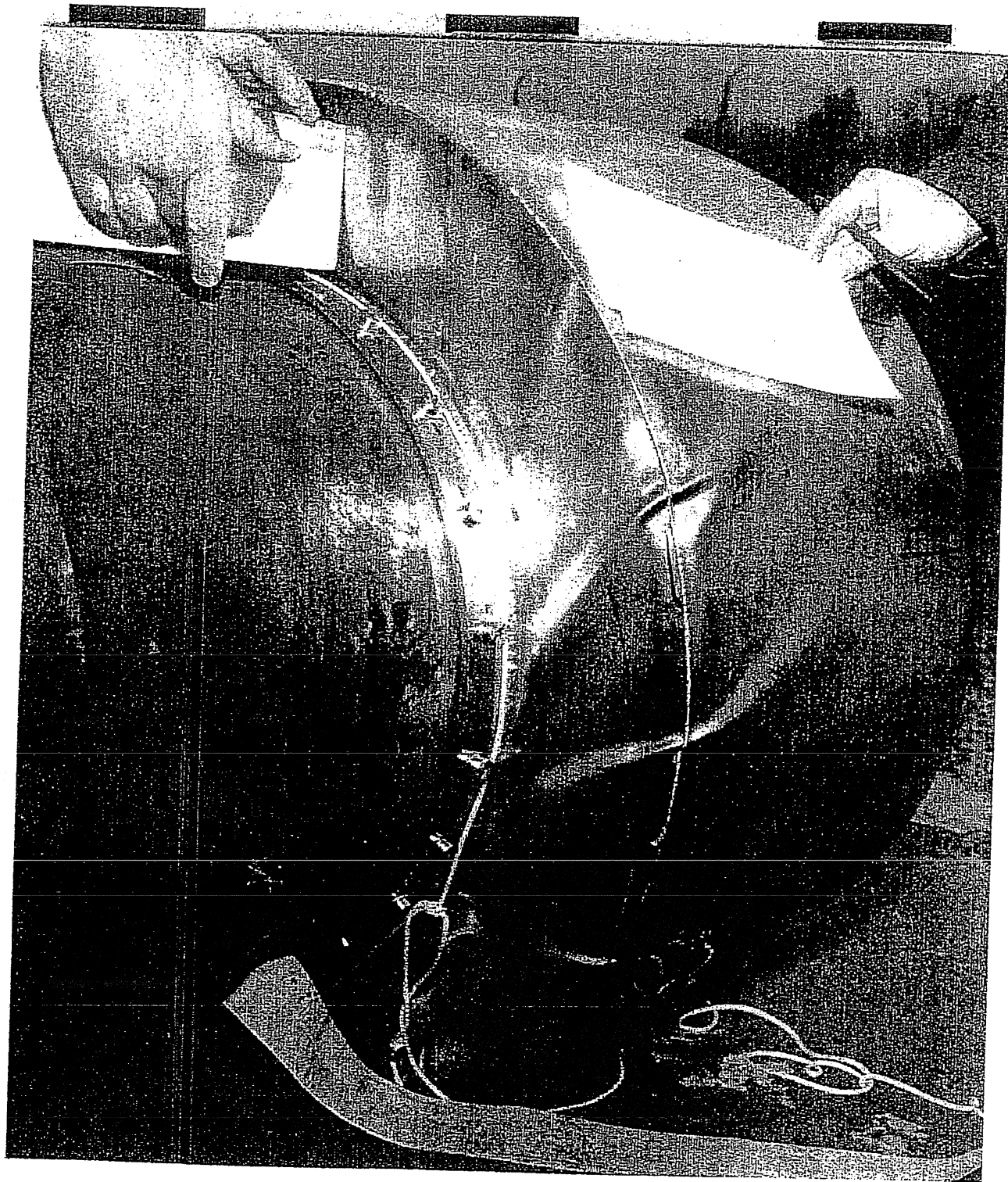


FIGURE 2.A.5.9 : 1/4 SCALE TOP IMPACT LIMITER AFTER SIDE DROP

HI-951251

REV. 10

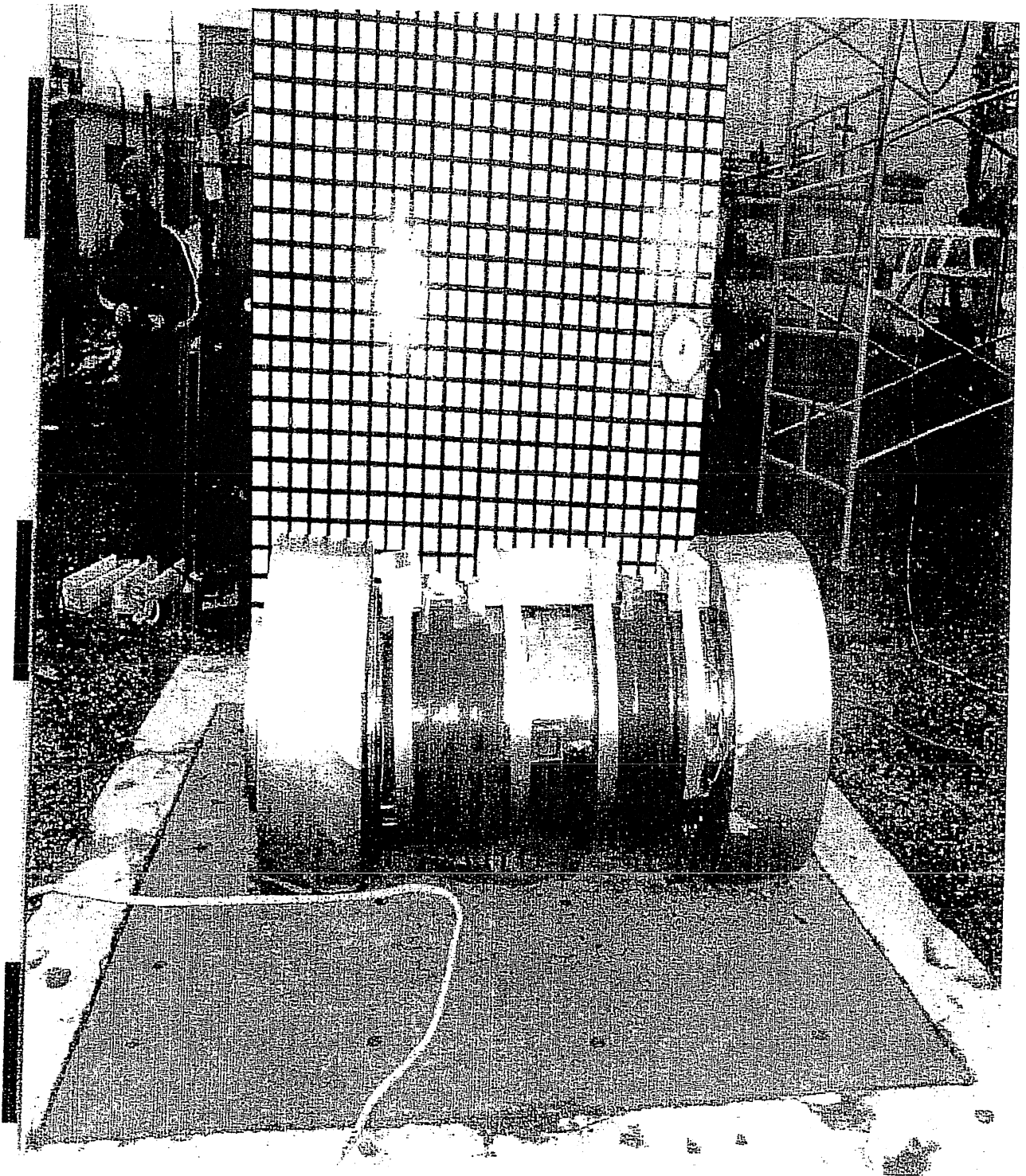


FIGURE 2.A.5.10 : 1/4 SCALE HI-STAR 100 PACKAGING AFTER SLAP DOWN DROP

HI-951251

REV. 10





**FIGURE 2.A.5.11 ; 1/4 SCALE IMPACT LIMITER AFTER C.G. OVER CORNER DROP**

HI-951251

**REV. 10**

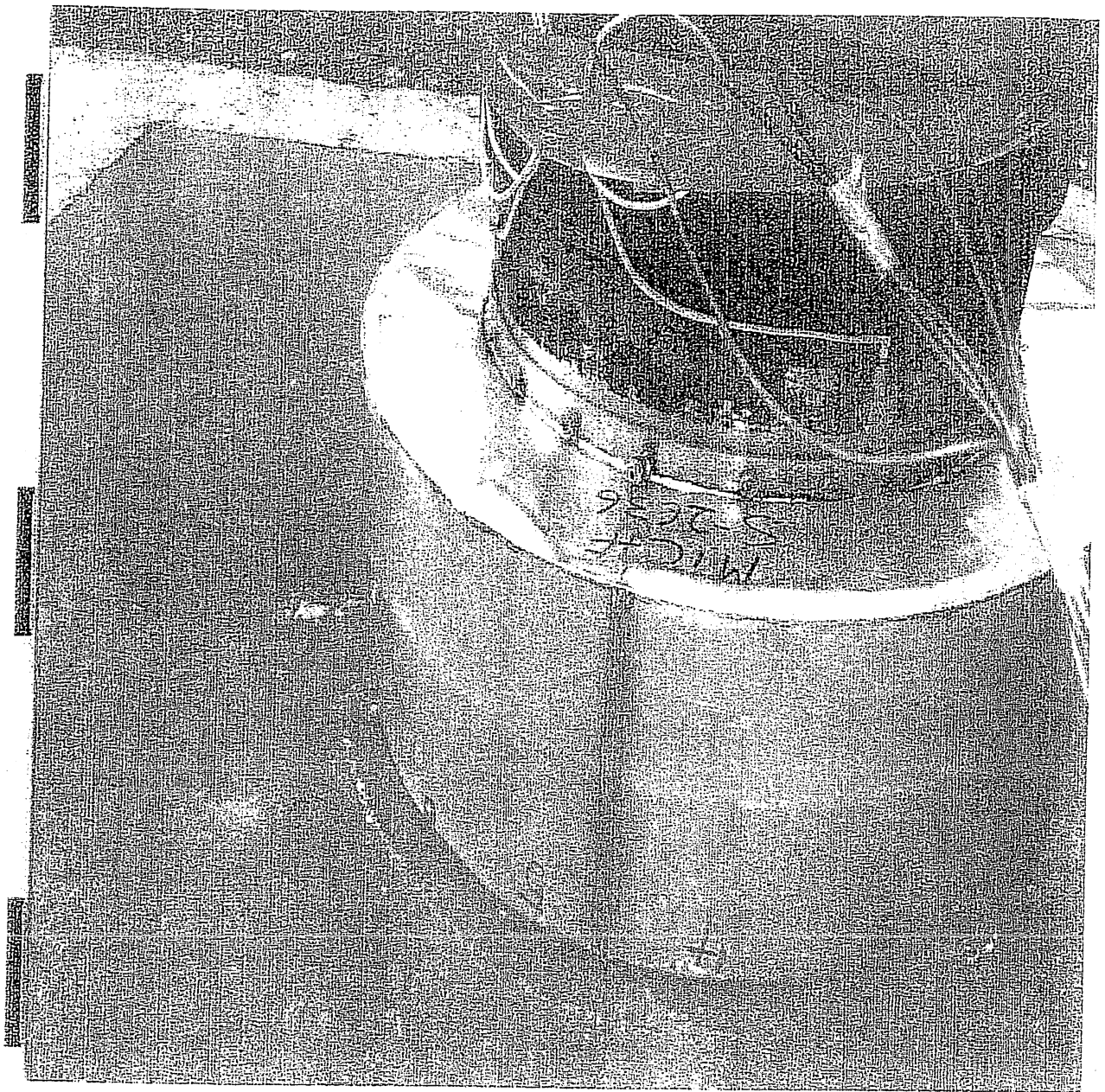


**FIGURE 2.A.5.12 ; 1/4 SCALE HI-STAR 100 PACKAGING AFTER TOP END DROP**

HI-951251

**REV. 10**



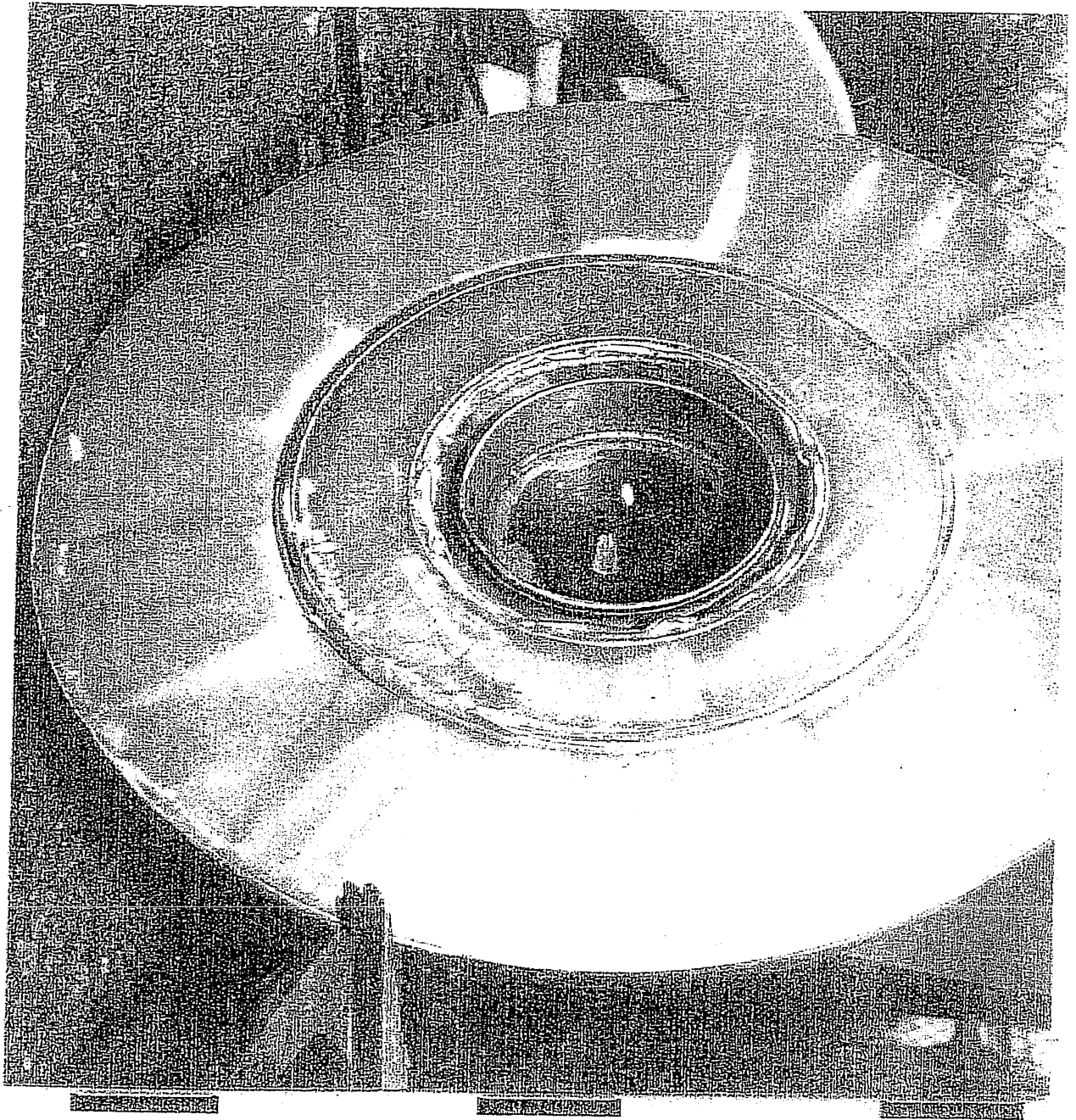


FIGURE 2.A.5.13 ; 1/4 SCALE IMPACT LIMITER TOP END DROP

HI-951251

REV. 10

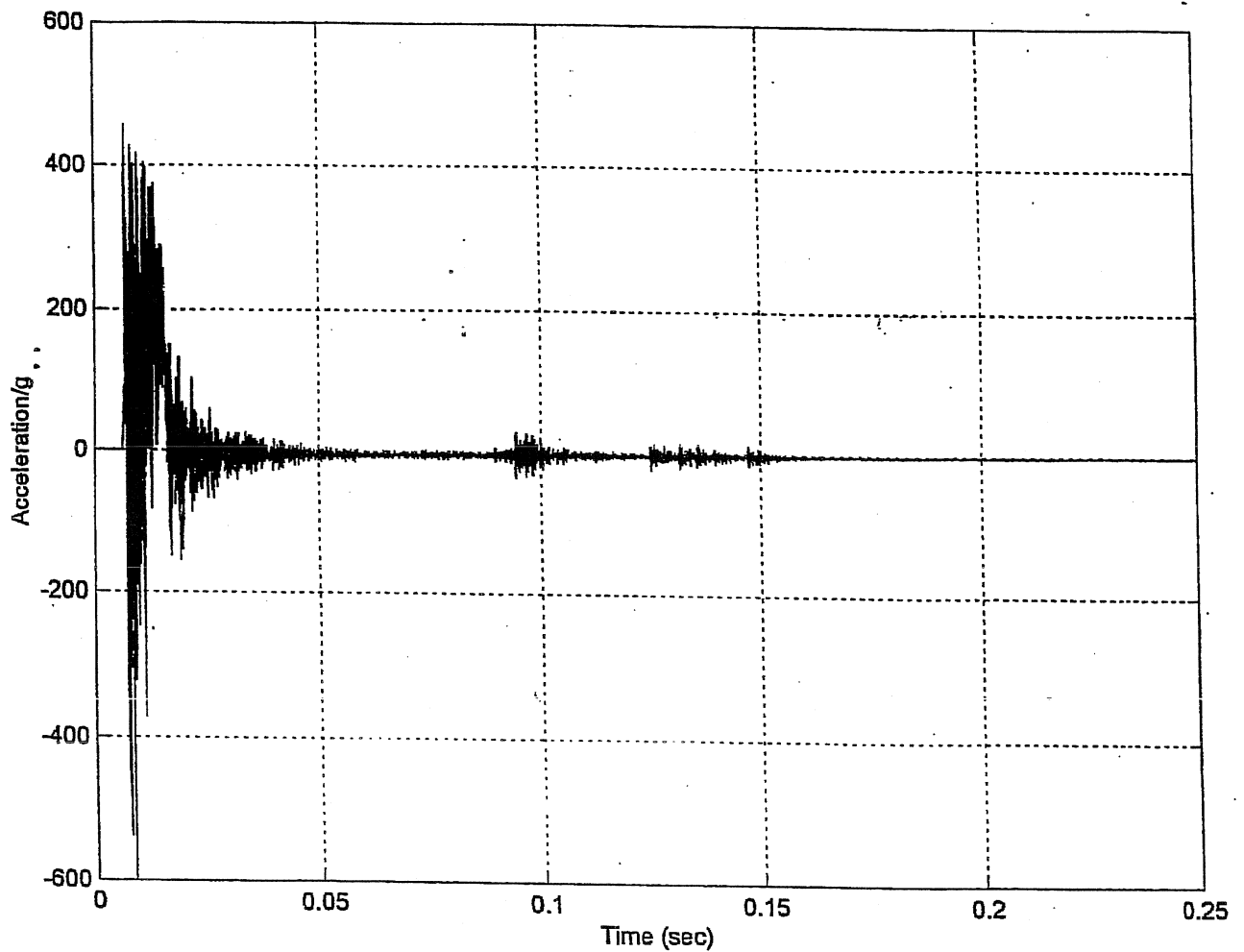


FIGURE 2.A.5.14 ; ACCELERATION RAW DATA FOR TOP END DROP

HI-951251

REV. 1C

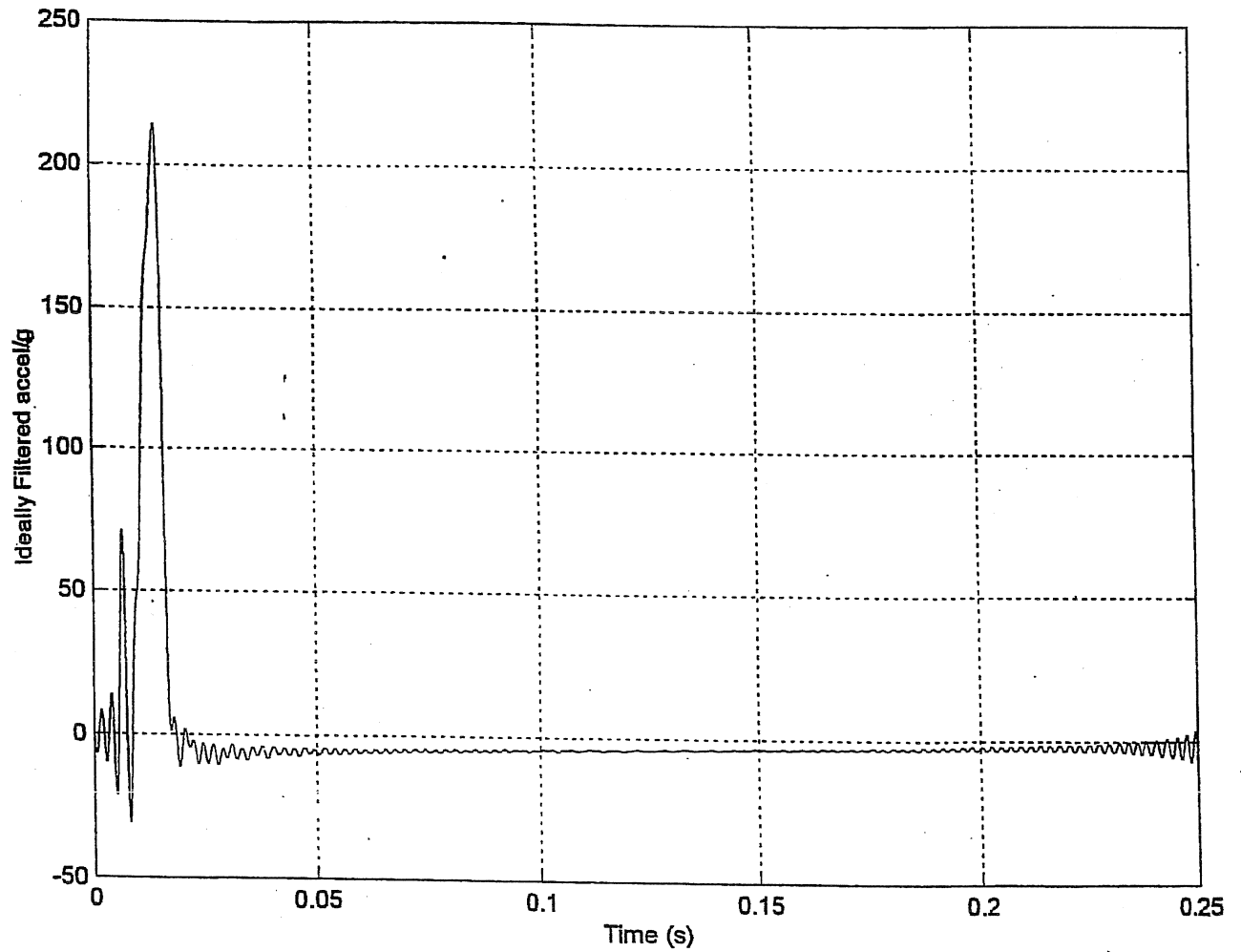
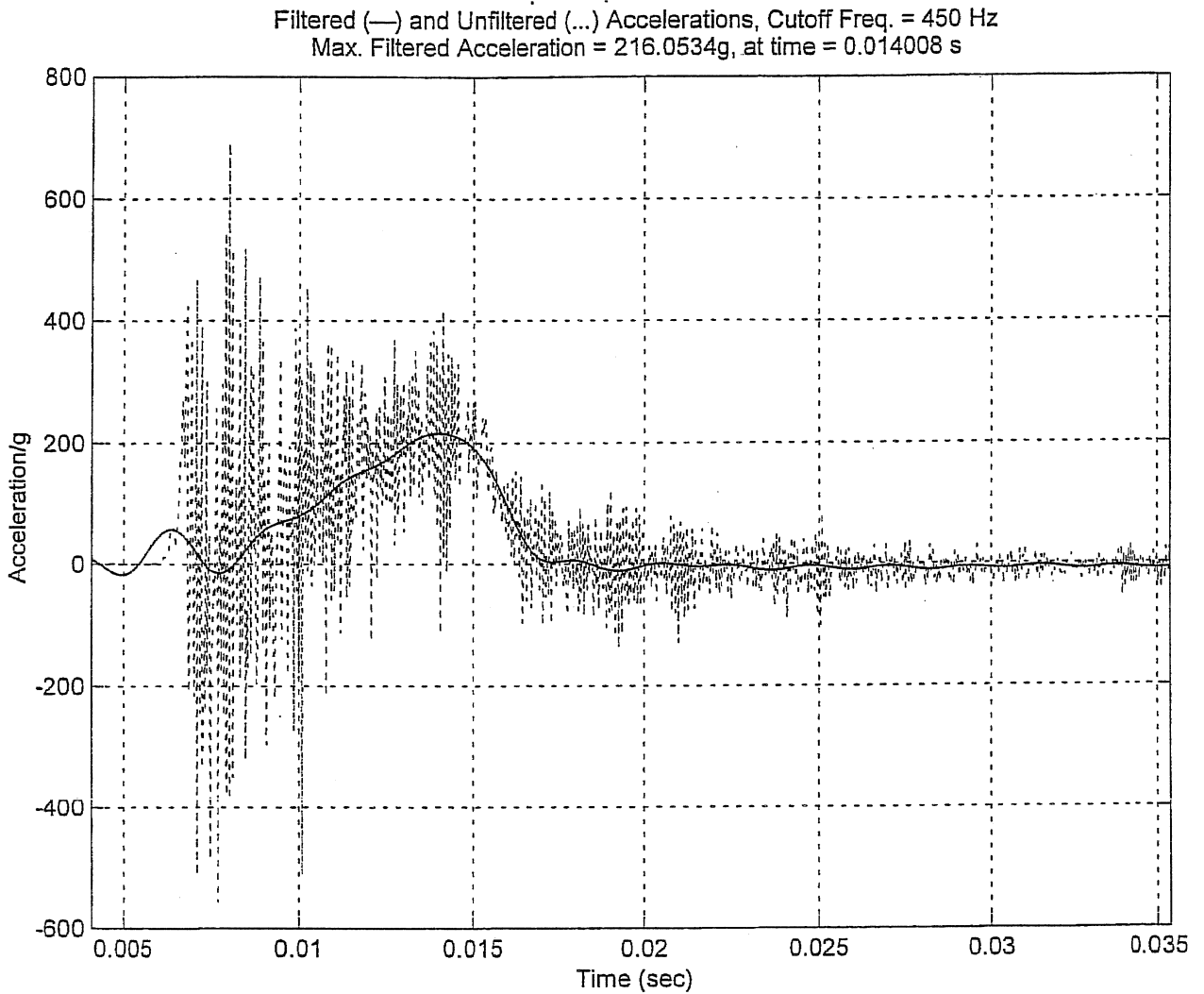


FIGURE 2.A.5.15 ; ACCELERATION DATA FILTERED AT 450 Hz FOR TOP END DROP

HI-951251

REV. 10

**FIGURE 2.A.5.15A ; TOP END DROP**

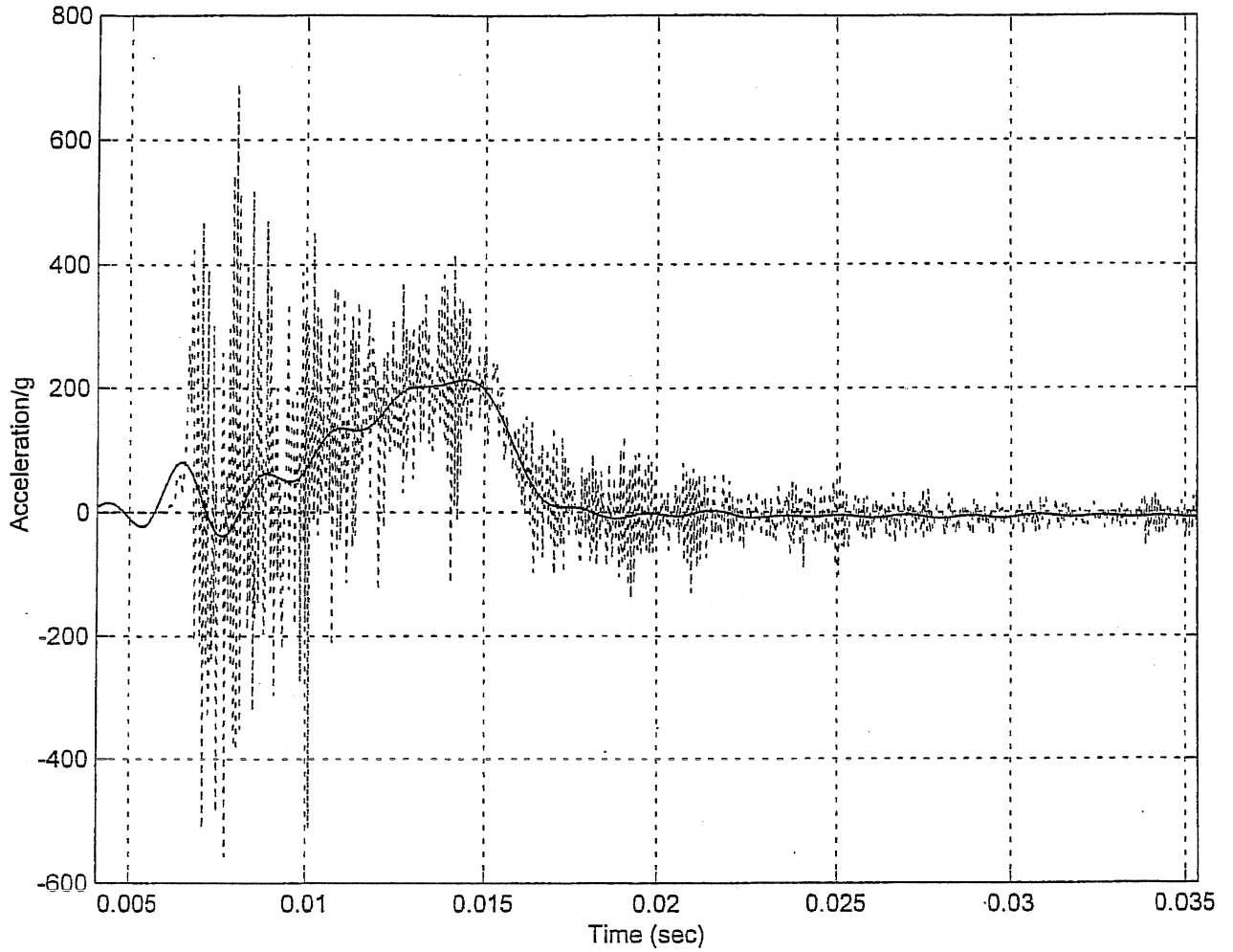


HI-951251

REV. 10

**FIGURE 2.A.5.15B ; TOP END DROP**

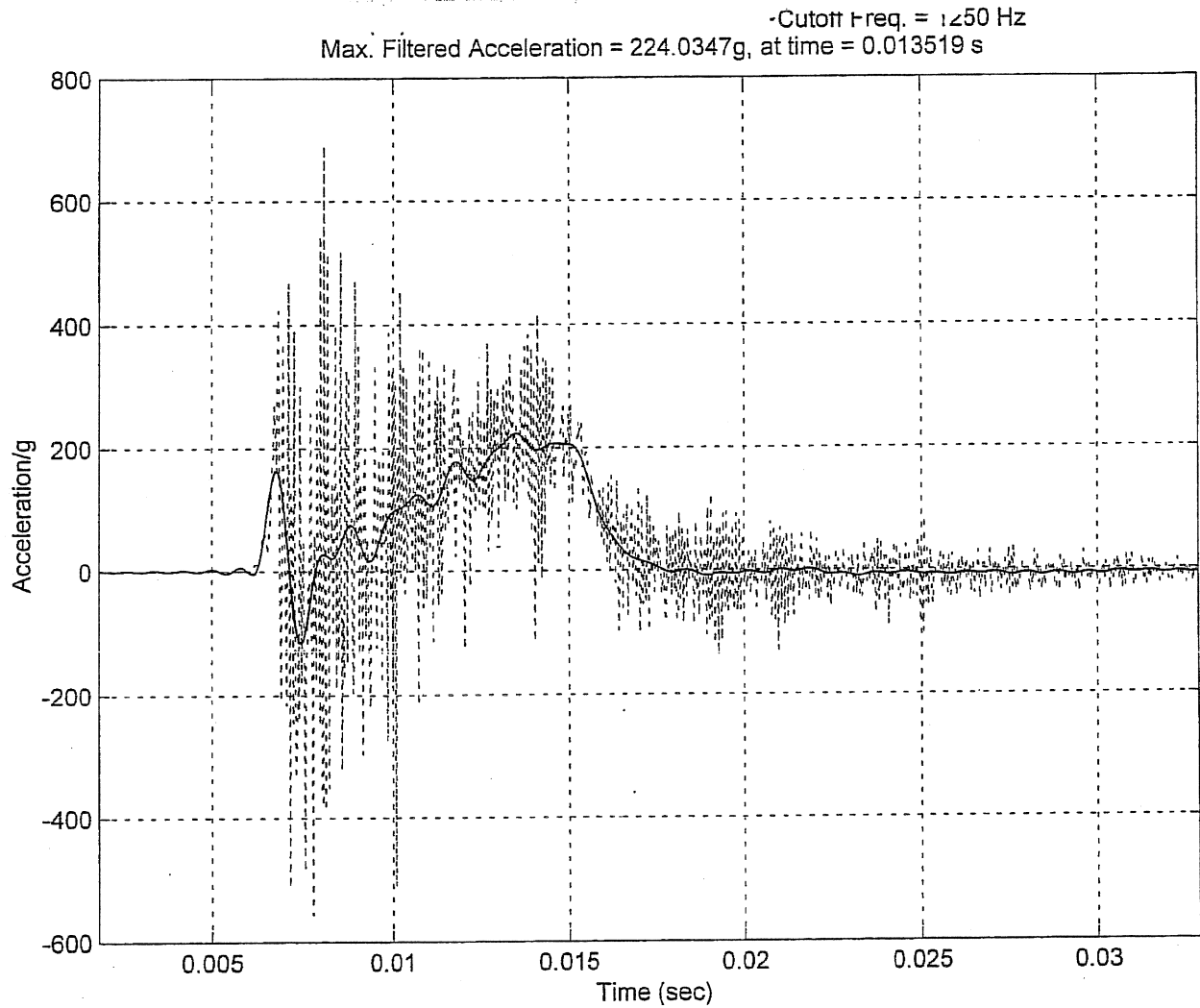
Filtered (—) and Unfiltered (...) Accelerations, Cutoff Freq. = 550 Hz  
 Max. Filtered Acceleration = 213.7848g, at time = 0.014465 s



HI-951251

REV. 10

**FIGURE 2.A.5.15C ; TOP END DROP**



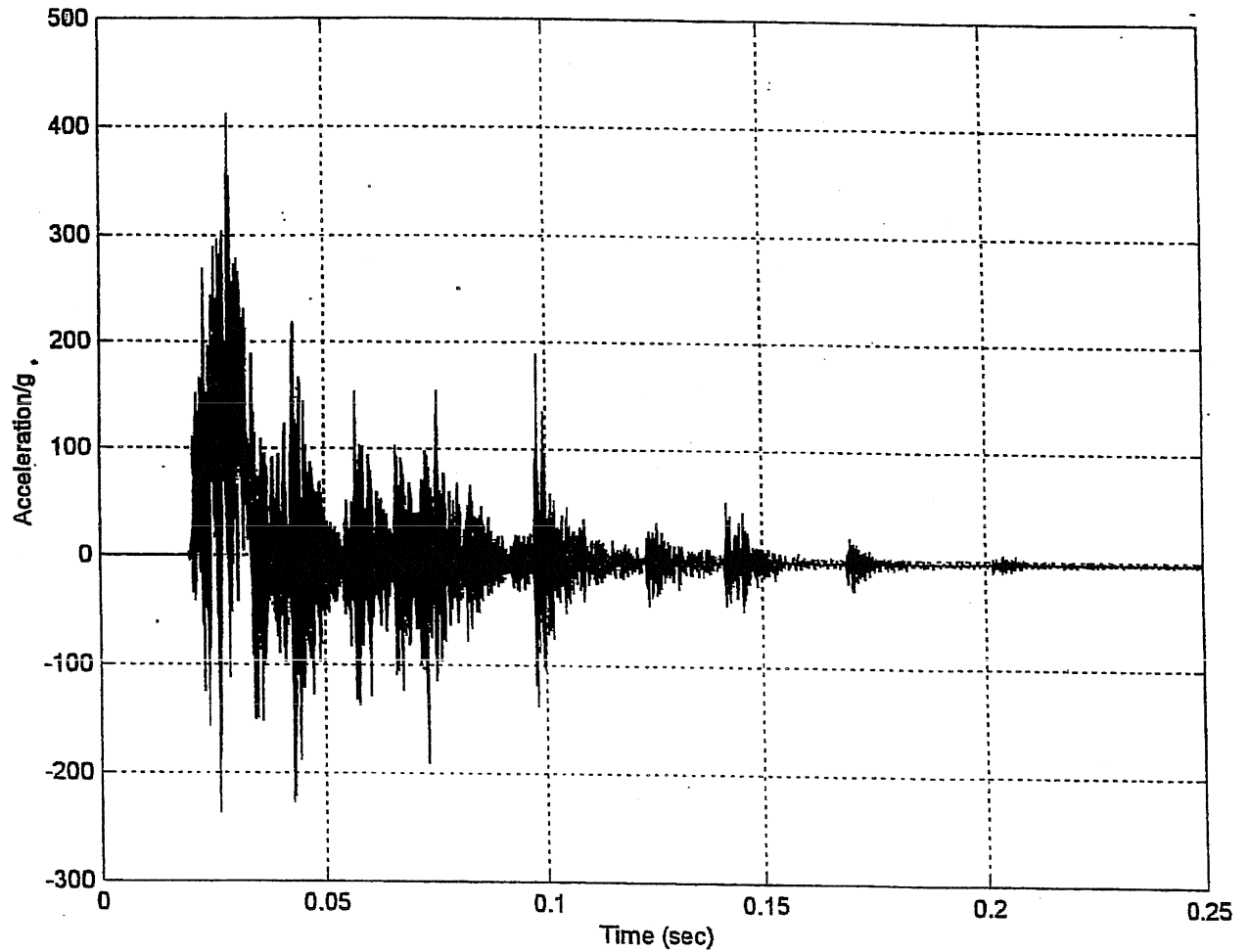


FIGURE 2.A.5.16 : ACCELERATION RAW DATA FOR C.G. OVER CORNER DROP

HI-951251

REV. 1

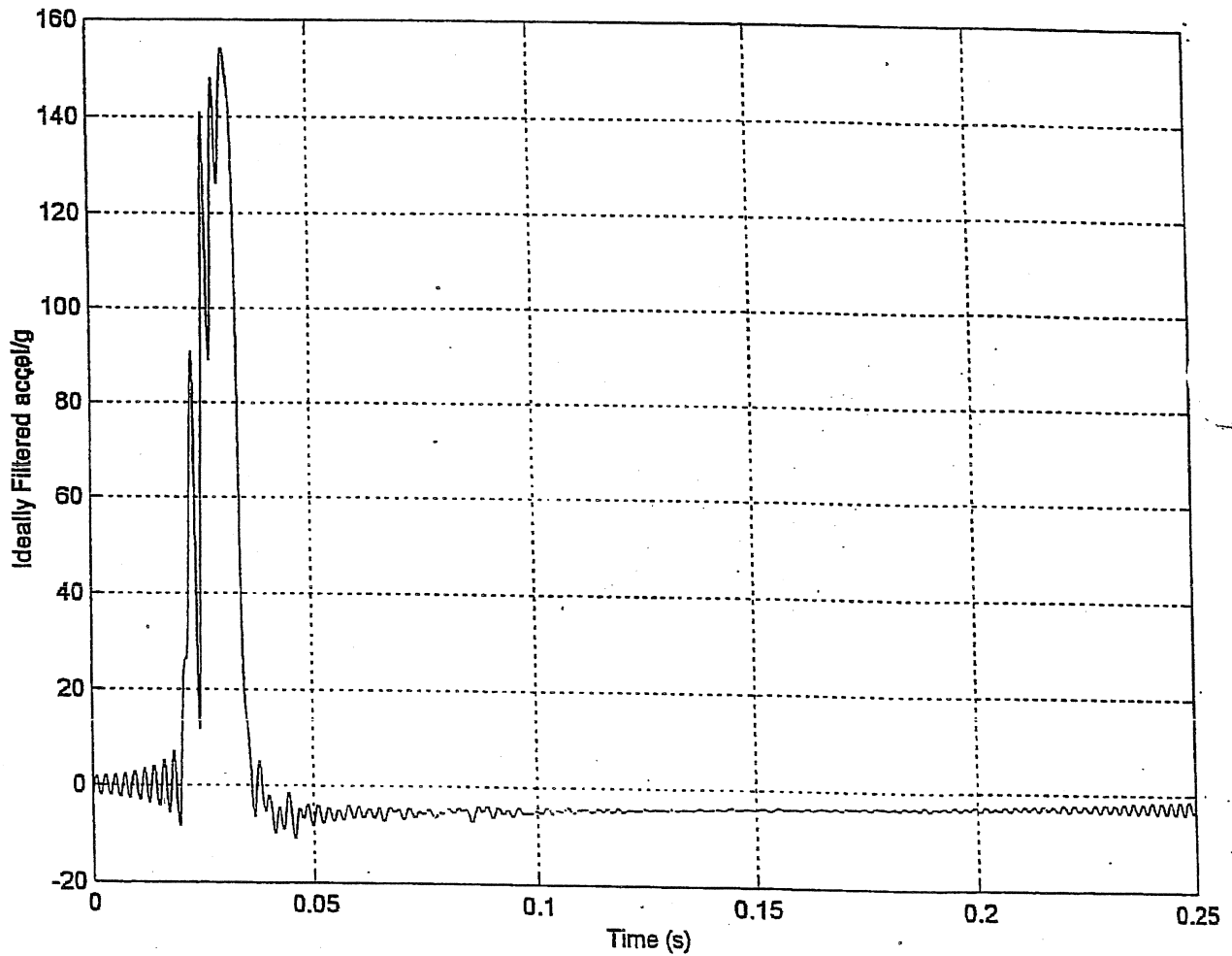


FIGURE 2.A.5.17 ; ACCELERATION DATA FILTERED AT 450 Hz FOR C.G. OVER CORNER

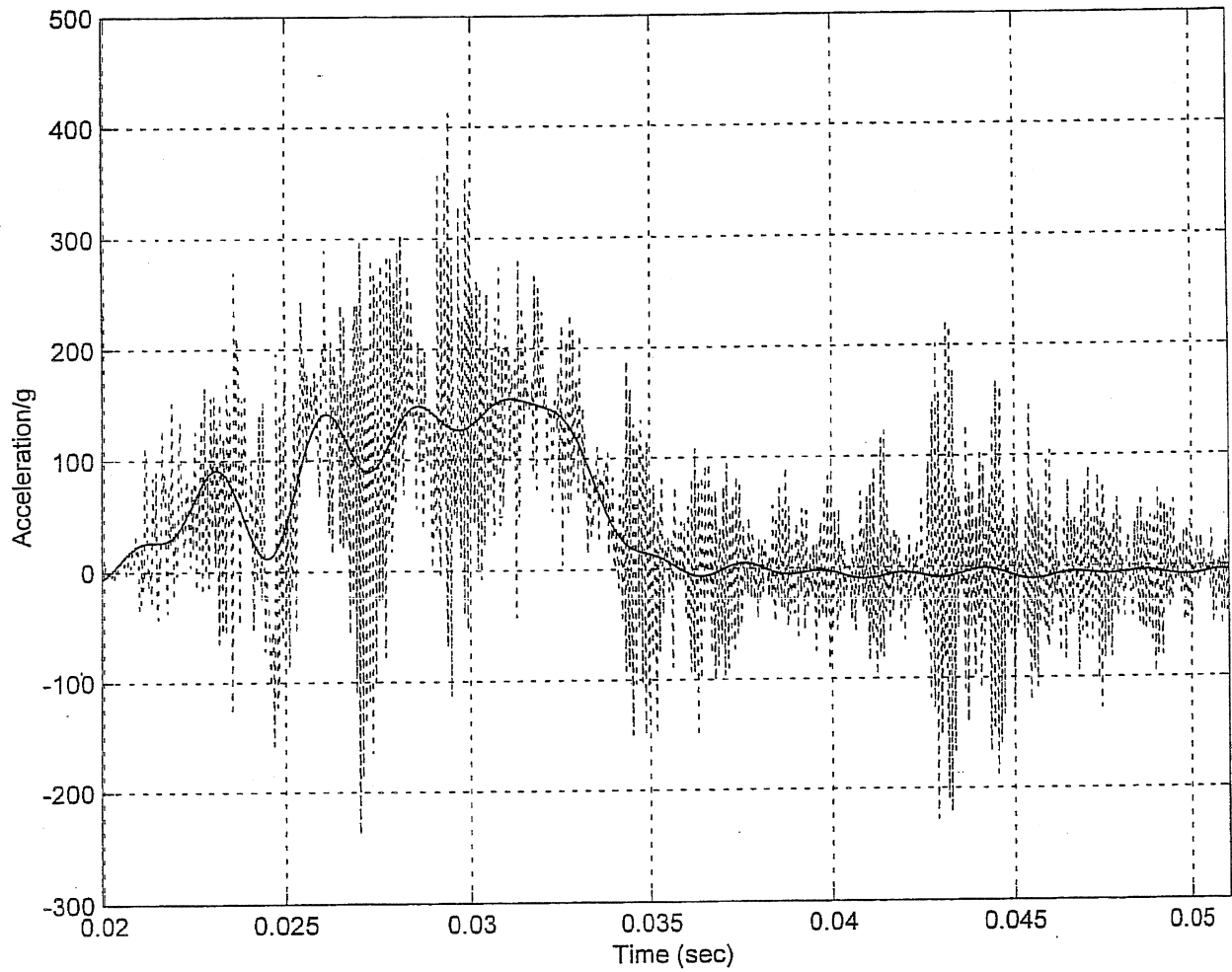
HI-951251

REV. 10



**FIGURE 2.A.5.17A : CG OVER CORNER**

Filtered (—) and Unfiltered (...) Accelerations, Cutoff Freq. = 450 Hz  
 Max. Filtered Acceleration = 154.2797g, at time = 0.031097 s



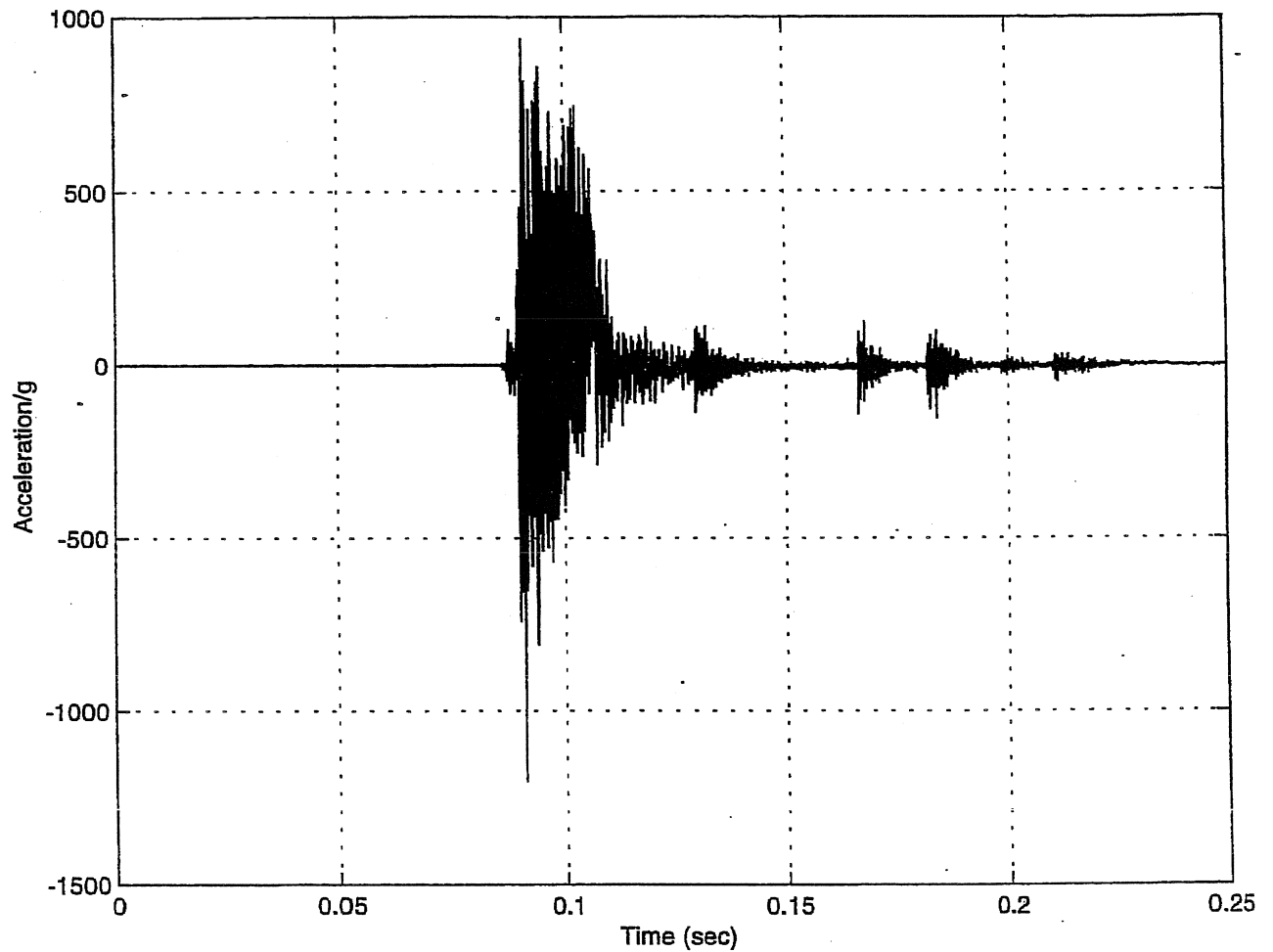


FIGURE 2.A.5.18 ; ACCELERATION RAW DATA AT BOTTOM END DURING SLAPDOWN DROP

HI-951251

REV. 10

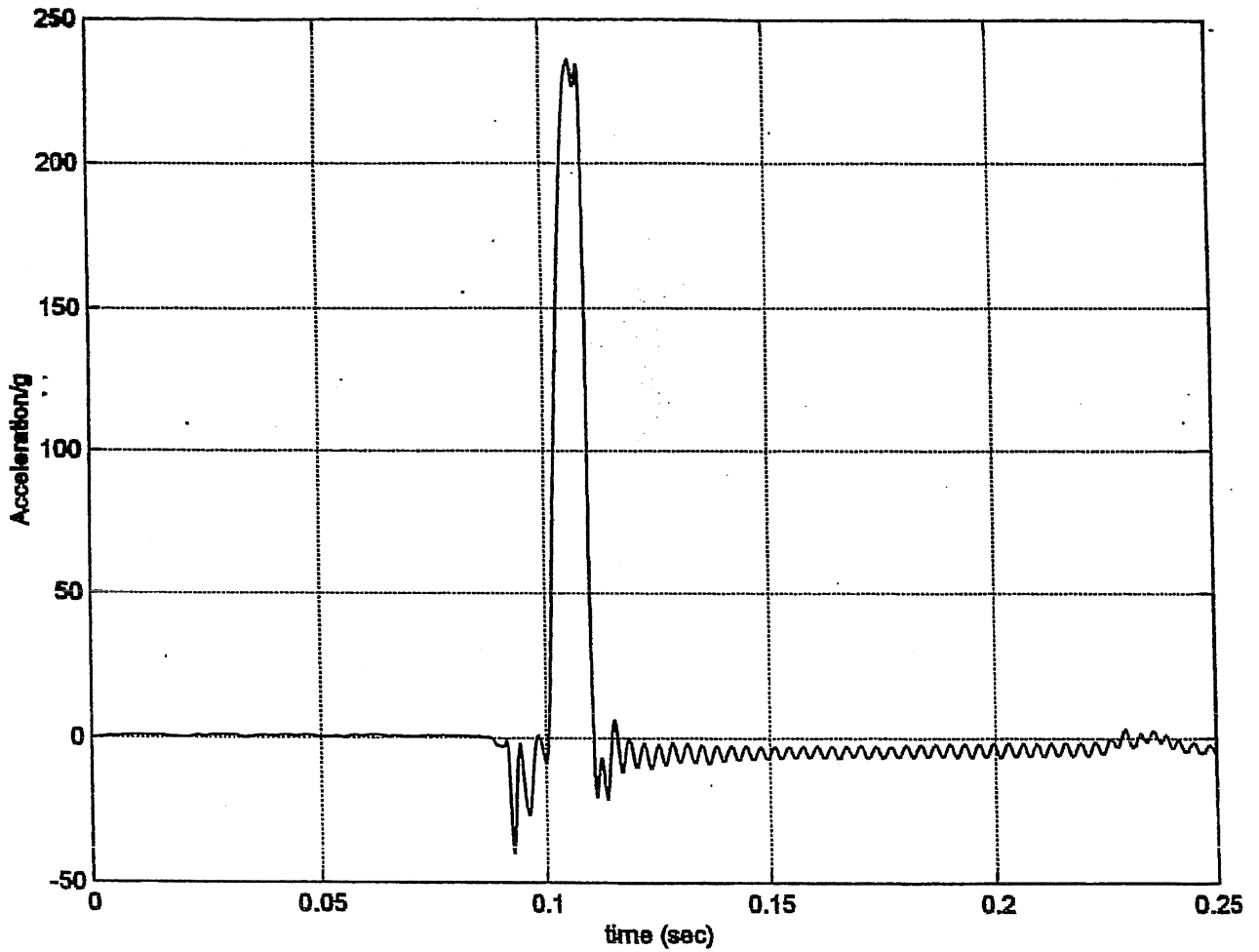
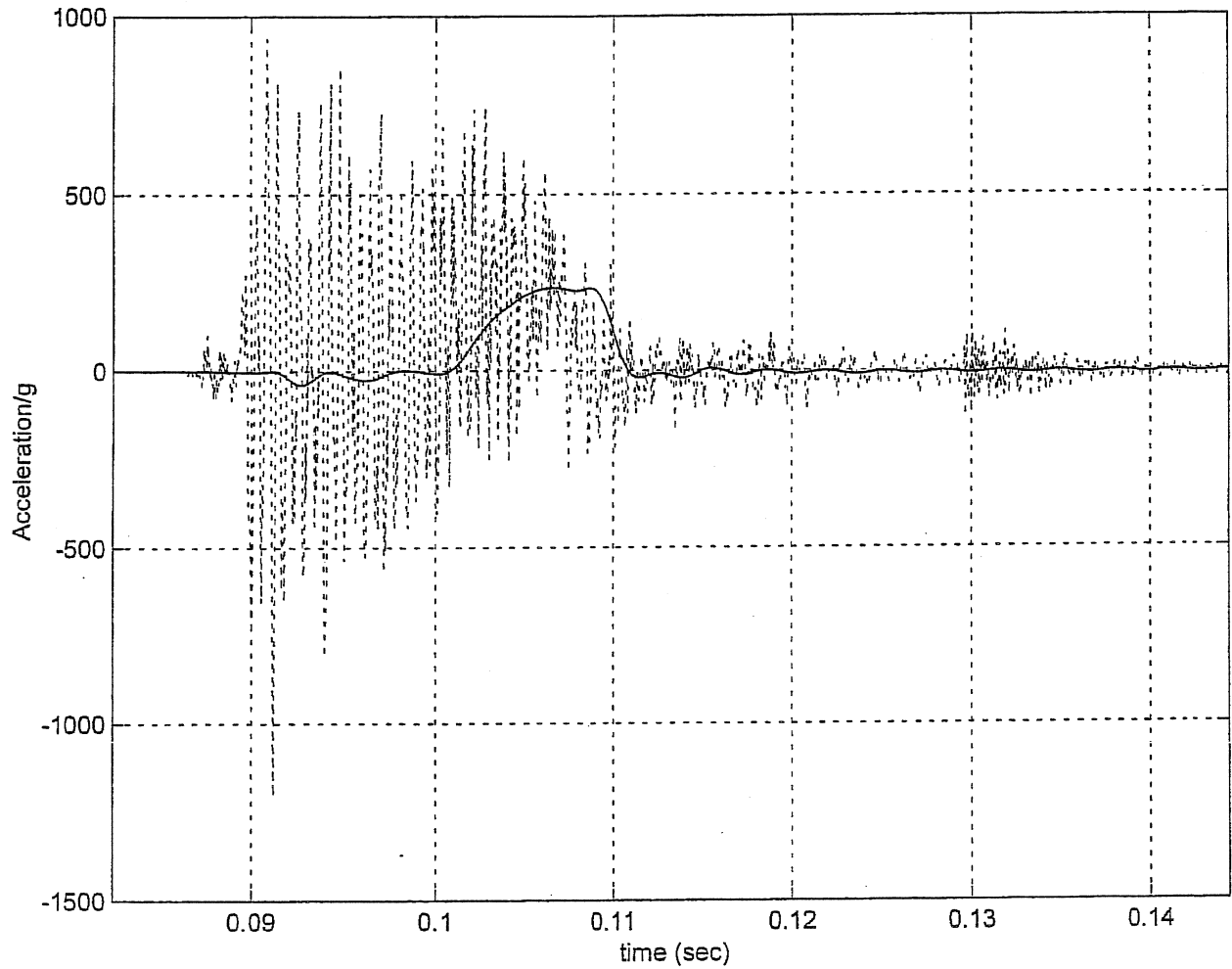


FIGURE 2.A.5.19 ; ACCELERATION DATA FILTERED AT 350 Hz FOR SLAPDOWN DROP  
 HI-951251 REV. 10

**FIGURE 2.A.5.19A ; : SLAP DOWN**

Filtered (—) and Unfiltered (...) Accelerations, Cutoff Freq. = 350 Hz  
Maximum Accel: for 1/4 scale model 236g; for prototype 59g  
From Program sl\_bw1.m



HI-951251

REV. 10

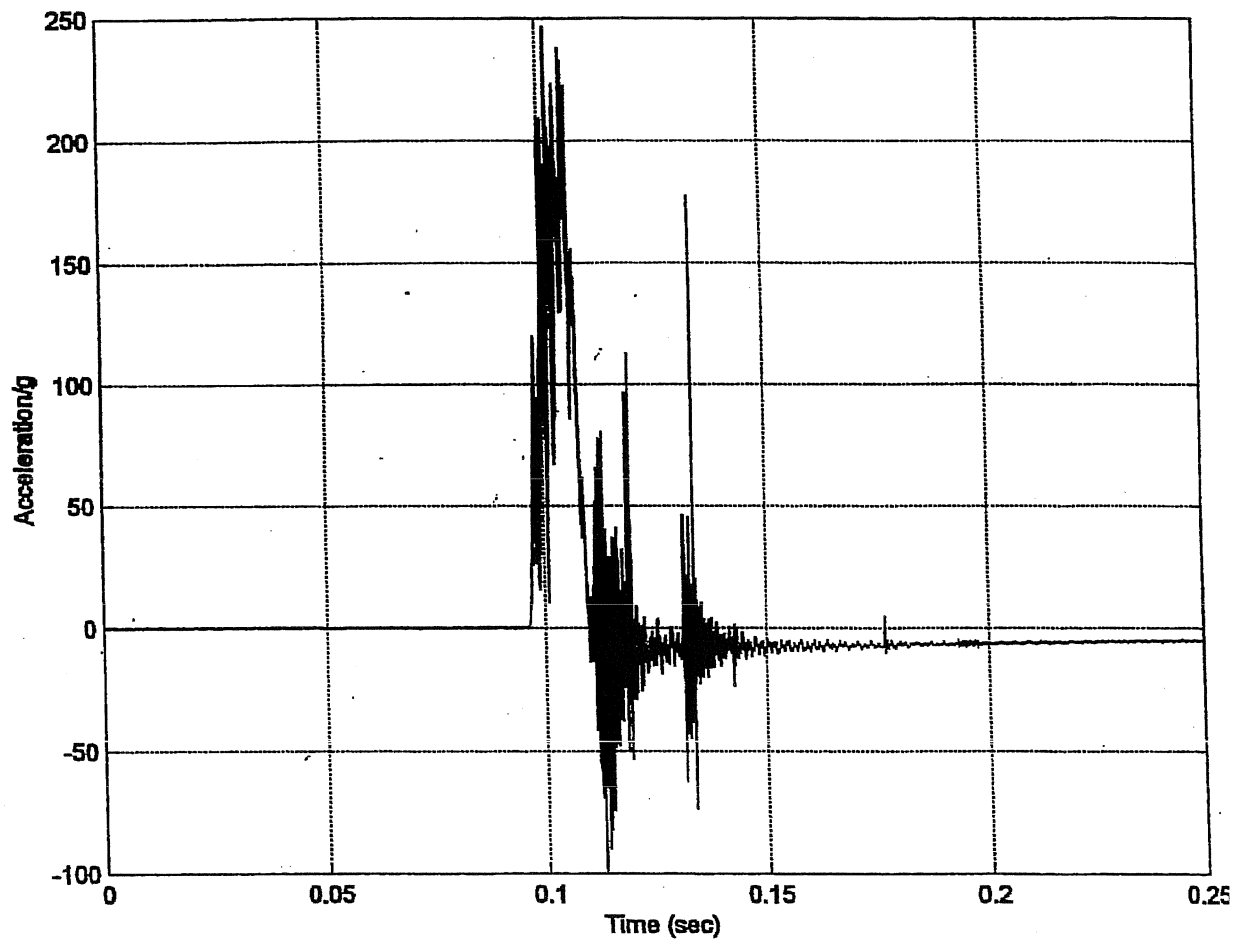


FIGURE 2.A.5.20 ; ACCELERATION RAW DATA FOR SIDE DROP

HI-951251

REV. 10

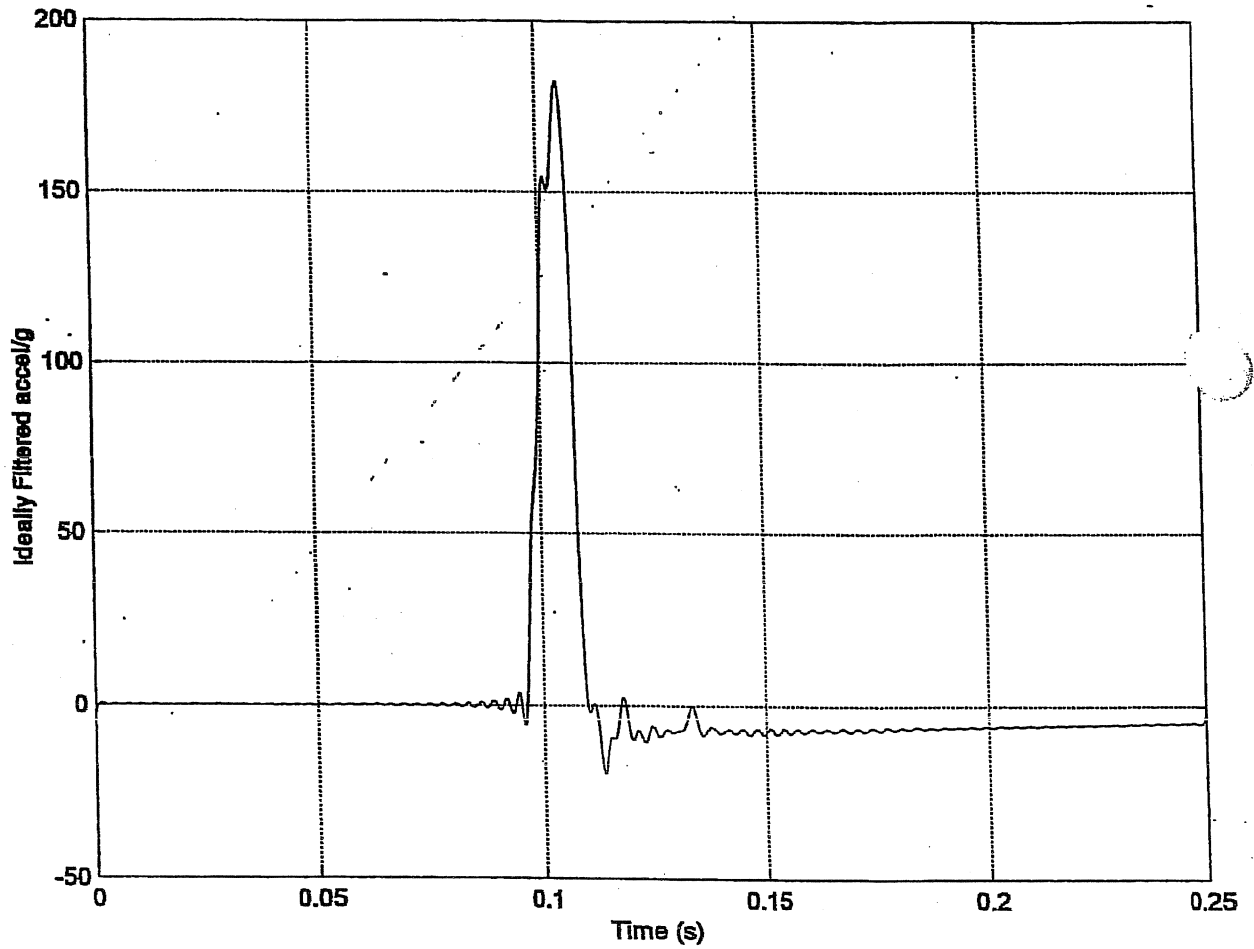
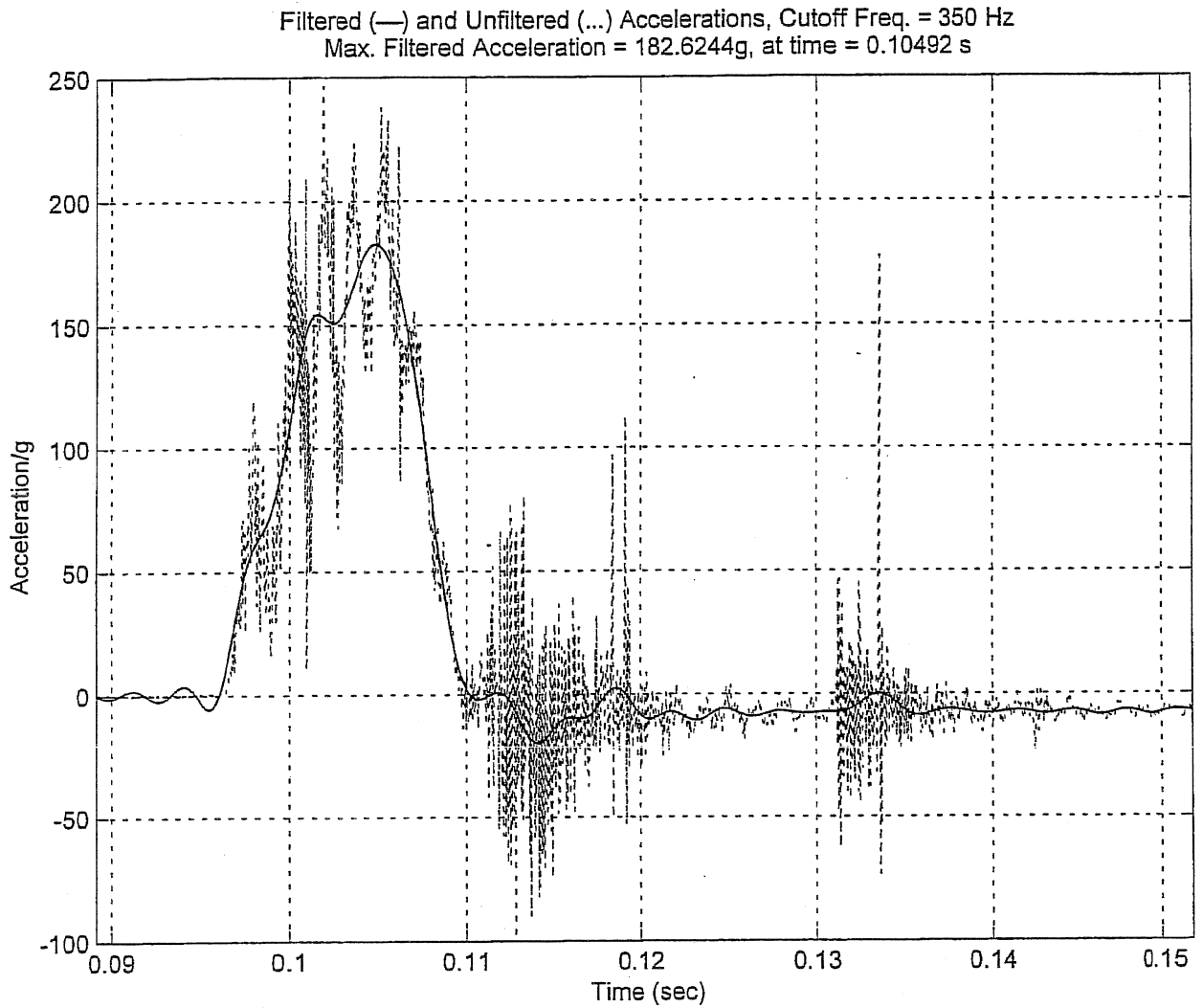


FIGURE 2.A.5.21 ; ACCELERATION DATA FILTERED AT 350 Hz FOR SIDE DROP

HI-951251

REV. 10

**FIGURE 2.A.5.21A**



HI-951251

REV. 10

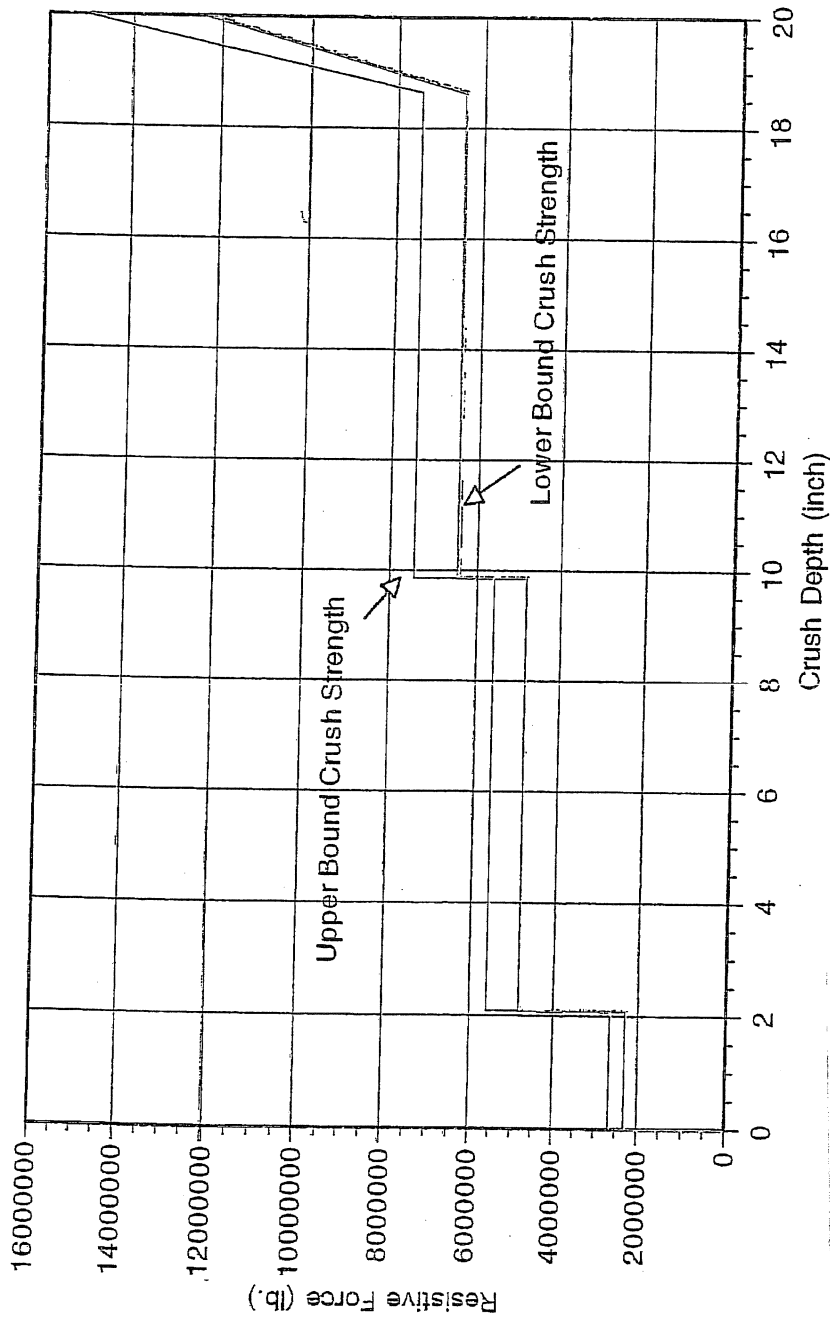


FIGURE 2.A.6.1 ; - Impact Limiter Force vs. Crush Depth ( $\theta = 90$  degrees)

HI-951251

REV. 10



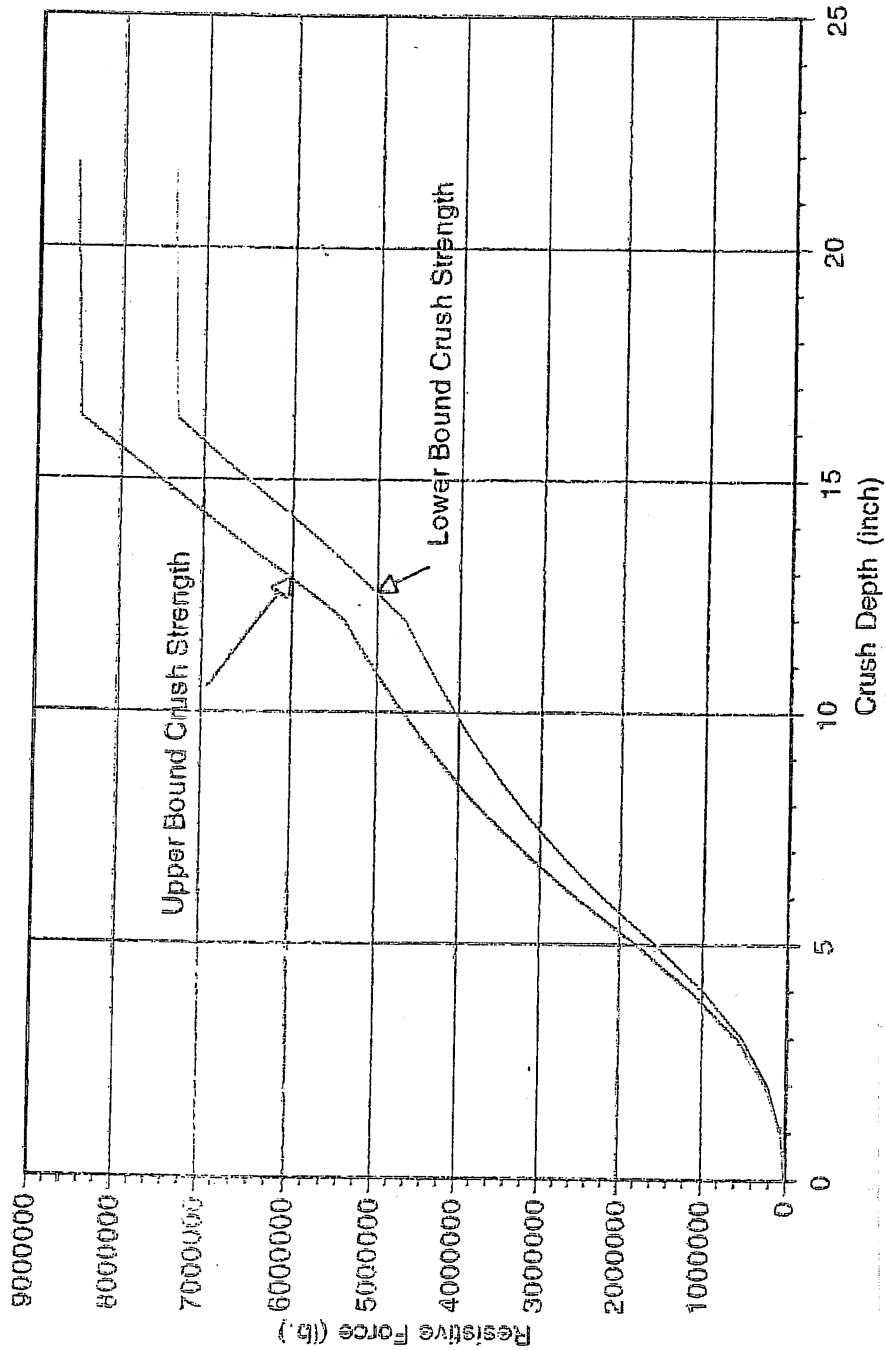


FIGURE 2.A.6.2 ; Impact Limiter Force vs. Crush Depth ( $\theta = 67.5$  degrees)

HI-951251

REV. 10

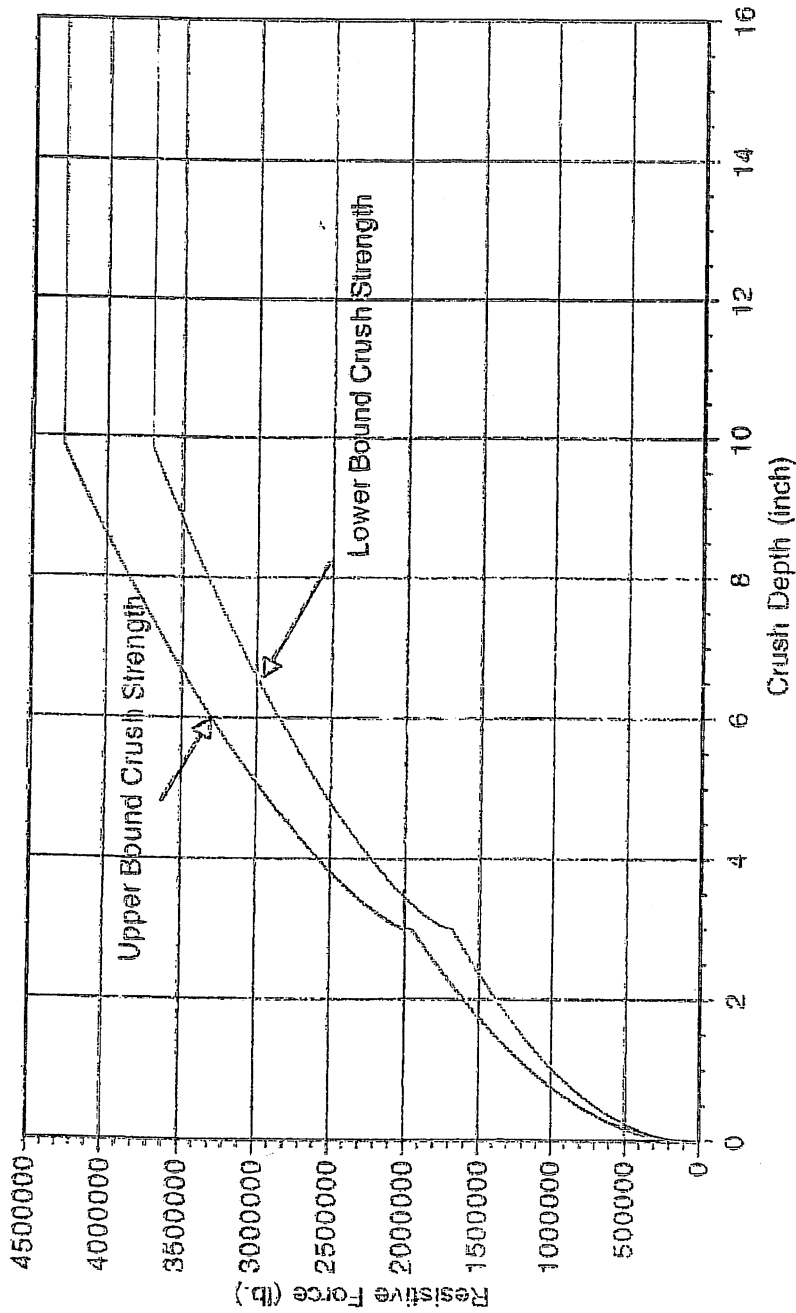


FIGURE 2.A.6.3 ; - Impact Limiter Force vs. Crush Depth ( $\theta = 0$  degrees)

HI-951251

REV. 10

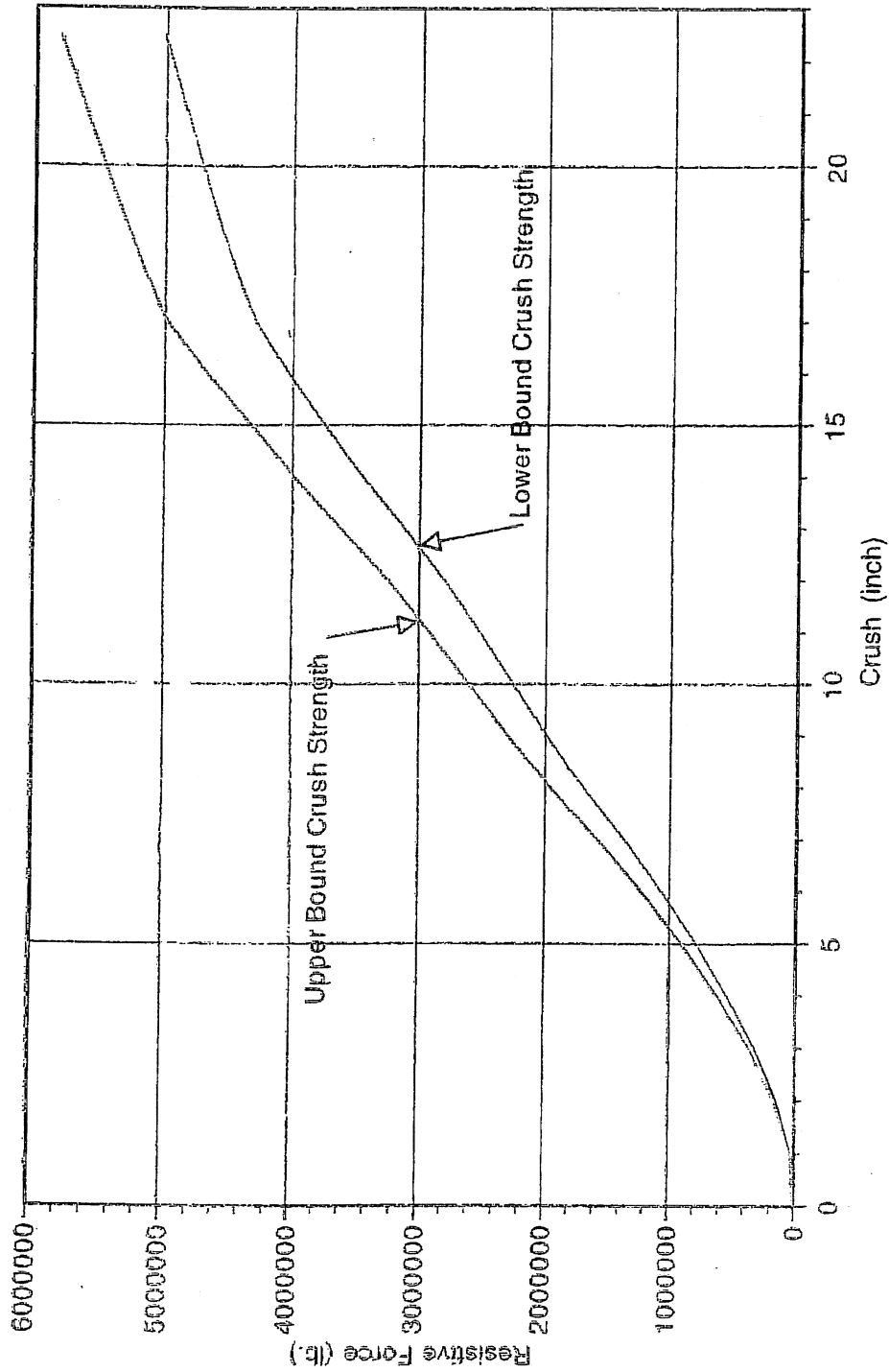


FIGURE 2.A.6.4 : Impact Limiter Force vs. Crush Depth ( $\theta = 15$  degrees)

HI-951251

REV. 10

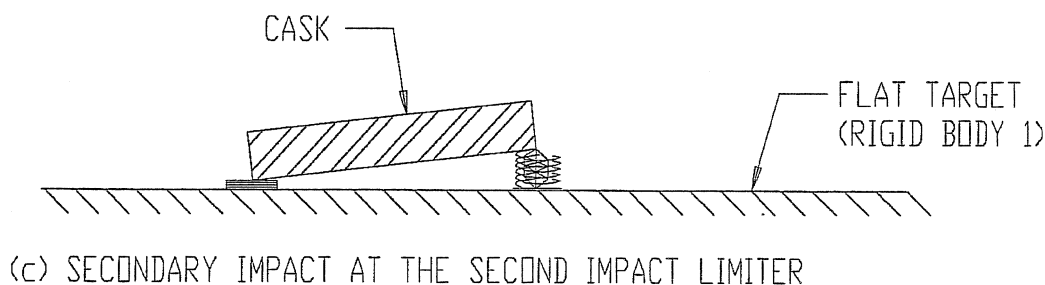
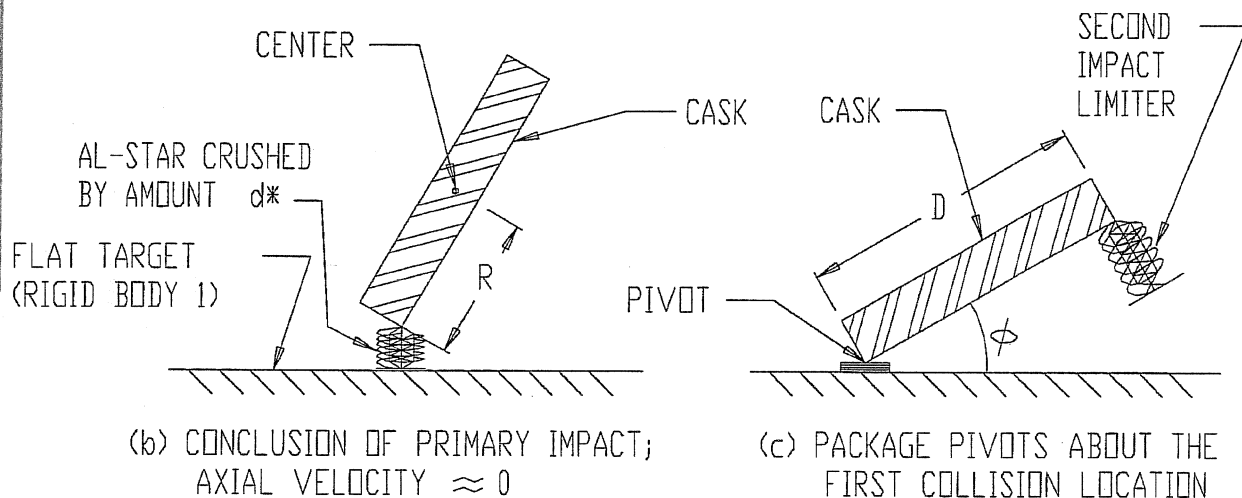
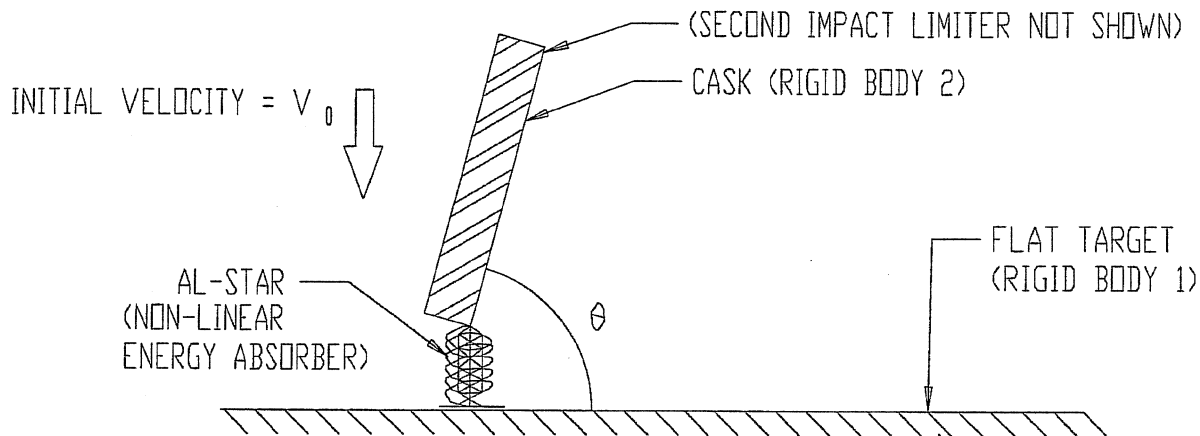
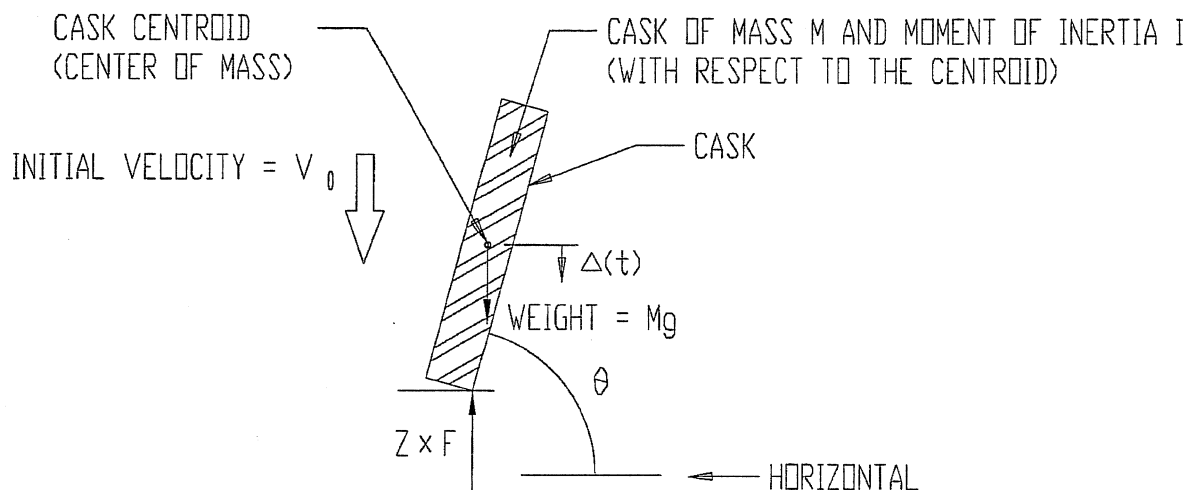
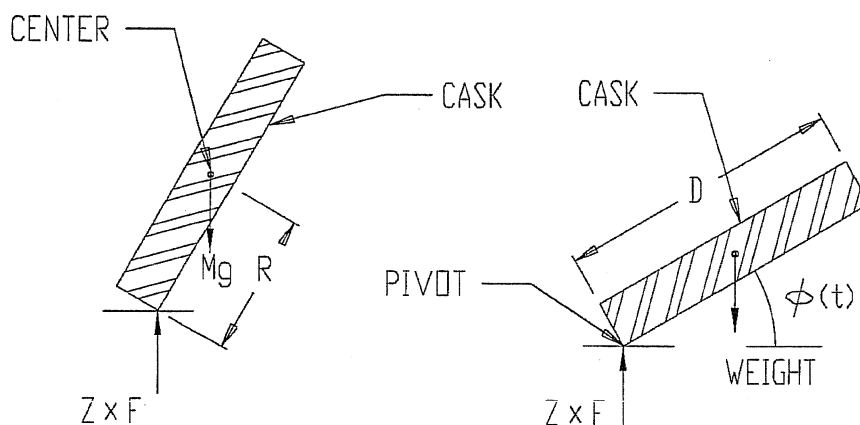


FIGURE 2.A.6.5; DYNAMIC MODEL FOR DUAL IMPACT SCENARIOS

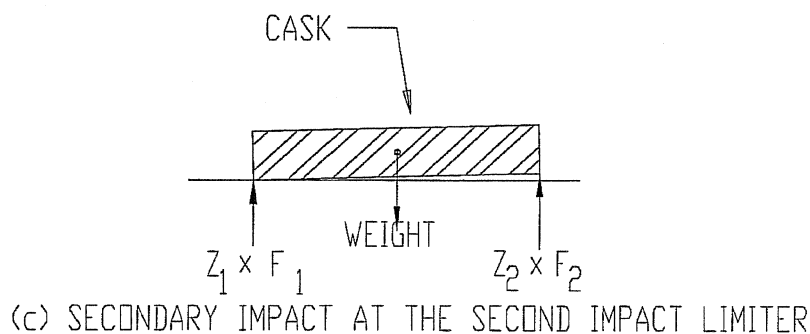


(a) INITIATION OF IMPACT AT AN OBLIQUE ANGLE ( $\theta \approx 67.5^\circ$ )



(b) CONCLUSION OF PRIMARY IMPACT;  
AXIAL VELOCITY  $\approx 0$

(c) PACKAGE PIVOTS ABOUT THE  
FIRST COLLISION LOCATION



(c) SECONDARY IMPACT AT THE SECOND IMPACT LIMITER

FIGURE 2.A.6.6; FREE-BODY DIAGRAM FOR IMPACT SCENARIOS

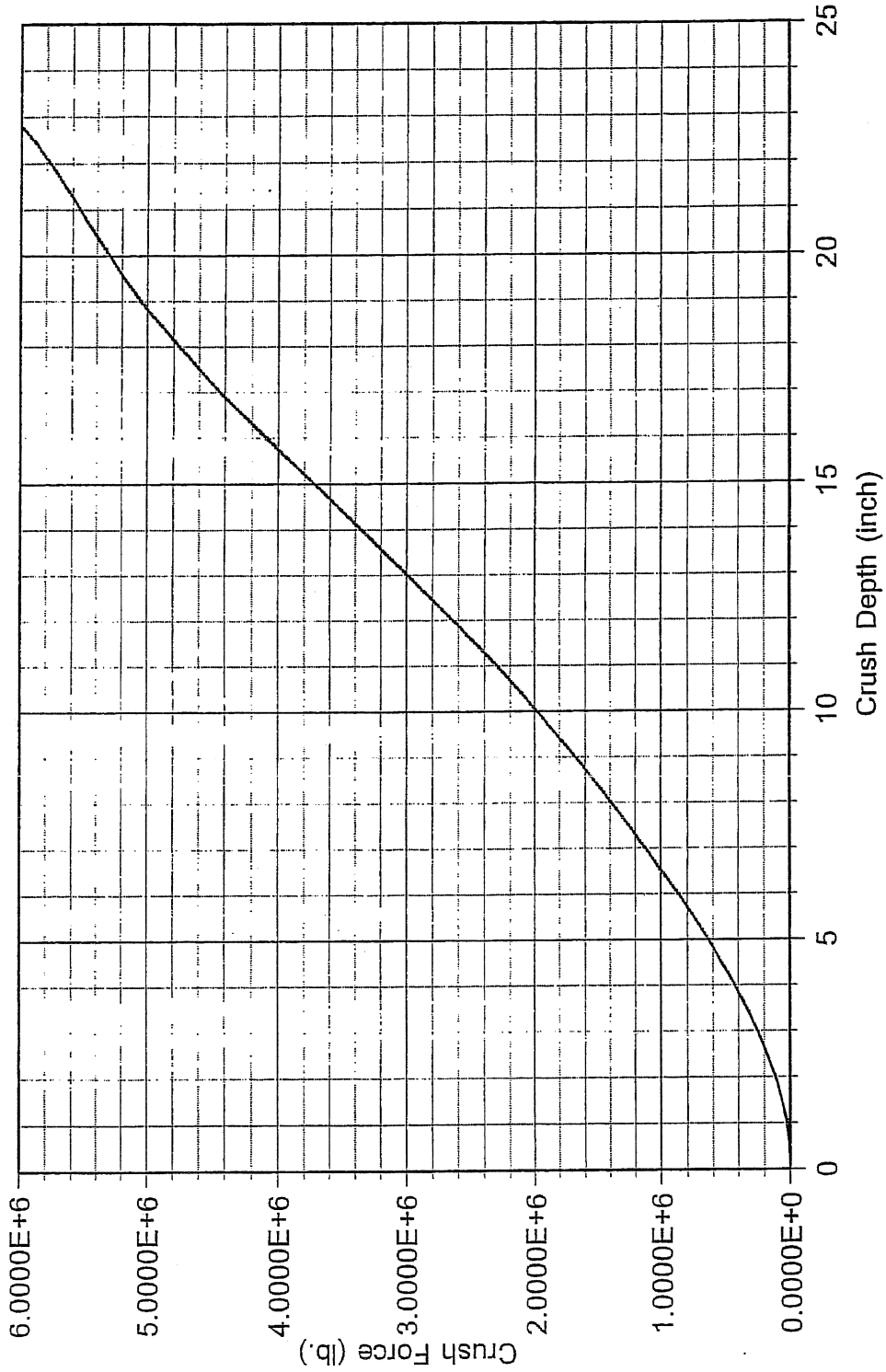


FIGURE 2.A.7.1 ; Static Crush Force vs Crush Depth - Impact at 30 Degrees with Horizontal Target

REV. 10

HI-951251

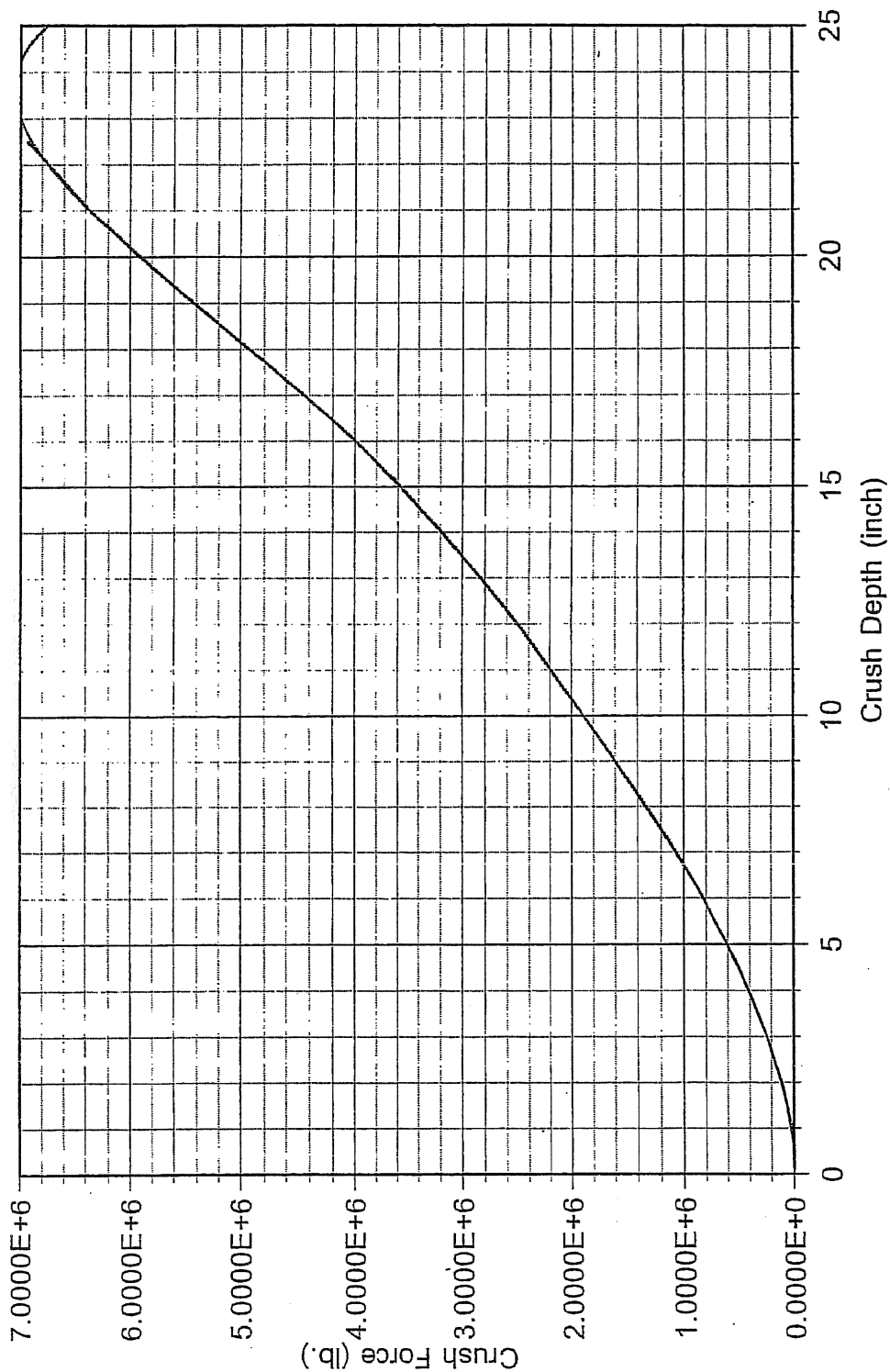


FIGURE 2.A.7.2 ; Static Crush Force vs Crush Depth - Impact at 45 Degrees with Horizontal Target

HI-951251

REV. 10

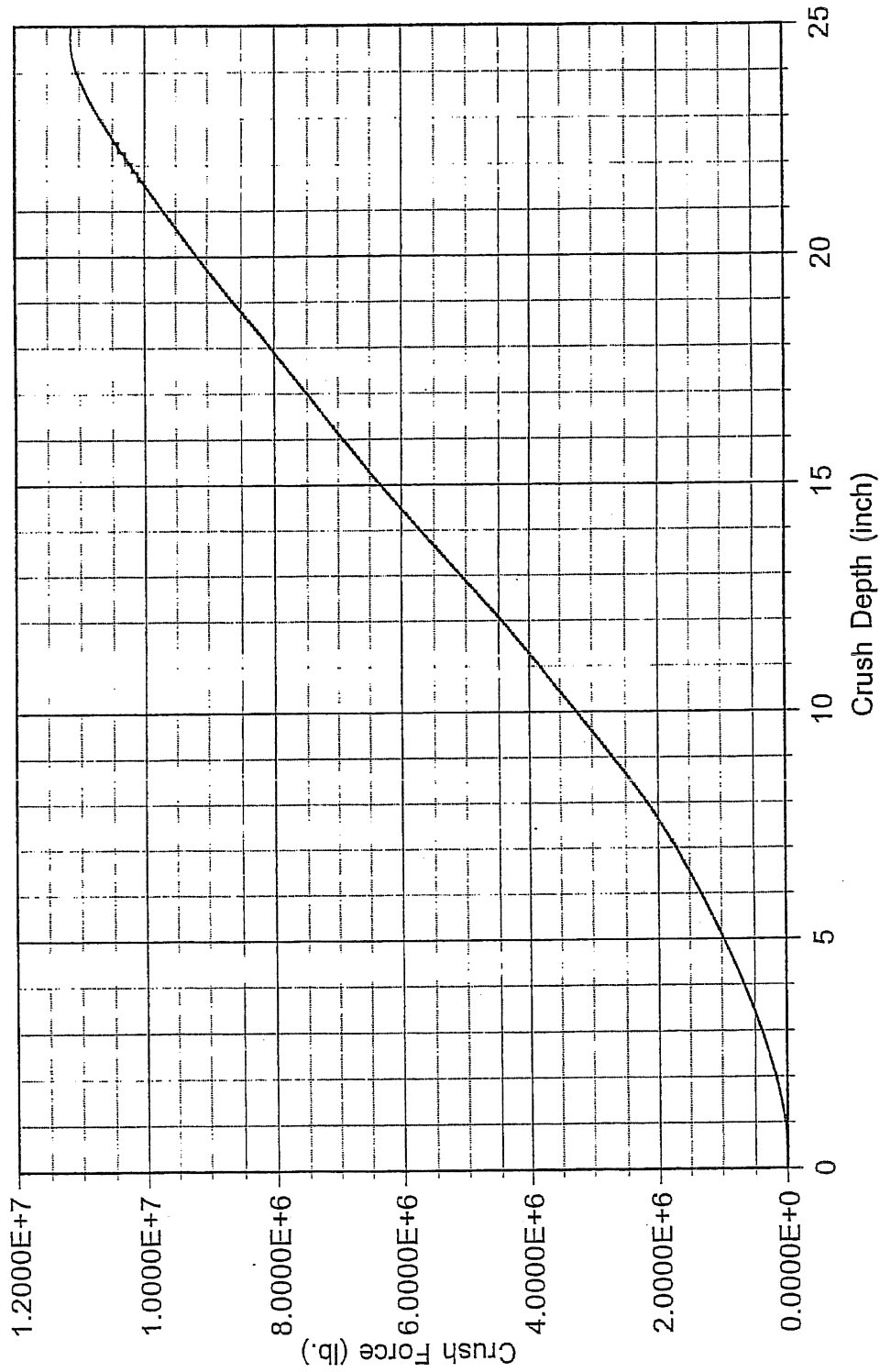


FIGURE 2A.7.3 ; Static Crush Force vs Crush Depth - Impact at 60 Degrees with Horizontal Target



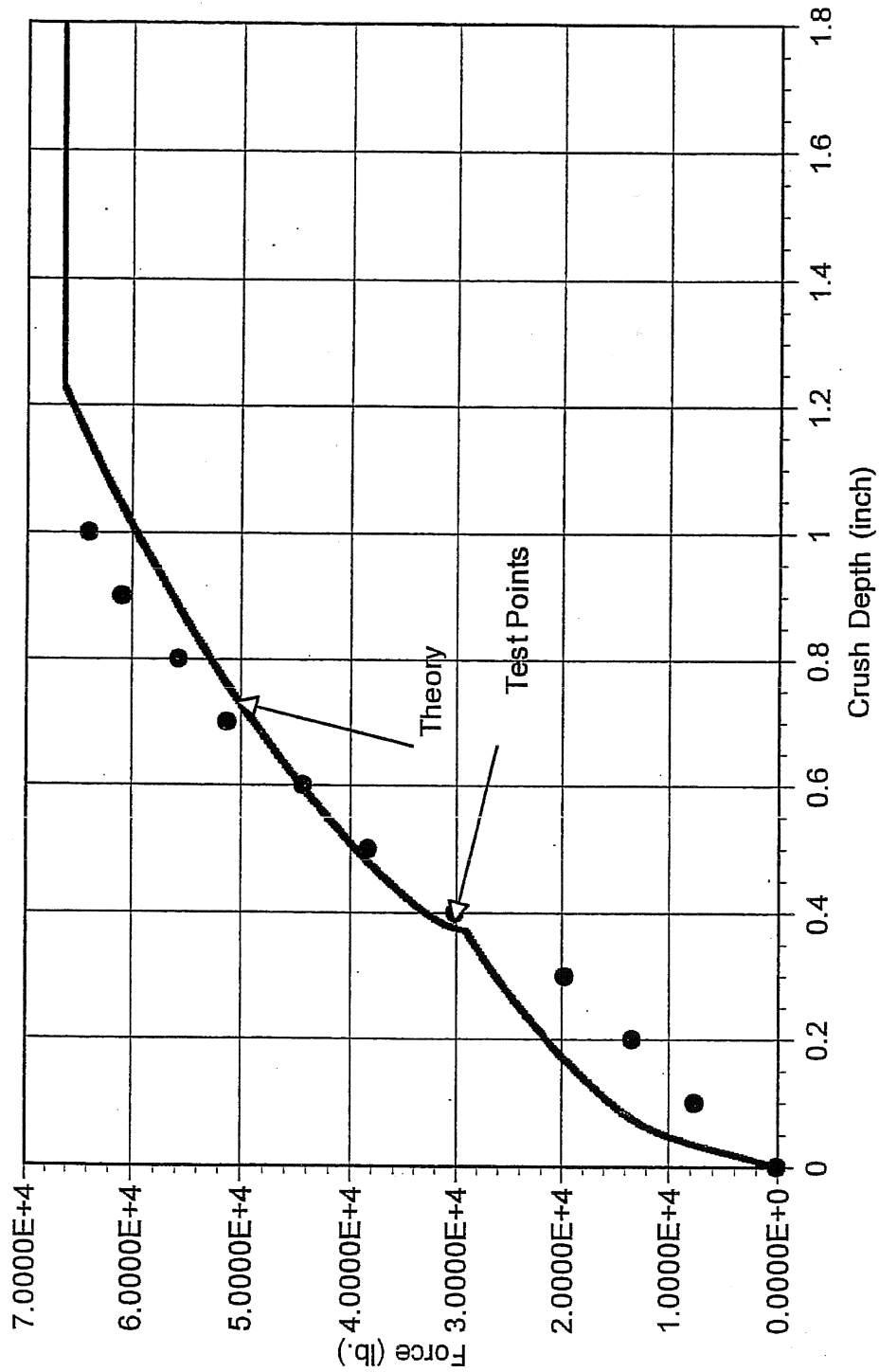


FIGURE 2A.10.1 ; 1/8th Scale Impact Limiter - Crush Force vs. Crush Depth - Side Orientation -  
HI-951251 REV. 10

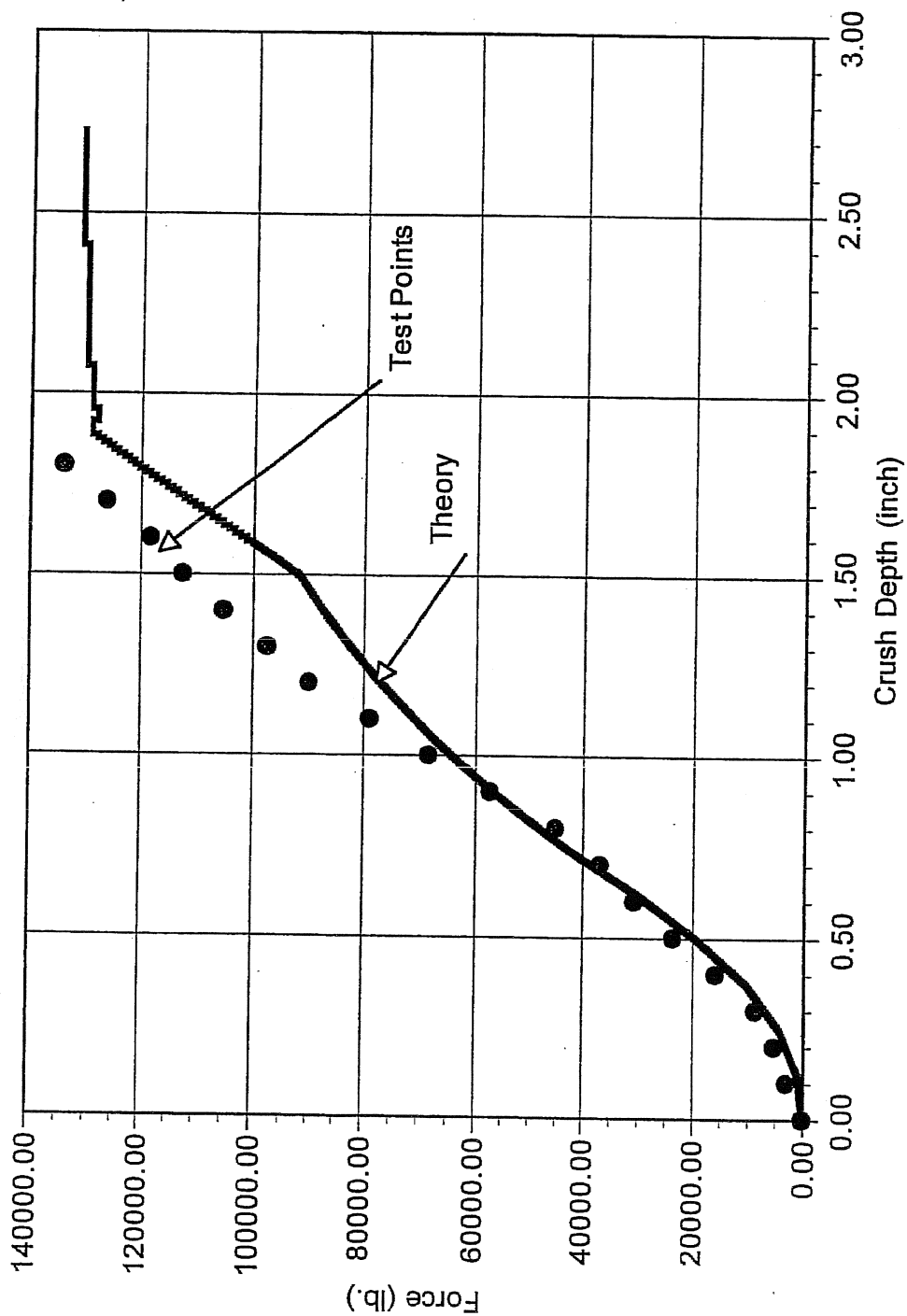


FIGURE 2.A.10.2 ; 1/8th Scale Impact Limiter - Crush Force vs. Crush Depth - Center of Gravity Over Corner Orientation  
HI-951251 REV. 10

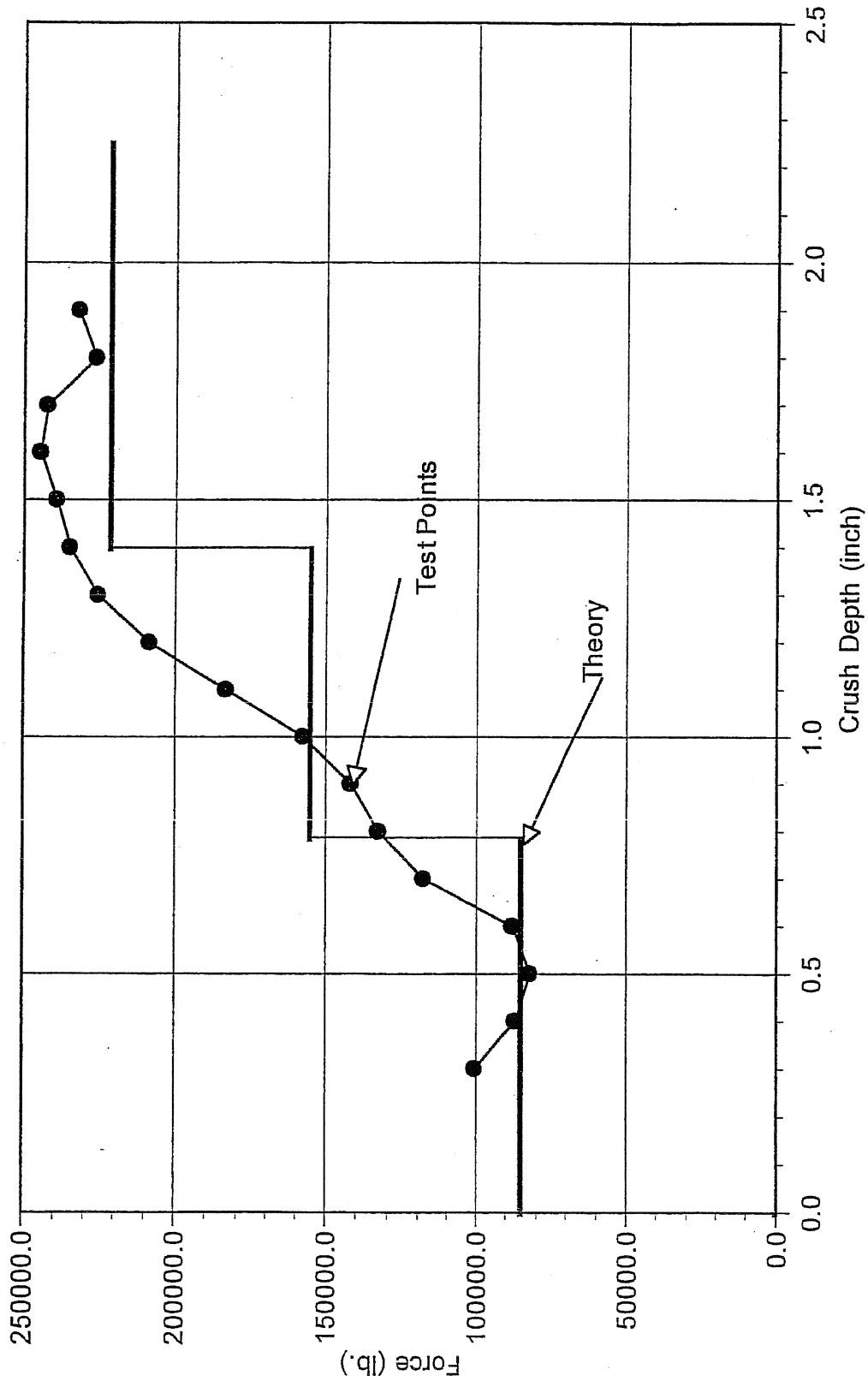


FIGURE 2.A.10.3 ; 1/8th Scale Impact Limiter - Crush Depth - End Orientation  
HI-951251 REV. 10

## Appendix 2.B

### SUMMARY OF RESULTS FOR STRUCTURAL INTEGRITY OF DAMAGED FUEL CANISTERS

#### 2.B.1 Introduction

Damaged Fuel Canisters or Containers (DFCs) to be deployed in the HI-STAR 100 System transport package have been evaluated to demonstrate that the canisters are structurally adequate to support the mechanical loads postulated during normal lifting operations while in long-term storage, and during a hypothetical end drop accident condition. The evaluations address the following damaged/failed fuel canisters for transportation in the Hi-STAR 100 System:

- Holtec-designed DFC for Dresden Unit 1 and Humboldt Bay fuel
- Transnuclear designed DFC for Dresden Unit 1 fuel
- Dresden Unit 1 Thoria Rod Canister
- Holtec-designed DFC for Trojan plant fuel
- Sierra Nuclear Corporation (SNC)-designed Failed Fuel Can for Trojan plant fuel

#### 2.B.2 Methodology

The structural load path in each of the analyzed canisters was evaluated using basic strength of materials formulations. The various structural components were modeled as axial or bending members and stresses computed. Depending on the particular DFC, the load path includes components such as the container sleeve and collar, various weld configurations, load tabs, closure components and lifting bolts. Axial plus bending stresses were computed, together with applicable bearing stresses and weld stresses. Comparison with appropriate allowable strengths at temperature was performed. Input data for all applicable DFC's came from the drawings. The design temperature for lifting evaluation was 150°F (since the DFC is in the spent fuel pool). The design temperature for accident conditions is 725°F.

For the SNC-designed Trojan Failed Fuel Can, the existing calculations prepared by SNC were reviewed by Holtec and determined to bound the loadings applicable to the HI-STAR 100 System. Therefore, no new calculations were prepared for the Trojan Failed Fuel Can.

#### 2.B.3 Acceptance Criteria

The upper closure assembly must meet the requirements set forth for special lifting devices used in nuclear applications [1]. The remaining components of the damaged fuel canister are governed by the stress limits of the ASME Code Section III, Subsection NG and Section III, Appendix F, as applicable [2].

#### 2.B.4 Assumptions

Buckling is not a concern during an accident since during a drop, the canister will be supported by the walls of the fuel basket.

The strength of welds is assumed to decrease the same as the base metal as temperatures increase.

An inertia load factor 1.15 is applied to all loads during a lifting analysis, except for the lifting analysis of the Trojan failed fuel can which assumes a 10% dynamic load factor.

#### 2.B.5 Summary of Results

Table 2.B.1 presents minimum safety factors for each DFC from among all of the computations and evaluations performed on the different damaged fuel canisters to be certified for transport in the HI-STAR 100 System.

#### 2.B.6 References

- [1] ANSI N14-6-1993, “American National Standard for Special Lifting Devices for Shipping Containers Weighing 10,000 Pounds (4,500 kg) or More for Nuclear Materials”, ANSI, Inc.
- [2] ASME Boiler and Pressure Vessel Code, Section III, Subsection NG and Appendix F, 1995.

Table 2.B.1

## SUMMARY OF SAFETY FACTORS FOR DAMAGED FUELCONTAINERS

Unit – (Maximum weight including contents -lbs)	Component	Calculated Stress (ksi)	Allowable Stress (ksi)	Safety Factor = (Allowable Value)/(Calculated Value)	Remarks
Holtec-designed Dresden (BWR) DFC	Lifting – Upper Closure Assembly	1.687	1.9251	1.141	Allowable weld stress includes a 0.35 quality factor
	60g end drop	10.667	37.920	3.6	Level D stress limits
Transnuclear DFC (550 lb.)	Lifting – Lid Frame Assembly	0.526	4.583	8.7	Bearing Stress
	60g end drop	12.316	37.920	3.1	Level D stress limits
Dresden Thoria Rod Canister (390 lb.)	Lifting – Lid Frame Assembly	0.3735	4.583	12.27	Bearing Stress
	60g end drop	8.733	37.920	4.3	Level D stress limits
Holtec-designed Trojan DFC (1680 lb.)	Lifting – Lifting Bolt	13.702	25.000	1.825	
	60g end drop	11.618	26.586	2.3	Spot welds
Trojan Failed Fuel Can	Lifting – Lifting Bar	6.2	6.37 <sup>†</sup>	1.03	Bending Stress
	124g end drop	8.25	11.7	1.42 <sup>††</sup>	Level D stress limits

<sup>†</sup> Allowable stress is equal to 1/3 of yield stress per [1].

<sup>††</sup> Conservatively based on bounding 124g vertical end drop used in SNC calculations. Per Table 2.1.10, the design basis deceleration for the HI-STAR 100 is 60g.

APPENDIX 2.C:  
EVALUATION OF AN IMPROVED HI-STAR 100 IMPACT LIMITER DESIGN  
BASED ON LS-DYNA DROP SIMULATIONS

**PROPRIETARY APPENDIX WITHHELD PER 10CFR2.390**

## **SUPPLEMENT 2.I: STRUCTURAL EVALUATION OF THE HI-STAR HB PACKAGE WITH MPC-HB**

### **2.I.0 OVERVIEW**

In this supplement, the structural adequacy of the HI-STAR HB is evaluated pursuant to the guidelines of NUREG-1617 and the requirements of 10CFR71. The organization of this supplement mirrors the format and content of Chapter 2 except it only contains material directly pertinent to the HI-STAR HB.

The HI-STAR HB is a shortened version of the HI-STAR 100 that is evaluated in Chapter 2. All dimensions (radius, thickness) of the HI-STAR HB are identical to those of the HI-STAR 100 except for the overall length of the layered cylinders, the threaded diameter of the lifting trunnions, and the enclosure shell radial gussets. The impact limiters are identical in all respects except for the crush strengths of the internal aluminum honeycomb material, which are reduced to ensure that the deceleration limits are met with the lighter weight HI-STAR HB. The HI-STAR HB is configured to carry the MPC HB that has the appropriate length and fuel basket design to carry 80 spent fuel assemblies from the closed Humboldt Bay Nuclear Plant. The qualification of the MPC HB to withstand a 60g deceleration has been documented in the Part 72 license for Humboldt Bay (Humboldt Bay ISFSI, Pacific Gas and Electric Company, Final Safety Analysis Report Update, Revision 0 January 2006, NRC Docket No. 72-27). Therefore, no new analyses of the MPC HB are required in this Supplement 2.I as long as the maximum cask deceleration remains bounded by 60g.

The applicable design codes and standards, and the design criteria for the HI-STAR HB are identical to those applied to the HI-STAR 100. Therefore, since the differences between the HI-STAR HB and HI-STAR 100 are limited to:

- Shorter overall length;
- Lower package weight;
- Reduced strength of impact limiter crush materials;
- Smaller diameter threads on lifting trunnions;
- Decreased number and length of enclosure shell radial gussets,



The supplement is focused on documenting the results from new evaluations required because of the reported differences in length, weight, impact limiter crush strength, thread diameter, and enclosure shell geometry. The reduced length and weight of the HI-STAR HB ensures that all stress-based evaluations performed on the HI-STAR 100 produce safety factors that are lower bounds for the same evaluation on the HI-STAR HB, except for the trunnion analysis discussed below. Therefore, no stress-based calculations need to be performed, except those that involve deceleration limits, because of the change in impact limiters, those that involve the lifting trunnions, because of the smaller diameter threads, and those that involve the enclosure shell, because of the modifications to the radial gussets; this supplement focuses only on providing summaries for the new evaluations performed for the HI-STAR HB, which are documented in Holtec calculation packages HI-2156708 [2.I.7.2] and HI-2033042 [2.I.7.3].

## 2.I.1 STRUCTURAL DESIGN

### 2.I.1.1 Discussion

The general discussion presented in Subsection 2.1.1 applies to the HI-STAR HB package. Drawings for the components of the HI-STAR HB package are provided in Section 1.I.4.

### 2.I.1.2 Design Criteria

The HI-STAR HB package meets the design criteria espoused in Section 2.1.2 in its entirety. For the HI-STAR HB overpack, however, the option to replace the SA203-E plate used for the 2.5” thick inner shell with comparable SA350 LF3 ring forgings, stacked to form the inner shell and welded together with full penetrant welds, has been added to the drawings. The Nil Ductility Transition Temperature is still required to be less than –70 degrees F when this option is used (per Subsection 2.1.2.3). Accordingly, Table 8.1.6 lists SA350 LF3 as an optional material for the inner shell. Similarly, Table 8.1.7 lists SA350 LF3 as an option for the port cover plates.

Further, all MPC HB’s shall be loaded to at least 60% of their capacity. Thus all MPC HB’s must have at least 48 fuel assemblies loaded. Additionally, the loading of the MPC should be symmetrical as described in Table 7.1.1 for generic MPC’s. These requirements ensure that the HI-STAR HB package remains in an “analyzed” condition, i.e., the handling of MPC’s and overpack is not affected, and the bounding deceleration limits for normal and hypothetical drop

events in Table 2.1.10 are satisfied. The detailed evaluations, which are based on the relation that the impact deceleration is inversely proportional to the square root of the weight [2.5.1], are documented in [2.I.1.1].

## 2.I.2 WEIGHTS AND CENTERS OF GRAVITY

Table 2.I.2.1 provides the weights of HI-STAR HB components as well as the total package weight. The weight of the impact limiter is also provided. Table 2.I.2.1 also provides the location of the calculated center of gravity for the HI-STAR HB package.

## 2.I.3 MECHANICAL PROPERTIES OF MATERIALS

Materials for the HI-STAR HB package are identical to those used for the HI-STAR 100 package.

## 2.I.4 GENERAL STANDARDS FOR ALL PACKAGES

The HI-STAR HB is a shorter and lighter version of the HI-STAR 100. Therefore, the features presented in Section 2.4 apply to the HI-STAR HB.

## 2.I.5 LIFTING AND TIE-DOWN STANDARDS

### 2.I.5.1 Lifting Configuration

The lifting **configuration** for the HI-STAR HB package **is** identical to **that of** the HI-STAR 100, except that the threaded portion of the lifting trunnions has a slightly smaller diameter. Therefore, even though the HI-STAR HB is lighter than the HI-STAR 100, the safety factors for the HI-STAR HB lifting trunnions and the top flange interface are recalculated based on the smaller trunnion diameter.

The embedded trunnion is analyzed as a cantilever beam in the same manner as described in Subsection 2.5.1.1. Calculations demonstrate that the stresses in the trunnions comply with NUREG-0612 **and Regulatory Guide 3.61 criteria**. Specifically, the following results are obtained.

Safety Factors from HI-STAR HB Lifting Trunnion Stress Analysis for a Bounding Lifted Load of 161,200 lb			
Item	Value (ksi) or (lb) or (lb-in)	Allowable (ksi) or (lb) or (lb-in)	Safety Factor
Bending stress (Comparison with Yield Stress/ <b>3</b> )	11.2	<b>49.0</b>	<b>4.38</b>
Shear stress (Comparison with Yield Stress/ <b>3</b> )	4.76	<b>29.4</b>	<b>6.18</b>
Bending Moment (Comparison with Ultimate Moment/10)	208,600	574,400	2.75
Shear Force (Comparison with Ultimate Force/10)	92,690	282,500	3.05

We note from the above that all safety factors are greater than 1.0. A factor of safety of exactly 1.0 means that the maximum stress, under apparent lift load D\*, is equal to the yield stress in tension or shear divided by **3**, or that the section moment or shear force is equal to the ultimate section moment capacity or section force capacity divided by 10.

It is also important to note that **the** safety factors associated with 10CFR71.45(a) are **inherently satisfied**.

The top flange interface with the trunnion under the lifted load is analyzed in the same manner as described in Subsection 2.5.1.2.2. The interface region is subject to the provisions of **RG 3.61**, and the thread shear stress and bearing stress are compared to  $1/3^{\text{rd}}$  of the top forging yield stress in shear or compression. The following table summarizes the results.

Top Flange B Minimum Safety Factors (Interface with Trunnion) for HI-STAR HB			
Item	Value (ksi)	Allowable (ksi)	Safety Factor
Bearing Stress ( <b>RG 3.61</b> Comparison)	2.555	<b>11.95</b>	<b>4.68</b>
Thread Shear Stress ( <b>RG 3.61</b> Comparison)	2.466	<b>7.17</b>	<b>2.91</b>
Stress Intensity ( <b>ASME</b> NB Comparison)	5.655	34.6	6.12

It is noted from the above that all safety factors are greater than 1.0 and that the safety factors for bearing stress and thread shear stress represent the additional margin over the factor of safety inherent in the member by virtue of the load multiplier mandated in **RG 3.61**.

#### 2.I.5.2 Tie-Down Devices

Since the HI-STAR HB is shorter and lighter, but otherwise identical to the HI-STAR 100, the **design of tie-down devices described in Subsection 2.5.2 will bound those for the HI-STAR HB.** The span between tie-down locations is less, reflecting the shorter overall length of the HI-STAR HB. **The tie-down arrangement is not a structural part of the HI-STAR HB Package. Therefore, 10CFR71.45(b) is not applicable.**

#### 2.I.5.3 Failure of Lifting and Tie-Down Devices

The discussion in Subsection 2.5.3 for the HI-STAR 100 also applies to the HI-STAR HB, except for the following. New calculations have been performed for the HI-STAR HB to demonstrate that the ultimate load carrying capacity of the lifting trunnions is governed by the cross section of the trunnion external to the overpack top forging rather than by any section within the top forging. It is concluded that the trunnion shank reaches ultimate load capacity limit prior to the top forging reaching its corresponding ultimate load capacity limit. Loss of the external shank of the lifting trunnion will not cause loss of any other structural or shielding function of the HI-STAR HB overpack; therefore, the requirement imposed by 10CFR71.45(a) is satisfied.

The following safety factors are established.

$$(\text{Ultimate Bearing Capacity at Trunnion/Top Forging Interface})/(\text{Ultimate Trunnion Load}) = \mathbf{4.68}$$

$$(\text{Ultimate Moment Capacity at Trunnion/Top Forging Interface})/(\text{Ultimate Trunnion Moment Capacity}) = \mathbf{2.75}$$

#### 2.I.5.4 Lifting of Humboldt Bay Damaged Fuel Container

The Humboldt Bay Damaged Fuel Container (DFC) has been analyzed in [2.I.1.1] for structural integrity during a lifting operation consistent with the methodology described in Appendix 2.B of the SAR. In order to lift the HB DFC and its contents, the DFC lid is temporarily removed and a

specially designed lifting tool is installed in its place. The lifting tool connects to the DFC through the four machined slots (one per side) near the top of the DFC tube. Once the DFC has been moved to its new location, the lifting tool is disengaged and the DFC lid is re-installed. The minimum safety factor for the HB DFC during lifting is provided in the following table, and shows that the factor of safety is greater than 1.0.

Unit	Component	Calculated Stress (ksi)	Allowable Stress (ksi)	Safety Factor = (Allowable Value)/(Calculated Value)
Holtec Designed HB DFC	Lifting – DFC Top Ring	19.042	30.000	1.575

## 2.1.6 NORMAL CONDITIONS OF TRANSPORT

The HI-STAR HB package, when subjected to the normal conditions of transport specified in 10CFR71.71, meets the design criteria in Subsection 2.1.2 (derived from the stipulations in 10CFR71.43 and 10CFR71.51). The HI-STAR HB is identical to the HI-STAR 100 in all respects except for the length of the overpack (and the MPC HB), the crush strength of the impact limiter material, the lifting trunnion thread diameter, and the configuration of the enclosure shell radial gussets; the total package weight is bounded by the package weights listed for the HI-STAR 100. Component diameters and thicknesses for the HI-STAR HB overpack and its closures are identical to those of the HI-STAR 100. Therefore, with the exception of the lifting trunnions and the enclosure shell, all stress analysis results associated with the HI-STAR HB overpack are bounded by the available results for the HI-STAR 100. No new analyses are reported in this supplement except for those associated with the performance of the impact limiter, the lifting trunnions, and the enclosure shell. Stress results for the MPC HB have been reported in detail in the Humboldt Bay ISFSI FSAR [2.1.6.1]; the MPC HB analyses were performed using the design basis deceleration.

### 2.1.6.1 Heat

Consistent with Regulatory Guide 7.9, the thermal evaluation of the HI-STAR HB is performed in Supplement 3.I and sets material temperatures, which are used in the structural evaluations discussed in this section and in Section 2.1.7. As the Humboldt Bay fuel is “old and cold”, the

operating temperatures are at or below comparable temperatures for the HI-STAR 100 analyses. This adds additional margins since the allowable strengths will generally be higher in a comparable strength analysis using the HI-STAR HB.

Design pressures and design temperatures for all conditions of transport are listed in Tables 2.1.1 and 2.1.2, respectively. All the design pressures and temperatures for the HI-STAR 100 and the HI-STAR HB are the same, except for the hypothetical accident internal pressure for MPC and overpack which is 200 psig for the HI-STAR HB. Since the design pressures and temperatures are bounded by the HI-STAR 100, and the HI-STAR HB is shorter than the HI-STAR 100, the stress analyses for the HI-STAR 100 in Section 2.6 give bounding results for the HI-STAR HB, except for the overpack enclosure shell.

In the HI-STAR HB, the number and length of the enclosure shell radial gussets have been reduced significantly as compared to the HI-STAR 100 (see drawings in Section 1.I.4). Therefore, a new analysis has been performed for the HI-STAR HB to demonstrate the structural integrity of the overpack enclosure shell and the overpack enclosure return under a bounding internal pressure. It is shown that large safety factors exist against overstress due to an internal pressure developing from off-gassing of the neutron shield material combined with a reduced external pressure. The minimum safety factors are summarized below:

Location	Calculated Stress (ksi)	Allowable Stress (ksi)	Safety Factor
Enclosure Shell Return (bottom)	1.00	26.3	26.3
Enclosure Shell Return (top)	3.55	26.3	7.42
Enclosure Shell	4.32	17.5	4.05
Weld Shear	0.46	10.5	22.8

The change in the enclosure shell radial gussets also has a minor effect on the global response of the HI-STAR HB overpack to a lateral drop because of the change in the gross metal cross section. Specifically, the area moment of inertia of the HI-STAR HB, at a cross section through the enclosure shell cavity, is roughly 5% lower than the HI-STAR 100 due to the difference in the enclosure shell radial gussets. However, this small decrease in the gross section properties is

completely offset by the almost 40% decrease in the cask containment cavity length. The net effect of the change in the enclosure shell radial gussets and the shorter cavity length is a HI-STAR HB overpack that is stronger in bending than the HI-STAR 100 overpack.

In summary, because of the lower weight and shorter length, all stress analyses performed for the HI-STAR 100 using the bounding deceleration inputs give stress results that are equal to or greater than results using the HI-STAR HB.

#### 2.I.6.1.1 Manufacturing Deviations

This subsection addresses specific manufacturing deviations that have occurred and potentially have an adverse impact on the structural performance of the HI-STAR HB.

HI-STAR HB Serial # 1020-012 has five closure lid bolt holes (out of 54) with useable thread lengths less than the minimum length specified on the licensing drawing. The worst case hole has a useable thread length of 1.5” compared to the design basis length of 3.25”. At these five locations the preload torque on the overpack closure plate bolts is reduced to a maximum of 750 ft-lb. The remaining 49 bolts are torqued per the requirements of Table 7.1.1. This deviation has been evaluated and determined to be acceptable because:

- i) the preload force associated with the 49 fully threaded hole locations is sufficient to maintain compression on the closure plate seals during normal operation of the HI-STAR HB system and to prevent gross unloading of all bolts during hypothetical accident conditions, and;
- ii) the thread engagement lengths at the 5 non-conforming hole locations are sufficient to meet ASME Section III, Subsection NB stress limits at 750 ft-lb of torque.

#### 2.I.6.2 Cold

No new or modified calculations or discussions are required for this subsection.

### 2.I.6.3 Reduced External Pressure

No new or modified calculations or discussions are required for this subsection. The stress analysis of the overpack enclosure shell in Subsection 2.I.6.1 conservatively bounds the effect of reduced external pressure (3.5 psia) by considering a higher pressure inside the enclosure shell cavity.

### 2.I.6.4 Increased External Pressure

No additional analyses need be performed here to demonstrate package performance of the HI-STAR HB.

### 2.I.6.5 Vibration

No new or modified calculations or discussions are required for this subsection.

### 2.I.6.6 Water Spray

The condition is not applicable to the HI-STAR HB System per Reg. Guide 7.8 [2.1.2].

### 2.I.6.7 Free Drop

The structural analysis of a 1-foot side drop has been performed for the HI-STAR 100 in Subsections 2.6.1 and 2.6.2 for heat and cold conditions of normal transport. As demonstrated in Subsections 2.6.1 and 2.6.2, safety factors are well over 1.0. Since the HI-STAR HB is shorter and lighter than the HI-STAR 100, the safety factors determined in Subsections 2.6.1 and 2.6.2 are lower bounds for comparable safety factors for the HI-STAR HB. As final verification, the decelerations for the free drop for the HI-STAR HB are determined in Section 2.I.7 and shown to be less than the design basis limits for the 1-foot free drop. Results for the 1-foot drop simulations are presented in Table 2.I.7.2.

### 2.I.6.8 Corner Drop

This condition is not applicable to the HI-STAR HB System per [2.1.2].

### 2.I.6.9 Compression

The condition is not applicable to the HI-STAR HB System per [2.1.2].



## 2.I.7 HYPOTHETICAL ACCIDENT CONDITIONS

The hypothetical accident conditions, as defined in 10CFR71.73 and Regulatory Guide 7.9, have been applied to the HI-STAR 100 System in the required sequence in Subsection 2.7.

It is shown in the following subsections that the HI-STAR HB System also meets the standards set forth in 10CFR71, when it is subjected to the hypothetical accident conditions specified in 10CFR71.73.

### 2.I.7.1 Free Drop

In this subsection the performance and structural integrity of the HI-STAR HB System is evaluated for the most severe drop events. The drop events that are potentially most damaging are the end drops (top or bottom), the side drop, the orientation for which the center of gravity is directly over the point of impact, an oblique drop where the angle of impact is somewhere between center of gravity over corner and a near side drop, and an orientation where package rotation after an impact at one end induces a larger impact deceleration when the other end impacts the target (i.e., slapdown).

As has been noted, the HI-STAR HB is shorter and lighter than the HI-STAR 100, but is identical to the HI-STAR in all other aspects of geometry. The impact limiter crush strengths are adjusted from those used in the HI-STAR 100 in order to ensure that the design basis deceleration limits for the HI-STAR family continue to be met. In Section 2.7, the analysis was performed in two parts. Initially, 1/8 and 1/4 scale testing was performed to establish the characteristics of the impact limiter and to demonstrate that the experimentally obtained decelerations for all orientations of the cask were below the design basis. Analytical models were developed and demonstrated to be capable of predicting the observed responses from the experimental results. These models were used to evaluate sensitivity to crush strength change and cask weight change. Once it was established that the impact limiter configuration and crush strengths successfully limited the rigid body decelerations of the cask to below the prescribed limits, various strength analyses were performed to assess the state of stress in the cask components and ensure that the prescribed stress limits were satisfied.

As the impact limiter for the HI-STAR HB has the same geometry as the HI-STAR 100 with the **primary** difference being the impact limiter crush material, no qualification testing is employed. In lieu of testing, the same analytical methodology (the differential equation method) is used to simulate the free drop tests and demonstrate the performance of the impact limiter for the HI-STAR HB. The key features of the differential equation method are presented in [2.I.7.1], which summarizes, in a single document, the general analysis method as it was first implemented for the HI-STAR 100 license under 10CFR71. **Further, the design of the HI-STAR 100 impact limiter is improved in Appendix 2.C by using only one type of honeycomb material, instead of four types used in the original design. Similarly, the HI-STAR HB impact limiter design is also improved in this subsection to use only one type of honeycomb material. Also, certain weld sizes have been reduced in the improved HI-STAR HB impact limiter design, as discussed in [2.I.7.2].**

The drop analysis of the HI-STAR HB Package using the differential equation method differs from the drop analysis for the HI-STAR 100 only to the extent that:

- the axial length of the cylindrical body is reduced;
- the nominal strength of the energy absorbing honeycomb material is reduced;
- the mass of the package is reduced;
- **the length of the impact limiter outer donut is increased;**
- **the size of certain welds is decreased.**

**Table 2.3.7** provides the reduced nominal crush strength used in the impact limiters for the HI-STAR HB.

The dynamic multipliers (or dynamic correlation function), which were originally determined for the HI-STAR 100, remain valid for the HI-STAR HB Package for the following reasons. The Hexcel manufacturer's catalog states that dynamic crush strengths are a function of impact velocity only; there is no information suggesting that the dynamic multipliers in the differential equation method are a function of crush material strength. Therefore, the drop analyses for the HI-STAR HB impact limiters use the same dynamic multipliers (represented as a linear function of the concomitant crush velocity) that were used for the HI-STAR 100. More information on the

dynamic multipliers, including the explicit form of the dynamic correlation function, is provided in [2.I.7.1].

The results from the four free drop simulations of the HI-STAR HB are documented in Table 2.I.7.1 using the **lower bound and upper bound** strengths of the honeycomb energy absorbing material. The results show that the HI-STAR HB impact limiters effectively protect the HI-STAR HB cask under the postulated 30-foot drop events by maintaining the peak cask rigid body deceleration below the design basis limit of 60 g's. Since the peak decelerations are below the values computed for the HI-STAR 100, it is assured that the pin/bolt connections between the HI-STAR HB impact limiters and the HI-STAR HB body maintain their structural integrity.

Consistent with the requirements for 1-foot free drops as part of the Normal Conditions of Transport, **the side drop condition is** also analyzed for the HI-STAR HB Package using the **lower bound and upper bound** strengths specified for the honeycomb energy absorbing material. The maximum decelerations sustained by the Package, as well as the maximum impact limiter crush and impact durations, are summarized in Table 2.I.7.2. The analyses leading to the reported results are documented in a supporting calculation package [2.I.7.2].

Analysis of the HB DFC to be transported in the HI-STAR 100 HB package is performed in [2.I.1.1] to demonstrate structural integrity under end drop condition consistent with those described in Appendix 2.B of the SAR. The safety factor for the HB DFC during a 60g end drop is provided in the following table, and shows that the factor of safety is greater than 1.0.

Unit	Component	Calculated Stress (ksi)	Allowable Stress (ksi)	Safety Factor = (Allowable Value)/(Calculated Value)	Remarks
Holtec Designed HB DFC	60g End Drop	13.260	26.586	2.00	Spot Welds

### 2.I.7.2 Puncture

No new or modified calculations need be performed to qualify the HI-STAR HB, as the structure at the puncture locations is unchanged from the HI-STAR 100.

### 2.I.7.3 Thermal

Thermal evaluation of the fire accident is presented in Supplement 3.I. No new or modified structural calculations need be performed to qualify the HI-STAR HB for the fire accident.

### 2.I.7.4 Immersion - Fissile Material

No new or modified calculations need be performed to qualify the HI-STAR HB.

### 2.I.7.5 Immersion - All Packages

No new or modified calculations need be performed to qualify the HI-STAR HB.

### 2.I.7.6 Summary of Damage

The results presented in Subsections 2.I.7.1 through 2.I.7.5 show that the HI-STAR HB System meets the requirements of 10CFR71.61 and 10CFR71.73. The results from simulation of the hypothetical drop conditions produce deceleration levels that are below the design basis levels for the HI-STAR 100 for the crush strength range specified for the HI-STAR HB impact limiters. Therefore, safety factors for the HI-STAR HB are greater than 1.0 by virtue of comparison with the corresponding calculations for the HI-STAR 100 for the Hypothetical Accident Conditions of Transport. Therefore, the HI-STAR 100 HB package, under the Hypothetical Accident Conditions of Transport, has adequate structural integrity to satisfy the subcriticality, containment, shielding, and temperature requirements of 10CFR71.

## 2.I.8 SPECIAL FORM

This section is not applicable to the HI-STAR HB System. This application does not seek approval for transport of special form radioactive material as defined in 10CFR71.4.

## 2.I.9 FUEL RODS

The Humboldt Bay fuel is shorter than the design basis fuel carried by the HI-STAR 100; therefore, the computations and conclusions in Section 2.9 encompass the HI-STAR HB. The

presence of “Undamaged Fuel Assemblies”, which are defined in Table 1.0.1 will have no significant effect on the structural response of the HI-STAR HB. This is because the only fuel parameters that have an influence on the structural analyses are the fuel mass and center of gravity height. Therefore, since an undamaged fuel assembly has essentially the same mass as an intact fuel assembly, and the exterior fuel rods serve to confine the interior fuel rods (with cladding in unknown condition) preventing them from dislocating and falling to the bottom of the fuel basket, the presence of undamaged fuel assemblies has no significant effect on the total amount of stored fuel mass or the center of gravity height used as input in the drop analysis for the HI-STAR HB.

## 2.I.10 MISCELLANEOUS ITEMS

No new appendices are introduced in Supplement 2.I. Also, since the HI-STAR 100 Package meets applicable NUREG 1617/10CFR71 requirements, so does the HI-STAR HB.

## 2.I.11 REFERENCES

- |           |  |  |
|-----------|--|--|
| [2.I.1.1] | Miscellaneous Calculations for the HI-STAR HB, HI-2033042, Rev. 4.   |  |
| [2.I.6.1] | Pacific Gas and Electric Company, NRC Docket Number 72-27, Humboldt Bay ISFSI, Final Safety Analysis Report Update, Revision 0, January 2006.        |  |
| [2.I.7.1] | A Classical Dynamics Based and Experimentally Benchmarked Impact Response Computation Methodology for Al-STAR Equipped Casks, HI-2084137, Rev. 0.    |  |
| [2.I.7.2] | <b>Analyses of HI-STAR HB Transport Package Drop Accidents Supporting an Improved Aluminum Honeycomb Impact Limiter Design</b> , HI-2156708, Rev. 0. |  |
| [2.I.7.3] | Miscellaneous Calculations for the HI-STAR HB, HI-2033042, Rev. 4.   |  |

***Table 2.I.2.1 PROPRIETARY INFORMATION WITHHELD PER 10CFR2.390***

**Table 2.I.7.1 –HI-STAR HB 30' DROP RESULTS**

CONFIGURATION	CRUSH STRENGTH	MAXIMUM DECELERATION (G'S)	MAXIMUM CRUSH (INCH)	DURATION OF IMPACT (SEC.)
30' END DROP	LOWER BOUND	55.6	18.4	0.056
30' END DROP	UPPER BOUND	57.5	16.7	0.056
30' SIDE DROP	LOWER BOUND	43.9	15.8	0.052
30' SIDE DROP	UPPER BOUND	34.1	13.0	0.048
30' CGOC	LOWER BOUND	40.5	24.8	0.070
30' CGOC	UPPER BOUND	47.0	22.4	0.062
30' SLAPDOWN	LOWER BOUND	57.1	-	-
30' SLAPDOWN	UPPER BOUND	44.3	-	-

**Table 2.I.7.2 –HI-STAR HB 1' DROP RESULTS**

COMMENTS	CRUSH STRENGTH	MAXIMUM DECELERATION (G'S)	MAXIMUM CRUSH (INCH)	DURATION OF IMPACT (SEC.)
1' SIDE DROP	LOWER BOUND	8.7	1.75	0.034
1' SIDE DROP	UPPER BOUND	11.0	1.39	0.030

## **SUPPLEMENT 2.II: STRUCTURAL EVALUATION OF THE HI-STAR HB GTCC PACKAGE WITH GWC-HB**

### **2.II.0 OVERVIEW**

In this supplement, the structural adequacy of the HI-STAR HB GTCC (Greater than Category C nuclear waste) transport package is evaluated pursuant to the guidelines of NUREG-1617 and the requirements of 10CFR71.

The HI-STAR HB GTCC transport package is essentially identical to the HI-STAR HB transport package in all key design characteristics (evaluated in Supplement 2.I). Both packages are protected by the HI-STAR HB impact limiters against potential drop accidents; the GTCC overpack shares identical materials, configurations and dimensions with the HI-STAR HB overpack except that the GTCC overpack need not be sealed nor have the neutron shielding layer. Finally, the GWC has identical dimensions to the MPC HB but is lighter than the MPC HB.

Compared with the spent fuel assemblies to be loaded in the MPC HB, the GTCC waste has a smaller thermal load; therefore, the temperatures of the GTCC structural components are considered to be bounded by those of the HI-STAR HB cask as justified in Subsection 2.II.6.1. Therefore, the HI-STAR HB GTCC structural components are structurally stronger than the counterparts of the HI-STAR HB transport cask.

Given the similarities between the two transport packages as discussed above, the structural evaluation of HI-STAR HB GTCC transport package is evaluated in a similar manner as the HI-STAR HB package. Namely, the same methodologies used to evaluate the HI-STAR HB transport package are employed herein for the structural qualification of the HI-STAR HB GTCC transport package. Note that the HI-STAR HB transport package is structurally qualified for the design basis decelerations of 60 g's for the 30' hypothetical drop event and 17 g's for the normal operation condition 1' drop event, respectively, as documented in Supplement 2.I.



## **2.II.1 STRUCTURAL DESIGN**

### **2.II.1.1 Discussion**

The general discussion presented in Subsection 2.1.1 and Supplement 2.I applies to the HI-STAR HB GTCC package. Drawings for the components of the HI-STAR HB GTCC package are provided in Section 1.II.4.

### **2.II.1.2 Design Criteria**

The HI-STAR HB GTCC package is designed to meet the same design criteria as the HI-STAR HB overpack (discussed in Supplement 2.I).

## **2.II.2 WEIGHTS AND CENTERS OF GRAVITY**

Table 2.II.2.1 provides the weights of HI-STAR HB GTCC components as well as the total package weight. The weight of the impact limiter is also provided. Table 2.II.2.1 also provides the location of the calculated center of gravity for the HI-STAR HB GTCC package.

## **2.II.3 MECHANICAL PROPERTIES OF MATERIALS**

Materials for the HI-STAR HB GTCC package are identical to those used for the HI-STAR HB package.

## **2.II.4 GENERAL STANDARDS FOR ALL PACKAGES**

The HI-STAR HB GTCC is the same length but a lighter version of the HI-STAR HB. Therefore, the features presented in Supplement 2.I apply to the HI-STAR HB GTCC.

## **2.II.5 LIFTING AND TIE-DOWN STANDARDS**

### **2.II.5.1 Lifting Configuration**

The lifting devices for the HI-STAR HB GTCC package are identical to those for the HI-STAR HB. Since the latter is slightly heavier as shown in Tables 2.I.2.1 and 2.II.2.1, safety factors for the HI-STAR HB GTCC lifting trunnions and the top flange interface are therefore greater than those for the HI-STAR HB, which are shown to have a minimum value of 2.75 in Subsection 2.I.5.1. The minimum safety factor was calculated following the NUREG-0612 and Reg. Guide 3.61 provisions. It should be pointed out that the requirements of 10CFR71.45(a) are inherently

satisfied since 10CFR71.45 only requires a factor of safety of 3 on the yield strength. Therefore, no new analyses are performed.

#### 2.II.5.2 Tie-Down Devices

Since the HI-STAR HB GTCC is lighter, but otherwise identical to the HI-STAR HB, the design of tie-down devices for the HI-STAR HB will bound those for the HI-STAR HB GTCC. The tie-down arrangement is not a structural part of the HI-STAR HB GTCC Package. Therefore, 10CFR71.45(b) is not applicable.

#### 2.II.5.3 Failure of Lifting and Tie-Down Devices

Since the HI-STAR HB GTCC is lighter than HI-STAR HB, the safety margins for the trunnion and the top forging reported in Subsection 2.I.5.3 will be exceeded in the case of HI-STAR HB GTCC and therefore no new calculations are performed.

## 2.II.6 NORMAL CONDITIONS OF TRANSPORT

The load combinations under normal condition of transportation for the HI-STAR HB GTCC are the same as the HI-STAR HB as defined in Subsection 2.I.6. The structural integrity of the GTCC is evaluated in detail below for each of the load combinations.

### 2.II.6.1 Heat

As described in Section 3.1.1.4 of the HB ISFSI SAR [2.II.6.1] “The ... decay heat attributed to the GTCC material is bounded by that assumed in the analysis performed for a HI-STAR HB cask containing spent nuclear fuel.” Because there is very low heat generation in the structures of the HI-STAR HB GTCC (i.e., all heat is conducted through the structures) and because the GTCC heat is no greater than the previously-assumed decay heat, it is apparent that the previously applied design temperatures for the HI-STAR HB can be conservatively applied to the HI-STAR HB GTCC as well. In fact, because the HI-STAR HB GTCC does not have the relatively low thermal conductivity Holtite neutron shield material around its perimeter like the fuel casks do, the HI-STAR HB GTCC component temperatures are bounded by the design temperatures of the HI-STAR HB.

In addition to lower temperatures, the GWC enclosure is subjected to the same internal pressure as the MPC HB, and GTCC overpack is subjected to a lower internal pressure than the HI-STAR HB, as listed in Table 1.II.2. Therefore, the safety factors of the HI-STAR HB GWC enclosure are the same as the MPC HB and GTCC overpack structural members are greater than those of the HI-STAR HB for the hot environment load combination under normal condition of transportation. No new or modified calculations or discussions are required for this subsection.

### 2.II.6.2 Cold

No new or modified calculations or discussions are required for this subsection, since the HI-STAR HB GTCC and HI-STAR HB are subjected to identical cold environment loads under the normal condition of transportation.

### 2.II.6.3 Reduced External Pressure

No additional analyses need be performed here to demonstrate package performance of the HI-STAR HB GTCC as the overpack is not sealed. Compared with the MPC HB, the GWC enclosure is expected to experience little stress/deformation as the unit is not sealed.

### 2.II.6.4 Increased External Pressure

No additional analyses need be performed here to demonstrate package performance of the HI-STAR HB GTCC as the overpack is not sealed.

### 2.II.6.5 Vibration

No new or modified calculations or discussions are required for this loading condition because of the reduced package weight and increased rigidity of the canister.

### 2.II.6.6 Water Spray

The condition is not applicable to the HI-STAR HB GTCC System per Reg. Guide 7.8 [2.1.2].

### 2.II.6.7 Free Drop

The bounding one-foot drop event analyzed in [2.II.6.2], for the minimum weight cask, indicates that the maximum deceleration of the HI-STAR HB GTCC transport package is 13.3 g's, which is less than the design basis deceleration (17 g's per Table 2.1.10) of the HI-STAR HB transport package.

### 2.II.6.8 Corner Drop

This condition is not applicable to the HI-STAR HB GTCC System per [2.1.2].

### 2.II.6.9 Compression

This condition is not applicable to the HI-STAR HB GTCC System per [2.1.2].

## 2.II.7 HYPOTHETICAL ACCIDENT CONDITIONS

The hypothetical accident conditions, as defined in 10CFR71.73 and Regulatory Guide 7.9, have been applied to the HI-STAR 100 System in the required sequence in Subsection 2.7.

It is shown in the following subsections that the HI-STAR HB GTCC System also meets the standards set forth in 10CFR71, when it is subjected to the hypothetical accident conditions specified in 10CFR71.73.

### 2.II.7.1 Free Drop

Calculations performed in [2.II.6.2] indicate that the maximum deceleration of the HI-STAR HB GTCC package in a 30' drop event is 31.5 g's, which is less than the design basis deceleration of the HI-STAR HB transport package for the 30' hypothetical drop condition (60 g's per Table 2.1.10).

It should be pointed out that the impact energy of the HI-STAR HB GTCC package in a 30' drop event is smaller than that of the HI-STAR HB transport package due to the weight difference. Since both packages are protected by identical impact limiters, the structural integrity of the impact limiter steel members (i.e., backbone and attachment bolts) of the HI-STAR HB GTCC transport package are expected to be maintained in a 30' hypothetical drop accident.

### 2.II.7.2 Puncture

No new or modified calculations need be performed to qualify the HI-STAR HB GTCC, as the structure at the puncture locations is unchanged from the HI-STAR HB.

### 2.II.7.3 Thermal

Thermal evaluation of the fire accident is presented in Supplement 3.II. No new or modified structural calculations need be performed to qualify the HI-STAR HB GWC enclosure and GTCC overpack for the fire accident as the design accident internal pressure is bounded by the MPC HB and HI-STAR HB overpack as listed in Table 1.II.2.

### 2.II.7.4 Immersion - Fissile Material

No new or modified calculations need be performed to qualify the HI-STAR HB GTCC.

### 2.II.7.5 Immersion - All Packages

In accordance with 10 CFR 71.61, a Type B package containing more than  $10^5$  A<sub>2</sub> of activity "must be designed so that its undamaged containment system can withstand an external water pressure of 2 MPa (290 psi) ... without collapse, buckling, or inleakage of water." Information in Appendix F of HI-2033047 [2.II.7.1] indicates that A<sub>2</sub> for the HB GTCC is about 26000 curies of Co-60. Per 10 CFR 71 Appendix A,  $10^5$  A<sub>2</sub> for Co-60 is 1,100,000 curies. Since the HI-STAR HB GTCC contains much less than  $10^5$  A<sub>2</sub> this external pressure event is not required. In Appendix D of [2.II.6.2], the stability of DWC shell is evaluated under a conservatively bounding external pressure of 100 psi.

### 2.II.7.6 Summary of Damage

The results presented in Subsections 2.II.7.1 through 2.II.7.5 show that the HI-STAR HB GTCC System meets the requirements of 10CFR71.61 and 10CFR71.73. The results from simulation of the hypothetical drop conditions produce deceleration levels that are below the design basis levels for the HI-STAR 100 for the crush strength range specified for the HI-STAR HB GTCC impact limiters. Therefore, safety factors for the HI-STAR HB GTCC are greater than 1.0 by virtue of comparison with the corresponding calculations for the HI-STAR 100 and the HI-STAR HB for the Hypothetical Accident Conditions of Transport. Therefore, the HI-STAR HB GTCC package, under the Hypothetical Accident Conditions of Transport, has adequate structural integrity to satisfy the subcriticality, containment, shielding, and temperature requirements of 10CFR71.

## 2.II.8 SPECIAL FORM

This section is not applicable to the HI-STAR HB GTCC System. This application does not seek approval for transport of special form radioactive material as defined in 10CFR71.4.

## 2.II.9 FUEL RODS

This section is not applicable to the HI-STAR HB GTCC System as no fuel rods are stored in the GWC.

## **2.II.10 MISCELLANEOUS ITEMS**

No new appendices are introduced in Supplement 2.II. Also, since the HI-STAR HB Package meets applicable NUREG 1617/10CFR71 requirements, so does the HI-STAR HB GTCC.

## **2.II.11 REFERENCES**

- [2.II.6.1] Pacific Gas and Electric Company, NRC Docket Number 72-27, Humboldt Bay ISFSI, Final Safety Analysis Report Update, Revision 0, January 2006.
- [2.II.6.2] Structural Evaluation of the HI-STAR HB GTCC Package, HI-2114941, Rev. 1.
- [2.II.7.1] ISFSI Dose Assessment for Humboldt Bay, HI-2033047, Rev. 0.

<i><b>Table 2.II.2.1 PROPRIETARY INFORMATION WITHHELD PER 10CFR2.390</b></i>
--



## **SUPPLEMENT 2.III: STRUCTURAL EVALUATION OF THE HI-STAR 100 PACKAGE WITH DIABLO CANYON MPC-32**

### **2.III.0 OVERVIEW**

In this supplement, the structural adequacy of the HI-STAR 100 with Diablo Canyon MPC-32 is evaluated pursuant to the guidelines of NUREG-1617 and the requirements of 10CFR71. The organization of this supplement mirrors the format and content of Chapter 2 except it only contains material directly pertinent to the HI-STAR 100 System with Diablo Canyon MPC-32.

The Diablo Canyon MPC-32 is a shortened version of the generic MPC-32 that is evaluated in Chapter 2. All dimensions (radius, thickness, etc.) of the Diablo Canyon MPC-32 are identical to those of the generic MPC-32 except for the overall length. A detailed description of the HI-STAR 100 System with Diablo Canyon MPC-32 is presented in Subsection 1.III.2. From a structural perspective, this package is very similar to the HI-STAR 100 with generic MPC-32 due to the use of a spacer ring that ensures the weight and the center of gravity of the two packages are comparable.

Given the similarities between the two transport packages as discussed above, the structural evaluation of HI-STAR 100 System with Diablo Canyon MPC-32 is evaluated in a similar manner as the HI-STAR 100 package. Namely, the same methodologies used to evaluate the HI-STAR 100 transport package are employed herein for the structural qualification of the HI-STAR 100 System with Diablo Canyon MPC-32.

### **2.III.1 STRUCTURAL DESIGN**

#### **2.III.1.1 Discussion**

The general discussion presented in Subsection 2.1.1 applies to the HI-STAR 100 System with Diablo Canyon MPC-32. Drawings for the components of the HI-STAR 100 System with Diablo Canyon MPC-32 are provided in Section 1.III.4.

### 2.III.1.2 Design Criteria

The HI-STAR 100 System with Diablo Canyon MPC-32 is designed to meet the same design criteria as the HI-STAR 100 overpack discussed in Subsection 2.1.2.

## 2.III.2 WEIGHTS AND CENTERS OF GRAVITY

Table 2.III.2.1 provides the weights of HI-STAR 100 System with Diablo Canyon MPC-32 components as well as the total package weight. The weight of the impact limiter is also provided. Table 2.III.2.2 provides the location of the calculated center of gravity for the HI-STAR 100 System with Diablo Canyon MPC-32.

## 2.III.3 MECHANICAL PROPERTIES OF MATERIALS

Materials for the HI-STAR 100 System with Diablo Canyon MPC-32 are identical to those used for the HI-STAR 100 package.

## 2.III.4 GENERAL STANDARDS FOR ALL PACKAGES

The HI-STAR 100 System with Diablo Canyon MPC-32 is the same length and similar weight as the HI-STAR 100 with generic MPC-32. Therefore, the features presented in Section 2.4 apply to the HI-STAR 100 System with Diablo Canyon MPC-32.

## 2.III.5 LIFTING AND TIE-DOWN STANDARDS

### 2.III.5.1 Lifting Configuration

The lifting devices for the HI-STAR 100 System with Diablo Canyon MPC-32 are identical to those for the HI-STAR 100. Since the latter is slightly heavier as shown in Tables 2.2.1 and 2.III.2.1, safety factors for the HI-STAR 100 System with Diablo Canyon MPC-32 are bounded by those for the HI-STAR 100 package presented in Subsection 2.5.1.

### 2.III.5.2 Tie-Down Devices

Since the HI-STAR 100 System with Diablo Canyon MPC-32 is slightly lighter, but otherwise identical to the HI-STAR 100, the design of tie-down devices described in Subsection 2.5.2 will be bounding. The tie-down arrangement is not a structural part of the HI-STAR 100 with Diablo Canyon MPC-32 Package. Therefore, 10CFR71.45(b) is not applicable.

#### 2.III.5.3 Failure of Lifting and Tie-Down Devices

Since the HI-STAR 100 System with Diablo Canyon MPC-32 is slightly lighter than HI-STAR 100, the safety margins for the trunnion and the top forging, reported in Subsection 2.5.3, will be maintained in the case of the HI-STAR 100 System with Diablo Canyon MPC-32 and therefore no new calculations are performed.

## 2.III.6 NORMAL CONDITIONS OF TRANSPORT

The load combinations under normal condition of transportation for the HI-STAR 100 System with Diablo Canyon MPC-32 are the same as the HI-STAR 100 as defined in Subsection 2.6. The structural integrity of the GTCC is evaluated in detail below for each of the load combinations.

### 2.III.6.1 Heat

Design pressures and design temperatures for all conditions of transport are listed in Tables 2.1.1 and 2.1.2, respectively. Since the design pressures and temperatures for the HI-STAR 100 with Diablo Canyon MPC-32 and the generic MPC-32 are the same, the stress analyses for the HI-STAR 100 in Section 2.6 give bounding results for the HI-STAR 100 with Diablo Canyon MPC-32.

### 2.III.6.2 Cold

No new or modified calculations or discussions are required for this subsection, since the HI-STAR 100 with Diablo Canyon MPC-32 and HI-STAR 100 are subjected to identical cold environment loads under the normal condition of transportation.

### 2.III.6.3 Reduced External Pressure

No new or modified calculations or discussions are required for this subsection, since the same HI-STAR 100 overpack is used with Diablo Canyon MPC-32 and generic MPC-32.

### 2.III.6.4 Increased External Pressure

No new or modified calculations or discussions are required for this subsection, since the same HI-STAR 100 overpack is used with Diablo Canyon MPC-32 and generic MPC-32.

### 2.III.6.5 Vibration

No new or modified calculations or discussions are required for this loading condition because the same HI-STAR 100 overpack is used and the Diablo Canyon MPC-32 is shorter, and therefore more rigid, than the generic MPC-32.

#### 2.III.6.6 Water Spray

This condition is not applicable to the HI-STAR 100 System per Reg. Guide 7.8 [2.1.2].

#### 2.III.6.7 Free Drop

Since the HI-STAR 100 System with Diablo Canyon MPC-32 is slightly lighter, but otherwise identical to the HI-STAR 100, the safety factors presented in subsection 2.6.7 are bounding. Therefore, no new analyses are performed.

#### 2.III.6.8 Corner Drop

This condition is not applicable to the HI-STAR 100 System per [2.1.2].

#### 2.III.6.9 Compression

This condition is not applicable to the HI-STAR 100 System per [2.1.2].

## **2.III.7 HYPOTHETICAL ACCIDENT CONDITIONS**

The hypothetical accident conditions, as defined in 10CFR71.73 and Regulatory Guide 7.9, have been applied to the HI-STAR 100 System in the required sequence in Subsection 2.7.

### **2.III.7.1 Free Drop**

Since the HI-STAR 100 System with Diablo Canyon MPC-32 is slightly lighter, but otherwise identical to the HI-STAR 100, the safety factors presented in subsection 2.7.1 are bounding. Therefore, no new analyses are performed.

It is noted that the HI-STAR 100 System with Diablo Canyon MPC-32 uses a MPC spacer ring between the top lid of the MPC and top lid of the HI-STAR 100. The Diablo Canyon MPC spacer ring is also bounded by the analysis performed on the generic spacer ring in Subsection 2.7.1.

### **2.III.7.2 Puncture**

No new or modified calculations need be performed to qualify the HI-STAR 100 System with Diablo Canyon MPC-32, as the structure at the puncture locations is unchanged from the HI-STAR 100.

### **2.III.7.3 Thermal**

Thermal evaluation of the fire accident is presented in Supplement 3.II. No new or modified structural calculations need be performed to qualify the HI-STAR 100 System with Diablo Canyon MPC-32 for the fire accident.

### **2.III.7.4 Immersion - Fissile Material**

No new or modified calculations need be performed to qualify the HI-STAR 100 System with Diablo Canyon MPC-32.

### **2.III.7.5 Immersion - All Packages**

No new or modified calculations need be performed to qualify the HI-STAR 100 System with Diablo Canyon MPC-32.

#### **2.III.7.6 Summary of Damage**

The results presented in Subsections 2.III.7.1 through 2.III.7.5 show that the HI-STAR 100 System with Diablo Canyon MPC-32 meets the requirements of 10CFR71.61 and 10CFR71.73. Since all analyses performed for the HI-STAR 100 system are applicable to the HI-STAR 100 System with Diablo Canyon MPC-32, all safety factors are greater than 1.0 for the hypothetical accident conditions of transport. Therefore, the HI-STAR HB GTCC package, under the Hypothetical Accident Conditions of Transport, has adequate structural integrity to satisfy the subcriticality, containment, shielding, and temperature requirements of 10CFR71.

#### **2.III.8 SPECIAL FORM**

This section is not applicable to the HI-STAR 100 System with Diablo Canyon MPC-32. This application does not seek approval for transport of special form radioactive material as defined in 10CFR71.4.

#### **2.III.9 FUEL RODS**

The Diablo Canyon fuel is shorter than the design basis fuel carried by the HI-STAR 100; therefore, the computations and conclusions in Section 2.9 encompass the HI-STAR 100 System with Diablo Canyon MPC-32. The presence of “Undamaged Fuel Assemblies”, which are defined in Table 1.0.1 will have no significant effect on the structural response of the HI-STAR 100. This is because the only fuel parameters that have an influence on the structural analyses are the fuel mass and center of gravity height. Therefore, since an undamaged fuel assembly has essentially the same mass as an intact fuel assembly, and the exterior fuel rods serve to confine the interior fuel rods (with cladding in unknown condition) preventing them from dislocating and falling to the bottom of the fuel basket, the presence of undamaged fuel assemblies has no significant effect on the total amount of stored fuel mass or the center of gravity height used as input in the drop analysis for the HI-STAR 100.

#### **2.III.10 MISCELLANEOUS ITEMS**

No new appendices are introduced in Supplement 2.III. Also, since the HI-STAR 100 Package meets applicable NUREG 1617/10CFR71 requirements, so does the HI-STAR 100 System with Diablo Canyon MPC-32.

## **2.III.11 REFERENCES**

- [2.III.6.1] Pacific Gas and Electric Company, NRC Docket Number 72-27, Humboldt Bay ISFSI, Final Safety Analysis Report Update, Revision 0, January 2006.
- [2.III.6.2] Structural Evaluation of the HI-STAR HB GTCC Package, HI-2114941, Rev. 1.
- [2.III.7.1] ISFSI Dose Assessment for Humboldt Bay, HI-2033047, Rev. 0.



***Table 2.III.2.1 PROPRIETARY INFORMATION WITHHELD PER 10CFR2.390***

***Table 2.III.2.2 PROPRIETARY INFORMATION WITHHELD PER 10CFR2.390***

## CHAPTER 3: THERMAL EVALUATION

### 3.0 INTRODUCTION

In this chapter, compliance of the HI-STAR System thermal performance to 10CFR71 requirements is established for normal transport and hypothetical accident conditions of transport. The analysis considers passive rejection of decay heat from the spent nuclear fuel (SNF) to an environment under the most severe 10CFR71 mandated design basis ambient conditions.

10CFR71 defines the requirements and acceptance criteria that must be fulfilled by the cask thermal design. The requirements and acceptance criteria applicable to the thermal analysis presented in this chapter are summarized here as follows:

1. The applicant must include a description of the proposed package in sufficient detail to identify the package accurately and provide a sufficient basis for the evaluation of the package. [71.33].

The description must include, with respect to the packaging, specific materials of construction, weights, dimensions, and fabrication methods of materials specifically used as nonfissile neutron absorbers or moderators [71.33(a)(5)(ii)]; and structural and mechanical means for the transfer and dissipation of heat [71.33(a)(5)(v)].

The description must include, with respect to the contents of the package, chemical and physical form [71.33(b)(3)]; maximum normal operating pressure [71.33(b)(5)]; maximum amount of decay heat [71.33(b)(7)]; and identification and volumes of any coolants [71.33(b)(8)].

2. A package must be designed, constructed, and prepared for shipment so that under normal conditions of transport there would be no substantial reduction in the effectiveness of the packaging [71.43(f) and 71.51(a)(1)].
3. A package must be designed, constructed, and prepared for shipment so that in still air at 100°F and in the shade, no accessible surface of the package would have a temperature exceeding 185°F in an exclusive use shipment [71.43(g)].
4. Compliance with the permitted activity release limits for a Type B package may not depend on filters or on a mechanical cooling system [71.51(c)].
5. With respect to the initial conditions for the events of normal conditions of transport and hypothetical accident conditions, the demonstration of compliance with the requirements of 10CFR71 must be based on the ambient temperature preceding and following the event remaining constant at that value between -20°F and 100°F which is most unfavorable for the feature

under consideration. The initial internal pressure within the containment system must be considered to be the maximum normal operating pressure, unless a lower internal pressure consistent with the ambient temperature considered to precede and follow the event is more unfavorable [71.71(b) and 71.73(b)].

6. For normal conditions of transport, a heat event consisting of an ambient temperature of 100°F in still air and prescribed insolation must be evaluated [71.71(c)(1)].
7. For normal conditions of transport, a cold event consisting of an ambient temperature of -40°F in still air and shade must be evaluated [71.71(c)(2)].
8. Evaluation for hypothetical accident conditions is to be based on sequential application of the specified events, in the prescribed order, to determine their cumulative effect on a package [71.73(a)].
9. For hypothetical accident conditions, a thermal event consisting of a fully engulfing hydrocarbon fuel/air fire with an average emissivity coefficient of at least 0.9, with an average flame temperature of at least 1475°F for a period of 30 minutes [71.73(c)(4)].

As demonstrated in this chapter, the HI-STAR System design and thermal analyses comply with all nine requirements and acceptance criteria listed above. Subsection 3.2 lists the material properties data required to perform the thermal analyses and Subsection 3.3 provides the applicable temperature limits criteria required to demonstrate the adequacy of the HI-STAR System design under all conditions. All thermal analyses to evaluate the normal conditions of transport performance of a HI-STAR System are described in Subsection 3.4. All thermal analyses for hypothetical accident conditions are described in Subsection 3.5. A summary discussion of regulatory compliance is included in Subsection 3.6.

### 3.1 DISCUSSION

Sectional views of the HI-STAR System have been presented earlier (see Figures 1.1.3 and 1.1.4). The system essentially consists of a loaded MPC situated inside an overpack equipped with a bolted closure. The fuel assemblies reside inside the MPC that has two redundant welded closures. The MPC contains a stainless steel honeycomb fuel basket that provides square-shaped fuel compartments of appropriate dimensions to facilitate insertion of fuel assemblies prior to welding of the MPC lid. Each fuel cell wall (except outer periphery MPC-32 and MPC-68 cell walls) is provided with thermal neutron absorber panels sandwiched between a stainless steel sheathing plate and the cell wall along the entire length of the active fuel region. Prior to sealing the MPC lid, the MPC is backfilled with helium to the levels specified in Table 1.2.3. This provides a stable and inert environment for the transport of the SNF. Additionally, the annular gap between the MPC and the overpack is backfilled with helium before the overpack vent and drain port plug plugs are installed. Heat is transferred from the SNF in the HI-STAR to the environment by passive heat transport mechanisms only.

The helium backfill gas is an integral part of the MPC and overpack thermal designs. The helium fills all the spaces between solid components and provides an improved conduction medium (compared to air) for dissipating decay heat in the MPC. Additionally, helium in the spaces between the fuel basket and the MPC shell is heated differentially and, therefore, subject to the “Rayleigh” effect which is discussed in detail later (Subsection 3.4.1.1.5). To ensure that the helium gas is retained and is not diluted by lower conductivity air, the MPC helium retention boundary is designed to comply with the provisions of the ASME B&PV Code Section III, Subsection NB, as an all-seal-welded pressure vessel with redundant closures. Similarly, the overpack containment boundary is designed as an ASME B&PV Code Section III, Subsection NB pressure vessel. The overpack containment boundary is required to meet maximum leakage rate requirements included in Section 8.1.4 of this SAR. The leakage rate criterion ensures the presence of helium during transport. The helium gas is therefore retained and undiluted, and may be credited in the thermal analyses.

An important thermal design criterion imposed on the HI-STAR System is to limit the maximum fuel cladding temperature during normal transport to below design basis limits (Table 1.2.3). An equally important design criterion is to reduce temperature gradients within the MPC to minimize thermal stresses. In order to meet these design objectives, the HI-STAR MPC basket is designed to possess certain distinctive characteristics, which are summarized in the following.

The MPC design minimizes resistance to heat transfer within the basket and basket periphery regions. This is ensured by a high structural integrity all-welded honeycomb structure. The MPC design incorporates top and bottom plenums with interconnected downcomer paths. The top plenum is formed between the MPC lid and the top of the honeycomb fuel basket with additional semicircular holes in the top of each fuel cell wall. The bottom plenum is formed by large elongated semicircular holes at the base of all cell walls. The MPC basket is designed to eliminate structural discontinuities (i.e., gaps) which introduce large thermal resistances to heat flow. Consequently, temperature gradients are minimized in this design, which results in lower thermal stresses within the basket. Low thermal stresses are also ensured by an MPC design that

permits unrestrained axial and radial growth of the basket to eliminate the possibility of thermally induced stresses due to restraint of free-end expansion.

The HI-STAR System is designed for transport of PWR and BWR spent fuel assemblies and features two distinct MPC fuel basket geometries. For intact PWR fuel a 24-assembly design (depicted in Figure 1.2.5) and a higher capacity canister (MPC-32) are available. A 68-assembly design for the transport of intact or specified damaged BWR fuel is shown in Figure 1.2.3. Damaged BWR fuel must be placed in a damaged fuel container for transport in the MPC-68. Extensively damaged BWR fuel assemblies (e.g. severed rods) classified as fuel debris shall be transported in the MPC-68F. The MPC-68F is identical to the MPC-68, except for the  $^{10}\text{B}$  loading of the neutron absorber panels for criticality control. Each basket design must comply with the required temperature limits under the imposed heat generation loads from the fuel assembly contents. For normal transport conditions, the maximum decay heat loads for the PWR and BWR MPCs are summarized in Table 1.2.3. The complete HI-STAR System consisting of the overpack and MPC under transport conditions is conservatively analyzed for the imposed design heat loads.

Thermal analysis of the HI-STAR System is based on including all three fundamental modes of heat transfer: conduction, natural convection and thermal radiation. Different combinations of these modes are active in different parts of the system. These modes are properly identified and conservatively analyzed within each region of the MPC and overpack, to enable bounding calculations of the temperature distribution within the HI-STAR System for both PWR and BWR MPC basket designs.

On the outside surface of the overpack, heat is dissipated to the environment by buoyancy induced convective air flow (natural convection) and thermal radiation. In the overpack internal metal structure, only conductive heat transport is possible. Between metal surfaces (e.g., between neighboring fuel rod surfaces) heat transport is due to a combination of conduction through a gaseous medium (helium) and thermal radiation. Finally, buoyancy-induced convective heat transport occurs within the open spaces of the MPC, aided by the MPC design which provides low pressure drop helium flow recirculation loops formed by the fuel cells, top plenum, downcomers, and bottom plenum. However, in the interest of conservatism, no credit for buoyancy-induced heat transport in the HI-STAR MPC basket is taken to satisfy either temperature or stress intensity limits. Heat transfer between the fuel basket external surface and MPC enclosure shell inside wall is further influenced by the so-called “Rayleigh” effect in differentially heated vertical cavities and “Rayleigh-Benard” effect in horizontal channels heated from below. A discussion on these effects is provided in Subsection 3.4.1.1.5.

The total heat generation in each assembly is non-uniformly distributed over the active fuel to account for design basis-fuel burnup distribution listed in Chapter 1 (Table 1.2.15 and Figures 1.2.13 and 1.2.14). As discussed later in this chapter (Subsection 3.4.6), an array of conservative assumptions bias the results of the thermal analysis towards much reduced computed margins than would be obtained by a rigorous analysis of the problem.

The complete thermal analysis is performed using the industry standard ANSYS finite element modeling package [3.1.1] and the finite volume Computational Fluid Dynamics (CFD) code FLUENT [3.1.2]. ANSYS has been previously used and accepted by the NRC on numerous dockets. The FLUENT CFD program is independently benchmarked and validated with a wide class of theoretical and experimental studies reported in the technical journals. Additionally, Holtec has confirmed the code's capability to reliably predict temperature fields in dry storage applications using independent full-scale test data from a loaded cask [3.1.3]. This study concluded that FLUENT can be used to model all modes of heat transfer, namely, conduction, convection, and radiation in dry cask systems.

### 3.2 SUMMARY OF THERMAL PROPERTIES OF MATERIALS

Materials present in the HI-STAR System include stainless steels, carbon steels, aluminum, neutron shield (Holtite-A), neutron absorber and helium. In Table 3.2.1, a summary of references used to obtain cask material properties for performing all thermal analyses is presented.

Tables 3.2.2, 3.2.3 and 3.2.9 provide numerical thermal conductivity data for all materials at several representative temperatures. The neutron absorber materials are made of aluminum powder and boron carbide powder. Although their manufacturing processes differ, from a thermal standpoint, their ability to conduct heat is virtually identical. Therefore, the value of conductivity of one neutron absorber (Boral) is used in the thermal calculations and is applicable to both neutron absorbers used in the HI-STAR 100 cask. Thermal properties of Boral are provided in Table 3.2.8.

Surface emissivity data for key materials of construction are provided in Table 3.2.4. [

PROPRIETARY INFORMATION WITHHELD PER 10CFR2.390

] A conservative solar absorptivity coefficient of 1.0 is applied to all exposed cask surfaces.

In Table 3.2.5, the heat capacity and density data of different cask materials is presented. These properties are used in performing transient (hypothetical fire accident condition, for example) analyses. MPC Rayleigh effect calculations use helium density, heat capacity, and gas viscosity properties data, which are listed in Tables 3.2.5 and 3.2.6.

The HI-STAR System's outside surface heat transfer coefficient is calculated by accounting for both natural convection heat transfer and radiation. The natural convection coefficient of a heated horizontal cylinder depends upon the product of the Grashof (Gr) and Prandtl (Pr) numbers. Following the approach developed by Jakob and Hawkins [3.2.9],  $GrPr$  is expressed as  $L^3 \Delta T Z$ , where  $L$  is the diameter of the cask,  $\Delta T$  is the HI-STAR System overpack surface-to-ambient temperature differential and  $Z$  is a parameter which depends upon air properties, which are known functions of temperature, evaluated at the average film temperature. The temperature dependence of  $Z$  for air is provided in Table 3.2.7.

The long-term thermal stability and radiation resistance of Holtite-A has been confirmed through qualification testing. The qualification test conditions exceed the Holtite-A thermal and radiation environment (gamma and neutron fluence) in the HI-STAR 100 cask. The Holtite-A thermal stability test temperature, 325°F, is well above the maximum operating temperature of Holtite-A (See Tables 3.4.10 and 3.4.11). The Holtite-A radiation test exposures exceed 50-year HI-STAR service neutron dose by a factor of 3.75 and gamma dose by a factor of 5.54 (See Table 3.2.10). The Holtite-A qualification test data is archived in the following reports:

- i) "Holtite A: Development history and thermal performance data", Holtec Report HI-2002396, Rev. 3.
- ii) "Holtite-A: Results of Pre-and-Post-Irradiation Tests and Measurements", Holtec Report HI-2002420, Rev. 1.



The testing referenced above confirms that Holtite-A does not degrade at elevated temperatures and Holtite-A is unaffected by high neutron fluence and megarad gamma doses. Even under very conservative assumptions (20-years of storage under the maximum temperature reached at the beginning of dry storage) only a 2% weight loss is computed (licensing basis commitment is 4%). Nevertheless, periodic thermal testing of HI-STAR 100 is required as specified in Chapter 8.

Table 3.2.1

**SUMMARY OF HI-STAR SYSTEM MATERIALS  
THERMAL PROPERTY REFERENCES**

<b>Material</b>	<b>Emissivity</b>	<b>Conductivity</b>	<b>Density</b>	<b>Heat Capacity</b>
Helium	NA	Handbook [3.2.2]	Ideal Gas Law	Handbook [3.2.2]
Air	NA	Handbook [3.2.2]	Ideal Gas Law	Handbook [3.2.2]
Zircaloy Cladding	EPRI [3.2.3]	NUREG [3.2.6], [3.2.7]	Rust [3.2.4]	Rust [3.2.4]
UO <sub>2</sub>	Not Used	NUREG [3.2.6], [3.2.7]	Rust [3.2.4]	Rust [3.2.4]
Stainless Steel (machined forgings)*	Kern [3.2.5]	ASME [3.2.8]	Marks [3.2.1]	Marks [3.2.1]
Stainless Steel Plates <sup>†</sup>	ORNL [3.2.12], [3.2.13]	ASME [3.2.8]	Marks [3.2.1]	Marks [3.2.1]
Carbon Steel	Kern [3.2.5]	ASME [3.2.8]	Marks [3.2.1]	Marks [3.2.1]
Aluminum Impact Limiters	Not Used	Note 1	Note 1	Note 1
Aluminum Alloy 1100 (Heat Conduction Elements) <sup>‡</sup>	Handbook [3.2.2]	ASME [3.2.8]	ASME [3.2.8]	ASME [3.2.8]
Boral <sup>†</sup>	Not Used	Test Data	Test Data	Test Data
Holtite-A	Not Used	Test Data [3.2.14]	Test Data [3.2.14]	Test Data [3.2.13]
METAMIC <sup>§</sup>	Not Used	Test Data [3.2.10], [3.2.11]	Test Data [3.2.10], [3.2.11]	Test Data [3.2.10], [3.2.11]
Note 1: Properties of solid aluminum are used during fire to maximize heat input and properties of air used during normal transport and post-fire cooldown to minimize heat dissipation. The solid aluminum properties are taken from the ASME Code [3.2.8] for alloy 5052, and thermal conductivity values are extrapolated linearly to 450°F and 700°F.				

- 
- \* Used in the MPC lid.  
<sup>†</sup> Used in the basket panels & sheathing, MPC shell& baseplate.  
<sup>‡</sup> Heat conduction elements used in certain early vintage MPCs  
<sup>†</sup> AAR Structures' Boral thermophysical test data.  
<sup>§</sup> Table lists all sources consulted for material properties.

Table 3.2.2

SUMMARY OF HI-STAR SYSTEM MATERIALS  
THERMAL CONDUCTIVITY DATA

<b>Material</b>	<b>@ 200°F (Btu/ft-hr-°F)</b>	<b>@ 450°F (Btu/ft-hr-°F)</b>	<b>@ 700°F (Btu/ft-hr-°F)</b>
Helium	0.0976	0.1289	0.1575
Air	0.0173	0.0225	0.0272
Alloy X	8.4	9.8	11.0
SA-515 Grade 70 (Carbon Steel Radial Connectors**)	29.2	27.1	24.6
SA-516 Grade 70 (Carbon Steel Gamma Shield Layers)	24.4	23.9	22.4
Aluminum Honeycomb Impact Limiter*	[PROPRIETARY INFORMATION WITHHELD PER 10CFR2.390]		
Holtite-A <sup>†</sup>	See Footnote		
Cryogenic Steel	23.8	23.7	22.3

\*\* Optionally, the radial connectors may be fabricated from SA-516 Grade 70.

\* Properties of solid Aluminum used during fire to maximize heat input and properties of air used during normal transport and post-fire cooldown to minimize heat dissipation.

† [PROPRIETARY INFORMATION WITHHELD PER 10CFR2.390]

Table 3.2.3

SUMMARY OF FUEL ELEMENT COMPONENTS  
THERMAL CONDUCTIVITY DATA

Fuel Cladding		Fuel (UO <sub>2</sub> )	
Temperature (°F)	Conductivity (Btu/ft-hr-°F)	Temperature (°F)	Conductivity (Btu/ft-hr-°F)
392	8.28 <sup>†</sup>	100	3.48
572	8.76	448	3.48
752	9.60	570	3.24
932	10.44	793	2.28 <sup>†</sup>

---

<sup>†</sup> Lowest value of conductivity is used in the thermal analysis for conservatism.

Table 3.2.4

[PROPRIETARY INFORMATION WITHHELD PER 10CFR2.390]

Table 3.2.5

[PROPRIETARY INFORMATION WITHHELD PER 10CFR2.390]

Table 3.2.6

HELIUM GAS VISCOSITY<sup>†</sup> VARIATION WITH TEMPERATURE

Temperature (°F)	Viscosity (Micropoise)
167.4	220.5
200.3	228.2
297.4	250.6
346.9	261.8
463.0	288.7
537.8	299.8
737.6	338.8

---

<sup>†</sup> Obtained from Rohsenow and Hartnett [3.2.2].

Table 3.2.7

VARIATION OF NATURAL CONVECTION PROPERTIES  
PARAMETER "Z" FOR AIR WITH TEMPERATURE

Temperature (°F)	Z (ft <sup>-3</sup> °F <sup>-1</sup> ) <sup>†</sup>
40	2.1×10 <sup>6</sup>
140	9.0×10 <sup>5</sup>
240	4.6×10 <sup>5</sup>
340	2.6×10 <sup>5</sup>
440	1.5×10 <sup>5</sup>

---

<sup>†</sup> Obtained from Jakob and Hawkins [3.2.9].



Table 3.2.8

BORAL COMPONENT MATERIALS\*  
THERMAL CONDUCTIVITY DATA

Temperature (°F)	B <sub>4</sub> C Core Conductivity (Btu/ft-hr-°F)	Aluminum Cladding Conductivity (Btu/ft-hr-°F)
212	48.09	100.00
392	48.03	104.51
572	47.28	108.04
752	46.35	109.43

---

\* Thermal properties of Boral used in the calculations are tabulated herein. As heat conduction properties of METAMIC are essentially same as Boral (See Section 3.2) tabulation of METAMIC properties is not necessary.

Table 3.2.9

HEAT CONDUCTION ELEMENTS (ALUMINUM ALLOY 1100)  
THERMAL CONDUCTIVITY DATA

<b>Temperature (°F)</b>	<b>Conductivity (Btu/ft×hr×°F)</b>
100	131.8
200	128.5
300	126.2
400	124.5

Table 3.2.10

## Holtite-A Radiation Exposure\*

	Under 50-Year Service Life	Test Exposure
Neutron Fluence (n/cm <sup>2</sup> )	$4 \times 10^{14}$	$1.28 \times 10^{15}$
Gamma Dose (rad)	$3.55 \times 10^5$	$1.7 \times 10^6$
Note: As tabulated above the Holtite-A qualification test exposures exceed 50-year service exposures by significant margins.		

---

\* "Holtite-A: Results of Pre-and-Post-Irradiation Tests and Measurements", Holtec Report HI-2002420, Rev. 1.

### 3.3 TECHNICAL SPECIFICATIONS FOR COMPONENTS

HI-STAR System materials and components which are required to be maintained within their safe operating temperature ranges to ensure their intended function are summarized in Table 3.3.1. Long-term stability and continued neutron shielding ability of the Holtite-A neutron shield material under normal transport conditions are ensured when material exposure temperatures are maintained below the maximum allowable limit. The overpack metallic seals will continue to ensure sealing of the closure plate, and drain and vent ports if the manufacturer's recommended design temperature limits are not exceeded. Integrity of SNF during transport requires demonstration of HI-STAR fuel cladding temperatures to remain below regulatory limits. Neutron absorber materials used in MPC baskets for criticality control are stable in excess of 1000°F. For conservatism temperature limits below the threshold of material integrity<sup>†</sup> are adopted (See Table 3.3.1).

Compliance to 10CFR71 requires evaluation of hypothetical accident conditions. The inherent mechanical stability characteristics of the HI-STAR System materials and components ensure that no significant functional degradation is possible due to exposure to short-term temperature excursions outside the normal long-term temperature limits. For evaluation of the HI-STAR System's thermal performance under hypothetical accident conditions, material temperature limits for short-duration events are also provided in Table 3.3.1. In this Table, the cladding temperature limits of ISG-11, Rev. 3 [3.1.5] are adopted for Commercial Spent Fuel (CSF). These limits are applicable to all fuel types, burnup levels and cladding materials approved by the NRC for power generation.

#### 3.3.1 Evaluation of Moderate Burnup Fuel

It is recognized that hydrides present in irradiated fuel rods (predominantly circumferentially oriented) dissolve at cladding temperatures above 400°C [3.3.8]. Upon cooling below a threshold temperature ( $T_p$ ), the hydrides precipitate and reorient to an undesirable (radial) direction if cladding stresses at the hydride precipitation temperature  $T_p$  are excessive. For moderate burnup fuel,  $T_p$  is conservatively estimated as 350°C [3.3.8].

Moderate Burnup Fuel (MBF) temperature limits for short term operations have been addressed in the PNNL report "Estimated Maximum Cladding Stresses for Bounding PWR Fuel Rods During Short Term Operations for Dry Cask Storage" published in Jan. 2004 [3.3.8]. In this report the potential for hydride re-orientation was evaluated in a simulated drying event in which fuel was heated to the cladding temperature limit (570°C (1058°F)) and then cooled below the hydride precipitation temperature  $T_p$ . The study concluded that hydride re-orientation is not a concern in moderate burnup fuel because the coincident cladding stress at the hydride precipitation temperature is below the critical cladding stress. Accordingly, the 570°C (1058°F) temperature limit is justified

---

<sup>†</sup> Neutron absorber materials are manufactured using B<sub>4</sub>C and aluminum. B<sub>4</sub>C is a refractory material that is unaffected by high temperatures and aluminum is solid at temperatures in excess of 1000°F.

for moderate burnup fuel and is adopted in the HI-STAR SAR for short-term operations with MBF fueled MPCs.

Table 3.3.1

## HI-STAR SYSTEM MATERIAL TEMPERATURE LIMITS

<b>Material</b>	<b>Normal Condition Temperature Limits</b>	<b>Short Term and Accident Temperature Limits</b>
CSF Cladding	752°F	1058°F
Neutron Absorber	800°F	1000°F
Overpack Closure Plate Mechanical Seals	See Table 4.1.1	See Table 4.1.1
Overpack Vent and Drain Port Plug Seals	See Table 4.1.1	See Table 4.1.1
Aluminum Alloy 5052	176°F <sup>††</sup>	1105°F <sup>†††</sup>
Holtite-A	300°F <sup>††††</sup>	N/A <sup>†††††</sup>
Aluminum Heat Conduction Elements (Alloy 1100) <sup>1</sup>	725°F	950°F

---

†† AL-STAR impact limiter aluminum honeycomb test data.

††† Melting range of alloy is 1105°F-1200°F [3.3.1].

†††† Neutron shield manufacturer's test data (Appendix 1.B).

††††† For shielding analysis (Chapter 5), Holtite-A is conservatively assumed to be lost during the fire accident.

1 Temperature limits provided to cover the use of aluminum heat conduction elements in certain early vintage MPCs.

---

Tables 3.3.2 through 3.3.8

[INTENTIONALLY DELETED]

### 3.4 THERMAL EVALUATION FOR NORMAL CONDITIONS OF TRANSPORT

#### 3.4.1 Thermal Model

The HI-STAR MPC basket designs consist of four distinct geometries engineered to hold 24 and 32 PWR (MPC-24, MPC-24E and MPC-32) or 68 BWR (MPC-68) fuel assemblies. The fuel basket forms a honeycomb matrix of square-shaped fuel compartments to retain the fuel assemblies during transport (refer to Figures 1.2.3 and 1.2.5 for an illustration of PWR and BWR baskets). The basket is formed by an interlocking honeycomb structure of steel plates and full-length edge welding of the cell corners to form an integral basket configuration. Individual cell walls (except outer periphery MPC-68 and MPC-32 cell walls) are provided with neutron absorber panels sandwiched between the cell wall and a stainless steel sheathing plate, for the full length of the active fuel region.

The design basis decay heat generation per PWR or BWR assembly for normal transport for each MPC type is specified in Table 1.2.13. The decay heat is considered to be non-uniformly distributed over the active fuel length based on the design basis axial burnup distribution specified in Chapter 1 (see Table 1.2.15 and Figures 1.2.13 and 1.2.14).

Transport of heat from the MPC basket interior to the basket periphery is accomplished by conduction through the MPC basket metal grid structure and the narrow helium gaps between the fuel assemblies and fuel cell walls. Heat dissipation in the MPC basket periphery-to-MPC shell gap is by a combination of helium conduction, natural convection (by means of the “Rayleigh” effect) and radiation across the gap. Between the MPC shell and the overpack inner shell is a small clearance, which is evacuated and backfilled with helium. Helium, besides being inert, is a better conductor of heat than air. Thus, heat conduction through the helium gap between the MPC and the overpack will minimize temperature differentials across this region.

The overpack, under normal transport conditions, passively rejects heat to the environment. Cooling of the exterior system surfaces is by natural convection and radiation. During transport, the HI-STAR System is placed in a horizontal position with stainless steel encased aluminum honeycomb impact limiters installed at both ends of the overpack. To conservatively maximize the calculated internal temperatures, the thermal conductivity of the impact limiters is set essentially equal to zero. Under normal transport conditions, the MPC shell rests on the overpack internal cavity surface forming an eccentric gap. Direct contact between the MPC and overpack surfaces is expected to minimize heat transfer resistance in this region of intimate contact. Significantly improved conductive heat transport due to reduction in the helium gap near the contact region is accounted for in the thermal analysis of the HI-STAR System. The HI-STAR System is conservatively analyzed assuming a minimum 0.02-inch gap at the line of metal-to-metal contact. Analytical modeling details of the various thermal transport mechanisms are provided in the following.

##### 3.4.1.1 Analytical Model - General Remarks

Transport of heat from the heat generation region (fuel assemblies) to the outside environment is analyzed broadly in terms of three interdependent thermal models.



- i. The first model considers transport of heat from the fuel assembly to the basket cell walls. This model recognizes the combined effects of conduction (through helium) and radiation, and is essentially a finite element technology-based update of the classical Wootton & Epstein [3.4.1] formulation (which considers radiative heat exchange between fuel rod surfaces).
- ii. The second model considers heat transport within an MPC cross section by conduction and radiation. The effective cross sectional thermal conductivity of the basket region obtained from the combined fuel assembly/basket heat conduction radiation model is applied to an axisymmetric thermal model of the HI-STAR System on the FLUENT [3.1.2] code.
- iii. The third model deals with the transmission of heat from the MPC exterior surface to the external environment (heat sink). From the MPC shell to the cask exterior surface, heat is conducted through an array of concentric shells representing the MPC-to-overpack helium gap, the overpack inner shell, the intermediate shells, the Holtite-A neutron shielding and finally the overpack outer shell. Heat rejection from the outside cask surfaces to ambient air is considered by accounting for natural convection and thermal radiation heat transfer mechanisms from the exposed cask surfaces. Insolation on exposed cask surfaces is based on 12-hour levels prescribed in 10CFR71, averaged over a 24-hour period.

The following subsections contain a systematic description of the mathematical models devised to articulate the temperature field in the HI-STAR System. Table 3.4.2 shows the relationship between the mathematical models and the corresponding regions (i.e., fuel, MPC, overpack, etc.) of the HI-STAR System. The description begins with the method to characterize the heat transfer behavior of the prismatic (square) opening referred to as the “fuel space” containing a heat emitting fuel assembly. The methodology utilizes a finite-volume procedure to replace the heterogeneous SNF/fuel space region with an equivalent solid body having a well-defined temperature-dependent conductivity. In the following subsection, the method to replace the composite walls of the fuel basket cells with equivalent “solid” walls is presented. Having created the mathematical equivalents for the SNF/fuel spaces and the fuel basket walls, the method to represent the MPC cylinder containing the fuel basket by an equivalent cylinder whose thermal conductivity is a function of the spatial location and coincident temperature is presented.

Following the approach of presenting descriptions starting from the inside and moving to the outer region of a cask, the next subsections present the mathematical model to simulate the overpack. Subsection 3.4.1.1.12 concludes the presentation with a description of how the different models for the specific regions within the HI-STAR System are assembled into the final finite element model.

#### 3.4.1.1.1 Overview of the Thermal Model

Thermal analysis of the HI-STAR System is performed by assuming that the system is subject to its maximum heat duty with each storage location occupied and with the heat generation rate in each stored fuel assembly equal to the design basis maximum value. While the assumption of equal heat generation imputes a certain symmetry to the cask thermal problem, the thermal model must incorporate three attributes of the physical problem to perform a rigorous analysis:

- i. While the rate of heat conduction through metals is a relatively weak function of temperature, radiation heat exchange is a nonlinear function of surface temperatures.
- ii. Heat generation in the MPC is axially non-uniform due to a non-uniform axial burnup profile in the fuel assemblies.
- iii. Inasmuch as the transfer of heat occurs from the inside of the basket region to the outside, the temperature field in the MPC is spatially distributed with the maximum values reached in the central region.

It is clearly impractical to explicitly model every fuel rod in every stored fuel assembly explicitly. Instead, the cross section bounded by the inside of the storage cell, which surrounds the assemblage of fuel rods and the interstitial helium gas, is replaced with an “equivalent” square (solid) section characterized by an effective thermal conductivity. Figure 3.4.1 pictorially illustrates the homogenization concept. Further details on this process for determining the effective conductivity is presented in Subsection 3.4.1.1.2. It suffices to state here that the effective conductivity of the cell space will be a function of temperature, because radiation heat transfer (a major component of the heat transport mechanism between the fuel rods to the basket metal square) is a strong function of the absolute temperatures of the participating bodies. Therefore, in effect, every storage cell location will have a different value of effective conductivity in the homogenized model. The process of determining the temperature-dependent effective conductivity is carried out using a finite volume procedure.

In the next step of homogenization, a planar section of MPC is considered. With each storage cell inside space replaced with an equivalent solid square, the MPC cross section consists of a metallic gridwork (basket cell walls with each cell space containing a solid fuel square with an effective thermal conductivity) circumscribed by a circular ring (MPC shell). There are four principal materials in this section that are included in all MPCs, namely the homogenized fuel cell squares, the Alloy X MPC structural materials in the MPC (including sheathing material), neutron absorber and helium gas. Aluminum heat conduction elements (AHCEs), included optionally in the MPC design, are appropriately ignored in the heat dissipation calculations. Each of the four constituent materials in this section has a different conductivity. As discussed earlier, the conductivity of the homogenized fuel cell is a strong function of temperature.

In order to replace this thermally heterogeneous MPC section with an equivalent conduction-only lamina, resort to the finite-element procedure is necessary. Because the rate of transport of heat within the MPC is influenced by radiation, which is a temperature-dependent effect, the equivalent conductivity of the MPC lamina must be computed as a function of temperature. Finally, it is recognized that the MPC section consists of two discrete regions, namely, the basket region and the periphery region. The periphery region is the space between the peripheral storage cells and the MPC enclosure shell. This space is essentially full of helium gas surrounded by Alloy X plates and optionally aluminum heat conduction elements. Accordingly, as illustrated in Figure 3.4.2 for MPC-68, the MPC cross section is replaced with two homogenized regions with temperature-dependent conductivities. In particular, the effective conductivity of the fuel cells is subsumed into the equivalent conductivity of the basket cross section using a finite element procedure. The ANSYS

finite-element code is the vehicle for all modeling efforts described in the foregoing.

In summary, appropriate finite element models are used to replace the MPC cross section with an equivalent two-region homogeneous conduction lamina whose local conductivity is a known function of coincident absolute temperature. Thus, the MPC cylinder containing discrete fuel assemblies, helium, neutron absorber, Alloy X and optionally AHCEs\* is replaced with a right circular cylinder whose material conductivity will vary with radial and axial position as a function of the coincident temperature.

The MPC-to-overpack gap is simply an annular space that is readily modeled with an equivalent conductivity that reflects the conduction and radiation modes of heat transfer. The overpack is a radially symmetric structure except for the neutron absorber region which is built from radial connectors and Holtite. Using the classical equivalence procedure as described in Section 3.4.1.1.9, this region is replaced with an equivalent radially symmetric annular cylinder.

The thermal analysis procedure described above makes frequent use of equivalent thermal properties to ease the geometric modeling of the cask components. These equivalent properties are rigorously calculated values based on detailed evaluations of actual cask system geometries. All these calculations are performed conservatively to ensure a bounding representation of the cask system. This process commonly referred to as submodeling, yields accurate (not approximate) results. Given the detailed nature of the submodeling process, experimental validation of the individual submodels is not necessary.

In this manner, a HI-STAR System overpack containing a loaded MPC is replaced with a right circular cylinder with spatially varying temperature-dependent conductivity. Heat is generated within the basket space in this cylinder in the manner of the prescribed axial distribution. In addition, heat is deposited from insulation on its external surface. Natural convection and thermal radiation to ambient air dissipate heat. Details of the elements of mathematical modeling are provided in the following sections.

#### 3.4.1.1.2 Fuel Region Effective Thermal Conductivity Calculation

Thermal properties of a large number of PWR and BWR fuel assembly configurations manufactured by the major fuel suppliers (i.e., Westinghouse, CE, B&W, and GE) have been evaluated for inclusion in the HI-STAR System thermal analysis. Bounding PWR and BWR fuel assembly configurations are determined using the simplified procedure described below. This is followed by the determination of temperature-dependent properties of the bounding PWR and BWR fuel assembly configurations to be used for cask thermal analysis using a finite-volume (FLUENT) approach.

To determine which of the numerous PWR assembly types listed in Table 3.4.4 should be used in the thermal model for the PWR fuel baskets, we must establish which assembly has the maximum thermal resistance. The same determination must be made for the MPC-68, out of the menu of SNF

---

\* In the thermal model, AHCEs are appropriately ignored.

types listed in Table 3.4.5. For this purpose, we utilize a simplified procedure that we describe below.

Each fuel assembly consists of a large array of fuel rods typically arranged on a square layout. Every fuel rod in this array is generating heat due to radioactive decay in the enclosed fuel pellets. There is a finite temperature difference required to transport heat from the innermost fuel rods to the storage cell walls. Heat transport within the fuel assembly is based on principles of conduction heat transfer combined with the highly conservative analytical model proposed by Wooton and Epstein [3.4.1]. The Wooton-Epstein model considers radiative heat exchange between individual fuel rod surfaces as a means to bound the hottest fuel rod cladding temperature.

Transport of heat energy within any cross section of a fuel assembly is due to a combination of radiative energy exchange and conduction through the helium gas that fills the interstices between the fuel rods in the array. With the assumption of uniform heat generation within any given horizontal cross section of a fuel assembly, the combined radiation and conduction heat transport effects result in the following heat flow equation:

$$Q = \sigma C_o F_\epsilon A [T_C^4 - T_B^4] + 13.5740 L K_{cs} [T_C - T_B]$$

where,

$$F_\epsilon = \text{Emissivity Factor} = \frac{1}{\left(\frac{1}{\epsilon_C} + \frac{1}{\epsilon_B} - 1\right)}$$

$\epsilon_C, \epsilon_B$  = emissivities of fuel cladding, fuel basket (see Table 3.2.4)

$C_o$  = Assembly Geometry Factor

$$= \frac{4N}{(N+1)^2} \text{ (when } N \text{ is odd)}$$

$$= \frac{4}{N+2} \text{ (when } N \text{ is even)}$$

$N$  = Number of rows or columns of rods arranged in a square array

$A$  = fuel assembly “box” heat transfer area  
=  $4 \times \text{width} \times \text{length (ft}^2\text{)}$

$L$  = fuel assembly length (ft)

$K_{cs}$  = fuel assembly constituent materials volume fraction weighted mixture conductivity (Btu/ft-hr-°F)

$T_C$	=	hottest fuel cladding temperature ( $^{\circ}\text{R}$ )
$T_B$	=	box temperature ( $^{\circ}\text{R}$ )
$Q$	=	net radial heat transport from the assembly interior (Btu/hr)
$\sigma$	=	Stefan-Boltzman Constant ( $0.1714 \times 10^{-8}$ Btu/ft <sup>2</sup> -hr- $^{\circ}\text{R}^4$ )

In the above heat flow equation, the first term is the Wooten-Epstein radiative heat flow contribution while the second term is the conduction heat transport contribution based on the classical solution to the temperature distribution problem inside a square shaped block with uniform heat generation [3.4.3]. The 13.574 factor in the conduction term of the equation is the shape factor for two-dimensional heat transfer in a square section. Planar fuel assembly heat transport by conduction occurs through a series of resistances formed by the interstitial helium fill gas, fuel cladding and enclosed fuel. An effective planar mixture conductivity is determined by a volume fraction weighted sum of the individual constituent materials resistances. For BWR assemblies, this formulation is applied to the region inside the fuel channel. A second conduction and radiation model is applied between the channel and the fuel basket gap. These two models are combined, in series, to yield a total effective conductivity.

The effective thermal conductivities of several representative intact PWR and BWR assemblies are presented in Tables 3.4.4 and 3.4.5. At higher temperatures (greater than 450°F), the zircaloy clad fuel assemblies with the lowest effective thermal conductivities are the Westinghouse 17×17 OFA (PWR) and the General Electric GE-11 9×9 (BWR). A discussion of fuel assembly conductivities for some of the newer 10×10 array and plant specific BWR fuel designs is presented near the end of this subsection. Based on this simplified analysis, the Westinghouse 17×17 OFA PWR and GE-11 9×9 BWR fuel assemblies are determined to be the bounding configurations for analysis at design basis maximum heat loads.

Several of the assemblies listed in Tables 3.4.5 were excluded from consideration when determining the bounding assembly because of their extremely low decay heat loads. The excluded assemblies, which were each used at a single reactor only, are physically small and have extremely low burnups and long cooling times. These factors combine to result in decay heat loads that are much lower than the design basis maximum. The excluded assemblies are:

- Dresden Unit 1 8×8
- Dresden Unit 1 6×6
- Allis-Chalmers 10×10 Stainless
- Exxon Nuclear 10×10 Stainless
- Humboldt Bay 7×7
- Quad<sup>+</sup> 8×8

The Allis-Chalmers and Exxon assemblies are used only in the LaCrosse reactor of the Dairyland Power Cooperative. The design basis assembly decay heat loads for Dresden Unit 1 and LaCrosse

SNF (Tables 1.2.14 and 1.2.19) are approximately 58% lower and 69% lower, respectively, than the MPC-68 design basis assembly maximum heat load (Table 1.2.13). Examining Table 3.4.5, the effective thermal conductivity of damaged Dresden Unit 1 fuel assemblies inside DFCs (the lowest of any Dresden Unit 1 assembly) and LaCrosse fuel assemblies are approximately 40% lower and 30% lower, respectively, than that of the bounding (GE-11 9×9) fuel assembly. Consequently, the fuel cladding temperatures in the HI-STAR System with Dresden Unit 1 and LaCrosse fuel assemblies (intact or damaged) will be bounded by design basis fuel cladding temperatures.

To accommodate Trojan Nuclear Plant (TNP) SNF in a HI-STAR System's MPC-24E canister\*, the discharged fuel characteristics at this permanently shutdown site are evaluated herein. To permit TNP fuel in the HI-STAR System, it is necessary to confirm that certain key fuel parameters, viz. burnup (B) and cask decay heat (D) are bounded by the thermal design limits (42,500 MWD/MTU and 20 kW for PWR MPCs). The TNP SNF is a member of the 17x17 class of fuel types. The bulk of the fuel inventory is from Westinghouse and balance from B&W. The B&W SNF configuration and cladding dimensions are same as that of the Westinghouse 17x17 SNF. The fuel is more than nine years old and the burnups are in the range of 5073 MWD/MTU to 41889 MWD/MTU. The TNP SNF burnups are bounded by the design maximum for PWR class of fuel (i.e.  $B < 42500$  MWD/MTU). Because the fuel decay heat is exponentially attenuating with time, it is conservative to evaluate decay heat on a date that precedes fuel loading. For this purpose, a reference date (RD) of 11/9/2001 is employed herein. The decay heat from the most emissive Trojan fuel is bounded by 725 W on RD. Postulating every cell location in an MPC-24E is occupied by this most heat emissive fuel assembly, a conservatively bounding  $D = 17.4 \text{ kW}^\dagger$  is computed. The Trojan MPC-24E heat loads are below the HI-STAR System design heat load (i.e.  $D < 20 \text{ kW}$ ) by a significant margin.

A limited number of Trojan assemblies have poison inserts (RCCAs and BPRAs) and other non-fuel hardware (Thimble Plugs). The inclusion of PWR non-fuel hardware influences the MPC thermal response in two ways: (i) The presence of non-fuel hardware increases the effective basket conductivity, thus enhancing heat dissipation and lowering fuel temperatures and (ii) Volume displaced by the mass of non-fuel hardware lowers the available cavity free volume for accommodating gas released in hypothetical rod rupture scenarios. For a conservatively bounding evaluation, the thermal modeling ignores the presence of non-fuel hardware and the MPC cavity volume is computed based on volume displacement by the heaviest fuel (bounding weight) with non-fuel hardware included.

Having established the governing (most resistive) PWR and BWR SNF types, a finite-volume code is used to determine the effective conductivities in a conservative manner. Detailed conduction-radiation finite-volume models of the bounding PWR and BWR fuel assemblies are developed in the FLUENT code as shown in Figures 3.4.7 and 3.4.8, respectively. The PWR model was originally developed on the ANSYS code which enables individual rod-to-rod and rod-to-basket wall view factor calculations to be performed using that code's AUX12 processor. Limitations of radiation modeling techniques implemented in ANSYS make it difficult to take advantage of the symmetry of the fuel assembly geometry. Unacceptably long CPU time and large workspace requirements

\* The height of MPC-24E for Trojan SNF is shorter than the height of generic HI-STAR MPCs.

† Projected MPC heat loads are much lower (in the range of 6 kW to 14.5 kW in circa 2003).

necessary for performing gray body radiation calculations for a complete fuel assembly geometry on ANSYS prompted the development of an alternate simplified model on the FLUENT code. The FLUENT model was benchmarked with the ANSYS model results for a Westinghouse 17×17 OFA fuel assembly geometry for the case of black body radiation (emissivities = 1). The FLUENT model was found to yield conservative results in comparison to the ANSYS model for the “black” surface case. The FLUENT model benchmarked in this manner is used to solve the gray body radiation problem to provide the necessary results for determining the effective thermal conductivity of the governing PWR fuel assembly. The same modeling approach using FLUENT is then applied to the governing BWR fuel assembly and the effective conductivity of GE-11 9×9 fuel is determined.

An equivalent homogeneous material that fills the basket opening replaces the combined fuel rods-helium matrix by the following two-step procedure. In the first step, the FLUENT-based fuel assembly model is solved by applying equal heat generation per unit length to the individual fuel rods and a uniform boundary temperature along the basket cell opening inside periphery. The temperature difference between the peak cladding and boundary temperatures is used to determine an effective conductivity as described in the next step. For this purpose, we consider a two-dimensional cross section of a square shaped block of size equal to 2L and a uniform volumetric heat source ( $q_g$ ) cooled at the periphery with a uniform boundary temperature. Under the assumption of constant material thermal conductivity (K), the temperature difference ( $\Delta T$ ) from the center of the cross section to the periphery is analytically given by [3.4.3]:

$$\Delta T = 0.29468 \frac{q_g L^2}{K}$$

This analytical formula is applied to determine the effective material conductivity from a known quantity of heat generation applied in the FLUENT model (smeared as a uniform heat source,  $q_g$ ), basket opening size and  $\Delta T$  calculated in the first step.

As discussed earlier, the effective fuel space conductivity is a function of the temperature coordinate. The above two step analysis is carried out for a number of reference temperatures. In this manner, the effective conductivity as a function of temperature is established.

In Table 3.4.25, 10×10 array type BWR fuel assembly effective thermal conductivity results from a simplified analysis are presented to determine the most resistive fuel assembly in this class. Using the simplified analysis procedure discussed earlier, the Atrium-10 fuel type is determined to be the most resistive in this class of fuel assemblies. A detailed finite-element model of this assembly type was developed to rigorously quantify the heat dissipation characteristics. The results of this study are presented in Table 3.4.26 and compared to the bounding BWR fuel assembly effective thermal conductivity depicted in Figure 3.4.13. The results of this study demonstrate that the bounding BWR fuel assembly effective thermal conductivity is conservative with respect to the 10×10 class of BWR assemblies. Table 3.4.34 summarizes plant specific fuel types’ effective conductivities. From these analytical results, the SPC-5 is determined to be the most resistive fuel assembly in this group of fuel types. A rigorous finite element model of SPC-5 fuel assembly was developed to confirm that its in-plane heat dissipation characteristics are bounded from below by the design basis BWR fuel

conductivities used in the HI-STAR thermal analysis.

Temperature-dependent effective conductivities of PWR and BWR design basis fuel assemblies (most resistive SNF types) are shown in Figure 3.4.13. The finite-volume results are also compared to results reported from independent technical sources. From this comparison, it is readily apparent that FLUENT-based fuel assembly conductivities are conservative. The FLUENT computed values (not the published literature data) are used in the MPC thermal analysis presented in this document.

#### 3.4.1.1.3 Effective Thermal Conductivity of Sheathing/Neutron Absorber/Cell Wall Sandwich

Each MPC basket cell wall (except outer periphery MPC-68 & MPC-32 cell walls) is manufactured with a neutron absorbing plate for criticality control. Each neutron absorbing plate is sandwiched in a sheathing-to-basket wall pocket. A schematic of the “Box Wall-Neutron Absorber-Sheathing” sandwich geometry of an MPC basket is illustrated in Figure 3.4.5. During fabrication, a uniformly applied normal pressure on each sheathing-Neutron Absorber-cell wall sandwich prior to stitch welding of the sheathing periphery to the box wall ensures adequate surface-to-surface contact for elimination of any macroscopic gaps. The mean coefficient of linear expansion of neutron absorber is higher than the basket materials thermal expansion coefficients. Consequently, basket heat-up from the contained SNF will further ensure a tight fit of the neutron absorber plate in the sheathing-to-cell wall pocket. The presence of small microscopic gaps due to less than perfect surface finish characteristics requires consideration of an interfacial contact resistance between the neutron absorber and the box and sheathing surfaces. A conservative contact resistance resulting from a 2 mils neutron absorber-to-pocket gap is applied to the analysis. Note that this gap would actually be filled with helium. In other words, no credit is taken for the interfacial pressure between neutron absorber and stainless plate/sheet stock produced by the fixturing and welding process.

Heat conduction properties of a composite “Box Wall-Neutron Absorber-Sheathing” sandwich in the two principal basket cross sectional directions as illustrated in Figure 3.4.5 (i.e., lateral “out-of-plane” and longitudinal “in-plane”) are unequal. In the lateral direction, heat is transported across layers of sheathing, helium-gap, neutron absorber, helium-gap, and cell wall resistances that are in series (except for the small helium filled end regions shown in Figure 3.4.6). Heat conduction in the longitudinal direction, in contrast, is through an array of essentially parallel resistances comprised of these same layers. For the ANSYS based MPC basket thermal model, corresponding non-isotropic effective thermal conductivities in the two orthogonal directions are determined and applied in the analysis.

The non-isotropic conductivities are determined by constructing ANSYS models of the composite “Box Wall-Neutron Absorber-Sheathing” sandwich for the “in-plane” and “out-of-plane” directions. For determining the effective conductivity ( $K_{eff}$ ), a heat flux is applied to one end of the sandwich and an ANSYS numerical solution to the sandwich temperature differential obtained. From Fourier equation for one-dimensional conduction heat transfer, the following equation for  $K_{eff}$  is obtained:

$$K_{eff} = \frac{qL}{\Delta T}$$



where:

$q$  = Sandwich heat flux

$L$  = Sandwich length in the direction of heat transfer

$\Delta T$  = Sandwich temperature differential (obtained from ANSYS solution)

In the equation above,  $L$  is the width or thickness of the sandwich, respectively, for in-plane or out-of-plane heat transfer directions.

#### 3.4.1.1.4 Modeling of Basket Conductive Heat Transport

Conduction of heat in a fuel basket is a combination of planar and axial contributions. These component contributions are individually calculated for each MPC basket design and combined (as described later in this subsection) to obtain an equivalent isotropic thermal conductivity. The heat rejection capability of each MPC design (i.e., MPC-24, MPC-24E, MPC-32 and MPC-68) is evaluated by developing a thermal model of the combined fuel assemblies and composite basket walls geometry on the ANSYS finite element code. The ANSYS model includes a geometric layout of the basket structure in which the “Box Wall-Neutron Absorber-Sheathing” sandwich is replaced by a “homogeneous wall” with an equivalent thermal conductivity. Since the thermal conductivity of the Alloy X material is a weakly varying function of temperature, the equivalent “homogeneous wall” must have a temperature-dependent effective conductivity. Similarly, as illustrated in Figure 3.4.6, the conductivities in the in-plane and through-thickness direction of the equivalent “homogeneous wall” are different. Finally, as discussed earlier, the fuel assemblies occupying the basket cell openings are modeled as homogeneous heat generating regions with effective temperature dependent in-plane conductivities. The methodology used to reduce the heterogeneous MPC basket - fuel assemblage to an equivalent homogeneous region with effective thermal properties is discussed in the following.

Consider a cylinder of height  $L$  and radius  $r_o$  with a uniform volumetric heat source term  $q_g$ , with insulated top and bottom faces and its cylindrical boundary maintained at a uniform temperature  $T_c$ . The maximum centerline temperature ( $T_h$ ) to boundary temperature difference is readily obtained from classical one-dimensional conduction relationships (for the case of a conducting region with constant thermal conductivity  $K_s$ ):

$$(T_h - T_c) = q_g r_o^2 / (4 K_s)$$

Noting that the total heat generated in the cylinder ( $Q_t$ ) is  $\pi r_o^2 L q_g$ , the above temperature rise formula can be reduced to the following simplified form in terms of the total heat generation per unit length ( $Q_t/L$ ):

$$(T_h - T_c) = (Q_t / L) / (4 \pi K_s)$$

This simple analytical approach is employed to determine an effective basket cross-sectional conductivity by applying an equivalence between the ANSYS finite element model of the basket and the analytical case. The equivalence principle employed in the HI-STAR System thermal analysis is depicted in Figure 3.4.2. The 2-dimensional ANSYS finite element model of the MPC basket is

solved by applying a uniform heat generation per unit length in each basket cell region and a constant basket periphery boundary temperature,  $T_c'$ . Noting that the basket region with uniformly distributed heat sources and a constant boundary temperature is equivalent to the analytical case of a cylinder with uniform volumetric heat source discussed earlier, an effective MPC basket conductivity ( $K_{eff}$ ) is readily derived from the analytical formula and the ANSYS solution leading to the following relationship:

$$K_{eff} = N (Q_f'/L) / (4 \pi [T_h' - T_c'])$$

where:

$N$  = number of fuel assemblies

$(Q_f'/L)$  = each fuel assembly heat generation per unit length applied in ANSYS model

$T_h'$  = peak basket cross-section temperature from ANSYS model

Cross sectional views of MPC basket ANSYS models are illustrated in Figures 3.4.10 and 3.4.11 for a PWR and BWR MPC. Notice that many of the basket supports and all shims have been conservatively neglected in the models. This conservative geometry simplification, coupled with the conservative neglect of thermal expansion which would minimize the gaps, yields conservative gap thermal resistances. Temperature dependent equivalent thermal conductivities of the fuel region and composite basket walls, as determined from analysis procedures described earlier, are applied to the ANSYS model. The planar ANSYS conduction model is solved by applying a constant basket periphery temperature with uniform heat generation in the fuel region. Table 3.4.6 summarizes effective thermal conductivity results of each basket design obtained from the ANSYS models. It is recalled that the equivalent thermal conductivity values presented in Table 3.4.6 are lower bound values because, among other elements of conservatism, the effective conductivity of the most resistive SNF type (Tables 3.4.4 and 3.4.5) is used in the MPC finite-element simulations.

The axial conductivity of a fuel basket is determined by calculating a cross-sectional area-weighted sum of the component conductivities (Helium, Alloy-X, neutron absorber and fuel cladding). In accordance with NUREG-1536 guidelines, credit for fuel rod axial heat conduction is conservatively limited to cladding.

Having obtained planar and axial thermal conductivities as described above, an equivalent isotropic conductivity (defined as the Square Root of the Mean Sum of Squares (SRMSS<sup>†</sup>)) is obtained as shown below:

$$k_{iso} = \sqrt{\frac{k_{rad}^2 + k_{ax}^2}{2}}$$

where:

$k_{iso}$  = equivalent isotropic thermal conductivity

<sup>†</sup> This formulation has been benchmarked for specific application to the MPC basket designs and confirmed to yield conservative results.

$k_{\text{rad}}$  = equivalent planar thermal conductivity  
 $k_{\text{ax}}$  = equivalent axial thermal conductivity

The equivalent isotropic conductivities are employed in the HI-STAR thermal modeling as discussed in Subsection 3.4.2.

#### 3.4.1.1.5 Heat Transfer in MPC Basket Peripheral Regions

Each of the MPC designs for storing PWR or BWR fuel are provided with relatively large helium filled regions formed between the relatively cooler MPC shell and hot basket peripheral panels. For a horizontally oriented cask under normal transport conditions, heat transfer in these helium-filled regions is similar to heat transfer in closed cavities under three cases listed below:

- i. differentially heated short vertical cavity
- ii. horizontal channel heated from below
- iii. horizontal channel heated from above

In a closed cavity (case i scenario), an exchange of hot and cold fluids occurs near the top and bottom ends of the cavity, resulting in a net transport of heat across the gap.

The case (ii) scenario is similar to the classical Rayleigh-Benard instability of a layer of fluid heated from below [3.4.6]. If the condition for onset of fluid motion is satisfied, then a multi-cellular natural convection pattern is formed. The flow pattern results in upward motion of heated fluid and downward motion of relatively cooler fluid from the top plate, resulting in a net transport of heat across the heated fluid channel.

The case (iii) is a special form of case (ii) with an inverted (stably stratified) temperature profile. No fluid motion is possible in this circumstance and heat transfer is thus limited to fluid (helium) conduction only.

The three possible cases of closed cavity natural convection are illustrated in Figure 3.4.3 for an MPC-68 basket geometry. Peripheral spaces labeled B and B' illustrate the case (i) scenario, the space labeled D illustrates the case (ii) scenario, and the space labeled D' illustrates the case (iii) scenario. The basket is oriented to conservatively maximize the number of peripheral spaces having *no* fluid motion. A small alteration in the basket orientation will result in a non-zero gravity component in the x-direction which will induce case (i) type fluid motion in the D' space. The rate of natural convection heat transfer is characterized by a Rayleigh number for the cavity defined as follows:

$$R_{aL} = \frac{C_p \rho^2 g \beta \Delta T L^3}{\mu K}$$

where:

$C_p$	=	fluid heat capacity
$\rho$	=	average fluid density
$g$	=	acceleration due to gravity
$\beta$	=	coefficient of thermal expansion (equal to reciprocal of absolute temperature for gases)
$\Delta T$	=	temperature difference between hot and cold surfaces
$L$	=	spacing between hot and cold surfaces
$\mu$	=	fluid viscosity
$K$	=	fluid conductivity

Hewitt et al. [3.4.5] report Nusselt number correlations for the closed cavity natural convection cases discussed earlier. A Nusselt number equal to unity implies heat transfer by fluid conduction only. A higher than unity Nusselt number is due to the so-called “Rayleigh” effect, which monotonically rises with increasing Rayleigh number. Nusselt numbers applicable to helium filled PWR and BWR MPCs in the peripheral voids are provided in Table 3.4.1. For conservatively maximizing HI-STAR normal transport temperatures, the heat dissipation enhancement due to Rayleigh effect is ignored.

#### 3.4.1.1.6 Effective Conductivity of Multi-Layered Intermediate Shell Region

Fabrication of the layered overpack intermediate shells is discussed in Section 1.2 of this SAR. In the thermal analysis, each intermediate shell metal-to-metal interface presents an additional resistance to heat transport. The contact resistance arises from microscopic pockets of air trapped between surface irregularities of the contacting surfaces. Since air is a relatively poor conductor of heat, this results in a reduction in the ability to transport heat across the interface compared to that of the base metal. Interfacial contact conductance depends upon three principal factors, namely: (i) base material conductivity, (ii) interfacial contact pressure, and (iii) surface finish.

Rohsenow and Hartnett [3.2.2] have reported results from experimental studies of contact conductance across air entrapped stainless steel surfaces with a typical 100  $\mu$ -inch surface finish. A minimum contact conductance of 350 Btu/ft-hr-°F is determined from extrapolation of results to zero contact pressure.

The thermal conductivity of carbon steel is about three times that of stainless steel. Thus the choice of carbon steel as the base material in a multi-layered construction significantly improves heat transport across interfaces. The fabrication process guarantees interfacial contact. Contact conductance values extrapolated to zero contact pressures are therefore conservative. The surface finish of hot-rolled carbon steel plate stock is generally in the range of 250-1000  $\mu$ -inch [3.2.1]. The

process of forming hot-rolled flat plate stock to cylindrical shapes to form the intermediate shells by rolling will result in a smoother surface finish. This results from the large surface pressures exerted by the hardened roller faces that flatten out any surface irregularities.

In the HI-STAR thermal analysis, a conservatively bounding interfacial contact conductance value is determined based on the following assumptions:

1. No credit is taken for high base metal conductivity.
2. No credit is taken for interfacial contact pressure.
3. No credit is taken for a smooth surface finish resulting from rolling of hot-rolled plate stock to cylindrical shapes.
4. Contact conductance is based on a uniform 2000  $\mu$ -inch (1000  $\mu$ -inch for each surface condition) interfacial air gap at all interfaces.
5. No credit for radiation heat exchange across this hypothetical inter-surface air gap.
6. Bounding low thermal conductivity at 200°F.

These assumptions guarantee a conservative assessment of heat dissipation characteristics of the multi-layered intermediate shell region. The resistances of the five carbon steel layers along with the associated interfacial resistances are combined as resistances in series to determine an effective conductivity of this region leading to the following relationship:

$$K_{gs} = r_o \ln \left[ \frac{r_5}{r_o} \right] \left[ \sum_{i=1}^5 \frac{\delta}{K_{air} r_i} + \frac{r_o \ln \left[ \frac{r_5}{r_o} \right]}{K_{cst}} \right]^{-1}$$

where (in conventional U.S. units):

$K_{gs}$	=	effective intermediate shell region thermal conductivity
$r_o$	=	inside radius of inner gamma shield layer
$r_i$	=	outer radius of $i^{th}$ intermediate shell layer
$\delta$	=	interfacial air gap (2000 $\mu$ -inch)
$K_{air}$	=	air thermal conductivity
$K_{cst}$	=	carbon steel thermal conductivity

#### 3.4.1.1.7 Heat Rejection from Overpack and Impact Limiter Outside Surfaces

Jakob and Hawkins [3.2.9] recommend the following correlations for natural convection heat transfer to air from heated vertical surfaces (flat impact limiter ends) and from single horizontal cylinders (overpack and impact limiter curved surfaces):

[PROPRIETARY INFORMATION WITHHELD PER 10CFR2.390]

[

PROPRIETARY INFORMATION WITHHELD PER 10CFR2.390

]

#### 3.4.1.1.8 Determination of Solar Heat Input

The intensity of solar radiation incident on an exposed surface depends on a number of time varying parameters. The solar heat flux strongly depends upon the time of the day as well as on latitude and day of the year. Also, the presence of clouds and other atmospheric conditions (dust, haze, etc.) can significantly attenuate solar intensity levels. Rapp [3.4.2] has discussed the influence of such factors in considerable detail.

The HI-STAR System thermal analysis is based upon insolation levels specified in 10CFR71, Subpart F, which are for a 12-hour daytime period. During normal transport conditions, the HI-STAR System is cyclically subjected to solar heating during the 12-hour daytime period followed by

cooling during the 12-hour nighttime. However, due to the large mass of metal and the size of the system, the inherent dynamic time lag in the temperature response is substantially larger than the 24-hour heating-cooling time period. Accordingly, the HI-STAR System cask model includes insolation at exposed surfaces averaged over a 24-hour time period. A bounding solar absorption coefficient of 1.0 is applied to cask exterior surfaces. The 10CFR71 mandated 12-hour average incident solar radiation levels are summarized in Table 3.4.7. The combined incident insolation heat flux absorbed by exposed cask surfaces and decay heat load from the MPC is rejected by natural convection and radiation to ambient air.

#### 3.4.1.1.9 Effective Thermal Conductivity of Radial Channels - Holtite Region

In order to minimize heat transfer resistance limitations due to the poor thermal conductivity of the Holtite-A neutron shield material, a large number of thick radial channels formed from high strength and conductivity carbon steel material are embedded in the neutron shield region. These radial channels form highly conductive heat transfer paths for efficient heat removal. Each channel is welded to the outside surface of the outermost intermediate shell and at the overpack enclosure shell, thereby providing a continuous path for heat removal to the ambient environment.

The effective thermal conductivity of the composite neutron shielding and radial channels region is determined by combining the heat transfer resistance of individual components in a parallel network. In determining the heat transfer capability of this region to the outside ambient environment for normal transport conditions, no credit is taken for conduction through the neutron shielding material. Thus, heat transport from the outer intermediate shell surface to the overpack outer shell is conservatively based on heat transfer through the carbon steel radial channel legs alone. Thermal conductivity of the parallel neutron shield and radial channel leg region is given by the following formula:

$$K_{ne} = \frac{K_R N_R t_R \ln \left[ \frac{r_B}{r_A} \right]}{2 \pi L_R} + \frac{K_{ns} N_R t_{ns} \ln \left[ \frac{r_B}{r_A} \right]}{2 \pi L_R}$$

where (in consistent U.S. units):

$K_{ne}$	=	effective thermal conductivity of neutron shield region
$r_A$	=	inner radius of neutron shielding
$r_B$	=	outer radius of neutron shielding
$K_R$	=	effective thermal conductivity of carbon steel radial channel leg
$N_R$	=	total number of radial channel legs (also equal number of neutron shield sections)
$t_R$	=	minimum (nominal) thickness of each radial channel leg
$L_R$	=	effective radial heat transport length through radial channel leg
$K_{ns}$	=	neutron shield thermal conductivity
$t_{ns}$	=	neutron shield circumferential thickness (between two radial channel legs)

The radial channel leg to outer intermediate shell surface weld thickness is **less than** the plate |

thickness. The additional weld resistance is accounted for by reducing the plate thickness in the weld region for a short radial span equal to the weld size. Conductivity of the radial carbon steel channel legs based on the full thickness for the entire radial span is correspondingly reduced. Figure 3.4.4 depicts a resistance network developed to combine the neutron shield and radial channel legs resistances to determine an effective conductivity of the neutron shield region. Note that in the resistance network analogy only the annulus region between overpack outer enclosure inner surface and intermediate shells outer surface is considered in this analysis. The effective thermal conductivity of neutron shield region is provided in Table 3.4.8.

#### 3.4.1.1.10 Effective Thermal Conductivity of the Eccentric MPC to Overpack Gap

During horizontal shipment of the HI-STAR System under normal transport conditions, the MPC will rest on the inside surface of the overpack. In the region of line contact, the resistance to heat transfer across the gap will be negligibly small due to a vanishingly small gap thickness. The resistance to heat transfer at other regions along the periphery of the MPC will, however, increase in direct proportion to the thickness of the local gap. This variation in gap thickness can be accounted for in the thermal model by developing a relation for the total heat transferred across the gap as given below:

$$Q_E = 2 \int_0^\pi \frac{K_{He}}{g(\theta)} L R_o \Delta T d\theta$$

where:

$Q_E$	=	total heat transfer across the gap (Btu/hr)
$K_{He}$	=	helium conductivity Btu/ft-hr-°F
$L$	=	length of MPC (ft.)
$R_o$	=	MPC radius (ft.)
$\theta$	=	angle from point of line contact
$g(\theta)$	=	variation of gap thickness with angle (ft.)
$\Delta T$	=	temperature difference across the gap (°F)

A corresponding relationship for heat transferred across a uniform gap is given by:

$$Q_c = \frac{K_{eff}}{(R_I - R_o)} 2\pi R_o L \Delta T$$

where  $R_I$  is the inside radius of the overpack and  $K_{eff}$  is the effective thermal conductivity of an equivalent concentric MPC/overpack gap configuration. From these two relationships, the ratio of effective gap conductivity to helium thermal conductivity in the MPC/overpack region is shown below:

$$\frac{K_{eff}}{K_{He}} = \frac{R_I - R_o}{\pi} \int_0^\pi \frac{1}{g(\theta)} d\theta$$

Based on an analysis of the geometry of a thin gap between two eccentrically positioned cylinders, the following relationship is developed for variation of the gap thickness with position:



$$g(\theta) = (R_I - R_0)(1 - \cos \theta) + \varepsilon \cos \theta$$

The above equation conservatively accounts for imperfect contact by postulating a minimum gap  $\varepsilon$  at the point where the two surfaces would ideally form a line of perfect contact. The relatively thin MPC shell is far more flexible than the much thicker overpack inner shell, and will ovalize to yield greater than line contact. The substantial weight of the fuel basket and contained fuel assemblies will also cause the MPC shell to conform to the overpack inner shell. An evaluation based on contact along a line would therefore be reasonable and conservative. However, a minimum gap is assumed to further increase conservatism in this calculation.

Based on an applied gap of 0.02-inch, which is conservative compared to contact along a line, the effective gap thermal conductivity determined from analytical integration [3.4.7] is in excess of 200% of the conductivity of helium gas. In the HI-STAR analysis, a conservative effective gap conductivity equal to twice the helium gas conductivity is applied to the performance evaluation.

#### 3.4.1.1.11 Effective Thermal Conductivity of MPC Basket-to-Shell Aluminum Heat Conduction Elements

The HI-STAR MPCs feature an option to install full-length heat conduction elements fabricated from aluminum alloy 1100 in the large MPC basket-to-shell gaps. Due to the high aluminum alloy 1100 thermal conductivity (about 15 times that of Alloy X), a significant rate of net heat transfer is possible along the thin plates. For conservatism, heat dissipation by the Aluminum Heat Conduction Elements (AHCEs) is ignored in normal transport analyses. This overstates the initial fuel temperature for hypothetical fire accident evaluation. To conservatively compute heating of MPC contents in a hypothetical fire condition, the presence of heat conduction elements in AHCE equipped MPCs is duly recognized.

Figure 3.4.12 shows a mathematical idealization of a heat conduction element inserted between basket periphery panels and the MPC shell. The aluminum insert is shown to cover the MPC basket Alloy X peripheral panel and MPC shell surfaces (Regions I and III depicted in Figure 3.4.12) along the full-length of the basket. Heat transport to and from the aluminum insert is conservatively postulated to occur across a thin helium gap as shown in the figure (i.e., no credit is considered for aluminum insert to Alloy X metal-to-metal contact). Aluminum surfaces inside the hollow region are sandblasted prior to fabrication to result in a rough surface finish which has a significantly higher emissivity compared to smooth surfaces of rolled aluminum. The untreated aluminum surfaces directly facing Alloy X panels have a smooth finish to minimize contact resistance.

Net heat transfer resistance from the hot basket periphery panel to the relatively cooler MPC shell along the aluminum heat conduction element pathway is a sum of three individual resistances in regions labeled I, II, and III. In Region I, heat is transported from the basket to the aluminum insert surface directly facing the basket panel across a thin helium resistance gap. Longitudinal transport of heat (in the  $z$  direction) in the aluminum plate (in Region I) will result in an axially non-uniform temperature distribution. Longitudinal one-dimensional heat transfer in the Region I aluminum plate is analytically formulated to result in the following ordinary differential equation for the non-uniform

temperature distribution:

$$t K_{Al} \frac{\partial^2 T}{\partial z^2} = - \frac{K_{He}}{h} (T_h - T) \quad (\text{Equation a})$$

### Boundary Conditions

$$\begin{aligned} \frac{\partial T}{\partial z} &= 0 \text{ at } z = 0 \\ T &= T_h' \text{ at } z = P \end{aligned} \quad (\text{Equation b})$$

where (see Figure 3.4.12):

$T(z)$	=	non-uniform aluminum metal temperature distribution
$t$	=	conduction element thickness
$K_{Al}$	=	conduction element conductivity
$K_{He}$	=	helium conductivity
$h$	=	helium gap thickness
$T_h$	=	hot basket temperature
$T_h'$	=	conduction element Region I boundary temperature at $z = P$
$P$	=	conduction element Region I length

Solution of this ordinary differential equation subject to the imposed boundary condition is:

$$(T_h - T) = (T_h - T_h') \left[ \frac{e^{\frac{z}{\sqrt{\alpha}}} + e^{-\frac{z}{\sqrt{\alpha}}}}{e^{\frac{P}{\sqrt{\alpha}}} + e^{-\frac{P}{\sqrt{\alpha}}}} \right] \quad (\text{Equation c})$$

where  $\alpha$  is a dimensional parameter equal to  $htK_{Al}/K_{He}$ . The net heat transfer ( $Q_I$ ) across the Region I helium gap can be determined by the following integrated heat flux to a conduction element of length  $L$  as:

$$Q_I = \int_0^P \frac{K_{He}}{h} (T_h - T) (L) dz \quad (\text{Equation d})$$

Substituting the analytical temperature distribution result obtained in Equation c into Equation d and

then integrating, the following expression for net heat transfer is obtained:

$$Q_I = \frac{K_{He} L \sqrt{\alpha}}{h} \left( 1 - \frac{1}{e^{\frac{P}{\sqrt{\alpha}}} + e^{-\frac{P}{\sqrt{\alpha}}}} \right) (T_h - T_h') \quad (\text{Equation e})$$

Based on this result, an expression for Region I resistance is obtained as shown below:

$$R_I = \frac{T_h - T_h'}{Q_I} = \frac{h}{K_{He} L \sqrt{\alpha}} \left( 1 - \frac{1}{e^{\frac{P}{\sqrt{\alpha}}} + e^{-\frac{P}{\sqrt{\alpha}}}} \right)^{-1} \quad (\text{Equation f})$$

Similarly, a Region III resistance expression can be analytically determined as shown below:

$$R_{III} = \frac{(T_c' - T_c)}{Q_{III}} = \frac{h}{K_{He} L \sqrt{\alpha}} \left( 1 - \frac{1}{e^{\frac{P}{\sqrt{\alpha}}} + e^{-\frac{P}{\sqrt{\alpha}}}} \right)^{-1} \quad (\text{Equation g})$$

A Region II resistance expression can be developed from the following net heat transfer equation in the vertical leg of the conduction element as shown below:

$$Q_{II} = \frac{K_{Al} L t}{W} (T_h' - T_c') \quad (\text{Equation h})$$

Hence,

$$R_{II} = \frac{T_h' - T_c'}{Q_{II}} = \frac{W}{K_{Al} L t} \quad (\text{Equation i})$$

This completes the analysis for the total thermal resistance attributable to the heat conduction elements equal to sum of the three individual resistances. The total resistance is smeared across the basket-to-MPC shell region as an effective uniform annular gap conductivity (see Figure 3.4.2). Note that heat transport along the conduction elements is an independent conduction path in parallel with conduction and radiation mechanisms in the large helium gaps. Helium conduction and radiation between the MPC basket and the MPC shell is accounted for separately in the ANSYS MPC models described earlier in this section. Therefore, the total MPC basket-to-MPC shell peripheral gaps conductivity will be the sum of the conduction elements effective conductivity and the helium conduction-radiation gap effective conductivity.

#### 3.4.1.1.12 FLUENT Model for HI-STAR Temperature Field Computation

In the preceding subsections, the series of analytical and numerical models to define the thermal characteristics of the various elements of the HI-STAR System are presented. The thermal modeling begins with the replacement of the SNF cross section and surrounding fuel cell space by a solid lamina with an equivalent conductivity. Since radiation is an important constituent of the heat transfer process in the SNF/storage cell space and the rate of radiation heat transfer is a strong function of the surface temperatures, it is necessary to treat the equivalent lamina conductivity as a function of temperature. In fact, because of the relatively large range of temperatures which will exist in a loaded HI-STAR System under the design basis heat loads, it is necessary to include the effect of variation in the thermal conductivity of materials with temperature throughout the system finite volume model. The presence of significant radiation effect in the storage cell spaces adds to the imperative to treat the equivalent lamina conductivity as temperature-dependent.

FLUENT finite volume simulations have been performed to establish the equivalent thermal conductivity as a function of temperature for the limiting (thermally most resistive) BWR and PWR spent fuel types. By utilizing the most limiting SNF (established through a simplified analytical process for comparing conductivities) the numerical idealization for the fuel space conductivity is ensured to be conservative for all non-limiting fuel types.

Having replaced the interior of the cell spaces by solid prismatic (square) columns possessing a temperature-dependent conductivity essentially renders the basket into a non-homogeneous three-dimensional solid where the non-homogeneity is introduced by the honeycomb basket structure. The basket panels themselves are a composite of Alloy X cell wall, neutron absorber, and Alloy X sheathing metal. A conservative approach to replace this composite section with an equivalent “solid wall” is described in a preceding subsection.

In the next step, a planar section of the MPC is considered. The MPC, externally radially symmetric, contains a non-symmetric basket lamina wherein the equivalent fuel space solid squares are separated by the “equivalent” solid metal walls. The space between the basket and the MPC, called the peripheral gap, is filled with helium gas and optionally aluminum heat conduction elements. The equivalent thermal conductivity of this MPC section is computed using a finite element procedure on ANSYS, as described previously. For hypothetical fire conditions the “helium-conduction-radiation” based peripheral gap conductivity and the effective conductivity of aluminum conduction elements are added to obtain a combined effective conductivity. At this stage in the thermal analysis, the SNF/basket/MPC assemblage has been replaced with a two-zone (Figure 3.4.2) cylindrical solid whose thermal conductivity is a strong function of temperature.

The idealization for the overpack is considerably more straightforward. The overpack is radially symmetric except for the Holtite region (discussed in Subsection 3.4.1.1.9). The procedure to replace the multiple shell layers, Holtite-A and radial connectors with an equivalent solid utilizes classical heat conduction analogies, as described in the preceding subsections.

In the final step of the analysis, the equivalent two-zone MPC cylinder, the equivalent overpack

shell, the top and bottom plates, and the impact limiters are assembled into a comprehensive finite volume model. A cross section of this axisymmetric model implemented on FLUENT is shown in Figure 3.4.14. A summary of the essential features of this model is presented in the following:

- The overpack shell is represented by  $840 \times 9$  elements. The effective thermal conductivity of the overpack shell elements is set down as a function of temperature based on the analyses described earlier.
- The overpack bottom plate and bolted closure plate are modeled by  $312 \times 9$  axisymmetric elements.
- The two-zone MPC “solid” is represented by  $1,144 \times 9$  axisymmetric elements.
- The space between the MPC “solid” and the overpack interior space is assumed to contain helium.
- Heat input due to insolation is applied to the impact limiter surfaces and the cylindrical surface of the overpack.
- The heat generation in the MPC solid basket region is assumed to be uniform in each horizontal plane, but to vary in the axial direction to correspond to the axial burnup distribution in the active fuel region postulated in Chapter 1.

The finite volume model constructed in this manner will produce an axisymmetric temperature distribution. The peak temperature will occur near the centerline and is expected to correspond to the axial location of peak heat generation. As is shown later, the results from the finite element solution bear out these observations.

#### 3.4.1.1.13 Effect of Fuel Cladding Crud Resistance

In this subsection, a conservatively bounding estimate of the temperature drop across a crud film adhering to a fuel rod during dry storage conditions is determined. The evaluation is performed for a BWR fuel assembly based on an upper bound crud thickness obtained from PNL-4835 report ([3.3.5], Table 3). The crud present on fuel assemblies is predominantly iron oxide mixed, with small quantities of other metals such as cobalt, nickel, chromium, etc. Consequently, the effective conductivity of the crud mixture is expected to be in the range of typical metal alloys. Metals have thermal conductivities several orders of magnitude larger than that of helium. In the interest of extreme conservatism, however, a film of helium with the same thickness replaces the crud layer. The calculation is performed in two steps. In the first step, a crud film resistance is determined based on bounding maximum crud layer thickness replaced as a helium film on the fuel rod surfaces. This is followed by a peak local cladding heat flux calculation for the smaller GE  $7 \times 7$  fuel assembly postulated to emit a conservatively bounding decay heat equal to 0.5kW. The temperature drop across the crud film obtained as a product of the heat flux and crud resistance terms is determined to be less than  $0.1^\circ\text{F}$ . The calculations are presented below:

Bounding Crud Thickness ( $\delta$ ) = 130 $\mu$ m ( $4.26 \times 10^{-4}$  ft)  
(PNL-4835)

Crud Conductivity (K) = 0.1 Btu/ft-hr-°F (conservatively assumed as helium)

GE 7×7 Fuel Assembly:

Rod O.D.	=	0.563"
Active Fuel Length	=	150"
Heat Transfer Area	=	$(7 \times 7) (\pi \times 0.563) \times 150 / 144$
	=	90.3 ft <sup>2</sup>
Axial Peaking Factor	=	1.195 (Burnup distribution Table 1.2.15)
Decay Heat	=	500W (conservative assumption)

$$\text{Crud Resistance} = \frac{\delta}{K} = \frac{4.26 \times 10^{-4}}{0.1} = 4.26 \times 10^{-3} \frac{\text{ft}^2 \cdot \text{hr} \cdot ^\circ\text{F}}{\text{Btu}}$$

$$\begin{aligned} \text{Peak Heat Flux} &= \frac{(500 \times 3.417) \text{ Btu/hr}}{90.3 \text{ ft}^2} \times 1.195 \\ &= 18.92 \times 1.195 = 22.6 \frac{\text{Btu}}{\text{ft}^2 \cdot \text{hr}} \end{aligned}$$

Temperature drop ( $\Delta T_c$ ) across crud film:

$$\begin{aligned} &= 4.26 \times 10^{-3} \frac{\text{ft}^2 \cdot \text{hr} \cdot ^\circ\text{F}}{\text{Btu}} \times 22.6 \frac{\text{Btu}}{\text{ft}^2 \cdot \text{hr}} \\ &= 0.096^\circ\text{F} \\ &\text{(i.e., less than } 0.1^\circ\text{F)} \end{aligned}$$

Therefore, it is concluded that deposition of crud does not materially change the SNF cladding temperature.

#### 3.4.1.1.14 Maximum Time Limit During Wet Transfer

While loading an empty HI-STAR System for transport directly from a spent fuel pool, water inside the MPC cavity is not permitted to boil. Consequently, uncontrolled pressures in the de-watering, purging, and recharging system that may result from two-phase condition are completely avoided. This requirement is accomplished by imposing a limit on the maximum allowable time duration for fuel to be submerged in water after a loaded HI-STAR cask is removed from the pool and prior to the start of vacuum drying operations.

When the HI-STAR overpack and the loaded MPC under water-flooded conditions are removed from the pool, the combined mass of the water, the fuel, the MPC, and the overpack will absorb the decay heat emitted by the fuel assemblies. This results in a slow temperature rise of the entire system

with time, starting from an initial temperature of the contents. The rate of temperature rise is limited by the thermal inertia of the HI-STAR system. To enable a bounding heat-up rate determination for the HI-STAR system, the following conservative assumptions are imposed:

- i. Heat loss by natural convection and radiation from the exposed HI-STAR surfaces to the pool building ambient air is neglected (i.e., an adiabatic temperature rise calculation is performed).
- ii. Design Basis maximum decay heat input from the loaded fuel assemblies is imposed on the HI-STAR system.
- iii. The smallest of the *minimum* MPC cavity-free volumes between the two MPC types is considered for flooded water mass determination.
- iv. Fifty percent of the water mass in the MPC cavity is credited towards water thermal inertia evaluation.

Table 3.4.19 summarizes the weights and thermal inertias of several components in the loaded HI-STAR system. The rate of temperature rise of the HI-STAR and its contents during an adiabatic heat-up is governed by the following equation:

$$\frac{dT}{d\tau} = \frac{Q}{C_h}$$

where:

Q = decay heat load (Btu/hr) [equal to Design Basis maximum (between the two MPC types) 20.0 kW (i.e., 68,260 Btu/hr)]

C<sub>h</sub> = combined thermal inertia of the loaded HI-STAR system (Btu/°F)

T = temperature of the contents (°F)

τ = time after HI-STAR system is removed from the pool (hr)

A bounding heat-up rate for the HI-STAR system contents is determined to be equal to 2.19°F/hr. From this adiabatic rate of temperature rise estimate, the maximum allowable time duration (t<sub>max</sub>) for fuel to be submerged in water is determined as follows:

$$t_{\max} = \frac{T_{\text{boil}} - T_{\text{initial}}}{dT/d\tau}$$

where:

T<sub>boil</sub> = boiling temperature of water (equal to 212°F at the water surface in the MPC cavity)

$T_{\text{initial}}$  = initial temperature of the HI-STAR contents when removed from the pool

Table 3.4.20 provides a summary of  $t_{\text{max}}$  at several initial HI-STAR contents temperatures.

As set forth in Section 7.4, in the unlikely event where the maximum allowable time provided in Table 3.4.20 is found to be insufficient to complete all wet transfer operations, a forced water circulation shall be initiated and maintained to remove the decay heat from the MPC cavity. In this case, relatively cooler water will enter via the MPC lid drain port connection and heated water will exit from the vent port. The minimum water flow rate required to maintain the MPC cavity water temperature below boiling with an adequate subcooling margin is determined as follows:

$$M_w = \frac{Q}{C_{pw}(T_{\text{max}} - T_{\text{in}})}$$

where:

$M_w$  = minimum water flow rate (lb/hr)

$C_{pw}$  = water heat capacity (Btu/lb-°F)

$T_{\text{max}}$  = maximum MPC cavity water mass temperature

$T_{\text{in}}$  = temperature of water supply to MPC

With the MPC cavity water temperature limited to 150°F, MPC inlet water maximum temperature equal to 125°F and at the design basis maximum heat load, the water flow rate is determined to be 2,731 lb/hr (5.5 gpm).

#### 3.4.1.1.15 Cask Cooldown and Reflood Analysis During Fuel Unloading Operation

Before a loaded HI-STAR System can be unloaded (i.e., fuel removed from the MPC) the cask must be cooled from the operating temperatures and reflooded with water<sup>†</sup>. Past industry experience generally supports cooldown of cask internals and fuel from hot storage conditions by direct water quenching. However, the extremely rapid cooldown rates that are typical during water injection, to which the hot cask internals and fuel cladding are subjected to, may result in uncontrolled thermal stresses and failure in the structural members. Moreover, water injection results in large amounts of steam generation and unpredictable transient two-phase flow conditions inside the MPC cavity, which may result in over-pressurization of the MPC helium retention boundary and a potentially unacceptable reduction in the safety margins to prevent criticality. To avoid potential safety concerns related to rapid cask cooldown by direct water quenching, the HI-STAR MPCs are designed to be cooled in a gradual manner, thereby eliminating thermal shock loads on the cask internals and fuel cladding.

<sup>†</sup> Certain fuel configurations in PWR MPCs require Borated water for criticality control (Chapter 6). Such MPCs are reflooded with Borated water.



In the unlikely event that a HI-STAR system is required to be unloaded, it will be transported back to the fuel handling building. Prior to reflooding the MPC cavity with water, a forced flow helium recirculation system with adequate flow capacity shall be operated to remove the decay heat and initiate a slow cask cooldown lasting for several days. The operating procedures in Section 7.2 provide a detailed description of the steps involved in the cask unloading. In this section, an analytical evaluation is presented to provide the basis for helium flow rates and time of forced cooling to meet the objective of eliminating thermal shock when the MPC cavity is eventually flooded with water.

Under a closed loop forced helium circulation condition, the helium gas is cooled via an external chiller, down to 100°F, and then introduced inside the MPC cavity from the drain line near the bottom baseplate. The helium gas enters the MPC basket from the bottom oversized flow holes and moves upward through the hot fuel assemblies, removing heat and cooling the MPC internals. The heated helium gas exits from the basket top and collects in the top plenum, from where it is expelled through the MPC lid vent connection to the helium recirculation and cooling system. The bulk average temperature reduction of the MPC contents as a function of time is principally dependent upon the rate of helium circulation. The temperature transient is governed by the following heat balance equation:

$$C_h \frac{dT}{d\tau} = Q_D - m C_p (T - T_i) - Q_c$$

Initial Condition:  $T = T_0$  at  $\tau = 0$

where:

$T =$  MPC bulk average temperature (°F)

$T_0 =$  initial MPC bulk average temperature in the HI-STAR system  
(483°F<sup>†</sup>)

$\tau =$  time after start of forced circulation (hr)

$Q_D =$  decay heat load (Btu/hr)  
(equal to Design Basis maximum 20.0 kW (i.e., 68,260 Btu/hr))

$m =$  helium circulation rate (lb/hr)

$C_p =$  helium heat capacity (Btu/lb-°F)  
(equal to 1.24 Btu/lb-°F)

$Q_c =$  heat rejection from cask exposed surfaces to ambient (Btu/hr)  
(conservatively neglected)

---

<sup>†</sup> Bounding for HI-STAR normal transport.

$C_h$  = thermal capacity of the loaded MPC (Btu/°F)  
 (For a bounding upper bound 100,000 lb loaded MPC weight, and heat capacity of Alloy X equal to 0.12 Btu/lb-°F, the heat capacity is equal to 12,000 Btu/°F)

$T_i$  = MPC helium inlet temperature (°F)

The differential equation is analytically solved, yielding the following expression for time-dependent MPC bulk temperature:

$$T(t) = \left( T_i + \frac{Q_D}{m C_p} \right) \left( 1 - e^{-\frac{m C_p t}{C_h}} \right) + T_o e^{-\frac{m C_p t}{C_h}}$$

This equation is used to determine the minimum helium mass flow rate that would cool the MPC cavity down from initially hot conditions to less than 200°F. For example, to cool the MPC to less than 200°F in 72 hours would required a helium mass flow rate of 574 lb/hr (i.e., 859 SCFM).

Once the helium gas circulation has cooled the MPC internals to less than 200°F, water can be injected to the MPC without risk of boiling and the associated thermal stress concerns. Because of the relatively long cooldown period, the thermal stress contribution to the total cladding stress would be negligible, and the total stress would therefore be bounded by the normal (dry) condition. The elimination of boiling eliminates any concern of over-pressurization due to steam production.

#### 3.4.1.1.16 MPC Evaluation Under Drying Conditions

The initial loading of SNF in the MPC requires that the water within the MPC be drained, residual moisture removed and MPC filled with helium. This operation on the HI-STAR MPCs will be carried out using a Forced Helium Dehydrator (FHD) for a “load-and-go” operation. A “load-and-go” operation is defined as an activity wherein an MPC is loaded for direct off-site shipment in a HI-STAR transport cask. MPCs prepared via other competent methods for MPC drying as approved by the NRC on other dockets (1008 and 1014) are duly recognized for transport under this docket.

To reduce moisture to trace levels in the MPC using a Forced Helium Dehydration (FHD) system, a closed loop system consisting of a condenser, a demister, a compressor, and a pre-heater is utilized to extract moisture from the MPC cavity through repeated displacement of its contained helium, accompanied by vigorous flow turbulence. Appendix 3.B contains detailed discussion of the design and operation criteria for the FHD system.

The FHD system provides concurrent fuel cooling during the moisture removal process through forced convective heat transfer. The attendant forced convection-aided heat transfer occurring during operation of the FHD system ensures that the fuel cladding temperature will remain below the applicable peak cladding temperature limit for normal conditions of transport (752°F) for all combinations of SNF type, burnup, decay heat, and cooling time. Because the FHD operation induces a state of forced convection heat transfer in the MPC, (in contrast to the quiescent mode of

natural convection in transport), it is readily concluded that the peak fuel cladding temperature under the latter condition will be greater than that during the FHD operation phase. In the event that the FHD system malfunctions, the forced convection state will degenerate to natural convection, which corresponds to the conditions of normal transport. As a result, the peak fuel cladding temperatures will approximate the values reached during normal transport as described elsewhere in this chapter.

#### 3.4.1.1.17 Effects of Helium Dilution from Fuel Rod Gases

In this subsection, the generic cask transportation accident issue raised in a USNRC Spent Fuel Project Office (SFPO) staff guidance letter<sup>†</sup> is addressed. This issue directs cask designers to evaluate the impact of fission gas release into the canister, from a 100% fuel rods rupture accident, on the cask component temperatures and pressures when the MNOP<sup>††</sup> is within 10% of the design pressure. To determine whether the HI-STAR System falls within the stipulated criteria, the MNOP results from Table 3.4.15 are examined. As shown in Table 3.4.15, the MNOPs are below the 90% threshold and an evaluation of the effect of fill gas dilution from fuel rod ruptures is not required.

#### 3.4.1.1.18 HI-STAR Temperature Field With Low Heat Emitting Fuel

The HI-STAR 100 thermal evaluations for BWR fuel are divided in two groups of fuel assemblies proposed for storage in MPC-68. These groups are classified as Low Heat Emitting (LHE) fuel assemblies and Design Basis (DB) fuel assemblies. The LHE group of fuel assemblies are characterized by low burnup, long cooling time, and short active fuel lengths. Consequently, their heat loads are dwarfed by the DB group of fuel assemblies. The Dresden-1 (6x6 and 8x8), QUAD+, and Humboldt Bay (7x7 and 6x6) fuel characteristics warrant their classification as LHE fuel. These characteristics, including burnup and cooling time limits imposed on this class of fuel, are presented in Table 1.2.23. This fuel (except Quad+) is permitted to be loaded when encased in Damaged Fuel Containers (DFCs). As a result of interruption of radiation heat exchange between the fuel assembly and the fuel basket by the DFC boundary, this loading configuration is bounding for thermal evaluation. In Subsection 3.4.1.1.2, two canister designs for encasing LHE fuel are evaluated – a previously approved Holtec Design (Figure 1.2.10) and an existing canister in which some of the Dresden-1 fuel is currently stored (Transnuclear D-1 Canister). The most resistive fuel assembly determined by analytical evaluation is considered for thermal evaluation (see Table 3.4.5). The MPC-68 basket effective conductivity, loaded with the most resistive fuel assembly from the LHE group of fuel (encased in a canister) is provided in Table 3.4.6. To this basket, LHE fuel decay heat load, is applied and a HI-STAR 100 System temperature field obtained. The low heat load burden limits the initial peak cladding temperature to less than 579°F which is substantially below the cladding temperature limit (Table 3.3.1).

<sup>†</sup> SFPO Director's Interim Staff Guidance Letter(s), W.F. Kane, (Interim Staff-Guidance-7), October 8, 1998.

<sup>††</sup> MNOP is a regulatory term defined in NUREG-1617 as the maximum gauge pressure that would develop in the containment in a period of 1 year under the heat condition specified in 10 CFR 71.71(c)(1) in the absence of venting, external ancillary cooling or operational controls.

A thorium rod canister designed to hold a maximum of 20 fuel rods arrayed in a 5x4 configuration is currently stored at the Dresden-1 spent fuel pool. The fuel rods contain a mixture of enriched  $\text{UO}_2$  and Thorium Oxide in the fuel pellets. The fuel rods were originally constituted as part of an 8x8 fuel assembly and used in the second and third cycle of Dresden-1 operation. The maximum fuel burnup of these rods is quite low ( $\sim 13,100$  MWD/MTU). The thorium rod canister internal design is a honeycomb structure formed from 12 gage stainless steel plates. The rods are loaded in individual square cells and are isolated from each other by the cell walls. The few number of rods (18 per assembly) and very low burnup of fuel stored in these Dresden-1 canisters render them as miniscule sources of decay heat. The canister all-metal internal honeycomb construction serves as an additional means of heat dissipation in the fuel cell space. In accordance with preferential fuel loading requirements, low burnup fuel shall be loaded toward the basket periphery (i.e., away from the hot central core of the fuel basket). All these considerations provide ample assurance that these fuel rods will be stored in a benign thermal environment and therefore remain protected during transport.

#### 3.4.1.2 Test Model

A detailed analytical model for evaluating the thermal design of the HI-STAR System was developed using the FLUENT CFD code and the industry standard ANSYS modeling system as discussed in Subsection 3.4.1.1. Furthermore, the analysis incorporates many conservative assumptions in order to demonstrate compliance with specified temperature limits for operation with adequate margins. In view of these considerations, the HI-STAR thermal design complies with the thermal criteria set forth in the design basis for normal transport conditions. Additional experimental verification of the thermal design is therefore not required. Acceptance and periodic thermal testing for the HI-STAR System is discussed in Sections 8.1 and 8.2.

#### 3.4.2 Maximum Temperatures Under Normal Transport Conditions

Both MPC-basket designs developed for the HI-STAR System have been analyzed to determine temperature distributions under normal transport conditions. In the HI-STAR System thermal analysis models developed on FLUENT, the overpack impact limiters are included in the finite volume geometry. However, no credit is considered for the presence of heat conducting aluminum honeycomb material. In other words, heat transmission through the ends is conservatively neglected in the analysis. The thermal results are therefore bounding with respect to impact limiter design. The MPC baskets are considered to be loaded at design-basis maximum heat load with PWR or BWR fuel assemblies, as appropriate.

As discussed in Subsection 3.4.1.1.1, the thermal analysis is performed using a submodeling process where the results of an analysis on an individual component are incorporated into the analysis of a larger set of components. Specifically, the submodeling process yields directly computed fuel temperatures from which fuel basket temperatures are indirectly calculated. This modeling process differs from previous analytical approaches wherein the basket temperatures were evaluated first and then a basket-to-cladding temperature difference calculation by Wooten-Epstein or other means provided a basis for cladding temperatures. Subsection 3.4.1.1.2 describes the calculation of an effective fuel assembly thermal conductivity for an equivalent homogenous region. It is important to

note that the result of this analysis is a function for thermal conductivity versus temperature. This function for fuel thermal conductivity is then input to the fuel basket effective thermal conductivity calculation described in Subsection 3.4.1.1.4. This calculation uses a finite-element methodology, wherein each fuel cell region containing multiple finite-elements has temperature varying thermal conductivity properties. The resultant temperature varying fuel basket thermal conductivity computed by this basket-fuel composite model is then input to the fuel basket region of the FLUENT cask model.

Because the FLUENT cask model incorporates the results of the fuel basket submodel, which in turn incorporates the fuel assembly submodel, the peak temperature reported from the FLUENT model is the peak temperature in any component. In a dry storage cask, the hottest components are the fuel assemblies. It should be noted that, because the fuel assembly models described in Subsection 3.4.1.1.2 include the fuel pellets, the FLUENT calculated peak temperatures reported in Tables 3.4.10 and 3.4.11 are actually peak pellet centerline temperatures which bound the peak cladding temperatures. We conservatively assume that the peak clad temperature is equal to the peak pellet centerline temperature.

From a thermal/hydraulic standpoint, the HI-STAR transport cask must cover two scenarios:

- i. MPCs equipped with AHCEs
- ii. MPCs without AHCEs

In the thermal analysis submitted in support of HI-STAR's original transport certification, which we now refer to as the Baseline Thermal Model (BTM), the AHCEs are included in the thermal models and the basket thermal model is constructed in an exceedingly conservative manner. In particular, the axial conductance of the basket fuel assemblage is assumed to be equal to the in-plane conductance (in reality, the in-plane conductance is much smaller than the axial conductance due to the presence of physical gaps between the fuel and the cell and within the fuel assemblies). For the Scenario (ii) analysis, such an overarching conservatism is removed while certain other less sweeping conservatisms are retained. The revised model, which we refer to as the Refined Thermal Model (RTM), forms the licensing basis for thermal evaluation. The conservatisms germane to the RTM are summarized in Appendix 3.A. To summarize, the principal difference between the BTM and RTM are as follows:

<i>Item</i>	<i>Description</i>	<i>BTM Assumption</i>	<i>RTM Assumption</i>
1	AHCE heat dissipation	Included	Excluded
2	Rayleigh effect	Included	Excluded
3	Basket Axial Conductivity	Grossly Understated	Realistic modeling of axial conductivity (See discussion in Subsection 3.4.1.1.4)

For representative PWR (MPC-24) and BWR (MPC-68) MPC-basket configurations with AHCEs installed, the temperature contours obtained with the Baseline Thermal Model (BTM) corresponding to steady-state hot conditions (100°F ambient, maximum design basis maximum decay heat and full

insolation) are shown in Figures 3.4.16 and 3.4.17. Figures 3.4.19 and 3.4.20 show the axial temperature variation of the hottest fuel rod in the MPC-24 and MPC-68 basket designs, respectively. Figures 3.4.22 and 3.4.23 show the radial temperature profile in the MPC-24 and MPC-68 basket designs, respectively, in the horizontal plane where maximum fuel cladding temperature is indicated. Tables 3.4.10 and 3.4.11 summarize maximum calculated temperatures in different parts of the HI-STAR System at design-basis maximum decay heat loads. **The maximum basket periphery temperatures therein are actually conservative lower bound values, which are included as inputs for thermal stress evaluations in Chapter 2 where larger center-to-periphery temperature gradients yield larger thermal stresses.** Tables 3.4.28 and 3.4.29 summarize the peak fuel cladding temperatures with heat loads lower than the design basis maximum. In Tables 3.4.22 and 3.4.23, maximum calculated temperatures in different parts of the HI-STAR System under steady-state cold conditions (-40°F ambient, maximum design basis maximum decay heat and no insolation) are summarized. **Again, maximum basket periphery temperatures therein are actually conservative lower bound values as larger center-to-periphery temperature gradients yield larger thermal stresses.** To confirm the BTM fuel temperatures provided herein are bounding for all MPCs without the AHCEs option (MPC-24, MPC-24E, MPC-32 and MPC-68) a Refined Thermal Model (RTM) is articulated as discussed in the preceding paragraph. As shown next, the results of the refined calculations confirm the BTM results are bounding.

Maximum Cladding Temperatures		
MPC Type	BTM [°F]	RTM [°F]
PWR	701	671 (MPC-24) 668 (MPC-24E) 699 (MPC-32)
BWR	713	642 (MPC-68)

The following additional observations can be derived by inspecting the temperature field obtained from the finite element analysis:

- The maximum fuel cladding temperature is well within the PNL recommended temperature limit.
- The maximum temperature of basket structural material is well within the stipulated design temperatures.
- The maximum temperature of the neutron absorber is below the material temperature limit.
- The maximum temperatures of the MPC helium retention boundary materials are well below their respective ASME Code limits.
- The maximum temperatures of the aluminum heat conduction elements are well below the stipulated design temperature limits.
- The maximum temperature of the HI-STAR containment boundary materials is well below their respective ASME Code limits.

- The neutron shielding material (Holtite-A) will not experience temperatures in excess of its qualified limit.

The above observations lead us to conclude that the temperature field in the HI-STAR System with a fully loaded MPC containing design-basis heat emitting SNF complies with all regulatory and industry thermal requirements for normal conditions of transport. In other words, the thermal environment in the HI-STAR System will be conducive to safe transport of spent nuclear fuel.

#### 3.4.2.1 Maximum Accessible Surface Temperatures

Access to the HI-STAR overpack cylindrical surface is restricted by the use of a personnel barrier (See Holtec Drawing 3930, Sheet 3 in Chapter 1, Section 1.4). Therefore, the HI-STAR System surfaces accessible during normal transport are the exposed impact limiter surfaces outside the personnel barrier. In this subsection, the exposed impact limiter surface temperatures are computed by including heat transmission from the hot overpack ends through the impact limiters. A conservatively bounding analysis is performed by applying the thermal conductivity of aluminum to the encased aluminum-honeycomb material in the impact limiter shells to the normal condition thermal model discussed earlier in this chapter. In this manner heat transport to the exposed surfaces from the hot overpack is maximized and accessible surface temperatures over estimated. The maximum exposed cask surface temperatures for a PWR MPC (MPC-24) and a BWR MPC (MPC-68) at design maximum heat loads are 142°F and 139°F respectively. In Figure 3.4.28, a color contour map of the regions of HI-STAR System less than 185°F (358°K) is depicted for the hotter MPC-24 basket design. From this map, it is apparent that the accessible (impact limiter) surface temperatures are below the 10CFR71.43(g) mandated limit by a significant margin.

#### 3.4.3 Minimum Temperatures

As specified in 10CFR71, the minimum ambient temperature conditions for the HI-STAR System are -20°F and a cold environment at -40°F. The HI-STAR System design does not have any minimum decay heat load restrictions for transport. Therefore, under zero decay heat load in combination with no solar input conditions, the temperature distribution will be uniformly equal to the imposed minimum ambient conditions. All HI-STAR System materials of construction would satisfactorily perform their intended function in the transport mode at this minimum postulated temperature condition. Evaluations in Chapter 2 demonstrate the acceptable structural performance of the overpack and MPC steel materials at low temperature. Shielding and criticality functions of the HI-STAR System materials (Chapters 5 and 6) are unaffected by exposure to this minimum temperature.

##### 3.4.3.1 Post Rapid Ambient Temperature Drop Overpack Cooldown Event

In this section, the thermal response of the HI-STAR overpack to a rapid ambient temperature drop is analyzed and evaluated. The ambient temperature is postulated to drop from the maximum to minimum temperature under normal condition of transport in a very short time (100°F to -40°F during a 1 hour period) and is assumed to hold steady at -40°F thereafter. The initial overpack

condition prior to this rapid temperature drop corresponds to normal steady state transport with maximum design basis heat load. During this postulated cooldown event, the outer surface of the overpack will initially cool more rapidly than the bulk of metal away from the exposed surfaces. Consequently, it is expected that the through-thickness temperature gradients will increase for a period of time, reach a maximum and follow an asymptotic return to the initial steady condition through thickness temperature gradients as the overpack temperature field approaches the  $-40^{\circ}\text{F}$  ambient steady condition. The results of the transient analysis reported in this sub-section verify these observations.

Noting that the state of thermal stress is influenced by changes in the overpack temperature field during the cooldown transient, a number of critical locations in the containment boundary depicted in Figure 3.4.24 are identified as pertinent to a structural integrity evaluation discussed in Subsection 2.6.2.3 of this SAR. Locations (1) and (2) are chosen to track the through-thickness temperature gradients in the overpack top forging which is directly exposed to the ambient. Locations (3) and (4) are chosen to track the overpack inner containment shell through-thickness temperature gradient in a plane of maximum heat generation (i.e. active fuel mid-height) where the heat fluxes and corresponding temperature gradients are highest. Locations (A) and (B) are similarly chosen to track the temperature differential in the multi-layered shells (outer-to-inner shells).

The normal transport condition thermal model discussed previously in this chapter is employed in the overpack cooldown transient analysis. This analysis is carried out by applying time-dependent thermal boundary conditions to the model and starting the transient solution in the FLUENT program. In the cooldown event, the ambient temperature is decreased from  $100^{\circ}\text{F}$  to  $-40^{\circ}\text{F}$  in  $10^{\circ}\text{F}$  steps every 4 minutes (i.e. a total of 14 steps lasting 56 minutes). The ambient temperature is held constant thereafter. The maximum design basis heat load cask (i.e. the MPC-24 design) was selected to maximize the thermal gradients (by Fourier's Law, thermal gradient is proportional to heat flow). The overpack cooldown event is tracked by the thermal model for a period of 24 hours and results are reported in Figures 3.4.25 through 3.4.27 as discussed below.

In Figure 3.2.25, the overpack containment through-thickness temperature gradient responses are plotted. From this figure, it is evident that the exposed surface of the overpack forging (location (2)) initially cools at a faster rate than the recessed location (1). A similar but less pronounced result is observed in the multi-layered shells temperature changes depicted in Figure 3.4.26. This out-of-phase rate of cooling results in an increasing temperature gradient through the overpack metal layers. The thermal response of deeply recessed locations (3) and (4) show gradual temperature changes that follow each other closely. In other words, while through-thickness temperature gradients in the forging are somewhat altered the overpack inner shell gradients are essentially unchanged during the cooldown period. A closer examination of the forging temperature gradient is therefore warranted.

In Figure 3.4.27, the time dependent forging through thickness temperature differential is depicted. The gradient increases to a maximum in a short time period followed by a slow return towards the starting state. In absolute terms, both the steady state and transient temperature gradients in the forging are quite modest. In the steady state the forging through thickness temperature gradient is approximately  $3^{\circ}\text{F}$ . This value reaches a maximum plateau of  $7^{\circ}\text{F}$  during the transient event (Figure 3.4.27). The incremental thermal stress arising from this short-term gradient elevation is computed



and discussed in Subsection 2.6.2.3 of this SAR.

#### 3.4.4 Maximum Internal Pressures

The MPC is initially filled with dry helium after fuel loading and prior to sealing the MPC lid port cover plates and closure ring. During normal transport conditions, the gas temperature within the MPC rises to its maximum operating temperature as determined by the thermal analysis methodology described earlier (see Subsection 3.4.1). The gas pressure inside the MPC will increase with rising temperature. The pressure rise is determined using the Ideal Gas Law which states that the absolute pressure of a fixed volume of entombed gas is proportional to its absolute temperature.

The HI-STAR Maximum Normal Operating Pressure (MNOP) is calculated for 10 CFR 71.71(c)(1) heat condition (100°F ambient & insolation) and the HI-STAR Overpack passively cooled at design maximum heat load. For other lower than design maximum heat load scenarios, (e.g. transport with Trojan fuel) the MNOP results are confirmed to be bounding. In Tables 3.4.13 and 3.4.14, summary calculations for determining net free volume in the PWR and BWR canisters are presented. Based on a 30% release of the significant radioactive gases, a 100% release of the rod fill gas from postulated cladding breaches, **release of gas from postulated breached components of non-fuel hardware installed in PWR fuel assemblies (BPRAs are limiting)**, the net free volume and the initial fill gas pressure, the MNOP results are given in Table 3.4.15. The overpack containment boundary MNOP for a hypothetical MPC breach condition is bounded by the MPC pressure results reported in this table.

#### 3.4.5 Maximum Thermal Stresses

Thermal expansion induced mechanical stresses due to imposed non-uniform temperature distributions have been determined and reported in Chapter 2. Tables 3.4.17 and 3.4.18 summarize the HI-STAR System components temperatures, under steady-state hot conditions, for structural evaluation. **The maximum basket periphery temperatures therein are actually conservative lower bound values, as larger temperature gradients yield larger thermal stresses.**

Additionally, Table 3.4.24 provides a summary of MPC helium retention boundary temperatures during normal transport conditions (steady state hot). Structural evaluations in Section 2.6 reference these temperature results to demonstrate the MPC helium retention boundary integrity.

#### 3.4.6 Evaluation of System Performance for Normal Conditions of Transport

The HI-STAR System thermal analysis is based on detailed and complete heat transfer models that properly account for radiation, conduction and natural convection modes of heat transfer. The thermal models incorporate many conservative assumptions that are listed below. A quantitative evaluation of HI-STAR conservatisms is provided in Appendix 3.A.

1. No credit for gap reduction between the MPC and overpack due to differential thermal expansion under hot condition is considered.

2. No credit is considered for MPC basket internal thermosiphon heat transfer. Under a perfectly horizontal transport condition, axial temperature gradients with peaking at active fuel mid-height induces buoyancy flows from both ends of the basket in each MPC cell. Buoyancy flow in shallow horizontal channels has been widely researched and reported in the technical literature [3.4.10 to 3.4.12]. An additional mode of heat transport due to thermosiphon flow within the basket cells is initiated for any cask orientation other than a perfectly horizontal condition. In practice this is a highly likely scenario. However, in the interest of conservatism, no credit is considered for this mode of heat transfer.
3. An upper bound solar absorbtivity of unity is applied to all exposed surfaces.
4. No credit considered for radiative heat transfer between the neutron absorber panels and the neutron absorber pocket walls.
5. A lower bound conductivity is considered for conduction through the neutron shielding materials of the radial connectors region.
6. No credit is considered for contact between fuel assemblies and the MPC basket wall or between the MPC basket and the MPC basket supports. The fuel assemblies and MPC basket are conservatively considered to be in concentric alignment.
7. No credit considered for presence of highly conducting aluminum honeycomb material inside impact limiters.
8. The fuel assembly contribution to MPC basket axial conductivity is conservatively limited to the fuel cladding only (i.e. axial heat transfer through fuel pellets is neglected).
9. The MPC is assumed to be loaded with the SNF type which has the maximum equivalent thermal resistance of all fuel types in its category (BWR or PWR), as applicable.
10. The design basis maximum decay heat loads are used for all thermal-hydraulic analyses. For casks loaded with fuel assemblies having decay heat generation rates less than design basis, additional thermal margins of safety will exist.
11. Interfacial contact conductance of multi-layered intermediate shell contacting layers was conservatively determined to bound surface finish, contact pressure, and base metal conductivity conditions.
12. Flow turbulation in the MPC space neglected.

Temperature distribution results obtained from a conservatively developed thermal model show that maximum fuel cladding temperature limits are met with adequate margins. Margins during actual normal transport conditions are expected to be greater due to the many conservative assumptions incorporated in the analysis. The maximum local temperatures in the neutron shield and overpack seals are lower than design limits. The maximum local MPC basket temperature level is below the

recommended limits for structural materials in terms of susceptibility to stress, corrosion and creep induced degradation. Furthermore, structural evaluation (Chapter 2) has demonstrated that stresses (including those induced due to imposed temperature gradients) are within ASME B&PV Code limits. Section 3.6 provides a discussion of compliance with the regulatory requirements and acceptance criteria listed in Section 3.0. As a result of the above-mentioned considerations, it is concluded that the HI-STAR thermal design is in compliance with 10CFR71 requirements for normal conditions of transport.

Table 3.4.1

CLOSED CAVITY NUSSELT NUMBER<sup>†</sup>  
RESULTS FOR HELIUM FILLED MPC PERIPHERAL VOIDS

	Case (i) Nusselt Number		Case (ii) Nusselt Number	
Temperature (°F)	MPC-24, MPC-24E, MPC-32	MPC-68	MPC-24, MPC-24E, MPC-32	MPC-68
200	6.93	4.72	5.45	3.46
450	5.44	3.71	4.09	2.58
700	4.60	3.13	3.36	2.12

---

<sup>†</sup> For conservatism, the heat dissipation enhancement due to Rayleigh effect discussed in Sub-section 3.4.1.1.5 is ignored

Table 3.4.2

RELATIONSHIP BETWEEN HI-STAR SYSTEM REGIONS  
AND MATHEMATICAL MODEL DESCRIPTIONS

<u>HI-STAR System Region</u>	<u>Mathematical Model</u>	<u>Subsections</u>
Fuel Assembly	Fuel Region Effective Thermal Conductivity	3.4.1.1.2
MPC	Effective Thermal Conductivity of Neutron Absorber/Sheathing/Box Wall Sandwich	3.4.1.1.3
	Basket In-Plane Conductive Heat Transport	3.4.1.1.4
	Heat Transfer in MPC Basket Peripheral Region	3.4.1.1.5
	Effective Thermal Conductivity of MPC Basket-to-Shell Aluminum Heat Conduction Elements	3.4.1.1.11
Overpack	Effective Conductivity of Multi-Layered Intermediate Shell Region	3.4.1.1.6
	Effective Thermal Conductivity of Holtite Neutron Shielding Region	3.4.1.1.9
Ambient Environment	Heat Rejection from Overpack Exterior Surfaces	3.4.1.1.7
	Solar Heat Input	3.4.1.1.8
Assembled Cask Model	Overview of the Thermal Model	3.4.1.1.1
	Effective Conductivity of MPC to Overpack Gap	3.4.1.1.10
	FLUENT Model for HI-STAR	3.4.1.1.12

Table 3.4.3

THIS TABLE IS INTENTIONALLY DELETED.

Table 3.4.4

SUMMARY OF PWR FUEL ASSEMBLIES  
EFFECTIVE THERMAL CONDUCTIVITIES

No.	Fuel	@ 200°F (Btu/ft-hr-°F)	@ 450°F (Btu/ft-hr-°F)	@ 700°F (Btu/ft-hr-°F)
1	<u>W</u> 17×17 OFA	0.182	0.277	<b>0.402</b>
2	<u>W</u> 17×17 Std	0.189	0.286	0.413
3	<u>W</u> 17×17 Vantage-5H	0.182	0.277	0.402
4	<u>W</u> 15×15 Std	0.191	0.294	0.430
5	<u>W</u> 14×14 Std	0.182	0.284	0.424
6	<u>W</u> 14×14 OFA	<b>0.175</b>	<b>0.275</b>	0.413
7	B&W 17×17	0.191	0.289	0.416
8	B&W 15×15	0.195	0.298	0.436
9	CE 16×16	0.183	0.281	0.411
10	CE 14×14	0.189	0.293	0.435
11	HN <sup>†</sup> 15×15 SS	0.180	0.265	0.370
12	<u>W</u> 14×14 SS	0.170	0.254	0.361
13	B&W 15×15 Mark B-11	0.187	0.289	0.424
14	CE 14×14 (MP2)	0.188	0.293	0.434

Note: Boldface values denote the lowest thermal conductivity in each column (excluding stainless steel clad fuel assemblies).

<sup>†</sup> Haddam Neck B&W or Westinghouse stainless steel clad fuel assemblies.

Table 3.4.5

## SUMMARY OF BWR FUEL ASSEMBLIES EFFECTIVE THERMAL CONDUCTIVITIES

No.	Fuel	@ 200°F (Btu/ft-hr-°F)	@ 450°F (Btu/ft-hr-°F)	@ 700°F (Btu/ft-hr-°F)
1	Dresden 1 8×8 <sup>†</sup>	0.119	0.201	0.319
2	Dresden 1 6×6	0.126	0.215	0.345
3	GE 7×7	0.171	0.286	0.449
4	GE 7×7R	0.171	0.286	0.449
5	GE 8×8	0.168	0.278	0.433
6	GE 8×8R	<b>0.166</b>	0.275	0.430
7	GE-10 8×8	0.168	0.280	0.437
8	GE-11 9×9	0.167	<b>0.273</b>	<b>0.422</b>
9	AC <sup>††</sup> 10×10 SS	0.152	0.222	0.309
10	Exxon 10×10 SS	0.151	0.221	0.308
11	Damaged Dresden 1 8×8 in a DFC <sup>†</sup>	0.107	0.169	0.254
12	Dresden-1 Thin Clad 6x6 <sup>†</sup>	0.124	0.212	0.343
13	Humboldt Bay-7x7 <sup>†</sup>	0.127	0.215	0.343
14	Damaged Dresden-1 8x8 (in TND-1 canister) <sup>†</sup>	0.107	0.168	0.252
15	8x8 QUAD+ Westinghouse <sup>†</sup>	0.164	0.278	0.435

Note: Boldface values denote the lowest thermal conductivity in each column (excluding Dresden and LaCrosse clad fuel assemblies).

<sup>†</sup> Low heat emitting fuel assemblies excluded from list of fuel assemblies (zircaloy clad) evaluated to determine the most resistive SNF type

<sup>††</sup> Allis-Chalmers stainless steel clad fuel assemblies



Table 3.4.6

**MPC BASKET EFFECTIVE THERMAL CONDUCTIVITY RESULTS  
FROM ANSYS MODELS**

<b>Basket</b>	<b>@200°F (Btu/ft-hr-°F)</b>	<b>@450°F (Btu/ft-hr-°F)</b>	<b>@700°F (Btu/ft-hr-°F)</b>
MPC-24 (Zircaloy Clad Fuel)	1.127	1.535	2.026
MPC-68 (Zircaloy Clad Fuel)	1.025	1.257	1.500
MPC-24 (Stainless Steel Clad Fuel) (Note 1)	0.901	1.230	1.615
MPC-68 (Stainless Steel Clad Fuel) (Note 1)	0.987	1.180	1.360
MPC-68 (Dresden-1 8x8 in canisters)	0.921	1.118	1.306
MPC-32 (Zircaloy Clad Fuel)	0.964	1.214	1.486
MPC-32 (Stainless Steel Clad Fuel) (Note 1)	0.762	0.936	1.104
MPC-24E (Zircaloy Clad Fuel)	1.211	1.635	2.137
MPC-24E (Stainless Steel Clad Fuel) (Note 1)	0.988	1.348	1.766

Note-1: Evaluated for a conservatively bounding configuration (fuel in a damaged fuel canister)

Table 3.4.7

## INSOLATION DATA SPECIFIED BY 10CFR71, SUBPART F

Surface Type	12-Hour Total Insolation Basis	
	(g-cal/cm <sup>2</sup> )	(Watts/m <sup>2</sup> )
Horizontally Transported Flat Surfaces		
- Base	None	None
- Other Surfaces	800	774.0
Non-Horizontal Flat Surfaces	200	193.5
Curved Surfaces	400	387.0

Table 3.4.8

EFFECTIVE THERMAL CONDUCTIVITY OF THE NEUTRON SHIELD/RADIAL  
CHANNELS REGION

<b>Condition/Temperature (°F)</b>	<b>Thermal Conductivity (Btu/ft-hr-°F)</b>
Normal Condition:	
200	1.953
450	1.812
700	1.645
Fire Condition:	
200	3.012
450	2.865
700	2.689

Table 3.4.9

THIS TABLE IS INTENTIONALLY DELETED.

Table 3.4.10

PROPRIETARY INFORMATION WITHHELD PER 10CFR2.390

Table 3.4.11

PROPRIETARY INFORMATION WITHHELD PER 10CFR2.390

Table 3.4.12

THIS TABLE IS INTENTIONALLY DELETED.

Table 3.4.13

SUMMARY OF BOUNDING MINIMUM  
FREE VOLUME CALCULATIONS (PWR MPCs)

<b>Item</b>	<b>MPC-24 Volume (ft<sup>3</sup>)</b>	<b>MPC-24E Volume (ft<sup>3</sup>)</b>	<b>MPC-32 Volume (ft<sup>3</sup>)</b>
Cavity Volume	367	367	367
Basket Metal Volume	45	52	25
Bounding Fuel Assemblies Volume	79	79	106
Basket Supports and Fuel Spacers Volume	7	7	9
Aluminum Conduction Elements <sup>†</sup>	6	6	6
Net Free Volume	230 (6512 liters)	223 (6314 liters)	221 (6258 liters)

---

<sup>†</sup> Bounding 1,000 lbs aluminum weight.



Table 3.4.14

SUMMARY OF BOUNDING MINIMUM  
MPC-68 FREE VOLUME CALCULATIONS

<b>Item</b>	<b>Volume (ft<sup>3</sup>)</b>
Cavity Volume	367
Basket Metal Volume	35
Bounding Fuel Assemblies Volume	93
Basket Supports and Fuel Spacers Volume	12
Aluminum Conduction Elements <sup>†</sup>	6
Net Free Volume	221 ( 6258 liters)

---

<sup>†</sup> Bounding 1,000 lbs aluminum weight.

Table 3.4.15

PROPRIETARY INFORMATION WITHHELD PER 10CFR2.390

Table 3.4.16

THIS TABLE IS INTENTIONALLY DELETED.

Table 3.4.17

PROPRIETARY INFORMATION WITHHELD PER 10CFR2.390

Table 3.4.18

PROPRIETARY INFORMATION WITHHELD PER 10CFR2.390

Table 3.4.19

PROPRIETARY INFORMATION WITHHELD PER 10CFR2.390

Table 3.4.20

MAXIMUM ALLOWABLE TIME DURATION  
FOR WET TRANSFER OPERATIONS

<b>Initial Temperature (°F)</b>	<b>Time Duration (hr)</b>
115	44.3
120	42.0
125	39.7
130	37.4
135	35.2
140	32.9
145	30.6
150	28.3

Table 3.4.21

THIS TABLE IS INTENTIONALLY DELETED.



Table 3.4.22

PROPRIETARY INFORMATION WITHHELD PER 10CFR2.390

Table 3.4.23

PROPRIETARY INFORMATION WITHHELD PER 10CFR2.390

Table 3.4.24

PROPRIETARY INFORMATION WITHHELD PER 10CFR2.390

Table 3.4.25

SUMMARY OF 10×10 ARRAY BWR FUEL ASSEMBLY TYPES  
EFFECTIVE THERMAL CONDUCTIVITIES<sup>†</sup>

<b>Fuel</b>	<b><math>k_{\text{eff}}</math> at 200°F [Btu/(ft-hr-°F)]</b>	<b><math>k_{\text{eff}}</math> at 450°F [Btu/(ft-hr-°F)]</b>	<b><math>k_{\text{eff}}</math> at 700°F [Btu/(ft-hr-°F)]</b>
GE-12/14	0.166	0.269	0.412
Atrium-10	0.164	0.266	0.409
SVEA-96	0.164	0.269	0.416

---

<sup>†</sup>

The conductivities reported in this table are obtained by the simplified method described in the beginning of Subsection 3.4.1.1.2.

Table 3.4.26

COMPARISON OF ATRIUM-10<sup>†</sup> AND BOUNDING<sup>††</sup> BWR FUEL ASSEMBLY  
EFFECTIVE THERMAL CONDUCTIVITIES

Temperature	Atrium-10 Assembly		Bounding BWR Assembly	
°F	Btu/(ft-hr-°F)	W/m-K	Btu/(ft-hr-°F)	W/m-K
200	0.225	0.389	0.171	0.296
450	0.345	0.597	0.271	0.469
700	0.504	0.872	0.410	0.710

---

<sup>†</sup> The reported effective thermal conductivity has been obtained from a rigorous finite-element modeling of the Atrium-10 assembly.

<sup>††</sup> The bounding BWR fuel assembly effective thermal conductivity applied in the MPC-68 basket thermal analysis.

Table 3.4.27

THIS TABLE IS INTENTIONALLY DELETED.

Table 3.4.28

PROPRIETARY INFORMATION WITHHELD PER 10CFR2.390

Table 3.4.29

PROPRIETARY INFORMATION WITHHELD PER 10CFR2.390



Table 3.4.30

INTENTIONALLY DELETED

|

Table 3.4.31

INTENTIONALLY DELETED

|

Table 3.4.32

INTENTIONALLY DELETED

|

Table 3.4.33

INTENTIONALLY DELETED

|

Table 3.4.34

## PLANT SPECIFIC BWR FUEL TYPES EFFECTIVE THERMAL CONDUCTIVITY\*

<b>Fuel</b>	<b>@200°F [Btu/ft-hr-°F]</b>	<b>@450°F [Btu/ft-hr-°F]</b>	<b>@700°F° [Btu/ft-hr-°F]</b>
Oyster Creek (7x7)	0.165	0.273	0.427
Oyster Creek (8x8)	0.162	0.266	0.413
TVA Browns Ferry (8x8)	0.160	0.264	0.411
SPC-5 (9x9)	0.149	0.245	0.380

---

\* The conductivities reported in this table are obtained by a simplified analytical method described in Subsection 3.4.1.1.2.

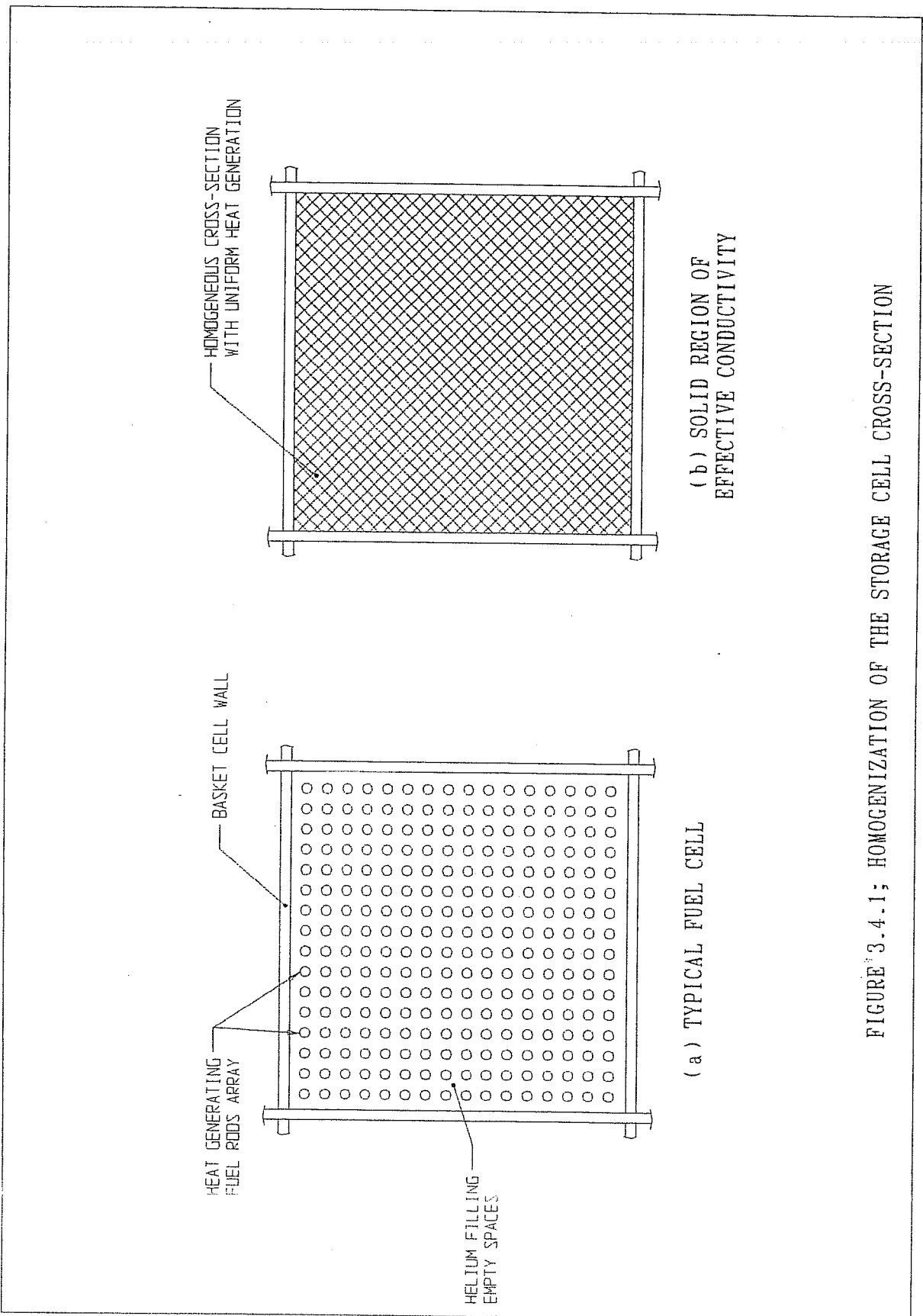


FIGURE 3.4.1; HOMOGENIZATION OF THE STORAGE CELL CROSS-SECTION

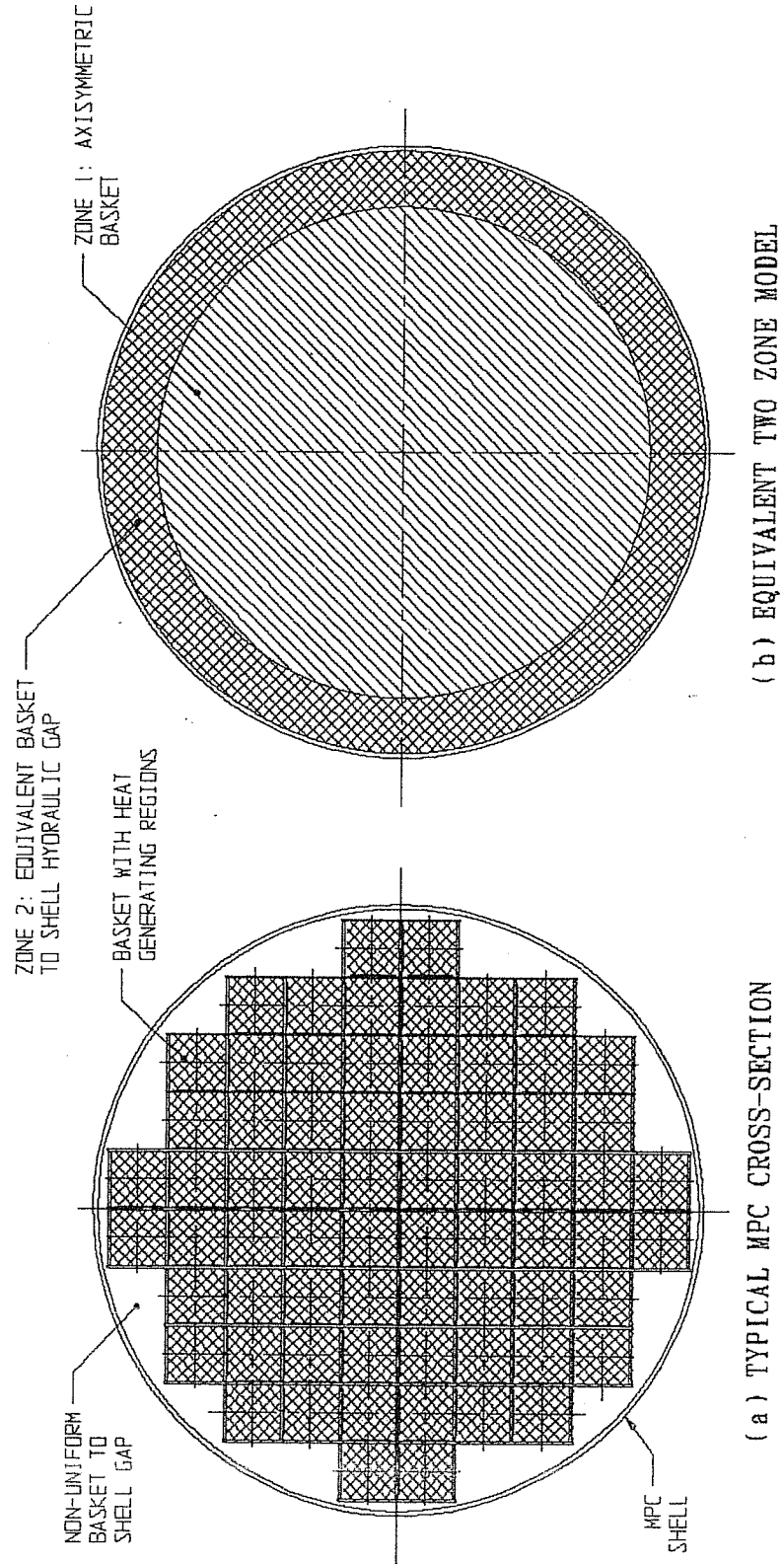


FIGURE 3.4.2; MPC CROSS-SECTION REPLACED WITH AN EQUIVALENT TWO ZONE AXISYMMETRIC BODY

PROJECTS\5014\HI951251\CH\_3\3\_4\_2

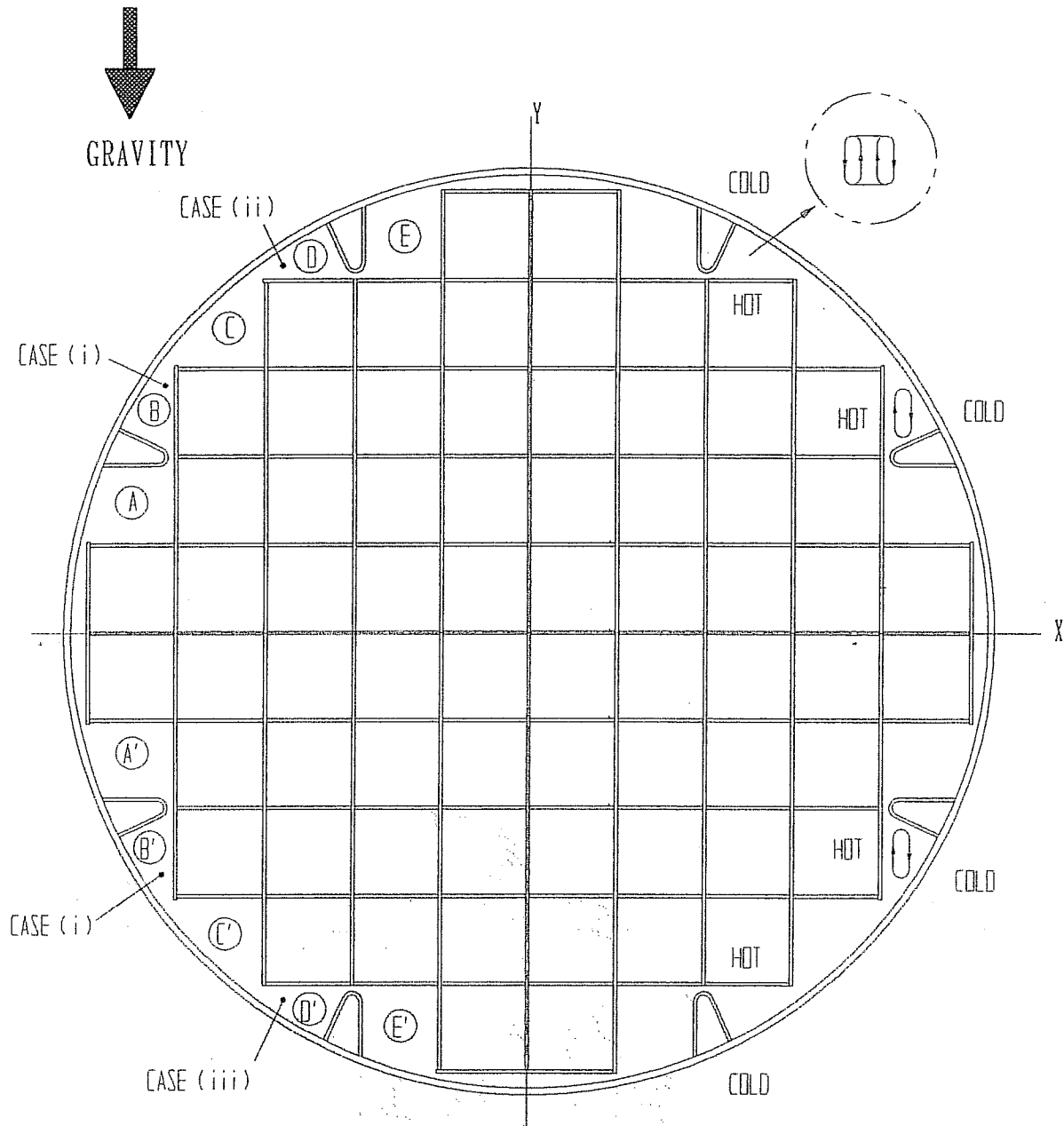


FIGURE 3.4.3; NATURAL CONVECTION IN MPC BASKET PERIPHERY REGION



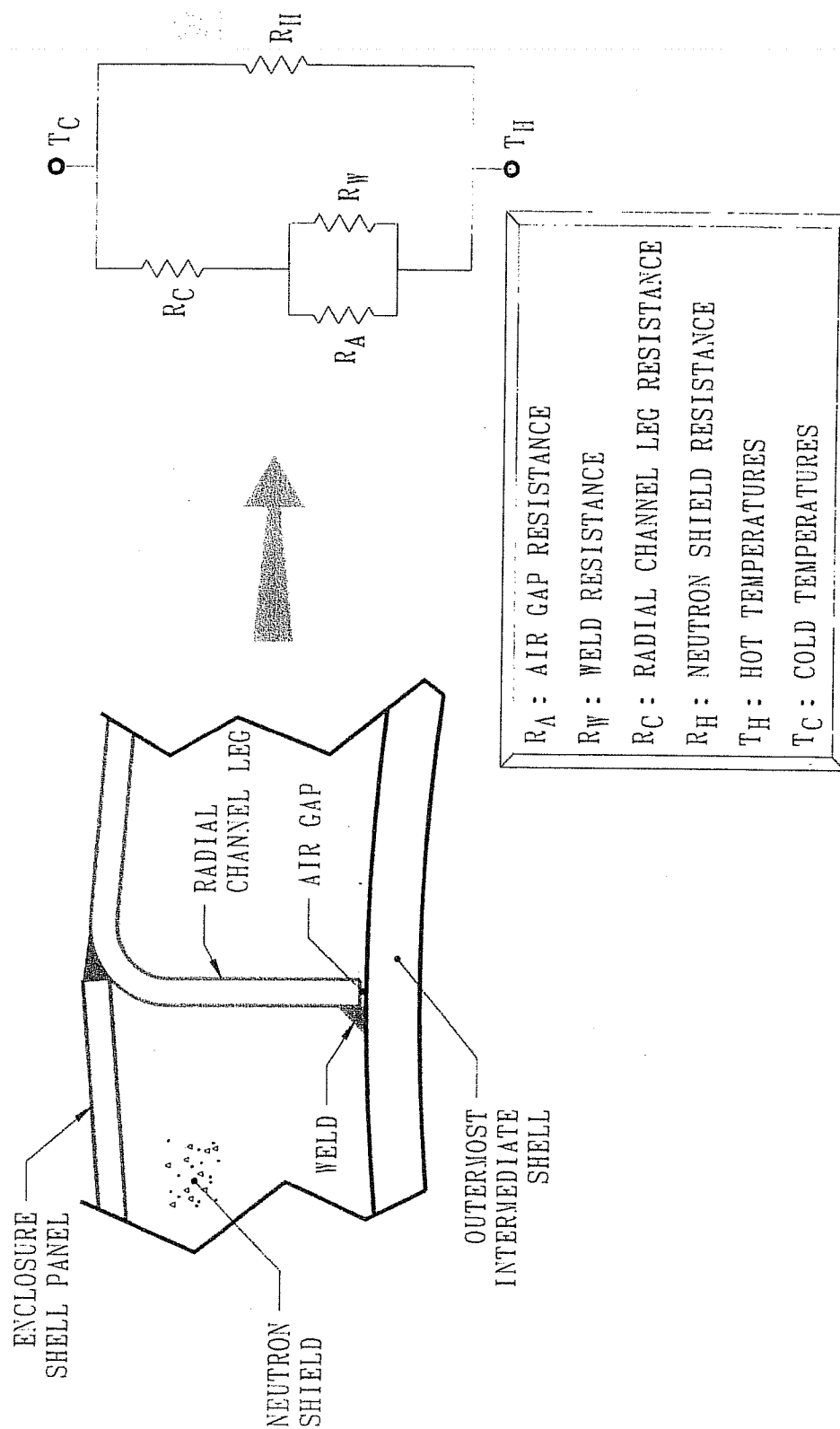


FIGURE 3.4.4; NEUTRON SHIELD REGION RESISTANCE NETWORK ANALOGY FOR EFFECTIVE CONDUCTIVITY CALCULATION

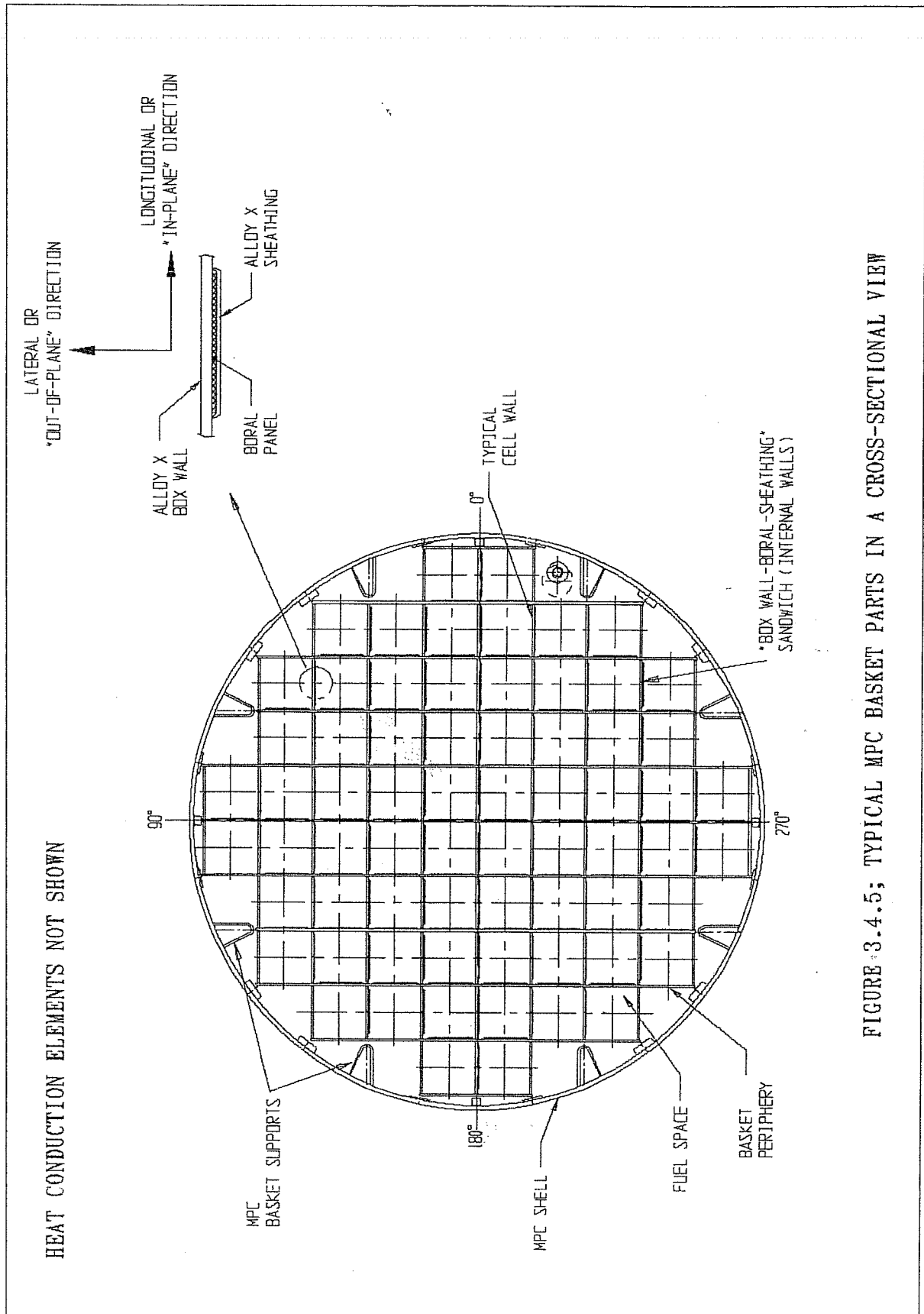


FIGURE 3.4.5; TYPICAL MPC BASKET PARTS IN A CROSS-SECTIONAL VIEW

VPROJECTS\5014\HI951251\CH\_3\3\_4\_5

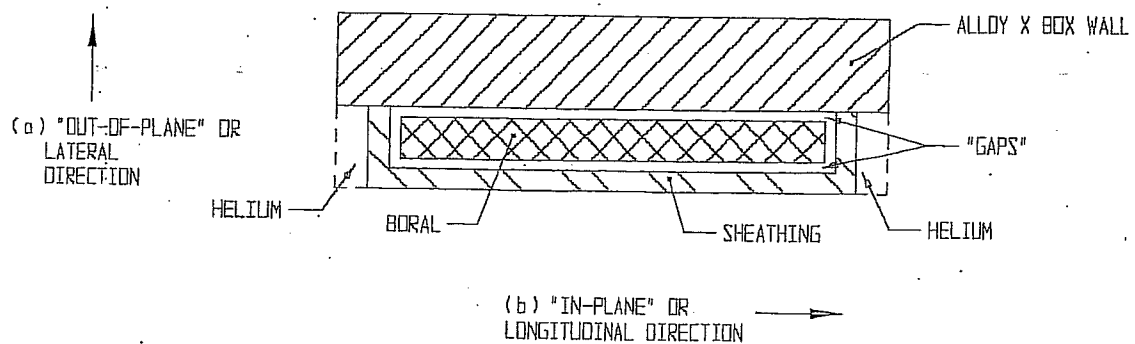


FIGURE 3.4.6: "BOX WALL-BORAL-SHEATHING" SANDWICH

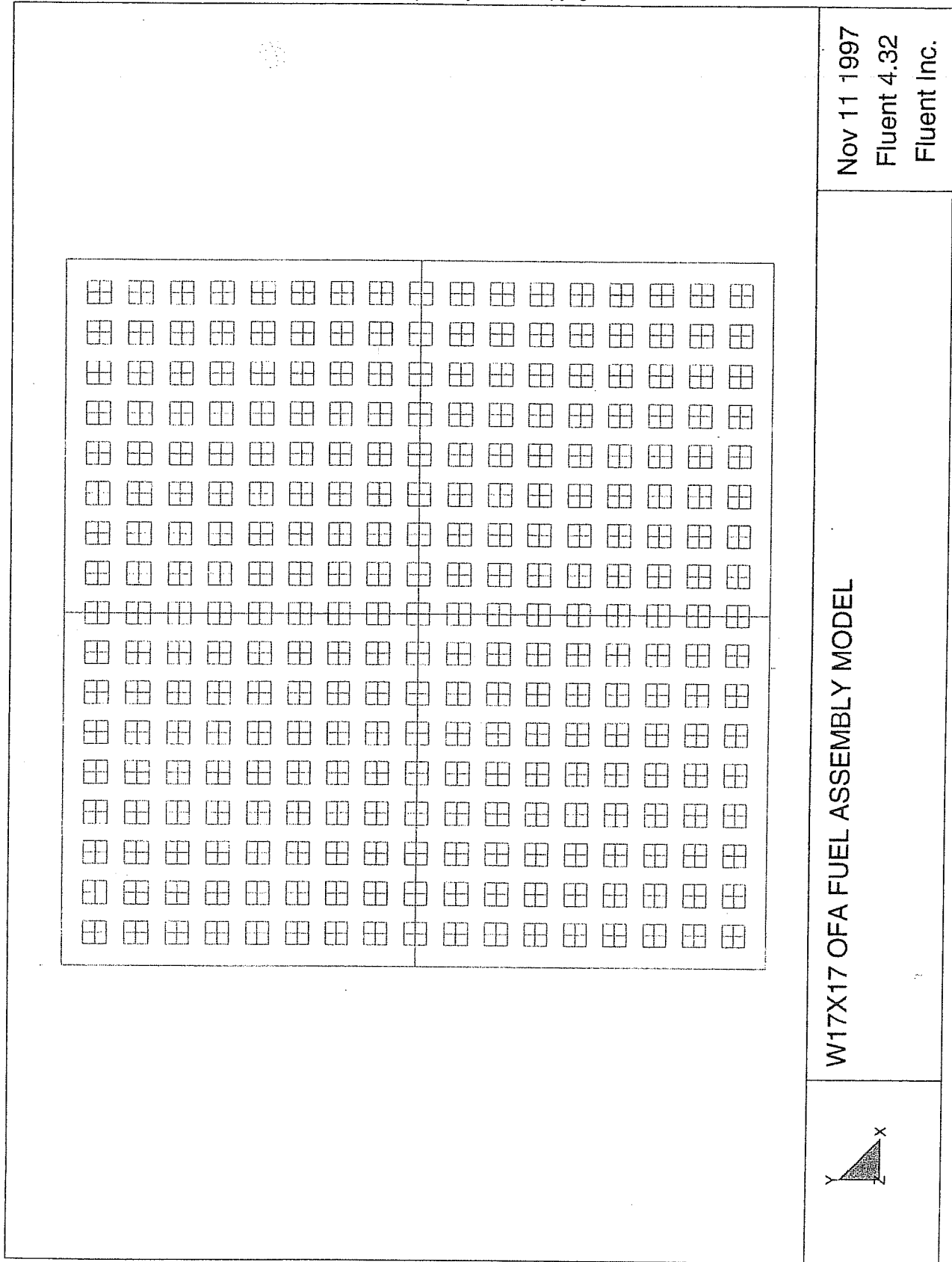


FIGURE 3.4.7: WESTINGHOUSE 17x17 OFA PWR FUEL ASSEMBLY MODEL

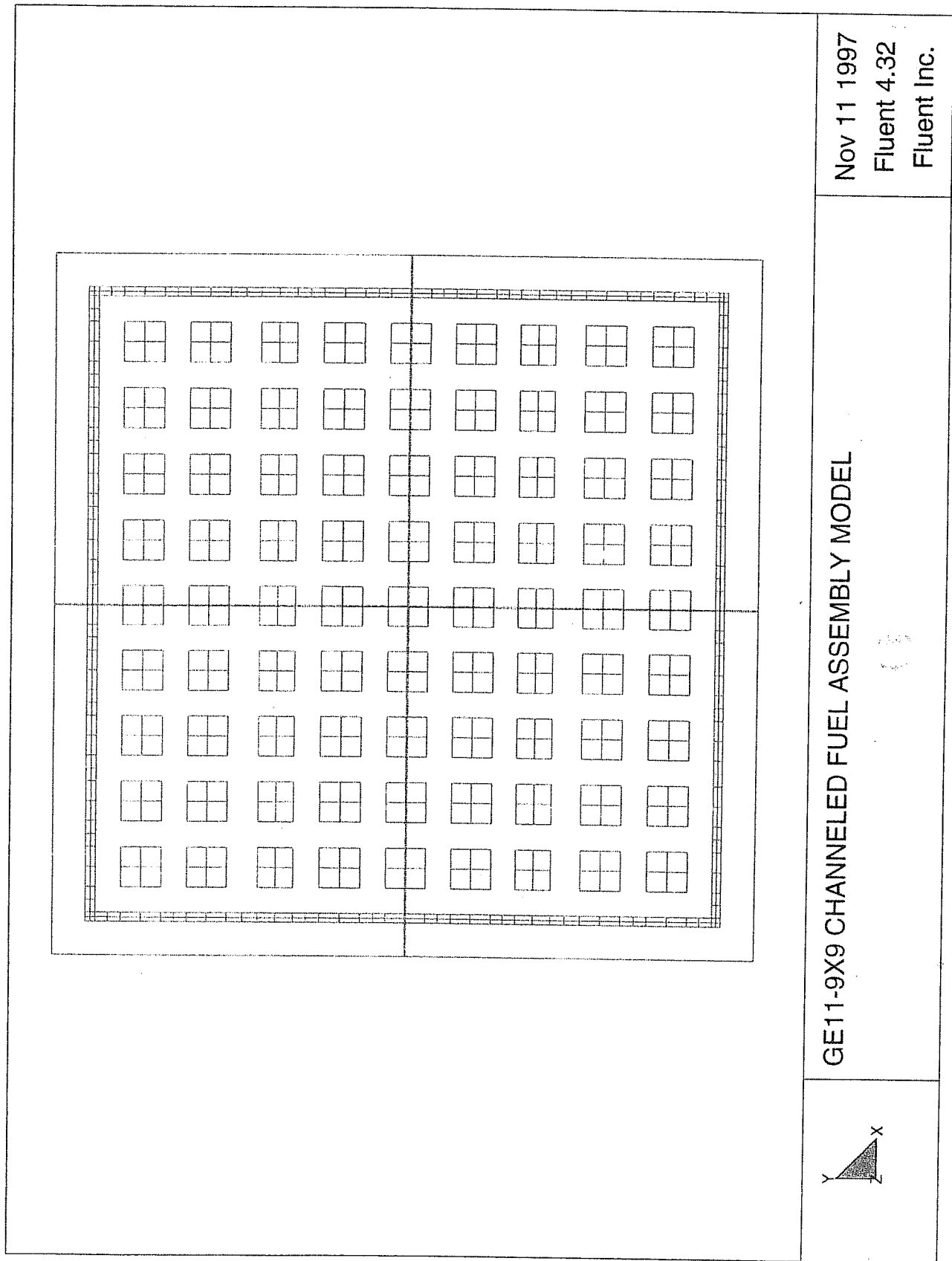


FIGURE 3.4.8: GENERAL ELECTRIC 9x9 BWR FUEL ASSEMBLY MODEL

FIGURE 3.4.9

THIS FIGURE IS INTENTIONALLY DELETED.

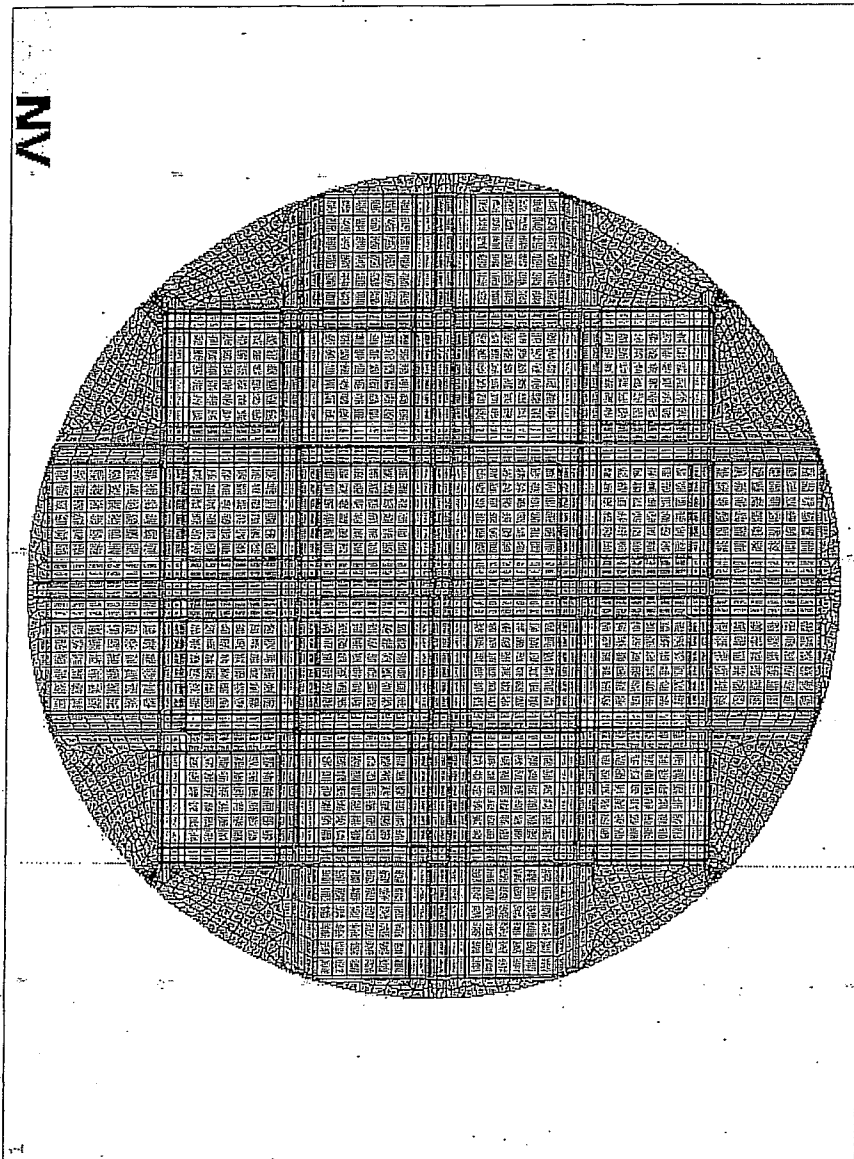


FIGURE 3.4.10: MPC-24 BASKET CROSS-SECTION ANSYS FINITE ELEMENT MODEL

REPORT HI-951251

Rev. 10

ANSYS 5.3  
NOV 13 1997  
11:28:39  
PLOT NO. 1  
ELEMENTS  
MAT NUM  
ZV =1  
\*DIST=37.606  
Z-BUFFER

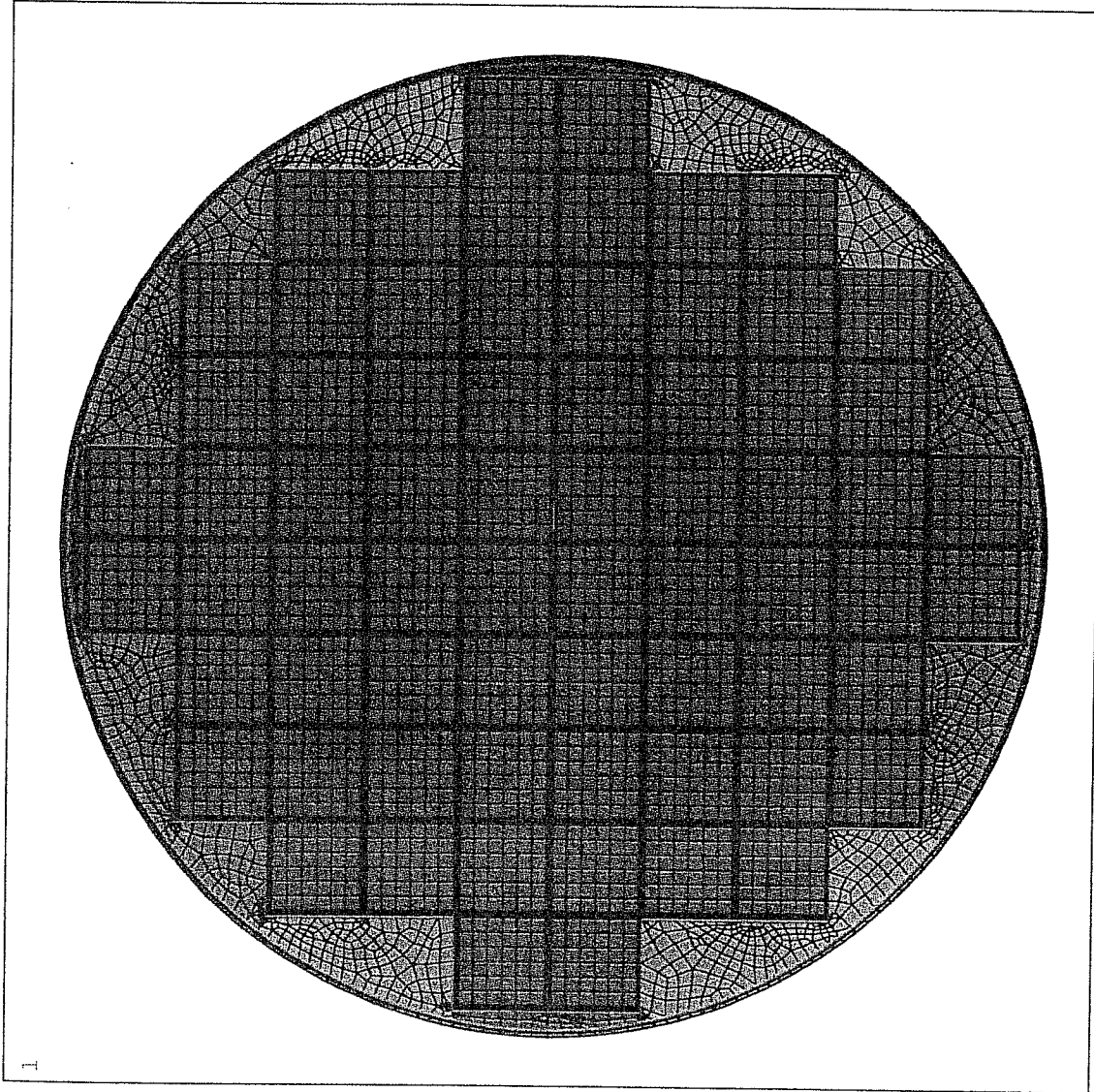
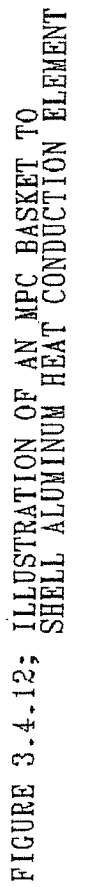
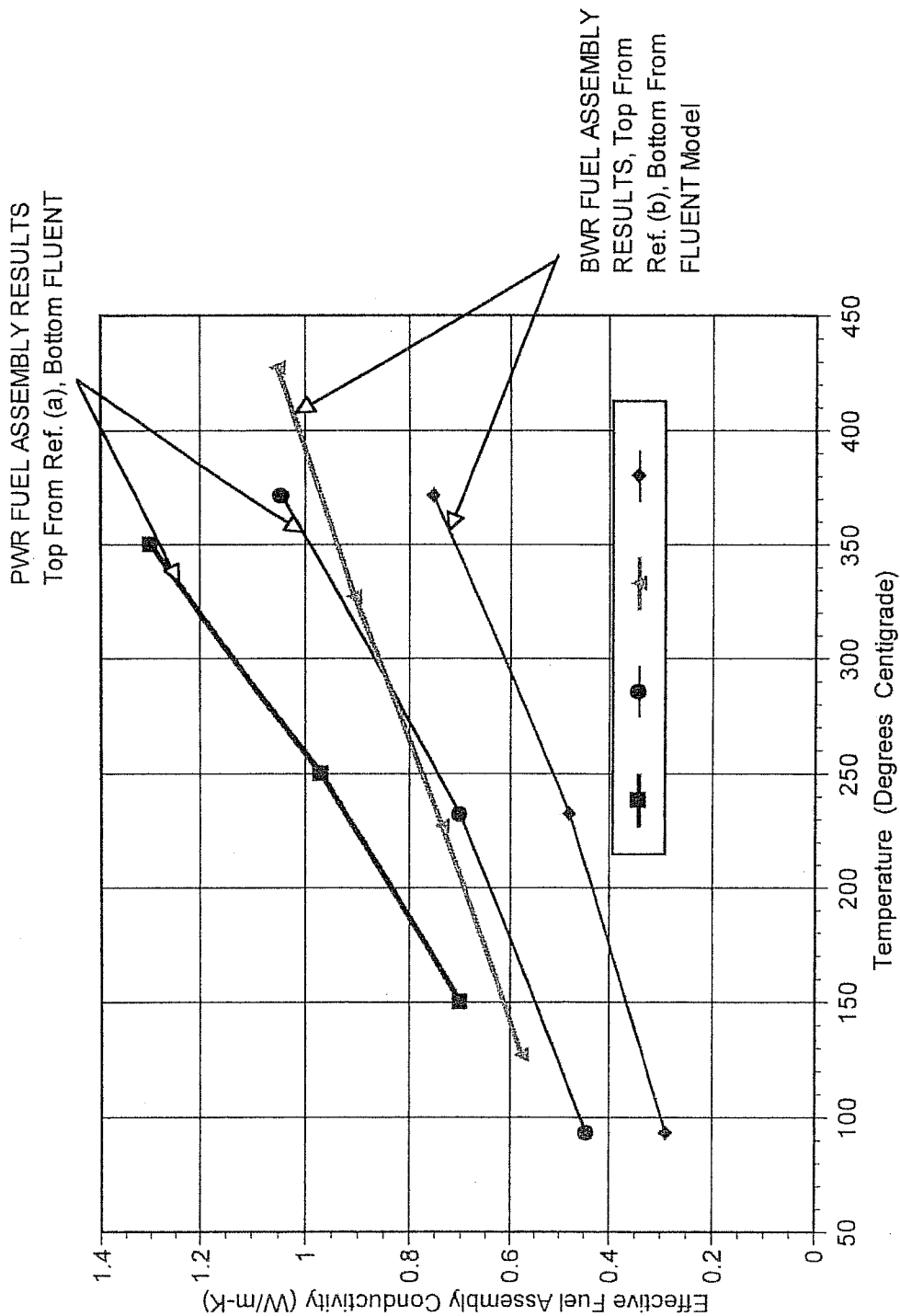


FIGURE 3.4.11; MPC-68 BASKET CROSS-SECTION ANSYS FINITE ELEMENT MODEL







(a) "Determination of SNF Peak Temperatures in the Waste Package", Bahney & Doering, *HLRWM Sixth Annual Conf.*, Pages 671-673, (April 30 - May 5, 1995)  
 (b) "A Method for Determining the Spent-Fuel Contribution to Transport Cask Containment Requirements", Sandia Report SAND90-2406, page II-132, (1992)

FIGURE 3.4.13: COMPARISON OF FLUENT BASED FUEL ASSEMBLY EFFECTIVE CONDUCTIVITY RESULTS WITH PUBLISHED TECHNICAL DATA

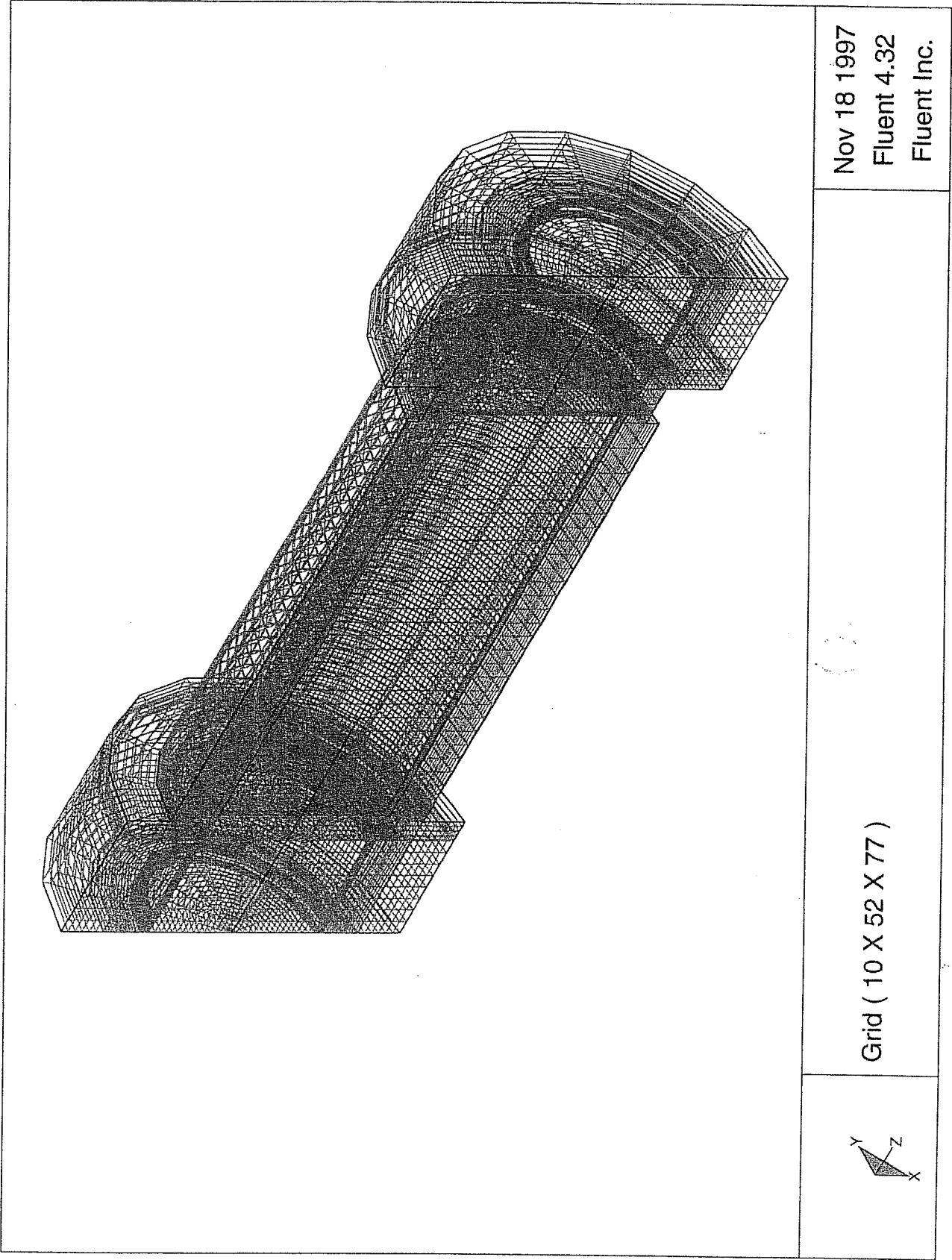


FIGURE 3.4.14: HI-STAR 100 SYSTEM FINITE ELEMENT MESH FOR THERMAL ANALYSIS

FIGURE 3.4.15

THIS FIGURE IS INTENTIONALLY DELETED.

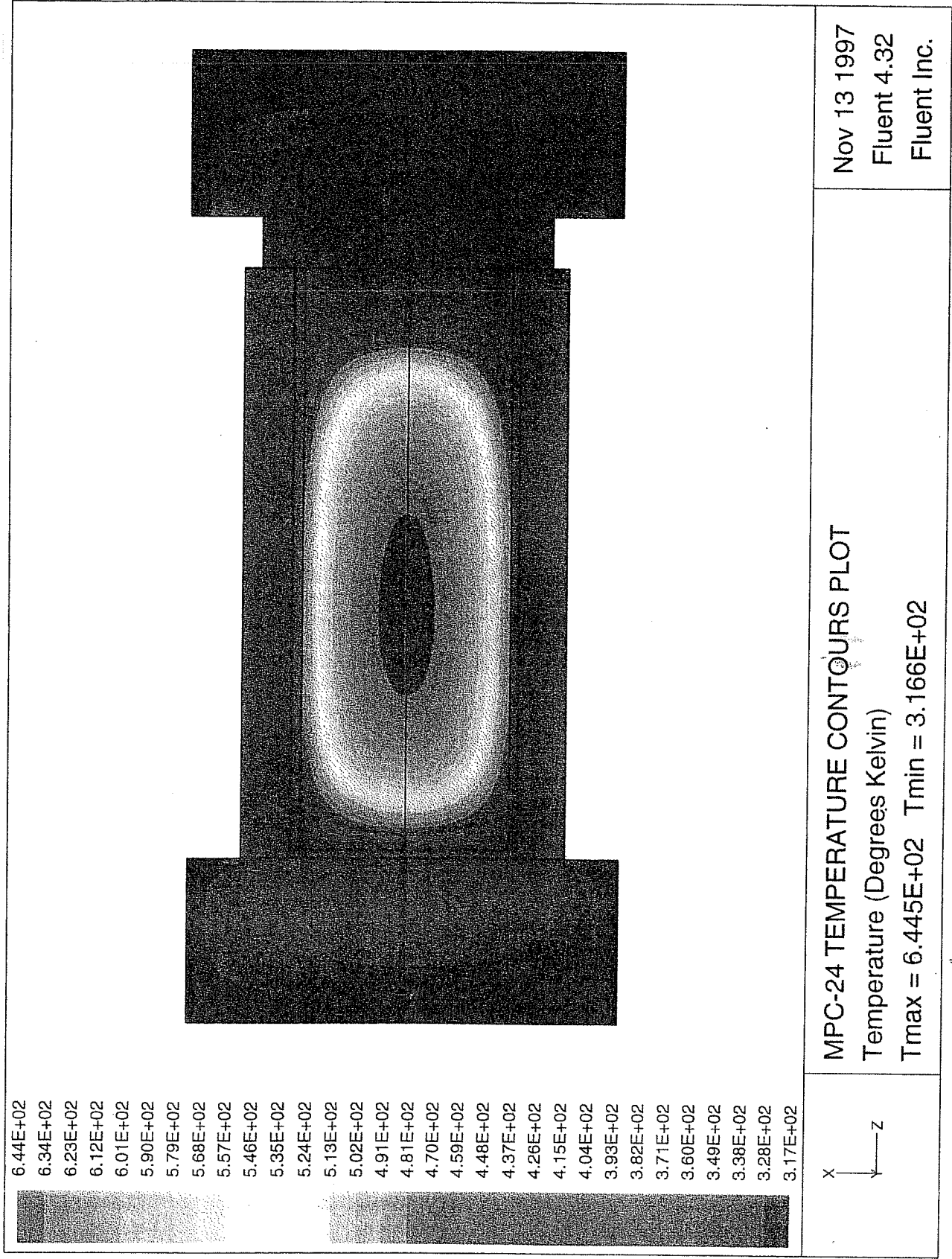
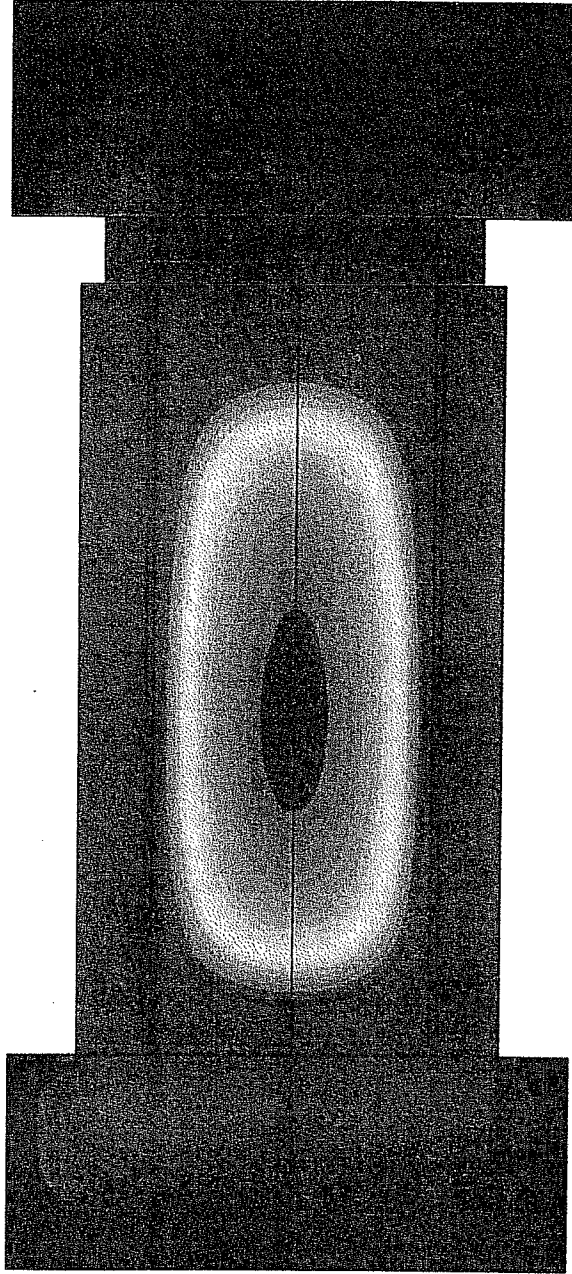


FIGURE 3.4.16: HI-STAR 100 SYSTEM NORMAL TRANSPORT CONDITION TEMPERATURE CONTOURS PLOT  
(MPC-24 BASKET)

6.51E+02  
6.40E+02  
6.29E+02  
6.18E+02  
6.07E+02  
5.96E+02  
5.84E+02  
5.73E+02  
5.62E+02  
5.51E+02  
5.40E+02  
5.29E+02  
5.18E+02  
5.07E+02  
4.95E+02  
4.84E+02  
4.73E+02  
4.62E+02  
4.51E+02  
4.40E+02  
4.29E+02  
4.18E+02  
4.06E+02  
3.95E+02  
3.84E+02  
3.73E+02  
3.62E+02  
3.51E+02  
3.40E+02  
3.29E+02  
3.17E+02



x  
z

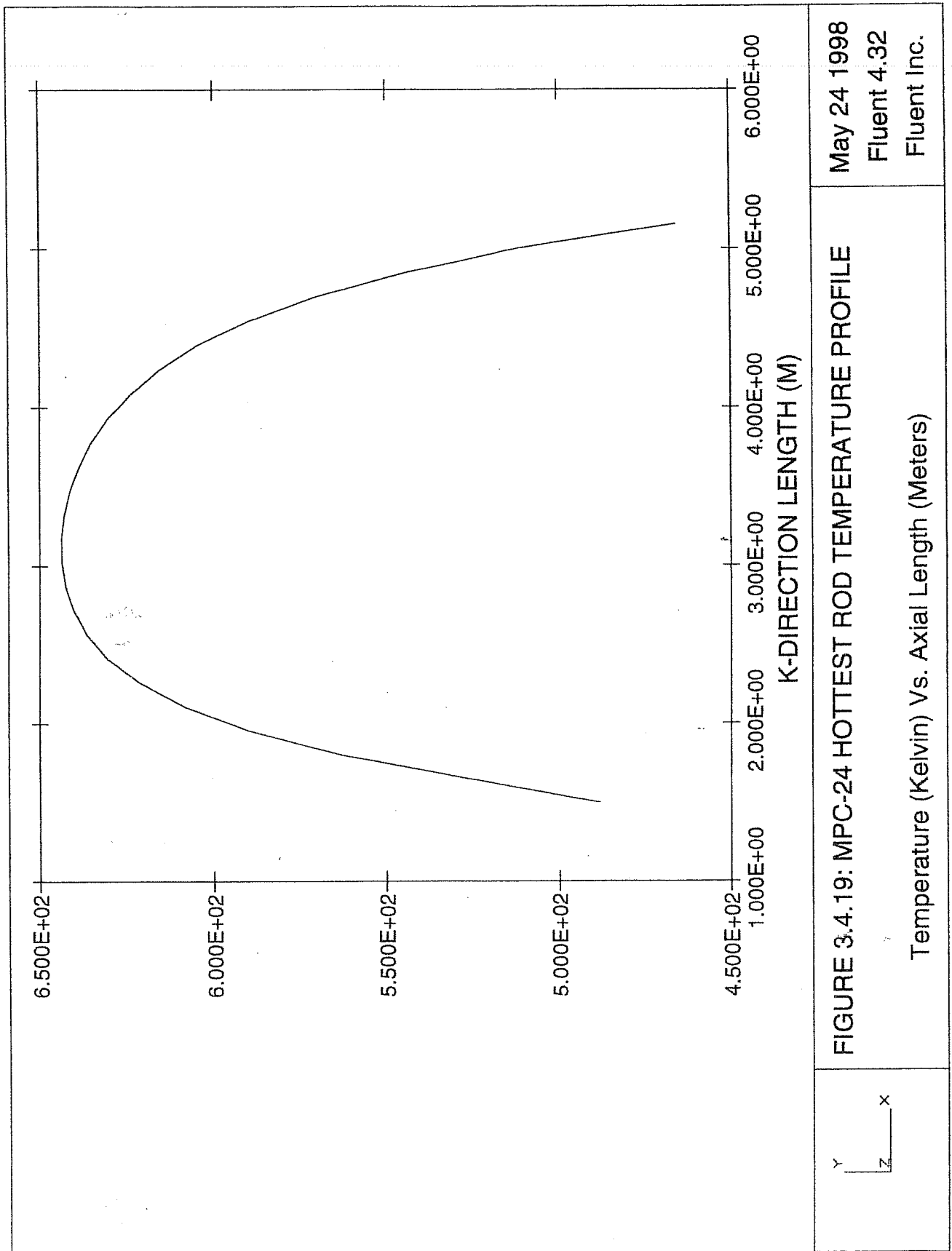
MPC-68 TEMPERATURE CONTOURS PLOT  
Temperature (Degrees Kelvin)  
Tmax = 6.512E+02 Tmin = 3.174E+02

Nov 13 1997  
Fluent 4.32  
Fluent Inc.

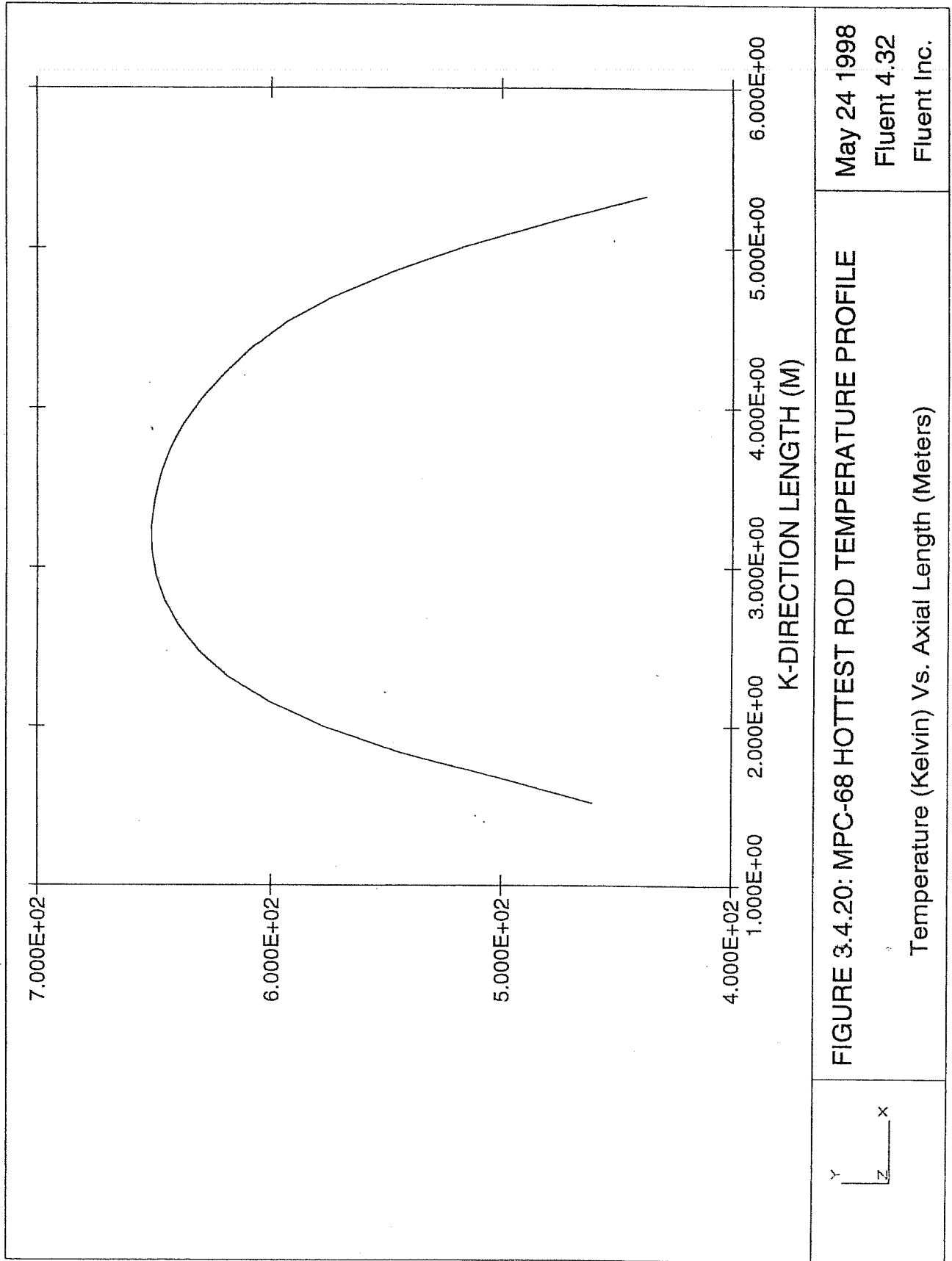
FIGURE 3.4.17: HI-STAR 100 SYSTEM NORMAL TRANSPORT CONDITION TEMPERATURE CONTOURS PLOT  
(MPC-68 BASKET)

FIGURE 3.4.18

THIS FIGURE IS INTENTIONALLY DELETED.



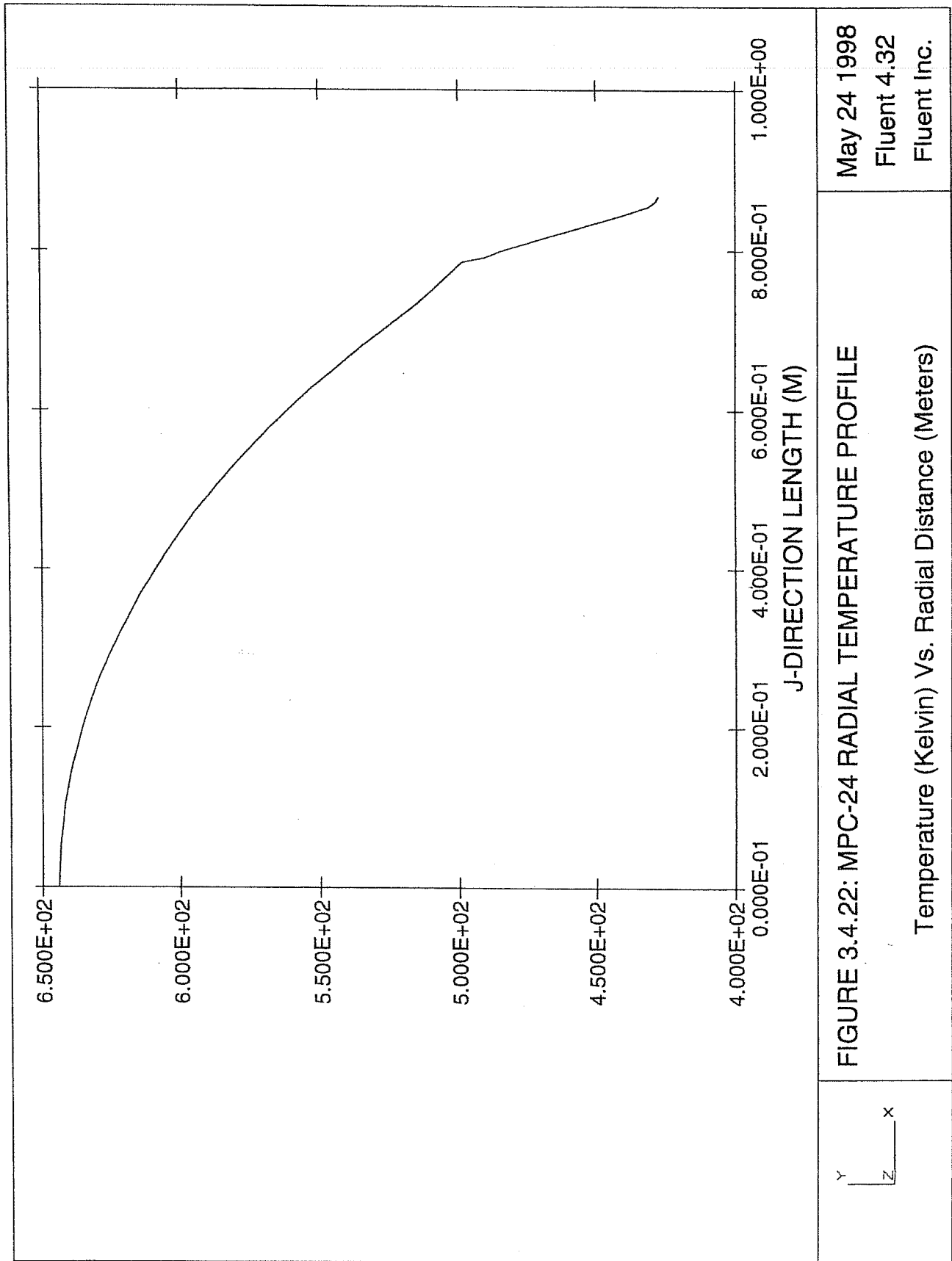


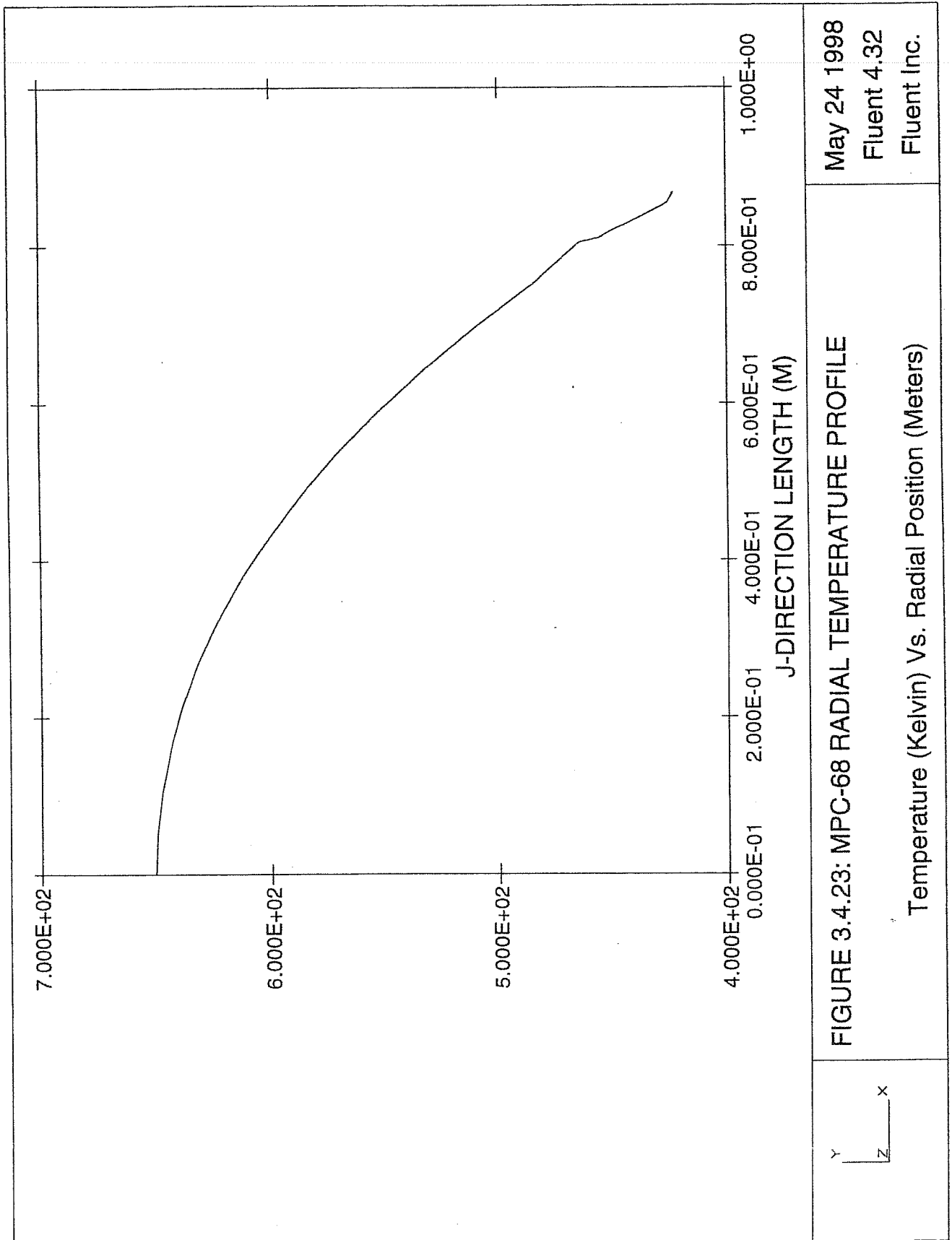


May 24 1998  
Fluent 4.32  
Fluent Inc.

FIGURE 3.4.21

THIS FIGURE IS INTENTIONALLY DELETED.





May 24 1998  
Fluent 4.32  
Fluent Inc.

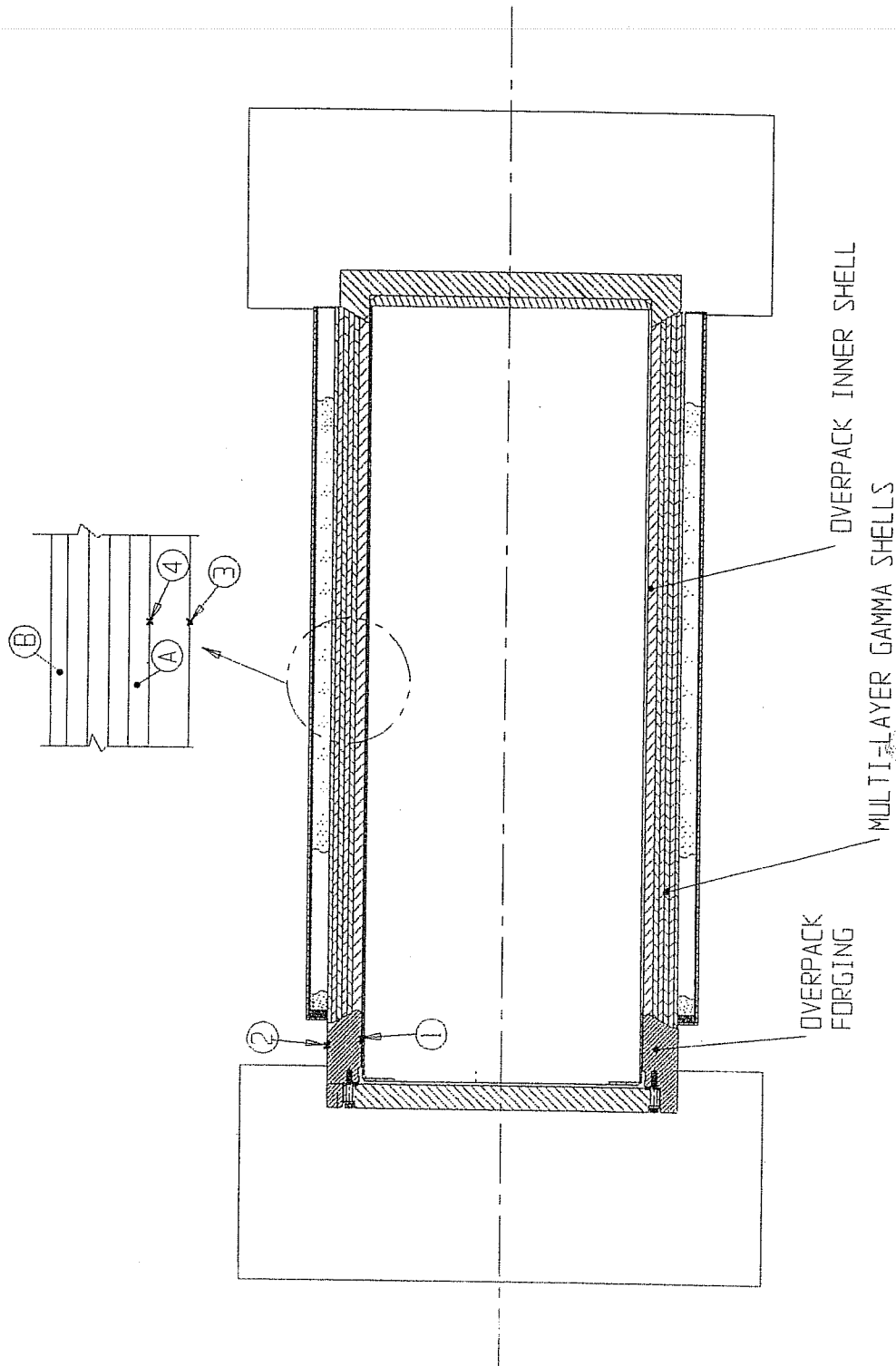


FIGURE 3.4.24; HI-STAR 100 PACKAGE CONTROL LOCATIONS TRACKED IN THE COOLDOWN EVENT

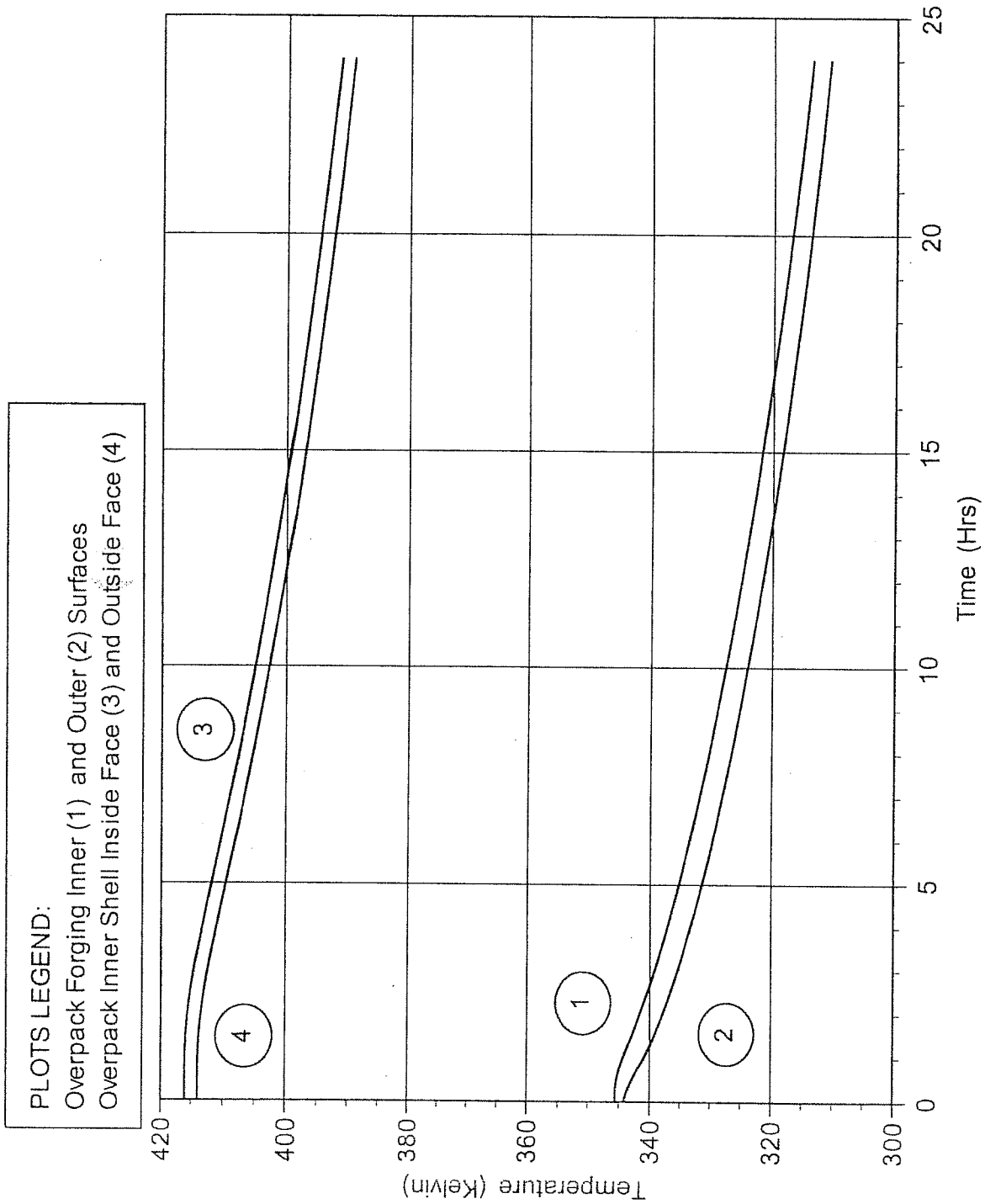


FIGURE 3.4.25: CONTAINMENT BOUNDARY COOLDOWN TEMPERATURE PROFILES

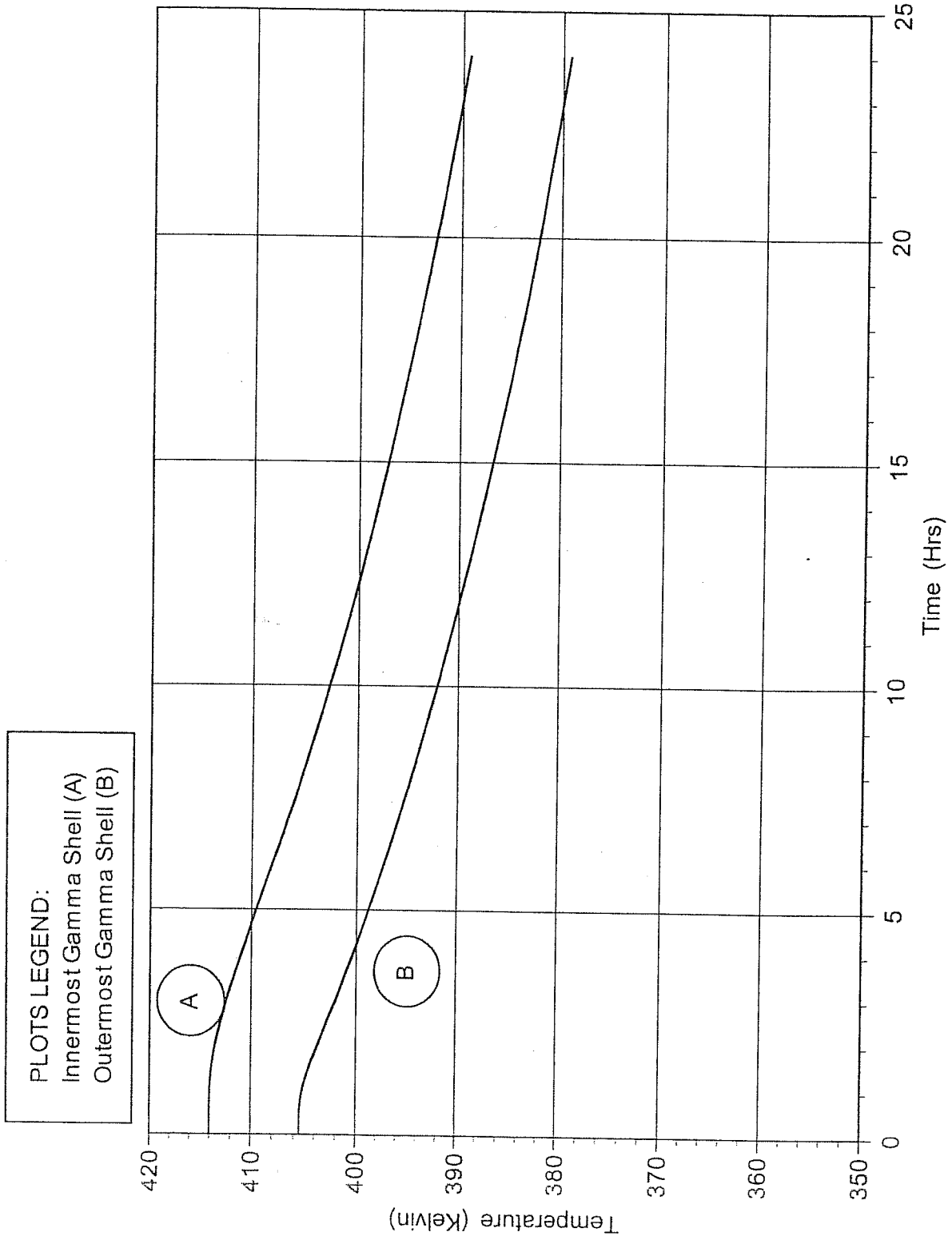


FIGURE 3.4.26: MULTI-LAYERED SHELLS COOLDOWN TEMPERATURE PROFILES

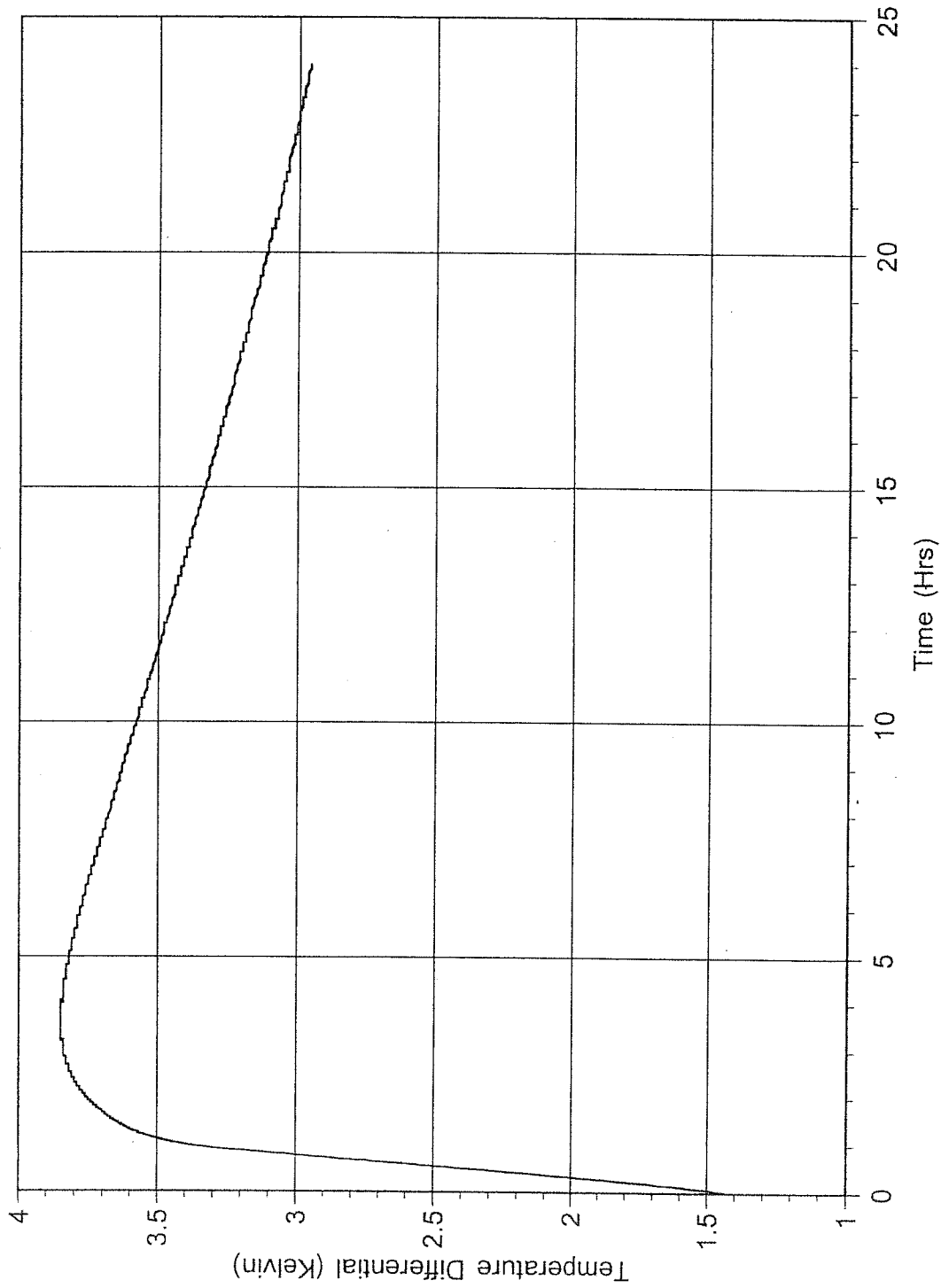
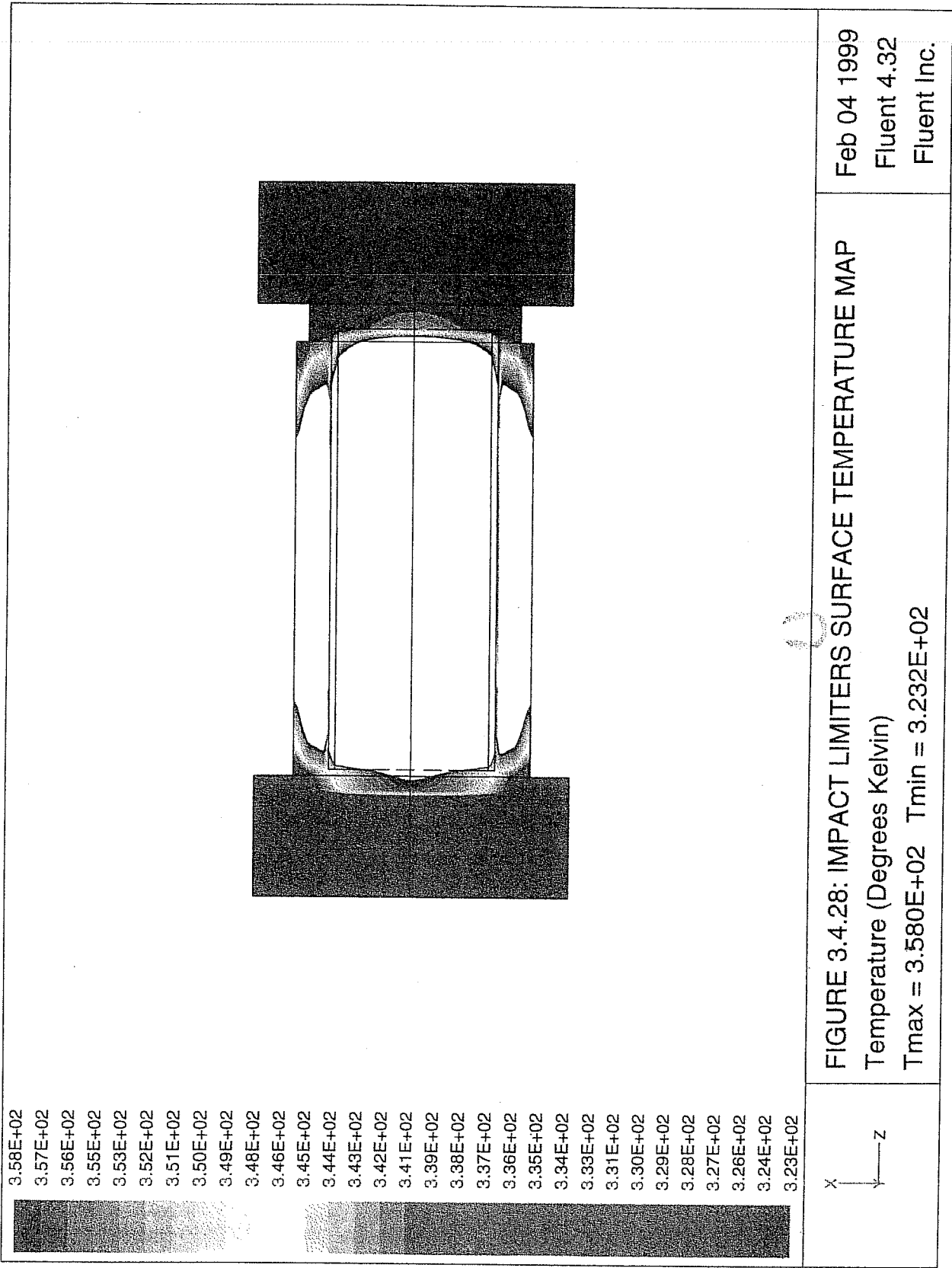


FIGURE 3.4.27: OVERPACK FORGING THROUGH THICKNESS TEMPERATURE GRADIENT DURING COOLDOWN TRANSIENT





### 3.5 HYPOTHETICAL ACCIDENT THERMAL EVALUATION

As mandated by 10CFR71 requirements, the HI-STAR System is subjected to a sequence of hypothetical accident conditions. The objective is to determine and assess the cumulative damage sustained by the system. The accident scenarios specified in order are: (1) a 30 foot free drop onto an unyielding surface; (2) a 40-inch drop onto a mild steel bar; and (3) exposure to a 30-minute fire at 1475°F. The initial conditions for the fire accident specify steady state at an ambient temperature between -20°F and 100°F [3.5.1]. In the HI-STAR System hypothetical fire accident evaluation, full effects of insolation before, during, and after the fire are considered. The effects of the first two drop accidents are evaluated in Chapter 2. In this section, the transient thermal response of the HI-STAR System to a 30-minute fire followed by a post-fire cooldown is determined. The fire accident evaluation is performed by consideration of a worst case combination of factors which conservatively overestimate heat input to the HI-STAR System during the fire followed by an underestimation of the ability of the cask to reject heat to the environment after the fire.

The impact limiters are designed to crush and absorb energy during the hypothetical drops. In the hypothetical fire accident evaluation, the impact limiter is assumed to be crushed to the bounding maximum condition of a solid block of highly conducting aluminum, resulting in increased heat input to the overpack ends through the reduced impact limiter thickness during the fire. The fire condition thermal analysis results are therefore bounding with respect to impact limiter design and amount of crush experienced during a hypothetical drop accident.

A puncture event may locally buckle some of the radial connector plates through the neutron shielding, thereby reducing the ability of the system to reject heat after the fire. As described in Section 2.7, the puncture bar is 6 inches in diameter and correspondingly has a face area of approximately 28.3 in<sup>2</sup>. The enclosure shell area is greater than 52,200 in<sup>2</sup>. Therefore, while the puncture bar would directly impact less than 0.06% of the exposed area, a conservative 10% reduction in the neutron shield region effective thermal conductivity is considered during the post-fire cooldown phase.

During the initial 30-minute fire event, some of the neutron shield will be exposed to high temperatures. Therefore, in determining heat input to the system, a conservative value maximizing the heat input is utilized for the neutron shield thermal conductivity. During the post-fire cooldown phase, no credit is considered for conduction through the neutron shield material. During the fire, a 10CFR71 mandated cask surface emissivity is considered to maximize radiant heat input to the cask. Destruction of the painted surfaces due to exposure to intense heat during the fire event is a credible possibility. Therefore, the lower emissivity of exposed carbon steel is conservatively considered for post-fire cooldown analysis.

The initial condition prior to the start of the fire accident is based on the bounding normal transport condition MPC basket temperature distribution. The smallest of the four baskets (MPC-24, MPC-24E, MPC-32 and MPC-68) average density and heat capacity are applied to the fire transient analysis. Thus, maximum basket heat load coincident with minimum thermal inertia provides a conservatively bounding response of the HI-STAR System to a fire accident condition.

In the fire event, analyzed in this Section of the SAR, the aim of the analysis is to bound two HI-STAR cask scenarios namely (a) MPCs installed with AHCEs and (b) MPCs without AHCEs. To achieve this objective, the analysis to characterize the response of the HI-STAR package in enveloping a Part 71 fire event assumes that the AHCE heat transfer bridge is present while the fire is raging so that the computed heat flow to the fuel is maximized. Further, the absorptivity of the overpack is increased from its normal operating condition value of 0.85 to the Part 71 value of 0.9. To account for the “no-AHCE” scenario, the emissivity of the overpack is reduced below its normal operating condition value (Table 3.5.2), as soon as the fire event ends, thus retarding the rejection of heat to the environment.

The temperature history of a number of critical control points in the HI-STAR System are monitored during the 30-minute fire and the subsequent relaxation of temperature profiles during the post-fire cooldown phase. The impact of transient temperature excursions on HI-STAR System materials is assessed in this section.

### 3.5.1 Thermal Model

#### 3.5.1.1 Analytical Model

A thermal transient simulation model to determine the fire condition temperature response is developed on the FLUENT CFD code [3.1.2]. The basic underlying finite volume model is based on the steady-state FLUENT model developed and described in Section 3.4. This basic model is modified by incorporating time dependent thermal loads on the exposed surfaces of the HI-STAR System for determining transient responses at every computational cell defined in the FLUENT model.

The HI-STAR System configuration during a hypothetical fire accident is schematically depicted in Figure 3.5.1. The initial thermal condition of the HI-STAR System prior to the accident condition is the normal transport steady-state temperature distribution. The HI-STAR System is then subjected to a 1475°F fire environment for 30 minutes. During this fire event, the impact limiters installed on both ends are assumed to be in a fully crushed state. This is a conservative assumption which results in an increased heat input to the overpack due to the higher thermal conductivity and reduced thickness of the crushed impact limiter. After 30 minutes, the ambient temperature is restored to 100°F and the HI-STAR System is allowed to proceed through a post-fire cooldown phase. During this entire transient event (fire and post-fire cooldown), the temperature history of several control points in the HI-STAR System is monitored. These points are schematically depicted in Figure 3.5.1.

Heat input to the HI-STAR System while it is engulfed in a fire is from a combination of radiation and forced convection heat transfer to all overpack/impact limiter exposed surfaces. This can be expressed by the following equation:

$$q_F = h_{fc} (T_F - T_s) + \sigma \varepsilon [(T_F + 460)^4 - (T_s + 460)^4]$$

where:

$q_F$  = surface heat input flux (Btu/ft<sup>2</sup>-hr)

- $T_F$  = fire condition temperature (1475°F)  
 $T_S$  = transient surface temperature (°F)  
 $h_{fc}$  = forced convection heat transfer coefficient [Btu/ft<sup>2</sup>-hr-°F]  
 $\varepsilon$  = surface emissivity = 0.9 (per 10CFR71)  
 $\sigma$  = Stefan-Boltzmann Constant (0.1714×10<sup>-8</sup> Btu/ft<sup>2</sup>-hr-°R<sup>4</sup>)

The forced convection heat transfer coefficient is calculated to bound the convective heat flux contribution to the exposed cask surfaces due to a fire induced air flow velocity of 15 m/s. For the case of air flow past a heated cylinder, Jakob [3.5.2] recommends the following correlation for convective heat transfer, obtained from experimental data:

$$Nu_{fc} = 0.028 Re^{0.8} \left[ 1 + 0.4 \left( \frac{L_{st}}{L_{tot}} \right)^{2.75} \right]$$

where:

- $L_{tot}$  = length traversed by flow  
 $L_{st}$  = length of unheated section  
 $K_f$  = thermal conductivity of air evaluated at the average film temperature  
 $Re$  = flow Reynolds Number based on  $L_{tot}$   
 $Nu_{fc}$  = Nusselt Number ( $h_{fc} L_{tot}/K_f$ )

Consideration of the wide range of temperatures to which the exposed surfaces are subjected to during the fire and the temperature dependent trend of air properties requires a careful selection of parameters to determine a conservatively large bounding value of the convective heat transfer coefficient. In Table 3.5.1, a summary of the parameter selections with justifications provides an appropriate basis for application of this correlation to determine forced convection heating of the HI-STAR System during the short-term fire event.

After the 30-minute fire event, the ambient temperature is restored to 100°F. The HI-STAR System cools down during this post-fire cooldown phase. Heat loss from outside exposed surfaces of the overpack is determined by the following equations:

$$q_s = 0.18 (T_S - T_A)^{4/3} + \sigma \varepsilon [(T_S + 460)^4 - (T_A + 460)^4]$$

where:

- $q_s$  = surface heat loss flux (Btu/ft<sup>2</sup>-hr)  
 $T_S$  = transient surface temperature (°F)  
 $T_A$  = ambient temperature (100°F)  
 $\varepsilon$  = surface emissivity  
 $\sigma$  = Stefan-Boltzmann Constant (0.1714×10<sup>-8</sup> Btu/ft<sup>2</sup>-hr-°R<sup>4</sup>)

During the fire event, some region of Holtite will be overheated and thus lose its ability to conduct heat. In the fire transient analysis, full credit is given to conduction through Holtite to conservatively increase heat input to the overpack. In the post-fire cooldown phase, all of the Holtite is conservatively assumed to be lost (no conduction through Holtite material).

During the 30-foot drop and puncture accident events, the mechanical integrity of the HI-STAR

System is maintained. From a thermal analysis standpoint, the impact limiters are crushed and there is at most localized damage to radial channels. While the resulting localized damage would not significantly degrade the heat transfer ability of the Holtite region, a 10% effective conductivity reduction is conservatively (as described earlier in Section 3.5) applied during the post-fire cooldown phase. In Table 3.5.2, a summary of inputs used in the determination of the effect of a hypothetical fire accident is provided.

#### 3.5.1.2 Test Model

For determining the transient response of the HI-STAR System under a hypothetical fire accident condition, a detailed finite volume model has been developed on the validated and benchmarked FLUENT code. The dynamic model features several conservative assumptions to bound temperature excursions during the heat up and cooldown phases of the accident. Accordingly, development of a separate test model to verify the results is not considered necessary. Evaluation of the HI-STAR System thermal design in the event of a hypothetical fire event is shown to be in compliance with 10CFR71 requirements.

#### 3.5.2 System Conditions and Environment

The HI-STAR System is shown to maintain its mechanical integrity following a 30 foot drop and puncture accident with stresses within applicable ASME Code requirements. The impact limiters absorb the impact forces and are crushed in the drop event. Completely crushed impact limiters provide a conservatively limiting situation for increased heat absorption during the 30-minute fire. The effect of a puncture accident results in localized damage to the radial connectors embedded in Holtite neutron shielding. This will *not* reduce the heat transfer capability of the region containing Holtite by a significant factor. The fire is specified to be at a temperature of 1475°F and last for 30 minutes. Emissivity of all exposed surfaces is set to 0.9. Some of the Holtite will decompose and lose its ability to conduct heat during the fire event due to exposure to severe temperature conditions. Thermal analysis of the HI-STAR System is performed by postulating worst case conditions whereby increased heat absorption takes place during the 30-minute fire and a reduced ability of the HI-STAR System to reject heat takes place during the post-fire cooldown phase.

#### 3.5.3 System Temperatures

The hypothetical fire accident condition is evaluated by imposing a 1475°F fire temperature for 30 minutes followed by a post-fire equilibrium phase that is followed for more than 30 hours. The temperature-time history of several control points is monitored. These points are selected because of their importance relating to safety evaluation. In Figures 3.5.2 to 3.5.4, the transient temperature profiles of the monitored points shown in Figure 3.5.1 are plotted. From these plots, the temperature of exposed surfaces is seen to increase rapidly and peak at about 1348°F at the end of the fire (i.e., 30 minutes). Figure 3.5.5 shows the peak axial fuel cladding temperature profile during post-fire cooldown. In the post-fire equilibrium phase, there is an initial rapid cooldown of the peak surface temperature followed by an asymptotic approach to the final steady-state condition. The closure bolts and mechanical seals peak temperatures are below short-term limits. The MPC basket center temperature rises sluggishly to a broad peak and then slowly decays to a final steady-state condition.

Portions of Holtite neutron shielding material near the overpack enclosure shell experience a short duration high temperature excursion. The crushed aluminum alloy inside the impact limiter begins to melt at 1105°F. The latent heat of melting of aluminum alloy during the melting phase would absorb the incident heat flux from the fire. This ablation mechanism will protect the cask by limiting the surface temperature excursion and restricting the amount of heat input to the overpack lid. In the HI-STAR System fire transient evaluation, credit for this protective feature is not considered.

The HI-STAR fire event model is depicted in Figure 3.5.6. Fire condition containment boundary through thickness temperature profiles are presented in Figures 3.5.7, 3.5.8, and 3.5.9 across Sections A-A, B-B, and C-C, as shown in Figure 3.5.6. The figures present through-thickness temperature profiles at the end of the 30-minute fire and 60 minutes after the start of the fire (30 minutes into the post-fire cooldown period).

In the fire event, the dominant heat input source is located on the outside of the cask. The temperature gradient, as seen in Figures 3.5.7, 3.5.8, and 3.5.9, is reversed from the normal condition, with the maximum temperature occurring at the outermost layer. From Figure 3.5.7, it is apparent that the overpack inner shell remains below the 500°F short-term design basis temperature limit. At the end of the 30-minute fire, the outermost layer of the multi-layered shells is heated to approximately 540°F. During the post-fire cooldown phase the temperature of this outer layer rapidly drops below 500°F, as shown on the 60-minute profile.

An examination of the overpack forging temperature profile (Section B-B, Figure 3.5.8) shows that the outer layers of the forging, directly adjacent to the surface exposed to the fire, are heated to in excess of 700°F during the fire. The bulk of the forging metal mass (in excess of 6 inches out of the total 8.5 inches) remains below the 700°F short-term design basis temperature limit. The portion of the overpack forging which is covered by the impact limiters remains below 700°F both during and after the fire. This is illustrated by the temperature profiles presented in Figure 3.5.9.

The following observations can be drawn from an examination of Figures 3.5.6 through 3.5.9:

- The containment boundary regions that are within the confines of the multi-layered shells remain below 500°F.
- The containment boundary regions that are within the confines of the impact limiters remain below 700°F.
- The bulk of the containment boundary in the regions that are directly exposed to the fire remain below 700°F.

The outer region of the HI-STAR 100 overpack consists of forty sector shaped annular spaces enclosed in half inch thick carbon steel plates. These annular spaces contain Holtite-A neutron absorber material. Holtite-A is a stable material under the environmental and thermal conditions corresponding to normal operation. Under a fire condition, the temperature in the enclosure shell cavity rises resulting in loosening of the water intermolecular bonds to the neutron shield material

leading to liberation of water vapor. For conservatism, a 6% weight loss factor for the neutron shield when exposed to a direct fire is assumed. Under a conservatively postulated scenario wherein all of the radial neutron shield material (approximately 12,850 lbs required to completely fill the forty spaces) is exposed to a direct fire, 771 lbs of water vapor (i.e 6% of neutron shield) generation in 30 minutes is required to be expelled from the neutron shield cavities. To protect the enclosure shell from overpressure, two rupture discs (each having the required vapor expulsion capacity) are incorporated in the HI-STAR overpack design. The rupture discs have a relatively low set pressure (30 psig) to relieve water vapor if the generation is rapid during a fire condition.

#### 3.5.4 Maximum Internal Pressure

Based on bounding transient temperature excursions calculated for the HI-STAR System during a hypothetical fire accident condition, maximum calculated cask internal pressures are reported in Table 3.5.3. **Although structural evaluations in Chapter 2 demonstrate there is no mechanical cause of fuel rod failures and this chapter demonstrates that fuel cladding temperatures are never exceeded, maximum pressure calculations conservatively assume 100% of the fuel rods and gas-containing components of non-fuel hardware (BPRAs are limiting) rupture non-mechanistically,** releasing conservatively determined rod fill gas and fission gases volumes into the MPC cavity.

#### 3.5.5 Maximum Thermal Stresses

Maximum thermal stresses generated during transient temperature excursions within the HI-STAR System are reported in Chapter 2.

#### 3.5.6 Evaluation of System Performance for the Hypothetical Accident Thermal Conditions

The HI-STAR System was subjected to a hypothetical fire accident condition with the impact limiters crushed and enclosure shell punctured as a result of previously imposed drop and puncture accidents. However, mechanical integrity of the overpack intermediate and inner shells, mechanical seals, and MPC shell is retained. During the fire accident event, portions of neutron shielding material in the overpack enclosure shell experience high transient temperature excursions and thus partially lose the ability to conduct heat and shield neutrons. Portions of aluminum alloy inside the crushed impact limiters near the exposed surfaces melt, but do not ignite.

For assessing the impact of transient temperature excursions on the integrity of the HI-STAR System, the significant components and quantities of interest are the closure plate bolts temperatures, the mechanical seals temperatures, the neutron shield temperature, the peak pressure and the peak fuel cladding temperature. The closure plate bolts maintain their ability to hold the seals. The neutron shield material in the post-accident shielding analysis is conservatively assumed to be completely lost. The peak system pressure remains below the design basis accident pressure. The fuel cladding temperature peak does not exceed short-term accident limits. Consequently, the HI-STAR System integrity during the most severe fire event followed by a post-fire cooldown phase is not compromised. In Table 3.5.4, a summary of peak HI-STAR System component temperatures during fire and post-fire accident conditions is provided. The calculated results demonstrate that the HI-

STAR System is in compliance with 10CFR71 thermal requirements for hypothetical accident conditions of transport.



Table 3.5.1

SUMMARY OF TEMPERATURE-DEPENDENT FORCED CONVECTION  
HEAT TRANSFER CORRELATION PARAMETERS FOR AIR

<b>Parameter</b>	<b>Trend with Increasing Temperatures</b>	<b>Criteria to Maximize <math>h_{fc}</math></b>	<b>Conservative Parameter Value</b>	<b>Evaluated At</b>
Temperature Range	100°F-1475°F	NA	NA	NA
Density	Decreases	Reynolds Number	High	100°F
Viscosity	Increases	Reynolds Number	Low	100°F
Conductivity ( $K_f$ )	Increases	$h_{fc}$ Proportional to $K_f$	High	1475°F

Table 3.5.2

## SUMMARY OF HYPOTHETICAL FIRE ACCIDENT INPUTS

	<b>Steady-State Initial<sup>†</sup> Condition</b>	<b>30-minute Fire</b>	<b>Post-Fire Equilibrium</b>
1. Conduction through Holtite	No	Yes	No
2. Holtite Region Conductivity Reduction (Loss of Radial Connectors)	No	No	Yes
3. Insolation	Yes	Yes	Yes
4. Radiation Heat Transfer	Yes	Yes	Yes
5. Surface Convection	Natural	Forced	Natural
6. Impact Limiters Installed <sup>††</sup>	Yes	Yes (crushed)	Yes (crushed)
7. Surface Emissivity	0.85	0.9	0.66

---

<sup>†</sup> A bounding initial temperature condition is imposed for fire transient analysis.

<sup>††</sup> Based on minimum 15,000 lbs impact limiter weight modeled as a solid aluminum cap to maximize heat input to cask.

Table 3.5.3

PROPRIETARY INFORMATION WITHHELD PER 10CFR2.390

Table 3.5.4

PROPRIETARY INFORMATION WITHHELD PER 10CFR2.390

LIST OF MONITORED POINTS:	
①	- ACTIVE FUEL MID-HEIGHT
②	- MPC SHELL
③	- HOLTITE INNER FACE
④	- HOLTITE OUTER FACE
⑤	- DRAIN PORT PLUG
⑥	- OVERPACK LID BOLT
⑦	- OVERPACK LID SEALS
⑧	- VENT PORT PLUG
⑨	- IMPACT LIMITER SURFACE

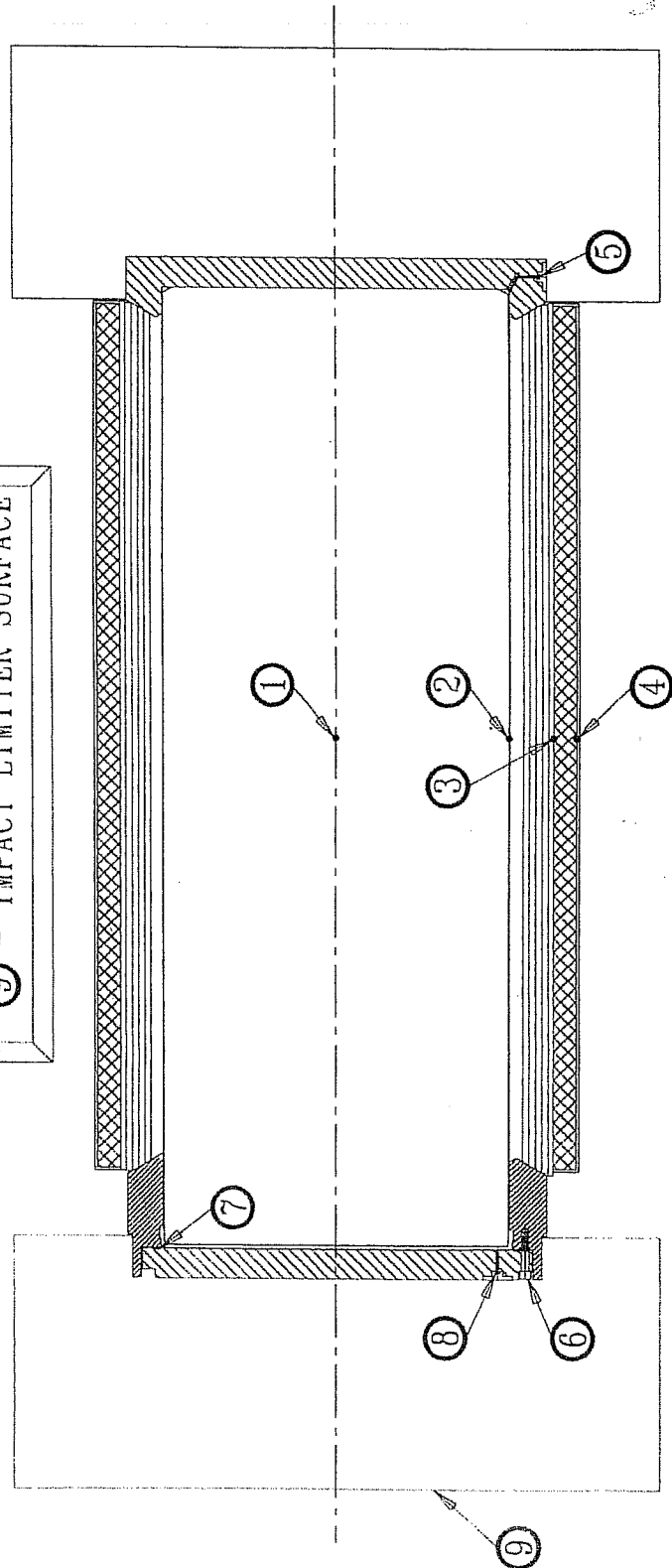


FIGURE 3.5.1; LOCATION OF HI-STAR 100 PACKAGE CONTROL POINTS MONITORED DURING HYPOTHETICAL FIRE ACCIDENT CONDITION

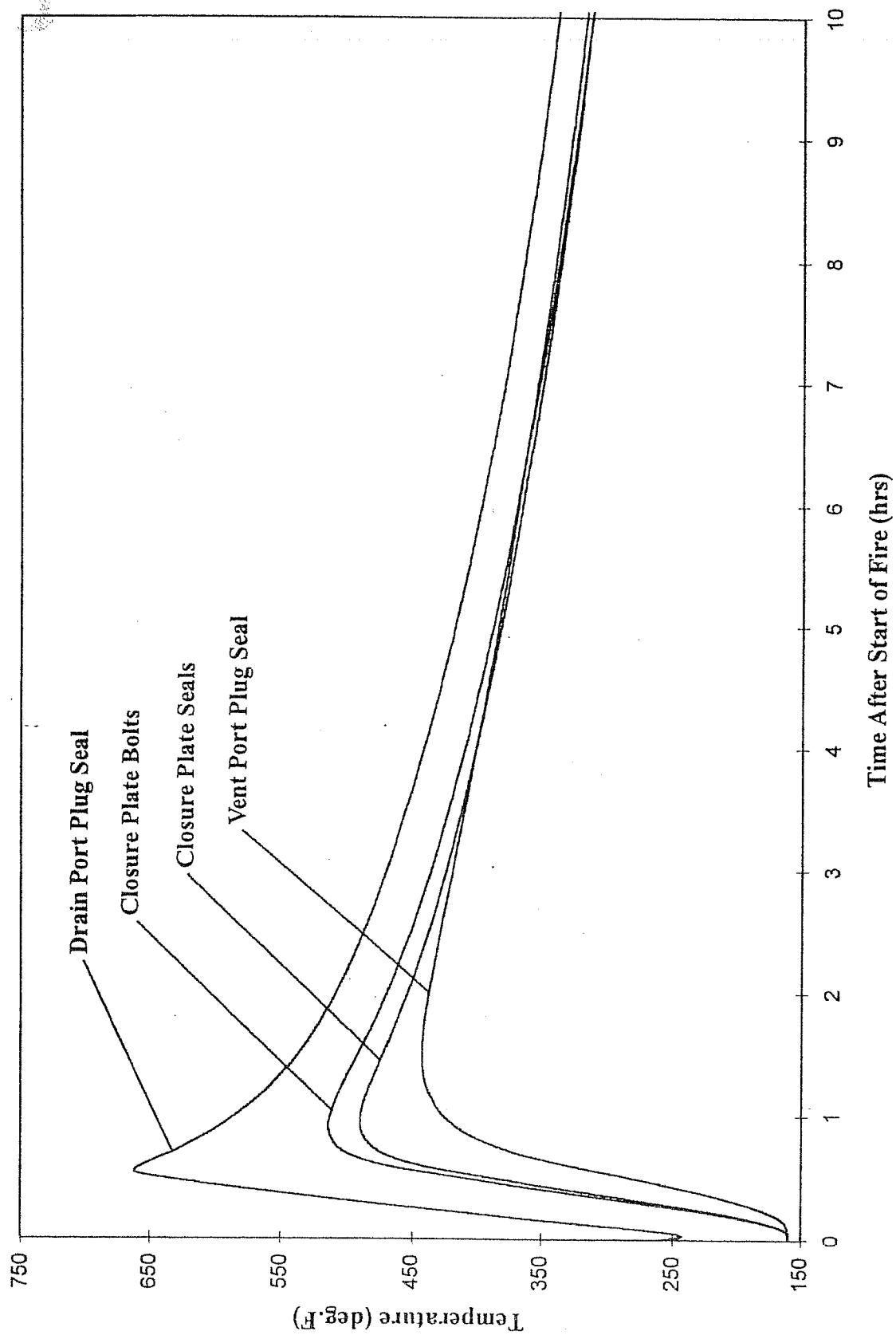


FIGURE 3.5.2; HI-STAR 100 PACKAGE CONTAINMENT BOUNDARY COMPONENTS FIRE ACCIDENT  
TRANSIENT TEMPERATURE RESPONSE

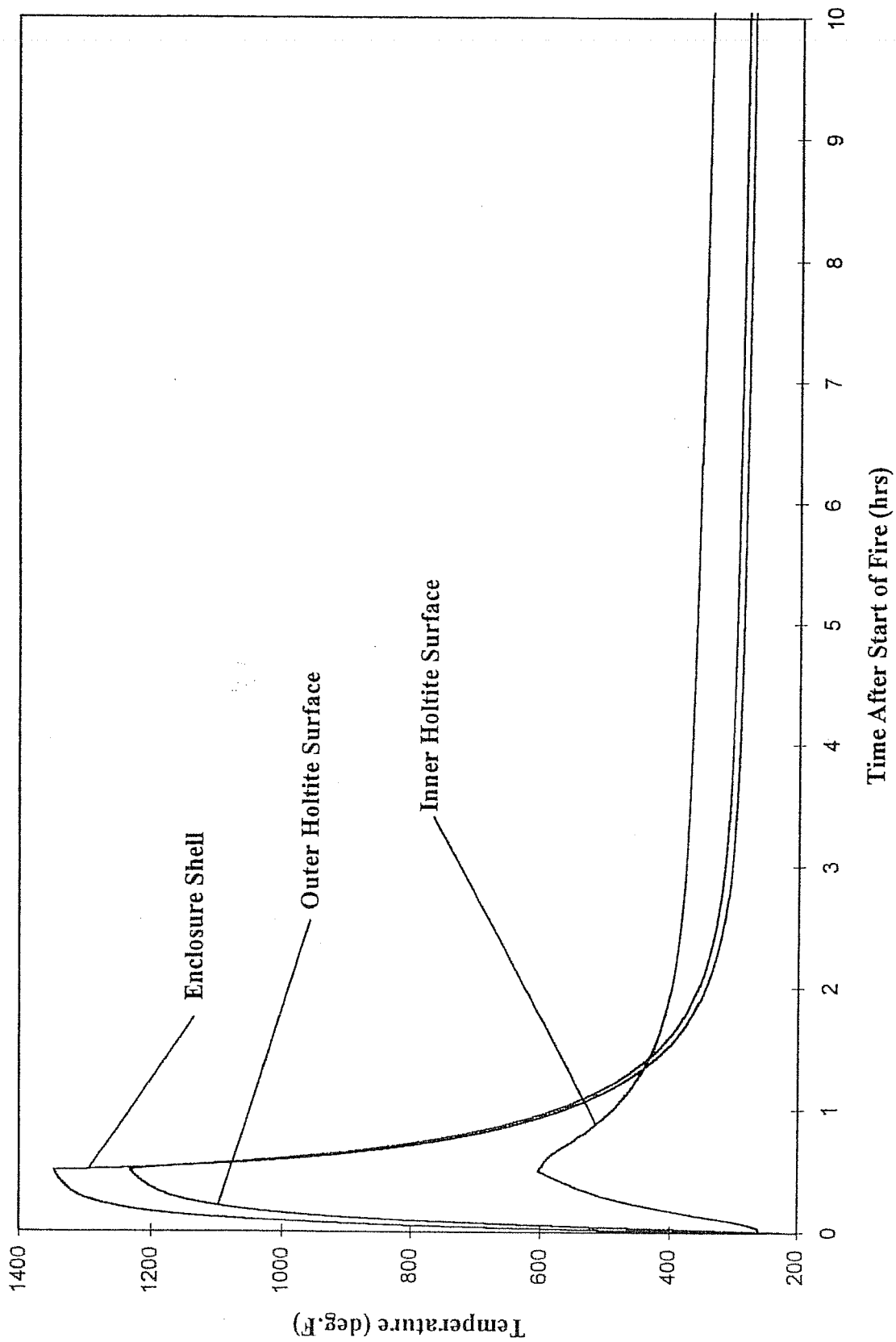


FIGURE 3.5.3; HI-STAR 100 PACKAGE NEUTRON SHIELDING REGION FIRE ACCIDENT TRANSIENT TEMPERATURE RESPONSE

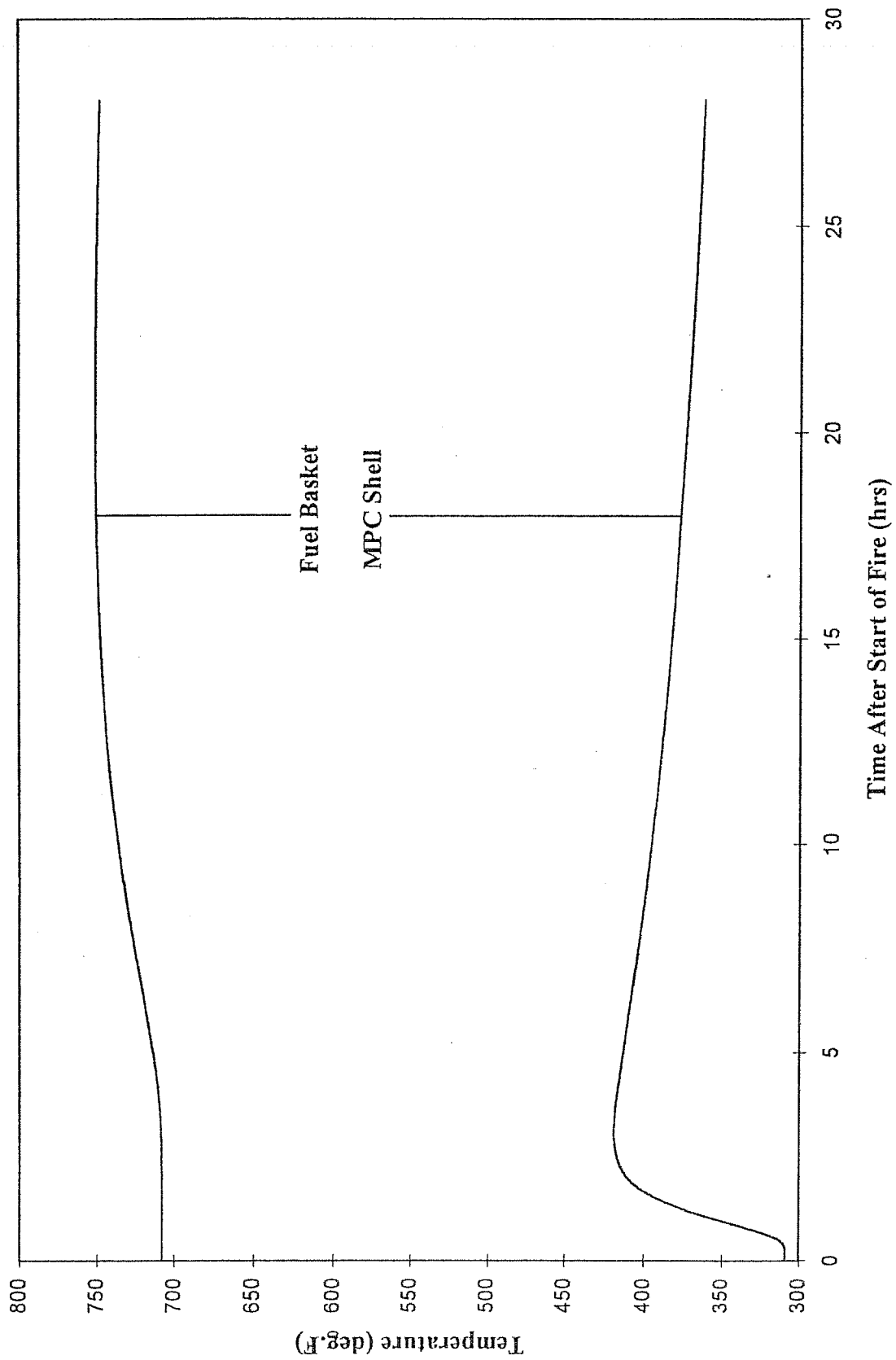


FIGURE 3.5.4; HI-STAR 100 PACKAGE MPC SHELL AND FUEL BASKET FIRE ACCIDENT  
TRANSIENT TEMPERATURE RESPONSE



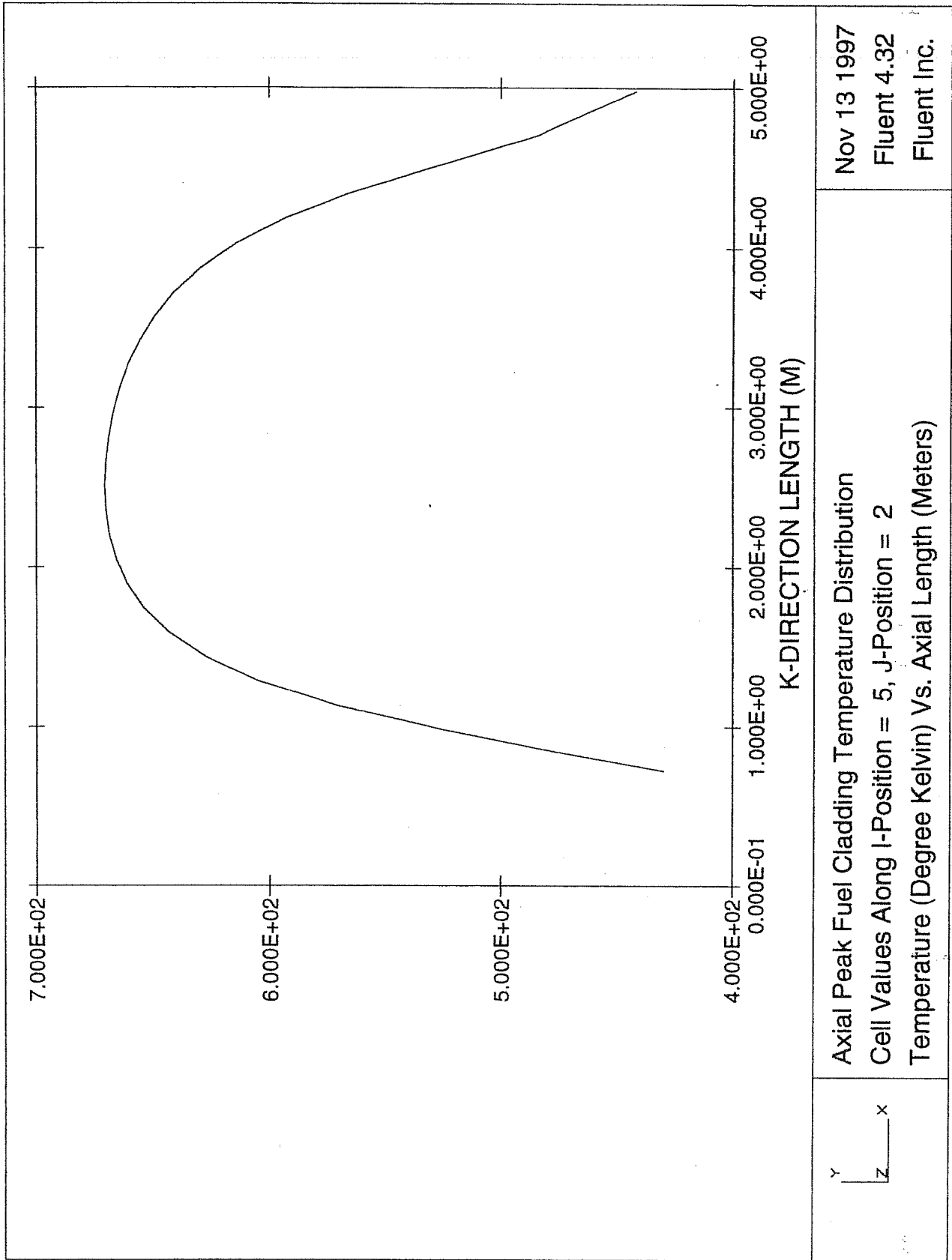


FIGURE 3.5.5: FUEL CLADDING PEAK AXIAL TEMPERATURE DISTRIBUTION DURING POST FIRE COOLDOWN

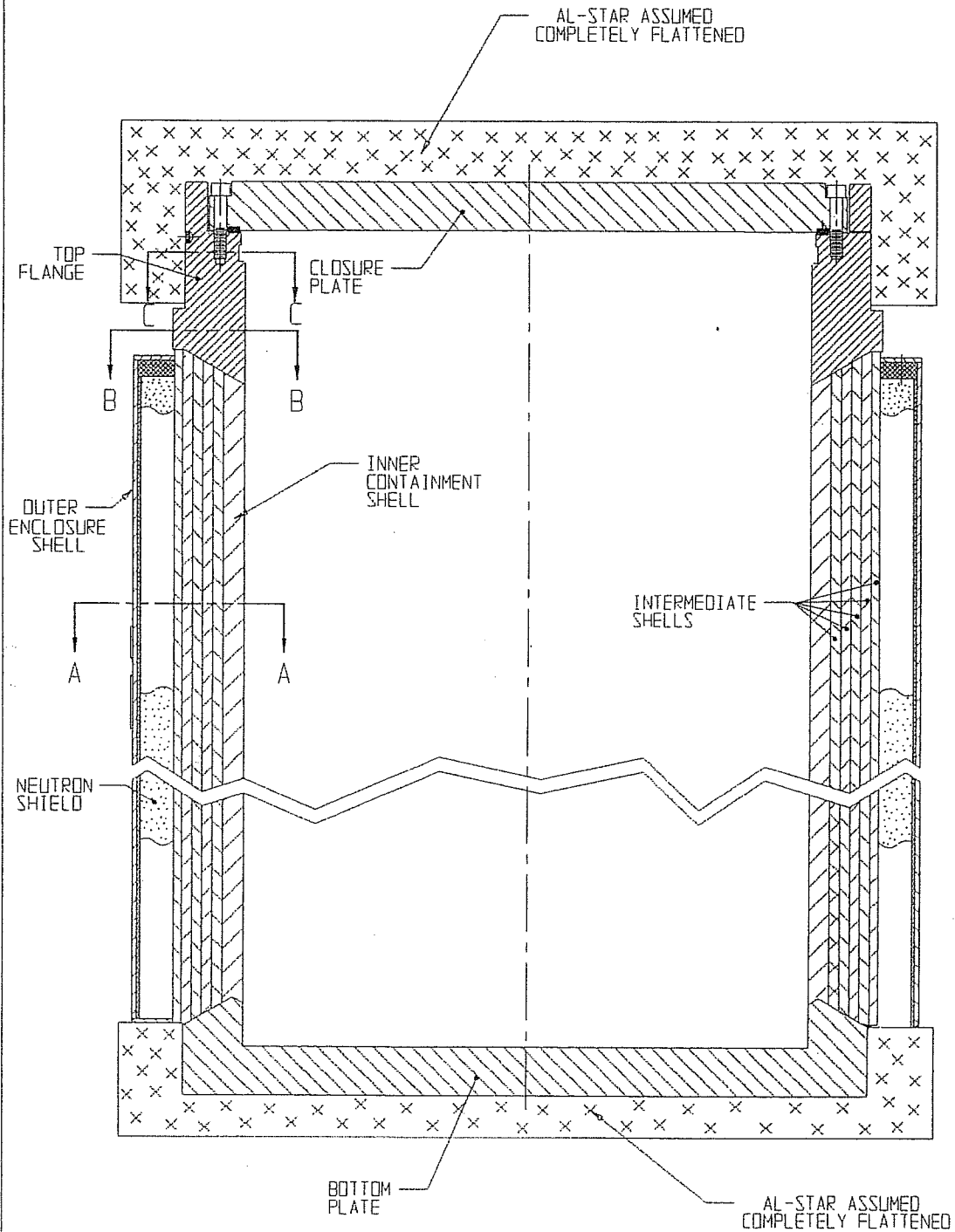


FIGURE 3.5.6; HI-STAR MODEL FOR TRANSPORT FIRE

REPORT HI-951251

REVISION 7

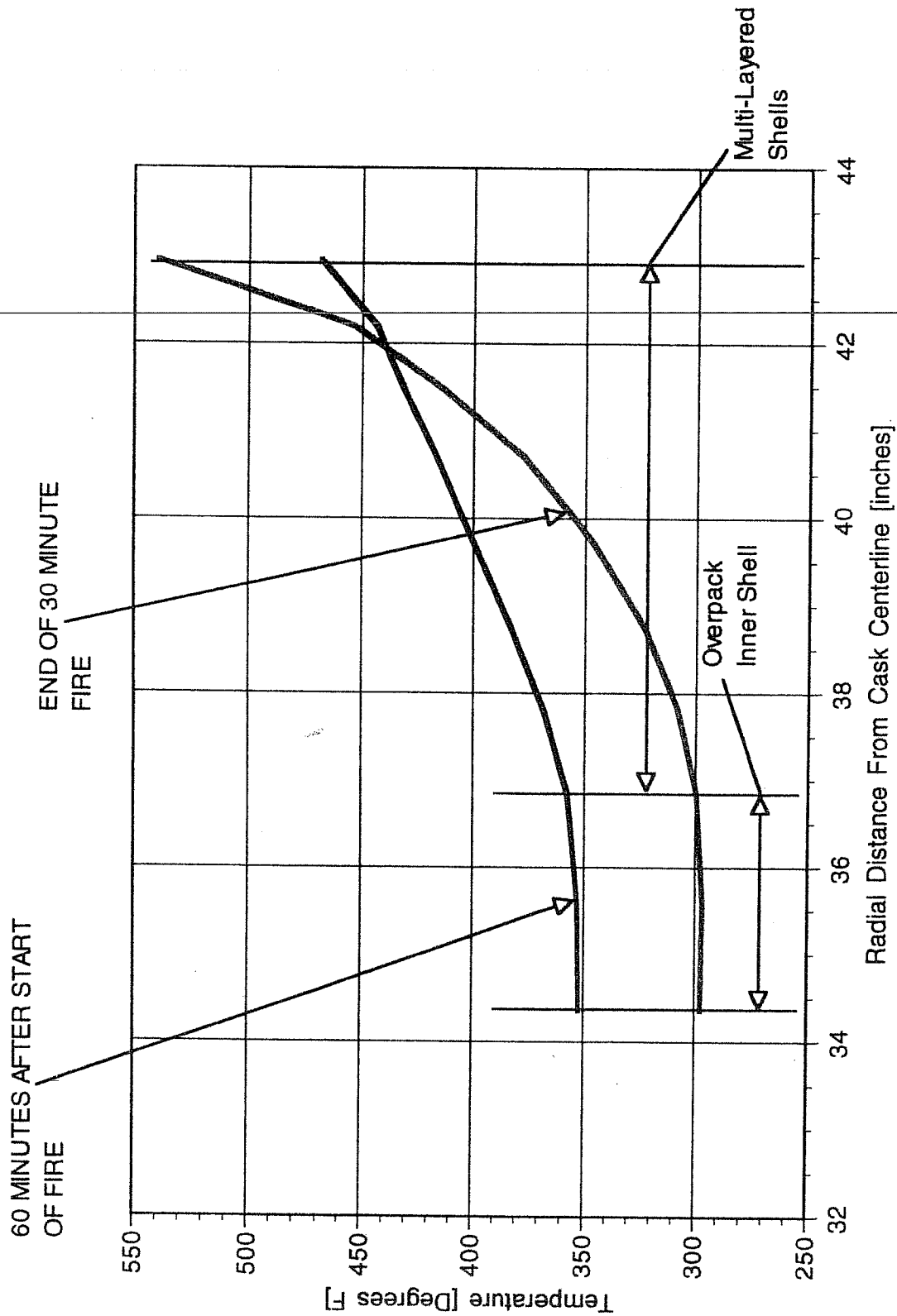


FIGURE 3.5.7: TRANSPORT FIRE CONDITION CONTAINMENT BOUNDARY AND LAYERED SHELLS TEMPERATURE DISTRIBUTIONS (SECTION A-A)

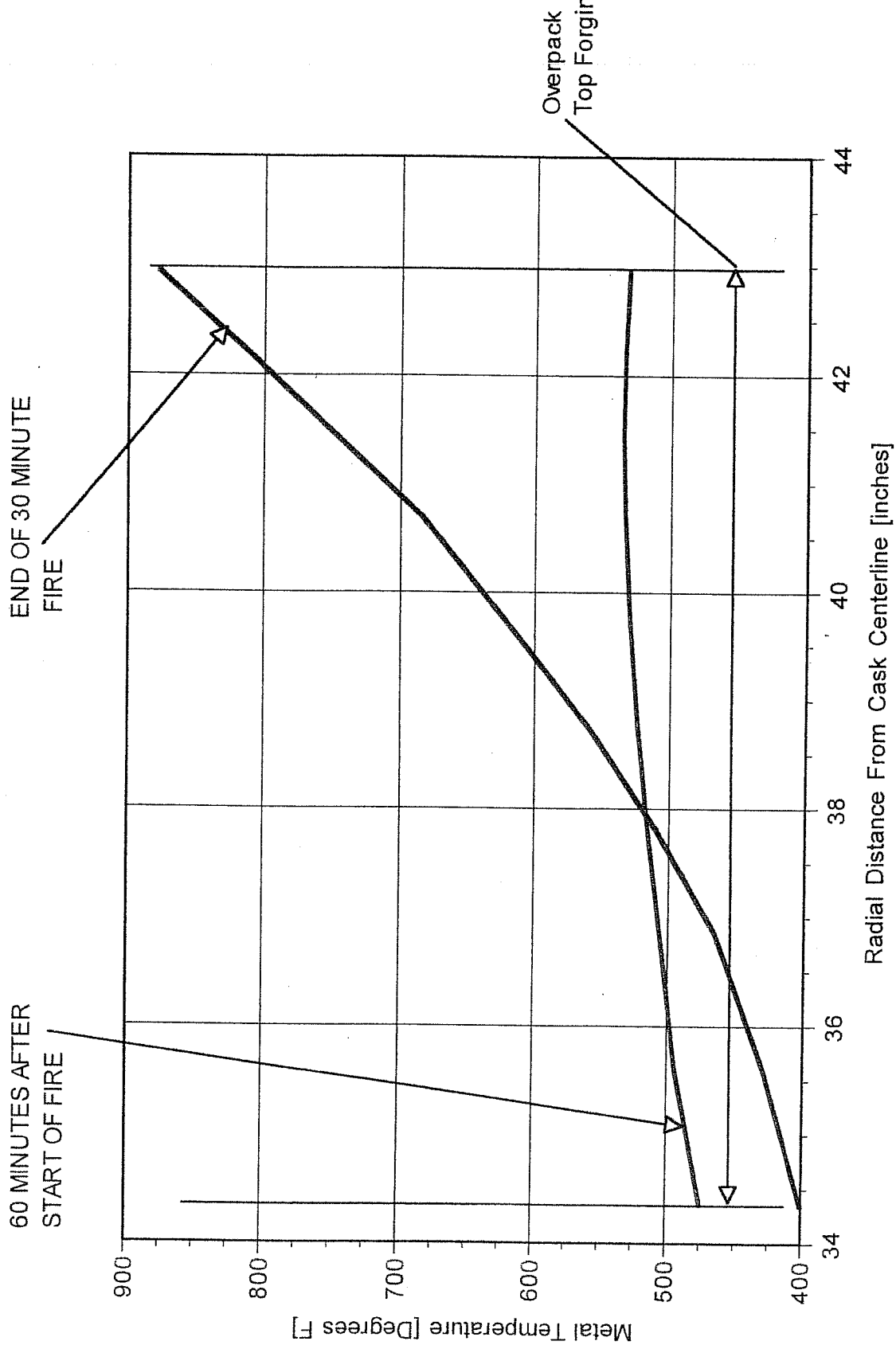


FIGURE 3.5.8: TRANSPORT FIRE CONDITION OVERPACK TOP FORGING TEMPERATURE DISTRIBUTIONS (SECTION B-B)

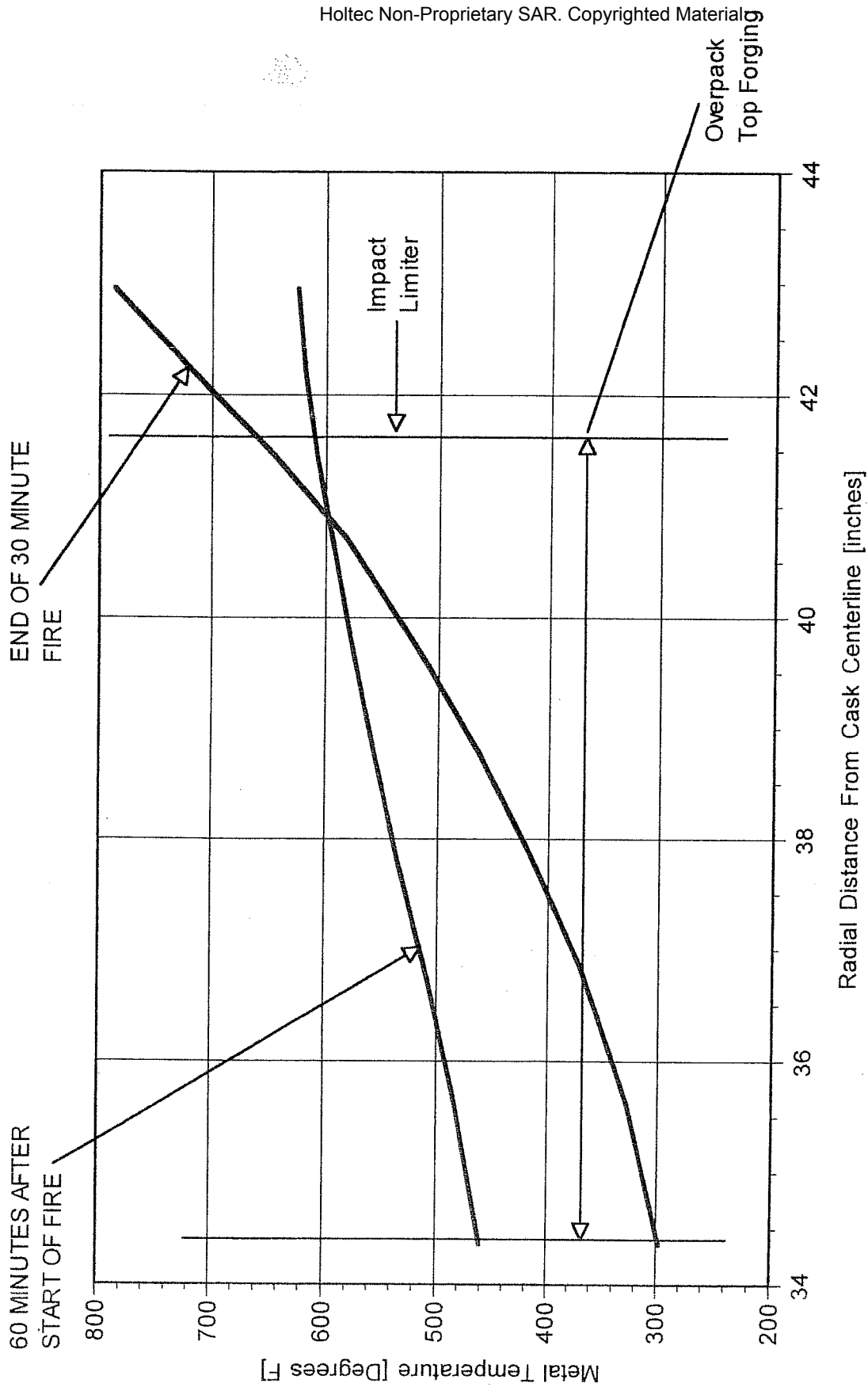


FIGURE 3.5.9: TRANSPORT FIRE CONDITION OVERPACK TOP FORGING TEMPERATURE DISTRIBUTIONS (SECTION C-C)

### 3.6 REGULATORY COMPLIANCE

Section 3.1 defines the requirements of 10CFR71 and ISG-11, Rev. 3 [3.1.5]) that must be met by the HI-STAR cask thermal design. The cask thermal evaluations in support of these requirements are provided in Sections 3.1 through 3.5. In this Section, a summary of the requirements and results of the evaluations are provided.

1. The applicant must include a description of the proposed package in sufficient detail to identify the package accurately and provide a sufficient basis for the evaluation of the package. The description must include, with respect to the packaging: specific materials of construction, weights, dimensions, and fabrication methods of materials specifically used as non-fissile neutron absorbers or moderators; and structural and mechanical means for the transfer and dissipation of heat. The description must include, with respect to the contents of the package: chemical and physical form; maximum normal operating pressure; maximum amount of decay heat; and identification and volumes of any coolants.

A general description of the HI-STAR System is included in Chapter 1. Descriptions of cask materials are presented in Subsection 1.2.1, Section 1.4 and Appendices 1.A, 1.B and 1.C. Shielding materials are specifically addressed in Subsection 1.2.1.4. Cask component weights are presented in Subsections 1.2.1.1 and 2.2. Cask component dimensions are presented in Subsection 1.2.1.2 and in engineering drawings included in Section 1.4. The transfer and dissipation of heat are discussed generally in Subsection 1.2.1.6, and in detail in this chapter.

General descriptions of and requirements for fuel assemblies for transport are presented in Subsection 1.2.3, including design basis maximum decay heat load specifications in Subsection 1.2.3.5. Maximum normal operating pressures are reported in Subsection 3.4.4. As stated in Subsection 1.2.1.7, there are no coolant volumes (reservoirs) in the HI-STAR System.

2. A package must be designed, constructed, and prepared for shipment so that under normal conditions of transport there would be no substantial reduction in the effectiveness of the packaging.

The results of thermal evaluations presented in Section 3.4 demonstrate that the HI-STAR System performs as designed under all normal conditions of transport.

3. A package must be designed, constructed, and prepared for shipment so that in still air at 100°F and in the shade, no accessible surface of the package would have a temperature exceeding 185°F in an exclusive use shipment.

Maximum exposed surface temperatures for the HI-STAR System are reported in Subsection 3.4.2. All impact limiter surface temperatures are shown to be below 185°F. The personnel

barrier, described in Chapter 7, renders the hot overpack enclosure shell surfaces inaccessible.

4. Compliance with the permitted activity release limits for a Type B package may not depend on filters or on a mechanical cooling system.

As stated in Section 3.1, all cooling mechanisms in the HI-STAR System are completely passive.

5. With respect to the initial conditions for the events of normal conditions of transport and hypothetical accident conditions, the demonstration of compliance with the requirements of 10CFR71 must be based on the ambient temperature preceding and following the event remaining constant at that value between -20°F and 100°F, which is most unfavorable for the feature under consideration. The initial internal pressure within the containment system must be considered to be the maximum normal operating pressure (MNOP), unless a lower internal pressure consistent with the ambient temperature considered to precede and follow the event is more unfavorable.

Hypothetical fire accident transient calculations for the HI-STAR System are described in Section 3.5. The initial condition for this event corresponds to the most severe steady-state solution for normal conditions of transport, which correspond to a 100°F ambient temperature with full insolation. These same environmental conditions are applied during the post-accident phase of the evaluation as well. All calculated temperatures for this event are below the specified design temperature limits.

Maximum calculated normal condition internal pressures (MNOPs) are reported in Subsection 3.4.4. Maximum calculated hypothetical accident condition internal pressures are reported in Subsection 3.5.4. All calculated MNOPs are below the design pressure limits for the MPC helium retention boundary and the overpack containment boundary.

6. For normal conditions of transport, a heat event consisting of an ambient temperature of 100°F in still air and prescribed insolation must be evaluated.

The maximum temperatures in the HI-STAR System reported in Subsection 3.4.2 correspond to the heat event. All calculated temperatures for this event are below the appropriate design temperature limits. As stated in Subsection 3.4.5, thermal stresses are determined and reported in Chapter 2.

7. For normal conditions of transport, a cold event consisting of an ambient temperature of -40°F in still air and shade must be evaluated.

The minimum temperatures in the HI-STAR System reported in Subsection 3.4.3 correspond to the cold event. All calculated temperatures for this event are below the appropriate design

temperature limits. As stated in Subsection 3.4.5, thermal stresses are determined and reported in Chapter 2.

8. Evaluation for hypothetical accident conditions is to be based on sequential application of the specified events, in the prescribed order, to determine their cumulative effect on a package.

As described in Section 3.5, the HI-STAR System hypothetical accident thermal condition (hydrocarbon fuel/air fire) evaluation incorporates bounding representations of the results of the preceding accident conditions. Specifically, the impact limiters are assumed to be completely crushed (drop event) and the heat transfer effectiveness of the radial channels region is reduced (puncture event). All calculated temperatures for this event are below the appropriate design temperature limits.

9. For hypothetical accident conditions, a thermal event consisting of a fully engulfing hydrocarbon fuel/air fire with an average emissivity coefficient of at least 0.9, with an average flame temperature of at least 1475°F for a period of 30 minutes.

The description of the HI-STAR System hypothetical accident thermal event model (Subsection 3.5.1.1) specifies the fire condition input parameters. All input parameters are in accordance with the requirements of 10CFR71.73(c)(4). All calculated temperatures for this event are below the appropriate design temperature limits.

The thermal evaluations in Sections 3.4, 3.5, 3.I.4 and 3.I.5 demonstrate compliance with ISG-11, Rev. 3 [3.1.5] temperature limits. Specifically, the maximum cladding temperatures for normal transport and accident conditions are below the prescribed limits (normal (752°F) and accident (1058°F)). The thermal evaluations provided in this SAR demonstrate that the HI-STAR and HI-STAR HB System description and evaluation satisfy the thermal requirements of 10 CFR Part 71. Specifically:

- The material properties and component specifications used in the thermal evaluation are sufficient to provide a basis for evaluation of the HI-STAR System against the thermal requirements of 10 CFR Part 71.
- The methods used in the thermal evaluation are described in sufficient detail to permit an independent review, with confirmatory calculations, of the HI-STAR System thermal design.
- The accessible surface temperatures of the HI-STAR System as it will be prepared for shipment satisfy 10 CFR 71.43(g) for exclusive use shipments.
- The HI-STAR System design, construction, and preparations for shipment ensure that the material and component temperatures will not extend beyond the specified allowable limits during normal conditions of transport consistent with 10 CFR 71.71.



- The HI-STAR System design, construction, and preparations for shipment ensure that the material and component temperatures will not exceed the specified allowable temperature limits during hypothetical accident conditions consistent with 10 CFR 71.73.

It is therefore concluded that the thermal design of the HI-STAR System is in compliance with 10 CFR Part 71, and that the applicable design and acceptance criteria have been satisfied. The evaluation of the thermal design provides reasonable assurance that the HI-STAR System will allow safe transport of spent fuel. This conclusion is based on the technical data and analyses presented in this chapter in conjunction with provisions of 10 CFR Part 71, appropriate regulatory guides, applicable codes and standards, and accepted engineering practices.

### 3.7 REFERENCES

- [3.1.1] ANSYS Finite Element Modeling Package, Swanson Analysis Systems, Inc., Houston, PA, 1993.
- [3.1.2] FLUENT Computational Fluid Dynamics Software (Fluent, Inc., Centerra Resource Park, 10 Cavendish Court, Lebanon, NH 03766).
- [3.1.3] Greer et al., “The TN-24P PWR Spent Fuel Storage Cask: Testing and Analyses,” EPRI NP-5128, PNL-6054, UC-85, (April 1987).
- [3.1.4] Deleted.
- [3.1.5] “Cladding Considerations for the Transportation and Storage of Spent Fuel”, Interim Staff Guidance – 11, Revision 3, (11/17/2003).
- [3.2.1] Baumeister, T., Avallone, E.A. and Baumeister III, T., “Marks’ Standard Handbook for Mechanical Engineers”, 8th Edition, McGraw Hill Book Company, 1978.
- [3.2.2] Rohsenow, W.M. and Hartnett, J.P., “Handbook of Heat Transfer,” McGraw Hill Book Company, New York, 1973.
- [3.2.3] Greer et al., “The TN-24P Spent Fuel Storage Cask: Testing and Analyses,” EPRI NP-5128, PNL-6054, UC-85, (April 1987).
- [3.2.4] Rust, J.H., “Nuclear Power Plant Engineering,” Haralson Publishing Company, (1979).
- [3.2.5] Kern, D.Q., “Process Heat Transfer,” McGraw Hill Kogakusha, (1950).
- [3.2.6] "A Handbook of Materials Properties for Use in the Analysis of Light Water Reactor Fuel Rod Behavior", NUREG/CR-0497, (August 1981).
- [3.2.7] “Safety Analysis Report for the NAC Storable Transport Cask,” Docket No. 71-9235.
- [3.2.8] ASME Boiler and Pressure Vessel Code, Section II, Part D, (1995).
- [3.2.9] Jakob, M. and Hawkins, G.A., “Elements of Heat Transfer,” John Wiley & Sons, New York, 1957.
- [3.2.10] “Qualification of METAMIC for Spent-Fuel Storage Application”, EPRI Report 1003137, (October 2001), EPRI, Palo Alto, CA.

- [3.2.11] “Sourcebook for METAMIC Performance Assessment”, Holtec Report HI-2043215, Holtec International, Marlton, NJ, 08053.
- [3.2.12] “Nuclear Systems Materials Handbook, Vol. 1, Design Data”, ORNL TID 26666.
- [3.2.13] “Scoping Design Analyses for Optimized Shipping Casks Containing 1-, 2-, 3-, 5-, 7-, or 10-Year-Old PWR Spent Fuel”, ORNL/CSD/TM-149 TTC-0316, (1983).
- [3.2.14] “Holtite A: Development History and Thermal Performance Data”, Holtec Report HI-2002396, Rev. 3., Holtec International, Marlton, NJ, 08053.
- [3.3.1] “Handbook of Aluminum,” Alcan Aluminum Corporation, 3rd Edition, page 170, (1970).
- [3.3.2] Deleted.
- [3.3.3] Deleted.
- [3.3.4] Deleted.
- [3.3.5] Johnson, Jr., A.B. and Gilbert, E.R., “Technical Basis for Storage of Zircaloy-Clad Spent Fuel in Inert Gases,” PNL-4835, (September 1983).
- [3.3.6] Deleted.
- [3.3.7] Deleted.
- [3.3.8] Lanning and Beyer, “Estimated Maximum Cladding Stresses for Bounding PWR Fuel Rod During Short Term Operations for Dry Cask Storage,” PNNL White Paper, (January 2004).
- [3.4.1] Wooton, R.O. and Epstein, H.M., “Heat Transfer from a Parallel Rod Fuel Element in a Shipping Container,” Battelle Memorial Institute, 1963.
- [3.4.2] Rapp, D., “Solar Energy,” Prentice-Hall, Inc., Englewood Cliffs, NJ, 1981.
- [3.4.3] Sanders et al., “A Method for Determining the Spent-Fuel Contribution to Transport Cask Containment Requirements,” Sandia Report SAND90-2406-TTC-1019UC-820, page II-127, (November 1992).
- [3.4.4] Holman, J.P., “Heat Transfer,” 6th ed., McGraw Hill Book Company, 1986.
- [3.4.5] Hewitt, G.F., Shires, G.L., and Bott, T.R., “Process Heat Transfer,” CRC Press,

(1994).

- [3.4.6] Chandrasekhar, S., “Hydrodynamic and Hydromagnetic Stability,” Dover, (1961).
- [3.4.7] Gradshteyn, I.S. and Ryzhik, I.M., “Table of Integrals Series and Products,” Academic Press, Fourth Edition, page 366, (1965).
- [3.4.8] Deleted.
- [3.4.9] Deleted.
- [3.4.10] Cormack, D.E., L.G. Leal and J. Imberger, “Natural Convection in a Shallow Cavity With Differentially Heated End Walls. Part 1 Asymptotic Theory,” J. Fluid Mechanics, 65, 209-229, (1974).
- [3.4.11] Cormack, D.E., L.G. Leal and J.H. Seinfeld, “Natural Convection in a Shallow Cavity With Differentially Heated End Walls. Part 2 Numerical Solutions,” J. Fluid Mechanics, 65, 231-246, (1974).
- [3.4.12] Imberger, J., “Natural Convection in a Shallow Cavity with Differentially Heated End Walls. Part 3 Experimental Results,” J. Fluid Mechanics, 65, 247-260, (1974).
- [3.4.13] Hagrman, Reymann and Mason, “MATPRO-Version 11 (Revision 2) A Handbook of Materials Properties for Use in the Analysis of Light Water Reactor Fuel Rod Behavior,” NUREG/CR-0497, Tree 1280, Rev. 2, EG&G Idaho, August 1981.
- [3.4.14] Deleted.
- [3.4.15] Deleted.
- [3.4.16] Deleted.
- [3.4.17] Deleted.
- [3.4.18] Perry and Green, “Perry’s Chemical Engineers’ Handbook”, 6<sup>th</sup> Edition, McGraw-Hill, 1984.
- [3.4.19] Reid, Prauznitz and Poling, “The Properties of Gases and Liquids”, Fourth Edition, McGraw-Hill, 1987.
- [3.5.1] 10CFR Part 71, Paragraph 71.73, (January 1, 1998).

[3.5.2] Jakob, M., “Heat Transfer,” John Wiley & Sons, Inc., page 555, (1967).

## APPENDIX 3.A: CONSERVATISMS IN THE THERMAL ANALYSIS OF THE HI-STAR SYSTEM

### 3.A.1 INTRODUCTION

The HI-STAR 100 overpack is a thick walled, multi-layered cylindrical vessel with an internal cavity suited for emplacement of a cylindrical canister containing spent nuclear fuel (SNF). The canister rests on the inside surface of a horizontally oriented overpack during transport. One principal safety function of the cask is to ensure that the Spent Nuclear Fuel (SNF) cladding temperatures remain below prescribed regulatory limits. For this purpose a thermal model is articulated with modeling assumptions that overstate the temperature of cask contents and provide a conservative upperbound to cladding temperature field that would be obtained inside the canister. In this appendix, the underlying modeling assumptions are evaluated and an assessment of thermal margins reported.

Storage of SNF in casks is characterized by relatively large temperature elevations above the ambient. The cladding temperature rise is the cumulative sum of temperature increments arising from individual elements of thermal resistance. To assure that cladding temperatures are below regulatory limits with robust margins, analytical assumptions adversely impacting heat transfer are chosen with particular attention given to those temperature increments which form the bulk of the temperature rise. In this appendix, a quantitative estimate of some of the principal conservatisms in the thermal model of the HI-STAR 100 System are presented to provide an insight into the extent of overall conservatism in the predicted peak cladding temperatures.

### 3.A.2 CONSERVATISM IN REPRESENTING HEAT DISSIPATION TO AMBIENT

Heat dissipation from a HI-STAR cask occurs principally by convection and radiation heat transfer to ambient air. The rate of decay heat dissipation from the external surfaces is, of course, influenced by several factors, some of which aid the process (e.g. wind), and others (radiation heating by sun) that oppose it. In the HI-STAR modeling, factors aiding heat transfer are neglected (still air) and those opposing it (insolation) are included. A concomitant effect of assuming no wind is that heat transfer is limited to natural convection cooling. To represent heat transfer from the HI-STAR cask, natural convection correlations for heat transfer (h) from heated surfaces are reported in Chapter 3 (Subsection 3.4.1.1.7). The numerical values obtained for the HI-STAR cask modeling are in the neighborhood of 1 Btu/ft<sup>2</sup>-hr-°F. As we show in the following, these h values are extremely conservative when the effects of wind are considered.

For considering the effects of wind, we present a heat transfer correlation from Jakob [3.A.1] for air flow past a heated cylinder [3.A.1].

$$\text{Nu} = 0.028 \text{ Re}^{0.8} [1 + 0.4 (L_h/L)^{2.75}] \quad [\text{Eq. 1}]$$

where:

L = Length of cylinder

L<sub>h</sub> = Length of heated section

Re = Reynolds number (LVρ/μ)

$V$  = Air velocity  
 $\rho$  = Air density  
 $\mu$  = Air viscosity  
 $Nu$  = Nusselt number ( $hL/k$ )  
 $k$  = Air conductivity

For illustrative purposes, let us consider a slight wind (10 MPH) and representative air properties ( $\rho = 0.075 \text{ lbm/ft}^3$ ,  $k = 0.015 \text{ Btu/ft-hr-}^\circ\text{F}$  and  $\mu = 180 \text{ } \mu\text{P}$ ). The length ( $L$ ) of the HI-STAR overpack cylinder is 203.125 inch (Section 1.4 HI-STAR Drawings). The length of overpack heating ( $L_h$ ) is assumed to be equal to a representative height of active fuel zone (12 ft). Employing consistent units,  $Re$  is computed as:

$$\begin{aligned}
 Re &= 16.92 \text{ ft} * 14.66 \text{ ft/s} * 0.075 \text{ lbm/ft}^3 / 1.2 \times 10^{-5} \text{ lbm/ft-s} \\
 &= 1.5 \times 10^6
 \end{aligned}$$

The Nusselt number is computed by substituting numerical values for  $Re$ ,  $L$  and  $L_h$  in Eq. 1. The numerical value is 2822. From the definition of  $Nu$  ( $=hL/k$ ),  $h$  is computed as  $2.5 \text{ Btu/ft}^2\text{-hr-}^\circ\text{F}$ . In other words, the principal mode of heat transfer – convection cooling of the HI-STAR cask – is approximately 150% greater than the values used in the thermal analysis.

### 3.A.3 CONSERVATISM IN REPRESENTING BASKET AXIAL RESISTANCE

Much of the elevation in fuel cladding temperatures in a HI-STAR cask occurs within the MPC<sup>1</sup>. Therefore, it stands to reason that conservatism in the basket thermal simulation would have a pronounced effect on the conservatism in the final solution. The thermal model of the fuel basket in the HI-STAR was accordingly constructed with a number of conservative assumptions to ensure robust margins. Most notable assumptions in this regard are:

- a) Axial heat dissipation in the fuel pellets ignored
- b) Convection heat transfer in the MPC space ignored

We illustrate these conservatisms by examining one of them (item a) in some detail in the following. It is recognized that the heat emission from a fuel assembly is axially non-uniform. The maximum heat generation occurs at about the mid-height region of the enriched uranium column, and tapers off toward its extremities. The axial heat conduction in the fuel basket would act to diffuse and levelize the temperature field in the basket. The axial conductivity of the basket, quite clearly, is the key determinant in how well the thermal field in the basket would be homogenized. In the interest of conservatism, axial heat dissipation in the fuel pellets is ignored. This assumption has the direct effect of throttling the axial flow of heat and thus of elevating the computed value of mid-height cladding temperature (where the peak temperature occurs) above its actual value. In actuality, the axial conductivity of the fuel basket is greater than used in the analysis. Had the axial conductivity of

<sup>1</sup> See for example temperature results Table 3.4.10 for PWR MPCs wherein the cladding is elevated 386°F above the MPC shell temperature. This elevation is 64% of the cladding temperature rise above ambient (601°F).

the basket been modeled less conservatively in the thermal analysis, the temperature peaking would be depressed and the temperature field would be more uniform.

To estimate the conservatism in restricting the basket axial resistance, we perform a numerical exercise using mathematical perturbation techniques. The axial conductivity ( $K_z$ ) of the MPC is, as explained previously, is higher than used in the analysis ( $K$ ). The thermal solution to the higher axial conductivity problem (i.e.  $K_z > K$ ) is mathematically expressed as a sum of a baseline solution  $T_o$  at  $K$  and a perturbation  $T^*$  which accounts for the higher axial conductivity. From Fourier's Law of heat conduction in solids, a perturbation equation for  $T^*$  is articulated below:

$$K_z \frac{d^2 T^*}{dz^2} = -\Delta K \frac{d^2 T_o}{dz^2}$$

Where,  $\Delta K$  is a perturbation parameter (axial conductivity offset  $\Delta K = K_z - K$ ). The boundary conditions for the perturbation solution are zero slope at peak cladding temperature location ( $dT^*/dz = 0$ ) (which occurs at about the active fuel mid-height) and  $T^* = 0$  at the ends of the active fuel length. The object of this calculation is to compute  $T^*$  where the peak fuel cladding temperature is reached. To this end, the baseline thermal solution  $T_o$  is employed to characterize  $d^2 T_o/dz^2$  for the hottest fuel cell. This is computed as  $(-\Delta T_{ax}/L^2)$  where  $\Delta T_{ax}$  is the cladding temperature rise from the ends of the active fuel length to mid-height and  $L$  is half the active fuel length ( $\sim 6$  ft). Conservatively postulating a lower bound  $\Delta T_{ax}$  of  $300^\circ\text{F}$   $d^2 T_o/dz^2$  is computed as  $-8.33^\circ\text{F}/\text{ft}^2$ . Integrating the perturbation equation shown above, the following formula for  $T^*$  is obtained:

$$T^* = \left( \frac{\Delta K}{K_z} \right) \frac{d^2 T_o}{dz^2} \frac{L^2}{2}$$

Employing a conservative low value for the  $(\Delta K/K_z)$  parameter of 0.05,  $T^*$  is computed as  $-7.5^\circ\text{F}$ . In other words, the baseline HI-STORM solution over predicts the peak cladding temperature by over  $7^\circ\text{F}$ , because of the conservatism in the value of axial conductivity.

### 3.A.4 CONSERVATISM IN REPRESENTING FUEL BASKET CONFIGURATION

The HI-STAR System is designed for normal transport in a horizontal orientation. This orientation ensures physical contact between: (i) Fuel assemblies and the fuel basket, (ii) Fuel basket and MPC (iii) MPC and HI-STAR overpack. From a heat transfer perspective, this is an optimal orientation because (a) Gap resistances are minimized and (b) Heat dissipation is maximized through physical contact. In the MPC modeling, we assume a physical configuration that is opposite of (a) and (b) for the MPC space. This configuration assumes:

- I. Each fuel assembly is levitating coaxially in it's storage cell
- II. Fuel basket is levitating coaxially in the MPC shell

The assumptions described in I and II maximize gap resistance and completely ignore physical contact. In the thermal analysis of the HI-STAR system the fuel storage cell space is modeled with a uniform gap between the fuel assembly envelope and the cell walls (See Figure 3.4.7). The fuel



basket-to-MPC space is modeled as a helium filled concentric annular gap (See Figure 3.4.2). Because gaps depress heat transfer, it follows that deliberately postulating gaps between physically contacting parts considerably elevates the MPC planar resistance and the computed fuel and basket temperatures. In the MPC-to-overpack space, the thermal modeling includes partial recognition of gap reduction (See Sub-section 3.4.1.1.10 for eccentric gap evaluation) and completely ignores physical contact between the MPC and overpack.

### 3.A.5 OTHER CONSERVATISMS

Section 3.4.6 of the SAR lists an array of conservatisms, of which certain unobvious and individually significant items are discussed in detail in this appendix. These conservatisms are primarily intrinsic to the solution methodology or are product of assumptions in the input data. Examples in the latter category are values assumed in the thermal analysis for key inputs such as insolation heat and ambient temperature. Apart from the input data and methodology related conservatisms, the modeling includes assumptions to under represent heat transfer. A listing of such conservatisms is summarized below:

- i) Insolation heating assumed with a bounding absorptivity of 1.0
- ii) Heat dissipation from the HI-STAR overpack ends ignored
- iii) Conduction heat transfer in Holtite is neglected.
- iv) MPCs are assumed to be loaded with the most thermally resistive fuel type in its category (BWR or PWR) as applicable

The assumptions inherent in the FLUENT methodology, in the thermal modeling and in the input data, are estimated to have an aggregate effect of overestimating cladding temperatures by a considerable amount, as estimated in Table 3.A.1.

### 3.A.6 CONCLUSIONS

The foregoing narrative provides a physical description of the many elements of conservatism in the HI-STORM 100 thermal model. The conservatisms may be broadly divided into two categories:

1. Those intrinsic to the FLUENT methodology.
2. Those arising from the input data and thermal modeling.

The conservatism in Category (1) may be identified by reviewing the Holtec International Benchmark Report [3.A.2], which shows that the FLUENT solution methodology, when applied to the prototype cask (TN 24P) over-predicts the peak cladding temperature by as much as 79 °F. and as much as 37°F relative to the PNNL results (see Attachment 1 to Reference [3.A.2]) from their COBRA SFS solution as compared against Holtec's FLUENT solution.

Category (2) conservatisms are those that we have deliberately embedded in the HI-STAR thermal models to ensure that the computed value of the peak fuel cladding temperature is further exaggerated. Table 3.A.1 contains a listing of the major conservatisms in the HI-STAR thermal

model, along with an estimate of the effect (increase) of each on the computed peak cladding temperature. Finally, we note that the computed peak cladding temperatures for all MPCs are also lower than the 400°C limit by varying amounts, which can be viewed as an additional thermal margin in the system.

The cumulative effect of conservatisms listed in Table 3.A.1 would be additive if the thermal resistances were all arrayed in series. In reality some resistances are in series and others in parallel. For obtaining a reasonable estimate of the cumulative effect, a square root of sum of squares of the individual conservatisms is computed and reported in the last row of the Table 3.A.1.

Table 3.A.1

[PROPRIETARY INFORMATION WITHHELD PER 10CFR2.390]

### 3.A.6 REFERENCES

[3.A.1] Jakob, M., “Heat Transfer”, John Wiley & Sons, Inc., (1967).

[3.A.2] “Topical Report on the HI-STAR/HI-STORM Thermal Model and its Benchmarking with Full-Size Cask Test Data”, Holtec Report HI-992252, Rev. 1.

## APPENDIX 3.B: THE FORCED HELIUM DEHYDRATION (FHD) SYSTEM

### 3.B.1 System Overview

The Forced Helium Dehydration (FHD) system is used to remove the remaining moisture in the MPC cavity after all of the water that can practically be removed through the drain line using a hydraulic pump or an inert gas has been expelled in the water blowdown operation. Expelling the water from the MPC using a conventional pump or a water displacement method using inert gas would remove practically all of the contained water except for the small quantity remaining on the MPC baseplate below the bottom of the drain line and an even smaller adherent amount wetting the internal surfaces. A skid-mounted, closed loop dehydration system will be used to remove the residual water from the MPC such that the partial pressure of the trace quantity of water vapor in the MPC cavity gas is brought down to  $\leq 3$  torr. The FHD system, engineered for this purpose, shall utilize helium gas as the working substance.

The FHD system, schematically illustrated in Figure 3.B.1, can be viewed as an assemblage of four thermal modules, namely, (i) the condensing module, (ii) the demister module, (iii) the helium circulator module and (iv) the pre-heater module. The condensing module serves to cool the helium/vapor mixture exiting the MPC to a temperature well below its dew point such that water may be extracted from the helium stream. The condensing module is equipped with suitable instrumentation to provide a direct assessment of the extent of condensation that takes place in the module during the operation of the FHD system. The demister module, engineered to receive partially cooled helium exiting the condensing module, progressively chills the recirculating helium gas to a temperature that is well below the temperature corresponding to the partial pressure of water vapor at 3 torr.

The motive energy to circulate helium is provided by the helium circulator module, which is sized to provide the pressure rise necessary to circulate helium at the requisite rate. The last item, labeled the pre-heater module, serves to pre-heat the flowing helium to the desired temperature such that it is sufficiently warm to boil off any water present in the MPC cavity.

The pre-heater module, in essence, serves to add supplemental heat energy to the helium gas (in addition to the heat generated by the stored SNF in the MPC) so as to facilitate rapid conversion of water into vapor form. The heat input from the pre-heater module can be adjusted in the manner of a conventional electric heater so that the recirculating helium entering the MPC is sufficiently dry and hot to evaporate water, but not unduly hot to place unnecessary thermal burden on the condensing module.

The FHD system described in the foregoing performs its intended function by continuously removing water entrained in the MPC through successive cooling, moisture removal and reheating of the working substance in a closed loop. In a classical system of the FHD genre, the moisture removal operation occurs in two discrete phases. In the beginning of the FHD system's operation (Phase 1), the helium exiting the MPC is laden with water vapor produced by boiling of the entrained bulk water. The condensing module serves as the principal device to condense out the water vapor from the helium stream in Phase 1. Phase 1 ends when all of the bulk water in the MPC cavity is

vaporized. At this point, the operation of the FHD system moves on to steadily lowering the relative humidity and bulk temperature of the circulating helium gas (Phase 2). The demoisturizer module, equipped with the facility to chill flowing helium, plays the principal role in the dehydration process in Phase 2.

### 3.B.2 Design Criteria

The design criteria set forth below are intended to ensure that design and operation of the FHD system will drive the partial pressure of the residual vapor in the MPC cavity to  $\leq 3$  torr if the temperature of helium exiting the demoisturizer has met the value and duration criteria provided in the HI-STORM technical specifications. The FHD system shall be designed to ensure that during normal operation (i.e., excluding startup and shutdown ramps) the following criteria are met:

- i. The temperature of helium gas in the MPC shall be at least 15°F higher than the saturation temperature at coincident pressure.
- ii. The pressure in the MPC cavity space shall be less than or equal to 60.3 psig (75 psia).
- iii. The recirculation rate of helium shall be sufficiently high (minimum hourly throughput equal to ten times the nominal helium mass backfilled into the MPC for fuel storage operations) so as to produce a turbulated flow regime in the MPC cavity.
- iv. The partial pressure of the water vapor in the MPC cavity will not exceed 3 torr if the helium temperature at the demoisturizer outlet is  $\leq 21^\circ\text{F}$  for a period of 30 minutes.

In addition to the above system design criteria, the individual modules shall be designed in accordance with the following criteria:

- i. The condensing module shall be designed to de-vaporize the recirculating helium gas to a dew point of 120°F or less.
- ii. The demoisturizer module shall be configured to be introduced into its helium conditioning function after the condensing module has been operated for the required length of time to assure that the bulk moisture vaporization in the MPC (defined as Phase 1 in Section 2.B.1) has been completed.
- iii. The helium circulator shall be sized to effect the minimum flow rate of circulation required by the system design criteria described above.
- iv. The pre-heater module shall be engineered to ensure that the temperature of the helium gas in the MPC meets the system design criteria described above.

### 3.B.3 Analysis Requirements

The design of the FHD system shall be subject to the confirmatory analyses listed below to ensure

that the system will accomplish the performance objectives set forth in this FSAR.

- i. System thermal analysis in Phase 1: Characterize the rate of condensation in the condensing module and helium temperature variation under Phase 1 operation (i.e., the scenario where there is some unevaporated water in the MPC) using a classical thermal-hydraulic model wherein the incoming helium is assumed to fully mix with the moist helium inside the MPC.
- ii. System thermal analysis in Phase 2: Characterize the thermal performance of the closed loop system in Phase 2 (no unvaporized moisture in the MPC) to predict the rate of condensation and temperature of the helium gas exiting the condensing and the demister modules. Establish that the system design is capable to ensure that partial pressure of water vapor in the MPC will reach  $\leq 3$  torr if the temperature of the helium gas exiting the demister is predicted to be at a maximum of 21°F for 30 minutes.
- iii. Fuel Cladding Temperature Analysis: A steady-state thermal analysis of the MPC under the forced helium flow scenario shall be performed using the methodology described in SAR Subsections 3.4.1.1.1 through 3.4.1.1.4 with due recognition of the forced convection process during FHD system operation. This analysis shall demonstrate that the peak temperature of the fuel cladding under the most adverse condition of FHD system operation (design maximum heat load, no moisture, and maximum helium inlet temperature), is below the peak cladding temperature limit for normal conditions of storage for the applicable fuel type (PWR or BWR) and cooling time at the start of dry storage.

#### 3.B.4 Acceptance Testing

The first FHD system designed and built for the MPC drying function required by HI-STORM's technical specifications shall be subject to confirmatory testing as follows:

- a. A representative quantity of water shall be placed in a manufactured MPC (or equivalent mock-up) and the closure lid and RVOAs installed and secured to create a hermetically sealed container.
- b. The MPC cavity drying test shall be conducted for the worst case scenario (no heat generation within the MPC available to vaporize water).
- c. The drain and vent line RVOAs on the MPC lid shall be connected to the terminals located in the pre-heater and condensing modules of the FHD system, respectively.
- d. The FHD system shall be operated through the moisture vaporization (Phase 1) and subsequent dehydration (Phase 2). The FHD system operation will be stopped after the temperature of helium exiting the demister module has been at or below 21°F for thirty minutes (nominal). Thereafter, a sample of the helium gas from the MPC will be

extracted and tested to determine the partial pressure of the residual water vapor in it. The FHD system will be deemed to have passed the acceptance testing if the partial pressure in the extracted helium sample is less than or equal to 3 torr.

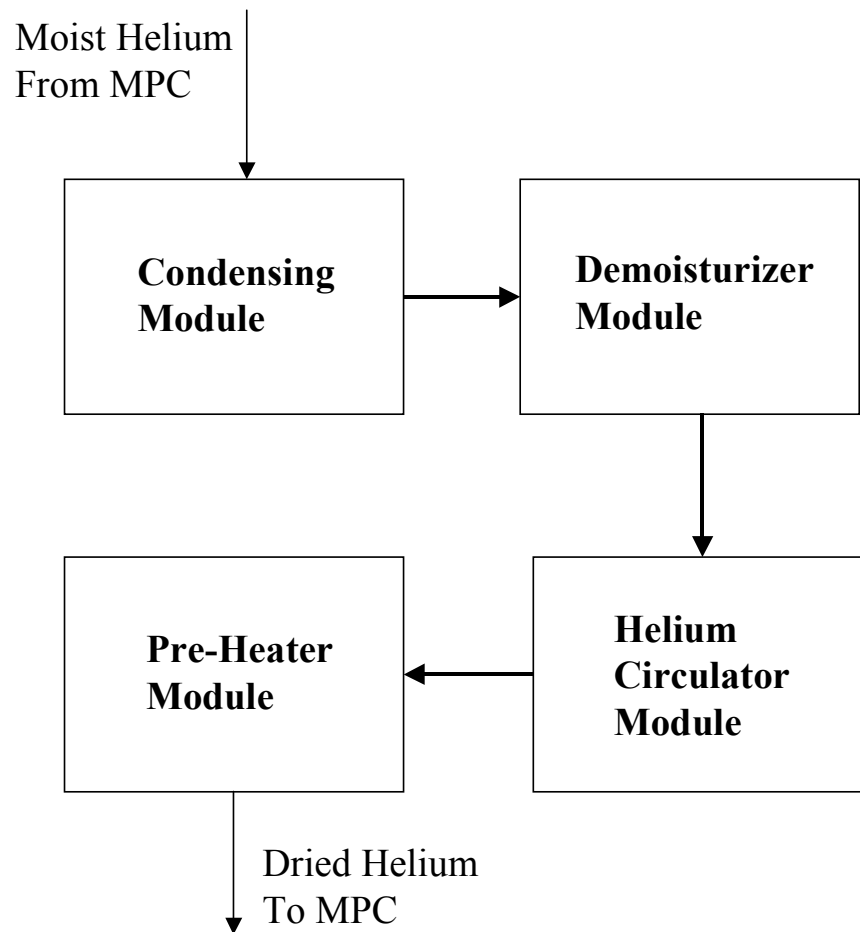


FIGURE 3.B.1: SCHEMATIC OF THE FORCED HELIUM DEHYDRATION SYSTEM



## SUPPLEMENT 3.I

### THERMAL EVALUATION OF **THE HI-STAR HB PACKAGE WITH MPC-HB**

#### 3.I.0 INTRODUCTION

The Humboldt Bay HI-STAR HB cask is licensed to store permanently shutdown Unit 3 BWR spent nuclear fuel (SNF) **and Greater-Than-Class C waste (GTCC)** at the Humboldt Bay ISFSI. In this supplement compliance of the HI-STAR HB cask to 10CFR71 and ISG-11, Rev. 3 thermal requirements are evaluated for transport. The analysis considers passive rejection of decay heat from the spent nuclear fuel **and GTCC** to an environment under the 10CFR71 mandated ambient conditions for normal and accident scenarios. The regulatory requirements and acceptance criteria for transport evaluation are listed in Section 3.0.

#### 3.I.1 DISCUSSION

The HI-STAR HB, with the exception noted below, is an essentially shortened version of the HI-STAR 100 cask. The HI-STAR 100 cask thermal design features discussed in Section 3.1 are applicable to the HI-STAR HB design. Prior to sealing the HI-STAR HB MPC lid, the MPC-HB is backfilled with helium to Table 1.I.2 specifications.

The HI-STAR HB overpack design features a neutron shield placed in the annulus region between the multi-layered shells and enclosure shell without connecting ribs. (See HI-STAR HB overpack dwg. 4082, Sht. 6 included in the Chapter 1 Supplement, Section 1.I.4). This feature is unique to the “HB” version of the generic HI-STAR 100 overpack design. As the annular shield is a thick layer of a low conductivity material, Holtite A, it retards the lateral transmission of fire heat during hypothetical accidents, thus minimizing the heating of HI-STAR HB package internals and the stored fuel during fires.

**The HI-STAR HB GTCC cask consists of a HI-STAR HB GTCC overpack and a GWC-HB. See HI-STAR HB GTCC overpack drawing 10315 and GWC-HB drawing 10316 (revisions listed in Chapter 1 Supplement II) for details. Prior to sealing the GWC-HB lid, the GWC-HB is backfilled with helium.**

**The Humboldt Bay GTCC contained in the GWC-HB has a negligible heat source term, particularly as compared to that of a fuel-bearing cask. As such the heat load of the HI-STAR HB GTCC cask is limited to insolation heat, so the resulting temperature and pressure fields are bounded by those of the HI-STAR HB and no further thermal analysis is required.**

#### 3.I.2 THERMAL PROPERTIES OF MATERIALS

The thermophysical data compiled in Section 3.2 of the SAR provides the required materials information except for Holtite thermal conductivity. Holtite conductivity data [3.I.1] is provided in Table 3.I.1.

Holtite-A is qualified to withstand the effects of much elevated temperatures and high radiation exposures reached in the generic HI-STAR 100 Cask (heat loads up to 20 kW). As the HI-STAR HB package heat loads (2 kW) are dwarfed by the generic design, much larger margins against thermal and radiation degradation are realized. The Holtite-A thermal characterization and qualification testing for use in dry storage casks are archived in references [3.I.1] and [3.I.2].

### 3.I.3 TECHNICAL SPECIFICATIONS OF COMPONENTS

The HI-STAR materials and components required to be maintained within safe operating limits are listed in Section 3.3. The temperature limits specified in this section are adopted for transport evaluation.

### 3.I.4 NORMAL TRANSPORT THERMAL EVALUATION

The HI-STAR HB cask features an all-welded multi-purpose canister (MPC) containing spent nuclear fuel emplaced in a bolted steel overpack. From a thermal standpoint the HI-STAR HB cask is identical to the generic HI-STAR cask except for the following differences:

- a) The height of the cask is reduced to be compatible with the short-length Humboldt Bay fuel.
- b) To accommodate the narrow width Humboldt Bay fuel the fuel storage cells count is increased to 80.
- c) Radial connectors in the neutron shield region are replaced with a continuous neutron shield ring to minimize streaming.

The thermal payload of the HI-STAR HB transport package is given in Table 3.I.2.

#### 3.I.4.1 Thermal Model

Thermal modeling of the HI-STAR HB adopts the same methodology used for HI-STAR thermal evaluation. An overview of the thermal methodology is given in the following.

Transport of heat from the HI-STAR HB to the ambient is analyzed broadly using three connected thermal models.

- i. The first model considers transport of heat from the fuel assembly to the basket cell walls. This model recognizes the combined effects of conduction (through helium) and radiation using finite element methods.
- ii. The second model considers heat transport within an MPC cross section by conduction and radiation. This model computes an effective cross sectional conductivity of the fuel basket.
- iii. The third model deals with the transmission of heat from the MPC exterior surface to the external environment (heat sink). From the MPC shell to the cask exterior surface, heat is conducted through an array of concentric shells

representing the MPC-to-overpack helium gap, the overpack inner shell, the intermediate shells, the Holtite-A neutron shielding and finally the overpack outer shell. Heat rejection from the outside cask surfaces to ambient air is considered by accounting for natural convection and thermal radiation heat transfer from the cask external surfaces. Insolation on exposed cask surfaces is based on 12-hour levels prescribed in 10CFR71, averaged over a 24-hour period.

Detailed descriptions of the above models are provided in Section 3.4. Using these steps, effective properties of the fuel, MPC and HI-STAR HB overpack are obtained and used in an axi-symmetric rendering of the cask geometry. For a conservative portrayal of cask temperatures the thermal evaluation incorporates the following assumptions:

- a) Fuel basket conductivity is understated.
- b) Neutron shield conductivity is understated.
- c) A theoretical bounding absorptivity of 1.0 assumed for insulation.
- d) Heat dissipation by internal helium motion is ignored.
- e) The ends of the overpack are assumed to be insulated.
- f) To conservatively bound the hottest fuel the cask decay heat is non-uniformly distributed with a robust peaking in the interior.

Thermal analysis results are provided in the next section.

#### 3.I.4.1.1 Evaluation of Damaged and Undamaged Fuel Assemblies

The HI-STAR HB cask is designed to store damaged and undamaged fuel assemblies (“Damaged” and “Undamaged Fuel Assemblies” are defined in Table 1.0.1). From a thermal perspective, damaged fuel assemblies storage is limiting because damaged fuel must be placed in a Damaged Fuel Container (DFC) which blocks radiation heat dissipation from the fuel assemblies. To bound the HI-STAR HB thermal condition in a conservative manner all fuel assemblies placed in the HI-STAR HB cask are assumed to be “Damaged” and in DFCs.

#### 3.I.4.2 Maximum Temperatures

As discussed in the previous section, an axi-symmetric model of the HI-STAR HB is constructed for thermal evaluation. This model adopts the same methodology used in the generic HI-STAR cask thermal analysis. To this model design basis heat loads (Table 3.I.2) and 10CFR71 inputs (100°F ambient temperature and Table 3.4.7 insolation) are imposed and steady state cask temperatures obtained. The results are provided in Table 3.I.3.

#### 3.I.4.3 Minimum Temperatures

As specified in 10CFR71, the minimum ambient temperature conditions for the HI-STAR System are -20°F and a cold environment at -40°F. The HI-STAR System design does not have any minimum decay heat load restrictions for transport. Therefore, under bounding cold conditions (zero decay heat and no insolation), the cask temperatures will approach ambient conditions. All HI-STAR System materials of construction satisfactorily perform their intended

function at these cold temperatures. Evaluations in Chapter 2 demonstrate the acceptable structural performance of the overpack and MPC steel materials at low temperature. Shielding and criticality functions of the cask materials are unaffected by cold.

#### 3.I.4.4 Maximum Internal Pressures

The Humboldt Bay multi-purpose canisters (MPC HB) are pressurized with helium prior to sealing the lid ports. In Table 3.I.4 the initial backfill pressures are listed. In response to higher than ambient transport temperatures the helium pressure rises above the initial backfill pressures. In accordance with NUREG-1617 the maximum normal operating pressure (MNOP) is computed assuming normal operating temperatures and 3% fuel rods are ruptured. For conservatism, the MPC HB is assumed to be backfilled at the maximum backfill pressure (See Table 3.I.4). The normal transport pressures are provided in Table 3.I.5.

#### 3.I.4.5 Maximum Thermal Stresses

Thermal expansion induced mechanical stresses are evaluated, using bounding temperature distributions, in Chapter 2.

#### 3.I.4.6 Evaluation of Normal Transport

Based on a comparison of HI-STAR HB normal transport conditions (Tables 3.I.3 and 3.I.5) with generic HI-STAR temperatures and pressures (Tables 3.4.10, 3.4.11 and 3.4.15) we conclude the following:

- a) Fuel temperatures are bounded by generic HI-STAR.
- b) Containment boundary temperatures are bounded by generic HI-STAR.
- c) Surface temperatures are bounded by generic HI-STAR.
- d) MNOP is bounded by generic HI-STAR.

As the HI-STAR HB temperatures and pressures are bounded by the generic HI-STAR package transport evaluation and the HI-STAR complies with 10CFR Part 71 and ISG 11, Rev. 3 requirements (See Section 3.6) we conclude that the HI-STAR HB package is in compliance with the 10CFR Part 71 and ISG 11, Rev. 3 requirements for normal transport.

### 3.I.5 HYPOTHETICAL ACCIDENT THERMAL EVALUATION

In compliance with 10CFR71 requirements, the HI-STAR System is evaluated for hypothetical accident conditions. The accident scenarios are: (1) a 30 foot free drop onto an unyielding surface; (2) a 40-inch drop onto a mild steel bar; and (3) exposure to a 30-minute fire at 1475°F. The effects of the drop accidents (items (1) and (2)) are evaluated in Chapter 2. In this section the effect of a 30-minute fire are evaluated.

The HI-STAR HB is a short height version of the generic HI-STAR overpack. This version includes a solid shell of a low conductivity material (Holtite-A) in the neutron shield region. The HI-STAR HB initial conditions (normal transport) are bounded by HI-STAR generic

temperatures and pressures. Based on the above information the following observations apply to HI-STAR HB fire evaluation:

Observation	Basis
Fire heat input to HI-STAR HB overpack is bounded by the generic HI-STAR	Exposed area of overpack is bounded by generic design
Rate of through-overpack fire heat transmission is bounded by generic HI-STAR	HI-STAR HB overpack design features a neutron shield ring without ribs (See discussion in Section 3.I.1)
Start of fire conditions are bounded by generic HI-STAR	See 3.I.4.6

Based on the observations above we conclude that the generic HI-STAR fire evaluation is bounding and the HI-STAR HB package complies with the 10CFR Part 71 requirements for hypothetical accidents.

### 3.I.6 REGULATORY COMPLIANCE

The Humboldt Bay cask evaluations for normal transport and hypothetical accident conditions show that the HI-STAR HB is bounded by the generic HI-STAR (See Sections 3.I.4.6 and 3.I.5). Accordingly, the regulatory compliance evaluated in Section 3.6 for HI-STAR cask applies to HI-STAR HB.

### 3.I.7 REFERENCES

- [3.I.1] “Holtite A: Development History and Thermal Performance Data”, Holtec Report HI-2002396, Rev. 3, Holtec International, Marlton, NJ, 08053.
- [3.I.2] “Holtite-A: Results of Pre-and-Post-Irradiation Tests and Measurements”, Holtec Report HI-2002420, Rev. 1.

Table 3.I.1: PROPRIETARY INFORMATION WITHHELD PER 10CFR2.390

Table 3.I.2: HI-STAR HB Thermal Payload

Fuel Decay Heat	2 kW
-----------------	------

Table 3.I.3: PROPRIETARY INFORMATION WITHHELD PER 10CFR2.390

Table 3.I.4: Helium Backfill Pressures

Minimum Pressure <sup>1</sup>	45.2 psig @ 70°F
Maximum Pressure	48.8 psig @ 70°F

<sup>1</sup> As MPC internal convection is conservatively neglected in transport evaluations the minimum required helium backfill pressure is 0 psig. This value is adopted in the transport CoC requirements for HI-STAR HB.

Table 3.I.5: PROPRIETARY INFORMATION WITHHELD PER 10CFR2.390

## **SUPPLEMENT 3.II**

### **THERMAL EVALUATION OF THE HI-STAR HB GTCC PACKAGE WITH GWC-HB**

#### **3.II.0 INTRODUCTION**

The Humboldt Bay HI-STAR HB cask is licensed to store permanently shutdown Unit 3 BWR spent nuclear fuel (SNF) and Greater-Than-Class C waste (GTCC) at the Humboldt Bay ISFSI. The GTCC package is discussed in Supplement 3.I along with the SNF-bearing package.



## SUPPLEMENT 3.III

### THERMAL EVALUATION OF THE HI-STAR 100 PACKAGE WITH DIABLO CANYON MPC-32

#### 3.III.0 INTRODUCTION

The Diablo Canyon MPC-32 is licensed to store Diablo Canyon PWR spent nuclear fuel (SNF) at the Diablo Canyon ISFSI in the HI-STORM 100SA overpack (U.S. NRC Materials License SNM-2511, Docket 72-26). As the HI-STORM 100SA is a storage-only overpack, the Diablo Canyon MPC-32 must be transferred to a HI-STAR 100 overpack for off-site transport. In this supplement compliance of the HI-STAR 100 overpack containing the Diablo Canyon MPC-32 to 10CFR71 and ISG-11, Rev. 3 thermal requirements are evaluated for transport. The analysis considers passive rejection of decay heat from the spent nuclear fuel to an environment under the 10CFR71 mandated ambient conditions for normal and accident scenarios. The regulatory requirements and acceptance criteria for transport evaluation are listed in Section 3.0.

#### 3.III.1 DISCUSSION

The Diablo Canyon MPC-32 is, essentially, a shortened version of the MPC-32. In addition to the MPC internal cavity and overall height being about 5% shorter, the fuel basket is also shorter and the normal threaded upper fuel spacers are replaced with I-beams welded to the MPC lid. The MPC thermal design features discussed in Section 3.1 are applicable to the Diablo MPC-32 design.

#### 3.III.2 THERMAL PROPERTIES OF MATERIALS

The thermophysical data compiled in Section 3.2 of the SAR provides the required materials information.

#### 3.III.3 TECHNICAL SPECIFICATIONS OF COMPONENTS

The HI-STAR materials and components required to be maintained within safe operating limits are listed in Section 3.3. The temperature limits specified in this section are adopted for transport evaluation.

#### 3.III.4 TRANSPORT THERMAL EVALUATION

In the fuel basket region, the generic and Diablo Canyon MPC-32 are geometrically the same (see Chapter 1 drawings). They also have the same enclosure shell diameter and thickness. So, the only differences from a thermal point of view are in the length as follows:

- The overall length of the Diablo Canyon MPC-32 is reduced compared to the generic MPC-32.

- The internal cavity length of the Diablo Canyon MPC-32 is reduced compared to the generic MPC-32.
- The length of the Diablo Canyon MPC-32 fuel basket is reduced compared to the generic MPC-32.

Given these relatively minor (all less than 10%) length differences between the generic and Diablo Canyon MPC-32 designs, the existing thermal model of the generic MPC-32 is leveraged to define the thermal performance of the Diablo Canyon design MPC-32.

The Diablo Canyon MPC-32 overall length is slightly smaller than that of the generic MPC-32, so a spacer ring will be placed above the MPC inside the HI-STAR 100 overpack. The presence of the spacer has the beneficial effect of lowering overpack lid and containment boundary seal temperatures. As described in Subsection 3.4.1, the impact limiters installed on the overpack during transportation are modeled with a thermal conductivity “set essentially equal to zero”, rendering the ends of the overpack as essentially adiabatic. Thus, heat transfer out of the cask in the axial direction is already throttled and the addition of the spacer would have little additional impact. As such, only heat transfer out of the cask in the radial direction is significant.

Recognizing that only radial direction heat transfer is significant, the reduced length of the Diablo Canyon MPC-32 will reduce the effective surface area for heat rejection. The thermal model of the HI-STAR 100 containing a generic MPC-32 will still bound the Diablo Canyon design if the design-basis decay heat load for Diablo Canyon design is reduced relative to that of the generic MPC-32 design. Ratios of the Diablo Canyon to generic MPC-32 length are determined for the overall MPC length, MPC internal cavity length and fuel basket length. The design-basis maximum decay heat load for the generic MPC-32 is multiplied by the smallest of these ratios to yield a conservative design-basis maximum decay heat load for the Diablo Canyon MPC-32.

The resulting value (rounded down to an integer value to ensure robust margins) is presented in Table 3.III.1. With the Diablo Canyon MPC-32 decay heat limited to the value from Table 3.III.1, all fuel and cask component temperatures reported in Chapter 3 for the generic MPC-32 (or PWR MPCs where only limiting values are reported) are applicable for the Diablo Canyon design. This is not true, however, for the MPC internal pressures because the Diablo Canyon design has a shorter cavity length and a higher backfill pressure.

The Diablo Canyon MPC-32 normal and accident condition pressures are reported in Table 3.III.2. Unlike the generic MPC-32, which can have up to 32 assemblies containing NFH, the Diablo Canyon MPC-32 may only contain 25 assemblies with NFH. BPRAs are the bounding NFH for MPC internal pressure, so all 25 assemblies are assumed to be equipped with a BPRA.

Based on consideration of transport conditions for a Diablo Canyon MPC-32 in a HI-STAR 100, it is concluded that a transportation package consisting of a Diablo Canyon MPC-32 in a HI-STAR 100 overpack is in compliance with the 10CFR Part 71 and ISG 11, Rev. 3 thermal requirements.

Table 3.III.1: HI-STAR 100 with Diablo Canyon MPC-32 Design-Basis Decay Heat

Design-Basis Decay Heat	18 kW
-------------------------	-------

Table 3.III.2: PROPRIETARY INFORMATION WITHHELD PER 10CFR2.390

## CHAPTER 4: CONTAINMENT

### 4.0 INTRODUCTION

This chapter demonstrates the HI-STAR 100 containment boundary compliance with the permitted activity release limits specified in 10CFR71, 71.51(a)(1) and 71.51(a)(2) for both normal and hypothetical accident conditions of transport [4.0.1]. Satisfaction of the containment criteria, expressed as the leakage rate acceptance criterion ( $\text{atm}\cdot\text{cm}^3/\text{sec}$ , Helium), ensures that the HI-STAR 100 package will not exceed the specified allowable radionuclide release rates. Leakage rates are determined in accordance with the recommendations of ANSI N14.5 [4.0.2], and utilizing NUREG/CR-6487, *Containment Analysis for Type B Packages Used to Transport Various Contents* [4.0.3], Regulatory Guide 7.4, *Leakage Tests on Packages for Shipment of Radioactive Materials* [4.0.4] as content guides, and Draft NUREG-1617, *Standard Review Plan for Transportation Packages for Spent Nuclear Fuel* [4.0.5].

The HI-STAR 100 packaging allowable leakage rates established herein ensures that the requirements of 10CFR71.51 are met. The containment system boundary for the HI-STAR 100 packaging consists of the overpack inner shell, the bottom plate, the top flange, the top closure plate, closure bolts, the overpack vent and drain port plugs, and their respective mechanical seals.

Chapter 2 of this SAR shows that all containment boundary components are maintained within their code-allowable stress limits during all normal and hypothetical accident conditions of transport as defined in 10CFR71.71 and 10CFR71.73. Chapter 3 of this SAR shows that the peak containment component temperatures and pressures are within the design basis limits for all normal and hypothetical accident conditions of transport as defined in 10CFR71.71 and 10CFR71.73. Since both the containment boundary is shown to remain intact, and the temperature and pressure design bases are not exceeded, the design basis leakage rates are not exceeded during normal or hypothetical accident conditions of transport.

The HI-STAR overpack is subjected to a containment system fabrication verification test before the first use as described in Chapter 8. The containment system fabrication verification test is performed at the factory as part of the HI-STAR 100 acceptance testing. The welds of the containment boundary, the closure plate inner seal, and the vent and drain port plug seals are helium leakage tested in accordance with ANSI N14.5. A containment system periodic verification test as described in Chapter 8, will be performed prior to each loaded transport. The mechanical seals of the HI-STAR 100 overpack will be replaced and retested each time the HI-STAR 100 is loaded.

As the containment system periodic verification leakage test shall be performed on the containment boundary prior to each loaded transport, this test takes the place of and is performed in lieu of the assembly verification.

## 4.1 CONTAINMENT BOUNDARIES

The containment system boundary for the HI-STAR 100 packaging consists of the overpack inner shell, the bottom plate, the top flange, the top closure plate, closure bolts, the overpack vent and drain port plugs, and their respective mechanical seals. The containment boundary system components for the HI-STAR 100 system are designed and fabricated in accordance with the requirements of ASME Code, Section III, Subsection NB [4.1.1], to the maximum extent practicable. Chapter 1 provides design criteria for the containment design. Section 1.3 provides applicable Code requirements. Exceptions to specific Code requirements with complete justifications are presented in Table 8.1.5. The containment boundary components are shown on Figure 4.1.1 with additional details provided in Figures 4.1.2 and 4.1.3.

Chapter 2 provides design criteria for the containment design. Section 1.3 provides applicable Code requirements. Alternatives to specific Code requirements with complete justifications are presented in Table 8.1.5.

### 4.1.1 Containment Vessel

The containment vessel for the HI-STAR 100 packaging consists of the overpack components which form the inner cavity volume used to house any of the MPC designs which contain spent nuclear fuel. The containment vessel is represented by the overpack inner shell, bottom plate, the top flange, and the closure plate. These components create an enclosed cylindrical cavity sufficient for insertion and enclosure of an MPC. The materials of construction for the packaging containment vessel are specified in the drawings in Section 1.4.

Table 4.1.1 provides a summary of the containment boundary design specifications.

### 4.1.2 Containment Penetrations

The containment system boundary penetrations for the HI-STAR 100 package include the closure plate test port plug, the vent port plug, the drain port plug, and their respective mechanical seals. Each penetration has redundant mechanical seals. The vent port is located in the closure plate and the drain port is located in the bottom plate. The closure configuration of the vent and drain ports is essentially identical (See Figure 4.1.3). The containment penetrations are designed and tested to ensure that the radionuclide release rates specified in 10CFR71.51 will not be exceeded.

### 4.1.3 Seals and Welds

The HI-STAR 100 containment vessel uses a combination of seals and welds designed and tested during normal transport conditions, and during and after the hypothetical transport accident conditions. Seals and welds are individually discussed below.

The seals and welds discussed below provides a containment system which is securely closed and cannot be opened unintentionally or by an internal pressure within the package as required in 10CFR71.43(c).

#### 4.1.3.1 Containment Seals

The HI-STAR 100 closure plate uses two concentric metallic seals to form the closure between the top flange surface and the closure plate. To protect the sealing surfaces against corrosion, a stainless steel weld inlay is provided during manufacturing on both the closure plate and mating overpack surfaces. The closure plate inner seal is tested for leakage through a small test port in the overpack closure plate (See Figure 4.1.2). The test port provides access to the volume between the two mechanical lid seals for leakage testing of the closure plate inner seal. Following leakage testing, a threaded plug with a metallic seal is installed in the test port hole to provide redundant closure.

Closure of the vent and drain ports is achieved via a threaded plug with a single metallic seal. The metallic seal is compressed between the underside of the threaded plug head and the overpack body to form the seal. The sealing surfaces are not subject to corrosion due to the presence of the cover plates and their seals preventing exposure of the seal surfaces to the elements. Each port plug seal is independently tested for leakage to verify containment performance. A bolted cover plate, with a machined seal groove, is installed over the vent and drain ports. A metallic seal, installed in the cover plate groove, is compressed between the cover plate and the overpack body during cover plate bolt torquing. These cover plates provide redundant closure of the drain and vent port penetrations.

Details on the seals are provided in the drawings in Section 1.4 and in Appendix 4.B. Table 4.1.1 contains reference information for the seals from the selected supplier. Note that the seals selected are designed and fabricated to meet the design requirements of the HI-STAR 100 System. The Chapter 7 procedures require replacement of any used seal after closure opening except for transportation of an empty overpack.

#### 4.1.3.2 Containment Welds

The containment boundary welds of the HI-STAR 100 overpack body include the welds forming the inner closure shell, the weld connecting the inner shell to the top flange, and the weld connecting the bottom plate to the inner shell. All containment boundary welds are fabricated and inspected in accordance with ASME Code Section III, Subsection NB (no stamp required). Full-penetration welds are specified for the plates that form the overpack inner shell. Full-penetration welds are also specified for the inner shell to the top flange and bottom plate welds. The weld details are shown in the drawings in Section 1.4. The containment boundary welds are volumetrically examined by radiography (RT) as described in Chapter 8.

#### 4.1.4 Closure

The HI-STAR 100 packaging closure plate is secured using multiple closure bolts around the perimeter. Torquing of the closure plate bolts compresses the closure plate concentric mechanical seals between the closure plate and the overpack flange forming the closure plate seal.

Closure of the overpack vent and drain ports is provided by a single threaded plug installed in each penetration (see Figure 4.1.3). The mechanical seal is compressed between the underside of the port plug head and the overpack body forming the port closure. A cover plate, containing a single metallic seal, is installed over each of the ports forming the redundant closure of the vent and drain port penetrations. The cover plate is secured by bolts. The closure plate test port is sealed using a port plug and mechanical seal in the same manner as the vent and drain port penetrations (see Figure 4.1.2).

The installation procedures, bolt torquing patterns, required lubrication, and torque values are provided in Table 7.1.1. The torque values are established to maintain containment during normal and accident conditions of transport. Torque values for the closure plate bolts were determined to preclude separation of the closure plate from the overpack flange. Appendix 4.A contains the calculations for the test, vent and drain port plugs and the vent and drain port cover plates bolt torques.

Table 4.1.2 provides a summary of the containment closure bolting for the HI-STAR 100 overpack penetrations.

#### 4.1.5 Damaged Fuel Container

Fuel assemblies classified as damaged fuel or fuel debris (assembly array/class 6x6A, 6x6B, 6x6C, 7x7A, and 8x8A for BWR fuel as specified in Table 1.2.11 and Trojan damaged fuel and fuel debris for PWR fuel as specified in Table 1.2.10) have been evaluated.

The MPC is designed to transport damaged fuel, fuel debris, or intact fuel. To aid in loading and unloading, damaged fuel assemblies and fuel debris will be loaded into stainless steel DFCs. The damaged fuel container (DFC) is shown in the drawings in Section 1.4. The DFC is designed to provide SNF loose component retention and handling capabilities. The DFC consists of a smooth-walled, welded stainless steel square canister with a removable lid. The canister lid provides the means of DFC closure and handling. The DFC is provided with stainless steel wire mesh screens in the top and bottom for draining, drying and helium backfill operations. The screens are specified as a 250-by-250-mesh with an effective opening of 0.0024 inches. There are no other openings in the DFC. Chapter 1 specifies the fuel assembly characteristics for damaged fuel acceptable for loading in the MPC-68, MPC-68F, or MPC-24EF and for fuel debris acceptable for loading in the MPC-68F or MPC-24EF.

Up to four (4) DFCs containing specified fuel debris may be placed in a custom-designed Trojan

MPC-24EF (Trojan PWR fuel debris) or an MPC-68F (BWR fuel debris). Up to 4 PWR damaged fuel assemblies in DFCs may be transported in a custom-designed Trojan MPC-24EF or up to 68 BWR damaged fuel assemblies in DFCs may be transported in an MPC-68 or MPC-68F, respectively. The quantity of fuel debris is limited to meet the off-site transportation requirements of 10CFR71, specifically, 10CFR71.51(a)(1). Analyses provided in this chapter conservatively assume 100% of the rods of the fuel debris are breached under normal conditions of transport. Therefore, 100% of the contents of the DFCs are available for release.



Table 4.1.1

## SUMMARY OF CONTAINMENT BOUNDARY DESIGN SPECIFICATIONS

Design Attribute	Design Rating
Closure Plate Mechanical Seals: <sup>††</sup> Design Temperature Pressure Rating Design Leakage Rate	1200°F 1,000 psig $1 \times 10^{-6}$ cm <sup>3</sup> /s, Helium
Overpack Vent and Drain Port Cover Plate Mechanical Seals: <sup>†,††</sup> Design Temperature Pressure Rating Design Leakage Rate	1200°F 1,000 psig $1 \times 10^{-6}$ cm <sup>3</sup> /sec, Helium
Overpack Vent and Drain Port Plug Mechanical Seals: <sup>††</sup> Design Temperature Pressure Rating Design Leakage Rate	1200°F 1,000 psig $1 \times 10^{-6}$ cm <sup>3</sup> /sec, Helium
Leakage Rate Acceptance Criterion	$4.3 \times 10^{-6}$ atm cm <sup>3</sup> /s, He
Leakage Rate Test Sensitivity	$2.15 \times 10^{-6}$ atm cm <sup>3</sup> /s, He

<sup>†</sup> No credit is taken for the overpack vent and drain port cover plate seals as part of the containment boundary. Specifications are provided for information.

<sup>††</sup> Per manufacturer's recommended operating limits.

Table 4.1.2

## CONTAINMENT CLOSURE BOLTING SUMMARY

<b>Item</b>	<b>Qty</b>	<b>Type</b>	<b>Material</b>
Closure Plate Bolt (Long)	52	1-5/8"-8 UNC x 7-3/8" LG Cap Screw	SB-637-N07718
Closure Plate Bolt (Short)	2	1-5/8"-8 UNC x 7-1/8" LG Cap Screw	SB-637-N07718
Vent/Drain Port Cover Plate Bolt	4 ea	3/8 -16 UNC x 5/8" LG Cap Screw	SA-193 GRADE B7
Vent/Drain/Closure Plate Test Port Plugs	1 ea	7/8" diameter Fabricated Plug	SA-193 GRADE B8

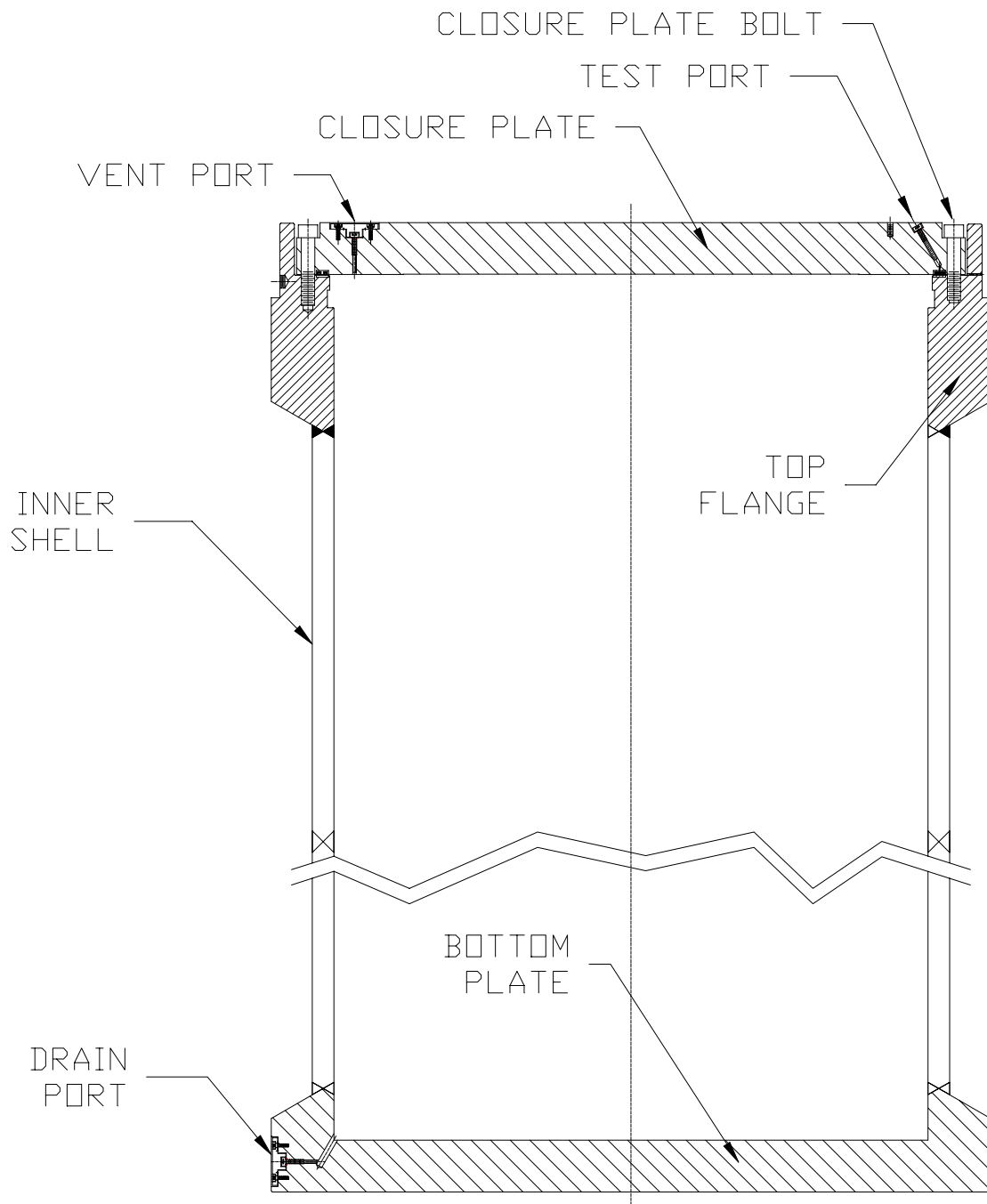


**FIGURE 4.1.1; HI-STAR 100 OVERPACK PRIMARY CONTAINMENT BOUNDARY COMPONENTS**

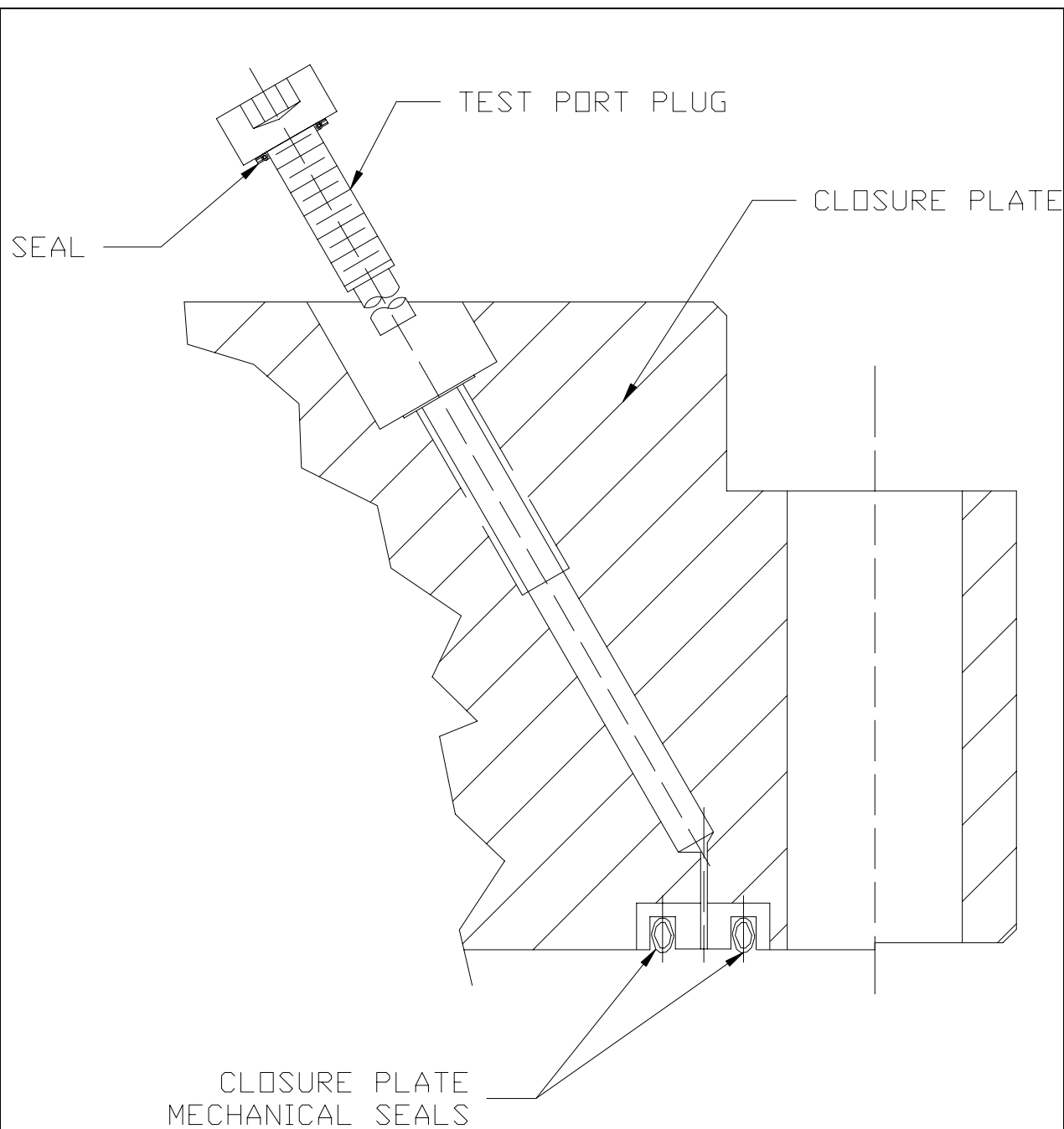


FIGURE 4.1.2; HI-STAR 100 CLOSURE PLATE CONTAINMENT DETAILS

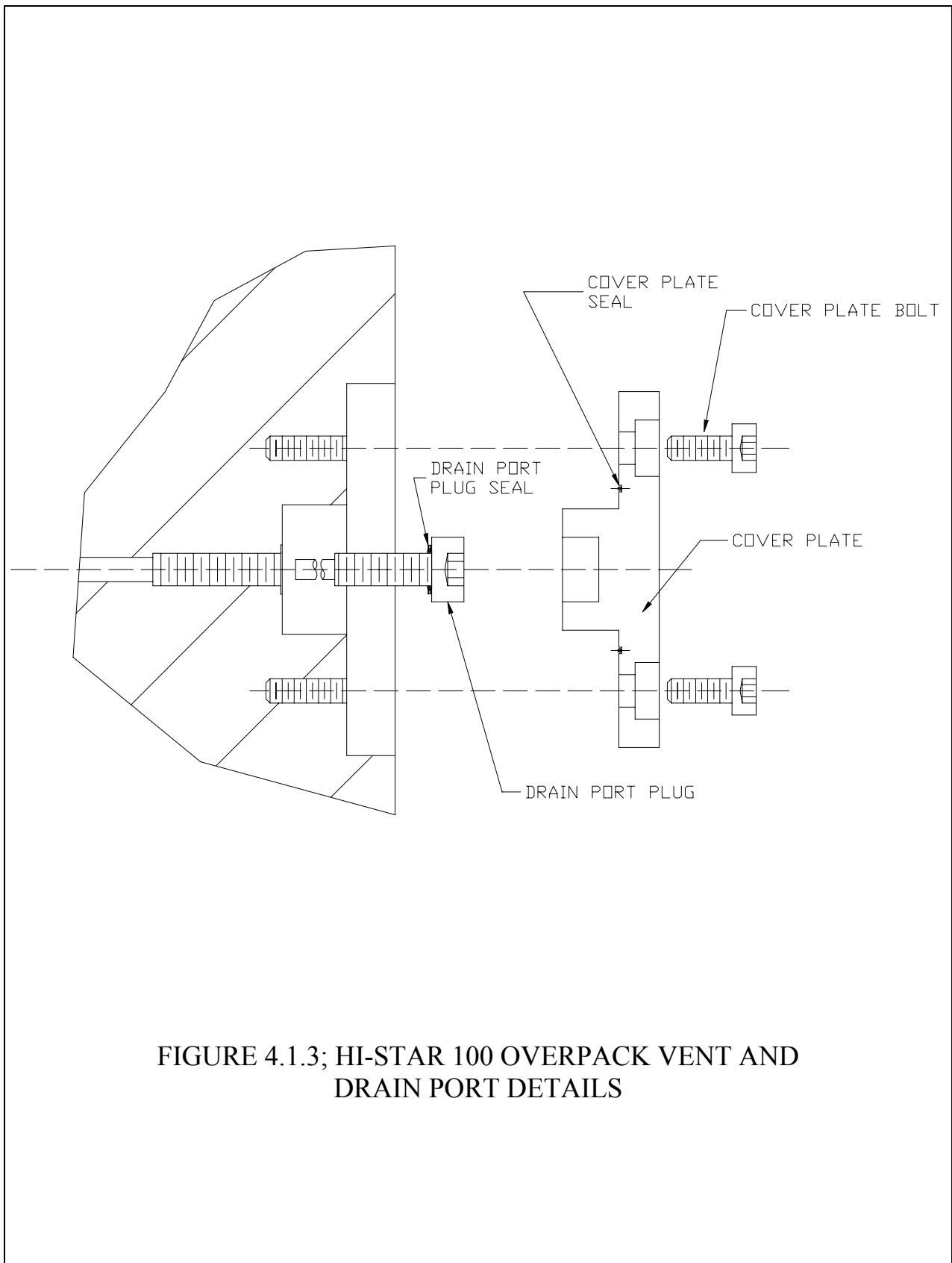


FIGURE 4.1.3; HI-STAR 100 OVERPACK VENT AND  
DRAIN PORT DETAILS

FIGURE 4.1.4;  
THIS FIGURE WAS INTENTIONALLY DELETED

## 4.2 REQUIREMENTS FOR NORMAL AND HYPOTHETICAL ACCIDENT CONDITIONS OF TRANSPORT

Chapter 2 shows that all containment components are maintained within their code-allowable stress limits during all normal and hypothetical accident conditions of transport as defined in 10CFR71.71 and 10CFR71.73 [4.0.1]. Chapter 3 shows that the peak containment component temperatures and pressure are within the design basis limits for all normal and hypothetical accident conditions of transport as defined in 10CFR71.71 and 10CFR71.73. Since the containment vessel remains intact, and the temperature and pressure design bases are not exceeded, the design basis leakage rate (see Table 4.1.1) will not be exceeded during normal or hypothetical accident conditions of transport.

### 4.2.1 Containment Criteria

The allowable leakage rates presented in this chapter were determined in accordance with ANSI N14.5-1997 [4.0.2] and shall be used for containment system fabrication verification and containment system periodic verification tests of the HI-STAR 100 containment boundary. Measured leakage rates shall not exceed the values presented in Table 4.1.1. Compliance with these leakage rates ensures that the radionuclide release rates specified in 10CFR71.51 will not be exceeded during normal or hypothetical accident conditions of transport.

### 4.2.2 Containment of Radioactive Material

The HI-STAR 100 packaging allowable leakage rate (See Table 4.1.1) ensures that the requirements of 10CFR71.51 are met. Section 4.2.5 determines the maximum leakage rate for normal and hypothetical accident conditions of transport and the allowable leakage rate criterion for the HI-STAR 100 packaging containing each of the MPC types. The maximum calculated leakage rates for normal transport conditions assume a full complement of design basis fuel assembly types with bounding radiological source terms. The calculations also assume 3% fuel rod rupture for normal conditions. This bounds all possible MPC fuel loading configurations. For calculating the maximum leakage rates for normal conditions of transport, the internal pressure is conservatively assumed to be greater than the MPC internal pressure for the most limiting MPC type determined in Chapter 3. Following testing, no credit is taken for the MPC as a containment boundary.

The allowable leakage rate is then conservatively chosen to be less than the calculated maximum leakage rates from all MPC types for normal conditions of transport. This ensures that the 10CFR71.51(a)(1) limit for radionuclide release are not exceeded.

### 4.2.3 Pressurization of Containment Vessel

The HI-STAR 100 overpack contains a sealed MPC during normal conditions of transport. Except for the small space between the MPC and overpack, the overpack internal cavity is essentially filled. This space (annulus) is drained, dried, evacuated and backfilled with helium gas prior to final closure

of the overpack; therefore, no vapors or gases are present which could cause a reaction or explosion inside the overpack. Procedural steps (Chapter 7) prevent overpack over-pressurization during closure operations. The enclosed MPC is also drained, dried, and backfilled with helium gas prior to final closure; therefore, any MPC leak would not introduce any explosive gases into the overpack cavity. Since the exterior of the MPC is entirely composed of stainless steel, there is no possibility of chemical reaction that would produce gas or vapor. The overpack accident condition design basis internal pressure analysis assumes a non-mechanistic event resulting in the loss of MPC closure welds, a full-complement of design basis fuel with 100% fill gas and 30% of significant fission gas release, and the hypothetical 10CFR71.73(c)(4) fire condition. Even in this event, structural integrity and containment of the HI-STAR 100 packaging are maintained.

As the MPC is drained, dried, evacuated and backfilled with helium gas, no vapors or gases are present which could cause a reaction or explosion inside the MPC. Procedural steps (Chapter 7) prevent MPC over-pressurization during closure operations. The interior of the MPC contains stainless steel, neutron absorber, and optional aluminum heat conductive inserts. There is no possibility of chemical reaction that would produce gas or vapor.

#### 4.2.4 Assumptions

The HI-STAR 100 System is designed to meet the radioactive release limit requirements of 10CFR71.51. Allowable leakage rates are determined in accordance with the requirements of ANSI N14.5, and utilizing NUREG/CR-6487, *Containment Analysis for Type B Packages Used to Transport Various Contents* [4.0.3] and Regulatory Guide 7.4, *Leakage Tests on Packages for Shipment of Radioactive Materials* [4.0.4] as guides.

The following assumptions have been used in determining the allowable leakage rates:

1. For MPCs other than the MPC-24EF with Trojan fuel debris and MPC-68F, three percent of the fuel rods are assumed to have failed during normal conditions of transportation. One-hundred percent of the fuel rods are assumed to have failed during hypothetical accident conditions.
2. Thirty percent of the radioactive gases are assumed to escape each failed fuel rod.
3. Fifteen percent of the  $^{60}\text{Co}$  from the crud on the surface of the fuel rods is released as an aerosol in normal conditions of transport. One-hundred percent of the  $^{60}\text{Co}$  is released as an aerosol from the surfaces of the fuel assemblies during accident conditions.
4. Since the overpack internals are never exposed to contaminants, the residual activity on the overpack interior surface and the MPC exterior surface is negligible compared to crud deposits on the fuel and is neglected as a source term.



5. Up to four (4) DFCs containing specified fuel debris may be placed in an MPC-24EF (only the custom-designed Trojan MPC-24EF) or an MPC-68F.
6. Crud spallation and cladding breaches occur instantaneously after fuel loading and container closure operations.
7. The calculation for normal transport conditions of an MPC containing fuel debris assumes 100% of the rods of the fuel debris are breached.
8. For containment analysis purposes, the MPC-24, MPC-24E or MPC-24EF contain up to 24 PWR assemblies, of which 4 of these in the custom-designed Trojan MPC-24EF may be DFCs with Trojan fuel debris, the MPC-32 contains up to 32 PWR assemblies, the MPC-68 contains up to 68 BWR assemblies, and the MPC-68F contains up to 68 intact BWR fuel assemblies, of which 4 of those may be specified BWR fuel debris in damaged fuel containers.
9. 0.003% of the total fuel mass contained in a rod is assumed to be released as fines if the cladding on the rod ruptures (i.e.,  $f_r=3 \times 10^{-5}$ ).
10. Bounding values for the crud surface activity for PWR rods is  $140 \times 10^{-6}$  Ci/cm<sup>2</sup> and for BWR rods is  $1254 \times 10^{-6}$  Ci/cm<sup>2</sup>.
11. The rod surface area per assembly is  $3 \times 10^5$  cm<sup>2</sup> for PWR and  $1 \times 10^5$  cm<sup>2</sup> for BWR fuel assemblies. These surface areas are also conservatively used for the surface area of damaged fuel or fuel debris..
12. The release fractions for volatiles (<sup>89</sup>Sr, <sup>90</sup>Sr, <sup>103</sup>Ru, <sup>106</sup>Ru, <sup>134</sup>Cs, <sup>135</sup>Cs, and <sup>137</sup>Cs) are all assumed to be  $2 \times 10^{-4}$  ( $f_v=2 \times 10^{-4}$ ).
13. In the analysis of the containment boundary, no credit is taken for the presence of the seal welded MPC.
14. In calculating the leakage rates of the containment system for normal conditions of transport, the internal pressure of the overpack is conservatively assumed to be larger than the maximum internal pressure of all MPC types determined in Chapter 3.
15. In calculating the leakage rates of the containment system for normal conditions of transport, the average cavity temperature of the overpack is conservatively assumed to be larger than the maximum cavity temperature of all MPC types determined in Chapter 3. The average cavity temperature for accident conditions is conservatively assumed to be the design basis peak cladding temperature of 1058°F (843K).

16. All of the activity associated with crud is assumed to be Cobalt-60.
17. It is assumed that the flow is unchoked for all leakage analyses.
18. Deleted
19. Deleted

#### 4.2.5 Analysis and Results

The allowable leakage rates for the containment boundary under normal and hypothetical accident conditions of transport at operating conditions for the HI-STAR 100 packaging containing each of the MPC types were determined and are presented in this chapter. To calculate the leakage rates for a particular contents type and transportation condition, the following were determined: the source term concentration for the releasable material; the effective  $A_2$  of the individual contributors; the releasable activity; the effective  $A_2$  for the total source term; the allowable radionuclide release rates; and the allowable leakage rates at transport (operating) conditions. Using the equations for continuum and molecular flow, the corresponding leakage hole diameters were calculated. Then, using these leak hole diameters, the corresponding allowable leakage rates at test conditions were calculated. Parameters were utilized in a way that ensured conservatism in the final leakage rates for the conditions, contents, and package arrangements considered.

The methodology and analysis results are summarized below.

##### 4.2.5.1 Volume in the Containment Vessel

As discussed above, the containment system boundary for the HI-STAR 100 packaging consists of the overpack inner shell and associated components.

Except for a small volume between the MPC and the overpack (the annulus), the overpack internal cavity is essentially filled. Therefore, the free gas volume for the containment boundary includes the free gas volume for the MPC plus the overpack annulus volume. The free gas volume in each of the MPC types is presented in Chapter 3. The free gas volumes of the containment system are repeated in Table 4.2.1 for completeness. The MPC-24E and MPC-24EF basket designed for Trojan are shorter to allow for storage in their overpacks. These shorter baskets are designated as the Trojan MPC-24E and Trojan MPC-24EF, respectively, where necessary. For calculating the free volume in the containment system (overpack) with either of the Trojan MPCs, the annulus space is assumed to be the same as that for the larger generic MPCs (i.e. the larger annulus space between the Trojan MPC and HI-STAR overpack is neglected). This will conservatively underestimate the free volume inside the containment boundary.

#### 4.2.5.2 Source Terms For Spent Nuclear Fuel Assemblies

In accordance with NUREG/CR-6487 [4.0.3], the following contributions are considered in determining the releasable source term for packages designed to transport irradiated fuel rods: (1) the radionuclides comprising the fuel rods, (2) the radionuclides on the surface of the fuel rods, and (3) the residual contamination on the inside surfaces of the vessel. NUREG/CR-6487 goes on to state that a radioactive aerosol can be generated inside a vessel when radioactive material from the fuel rods or from the inside surfaces of the container become airborne. The sources for the airborne material are (1) residual activity on the cask interior, (2) fission and activation-product activity associated with corrosion-deposited material (crud) on the fuel assembly surface, and (3) the radionuclides within the individual fuel rods. In accordance with NUREG/CR-6487, contamination due to residual activity on the cask interior surfaces is negligible as compared to crud deposits on the fuel rods themselves and therefore may be neglected. The source term considered for this calculation results from the spallation of crud from the fuel rods and from the fines, gases and volatiles which result from cladding breaches.

The inventory for isotopes other than  $^{60}\text{Co}$  is calculated with the SAS2H and ORIGEN-S modules of the SCALE 4.3 system as described in Chapter 5. The inventory for the MPC-24, MPC-24E, MPC-24EF, and MPC-32 was conservatively based on the B&W 15x15 fuel assembly with a burnup of 45,000 MWD/MTU, 5 years of cooling time, and an enrichment of 3.6%. The inventory for the Trojan MPCs (Trojan MPC-24E, Trojan MPC-24EF) was based on the Westinghouse 17x17 fuel assembly with a burnup of 42,000 MWD/MTU, 9 years cooling time, and an enrichment of 3.09%. The inventory for the MPC-68 was based the GE 7x7 fuel assembly with a burnup of 45,000 MWD/MTU, 5 years of cooling time, and 3.2% enrichment. The inventory for the MPC-68F was based on the GE 6x6 fuel assembly with a burnup of 30,000 MWD/MTU, 18 years of cooling time, and 1.8% enrichment. Additionally, an MPC-68F was analyzed containing 67 GE 6x6 assemblies and a DFC containing 18 thorium rods. Finally, an Sb-Be source stored in one fuel rod in one assembly with 67 GE 6x6 assemblies was analyzed. The isotopes which contribute greater than 0.01% to the total curie inventory for the fuel assembly are considered in the evaluation as fines. Additionally, isotopes with  $A_2$  values less than 1.0 in Table A-1, Appendix A, 10CFR71 are included as fines. Isotopes which contribute greater than 0.01% but which do not have an assigned  $A_2$  value in Table A-1 are assigned an  $A_2$  value based on the guidance in Table A-3, Appendix A, 10CFR71. Finally, those radionuclides that have no  $A_2$  value in Table A-1 from Appendix A of 10CFR71, have a half-life shorter than 10 days, and have a half-life less than their parent radionuclide (i.e, are in secular equilibrium with their parent nuclide), are in accordance with 10CFR71, Appendix A, III treated as a single radionuclide along with the parent nuclide. Table 4.2.2 presents the isotope inventory used in the calculation.

##### A. Source Activity Due to Crud Spallation from Fuel Rods

The majority of the activity associated with crud is due to  $^{60}\text{Co}$  [4.0.3]. The inventory for  $^{60}\text{Co}$  was determined by using the crud surface activity for PWR rods ( $140 \times 10^{-6} \text{ Ci/cm}^2$ ) and for BWR rods

( $1254 \times 10^{-6}$  Ci/cm<sup>2</sup>) provided in NUREG/CR-6487 [4.0.3] multiplied by the surface area per assembly ( $3 \times 10^5$  cm<sup>2</sup> and  $1 \times 10^5$  cm<sup>2</sup> for PWR and BWR, respectively, also provided in NUREG/CR-6487).

The source terms were then decay corrected (5 years for the MPC-24, MPC-24E, MPC-24EF, MPC-32 and the MPC-68; 18 years for the MPC-68F; 9 years for the Trojan MPCs) using the basic radioactive decay equation:

$$A(t) = A_0 e^{-\lambda t} \quad (4-1)$$

where:

$A(t)$  is activity at time  $t$  [Ci]  
 $A_0$  is the initial activity [Ci]  
 $\lambda$  is the  $\ln 2/t_{1/2}$  (where  $t_{1/2} = 5.272$  years for  $^{60}\text{Co}$ )  
 $t$  is the time in years (5 years for the MPC-24, MPC-24E, MPC-24EF, MPC-32 and the MPC-68; 18 years for the MPC-68F; 9 years for the Trojan MPCs)

The inventory for  $^{60}\text{Co}$  was determined using the methodology described above with the following results:

#### **PWR**

Surface area per Assy =  $3.0\text{E}+05$  cm<sup>2</sup>  
 $140 \mu\text{Ci}/\text{cm}^2 \times 3.0\text{E}+05 \text{ cm}^2 = 42.0 \text{ Ci/assy}$

#### **BWR**

Surface area per Assy =  $1.0\text{E}+05$  cm<sup>2</sup>  
 $1254 \mu\text{Ci}/\text{cm}^2 \times 1.0\text{E}+05 \text{ cm}^2 = 125.4 \text{ Ci/assy}$

$^{60}\text{Co}(t) = ^{60}\text{Co}_0 e^{-(\lambda t)}$ , where  $\lambda = \ln 2/t_{1/2}$ ,  $t = 5$  years (for the MPC-24, MPC-24E, MPC-24EF, MPC-32 and MPC-68),  $t = 18$  years (MPC-68F),  $t = 9$  years (Trojan MPCs),  $t_{1/2} = 5.272$  years for  $^{60}\text{Co}$  [4.2.4]

MPC-24, MPC-24E, MPC-24EF, MPC-32

$$^{60}\text{Co}(5) = 42.0 \text{ Ci } e^{-(\ln 2/5.272)(5)}$$

$$^{60}\text{Co}(5) = 21.77 \text{ Ci/assy}$$

MPC-68

$$^{60}\text{Co}(5) = 125.4 \text{ Ci } e^{-(\ln 2/5.272)(5)}$$

$$^{60}\text{Co}(5) = 64.98 \text{ Ci/assy}$$

Trojan MPC-24E, Trojan MPC-24EF

$$^{60}\text{Co}(5) = 42.0 \text{ Ci } e^{-(\ln 2/5.272)(9)}$$

$$^{60}\text{Co}(5) = 12.86 \text{ Ci/assy}$$

MPC-68F

$$^{60}\text{Co}(18) = 125.4 \text{ Ci } e^{-(\ln 2/5.272)(18)}$$

$$^{60}\text{Co}(18) = 11.76 \text{ Ci/assy}$$

A summary of the  $^{60}\text{Co}$  inventory available for release is provided in Table 4.2.2.

The activity density that results inside the containment vessel as a result of crud spallation from spent fuel rods can be formulated as:

$$C_{\text{crud}} = \frac{f_C M_A N_A}{V} \quad (4-2)$$

where:

$C_{\text{crud}}$  is the activity density inside the containment vessel as a result of crud spallation [Ci/cm<sup>3</sup>],  
 $M_A$  is the total crud activity inventory per assembly [Ci/assy],  
 $f_C$  is the crud spallation fraction,  
 $N_A$  is the number of assemblies, and  
 $V$  is the free volume inside the containment vessel [cm<sup>3</sup>].

NUREG/CR-6487 states that measurements have shown 15% to be a reasonable value for the percent of crud spallation for both PWR and BWR fuel rods under normal transportation conditions. For hypothetical accident conditions, it is assumed that there is 100% crud spallation [4.0.3].

#### B. Source Activity Due to Releases of Fines from Cladding Breaches

A breach in the cladding of a fuel rod may allow radionuclides to be released from the resulting cladding defect into the interior of the MPC. If there is a leak in the containment vessel, then the radioisotopes emitted from a cladding breach that were aerosolized may be entrained in the gases escaping from the package and result in a radioactive release to the environment.

NUREG/CR-6487 suggests that a bounding value of 3% of the rods develop cladding breaches during normal transportation (i.e.,  $f_B=0.03$ ). For hypothetical accident conditions, it is assumed that all of the rods develop a cladding breach (i.e.,  $f_B=1.0$ ). These values were used for both PWR and BWR fuel rods. As described in NUREG/CR-6487, roughly 0.003% of the fuel mass contained in a rod is released as fines if the cladding on the rod ruptures (i.e.,  $f_f=3 \times 10^{-5}$ ).

The calculation for normal transport conditions of either a Trojan MPC-24EF or an MPC-68F containing four (4) DFCs containing fuel debris assumes that for the four DFCs, 100% of the rods of the fuel debris are breached. The remaining 20 or 64 assemblies in either the Trojan MPC-24EF or the MPC-68F, respectively, were assumed to have a 3% cladding rupture. Therefore,  $f_B$  for a Trojan MPC-24EF or an MPC-68F containing fuel debris is:

$$f_B = (0.03) \frac{20}{24} + (1.0) \frac{4}{20} \quad (4-3a)$$

$$f_B = 0.192$$

$$f_B = (0.03) \frac{64}{68} + (1.0) \frac{4}{68}$$

(4-3b)

The activity concentration inside the containment vessel due to fines being released from cladding breaches is given by:

$$C_{\text{fines}} = \frac{f_f I_{\text{fines}} N_A f_B}{V} \quad (4-4)$$

where:

- $C_{\text{fines}}$  is the activity concentration inside the containment vessel as a result of fines released from cladding breaches [Ci/cm<sup>3</sup>],
- $f_f$  is the fraction of a fuel rod's mass released as fines as a result of a cladding breach ( $f_f=3 \times 10^{-5}$ ),
- $I_{\text{fines}}$  is the total activity inventory [Ci/assy],
- $N_A$  is the number of assemblies,
- $f_B$  is the fraction of rods that develop cladding breaches, and
- $V$  is the free volume inside the containment vessel [cm<sup>3</sup>].

#### C. Source Activity from Gases due to Cladding Breaches

If a cladding failure occurs in a fuel rod, a large fraction of the gap fission gases will be introduced into the free volume of the system. Tritium and Krypton-85 are typically the major sources of radioactivity among the gases present [4.0.3]. NUREG/CR-6487 suggests that a bounding value of 30% of the fission product gases escape from a fuel rod as a result of a cladding breach (i.e.,  $f_g=0.3$ ).

The activity concentration due to the release of gases from a cladding breach is given by:

$$C_{\text{gases}} = \frac{f_g I_{\text{gases}} N_A f_B}{V} \quad (4-5)$$

where:

- $C_{\text{gases}}$  is the releasable activity concentration inside the containment vessel due to gases released from cladding breaches [Ci/cm<sup>3</sup>],
- $f_g$  is the fraction of gas that would escape from a fuel rod that developed a cladding breach,
- $I_{\text{gases}}$  is the gas activity inventory [<sup>3</sup>H, <sup>129</sup>I, <sup>85</sup>Kr, <sup>81</sup>Kr, <sup>127</sup>Xe] [Ci/assy],
- $N_A$  is the number of assemblies,
- $f_B$  is the fraction of rods that develop cladding breaches, and
- $V$  is the free volume inside the containment vessel [cm<sup>3</sup>].

#### D. Source Activity from Volatiles due to Cladding Breaches

Volatiles such as cesium, strontium, and ruthenium, can also be released from a fuel rod as a result of a cladding breach. NUREG/CR-6487 estimates that  $2 \times 10^{-4}$  is a conservative bounding value for the fraction of the volatiles released from a fuel rod (i.e.,  $f_v = 2 \times 10^{-4}$ ).

The activity concentration due to the release of volatiles is given by:

$$C_{vol} = \frac{f_v I_{vol} N_A f_B}{V} \quad (4-6)$$

where:

- $C_{vol}$  is the releasable activity concentration inside the containment vessel due to volatiles released from cladding breaches [Ci/cm<sup>3</sup>],
- $f_v$  is the fraction of volatiles that would escape from a fuel rod that developed a cladding breach,
- $I_{vol}$  is the volatile activity inventory [<sup>89</sup>Sr, <sup>90</sup>Sr, <sup>134</sup>Cs, <sup>135</sup>Cs, <sup>137</sup>Cs, <sup>134</sup>Cs, <sup>103</sup>Ru, <sup>106</sup>Ru] [Ci/assy],
- $N_A$  is the number of assemblies,
- $f_B$  is the fraction of rods that develop cladding breaches, and
- $V$  is the free volume inside the containment vessel [cm<sup>3</sup>].

#### E. Total Source Term for the HI-STAR 100 System

The total source term was determined by combining Equations 4-2, 4-4, 4-5, and 4-6:

$$C_{total} = C_{crud} + C_{fines} + C_{gases} + C_{vol} \quad (4-7)$$

where  $C_{total}$  has units of Ci/cm<sup>3</sup>.

Table 4.2.3 presents the total source term determined using the above methodology. Table 4.2.4 summarizes the parameters from NUREG/CR-6487 used in this analysis.

##### 4.2.5.3 Effective $A_2$ of Individual Contributors (Crud, Fines, Gases, and Volatiles)

The  $A_2$  of the individual contributions (i.e., crud, fines, gases, and volatiles) were determined in accordance with NUREG/CR-6487. As previously described, the majority of the activity due to crud is from Cobalt-60. Therefore, the  $A_2$  value of 10.8 Ci used for crud for both PWR and BWR fuel is the same as that for Cobalt-60 found in 10CFR71, Appendix A.

In accordance with 10CFR71.51(b) the methodology presented in 10CFR71, Appendix A for mixtures of different radionuclides was used to determine the  $A_2$  values for the gases, fines and volatiles.

$$A_2 \text{ for a mixture} = \frac{1}{\sum_{i=1}^I \frac{f_i}{(A_2)_i}}$$

Where  $f(i)$  is the fraction of activity of nuclide  $I$  in the mixture and  $A_2(i)$  is the appropriate  $A_2$  value for the nuclide  $I$ .

10CFR71.51(b) also states that for Krypton-85, an effective  $A_2$  value equal to 10  $A_2$  may be used. Table 4.2.5 summarizes the effective  $A_2$  for all individual contributors.

#### 4.2.5.4 Releasable Activity

The releasable activity is the product of the respective activity concentrations ( $C_{\text{fines}}$ ,  $C_{\text{gas}}$ ,  $C_{\text{crud}}$ , and  $C_{\text{vol}}$ ) and the respective MPC volume. The releasable activity of fines, volatiles, gases, and crud were determined using this methodology.

$$\text{Releasable Activity [Ci]} = \text{Activity Concentration} \left[ \frac{\text{Ci}}{\text{cm}^3} \right] \times \text{Volume} [\text{cm}^3]$$

#### 4.2.5.5 Effective $A_2$ for the Total Source Term

Using the releasable activity and the effective  $A_2$  values from the individual contributors (i.e., crud, fines, gases, and volatiles), the effective  $A_2$  for the total source term was calculated for each MPC type, for normal transportation and hypothetical accident conditions. The methodology used to determine the effective  $A_2$  is the same as that used for a mixture, which is provided in Equation 4-8.

The results are summarized in Table 4.2.6. As stated in 4.2.5.3, the effective  $A_2$  used for Krypton-85 is 10  $A_2$  (2700 Ci).

#### 4.2.5.6 Allowable Radionuclide Release Rates

The containment criterion for the HI-STAR 100 System under normal conditions of transport is given in 10CFR71.51(a)(1). This criterion requires that a package have a radioactive release rate less than  $A_2 \times 10^{-6}$  in one hour, where  $A_2$  is the effective  $A_2$  for the total source term in the packaging determined in 4.2.5.5. Additionally, 10CFR71.51(b)(2) specifies that for hypothetical accident conditions, the quantity that may be released in one week is  $A_2$  (effective  $A_2$  for the total source term).



determined in 4.2.5.5).

NUREG/CR-6487 and ANSI N14.5 provides the following equations for the allowable release rates.

Release rate for normal conditions of transport:

$$R_N = L_N C_N \leq A_2 \times 2.78 \times 10^{-10} / \text{second} \quad (4-10)$$

where:

$R_N$  is the release rate for normal transport [Ci/s]  
 $L_N$  is the volumetric gas leakage rate [cm<sup>3</sup>/s]  
 $C_N$  is the total source term activity concentration [Ci/cm<sup>3</sup>]  
 $A_2$  is the appropriate effective  $A_2$  value [Ci].

Release rate for hypothetical accident conditions:

$$R_A = L_A C_A \leq A_2 \times 1.65 \times 10^{-6} / \text{second} \quad (4-11)$$

where:

$R_A$  is the release rate for hypothetical accident conditions [Ci/s]  
 $L_A$  is the volumetric gas leakage rate [cm<sup>3</sup>/s]  
 $C_A$  is the total source term activity concentration [Ci/cm<sup>3</sup>]  
 $A_2$  is the appropriate effective  $A_2$  value [Ci].

Equations 4-10 and 4-11 were used to determine the allowable radionuclide release rates for each MPC type and transport condition. The release rates are summarized in Table 4.2.7.

#### 4.2.5.7 Allowable Leakage Rates at Operating Conditions

The allowable leakage rates at operating conditions were determined by dividing the allowable release rates by the appropriate source term activity concentration (modifying Equations 4-10 and 4-11).

$$L_N = \frac{R_N}{C_N} \quad \text{or} \quad L_A = \frac{R_A}{C_A} \quad (4-12)$$

where,

$L_N$  or  $L_A$  is the allowable leakage rate at the upstream pressure for normal (N) or accident (A) conditions [cm<sup>3</sup>/s],

$R_N$  or  $R_A$  is the allowable release rate for normal (N) or accident (A) conditions [Ci/s], and  
 $C_N$  or  $C_A$  is the allowable release rate for normal (N) or accident (A) conditions [Ci/cm<sup>3</sup>].

The allowable leakage rates determined using Equation 4-12 are the allowable leakage rates at the upstream pressure. Table 4.2.9 summarizes the allowable leakage rates at the upstream pressures. The most limiting allowable leakage rate presented in Table 4.2.9 was conservatively selected and used to determine the leakage rate acceptance criterion.

Equation deleted (4-13)

#### 4.2.5.8 Leakage Rate Acceptance Criteria for Test Conditions

The leakage rates discussed thus far were determined at operating conditions (see normal and accident conditions in Table 4.2.12). The following provides details of the methodology used to convert the allowable leakage rate at operating conditions to a leakage rate acceptance criterion at reference test conditions.

For conservatism, unchoked flow correlations were used as the unchoked flow correlations better approximate the true measured flow rate for the leakage rates associated with transportation packages. Using the equations for molecular and continuum flow provided in NUREG/CR-6487, the corresponding leak hole diameter was calculated by solving Equation 4-14a for  $D$ , the leak hole diameter. The capillary length required for Equation 4-14a for the containment was conservatively chosen as the closure plate inner seal seating width which is 0.25 cm.

$$L_{@P_u} = \left[ \frac{2.49 \times 10^6 D^4}{a u} + \frac{3.81 \times 10^3 D^3 \sqrt{\frac{T}{M}}}{a P_a} \right] [P_u - P_d] \frac{P_a}{P_u}$$

where:

$L_{@P_u}$  is the allowable leakage rate at the upstream pressure for normal and accident conditions [cm<sup>3</sup>/s],  
 $a$  is the capillary length [cm],  
 $T$  is the temperature for normal and accident conditions [K],  
 $M$  is the gas molecular weight [g/mole] = 4.0 from ANSI N14.5, Table B1 [4.0.2],  
 $u$  is the fluid viscosity for helium [cP] from Rosenhow and Hartnett [4.2.3]  
 $P_u$  is the upstream pressure [ATM],  
 $D$  leak hole diameter [cm],  
 $P_d$  is the downstream pressure for normal and accident conditions [ATM], and  
 $P_a$  is the average pressure;  $P_a = (P_u + P_d)/2$  for normal and accident conditions [ATM].

The actual leakage tests performed on the containment boundary are typically not performed under exactly the same conditions every time. Therefore, reference test conditions are specified to provide a consistent comparison of the measured leakage rate to the leakage rate acceptance criterion. The reference test conditions, and approximate actual test conditions are specified in Table 4.2.12.

The corresponding leak hole diameter at operating conditions was determined by solving Equation 4-14a for 'D' where  $L_{@P_u}$  is the most restrictive allowable leakage rate at the upstream pressure from Table 4.2.9 and using the parameters for normal conditions of transport presented in Table 4.2.12.

Using this leak hole diameter and the temperature and pressure specified for reference test conditions provided in Table 4.2.12, Equation 4-14a was solved for the volumetric leakage rate at reference test conditions.

Equation B-1 of ANSI N14.5-1997 [4.0.2] is used to express this volumetric leakage rate into a mass-like helium flow rate ( $Q_u$ ) as follows:

$$Q_u = L_u * P_u \text{ (atm-cm}^3\text{/sec)} \quad (4-14b)$$

where:

$L_u$  is the upstream volumetric leakage rate [cm<sup>3</sup>/sec],  
 $Q_u$  is the mass-like helium leak rate [atm-cm<sup>3</sup>/sec], and  
 $P_u$  is the upstream pressure [atm].

Using Equation 4-14b to convert the volumetric flow rate into a mass-like flow, the leakage rate acceptance criteria is calculated and conservatively reduced to the value presented in Table 4.1.1.

Table 4.2.12 provides additional parameters used in the analysis.

#### 4.2.5.9 Leak Test Sensitivity

The sensitivity for the overpack leakage test procedures is equal to one-half of the allowable leakage rate. The HI-STAR 100 containment packaging tests in Chapter 8 incorporate the appropriate leakage test procedure sensitivity. The leakage rates for the HI-STAR 100 containment packaging with its corresponding sensitivity are presented in Table 4.1.1.

Table 4.2.1

## FREE GAS VOLUME OF THE CONTAINMENT SYSTEM

<b>MPC Type</b>	Containment Volume (cm <sup>3</sup> )
MPC-24	6.70 x 10 <sup>6</sup>
<b>MPC-24E</b> <b>MPC-24EF</b>	6.55 x 10 <sup>6</sup>
Trojan MPC-24E Trojan MPC-24EF	6.12 x 10 <sup>6</sup>
MPC-32	6.35 x 10 <sup>6</sup>
MPC-68	6.15 x 10 <sup>6</sup>
MPC-68F	6.15 x 10 <sup>6</sup>

**Table 4.2.2**

ISOTOPE INVENTORY  
Ci/Assembly

Security-Related Information Figure  
Withheld Under 10 CFR 2.390.

Table 4.2.2 (continued)  
ISOTOPE INVENTORY

Security-Related Information Figure  
Withheld Under 10 CFR 2.390.

Table 4.2.2 (continued)

**ISOTOPE INVENTORY**

Ci/Assembly

Security-Related Information Figure  
Withheld Under 10 CFR 2.390.

Table 4.2.2 (continued)  
**ISOTOPE INVENTORY**  
Ci/Assembly

Security-Related Information Figure  
Withheld Under 10 CFR 2.390.



Table 4.2.2 (continued)  
ISOTOPE INVENTORY  
Ci/Assembly

## Security-Related Information Figure Withheld Under 10 CFR 2.390.

Note: The isotopes which contribute greater than 0.01% to the total curie inventory for the fuel assembly are considered in the evaluation as fines. Additionally, isotopes with  $A_2$  values less than 1.0 in Table A-1, Appendix A, 10CFR71 are included as fines and are designated in the table by an “\*\*”.

Table 4.2.3

TOTAL SOURCE TERM FOR THE HI-STAR 100 SYSTEM (Ci/cm<sup>3</sup>)

Security-Related Information Figure  
Withheld Under 10 CFR 2.390.

Table 4.2.4

VARIABLES FOUND IN NUREG/CR-6487 USED IN THE  
LEAKAGE RATE ANALYSIS

Variable	PWR		BWR	
	Normal	Accident	Normal	Accident
Fraction of crud that spalls, $f_C$	0.15	1.0	0.15	1.0
Crud surface activity (Ci/cm <sup>2</sup> )	$140 \times 10^{-06}$	$140 \times 10^{-06}$	$1254 \times 10^{-06}$	$1254 \times 10^{-06}$
Surface area per assembly, cm <sup>2</sup>	$3 \times 10^5$	$3 \times 10^5$	$1 \times 10^5$	$1 \times 10^5$
Fraction of rods that develop cladding breach, $f_B^\dagger$	0.03	1.0	0.03	1.0
Fraction of fines that are released, $f_f$	$3 \times 10^{-5}$	$3 \times 10^{-5}$	$3 \times 10^{-5}$	$3 \times 10^{-5}$
Fraction of gases that are released, $f_G$	0.3	0.3	0.3	0.3
Fraction of volatiles that are released, $f_v$	$2 \times 10^{-04}$	$2 \times 10^{-04}$	$2 \times 10^{-04}$	$2 \times 10^{-04}$

<sup>†</sup> The calculation for normal transport conditions of the Trojan MPC-24EF and MPC-68F each containing four (4) DFCs with fuel debris assumes that for the four DFCs, 100% of the rods of the fuel debris are breached. The remaining 20 or 64 assemblies in the Trojan MPC-24EF and MPC-68F, respectively, were assumed to have a 3% cladding rupture. Therefore,  $f_B$  for the Trojan MPC-24EF and the MPC-68F containing fuel debris is 0.192 and 0.087, respectively.

Table 4.2.5

INDIVIDUAL CONTRIBUTOR EFFECTIVE  $A_2$   
FOR GASES, CRUD, FINES, AND VOLATILES

<b>MPC Type</b>	<b><math>A_2</math> (Ci)</b>
<b>Gases</b>	
PWR MPCs	282
MPC-68	282
MPC-68F	285
Trojan MPCs	479
<b>Crud</b>	
All MPCs	10.8
<b>Fines</b>	
PWR MPCs	0.889
MPC-68	0.812
MPC-68F	0.351
Trojan MPCs	0.494
<b>Volatiles</b>	
PWR MPCs	9.72
MPC-68	9.90
MPC-68F	11.8
Trojan MPCs	11.8

Table 4.2.6

TOTAL SOURCE TERM EFFECTIVE  $A_2$  FOR  
NORMAL AND HYPOTHETICAL  
ACCIDENT CONDITIONS

<b>Normal Transport Conditions</b>	
	Effective $A_2$ (Ci)
MPC-24	60.3
MPC-24E MPC-24EF	60.3
Trojan MPC-24E	62.6
Trojan MPC-24EF	87.7
MPC-32	60.3
MPC-68	24.9
MPC-68F	30.6
<b>Accident Conditions</b>	
MPC-24	81.0
MPC-24E MPC-24EF	81.0
Trojan MPC-24E	85.8
Trojan MPC-24EF	85.8
MPC-32	81.0
MPC-68	52.1
MPC-68F	37.0

Table 4.2.7

## RADIONUCLIDE RELEASE RATES

	Allowable Release Rate ( $R_N$ or $R_A$ ) (Ci/s)
Normal Conditions	
MPC-24	1.68E-08
MPC-24E, MPC-24EF	1.68E-08
Trojan MPC-24E	1.74E-08
Trojan MPC-24EF	2.44E-08
MPC-32	1.68E-08
MPC-68	6.93E-09
MPC-68F	8.51E-09
Accident Conditions	
MPC-24	1.34E-04
MPC-24E, MPC-24EF	1.34E-04
Trojan MPC-24E	1.42E-04
Trojan MPC-24EF	1.42E-04
MPC-32	1.34E-04
MPC-68	8.59E-05
MPC-68F	6.10E-05

Table 4.2.8

Table Deleted

Table 4.2.9

## ALLOWABLE LEAKAGE RATES AT UPSTREAM PRESSURE

	$C_{\text{total}}$ (Ci/cm <sup>3</sup> )	Allowable Leakage Rate at $P_u$ $L_N$ or $L_A$ (cm <sup>3</sup> /s)
Normal Transport Conditions		
MPC-24	1.77E-04	9.47E-05
MPC-24E, MPC-24EF	1.81E-04	9.26E-05
Trojan MPC-24E	1.14E-04	1.53E-04
Trojan MPC-24EF	6.87E-04	3.55E-05
MPC-32	2.49E-04	6.73E-05
MPC-68	3.03E-04	2.29E-05
MPC-68F	9.56E-05	8.91E-05
Accident Conditions		
MPC-24	5.59E-03	2.39E-02
MPC-24E, MPC-24EF	5.72E-03	2.34E-02
Trojan MPC-24E	3.59E-03	3.95E-02
Trojan MPC-24EF	3.59E-03	3.95E-02
MPC-32	7.86E-03	1.70E-02
MPC-68	7.22E-03	1.19E-02
MPC-68F	1.00E-03	6.07E-02



Table 4.2.10

Table Deleted

Table 4.2.11

DELETED

Table 4.2.12

PARAMETERS FOR NORMAL, HYPOTHETICAL ACCIDENT  
AND TEST CONDITIONS

Parameter	Normal Conditions	Hypothetical Accident Conditions	Reference Test Conditions	Actual Test Conditions
$P_u$	114.7 psia (7.80 ATM)	239.7 psia (16.31 ATM)	1.68 ATM	1.68 ATM (min)
$P_d$	14.7 psia (1 ATM)	14.7 psia (1 ATM)	14.7 psia (1 ATM)	14.7 psia (1 ATM)
T	540°F (555 K)	1058°F (843 K)	373 K	373 K (max)
M	4 g/mol	4 g/mol	4 g/mol	4 g/mol
u	0.0304 cP	0.0397 cP	0.0231 cP	0.0231 cP
a	0.25 cm	0.25 cm	0.25 cm	0.25 cm

Table 4.2.13  
DELETED

Table 4.2.14  
DELETED

### 4.3 REGULATORY COMPLIANCE

Chapter 4 of this SAR has been prepared to summarize the containment features and capabilities of the HI-STAR 100 packaging. The containment boundary of the HI-STAR 100 packaging are designed and tested to ensure that the radionuclide release rates specified in 10CFR71.51 [4.0.1] will not be exceeded.

Leakage rates presented in Chapter 4 are determined in accordance with the requirements of ANSI N14.5 [4.0.2], and utilizing NUREG/CR-6487, *Containment Analysis for Type B Packages Used to Transport Various Contents* [4.0.3], Regulatory Guide 7.4, *Leakage Tests on Packages for Shipment of Radioactive Materials* [4.0.4] as content guides, and NUREG-1617, Standard Review Plan for Transportation Packages for Spent Nuclear Fuel [4.0.5].

The containment features and capabilities of the HI-STAR 100 packaging can be summarized in the following evaluation statements:

18. The HI-STAR 100 packaging, as presented in Chapter 4, complies with all applicable codes and standards for the containment system as identified in the chapter.
19. The containment boundary is securely closed by using multiple bolts and plugs. The closure of the containment boundary is sufficient to prevent unintentional opening or opening by pressure that may arise in the package as required by 10CFR71.43(c).
20. The materials of construction for the packaging containment are specified in the Bills-of-Material in Section 1.4. All materials and construction assure that there will be no significant chemical, galvanic, or other reaction as required by 10CFR71.43(d).
21. The overpack and MPC penetrations are designed to prevent leakage and protect against unauthorized operation by using cover plates to provide redundant closure as required by 10CFR71.43(e).
22. The containment system boundary for the HI-STAR 100 packaging consists of the overpack inner shell, the bottom plate, the top flange, the top closure plate, closure bolts, the overpack vent and drain port plugs, and their respective mechanical seals.

23. The HI-STAR 100 packaging is design, constructed, and prepared for shipment so that under the tests specified in 10CFR71.71 (normal conditions of transport), the package satisfies the containment requirement of 10CFR71.43(f) and 10CFR71.51(a)(1) for normal conditions of transport and 10CFR71.51(a)(2) for hypothetical accident conditions with no dependence on filters or a mechanical cooling system as required by 10CFR71.51(c).
24. The HI-STAR 100 packaging satisfies the containment requirements of 10CFR71, and the packaging meets the containment criteria of ANSI N14.5.

#### 4.4 REFERENCES

- [4.0.1] 10CFR71. "Packaging and Transportation of Radioactive Material." 2006
- [4.0.2] ANSIN14.5-1997. "American National Standard for Radioactive Materials-Leakage Tests on Packages for Shipment."
- [4.0.3] B.L. Anderson et al. *Containment Analysis for Type B Packages Used to Transport Various Contents*. NUREG/CR-6487, UCRL-ID-124822. Lawrence Livermore National Laboratory, November 1996.
- [4.0.4] U.S. Nuclear Regulatory Commission, Regulatory Guide 7.4, *Leakage Tests on Packages for Shipment of Radioactive Materials*, June 1975.
- [4.0.5] NUREG-1617, "Standard Review Plan for Transportation Packages for Spent Nuclear Fuel", Draft Report for Comment, March 1998.
- [4.1.1] American Society of Mechanical Engineers (ASME), Boiler and Pressure Vessel Code, Section III, Division 1, Subsection NB, Class 1 Components, 1995 Edition.
- [4.2.1] Deleted.
- [4.2.2] Deleted.
- [4.2.3] Rosenhow, W.M. and Hartnett, J.P., *Handbook of Heat Transfer*, Hemisphere Publishing Corporation, New York, 1973.
- [4.2.4] Shleien, B., *The Health Physics and Radiological Health Handbook*, Scinta, Inc. Silver Spring, MD, 1992.



## APPENDIX 4.A: BOLT AND PLUG TORQUES

This appendix provides the calculations used to determine the torque values for the vent and drain port plugs and cover plate bolts.

### 4.A.1 HI-STAR 100 Vent and Drain Port Plug Torques<sup>†</sup>

The HI-STAR 100 vent and drain port are sealed with plugs under which a mechanical seal is compressed. The objective of this calculation is to determine the torque required on the plug and to provide the required compressive load.

Given:

O-Ring (Mechanical Seal) Diameter:  $D_{OR} = 0.683$  in

O-Ring Compression:  $q_{OR} = 800$  lbf/in (pound force per linear inch)

Internal Pressure:  $p_i = 100$  psi

Plug Diameter:  $D_B = 0.5$  inch

Load due to internal overpack pressure:  $q_i = p_i \pi D_B^2 / 4 = 19.6$  lbf

Determine the required seating load:

The circumference of the O-Ring is:  $C_{OR} = \pi D_{OR}$   $C_{OR} = 2.14$  in

The required seating load is:  $F_i = q_i + P_{OR}$

$p_{OR} = C_{OR} q_{OR}$   $p_{OR} = 1712$  lbf

$F_i = 1732$  lbf

The procedure presented here is taken from Shingley, Joseph Edward and Mischke, Charles R., Mechanical Engineering Design, Fifth Edition, McGraw Hill, p. 344-346.

---

<sup>†</sup> Since the closure plate test port plug is the same material, diameter and uses the same seal, this calculation also applies to the closure plate test port plug.

Given a torque factor  $K = 0.30$  (for non-plated, non-lubricated plug).

Determine the required torque:

$$T = K F_i D_B$$

$$T = 0.30 (1732 \text{ lbf}) 0.5 \text{ in} \quad T = 259 \text{ in-lbf} \quad T = 22 \text{ ft-lbf}$$

#### 4.A.2 HI-STAR 100 Vent and Drain Port Cover Plate Bolt Torques

The HI-STAR 100 vent and drain port cover plates are sealed with a mechanical seal that is compressed under a bolted cover plate. The objective of this calculation is to determine the torque required on the bolts and to provide the required compressive load.

Given:

O-Ring (Mechanical Seal) Diameter:  $D_{OR} = 2.5 \text{ in}$

Required O-Ring Compression:  $q_{OR} = 1150 \text{ lbf/in}$  (pound force per linear inch)

Internal Pressure:  $p_i = 100 \text{ psi}$  (assumed)

Bolt Diameter:  $D_B = 0.375 \text{ inch}$

Number of Bolts:  $n = 4 \text{ bolts}$

Determine the required seating load:

The circumference of the O-Ring is:  $C_{OR} = \pi D_{OR} \quad C_{OR} = 7.85 \text{ in}$

The required seating load per bolt is:  $F_i = q_i + P_{OR}/n$

$$q_i = p_i \pi D_{OR}^2 / 4 \quad q_i = 491 \text{ lbf}$$

$$P_{OR} = C_{OR} q_{OR} \quad P_{OR} = 9028 \text{ lbf}$$

$$F_i = 9516 \text{ lbf} / 4 \quad F_i = 2380 \text{ ft-lbf}$$

The procedure presented here is taken from Shingley, Joseph Edward and Mischke, Charles R., Mechanical Engineering Design, Fifth Edition, McGraw Hill, p. 344-346.

Given a torque factor  $K = 0.15$  (See technical Bulletin for FELPRO N-5000 in Appendix 1.C).

For conservatism, the torque factor is increased by an additional 5 percent in the following calculation.

Determine the required torque:

$$T = K F_i D_B$$

$$T = 0.1575 (2380 \text{ lbf}) (0.375 \text{ in}) \quad T = 141 \text{ in-lbf} \quad T = 11.8 \text{ ft-lbf}$$

## APPENDIX 4.B: Manufacturer Seal Information (Total of 5 Pages Including This Page)

The information provided in this appendix provides additional details on the mechanical seals specified to ensure containment. The following is a listing of the drawings provided in this appendix.

- ASE Drawing No. 050038-TAB, Rev B, ".375 C-Ring, Spring Ener., Internal Pressure" (Detail of Closure Plate Mechanical Seals, Holtec Dwg. 1397 and Bill-of-Material 1476, Items 26 and 27)
- ASE Drawing No. 050033, Rev. B, "C-Ring, .062 Spring Energized, Internal Pressure" (Detail of Port Plug Mechanical Seal, Holtec Dwg. 1397 and Bill-of-Material 1476, Item 19)
- ASE Drawing No. 050118, Rev. A, ".062 C-Ring, Spring Ener., Internal Pressure" (Detail of Port Cover Mechanical Seal, Holtec Dwg. 1398 and Bill-of-Material 1476, Item 30)

The detailed dimensions, materials, and groove requirements are provided below for each mechanical seal.

### Closure Plate Outer Seal:

Holtec Item No.	27
ASE Part No.	ASE050038-TAB-1
Seal Type	Spring energized C-ring, internal pressure
Seal Size	72.50 OD x 3/8 free height
Material	Jacket Alloy X750
	Spring Alloy X750
Plating	Silver
Groove OD	72.545 inches nominal
Groove ID	71.685 inches nominal
Groove Depth	0.300 inches nominal

Closure Plate Inner Seal:

Holtec Item No.	26
ASE Part No.	ASE050038-TAB-2
Seal Type	Spring energized C-ring, internal pressure
Seal Size	71.00 OD x 3/8 free height
Material	Jacket Alloy X750
	Spring Alloy X750
Plating	Silver
Groove OD	71.045 inches nominal
Groove ID	70.175 inches nominal
Groove Depth	0.300 inches nominal

Port Plug Seal:

Holtec Item No.	19
ASE Part No.	ASE050033
Seal Type	Spring energized C-ring, internal pressure
Seal Size	0.75 OD x 0.062 free height
Material	Jacket Alloy X750
	Spring Alloy X750
Plating	Silver
Groove OD	0.760 inches nominal
Groove Depth	0.052 inches nominal

Port Cover Seal:

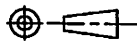
Holtec Item No.	30
ASE Part No.	ASE050118
Seal Type	Spring energized C-ring, internal pressure
Seal Size	2.50 OD x 0.062 free height
Material	Jacket Alloy X750
	Spring Alloy X750
Plating	Silver
Groove OD	2.52 inches nominal
Groove ID	2.31 inches nominal
Groove Depth	0.052 inches nominal

4.B-3

# Security-Related Information Figure Withheld Under 10 CFR 2.390.

DRAWING NO.	REV
050038-TAB	B

REVISIONS				
LTR.	DESCRIPTION	ECO	DATE	APPROVED
-	INITIAL RELEASE	96021	11-12-97	CAP
A	ADDED TESTING NOTE 8.	96021	06-10-98	CAP
B	LOAD INCREASED TO 1700-2200 LB	96021	12-01-99	CAP

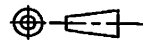
UNLESS OTHERWISE SPECIFIED		DRAWN	CAP	11-12-97	American Seal & Engineering Co., Inc. 156 Gando Drive New Haven, CT 06513, USA			
1. DECIMALS: JXX ±.010 JXX ±.005		CHECKED	JRP	11-12-97				
2. ANGLES: ±2°		D.A.	CAP	11-12-97				
3. FRACTIONS: ±1/64		ENGR.	CAP	11-12-97				
4. ALL DIMENSIONS ARE IN INCHES		MATERIAL: AS NOTED			TITLE: .375 C-RING, SPRING ENER., INTERNAL PRESSURE			
5. INTERPRET PER MIL-STD-100								
6. SURFACE ROUGHNESS 125/		TEMPER: AS NOTED			SIZE	CAGE NUMBER	DRAWING NO.	REV.
THIRD ANGLE PROJECTION					FINISH: AS NOTED	B	9G389	050038-TAB
					SCALE: NOTED	NEXT ASSY: -		SHEET: 1 OF 1

4.B-4

# Security-Related Information Figure Withheld Under 10 CFR 2.390.

DRAWING NO.	050033	REV	B
-------------	--------	-----	---

REVISIONS				
LTR.	DESCRIPTION	ECO	DATE	APPROVED
-	INITIAL RELEASE	96012	09-06-96	CAP
A	REDRAWN TO LATEST STD.	96012	01-13-98	CAP
B	Ag PER AMS 2410 WAS NI PER AMS 2424	96012	07-21-00	CAP

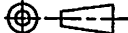
UNLESS OTHERWISE SPECIFIED			DRAWN	CAP	09-06-96	American Seal & Engineering Co., Inc. 156 Gando Drive New Haven, CT 06513, USA		
1. DECIMALS: JOX ±.010 JOX ±.005			CHECKED	JRP	09-06-98			
2. ANGLES: ±2°			D.A.	CAP	09-06-96			
3. FRACTIONS: ±1/64			ENGR.	CAP	09-06-96	TITLE .062 C-RING, SPRING ENER., INTERNAL PRESSURE		
4. ALL DIMENSIONS ARE IN INCHES			MATERIAL: AS NOTED					
5. INTERPRET PER MIL-STD-100			TEMPER: AS NOTED			SIZE	CAGE NUMBER	DRAWING NO.
6. SURFACE ROUGHNESS 125/✓			FINISH: AS NOTED			B	9G389	050033
THIRD ANGLE PROJECTION 						SCALE	NOTED	NEXT ASSY: -
						SHEET: 1 OF 1		

4.B-5

# Security-Related Information Figure Withheld Under 10 CFR 2.390.

DRAWING NO.	050118	REV	A
-------------	--------	-----	---

REVISIONS				
LTR.	DESCRIPTION	ECO	DATE	APPROVED
-	INITIAL RELEASE	97141	12-17-97	CAP
A	Ag PER AMS 2410 WAS NI PER AMS 2424	97141	07-21-00	CAP

UNLESS OTHERWISE SPECIFIED		DRAWN	CAP	12-17-97	American Seal & Engineering Co., Inc. 136 Gando Drive New Haven, CT 06513, USA
1. DECIMALS: JOX ±.010 JOKK ±.005		CHECKED	JRP	12-17-97	
2. ANGLES: ±2°		D.A.	CAP	12-17-97	
3. FRACTIONS: 1/164		ENGR.	CAP	12-17-97	
4. ALL DIMENSIONS ARE IN INCHES		MATERIAL			TITLE: .062 C-RING, SPRING ENER, INTERNAL PRESSURE
5. INTERPRET PER MIL-STD-100		AS NOTED			
6. SURFACE ROUGHNESS 125		TEMPER			SIZE
THIRD ANGLE PROJECTION		AS NOTED			CAGE NUMBER
		FINISH			DRAWING NO.
		AS NOTED			REV.
		SCALE: NOTED		NEXT ASSY: -	SHEET: 1 OF 1



## SUPPLEMENT 4.I

### CONTAINMENT EVALUATION OF THE HI-STAR HB **PACKAGE WITH MPC-HB**

#### 4.I.0 INTRODUCTION

This supplement is focused on providing containment evaluations for fuel from the Humboldt Bay Power Plant (HBPP) in the HI-STAR HB. The evaluation presented herein supplements those evaluations contained in the main body of Chapter 4 of this FSAR, and information in the main body of Chapter 4 is not repeated in this supplement. To aid the reader, the sections in this supplement are numbered in the same fashion as the corresponding sections in the main body of this chapter, i.e., Sections 4.I.1 through 4.I.3 correspond to Sections 4.1 through 4.3. Tables and figures in this supplement are labeled sequentially. The results of the evaluations in this supplement demonstrates the HI-STAR HB containment boundary compliance with the permitted activity release limits specified in 10 CFR 71, 71.51(a)(1) and 71.51(a)(2) for both normal and hypothetical accident conditions of transport.

#### 4.I.1 CONTAINMENT BOUNDARIES

The containment system boundary for the HI-STAR HB is identical to that of the HI-STAR 100 System described in Section 4.1. Therefore, the discussion provided in the main part of the chapter on the containment vessel, penetrations, seals, welds, closure and damaged fuel containers for the HI-STAR 100 System are directly applicable to the HI-STAR HB.

#### 4.I.2 REQUIREMENTS FOR NORMAL AND HYPOTHETICAL ACCIDENT CONDITIONS OF TRANSPORT

Supplement 2.I shows that all containment components for the HI-STAR HB are maintained within their code-allowable stress limits during all normal and hypothetical accident conditions of transport as defined in 10CFR71.71 and 10CFR71.73 [4.0.1]. Supplement 3.I shows that the peak containment component temperatures and pressure are within the design basis limits for all normal and hypothetical accident conditions of transport as defined in 10CFR71.71 and 10CFR71.73. Since the containment vessels remain intact, and the temperature and pressure design bases are not exceeded, the design basis leakage rate will not be exceeded during normal or hypothetical accident conditions of transport.

##### 4.I.2.1 Containment Criteria

The containment criteria are identical to those identified in Section 4.2.1 of the main part of the chapter.

#### 4.I.2.2 Containment of Radioactive Material

The HI-STAR HB packaging allowable leakage rate ensures that the requirements of 10CFR71.51 are met. Section 4.I.2.5 determines the maximum leakage rate for normal and hypothetical accident conditions of transport and the allowable leakage rate criterion for the HI-STAR HB packaging containing the MPC-HB. Following testing, no credit is taken for the MPC as a containment boundary for the transport of spent fuel.

#### 4.I.2.3 Pressurization of Containment Vessel

The HI-STAR HB is drained, dried, evacuated and backfilled with helium gas prior to final closure of the overpack in an identical way as the HI-STAR 100 System described in the main part of the chapter.

#### 4.I.2.4 Assumptions

The following assumptions have been used in determining the allowable leakage rates in addition to those already listed in Section 4.2.4:

1. The MPC-HB contains 80 Humboldt Bay fuel assemblies of which up to forty (40) may be DFCs containing specified fuel debris or damaged fuel.
2. In calculating the leakage rates of the containment system for normal conditions of transport, the internal pressure of the overpack is assumed to be equal to the maximum internal pressure determined in Supplement 3.I with 3% rod rupture.
3. The average cavity temperature for normal conditions is conservatively assumed to be the maximum cladding temperature from Supplement 3.I.
4. The average cavity temperature for hypothetical accident conditions is conservatively assumed to be the design basis peak cladding temperature.

#### 4.I.2.5 Analysis and Results

The methodology to determine the allowable leakage rates from the HI-STAR HB for normal and hypothetical accident conditions is identical to the methodology employed in the main part of the chapter for the HI-STAR 100 System. The only differences are in the input information, which is detailed in the following sections.

##### 4.I.2.5.1 Volume in the Containment Vessel

The free gas volume in the MPC-HB is presented in Table 4.I.2.1. For calculating the free volume in the containment system (overpack) the volume of the annulus space is added to the

free volume of the MPC-HB. This will conservatively underestimate the free volume inside the containment boundary.

#### 4.I.2.5.2 Source Terms for Spent Nuclear Fuel Assemblies

The inventory for isotopes other than  $^{60}\text{Co}$  is calculated with the SAS2H and ORIGEN-S modules of the SCALE 4.3 system as described in Chapter 5. The inventory for the MPC-HB was based the Humboldt Bay 6x6 fuel assembly with a burnup of 23,000 MWD/MTU, 29 years of cooling time, and 2.09 wt% enrichment. The isotopes which contribute greater than 0.01% to the total curie inventory for the fuel assembly are considered in the evaluation as fines. Additionally, isotopes with  $A_2$  values less than 1.0 in Table A-1, Appendix A, 10CFR71 are included as fines. Isotopes which contribute greater than 0.01% but which do not have an assigned  $A_2$  value in Table A-1 are assigned an  $A_2$  value based on the guidance in Table A-3, Appendix A, 10CFR71. Isotopes which contribute greater than 0.01% but have a radiological half life less than 10 days are neglected. Table 4.I.2.2 presents the isotope inventory used in the calculation.

##### A. Source Activity Due to Crud Spallation from Fuel Rods

The source term activity associated with crud for the Humboldt Bay fuel was calculated in the same way as in the main part of the chapter. The inventory for  $^{60}\text{Co}$  was determined by using the crud surface activity for BWR rods ( $1254 \times 10^{-6} \text{ Ci/cm}^2$ ) provided in NUREG/CR-6487 [4.0.3] multiplied by the surface area per assembly ( $1 \times 10^5 \text{ cm}^2$  for BWR fuel, also provided in NUREG/CR-6487). The source terms were then decay corrected 29 years using equation 4-1.

##### **BWR**

$$\begin{aligned} \text{Surface area per Assy} &= 1.0\text{E}+05 \text{ cm}^2 \\ 1254 \mu\text{Ci/cm}^2 \times 1.0\text{E}+05 \text{ cm}^2 &= 125.4 \text{ Ci/assy} \end{aligned}$$

##### **MPC-HB**

$$\begin{aligned} {}^{60}\text{Co}(29) &= 125.4 \text{ Ci } e^{-(\ln 2/5.272)(29)} \\ {}^{60}\text{Co}(29) &= 2.769 \text{ Ci/assy} \end{aligned}$$

A summary of the  $^{60}\text{Co}$  inventory available for release is provided in Table 4.I.2.2.

The activity density that results inside the HI-STAR HB containment vessel as a result of crud spallation from spent fuel rods is calculated using Equation 4-2.

##### B. Source Activity Due to Releases of Fines from Cladding Breaches

The source term activity associated with fines for the Humboldt Bay fuel was calculated in the same way as in the main part of the chapter.

The calculation for normal transport conditions of a MPC-HB containing forty (40) DFCs containing fuel debris assumes that for the forty DFCs, 100% of the rods of the fuel debris are breached. The remaining 40 in the MPC-HB were assumed to have a 3% cladding rupture. Therefore,  $f_B$  for an MPC-HB containing fuel debris is:

$$f_B = (0.03)\frac{40}{80} + (1.0)\frac{40}{80} \quad (4.I-1)$$

$$f_B = 0.515$$

The activity concentration inside the containment vessel due to fines being released from cladding breaches is given by Equation 4-4.

#### C. Source Activity from Gases due to Cladding Breaches

The source term activity associated with gases for the Humboldt Bay fuel was calculated in the same way as in the main part of the chapter.

The activity concentration due to the release of gases from a cladding breach is given by Equation 4-5.

#### D. Source Activity from Volatiles due to Cladding Breaches

The source term activity associated with volatiles for the Humboldt Bay fuel was calculated in the same way as in the main part of the chapter.

The activity concentration due to the release of volatiles from a cladding breach is given by Equation 4-6.

#### E. Total Source Term for the HI-STAR HB System

The total source term was determined using Equation 4-7. Table 4.I.2.3 presents the total source term determined using the above methodology.

##### 4.I.2.5.3 Effective $A_2$ of Individual Contributors (Crud, Fines, Gases, and Volatiles)

Table 4.I.2.3 presents the total source term determined using the above methodology. Table 4.2.4 in the main part of the chapter summarizes the parameters from NUREG/CR-6487 used in this analysis, with the exception of the fraction of rods that develop cladding breaches, which is explained in the previous section. Table 4.I.2.4 summarizes the effective  $A_2$  for all individual contributors.

##### 4.I.2.5.4 Releasable Activity

The release activity of fines, volatiles, gases, and crud were determined using Equation 4-9.

#### 4.I.2.5.5 Effective $A_2$ for the Total Source Term

The total source term effective  $A_2$  was calculated in the same way as in the main chapter. The results are summarized in Table 4.I.2.5

#### 4.I.2.5.6 Allowable Radionuclide Release Rates

The HI-STAR HB containment system is designed to the same containment criteria as the HI-STAR 100 System. These criterion are given in 10CFR71.51(a)(1) for normal conditions and 10CFR71.51(b)(2) for hypothetical accident conditions.

Equations 4-10 and 4-11 were used to determine the allowable radionuclide release rate for the MPC-HB under normal and hypothetical accident conditions. The release rates for the MPC-HB are summarized in Table 4.I.2.6.

#### 4.I.2.5.7 Allowable Leakage Rates at Operating Conditions

The allowable leakage rates at operating conditions were determined using Equation 4-12. Table 4.I.2.7 summarizes the allowable leakage rates at the upstream pressures. The most limiting allowable leakage rate presented in Table 4.I.2.7 was conservatively selected and used to determine the leakage rate acceptance criterion for the MPC-HB.

#### 4.I.2.5.8 Leakage Rate Acceptance Criteria for Test Conditions

The leakage rate acceptance criteria for test conditions was determined using the same methodology presented in Section 4.2.5.8 of the main part of the chapter. The reference test conditions, and approximate actual test conditions for the MPC-HB are specified in Table 4.I.2.8.

#### 4.I.2.5.9 Leak Test Sensitivity

The sensitivity for the overpack leakage test procedures is equal to one-half of the allowable leakage rate. The HI-STAR HB containment packaging tests in Chapter 8 incorporate the appropriate leakage test procedure sensitivity. The leakage rates for the HI-STAR 100 containment packaging with its corresponding sensitivity are presented in Table 4.1.1.

### 4.I.3 REGULATORY COMPLIANCE

The HI-STAR HB is identical to the HI-STAR 100 System in that it is designed and tested to ensure compliance with the radionuclide release rates specified in 10CFR71.51 [4.0.1] for normal and hypothetical accident transport conditions.

Table 4.I.2.1

FREE GAS VOLUME OF THE HI-STAR HB CONTAINMENT SYSTEM

Containment Volume [cm <sup>3</sup> ]	3.40 x 10 <sup>6</sup>
--	------------------------

Table 4.I.2.2

Isotopic Inventory for the HI-STAR HB

Security-Related Information Figure  
Withheld Under 10 CFR 2.390.

Table 4.I.2.2 (continued)  
ISOTOPE INVENTORY

Security-Related Information Figure  
Withheld Under 10 CFR 2.390.



Table 4.I.2.2 (continued)  
ISOTOPE INVENTORY

Security-Related Information Figure  
Withheld Under 10 CFR 2.390.

Table 4.I.2.2 (continued)  
ISOTOPE INVENTORY

Security-Related Information Figure  
Withheld Under 10 CFR 2.390.

Table 4.I.2.3

TOTAL SOURCE TERM FOR THE HI-STAR HB (Ci/cm<sup>3</sup>)

	$C_{\text{crud}}$ (Ci/cm <sup>3</sup> )	$C_{\text{fines}}$ (Ci/cm <sup>3</sup> )	$C_{\text{gas}}$ (Ci/cm <sup>3</sup> )	$C_{\text{vol}}$ (Ci/cm <sup>3</sup> )	Total (Ci/cm <sup>3</sup> )
Normal Transport Conditions					
HI-STAR HB	9.77E-06	1.43E-06	2.82E-04	1.22E-05	3.06E-04
Accident Conditions					
HI-STAR HB	6.52E-05	2.78E-06	5.48E-04	2.36E-05	6.40E-04

Table 4.I.2.4

INDIVIDUAL CONTRIBUTOR EFFECTIVE  $A_2$  FOR GASES, CRUD, FINES, AND  
VOLATILES FOR THE HI-STAR HB

HI-STAR HB	$A_2$ (Ci)
Gases	2.46E+03
Crud	10.8
Fines	3.13E-01
Volatiles	1.16E+01

Table 4.I.2.5

TOTAL SOURCE TERM EFFECTIVE  $A_2$  FOR NORMAL  
AND HYPOTHETICAL ACCIDENT CONDITIONS FOR THE HI-STAR HB

	Effective $A_2$ (Ci)
Normal Transport Conditions	
HI-STAR HB	46.1
Accident Conditions	
HI-STAR HB	37.3

Table 4.I.2.6

## RADIONUCLIDE RELEASE RATES FOR THE HI-STAR HB

	Allowable Release Rate ( $R_N$ or $R_A$ ) (Ci/s)
Normal Conditions	
HI-STAR HB	1.28E-08
Accident Conditions	
HI-STAR HB	6.15E-05

Table 4.I.2.7

## ALLOWABLE LEAKAGE RATES AT UPSTREAM PRESSURE FOR THE HI-STAR HB

	Allowable Leakage Rate at $P_u L_N$ or $L_A$ ( $\text{cm}^3/\text{s}$ )
Normal Transport Conditions	
HI-STAR HB	4.19E-05
Accident Conditions	
HI-STAR HB	9.61E-02

Table 4.I.2.8

PARAMETERS FOR NORMAL, HYPOTHETICAL ACCIDENT  
AND TEST CONDITIONS FOR THE HI-STAR HB

Parameter	Normal Conditions	Hypothetical Accident Conditions	Reference Test Conditions	Actual Test Conditions
$P_u$	84.4 psia (5.74 ATM)	214.7 psia (14.61 ATM)	1.68 ATM	1.68 ATM (min)
$P_d$	14.7 psia (1 ATM)	14.7 psia (1 ATM)	14.7 psia (1 ATM)	14.7 psia (1 ATM)
T	419°F (488 K)	1058°F (843 K)	373 K	373 K (max)
M	4 g/mol	4 g/mol	4 g/mol	4 g/mol
$\mu$	0.0276 cP	0.0397 cP	0.0231 cP	0.0231 cP
a	0.25 cm	0.25 cm	0.25 cm	0.25 cm



## SUPPLEMENT 4.II

### CONTAINMENT EVALUATION OF THE HI-STAR HB GTCC with GWC-HB

#### 4.II.0 INTRODUCTION

This supplement is focused on providing containment evaluations for Greater-Than-Class C Low-Level Radioactive Waste (GTCC) in the HI-STAR 100 Version HB GTCC (HI-STAR HB GTCC) with GTCC waste container (GWC-HB). The evaluation presented herein supplements those evaluations contained in the main body of Chapter 4 of this FSAR, and information in the main body of Chapter 4 is not repeated in this supplement. To aid the reader, the sections in this supplement are numbered in the same fashion as the corresponding sections in the main body of this chapter, i.e., Sections 4.II.1 through 4.II.3 correspond to Sections 4.1 through 4.3. Tables and figures in this supplement are labeled sequentially. The results of the evaluations in this supplement demonstrates the HI-STAR HB GTCC containment boundary compliance with the permitted activity release limits specified in 10 CFR 71, 71.51(a)(1) and 71.51(a)(2) for both normal and hypothetical accident conditions of transport.

GWC-HB is vacuum dried, backfilled with helium and leak tested by hydrostatic pressure test while the HI-STAR HB GTCC overpack is not vacuum dried, helium backfilled or pressure tested and the closure lid of the overpack features no containment seal, as described in Section 1.II.2.

#### 4.II.1 CONTAINMENT BOUNDARIES

Since the HI-STAR HB GTCC overpack lacks containment seals, the GWC-HB contained in the HI-STAR HB GTCC overpack takes on the role of containment system boundary, while the HI-STAR HB GTCC overpack only takes on a structural (support and protection) role. The GWC-HB is similar to the Multiple-Purpose Canister (MPC) with a spent fuel cask. The GWC-HB enclosure vessel is credited as the sole containment boundary which consists of the base plate, top and bottom lids, upper and lower outer GWC-HB canister shell plates, closure ring, and vent and drain port cover plates. The containment boundary system components for the HI-STAR HB GTCC system are designed and fabricated in accordance with the requirements of ASME Code, Section III, Subsection NB [4.1.1] to the maximum extent practicable. Chapter 1 provides design criteria for the containment design. Section 1.II.3 provides applicable code requirement. The containment components are shown in Figure 4.II.1.1 with additional details provided in drawings listed in Section 1.II.4.

##### 4.II.1.1 Containment Vessel

The containment vessel for the GWC-HB consists of the components which form the inner cavity volume that contains GTCC. The HI-STAR HB GTCC overpack which houses GWC-HB does not provide containment function. The containment vessel components create an enclosed cylindrical cavity sufficient for insertion and enclosure of the GTCC. The materials of construction for the packaging containment vessel are specified in the drawings in Section 1.II.4.

#### 4.II.1.2 Containment Penetrations

The only containment system boundary penetration for the GWC-HB is the drain port. The penetration has redundant mechanical seals. The lift hole and the top handling hole located in the lid of GWC-HB do not penetrate the containment system boundary. The containment penetrations are designed and tested to ensure that the radionuclide release rates specified in 10CFR71.51 will not be exceeded.

#### 4.II.1.3 Seals and Welds

The GWC-HB of HI-STAR HB GTCC uses a combination of seals and welds designed and tested to provide containment. Seals and welds are individually discussed below. The seals and welds provide a containment system, which is securely closed, cannot be opened unintentionally or by an internal pressure within the package as required in 10CFR71.43(c).

##### 4.II.1.3.1 Containment Seals

The HI-STAR HB GTCC overpack lacks containment seals thus the GWC-HB takes on the role of containment.

The process waste is contained in a Process Waste Container (PWC) which is placed with the Outer Container welded to the bottom of the GWC-HB. The PWC is not-important-to-safety mechanically sealed, vacuum dried, helium-backfilled and leak tested and provides no safety function for transportation.

The closure of vent port and drain port of GWC-HB is provided by the port cover plates with corresponding seals and secured with bolts.

Chapter 7 describes the operating procedures required for proper seal function. Seal and closure details are provided in the drawing package in Section 1.II.4.

##### 4.II.1.3.2 Containment Welds

The containment boundary welds for the GWC-HB include:

- welds forming the shell plates,
- welds connecting the shell plates to the top lid, and
- welds connecting the shell plates to the base plate.

Full-penetration welds are specified for the plates that form the containment shell. Full-penetration welds are also specified for the shell to the top lid and base plate welds. The weld fabrication and inspection details are shown in the drawings in Section 1.II.4.

#### 4.II.1.4 Closure

The GWC-HB consists of a smooth walled, welded stainless steel cylindrical canister with a removable lid. After loading the GTCC waste into the GWC-HB, a lid is placed on top of the GWC-HB and is welded to the shell to provide the means of GWC-HB closure and handling. An inflatable annulus seal is also installed in the top part of the overpack-to-GWC-HB annulus to minimum the risk of contamination the external shell of the GWC-HB. The GWC-HB is vacuum dried, backfilled with helium and leak tested. Then a lid is placed on top of the HI-STAR HB GTCC Overpack and bolted shut.

#### 4.II.2 REQUIREMENTS FOR NORMAL AND HYPOTHETICAL ACCIDENT CONDITIONS OF TRANSPORT

Supplement 2.II shows that all containment components for the HI-STAR HB GTCC are maintained within their code-allowable stress limits during all normal and hypothetical accident conditions of transport as defined in 10CFR71.71 and 10CFR71.73 [4.0.1]. Supplement 3.II shows that the peak containment component temperatures and pressure are within the design basis limits for all normal and hypothetical accident conditions of transport as defined in 10CFR71.71 and 10CFR71.73. Since the containment vessels remain intact, and the temperature and pressure design bases are not exceeded, the design basis leakage rate will not be exceeded during normal or hypothetical accident conditions of transport.

##### 4.II.2.1 Containment Criteria

The allowable leakage rates presented in this supplement were determined in accordance with ANSI N14.5-1997 [4.0.2] and shall be used for containment system fabrication verification and containment system periodic verification tests of the HI-STAR HB GTCC containment boundary. Measured leakage rates shall not exceed the values presented in Table 4.II.2.9.

##### 4.II.2.2 Containment of Radioactive Material

The HI-STAR HB GTCC packaging allowable leakage rate ensures that the requirements of 10CFR71.51 are met. Section 4.II.2.5 determines the maximum leakage rate for normal and hypothetical accident conditions of transport and the allowable leakage rate criterion for the GWC-HB contained in the HI-STAR HB GTCC packaging. Following testing, no credit is taken for the HI-STAR HB GTCC overpack as a containment boundary for the transport of radioactive waste.

#### 4.II.2.3 Pressurization of Containment Vessel

The enclosed GWC-HB takes on the role of containment boundary for the HI-STAR HB GTCC packaging. The GWC-HB is drained, dried, evacuated and backfilled with helium gas prior to its final closure; and the interior of the GWC-HB contains metallic waste at relatively low temperatures. Therefore, there is no possibility of chemical reaction that would produce gas or vapor to significantly affect the internal pressure of the containment vessel. The potential for an explosive level of gases due to radiological decomposition in the containment vessel cavity is eliminated by excluding foreign materials in the package.

#### 4.II.2.4 Assumptions

The following assumptions have been used in determining the allowable leakage rates for the GWC-HB:

[

PROPRIETARY INFORMATION WITHHELD PER 10CFR2.390

]

[

PROPRIETARY INFORMATION WITHHELD PER 10CFR2.390

]

#### 4.II.2.5 Analysis and Results

The waste transported in HI-STAR HB GTCC is limited to GTCC radioactive waste. The specific guidance in NUREG/CR-6487, Chapter 4 “Solid Byproduct or Special Nuclear

Materials” is followed in determining the appropriate source terms for waste transported in HI-STAR HB GTCC. More specifically, the guidance on both non-dispersible solids that have releasable surface contamination and dispersible radioactive solids is followed.

#### 4.II.2.5.1 Volume in the Containment Vessel

The free gas volume of the GWC-HB is used as free volume in the containment vessel and presented in Table 4.II.2.1.

#### 4.II.2.5.2 Source Terms

##### A. Source Terms for Non-Dispersible Solids

The source-terms from releasable activity arise from surface activity of transported waste for non-dispersible solids. Similar to the treatment of crud on the surface of irradiated nuclear fuel rods, the crud spallation fractions for normal and accident conditions are assumed. The majority of the activity associated with crud is due to  $^{60}\text{Co}$  per NUREG/CR-6487. Therefore all surface activity is assumed to be  $^{60}\text{Co}$  and the amount is presented in Table 4.II.2.3.

In transportation packages holding non-dispersible solids, the releasable material consists of fine particulates that spall-off the surface of the solids to create a powder aerosol inside the containment vessel. The activity concentration of the powder aerosol can be formulated as:

$$C_n = \frac{f_n A_s}{V} \quad (4-II-1)$$

where,

$C_n$  is the activity concentration as a result of crud spallation for non-dispersible solids [ $\text{Ci}/\text{cm}^3$ ],

$f_n$  is the activity fraction of the surface contamination that spalls-off the surface contaminated solids, the value is 15% for normal conditions and 100% for hypothetical accident conditions, as shown in Table 4.II.2.3,

$A_s$  is the surface activity [ $\text{Ci}$ ].  $A_s = S_{AS} \times A_{SC}$ , where  $S_{AS}$  is total surface area of the contaminated solids [ $\text{cm}^2$ ] shown in Table 4.II.2.3, and  $A_{SC}$  is activity surface density of the contaminated solids [ $\text{Ci}/\text{cm}^2$ ] shown in Table 4.II.2.3,

$V$  is the free volume inside the containment vessel [ $\text{cm}^3$ ].

The activity density that results inside the HI-STAR HB GTCC containment vessel as a result of crud spallation from spent fuel rods is calculated using Equation 4-2. Calculated activity concentrations for normal and hypothetical accident conditions are provided in Table 4.II.2.5.

##### B. Source Terms for Dispersible Solids

Dispersible solid materials will tend to fracture and crumble due to handling, vibration, or accident conditions. These conditions will tend to cause the radioactive solid material inside the containment vessel to produce a powder aerosol. According to NUREG/CR-6487, the source-term concentration of dispersible solids can be formulated as:

$$C_d = a_d \rho_d \quad (4-II-2)$$

where,

$C_d$  is the activity concentration of the dispersible solids [Ci/cm<sup>3</sup>],  
 $a_d$  is the specific activity of the dispersible solids [Ci/g], as shown in Table 4.II.2.4,  
 $\rho_d$  is the aerosol mass density of the dispersible solids [g/cm<sup>3</sup>]. A reasonable bounding value of the mass density of a powder aerosol is shown in Table 4.II.2.4 based on discussion in Chapter 4 of NUREG/CR-6487.

Calculated activity concentrations for normal and hypothetical accident conditions are provided in Table 4.II.2.5.

#### C. Total Source Term for the HI-STAR HB GTCC System

The total source term was determined by combining Equations 4-II-2 and 4-II-3:

$$C_{\text{total}} = C_n + C_d \quad (4-II-3)$$

where  $C_{\text{total}}$  has units of Ci/cm<sup>3</sup>.

Table 4.II.2.5 presents the total source term determined using the above methodology and the parameters from NUREG/CR-6487 used in this analysis.

##### 4.II.2.5.3 Effective $A_2$ Value of Individual Contributors

The  $A_2$  of the individual contributions (i.e., non-dispersible solids and dispersible solids) were determined in accordance with NUREG/CR-6487. As described in Subparagraph 4.II.2.5.2, source-terms from non-dispersible solids arise from surface activity and all activity is assumed to be <sup>60</sup>Co.  $A_2$  value for <sup>60</sup>Co is provided in 10CFR71, Appendix A and reproduced in Table 4.II.2.6.

In accordance with methodology presented in 10CFR71, Appendix A for mixtures of different radionuclides, Equation 4-8 was used to determine the  $A_2$  values for the dispersible solids. Table 4.II.2.6 summarizes the effective  $A_2$  for the dispersible solids.

##### 4.II.2.5.4 Releasable Activity

The releasable activity is the product of the activity concentration and free volume in containment boundary of HI-STAR HB GTCC package.

The releasable activities of non-dispersible solids and dispersible solids were determined using Equation 4-9.

#### 4.II.2.5.5 Effective $A_2$ for the Total Source Term

Using the releasable activity and the effective  $A_2$  values from the individual contributors (i.e., non-dispersible solids and dispersible solids), the effective  $A_2$  for the total source term was calculated for normal transportation and hypothetical accident conditions. The methodology used to determine the effective  $A_2$  is the same as that used for a mixture, which is provided in Equation 4-8. The results are summarized in Table 4.II.2.6.

#### 4.II.2.5.6 Allowable Radionuclide Release Rates

The HI-STAR HB GTCC containment system is designed to the same containment criteria as the HI-STAR 100 System. These criteria are given in 10CFR71.51(a)(1) for normal conditions and 10CFR71.51(a)(2) for hypothetical accident conditions.

Equations 4-10 and 4-11 were used to determine the allowable radionuclide release rate for the GWC-HB under normal and hypothetical accident conditions. The release rates for the GWC-HB are summarized in Table 4.II.2.7.

#### 4.II.2.5.7 Allowable Leakage Rates at Operating Conditions

The allowable leakage rates at operating conditions were determined using Equation 4-12. Table 4.II.2.8 summarizes the allowable leakage rates at the upstream pressures. The most limiting allowable leakage rate presented in Table 4.II.2.8 was conservatively selected and used to determine the leakage rate acceptance criterion for the GWC-HB.

#### 4.II.2.5.8 Leakage Rate Acceptance Criteria for Test Conditions

The leakage rate acceptance criteria for test conditions were determined using the same methodology presented in Section 4.2.5.8 of the main part of the chapter. The reference test conditions for the GWC-HB are specified in Table 4.II.2.2.

#### 4.II.2.5.9 Leak Test Sensitivity



The sensitivity for the overpack leakage test procedures is equal to one-half of the allowable leakage rate. The leakage rates for the HI-STAR HB GTCC containment packaging with its corresponding sensitivity are presented in Table 4.II.2.9.

#### 4.II.3 REGULATORY COMPLIANCE

The HI-STAR HB GTCC is designed and tested to ensure compliance with the radionuclide release rates specified in 10CFR71.51 [4.0.1] for normal and hypothetical accident transport conditions.

#### 4.II.4 REFERENCE

- [4.II.2.1] “Humboldt Bay Power Plant Unit 3 Reactor Vessel and Internals Activation Evaluation”, WMG Reports WMG-09-026-RE-132, Revision 2, Pacific Gas & Electric, July 2011.
- [4.II.2.2] “Radiological Characterization of Shut Down Nuclear Reactors for Decommissioning Purposes”, Technical Reports Series No. 389, Activities in Tables XVI to XXI, and Surface Activity Densities in Annexes I-1 to I-9 International Atomic Energy Agency, Vienna, 1998.
- [4.II.2.3] “Supplemental Characterization of Container ISC-18 at the Humboldt Bay Power Plant Unit 3”, DW James Calculation DAC-2003, Revision 0, July 2009.

Figure 4.II.1.1: PROPRIETARY INFORMATION WITHHELD PER 10CFR2.390

Table 4.II.2.1

FREE GAS VOLUME OF THE HI-STAR HB CONTAINMENT SYSTEM

HI-STAR HB GTCC Containment Volume [cm <sup>3</sup> ]	PROPRIETARY INFORMATION WITHHELD PER 10CFR2.390
--	--

Table 4.II.2.2

PARAMETERS FOR NORMAL, HYPOTHETICAL ACCIDENT  
AND TEST CONDITIONS FOR THE HI-STAR HB GTCC

Parameter	Normal Conditions	Hypothetical Accident Conditions	Reference Test Conditions
$P_u$	32.6 psia (2.22 ATM)	Refer to Table 4.I.2.8	Refer to Table 4.I.2.8
$P_d$	14.7 psia (1 ATM)		
T	150°F (339 K)		
M	4 g/mol		
$\mu$	0.0217 cP		
a	0.25 cm		

Table 4.II.2.3

PROPRIETARY INFORMATION WITHHELD PER 10CFR2.390

Table 4.II.2.4

PROPRIETARY INFORMATION WITHHELD PER 10CFR2.390

Table 4.II.2.5

PROPRIETARY INFORMATION WITHHELD PER 10CFR2.390

Table 4.II.2.6

PROPRIETARY INFORMATION WITHHELD PER 10CFR2.390



Table 4.II.2.7

PROPRIETARY INFORMATION WITHHELD PER 10CFR2.390

Table 4.II.2.8

PROPRIETARY INFORMATION WITHHELD PER 10CFR2.390

Table 4.II.2.9

SUMMARY OF CONTAINMENT BOUNDARY DESIGN SPECIFICATIONS FOR  
THE HI-STAR HB GTCC

Design Attribute	Design Rating
Leakage Rate Acceptance Criterion	$2.0 \times 10^{-2}$ atm-cm <sup>3</sup> /s, He
Leakage Rate Test Sensitivity	$1.0 \times 10^{-2}$ atm-cm <sup>3</sup> /s, He

## SUPPLEMENT 4.III

### CONTAINMENT EVALUATION OF OF THE HI-STAR 100 SYSTEM WITH DIABLO CANYON MPC-32

#### 4.III.0 INTRODUCTION

This supplement is focused on providing containment evaluations for fuel from the Diablo Canyon Nuclear Plant (DCNPP) in the HI-STAR 100 system with Diablo Canyon MPC-32. The evaluation presented herein supplements those evaluations contained in the main body of Chapter 4 of this FSAR, and information in the main body of Chapter 4 is not repeated in this supplement. To aid the reader, the sections in this supplement are numbered in the same fashion as the corresponding sections in the main body of this chapter, i.e., Sections 4.III.1 through 4.III.3 correspond to Sections 4.1 through 4.3. Tables and figures in this supplement are labeled sequentially. The results of the evaluations in this supplement demonstrates the containment boundary of the HI-STAR 100 with Diablo Canyon MPC-32 compliance with the permitted activity release limits specified in 10 CFR 71, 71.51(a)(1) and 71.51(a)(2) for both normal and hypothetical accident conditions of transport.

#### 4.III.1 CONTAINMENT BOUNDARIES

The containment system boundary is identical to that of the HI-STAR 100 System described in Section 4.1. Therefore, the discussion provided in the main part of the chapter on the containment vessel, penetrations, seals, welds, closure and damaged fuel containers for the HI-STAR 100 System are directly applicable to the HI-STAR HB.

#### 4.III.2 REQUIREMENTS FOR NORMAL AND HYPOTHETICAL ACCIDENT CONDITIONS OF TRANSPORT

Supplement 2.III shows that all containment components for the HI-STAR 100 with Diablo Canyon MPC-32 are maintained within their code-allowable stress limits during all normal and hypothetical accident conditions of transport as defined in 10CFR71.71 and 10CFR71.73 [4.0.1]. Supplement 3.II shows that the peak containment component temperatures and pressure are within the design basis limits for all normal and hypothetical accident conditions of transport as defined in 10CFR71.71 and 10CFR71.73. Since the containment vessels remain intact, and the temperature and pressure design bases are not exceeded, the design basis leakage rate will not be exceeded during normal or hypothetical accident conditions of transport.

##### 4.III.2.1 Containment Criteria

The containment criteria are identical to those identified in Section 4.2.1 of the main part of the chapter.

#### 4.III.2.2 Containment of Radioactive Material

The packaging of HI-STAR 100 with Diablo Canyon MPC-32 allowable leakage rate ensures that the requirements of 10CFR71.51 are met. Section 4.III.2.5 determines the maximum leakage rate for normal and hypothetical accident conditions of transport and the allowable leakage rate criterion for the HI-STAR 100 packaging containing the Diablo Canyon MPC-32. Following testing, no credit is taken for the MPC as a containment boundary for the transport of spent fuel.

#### 4.III.2.3 Pressurization of Containment Vessel

The HI-STAR 100 with Diablo Canyon MPC-32 is drained, dried, evacuated and backfilled with helium gas prior to final closure of the overpack in an identical way as the HI-STAR 100 System described in the main part of the chapter.

#### 4.III.2.4 Assumptions

The assumptions used in determining the allowable leakage rates are the same as those already listed in Section 4.2.4 for the standard length MPC-32.

#### 4.III.2.5 Analysis and Results

The methodology to determine the allowable leakage rates from the HI-STAR 100 with Diablo Canyon MPC-32 for normal and hypothetical accident conditions is identical to the methodology employed in the main part of the chapter for the HI-STAR 100 System. The only differences are in the input information, which is detailed in the following sections.

##### 4.III.2.5.1 Volume in the Containment Vessel

The free gas volume in the Diablo Canyon MPC is presented in Table 4.III.2.1. For calculating the free volume in the containment system (overpack) the volume of the annulus space is added to the free volume of the Diablo Canyon MPC-32. This will conservatively underestimate the free volume inside the containment boundary.

##### 4.III.2.5.2 Source Terms for Spent Nuclear Fuel Assemblies

The inventory for the Diablo Canyon MPC-32 was assumed as the same as that for the PWR MPCs described in Paragraph 4.2.5.2 and Table 4.2.2.2.

##### 4.III.2.5.3 Effective $A_2$ of Individual Contributors (Crud, Fines, Gases, and Volatiles)

Table 4.III.2.2 presents the total source term determined using the above methodology. Table 4.2.4 in the main part of the chapter summarizes the parameters from NUREG/CR-6487 used in this analysis, with the exception of the fraction of rods that develop cladding breaches, which is

explained in the previous section. Table 4.III.2.3 summarizes the effective  $A_2$  for all individual contributors.

#### 4.III.2.5.4 Releasable Activity

The release activity of fines, volatiles, gases, and crud were determined using Equation 4-9.

#### 4.III.2.5.5 Effective $A_2$ for the Total Source Term

The total source term effective  $A_2$  was calculated in the same way as in the main chapter. The results are summarized in Table 4.III.2.4.

#### 4.III.2.5.6 Allowable Radionuclide Release Rates

The containment system of HI-STAR 100 with Diablo Canyon MPC-32 is designed to the same containment criteria as the HI-STAR 100 System. These criterion are given in 10CFR71.51(a)(1) for normal conditions and 10CFR71.51(b)(2) for hypothetical accident conditions.

Equations 4-10 and 4-11 were used to determine the allowable radionuclide release rate for the Diablo Canyon MPC-32 under normal and hypothetical accident conditions. The release rates for the Diablo Canyon MPC-32 are summarized in Table 4.III.2.5.

#### 4.III.2.5.7 Allowable Leakage Rates at Operating Conditions

The allowable leakage rates at operating conditions were determined using Equation 4-12. Table 4.III.2.6 summarizes the allowable leakage rates at the upstream pressures. The most limiting allowable leakage rate presented in Table 4.III.2.6 was conservatively selected and used to determine the leakage rate acceptance criterion for the Diablo Canyon MPC-32.

#### 4.III.2.5.8 Leakage Rate Acceptance Criteria for Test Conditions

The leakage rate acceptance criteria for test conditions was determined using the same methodology presented in Section 4.2.5.8 of the main part of the chapter. The reference test conditions for the Diablo Canyon MPC-32 are specified in Table 4.2.12.

#### 4.III.2.5.9 Leak Test Sensitivity

The sensitivity for the overpack leakage test procedures is equal to one-half of the allowable leakage rate. The HI-STAR 100 containment packaging tests in Chapter 8 incorporate the appropriate leakage test procedure sensitivity. The leakage rates for the HI-STAR 100 containment packaging with its corresponding sensitivity are presented in Table 4.1.1.

#### 4.III.3 REGULATORY COMPLIANCE

The HI-STAR 100 with Diablo Canyon MPC-32 is identical to the HI-STAR 100 System in the main body of Chapter 4 of this FSAR in that it is designed and tested to ensure compliance with the radionuclide release rates specified in 10CFR71.51 [4.0.1] for normal and hypothetical accident transport conditions.

Table 4.III.2.1

FREE GAS VOLUME OF THE CONTAINMENT SYSTEM FOR THE HI-STAR 100 WITH  
DIABLO CANYON MPC-32

Containment Volume [cm <sup>3</sup> ]	PROPRIETARY INFORMATION WITHHELD PER 10CFR2.390
--	--



Table 4.III.2.2

TOTAL SOURCE TERM FOR THE HI-STAR HB (Ci/cm<sup>3</sup>)

	$C_{\text{crud}}$ (Ci/cm <sup>3</sup> )	$C_{\text{fines}}$ (Ci/cm <sup>3</sup> )	$C_{\text{gas}}$ (Ci/cm <sup>3</sup> )	$C_{\text{vol}}$ (Ci/cm <sup>3</sup> )	Total (Ci/cm <sup>3</sup> )
Normal Transport Conditions					
HI-STAR 100 WITH DIABLO CANYON MPC- 32	1.69E-05	1.07E-06	2.32E-04	6.44E-06	2.56E-04
Accident Conditions					
HI-STAR 100 WITH DIABLO CANYON MPC- 32	1.13E-04	3.55E-05	7.72E-03	2.15E-04	8.09E-03

Table 4.III.2.3

INDIVIDUAL CONTRIBUTOR EFFECTIVE  $A_2$  FOR GASES, CRUD, FINES, AND  
VOLATILES FOR THE HI-STAR HB

<b>HI-STAR 100 WITH DIABLO CANYON MPC-32</b>	<b><math>A_2</math> (Ci)</b>
Gases	2.82E+02
Crud	10.8
Fines	8.89E-01
Volatiles	9.72E+00

Table 4.III.2.4

TOTAL SOURCE TERM EFFECTIVE  $A_2$  FOR NORMAL  
AND HYPOTHETICAL ACCIDENT CONDITIONS FOR THE HI-STAR 100 WITH DIABLO  
CANYON MPC-32

	Effective $A_2$ (Ci)
Normal Transport Conditions	
HI-STAR 100 WITH DIABLO CANYON MPC-32	60.3
Accident Conditions	
HI-STAR 100 WITH DIABLO CANYON MPC-32	81.0

Table 4.III.2.5

RADIONUCLIDE RELEASE RATES FOR THE HI-STAR 100 WITH DIABLO CANYON  
MPC-32

	Allowable Release Rate ( $R_N$ or $R_A$ ) (Ci/s)
Normal Conditions	
HI-STAR 100 WITH DIABLO CANYON MPC-32	1.68E-08
Accident Conditions	
HI-STAR 100 WITH DIABLO CANYON MPC-32	1.34E-04

Table 4.III.2.6

**ALLOWABLE LEAKAGE RATES AT UPSTREAM PRESSURE FOR THE HI-STAR 100  
WITH DIABLO CANYON MPC-32**

	Allowable Leakage Rate at $P_u L_N$ or $L_A$ ( $\text{cm}^3/\text{s}$ )
Normal Transport Conditions	
HI-STAR 100 WITH DIABLO CANYON MPC-32	6.54E-05
Accident Conditions	
HI-STAR 100 WITH DIABLO CANYON MPC-32	1.65E-02

## CHAPTER 5: SHIELDING EVALUATION

### 5.0 INTRODUCTION

The shielding analysis of the HI-STAR 100 System is presented in this chapter. The HI-STAR 100 System is designed to accommodate different MPCs within one standard HI-STAR 100 overpack. The MPCs are designated as MPC-24, MPC-24E, and MPC-24EF (24 PWR fuel assemblies), MPC-32 (32 PWR fuel assemblies), and MPC-68 and MPC-68F (68 BWR fuel assemblies). The MPC-24E and MPC-24EF are essentially identical to the MPC-24 from a shielding perspective. Therefore, only the MPC-24 is analyzed in this chapter. Throughout this chapter, unless stated otherwise, MPC-24 refers to either the MPC-24, MPC-24E, or MPC-24EF and MPC-68 refers to the MPC-68 or MPC-68F.

In addition to housing intact PWR and BWR fuel assemblies, the HI-STAR 100 System is designed to transport damaged BWR fuel assemblies and BWR fuel debris. Damaged fuel assemblies and fuel debris are defined in Subsection 1.2.3. Both damaged BWR fuel assemblies and BWR fuel debris are required to be loaded into Damaged Fuel Containers (DFCs). DFCs containing BWR fuel debris must be stored in the MPC-68F. DFCs containing BWR damaged fuel assemblies may be stored in either the MPC-68 or the MPC-68F. Only the fuel assemblies in the Dresden 1 and Humboldt Bay fuel assembly classes identified in Table 1.2.9 are authorized as contents for transport in the HI-STAR 100 system as either BWR damaged fuel or fuel debris.

The MPC-68 and MPC-68F are also capable of transporting Dresden Unit 1 antimony-beryllium neutron sources and the single Thoria rod canister which contains 18 thoria rods that were irradiated in two separate fuel assemblies.

Slightly modified versions of the MPC-24E and MPC-24EF are being used for the transportation of Trojan nuclear power plant spent nuclear fuel, non-fuel hardware, neutron sources, and damaged fuel and fuel debris as described in Subsection 1.2.3. These MPCs are referred to as the Trojan MPC-24E and Trojan MPC-24EF. The Trojan MPC-24E/EF is explicitly analyzed in this chapter for the inclusion of the Trojan non-fuel hardware, damaged fuel, and Antimony-Beryllium and Californium neutron sources.

The PWR fuel assemblies loaded into the MPC-32 may contain burnable poison rod assemblies (BPRAs), with any number of full-length rods and thimble plug rodlets in the locations without a full-length rod, thimble plug devices (TPDs), control rod assemblies (CRAs), neutron source assemblies (NSAs), or similarly named devices. These non-fuel hardware devices are an integral yet removable part of PWR fuel assemblies. Since each device occupies the same location within a fuel assembly, a single PWR fuel assembly will not contain multiple devices, with the exception of instrument tube tie rods (ITTRs), which may be stored in the assembly along with other types of non-fuel hardware.

This chapter contains the following information:

- A description of the shielding features of the HI-STAR 100 System.
- A description of the bounding source terms.
- A general description of the shielding analysis methodology.
- A description of the analysis assumptions and results for the HI-STAR 100 System.
- Analyses for the HI-STAR 100 System's content conditions to show that the 10CFR71.47 radiation limits are met during normal conditions of transport and that the 10CFR71.51 dose rate limit is not exceeded following hypothetical accident conditions.
- Analyses which demonstrate that the storage of BWR damaged fuel in the HI-STAR 100 System is bounded by the BWR intact fuel analysis during normal and hypothetical accident conditions.
- Analyses for the Trojan Nuclear Power Plant spent fuel contents, including damaged fuel and fuel debris, and non-fuel hardware.

## 5.1 DISCUSSION AND RESULTS

The principal sources of radiation in the HI-STAR 100 System are:

- Gamma radiation originating from the following sources
  1. Decay of radioactive fission products
  2. Hardware activation products generated during core operations
  3. Secondary photons from neutron capture in fissile and non-fissile nuclides
- Neutron radiation originating from the following sources
  1. Spontaneous fission
  2.  $\alpha, n$  reactions in fuel materials
  3. Secondary neutrons produced by fission from subcritical multiplication
  4.  $\gamma, n$  reactions (this source is negligible)
  5. Dresden Unit 1 and Trojan neutron sources

Shielding from gamma radiation is provided by the steel structure of the MPC and overpack. In order for the neutron shielding to be effective, the neutrons must be thermalized and then absorbed in a material of high neutron cross section. In the HI-STAR 100 System design, a neutron shielding material, Holtite-A, is used to thermalize the neutrons. Boron carbide, dispersed in the neutron shield, utilizes the high neutron absorption cross section of  $^{10}\text{B}$  to absorb the thermalized neutrons.

The shielding analyses were performed with MCNP-4A [5.1.1] from Los Alamos National Laboratory. The source terms for the design basis fuels were calculated with the SAS2H and ORIGEN-S sequences from the SCALE 4.3 system [5.1.2, 5.1.3] from Oak Ridge National Laboratory. The source terms for the Trojan specific inventory were calculated with the SAS2H and ORIGEN-S sequences from the SCALE 4.4 system [5.1.4, 5.1.5] as described in the Trojan FSAR [5.1.6]. A detailed description of the MCNP models and the source term calculations are presented in Sections 5.3 and 5.2, respectively.

The design basis intact zircaloy clad fuels used in calculating the dose rates presented in this chapter are the B&W 15x15 (with zircaloy and non-zircaloy incore spacers) and the GE 7x7, for PWR and BWR fuel types, respectively. The design basis intact 6x6, damaged, and mixed oxide (MOX) fuel assemblies are the GE 6x6. Tables 1.2.22 through 1.2.27 specify the acceptable intact zircaloy clad fuel characteristics for transport. Tables 1.2.23 and 1.2.24 specify the acceptable damaged and MOX zircaloy clad fuel characteristics for transport.

The design bases intact stainless steel clad fuels are the WE 15x15 and the AC 10x10, for PWR and BWR fuel types, respectively. Tables 1.2.22, 1.2.23, 1.2.25, and 1.2.26 specify the acceptable fuel characteristics of stainless steel clad fuel for transport.



The Trojan spent fuel contents were analyzed separately, as discussed in later sections, and therefore are not covered by the design basis fuel assemblies mentioned above.

Tables 1.2.28 through 1.2.33 specify, in tabular form, the minimum enrichment, burnup and cooling time combinations for spent nuclear fuel that were analyzed for transport in the MPC-24, MPC-32, and MPC-68. Each combination provides a dose rate equal to or below the maximum values reported in this section. These tables represent the fuel assembly acceptance criteria.

The burnup, cooling time, and minimum enrichment combinations specified in Tables 1.2.28 through 1.2.33 were determined strictly based on the shielding analysis in this chapter. Each combination was specifically analyzed and it was verified that the calculated dose rates were less than the regulatory limits. Detailed results (e.g. dose from gammas, neutrons, co-60, etc...) are not presented in this chapter for each burnup, cooling time, and minimum enrichment combination analyzed. Rather, the detailed results for the combination that produced the highest dose rate for each of the three regulatory acceptance criteria and locations (i.e. surface normal condition, 2 meter normal condition, 1 meter accident condition) in a specific MPC are presented in this section. However, the total dose rates for all approved burnup and cooling time combinations are presented in Section 5.4. The choice of burnup and cooling time combinations for which detailed (i.e. individual dose components in addition to total) results are provided is discussed further in the following subsections.

Unless otherwise stated, all dose rates reported in this chapter are average surface dose rates. The effect of radiation peaking due to azimuthal variations in the fuel loading pattern and the steel radial channels is specifically addressed in Subsection 5.4.1.

#### 5.1.1 Normal Operations

The 10CFR71.47 external radiation requirements during normal transport operations for an exclusive use shipment are:

1. 200 mrem/hr (2 mSv/hr) on the external surface of the package, unless the following conditions are met, in which case the limit is 1000 mrem/hr (10 mSv/hr).
  - i. The shipment is made in a closed transport vehicle;
  - ii. The package is secured within the vehicle so that its position remains fixed during transportation; and
  - iii. There are no loading and unloading operations between the beginning and end of the transportation.
2. 200 mrem/hr (2 mSv/hr) at any point on the outer surface of the vehicle, including the top and underside of the vehicle; or in the case of a flat-bed style vehicle, at any point on the vertical planes projected from the outer edges of the vehicle, on the upper surface of the load or enclosure, if used, and on the lower external surface of the vehicle.

3. 10 mrem/hr (0.1 mSv/hr) at any point 2 meters (80 in) from the outer lateral surfaces of the vehicle (excluding the top and underside of the vehicle); or in the case of a flat-bed style vehicle, at any point 2 meters (6.6 feet) from the vertical planes projected by the outer edges of the vehicle (excluding the top and underside of the vehicle).
4. 2 mrem/h (0.02 mSv/hr) in any normally occupied space, except that this provision does not apply to private carriers, if exposed personnel under their control wear radiation dosimetry devices in conformance with 10CFR20.1502.

The Standard Review Plan for Transportation Packages of Spent Nuclear Fuel, NUREG-1617 [5.2.1] states that “Personnel barriers and similar devices that are attached to the conveyance, rather than the package, can, however, qualify the vehicle as a closed vehicle (NUREG/CR-5569A and NUREG/CR-5569B) as defined in 49 CFR 173.403.”

When the HI-STAR is transported, a personnel barrier will be placed over the HI-STAR as depicted in Figure 1.2.8. This personnel barrier spans the distance between the impact limiters. The outer radial location of the personnel barrier is equal to the outer radial surface of the impact limiters and the personnel barrier is attached to the saddle on the rail car rather than the HI-STAR overpack. Therefore, the personnel barrier acts as an enclosure for the main body of the HI-STAR overpack. Consequently, the 1000 mrem/hr limit for the enclosed package is applicable for the outer radial surface of the overpack in the region between the impact limiters. Since the impact limiters are not enclosed, the surface of the impact limiters is required to meet the lower 200 mrem/hr limit for the package.

The HI-STAR 100 System will be transported on either a flat-bed rail car, heavy haul vehicle, or a barge. The smallest width of a transport vehicle is equivalent to the width of the impact limiters. Therefore, the vertical planes projected by the outer side edges of the transport vehicle are equivalent to the outer edge of the impact limiters. The minimum length of any transport vehicle will be 12 feet longer than the length of the overpack, with impact limiters attached. The bottom impact limiter of the HI-STAR 100 System will be conservatively positioned a minimum of 9 feet from the end of the transport vehicle. Therefore, the vertical planes projected from the outer edge of the ends of the vehicle will be taken as the end of the top impact limiter and 9 feet from the end of the bottom impact limiter.

Figure 5.1.1 shows the HI-STAR 100 System during normal transport conditions. The impact limiters and personnel barrier are outlined on the figure and various dose point locations are shown on the surface of the enclosure (personnel barrier) and the HI-STAR 100 System. The dose values reported at the locations shown on Figure 5.1.1 are averaged over a region that is approximately 1 foot in width. Each of the dose locations in Figure 5.1.1 (with the exception of 2a and 3a) has a corresponding location at 2 meters from the surface of the transport vehicle as defined above.

Dose locations 2a, 3a, and 2 shown in Figure 5.1.1 and Figure 5.1.2 (discussed below) do not correspond to single dose locations. Rather the dose rate for multiple axial segments of approximately 1 foot or less were calculated and the highest value was chosen for the corresponding dose location. Dose locations 2a and 2 encompass 14 axial segments that range from the pocket trunnion to the top of the Holtite. The highest dose rate of these 14 axial segments was chosen as the value for dose locations 2a and 2. Dose location 3a corresponds to two axial segments while dose locations 1, 3, and 4 correspond to a single axial segment. Dose locations 5 and 6 correspond to either the center radial segment of the overpack along the axis or the adjacent location radial segment.

Tables 5.1.1 through 5.1.3, 5.1.10, 5.1.11, and 5.1.16 provide the maximum dose rates on the surface of the system during normal transport conditions for the MPC-24, MPC-32, and MPC-68 with design basis intact zircaloy clad fuel. Tables 5.1.4 through 5.1.6, 5.1.12, 5.1.13, and 5.1.17 list the maximum dose rates two meters from the edge of the transport vehicle during normal conditions. Section 5.4 provides a detailed list of the total dose rates at several cask locations for all burnup and cooling times analyzed. The burnup and cooling time combinations chosen for the tables mentioned above was the combination that resulted in the absolute highest dose rate for the normal condition regulatory locations (i.e. surface and 2 meter). For example, Table 5.1.1 presents the burnup and cooling time combination that results in the highest dose rate from a review of the dose rates, in Table 5.4.8, for locations 2a, 3a, and 1-6 for all allowable burnup and cooling time combinations. This combination may not result in the highest dose rate at each individual dose location (e.g. 2a, 3a, 1-6) but it is the combination that results in the absolute highest dose rate for the surface or 2 meter locations.

Subsections 5.2.1 and 5.2.2 list the gamma and neutron sources for the design basis zircaloy clad intact, zircaloy clad damaged and MOX fuel assemblies. Since the source strengths of the damaged and MOX fuel are significantly smaller in all energy groups than the intact design basis fuel source strengths, the damaged and MOX fuel dose rates for normal conditions are bounded by the MPC-68 analysis with design basis intact fuel. Therefore, no explicit analysis of the MPC-68 with either damaged or MOX fuel for normal conditions is required to demonstrate that the MPC-68 with damaged fuel or MOX fuel will meet the normal condition regulatory requirements.

Subsection 5.2.6 lists the gamma and neutron sources from the Dresden Unit 1 Thoria rod canister and demonstrates that the Thoria rod canister is bounded by the design basis 6x6 intact fuel.

Subsection 5.4.5 demonstrates that the Dresden Unit 1 fuel assemblies containing antimony-beryllium neutron sources are bounded by the shielding analysis presented in this section.

Subsections 5.4.7 and 5.4.8 present the results for the Trojan contents in the MPC-24E/EF and demonstrate that these contents are acceptable for transportation.

Subsection 5.2.3 lists the gamma and neutron sources for the design basis intact stainless steel clad fuels. The dose rates from these fuels are provided in Subsection 5.4.4.

Tables 5.1.4 through 5.1.6, 5.1.12, 5.1.13, and 5.1.17 show that the dose rate at Dose Location #5 (the top of the HI-STAR 100 System, see Figure 5.1.1) at 2 meters from the edge of the transport vehicle is less than 2 mrem/hr. It is, therefore, recommended that the HI-STAR 100 System be positioned such that the top impact limiter is facing the normally occupied space. If this is the orientation, radiation dosimetry will not be required as long as the normally occupied space is a minimum of 2 meters from the impact limiter on the top of the HI-STAR 100 System. If a different orientation is chosen for the HI-STAR 100 System, the dose rate in the normally occupied space will have to be evaluated against the dose requirement for the normally occupied space to determine if radiation dosimetry is required.

The analyses summarized in this section demonstrate the HI-STAR 100 System's compliance with the 10CFR71.47 limits.

### 5.1.2 Hypothetical Accident Conditions

The 10CFR71.51 external radiation dose limit for design basis accidents is:

- The external radiation dose rate shall not exceed 1 rem/hr (10 mSv/hr) at 1 m (40 in.) from the external surface of the package.

The hypothetical accident conditions of transport have two bounding consequences which affect the shielding materials. They are the damage to the neutron shield as a result of the design basis fire and damage of the impact limiters as a result of the 30 foot drop. In a conservative fashion, the dose analysis assumes that as a result of the fire, the neutron shield is completely destroyed and replaced by a void. Additionally, the impact limiters are assumed to have been lost. These are highly conservative assumptions since some portion of the neutron shield would be expected to remain after the fire as the neutron shield material is fire retardant, and the impact limiters have been shown by 1/4-scale testing to remain attached following impact.

Throughout the hypothetical accident condition the axial location of the fuel will remain fixed within the MPC because of the fuel spacers or by the MPC lid and baseplate if spacers are not used. Chapter 2 provides an analysis to show that the fuel spacers do not fail under all normal and hypothetical accident conditions. Chapter 2 also shows that the inner shell, intermediate shell, radial channels, and outer enclosure shell of the overpack remain unaltered throughout the hypothetical accident conditions. Localized damage of the overpack outer enclosure shell could be experienced during the pin puncture. However, the localized deformations will have only a negligible impact on the dose rate at 1 meter from the surface.

Figure 5.1.2 shows the HI-STAR 100 System after the postulated accident. The various dose point locations at 1 meter from the HI-STAR 100 System are shown on the figure. Tables 5.1.7

through 5.1.9, 5.1.14, 5.1.15, and 5.1.18 provide the maximum dose rates at 1 meter for the accident conditions. The burnup and cooling time combinations chosen for the aforementioned tables were the combinations that resulted in the absolute highest dose rate for the accident condition regulatory location (i.e. 1 meter).

The consequences of the hypothetical accident conditions for the MPC-68F storing either damaged or MOX (which can also be considered damaged) fuel differ slightly from those with intact fuel. For this accident condition, it is conservatively assumed that during a drop accident the damaged fuel collapses and the pellets rest in the bottom of the damaged fuel container. The analysis presented in Subsections 5.4.2 and 5.4.3 demonstrate that the damaged fuel in the post-accident condition has lower source terms (both gamma and neutron) per inch than the intact BWR design basis fuel. Therefore, the damaged fuel post-accident dose rates are bounded by the BWR intact fuel post-accident dose rates.

Subsections 5.4.7 and 5.4.8 present the results for the Trojan contents in the MPC-24E/EF and demonstrate that these contents are acceptable for transportation.

Analyses summarized in this section demonstrate the HI-STAR 100 System's compliance with the 10CFR71.51 radiation dose limit.

Table 5.1.1

DOSE RATES ON THE SURFACE OF THE HI-STAR 100 SYSTEM FOR NORMAL CONDITIONS  
MPC-24 WITH DESIGN BASIS ZIRCALOY CLAD FUEL WITH ZIRCALOY INCORE SPACERS  
**WITHOUT NON-FUEL HARDWARE**  
AT WORST CASE BURNUP AND COOLING TIME  
44,500 MWD/MTU AND 14-YEAR COOLING

Dose Point <sup>†</sup> Location	[PROPRIETARY INFORMATION WITHHELD PER 10CFR2.390]				Totals (mrem/hr)	10 CFR 71.47 Limit
2a					46.19	1000
3a					138.47	1000
1					34.85	200
2					28.24	200
3					30.19	200
4					28.05	200
5					4.15	200
6					90.02	200

<sup>†</sup> Refer to Figure 5.1.1.

Table 5.1.2

DOSE RATES ON THE SURFACE OF THE HI-STAR 100 SYSTEM FOR NORMAL CONDITIONS  
MPC-24 WITH DESIGN BASIS ZIRCALOY CLAD FUEL WITH NON-ZIRCALOY INCORE SPACERS  
**WITHOUT NON-FUEL HARDWARE**  
AT WORST CASE BURNUP AND COOLING TIME  
44,500 MWD/MTU AND 18-YEAR COOLING

Dose Point <sup>†</sup> Location	[PROPRIETARY INFORMATION WITHHELD PER 10CFR2.390]				Totals (mrem/hr)	10 CFR 71.47 Limit
2a					46.24	1000
3a					111.87	1000
1					26.75	200
2					28.62	200
3					23.47	200
4					21.85	200
5					3.58	200
6					63.35	200

<sup>†</sup> Refer to Figure 5.1.1.

Table 5.1.3

DOSE RATES ON THE SURFACE OF THE HI-STAR 100 SYSTEM FOR NORMAL CONDITIONS  
MPC-68 WITH DESIGN BASIS ZIRCALOY CLAD FUEL AT  
WORST CASE BURNUP AND COOLING TIME  
20,000 MWD/MTU AND 7-YEAR COOLING

<b>Dose Point<sup>†</sup> Location</b>	<b>[PROPRIETARY INFORMATION WITHHELD PER 10CFR2.390]</b>				<b>Totals (mrem/hr)</b>	<b>10 CFR 71.47 Limit</b>
2a					52.69	1000
3a					154.42	1000
1					39.29	200
2					27.53	200
3					37.75	200
4					35.76	200
5					0.60	200
6					121.21	200

---

<sup>†</sup> Refer to Figure 5.1.1.



Table 5.1.4

DOSE RATES AT TWO METERS FOR NORMAL CONDITIONS  
MPC-24 WITH DESIGN BASIS ZIRCALOY CLAD FUEL WITH ZIRCALOY INCORE SPACERS  
**WITHOUT NON-FUEL HARDWARE**  
AT WORST CASE BURNUP AND COOLING TIME  
24,500 MWD/MTU AND 6-YEAR COOLING

Dose Point <sup>†</sup> Location	[PROPRIETARY INFORMATION WITHHELD PER 10CFR2.390]				Totals (mrem/hr)
1					7.41
2					9.57
3					6.72
4					6.16
5					0.09
6					8.39
10CFR71.47 Limit					10.00

---

<sup>†</sup> Refer to Figure 5.1.1.

Table 5.1.5

DOSE RATES AT TWO METERS FOR NORMAL CONDITIONS  
MPC-24 WITH DESIGN BASIS ZIRCALOY CLAD FUEL WITH NON-ZIRCALOY INCORE SPACERS  
**WITHOUT NON-FUEL HARDWARE**  
AT WORST CASE BURNUP AND COOLING TIME  
24,500 MWD/MTU AND 9-YEAR COOLING

Dose Point <sup>†</sup> Location	[PROPRIETARY INFORMATION WITHHELD PER 10CFR2.390]				Totals (mrem/hr)
1					6.42
2					9.51
3					5.68
4					5.08
5					0.08
6					5.84
10CFR71.47 Limit					10.00

---

<sup>†</sup> Refer to Figure 5.1.1.

Table 5.1.6

DOSE RATES AT TWO METERS FOR NORMAL CONDITIONS  
 MPC-68 WITH DESIGN BASIS ZIRCALOY CLAD FUEL  
 AT WORST CASE BURNUP AND COOLING TIME  
 34,500 MWD/MTU AND 11-YEAR COOLING

<b>Dose Point<sup>†</sup> Location</b>	<b>[PROPRIETARY INFORMATION WITHHELD PER 10CFR2.390]</b>				<b>Totals (mrem/hr)</b>
1					7.59
2					9.62
3					6.62
4					6.32
5					0.15
6					5.01
10CFR71.47 Limit					10.00

---

<sup>†</sup> Refer to Figure 5.1.1.

Table 5.1.7

DOSE RATES AT ONE METER FOR ACCIDENT CONDITIONS  
MPC-24 WITH DESIGN BASIS ZIRCALOY CLAD FUEL WITH ZIRCALOY INCORE SPACERS  
**WITHOUT NON-FUEL HARDWARE**  
AT WORST CASE BURNUP AND COOLING TIME  
29,500 MWD/MTU AND 7-YEAR COOLING

<b>Dose Point<sup>†</sup> Location</b>	<b>[PROPRIETARY INFORMATION WITHHELD PER 10CFR2.390]</b>			<b>Totals (mrem/hr)</b>
1				97.55
2				224.23
3				64.41
4				47.12
5				6.59
6				687.08
10CFR71.51 Limit				1000.00

<sup>†</sup> Refer to Figure 5.1.2.

Table 5.1.8

DOSE RATES AT ONE METER FOR ACCIDENT CONDITIONS  
MPC-24 WITH DESIGN BASIS ZIRCALOY CLAD FUEL WITH NON-ZIRCALOY INCORE SPACERS  
**WITHOUT NON-FUEL HARDWARE**  
AT WORST CASE BURNUP AND COOLING TIME  
24,500 MWD/MTU AND 9-YEAR COOLING

<b>Dose Point<sup>†</sup> Location</b>	<b>[PROPRIETARY INFORMATION WITHHELD PER 10CFR2.390]</b>			<b>Totals (mrem/hr)</b>
1				62.33
2				145.00
3				40.70
4				29.39
5				3.59
6				478.28
10CFR71.51 Limit				1000.00

---

<sup>†</sup> Refer to Figure 5.1.2.

Table 5.1.9

DOSE RATES AT ONE METER FOR ACCIDENT CONDITIONS  
MPC-68 WITH DESIGN BASIS ZIRCALOY CLAD FUEL  
AT WORST CASE BURNUP AND COOLING TIME  
20,000 MWD/MTU AND 7-YEAR COOLING

<b>Dose Point<sup>†</sup> Location</b>	<b>[PROPRIETARY INFORMATION WITHHELD PER 10CFR2.390]</b>			<b>Totals (mrem/hr)</b>
1				86.18
2				172.74
3				49.39
4				39.33
5				2.70
6				668.09
10CFR71.51 Limit				1000.00

---

<sup>†</sup> Refer to Figure 5.1.2.

Table 5.1.10

DOSE RATES ON THE SURFACE OF THE HI-STAR 100 SYSTEM FOR NORMAL CONDITIONS  
MPC-32 WITH DESIGN BASIS ZIRCALOY CLAD FUEL WITH ZIRCALOY INCORE SPACERS  
**WITHOUT NON-FUEL HARDWARE**  
AT WORST CASE BURNUP AND COOLING TIME  
44,500 MWD/MTU AND 19-YEAR COOLING

<b>Dose Point<sup>†</sup> Location</b>	<b>[PROPRIETARY INFORMATION WITHHELD PER 10CFR2.390]</b>				<b>Totals (mrem/hr)</b>	<b>10 CFR 71.47 Limit</b>
2a					50.90	1000
3a					263.95	1000
1					42.51	200
2					35.48	200
3					49.68	200
4					47.31	200
5					8.46	200
6					95.45	200

<sup>†</sup> Refer to Figure 5.1.1.

Table 5.1.11

DOSE RATES ON THE SURFACE OF THE HI-STAR 100 SYSTEM FOR NORMAL CONDITIONS  
MPC-32 WITH DESIGN BASIS ZIRCALOY CLAD FUEL WITH NON-ZIRCALOY INCORE SPACERS  
**WITHOUT NON-FUEL HARDWARE**  
AT WORST CASE BURNUP AND COOLING TIME  
42,500 MWD/MTU AND 20-YEAR COOLING

<b>Dose Point<sup>†</sup> Location</b>	<b>[PROPRIETARY INFORMATION WITHHELD PER 10CFR2.390]</b>				<b>Totals (mrem/hr)</b>	<b>10 CFR 71.47 Limit</b>
2a					44.54	1000
3a					213.21	1000
1					35.33	200
2					29.93	200
3					40.74	200
4					38.57	200
5					6.79	200
6					79.64	200

<sup>†</sup> Refer to Figure 5.1.1.



Table 5.1.12

DOSE RATES AT TWO METERS FOR NORMAL CONDITIONS  
MPC-32 WITH DESIGN BASIS ZIRCALOY CLAD FUEL WITH ZIRCALOY INCORE SPACERS  
AT WORST CASE BURNUP AND COOLING TIME  
**WITHOUT NON-FUEL HARDWARE**  
39,500 MWD/MTU AND 14-YEAR COOLING

<b>Dose Point<sup>†</sup> Location</b>	<b>[PROPRIETARY INFORMATION WITHHELD PER 10CFR2.390]</b>				<b>Totals (mrem/hr)</b>
1					8.43
2					9.65
3					9.10
4					8.79
5					0.55
6					5.66
10CFR71.47 Limit					10.00

---

<sup>†</sup> Refer to Figure 5.1.1.

Table 5.1.13

DOSE RATES AT TWO METERS FOR NORMAL CONDITIONS  
MPC-32 WITH DESIGN BASIS ZIRCALOY CLAD FUEL WITH NON-ZIRCALOY INCORE SPACERS  
**WITHOUT NON-FUEL HARDWARE**  
AT WORST CASE BURNUP AND COOLING TIME  
42,500 MWD/MTU AND 20-YEAR COOLING

Dose Point <sup>†</sup> Location	[PROPRIETARY INFORMATION WITHHELD PER 10CFR2.390]				Totals (mrem/hr)
1					7.13
2					9.61
3					7.71
4					7.36
5					0.53
6					3.24
10CFR71.47 Limit					10.00

---

<sup>†</sup> Refer to Figure 5.1.1.

Table 5.1.14

DOSE RATES AT ONE METER FOR ACCIDENT CONDITIONS  
MPC-32 WITH DESIGN BASIS ZIRCALOY CLAD FUEL WITH ZIRCALOY INCORE SPACERS  
**WITHOUT NON-FUEL HARDWARE**  
AT WORST CASE BURNUP AND COOLING TIME  
29,500 MWD/MTU AND 9-YEAR COOLING

Dose Point <sup>†</sup> Location	[PROPRIETARY INFORMATION WITHHELD PER 10CFR2.390]			Totals (mrem/hr)
1				117.99
2				249.47
3				89.91
4				66.55
5				15.09
6				817.16
10CFR71.51 Limit				1000.00

<sup>†</sup> Refer to Figure 5.1.2.

Table 5.1.15

DOSE RATES AT ONE METER FOR ACCIDENT CONDITIONS  
MPC-32 WITH DESIGN BASIS ZIRCALOY CLAD FUEL WITH NON-ZIRCALOY INCORE SPACERS  
**WITHOUT NON-FUEL HARDWARE**  
AT WORST CASE BURNUP AND COOLING TIME  
24,500 MWD/MTU AND 12-YEAR COOLING

<b>Dose Point<sup>†</sup> Location</b>	<b>[PROPRIETARY INFORMATION WITHHELD PER 10CFR2.390]</b>			<b>Totals (mrem/hr)</b>
1				69.80
2				152.61
3				52.15
4				38.31
5				7.89
6				500.54
10CFR71.51 Limit				1000.00

<sup>†</sup> Refer to Figure 5.1.2.

Table 5.1.16

DOSE RATES ON THE SURFACE OF THE HI-STAR 100 SYSTEM FOR NORMAL CONDITIONS  
MPC-32 WITH DESIGN BASIS ZIRCALOY CLAD FUEL WITH NON-ZIRCALOY INCORE SPACERS  
WITH NON-FUEL HARDWARE  
AT WORST CASE BURNUP AND COOLING TIME  
24,500 MWD/MTU AND 13-YEAR COOLING

<b>Dose Point<sup>†</sup> Location</b>	<b>[PROPRIETARY INFORMATION WITHHELD PER 10CFR2.390]</b>			<b>Totals (mrem/hr)</b>	<b>10 CFR 71.47 Limit</b>
2a				47.29	1000
3a				114.54	1000
1				26.48	200
2				26.68	200
3				29.44	200
4				27.17	200
5				0.92	200
6				117.05	200

<sup>†</sup> Refer to Figure 5.1.1.

Table 5.1.17

DOSE RATES AT TWO METERS FOR NORMAL CONDITIONS  
MPC-32 WITH DESIGN BASIS ZIRCALOY CLAD FUEL WITH NON-ZIRCALOY INCORE SPACERS  
WITHOUT NON-FUEL HARDWARE  
AT WORST CASE BURNUP AND COOLING TIME  
24,500 MWD/MTU AND 13-YEAR COOLING

Dose Point <sup>†</sup> Location	[PROPRIETARY INFORMATION WITHHELD PER 10CFR2.390]			Totals (mrem/hr)
1				6.41
2				9.46
3				6.93
4				6.43
5				0.09
6				5.72
10CFR71.47 Limit				10.00

<sup>†</sup> Refer to Figure 5.1.1.

Table 5.1.18

DOSE RATES AT ONE METER FOR ACCIDENT CONDITIONS  
MPC-32 WITH DESIGN BASIS ZIRCALOY CLAD FUEL WITH NON-ZIRCALOY INCORE SPACERS  
WITH NON-FUEL HARDWARE  
AT WORST CASE BURNUP AND COOLING TIME  
24,500 MWD/MTU AND 13-YEAR COOLING

Dose Point <sup>†</sup> Location	[PROPRIETARY INFORMATION WITHHELD PER 10CFR2.390]			Totals (mrem/hr)
1				66.34
2				151.09
3				49.23
4				37.67
5				3.83
6				623.24
10CFR71.51 Limit				1000.00

<sup>†</sup> Refer to Figure 5.1.2.

FIGURES 5.1.1 AND 5.1.2: [PROPRIETARY INFORMATION WITHHELD PER  
10CFR2.390]



## 5.2 SOURCE SPECIFICATION

The neutron and gamma source terms, decay heat values, and quantities of radionuclides available for release were calculated with the SAS2H and ORIGEN-S modules of the SCALE 4.3 system [5.1.2, 5.1.3]. The source terms for the Trojan specific inventory were calculated with the SAS2H and ORIGEN-S sequences from the SCALE 4.4 system [5.1.4, 5.1.5] as described in the Trojan FSAR [5.1.6]. Sample input files for SAS2H and ORIGEN-S are provided in Appendices 5.A and 5.B, respectively. The gamma source term is actually comprised of three distinct sources. The first is a gamma source term from the active fuel region due to decay of fission products. The second source term is from  $^{60}\text{Co}$  activity of the steel structural material in the fuel assembly above and below the active fuel region. The third source is from (n, $\gamma$ ) reactions described below.

A description of the design basis intact zircaloy clad fuel for the source term calculations is provided in Table 5.2.1. The PWR fuel assembly described is the assembly that produces the highest neutron and gamma sources and the highest decay heat load from the following fuel assembly classes listed in Table 1.2.8: B&W 15x15, B&W 17x17, CE 14x14, CE 16x16, WE 14x14, WE 15x15, WE 17x17, St. Lucie, and Ft. Calhoun. The BWR fuel assembly described is the assembly that produces the highest neutron and gamma sources and the highest decay heat load from the following fuel assembly classes listed in Table 1.2.9: GE BWR/2-3, GE BWR/4-6, Humboldt Bay 7x7, and Dresden 1 8x8. Multiple SAS2H and ORIGEN-S calculations were performed to confirm that the B&W 15x15 and the GE 7x7, which have the highest  $\text{UO}_2$  mass, bound all other PWR and BWR fuel assemblies, respectively. Subsection 5.2.5 discusses, in detail, the determination of the design basis fuel assemblies.

The design basis Humboldt Bay and Dresden 1 6x6 fuel assembly, which is also the design basis damaged fuel assembly for the Humboldt Bay and Dresden 1 damaged fuel or fuel debris, is described in Table 5.2.2. The design basis damaged fuel assembly is also the design basis fuel assembly for fuel debris. The fuel assembly type listed produces the highest total neutron and gamma sources from the fuel assemblies at Dresden 1 and Humboldt Bay. Table 5.2.15 provides a description of the design basis Dresden 1 MOX fuel assembly used in this analysis. The design basis 6x6, damaged, and MOX fuel assemblies which are smaller than the GE 7x7, are assumed to have the same hardware characteristics as the GE 7x7. This is conservative because the larger hardware mass of the GE 7x7 results in a larger  $^{60}\text{Co}$  activity.

The design basis stainless steel clad fuel assembly for the Indian Point 1, Haddam Neck and San Onofre 1 assembly classes is described in Table 5.2.18. This table also describes the design basis stainless steel clad LaCrosse fuel assembly.

Since the MPC-24E being used for Trojan fuel is slightly different than the standard MPC-24E, the Trojan contents were specifically analyzed and are not covered by the design basis PWR fuel assembly described above. The design basis Trojan WE 17x17 fuel assembly is described in Table 5.2.32 and was taken from the site specific Trojan FSAR analysis [5.1.6].

In performing the SAS2H and ORIGEN-S calculations, a single full power cycle was used to achieve the desired burnup. This assumption, in conjunction with the above-average specific powers listed in Tables 5.2.1, 5.2.2, 5.2.15, 5.2.18, and 5.2.32 resulted in conservative source term calculations.

Subsections 5.2.1 and 5.2.2 describe the calculation of the gamma and neutron source terms for zircaloy clad fuel while Subsection 5.2.3 discusses the calculation of the gamma and neutron source terms for the stainless steel clad fuel.

#### 5.2.1 Gamma Source

Tables 5.2.3 through 5.2.6, 5.2.33, 5.2.40, and 5.2.41 provide the gamma source in MeV/s and photons/s as calculated with SAS2H and ORIGEN-S for the design bases intact fuels for the MPC-24, MPC-32, MPC-68, the design basis damaged fuel, and the Trojan fuel. Table 5.2.16 provides the gamma source in MeV/s and photons/s for the design basis MOX fuel. NUREG-1617 [5.2.1] states that "In general, only gammas from approximately 0.8 MeV-2.5 MeV will contribute significantly to the external radiation levels." [

PROPRIETARY INFORMATION WITHHELD PER 10CFR2.390

]

PWR fuel assemblies are currently manufactured with zircaloy incore grid spacers (the plenum spacer and the lower spacer are still inconel in some cases). However, earlier assemblies were manufactured with inconel incore grid spacers. Since the mass of the spacers is significant and since the cobalt impurity level assumed for inconel is very conservative, the Cobalt-60 activity from the incore spacers contributes significantly to the external dose rate. As a result, separate burnup and cooling times were developed for PWR assemblies that utilize zircaloy and non-zircaloy incore spacers. Since steel has a lower cobalt impurity level than inconel, any zircaloy clad PWR assemblies with stainless steel grid spacers are bounded by the analysis performed in this chapter utilizing inconel grid spacers.

It should be noted that some utilities use fuel straps for PWR fuel assemblies in the core periphery locations. These fuel straps provide additional support, along with grid spacers, for the fuel rods. The activation of these fuel straps is not explicitly analyzed in this section since a bounding cobalt-59 impurity level for non-zircaloy grid spacers is used in shielding analysis. Also, these fuel straps increase the fuel assembly mass, which results in larger self-shielding.

The BWR assembly grid spacers are zircaloy, however, some assembly designs have inconel springs in conjunction with the grid spacers. The gamma source for the BWR fuel assembly includes the activation of these springs associated with the grid spacers.

The non-fuel data listed in Table 5.2.1 was taken from References [5.2.3], [5.2.4], and [5.2.5] while the non-fuel data listed in Table 5.2.32 was taken from References [5.2.5] and [5.2.8]. The BWR masses are for an 8x8 fuel assembly. These masses are also appropriate for the 7x7 assembly since the masses of the non-fuel hardware from a 7x7 and an 8x8 are approximately the same. The masses listed are those of the steel components. The zircaloy in these regions was not included because zircaloy does not produce significant activation. These masses are larger than most other fuel assemblies from other manufacturers. This, in combination with the conservative  $^{59}\text{Co}$  impurity level, results in a conservative estimate of the  $^{60}\text{Co}$  activity.

The masses in Table 5.2.1 and 5.2.32 were used to calculate a  $^{59}\text{Co}$  impurity level in the fuel material. The grams of impurity were then used in ORIGEN-S to calculate a  $^{60}\text{Co}$  activity level for the desired burnup and decay time. The methodology used to determine the activation level was developed from Reference [5.2.2] and is described here.

1. The activity of the  $^{60}\text{Co}$  is calculated using ORIGEN-S. The flux used in the calculation was the in-core fuel region flux at full power.
2. The activity calculated in Step 1 for the region of interest was modified by the appropriate scaling factors listed in Table 5.2.7. These scaling factors were taken from Reference [5.2.2]. In the case of the Trojan fuel, the higher value of 0.2 was used for both the gas plenum springs and spacer consistent with the Trojan FSAR [5.1.6].

Tables 5.2.8 through 5.2.10, 5.2.34, 5.2.42, and 5.2.43 provide the  $^{60}\text{Co}$  activity utilized in the shielding calculations in the non-fuel regions of the assemblies for the MPC-24, MPC-32, MPC-68, and Trojan fuel. The design basis damaged and MOX fuel assemblies are conservatively assumed to have the same  $^{60}\text{Co}$  source strength as the BWR intact design basis fuel. This is a conservative assumption as the design basis damaged fuel and MOX fuel are limited to a significantly lower burnup and longer cooling time than the intact design basis zircaloy clad fuel.

[

PROPRIETARY INFORMATION WITHHELD PER 10CFR2.390

]

### 5.2.2 Neutron Source

It is well known that the neutron source strength increases as enrichment decreases, for a constant burnup and decay time. This is due to the increase in Pu content in the fuel which increases the inventory of other transuranium nuclides such as Cm. The gamma source also varies with enrichment, although only slightly. Because of this effect and in order to obtain conservative source terms, low initial fuel enrichments were chosen for the BWR and PWR design basis fuel assemblies as a function of burnup and cooling time. Conservatively, the minimum enrichments used to develop the source terms and dose rates presented in this chapter are specified in Tables 1.2.28 through 1.2.33 as fuel assembly acceptance criteria. The minimum enrichments for the design basis PWR and BWR assemblies are also listed in Table 5.2.23 for convenience.

The neutron source calculated for the design basis intact fuel assemblies for the MPC-24, MPC-32, MPC-68, Trojan fuel, and the design basis damaged fuel are listed in Tables 5.2.11 through 5.2.14, 5.2.35, 5.2.44, and 5.2.45 in neutrons/s. Table 5.2.17 provides the neutron source in neutrons/sec for the design basis MOX fuel assembly. [

PROPRIETARY INFORMATION WITHHELD PER 10CFR2.390

]

### 5.2.3 Stainless Steel Clad Fuel Source

Table 5.2.18 lists the characteristics of the design basis stainless steel clad fuel. The fuel characteristics listed in this table are the input parameters that were used in the shielding calculations described in this chapter. The active fuel length listed in the table is actually longer than the true active fuel length of 122 inches for the W15x15 and 83 inches for the A/C 10x10. Since the true active fuel length is shorter than the design basis zircaloy clad active fuel length, it would be incorrect to calculate source terms for the stainless steel fuel using the actual fuel length and compare them directly to the source terms from the zircaloy clad fuel with a longer

active fuel length.

In order to eliminate the potential confusion when comparing source terms, the stainless steel clad fuel source terms were calculated with the same active fuel length as the design basis zircaloy clad fuel. Reference [5.2.3] indicates that the Cobalt-59 impurity level in steel is 800 ppm or 0.8 gm/kg and in inconel is approximately 4700 ppm or 4.7 gm/kg. In the early to mid 1980s, the fuel vendors reduced the Cobalt-59 impurity level in both inconel and steel to less than 500 ppm or 0.5 gm/kg. Prior to that, the impurity level in inconel in fuel assemblies was typically less than 1200 ppm or 1.2 gm/kg. Nevertheless, a conservative Cobalt-59 impurity level of 0.8 gm/kg was used for the stainless steel cladding and a highly conservative impurity level of 4.7 gm/kg was used for the inconel incore spacers. It is assumed that the end fitting masses of the stainless steel clad fuel are the same as the end fittings masses of the zircaloy clad fuel. Therefore, separate source terms are not provided for the end fittings of the stainless steel fuel.

Tables 5.2.19 through 5.2.22 list the neutron and gamma source strengths for the design basis stainless steel clad fuel. The gamma source strengths include the contribution from the cobalt activation in the incore spacers. Subsection 5.4.4 presents the dose rates around the HI-STAR 100 for the normal and hypothetical accident conditions for the stainless steel fuel. In the calculation of these dose rates the length of the active fuel was conservatively assumed to be 144 inches. In addition, the fuel assembly configuration used in the MCNP calculations was identical to the configuration used for the design basis fuel assemblies as described in Table 5.3.1.

#### 5.2.4 Non-fuel Hardware

Generic PWR non-fuel hardware is not permitted for transport in the HI-STAR 100 system **with MPC-24 (24 PWR assemblies)**. However, certain non-fuel hardware from the Trojan Nuclear plant has been analyzed and is approved for transportation. These components include rod cluster control assemblies (RCCAs), burnable poison rod assemblies (BPRAs) and thimble plug devices (TPDs). The methodology for analyzing the non-fuel hardware authorized for transportation is described below and has been previously approved in the HI-STORM 100 FSAR [5.2.9].

**Burnable poison rod assemblies (BPRAs), thimble plug devices (TPDs), and rod cluster control assemblies (RCCAs) are permitted for transportation in the HI-STAR 100 system with MPC-32 as an integral part of a PWR fuel assembly. BPRAs and TPDs may be stored in any fuel cell location while RCCAs are required to be stored in the fuel cell locations of the MPC-32 basket specified in Subsection 1.2.3.**

**It should be noted that currently the loading of axial power shaping rods (APSRs) are not allowed.**

##### 5.2.4.1 BPRAs and TPDs

Burnable poison rod assemblies (BPRA) and thimble plug devices (TPD) are an integral, yet removable, part of a large portion of PWR fuel. The TPDs are not used in all assemblies in a reactor core but are reused from cycle to cycle. Therefore, these devices can achieve very high burnups. In contrast, BPRAs are burned with a fuel assembly in core and are not reused. In fact, many BPRAs are removed after one or two cycles before the fuel assembly is discharged. Therefore, the achieved burnup for BPRAs is not significantly different than fuel assemblies.

TPDs are made of stainless steel and may contain a small amount of inconel. These devices extend down into the plenum region of the fuel assembly but do not extend into the active fuel region. Since these devices are made of stainless steel, there is a significant amount of cobalt-60 produced during irradiation. This is the only significant radiation source from the activation of steel and inconel.

BPRAs are made of stainless steel in the region above the active fuel zone and may contain a small amount of inconel in this region. Within the active fuel zone the BPRAs may contain 2-24 rodlets which are burnable absorbers clad in either zircaloy or stainless steel. The stainless steel clad BPRAs create a significant radiation source (Co-60) while the zircaloy clad BPRAs create a negligible radiation source. Therefore the stainless steel clad BPRAs are bounding.

#### 5.2.4.1.1 MPC-32 Design Basis BPRA and TPD

The MPC-32 design basis BPRA and TPD used in current calculations are based on information provided in Chapter 5 the HI-STORM 100 FSAR [5.2.9] for BPRAs and TPDs. Table 5.2.46 provides the description of design basis BPRA and TPD. Table 5.2.47 provides the BPRA and TPD Co-60 activities used in the current analyses.

#### 5.2.4.1.2 Trojan's BPRAs and TPDs

SAS2H and ORIGEN-S were used to calculate a radiation source term for the Trojan TPDs and BPRAs. In the ORIGEN-S calculations the cobalt-59 impurity level was conservatively assumed to be 0.8 gm/kg for stainless steel and 4.7 gm/kg for inconel. These calculations were performed by irradiating the appropriate mass of steel and inconel using the flux calculated for the design basis Trojan 17x17 fuel assembly. The mass of material in the regions above the active fuel zone was scaled by the appropriate scaling factors listed in Table 5.2.7 in order to account for the reduced flux levels above the fuel assembly. The total curies of cobalt were calculated for the Trojan TPDs and BPRAs for the actual burnups and cooling times (the BPRAs were only used in the first cycle whereas the TPDs were used in all but the last cycle). The accumulated burnup and cooling time for the BPRAs and TPDs are 15,998 MWD/MTU and 24 years cooling and 118,674 MWD/MTU and 11 years cooling, respectively. Since the operating history of the shutdown Trojan reactor is well known the actual cycle lengths and conservatively short downtimes between cycles were used in the calculation of the source terms. In the ORIGEN-S calculations it was assumed that the burned fuel assembly was replaced with a fresh fuel assembly after every

cycle. This was achieved in ORIGEN-S by resetting the flux levels and cross sections to the 0 MWD/MTU condition after every cycle.

Currently only the Trojan non-fuel hardware is permitted for transportation in the HI-STAR 100 System. The masses of the Trojan TPD and BPRA are listed in Table 5.2.36. This information was taken from references [5.2.5] and [5.2.7] and is the same information used in the Trojan FSAR [5.1.6].

Table 5.2.37 shows the curies of Co-60 that were calculated for BPRAs and TPDs in each region of the fuel assembly (e.g. incore, plenum, top). An allowable cooling time, separate from the fuel assemblies, of 24 years and 11 years is used for the Trojan BPRAs and TPDs, respectively.

Subsection 5.4.7 discusses the analysis of cask dose rates from Trojan fuel including the effect of the insertion of BPRAs or TPDs into Trojan fuel assemblies.

#### 5.2.4.2 RCCAs

Rod cluster control assemblies (RCCAs) are an integral, yet reusable, portion of a PWR fuel assembly. These devices are utilized for many years (upwards of 20 years) prior to discharge into the spent fuel pool. The manner in which the RCCAs are utilized varies from plant to plant. Some utilities maintain the RCCAs fully withdrawn during normal operation while others may operate with a bank of rods partially inserted (approximately 10%) during normal operation. Even when fully withdrawn, the ends of the RCCAs are present in the upper portion of the fuel assembly since they are never fully removed from the fuel assembly during operation. The result of the different operating styles is a variation in the source term for the RCCAs. In all cases, however, only the lower portion of the RCCAs will be significantly activated. Therefore, when the RCCAs are stored with the PWR fuel assembly, the activated portion of the RCCAs will be in the lower portion of the cask. RCCAs are fabricated of various materials. The cladding is typically stainless steel, although inconel has been used. The absorber can be a single material or a combination of materials. AgInCd is possibly the most common absorber although B<sub>4</sub>C in aluminum is used, and hafnium has also been used. AgInCd produces a noticeable source term in the 0.3-1.0 MeV range due to the activation of Ag.

##### 5.2.4.2.1 MPC-32 Design Basis RCCA

The MPC-32 design basis RCCA used in current calculations is based on information provided in Chapter 5 of the HI-STORM 100 FSAR [5.2.9] for RCCAs (i.e., Control Rod Assemblies, CRAs). Two configurations are evaluated for RCCAs in Chapter 5 of Reference [5.2.9], showing that Configuration 1 (10% RCCA insertion) bounds Configuration 2 (fully removed RCCA) from dose rate perspective. Thus, the shielding calculations in this chapter are only performed for Configuration 1. Table 5.2.48 provides the description of design basis RCCA. Table 5.2.49

provides the RCCA Co-60 and other activities (from the activation of AgInCd) used for the current analyses.

It should be noted that RCCAs are required to be stored in the fuel cell locations of the MPC-32 basket specified in Subsection 1.2.3.

#### 5.2.4.2.2 Trojan's RCCAs

The Trojan RCCAs, the only RCCAs currently authorized for transport, were made of AgInCd clad in stainless steel.

In order to determine the impact on the dose rates around the HI-STAR 100 System, source terms for the Trojan RCCAs were calculated using SAS2H and ORIGEN-S. In the ORIGEN-S calculations the cobalt-59 impurity level was conservatively assumed to be 0.8 gm/kg for stainless steel and 4.7 gm/kg for inconel. These calculations were performed by irradiating 1 kg of steel, inconel, and AgInCd using the flux calculated for the Trojan W 17x17 fuel assembly. The total curies of cobalt for the steel and inconel and the 0.3-1.0 MeV source for the AgInCd were calculated for a single burnup, 125,515 MWD/MTU, and cooling time, 9 years, corresponding to the lifetime operation of the Trojan reactor. Since the operating history of the shutdown Trojan reactor is well known the actual cycle lengths and conservatively short downtimes between cycles were used in the calculation of the source terms. In the ORIGEN-S calculations it was assumed that the burned fuel assembly was replaced with a fresh fuel assembly after every cycle. This was achieved in ORIGEN-S by resetting the flux levels and cross sections to the 0 MWD/MTU condition after every cycle. The sources were then scaled by the appropriate mass using the flux weighting factors for the different regions of the assembly to determine the final source term. Since the Trojan reactor normally operated with all RCCA rods fully withdrawn only one configuration was analyzed for the RCCAs. The configuration, which is summarized below, is described in Table 5.2.38 for the RCCAs. The masses of the materials listed in these tables were determined from reference [5.2.5]. The masses listed in Table 5.2.38 do not match exact values from [5.2.5] because the values in the reference were adjusted to the lengths shown in the tables.

#### RCCA Configuration

This configuration represents a fully removed RCCA during normal core operations. The activated portion corresponds to the upper portion of a fuel assembly above the active fuel length with the appropriate flux weighting factors used.

Table 5.2.38 presents the source terms that were calculated for the Trojan RCCAs. The only significant source from the activation of inconel or steel is Co-60 and the only significant source from the activation of AgInCd is from 0.3-1.0 MeV.



Subsection 5.4.7 discusses the analysis of cask dose rates from Trojan fuel including the effect of the insertion of RCCAs into Trojan fuel assemblies.

### 5.2.5 Choice of Design Basis Assembly

The analysis presented in this chapter was performed to bound the fuel assembly classes listed in Tables 1.2.8 and 1.2.9. In order to perform a bounding analysis, a design basis fuel assembly must be chosen. Therefore, a fuel assembly from each fuel class was analyzed and a comparison of the neutrons/sec, photons/sec, and thermal power (watts) was performed. The fuel assembly which produced the highest source for a specified burnup, cooling time, and enrichment was chosen as the design basis fuel assembly. A separate design basis assembly was chosen for the PWR baskets (MPC-24 and MPC-32) and the BWR basket (MPC-68).

#### 5.2.5.1 PWR Design Basis Assembly

Table 1.2.8 lists the PWR fuel assembly classes that were evaluated to determine the design basis PWR fuel assembly. Within each class, the fuel assembly with the highest  $\text{UO}_2$  mass was analyzed. Since the variations of fuel assemblies within a class are very minor (pellet diameter, clad thickness, etc.), it is conservative to choose the assembly with the highest  $\text{UO}_2$  mass. For a given class of assemblies, the one with the highest  $\text{UO}_2$  mass will produce the highest radiation source because, for a given burnup (MWD/MTU) and enrichment, the highest  $\text{UO}_2$  mass will have produced the most energy and therefore the most fission products.

Table 5.2.24 presents the characteristics of the fuel assemblies analyzed to determine the design basis zircaloy clad PWR fuel assembly. The fuel assembly listed for each class is the assembly with the highest  $\text{UO}_2$  mass. The St. Lucie and Ft. Calhoun classes are not present in Table 5.2.24. These assemblies are shorter versions of the CE 16x16 and CE 14x14 assembly classes, respectively. Therefore, these assemblies are bounded by the CE 16x16 and CE 14x14 classes and were not explicitly analyzed. Since the Haddam Neck and San Onofre 1 classes are stainless steel clad fuel, these classes were analyzed separately and are discussed below. All fuel assemblies in Table 5.2.24 were analyzed at the same burnup and cooling time. The results of the comparison are provided in Table 5.2.26. These results indicate that the B&W 15x15 fuel assembly has the highest radiation source term of the zircaloy clad fuel assembly classes considered in Table 1.2.8. This fuel assembly also has the highest  $\text{UO}_2$  mass (see Table 5.2.24) which confirms that, for a given initial enrichment, burnup, and cooling time, the assembly with the highest  $\text{UO}_2$  mass produces the highest radiation source term.

The Haddam Neck and San Onofre 1 classes are shorter stainless steel clad versions of the WE 15x15 and WE 14x14 classes, respectively. Since these assemblies have stainless steel clad, they were analyzed separately as discussed in Subsection 5.2.3. Based on the results in Table 5.2.26, which show that the WE 15x15 assembly class has a higher source term than the WE 14x14

assembly class, the Haddam Neck, WE 15x15, fuel assembly was analyzed as the bounding PWR stainless steel clad fuel assembly.

#### 5.2.5.2 BWR Design Basis Assembly

Table 1.2.9 lists the BWR fuel assembly classes that were evaluated to determine the design basis BWR fuel assembly. Since there are minor differences between the array types in the GE BWR/2-3 and GE BWR/4-6 assembly classes, these assembly classes were not considered individually but rather as a single class. Within that class, the array types, 7x7, 8x8, 9x9, and 10x10 were analyzed to determine the bounding BWR fuel assembly. Since the Humboldt Bay 7x7 and Dresden 1 8x8 are smaller versions of the 7x7 and 8x8 assemblies they are bounded by the 7x7 and 8x8 assemblies in the GE BWR/2-3 and GE BWR/4-6 classes. Within each array type, the fuel assembly with the highest  $\text{UO}_2$  mass was analyzed. Since the variations of fuel assemblies within an array type are very minor, it is conservative to choose the assembly with the highest  $\text{UO}_2$  mass. For a given array type of assemblies, the one with the highest  $\text{UO}_2$  mass will produce the highest radiation source because, for a given burnup (MWD/MTU) and enrichment, it will have produced the most energy and therefore the most fission products. The Humboldt Bay 6x6, Dresden 1 6x6, and LaCrosse assembly classes were not considered in the determination of the bounding fuel assembly. However, these assemblies were analyzed explicitly as discussed below.

Table 5.2.25 presents the characteristics of the fuel assemblies analyzed to determine the design basis zircaloy clad BWR fuel assembly. The fuel assembly listed for each array type is the assembly that has the highest  $\text{UO}_2$  mass. All fuel assemblies in Table 5.2.25 were analyzed at the same burnup and cooling time. The results of the comparison are provided in Table 5.2.27. These results indicate that the 7x7 fuel assembly has the highest radiation source term of the zircaloy clad fuel assembly classes considered in Table 1.2.9. This fuel assembly also has the highest  $\text{UO}_2$  mass which confirms that, for a given initial enrichment, burnup, and cooling time, the assembly with the highest  $\text{UO}_2$  mass produces the highest radiation source term. According to Reference [5.2.6], the last discharge of a 7x7 assembly was in 1985 and the maximum average burnup for a 7x7 during their operation was 29,000 MWD/MTU. This clearly indicates that the existing 7x7 assemblies have an average burnup and minimum cooling time that is well within the burnup and cooling time limits in Table 1.2.20. Therefore, the 7x7 assembly has never reached the burnup level analyzed in this chapter. However, in the interest of conservatism the 7x7 was chosen as the bounding fuel assembly array type.

Since the LaCrosse fuel assembly type is a stainless steel clad 10x10 assembly, it was analyzed separately. The maximum burnup and minimum cooling times for this assembly are limited to 22,500 MWD/MTU and 15-year cooling as specified in Table 1.2.19. This assembly type is discussed further in Subsection 5.2.3.

The Humboldt Bay 6x6 and Dresden 1 6x6 fuel are older and shorter than the other array types analyzed and therefore are considered separately. The Dresden 1 6x6 was chosen as the design basis fuel assembly for the Humboldt Bay 6x6 and Dresden 1 6x6 fuel assembly classes because it has the higher  $\text{UO}_2$  mass. Dresden 1 also contains a few 6x6 MOX fuel assemblies which were explicitly analyzed as well.

Reference [5.2.6] indicates that the Dresden 1 6x6 fuel assembly has a higher  $\text{UO}_2$  mass than the Dresden 1 8x8 or the Humboldt Bay fuel (6x6 and 7x7). Therefore, the Dresden 1 6x6 fuel assembly was also chosen as the bounding assembly for damaged fuel and fuel debris for the Humboldt Bay and Dresden 1 fuel assembly classes.

Since the design basis damaged fuel assembly and the design basis intact 6x6 fuel assembly are identical, the analysis presented in Subsection 5.4.2 for the damaged fuel assembly also demonstrates the acceptability of transporting intact 6x6 fuel assemblies from the Dresden 1 and Humboldt Bay fuel assembly classes.

#### 5.2.5.3 Decay Heat Loads

The decay heat values per assembly were calculated using the methodology described in Section 5.2. As demonstrated in Tables 5.2.26 and 5.2.27, the design basis fuel assembly produces a higher decay heat value than the other assembly types considered. This is due to the higher heavy metal mass in the design basis fuel assemblies. Conservatively, Tables 1.2.10 and 1.2.11 limit the heavy metal mass of the design basis fuel assembly classes to a value less than the design basis value utilized in this chapter. This provides additional assurance that the radiation source terms are bounding values.

As further demonstration that the decay heat values (calculated using the design basis fuel assemblies) are conservative, a comparison between these calculated decay heats and the decay heats reported in Reference [5.2.7] are presented in Table 5.2.28. This comparison is made for a burnup of 30,000 MWD/MTU and a cooling time of 5 years. The burnup was chosen based on the limited burnup data available in Reference [5.2.7].

The heavy metal mass of the non-design basis fuel assembly classes in Tables 1.2.10 and 1.2.11 are limited to the masses used in Tables 5.2.24 and 5.2.25. No margin is applied between the allowable mass and the analyzed mass of heavy metal for the non-design basis fuel assemblies. This is acceptable because additional assurance that the radiation source terms for the non-design basis fuel assemblies are bounding values is obtained by using the radiation source terms for the design basis fuel assemblies in determining the acceptable loading criteria for all fuel assemblies.

#### 5.2.6 Thoria Rod Canister

Dresden Unit 1 has a single DFC containing 18 thoria rods which have obtained a relatively low burnup, 16,000 MWD/MTU. These rods were removed from two 8x8 fuel assemblies which contained 9 rods each. The irradiation of thorium produces an isotope which is not commonly found in depleted uranium fuel. Th-232 when irradiated produces U-233. The U-233 can undergo an (n,2n) reaction which produces U-232. The U-232 decays to produce Tl-208 which produces a 2.6 MeV gamma during Beta decay. This results in a significant source in the 2.5-3.0 MeV range which is not commonly present in depleted uranium fuel. Therefore, this single DFC container was analyzed to determine if it was bounded by the current shielding analysis.

A radiation source term was calculated for the 18 thoria rods using SAS2H and ORIGEN-S for a burnup of 16,000 MWD/MTU and a cooling time of 18 years. Table 5.2.29 describes the 8x8 fuel assembly that contains the thoria rods. Table 5.2.30 and 5.2.31 show the gamma and neutron source terms, respectively, that were calculated for the 18 thoria rods in the thoria rod canister. Comparing these source terms to the design basis 6x6 source terms for Dresden Unit 1 fuel in Tables 5.2.6 and 5.2.14 clearly indicates that the design basis source terms bound the thoria rods source terms in all neutron groups and in all gamma groups except the 2.5-3.0 MeV group. As mentioned above, the thoria rods have a significant source in this energy range due to the decay of Tl-208.

Subsection 5.4.6 provides a further discussion of the thoria rod canister and its acceptability for transport in the HI-STAR 100 System.

## 5.2.7 Fuel Assembly Neutron Sources

Neutron sources are used in reactors during initial startup of reactor cores. There are different types of neutron sources (e.g. californium, americium-beryllium, plutonium-beryllium, antimony-beryllium). These neutron sources are typically inserted into the water rod of a fuel assembly and are usually removable.

The neutron source from Dresden Unit 1 and Trojan Nuclear Plant is permitted for transport in the HI-STAR 100 System. Also, the design basis neutron source is permitted for transport in the HI-STAR 100 System with MPC-32. These neutron sources assemblies are discussed below.

### 5.2.7.1 Dresden Unit 1 Neutron Source Assemblies

Dresden Unit 1 has a few antimony-beryllium neutron sources. These sources have been analyzed in Subsection 5.4.5 to demonstrate that they are acceptable for transport in the HI-STAR 100 System.

### 5.2.7.2 Trojan Nuclear Plant Neutron Source Assemblies

Trojan Nuclear Power has two primary (californium) neutron source assemblies and four secondary (antimony-beryllium) neutron source assemblies. The neutron source assemblies are basically BPRAs with the source material placed in a few of the rods instead of burnable absorber. In the case of the californium source, a single rod contained a nominally 1.5 inch long californium capsule while the remaining locations consisted of 19 burnable poison rods and 4 thimble plug rods. The initial source strength of the primary sources were approximately  $6.0\text{E}+8$  neutrons/sec. Since these devices were delivered prior to startup, they have realized more than 24 years of decay time. Based on the half-life of Cf-252 (2.65 years), the neutron source strength of these devices would be less than  $1.2\text{E}+6$  neutrons/sec after 24 years of decay time. Therefore, the neutron contribution from these devices is negligible and is not considered in the analysis in this chapter. Since these devices are clad in stainless steel, there is the potential for significant Co-60 activation from in-core activation of the cladding material. The primary sources were only operated during the first cycle of the Trojan nuclear plant and as a result achieved a burnup of 15,998 MWD/MTU and have a cooling time of more than 24 years. This burnup and cooling time is identical to the burnup and cooling time for the Trojan BPRAs as discussed in Subsection 5.2.4.1. Therefore, the primary sources are not explicitly considered in this analysis but are bounded by the analysis of the BPRAs.

The Trojan Nuclear Plant secondary neutron source assemblies used 4 rods for the antimony-beryllium source and the remaining rods were either burnable poison rods or thimble plug rods. The 4 source rods in a secondary neutron source assembly each contained 88 inches of antimony-beryllium. Since the antimony-beryllium neutron sources are regenerative sources they will be producing a steady state level of neutrons while in the MPC. This production of neutrons has been explicitly analyzed in Subsection 5.4.8. In addition to the neutron source from the secondary sources, there will be a substantial Co-60 source from the activation of the stainless steel cladding. There are two different levels of activation since the first two source assemblies were used in-core for cycles 1-4 and the latter two source assemblies were used in-core for cycles 4-14. The operating history for these devices results in a burnup of 45,361 MWD/MTU and a cooling time of 19 years for the source assemblies that operated in the first four cycles. The burnup and cooling time for the other two source assemblies is 88,547 MWD/MTU and 9 years. In addition to the difference in the burnup and cooling times between the two sets of secondary source assemblies, the number of burnable poison rods and thimble plug rods is different. The two source assemblies used in Cycles 1-4 each contained 4 source rods, 16 burnable poison rods and 4 thimble plug rods. The two source assemblies used in Cycles 4-14 each contained 4 source rods and 20 thimble plug rods. Table 5.2.39 shows the physical description of these devices that was used in the source term calculation and the resultant Co-60 source term in each region. Subsection 5.4.8 discusses the effect of the secondary source assemblies on the calculated dose rates and demonstrates that these devices are acceptable for transport.

### 5.2.7.3 MPC-32 Design Basis Neutron Source Assemblies

The MPC-32 design basis NSA used in current analysis is based on information provided in Chapter 5 the HI-STORM 100 FSAR [5.2.9] for PWR NSAs. It is stated in Paragraph 5.2.7.1 of Reference [5.2.9] that the total activation of a primary or secondary source is bounded by the total activation of a BPRA. Thus, no further shielding analysis is performed in this SAR.

It should be noted only one NSA is permitted for loading in each HI-STAR 100 System with MPC-32. The NSA is required to be stored in the fuel storage locations of the MPC-32 basket specified in Subsection 1.2.3.

### 5.2.8 Trojan Non-Fuel Bearing Components, Damaged Fuel and Fuel Debris

Trojan Nuclear Power has failed fuel cans containing fuel process can capsules and fuel debris. The fuel process can capsules contain only a limited amount of fuel in the form of fuel debris (metal fragments). The source term from the fuel process can capsules is therefore bounded by the source from a fuel assembly.

The fuel assemblies classified as fuel debris consist of a few assemblies with each containing a maximum of 17 rods. There is also a single damaged fuel container that has 23 individual rods not bound in a fuel assembly configuration. If it is assumed that the 23 individual rods are from a design basis Trojan fuel assembly and have not collapsed, then the source strength per inch of active fuel is a small fraction (23 rods/264 rods in an intact assembly) of the source in an intact assembly. If it is assumed that the source strength per rod is "A" then the source per inch in an intact assembly is  $264A/144 = 1.833A$ . The damaged fuel assembly with 23 rods would have to collapse from 144 inches in height to 12.5 inches (height =  $23A/1.833A$ ) in order for the source strength per unit inch in the collapsed assembly to be equivalent to the source strength per unit inch in an intact assembly. Further collapse would increase the source strength per inch beyond that of a design basis assembly but it is not considered likely that this would occur. Therefore, even in a collapsed state which might exist after a transport accident, this fuel debris is bounded by an intact fuel assembly and therefore is not explicitly considered in the analysis in this chapter.

There are also a couple of fuel assemblies classified as damaged fuel because of missing rods. These assemblies are also bounded by an intact assembly and during the transport accident it is expected that these damaged assemblies would react the same as intact assemblies. Therefore, the Trojan damaged fuel assemblies were not explicitly considered in the analysis in this chapter.

Trojan fuel assembly hardware, non-fuel bearing components and one fuel skeleton will also be transported. These components are made of stainless steel, zircaloy and inconel. The source term from these additional components were not explicitly considered but are bounded by intact fuel assemblies. Therefore, the source term from these components were not explicitly considered.

Table 5.2.1

PROPRIETARY INFORMATION WITHHELD PER 10CFR2.390

Table 5.2.1 (continued)

PROPRIETARY INFORMATION WITHHELD PER 10CFR2.390



Table 5.2.2

PROPRIETARY INFORMATION WITHHELD PER 10CFR2.390

Table 5.2.3  
CALCULATED MPC-24 PWR FUEL GAMMA SOURCE PER ASSEMBLY FOR DESIGN BASIS ZIRCALOY CLAD  
FUEL WITH NON-ZIRCALOY INCORE SPACERS FOR VARYING BURNUPS AND COOLING TIMES

<b>Lower Energy</b>	<b>Upper Energy</b>	<b>24,500 MWD/MTU 9 Year Cooling</b>		<b>29,500 MWD/MTU 11 Year Cooling</b>		<b>34,500 MWD/MTU 13 Year Cooling</b>	
(MeV)	(MeV)	(MeV/s)	(Photons/s)	(MeV/s)	(Photons/s)	(MeV/s)	(Photons/s)
0.45	0.7	7.61E+14	1.32E+15	8.35E+14	1.45E+15	9.05E+14	1.57E+15
0.7	1.0	8.94E+13	1.05E+14	6.95E+13	8.18E+13	5.54E+13	6.52E+13
1.0	1.5	3.29E+13	2.63E+13	3.33E+13	2.67E+13	3.41E+13	2.73E+13
1.5	2.0	1.70E+12	9.74E+11	1.73E+12	9.91E+11	1.84E+12	1.05E+12
2.0	2.5	2.19E+11	9.71E+10	5.49E+10	2.44E+10	1.89E+10	8.40E+09
2.5	3.0	1.32E+10	4.81E+09	4.06E+09	1.47E+09	1.49E+09	5.42E+08
Totals		8.85E+14	1.46E+15	9.39E+14	1.56E+15	9.96E+14	1.67E+15
<b>Lower Energy</b>	<b>Upper Energy</b>	<b>39,500 MWD/MTU 15 Year Cooling</b>		<b>44,500 MWD/MTU 18 Year Cooling</b>			
(MeV)	(MeV)	(MeV/s)	(Photons/s)	(MeV/s)	(Photons/s)		
0.45	0.7	9.70E+14	1.69E+15	1.00E+15	1.74E+15		
0.7	1.0	4.49E+13	5.28E+13	3.32E+13	3.90E+13		
1.0	1.5	3.39E+13	2.71E+13	3.07E+13	2.46E+13		
1.5	2.0	1.89E+12	1.08E+12	1.78E+12	1.02E+12		
2.0	2.5	1.11E+10	4.92E+09	9.00E+09	4.00E+09		
2.5	3.0	8.82E+08	3.21E+08	8.14E+08	2.96E+08		
Totals		1.05E+15	1.77E+15	1.07E+15	1.81E+15		

Table 5.2.4  
CALCULATED MPC-24 PWR FUEL GAMMA SOURCE PER ASSEMBLY FOR DESIGN BASIS ZIRCALOY CLAD  
FUEL WITH ZIRCALOY INCORE SPACERS FOR VARYING BURNUPS AND COOLING TIMES

<b>Lower Energy</b>	<b>Upper Energy</b>	<b>24,500 MWD/MTU 6 Year Cooling</b>		<b>29,500 MWD/MTU 7 Year Cooling</b>		<b>34,500 MWD/MTU 9 Year Cooling</b>	
(MeV)	(MeV)	(MeV/s)	(Photons/s)	(MeV/s)	(Photons/s)	(MeV/s)	(Photons/s)
0.45	0.7	9.60E+14	1.67E+15	1.06E+15	1.85E+15	1.08E+15	1.88E+15
0.7	1.0	2.17E+14	2.55E+14	2.09E+14	2.46E+14	1.48E+14	1.74E+14
1.0	1.5	5.67E+13	4.54E+13	5.96E+13	4.77E+13	5.44E+13	4.35E+13
1.5	2.0	3.71E+12	2.12E+12	3.24E+12	1.85E+12	2.70E+12	1.54E+12
2.0	2.5	2.48E+12	1.10E+12	1.19E+12	5.27E+11	2.57E+11	1.14E+11
2.5	3.0	1.02E+11	3.70E+10	5.83E+10	2.12E+10	1.67E+10	6.08E+09
Totals		1.24E+15	1.97E+15	1.33E+15	2.14E+15	1.29E+15	2.10E+15
<b>Lower Energy</b>	<b>Upper Energy</b>	<b>39,500 MWD/MTU11 Year Cooling</b>		<b>44,500 MWD/MTU14 Year Cooling</b>			
(MeV)	(MeV)	(MeV/s)	(Photons/s)	(MeV/s)	(Photons/s)		
0.45	0.7	1.12E+15	1.94E+15	1.12E+15	1.95E+15		
0.7	1.0	1.05E+14	1.24E+14	6.36E+13	7.48E+13		
1.0	1.5	5.06E+13	4.05E+13	4.35E+13	3.48E+13		
1.5	2.0	2.58E+12	1.47E+12	2.37E+12	1.35E+12		
2.0	2.5	6.36E+10	2.83E+10	1.55E+10	6.89E+09		
2.5	3.0	5.07E+09	1.84E+09	1.41E+09	5.12E+08		
Totals		1.28E+15	2.11E+15	1.23E+15	2.06E+15		

Table 5.2.5  
CALCULATED MPC-68 BWR FUEL GAMMA SOURCE PER ASSEMBLY FOR DESIGN BASIS ZIRCALOY CLAD  
FUEL FOR VARYING BURNUPS AND COOLING TIMES

<b>Lower Energy</b>		<b>Upper Energy</b>		<b>10,000 MWD/MTU 5 Year Cooling</b>		<b>20,000 MWD/MTU 7 Year Cooling</b>		<b>24,500 MWD/MTU 8 Year Cooling</b>		<b>29,500 MWD/MTU 9 Year Cooling</b>	
(MeV)	(MeV)	(MeV/s)	(Photons/s)	(MeV/s)	(Photons/s)	(MeV/s)	(Photons/s)	(MeV/s)	(Photons/s)	(MeV/s)	(Photons/s)
0.45	0.7	1.68E+14	2.93E+14	2.83E+14	4.92E+14	3.21E+14	5.57E+14	3.64E+14	6.34E+14		
0.7	1.0	3.28E+13	3.86E+13	4.89E+13	5.75E+13	4.54E+13	5.34E+13	4.46E+13	5.25E+13		
1.0	1.5	9.61E+12	7.69E+12	1.42E+13	1.13E+13	1.46E+13	1.17E+13	1.63E+13	1.30E+13		
1.5	2.0	1.11E+12	6.34E+11	8.42E+11	4.81E+11	7.68E+11	4.39E+11	8.20E+11	4.69E+11		
2.0	2.5	1.22E+12	5.40E+11	3.47E+11	1.54E+11	1.65E+11	7.34E+10	8.09E+10	3.60E+10		
2.5	3.0	4.73E+10	1.72E+10	1.87E+10	6.82E+09	9.32E+09	3.39E+09	5.31E+09	1.93E+09		
Total		2.13E+14	3.40E+14	3.47E+14	5.62E+14	3.82E+14	6.23E+14	4.26E+14	7.00E+14		
<b>Lower Energy</b>		<b>Upper Energy</b>		<b>34,500 MWD/MTU 11 Year Cooling</b>		<b>39,500 MWD/MTU 14 Year Cooling</b>		<b>44,500 MWD/MTU 19 Year Cooling</b>			
(MeV)	(MeV)	(MeV/s)	(Photons/s)	(MeV/s)	(Photons/s)	(MeV/s)	(Photons/s)	(MeV/s)	(Photons/s)		
0.45	0.7	3.87E+14	6.73E+14	3.96E+14	6.89E+14	3.87E+14	6.73E+14				
0.7	1.0	3.31E+13	3.89E+13	2.03E+13	2.39E+13	1.09E+13	1.28E+13				
1.0	1.5	1.57E+13	1.26E+13	1.38E+13	1.10E+13	1.05E+13	8.38E+12				
1.5	2.0	8.10E+11	4.63E+11	7.59E+11	4.34E+11	6.17E+11	3.53E+11				
2.0	2.5	2.05E+10	9.10E+09	5.27E+09	2.34E+09	3.33E+09	1.48E+09				
2.5	3.0	1.62E+09	5.91E+08	4.16E+08	1.51E+08	2.84E+08	1.03E+08				
Total		4.36E+14	7.25E+14	4.31E+14	7.24E+14	4.09E+14	6.95E+14				

Table 5.2.6

CALCULATED MPC-68 and MPC-68F BWR FUEL GAMMA  
SOURCE PER ASSEMBLY FOR DESIGN BASIS  
ZIRCALOY CLAD DAMAGED FUEL

<b>Lower Energy</b>	<b>Upper Energy</b>	<b>30,000 MWD/MTU 18 Year Cooling</b>	
(MeV)	(MeV)	(MeV/s)	(Photons/s)
0.45	0.7	1.52E+14	2.65E+14
0.7	1.0	4.14E+12	4.87E+12
1.0	1.5	3.91E+12	3.13E+12
1.5	2.0	2.28E+11	1.30E+11
2.0	2.5	1.17E+09	5.21E+08
2.5	3.0	7.48E+07	2.72E+07
Totals		1.60E+14	2.73E+14

Table 5.2.7

PROPRIETARY INFORMATION WITHHELD PER 10CFR2.390

Table 5.2.8

CALCULATED MPC-24  $^{60}\text{Co}$  SOURCE PER ASSEMBLY FOR DESIGN BASIS ZIRCALOY CLAD FUEL  
WITH NON-ZIRCALOY INCORE SPACERS AT VARYING BURNUPS AND COOLING TIMES

<b>Location</b>	<b>24,500 MWD/MTU 9 Year Cooling (curies)</b>	<b>29,500 MWD/MTU 11 Year Cooling (curies)</b>	<b>34,500 MWD/MTU 13 Year Cooling (curies)</b>	<b>39,500 MWD/MTU 15 Year Cooling (curies)</b>	<b>44,500 MWD/MTU 18 Year Cooling (curies)</b>
Lower end fitting	95.83	81.89	68.71	56.79	41.33
Gas plenum springs	18.64	15.93	13.37	11.05	8.04
Gas plenum spacer	10.70	9.14	7.67	6.34	4.61
Expansion springs	N/A	N/A	N/A	N/A	N/A
Grid spacers	870.53	743.87	624.11	515.87	375.39
Upper end fitting	35.08	29.97	25.15	20.79	15.13
Handle	N/A	N/A	N/A	N/A	N/A

Table 5.2.9

CALCULATED MPC-24  $^{60}\text{Co}$  SOURCE PER ASSEMBLY FOR DESIGN BASIS ZIRCALOY CLAD FUEL  
WITH ZIRCALOY INCORE SPACERS AT VARYING BURNUPS AND COOLING TIMES

<b>Location</b>	<b>24,500 MWD/MTU 6 Year Cooling (curies)</b>	<b>29,500 MWD/MTU 7 Year Cooling (curies)</b>	<b>34,500 MWD/MTU 9 Year Cooling (curies)</b>	<b>39,500 MWD/MTU 11 Year Cooling (curies)</b>	<b>44,500 MWD/MTU 14 Year Cooling (curies)</b>
Lower end fitting	142.23	138.68	116.12	96.09	69.72
Gas plenum springs	27.67	26.98	22.59	18.69	13.56
Gas plenum spacer	15.88	15.48	12.96	10.73	7.78
Expansion springs	N/A	N/A	N/A	N/A	N/A
Grid spacers <sup>†</sup>	N/A	N/A	N/A	N/A	N/A
Upper end fitting	52.06	50.76	42.50	35.17	25.52
Handle	N/A	N/A	N/A	N/A	N/A

<sup>†</sup> These burnup and cooling times represent fuel with zircaloy grid spacers. Therefore, the cobalt activation is negligible.



Table 5.2.10

CALCULATED MPC-68 <sup>60</sup>CO SOURCE PER ASSEMBLY FOR DESIGN BASIS ZIRCALOY CLAD FUEL  
AT VARYING BURNUPS AND COOLING TIMES

<b>Location</b>	<b>10,000 MWD/MTU 5 Year Cooling (curies)</b>	<b>20,000 MWD/MTU 7 Year Cooling (curies)</b>	<b>24,500 MWD/MTU 8 Year Cooling (curies)</b>	<b>29,500 MWD/MTU 9 Year Cooling (curies)</b>	<b>34,500 MWD/MTU 11 Year Cooling (curies)</b>	<b>39,500 MWD/MTU 14 Year Cooling (curies)</b>	<b>44,500 MWD/MTU 19 Year Cooling (curies)</b>
Lower end fitting	39.71	40.80	34.04	30.55	27.49	19.64	11.08
Gas plenum springs	12.13	12.47	10.40	9.33	8.40	6.00	3.39
Gas plenum spacer	N/A	N/A	N/A	N/A	N/A	N/A	N/A
Expansion springs	2.21	2.27	1.89	1.70	1.53	1.09	0.62
Grid spacers	85.54	87.89	73.32	65.80	59.22	42.30	23.88
Upper end fitting	11.03	11.33	9.45	8.48	7.64	5.45	3.08
Handle	1.38	1.42	1.18	1.06	0.95	0.68	0.38

Table 5.2.11

CALCULATED MPC-24 PWR NEUTRON SOURCE PER ASSEMBLY  
FOR DESIGN BASIS ZIRCALOY CLAD FUEL WITH NON-ZIRCALOY  
INCORE SPACERS FOR VARYING BURNUPS AND COOLING TIMES

<b>Lower Energy (MeV)</b>	<b>Upper Energy (MeV)</b>	<b>24,500 MWD/MTU 9 Year Cooling (Neutrons/s)</b>	<b>29,500 MWD/MTU 11 Year Cooling (Neutrons/s)</b>	<b>34,500 MWD/MTU 13 Year Cooling (Neutrons/s)</b>	<b>39,500 MWD/MTU 15 Year Cooling (Neutrons/s)</b>	<b>44,500 MWD/MTU 18 Year Cooling (Neutrons/s)</b>
1.0E-01	4.0E-01	2.50E+06	4.04E+06	6.01E+06	8.09E+06	1.05E+07
4.0E-01	9.0E-01	1.28E+07	2.06E+07	3.07E+07	4.13E+07	5.35E+07
9.0E-01	1.4	1.18E+07	1.90E+07	2.82E+07	3.79E+07	4.91E+07
1.4	1.85	8.77E+06	1.41E+07	2.09E+07	2.81E+07	3.63E+07
1.85	3.0	1.58E+07	2.52E+07	3.73E+07	5.00E+07	6.47E+07
3.0	6.43	1.40E+07	2.25E+07	3.35E+07	4.50E+07	5.82E+07
6.43	20.0	1.23E+06	1.98E+06	2.94E+06	3.96E+06	5.13E+06
TOTALS		6.69E+07	1.07E+08	1.60E+08	2.14E+08	2.77E+08

Table 5.2.12

CALCULATED MPC-24 PWR NEUTRON SOURCE PER ASSEMBLY  
FOR DESIGN BASIS ZIRCALOY CLAD FUEL WITH ZIRCALOY  
INCORE SPACERS FOR VARYING BURNUPS AND COOLING TIMES

<b>Lower Energy (MeV)</b>	<b>Upper Energy (MeV)</b>	<b>24,500 MWD/MTU 6 Year Cooling (Neutrons/s)</b>	<b>29,500 MWD/MTU 7 Year Cooling (Neutrons/s)</b>	<b>34,500 MWD/MTU 9 Year Cooling (Neutrons/s)</b>	<b>39,500 MWD/MTU 11 Year Cooling (Neutrons/s)</b>	<b>44,500 MWD/MTU 14 Year Cooling (Neutrons/s)</b>
1.0E-01	4.0E-01	2.80E+06	4.69E+06	6.98E+06	9.40E+06	1.22E+07
4.0E-01	9.0E-01	1.43E+07	2.40E+07	3.57E+07	4.80E+07	6.22E+07
9.0E-01	1.4	1.32E+07	2.20E+07	3.27E+07	4.40E+07	5.70E+07
1.4	1.85	9.76E+06	1.63E+07	2.42E+07	3.26E+07	4.21E+07
1.85	3.0	1.75E+07	2.90E+07	4.30E+07	5.78E+07	7.47E+07
3.0	6.43	1.56E+07	2.61E+07	3.88E+07	5.22E+07	6.75E+07
6.43	20.0	1.37E+06	2.29E+06	3.42E+06	4.60E+06	5.96E+06
TOTALS		7.45E+07	1.24E+08	1.85E+08	2.49E+08	3.22E+08

Table 5.2.13

CALCULATED MPC-68 BWR NEUTRON SOURCE PER ASSEMBLY  
FOR DESIGN BASIS ZIRCALOY CLAD FUEL  
FOR VARYING BURNUPS AND COOLING TIMES

<b>Lower Energy (MeV)</b>	<b>Upper Energy (MeV)</b>	<b>10,000 MWD/MTU 5 Year Cooling (Neutrons/s)</b>	<b>20,000 MWD/MTU 7 Year Cooling (Neutrons/s)</b>	<b>24,500 MWD/MTU 8 Year Cooling (Neutrons/s)</b>	<b>29,500 MWD/MTU 9 Year Cooling (Neutrons/s)</b>	<b>34,500 MWD/MTU 11 Year Cooling (Neutrons/s)</b>	<b>39,500 MWD/MTU 14 Year Cooling (Neutrons/s)</b>	<b>44,500 MWD/MTU 19 Year Cooling (Neutrons/s)</b>
1.0E-01	4.0E-01	1.62E+05	1.01E+06	1.08E+06	1.81E+06	2.80E+06	3.61E+06	4.57E+06
4.0E-01	9.0E-01	8.29E+05	5.15E+06	5.52E+06	9.23E+06	1.43E+07	1.84E+07	2.33E+07
9.0E-01	1.4	7.68E+05	4.72E+06	5.08E+06	8.47E+06	1.31E+07	1.69E+07	2.14E+07
1.4	1.85	5.79E+05	3.50E+06	3.77E+06	6.27E+06	9.71E+06	1.25E+07	1.58E+07
1.85	3.0	1.07E+06	6.25E+06	6.75E+06	1.12E+07	1.73E+07	2.22E+07	2.80E+07
3.0	6.43	9.26E+05	5.61E+06	6.04E+06	1.01E+07	1.56E+07	2.00E+07	2.53E+07
6.43	20.0	7.91E+04	4.93E+05	5.29E+05	8.84E+05	1.37E+06	1.77E+06	2.24E+06
TOTALS		4.41E+06	2.67E+07	2.88E+07	4.79E+07	7.42E+07	9.54E+07	1.21E+08

Table 5.2.14

CALCULATED MPC-68 and MPC-68F BWR NEUTRON  
SOURCE PER ASSEMBLY FOR DESIGN BASIS  
DAMAGED ZIRCALOY CLAD FUEL

<b>Lower Energy (MeV)</b>	<b>Upper Energy (MeV)</b>	<b>30,000 MWD/MTU 18 Year Cooling (Neutrons/s)</b>
1.0E-01	4.0E-01	1.59E+6
4.0E-01	9.0E-01	8.10E+6
9.0E-01	1.4	7.43E+6
1.4	1.85	5.49E+6
1.85	3.0	9.76E+6
3.0	6.43	8.80E+6
6.43	20.0	7.76E+5
Totals		4.19E+7

Table 5.2.15

[PROPRIETARY INFORMATION WITHHELD PER 10CFR2.390]

Table 5.2.16

CALCULATED MPC-68 BWR FUEL GAMMA SOURCE PER ASSEMBLY  
FOR DESIGN BASIS ZIRCALOY CLAD MIXED OXIDE FUEL

<b>Lower Energy</b>	<b>Upper Energy</b>	<b>30,000 MWD/MTU 18-Year Cooling</b>	
(MeV)	(MeV)	(MeV/s)	(Photons/s)
0.45	0.7	1.45E+14	2.52E+14
0.7	1.0	3.95E+12	4.65E+12
1.0	1.5	3.82E+12	3.06E+12
1.5	2.0	2.22E+11	1.27E+11
2.0	2.5	1.11E+9	4.93E+8
2.5	3.0	9.31E+7	3.39E+7
Totals		1.53E+14	2.60E+14

Table 5.2.17

**CALCULATED MPC-68 BWR NEUTRON SOURCE PER ASSEMBLY  
FOR DESIGN BASIS ZIRCALOY CLAD MIXED OXIDE FUEL**

<b>Lower Energy (MeV)</b>	<b>Upper Energy (MeV)</b>	<b>30,000 MWD/MTU 18-Year Cooling (Neutrons/s)</b>
1.0E-01	4.0E-01	1.50E+6
4.0E-01	9.0E-01	7.67E+6
9.0E-01	1.4	7.09E+6
1.4	1.85	5.31E+6
1.85	3.0	9.67E+6
3.0	6.43	8.47E+6
6.43	20.0	7.33E+5
Totals		4.04E+7



Table 5.2.18

[PROPRIETARY INFORMATION WITHHELD PER 10CFR2.390]

Table 5.2.19

CALCULATED BWR FUEL GAMMA SOURCE PER ASSEMBLY  
FOR STAINLESS STEEL CLAD FUEL

<b>Lower Energy</b>	<b>Upper Energy</b>	<b>22,500 MWD/MTU 16-Year Cooling</b>	
(MeV)	(MeV)	(MeV/s)	(Photons/s)
0.45	0.7	2.26E+14	3.94E+14
0.7	1.0	6.02E+12	7.08E+12
1.0	1.5	4.04E+13	3.23E+13
1.5	2.0	2.90E+11	1.66E+11
2.0	2.5	2.94E+9	1.31E+9
2.5	3.0	7.77E+7	2.83E+7
Totals		2.73E+14	4.33E+14

Note:

1. These source terms were calculated for a 144 inch active fuel length. The actual active fuel length is 83 inches.
2. The  $^{60}\text{Co}$  activation from incore spacers is included in the 1.0-1.5 MeV energy group.

Table 5.2.20

CALCULATED PWR FUEL GAMMA SOURCE PER ASSEMBLY  
FOR STAINLESS STEEL CLAD FUEL

<b>Lower Energy</b>	<b>Upper Energy</b>	<b>30,000 MWD/MTU 19-Year Cooling</b>		<b>40,000 MWD/MTU 24-Year Cooling</b>	
(MeV)	(MeV)	(MeV/s)	(Photons/s)	(MeV/s)	(Photons/s)
0.45	0.7	6.81E+14	1.18E+15	7.97E+14	1.39E+15
0.7	1.0	1.83E+13	2.16E+13	1.70E+13	2.01E+13
1.0	1.5	1.13E+14	9.06E+13	8.24E+13	6.60E+13
1.5	2.0	1.06E+12	6.04E+11	1.12E+12	6.42E+11
2.0	2.5	7.25E+9	3.22E+9	7.42E+9	3.30E+9
2.5	3.0	3.52E+8	1.28E+8	6.43E+8	2.34E+8
Totals		8.14E+14	1.30E+15	8.98E+14	1.47E+15

Note:

1. These source terms were calculated for a 144 inch active fuel length. The actual active fuel length is 122 inches.
2. The  $^{60}\text{Co}$  activation from incore spacers is included in the 1.0-1.5 MeV energy group.

Table 5.2.21

CALCULATED BWR NEUTRON SOURCE PER ASSEMBLY  
FOR STAINLESS STEEL CLAD FUEL

<b>Lower Energy (MeV)</b>	<b>Upper Energy (MeV)</b>	<b>22,500 MWD/MTU 16-Year Cooling (Neutrons/s)</b>
1.0E-01	4.0E-01	1.81E+5
4.0E-01	9.0E-01	9.26E+5
9.0E-01	1.4	8.75E+5
1.4	1.85	6.85E+5
1.85	3.0	1.34E+6
3.0	6.43	1.08E+6
6.43	20.0	8.77E+4
Total		5.18E+6

Note:

These source terms were calculated for a 144 inch active fuel length. The actual active fuel length is 83 inches.

Table 5.2.22

**CALCULATED PWR NEUTRON SOURCE PER ASSEMBLY  
FOR STAINLESS STEEL CLAD FUEL**

<b>Lower Energy (MeV)</b>	<b>Upper Energy (MeV)</b>	<b>30,000 MWD/MTU 19-Year Cooling (Neutrons/s)</b>	<b>40,000 MWD/MTU 24-Year Cooling (Neutrons/s)</b>
1.0E-01	4.0E-01	2.68E+6	7.07E+6
4.0E-01	9.0E-01	1.37E+7	3.61E+7
9.0E-01	1.4	1.27E+7	3.32E+7
1.4	1.85	9.50E+6	2.47E+7
1.85	3.0	1.74E+7	4.43E+7
3.0	6.43	1.52E+7	3.95E+7
6.43	20.0	1.31E+6	3.46E+6
Totals		7.24E+7	1.88E+8

Note:

These source terms were calculated for a 144 inch active fuel length. The actual active fuel length is 122 inches.

Table 5.2.23

MINIMUM ENRICHMENTS AS A FUNCTION OF BURNUP  
FOR THE SHIELDING ANALYSIS

Minimum Enrichment (wt.% $^{235}\text{U}$ )	Maximum Burnup Analyzed (MWD/MTU)	
PWR assemblies with non-zircaloy incore spacers	MPC-24	MPC-32
2.3	24,500	24,500
2.6	29,500	29,500
2.9	34,500	34,500
3.2	39,500	39,500
3.4	44,500	42,500
3.6	N/A	45,000
PWR assemblies with zircaloy incore spacers	MPC-24	MPC-32
2.3	24,500	24,500
2.6	29,500	29,500
2.9	34,500	34,500
3.2	39,500	39,500
3.4	44,500	44,500
3.6	N/A	45,000
MPC-68		
0.7	10,000	
1.35	20,000	
2.1	24,500	
2.4	29,500	
2.6	34,500	
2.9	39,500	
3.0	44,500	

Table 5.2.24

## DESCRIPTION OF EVALUATED INTACT ZIRCALOY CLAD PWR FUEL

Assembly class	WE 14×14	WE 15×15	WE 17×17	CE 14×14	CE 16×16	B&W 15×15	B&W 17×17
Active fuel length (in.)	144	144	144	144	150	144	144
No. of fuel rods	179	204	264	176	236	208	264
Rod pitch (in.)	0.556	0.563	0.496	0.580	0.5063	0.568	0.502
Cladding material	Zr-4	Zr-4	Zr-4	Zr-4	Zr-4	Zr-4	Zr-4
Rod diameter (in.)	0.422	0.422	0.374	0.440	0.382	0.428	0.377
Cladding thickness (in.)	0.0243	0.0245	0.0225	0.0280	0.0250	0.0230	0.0220
Pellet diameter (in.)	0.3659	0.366	0.3225	0.377	0.3255	0.3742	0.3252
Pellet material	UO <sub>2</sub>	UO <sub>2</sub>	UO <sub>2</sub>	UO <sub>2</sub>	UO <sub>2</sub>	UO <sub>2</sub>	UO <sub>2</sub>
Pellet density (gm/cc) (95% of theoretical)	10.412	10.412	10.412	10.412	10.412	10.412	10.412
Enrichment (wt.% <sup>235</sup> U)	3.4	3.4	3.4	3.4	3.4	3.4	3.4
Burnup (MWD/MTU)	40,000	40,000	40,000	40,000	40,000	40,000	40,000
Cooling time (years)	5	5	5	5	5	5	5
Specific power (MW/MTU)	40	40	40	40	40	40	40
Weight of UO <sub>2</sub> (kg) <sup>†</sup>	462.451	527.327	529.848	482.706	502.609	562.029	538.757
Weight of U (kg) <sup>†</sup>	407.697	464.891	467.114	425.554	443.100	495.485	474.968
No. of Guide Tubes	17	21	25	5	5	17	25
Guide Tube O.D. (in.)	0.539	0.546	0.474	1.115	0.98	0.53	0.564
Guide Tube Thickness (in.)	0.0170	0.0170	0.0160	0.0400	0.0400	0.0160	0.0175

<sup>†</sup> Derived from parameters in this table.

Table 5.2.25

## DESCRIPTION OF EVALUATED INTACT ZIRCALOY CLAD BWR FUEL

Array Type	7×7	8×8	9×9	10×10
Active fuel length (in.)	144	144	144	144
No. of fuel rods	49	63	74	92
Rod pitch (in.)	0.738	0.640	0.566	0.510
Cladding material	Zr-2	Zr-2	Zr-2	Zr-2
Rod diameter (in.)	0.570	0.493	0.440	0.404
Cladding thickness (in.)	0.0355	0.0340	0.0280	0.0260
Pellet diameter (in.)	0.488	0.416	0.376	0.345
Pellet material	UO <sub>2</sub>	UO <sub>2</sub>	UO <sub>2</sub>	UO <sub>2</sub>
Pellet density (gm/cc) (95% of theoretical)	10.412	10.412	10.412	10.412
Enrichment (wt.% <sup>235</sup> U)	3.0	3.0	3.0	3.0
Burnup (MWD/MTU)	40,000	40,000	40,000	40,000
Cooling time (years)	5	5	5	5
Specific power (MW/MTU)	30	30	30	30
Weight of UO <sub>2</sub> (kg) <sup>†</sup>	225.177	210.385	201.881	211.307
Weight of U (kg) <sup>†</sup>	198.516	185.475	177.978	186.288
No. of Water Rods	0	1	2	2
Water Rod O.D. (in.)	n/a	0.493	0.980	0.980
Water Rod Thickness (in.)	n/a	0.0340	0.0300	0.0300

<sup>†</sup> Derived from parameters in this table.



Table 5.2.26

COMPARISON OF SOURCE TERMS FOR INTACT ZIRCALOY CLAD PWR FUEL  
3.4 wt.%  $^{235}\text{U}$  - 40,000 MWD/MTU - 5 years cooling

Assembly class	WE 14x14	WE 15x15	WE 17x17	CE 14x14	CE 16x16	B&W 15x15	B&W 17x17
Neutrons/sec	2.29E+8 / 2.31E+8	2.63E+8 / 2.65E+8	2.62E+8	2.31E+8	2.34E+8	2.94E+8	2.64E+8
Photons/sec (0.45-3.0 MeV)	3.28E+15/ 3.33E+15	3.74E+15/ 3.79E+15	3.76E+15	3.39E+15	3.54E+15	4.01E+15	3.82E+15
Thermal power (watts)	926.6 / 936.8	1056 / 1068	1062	956.6	995.7	1137	1077

Note:

The WE 14x14 and WE 15x15 have both zircaloy and stainless steel guide tubes. The first value presented is for the assembly with zircaloy guide tubes and the second value is for the assembly with stainless steel guide tubes.

Table 5.2.27

COMPARISON OF SOURCE TERMS FOR INTACT ZIRCALOY CLAD BWR FUEL  
 3.0 wt.%  $^{235}\text{U}$  - 40,000 MWD/MTU - 5 years cooling

Assembly class	7×7	8×8	9×9	10×10
Neutrons/sec	1.33E+8	1.17E+8	1.11E+8	1.22E+8
Photons/sec (0.45-3.0 MeV)	1.55E+15	1.44E+15	1.38E+15	1.46E+15
Thermal power (watts)	435.5	402.3	385.3	407.4

Table 5.2.28

COMPARISON OF CALCULATED DECAY HEATS FOR DESIGN BASIS FUEL  
AND VALUES REPORTED IN THE  
DOE CHARACTERISTICS DATABASE <sup>†</sup> FOR  
30,000 MWD/MTU AND 5-YEAR COOLING

Fuel Assembly Class	Decay Heat from the DOE Database (watts/assembly)	Decay Heat from Design Basis Fuel (watts/assembly)
PWR Fuel		
B&W 15x15	752.0	827.5
B&W 17x17	732.9	827.5
CE 16x16	653.7	827.5
CE 14x14	601.3	827.5
WE 17x17	742.5	827.5
WE 15x15	762.2	827.5
WE 14x14	649.6	827.5
BWR Fuel		
7x7	310.9	315.7
8x8	296.6	315.7
9x9	275.0	315.7

## Notes:

1. The PWR and BWR design basis fuels are the B&W 15x15 and the GE 7x7, respectively.
2. The decay heat values from the database include contributions from in-core material (e.g. spacer grids).
3. Information on the 10x10 was not available in the DOE database. However, based on the results in Table 5.2.27, the actual decay heat values from the 10x10 would be very similar to the values shown above for the 8x8.

---

<sup>†</sup> Reference [5.2.7].

Table 5.2.29

[PROPRIETARY INFORMATION WITHHELD PER 10CFR2.390]

Table 5.2.30

CALCULATED FUEL GAMMA SOURCE FOR THORIA ROD  
CANISTER CONTAINING EIGHTEEN THORIA RODS

<b>Lower Energy</b>	<b>Upper Energy</b>	<b>16,000 MWD/MTIHM 18-Year Cooling</b>	
(MeV)	(MeV)	(MeV/s)	(Photons/s)
7.0E-01	1.0	5.79E+11	6.81E+11
1.0	1.5	3.79E+11	3.03E+11
1.5	2.0	4.25E+10	2.43E+10
2.0	2.5	4.16E+8	1.85E+8
2.5	3.0	2.31E+11	8.39E+10
Totals		1.23E+12	1.09E+12

Table 5.2.31

CALCULATED FUEL NEUTRON SOURCE FOR THORIA ROD  
CANISTER CONTAINING EIGHTEEN THORIA RODS

<b>Lower Energy (MeV)</b>	<b>Upper Energy (MeV)</b>	<b>16,000 MWD/MTIHM 18-Year Cooling (Neutrons/s)</b>
1.0E-01	4.0E-01	5.65E+2
4.0E-01	9.0E-01	3.19E+3
9.0E-01	1.4	6.79E+3
1.4	1.85	1.05E+4
1.85	3.0	3.68E+4
3.0	6.43	1.41E+4
6.43	20.0	1.60E+2
Totals		7.21E+4

Table 5.2.32

[PROPRIETARY INFORMATION WITHHELD PER 10CFR2.390]

Table 5.2.33  
CALCULATED TROJAN PWR FUEL GAMMA SOURCE PER ASSEMBLY

<b>Lower Energy</b>	<b>Upper Energy</b>	<b>30,000 MWD/MTU 16 Year Cooling</b>		<b>37,500 MWD/MTU 16 Year Cooling</b>		<b>42,000 MWD/MTU 16 Year Cooling</b>	
(MeV)	(MeV)	(MeV/s)	(Photons/s)	(MeV/s)	(Photons/s)	(MeV/s)	(Photons/s)
0.45	0.7	6.80E+14	1.18E+15	8.46E+14	1.47E+15	9.44E+14	1.64E+15
0.7	1.0	2.52E+13	2.96E+13	3.35E+13	3.94E+13	3.82E+13	4.50E+13
1.0	1.5	2.04E+13	1.64E+13	2.71E+13	2.17E+13	3.09E+13	2.47E+13
1.5	2.0	1.16E+12	6.65E+11	1.53E+12	8.77E+11	1.75E+12	9.99E+11
2.0	2.5	6.72E+09	2.99E+09	8.28E+09	3.68E+09	9.33E+09	4.15E+09
2.5	3.0	4.10E+08	1.49E+08	6.13E+08	2.23E+08	7.47E+08	2.72E+08
Totals		7.26E+14	1.23E+15	9.08E+14	1.53E+15	1.01E+15	1.71E+15



Table 5.2.34  
CALCULATED TROJAN FUEL  $^{60}\text{Co}$  SOURCE PER ASSEMBLY

<b>Location</b>	<b>30,000 MWD/MTU 16 Year Cooling (curies)</b>	<b>37,500 MWD/MTU 16 Year Cooling (curies)</b>	<b>42,000 MWD/MTU 16 Year Cooling (curies)</b>
Lower End Fitting	21.48	23.72	24.19
Gas Plenum Springs	4.19	4.62	4.72
Gas Plenum Spacer	15.99	17.66	18.02
Grid Spacers	419.15	462.90	472.12
Upper End Fitting	18.29	20.20	20.60

Table 5.2.35  
CALCULATED TROJAN FUEL NEUTRON SOURCE PER ASSEMBLY

<b>Lower Energy (MeV)</b>	<b>Upper Energy (MeV)</b>	<b>30,000 MWD/MTU 16 Year Cooling (Neutrons/s)</b>	<b>37,500 MWD/MTU 16 Year Cooling (Neutrons/s)</b>	<b>42,000 MWD/MTU 16 Year Cooling (Neutrons/s)</b>
1.0E-01	4.0E-01	4.71E+06	8.11E+06	9.55E+06
4.0E-01	9.0E-01	2.41E+07	4.15E+07	4.88E+07
9.0E-01	1.4	2.21E+07	3.80E+07	4.47E+07
1.4	1.85	1.64E+07	2.81E+07	3.31E+07
1.85	3.0	2.93E+07	5.00E+07	5.88E+07
3.0	6.43	2.63E+07	4.51E+07	5.30E+07
6.43	20.0	2.30E+06	3.97E+06	4.67E+06
Total		1.25E+08	2.15E+08	2.53E+08

Table 5.2.36

DESCRIPTION OF TROJAN BURNABLE POISON ROD ASSEMBLY  
AND THIMBLE PLUG DEVICE

<b>Region</b>	<b>BPRA</b>	<b>TPD</b>
Upper End Fitting (kg of steel)	2.62	2.31
Upper End Fitting (kg of inconel)	0.42	0.42
Gas Plenum Spacer (kg of steel)	0.72	1.6
Gas Plenum Springs (kg of steel)	0.73	1.6
In-core (kg of steel)	12.10	N/A

Table 5.2.37

COBALT-60 ACTIVITIES FOR TROJAN BURNABLE POISON ROD  
ASSEMBLIES AND THIMBLE PLUG DEVICES

<b>Region</b>	<b>BPRA</b>	<b>TPD</b>
Burnup (MWD/MTU)	15,998	118,674
Cooling Time (years)	24	11
Upper End Fitting (curies Co-60)	1.20	18.86
Gas Plenum Spacer (curies Co-60)	0.34	12.80
Gas Plenum Springs (curies Co-60)	0.34	12.80
In-core (curies Co-60)	28.68	N/A

Table 5.2.38

DESCRIPTION OF TROJAN ROD CLUSTER CONTROL ASSEMBLY  
FOR SOURCE TERM CALCULATIONS

Physical Description

Axial Dimensions Relative to Bottom of Active Fuel			Flux Weighting Factor	Mass of cladding (kg Steel)	Mass of absorber (kg AgInCd)
Start (in)	Finish (in)	Length (in)			
Configuration - Fully Removed					
0.0	8.358	8.358	0.2	0.76	3.18
8.358	12.028	3.67	0.1	0.34	1.40

Radiological Description

125,515 MWD/MTU

9 Year Cooling

Axial Dimensions Relative to Bottom of Active Fuel			Photons/sec from AgInCd			Curies Co-60 from Steel
Start (in)	Finish (in)	Length (in)	0.3-0.45 MeV	0.45-0.7 MeV	0.7-1.0 MeV	
Configuration - Fully Removed						
0.0	8.358	8.358	7.66E+12	7.12E+12	5.66E+12	7.34
8.358	12.028	3.67	1.68E+12	1.56E+13	1.24E+12	1.61

Table 5.2.39

## DESCRIPTION OF TROJAN SECONDARY SOURCE ASSEMBLIES

## Physical Description

<b>Region</b>	<b>Source in Cycles 1-4</b>	<b>Sources in Cycles 4-14</b>
Upper End Fitting (kg of steel)	2.62	2.62
Upper End Fitting (kg of inconel)	0.42	0.42
Gas Plenum Spacer (kg of steel)	1.6	1.6
Gas Plenum Springs (kg of steel)	1.6	1.6
In-core (kg of steel)	10.08	2.02

## Radiological Description

<b>Region</b>	<b>Source in Cycles 1-4</b>	<b>Sources in Cycles 4-14</b>
Burnup (MWD/MTU)	45,361	88,547
Cooling Time (years)	19	9
Upper End Fitting (curies Co-60)	10.08	45.09
Gas Plenum Spacer (curies Co-60)	3.18	14.30
Gas Plenum Springs (curies Co-60)	3.18	14.30
In-core (curies Co-60)	100.20	90.29

Table 5.2.40  
 CALCULATED MPC-32 PWR FUEL GAMMA SOURCE PER ASSEMBLY FOR DESIGN BASIS ZIRCALOY CLAD  
 FUEL WITH NON-ZIRCALOY INCORE SPACERS FOR **SELECTED** BURNUPS AND COOLING TIMES

<b>Lower Energy</b>	<b>Upper Energy</b>	<b>24,500 MWD/MTU 12 Year Cooling</b>		<b>29,500 MWD/MTU 14 Year Cooling</b>		<b>34,500 MWD/MTU 16 Year Cooling</b>	
(MeV)	(MeV)	(MeV/s)	(Photons/s)	(MeV/s)	(Photons/s)	(MeV/s)	(Photons/s)
0.45	0.7	6.67E+14	1.16E+15	7.51E+14	1.31E+15	8.26E+14	1.44E+15
0.7	1.0	4.19E+13	4.94E+13	3.59E+13	4.23E+13	3.18E+13	3.74E+13
1.0	1.5	2.29E+13	1.83E+13	2.45E+13	1.96E+13	2.59E+13	2.07E+13
1.5	2.0	1.23E+12	7.05E+11	1.36E+12	7.80E+11	1.48E+12	8.47E+11
2.0	2.5	2.57E+10	1.14E+10	1.14E+10	5.06E+09	8.42E+09	3.74E+09
2.5	3.0	1.87E+09	6.78E+08	7.75E+08	2.82E+08	5.66E+08	2.06E+08
Totals		7.33E+14	1.23E+15	8.13E+14	1.37E+15	8.85E+14	1.50E+15
<b>Lower Energy</b>	<b>Upper Energy</b>	<b>39,500 MWD/MTU 19 Year Cooling</b>		<b>42,500 MWD/MTU 20 Year Cooling</b>		<b>45,000 MWD/MTU 24 Year Cooling</b>	
(MeV)	(MeV)	(MeV/s)	(Photons/s)	(MeV/s)	(Photons/s)	(MeV/s)	(Photons/s)
0.45	0.7	8.72E+14	1.52E+15	9.13E+14	1.59E+15	8.76E+14	1.52E+15
0.7	1.0	2.51E+13	2.95E+13	2.46E+13	2.89E+13	1.84E+13	2.17E+13
1.0	1.5	2.42E+13	1.94E+13	2.46E+13	1.97E+13	1.96E+13	1.57E+13
1.5	2.0	1.43E+12	8.17E+11	1.46E+12	8.35E+11	1.21E+12	6.90E+11
2.0	2.5	7.78E+09	3.46E+09	8.08E+09	3.59E+09	7.68E+09	3.41E+09
2.5	3.0	5.98E+08	2.17E+08	6.89E+08	2.51E+08	7.54E+08	2.74E+08
Totals		9.22E+14	1.57E+15	9.63E+14	1.64E+15	9.15E+14	1.56E+15

Table 5.2.41  
CALCULATED MPC-32 PWR FUEL GAMMA SOURCE PER ASSEMBLY FOR DESIGN BASIS ZIRCALOY CLAD  
FUEL WITH ZIRCALOY INCORE SPACERS FOR VARYING BURNUPS AND COOLING TIMES

<b>Lower Energy</b>	<b>Upper Energy</b>	<b>24,500 MWD/MTU 8 Year Cooling</b>		<b>29,500 MWD/MTU 9 Year Cooling</b>		<b>34,500 MWD/MTU 12 Year Cooling</b>	
(MeV)	(MeV)	(MeV/s)	(Photons/s)	(MeV/s)	(Photons/s)	(MeV/s)	(Photons/s)
0.45	0.7	8.09E+14	1.41E+15	9.20E+14	1.60E+15	9.38E+14	1.63E+15
0.7	1.0	1.19E+14	1.40E+14	1.17E+14	1.38E+14	6.91E+13	8.13E+13
1.0	1.5	3.84E+13	3.07E+13	4.30E+13	3.44E+13	3.78E+13	3.02E+13
1.5	2.0	2.04E+12	1.17E+12	2.17E+12	1.24E+12	1.99E+12	1.14E+12
2.0	2.5	4.83E+11	2.15E+11	2.40E+11	1.07E+11	3.18E+10	1.41E+10
2.5	3.0	2.60E+10	9.46E+09	1.51E+10	5.48E+09	2.53E+09	9.20E+08
Totals		9.69E+14	1.58E+15	1.08E+15	1.77E+15	1.05E+15	1.74E+15
<b>Lower Energy</b>	<b>Upper Energy</b>	<b>39,500 MWD/MTU 14 Year Cooling</b>		<b>44,500 MWD/MTU 19 Year Cooling</b>		<b>45,000 MWD/MTU 20 Year Cooling</b>	
(MeV)	(MeV)	(MeV/s)	(Photons/s)	(MeV/s)	(Photons/s)	(MeV/s)	(Photons/s)
0.45	0.7	1.00E+15	1.74E+15	9.78E+14	1.70E+15	9.64E+14	1.68E+15
0.7	1.0	5.41E+13	6.37E+13	2.92E+13	3.44E+13	2.65E+13	3.12E+13
1.0	1.5	3.71E+13	2.97E+13	2.84E+13	2.27E+13	2.66E+13	2.13E+13
1.5	2.0	2.03E+12	1.16E+12	1.66E+12	9.50E+11	1.58E+12	9.03E+11
2.0	2.5	1.42E+10	6.32E+09	8.63E+09	3.84E+09	8.55E+09	3.80E+09
2.5	3.0	1.17E+09	4.25E+08	7.88E+08	2.87E+08	7.93E+08	2.89E+08
Totals		1.09E+15	1.83E+15	1.04E+15	1.76E+15	1.02E+15	1.73E+15



Table 5.2.42

CALCULATED MPC-32  $^{60}\text{Co}$  SOURCE PER ASSEMBLY FOR DESIGN BASIS ZIRCALOY CLAD FUEL  
WITH NON-ZIRCALOY INCORE SPACERS **FOR SELECTED** BURNUPS AND COOLING TIMES

Location	<b>24,500 MWD/MTU 12 Year Cooling (curies)</b>	<b>29,500 MWD/MTU 14 Year Cooling (curies)</b>	<b>34,500 MWD/MTU 16 Year Cooling (curies)</b>	<b>39,500 MWD/MTU 19 Year Cooling (curies)</b>	<b>42,500 MWD/MTU 20 Year Cooling (curies)</b>	<b>45,000 MWD/MTU 24 Year Cooling (curies)</b>	
Lower end fitting	64.65	55.27	46.40	33.47	30.42	18.33	
Gas plenum springs	12.58	10.75	9.03	6.51	5.92	3.58	
Gas plenum spacer	7.22	6.17	5.18	3.74	3.40	2.05	
Expansion springs	N/A	N/A	N/A	N/A	N/A	N/A	
Grid spacers	587.27	502.05	421.45	304.00	276.36	166.97	
Upper end fitting	23.66	20.23	16.98	12.25	11.14	6.73	
Handle	N/A	N/A	N/A	N/A	N/A	N/A	

Table 5.2.43

CALCULATED MPC-32  $^{60}\text{Co}$  SOURCE PER ASSEMBLY FOR DESIGN BASIS ZIRCALOY CLAD FUEL  
WITH ZIRCALOY INCORE SPACERS AT VARYING BURNUPS AND COOLING TIMES

Location	24,500 MWD/MTU 8 Year Cooling (curies)	29,500 MWD/MTU 9 Year Cooling (curies)	34,500 MWD/MTU 12 Year Cooling (curies)	39,500 MWD/MTU 14 Year Cooling (curies)	44,500 MWD/MTU 19 Year Cooling (curies)	45,000 MWD/MTU 20 Year Cooling (curies)	
Lower end fitting	109.27	106.74	78.34	64.65	36.25	31.09	
Gas plenum springs	21.26	20.77	15.24	12.58	7.05	6.07	
Gas plenum spacer	12.20	11.91	8.74	7.22	4.05	3.48	
Expansion springs	N/A	N/A	N/A	N/A	N/A	N/A	
Grid spacers <sup>†</sup>	N/A	N/A	N/A	N/A	N/A	N/A	
Upper end fitting	40.00	39.07	28.68	23.66	13.27	11.41	
Handle	N/A	N/A	N/A	N/A	N/A	N/A	

<sup>†</sup> These burnup and cooling times represent fuel with zircaloy grid spacers. Therefore, the cobalt activation is negligible.

Table 5.2.44

CALCULATED MPC-32 PWR NEUTRON SOURCE PER ASSEMBLY  
FOR DESIGN BASIS ZIRCALOY CLAD FUEL WITH NON-ZIRCALOY  
INCORE SPACERS FOR **SELECTED** BURNUPS AND COOLING TIMES

Lower Energy (MeV)	Upper Energy (MeV)	24,500 MWD/MTU 12 Year Cooling (Neutrons/s)	29,500 MWD/MTU 14 Year Cooling (Neutrons/s)	34,500 MWD/MTU 16 Year Cooling (Neutrons/s)	39,500 MWD/MTU 19 Year Cooling (Neutrons/s)	42,500 MWD/MTU 20 Year Cooling (Neutrons/s)	45,000 MWD/MTU 24 Year Cooling (Neutrons/s)	
1.0E-01	4.0E-01	2.24E+06	3.61E+06	5.37E+06	6.97E+06	8.08E+06	7.98E+06	
4.0E-01	9.0E-01	1.15E+07	1.84E+07	2.74E+07	3.56E+07	4.13E+07	4.08E+07	
9.0E-01	1.4	1.06E+07	1.70E+07	2.52E+07	3.27E+07	3.79E+07	3.75E+07	
1.4	1.85	7.88E+06	1.26E+07	1.87E+07	2.43E+07	2.81E+07	2.78E+07	
1.85	3.0	1.43E+07	2.27E+07	3.35E+07	4.34E+07	5.02E+07	4.98E+07	
3.0	6.43	1.26E+07	2.02E+07	3.00E+07	3.89E+07	4.50E+07	4.45E+07	
6.43	20.0	1.10E+06	1.76E+06	2.63E+06	3.41E+06	3.95E+06	3.90E+06	
TOTALS		6.01E+07	9.63E+07	1.43E+08	1.85E+08	2.15E+08	2.12E+08	

Table 5.2.45

CALCULATED MPC-32 PWR NEUTRON SOURCE PER ASSEMBLY  
FOR DESIGN BASIS ZIRCALOY CLAD FUEL WITH ZIRCALOY  
INCORE SPACERS FOR VARYING BURNUPS AND COOLING TIMES

Lower Energy (MeV)	Upper Energy (MeV)	24,500 MWD/MTU 8 Year Cooling (Neutrons/s)	29,500 MWD/MTU 9 Year Cooling (Neutrons/s)	34,500 MWD/MTU 12 Year Cooling (Neutrons/s)	39,500 MWD/MTU 14 Year Cooling (Neutrons/s)	44,500 MWD/MTU 19 Year Cooling (Neutrons/s)	45,000 MWD/MTU 20 Year Cooling (Neutrons/s)	
1.0E-01	4.0E-01	2.60E+06	4.35E+06	6.24E+06	8.40E+06	1.01E+07	9.26E+06	
4.0E-01	9.0E-01	1.33E+07	2.22E+07	3.19E+07	4.29E+07	5.16E+07	4.73E+07	
9.0E-01	1.4	1.22E+07	2.04E+07	2.92E+07	3.94E+07	4.73E+07	4.34E+07	
1.4	1.85	9.08E+06	1.51E+07	2.17E+07	2.91E+07	3.50E+07	3.22E+07	
1.85	3.0	1.63E+07	2.70E+07	3.86E+07	5.19E+07	6.24E+07	5.74E+07	
3.0	6.43	1.45E+07	2.42E+07	3.47E+07	4.67E+07	5.61E+07	5.16E+07	
6.43	20.0	1.27E+06	2.13E+06	3.05E+06	4.11E+06	4.94E+06	4.53E+06	
TOTALS		6.93E+07	1.16E+08	1.65E+08	2.23E+08	2.67E+08	2.46E+08	

Table 5.2.46

DESCRIPTION OF DESIGN BASIS BURNABLE POISON ROD ASSEMBLY  
AND THIMBLE PLUG DEVICE [5.2.9]

<b>Region</b>	<b>BPRA</b>	<b>TPD</b>
Upper End Fitting (kg of steel)	2.62	2.3
Upper End Fitting (kg of inconel)	0.42	0.42
Gas Plenum Spacer (kg of steel)	0.77488	1.71008
Gas Plenum Springs (kg of steel)	0.67512	1.48992
In-core (kg of steel)	13.2	N/A

Table 5.2.47

**COBALT-60 ACTIVITIES FOR DESIGN BASIS BURNABLE POISON ROD  
ASSEMBLIES AND THIMBLE PLUG DEVICES [5.2.9] (Note 1)**

<b>Region</b>	<b>BPRA</b>	<b>TPD</b>
Upper End Fitting (curies Co-60)	6.75	5.2
Gas Plenum Spacer (curies Co-60)	1.03	1.87
Gas Plenum Springs (curies Co-60)	1.84	3.25
In-core (curies Co-60)	175.12	N/A

Note 1: The cobalt-60 activities provided in this table are consistent with design basis cobalt-60 activities for BPRAs and TPDs in Chapter 5 of Reference [5.2.9], but 12 years additional cooling time is considered.

Table 5.2.48

DESCRIPTION OF DESIGN BASIS ROD CLUSTER CONTROL ASSEMBLY  
CONFIGURATIONS FOR SOURCE TERM CALCULATIONS [5.2.9]

Axial Dimensions Relative to Bottom of Active Fuel			Flux Weighting Factor	Mass of cladding (kg Inconel)	Mass of absorber (kg AgInCd)
Start (in.)	Finish (in.)	Length (in.)			
Configuration 1 - 10% Inserted					
0.0	15.0	15.0	1.0	1.32	7.27
15.0	18.8125	3.8125	0.2	0.34	1.85
18.8125	28.25	9.4375	0.1	0.83	4.57

Table 5.2.49

## DESIGN BASIS SOURCE TERMS FOR ROD CLUSTER CONTROL ASSEMBLY CONFIGURATIONS [5.2.9] (Note 1)

Axial Dimensions Relative to Bottom of Active Fuel			Photons/sec from AgInCd			Curies Co-60 from Inconel
Start (in.)	Finish (in.)	Length (in.)	0.3-0.45 MeV	0.45-0.7 MeV	0.7-1.0 MeV	
Configuration 1 - 10% Inserted						
0.0	15.0	15.0	1.91e+14	1.78e+14	1.42e+14	229.4
15.0	18.8125	3.8125	9.71e+12	9.05e+12	7.20e+12	11.7
18.8125	28.25	9.4375	1.20e+13	1.12e+13	8.92e+12	14.4

Note 1: The cobalt-60 activities provided in this table are consistent with design basis cobalt-60 activities for CRAs in Chapter 5 of Reference [5.2.9], but 12 years additional cooling time is considered.



### 5.3 MODEL SPECIFICATIONS

The shielding analysis of the HI-STAR 100 System was performed with MCNP-4A [5.1.1]. MCNP is a Monte Carlo transport code that offers a full three-dimensional combinatorial geometry modeling capability including such complex surfaces as cones and tori. This means that no gross approximations were required to represent the HI-STAR 100 System in the shielding analysis. A sample input file for MCNP is provided in Appendix 5.C.

Subsection 5.1.2 discussed the accident conditions and stated that the only accident that would impact the shielding analysis would be a loss of the neutron shield and impact limiters. Therefore, the MCNP models of the HI-STAR 100 System normal condition have the neutron shield and impact limiters in place while the hypothetical accident condition replaces the neutron shield with void and removes the impact limiters. The aluminum honeycomb in the impact limiters was conservatively neglected in the MCNP modeling. However, credit was taken for the outer dimensions of the impact limiters.

#### 5.3.1 Description of the Radial and Axial Shielding Configuration

Section 1.4 provides the drawings that describe the HI-STAR 100 System. These drawings were used to create the MCNP models used in the radiation transport calculations. Figures 5.3.1 through 5.3.3 show cross sectional views of the HI-STAR 100 overpack and MPC as it was modeled in MCNP for each of the MPCs. These figures were created with the MCNP two-dimensional plotter and are drawn to scale. The figures clearly illustrate the radial steel fins and pocket trunnions in the neutron shield region. Since the fins and pocket trunnions were modeled explicitly, neutron streaming through these components is accounted for in the calculations of the dose adjacent to the overpack and 1 meter dose. In Subsection 5.4.1, the dose effect of localized streaming through these compartments is analyzed. Figures 5.3.4 through 5.3.6 show the MCNP models of the MPC-32, MPC-24, and MPC-68 fuel baskets including the as-modeled dimensions. Figure 5.3.9 shows a cross sectional view of the HI-STAR 100 overpack with the as-modeled thickness of the various materials. Figure 5.3.10 is an axial representation of the HI-STAR 100 overpack with the various as-modeled dimensions indicated. As Figure 5.3.10 indicates, the thickness of the MPC lid is 9.5 inches. Earlier versions of the MPC-68 used a 10 inch thick lid with a correspondingly smaller MPC-internal cavity height. The analysis in this chapter conservatively represents the 9.5 inch thick lid. Figures 5.3.11 and 5.3.12 provide the as-modeled dimensions of the impact limiters during normal conditions. The aluminum honeycomb material in the impact limiter is not shown in Figure 5.3.11 because it was conservatively not modeled in the MCNP calculations.

Calculations were performed to determine the acceptability of homogenizing the fuel assembly versus explicit modeling. Based on these calculations it was concluded that it was acceptable to homogenize the fuel assembly without loss of accuracy. The width of the PWR and BWR homogenized fuel assembly is equal to 15 times the pitch and 7 times the pitch, respectively.

Several conservative approximations were made in modeling the MPC and overpack. The conservative approximations are listed below.

[

PROPRIETARY INFORMATION WITHHELD PER 10CFR2.390

]

During this project several design changes occurred that affected the drawings, but did not significantly affect the MCNP models of the HI-STAR 100 overpack or MPC. Therefore, in some cases, these models do not exactly represent the drawings. The discrepancies between models and drawings are listed and discussed here.

[

PROPRIETARY INFORMATION WITHHELD PER 10CFR2.390

1

#### 5.3.1.1 Fuel Configuration

As described above, the active fuel region is modeled as a homogenous zone. The end fittings and the plenum regions are also modeled as homogenous regions of steel. The masses of steel used in these regions are shown in Tables 5.2.1 and 5.2.32. The axial description of the design basis fuel assemblies is provided in Table 5.3.1. The axial description of the Trojan fuel assembly is provided in Table 5.3.4. Figures 5.3.7 and 5.3.8 graphically depict the location of the

PWR and BWR fuel assemblies within the HI-STAR 100 System. The impact limiters are not depicted in the figures for clarity. The axial locations of the Boral, basket, pocket trunnion, and transition areas are shown in these figures.

The axial position of the fuel assembly within the basket is maintained with the use of the upper and lower fuel spacers. These fuel spacers are used to position the active fuel region next to the Boral. Chapter 2 demonstrates that these fuel spacers do not fail under all normal and hypothetical accident conditions. Therefore, movement of the fuel assembly during transport is not considered.

#### 5.3.1.2 Streaming Considerations

The streaming from the radial channels and pocket trunnions in the neutron shield is evaluated in Subsection 5.4.1. The MCNP model of the HI-STAR 100 completely describes the radial channels and pocket trunnions, thereby properly accounting for the streaming effect. In newer designs of the HI-STAR 100 overpack, the pocket trunnion has been removed. However, the analysis presented in this chapter using the pocket trunnion bounds the new configuration due to the reduction in streaming when the pocket trunnion is not present.

The design of the HI-STAR 100 System, as described in the drawings in Section 1.4, has eliminated all other possible streaming paths. Therefore, the MCNP model does not represent any additional streaming paths. A brief justification of this assumption is provided for each penetration.

- The lifting trunnions will remain installed in the overpack top flange. No credit is taken for any part of the trunnion that extends outside of the overpack.
- The pocket trunnions are modeled as solid blocks of steel. The pocket trunnion will be filled with a solid steel rotation trunnion attached to the transport frame during handling and shipping or a plug will be installed if rotation trunnions are not inserted into the pocket trunnion.
- The threaded holes in the MPC lid are plugged with solid plugs during shipping and, therefore, do not create a void in the MPC lid.
- The drain and vent ports in the MPC lid are designed to eliminate streaming paths. The steel lost in the MPC lid at the port location is replaced with a block of steel approximately 6 inches thick below the port opening and attached to the underside of the lid. This design feature is shown on the drawings in Section 1.4. The MCNP model did not explicitly represent this arrangement but, rather, modeled the MPC lid as a solid piece.

- The penetrations in the overpack are filled with bolts that extend into the penetration, thereby eliminating any potential direct streaming paths. Cover plates are also designed in such a way as to maintain the thickness of the overpack to the maximum extent practical. Therefore, the MCNP model does not represent any streaming paths due to penetrations in the overpack.

### 5.3.2 Regional Densities

Composition and densities of the various materials used in the HI-STAR 100 System shielding analyses are given in Tables 5.3.2 and 5.3.3. All of the materials and their actual geometries are represented in the MCNP model. All steel in the MPC was modeled as stainless steel and all steel in the overpack was modeled as carbon steel.

The MPCs in the HI-STAR 100 System can be manufactured with one of two possible neutron absorbing materials: Boral or Metamic. Both materials are made of aluminum and B<sub>4</sub>C powder. The Boral contains an aluminum and B<sub>4</sub>C powder mixture sandwiched between two aluminum plates while the Metamic is a single plate. The thickness and minimum <sup>10</sup>B areal density are the same for Boral and Metamic while the thicknesses are essentially the same. Therefore, the mass of Aluminum and B<sub>4</sub>C are essentially equivalent and there is no distinction between the two materials from a shielding perspective. As a result, Table 5.3.2 identifies the composition for Boral and no explicit calculations were performed with Metamic.

Section 3.4 demonstrates that all materials used in the HI-STAR 100 System remain below their design temperatures as specified in Table 2.1.2 during all normal conditions. Therefore, the shielding analysis does not address changes in the material density or composition as a result of temperature changes.

During normal operations, the depletion of B-10 in the Boral and the Holtite-A neutron shield is negligible. The fraction of B-10 atoms that are depleted in 50 years is approximately 3.0E-9 and 4.0E-8 in the Boral and Holtite-A, respectively. Therefore, the shielding analysis does not address changes in the composition of the Boral or Holtite-A as a result of neutron absorption.

As discussed in Section 1.2.1.4.2, the density of the Holtite-A during normal condition was reduced by approximately 4% to account for any potential water loss. In addition, the Hydrogen weight percent was conservatively reduced from 6% to 5.92%.

Section 3.5 discusses the effect of the hypothetical accident condition (fire) on the temperatures of the shielding materials and the resultant impact on their shielding effectiveness. As stated in Subsection 5.1.2, the only consequence that has any significant impact on the shielding configuration is the loss of the neutron shield in the HI-STAR 100 System as a result of fire. The

change in the neutron shield was conservatively analyzed by assuming that the entire volume of the neutron shield was replaced by void.

Table 5.3.1

[PROPRIETARY INFORMATION WITHHELD PER 10CFR2.390]

Table 5.3.2

[PROPRIETARY INFORMATION WITHHELD PER 10CFR2.390]



Table 5.3.2 (continued)

[PROPRIETARY INFORMATION WITHHELD PER 10CFR2.390]

Table 5.3.2 (continued)

[PROPRIETARY INFORMATION WITHHELD PER 10CFR2.390]

Table 5.3.3

[PROPRIETARY INFORMATION WITHHELD PER 10CFR2.390]

Table 5.3.4

[PROPRIETARY INFORMATION WITHHELD PER 10CFR2.390]

FIGURES 5.3.1 THROUGH 5.3.12: [PROPRIETARY INFORMATION WITHHELD PER  
10CFR2.390]

## 5.4 SHIELDING EVALUATION

The MCNP-4A code[5.1.1] was used for all of the shielding analyses. MCNP is a continuous energy, three-dimensional, coupled neutron-photon-electron Monte Carlo transport code. Continuous energy cross section data is represented with sufficient energy points to permit linear-linear interpolation between these points. The individual cross section libraries used for each nuclide are those recommended by the MCNP manual. All of these data are based on ENDF/B-V data. MCNP has been extensively benchmarked against experimental data by the large user community. References [5.4.2], [5.4.3], and [5.4.4] are three examples of the benchmarking that has been performed.

The energy distribution of the source term, as described earlier, is used explicitly in the MCNP model. A different MCNP calculation is performed for each of the three source terms (neutron, decay gamma, and  $^{60}\text{Co}$ ). The axial distribution of the fuel source term is described in Table 1.2.15 and Figures 1.2.13 and 1.2.14. The PWR and BWR axial burnup distributions were obtained from References [5.4.5] and [5.4.6] respectively. These axial distributions were obtained from operating plants and are representative of PWR and BWR fuel with burnups greater than 30,000 MWD/MTU. The  $^{60}\text{Co}$  source in the hardware was assumed to be uniformly distributed over the appropriate regions. The axial distribution used for the Trojan Plant fuel was similar but not identical to the generic PWR distribution. Table 1.2.15 and Figure 1.2.13a present the axial burnup distribution used for the Trojan Plant fuel taken from the Trojan FSAR [5.1.6].

[

PROPRIETARY INFORMATION WITHHELD PER 10CFR2.390

]

MCNP was used to calculate dose at the various desired locations. MCNP calculates neutron or photon flux and these values can be converted into dose by the use of dose response functions. This is done internally in MCNP and the dose response functions are listed in the input file. The response functions used in these calculations are listed in Table 5.4.1 and were taken from ANSI/ANS 6.1.1, 1977 [5.4.1].

[

PROPRIETARY INFORMATION WITHHELD PER 10CFR2.390

]

#### 5.4.1 Streaming Through Radial Steel Fins and Pocket Trunnions

The HI-STAR 100 overpack utilizes 0.5 inch thick radial channels for structural support and cooling. The attenuation of neutrons through steel is substantially less than the attenuation of neutrons through the neutron shield. Therefore, it is possible to have neutron streaming through the channels which could result in a localized dose peak. The reverse is true for photons which would result in a localized reduction in the photon dose. Analyses were performed to determine the magnitude of the dose peaks and depressions and the impact on localized dose as compared to average total dose. This effect was evaluated at the radial surface of the HI-STAR 100 System and a distance of two meters.

In addition to the radial channels, the pocket trunnions are essentially blocks of steel that are approximately 12 inches wide and 12 inches high. The effect of the pocket trunnion on neutron streaming and photon transmission will be more substantial than the effect of a single fin. Therefore, analyses were performed to quantify this effect. Figures 5.3.7 and 5.3.8 illustrate the location of the pocket trunnion and its axial position relative to the active fuel.

The fuel loading pattern in the MPC-32, MPC-24 and the MPC-68, as depicted in Figures 5.3.1 through 5.3.3, is not cylindrical. Therefore, there is a potential to experience peaking as a result of azimuthal variations in the fuel loading. Since the MCNP models represent the fuel in the correct positions (i.e., cylindrical homogenization is not performed) the effect of azimuthal variations in the loading pattern is automatically accounted for in the calculations that are discussed below.

The effect of streaming through the pocket trunnion and the radial channels was analyzed using the full three-dimensional MCNP models of the MPC-24 and the MPC-68. The effect of peaking was calculated on the surface of the overpack adjacent to the pocket trunnion and dose locations 2a and 3a in Figures 5.1.1. The effect of peaking was also analyzed at 2 meters from the overpack at dose location 2 and at the axial height of the impact limiter. Dose location 3 was not analyzed at two meters because the dose at that point is less than the dose at location 2 as demonstrated in the tables at the end of this section. Figure 5.4.1 shows a quarter of the HI-STAR 100 overpack with 41 azimuthal bins drawn. There is one bin per steel fin and 3 bins in each neutron shield region. This azimuthal binning structure was used over the axial height of the overpack. The dose was calculated in each of these bins and then compared to the average dose calculated over the surface to determine a peak-to-average ratio for the dose in that bin. The azimuthal location of the pocket trunnion is shown in Figure 5.4.1. The pocket trunnion was modeled as solid steel. During shipping, a steel rotation trunnion or plug shall be placed in the pocket trunnion recess. To conservatively evaluate the peak to average ratio, the pocket trunnion is assumed to be solid steel.

Table 5.4.14 provides representative peak-to-average ratios that were calculated for the various dose components and locations. Table 5.4.15 presents the dose rates at the dose locations analyzed including the effect of peaking. These results can be compared with the surface average results in Tables 5.1.1, 5.1.3, 5.1.4, and 5.1.6. The peak dose on the surface of the overpack at dose location 2a occurs at a steel channel (fin). This is evident by the high neutron peaking at dose location 2a on the surface of the overpack. The dose rate at the pocket trunnion, in those overpacks containing pocket trunnions, is higher than the dose rate at dose location 2 on the surface of the overpack. However, these results clearly indicate that, at two meters, the peaking associated with the pocket trunnion is not present and that the peak dose location is #2.

The MPC-32 was not explicitly analyzed to determine peak-to-average ratios. This is acceptable because the peaking outside the HI-STAR for the MPC-32 will be similar if not smaller than in the MPC-24 due to the fact that the fuel assemblies in the MPC-24 are not as closely positioned



to each other as in the MPC-32. Section 5.5, Regulatory Compliance, presents results which take into account peaking due to radiation streaming or azimuthal variation. For the MPC-32, the peak-to-average values calculated for the MPC-24 were used.

#### 5.4.2 Damaged Fuel Post-Accident Shielding Evaluation

As discussed in Subsection 5.2.5.2, the analysis presented below, even though it is for damaged fuel, demonstrates the acceptability of transporting intact Humboldt Bay 6x6 and intact Dresden 1 6x6 fuel assemblies. As discussed in Subsection 5.2.8, the Trojan damaged fuel and fuel debris were not explicitly analyzed because they are bounded by the intact fuel assemblies.

For the damaged fuel and fuel debris accident condition, it is conservatively assumed the damaged fuel cladding ruptures and all the fuel pellets fall and collect at the bottom of the damaged fuel container. The inner dimension of the damaged fuel container, specified in the Design Drawings of Section 1.4, and the design basis damaged fuel and fuel debris assembly dimensions in Table 5.2.2 are used to calculate the axial height of the rubble in the damaged fuel container assuming 50% compaction. Neglecting the fuel pellet to cladding inner diameter gap, the volume of cladding and fuel pellets available for deposit is calculated assuming the fuel rods are solid. Using the volume in conjunction with the damaged fuel container, the axial height of rubble is calculated to be 80 inches.

Some of the 6x6 assemblies described in Table 5.2.2 were manufactured with Inconel grid spacers (the mass of inconel is listed in Table 5.2.2). The calculated  $^{60}\text{Co}$  activity from these spacers was 66.7 curies for a burnup of 30,000 MWD/MTU and a cooling time of 18 years. Including this source with the total fuel gamma source for damaged fuel in Table 5.2.6 and dividing by the 80 inch rubble height provides a gamma source per inch of  $3.47\text{E}+12$  photon/s. Dividing the total neutron source for damaged fuel in Table 5.2.14 by 80 inches provides a neutron source per inch of  $5.24\text{E}+5$  neutron/s. These values are both bounded by the BWR design basis fuel gamma source per inch and neutron source per inch values of  $5.03\text{E}+12$  photon/s and  $6.63\text{E}+5$  neutron/s. These BWR design basis values were calculated by dividing the total source strengths as calculated from Tables 5.2.5 and 5.2.13 (39,500 MWD/MTU and 14 year cooling values) by the active fuel length of 144 inches. Additionally, a separate analysis added the calculated  $^{60}\text{Co}$  activity from the Inconel grid spacers to the 1.0 to 1.5 MeV energy range of the gamma source rather than to the total of the fuel gamma source. While the gamma source in the 1.0 to 1.5 MeV range is not bounded, the resulting dose rate is still below the limit, since the contribution from the other energy ranges are lower. The resulting side dose rates from the damaged fuel assemblies are approximately 20 to 25% lower than the side dose rates from the design basis BWR intact fuel assemblies. Therefore, the design basis damaged fuel assembly is bounded by the design basis intact BWR fuel assembly for accident conditions. No explicit analysis of the damaged fuel dose rates are provided as they are bounded by the intact fuel analysis.

### 5.4.3 Mixed Oxide Fuel Evaluation

The source terms calculated for the Dresden Unit 1 GE 6x6 MOX fuel assemblies can be compared to the design basis source terms for the BWR assemblies which demonstrates that the MOX fuel source terms are bounded by the design basis source terms and no additional shielding analysis is needed.

Since the active fuel length of the MOX fuel assemblies is shorter than the active fuel length of the design basis fuel, the source terms must be compared on a per inch basis. Including the  $^{60}\text{Co}$  source from grid spacers as calculated in the previous subsection (66.7 curies) with the total fuel gamma source for the MOX fuel in Table 5.2.16 and dividing by the 110 inch active fuel height provides a gamma source per inch of  $2.41\text{E}+12$  photons/s. Dividing the total neutron source for the MOX fuel assemblies in Table 5.2.17 by 110 inches provides a neutron source strength per inch of  $3.67\text{E}+5$  neutrons/s. These values are both bounded by the BWR design basis fuel gamma source per inch and neutron source per inch values of  $5.03\text{E}+12$  photons/s and  $6.63\text{E}+5$  neutrons/s. These BWR design basis values were calculated by dividing the total source strengths as calculated from Tables 5.2.5 and 5.2.13 (39,500 MWD/MTU and 14 year cooling values) by the active fuel length of 144 inches. This comparison shows that the MOX fuel source terms are bound by the design basis source terms. Therefore, no explicit analysis of dose rates is provided for MOX fuel.

Since the MOX fuel assemblies are Dresden Unit 1 6x6 assemblies, they can also be considered as damaged fuel. Using the same methodology as described in Subsection 5.4.2, the source term for the MOX fuel is calculated on a per inch basis assuming a post-accident rubble height of 80 inches. The resulting gamma and neutron source strengths are  $3.31\text{E}+12$  photons/s and  $5.05\text{E}+5$  neutrons/s. These values are also bounded by the design basis fuel gamma source per inch and neutron source per inch. Therefore, no explicit analysis of dose rates is provided for MOX fuel in a post-accident configuration.

### 5.4.4 Stainless Steel Clad Fuel Evaluation

Tables 5.4.22 through 5.4.24 present the dose rates from the stainless steel clad fuel at various dose locations around the HI-STAR 100 overpack for the MPC-24 and the MPC-68 for normal and hypothetical accident conditions. These dose rates are below the regulatory limits indicating that these fuel assemblies are acceptable for transport.

As described in Subsection 5.2.3, the source term for the stainless steel fuel was calculated conservatively with an artificial active fuel length of 144 inches. The end fitting masses of the stainless steel clad fuel are also assumed to be identical to the end fitting masses of the zircaloy clad fuel. In addition, the fuel assembly configuration used in the MCNP calculations was identical to the configuration used for the design basis fuel assemblies as described in Table 5.3.1.

#### 5.4.5 Dresden Unit 1 Antimony-Beryllium Neutron Sources

Dresden Unit 1 has antimony-beryllium neutron sources which are placed in the water rod location of their fuel assemblies. These sources are steel rods which contain a cylindrical antimony-beryllium source which is 77.25 inches in length. The steel rod is approximately 95 inches in length. Information obtained from Dresden Unit 1 characterizes these sources in the following manner: "About one-quarter pound of beryllium will be employed as a special neutron source material. The beryllium produces neutrons upon gamma irradiation. The gamma rays for the source at initial start-up will be provided by neutron-activated antimony (about 865 curies). The source strength is approximately  $1\text{E}+8$  neutrons/second."

As stated above, beryllium produces neutrons through gamma irradiation and in this particular case antimony is used as the gamma source. The threshold gamma energy for producing neutrons from beryllium is 1.666 MeV. The outgoing neutron energy increases as the incident gamma energy increases. Sb-124, which decays by Beta decay with a half life of 60.2 days, produces a gamma of energy 1.69 MeV which is just energetic enough to produce a neutron from beryllium. Approximately 54% of the Beta decays for Sb-124 produce gammas with energies greater than or equal to 1.69 MeV. Therefore, the neutron production rate in the neutron source can be specified as  $5.8\text{E}-6$  neutrons per gamma ( $1\text{E}+8/865/3.7\text{E}+10/0.54$ ) with energy greater than 1.666 MeV or  $1.16\text{E}+5$  neutrons/curie ( $1\text{E}+8/865$ ) of Sb-124.

With the short half life of 60.2 days all of the initial Sb-124 is decayed and any Sb-124 that was produced while the neutron source was in the reactor is also decayed since these neutron sources are assumed to have the same minimum cooling time as the Dresden 1 fuel assemblies (array classes 6x6A, 6x6B, 6x6C, and 8x8A) of 18 years. Therefore, there are only two possible gamma sources which can produce neutrons from this antimony-beryllium source. The first is the gammas from the decay of fission products in the fuel assemblies in the MPC. The second gamma source is from Sb-124 which is being produced in the MPC from neutron activation from neutrons from the decay of fission products.

MCNP calculations were performed to determine the gamma source as a result of decay gammas from fuel assemblies and Sb-124 activation. The calculations explicitly modeled the 6x6 fuel assembly described in Table 5.2.2. A single fuel rod was removed and replaced by a guide tube. In order to determine the amount of Sb-124 that is being activated from neutrons in the MPC it was necessary to estimate the amount of antimony in the neutron source. The O.D. of the source was assumed to be the I.D. of the steel rod encasing the source (0.345 in.). The length of the source is 77.25 inches. The beryllium is assumed to be annular in shape encompassing the antimony. Using the assumed O.D. of the beryllium and the mass and length, the I.D. of the beryllium was calculated to be 0.24 inches. The antimony is assumed to be a solid cylinder with an O.D. equal to the I.D. of the beryllium. These assumptions are conservative since the antimony and beryllium are probably encased in another material which would reduce the mass

of antimony. A larger mass of antimony is conservative since the calculated activity of Sb-124 is directly proportional to the initial mass of antimony.

The number of gammas from fuel assemblies with energies greater than 1.666 MeV entering the 77.25 inch long neutron source was calculated to be  $1.04\text{E}+8$  gammas/sec which would produce a neutron source of 603.2 neutrons/sec ( $1.04\text{E}+8 * 5.8\text{E}-6$ ). The steady state amount of Sb-124 activated in the antimony was calculated to be 39.9 curies. This activity level would produce a neutron source of  $4.63\text{E}+6$  neutrons/sec ( $39.9 * 1.16\text{E}+5$ ) or  $6.0\text{E}+4$  neutrons/sec/inch ( $4.63\text{E}+6/77.25$ ). These calculations conservatively neglect the reduction in antimony and beryllium which would have occurred while the neutron sources were in the core and being irradiated at full reactor power.

Since this is a localized source (77.25 inches in length) it is appropriate to compare the neutron source per inch from the design basis Dresden Unit 1 fuel assembly, 6x6, containing an Sb-Be neutron source to the design basis fuel neutron source per inch. This comparison, presented in Table 5.4.25, demonstrates that a Dresden Unit 1 fuel assembly containing an Sb-Be neutron source is bounded by the design basis fuel.

As stated above, the Sb-Be source is encased in a steel rod. Therefore, the gamma source from the activation of the steel was considered assuming a burnup of 120,000 MWD/MTU which is the maximum burnup assuming the Sb-Be source was in the reactor for the entire 18 year life of Dresden Unit 1. The cooling time assumed was 18 years which is the minimum cooling time for Dresden Unit 1 fuel. The source from the steel was bounded by the design basis fuel assembly. In conclusion, transport of a Dresden Unit 1 Sb-Be neutron source in a Dresden Unit 1 fuel assembly is acceptable and bounded by the current analysis.

#### 5.4.6 Thoria Rod Canister

Based on a comparison of the gamma spectra from Tables 5.2.30 and 5.2.6 for the thoria rod canister and design basis 6x6 fuel assembly, respectively, it is difficult to determine if the thoria rods will be bounded by the 6x6 fuel assemblies. However, it is obvious that the neutron spectra from the 6x6, Table 5.2.14, bounds the thoria rod neutron spectra, Table 5.2.31, with a significant margin. In order to demonstrate that the gamma spectrum from the single thoria rod canister is bounded by the gamma spectrum from the design basis 6x6 fuel assembly, the gamma dose rate on the outer radial surface of the overpack was estimated conservatively assuming an MPC full of thoria rod canisters. This gamma dose rate was compared to an estimate of the dose rate from an MPC full of design basis 6x6 fuel assemblies. The gamma dose rate from the 6x6 fuel was higher than the dose rate from an MPC full of thoria rod canisters. This in conjunction with the significant margin in neutron spectrum and the fact that there is only one thoria rod canister clearly demonstrates that the thoria rod canister is acceptable for transport in the MPC-68 or the MPC-68F.

#### 5.4.7 Trojan Fuel Contents

Tables 5.4.26 through 5.4.28 present the results for the Trojan MPC-24E for normal surface and 2 meter as well as accident results. These results are presented for a single burnup and cooling time of 42,000 MWD/MTU and 16 year cooling. This burnup and cooling time combination is shown in Tables 5.2.33 through 5.2.35 to bound the other allowable burnup and cooling time combinations for Trojan fuel. Since the Trojan MPCs will contain BPRAs, RCCAs, and TPDs, the source from these devices was considered in the analysis. The source from BPRAs and TPDs were added to the fuel source in the appropriate location. The mass from these devices was conservatively neglected. Separate calculations were performed for the BPRAs and the TPDs since both devices can not be present in the same fuel assembly. The results presented in Tables 5.4.26 through 5.4.28 represent the configuration (fuel plus non-fuel hardware: BPRa or TPD) that produces the highest dose rate at that location. Separate results for the different non-fuel hardware are not provided. Separate MCNP calculations were performed for the consideration of the RCCAs since this source is localized at the bottom of the MPC. The results for the RCCAs indicate that the presence of RCCAs will increase the dose rate on the surface of the overpack by a maximum of 1.3 mrem/hr and the dose rate at 2 meters will increase by a maximum of 0.09 mrem/hr for normal conditions. During accident conditions the dose rate will increase by a maximum of 6 mrem/hr with the presence of RCCAs.

These dose rates are less than the regulatory limits and therefore the Trojan contents are approved for transportation.

#### 5.4.8 Trojan Antimony-Beryllium Neutron Sources

The analysis of the Trojan secondary antimony-beryllium neutron sources was performed in a manner very similar to that described above in Subsection 5.4.5. The secondary sources are basically BPRAs with four rods containing the antimony-beryllium with a length of 88 inches in each rod. As mentioned in Subsection 5.4.5, the antimony-beryllium source is a regenerative source in which the antimony is activated and the gammas released from the antimony induce a gamma,n reaction in the beryllium.

The steady state production of neutrons from this antimony-beryllium source was conservatively calculated in the MPC using an approach very similar to that described in Subsection 5.4.5. The depletion of antimony from the operation in the reactor core was conservatively neglected in the analysis. MCNP calculations were performed with explicitly modeled fuel assemblies in a Trojan MPC model to calculate the steady state activity of Sb-124 in the antimony-beryllium source due to the neutrons from the spent fuel. This activity level was used in a subsequent MCNP calculation to determine the gamma,n reaction rate in the beryllium. The gamma,n cross section for beryllium, which exhibits peaks at  $1.5\text{E-}3$  with lows at approximately  $0.3\text{E-}3$  barns, was used in MCNP as a reaction rate multiplier for the flux tallies. Additionally, the gamma,n reaction rate due to gammas from the spent fuel was determined. In the latter case, gammas from the spent

fuel with energies up to 11 MeV were considered in the analysis compared to an upper limit of 3 MeV for the cask dose rate analysis. Finally, the gamma,n reaction rate was converted to neutrons/sec to yield the neutron source per secondary source assembly. In this conversion process the spectrum of neutrons emitted from the Sb-Be source was determined based on the energy spectrum of the gammas reacting in the beryllium [5.4.7]. The neutron source strength per secondary source assembly was calculated to be  $9.9\text{E}+5$  neutrons/sec with more than 99% of these having an upper energy of 0.03 MeV. The remaining 1% of the secondary source neutrons had energies up to 0.74 MeV. This is a conservative estimate of the neutrons/sec from the secondary source because it neglects depletion of the antimony that has occurred during core operation and it assumes that all assemblies in the MPC are design basis Trojan fuel assemblies.

In order to determine the impact of the secondary neutron sources on the dose rates, MCNP calculations were performed. Since the dose rate that is closest to the regulatory limit is at 2 meters from the overpack, this was the only location considered in the analysis. Rather than calculate the average dose rate around the overpack at the 2 meter location, the dose rate was calculated for a specific location. Figure 5.4.2 shows the location where the dose rate was calculated. This location (an 8.2 inch diameter cylinder) is at 2 meters from the transport vehicle on a line drawn from the center of the MPC through the center of a corner assembly. The dose rate in this cylinder was calculated using the same axial segmentation as in the design basis calculations. In this analysis, the corner assembly was the only assembly considered to have the secondary source assembly. This choice of assembly position and dose location bounds all other possible locations for the single Trojan secondary source assembly permitted in any MPC.

The dose rates were calculated for the following combinations of fuel assemblies and non-fuel hardware inserts. In all dose rate calculations, both the neutron and gamma source from the secondary sources was considered.

1. One fuel assembly with secondary source assembly from cycles 1-4 and the remaining 23 fuel assemblies with BPRAs.
2. One fuel assembly with secondary source assembly from cycles 1-4 and the remaining 23 fuel assemblies with TPDs.
3. One fuel assembly with secondary source assembly from cycles 4-14 and the remaining 23 fuel assemblies with BPRAs.
4. One fuel assembly with secondary source assembly from cycles 4-14 and the remaining 23 fuel assemblies with TPDs.

The worst case dose rate from the configurations listed above was less than 9.8 mrem/hr from configuration 4. This value was conservatively calculated assuming all fuel assemblies were identical design basis Trojan fuel assemblies with design basis Trojan non-fuel hardware. This dose rate is slightly higher than the design basis dose rates for the Trojan fuel. However, this value is still below the regulatory limit of 10.0 mrem/hr. Therefore, the insertion of a single secondary source assembly into a Trojan MPC is acceptable for transport.

#### 5.4.9 MPC-32 with Non-Fuel Hardware

As discussed in Section 5.2.4, non-fuel hardware devices in the form of BPRAs, TPDs, and RCCAs are permitted for transport, integral with a PWR fuel assembly, in the HI-STAR 100 System. Since each of these devices occupy the same location within an assembly (i.e., the guide tubes), only one of these devices will be present in a given assembly.<sup>1</sup> ITTRs, which are installed after core discharge and do not contain radioactive material, may also be stored in the assembly. BPRAs, TPDs, and ITTRs are authorized for unrestricted storage in an MPC. The RCCAs are restricted to the inner-region cells in an MPC-32. The calculation of the source term and a description of the bounding fuel devices are provided in Section 5.2.4.

In shielding analysis of non-fuel hardware devices, conservatively it is assumed each inner-region cell has BPRA, TPD and RCCA, and each outer-region cell has both BPRA and TPD. It is conservative since a fuel assembly cannot have all these two or three non-fuel hardware devices at the same time. The permissible cells for non-fuel hardware devices are provided in Table 1.2.27. Also, it is assumed that calculations are only performed for the MPC-32 design basis zircaloy clad fuel with non-zircaloy incore spacers. This fuel bounds the fuel with zircaloy incore spacers, from shielding perspective, for the same burnup, cooling time and enrichment combination.

Table 5.4.35 and Table 5.4.36 provide, respectively, the surface and 2-meter dose rates at various locations of HI-STAR 100 with MPC-32 for normal conditions. Table 5.4.37 provides the 1-meter dose rates at various locations of HI-STAR 100 with MPC-32 for accident conditions.

---

<sup>1</sup> As it is stated in Section 5.0, some types of BPRAs may have thimble plug rodlets in the locations without a full-length rod.

Table 5.4.1

FLUX-TO-DOSE CONVERSION FACTORS  
(FROM [5.4.1])

<b>Gamma Energy (MeV)</b>	<b>(rem/hr)/(photon/cm<sup>2</sup>-s)</b>
0.01	3.96E-06
0.03	5.82E-07
0.05	2.90E-07
0.07	2.58E-07
0.1	2.83E-07
0.15	3.79E-07
0.2	5.01E-07
0.25	6.31E-07
0.3	7.59E-07
0.35	8.78E-07
0.4	9.85E-07
0.45	1.08E-06
0.5	1.17E-06
0.55	1.27E-06
0.6	1.36E-06
0.65	1.44E-06
0.7	1.52E-06
0.8	1.68E-06
1.0	1.98E-06
1.4	2.51E-06
1.8	2.99E-06
2.2	3.42E-06



Table 5.4.1 (continued)

FLUX-TO-DOSE CONVERSION FACTORS  
(FROM [5.4.1])

<b>Gamma Energy (MeV)</b>	<b>(rem/hr)/(photon/cm<sup>2</sup>-s)</b>
2.6	3.82E-06
2.8	4.01E-06
3.25	4.41E-06
3.75	4.83E-06
4.25	5.23E-06
4.75	5.60E-06
5.0	5.80E-06
5.25	6.01E-06
5.75	6.37E-06
6.25	6.74E-06
6.75	7.11E-06
7.5	7.66E-06
9.0	8.77E-06
11.0	1.03E-05
13.0	1.18E-05
15.0	1.33E-05

Table 5.4.1 (continued)

FLUX-TO-DOSE CONVERSION FACTORS  
(FROM [5.4.1])

Neutron Energy (MeV)	Quality Factor	(rem/hr)/(n/cm <sup>2</sup> -s) <sup>†</sup>
2.5E-8	2.0	3.67E-6
1.0E-7	2.0	3.67E-6
1.0E-6	2.0	4.46E-6
1.0E-5	2.0	4.54E-6
1.0E-4	2.0	4.18E-6
1.0E-3	2.0	3.76E-6
1.0E-2	2.5	3.56E-6
0.1	7.5	2.17E-5
0.5	11.0	9.26E-5
1.0	11.0	1.32E-4
2.5	9.0	1.25E-4
5.0	8.0	1.56E-4
7.0	7.0	1.47E-4
10.0	6.5	1.47E-4
14.0	7.5	2.08E-4
20.0	8.0	2.27E-4

---

<sup>†</sup> Includes the Quality Factor.

Table 5.4.2

DELETED

Table 5.4.3

DELETED

Table 5.4.4

DELETED

Table 5.4.5

DELETED

Table 5.4.6

DELETED

Table 5.4.7

DELETED



Table 5.4.8

TOTAL DOSE RATES  
DOSE LOCATION ON THE SURFACE OF THE HI-STAR 100 SYSTEM FOR NORMAL CONDITIONS  
MPC-24 DESIGN BASIS ZIRCALOY CLAD FUEL WITH ZIRCALOY INCORE SPACERS  
AT VARYING BURNUPS AND COOLING TIMES

<b>Dose Point<sup>†</sup> Location</b>	<b>24,500 MWD/MTU 6 Year Cooling (mrem/hr)</b>	<b>29,500 MWD/MTU 7 Year Cooling (mrem/hr)</b>	<b>34,500 MWD/MTU 9 Year Cooling (mrem/hr)</b>	<b>39,500 MWD/MTU 11 Year Cooling (mrem/hr)</b>	<b>44,500 MWD/MTU 14 Year Cooling (mrem/hr)</b>
2a	49.81	50.88	46.38	43.02	46.19
3a	95.80	108.16	113.72	124.43	138.47
1	35.33	37.42	36.18	35.89	34.85
2	29.01	28.87	26.11	26.57	28.24
3	27.02	29.30	29.26	29.94	30.19
4	23.73	26.05	26.43	27.40	28.05
5	1.00	1.64	2.41	3.22	4.15
6	125.44	127.01	114.18	104.20	90.02
10CFR71.47 Limit	1000.00 (2a,3a) 200.00 (1-6)	1000.00 (2a,3a) 200.00 (1-6)	1000.00 (2a,3a) 200.00 (1-6)	1000.00 (2a,3a) 200.00 (1-6)	1000.00 (2a,3a) 200.00 (1-6)

<sup>†</sup> Refer to Figure 5.1.1.

Table 5.4.9

TOTAL DOSE RATES  
DOSE LOCATION ON THE SURFACE OF THE HI-STAR 100 SYSTEM FOR NORMAL CONDITIONS  
MPC-68 DESIGN BASIS ZIRCALOY CLAD FUEL AT VARYING BURNUPS AND COOLING TIMES

<b>Dose Point<sup>†</sup> Location</b>	<b>10,000 MWD/MTU 5 Year Cooling (mrem/hr)</b>	<b>20,000 MWD/MTU 7 Year Cooling (mrem/hr)</b>	<b>24,500 MWD/MTU 8 Year Cooling (mrem/hr)</b>	<b>29,500 MWD/MTU 9 Year Cooling (mrem/hr)</b>	<b>34,500 MWD/MTU 11 Year Cooling (mrem/hr)</b>	<b>39,500 MWD/MTU 14 Year Cooling (mrem/hr)</b>	<b>44,500 MWD/MTU 19 Year Cooling (mrem/hr)</b>
2a	49.51	52.69	44.53	44.60	50.12	52.65	55.25
3a	139.50	154.42	132.09	129.62	132.20	115.66	103.70
1	34.25	39.29	34.23	35.33	37.96	35.72	33.64
2	25.50	27.53	24.21	27.97	31.12	32.05	33.07
3	34.44	37.75	32.25	31.43	31.69	27.33	22.81
4	32.63	35.76	30.52	29.69	29.91	25.74	21.42
5	0.14	0.60	0.64	1.03	1.58	2.01	2.53
6	112.26	121.21	103.06	98.97	97.96	82.26	65.73
10CFR71.47 Limit	1000.00 (2a,3a) 200.00 (1-6)	1000.00 (2a,3a) 200.00 (1-6)	1000.00 (2a,3a) 200.00 (1-6)	1000.00 (2a,3a) 200.00 (1-6)	1000.00 (2a,3a) 200.00 (1-6)	1000.00 (2a,3a) 200.00 (1-6)	1000.00 (2a,3a) 200.00 (1-6)

<sup>†</sup> Refer to Figure 5.1.1.

Table 5.4.10

TOTAL DOSE RATES  
DOSE LOCATION AT TWO METERS FOR NORMAL CONDITIONS  
MPC-24 DESIGN BASIS ZIRCALOY CLAD FUEL WITH ZIRCALOY INCORE SPACERS  
AT VARYING BURNUPS AND COOLING TIMES

<b>Dose Point<sup>†</sup> Location</b>	<b>24,500 MWD/MTU 6 Year Cooling (mrem/hr)</b>	<b>29,500 MWD/MTU 7 Year Cooling (mrem/hr)</b>	<b>34,500 MWD/MTU 9 Year Cooling (mrem/hr)</b>	<b>39,500 MWD/MTU 11 Year Cooling (mrem/hr)</b>	<b>44,500 MWD/MTU 14 Year Cooling (mrem/hr)</b>
1	7.41	7.61	7.26	7.31	7.27
2	9.57	9.45	8.77	8.95	9.10
3	6.72	6.93	6.61	6.64	6.59
4	6.16	6.39	6.13	6.16	6.11
5	0.09	0.15	0.21	0.28	0.35
6	8.39	8.34	7.26	6.36	5.15
10CFR71.47 Limit	10.00	10.00	10.00	10.00	10.00

---

<sup>†</sup> Refer to Figure 5.1.1.

Table 5.4.11

TOTAL DOSE RATES  
DOSE LOCATION AT TWO METERS FOR NORMAL CONDITIONS  
MPC-68 DESIGN BASIS ZIRCALOY CLAD FUEL AT VARYING BURNUPS AND COOLING TIMES

<b>Dose Point<sup>†</sup> Location</b>	<b>10,000 MWD/MTU 5 Year Cooling (mrem/hr)</b>	<b>20,000 MWD/MTU 7 Year Cooling (mrem/hr)</b>	<b>24,500 MWD/MTU 8 Year Cooling (mrem/hr)</b>	<b>29,500 MWD/MTU 9 Year Cooling (mrem/hr)</b>	<b>34,500 MWD/MTU 11 Year Cooling (mrem/hr)</b>	<b>39,500 MWD/MTU 14 Year Cooling (mrem/hr)</b>	<b>44,500 MWD/MTU 19 Year Cooling (mrem/hr)</b>
1	6.67	7.33	6.58	7.05	7.59	7.34	7.07
2	8.32	8.71	8.03	8.94	9.62	9.55	9.39
3	6.66	7.20	6.31	6.44	6.62	6.02	5.36
4	6.43	6.98	6.09	6.15	6.32	5.70	5.03
5	0.02	0.06	0.07	0.10	0.15	0.19	0.24
6	6.55	6.85	5.77	5.34	5.01	3.87	2.65
10CFR71.47 Limit	10.00	10.00	10.00	10.00	10.00	10.00	10.00

<sup>†</sup> Refer to Figure 5.1.1.

Table 5.4.12

TOTAL DOSE RATES  
DOSE LOCATION AT ONE METER FOR ACCIDENT CONDITIONS  
MPC-24 DESIGN BASIS ZIRCALOY CLAD FUEL WITH ZIRCALOY INCORE SPACERS  
AT VARYING BURNUPS AND COOLING TIMES

<b>Dose Point<sup>†</sup> Location</b>	<b>24,500 MWD/MTU 6 Year Cooling (mrem/hr)</b>	<b>29,500 MWD/MTU 7 Year Cooling (mrem/hr)</b>	<b>34,500 MWD/MTU 9 Year Cooling (mrem/hr)</b>	<b>39,500 MWD/MTU 11 Year Cooling (mrem/hr)</b>	<b>44,500 MWD/MTU 14 Year Cooling (mrem/hr)</b>
1	76.55	97.55	117.95	141.21	166.93
2	153.26	224.23	307.31	399.33	504.35
3	49.37	64.41	79.67	96.85	116.00
4	35.97	47.12	58.44	71.10	85.20
5	4.06	6.59	9.62	12.83	16.51
6	685.36	687.08	605.96	539.45	447.78
10CFR71.51 Limit	1000.00	1000.00	1000.00	1000.00	1000.00

<sup>†</sup> Refer to Figure 5.1.2.

Table 5.4.13

TOTAL DOSE RATES  
DOSE LOCATION AT ONE METER FOR ACCIDENT CONDITIONS  
MPC-68 DESIGN BASIS ZIRCALOY CLAD FUEL AT VARYING BURNUPS AND COOLING TIMES

<b>Dose Point<sup>†</sup> Location</b>	<b>10,000 MWD/MTU 5 Year Cooling (mrem/hr)</b>	<b>20,000 MWD/MTU 7 Year Cooling (mrem/hr)</b>	<b>24,500 MWD/MTU 8 Year Cooling (mrem/hr)</b>	<b>29,500 MWD/MTU 9 Year Cooling (mrem/hr)</b>	<b>34,500 MWD/MTU 11 Year Cooling (mrem/hr)</b>	<b>39,500 MWD/MTU 14 Year Cooling (mrem/hr)</b>	<b>44,500 MWD/MTU 19 Year Cooling (mrem/hr)</b>
1	51.38	86.18	82.43	108.56	145.23	169.25	198.52
2	62.71	172.74	179.75	275.87	403.87	504.00	622.86
3	31.39	49.39	46.51	59.30	77.64	88.84	102.65
4	26.31	39.33	36.57	45.32	58.13	65.34	74.36
5	0.66	2.70	2.84	4.55	6.92	8.80	11.04
6	629.12	668.09	564.75	530.59	509.65	408.69	300.71
10CFR71.51 Limit	1000.00	1000.00	1000.00	1000.00	1000.00	1000.00	1000.00

<sup>†</sup> Refer to Figure 5.1.2.

Table 5.4.14

PEAK-TO-AVERAGE RATIOS FOR THE DOSE COMPONENTS  
AT VARIOUS LOCATIONS

Location	Fuel Gammas	Gammas from Neutrons	<sup>60</sup> Co Gammas	Neutron
<b>MPC-24</b>				
Surface				
Pocket Trunnion	0.081	0.262	0.075	6.695
2a	0.713	0.955	0.407	2.362
3a	1.317	1.011	1.005	1.177
2 meter				
Pocket Trunnion	1.109	1.232	1.059	0.809
2	1.034	0.974	1.086	0.990
<b>MPC-68</b>				
Surface				
Pocket Trunnion	0.070	0.432	0.074	7.340
2a	0.737	0.977	1.123	2.284
3a	0.908	0.816	1.217	0.940
2 meter				
Pocket Trunnion	1.121	0.982	1.144	1.171
2	1.070	0.939	1.146	0.950

Table 5.4.15

DOSE RATES FOR NORMAL CONDITIONS SHOWING THE  
EFFECT OF PEAKING

<b>Dose Point<sup>†</sup> Location</b>	<b>Fuel Gammas (mrem/hr)</b>	<b>Gammas from Neutrons (mrem/hr)</b>	<b><sup>60</sup>Co Gammas (mrem/hr)</b>	<b>Neutrons (mrem/hr)</b>	<b>Total (mrem/hr)</b>
<b>MPC-24</b>					
Surface 44,500 MWD/MTU 14-Year Cooling					
Pocket Trunnion	0.15	0.37	1.98	97.92	100.42
2a	12.30	6.35	0.00	52.60	71.26
3a	0.40	0.67	28.67	128.27	158.01
2 meter 24,500 MWD/MTU 6-Year Cooling					
Pocket Trunnion	4.03	0.17	3.50	0.64	8.34
2	7.55	0.21	1.26	0.87	9.90
<b>MPC-68</b>					
Surface 34,500 MWD/MTU 11-Year Cooling					
Pocket Trunnion	0.25	0.45	1.97	77.42	80.09
2a	19.24	5.35	0.02	42.33	66.93
3a	0.33	0.12	115.34	34.69	150.49
2 meter 34,500 MWD/MTU 11-Year Cooling					
Pocket Trunnion	3.23	0.46	2.06	3.03	8.77
2	5.80	0.68	0.74	2.69	9.91

---

<sup>†</sup> Refer to Figure 5.1.1.



Table 5.4.16

DELETED

Table 5.4.17

DELETED

Table 5.4.18

DELETED

Table 5.4.19

TOTAL DOSE RATES  
DOSE LOCATION ON THE SURFACE OF THE HI-STAR 100 SYSTEM FOR NORMAL CONDITIONS  
MPC-24 DESIGN BASIS ZIRCALOY CLAD FUEL WITH NON-ZIRCALOY INCORE SPACERS  
AT VARYING BURNUPS AND COOLING TIMES

<b>Dose Point<sup>†</sup> Location</b>	<b>24,500 MWD/MTU 9 Year Cooling (mrem/hr)</b>	<b>29,500 MWD/MTU 11 Year Cooling (mrem/hr)</b>	<b>34,500 MWD/MTU 13 Year Cooling (mrem/hr)</b>	<b>39,500 MWD/MTU 15 Year Cooling (mrem/hr)</b>	<b>44,500 MWD/MTU 18 Year Cooling (mrem/hr)</b>
2a	42.91	42.11	43.11	45.08	46.24
3a	69.70	74.06	83.00	96.79	111.87
1	25.77	25.19	25.54	26.31	26.75
2	26.97	26.54	27.34	28.35	28.62
3	19.70	19.86	20.87	22.23	23.47
4	17.23	17.64	18.84	20.37	21.85
5	0.89	1.40	2.07	2.77	3.58
6	87.60	80.03	74.35	69.97	63.35
10CFR71.47 Limit	1000.00 (2a,3a) 200.00 (1-6)	1000.00 (2a,3a) 200.00 (1-6)	1000.00 (2a,3a) 200.00 (1-6)	1000.00 (2a,3a) 200.00 (1-6)	1000.00 (2a,3a) 200.00 (1-6)

<sup>†</sup> Refer to Figure 5.1.1.

Table 5.4.20

TOTAL DOSE RATES  
DOSE LOCATION AT TWO METERS FOR NORMAL CONDITIONS  
MPC-24 DESIGN BASIS ZIRCALOY CLAD FUEL WITH NON-ZIRCALOY INCORE SPACERS  
AT VARYING BURNUPS AND COOLING TIMES

<b>Dose Point<sup>†</sup> Location</b>	<b>24,500 MWD/MTU 9 Year Cooling (mrem/hr)</b>	<b>29,500 MWD/MTU 11 Year Cooling (mrem/hr)</b>	<b>34,500 MWD/MTU 13 Year Cooling (mrem/hr)</b>	<b>39,500 MWD/MTU 15 Year Cooling (mrem/hr)</b>	<b>44,500 MWD/MTU 18 Year Cooling (mrem/hr)</b>
1	6.42	6.24	6.29	6.42	6.40
2	9.51	9.16	9.18	9.27	9.09
3	5.68	5.52	5.58	5.70	5.71
4	5.08	4.96	5.03	5.16	5.19
5	0.08	0.12	0.18	0.24	0.30
6	5.84	5.19	4.62	4.13	3.47
10CFR71.47 Limit	10.00	10.00	10.00	10.00	10.00

---

<sup>†</sup> Refer to Figure 5.1.1.

Table 5.4.21

TOTAL DOSE RATES  
DOSE LOCATION AT ONE METER FOR ACCIDENT CONDITIONS  
MPC-24 DESIGN BASIS ZIRCALOY CLAD FUEL WITH NON-ZIRCALOY INCORE SPACERS  
AT VARYING BURNUPS AND COOLING TIMES

<b>Dose Point<sup>†</sup> Location</b>	<b>24,500 MWD/MTU 9 Year Cooling (mrem/hr)</b>	<b>29,500 MWD/MTU 11 Year Cooling (mrem/hr)</b>	<b>34,500 MWD/MTU 13 Year Cooling (mrem/hr)</b>	<b>39,500 MWD/MTU 15 Year Cooling (mrem/hr)</b>	<b>44,500 MWD/MTU 18 Year Cooling (mrem/hr)</b>
1	62.33	76.36	95.99	117.23	140.85
2	145.00	201.06	275.44	354.15	442.83
3	40.70	51.15	65.54	81.04	98.36
4	29.39	37.13	47.76	59.20	72.01
5	3.59	5.63	8.26	11.03	14.21
6	478.28	429.22	388.56	354.69	306.90
10CFR71.51 Limit	1000.00	1000.00	1000.00	1000.00	1000.00

---

<sup>†</sup> Refer to Figure 5.1.2.

Table 5.4.22

DOSE RATES FOR  
MPC-68 DESIGN BASIS STAINLESS STEEL CLAD FUEL  
22,500 MWD/MTU AND 16-YEAR COOLING

Dose Point <sup>†</sup> Location	Fuel Gammas <sup>††</sup> (mrem/hr)	<sup>60</sup> Co Gammas (mrem/hr)	Neutrons (mrem/hr)	Totals (mrem/hr)
<b>Dose Location at Surface for Normal Condition</b>				
1	2.91	9.19	1.00	13.09
2a	39.68	0.00	1.20	40.88
3a	0.62	40.84	2.60	44.07
4	0.45	9.49	0.53	10.47
5	0.02	0.01	0.10	0.12
6	2.37	32.43	1.37	36.18
10CFR71.47 Limit				200.00
<b>Dose Location at Two Meters for Normal Condition</b>				
1	3.45	1.00	0.17	4.63
2	7.71	0.27	0.19	8.18
3	2.26	1.35	0.12	3.73
4	1.67	1.43	0.11	3.21
5	0.00	0.00	0.01	0.01
6	0.20	1.89	0.03	2.12
10CFR71.47 Limit				10.00
<b>Dose Location at One Meter for Accident Condition</b>				
1	9.43	10.90	7.95	28.29
2	46.22	0.23	25.97	72.42
3	3.58	7.41	4.06	15.05
4	2.00	6.60	2.91	11.51
5	0.01	0.07	0.48	0.57
6	11.14	183.23	5.34	199.71
10CFR71.51 Limit				1000.00

Note: The more conservative limit of 200 mrem/hr was applied for dose locations 2a and 3a while dose locations 2 and 3 were not analyzed.

<sup>†</sup> Refer to Figures 5.1.1 and 5.1.2.

<sup>††</sup> Gammas generated by neutron capture and gammas from incore spacers are included with fuel gammas.

Table 5.4.23

DOSE RATES FOR  
MPC-24 DESIGN BASIS STAINLESS STEEL CLAD FUEL  
30,000 MWD/MTU AND 19-YEAR COOLING

<b>Dose Point<sup>†</sup> Location</b>	<b>Fuel Gammas<sup>††</sup> (mrem/hr)</b>	<b><sup>60</sup>Co Gammas (mrem/hr)</b>	<b>Neutrons (mrem/hr)</b>	<b>Totals (mrem/hr)</b>
<b>Dose Location at Surface for Normal Condition</b>				
1	2.40	5.54	4.27	12.22
2a	35.54	0.01	4.41	39.96
3a	0.66	11.31	24.60	36.57
4	0.73	3.65	4.11	8.49
5	0.12	0.01	0.82	0.94
6	4.36	22.14	6.65	33.15
10CFR71.47 Limit				200.00
<b>Dose Location at Two Meters for Normal Condition</b>				
1	3.05	0.69	0.76	4.50
2	7.23	0.23	0.83	8.29
3	2.47	0.66	0.72	3.85
4	1.95	0.67	0.69	3.30
5	0.01	0.00	0.07	0.08
6	0.30	1.53	0.25	2.08
10CFR71.47 Limit				10.00
<b>Dose Location at One Meter for Accident Condition</b>				
1	7.57	6.83	32.78	47.18
2	39.78	0.24	108.52	148.54
3	4.96	3.96	23.27	32.19
4	2.85	3.00	17.13	22.99
5	0.02	0.05	3.69	3.76
6	22.73	123.24	28.03	174.00
10CFR71.51 Limit				1000.00

Note: The more conservative limit of 200 mrem/hr was applied for dose locations 2a and 3a while dose locations 2 and 3 were not analyzed.

<sup>†</sup> Refer to Figures 5.1.1 and 5.1.2.

<sup>††</sup> Gammas generated by neutron capture and gammas from incore spacers are included with fuel gammas.



Table 5.4.24

DOSE RATES FOR  
MPC-24 DESIGN BASIS STAINLESS STEEL CLAD FUEL  
40,000 MWD/MTU AND 24-YEAR COOLING

<b>Dose Point<sup>†</sup> Location</b>	<b>Fuel Gammas<sup>††</sup> (mrem/hr)</b>	<b><sup>60</sup>Co Gammas (mrem/hr)</b>	<b>Neutrons (mrem/hr)</b>	<b>Totals (mrem/hr)</b>
<b>Dose Location at Surface for Normal Condition</b>				
1	2.12	5.80	11.10	19.02
2a	28.04	0.00	13.06	41.10
3a	0.78	11.82	63.88	76.48
4	0.66	3.82	10.68	15.16
5	0.30	0.01	2.13	2.43
6	4.44	23.15	17.25	44.84
10CFR71.47 Limit				200.00
<b>Dose Location at Two Meters for Normal Condition</b>				
1	2.55	0.72	1.98	5.26
2	5.82	0.24	2.23	8.29
3	2.06	0.69	1.86	4.62
4	1.64	0.70	1.78	4.11
5	0.02	0.00	0.19	0.21
6	0.25	1.60	0.65	2.49
10CFR71.47 Limit				10.00
<b>Dose Location at One Meter for Accident Condition</b>				
1	5.88	7.14	85.12	98.14
2	30.69	0.25	281.83	312.76
3	3.85	4.14	60.42	68.41
4	2.24	3.14	44.48	49.86
5	0.04	0.05	9.57	9.66
6	17.44	128.89	72.74	219.07
10CFR71.51 Limit				1000.00

Note: The more conservative limit of 200 mrem/hr was applied for dose locations 2a and 3a while dose locations 2 and 3 were not analyzed.

<sup>†</sup> Refer to Figures 5.1.1 and 5.1.2.

<sup>††</sup> Gammas generated by neutron capture and gammas from incore spacers are included with fuel gammas.

Table 5.4.25

COMPARISON OF NEUTRON SOURCE PER INCH PER SECOND FOR  
DESIGN BASIS 7X7 FUEL AND DESIGN BASIS DRESDEN UNIT 1 FUEL

<b>Assembly</b>	<b>Active fuel length (inch)</b>	<b>Neutrons per sec per inch</b>	<b>Neutrons per sec per inch with Sb-Be source</b>	<b>Reference for neutrons per sec per inch</b>
7x7 design basis	144	6.63E+5	N/A	Table 5.2.13 39.5 GWD/MTU and 14 year cooling
6x6 design basis	110	3.81E+5	4.41E+5	Table 5.2.14
6x6 design basis MOX	110	3.67E+5	4.27E+5	Table 5.2.17

Table 5.4.26

DOSE RATES AT THE SURFACE OF THE HI-STAR 100 SYSTEM FOR NORMAL CONDITIONS  
MPC-24 WITH TROJAN ZIRCALOY CLAD FUEL WITH NON-ZIRCALOY INCORE SPACERS  
42,000 MWD/MTU AND 16-YEAR COOLING

<b>Dose Point<sup>†</sup> Location</b>	<b>Fuel Gammas<sup>††</sup> (mrem/hr)</b>	<b>Gammas from Incore Spacers (mrem/hr)</b>	<b><sup>60</sup>Co Gammas (mrem/hr)</b>	<b>Neutrons (mrem/hr)</b>	<b>Totals (mrem/hr)</b>	<b>10 CFR 71.47 Limit</b>
2a	3.72	2.48	38.39	2.25	46.84	1000
3a	0.39	0.07	14.34	49.81	64.61	1000
1	1.62	1.09	4.54	14.43	21.68	200
2	10.94	7.72	0.05	9.69	28.40	200
3	0.62	0.32	10.66	8.00	19.60	200
4	0.36	0.16	5.01	7.80	13.34	200
5	0.36 <sup>†††</sup>	-	0.08	2.88	3.32	200
6	7.35 <sup>†††</sup>	-	22.44	21.29	51.08	200

---

<sup>†</sup> Refer to Figure 5.1.1.

<sup>††</sup> Gammas generated by neutron capture are included with fuel gammas.

<sup>†††</sup> Gammas from incore spacers are included with fuel gammas.

Table 5.4.27

DOSE RATES AT TWO METERS FROM THE HI-STAR 100 SYSTEM FOR NORMAL CONDITIONS  
MPC-24 WITH TROJAN ZIRCALOY CLAD FUEL WITH NON-ZIRCALOY INCORE SPACERS  
42,000 MWD/MTU AND 16-YEAR COOLING

<b>Dose Point<sup>†</sup> Location</b>	<b>Fuel Gammas<sup>††</sup> (mrem/hr)</b>	<b>Gammas from Incore Spacers (mrem/hr)</b>	<b><sup>60</sup>Co Gammas (mrem/hr)</b>	<b>Neutrons (mrem/hr)</b>	<b>Totals (mrem/hr)</b>
1	1.52	1.11	0.55	2.52	5.69
2	3.41	2.53	0.64	2.67	9.24
3	1.20	0.82	2.31	1.71	6.05
4	0.97	0.62	2.13	1.50	5.21
5	0.02 <sup>†††</sup>	-	0.07	0.22	0.31
6	0.62 <sup>†††</sup>	-	2.25	0.80	3.68
10CFR71.47 Limit					10.00

---

<sup>†</sup> Refer to Figure 5.1.1.

<sup>††</sup> Gammas generated by neutron capture are included with fuel gammas.

<sup>†††</sup> Gammas from incore spacers are included with fuel gammas.

Table 5.4.28

DOSE RATES AT ONE METER FOR ACCIDENT CONDITIONS  
MPC-24 WITH TROJAN ZIRCALOY CLAD FUEL WITH NON- ZIRCALOY INCORE SPACERS  
42,000 MWD/MTU AND 16-YEAR COOLING

<b>Dose Point<sup>†</sup> Location</b>	<b>Fuel Gammas<sup>††</sup> (mrem/hr)</b>	<b><sup>60</sup>Co Gammas (mrem/hr)</b>	<b>Neutrons (mrem/hr)</b>	<b>Totals (mrem/hr)</b>
1	7.01	5.69	106.18	118.88
2	31.31	0.30	356.39	387.99
3	3.27	15.94	69.43	88.64
4	1.86	8.65	49.17	59.68
5	0.11	0.25	12.42	12.78
6	34.74	128.20	82.48	245.42
10CFR71.51 Limit				1000.00

---

<sup>†</sup> Refer to Figure 5.1.2.

<sup>††</sup> Gammas generated by neutron capture and gammas from incore spacers are included with fuel gammas.

Table 5.4.29

TOTAL DOSE RATES  
DOSE LOCATION ON THE SURFACE OF THE HI-STAR 100 SYSTEM FOR NORMAL CONDITIONS  
MPC-32 DESIGN BASIS ZIRCALOY CLAD FUEL WITH ZIRCALOY INCORE SPACERS  
**WITHOUT NON-FUEL HARDWARE**  
AT VARYING BURNUPS AND COOLING TIMES

<b>Dose Point<sup>†</sup> Location</b>	<b>24,500 MWD/MTU 8 Year Cooling (mrem/hr)</b>	<b>29,500 MWD/MTU 9 Year Cooling (mrem/hr)</b>	<b>34,500 MWD/MTU 12 Year Cooling (mrem/hr)</b>	<b>39,500 MWD/MTU 14 Year Cooling (mrem/hr)</b>	<b>44,500 MWD/MTU 19 Year Cooling (mrem/hr)</b>	<b>45,000 MWD/MTU 20 Year Cooling (mrem/hr)</b>
2a	62.31	66.79	58.99	59.34	50.90	43.28
3a	162.02	192.08	205.87	245.88	263.95	133.57
1	44.46	48.87	45.01	46.94	42.51	29.92
2	34.63	38.55	36.17	38.33	35.48	26.53
3	40.30	46.47	46.08	50.81	49.68	28.44
4	37.52	43.47	43.40	48.09	47.31	27.12
5	2.24	3.70	5.26	7.06	8.46	3.72
6	149.23	154.74	128.70	122.42	95.45	68.45
10CFR71.47 Limit	1000.00 (2a,3a) 200.00 (1-6)	1000.00 (2a,3a) 200.00 (1-6)	1000.00 (2a,3a) 200.00 (1-6)	1000.00 (2a,3a) 200.00 (1-6)	1000.00 (2a,3a) 200.00 (1-6)	1000.00 (2a,3a) 200.00 (1-6)

<sup>†</sup> Refer to Figure 5.1.1.

Table 5.4.30

TOTAL DOSE RATES  
DOSE LOCATION AT TWO METERS FOR NORMAL CONDITIONS  
MPC-32 DESIGN BASIS ZIRCALOY CLAD FUEL WITH ZIRCALOY INCORE SPACERS  
**WITHOUT NON-FUEL HARDWARE**  
AT VARYING BURNUPS AND COOLING TIMES

Dose Point <sup>†</sup> Location	24,500 MWD/MTU 8 Year Cooling (mrem/hr)	29,500 MWD/MTU 9 Year Cooling (mrem/hr)	34,500 MWD/MTU 12 Year Cooling (mrem/hr)	39,500 MWD/MTU 14 Year Cooling (mrem/hr)	44,500 MWD/MTU 19 Year Cooling (mrem/hr)	45,000 MWD/MTU 20 Year Cooling (mrem/hr)
1	7.85	8.67	8.01	8.43	7.69	6.43
2	8.22	9.28	8.86	9.65	9.19	8.37
3	7.83	8.83	8.44	9.10	8.59	6.00
4	7.50	8.48	8.14	8.79	8.34	5.59
5	0.18	0.29	0.41	0.55	0.66	0.33
6	8.22	8.21	6.37	5.66	3.83	2.93
10CFR71.47 Limit	10.00	10.00	10.00	10.00	10.00	10.00

<sup>†</sup> Refer to Figure 5.1.1.

Table 5.4.31

TOTAL DOSE RATES  
DOSE LOCATION AT ONE METER FOR ACCIDENT CONDITIONS  
MPC-32 DESIGN BASIS ZIRCALOY CLAD FUEL WITH ZIRCALOY INCORE SPACERS  
**WITHOUT NON-FUEL HARDWARE**  
AT VARYING BURNUPS AND COOLING TIMES

Dose Point <sup>†</sup> Location	24,500 MWD/MTU 8 Year Cooling (mrem/hr)	29,500 MWD/MTU 9 Year Cooling (mrem/hr)	34,500 MWD/MTU 12 Year Cooling (mrem/hr)	39,500 MWD/MTU 14 Year Cooling (mrem/hr)	44,500 MWD/MTU 19 Year Cooling (mrem/hr)	45,000 MWD/MTU 20 Year Cooling (mrem/hr)
1	91.38	117.99	134.85	162.88	176.78	156.03
2	160.99	249.47	334.77	439.98	516.93	476.21
3	66.27	89.91	108.35	134.66	150.49	106.95
4	49.53	66.55	79.40	98.17	109.14	81.59
5	9.17	15.09	21.41	28.69	34.38	15.28
6	802.16	817.16	656.05	601.72	437.06	334.78
10CFR71.51 Limit	1000.00	1000.00	1000.00	1000.00	1000.00	1000.00

<sup>†</sup> Refer to Figure 5.1.2.



Table 5.4.32

TOTAL DOSE RATES  
DOSE LOCATION ON THE SURFACE OF THE HI-STAR 100 SYSTEM FOR NORMAL CONDITIONS  
MPC-32 DESIGN BASIS ZIRCALOY CLAD FUEL WITH NON-ZIRCALOY INCORE SPACERS  
**WITHOUT NON-FUEL HARDWARE**  
AT VARYING BURNUPS AND COOLING TIMES

Dose Point <sup>†</sup> Location	24,500 MWD/MTU 12 Year Cooling (mrem/hr)	29,500 MWD/MTU 14 Year Cooling (mrem/hr)	34,500 MWD/MTU 16 Year Cooling (mrem/hr)	39,500 MWD/MTU 19 Year Cooling (mrem/hr)	42,500 MWD/MTU 20 Year Cooling (mrem/hr)	<b>45,000 MWD/MTU 24 Year Cooling (mrem/hr)</b>
2a	40.66	40.41	42.78	42.27	44.54	<b>41.20</b>
3a	110.58	127.81	162.16	189.57	213.21	<b>109.08</b>
1	29.82	30.69	32.88	33.09	35.33	<b>23.43</b>
2	24.88	25.46	27.44	27.93	29.93	<b>25.41</b>
3	27.57	30.30	34.70	37.26	40.74	<b>22.51</b>
4	25.39	28.15	32.50	35.17	38.57	<b>21.42</b>
5	1.93	3.07	4.54	5.87	6.79	<b>3.21</b>
6	94.26	89.20	86.67	78.04	79.64	<b>49.25</b>
10CFR71.47 Limit	1000.00 (2a,3a) 200.00 (1-6)	1000.00 (2a,3a) 200.00 (1-6)	1000.00 (2a,3a) 200.00 (1-6)	1000.00 (2a,3a) 200.00 (1-6)	1000.00 (2a,3a) 200.00 (1-6)	<b>1000.00 (2a,3a) 200.00 (1-6)</b>

<sup>†</sup> Refer to Figure 5.1.1.

Table 5.4.33

TOTAL DOSE RATES  
DOSE LOCATION AT TWO METERS FOR NORMAL CONDITIONS  
MPC-32 DESIGN BASIS ZIRCALOY CLAD FUEL WITH NON-ZIRCALOY INCORE SPACERS  
**WITHOUT NON-FUEL HARDWARE**  
AT VARYING BURNUPS AND COOLING TIMES

Dose Point <sup>†</sup> Location	24,500 MWD/MTU 12 Year Cooling (mrem/hr)	29,500 MWD/MTU 14 Year Cooling (mrem/hr)	34,500 MWD/MTU 16 Year Cooling (mrem/hr)	39,500 MWD/MTU 19 Year Cooling (mrem/hr)	42,500 MWD/MTU 20 Year Cooling (mrem/hr)	<b>45,000 MWD/MTU 24 Year Cooling (mrem/hr)</b>
1	6.55	6.64	6.95	6.78	7.13	<b>5.56</b>
2	8.99	9.14	9.54	9.21	9.61	<b>7.98</b>
3	6.38	6.65	7.17	7.23	7.71	<b>5.13</b>
4	5.93	6.21	6.76	6.88	7.36	<b>4.72</b>
5	0.15	0.24	0.35	0.46	0.53	<b>0.28</b>
6	5.10	4.55	4.08	3.32	3.24	<b>1.96</b>
10CFR71.47 Limit	10.00	10.00	10.00	10.00	10.00	<b>10.00</b>

<sup>†</sup> Refer to Figure 5.1.1.

Table 5.4.34

TOTAL DOSE RATES  
DOSE LOCATION AT ONE METER FOR ACCIDENT CONDITIONS  
MPC-32 DESIGN BASIS ZIRCALOY CLAD FUEL WITH NON-ZIRCALOY INCORE SPACERS  
**WITHOUT NON-FUEL HARDWARE**  
AT VARYING BURNUPS AND COOLING TIMES

Dose Point <sup>†</sup> Location	24,500 MWD/MTU 12 Year Cooling (mrem/hr)	29,500 MWD/MTU 14 Year Cooling (mrem/hr)	34,500 MWD/MTU 16 Year Cooling (mrem/hr)	39,500 MWD/MTU 19 Year Cooling (mrem/hr)	42,500 MWD/MTU 20 Year Cooling (mrem/hr)	45,000 MWD/MTU 24 Year Cooling (mrem/hr)
1	69.80	86.91	110.36	128.98	144.97	132.33
2	152.64	217.18	301.81	373.81	428.78	416.20
3	52.15	68.42	90.21	108.35	122.82	91.02
4	38.31	49.93	65.54	78.49	88.90	69.25
5	7.89	12.51	18.46	23.84	27.60	13.19
6	500.54	460.23	430.39	368.33	367.17	234.35
10CFR71.51 Limit	1000.00	1000.00	1000.00	1000.00	1000.00	1000.00

<sup>†</sup> Refer to Figure 5.1.2.

Table 5.4.35

TOTAL DOSE RATES  
DOSE LOCATION ON THE SURFACE OF THE HI-STAR 100 SYSTEM FOR NORMAL CONDITIONS  
MPC-32 DESIGN BASIS ZIRCALOY CLAD FUEL WITH NON-ZIRCALOY INCORE SPACERS  
WITH NON-FUEL HARDWARE  
AT VARYING BURNUPS AND COOLING TIMES

Dose Point <sup>†</sup> Location	24,500 MWD/MTU 13 Year Cooling (mrem/hr)	29,500 MWD/MTU 16 Year Cooling (mrem/hr)	34,500 MWD/MTU 18 Year Cooling (mrem/hr)	39,500 MWD/MTU 21 Year Cooling (mrem/hr)	42,500 MWD/MTU 23 Year Cooling (mrem/hr)	45,000 MWD/MTU 25 Year Cooling (mrem/hr)
2a	47.29	42.24	43.18	44.47	44.95	44.48
3a	114.54	112.01	121.05	125.89	128.21	128.02
1	26.48	24.11	25.05	24.72	24.45	23.79
2	26.68	25.33	27.46	28.00	28.11	27.68
3	29.44	28.04	29.51	29.90	30.03	29.70
4	27.17	26.05	27.60	28.16	28.40	28.16
5	0.92	1.39	2.04	2.62	2.94	3.11
6	117.05	103.13	99.29	91.62	87.23	82.96
10CFR71.47 Limit	1000.00 (2a,3a) 200.00 (1-6)	1000.00 (2a,3a) 200.00 (1-6)	1000.00 (2a,3a) 200.00 (1-6)	1000.00 (2a,3a) 200.00 (1-6)	1000.00 (2a,3a) 200.00 (1-6)	1000.00 (2a,3a) 200.00 (1-6)

<sup>†</sup> Refer to Figure 5.1.1.

Table 5.4.36

TOTAL DOSE RATES  
DOSE LOCATION AT TWO METERS FOR NORMAL CONDITIONS  
MPC-32 DESIGN BASIS ZIRCALOY CLAD FUEL WITH NON-ZIRCALOY INCORE SPACERS  
WITH NON-FUEL HARDWARE  
AT VARYING BURNUPS AND COOLING TIMES

Dose Point <sup>†</sup> Location	24,500 MWD/MTU 13 Year Cooling (mrem/hr)	29,500 MWD/MTU 16 Year Cooling (mrem/hr)	34,500 MWD/MTU 18 Year Cooling (mrem/hr)	39,500 MWD/MTU 21 Year Cooling (mrem/hr)	42,500 MWD/MTU 23 Year Cooling (mrem/hr)	45,000 MWD/MTU 25 Year Cooling (mrem/hr)
1	6.41	5.96	6.23	6.16	6.09	5.92
2	9.46	8.96	9.42	9.33	9.21	8.97
3	6.93	6.50	6.75	6.68	6.61	6.46
4	6.43	6.03	6.26	6.21	6.15	6.02
5	0.09	0.13	0.18	0.23	0.26	0.27
6	5.72	4.76	4.35	3.73	3.38	3.08
10CFR71.47 Limit	10.00	10.00	10.00	10.00	10.00	10.00

<sup>†</sup> Refer to Figure 5.1.1.

Table 5.4.37

TOTAL DOSE RATES  
DOSE LOCATION AT ONE METER FOR ACCIDENT CONDITIONS  
MPC-32 DESIGN BASIS ZIRCALOY CLAD FUEL WITH NON-ZIRCALOY INCORE SPACERS  
WITH NON-FUEL HARDWARE  
AT VARYING BURNUPS AND COOLING TIMES

Dose Point <sup>†</sup> Location	24,500 MWD/MTU 13 Year Cooling (mrem/hr)	29,500 MWD/MTU 16 Year Cooling (mrem/hr)	34,500 MWD/MTU 18 Year Cooling (mrem/hr)	39,500 MWD/MTU 21 Year Cooling (mrem/hr)	42,500 MWD/MTU 23 Year Cooling (mrem/hr)	45,000 MWD/MTU 25 Year Cooling (mrem/hr)
1	66.34	77.61	98.96	116.54	125.74	130.10
2	151.09	204.52	283.20	352.00	388.26	407.51
3	49.23	57.67	72.81	85.44	92.07	95.29
4	37.67	44.10	55.63	65.27	70.34	72.81
5	3.83	5.75	8.40	10.81	12.08	12.79
6	623.24	540.64	511.67	462.29	434.31	408.68
10CFR71.51 Limit	1000.00	1000.00	1000.00	1000.00	1000.00	1000.00

<sup>†</sup> Refer to Figure 5.1.2.

FIGURES 5.4.1 AND 5.4.2: [PROPRIETARY INFORMATION WITHHELD PER  
10CFR2.390]

## 5.5 REGULATORY COMPLIANCE

The analysis presented in this chapter has shown that the external radiation levels will not increase during normal conditions of transport consistent with the tests specified in 10CFR71.71. This chapter also confirms that the external dose rates from HI-STAR 100 System, when fully loaded with fuel assemblies that meet the acceptance criteria specified in Chapter 1, are less than the regulatory limits specified in 10CFR71.47.

This chapter also demonstrates that the maximum external radiation level at one meter from the external surface of the package does not exceed 1 Rem/hr (10 mSv/hr) during the hypothetical accident conditions consistent with the tests specified in 10CFR71.73.

Tables 5.5.1 through 5.5.3 summarize the maximum dose rates, including the effect of radiation peaking as discussed in Subsection 5.4.1, and demonstrate the HI-STAR 100 System's compliance with the regulatory requirements of 10CFR71.47 and 10CFR71.51. Since these dose rates include the effect of peaking, they may not be equivalent to values reported earlier in this chapter which were surface average dose rates. In these tables "Side" refers to the dose point location that has the maximum dose rate from locations 1-4 (including the pocket trunnion) on Figures 5.1.1 and 5.1.2; "Top" and "Bottom" refer to locations 5 and 6, respectively, on Figures 5.1.1 and 5.1.2. Dose location 2a and 3a from Figure 5.1.1 are not used in Tables 5.5.1 through 5.5.3. Since the maximum dose rate at each location is provided, the corresponding burnup and cooling time may be different between locations and therefore is not listed in the tables. Some of the dose rates in these tables are very close to the regulatory limit. These high dose rates are acceptable because the analysis has been demonstrated to be conservative. In addition, it is extremely unlikely that the casks would be loaded with all fuel assemblies containing the same identical burnup and cooling time analyzed. Finally, the ultimate demonstration of compliance with the 10 CFR 71 regulations will be the measurements that are taken before shipment of the fuel.



Table 5.5.1  
MAXIMUM EXTERNAL DOSE RATES FOR THE  
HI-STAR 100 SYSTEM CONTAINING THE MPC-24

<b>Normal Conditions of Transport</b>			
	<b>External Surface of Package</b>		
<b>Radiation (mrem/hr)</b>	<b>Top</b>	<b>Side</b>	<b>Bottom</b>
Gamma <sup>†</sup>	0.52	1.35	115.63
Neutron	3.63	78.65	11.38
Total	4.15	80.00	127.01
10 CFR 71.47(b)(1) Limit	200	200	200
	<b>2 Meters from Vehicle Outer Surface<sup>††</sup></b>		
<b>Radiation (mrem/hr)</b>	<b>Top</b>	<b>Side</b>	<b>Bottom</b>
Gamma <sup>†</sup>	0.03	9.04	8.13
Neutron	0.32	0.87	0.26
Total	0.35	9.91	8.39
10 CFR 71.47(b)(3) Limit	10	10	10
<b>Hypothetical Accident Conditions</b>			
	<b>1 Meter from Surface of Package<sup>†††</sup></b>		
<b>Radiation (mrem/hr)</b>	<b>Top</b>	<b>Side</b>	<b>Bottom</b>
Gamma <sup>†</sup>	0.18	23.43	639.09
Neutron	16.33	480.92	47.99
Total	16.51	504.35	687.08
10 CFR 71.51(a)(2) Limit	1000	1000	1000

<sup>†</sup> This includes fuel gammas, gammas from hardware activation including incore spacers, and gammas generated by neutron capture.

<sup>††</sup> The vehicle outer surface is the outer radial surface of the impact limiters, the end of the top impact limiter, and 9 feet from the end of the bottom impact limiter.

<sup>†††</sup> The impact limiters are not present.

Table 5.5.2

**MAXIMUM EXTERNAL DOSE RATES FOR THE  
HI-STAR 100 SYSTEM CONTAINING THE MPC-32**

<b>Normal Conditions of Transport</b>			
	<b>External Surface of Package</b>		
<b>Radiation (mrem/hr)</b>	<b>Top</b>	<b>Side</b>	<b>Bottom</b>
Gamma <sup>†</sup>	0.95	1.19	135.06
Neutron	7.52	112.38	19.68
Total	8.46	113.57	154.74
10 CFR 71.47(b)(1) Limit	200	200	200
	<b>2 Meters from Vehicle Outer Surface<sup>††</sup></b>		
<b>Radiation (mrem/hr)</b>	<b>Top</b>	<b>Side</b>	<b>Bottom</b>
Gamma <sup>†</sup>	0.08	5.89	7.98
Neutron	0.58	4.09	0.23
Total	0.66	9.98	8.22
10 CFR 71.47(b)(3) Limit	10	10	10
<b>Hypothetical Accident Conditions</b>			
	<b>1 Meter from Surface of Package<sup>†††</sup></b>		
<b>Radiation (mrem/hr)</b>	<b>Top</b>	<b>Side</b>	<b>Bottom</b>
Gamma <sup>†</sup>	0.22	21.52	739.52
Neutron	34.16	495.41	77.64
Total	34.38	516.93	817.16
10 CFR 71.51(a)(2) Limit	1000	1000	1000

<sup>†</sup> This includes fuel gammas, gammas from hardware activation including incore spacers, and gammas generated by neutron capture.

<sup>††</sup> The vehicle outer surface is the outer radial surface of the impact limiters, the end of the top impact limiter, and 9 feet from the end of the bottom impact limiter.

<sup>†††</sup> The impact limiters are not present.

Table 5.5.3  
MAXIMUM EXTERNAL DOSE RATES FOR THE  
HI-STAR 100 SYSTEM CONTAINING THE MPC-68

<b>Normal Conditions of Transport</b>			
	<b>External Surface of Package</b>		
<b>Radiation (mrem/hr)</b>	<b>Top</b>	<b>Side</b>	<b>Bottom</b>
Gamma <sup>†</sup>	0.34	1.15	114.21
Neutron	2.19	99.04	7.00
Total	2.53	100.19	121.21
10 CFR 71.47(b)(1) Limit	200	200	200
	<b>2 Meters from Vehicle Outer Surface<sup>††</sup></b>		
<b>Radiation (mrem/hr)</b>	<b>Top</b>	<b>Side</b>	<b>Bottom</b>
Gamma <sup>†</sup>	0.03	5.92	6.69
Neutron	0.21	4.05	0.16
Total	0.24	9.97	6.85
10 CFR 71.47(b)(3) Limit	10	10	10
<b>Hypothetical Accident Conditions</b>			
	<b>1 Meter from Surface of Package<sup>†††</sup></b>		
<b>Radiation (mrem/hr)</b>	<b>Top</b>	<b>Side</b>	<b>Bottom</b>
Gamma <sup>†</sup>	0.11	22.15	640.72
Neutron	10.93	600.71	27.37
Total	11.04	622.86	668.09
10 CFR 71.51(a)(2) Limit	1000	1000	1000

<sup>†</sup> This includes fuel gammas, gammas from hardware activation including incore spacers, and gammas generated by neutron capture.

<sup>††</sup> The vehicle outer surface is the outer radial surface of the impact limiters, the end of the top impact limiter, and 9 feet from the end of the bottom impact limiter.

<sup>†††</sup> The impact limiters are not present.

## 5.6 REFERENCES

- [5.1.1] J.F. Briesmeister, Ed., "MCNP - A General Monte Carlo N-Particle Transport Code, Version 4A." Los Alamos National Laboratory, LA-12625-M (1993).
- [5.1.2] O.W. Hermann, C.V. Parks, "SAS2H: A Coupled One-Dimensional Depletion and Shielding Analysis Module," NUREG/CR-0200, Revision 5, (ORNL/NUREG/CSD-2/V2/R5), Oak Ridge National Laboratory, September 1995.
- [5.1.3] O.W. Hermann, R.M. Westfall, "ORIGEN-S: SCALE System Module to Calculate Fuel Depletion, Actinide Transmutation, Fission Product Buildup and Decay, and Associated Radiation Source Terms," NUREG/CR-0200, Revision 5, (ORNL/NUREG/CSD-2/V2/R5), Oak Ridge National Laboratory, September 1995.
- [5.1.4] O.W. Hermann, C.V. Parks, "SAS2H: A Coupled One-Dimensional Depletion and Shielding Analysis Module," NUREG/CR-0200, Revision 6, (ORNL/NUREG/CSD-2/V2/R6), Oak Ridge National Laboratory, September 1998.
- [5.1.5] O.W. Hermann, R.M. Westfall, "ORIGEN-S: SCALE System Module to Calculate Fuel Depletion, Actinide Transmutation, Fission Product Buildup and Decay, and Associated Radiation Source Terms," NUREG/CR-0200, Revision 6, (ORNL/NUREG/CSD-2/V2/R6), Oak Ridge National Laboratory, September 1998.
- [5.1.6] Trojan ISFSI Safety Analysis Report, Revision 3, USNRC Docket 72-0017.
- [5.2.1] NUREG-1617, SRP for Transportation Packages for Spent Nuclear Fuel, USNRC, Washington, DC, March 2000.
- [5.2.2] A. Luksic, "Spent Fuel Assembly Hardware: Characterization and 10CFR 61 Classification for Waste Disposal," PNL-6906-vol. 1, Pacific Northwest Laboratory, June 1989.
- [5.2.3] A.G. Croff, M.A. Bjerke, G.W. Morrison, L.M. Petrie, "Revised Uranium-Plutonium Cycle PWR and BWR Models for the ORIGEN Computer Code," ORNL/TM-6051, Oak Ridge National Laboratory, September 1978.

- [5.2.4] J.W. Roddy et al., "Physical and Decay Characteristics of Commercial LWR Spent Fuel," ORNL/TM-9591/V1&R1, Oak Ridge National Laboratory, January 1996.
- [5.2.5] "Characteristics of Spent Fuel, High Level Waste, and Other Radioactive Wastes Which May Require Long-Term Isolation," DOE/RW-0184, U.S. Department of Energy, December 1987.
- [5.2.6] "Spent Nuclear Fuel Discharges from U.S. Reactors 1994," SR/CNEAF/96-01, Energy Information Administration, U.S. Department of Energy, February 1996.
- [5.2.7] "Characteristics Database System LWR Assemblies Database," DOE/RW-0184-R1, U.S. Department of Energy, July 1992.
- [5.2.8] S.B. Ludwig and J.P. Renier, "Standard and Extended Burnup PWR and BWR Reactor Models for the ORIGEN2 Computer Code," ORNL/TM-11018, Oak Ridge National Laboratory, December 1989.
- [5.2.9] "HI-STORM 100 Final Safety Analysis Report", HI-2002444, Revision 12, Holtec International, Docket No. 72-1014.
- [5.4.1] "American National Standard Neutron and Gamma-Ray Flux-to-Dose Rate Factors", ANSI/ANS-6.1.1-1977.
- [5.4.2] D. J. Whalen, et al., "MCNP: Photon Benchmark Problems," LA-12196, Los Alamos National Laboratory, September 1991.
- [5.4.3] D. J. Whalen, et al., "MCNP: Neutron Benchmark Problems," LA-12212, Los Alamos National Laboratory, November 1991.
- [5.4.4] J. C. Wagner, et al., "MCNP: Criticality Safety Benchmark Problems," LA-12415, Los Alamos National Laboratory, October 1992.
- [5.4.5] S. E. Turner, "Uncertainty Analysis - Axial Burnup Distribution Effects," presented in "Proceedings of a Workshop on the Use of Burnup Credit in Spent Fuel Transport Casks," SAND-89-0018, Sandia National Laboratory, Oct. 1989.
- [5.4.6] Commonwealth Edison Company, Letter No. NFS-BND-95-083, Chicago, Illinois.

- [5.4.8] S. Cierjacks, "Neutron Sources for Basic Physics and Applications," Pergamon Press, 1983.

**APPENDIX 5.A**

**PROPRIETARY APPENDIX WITHHELD IN  
ITS ENTIRETY PER 10CFR2.390**

**APPENDIX 5.B**

**PROPRIETARY APPENDIX WITHHELD IN  
ITS ENTIRETY PER 10CFR2.390**



## **APPENDIX 5.C**

**PROPRIETARY APPENDIX WITHHELD IN  
ITS ENTIRETY PER 10CFR2.390**

## SUPPLEMENT 5.I

### SHIELDING EVALUATION OF THE **HI-STAR HB PACKAGE WITH MPC-HB**

#### 5.I.0 INTRODUCTION

This supplement is focused on providing a shielding evaluation of the HI-STAR 100 System with the MPC-HB. The evaluation presented herein supplements those evaluations of the HI-STAR System contained in the main body of Chapter 5 of this SAR and information in the main body of Chapter 5 that remains applicable to the HI-STAR 100 System with the MPC-HB is not repeated in this supplement. To aid the reader, the sections in this supplement are numbered in the same fashion as the corresponding sections in the main body of this chapter, i.e., Sections 5.I.1 through 5.I.5 correspond to Sections 5.1 through 5.5. Tables and figures in this supplement are labeled sequentially.

#### 5.I.1 DISCUSSION AND RESULTS

The MPC-HB is designed to accommodate 80 Humboldt Bay fuel assemblies. The maximum burnup, minimum cooling time, and the minimum enrichment are provided in Supplement 1.I. Since the burnup of these assemblies is very low and the cooling time is long, an explicit evaluation of the dose rate outside a HI-STAR 100 overpack is not performed. Rather, the neutron and gamma source and assembly hardware activation inside an MPC-HB is compared to the corresponding values from an MPC-68 with design basis fuel to demonstrate that the MPC-HB is bounded by the analysis of the MPC-68. This comparison is performed in Section 5.I.4.

#### 5.I.2 SOURCE SPECIFICATION

The neutron and gamma source term for the Humboldt Bay fuel assemblies were calculated using the same techniques described in Section 5.2. Table 5.I.1 provides the fuel characteristics for the Humboldt Bay fuel assemblies as analyzed in this supplement. These fuel characteristics are the same as those used in reference [5.I.1], except for an additional amount of 1.5 kg of stainless steel cladding that has been added for the DFCs. This is to allow for loading of stainless steel clad fuel rod fragments, should this be necessary. The value of 1.5 kg is a conservative upper bound value of the expected amount, based on the expected total amount of fuel fragments to be loaded, and the assumption that all those fragments have stainless steel clad.

Table 5.I.2 and 5.I.3 provide the neutron and gamma source term for Humboldt Bay fuel. Table 5.I.4 shows the fuel hardware activation. The activity of the stainless steel cladding fragments is directly derived from the activity of the lower tie plate by adjustment for the difference in steel weight (5.73 vs 1.5) and the flux factor (0.2 vs 1). Note that the source for the stainless steel clad is for the entire amount of steel, while all other values are per assembly. Note that the stainless steel clad source is smaller than the total source from steel from a single assembly, and therefore negligible compared to the total source from steel activation in an entire MPC with 80 assemblies.

### 5.I.3 MODEL SPECIFICATIONS

Generally, the same as in Section 5.3. However, the Holtite thickness in the **body of HI-STAR HB** is only 4.0 inches, compared to 4.3 Inches in the HI-STAR 100. A study shows that this could result in an increase in neutron dose rates of up to 30%. This increase is considered in the source term comparison in Section 5.I.4 below. Additionally, the Holtite composition for the HI-STAR HB is slightly different from the composition described in Section 5.3, with a Hydrogen content of 5.6 wt% instead of 5.92 wt%. A study shows that the effect on dose rates of this difference is less than 5%. This is more than compensated by the margins in the source terms discussed in Section 5.I.4 below. The Holtite composition with 5.6 wt% Hydrogen is therefore acceptable for the HI-STAR HB.

**Also, the HI-STAR HB impact limiters do not have Holtite. This is acceptable since the HB fuel assemblies have low burnup and high cooling time. As it is shown in this supplement, the neutron source for the HB fuel assembly is significantly lower than that for the design basis fuel assembly.**

The MPC-HB is manufactured with Metamic neutron absorbing materials, while the MPCs discussed in the main part of this chapter are manufactured with Boral neutron absorber material. Both materials are made of aluminum and B<sub>4</sub>C powder. The Boral contains an aluminum and B<sub>4</sub>C powder mixture sandwiched between two aluminum plates while the Metamic is a single plate of aluminum and B<sub>4</sub>C. The materials are therefore essentially equivalent and there is no distinction between the two materials from a shielding perspective.

### 5.I.4 SHIELDING EVALUATION

#### 5.I.4.1 Normal Condition

The acceptability of transporting the MPC-HB was determined by comparing the source terms for the MPC-HB to the source terms for an MPC-68 containing BWR fuel with a burnup and cooling time of 24,500 MWD/MTU and 8 years. The neutron and gamma source terms for this burnup and cooling time can be found in Tables 5.2.5 and 5.2.13 in the main portion of this chapter, respectively. The source term in each energy group was multiplied by the number of assemblies and then divided by the active fuel length (144 inches for the MPC-68 and 77.5 inches for the MPC-HB) to determine the source strength per unit length. For neutrons, the total number of assemblies in the basket (68 or 80) is used for the comparison. For gammas, where the dose rates are dominated by the contributions of the assemblies on the periphery of the basket, the number of assemblies in the outer rows of the basket is used. These are 36 for the MPC-68, and 48 for the MPC-HB. Additionally, for neutrons in the HI-STAR HB, an increase of 30% (factor of 1.3) is applied as discussed in 5.I.3. In all cases, the design basis source term for the MPC-68 bounds the source term for the MPC-HB, and in most cases by a substantial margin. Therefore, the dose rates from a HI-STAR containing the MPC-HB will be bounded by the dose rates from a HI-STAR containing the MPC-68 under normal conditions.

### 5.I.4.2 Accident Condition

The accident condition was evaluated in the same manner as the normal condition. However, similar to the analysis in Section 5.4.2, it was assumed that fuel assemblies that are not intact are compacted. The effect of this compaction is discussed below for damaged and undamaged assemblies.

- For damaged fuel in DFCs, it is assumed that 50% of the volume in the DFC cross-section is filled with fuel rods and cladding. Given the amount of fuel and cladding in a HB assembly, this corresponds to an active fuel height of 55 inches inside the DFC, i.e. an increase in the source per unit of active length by a factor of  $77.5/55 = 1.41$ .
- For the undamaged assemblies, fuel relocation would be limited by the intact peripheral rods, so the compaction, if any, would also be limited. For a 6x6 assembly it is reasonable to assume that the 4x4 rods inside of the periphery could at most be replaced by a 5x5 rod array, resulting in a maximum number of rods in a cross section of  $6 \times 6 - 4 \times 4 + 5 \times 5 = 45$  rods. This represents an increase by factor 1.25 compared to the intact assembly. Correspondingly, for a 7x7 assembly the maximum number would be  $7 \times 7 - 5 \times 5 + 6 \times 6 = 60$ , or an increase by factor 1.22.

As a bounding approach, an increase in source term per unit of active length of 1.41, corresponding to an active length reduced to 55 inch, was assumed for all assemblies in the basket, i.e. for both damaged and undamaged assemblies. The source term for the MPC-68, assuming an active height of 144 inches, was then compared, on a per inch basis, to the source term from the MPC-HB for an active height of 55 inches. In all neutron and gamma energy groups, the design basis source term for the MPC-68 bounds the source term for the MPC-HB, in most cases by a substantial margin. Therefore, the dose rates from a HI-STAR containing the MPC-HB will be bounded by the dose rates from a HI-STAR containing the MPC-68 during the design basis accident for all assembly conditions.

### 5.I.5 REGULATORY COMPLIANCE

In summary it can be concluded that dose rates from the HI-STAR 100 System with the MPC-HB are bounded by the dose rates for the MPCs analyzed in the main body of the report. The shielding system of the HI-STAR 100 System is therefore in compliance with 10CFR71.

### 5.I.6 REFERENCES

- [5.I.1] “Humboldt Bay Independent Spent Fuel Storage Installation Safety Analysis Report”, Pacific Gas and Electric Company, Docket No. 72-27.

Table 5.I.1

[PROPRIETARY INFORMATION WITHHELD IN ACCORDANCE WITH 10CFR2.390]

Table 5.I.2

CALCULATED NEUTRON SOURCE PER ASSEMBLY  
FOR HUMBOLDT BAY FUEL

<b>Lower Energy (MeV)</b>	<b>Upper Energy (MeV)</b>	<b>23,000 MWD/MTU 29-Year Cooling (Neutrons/sec)</b>
1.0E-01	4.0E-01	1.27E+05
4.0E-01	9.0E-01	6.48E+05
9.0E-01	1.4	6.06E+05
1.4	1.85	4.66E+05
1.85	3.0	8.85E+05
3.0	6.43	7.41E+05
6.43	20.0	6.17E+04
Total		3.53E+06

Table 5.I.3

CALCULATED FUEL GAMMA SOURCE PER ASSEMBLY  
FOR HUMBOLDT BAY FUEL

<b>Lower Energy</b>	<b>Upper Energy</b>	<b>23,000 MWD/MTU 29-Year Cooling</b>	
(MeV)	(MeV)	(MeV/s)	(Photons/s)
0.45	0.7	6.31E+13	1.10E+14
0.7	1.0	7.96E+11	9.37E+11
1.0	1.5	7.47E+11	5.98E+11
1.5	2.0	5.26E+10	3.01E+10
2.0	2.5	5.67E+08	2.52E+08
2.5	3.0	1.94E+07	7.04E+06
Totals		6.47E+13	1.12E+14

Table 5.I.4

Non Fuel Hardware Sources  
(23,000 MWD/MTU Burnup)

<b>Location</b>	<b>29-Year Cooling (curies)</b>
Lower Tie Plate	2.218
Active Fuel Zone (grid spacers)	4.107
Plenum Springs	0.065
Compression / Expansion Springs	0.133
Upper Tie Plate	0.400
Stainless Steel Cladding Fragments	2.9

## SUPPLEMENT 5.II

### SHIELDING EVALUATION OF HI-STAR HB GTCC PACKAGE WITH GWC-HB

#### 5.II.0 INTRODUCTION

This supplement documents the radiation shielding analysis of a single HI-STAR HB GTCC Package with GWC-HB filled with GTCC during transportation for the Humboldt Bay Power Plant (HBPP). Dose rates at various locations around HI-STAR HB GTCC with GWC-HB are calculated. The objective of this analysis is to verify that the cask will meet the 10CFR71 requirements for normal and accident scenarios.

The GTCC waste includes neutron activated components and process waste materials at HBPP. The process waste is contained in the Process Waste Container (PWC), which is inside a secondary waste basket. The authorized to load GTCC information is provided in Supplement 1.II.

The evaluation presented herein supplements those evaluations of the HI-STAR System contained in the main body of Chapter 5 of this SAR and information in the main body of Chapter 5 that remains applicable to HB GTCC with GWC-HB is not repeated in this supplement. To aid the reader, the sections in this supplement are numbered in the same fashion as the corresponding sections in the main body of this chapter, i.e., Sections 5.II.1 through 5.II.5 correspond to Sections 5.1 through 5.5. Tables and figures in this supplement are labeled sequentially.

#### 5.II.1 DISCUSSION AND RESULTS

The source specification is provided in Subsection 5.II.2. The transport acceptance criteria are provided in Section 5.1 of the main part of this chapter.

Surface and 2 meters dose rates are calculated for normal conditions, and 1 meter dose rates are calculated for accident conditions. The maximum dose rates along different sides of the HI-STAR HB GTCC with GWC-HB are summarized in Table 5.II.1 through Table 5.II.3. The dose locations are shown on Figure 5.II.1.

The analyses summarized in this supplement demonstrate HI-STAR HB GTCC with GWC-HB compliance with the 10CFR71 dose rate limits.

#### 5.II.2 SOURCE SPECIFICATION

NUREG-1617 states that “In general, only gammas from approximately 0.8 MeV-2.5 MeV will contribute significantly to the external radiation levels” [5.2.1]. Cobalt-60 is the most substantial high-activity gamma emitter in this gamma energy range. Table 5.II.4 lists the Co-60 source that is used in the MCNP calculations. The Co-60 used in shielding analysis bounds the authorized to load Co-60 activity (stated in Supplement 1.II).



The process waste is modeled in PWC, which is the Inner Region. The remaining waste is modeled in both the Outer Region and the Inner Region. It is assumed that the waste is uniformly distributed.

### 5.II.3 MODEL SPECIFICATIONS

MCNP calculations are performed to determine dose rates along the top, bottom and side of the HI-STAR HB GTCC loaded with GTCC waste (activated metals). Dose rates are calculated at the surface and 2 meters from HI-STAR HB GTCC for the normal conditions, and at 1 meter for accident conditions. The end plate/shielding disk of the Impact limiter is added to the bottom of HI-STAR HB GTCC as a shielding material (this disk is attached to the bottom plate of the HI-STAR HB GTCC using screws; and therefore, the disk remains in place after an accident).

The HI-STAR HB GTCC Package with GWC-HB is modeled in full three-dimensional detail using MCNP. The GTCC waste is modeled as homogenized material, with densities provided in Table 5.II.4.

### 5.II.4 SHIELDING EVALUATION

#### 5.II.4.1 Sensitivity Analysis Dose Rates

The inner shell of HI-STAR HB GTCC with GWC-HB does not have lid. Also, it is possible its welds break during normal or accident conditions of transport. Although the waste is large so that the majority of the waste stays in place, there is possibility that small part of the source would pass the inner shell. Also, the secondary waste basket cover plate may not stay in place during normal or accident conditions of transport. As a consequence, side dose rates may potentially increase.

As a defense in depth, a sensitivity study is performed by voiding the inner shell. This is an overly conservative assumption since a significant amount of shielding material is removed. The sensitivity-study dose rates are summarized in Tables 5.II.1 through 5.II.3.

#### 5.II.4.2 Flux to Dose Rate Conversion Factors

All results presented in this supplement are calculated using the ANSI/ANS-6.1.1-1977 flux to dose rate conversion factors [5.4.1].

### 5.II.5 REGULATORY COMPLIANCE

In summary it is concluded that the shielding system of HI-STAR HB GTCC with GWC-HB is in compliance with 10CFR71 dose rate requirements.

Table 5.II.1

MAXIMUM DOSE RATES ON THE SURFACE OF HI-STAR HB GTCC WITH GWC-HB  
FOR NORMAL CONDITIONS

<b>Dose Location</b>	<b>Maximum Dose Rate (mrem/hr)</b>	
	<b>Design Basis</b>	<b>Sensitivity Analysis</b>
1	4.81	23.71
2	8.04	40.17
3	7.66	25.38
4	0.05	0.08
5	2.22	2.23
10CFR71.47 Limit	200	

Table 5.II.2

MAXIMUM DOSE RATES AT TWO METERS FROM HI-STAR HB GTCC WITH GWC-HB  
FOR NORMAL CONDITIONS

<b>Dose Location</b>	<b>Maximum Dose Rate (mrem/hr)</b>	
	<b>Design Basis</b>	<b>Sensitivity Analysis</b>
2	1.76	8.43
4	0.03	0.10
5	0.40	0.49
10CFR71.47 Limit	10	

Table 5.II.3

MAXIMUM DOSE RATES AT ONE METER FROM HI-STAR HB GTCC WITH GWC-HB  
FOR HYPOTHETICAL ACCIDENT CONDITIONS

<b>Dose Location</b>	<b>Maximum Dose Rate (mrem/hr)</b>	
	<b>Design Basis</b>	<b>Sensitivity Analysis</b>
2	3.30	16.19
4	0.11	0.33
5	0.93	1.01
10CFR71.51 Limit	1000	

Table 5.II.4

[PROPRIETARY INFORMATION WITHHELD PER 10CFR2.390]

FIGURE 5.II.1: [PROPRIETARY INFORMATION WITHHELD PER 10CFR2.390]

## SUPPLEMENT 5.III

### SHIELDING EVALUATION OF HI-STAR 100 PACKAGE WITH DIABLO CANYON MPC-32

#### 5.III.0 INTRODUCTION

The HI-STAR 100 System is to be used for the transportation of Diablo Canyon fuel assemblies. The general information about the Diablo Canyon HI-STAR 100 Package is provided in Supplement 1.III.

#### 5.III.1 DISCUSSION AND RESULTS

The shielding analysis provided in the main part of this chapter bounds the Diablo Canyon HI-STAR 100 MPC/fuel configuration since:

1. As discussed in Section 5.2, the PWR fuel analyzed in the main part of the report has the highest  $\text{UO}_2$ , thus it bounds other PWR fuel assemblies.
2. As discussed in Supplement 1.III, the number of non-fuel hardware devices that can be loaded into the HI-STAR 100 System with Diablo Canyon MPC-32 is limited, and is less than the number of non-fuel hardware devices analyzed in the main part of this chapter.

Thus, no further analysis is provided.

## CHAPTER 6: CRITICALITY EVALUATION

This chapter documents the criticality evaluation of the HI-STAR 100 System for the packaging and transportation of radioactive materials (spent nuclear fuel) in accordance with 10CFR71. The results of this evaluation demonstrate that, for the designated fuel assembly classes and basket configurations, an infinite number of HI-STAR 100 Systems with variations in internal and external moderation remain subcritical with a margin of subcriticality greater than  $0.05\Delta k$ . This corresponds to a Criticality Safety Index (CSI) of zero (0) and demonstrates compliance with 10CFR71 criticality requirements for normal and hypothetical accident conditions of transport.

The criticality design is based on favorable geometry, fixed neutron poisons, an administrative limit on the maximum allowable enrichment, and an administrative limit on the minimum average assembly burnup for the MPC-32. Criticality safety of the HI-STAR 100 System does *not* rely on credit for: (1) fuel burnup except for the MPC-32; (2) fuel-related burnable absorbers; or (3) more than 75% of the manufacturer's minimum B-10 content for the fixed neutron absorber when subject to standard acceptance tests<sup>†</sup>.

In addition to demonstrating that the criticality safety acceptance criteria are satisfied, this chapter describes the HI-STAR 100 System design structures and components important to criticality safety and limiting fuel characteristics in sufficient detail to identify the package accurately and provide a sufficient basis for the evaluation of the package.

---

<sup>†</sup> For greater credit allowance, fabrication tests capable of verifying the presence and uniformity of the neutron absorber are needed.

## 6.1 DISCUSSION AND RESULTS

In conformance with the principles established in 10CFR71 [6.1.1], NUREG-1617 [6.1.2], and NUREG-0800 Section 9.1.2 [6.1.3], the results in this chapter demonstrate that the effective multiplication factor ( $k_{\text{eff}}$ ) of the HI-STAR 100 System, including all biases and uncertainties evaluated with a 95% probability at the 95% confidence level, does not exceed 0.95 under all credible normal and hypothetical accident conditions of transport. This criterion provides a large subcritical margin, sufficient to assure the criticality safety of the HI-STAR 100 System when fully loaded with fuel of the highest permissible reactivity. In addition, the results of this evaluation demonstrate that the HI-STAR 100 System is in full compliance with the requirements outlined in the Standard Review Plan for Dry Cask Storage Systems, NUREG-1536.

Criticality safety of the HI-STAR 100 System depends on the following four principal design parameters:

1. The inherent geometry of the fuel basket designs within the MPC (and the flux-trap water gaps in the MPC-24),
2. The incorporation of permanent fixed neutron-absorbing panels in the fuel basket structure, and
3. An administrative limit on the maximum average enrichment for PWR fuel and maximum planar-average enrichment for BWR fuel, and
4. An administrative limit on the minimum average assembly burnup for PWR fuel in the MPC-32.

The HI-STAR 100 System is designed such that the fixed neutron absorber will remain effective for a period greater than 20 years, and there are no credible means to lose it. Therefore, there is no need to provide a surveillance or monitoring program to verify the continued efficacy of the neutron absorber.

Criticality safety of the HI-STAR 100 System does not rely on the use of any of the following credits:

- burnup of fuel, except for the MPC-32
- fuel-related burnable neutron absorbers
- more than 75 percent of the B-10 content for the Boral fixed neutron absorber.



- more than 90 percent of the B-10 content for the Metamic fixed neutron absorber, with comprehensive fabrication tests as described in Chapter 8.

The following basket designs are available for use in the HI-STAR 100 System:

- a 24-cell basket (MPC-24), designed for intact PWR fuel assemblies with a specified maximum enrichment.
- a 24-cell basket (MPC-24E/EF), designed for intact and damaged PWR fuel assemblies, and fuel debris. This is a variation of the MPC-24, with increased  $^{10}\text{B}$  content in the fixed neutron absorber and with four cells capable of accommodating either intact fuel or a damaged fuel container (DFC). The MPC-24E and MPC-24EF is designed for fuel assemblies with a specified maximum enrichment. Although the MPC-24E/EF is designed and analyzed for damaged fuel and fuel debris, it is only certified for intact fuel assemblies.
- a 24-cell basket (MPC-24E/EF Trojan), design for intact and damaged PWR fuel assemblies, and fuel debris from the Trojan Nuclear Plant (TNP). This is a variation of the MPC-24E/EF, with a slightly reduced height, and increased cell sizes for the cells designated for damaged fuel and fuel debris. This increased cell size is required to accommodate the Trojan specific Failed Fuel Cans and DFCs.
- a 32-cell basket (MPC-32), designed for intact PWR fuel assemblies of a specified minimum burnup, and
- a 68-cell basket (MPC-68), designed for both intact and damaged BWR fuel assemblies with a specified maximum planar-average enrichment. Additionally, a variation in the MPC-68, designated MPC-68F, is designed for damaged BWR fuel assemblies and BWR fuel debris with a specified maximum planar-average enrichment.
- a 80-cell basket (MPC-HB), designed for Humboldt Bay fuel. See Supplement 6.I for details and evaluations for this basket version.

Two interchangeable neutron absorber materials are used in these baskets, Boral and Metamic. [

PROPRIETARY INFORMATION WITHHELD PER 10CFR2.390

]

During the normal conditions of transport, the HI-STAR 100 System is dry (no moderator), and thus, the reactivity is very low ( $k_{\text{eff}} < 0.50$ ). However, the HI-STAR 100 System for loading and unloading operations, as well as for the hypothetical accident conditions, is flooded, and thus, represents the limiting case in terms of reactivity. The calculational models for these conditions conservatively include: full flooding with ordinary water, corresponding to the highest reactivity, and the worst case (most conservative) combination of manufacturing and fabrication tolerances.

The MPC-24EF contains the same basket as the MPC-24E. More specifically, all dimensions relevant to the criticality analyses are identical between the MPC-24E and MPC-24EF. Therefore, all criticality results obtained for the MPC-24E are valid for the MPC-24EF and no separate analyses for the MPC-24EF are necessary.

Confirmation of the criticality safety of the HI-STAR 100 Systems under flooded conditions, when filled with fuel of the maximum permissible reactivity for which they are designed, was accomplished with the three-dimensional Monte Carlo code MCNP4a [6.1.4]. Independent confirmatory calculations were made with NITAWL-KENO5a from the SCALE-4.3 package. KENO5a [6.1.5] calculations used the 238-group SCALE cross-section library in association with the NITAWL-II program [6.1.6], which adjusts the uranium-238 cross sections to compensate for resonance self-shielding effects. The Dancoff factors required by NITAWL-II were calculated with the CELLDAN code [6.1.13], which includes the SUPERDAN code [6.1.7] as a subroutine. K-factors for one-sided statistical tolerance limits with 95% probability at the 95% confidence level were obtained from the National Bureau of Standards (now NIST) Handbook 91 [6.1.8].

For the burnup credit calculations, CASMO-4, a two-dimensional transport theory code [6.1.10-6.1.12] for fuel assemblies, was used to calculate the isotopic composition of the spent fuel. The criticality evaluations for burnup credit were performed with MCNP4a [6.1.4].

To assess the incremental reactivity effects due to manufacturing tolerances, CASMO and MCNP4a [6.1.4] were used. The CASMO and MCNP4a calculations identify those tolerances that cause a positive reactivity effect, enabling the Monte Carlo code input to define the worst case (most conservative) conditions. CASMO was not used for quantitative criticality evaluations, but only to qualitatively indicate the direction and approximate magnitude of the reactivity effects of the manufacturing tolerances.

Benchmark calculations were made to compare the primary code packages (MCNP4a, CASMO and KENO5a) with experimental data, using experiments selected to encompass, insofar as practical, the design parameters of the HI-STAR 100 System. The most important parameters are (1) the enrichment, (2) the water-gap size (MPC-24) or cell spacing (MPC-32 and MPC-68), (3)

the  $^{10}\text{B}$  loading of the neutron absorber panels, and (4) the assembly burnup (MPC-32 only). Benchmark calculations are presented in Appendix 6.A, Appendix 6.E and Appendix 6.C. |

Applicable codes, standards, and regulations, or pertinent sections thereof, include the following:

- U.S. Code of Federal Regulations, “Packaging and Transportation of Radioactive Materials,” Title 10, Part 71.
- NUREG-1617, “Standard Review Plan for Transportation Packages for Spent Nuclear Fuel” USNRC, Washington D.C., March 2000.
- U.S. Code of Federal Regulations, “Prevention of Criticality in Fuel Storage and Handling,” Title 10, Part 50, Appendix A, General Design Criterion 62.
- USNRC Standard Review Plan, NUREG-0800, Section 9.1.2, Spent Fuel Storage, Rev. 3, July 1981.
- USNRC Interim Staff Guidance 8 (ISG-8), Revision 2, “Burnup Credit in the Criticality Safety Analyses of PWR Spent Fuel in Transport and Storage Casks”.

To assure the true reactivity will always be less than the calculated reactivity, the following conservative assumptions were made:

[

PROPRIETARY INFORMATION WITHHELD PER 10CFR2.390

]

[

PROPRIETARY INFORMATION WITHHELD PER 10CFR2.390

]

The principal calculational results, which address the following conditions:

- A single package, under the conditions of 10 CFR 71.55(b), (d), and (e);
- An array of undamaged packages, under the conditions of 10 CFR 71.59(a)(1); and
- An array of damaged packages, under the conditions of 10 CFR 71.59(a)(2)

are summarized in Table 6.1.4 for all MPCs and for the most reactive configuration and fuel condition in each MPC. These results demonstrate that the HI-STAR 100 System is in full compliance with 10CFR71 (71.55(b), (d), and (e) and 71.59(a)(1) and (a)(2)). The calculations for package arrays are performed for infinite arrays of HI-STAR 100 Systems under flooded conditions. Therefore, the Criticality Safety Index (CSI) is zero (0). It is noted that the results for the internally flooded single package and package arrays are statistically equivalent for each basket. This shows that the physical separation between overpacks and the steel radiation shielding are each adequate to preclude any significant neutronic coupling between casks in an array configuration. In addition, the table shows the result for an unreflected, internally flooded cask for each MPC. This configuration is used in many calculations and studies throughout this chapter, and is shown to yield results that are statistically equivalent to the results for the corresponding reflected package. Further analyses for the various conditions of flooding that support the conclusion that the fully flooded condition corresponds to the highest reactivity, and thus is most limiting, are presented in Section 6.4. These analyses also include cases with various internal and external moderator densities and various cask-to-cask spacings.

Additional results of the design basis criticality safety calculations for single unreflected, internally flooded casks (limiting cases) are listed in Tables 6.1.1 through 6.1.3 and 6.1.5 through 6.1.7, conservatively evaluated for the worst combination of manufacturing tolerances (as identified in Section 6.3), and including the calculational bias, uncertainties, and calculational statistics. For each of the MPC designs and fuel assembly classes<sup>†</sup>, Tables 6.1.1 through 6.1.3 and 6.1.5 through 6.1.7 list the bounding maximum  $k_{\text{eff}}$  value, the associated maximum allowable enrichment, and the minimum required assembly average burnup (if applicable), as required by 10CFR71.33(b)(2). The maximum enrichment and minimum burnup acceptance criteria are defined in Chapter 1. Additional results for each of the candidate fuel assemblies, that are bounded by those listed in Tables 6.1.1 through 6.1.3, are given in Section 6.2 for the MPC-24, MPC-68 and MPC-68F. The tables in Section 6.2 list the maximum  $k_{\text{eff}}$  (including bias, uncertainties, and calculational statistics), calculated  $k_{\text{eff}}$ , standard deviation, and energy of the average lethargy causing fission (EALF) for each of the candidate fuel assemblies and basket configurations analyzed. The capability of the MPC-68F to safely accommodate Dresden-1 and Humboldt Bay damaged fuel (fuel assembly classes 6x6A, 6x6B, 6x6C, 7x7A, and 8x8A) is demonstrated in Subsection 6.4.4.

In Summary, these results confirm that the maximum  $k_{\text{eff}}$  values for the HI-STAR 100 System are below the limiting design criteria ( $k_{\text{eff}} < 0.95$ ) when fully flooded and loaded with any of the candidate fuel assemblies and basket configurations. The Criticality Safety Index is zero (0).

---

<sup>†</sup> For each array size (e.g., 6x6, 7x7, 14x14, etc.), the fuel assemblies have been subdivided into a number of assembly classes, where an assembly class is defined in terms of the (1) number of fuel rods; (2) pitch; (3) number and location of guide tubes (PWR) or water rods (BWR); and (4) cladding material. The assembly classes for BWR and PWR fuel are defined in Section 6.2.

Table 6.1.1

BOUNDING MAXIMUM  $k_{\text{eff}}$  VALUES FOR EACH ASSEMBLY CLASS IN THE MPC-24

Fuel Assembly Class	Maximum Allowable Enrichment (wt% $^{235}\text{U}$ )	Maximum <sup>†</sup> $k_{\text{eff}}$
14x14A	4.6	0.9296
14x14B	4.6	0.9228
14x14C	4.6	0.9307
14x14D	4.0	0.8507
14x14E	5.0	0.7627
15x15A	4.1	0.9227
15x15B	4.1	0.9388
15x15C	4.1	0.9361
15x15D	4.1	0.9367
15x15E	4.1	0.9392
15x15F	4.1	0.9410
15x15G	4.0	0.8907
15x15H	3.8	0.9337
16x16A	4.6	0.9287
17x17A	4.0	0.9368
17x17B	4.0	0.9355
17x17C	4.0	0.9349

Note: These calculations are for single unreflected, fully flooded casks. However, comparable reactivities were obtained for fully reflected casks and for arrays of casks.

---

† The term "maximum  $k_{\text{eff}}$ " as used here, and elsewhere in this document, means the highest possible k-effective, including bias, uncertainties, and calculational statistics, evaluated for the worst case combination of manufacturing tolerances.

Table 6.1.2

BOUNDING MAXIMUM  $k_{\text{eff}}$  VALUES FOR EACH ASSEMBLY CLASS IN THE MPC-68

Fuel Assembly Class	Maximum Allowable Planar-Average Enrichment (wt% $^{235}\text{U}$ )	Maximum <sup>†</sup> $k_{\text{eff}}$
6x6A	2.7 <sup>††</sup>	0.7888 <sup>†††</sup>
6x6B <sup>‡</sup>	2.7 <sup>††</sup>	0.7824 <sup>†††</sup>
6x6C	2.7 <sup>††</sup>	0.8021 <sup>†††</sup>
7x7A	2.7 <sup>††</sup>	0.7974 <sup>†††</sup>
7x7B	4.2	0.9386
8x8A	2.7 <sup>††</sup>	0.7697 <sup>†††</sup>
8x8B	4.2	0.9416
8x8C	4.2	0.9425
8x8D	4.2	0.9403
8x8E	4.2	0.9312
8x8F	4.0	0.9459

Note: These calculations are for single unreflected, fully flooded casks. However, comparable reactivities were obtained for fully reflected casks and for arrays of casks.

- 
- † The term "maximum  $k_{\text{eff}}$ " as used here, and elsewhere in this document, means the highest possible k-effective, including bias, uncertainties, and calculational statistics, evaluated for the worst case combination of manufacturing tolerances.
- †† This calculation was performed for 3.0% planar-average enrichment, however, the authorized contents are limited to maximum planar-average enrichment of 2.7%. Therefore, the listed maximum  $k_{\text{eff}}$  value is conservative.
- ††† This calculation was performed for a  $^{10}\text{B}$  loading of 0.0067 g/cm<sup>2</sup>, which is 75% of a minimum  $^{10}\text{B}$  loading of 0.0089 g/cm<sup>2</sup>. The minimum  $^{10}\text{B}$  loading in the MPC-68 is at least 0.0310 g/cm<sup>2</sup>. Therefore, the listed maximum  $k_{\text{eff}}$  value is conservative.
- ‡ Assemblies in this class contain both MOX and UO<sub>2</sub> pins. The composition of the MOX fuel pins is given in Table 6.3.4. The maximum allowable planar-average enrichment for the MOX pins is given in the specification of authorized contents, Chapter 1.

Table 6.1.2 (continued)

BOUNDING MAXIMUM  $k_{\text{eff}}$  VALUES FOR EACH ASSEMBLY CLASS IN THE MPC-68

Fuel Assembly Class	Maximum Allowable Planar-Average Enrichment (wt% $^{235}\text{U}$ )	Maximum <sup>†</sup> $k_{\text{eff}}$
9x9A	4.2	0.9417
9x9B	4.2	0.9436
9x9C	4.2	0.9395
9x9D	4.2	0.9394
9x9E	4.0	0.9486
9x9F	4.0	0.9486
9x9G	4.2	0.9383
10x10A	4.2	0.9457 <sup>††</sup>
10x10B	4.2	0.9436
10x10C	4.2	0.9433
10x10D	4.0	0.9376
10x10E	4.0	0.9185

Note: These calculations are for single unreflected, fully flooded casks. However, comparable reactivities were obtained for fully reflected casks and for arrays of casks.

---

† The term "maximum  $k_{\text{eff}}$ " as used here, and elsewhere in this document, means the highest possible k-effective, including bias, uncertainties, and calculational statistics, evaluated for the worst case combination of manufacturing tolerances.

†† KENO5a verification calculation resulted in a maximum  $k_{\text{eff}}$  of 0.9453.



Table 6.1.3

BOUNDING MAXIMUM  $k_{\text{eff}}$  VALUES FOR EACH ASSEMBLY CLASS IN THE MPC-68F

Fuel Assembly Class	Maximum Allowable Planar-Average Enrichment (wt% $^{235}\text{U}$ )	Maximum $^{\dagger} k_{\text{eff}}$
6x6A	2.7 $^{\dagger\dagger}$	0.7888
6x6B $^{\dagger\dagger\dagger}$	2.7	0.7824
6x6C	2.7	0.8021
7x7A	2.7	0.7974
8x8A	2.7	0.7697

Note:

1. These calculations are for single unreflected, fully flooded casks. However, comparable reactivities were obtained for fully reflected casks and for arrays of casks.
2. These calculations were performed for a  $^{10}\text{B}$  loading of  $0.0067 \text{ g/cm}^2$ , which is 75% of a minimum  $^{10}\text{B}$  loading of  $0.0089 \text{ g/cm}^2$ . The minimum  $^{10}\text{B}$  loading in the MPC-68F is  $0.010 \text{ g/cm}^2$ . Therefore, the listed maximum  $k_{\text{eff}}$  values are conservative.

---

$^{\dagger}$  The term "maximum  $k_{\text{eff}}$ " as used here, and elsewhere in this document, means the highest possible k-effective, including bias, uncertainties, and calculational statistics, evaluated for the worst case combination of manufacturing tolerances.

$^{\dagger\dagger}$  These calculations were performed for 3.0% planar-average enrichment, however, the authorized contents are limited to a maximum planar-average enrichment of 2.7%. Therefore, the listed maximum  $k_{\text{eff}}$  values are conservative.

$^{\dagger\dagger\dagger}$  Assemblies in this class contain both MOX and  $\text{UO}_2$  pins. The composition of the MOX fuel pins is given in Table 6.3.4. The maximum allowable planar-average enrichment for the MOX pins is given in the specification of authorized contents, Chapter 1.

Table 6.1.4  
SUMMARY OF THE CRITICALITY RESULTS FOR THE MOST REACTIVE ASSEMBLY FROM  
THE ASSEMBLY CLASSES IN EACH MPC<sup>†</sup>  
TO DEMONSTRATE COMPLIANCE WITH 10CFR71.55 AND 10CFR71.59

MPC-24, Assembly Class 15x15F, 4.1 wt% <sup>235</sup> U				
Configuration	% Internal Moderation	% External Moderation	Applicable Requirement	Maximum $k_{eff}$ <sup>‡</sup>
Single Package, unreflected	100%	0%	n/a	0.9410
Single Package, fully reflected	100%	100%	10CFR71.55 (b), (d), and (e)	0.9397
Containment, fully reflected	100%	100%		0.9397
Infinite Array of Damaged Packages	100%	100%	10CFR71.59 (a)(2)	0.9436
Infinite Array of Undamaged Packages	0%	0%	10CFR71.59 (a)(1)	0.3950
MPC-68, Assembly Class 9x9E/F, 4.0 wt% <sup>235</sup> U				
Configuration	% Internal Moderation	% External Moderation	Applicable Requirement	Maximum $k_{eff}$
Single Package, unreflected	100%	0%	n/a	0.9486
Single Package, fully reflected	100%	100%	10CFR71.55 (b), (d), and (e)	0.9470
Containment, fully reflected	100%	100%		0.9461
Infinite Array of Damaged Packages	100%	100%	10CFR71.59 (a)(2)	0.9468
Infinite Array of Undamaged Packages	0%	0%	10CFR71.59 (a)(1)	0.3808
MPC-68F, Assembly Class 6x6C, 2.7 wt% <sup>235</sup> U				
Configuration	% Internal Moderation	% External Moderation	Applicable Requirement	Maximum $k_{eff}$
Single Package, unreflected	100%	0%	n/a	0.8021
Single Package, fully reflected	100%	100%	10CFR71.55 (b), (d), and (e)	0.8033
Containment, fully reflected	100%	100%		0.8033
Infinite Array of Damaged Packages	100%	100%	10CFR71.59 (a)(2)	0.8026
Infinite Array of Undamaged Packages	0%	0%	10CFR71.59 (a)(1)	0.3034

<sup>†</sup> See Supplement 6.I, Table 6.I.1 for results for the MPC-HB.

<sup>‡</sup> The maximum  $k_{eff}$  is equal to the sum of the calculated  $k_{eff}$ , two standard deviations, the code bias, and the uncertainty in the code bias. For cases with 100% internal moderation, the standard deviation is between 0.0007 and 0.0009, for cases with 0% internal moderation, the standard deviation is between 0.0002 and 0.0004.

Table 6.1.4 (continued)  
SUMMARY OF THE CRITICALITY RESULTS FOR THE MOST REACTIVE ASSEMBLY FROM  
THE ASSEMBLY CLASSES IN EACH MPC<sup>†</sup>  
TO DEMONSTRATE COMPLIANCE WITH 10CFR71.55 AND 10CFR71.59

MPC-24E/EF, Assembly Class 15x15F, 4.5 wt% <sup>235</sup> U				
Configuration	% Internal Moderation	% External Moderation	Applicable Requirement	Maximum <sup>‡</sup> k <sub>eff</sub>
Single Package, unreflected	100%	0%	n/a	0.9495
Single Package, fully reflected	100%	100%	10CFR71.55 (b), (d), and (e)	0.9485
Containment, fully reflected	100%	100%		0.9486
Infinite Array of Damaged Packages	100%	100%	10CFR71.59 (a)(2)	0.9495
Infinite Array of Undamaged Packages	0%	0%	10CFR71.59 (a)(1)	0.4026
MPC-24E/EF TROJAN, Trojan Intact and Damaged Fuel, 3.7 wt% <sup>235</sup> U				
Configuration	% Internal Moderation	% External Moderation	Applicable Requirement	Maximum k <sub>eff</sub>
Single Package, unreflected	100%	0%	n/a	0.9377
Single Package, fully reflected	100%	100%	10CFR71.55 (b), (d), and (e)	0.9366
Containment, fully reflected	100%	100%		0.9377
Infinite Array of Damaged Packages	100%	100%	10CFR71.59 (a)(2)	0.9383
Infinite Array of Undamaged Packages	0%	0%	10CFR71.59 (a)(1)	0.3518
MPC-32, Assembly Class 15x15F and 17x17B				
Configuration	% Internal Moderation	% External Moderation	Applicable Requirement	Maximum k <sub>eff</sub>
Single Package, unreflected	100%	0%	n/a	0.9450
Single Package, fully reflected	100%	100%	10CFR71.55 (b), (d), and (e)	0.9448
Containment, fully reflected	100%	100%		0.9450
Infinite Array of Damaged Packages	100%	100%	10CFR71.59 (a)(2)	0.9452
Infinite Array of Undamaged Packages	0%	0%	10CFR71.59 (a)(1)	0.4420

<sup>†</sup> See Supplement 6.I, Table 6.I.1 for results for the MPC-HB.

<sup>‡</sup> The maximum k<sub>eff</sub> is equal to the sum of the calculated k<sub>eff</sub>, two standard deviations, the code bias, and the uncertainty in the code bias. For cases with 100% internal moderation, the standard deviation is between 0.0004 and 0.0009, for cases with 0% internal moderation, the standard deviation is between 0.0002 and 0.0004.

Table 6.1.5

BOUNDING MAXIMUM  $k_{\text{eff}}$  VALUES FOR EACH ASSEMBLY CLASS IN THE MPC-24E/EF

Fuel Assembly Class	Maximum Allowable Enrichment (wt% $^{235}\text{U}$ )	Maximum <sup>†</sup> $k_{\text{eff}}$
14x14A	5.0	0.9380
14x14B	5.0	0.9312
14x14C	5.0	0.9365
14x14D	5.0	0.8875
14x14E	5.0	0.7651
15x15A	4.5	0.9336
15x15B	4.5	0.9487
15x15C	4.5	0.9462
15x15D	4.5	0.9445
15x15E	4.5	0.9471
15x15F	4.5	0.9495
15x15G	4.5	0.9062
15x15H	4.2	0.9455
16x16A	5.0	0.9358
17x17A	4.4	0.9447
17x17B	4.4	0.9438
17x17C	4.4	0.9433

---

† The term "maximum  $k_{\text{eff}}$ " as used here, and elsewhere in this document, means the highest possible k-effective, including bias, uncertainties, and calculational statistics, evaluated for the worst case combination of manufacturing tolerances.

Table 6.1.6

BOUNDING MAXIMUM  $k_{\text{eff}}$  VALUES IN THE MPC-24E/EF TROJAN

Fuel Assembly Class	Maximum Allowable Enrichment (wt% $^{235}\text{U}$ )	Content	Maximum <sup>†</sup> $k_{\text{eff}}$
17x17B	3.7	Intact Fuel	0.9187
17x17B	3.7	Intact Fuel, Damaged Fuel and Fuel Debris	0.9377

---

† The term "maximum  $k_{\text{eff}}$  " as used here, and elsewhere in this document, means the highest possible k-effective, including bias, uncertainties, and calculational statistics, evaluated for the worst case combination of manufacturing tolerances.

Table 6.1.7

BOUNDING MAXIMUM  $k_{\text{eff}}$  VALUES IN THE MPC-32  
FOR ASSEMBLIES NOT EXPOSED TO CONTROL RODS DURING DEPLETION<sup>‡</sup>

Fuel Assembly Class	Maximum Allowable Enrichment <sup>††</sup> (wt% <sup>235</sup> U)	Minimum Required Assembly Average Burnup <sup>††</sup> (GWd/MTU)	Maximum <sup>†</sup> $k_{\text{eff}}$
15x15D, E, F, H	1.8 <sup>‡</sup>	0	0.9281
	2.0	9.07	0.9440
	3.0	27.65	0.9444
	4.0	38.32	0.9462
	5.0	48.43	0.9454
17x17A, B, C	1.8 <sup>‡</sup>	0	0.9226
	2.0	6.65	0.9453
	3.0	25.06	0.9448
	4.0	37.96	0.9451
	5.0	49.38	0.9455

<sup>‡</sup> The result for 1.8 wt% <sup>235</sup>U is not impacted by the changes discussed in Appendix 6.C.

<sup>††</sup> Other combinations of maximum enrichment and minimum burnup have been evaluated which result in the same maximum  $k_{\text{eff}}$ . See Appendix 6.C for a bounding polynomial function.

<sup>†</sup> The term "maximum  $k_{\text{eff}}$  " as used here, and elsewhere in this document, means the highest possible k-effective, including bias, uncertainties, and calculational statistics, evaluated for the worst case combination of manufacturing tolerances.

## 6.2 SPENT FUEL LOADING

Specifications for the BWR and PWR fuel assemblies that were analyzed in this criticality evaluation are given in Tables 6.2.1 and 6.2.2, respectively. For the BWR fuel characteristics, the number and dimensions for the water rods are the actual number and dimensions. For the PWR fuel characteristics, the actual number and dimensions of the control rod guide tubes and thimbles are used. Table 6.2.1 lists 72 unique BWR assemblies while Table 6.2.2 lists 46 unique PWR assemblies, all of which were explicitly analyzed for this evaluation. Examination of Tables 6.2.1 and 6.2.2 reveals that there are a large number of minor variations in fuel assembly dimensions.

Due to the large number of minor variations in fuel assembly dimensions, the use of explicit dimensions in defining the authorized contents could limit the applicability of the HI-STAR 100 System. To resolve this limitation, bounding criticality analyses are presented in this section for a number of defined fuel assembly classes for both fuel types (PWR and BWR). The results of the bounding criticality analyses justify using bounding fuel dimensions for defining the authorized contents.

### 6.2.1 Definition of Assembly Classes

For each array size (e.g., 6x6, 7x7, 15x15, etc.), the fuel assemblies have been subdivided into a number of defined classes, where a class is defined in terms of the (1) number of fuel rods; (2) pitch; (3) number and locations of guide tubes (PWR) or water rods (BWR); and (4) cladding material. The assembly classes for BWR and PWR fuel are defined in Tables 6.2.1 and 6.2.2, respectively. It should be noted that these assembly classes are unique to this evaluation and are not known to be consistent with any class designations in the open literature.

For each assembly class, calculations have been performed for all of the dimensional variations for which data is available (i.e., all data in Tables 6.2.1 and 6.2.2). These calculations demonstrate that the maximum reactivity corresponds to:

- maximum active fuel length,
- maximum fuel pellet diameter,
- minimum cladding outside diameter (OD),
- maximum cladding inside diameter (ID),
- minimum guide tube/water rod thickness, and
- maximum channel thickness (for BWR assemblies only).

Therefore, for each assembly class, a bounding assembly was defined based on the above characteristics and a calculation for the bounding assembly was performed to demonstrate compliance with the regulatory requirement of  $k_{\text{eff}} < 0.95$ . In some assembly classes this bounding assembly corresponds directly to one of the actual (real) assemblies; while in most assembly classes, the bounding assembly is artificial (i.e., based on bounding dimensions from

more than one of the actual assemblies). In classes where the bounding assembly is artificial, the reactivity of the actual (real) assemblies is typically much less than that of the bounding assembly; thereby providing additional conservatism. As a result of these analyses, the authorized contents (Chapter 1) are defined in terms of the bounding assembly parameters for each class.

To demonstrate that the aforementioned characteristics are bounding, a parametric study was performed for a reference BWR assembly, designated herein as 8x8C04 (identified generally as a GE8x8R). The results of this study are shown in Table 6.2.3, and verify the positive reactivity effect associated with (1) increasing the pellet diameter, (2) maximizing the cladding ID (while maintaining a constant cladding OD), (3) minimizing the cladding OD (while maintaining a constant cladding ID), (4) decreasing the water rod thickness, (5) artificially replacing the Zircaloy water rod tubes with water, (6) maximizing the channel thickness, and (7) increasing the active length. These results, and the many that follow, justify the approach for using bounding dimensions for defining the authorized contents. Where margins permit, the Zircaloy water rod tubes (BWR assemblies) are artificially replaced by water in the bounding cases to remove the requirement for water rod thickness from the specification of authorized contents.

As mentioned, the bounding approach used in these analyses often results in a maximum  $k_{\text{eff}}$  value for a given class of assemblies that is much greater than the reactivity of any of the actual (real) assemblies within the class, and yet, is still below the 0.95 regulatory limit.

### 6.2.2 PWR Fuel Assemblies in the MPC-24

For PWR fuel assemblies (specifications listed in Table 6.2.2) the 15x15F01 fuel assembly at 4.1% enrichment has the highest reactivity (see Table 6.2.13). The 17x17A01 assembly (otherwise known as a Westinghouse 17x17 OFA) has a similar reactivity (see Table 6.2.17) and was used throughout this criticality evaluation as a reference PWR assembly. The 17x17A01 assembly is a representative PWR fuel assembly in terms of design and reactivity and is useful for the reactivity studies presented in Sections 6.3 and 6.4. Calculations for the various PWR fuel assemblies in the MPC-24 are summarized in Tables 6.2.4 through 6.2.19 and 6.2.43 for the fully flooded condition with the fuel centered in each fuel storage location.

Tables 6.2.4 through 6.2.19 and 6.2.43 show the maximum  $k_{\text{eff}}$  values for the assembly classes that are acceptable for storage in the MPC-24. All maximum  $k_{\text{eff}}$  values include the bias, uncertainties, and calculational statistics, evaluated for the worst combination of manufacturing tolerances. All calculations for the MPC-24 were performed for a  $^{10}\text{B}$  loading of  $0.020 \text{ g/cm}^2$ , which is 75% of the minimum loading of  $0.0267 \text{ g/cm}^2$  for Boral, or 90% of the minimum loading of  $0.0223 \text{ g/cm}^2$  for Metamic, specified for the MPC-24 in Section 1.4. The maximum allowable enrichment in the MPC-24 varies from 3.8 to 5.0 wt%  $^{235}\text{U}$ , depending on the assembly class, and is defined in Tables 6.2.4 through 6.2.19 and 6.2.43. It should be noted that the maximum allowable enrichment does not vary within an assembly class. Table 6.1.1



summarizes the maximum allowable enrichments for each of the assembly classes that are acceptable for storage in the MPC-24.

Tables 6.2.4 through 6.2.19 and 6.2.43 are formatted with the assembly class information in the top row, the unique assembly designations, dimensions, and  $k_{\text{eff}}$  values in the following rows above the bold double lines, and the bounding dimensions selected to define the authorized contents and corresponding bounding  $k_{\text{eff}}$  values in the final rows. Where the bounding assembly corresponds directly to one of the actual assemblies, the fuel assembly designation is listed in the bottom row in parentheses (e.g., Table 6.2.4). Otherwise, the bounding assembly is given a unique designation. For an assembly class that contains only a single assembly (e.g., 14x14D, see Table 6.2.7), the authorized contents dimensions are based on the assembly dimensions from that single assembly. Generally, the maximum  $k_{\text{eff}}$  values corresponding to the selected bounding dimensions are greater than or equal to those for the actual assembly dimensions, and all maximum  $k_{\text{eff}}$  values are below the 0.95 regulatory limit.

The results of the analyses for the MPC-24, which were performed for all assemblies in each class, further confirm the validity of the bounding dimensions established in Subsection 6.2.1. Thus, for all following calculations, namely analyses of the MPC-24E, only the bounding assembly in a class is analyzed. For the MPC-32 with burnup credit, the validity of the bounding dimensions is verified in Appendix 6.C and Appendix 6.E.

### 6.2.3 BWR Fuel Assemblies in the MPC-68

For BWR fuel assemblies (specifications listed in Table 6.2.1) the artificial bounding assembly for the 10x10A assembly class at 4.2% enrichment has the highest reactivity (see Table 6.2.32). Calculations for the various BWR fuel assemblies in the MPC-68 are summarized in Tables 6.2.20 through 6.2.36 and 6.2.44 for the fully flooded condition. In all cases, the gadolinia ( $\text{Gd}_2\text{O}_3$ ) normally incorporated in BWR fuel was conservatively neglected and the fuel assembly was assumed to be centered in the fuel storage location.

For calculations involving BWR assemblies, the use of a uniform (planar-average) enrichment, as opposed to the distributed enrichments normally used in BWR fuel, produces conservative results. Calculations confirming this statement are presented in Appendix 6.B for several representative BWR fuel assembly designs. These calculations justify the specification of planar-average enrichments to define acceptability of BWR fuel for loading into the MPC-68.

Tables 6.2.20 through 6.2.36 and 6.2.44 show the maximum  $k_{\text{eff}}$  values for assembly classes that are acceptable for storage in the MPC-68. All maximum  $k_{\text{eff}}$  values include the bias, uncertainties, and calculational statistics, evaluated for the worst combination of manufacturing tolerances. With the exception of assembly classes 6x6A, 6x6B, 6x6C, 7x7A, and 8x8A, which will be discussed in Section 6.2.4, all calculations for the MPC-68 were performed with a  $^{10}\text{B}$  loading of  $0.0279 \text{ g/cm}^2$ , which is 75% of the minimum loading of  $0.0372 \text{ g/cm}^2$  for Boral, or 90% of the minimum loading of  $0.031 \text{ g/cm}^2$  for Metamic, specified for the MPC-68 in Section

1.4. Calculations for assembly classes 6x6A, 6x6B, 6x6C, 7x7A, and 8x8A were conservatively performed with a  $^{10}\text{B}$  loading of  $0.0067 \text{ g/cm}^2$ . The maximum allowable enrichment in the MPC-68 varies from 2.7 to 4.2 wt%  $^{235}\text{U}$ , depending on the assembly class. It should be noted that the maximum allowable enrichment does not vary within an assembly class. Table 6.1.2 summarizes the maximum allowable enrichments for all assembly classes that are acceptable for storage in the MPC-68.

Tables 6.2.20 through 6.2.36 and 6.2.44 are formatted with the assembly class information in the top row, the unique assembly designations, dimensions, and  $k_{\text{eff}}$  values in the following rows above the bold double lines, and the bounding dimensions selected to define the authorized contents and corresponding bounding  $k_{\text{eff}}$  values in the final rows. Where an assembly class contains only a single assembly (e.g., 8x8E, see Table 6.2.24), the authorized contents dimensions are based on the assembly dimensions from that single assembly. For assembly classes that are suspected to contain assemblies with thicker channels (e.g., 120 mils), bounding calculations are also performed to qualify the thicker channels (e.g. 7x7B, see Table 6.2.20). All of the maximum  $k_{\text{eff}}$  values corresponding to the selected bounding dimensions are shown to be greater than or equal to those for the actual assembly dimensions and are below the 0.95 regulatory limit.

For assembly classes that contain partial length rods (i.e., 9x9A, 10x10A, and 10x10B), calculations were performed for the actual (real) assembly configuration and for the axial segments (assumed to be full length) with and without the partial length rods. In all cases, the axial segment with only the full length rods present (where the partial length rods are absent) is bounding. Therefore, the bounding maximum  $k_{\text{eff}}$  values reported for assembly classes that contain partial length rods bound the reactivity regardless of the active fuel length of the partial length rods. As a result, the specification of authorized contents has no minimum requirement for the active fuel length of the partial length rods.

For BWR fuel assembly classes where margins permit, the Zircaloy water rod tubes are artificially replaced by water in the bounding cases to remove the requirement for water rod thickness from the specification of authorized contents. For these cases, the bounding water rod thickness is listed as zero.

As mentioned, the highest observed maximum  $k_{\text{eff}}$  value† corresponds to the artificial bounding assembly in the 10x10A assembly class. This assembly has the following bounding characteristics: (1) the partial length rods are assumed to be zero length (most reactive configuration); (2) the channel is assumed to be 120 mils thick; and (3) the active fuel length of the full length rods is 155 inches.

---

† Assuming assemblies are centered in their basket position. For cases with eccentric positioning see Section 6.3.3.

#### 6.2.4 Damaged BWR Fuel Assemblies and BWR Fuel Debris

In addition to storing intact PWR and BWR fuel assemblies, the HI-STAR 100 System is designed to store damaged BWR fuel assemblies and BWR fuel debris. Damaged fuel assemblies and fuel debris are defined in Chapter 1. Both damaged BWR fuel assemblies and BWR fuel debris are required to be loaded into Damaged Fuel Containers (DFCs). Two different DFC types with slightly different cross sections are considered. DFCs containing fuel debris are only analyzed in the MPC-68F. DFCs containing damaged fuel assemblies may be stored in either the MPC-68 or MPC-68F. The criticality evaluation of various possible damaged conditions of the fuel is presented in Subsection 6.4.4 for both DFC types.

Tables 6.2.37 through 6.2.41 show the maximum  $k_{\text{eff}}$  values for the six assembly classes that may be stored as damaged fuel or fuel debris. All maximum  $k_{\text{eff}}$  values include the bias, uncertainties, and calculational statistics, evaluated for the worst combination of manufacturing tolerances. All calculations were performed for a  $^{10}\text{B}$  loading of  $0.0067 \text{ g/cm}^2$ , which is 75% of a minimum loading,  $0.0089 \text{ g/cm}^2$ . However, because the practical manufacturing lower limit for minimum  $^{10}\text{B}$  loading is  $0.01 \text{ g/cm}^2$ , the minimum  $^{10}\text{B}$  loading of  $0.01 \text{ g/cm}^2$  is specified in Section 1.4, for the MPC-68F. As an additional level of conservatism in the analyses, the calculations were performed for an enrichment of 3.0 wt%  $^{235}\text{U}$ , while the maximum allowable enrichment for these assembly classes is limited to 2.7 wt%  $^{235}\text{U}$  in the specification of authorized contents. Therefore, the maximum  $k_{\text{eff}}$  values for damaged BWR fuel assemblies and fuel debris are conservative. Calculations for the various BWR fuel assemblies in the MPC-68F are summarized in Tables 6.2.37 through 6.2.41 for the fully flooded condition.

For the assemblies that may be stored as damaged fuel or fuel debris, the 6x6C01 assembly at 3.0 wt%  $^{235}\text{U}$  enrichment has the highest reactivity (see Table 6.2.39). Considering all of the conservatism built into this analysis (e.g., higher than allowed enrichment and lower than actual  $^{10}\text{B}$  loading), the actual reactivity will be lower.

Because the analysis for the damaged BWR fuel assemblies and fuel debris was performed for a minimum  $^{10}\text{B}$  loading of  $0.0089 \text{ g/cm}^2$ , which conservatively bounds damaged BWR fuel assemblies in a standard MPC-68 with a minimum  $^{10}\text{B}$  loading of at least  $0.0310 \text{ g/cm}^2$ , damaged BWR fuel assemblies may also be stored in the standard MPC-68. However, fuel debris is limited to the MPC-68F by the specification of authorized contents in Chapter 1.

Tables 6.2.37 through 6.2.41 are formatted with the assembly class information in the top row, the unique assembly designations, dimensions, and  $k_{\text{eff}}$  values in the following rows above the bold double lines, and the bounding dimensions selected to define the authorized contents and corresponding bounding  $k_{\text{eff}}$  values in the final rows. Where an assembly class contains only a single assembly (e.g., 6x6C, see Table 6.2.39), the authorized contents dimensions are based on the assembly dimensions from that single assembly. All of the maximum  $k_{\text{eff}}$  values corresponding to the selected bounding dimensions are greater than or equal to those for the actual assembly dimensions and are well below the 0.95 regulatory limit.

### 6.2.5 Thoria Rod Canister

Additionally, the HI-STAR 100 System is designed to store a Thoria Rod Canister in the MPC68 or MPC68F. The canister is similar to a DFC and contains 18 intact Thoria Rods placed in a separator assembly. The reactivity of the canister in the MPC68 or MPC68F is very low compared to the reactivity of the approved fuel assemblies (The  $^{235}\text{U}$  content of these rods corresponds to  $\text{UO}_2$  rods with an initial enrichment of approximately 1.5 wt%  $^{235}\text{U}$ ). It is therefore permissible to store the Thoria Rod Canister together with any other approved content in a MPC68 or MPC68F. Specifications of the canister and the Thoria Rods that are used in the criticality evaluation are given in Table 6.2.42. The criticality evaluation is presented in Subsection 6.4.6.

### 6.2.6 PWR Assemblies in the MPC-24E and MPC-24EF

The MPC-24E and MPC-24EF are variations of the MPC-24, which provide for transportation of higher enriched fuel than the MPC-24 through an increased  $^{10}\text{B}$  loading in the neutron absorber. The maximum allowable fuel enrichment varies between 4.2 and 5.0 wt%  $^{235}\text{U}$ , depending on the assembly class. The maximum allowable enrichment for each assembly class is listed in Table 6.1.5, together with the maximum  $k_{\text{eff}}$  for the bounding assembly in the assembly class. All maximum  $k_{\text{eff}}$  values are below the 0.95 regulatory limit. The 15x15F assembly class at 4.5% enrichment has the highest reactivity.

### 6.2.7 PWR Intact Fuel, Damaged Fuel and Fuel Debris in the Trojan MPC-24E/EF

The Trojan MPC-24E and MPC-24EF are variations of the MPC-24E/EF, designed to transport Trojan intact and damaged PWR fuel assemblies and fuel debris. Damaged PWR fuel assemblies and fuel debris are required to be loaded into PWR Damaged Fuel Containers (DFCs) or Failed Fuel Cans. Up to four DFCs may be loaded in the MPC-24E or MPC-24EF. The maximum enrichment for intact fuel, damaged fuel and fuel debris is 3.7 wt%  $^{235}\text{U}$ . Only the assembly class 17x17B is certified for the Trojan MPC-24E/EF. The maximum  $k_{\text{eff}}$  is listed in Table 6.1.6. The criticality evaluation of the damaged fuel is presented in Subsection 6.4.9.

### 6.2.8 PWR Assemblies in the MPC-32

Burnup credit is necessary to store PWR assemblies in the MPC-32, i.e. a required minimum average assembly burnup is specified as a function of the assembly initial enrichment. Only the assembly classes 15x15D, E, F, H and 17x17A, B, C are certified for transportation in the MPC-32. The maximum initial enrichment is 5.0 wt%  $^{235}\text{U}$ . The criticality evaluations for burnup credit are presented in Appendix 6.C and Appendix 6.E.

Table 6.2.1 (page 1 of 6)  
 BWR FUEL CHARACTERISTICS AND ASSEMBLY CLASS DEFINITIONS  
 (all dimensions are in inches)

Fuel Assembly Designation	Clad Material	Pitch	Number of Fuel Rods	Cladding OD	Cladding Thickness	Pellet Diameter	Active Fuel Length	Number of Water Rods	Water Rod OD	Water Rod ID	Channel Thickness	Channel ID
6x6A Assembly Class												
6x6A01	Zr	0.694	36	0.5645	0.0350	0.4940	110.0	0	n/a	n/a	0.060	4.290
6x6A02	Zr	0.694	36	0.5645	0.0360	0.4820	110.0	0	n/a	n/a	0.060	4.290
6x6A03	Zr	0.694	36	0.5645	0.0350	0.4820	110.0	0	n/a	n/a	0.060	4.290
6x6A04	Zr	0.694	36	0.5550	0.0350	0.4820	110.0	0	n/a	n/a	0.060	4.290
6x6A05	Zr	0.696	36	0.5625	0.0350	0.4820	110.0	0	n/a	n/a	0.060	4.290
6x6A06	Zr	0.696	35	0.5625	0.0350	0.4820	110.0	1	0.0	0.0	0.060	4.290
6x6A07	Zr	0.700	36	0.5555	0.03525	0.4780	110.0	0	n/a	n/a	0.060	4.290
6x6A08	Zr	0.710	36	0.5625	0.0260	0.4980	110.0	0	n/a	n/a	0.060	4.290
6x6B (MOX) Assembly Class												
6x6B01	Zr	0.694	36	0.5645	0.0350	0.4820	110.0	0	n/a	n/a	0.060	4.290
6x6B02	Zr	0.694	36	0.5625	0.0350	0.4820	110.0	0	n/a	n/a	0.060	4.290
6x6B03	Zr	0.696	36	0.5625	0.0350	0.4820	110.0	0	n/a	n/a	0.060	4.290
6x6B04	Zr	0.696	35	0.5625	0.0350	0.4820	110.0	1	0.0	0.0	0.060	4.290
6x6B05	Zr	0.710	35	0.5625	0.0350	0.4820	110.0	1	0.0	0.0	0.060	4.290
6x6C Assembly Class												
6x6C01	Zr	0.740	36	0.5630	0.0320	0.4880	77.5	0	n/a	n/a	0.060	4.542
7x7A Assembly Class												
7x7A01	Zr	0.631	49	0.4860	0.0328	0.4110	80	0	n/a	n/a	0.060	4.542

HI-STAR SAR

REPORT HI-951251

Rev. 16

6.2-7

Table 6.2.1 (page 2 of 6)  
 BWR FUEL CHARACTERISTICS AND ASSEMBLY CLASS DEFINITIONS  
 (all dimensions are in inches)

Fuel Assembly Designation	Clad Material	Pitch	Number of Fuel Rods	Cladding OD	Cladding Thickness	Pellet Diameter	Active Fuel Length	Number of Water Rods	Water Rod OD	Water Rod ID	Channel Thickness	Channel ID
7x7B Assembly Class												
7x7B01	Zr	0.738	49	0.5630	0.0320	0.4870	150	0	n/a	n/a	0.080	5.278
7x7B02	Zr	0.738	49	0.5630	0.0370	0.4770	150	0	n/a	n/a	0.102	5.291
7x7B03	Zr	0.738	49	0.5630	0.0370	0.4770	150	0	n/a	n/a	0.080	5.278
7x7B04	Zr	0.738	49	0.5700	0.0355	0.4880	150	0	n/a	n/a	0.080	5.278
7x7B05	Zr	0.738	49	0.5630	0.0340	0.4775	150	0	n/a	n/a	0.080	5.278
7x7B06	Zr	0.738	49	0.5700	0.0355	0.4910	150	0	n/a	n/a	0.080	5.278
8x8A Assembly Class												
8x8A01	Zr	0.523	64	0.4120	0.0250	0.3580	110	0	n/a	n/a	0.100	4.290
8x8A02	Zr	0.523	63	0.4120	0.0250	0.3580	120	0	n/a	n/a	0.100	4.290

Table 6.2.1 (page 3 of 6)  
 BWR FUEL CHARACTERISTICS AND ASSEMBLY CLASS DEFINITIONS  
 (all dimensions are in inches)

Fuel Assembly Designation	Clad Material	Pitch	Number of Fuel Rods	Cladding OD	Cladding Thickness	Pellet Diameter	Active Fuel Length	Number of Water Rods	Water Rod OD	Water Rod ID	Channel Thickness	Channel ID
8x8B Assembly Class												
8x8B01	Zr	0.641	63	0.4840	0.0350	0.4050	150	1	0.484	0.414	0.100	5.278
8x8B02	Zr	0.636	63	0.4840	0.0350	0.4050	150	1	0.484	0.414	0.100	5.278
8x8B03	Zr	0.640	63	0.4930	0.0340	0.4160	150	1	0.493	0.425	0.100	5.278
8x8B04	Zr	0.642	64	0.5015	0.0360	0.4195	150	0	n/a	n/a	0.100	5.278
8x8C Assembly Class												
8x8C01	Zr	0.641	62	0.4840	0.0350	0.4050	150	2	0.484	0.414	0.100	5.278
8x8C02	Zr	0.640	62	0.4830	0.0320	0.4100	150	2	0.591	0.531	0.000	no channel
8x8C03	Zr	0.640	62	0.4830	0.0320	0.4100	150	2	0.591	0.531	0.080	5.278
8x8C04	Zr	0.640	62	0.4830	0.0320	0.4100	150	2	0.591	0.531	0.100	5.278
8x8C05	Zr	0.640	62	0.4830	0.0320	0.4100	150	2	0.591	0.531	0.120	5.278
8x8C06	Zr	0.640	62	0.4830	0.0320	0.4110	150	2	0.591	0.531	0.100	5.278
8x8C07	Zr	0.640	62	0.4830	0.0340	0.4100	150	2	0.591	0.531	0.100	5.278
8x8C08	Zr	0.640	62	0.4830	0.0320	0.4100	150	2	0.493	0.425	0.100	5.278
8x8C09	Zr	0.640	62	0.4930	0.0340	0.4160	150	2	0.493	0.425	0.100	5.278
8x8C10	Zr	0.640	62	0.4830	0.0340	0.4100	150	2	0.591	0.531	0.120	5.278
8x8C11	Zr	0.640	62	0.4830	0.0340	0.4100	150	2	0.591	0.531	0.120	5.215
8x8C12	Zr	0.636	62	0.4830	0.0320	0.4110	150	2	0.591	0.531	0.120	5.215

Table 6.2.1 (page 4 of 6)  
 BWR FUEL CHARACTERISTICS AND ASSEMBLY CLASS DEFINITIONS  
 (all dimensions are in inches)

Fuel Assembly Designation	Clad Material	Pitch	Number of Fuel Rods	Cladding OD	Cladding Thickness	Pellet Diameter	Active Fuel Length	Number of Water Rods	Water Rod OD	Water Rod ID	Channel Thickness	Channel ID
8x8D Assembly Class												
8x8D01	Zr	0.640	60	0.4830	0.0320	0.4110	150	2 large/ 2 small	0.591/ 0.483	0.531/ 0.433	0.100	5.278
8x8D02	Zr	0.640	60	0.4830	0.0320	0.4110	150	4	0.591	0.531	0.100	5.278
8x8D03	Zr	0.640	60	0.4830	0.0320	0.4110	150	4	0.483	0.433	0.100	5.278
8x8D04	Zr	0.640	60	0.4830	0.0320	0.4110	150	1	1.34	1.26	0.100	5.278
8x8D05	Zr	0.640	60	0.4830	0.0320	0.4100	150	1	1.34	1.26	0.100	5.278
8x8D06	Zr	0.640	60	0.4830	0.0320	0.4110	150	1	1.34	1.26	0.120	5.278
8x8D07	Zr	0.640	60	0.4830	0.0320	0.4110	150	1	1.34	1.26	0.080	5.278
8x8D08	Zr	0.640	61	0.4830	0.0300	0.4140	150	3	0.591	0.531	0.080	5.278
8x8E Assembly Class												
8x8E01	Zr	0.640	59	0.4930	0.0340	0.4160	150	5	0.493	0.425	0.100	5.278
8x8F Assembly Class												
8x8F01	Zr	0.609	64	0.4576	0.0290	0.3913	150	4 <sup>†</sup>	0.291 <sup>†</sup>	0.228 <sup>†</sup>	0.055	5.390
9x9A Assembly Class												
9x9A01	Zr	0.566	74	0.4400	0.0280	0.3760	150	2	0.98	0.92	0.100	5.278
9x9A02	Zr	0.566	66	0.4400	0.0280	0.3760	150	2	0.98	0.92	0.100	5.278
9x9A03	Zr	0.566	74/66	0.4400	0.0280	0.3760	150/90	2	0.98	0.92	0.100	5.278
9x9A04	Zr	0.566	66	0.4400	0.0280	0.3760	150	2	0.98	0.92	0.120	5.278

<sup>†</sup> Four rectangular water cross segments dividing the assembly into four quadrants

HI-STAR SAR

Rev. 16

REPORT HI-951251

6.2-10



Table 6.2.1 (page 5 of 6)  
 BWR FUEL CHARACTERISTICS AND ASSEMBLY CLASS DEFINITIONS  
 (all dimensions are in inches)

Fuel Assembly Designation	Clad Material	Pitch	Number of Fuel Rods	Cladding OD	Cladding Thickness	Pellet Diameter	Active Fuel Length	Number of Water Rods	Water Rod OD	Water Rod ID	Channel Thickness	Channel ID
9x9B Assembly Class												
9x9B01	Zr	0.569	72	0.4330	0.0262	0.3737	150	1	1.516	1.459	0.100	5.278
9x9B02	Zr	0.569	72	0.4330	0.0260	0.3737	150	1	1.516	1.459	0.100	5.278
9x9B03	Zr	0.572	72	0.4330	0.0260	0.3737	150	1	1.516	1.459	0.100	5.278
9x9C Assembly Class												
9x9C01	Zr	0.572	80	0.4230	0.0295	0.3565	150	1	0.512	0.472	0.100	5.278
9x9D Assembly Class												
9x9D01	Zr	0.572	79	0.4240	0.0300	0.3565	150	2	0.424	0.364	0.100	5.278
9x9E Assembly Class <sup>†</sup>												
9x9E01	Zr	0.572	76	0.4170	0.0265	0.3530	150	5	0.546	0.522	0.120	5.215
9x9E02	Zr	0.572	48 28	0.4170 0.4430	0.0265 0.0285	0.3530 0.3745	150	5	0.546	0.522	0.120	5.215
9x9F Assembly Class <sup>†</sup>												
9x9F01	Zr	0.572	76	0.4430	0.0285	0.3745	150	5	0.546	0.522	0.120	5.215
9x9F02	Zr	0.572	48 28	0.4170 0.4430	0.0265 0.0285	0.3530 0.3745	150	5	0.546	0.522	0.120	5.215
9x9G Assembly Class												
9x9G01	Zr	0.572	72	0.4240	0.0300	0.3565	150	1	1.668	1.604	0.120	5.278

<sup>†</sup> The 9x9E and 9x9F fuel assembly classes represent a single fuel type containing fuel rods with different dimensions (SPC 9x9-5). In addition to the actual configuration (9x9E02 and 9x9F02), the 9x9E class contains a hypothetical assembly with only small fuel rods (9x9E01), and the 9x9F class contains a hypothetical assembly with only large rods (9x9F01). This was done in order to simplify the specification of this assembly for the authorized contents.

Table 6.2.1 (page 6 of 6)  
BWR FUEL CHARACTERISTICS AND ASSEMBLY CLASS DEFINITIONS  
(all dimensions are in inches)

Fuel Assembly Designation	Clad Material	Pitch	Number of Fuel Rods	Cladding OD	Cladding Thickness	Pellet Diameter	Active Fuel Length	Number of Water Rods	Water Rod OD	Water Rod ID	Channel Thickness	Channel ID
10x10A Assembly Class												
10x10A01	Zr	0.510	92	0.4040	0.0260	0.3450	155	2	0.980	0.920	0.100	5.278
10x10A02	Zr	0.510	78	0.4040	0.0260	0.3450	155	2	0.980	0.920	0.100	5.278
10x10A03	Zr	0.510	92/78	0.4040	0.0260	0.3450	155/90	2	0.980	0.920	0.100	5.278
10x10B Assembly Class												
10x10B01	Zr	0.510	91	0.3957	0.0239	0.3413	155	1	1.378	1.321	0.100	5.278
10x10B02	Zr	0.510	83	0.3957	0.0239	0.3413	155	1	1.378	1.321	0.100	5.278
10x10B03	Zr	0.510	91/83	0.3957	0.0239	0.3413	155/90	1	1.378	1.321	0.100	5.278
10x10C Assembly Class												
10x10C01	Zr	0.488	96	0.3780	0.0243	0.3224	150	5	1.227	1.165	0.055	5.457
10x10D Assembly Class												
10x10D01	SS	0.565	100	0.3960	0.0200	0.3500	83	0	n/a	n/a	0.08	5.663
10x10E Assembly Class												
10x10E01	SS	0.557	96	0.3940	0.0220	0.3430	83	4	0.3940	0.3500	0.08	5.663

Table 6.2.2 (page 1 of 4)  
PWR FUEL CHARACTERISTICS AND ASSEMBLY CLASS DEFINITIONS  
(all dimensions are in inches)

Fuel Assembly Designation	Clad Material	Pitch	Number of Fuel Rods	Cladding OD	Cladding Thickness	Pellet Diameter	Active Fuel Length	Number of Guide Tubes	Guide Tube OD	Guide Tube ID	Guide Tube Thickness
14x14A Assembly Class											
14x14A01	Zr	0.556	179	0.400	0.0243	0.3444	150	17	0.527	0.493	0.0170
14x14A02	Zr	0.556	179	0.400	0.0243	0.3444	150	17	0.528	0.490	0.0190
14x14A03	Zr	0.556	179	0.400	0.0243	0.3444	150	17	0.526	0.492	0.0170
14x14B Assembly Class											
14x14B01	Zr	0.556	179	0.422	0.0243	0.3659	150	17	0.539	0.505	0.0170
14x14B02	Zr	0.556	179	0.417	0.0295	0.3505	150	17	0.541	0.507	0.0170
14x14B03	Zr	0.556	179	0.424	0.0300	0.3565	150	17	0.541	0.507	0.0170
14x14B04	Zr	0.556	179	0.426	0.0310	0.3565	150	17	0.541	0.507	0.0170
14x14C Assembly Class											
14x14C01	Zr	0.580	176	0.440	0.0280	0.3765	150	5	1.115	1.035	0.0400
14x14C02	Zr	0.580	176	0.440	0.0280	0.3770	150	5	1.115	1.035	0.0400
14x14C03	Zr	0.580	176	0.440	0.0260	0.3805	150	5	1.111	1.035	0.0380
14x14D Assembly Class											
14x14D01	SS	0.556	180	0.422	0.0165	0.3835	144	16	0.543	0.514	0.0145

Table 6.2.2 (page 2 of 4)  
PWR FUEL CHARACTERISTICS AND ASSEMBLY CLASS DEFINITIONS  
(all dimensions are in inches)

Fuel Assembly Designation	Clad Material	Pitch	Number of Fuel Rods	Cladding OD	Cladding Thickness	Pellet Diameter	Active Fuel Length	Number of Guide Tubes	Guide Tube OD	Guide Tube ID	Guide Tube Thickness
14x14E Assembly Class											
14x14E01†	SS	0.453 and 0.441	162 3 8	0.3415 0.3415 0.3415	0.0120 0.0285 0.0200	0.313 0.280 0.297	102	0	n/a	n/a	n/a
14x14E02†	SS	0.453 and 0.441	173	0.3415	0.0120	0.313	102	0	n/a	n/a	n/a
14x14E03†	SS	0.453 and 0.441	173	0.3415	0.0285	0.280	102	0	n/a	n/a	n/a
15x15A Assembly Class											
15x15A01	Zr	0.550	204	0.418	0.0260	0.3580	150	21	0.533	0.500	0.0165

† This is the fuel assembly used at Indian Point 1 (IP-1). This assembly is a 14x14 assembly with 23 fuel rods omitted to allow passage of control rods between assemblies. It has a different pitch in different sections of the assembly, and different fuel rod dimensions in some rods.

Table 6.2.2 (page 3 of 4)  
PWR FUEL CHARACTERISTICS AND ASSEMBLY CLASS DEFINITIONS  
(all dimensions are in inches)

Fuel Assembly Designation	Clad Material	Pitch	Number of Fuel Rods	Cladding OD	Cladding Thickness	Pellet Diameter	Active Fuel Length	Number of Guide Tubes	Guide Tube OD	Guide Tube ID	Guide Tube Thickness
15x15B Assembly Class											
15x15B01	Zr	0.563	204	0.422	0.0245	0.3660	150	21	0.533	0.499	0.0170
15x15B02	Zr	0.563	204	0.422	0.0245	0.3660	150	21	0.546	0.512	0.0170
15x15B03	Zr	0.563	204	0.422	0.0243	0.3660	150	21	0.533	0.499	0.0170
15x15B04	Zr	0.563	204	0.422	0.0243	0.3659	150	21	0.545	0.515	0.0150
15x15B05	Zr	0.563	204	0.422	0.0242	0.3659	150	21	0.545	0.515	0.0150
15x15B06	Zr	0.563	204	0.420	0.0240	0.3671	150	21	0.544	0.514	0.0150
15x15C Assembly Class											
15x15C01	Zr	0.563	204	0.424	0.0300	0.3570	150	21	0.544	0.493	0.0255
15x15C02	Zr	0.563	204	0.424	0.0300	0.3570	150	21	0.544	0.511	0.0165
15x15C03	Zr	0.563	204	0.424	0.0300	0.3565	150	21	0.544	0.511	0.0165
15x15C04	Zr	0.563	204	0.417	0.0300	0.3565	150	21	0.544	0.511	0.0165
15x15D Assembly Class											
15x15D01	Zr	0.568	208	0.430	0.0265	0.3690	150	17	0.530	0.498	0.0160
15x15D02	Zr	0.568	208	0.430	0.0265	0.3686	150	17	0.530	0.498	0.0160
15x15D03	Zr	0.568	208	0.430	0.0265	0.3700	150	17	0.530	0.499	0.0155
15x15D04	Zr	0.568	208	0.430	0.0250	0.3735	150	17	0.530	0.500	0.0150
15x15E Assembly Class											
15x15E01	Zr	0.568	208	0.428	0.0245	0.3707	150	17	0.528	0.500	0.0140
15x15F Assembly Class											
15x15F01	Zr	0.568	208	0.428	0.0230	0.3742	150	17	0.528	0.500	0.0140

Table 6.2.2 (page 4 of 4)  
PWR FUEL CHARACTERISTICS AND ASSEMBLY CLASS DEFINITIONS  
(all dimensions are in inches)

Fuel Assembly Designation	Clad Material	Pitch	Number of Fuel Rods	Cladding OD	Cladding Thickness	Pellet Diameter	Active Fuel Length	Number of Guide Tubes	Guide Tube OD	Guide Tube ID	Guide Tube Thickness
15x15G Assembly Class											
15x15G01	SS	0.563	204	0.422	0.0165	0.3825	144	21	0.543	0.514	0.0145
15x15H Assembly Class											
15x15H01	Zr	0.568	208	0.414	0.0220	0.3622	150	17	0.528	0.500	0.0140
16x16A Assembly Class											
16x16A01	Zr	0.506	236	0.382	0.0250	0.3255	150	5	0.980	0.900	0.0400
16x16A02	Zr	0.506	236	0.382	0.0250	0.3250	150	5	0.980	0.900	0.0400
17x17A Assembly Class											
17x17A01	Zr	0.496	264	0.360	0.0225	0.3088	150	25	0.474	0.442	0.0160
17x17A02	Zr	0.496	264	0.360	0.0250	0.3030	150	25	0.480	0.448	0.0160
17x17B Assembly Class											
17x17B01	Zr	0.496	264	0.374	0.0225	0.3225	150	25	0.482	0.450	0.0160
17x17B02	Zr	0.496	264	0.374	0.0225	0.3225	150	25	0.474	0.442	0.0160
17x17B03	Zr	0.496	264	0.376	0.0240	0.3215	150	25	0.480	0.448	0.0160
17x17B04	Zr	0.496	264	0.372	0.0205	0.3232	150	25	0.427	0.399	0.0140
17x17B05	Zr	0.496	264	0.374	0.0240	0.3195	150	25	0.482	0.450	0.0160
17x17B06	Zr	0.496	264	0.372	0.0205	0.3232	150	25	0.480	0.452	0.0140
17x17C Assembly Class											
17x17C01	Zr	0.502	264	0.379	0.0240	0.3232	150	25	0.472	0.432	0.0200
17x17C02	Zr	0.502	264	0.377	0.0220	0.3252	150	25	0.472	0.432	0.0200

Table 6.2.3  
[PROPRIETARY INFORMATION WITHHELD PER 10CFR2.390]

Table 6.2.4  
 MAXIMUM  $K_{\text{EFF}}$  VALUES FOR THE 14X14A ASSEMBLY CLASS IN THE MPC-24  
 (all dimensions are in inches)

14x14A (4.6% Enrichment, Fixed neutron absorber $^{10}\text{B}$ minimum loading of 0.02 g/cm <sup>2</sup> ) 179 fuel rods, 17 guide tubes, pitch=0.556, Zr clad										
Fuel Assembly Designation	maximum $k_{\text{eff}}$	calculated $k_{\text{eff}}$	standard deviation	EALF	cladding OD	cladding ID	cladding thickness	pellet OD	fuel length	guide tube thickness
14x14A01	0.9295	0.9252	0.0008	0.2084	0.400	0.3514	0.0243	0.3444	150	0.017
14x14A02	0.9286	0.9242	0.0008	0.2096	0.400	0.3514	0.0243	0.3444	150	0.019
14x14A03	0.9296	0.9253	0.0008	0.2093	0.400	0.3514	0.0243	0.3444	150	0.017
Dimensions Listed for Authorized Contents					0.400 (min.)	0.3514 (max.)		0.3444 (max.)	150 (max.)	0.017 (min.)
bounding dimensions (14x14A03)	0.9296	0.9253	0.0008	0.2093	0.400	0.3514	0.0243	0.3444	150	0.017



Table 6.2.5  
 MAXIMUM  $K_{\text{EFF}}$  VALUES FOR THE 14X14B ASSEMBLY CLASS IN THE MPC-24  
 (all dimensions are in inches)

14x14B (4.6% Enrichment, Fixed neutron absorber $^{10}\text{B}$ minimum loading of 0.02 g/cm <sup>2</sup> ) 179 fuel rods, 17 guide tubes, pitch=0.556, Zr clad										
Fuel Assembly Designation	maximum $k_{\text{eff}}$	calculated $k_{\text{eff}}$	standard deviation	EALF	cladding OD	cladding ID	cladding thickness	pellet OD	fuel length	guide tube thickness
14x14B01	0.9159	0.9117	0.0007	0.2727	0.422	0.3734	0.0243	0.3659	150	0.017
14x14B02	0.9169	0.9126	0.0008	0.2345	0.417	0.3580	0.0295	0.3505	150	0.017
14x14B03	0.9110	0.9065	0.0009	0.2545	0.424	0.3640	0.0300	0.3565	150	0.017
14x14B04	0.9084	0.9039	0.0009	0.2563	0.426	0.3640	0.0310	0.3565	150	0.017
Dimensions Listed for Authorized Contents					0.417 (min.)	0.3734 (max.)		0.3659 (max.)	150 (max.)	0.017 (min.)
bounding dimensions (B14x14B01)	0.9228	0.9185	0.0008	0.2675	0.417	0.3734	0.0218	0.3659	150	0.017

Table 6.2.6  
 MAXIMUM  $K_{\text{EFF}}$  VALUES FOR THE 14X14C ASSEMBLY CLASS IN THE MPC-24  
 (all dimensions are in inches)

14x14C (4.6% Enrichment, Fixed neutron absorber $^{10}\text{B}$ minimum loading of 0.02 g/cm <sup>2</sup> ) 176 fuel rods, 5 guide tubes, pitch=0.580, Zr clad										
Fuel Assembly Designation	maximum $k_{\text{eff}}$	calculated $k_{\text{eff}}$	standard deviation	EALF	cladding OD	cladding ID	cladding thickness	pellet OD	fuel length	guide tube thickness
14x14C01	0.9258	0.9215	0.0008	0.2729	0.440	0.3840	0.0280	0.3765	150	0.040
14x14C02	0.9265	0.9222	0.0008	0.2765	0.440	0.3840	0.0280	0.3770	150	0.040
14x14C03	0.9287	0.9242	0.0009	0.2825	0.440	0.3880	0.0260	0.3805	150	0.038
Dimensions Listed for Authorized Contents					0.440 (min.)	0.3880 (max.)		0.3805 (max.)	150 (max.)	0.038 (min.)
bounding dimensions (14x14C03)	0.9287	0.9242	0.0009	0.2825	0.440	0.3880	0.0260	0.3805	150	0.038

Table 6.2.7  
 MAXIMUM  $K_{\text{EFF}}$  VALUES FOR THE 14X14D ASSEMBLY CLASS IN THE MPC-24  
 (all dimensions are in inches)

14x14D (4.0% Enrichment, Fixed neutron absorber $^{10}\text{B}$ minimum loading of 0.02 g/cm <sup>2</sup> ) 180 fuel rods, 16 guide tubes, pitch=0.556, SS clad										
Fuel Assembly Designation	maximum $k_{\text{eff}}$	calculated $k_{\text{eff}}$	standard deviation	EALF	cladding OD	cladding ID	cladding thickness	pellet OD	fuel length	guide tube thickness
14x14D01	0.8507	0.8464	0.0008	0.3308	0.422	0.3890	0.0165	0.3835	144	0.0145
Dimensions Listed for Authorized Contents					0.422 (min.)	0.3890 (max.)		0.3835 (max.)	144 (max.)	0.0145 (min.)

Table 6.2.8  
 MAXIMUM  $K_{\text{EFF}}$  VALUES FOR THE 15X15A ASSEMBLY CLASS IN THE MPC-24  
 (all dimensions are in inches)

15x15A (4.1% Enrichment, Fixed neutron absorber $^{10}\text{B}$ minimum loading of 0.02 g/cm <sup>2</sup> ) 204 fuel rods, 21 guide tubes, pitch=0.550, Zr clad										
Fuel Assembly Designation	maximum $k_{\text{eff}}$	calculated $k_{\text{eff}}$	standard deviation	EALF	cladding OD	cladding ID	cladding thickness	pellet OD	fuel length	guide tube thickness
15x15A01	0.9204	0.9159	0.0009	0.2608	0.418	0.3660	0.0260	0.3580	150	0.0165
Dimensions Listed for Authorized Contents					0.418 (min.)	0.3660 (max.)		0.3580 (max.)	150 (max.)	0.0165 (min.)

Table 6.2.9  
 MAXIMUM  $K_{\text{EFF}}$  VALUES FOR THE 15X15B ASSEMBLY CLASS IN THE MPC-24  
 (all dimensions are in inches)

15x15B (4.1% Enrichment, Fixed neutron absorber $^{10}\text{B}$ minimum loading of 0.02 g/cm <sup>2</sup> ) 204 fuel rods, 21 guide tubes, pitch=0.563, Zr clad										
Fuel Assembly Designation	maximum $k_{\text{eff}}$	calculated $k_{\text{eff}}$	standard deviation	EALF	cladding OD	cladding ID	cladding thickness	pellet OD	fuel length	guide tube thickness
15x15B01	0.9369	0.9326	0.0008	0.2632	0.422	0.3730	0.0245	0.3660	150	0.017
15x15B02	0.9338	0.9295	0.0008	0.2640	0.422	0.3730	0.0245	0.3660	150	0.017
15x15B03	0.9362	0.9318	0.0008	0.2632	0.422	0.3734	0.0243	0.3660	150	0.017
15x15B04	0.9370	0.9327	0.0008	0.2612	0.422	0.3734	0.0243	0.3659	150	0.015
15x15B05	0.9356	0.9313	0.0008	0.2606	0.422	0.3736	0.0242	0.3659	150	0.015
15x15B06	0.9366	0.9324	0.0007	0.2638	0.420	0.3720	0.0240	0.3671	150	0.015
Dimensions Listed for Authorized Contents					0.420 (min.)	0.3736 (max.)		0.3671 (max.)	150 (max.)	0.015 (min.)
bounding dimensions (B15x15B01)	0.9388	0.9343	0.0009	0.2626	0.420	0.3736	0.0232	0.3671	150	0.015

Table 6.2.10  
 MAXIMUM  $K_{\text{EFF}}$  VALUES FOR THE 15X15C ASSEMBLY CLASS IN THE MPC-24  
 (all dimensions are in inches)

15x15C (4.1% Enrichment, Fixed neutron absorber $^{10}\text{B}$ minimum loading of 0.02 g/cm <sup>2</sup> ) 204 fuel rods, 21 guide tubes, pitch=0.563, Zr clad										
Fuel Assembly Designation	maximum $k_{\text{eff}}$	calculated $k_{\text{eff}}$	standard deviation	EALF	cladding OD	cladding ID	cladding thickness	pellet OD	fuel length	guide tube thickness
15x15C01	0.9255	0.9213	0.0007	0.2493	0.424	0.3640	0.0300	0.3570	150	0.0255
15x15C02	0.9297	0.9255	0.0007	0.2457	0.424	0.3640	0.0300	0.3570	150	0.0165
15x15C03	0.9297	0.9255	0.0007	0.2440	0.424	0.3640	0.0300	0.3565	150	0.0165
15x15C04	0.9311	0.9268	0.0008	0.2435	0.417	0.3570	0.0300	0.3565	150	0.0165
Dimensions Listed for Authorized Contents					0.417 (min.)	0.3640 (max.)		0.3570 (max.)	150 (max.)	0.0165 (min.)
bounding dimensions (B15x15C01)	0.9361	0.9316	0.0009	0.2385	0.417	0.3640	0.0265	0.3570	150	0.0165

Table 6.2.11  
MAXIMUM  $K_{\text{EFF}}$  VALUES FOR THE 15X15D ASSEMBLY CLASS IN THE MPC-24  
(all dimensions are in inches)

15x15D (4.1% Enrichment, Fixed neutron absorber $^{10}\text{B}$ minimum loading of 0.02 g/cm <sup>2</sup> ) 208 fuel rods, 17 guide tubes, pitch=0.568, Zr clad										
Fuel Assembly Designation	maximum $k_{\text{eff}}$	calculated $k_{\text{eff}}$	standard deviation	EALF	cladding OD	cladding ID	cladding thickness	pellet OD	fuel length	guide tube thickness
15x15D01	0.9341	0.9298	0.0008	0.2822	0.430	0.3770	0.0265	0.3690	150	0.0160
15x15D02	0.9367	0.9324	0.0008	0.2802	0.430	0.3770	0.0265	0.3686	150	0.0160
15x15D03	0.9354	0.9311	0.0008	0.2844	0.430	0.3770	0.0265	0.3700	150	0.0155
15x15D04	0.9339	0.9292	0.0010	0.2958	0.430	0.3800	0.0250	0.3735	150	0.0150
Dimensions Listed for Authorized Contents					0.430 (min.)	0.3800 (max.)		0.3735 (max.)	150 (max.)	0.0150 (min.)
bounding dimensions (15x15D04)	0.9339 <sup>†</sup>	0.9292	0.0010	0.2958	0.430	0.3800	0.0250	0.3735	150	0.0150

<sup>†</sup> The  $k_{\text{eff}}$  value listed for the 15x15D02 case is slightly higher than that for the case with the bounding dimensions. However, calculations with significantly increased number of particles show that the two cases are statistically equivalent, with a maximum  $k_{\text{eff}}$  value of 0.9339. Nevertheless, the 15x15D02 case is used in Table 6.3.5 for the eccentric positioning analysis.

Table 6.2.12  
 MAXIMUM  $K_{\text{EFF}}$  VALUES FOR THE 15X15E ASSEMBLY CLASS IN THE MPC-24  
 (all dimensions are in inches)

15x15E (4.1% Enrichment, Fixed neutron absorber $^{10}\text{B}$ minimum loading of 0.02 g/cm <sup>2</sup> ) 208 fuel rods, 17 guide tubes, pitch=0.568, Zr clad										
Fuel Assembly Designation	maximum $k_{\text{eff}}$	calculated $k_{\text{eff}}$	standard deviation	EALF	cladding OD	cladding ID	cladding thickness	pellet OD	fuel length	guide tube thickness
15x15E01	0.9368	0.9325	0.0008	0.2826	0.428	0.3790	0.0245	0.3707	150	0.0140
Dimensions Listed for Authorized Contents					0.428 (min.)	0.3790 (max.)		0.3707 (max.)	150 (max.)	0.0140 (min.)



Table 6.2.13  
 MAXIMUM  $K_{\text{EFF}}$  VALUES FOR THE 15X15F ASSEMBLY CLASS IN THE MPC-24  
 (all dimensions are in inches)

15x15F (4.1% Enrichment, Fixed neutron absorber $^{10}\text{B}$ minimum loading of 0.02 g/cm <sup>2</sup> ) 208 fuel rods, 17 guide tubes, pitch=0.568, Zr clad										
Fuel Assembly Designation	maximum $k_{\text{eff}}$	calculated $k_{\text{eff}}$	standard deviation	EALF	cladding OD	cladding ID	cladding thickness	pellet OD	fuel length	guide tube thickness
15x15F01	0.9395 <sup>†</sup>	0.9350	0.0009	0.2903	0.428	0.3820	0.0230	0.3742	150	0.0140
Dimensions Listed for Authorized Contents					0.428 (min.)	0.3820 (max.)		0.3742 (max.)	150 (max.)	0.0140 (min.)

<sup>†</sup> KENO5a verification calculation resulted in a maximum  $k_{\text{eff}}$  of 0.9378.

Table 6.2.14  
 MAXIMUM  $K_{\text{EFF}}$  VALUES FOR THE 15X15G ASSEMBLY CLASS IN THE MPC-24  
 (all dimensions are in inches)

15x15G (4.0% Enrichment, Fixed neutron absorber $^{10}\text{B}$ minimum loading of 0.02 g/cm <sup>2</sup> ) 204 fuel rods, 21 guide tubes, pitch=0.563, SS clad										
Fuel Assembly Designation	maximum $k_{\text{eff}}$	calculated $k_{\text{eff}}$	standard deviation	EALF	cladding OD	cladding ID	cladding thickness	pellet OD	fuel <sup>†</sup> length	guide tube thickness
15x15G01	0.8876	0.8833	0.0008	0.3357	0.422	0.3890	0.0165	0.3825	144	0.0145
Dimensions Listed for Authorized Contents					0.422 (min.)	0.3890 (max.)		0.3825 (max.)	144 (max.)	0.0145 (min.)

---

<sup>†</sup> Calculations were conservatively performed for a fuel length of 150 inches.

Table 6.2.15  
 MAXIMUM  $K_{\text{EFF}}$  VALUES FOR THE 15X15H ASSEMBLY CLASS IN THE MPC-24  
 (all dimensions are in inches)

15x15H (3.8% Enrichment, Fixed neutron absorber $^{10}\text{B}$ minimum loading of 0.02 g/cm <sup>2</sup> ) 208 fuel rods, 17 guide tubes, pitch=0.568, Zr clad										
Fuel Assembly Designation	maximum $k_{\text{eff}}$	calculated $k_{\text{eff}}$	standard deviation	EALF	cladding OD	cladding ID	cladding thickness	pellet OD	fuel length	guide tube thickness
15x15H01	0.9337	0.9292	0.0009	0.2349	0.414	0.3700	0.0220	0.3622	150	0.0140
Dimensions Listed for Authorized Contents					0.414 (min.)	0.3700 (max.)		0.3622 (max.)	150 (max.)	0.0140 (min.)

Table 6.2.16  
 MAXIMUM  $K_{\text{EFF}}$  VALUES FOR THE 16X16A ASSEMBLY CLASS IN THE MPC-24  
 (all dimensions are in inches)

16x16A (4.6% Enrichment, Fixed neutron absorber $^{10}\text{B}$ minimum loading of $0.02 \text{ g/cm}^2$ ) 236 fuel rods, 5 guide tubes, pitch=0.506, Zr clad										
Fuel Assembly Designation	maximum $k_{\text{eff}}$	calculated $k_{\text{eff}}$	standard deviation	EALF	cladding OD	cladding ID	cladding thickness	pellet OD	fuel length	guide tube thickness
16x16A01	0.9287	0.9244	0.0008	0.2704	0.382	0.3320	0.0250	0.3255	150	0.0400
16x16A02	0.9263	0.9221	0.0007	0.2702	0.382	0.3320	0.0250	0.3250	150	0.0400
Dimensions Listed for Authorized Contents					0.382 (min.)	0.3320 (max.)		0.3255 (max.)	150 (max.)	0.0400 (min.)
bounding dimensions (16x16A01)	0.9287	0.9244	0.0008	0.2704	0.382	0.3320	0.0250	0.3255	150	0.0400

Table 6.2.17  
 MAXIMUM  $K_{\text{EFF}}$  VALUES FOR THE 17X17A ASSEMBLY CLASS IN THE MPC-24  
 (all dimensions are in inches)

17x17A (4.0% Enrichment, Fixed neutron absorber $^{10}\text{B}$ minimum loading of 0.02 g/cm <sup>2</sup> ) 264 fuel rods, 25 guide tubes, pitch=0.496, Zr clad										
Fuel Assembly Designation	maximum $k_{\text{eff}}$	calculated $k_{\text{eff}}$	standard deviation	EALF	cladding OD	cladding ID	cladding thickness	pellet OD	fuel length	guide tube thickness
17x17A01	0.9368	0.9325	0.0008	0.2131	0.360	0.3150	0.0225	0.3088	150	0.016
17x17A02	0.9329	0.9286	0.0008	0.2018	0.360	0.3100	0.0250	0.3030	150	0.016
Dimensions Listed for Authorized Contents					0.360 (min.)	0.3150 (max.)		0.3088 (max.)	150 (max.)	0.016 (min.)
bounding dimensions (17x17A01)	0.9368	0.9325	0.0008	0.2131	0.360	0.3150	0.0225	0.3088	150	0.016

Table 6.2.18  
MAXIMUM  $K_{\text{EFF}}$  VALUES FOR THE 17X17B ASSEMBLY CLASS IN THE MPC-24  
(all dimensions are in inches)

17x17B (4.0% Enrichment, Fixed neutron absorber $^{10}\text{B}$ minimum loading of 0.02 g/cm <sup>2</sup> ) 264 fuel rods, 25 guide tubes, pitch=0.496, Zr clad										
Fuel Assembly Designation	maximum $k_{\text{eff}}$	calculated $k_{\text{eff}}$	standard deviation	EALF	cladding OD	cladding ID	cladding thickness	pellet OD	fuel length	guide tube thickness
17x17B01	0.9288	0.9243	0.0009	0.2607	0.374	0.3290	0.0225	0.3225	150	0.016
17x17B02	0.9290	0.9247	0.0008	0.2596	0.374	0.3290	0.0225	0.3225	150	0.016
17x17B03	0.9243	0.9199	0.0008	0.2625	0.376	0.3280	0.0240	0.3215	150	0.016
17x17B04	0.9324	0.9279	0.0009	0.2576	0.372	0.3310	0.0205	0.3232	150	0.014
17x17B05	0.9266	0.9222	0.0008	0.2539	0.374	0.3260	0.0240	0.3195	150	0.016
17x17B06	0.9311	0.9268	0.0008	0.2593	0.372	0.3310	0.0205	0.3232	150	0.014
Dimensions Listed for Authorized Contents					0.372 (min.)	0.3310 (max.)		0.3232 (max.)	150 (max.)	0.014 (min.)
bounding dimensions (17x17B06)	0.9311 <sup>†</sup>	0.9268	0.0008	0.2593	0.372	0.3310	0.0205	0.3232	150	0.014

<sup>†</sup> The  $k_{\text{eff}}$  value listed for the 17x17B04 case is slightly higher than that for the case with the bounding dimensions. However, the difference (0.0013) is well within the statistical uncertainties, and thus, the two values are statistically equivalent (within  $2\sigma$ ). Nevertheless, the 17x17B04 case is used in Table 6.3.5 for the eccentric analysis.

Table 6.2.19  
 MAXIMUM  $K_{\text{EFF}}$  VALUES FOR THE 17X17C ASSEMBLY CLASS IN THE MPC-24  
 (all dimensions are in inches)

17x17C (4.0% Enrichment, Fixed neutron absorber $^{10}\text{B}$ minimum loading of $0.02 \text{ g/cm}^2$ ) 264 fuel rods, 25 guide tubes, pitch=0.502, Zr clad										
Fuel Assembly Designation	maximum $k_{\text{eff}}$	calculated $k_{\text{eff}}$	standard deviation	EALF	cladding OD	cladding ID	cladding thickness	pellet OD	fuel length	guide tube thickness
17x17C01	0.9293	0.9250	0.0008	0.2595	0.379	0.3310	0.0240	0.3232	150	0.020
17x17C02	0.9336	0.9293	0.0008	0.2624	0.377	0.3330	0.0220	0.3252	150	0.020
Dimensions Listed for Authorized Contents					0.377 (min.)	0.3330 (max.)		0.3252 (max.)	150 (max.)	0.020 (min.)
bounding dimensions (17x17C02)	0.9336	0.9293	0.0008	0.2624	0.377	0.3330	0.0220	0.3252	150	0.020

Table 6.2.20  
 MAXIMUM K<sub>EFF</sub> VALUES FOR THE 7X7B ASSEMBLY CLASS IN THE MPC-68  
 (all dimensions are in inches)

7x7B (4.2% Enrichment, Fixed neutron absorber <sup>10</sup> B minimum loading of 0.0279 g/cm <sup>2</sup> ) 49 fuel rods, 0 water rods, pitch=0.738, Zr clad											
Fuel Assembly Designation	maximum k <sub>eff</sub>	calculated k <sub>eff</sub>	standard deviation	EALF	cladding OD	cladding ID	cladding thickness	pellet OD	fuel length	water rod thickness	channel thickness
7x7B01	0.9372	0.9330	0.0007	0.3658	0.5630	0.4990	0.0320	0.4870	150	n/a	0.080
7x7B02	0.9301	0.9260	0.0007	0.3524	0.5630	0.4890	0.0370	0.4770	150	n/a	0.102
7x7B03	0.9313	0.9271	0.0008	0.3438	0.5630	0.4890	0.0370	0.4770	150	n/a	0.080
7x7B04	0.9311	0.9270	0.0007	0.3816	0.5700	0.4990	0.0355	0.4880	150	n/a	0.080
7x7B05	0.9350	0.9306	0.0008	0.3382	0.5630	0.4950	0.0340	0.4775	150	n/a	0.080
7x7B06	0.9298	0.9260	0.0006	0.3957	0.5700	0.4990	0.0355	0.4910	150	n/a	0.080
Dimensions Listed for Authorized Contents					0.5630 (min.)	0.4990 (max.)		0.4910 (max.)	150 (max.)	n/a	0.120 (max.)
bounding dimensions (B7x7B01)	0.9375	0.9332	0.0008	0.3887	0.5630	0.4990	0.0320	0.4910	150	n/a	0.102
bounding dimensions with 120 mil channel (B7x7B02)	0.9386	0.9344	0.0007	0.3983	0.5630	0.4990	0.0320	0.4910	150	n/a	0.120



Table 6.2.21  
 MAXIMUM  $K_{\text{EFF}}$  VALUES FOR THE 8X8B ASSEMBLY CLASS IN THE MPC-68  
 (all dimensions are in inches)

8x8B (4.2% Enrichment, Fixed neutron absorber $^{10}\text{B}$ minimum loading of 0.0279 g/cm <sup>2</sup> ) 63 or 64 fuel rods, 1 or 0 water rods, pitch <sup>†</sup> = 0.636-0.642, Zr clad													
Fuel Assembly Designation	maximum $k_{\text{eff}}$	calculated $k_{\text{eff}}$	standard deviation	EALF	Fuel rods	pitch	cladding OD	cladding ID	cladding thickness	pellet OD	fuel length	water rod thickness	channel thickness
8x8B01	0.9310	0.9265	0.0009	0.2935	63	0.641	0.4840	0.4140	0.0350	0.4050	150	0.035	0.100
8x8B02	0.9227	0.9185	0.0007	0.2993	63	0.636	0.4840	0.4140	0.0350	0.4050	150	0.035	0.100
8x8B03	0.9299	0.9257	0.0008	0.3319	63	0.640	0.4930	0.4250	0.0340	0.4160	150	0.034	0.100
8x8B04	0.9236	0.9194	0.0008	0.3700	64	0.642	0.5015	0.4295	0.0360	0.4195	150	n/a	0.100
Dimensions Listed for Authorized Contents					63 or 64	0.636-0.642	0.4840 (min.)	0.4295 (max.)		0.4195 (max.)	150 (max.)	0.034	0.120 (max.)
bounding (pitch=0.636) (B8x8B01)	0.9346	0.9301	0.0009	0.3389	63	0.636	0.4840	0.4295	0.02725	0.4195	150	0.034	0.120
bounding (pitch=0.640) (B8x8B02)	0.9385	0.9343	0.0008	0.3329	63	0.640	0.4840	0.4295	0.02725	0.4195	150	0.034	0.120
bounding (pitch=0.641) (B8x8B03)	0.9416	0.9375	0.0007	0.3293	63	0.642	0.4840	0.4295	0.02725	0.4195	150	0.034	0.120

<sup>†</sup> This assembly class was analyzed and qualified for a small variation in the pitch and a variation in the number of fuel and water rods.

Table 6.2.22  
 MAXIMUM  $K_{\text{EFF}}$  VALUES FOR THE 8X8C ASSEMBLY CLASS IN THE MPC-68  
 (all dimensions are in inches)

8x8C (4.2% Enrichment, Fixed neutron absorber $^{10}\text{B}$ minimum loading of 0.0279 g/cm <sup>2</sup> ) 62 fuel rods, 2 water rods, pitch <sup>†</sup> = 0.636-0.641, Zr clad												
Fuel Assembly Designation	maximum $k_{\text{eff}}$	calculated $k_{\text{eff}}$	standard deviation	EALF	pitch	cladding OD	cladding ID	cladding thickness	pellet OD	fuel length	water rod thickness	channel thickness
8x8C01	0.9315	0.9273	0.0007	0.2822	0.641	0.4840	0.4140	0.0350	0.4050	150	0.035	0.100
8x8C02	0.9313	0.9268	0.0009	0.2716	0.640	0.4830	0.4190	0.0320	0.4100	150	0.030	0.000
8x8C03	0.9329	0.9286	0.0008	0.2877	0.640	0.4830	0.4190	0.0320	0.4100	150	0.030	0.800
8x8C04	0.9348 <sup>††</sup>	0.9307	0.0007	0.2915	0.640	0.4830	0.4190	0.0320	0.4100	150	0.030	0.100
8x8C05	0.9353	0.9312	0.0007	0.2971	0.640	0.4830	0.4190	0.0320	0.4100	150	0.030	0.120
8x8C06	0.9353	0.9312	0.0007	0.2944	0.640	0.4830	0.4190	0.0320	0.4110	150	0.030	0.100
8x8C07	0.9314	0.9273	0.0007	0.2972	0.640	0.4830	0.4150	0.0340	0.4100	150	0.030	0.100
8x8C08	0.9339	0.9298	0.0007	0.2915	0.640	0.4830	0.4190	0.0320	0.4100	150	0.034	0.100
8x8C09	0.9301	0.9260	0.0007	0.3183	0.640	0.4930	0.4250	0.0340	0.4160	150	0.034	0.100
8x8C10	0.9317	0.9275	0.0008	0.3018	0.640	0.4830	0.4150	0.0340	0.4100	150	0.030	0.120
8x8C11	0.9328	0.9287	0.0007	0.3001	0.640	0.4830	0.4150	0.0340	0.4100	150	0.030	0.120
8x8C12	0.9285	0.9242	0.0008	0.3062	0.636	0.4830	0.4190	0.0320	0.4110	150	0.030	0.120
Dimensions Listed for Authorized Contents					0.636-0.641	0.4830 (min.)	0.4250 (max.)		0.4160 (max.)	150 (max.)	0.000 (min.)	0.120 (max.)
bounding (pitch=0.636) (B8x8C01)	0.9357	0.9313	0.0009	0.3141	0.636	0.4830	0.4250	0.0290	0.4160	150	0.000	0.120
bounding (pitch=0.640) (B8x8C02)	0.9425	0.9384	0.0007	0.3081	0.640	0.4830	0.4250	0.0290	0.4160	150	0.000	0.120
bounding (pitch=0.641) (B8x8C03)	0.9418	0.9375	0.0008	0.3056	0.641	0.4830	0.4250	0.0290	0.4160	150	0.000	0.120

<sup>†</sup> This assembly class was analyzed and qualified for a small variation in the pitch.

<sup>††</sup> KENO5a verification calculation resulted in a maximum  $k_{\text{eff}}$  of 0.9343.

HI-STAR SAR

Rev. 16

REPORT HI-951251

6.2-36

Table 6.2.23  
 MAXIMUM  $K_{\text{EFF}}$  VALUES FOR THE 8X8D ASSEMBLY CLASS IN THE MPC-68  
 (all dimensions are in inches)

8x8D (4.2% Enrichment, Fixed neutron absorber $^{10}\text{B}$ minimum loading of $0.0279 \text{ g/cm}^2$ ) 60 or 61 fuel rods, 1-4 water rods†, pitch=0.640, Zr clad											
Fuel Assembly Designation	maximum $k_{\text{eff}}$	calculated $k_{\text{eff}}$	standard deviation	EALF	cladding OD	cladding ID	cladding thickness	pellet OD	fuel length	water rod thickness	channel thickness
8x8D01	0.9342	0.9302	0.0006	0.2733	0.4830	0.4190	0.0320	0.4110	150	0.03/0.025	0.100
8x8D02	0.9325	0.9284	0.0007	0.2750	0.4830	0.4190	0.0320	0.4110	150	0.030	0.100
8x8D03	0.9351	0.9309	0.0008	0.2731	0.4830	0.4190	0.0320	0.4110	150	0.025	0.100
8x8D04	0.9338	0.9296	0.0007	0.2727	0.4830	0.4190	0.0320	0.4110	150	0.040	0.100
8x8D05	0.9339	0.9294	0.0009	0.2700	0.4830	0.4190	0.0320	0.4100	150	0.040	0.100
8x8D06	0.9365	0.9324	0.0007	0.2777	0.4830	0.4190	0.0320	0.4110	150	0.040	0.120
8x8D07	0.9341	0.9297	0.0009	0.2694	0.4830	0.4190	0.0320	0.4110	150	0.040	0.080
8x8D08	0.9376	0.9332	0.0009	0.2841	0.4830	0.4230	0.0300	0.4140	150	0.030	0.080
Dimensions Listed for Authorized Contents					0.4830 (min.)	0.4230 (max.)		0.4140 (max.)	150 (max.)	0.000 (min.)	0.120 (max.)
bounding dimensions (B8x8D01)	0.9403	0.9363	0.0007	0.2778	0.4830	0.4230	0.0300	0.4140	150	0.000	0.120

† Fuel assemblies 8x8D01 through 8x8D03 have 4 water rods that are similar in size to the fuel rods, while assemblies 8x8D04 through 8x8D07 have 1 large water rod that takes the place of the 4 water rods. Fuel assembly 8x8D08 contains 3 water rods that are similar in size to the fuel rods.

Table 6.2.24  
 MAXIMUM  $K_{\text{EFF}}$  VALUES FOR THE 8X8E ASSEMBLY CLASS IN THE MPC-68  
 (all dimensions are in inches)

8x8E (4.2% Enrichment, Fixed neutron absorber $^{10}\text{B}$ minimum loading of 0.0279 g/cm <sup>2</sup> ) 59 fuel rods, 5 water rods, pitch=0.640, Zr clad											
Fuel Assembly Designation	maximum $k_{\text{eff}}$	calculated $k_{\text{eff}}$	standard deviation	EALF	cladding OD	cladding ID	cladding thickness	pellet OD	fuel length	water rod thickness	channel thickness
8x8E01	0.9312	0.9270	0.0008	0.2831	0.4930	0.4250	0.0340	0.4160	150	0.034	0.100
Dimensions Listed for Authorized Contents					0.4930 (min.)	0.4250 (max.)		0.4160 (max.)	150 (max.)	0.034 (min.)	0.100 (max.)

Table 6.2.25  
 MAXIMUM  $K_{\text{EFF}}$  VALUES FOR THE 8X8F ASSEMBLY CLASS IN THE MPC-68  
 (all dimensions are in inches)

8x8F (4.0% Enrichment, Fixed neutron absorber $^{10}\text{B}$ minimum loading of 0.0279 g/cm <sup>2</sup> ) 64 fuel rods, 4 rectangular water cross segments dividing the assembly into four quadrants, pitch=0.609, Zr clad											
Fuel Assembly Designation	maximum $k_{\text{eff}}$	calculated $k_{\text{eff}}$	standard deviation	EALF	cladding OD	cladding ID	cladding thickness	pellet OD	fuel length	water rod thickness	channel thickness
8x8F01	0.9411	0.9366	0.0009	0.2264	0.4576	0.3996	0.0290	0.3913	150	0.0315	0.055
Dimensions Listed for Authorized Contents					0.4576 (min.)	0.3996 (max.)		0.3913 (max.)	150 (max.)	0.0315 (min.)	0.055 (max.)

Table 6.2.26  
 MAXIMUM  $K_{\text{EFF}}$  VALUES FOR THE 9X9A ASSEMBLY CLASS IN THE MPC-68  
 (all dimensions are in inches)

9x9A (4.2% Enrichment, Fixed neutron absorber $^{10}\text{B}$ minimum loading of 0.0279 g/cm <sup>2</sup> ) 74/66 fuel rods†, 2 water rods, pitch=0.566, Zr clad											
Fuel Assembly Designation	maximum $k_{\text{eff}}$	calculated $k_{\text{eff}}$	standard deviation	EALF	cladding OD	cladding ID	cladding thickness	pellet OD	fuel length	water rod thickness	channel thickness
9x9A01 (axial segment with all rods)	0.9353	0.9310	0.0008	0.2875	0.4400	0.3840	0.0280	0.3760	150	0.030	0.100
9x9A02 (axial segment with only the full length rods)	0.9388	0.9345	0.0008	0.2228	0.4400	0.3840	0.0280	0.3760	150	0.030	0.100
9x9A03 (actual three-dimensional representation of all rods)	0.9351	0.9310	0.0007	0.2837	0.4400	0.3840	0.0280	0.3760	150/90	0.030	0.100
9x9A04 (axial segment with only the full length rods)	0.9396	0.9355	0.0007	0.2262	0.4400	0.3840	0.0280	0.3760	150	0.030	0.120
Dimensions Listed for Authorized Contents					0.4400 (min.)	0.3840 (max.)		0.3760 (max.)	150 (max.)	0.000 (min.)	0.120 (max.)
bounding dimensions (axial segment with only the full length rods) (B9x9A01)	0.9417	0.9374	0.0008	0.2236	0.4400	0.3840	0.0280	0.3760	150	0.000	0.120

† This assembly class contains 66 full length rods and 8 partial length rods. In order to eliminate a requirement on the length of the partial length rods, separate calculations were performed for the axial segments with and without the partial length rods.

Table 6.2.27  
 MAXIMUM  $K_{\text{EFF}}$  VALUES FOR THE 9X9B ASSEMBLY CLASS IN THE MPC-68  
 (all dimensions are in inches)

9x9B (4.2% Enrichment, Fixed neutron absorber $^{10}\text{B}$ minimum loading of 0.0279 g/cm <sup>2</sup> ) 72 fuel rods, 1 water rod (square, replacing 9 fuel rods), pitch=0.569 to 0.572†, Zr clad												
Fuel Assembly Designation	maximum $k_{\text{eff}}$	calculated $k_{\text{eff}}$	standard deviation	EALF	pitch	cladding OD	cladding ID	cladding thickness	pellet OD	fuel length	water rod thickness	channel thickness
9x9B01	0.9380	0.9336	0.0008	0.2576	0.569	0.4330	0.3807	0.0262	0.3737	150	0.0285	0.100
9x9B02	0.9373	0.9329	0.0009	0.2578	0.569	0.4330	0.3810	0.0260	0.3737	150	0.0285	0.100
9x9B03	0.9417	0.9374	0.0008	0.2545	0.572	0.4330	0.3810	0.0260	0.3737	150	0.0285	0.100
Dimensions Listed for Authorized Contents					0.572	0.4330 (min.)	0.3810 (max.)		0.3740 (max.)	150 (max.)	0.000 (min.)	0.120 (max.)
bounding dimensions (B9x9B01)	0.9436	0.9394	0.0008	0.2506	0.572	0.4330	0.3810	0.0260	0.3740† †	150	0.000	0.120

† This assembly class was analyzed and qualified for a small variation in the pitch.

†† This value was conservatively defined to be larger than any of the actual pellet diameters.

HI-STAR SAR

Rev. 16

REPORT HI-951251

6.2-41

Table 6.2.28  
 MAXIMUM  $K_{\text{EFF}}$  VALUES FOR THE 9X9C ASSEMBLY CLASS IN THE MPC-68  
 (all dimensions are in inches)

9x9C (4.2% Enrichment, Fixed neutron absorber $^{10}\text{B}$ minimum loading of $0.0279 \text{ g/cm}^2$ ) 80 fuel rods, 1 water rods, pitch=0.572, Zr clad											
Fuel Assembly Designation	maximum $k_{\text{eff}}$	calculated $k_{\text{eff}}$	standard deviation	EALF	cladding OD	cladding ID	cladding thickness	pellet OD	fuel length	water rod thickness	channel thickness
9x9C01	0.9395	0.9352	0.0008	0.2698	0.4230	0.3640	0.0295	0.3565	150	0.020	0.100
Dimensions Listed for Authorized Contents					0.4230 (min.)	0.3640 (max.)		0.3565 (max.)	150 (max.)	0.020 (min.)	0.100 (max.)



Table 6.2.29  
 MAXIMUM  $K_{\text{EFF}}$  VALUES FOR THE 9X9D ASSEMBLY CLASS IN THE MPC-68  
 (all dimensions are in inches)

9x9D (4.2% Enrichment, Fixed neutron absorber $^{10}\text{B}$ minimum loading of $0.0279 \text{ g/cm}^2$ ) 79 fuel rods, 2 water rods, pitch=0.572, Zr clad											
Fuel Assembly Designation	maximum $k_{\text{eff}}$	calculated $k_{\text{eff}}$	standard deviation	EALF	cladding OD	cladding ID	cladding thickness	pellet OD	fuel length	water rod thickness	channel thickness
9x9D01	0.9394	0.9350	0.0009	0.2625	0.4240	0.3640	0.0300	0.3565	150	0.0300	0.100
Dimensions Listed for Authorized Contents					0.4240 (min.)	0.3640 (max.)		0.3565 (max.)	150 (max.)	0.0300 (min.)	0.100 (max.)

Table 6.2.30  
 MAXIMUM  $K_{\text{EFF}}$  VALUES FOR THE 9X9E ASSEMBLY CLASS IN THE MPC-68  
 (all dimensions are in inches)

9x9E (4.0% Enrichment, Fixed neutron absorber $^{10}\text{B}$ minimum loading of 0.0279 g/cm <sup>2</sup> ) 76 fuel rods, 5 water rods, pitch=0.572, Zr clad											
Fuel Assembly Designation	maximum $k_{\text{eff}}$	calculated $k_{\text{eff}}$	standard deviation	EALF	cladding OD	cladding ID	cladding thickness	pellet OD	fuel length	water rod thickness	channel thickness
9x9E01	0.9334	0.9293	0.0007	0.2227	0.4170	0.3640	0.0265	0.3530	150	0.0120	0.120
9x9E02	0.9401	0.9359	0.0008	0.2065	0.4170 0.4430	0.3640 0.3860	0.0265 0.0285	0.3530 0.3745	150	0.0120	0.120
Dimensions Listed for Authorized Contents†					0.4170 (min.)	0.3640 (max.)		0.3530 (max.)	150 (max.)	0.0120 (min.)	0.120 (max.)
bounding dimensions (9x9E02)	0.9401	0.9359	0.0008	0.2065	0.4170 0.4430	0.3640 0.3860	0.0265 0.0285	0.3530 0.3745	150	0.0120	0.120

† This fuel assembly, also known as SPC 9x9-5, contains fuel rods with different cladding and pellet diameters which do not bound each other. To be consistent in the way fuel assemblies are listed for Authorized Contents, two assembly classes (9x9E and 9x9F) are required to specify this assembly. Each class contains the actual geometry (9x9E02 and 9x9F02), as well as a hypothetical geometry with either all small rods (9x9E01) or all large rods (9x9F01). The Authorized Content lists the small rod dimensions for class 9x9E and the large rod dimensions for class 9x9F, and a note that both classes are used to qualify the assembly. The analyses demonstrate that all configurations, including the actual geometry, are acceptable.

Table 6.2.31  
 MAXIMUM  $K_{\text{EFF}}$  VALUES FOR THE 9X9F ASSEMBLY CLASS IN THE MPC-68  
 (all dimensions are in inches)

9x9F (4.0% Enrichment, Fixed neutron absorber $^{10}\text{B}$ minimum loading of 0.0279 g/cm <sup>2</sup> ) 76 fuel rods, 5 water rods, pitch=0.572, Zr clad											
Fuel Assembly Designation	maximum $k_{\text{eff}}$	calculated $k_{\text{eff}}$	standard deviation	EALF	cladding OD	cladding ID	cladding thickness	pellet OD	fuel length	water rod thickness	channel thickness
9x9F01	0.9307	0.9265	0.0007	0.2899	0.4430	0.3860	0.0285	0.3745	150	0.0120	0.120
9x9F02	0.9401	0.9359	0.0008	0.2065	0.4170 0.4430	0.3640 0.3860	0.0265 0.0285	0.3530 0.3745	150	0.0120	0.120
Dimensions Listed for Authorized Contents†					0.4430 (min.)	0.3860 (max.)		0.3745 (max.)	150 (max.)	0.0120 (min.)	0.120 (max.)
bounding dimensions (9x9F02)	0.9401	0.9359	0.0008	0.2065	0.4170 0.4430	0.3640 0.3860	0.0265 0.0285	0.3530 0.3745	150	0.0120	0.120

† This fuel assembly, also known as SPC 9x9-5, contains fuel rods with different cladding and pellet diameters which do not bound each other. To be consistent in the way fuel assemblies are listed for Authorized Contents, two assembly classes (9x9E and 9x9F) are required to specify this assembly. Each class contains the actual geometry (9x9E02 and 9x9F02), as well as a hypothetical geometry with either all small rods (9x9E01) or all large rods (9x9F01). The Authorized Content lists the small rod dimensions for class 9x9E and the large rod dimensions for class 9x9F, and a note that both classes are used to qualify the assembly. The analyses demonstrate that all configurations, including the actual geometry, are acceptable.

Table 6.2.32  
MAXIMUM  $K_{\text{EFF}}$  VALUES FOR THE 10X10A ASSEMBLY CLASS IN THE MPC-68  
(all dimensions are in inches)

10x10A (4.2% Enrichment, Fixed neutron absorber $^{10}\text{B}$ minimum loading of 0.0279 g/cm <sup>2</sup> ) 92/78 fuel rods†, 2 water rods, pitch=0.510, Zr clad											
Fuel Assembly Designation	maximum $k_{\text{eff}}$	calculated $k_{\text{eff}}$	standard deviation	EALF	cladding OD	cladding ID	cladding thickness	pellet OD	fuel length	water rod thickness	channel thickness
10x10A01 (axial segment with all rods)	0.9377	0.9335	0.0008	0.3170	0.4040	0.3520	0.0260	0.3450	155	0.030	0.100
10x10A02 (axial segment with only the full length rods)	0.9426	0.9386	0.0007	0.2159	0.4040	0.3520	0.0260	0.3450	155	0.030	0.100
10x10A03 (actual three-dimensional representation of all rods)	0.9396	0.9356	0.0007	0.3169	0.4040	0.3520	0.0260	0.3450	155/90	0.030	0.100
Dimensions Listed for Authorized Contents					0.4040 (min.)	0.3520 (max.)		0.3455 (max.)	150†† (max.)	0.030 (min.)	0.120 (max.)
bounding dimensions (axial segment with only the full length rods) (B10x10A01)	0.9457†††	0.9414	0.0008	0.2212	0.4040	0.3520	0.0260	0.3455‡	155	0.030	0.120

† This assembly class contains 78 full-length rods and 14 partial-length rods. In order to eliminate the requirement on the length of the partial length rods, separate calculations were performed for axial segments with and without the partial length rods.

†† Although the analysis qualifies this assembly for a maximum active fuel length of 155 inches, the specification for authorized contents limits the active fuel length to 150 inches. This is due to the fact that the Fixed neutron absorber panels are 156 inches in length.

††† KENO5a verification calculation resulted in a maximum  $k_{\text{eff}}$  of 0.9453.

‡ This value was conservatively defined to be larger than any of the actual pellet diameters.

Table 6.2.33  
 MAXIMUM  $K_{\text{EFF}}$  VALUES FOR THE 10X10B ASSEMBLY CLASS IN THE MPC-68  
 (all dimensions are in inches)

10x10B (4.2% Enrichment, Fixed neutron absorber $^{10}\text{B}$ minimum loading of 0.0279 g/cm <sup>2</sup> ) 91/83 fuel rods†, 1 water rods (square, replacing 9 fuel rods), pitch=0.510, Zr clad											
Fuel Assembly Designation	maximum $k_{\text{eff}}$	calculated $k_{\text{eff}}$	standard deviation	EALF	cladding OD	cladding ID	cladding thickness	pellet OD	fuel length	water rod thickness	channel thickness
10x10B01 (axial segment with all rods)	0.9384	0.9341	0.0008	0.2881	0.3957	0.3480	0.0239	0.3413	155	0.0285	0.100
10x10B02 (axial segment with only the full length rods)	0.9416	0.9373	0.0008	0.2333	0.3957	0.3480	0.0239	0.3413	155	0.0285	0.100
10x10B03 (actual three-dimensional representation of all rods)	0.9375	0.9334	0.0007	0.2856	0.3957	0.3480	0.0239	0.3413	155/90	0.0285	0.100
Dimensions Listed for Authorized Contents					0.3957 (min.)	0.3480 (max.)		0.3420 (max.)	150†† (max.)	0.000 (min.)	0.120 (max.)
bounding dimensions (axial segment with only the full length rods) (B10x10B01)	0.9436	0.9395	0.0007	0.2366	0.3957	0.3480	0.0239	0.3420††† †	155	0.000	0.120

† This assembly class contains 83 full length rods and 8 partial length rods. In order to eliminate a requirement on the length of the partial length rods, separate calculations were performed for the axial segments with and without the partial length rods.

†† Although the analysis qualifies this assembly for a maximum active fuel length of 155 inches, the specification for authorized contents limits the active fuel length to 150 inches. This is due to the fact that the Fixed neutron absorber panels are 156 inches in length.

††† This value was conservatively defined to be larger than any of the actual pellet diameters.

Table 6.2.34  
 MAXIMUM  $K_{\text{EFF}}$  VALUES FOR THE 10X10C ASSEMBLY CLASS IN THE MPC-68  
 (all dimensions are in inches)

10x10C (4.2% Enrichment, Fixed neutron absorber $^{10}\text{B}$ minimum loading of $0.0279 \text{ g/cm}^2$ ) 96 fuel rods, 5 water rods (1 center diamond and 4 rectangular), pitch=0.488, Zr clad											
Fuel Assembly Designation	maximum $k_{\text{eff}}$	calculated $k_{\text{eff}}$	standard deviation	EALF	cladding OD	cladding ID	cladding thickness	pellet OD	fuel length	water rod thickness	channel thickness
10x10C01	0.9433	0.9392	0.0007	0.2416	0.3780	0.3294	0.0243	0.3224	150	0.031	0.055
Dimensions Listed for Authorized Contents					0.3780 (min.)	0.3294 (max.)		0.3224 (max.)	150 (max.)	0.031 (min.)	0.055 (max.)

Table 6.2.35  
 MAXIMUM  $K_{\text{EFF}}$  VALUES FOR THE 10X10D ASSEMBLY CLASS IN THE MPC-68  
 (all dimensions are in inches)

10x10D (4.0% Enrichment, Fixed neutron absorber $^{10}\text{B}$ minimum loading of 0.0279 g/cm <sup>2</sup> ) 100 fuel rods, 0 water rods, pitch=0.565, SS clad											
Fuel Assembly Designation	maximum $k_{\text{eff}}$	calculated $k_{\text{eff}}$	standard deviation	EALF	cladding OD	cladding ID	cladding thickness	pellet OD	fuel length	water rod thickness	channel thickness
10x10D01	0.9376	0.9333	0.0008	0.3355	0.3960	0.3560	0.0200	0.350	83	n/a	0.080
Dimensions Listed for Authorized Contents					0.3960 (min.)	0.3560 (max.)		0.350 (max.)	83 (max.)	n/a	0.080 (max.)

Table 6.2.36  
 MAXIMUM  $K_{\text{EFF}}$  VALUES FOR THE 10X10E ASSEMBLY CLASS IN THE MPC-68  
 (all dimensions are in inches)

10x10E (4.0% Enrichment, Fixed neutron absorber $^{10}\text{B}$ minimum loading of 0.0279 g/cm <sup>2</sup> ) 96 fuel rods, 4 water rods, pitch=0.557, SS clad											
Fuel Assembly Designation	maximum $k_{\text{eff}}$	calculated $k_{\text{eff}}$	standard deviation	EALF	cladding OD	cladding ID	cladding thickness	pellet OD	fuel length	water rod thickness	channel thickness
10x10E01	0.9185	0.9144	0.0007	0.2936	0.3940	0.3500	0.0220	0.3430	83	0.022	0.080
Dimensions Listed for Authorized Contents					0.3940 (min.)	0.3500 (max.)		0.3430 (max.)	83 (max.)	0.022 (min.)	0.080 (max.)



Table 6.2.37  
 MAXIMUM K<sub>EFF</sub> VALUES FOR THE 6X6A ASSEMBLY CLASS IN THE MPC-68F  
 (all dimensions are in inches)

6x6A (3.0% Enrichment†, Fixed neutron absorber <sup>10</sup> B minimum loading of 0.0067 g/cm <sup>2</sup> ) 35 or 36 fuel rods††, 1 or 0 water rods††, pitch=0.694 to 0.710††, Zr clad													
Fuel Assembly Designation	maximum k <sub>eff</sub>	calculated k <sub>eff</sub>	standard deviation	EALF	pitch	fuel rods	cladding OD	cladding ID	cladding thickness	pellet OD	fuel length	water rod thickness	channel thickness
6x6A01	0.7539	0.7498	0.0007	0.2754	0.694	36	0.5645	0.4945	0.0350	0.4940	110	n/a	0.060
6x6A02	0.7517	0.7476	0.0007	0.2510	0.694	36	0.5645	0.4925	0.0360	0.4820	110	n/a	0.060
6x6A03	0.7545	0.7501	0.0008	0.2494	0.694	36	0.5645	0.4945	0.0350	0.4820	110	n/a	0.060
6x6A04	0.7537	0.7494	0.0008	0.2494	0.694	36	0.5550	0.4850	0.0350	0.4820	110	n/a	0.060
6x6A05	0.7555	0.7512	0.0008	0.2470	0.696	36	0.5625	0.4925	0.0350	0.4820	110	n/a	0.060
6x6A06	0.7618	0.7576	0.0008	0.2298	0.696	35	0.5625	0.4925	0.0350	0.4820	110	0.0	0.060
6x6A07	0.7588	0.7550	0.0007	0.2360	0.700	36	0.5555	0.4850	0.03525	0.4780	110	n/a	0.060
6x6A08	0.7808	0.7766	0.0007	0.2527	0.710	36	0.5625	0.5105	0.0260	0.4980	110	n/a	0.060
Dimensions Listed for Authorized Contents					0.710 (max.)	35 or 36	0.5550 (min.)	0.5105 (max.)	0.02225	0.4980 (max.)	120 (max.)	0.0	0.060 (max.)
bounding dimensions (B6x6A01)	0.7727	0.7685	0.0007	0.2460	0.694	35	0.5550	0.5105	0.02225	0.4980	120	0.0	0.060
bounding dimensions (B6x6A02)	0.7782	0.7738	0.0008	0.2408	0.700	35	0.5550	0.5105	0.02225	0.4980	120	0.0	0.060
bounding dimensions (B6x6A03)	0.7888	0.7846	0.0007	0.2310	0.710	35	0.5550	0.5105	0.02225	0.4980	120	0.0	0.060

† Although the calculations were performed for 3.0%, the enrichment is limited in the specification for authorized contents to 2.7%.

†† This assembly class was analyzed and qualified for a small variation in the pitch and a variation in the number of fuel and water rods.

HI-STAR SAR

Rev. 16

REPORT HI-951251

6.2-51

Table 6.2.38  
 MAXIMUM  $K_{\text{EFF}}$  VALUES FOR THE 6X6B ASSEMBLY CLASS IN THE MPC-68F  
 (all dimensions are in inches)

6x6B (3.0% Enrichment <sup>†</sup> , Fixed neutron absorber <sup>10</sup> B minimum loading of 0.0067 g/cm <sup>2</sup> ) 35 or 36 fuel rods <sup>††</sup> (up to 9 MOX rods), 1 or 0 water rods <sup>††</sup> , pitch=0.694 to 0.710 <sup>††</sup> , Zr clad													
Fuel Assembly Designation	maximum $k_{\text{eff}}$	calculated $k_{\text{eff}}$	standard deviation	EALF	pitch	fuel rods	cladding OD	cladding ID	cladding thickness	pellet OD	fuel length	water rod thickness	channel thickness
6x6B01	0.7604	0.7563	0.0007	0.2461	0.694	36	0.5645	0.4945	0.0350	0.4820	110	n/a	0.060
6x6B02	0.7618	0.7577	0.0007	0.2450	0.694	36	0.5625	0.4925	0.0350	0.4820	110	n/a	0.060
6x6B03	0.7619	0.7578	0.0007	0.2439	0.696	36	0.5625	0.4925	0.0350	0.4820	110	n/a	0.060
6x6B04	0.7686	0.7644	0.0008	0.2286	0.696	35	0.5625	0.4925	0.0350	0.4820	110	0.0	0.060
6x6B05	0.7824	0.7785	0.0006	0.2184	0.710	35	0.5625	0.4925	0.0350	0.4820	110	0.0	0.060
Dimensions Listed for Authorized Contents					0.710 (max.)	35 or 36	0.5625 (min.)	0.4945 (max.)		0.4820 (max.)	120 (max.)	0.0	0.060 (max.)
bounding dimensions (B6x6B01)	0.7822 <sup>†††</sup>	0.7783	0.0007	0.2190	0.710	35	0.5625	0.4945	0.0340	0.4820	120	0.0	0.060

Note:

1. These assemblies contain up to 9 MOX pins. The composition of the MOX fuel pins is given in Table 6.3.4.

<sup>†</sup> The <sup>235</sup>U enrichment of the MOX and UO<sub>2</sub> pins is assumed to be 0.711% and 3.0%, respectively.

<sup>††</sup> This assembly class was analyzed and qualified for a small variation in the pitch and a variation in the number of fuel and water rods.

<sup>†††</sup> The  $k_{\text{eff}}$  value listed for the 6x6B05 case is slightly higher than that for the case with the bounding dimensions. However, the difference (0.0002) is well within the statistical uncertainties, and thus, the two values are statistically equivalent (within 1 $\sigma$ ). Therefore, the 0.7824 value is listed in Tables 6.1.2 and 6.1.3 as the maximum.

HI-STAR SAR

Rev. 16

REPORT HI-951251

6.2-52

Table 6.2.39  
 MAXIMUM  $K_{\text{EFF}}$  VALUES FOR THE 6X6C ASSEMBLY CLASS IN THE MPC-68F  
 (all dimensions are in inches)

6x6C (3.0% Enrichment <sup>†</sup> , Fixed neutron absorber $^{10}\text{B}$ minimum loading of 0.0067 g/cm <sup>2</sup> ) 36 fuel rods, 0 water rods, pitch=0.740, Zr clad											
Fuel Assembly Designation	maximum $k_{\text{eff}}$	calculated $k_{\text{eff}}$	standard deviation	EALF	cladding OD	cladding ID	cladding thickness	pellet OD	fuel length	water rod thickness	channel thickness
6x6C01	0.8021	0.7980	0.0007	0.2139	0.5630	0.4990	0.0320	0.4880	77.5	n/a	0.060
Dimensions Listed for Authorized Contents					0.5630 (min.)	0.4990 (max.)		0.4880 (max.)	77.5 (max.)	n/a	0.060 (max.)

---

<sup>†</sup> Although the calculations were performed for 3.0%, the enrichment is limited in the specification for authorized contents to 2.7%.

Table 6.2.40  
 MAXIMUM  $K_{\text{EFF}}$  VALUES FOR THE 7X7A ASSEMBLY CLASS IN THE MPC-68F  
 (all dimensions are in inches)

7x7A (3.0% Enrichment <sup>†</sup> , Fixed neutron absorber $^{10}\text{B}$ minimum loading of 0.0067 g/cm <sup>2</sup> ) 49 fuel rods, 0 water rods, pitch=0.631, Zr clad											
Fuel Assembly Designation	maximum $k_{\text{eff}}$	calculated $k_{\text{eff}}$	standard deviation	EALF	cladding OD	cladding ID	cladding thickness	pellet OD	fuel length	water rod thickness	channel thickness
7x7A01	0.7974	0.7932	0.0008	0.2015	0.4860	0.4204	0.0328	0.4110	80	n/a	0.060
Dimensions Listed for Authorized Contents					0.4860 (min.)	0.4204 (max.)		0.4110 (max.)	80 (max.)	n/a	0.060 (max.)

---

<sup>†</sup> Although the calculations were performed for 3.0%, the enrichment is limited in the specification for authorized contents to 2.7%.

Table 6.2.41  
 MAXIMUM  $K_{\text{EFF}}$  VALUES FOR THE 8X8A ASSEMBLY CLASS IN THE MPC-68F  
 (all dimensions are in inches)

8x8A (3.0% Enrichment <sup>†</sup> , Fixed neutron absorber <sup>10</sup> B minimum loading of 0.0067 g/cm <sup>2</sup> ) 63 or 64 fuel rods <sup>††</sup> , 0 water rods, pitch=0.523, Zr clad												
Fuel Assembly Designation	maximum $k_{\text{eff}}$	calculated $k_{\text{eff}}$	standard deviation	EALF	fuel rods	cladding OD	cladding ID	cladding thickness	pellet OD	fuel length	water rod thickness	channel thickness
8x8A01	0.7685	0.7644	0.0007	0.2227	64	0.4120	0.3620	0.0250	0.3580	110	n/a	0.100
8x8A02	0.7697	0.7656	0.0007	0.2158	63	0.4120	0.3620	0.0250	0.3580	120	n/a	0.100
Dimensions Listed for Authorized Contents					63	0.4120 (min.)	0.3620 (max.)		0.3580 (max.)	110 (max.)	n/a	0.100 (max.)
bounding dimensions (8x8A02)	0.7697	0.7656	0.0007	0.2158	63	0.4120	0.3620	0.0250	0.3580	120	n/a	0.100

<sup>†</sup> Although the calculations were performed for 3.0%, the enrichment is limited in the specification for authorized contents to 2.7%.

<sup>††</sup> This assembly class was analyzed and qualified for a variation in the number of fuel rods.

Table 6.2.42

## SPECIFICATION OF THE THORIA ROD CANISTER AND THE THORIA RODS

Canister ID	4.81"
Canister Wall Thickness	0.11"
Separator Assembly Plates Thickness	0.11"
Cladding OD	0.412"
Cladding ID	0.362"
Pellet OD	0.358"
Active Length	110.5"
Fuel Composition	1.5% UO <sub>2</sub> and 98.5% ThO <sub>2</sub> <sup>1</sup>
Initial Enrichment	93.5 wt% <sup>235</sup> U for 1.5% of the fuel
Maximum k <sub>eff</sub>	0.1813
Calculated k <sub>eff</sub>	0.1779
Standard Deviation	0.0004

<sup>1</sup> Reducing the UO<sub>2</sub> content to 1.5% results in a reduction in reactivity from the original calculation, thus no new calculation is needed.

Table 6.2.43  
 MAXIMUM  $K_{\text{EFF}}$  VALUES FOR THE 14X14E ASSEMBLY CLASS IN THE MPC-24  
 (all dimensions are in inches)

14x14E (5.0% Enrichment, Fixed neutron absorber $^{10}\text{B}$ minimum loading of 0.02 g/cm <sup>2</sup> ) 173 fuel rods, 0 guide tubes, pitch=0.453 and 0.441, SS clad†										
Fuel Assembly Designation	maximum $k_{\text{eff}}$	calculated $k_{\text{eff}}$	standard deviation	EALF	cladding OD	cladding ID	cladding thickness	pellet OD	fuel length††	guide tube thickness
14x14E01	0.7598	0.7555	0.0008	0.3890	0.3415	0.3175 0.2845 0.3015	0.0120 0.0285 0.0200	0.3130 0.2800 0.2970	102	0.0000
14x14E02	0.7627	0.7586	0.0007	0.3607	0.3415	0.3175	0.0120	0.3130	102	0.0000
14x14E03	0.6952	0.6909	0.0008	0.2905	0.3415	0.2845	0.0285	0.2800	102	0.0000
Dimensions Listed for Authorized Contents					0.3415 (min.)	0.3175 (max.)		0.3130 (max.)	102 (max.)	0.0000 (min.)
Bounding dimensions (14x14E02)	0.7627	0.7586	0.0007	0.3607	0.3415	0.3175	0.0120	0.3130	102	0.0000

† This is the IP-1 fuel assembly at Indian Point. This assembly is a 14x14 assembly with 23 fuel rods omitted to allow passage of control rods between assemblies. Fuel rod dimensions are bounding for each of the three types of rods found in the IP-1 fuel assembly.

†† Calculations were conservatively performed for a fuel length of 150 inches.

Table 6.2.44  
 MAXIMUM  $K_{\text{EFF}}$  VALUES FOR THE 9X9G ASSEMBLY CLASS IN THE MPC-68 and MPC-68FF  
 (all dimensions are in inches)

9x9G (4.2% Enrichment, Fixed neutron absorber $^{10}\text{B}$ minimum loading of $0.0279 \text{ g/cm}^2$ ) 72 fuel rods, 1 water rod (square, replacing 9 fuel rods), pitch=0.572, Zr clad											
Fuel Assembly Designation	maximum $k_{\text{eff}}$	calculated $k_{\text{eff}}$	standard deviation	EALF	cladding OD	cladding ID	cladding thickness	pellet OD	fuel length	water rod thickness	channel thickness
9x9G01	0.9309	0.9265	0.0008	0.2191	0.4240	0.3640	0.0300	0.3565	150	0.0320	0.120
Dimensions Listed for Authorized Contents					0.4240 (min.)	0.3640 (max.)		0.3565 (max.)	150 (max.)	0.0320 (min.)	0.120 (max.)



### 6.3 MODEL SPECIFICATION

In compliance with the requirements of 10CFR71.31(a)(1), 10CFR71.33(a)(5), and 10CFR71.33(b), this section provides a description of the HI-STAR 100 System in sufficient detail to identify the package accurately and provide a sufficient basis for the evaluation of the package.

#### 6.3.1 Description of Calculational Model

Figures 6.3.1 through 6.3.3 show representative horizontal cross sections of the four types of cells used in the calculations, and Figures 6.3.4 through 6.3.6 illustrate the basket configurations used. Four different MPC fuel basket designs were evaluated as follows:

- a 24 PWR assembly basket,
- an optimized 24 PWR assembly basket (MPC-24E/EF and Trojan MPC-24E/EF),
- a 32 PWR assembly basket, and
- a 68 BWR assembly basket.

For all basket designs, the same techniques and the same level of detail are used in the calculational models.

[

PROPRIETARY INFORMATION WITHHELD PER 10CFR2.390

]

[

PROPRIETARY INFORMATION WITHHELD PER 10CFR2.390

]

As indicated in Figures 6.3.1 through 6.3.3 and in Tables 6.3.1 and 6.3.2, calculations were made with dimensions assumed to be at their most conservative value with respect to criticality. CASMO and MCNP4a were used to determine the direction of the manufacturing tolerances which produced the most adverse effect on criticality. After the directional effect (positive effect with an increase in reactivity; or negative effect with a decrease in reactivity) of the manufacturing tolerances was determined, the criticality analyses were performed using the worst case tolerances in the direction which would increase reactivity.

CASMO-3 and -4 were used for one of each of the two principal basket designs, i.e. for the fluxtrap design MPC-24 and for the non-fluxtrap design MPC-68. The effects are shown in Table 6.3.1 which also identifies the approximate magnitude of the tolerances on reactivity. The conclusions in Table 6.3.1 are directly applicable to the MPC-24E/EF and the MPC-32, due to the similarity in the basket designs.

Additionally, MCNP4a calculations are performed to evaluate the tolerances of the various basket dimensions of the MPC-68, MPC-24 and MPC-32 in further detail. [

PROPRIETARY INFORMATION WITHHELD PER 10CFR2.390

]

[ PROPRIETARY INFORMATION WITHHELD PER 10CFR2.390 ]

Based on the MCNP4a and CASMO calculations, the conservative dimensional assumptions listed in Table 6.3.3 were determined for the MPC basket designs. Because the reactivity effect (positive or negative) of the manufacturing tolerances are not assembly dependent, these dimensional assumptions were employed for the criticality analyses.

The design parameters important to criticality safety are: fuel enrichment, the inherent geometry of the fuel basket structure, and the fixed neutron absorbing panels. None of these parameters are affected by the hypothetical accident conditions of transport.

During the hypothetical accident conditions of transport, the HI-STAR 100 System is assumed to be flooded to such an extent as to cause the maximum reactivity and to have full water reflection to such an extent as to cause the maximum reactivity. Further, arrays of packages under the hypothetical accident conditions must be evaluated to determine the maximum number of packages that may be transported in a single shipment. Thus, the only differences between the normal and hypothetical accident condition calculational models are the internal/external moderator densities and the boundary conditions (to simulate an infinite array of HI-STAR 100 Systems).

### 6.3.2 Cask Regional Densities

Composition of the various components of the principal designs of the HI-STAR 100 Systems are listed in Table 6.3.4. In this table, only the composition of fresh fuel is listed. For a discussion on the composition of spent fuel for burnup credit in the MPC-32 see Appendix 6.C and Appendix 6.E.

The HI-STAR 100 System is designed such that the fixed neutron absorber will remain effective for a period greater than 20 years, and there are no credible means to lose it. A detailed physical description, historical applications, unique characteristics, service experience, and manufacturing quality assurance of fixed neutron absorbers are provided in Subsection 1.2.1.4.1.

The continued efficacy of the fixed neutron absorber is assured by acceptance testing, documented in Chapter 8, to validate the  $^{10}\text{B}$  (poison) concentration in the fixed neutron absorber. To demonstrate that the neutron flux from the irradiated fuel results in a negligible depletion of the poison material, an MCNP4a calculation of the number of neutrons absorbed in the  $^{10}\text{B}$  was performed. The calculation conservatively assumed a constant neutron source for 50 years equal to the initial source for the design basis fuel, as determined in Section 5.2, and shows that the fraction of  $^{10}\text{B}$  atoms destroyed is only 2.6E-09 in 50 years. Thus, the reduction in  $^{10}\text{B}$  concentration in the fixed neutron absorber by neutron absorption is negligible. In addition, the

structural analysis demonstrates that the sheathing, which affixes the fixed neutron absorber panel, remains in place during all hypothetical accident conditions, and thus, the fixed neutron absorber panel remains permanently fixed. Therefore, there is no need to provide a surveillance or monitoring program to verify the continued efficacy of the neutron absorber.

### 6.3.3 Eccentric Positioning of Assemblies in Fuel Storage Cells

Up to and including Revision 9 of this SAR, all criticality calculations were performed with fuel assemblies centered in the fuel storage locations since the effect of credible eccentric fuel positioning was judged to be not significant. Starting in Revision 10 of this SAR, the potential reactivity effect of eccentric positioning of assemblies in the fuel storage locations is accounted for in a conservatively bounding fashion, as described further in this subsection, for all new or changed MPC designs or assembly classes. The calculations in this subsection serve to determine the highest maximum  $k_{\text{eff}}$  value for each of these assembly class and basket combinations, that is then reported in the summary tables in Section 6.1 and the results tables in Section 6.4. Further, the calculations in this subsection are used to determine the assembly class in each basket with the highest maximum  $k_{\text{eff}}$  that is then used to demonstrate compliance with the requirements of 10CFR71.55 and 10CFR71.59. All other calculations throughout this chapter, such as studies to determine bounding fuel dimension, bounding basket dimensions, or bounding moderation conditions, are performed with assemblies centered in the fuel storage locations.

To conservatively account for eccentric fuel positioning in the fuel storage cells, three different configurations are analyzed, and the results are compared to determine the bounding configuration:

- Cell Center Configuration: All assemblies centered in their fuel storage cell; same configuration that is used in Section 6.2 and Section 6.3.1;
- Basket Center Configuration: All assemblies in the basket are moved as closely to the center of the basket as permitted by the basket geometry; and
- Basket Periphery Configuration: All assemblies in the basket are moved furthest away from the basket center, and as closely to the periphery of the basket as possible.

It needs to be noted that the two eccentric configurations are hypothetical, since there is no known physical effect that could move all assemblies within a basket consistently to the center or periphery. Instead, the most likely configuration would be that all assemblies are moved in the same direction when the cask is in a horizontal position, and that assemblies are positioned randomly when the cask is in a vertical position. Further, it is not credible to assume that any such configuration could exist by chance. Even if the probability for a single assembly placed in the corner towards the basket center would be  $1/5$  (i.e. assuming only the center and four corner positions in each cell, all with equal probability), then the probability that all assemblies would be located towards the center would be  $(1/5)^{24}$  or approximately  $10^{-17}$  for the MPC-24,  $(1/5)^{32}$  or

approximately  $10^{-23}$  for the MPC-32, and  $(1/5)^{68}$  or approximately  $10^{-48}$  for the MPC-68. However, since the configurations listed above bound all credible configurations, they are conservatively used in the analyses.

The results are presented in Table 6.3.5 for the MPC-24, Table 6.3.6 for the MPC-24E/EF, Table 6.3.7 for the Trojan MPC-24E/EF, and Table 6.3.8 for the MPC-68. For evaluations of eccentric fuel positions in the MPC-32 with burnup credit see Appendix 6.C and Appendix 6.E. Each table shows the maximum  $k_{\text{eff}}$  value for centered and the two eccentric configurations for each of the assembly classes, and indicates the bounding configuration. The results are summarized as follows:

- In all cases, moving the assemblies to the periphery of the basket results in a reduction in reactivity, compared to the cell centered position.
- Most cases show the maximum reactivity for the basket center configuration, however, in some cases the reactivity is higher for the cell center configuration.

For each of the assembly class and basket combinations listed in Tables 6.3.5 through Table 6.3.8, the configuration showing the highest reactivity is used as the bounding configuration, and listed in the respective tables in Section 6.1. and 6.4. For evaluations of eccentric fuel positions in the MPC-32 with burnup credit see Appendix 6.C and Appendix 6.E.

Table 6.3.1

[PROPRIETARY INFORMATION WITHHELD PER 10CFR2.390]

Table 6.3.1 (continued)

[PROPRIETARY INFORMATION WITHHELD PER 10CFR2.390]

---

HI-STAR SAR

Rev. 16

REPORT HI-951251

6.3-7

Table 6.3.2

[PROPRIETARY INFORMATION WITHHELD PER 10CFR2.390]



Table 6.3.2 (cont.)

[PROPRIETARY INFORMATION WITHHELD PER 10CFR2.390]

Table 6.3.3

[PROPRIETARY INFORMATION WITHHELD PER 10CFR2.390]

Table 6.3.4

[PROPRIETARY INFORMATION WITHHELD PER 10CFR2.390]

Table 6.3.4 (continued)

[PROPRIETARY INFORMATION WITHHELD PER 10CFR2.390]

Table 6.3.4 (continued)

[PROPRIETARY INFORMATION WITHHELD PER 10CFR2.390]

Table 6.3.4 (continued)

[PROPRIETARY INFORMATION WITHHELD PER 10CFR2.390]

Table 6.3.5

[PROPRIETARY INFORMATION WITHHELD PER 10CFR2.390]

Table 6.3.6

[PROPRIETARY INFORMATION WITHHELD PER 10CFR2.390]



Table 6.3.7

[PROPRIETARY INFORMATION WITHHELD PER 10CFR2.390]

Table 6.3.8

[PROPRIETARY INFORMATION WITHHELD PER 10CFR2.390]

FIGURES 6.3.1 THROUGH 6.3.7: [PROPRIETARY INFORMATION WITHHELD PER  
10CFR2.390]

## 6.4 CRITICALITY CALCULATIONS

### 6.4.1 Calculational or Experimental Method

The principal method for the criticality analysis is the general three-dimensional continuous energy Monte Carlo N-Particle code MCNP4a [6.1.4] developed at the Los Alamos National Laboratory. MCNP4a was selected because it has been extensively used and verified and has all of the necessary features for this analysis. MCNP4a calculations used continuous energy cross-section data based on ENDF/B-V<sup>†</sup>, as distributed with the code [6.1.4]. Independent verification calculations were performed with NITAWL-KENO5a [6.1.5], which is a three-dimensional multigroup Monte Carlo code developed at the Oak Ridge National Laboratory. The KENO5a calculations used the 238-group cross-section library, which is based on ENDF/B-V data and is distributed as part of the SCALE-4.3 package [6.4.1], in association with the NITAWL-II program [6.1.6], which adjusts the uranium-238 cross sections to compensate for resonance self-shielding effects. The Dancoff factors required by NITAWL-II were calculated with the CELLDAN code [6.1.13], which includes the SUPERDAN code [6.1.7] as a subroutine.

The convergence of a Monte Carlo criticality problem is sensitive to the following parameters: (1) number of histories per cycle, (2) the number of cycles skipped before averaging, (3) the total number of cycles and (4) the initial source distribution. The MCNP4a criticality output contains a great deal of useful information that may be used to determine the acceptability of the problem convergence. This information was used in parametric studies to develop appropriate values for the aforementioned criticality parameters to be used in the criticality calculations for this submittal. Based on these studies, calculations assuming fresh fuel used a minimum of 5,000 simulated histories per cycle, a minimum of 20 cycles were skipped before averaging, a minimum of 100 cycles were accumulated, and the initial source was specified as uniform over the fueled regions (assemblies). For parameters used in the burnup credit calculations see Appendix 6.C and Appendix 6.E. Further, the output was examined to ensure that each calculation achieved acceptable convergence. These parameters represent an acceptable compromise between calculational precision and computational time. Appendix 6.D provides sample input files for the MPC-24 and MPC-68 basket in the HI-STAR 100 System.

CASMO-4 [6.1.10-6.1.12] was used for determining the small incremental reactivity effects of manufacturing tolerances. Although CASMO has been extensively benchmarked, these calculations are used only to establish direction of reactivity uncertainties due to manufacturing tolerances (and their magnitude). This allows the MCNP4a calculational model to use the worst combination of manufacturing tolerances. Table 6.3.1 shows results of the CASMO calculations.

---

<sup>†</sup> For burnup credit calculations in the MPC-32, ENDF/B-VI cross sections are used for nuclides where ENDF/B-V cross sections are not available. Also see Appendix 6.C.

Additionally, CASMO-4 was used to determine the isotopic composition of spent fuel for burnup credit in the MPC-32 (see Appendix 6.C and Appendix 6.E).

#### 6.4.2 Fuel Loading or Other Contents Loading Optimization

The basket designs are intended to safely accommodate the candidate fuel assemblies with enrichments indicated in Tables 6.1.1 through 6.1.3 and 6.1.5 through 6.1.7. The calculations were based on the assumption that the HI-STAR 100 System was fully flooded with water. In all cases, the calculations include bias and calculational uncertainties, as well as the reactivity effects of manufacturing tolerances, determined by assuming the worst case geometry.

##### 6.4.2.1 Internal and External Moderation

The regulations in 10CFR71.55 include the requirement that the system remains subcritical when assuming moderation to the most reactive credible extent. The regulations in 10CFR71.59 require subcriticality for package arrays under different moderation conditions. The calculations in this section demonstrate that the HI-STAR 100 System remains subcritical for all credible conditions of moderation, and that the system fulfills all requirements of 10CFR71.55 and 10CFR71.59. The following subsections 6.4.2.1.1 through 6.4.2.4 present various studies to confirm or identify the most reactive configuration or moderation condition. Specifically, the following conditions are analyzed:

- Reduced internal and external water density for single packages (6.4.2.1.1) and package arrays (6.4.2.1.2);
- Variation in package to package distance in package arrays (6.4.2.1.2);
- Partial internal flooding of package (6.4.2.2);
- Flooding of pellet to cladding gap of the fuel rods (6.4.2.3); and
- Preferential flooding, i.e. uneven flooding inside the package (6.4.2.4).

The calculations that specifically demonstrate compliance with the individual requirements of 10CFR71.55 and 10CFR71.59 are presented in Section 6.4.3. These calculations are performed for all MPCs.

The studies in subsections 6.4.2.1.1 through 6.4.2.4 have been performed for both principal basket designs (flux-trap and non-flux-trap) and for both fuel designs (BWR and PWR). Specifically, the studies are performed with the MPC-24 (flux-trap design / PWR fuel) and the MPC-68 (non-flux-trap design / BWR fuel). The results of the studies show a consistent behavior of the different basket designs and fuel types for different moderation conditions. Consequently, the conclusions drawn from these studies are directly applicable to the remaining baskets, namely the MPC-24E/EF (flux-trap design, PWR), MPC-32 (non-flux-trap design, PWR) and MPC-68F (non-flux-trap design, BWR), and no further studies are required for these baskets.

The studies in subsection 6.4.2.1.1 through 6.4.2.4 have been performed with the fuel assemblies centered in each storage location in the basket, which is not necessarily the most reactive position. However, this assumption is acceptable since the objective of these studies is to determine the most reactive moderation condition, not the highest reactivity. The calculations in Section 6.4.3 that demonstrate compliance with 10CFR71.55 and 19CFR71.59 are performed with the most reactive assembly position as discussed in Section 6.3.3.

Regarding the effect of low moderator density it is noted that with a neutron absorber present (i.e., the fixed neutron absorber sheets on the steel walls of the storage compartments), the phenomenon of a peak in reactivity at a hypothetical low moderator density (sometimes called "optimum" moderation) does not occur to any significant extent. In a definitive study, Cano, et al. [6.4.2] has demonstrated that the phenomenon of a peak in reactivity at low moderator densities does not occur when strong neutron absorbing material is present or in the absence of large water spaces between fuel assemblies in storage. Nevertheless, calculations for a single reflected cask and for infinite arrays of casks were made to confirm that the phenomenon does not occur with low density water inside or outside the HI-STAR 100 Systems.

#### 6.4.2.1.1 Single Package Evaluation

Calculations for a single package are performed for the MPC-24 and MPC-68. The Calculational model consists of the HI-STAR System surrounded by a rectangular box filled with water. The neutron absorber on the outside of the HI-STAR is neglected, since it might be damaged under accident conditions, and since it is conservative to replace the neutron absorber (Holtite-A) with a neutron reflector (water). The minimum water thickness on each side of the cask is 30 cm, which effectively represents full water reflection. The outer surfaces of the surrounding box are conservatively set to be fully reflective, which effectively models a three dimensional array of cask systems with a minimum surface to surface distance of 60 cm. The calculations with internal and external moderators of various densities are shown in Table 6.4.1. For comparison purposes, a calculation for a single unreflected cask (Case 1) is also included in Table 6.4.1. At 100% external moderator density, Case 2 corresponds to a single fully-flooded cask, fully reflected by water. Figure 6.4.9 plots calculated  $k_{\text{eff}}$  values ( $\pm 2\sigma$ ) as a function of internal moderator density for both MPC designs with 100% external moderator density (i.e., full water reflection).

Results listed in Table 6.4.1 and plotted in Figure 6.4.9 support the following conclusions:

- The calculated  $k_{\text{eff}}$  for a fully-flooded cask is independent of the external moderator (the small variations in the listed values are due to statistical uncertainties which are inherent to the calculational method (Monte Carlo)), and

- Reducing the internal moderation results in a monotonic reduction in reactivity, with no evidence of any optimum moderation. Thus, the fully flooded condition corresponds to the highest reactivity, and the phenomenon of optimum low-density moderation does not occur and is not applicable to the HI-STAR 100 System.

#### 6.4.2.1.2 Evaluation of Package Arrays

In terms of reactivity, the normal conditions of transport (i.e., no internal or external moderation) are bounded by the hypothetical accident conditions of transport. Therefore, the calculations in this section evaluate arrays of HI-STAR 100 Systems under hypothetical accident conditions (i.e., internal and external moderation by water to the most reactive credible extent and no neutron shield present).

In accordance with 10CFR71.59 requirements, calculations were performed to simulate an infinite three-dimensional square array of internally fully-flooded (highest reactivity) casks with varying cask spacing and external moderation density. The MPC-24 was used for this analysis. The maximum  $k_{\text{eff}}$  results of these calculations are listed in Table 6.4.2 and confirm that the individual casks in a square-pitched array are independent of external moderation and cask spacing. The maximum value listed in Table 6.4.2 is statistically equivalent (within three standard deviations) to the reference value (Case 1 shown in Table 6.4.1) for a single unreflected fully flooded cask.

To further investigate the reactivity effects of array configurations, calculations were also performed to simulate an infinite three-dimensional hexagonal (triangular-pitched) array of internally fully-flooded (highest reactivity) MPC-24 casks with varying cask spacing and external moderation density. The maximum  $k_{\text{eff}}$  results of these calculations are listed in Table 6.4.3 and confirm that the individual casks in a hexagonal (triangular pitched) array are effectively independent of external moderation and cask spacing. The maximum value listed in Table 6.4.3 is statistically equivalent (within two standard deviations) to the reference value (Case 1 shown in Table 6.4.1) for a single unreflected fully flooded cask.

To assure that internal moderation does not result in increased reactivity, hexagonal array calculations were also performed for 10% internal moderator with 10% and 100% external moderation for varying cask spacing. Maximum  $k_{\text{eff}}$  results are summarized in Table 6.4.4 and confirm the very low values of  $k_{\text{eff}}$  for low values of internal moderation.

The results presented thus far indicate that neutronic interaction between casks is not enhanced by the neighboring casks or the water between the neighboring casks, and thus, the most reactive arrangement of casks corresponds to a tightly packed array with the cask surfaces touching. Therefore, calculations were performed for an infinite hexagonal (triangular pitched) array of touching casks (neglecting the Holtite-A neutron shield). These calculations were performed for

the MPC-24 and the MPC-68 designs, in the internally flooded (highest reactivity) and internally dry conditions, with and without external flooding. The results of these calculations are listed in Table 6.4.5. For both the MPC-24 and MPC-68, the maximum  $k_{\text{eff}}$  values are shown to be statistically equivalent (within one standard deviation) to that of a single internally flooded unreflected cask and are below the regulatory limit of 0.95.

The calculations demonstrate that the thick steel wall of the overpack is more than sufficient to preclude neutron coupling between casks, consistent with the findings of Cano, et al. Neglecting the Holtite-A neutron shielding in the calculational model provides further assurance of conservatism in the calculations.

#### 6.4.2.2 Partial Flooding

To demonstrate that the HI-STAR 100 System would remain subcritical if water were to leak into the containment system, as required by 10CFR71.55, calculations in this section address partial flooding in the HI-STAR 100 System and demonstrate that the fully flooded condition is the most reactive.

The reactivity changes during the flooding process were evaluated in both the vertical and horizontal positions for the MPC-24 and MPC-68 designs. For these calculations, the cask is partially filled (at various levels) with full density (1.0 g/cc) water and the remainder of the cask is filled with steam consisting of ordinary water at partial density (0.002 g/cc). Results of these calculations are shown in Table 6.4.6. In all cases, the reactivity increases monotonically as the water level rises, confirming that the most reactive condition is fully flooded. This conclusion is also true for the other baskets that were not analyzed under partial flooding conditions, since increasing the water level always improves the moderation condition of the fuel and therefore results in an increase in reactivity<sup>†</sup>. The fully flooded case therefore represents the bounding condition for all MPC basket types.

#### 6.4.2.3 Clad Gap Flooding

The reactivity effect of flooding the fuel rod pellet-to-clad gap regions, in the fully flooded condition, has been investigated. Table 6.4.7 presents maximum  $k_{\text{eff}}$  values that demonstrate the positive reactivity effect associated with flooding the pellet-to-clad gap regions. These results confirm that it is conservative to assume that the pellet-to-clad gap regions are flooded. For all cases that involve flooding, the pellet-to-clad gap regions are assumed to be flooded.

---

<sup>†</sup> The rate of increase in reactivity along the fuel length, though, could be different between different MPC designs. An example would be the MPC-32 with burnup credit where the reactivity is strongly affected by the lower burned ends of the fuel.

---



#### 6.4.2.4 Preferential Flooding

Two different potential conditions of preferential flooding are considered: preferential flooding of the MPC basket itself (i.e. different water levels in different basket cells), and preferential flooding involving Damaged Fuel Containers.

Preferential flooding of the MPC basket itself for any of the MPC fuel basket designs is not possible [

PROPRIETARY INFORMATION WITHHELD PER 10CFR2.390

]

[PROPRIETARY INFORMATION WITHHELD PER 10CFR2.390  
]

In summary, it is concluded that the MPC fuel baskets cannot be preferentially flooded, and that the potential preferential flooding conditions involving DFCs are bounded by the result for the fully flooded condition listed in Subsections 6.4.4 and 6.4.9.

#### 6.4.2.5 Hypothetical Accidents Conditions of Transport

The analyses presented in Section 2.7 of Chapter 2 and Section 3.5 of Chapter 3 demonstrate that the damage resulting from the hypothetical accident conditions of transport are limited to a loss of the neutron shield material as a result of the hypothetical fire accident. Because the criticality analyses do not take credit for the neutron shield material (Holtite-A), this condition has no effect on the criticality analyses.

As reported in Table 2.7.1, the minimum factor of safety for all MPCs as a result of the hypothetical accident conditions of transport is larger than 1.0 against the Level D allowables for Subsection NG, Section III of the ASME Code. Therefore, because the maximum box wall stresses are well within the ASME Level D allowables, the flux-trap gap change in the MPC-24 and MPC-24E/EF will be insignificant compared to the characteristic dimension of the flux trap.

Regarding the fuel assembly integrity, SAR Section 2.9 contains an evaluation of the fuel under accident conditions that concludes that the fuel rod cladding remains intact under the design basis deceleration levels set for the HI-STAR 100.

In summary, the hypothetical transport accidents have no adverse effect on the geometric form of the package contents important to criticality safety, and thus, are limited to the effects on internal and external moderation evaluated in Subsection 6.4.2.1.

#### 6.4.3 Criticality Results

In calculating the maximum reactivity, the analysis used the following equation:

$$k_{eff}^{max} = k_c + K_c \sigma_c + Bias + \sigma_B$$

where:

- ⇒  $k_c$  is the calculated  $k_{eff}$  under the worst combination of tolerances;
- ⇒  $K_c$  is the K multiplier for a one-sided statistical tolerance limit with 95% probability at the 95% confidence level [6.1.8]. Each final  $k_{eff}$  value calculated by MCNP4a (or KENO5a) is the result of averaging 100 (or more) cycle  $k_{eff}$  values, and thus, is based on a sample size of 100. The K multiplier corresponding to a sample size of 100 is 1.93.

However, for this analysis a value of 2.00 was assumed for the K multiplier, which is larger (more conservative) than the value corresponding to a sample size of 100;

- ⇒  $\sigma_c$  is the standard deviation of the calculated  $k_{eff}$ , as determined by the computer code (MCNP4a or KENO5a);
- ⇒ **Bias** is the systematic error in the calculations (code dependent) determined by comparison with critical experiments; and
- ⇒  $\sigma_B$  is the standard error of the bias (which includes the K multiplier for 95% probability at the 95% confidence level).

Appendix 6.A presents the critical experiment benchmarking for fresh UO<sub>2</sub> and MOX fuel and the derivation of the corresponding bias and standard error of the bias (95% probability at the 95% confidence level).

See Appendix 6.C and Appendix 6.E for the critical experiment benchmarking for spent fuel.

The studies in sections 6.4.2.1 through 6.4.2.4 demonstrate that the moderation by water to the most reactive credible extent corresponds to the internally fully flooded condition of the MPC, with the pellet-to-clad gap in the fuel rods also flooded with water. The external moderation and/or the presence of other surrounding packages, however, has a statistically negligible effect. To demonstrate compliance with 10CFR71.55 and 10CFR71.59, the following set of four calculations is performed for each of the MPC designs:

- Single containment with full internal and external water moderation. The full external water moderation is modeled through an infinite array of containments with a 60cm surface to surface distance. The containment system corresponds to the 2.5 inch inner shell of the overpack. This case addresses the requirement of 10CFR71.55 (b).
- Single cask with full internal and external water moderation. As for the single containment, the full external water moderation is modeled through an infinite array. The external neutron moderator is conservatively neglected in the model. This case also addresses the requirement of 10CFR71.55 (b).
- Hexagonal array of touching casks with full internal and external water reflection. This addresses the requirement of 10CFR71.59 (a)(2) and the determination of the transport index based on criticality control according to 10CFR71.59 (b).
- Hexagonal array of touching casks, internally and externally dry. This addresses the requirement of 10CFR71.59 (a) (1) and the determination of the transport index based on criticality control according to 10CFR71.59 (b). This also addresses the requirement of 10CFR71.55 (d)(1).

To satisfy the requirements of 10CFR71.55 (b)(1), the calculations are performed

- with the assembly type that results in the highest reactivity in the MPC. This is the assembly class 15x15F for the MPC-24, MPC-24E/EF and MPC-32, the assembly class 17x17B with intact and damaged assemblies in the Trojan MPC-24E/EF, the assembly class 9x9E/F in the MPC-68, and the assembly class 6x6C for the MPC-68F; and
- with the bounding basket dimensions as determined in Section 6.3.1 for each basket; and
- with eccentric fuel positioning as necessary, as discussed in Section 6.3.3.

The maximum  $k_{\text{eff}}$  values for all these cases, calculated with 95% probability at the 95% confidence level, are listed in Table 6.4.12. Results of the criticality safety calculations for other assembly classes under the condition of full internal flooding with water are summarized in Section 6.1. Corresponding detailed results including the maximum  $k_{\text{eff}}$ , standard deviation and energy of the average lethargy causing fission (EALF) are listed for all MPCs except the MPC-32 in Tables 6.4.13 through 6.4.17. Results for the MPC-32 are presented in Appendix 6.C and Appendix 6.E. Overall, these results confirm that for each of the candidate fuel assemblies and basket configurations the effective multiplication factor ( $k_{\text{eff}}$ ), including all biases and uncertainties at a 95-percent confidence level, do not exceed 0.95 under all credible normal and hypothetical accident conditions of transport. Therefore, compliance with 10CFR71.55 for single packages and 10CFR71.59 for package arrays in both normal and hypothetical accident conditions of transport is demonstrated for all of the fuel assembly classes and basket configurations listed in Tables 6.1.1 through 6.1.3 and 6.1.5 through 6.1.7. It further demonstrates that the transportation index for criticality control is zero because an infinite number of HI-STAR 100 casks will remain subcritical ( $k_{\text{eff}} < 0.95$ ) under both normal and hypothetical accident conditions of transport.

Additional calculations (CASMO-4) at elevated temperatures confirm that the temperature coefficients of reactivity are negative as shown in Table 6.3.1. This confirms that the calculations for the storage baskets are conservative.

Tables listing the maximum  $k_{\text{eff}}$ , calculated  $k_{\text{eff}}$ , standard deviation, and energy of the average lethargy causing fission (EALF) for each of the candidate fuel assemblies in each assembly class for the MPC-24, MPC-68 and MPC-68F basket configurations, and with assemblies centered in the fuel storage locations, are provided in Section 6.2.

#### 6.4.4 Damaged Fuel Container for BWR Fuel

Both damaged BWR fuel assemblies and BWR fuel debris are required to be loaded into Damaged Fuel Containers (DFCs). Two different DFC types with slightly different cross sections are analyzed. DFCs containing fuel debris are only analyzed in the MPC-68F. DFCs containing damaged fuel assemblies may be stored in either the MPC-68 or MPC-68F. Evaluation of the capability of storing damaged fuel and fuel debris (loaded in DFCs) is limited to very low reactivity fuel in the MPC-68F. Because the MPC-68 has a higher specified  $^{10}\text{B}$

loading, the evaluation of the MPC-68F conservatively bounds the storage of damaged BWR fuel assemblies in a standard MPC-68. Although the maximum planar-average enrichment of the damaged fuel is limited to 2.7%  $^{235}\text{U}$  as specified in Chapter 1, analyses have been made for three possible scenarios, conservatively assuming fuel†† of 3.0% enrichment. The scenarios considered included the following:

1. Lost or missing fuel rods, calculated for various numbers of missing rods in order to determine the maximum reactivity. The configurations assumed for analysis are illustrated in Figures 6.4.1 through 6.4.7.
2. Broken fuel assembly with the upper segments falling into the lower segment creating a close-packed array (described as a 8x8 array). For conservatism, the array analytically retained the same length as the original fuel assemblies in this analysis. This configuration is illustrated in Figure 6.4.8.
3. Fuel pellets lost from the assembly and forming powdered fuel dispersed through a volume equivalent to the height of the original fuel. (Flow channel and clad material assumed to disappear).

Results of the analyses, shown in Table 6.4.8, confirm that, in all cases, the maximum reactivity is well below the regulatory limit. There is no significant difference in reactivity between the two DFC types. Collapsed fuel reactivity (simulating fuel debris) is low because of the reduced moderation. Dispersed powdered fuel results in low reactivity because of the increase in  $^{238}\text{U}$  neutron capture (higher effective resonance integral for  $^{238}\text{U}$  absorption).

The loss of fuel rods results in a small increase in reactivity (i.e., rods assumed to collapse, leaving a smaller number of rods still intact). The peak reactivity occurs for 8 missing rods, and a smaller (or larger) number of intact rods will have a lower reactivity, as indicated in Table 6.4.8.

The analyses performed and summarized in Table 6.4.8 provides the relative magnitude of the effects on the reactivity. This information in combination with the maximum  $k_{\text{eff}}$  values listed in Table 6.1.3 and the conservatism in the analyses, demonstrate that the maximum  $k_{\text{eff}}$  of the damaged fuel in the most adverse post-accident condition will remain well below the regulatory requirement of  $k_{\text{eff}} < 0.95$ .

Appendix 6.D provides sample input files for the damaged fuel analysis.

#### 6.4.5 Fuel Assemblies with Missing Rods

For fuel assemblies that are qualified for damaged fuel storage, missing and/or damaged fuel rods are acceptable. However, for fuel assemblies to meet the limitations of intact fuel assembly

---

†† 6x6A01 and 7x7A01 fuel assemblies were used as representative assemblies.

storage, missing fuel rods must be replaced with dummy rods that displace a volume of water that is equal to, or larger than, that displaced by the original rods.

#### 6.4.6 Thoria Rod Canister

The Thoria Rod Canister is similar to a DFC with an internal separator assembly containing 18 intact fuel rods. The configuration is illustrated in Figure 6.4.10. The  $k_{\text{eff}}$  value for an MPC-68F filled with Thoria Rod Canisters is calculated to be 0.1813. This low reactivity is attributed to the relatively low content in  $^{235}\text{U}$  (equivalent to  $\text{UO}_2$  fuel with an enrichment of approximately 1.5 wt%  $^{235}\text{U}$ ), the large spacing between the rods (the pitch is approximately 1", the cladding OD is 0.412") and the absorption in the separator assembly. Together with the maximum  $k_{\text{eff}}$  values listed in Tables 6.1.2 and 6.1.3 this result demonstrates, that the  $k_{\text{eff}}$  for a Thoria Rod Canister loaded into the MPC68 or the MPC68F together with other approved fuel assemblies or DFCs will remain well below the regulatory requirement of  $k_{\text{eff}} < 0.95$ .

#### 6.4.7 Sealed Rods Replacing BWR Water Rods

Some BWR fuel assemblies contain sealed rods filled with a non-fissile instead of water rods. Compared to the configuration with water rods, the configuration with sealed rods has a reduced amount of moderator, while the amount of fissile material is maintained. Thus, the reactivity of the configuration with sealed rods will be lower compared to the configuration with water rods. Any configuration containing sealed rods instead of water rods is therefore bounded by the analysis for the configuration with water rods and no further analysis is required to demonstrate the acceptability. Therefore, for all BWR fuel assemblies analyzed, it is permissible that water rods are replaced by sealed rods filled with a non-fissile material.

#### 6.4.8 Neutron Sources in Fuel Assemblies

Fuel assemblies containing start-up neutron sources are permitted for storage in the HI-STAR 100 System. The reactivity of a fuel assembly is not affected by the presence of a neutron source (other than by the presence of the material of the source, which is discussed later). This is true because in a system with a  $k_{\text{eff}}$  less than 1.0, any given neutron population at any time, regardless of its origin or size, will decrease over time. Therefore, a neutron source of any strength will not increase reactivity, but only the neutron flux in a system, and no additional criticality analyses are required. Sources are inserted as rods into fuel assemblies, i.e. they replace either a fuel rod or water rod (moderator). Therefore, the insertion of the material of the source into a fuel assembly will not lead to an increase of reactivity either.

#### 6.4.9 PWR Damaged Fuel and Fuel Debris

The MPC-24E, MPC-24EF, and Trojan MPC-24E and MPC-24EF are designed to contain

damaged fuel and fuel debris, loaded into Damaged Fuel Containers (DFCs) or Failed Fuel Cans (FFCs). There is one generic DFC for the MPC-24E/EF, and two containers, a Holtec DFC and a Trojan FFC for the Trojan MPC-24E/EF. In this section, the term “DFC” is used to specify either of these components. In any case, the number of DFCs is limited to 4, and the permissible locations of the DFCs are shown in Figure 6.4.11.

Only the Trojan MPC-24E/EF is certified for damaged fuel and fuel debris. However, the generic MPC-24E/EF is also designed to accommodate damaged fuel and fuel debris, and the majority of criticality evaluations for damaged fuel and fuel debris are performed for the generic MPC-24E/EF, with only a smaller number of calculations performed for the Trojan MPCs. Therefore, criticality evaluations for both the generic MPC-24E/EF and the Trojan MPC-24E/EF are presented in this subsection, even though the Trojan MPC-24E/EF are the only MPCs authorized to transport damaged fuel and fuel debris.

Damaged fuel assemblies are assemblies with known or suspected cladding defects greater than pinholes or hairlines, or with missing rods, but excluding fuel assemblies with gross defects (for a full definition see Chapter 1). Therefore, apart from possible missing fuel rods, damaged fuel assemblies have the same geometric configuration as intact fuel assemblies and consequently the same reactivity. Missing fuel rods can result in a slight increase of reactivity. After a drop accident, however, it can not be assumed that the initial geometric integrity is still maintained. For a drop on either the top or bottom of the cask, the damaged fuel assemblies could collapse. This would result in a configuration with a reduced length, but increased amount of fuel per unit length. For a side drop, fuel rods could be compacted to one side of the DFC. In either case, a significant relocation of fuel within the DFC is possible, which creates a greater amount of fuel in some areas of the DFC, whereas the amount of fuel in other areas is reduced. Fuel debris can include a large variety of configurations ranging from whole fuel assemblies with severe damage down to individual fuel pellets.

In the cases of fuel debris or relocated damaged fuel, there is the potential that fuel could be present in axial sections of the DFCs that are outside the basket height covered with fixed neutron absorber. However, in these sections, the DFCs are not surrounded by any intact fuel, only by basket cell walls, non-fuel hardware and water. Studies have shown that this condition does not result in any significant effect on reactivity, compared to a condition where the damaged fuel and fuel debris is restricted to the axial section of the basket covered by fixed neutron absorber. All calculations for damaged fuel and fuel debris are therefore performed assuming that fuel is present only in the axial sections covered by the fixed neutron absorber, and the results are directly applicable to any situation where damaged fuel and fuel debris is located outside these sections in the DFCs.

To address all the situations listed above and identify the configuration or configurations leading to the highest reactivity, it is impractical to analyze a large number of different geometrical

configurations for each of the fuel classes. Instead, a bounding approach is taken which is based on the analysis of regular arrays of bare fuel rods without cladding. Details and results of the analyses are discussed in the following sections.

All calculations for generic damaged fuel and fuel debris are performed using a full cask model with the maximum permissible number of Damaged Fuel Containers. For the MPC-24E and MPC-24EF, the model consists of 20 intact assemblies, and 4 DFCs in the locations shown in Figure 6.4.11. The bounding assumptions regarding the intact assemblies and the modeling of the damaged fuel and fuel debris in the DFCs are discussed in the following sections.

#### 6.4.9.1 Bounding Intact Assemblies

Intact PWR assemblies stored together with DFCs in the MPC-24E/EF are limited to a maximum enrichment of 4.0 wt%  $^{235}\text{U}$ , regardless of the fuel class. Results presented in Table 6.1.5 for the MPC-24E/EF loaded with intact assemblies only are for different enrichments for each class, ranging between 4.2 and 5.0 wt%  $^{235}\text{U}$ , making it difficult to directly identify the bounding assembly. However, the assembly class 15x15H is among the classes with the highest reactivity, but has the lowest initial enrichment. Therefore, the 15x15H assembly is used as the intact PWR assembly for all calculations with DFCs.

The Trojan MPC-24E/EF is only certified for the assembly class 17x17B, which bounds the fuel types used at the Trojan plant. Consequently, the assembly class 17x17B is used as the intact assembly in all calculations for the Trojan MPC-24E/EF.

#### 6.4.9.2 Bare Fuel Rod Arrays

A conservative approach is used to model both damaged fuel and fuel debris in the DFCs, using arrays of bare fuel rods:

- Fuel in the DFCs is arranged in regular, rectangular arrays of bare fuel rods, i.e. all cladding and other structural material in the DFC is replaced by water.
- The active length of these rods is chosen to be the maximum active fuel length of all fuel assemblies listed in Section 6.2, which is 150 inch for PWR fuel.
- To ensure the configuration with optimum moderation and highest reactivity is analyzed, the amount of fuel per unit length of the DFC is varied over a large range. This is achieved by changing the number of rods in the array and the rod pitch. The number of rods are varied between 64 (8x8) and 729 (27x27) for PWR fuel.



- Analyses are performed for the minimum, maximum and typical pellet diameter of the fuel.

This is a very conservative approach to model damaged fuel, and to model fuel debris configurations such as severely damaged assemblies and bundles of individual fuel rods, as the absorption in the cladding and structural material is neglected.

This is also a conservative approach to model fuel debris configurations such as bare fuel pellets due to the assumption of an active length of 150 inch. For some of the analyzed cases, this assumption results in more uranium mass being modeled in the DFCs than is permitted by the uranium mass loading restrictions listed in Chapter 1.

To demonstrate the level of conservatism, additional analyses are performed with the DFC containing various realistic assembly configurations such as intact assemblies, assemblies with missing fuel rods and collapsed assemblies, i.e. assemblies with increased number of rods and decreased rod pitch.

As discussed in Subsection 6.4.9, all calculations are performed for full cask models, containing the maximum permissible number of DFCs together with intact assemblies.

Graphical presentations of the calculated maximum  $k_{\text{eff}}$  for each case as a function of the fuel mass per unit length of the DFC are shown in Figure 6.4.12. The results for the bare fuel rods show a distinct peak in the maximum  $k_{\text{eff}}$  at about 3.5 kgUO<sub>2</sub>/inch.

The realistic assembly configurations are typically about 0.01 (delta-k) or more below the peak results for the bare fuel rods, demonstrating the conservatism of this approach to model damaged fuel and fuel debris configurations such as severely damaged assemblies and bundles of fuel rods.

For fuel debris configurations consisting of bare fuel pellets only, the fuel mass per unit length would be beyond the value corresponding to the peak reactivity. For example, for DFCs filled with a mixture of 60 vol% fuel and 40 vol% water the fuel mass per unit length is 7.92 kgUO<sub>2</sub>/inch for the PWR DFC. The corresponding reactivities are significantly below the peak reactivities. The difference is about 0.01 (delta-k) or more for PWR fuel. Furthermore, the filling height of the DFC would be less than 70 inches in these examples due to the limitation of the fuel mass per basket position, whereas the calculation is conservatively performed for a height of 150 inch. These results demonstrate that even for the fuel debris configuration of bare fuel pellets, the model using bare fuel rods is a conservative approach.

To demonstrate that the bare fuel rod approach also bounds the potential presence of fuel fragments in the DFCs, additional calculations were performed with fuel fragments in the DFCs

instead of bare fuel rods. The fuel fragments are modeled as regular 3-dimensional arrays of fuel cubes positioned inside water cubes. Both the dimension of the fuel cubes and the fuel-to-water-volume ratio are varied over a wide range. Calculations are performed for the MPC-24E/EF Trojan, and the results are presented in Table 6.4.18. The highest maximum  $k_{\text{eff}}$  is 0.9320 for a fragment outer dimension of 0.2 inches and a fuel to water volume ratio of 0.4. This maximum  $k_{\text{eff}}$  value is lower than the corresponding value for the bare fuel rod model, which is 0.9377 as shown in Table 6.4.17. The damaged fuel and fuel debris model based on bare fuel rods therefore bounds any condition involving fuel fragments in the DFCs.

#### 6.4.9.3 Results for MPC-24E and MPC-24EF

The MPC-24E/EF is designed for the storage of up to four DFCs with damaged fuel or fuel debris in the four outer fuel baskets cells shaded in Figure 6.4.11. These locations are designed with a larger box ID to accommodate the DFCs. For an enrichment of 4.0 wt%  $^{235}\text{U}$  for the intact fuel, damaged fuel and fuel debris, the results for the various configurations outlined in Subsection 6.4.9.2 are summarized in Figure 6.4.12 and in Table 6.4.11. Figure 6.4.12 shows the maximum  $k_{\text{eff}}$ , including bias and calculational uncertainties, for various actual and hypothetical damaged fuel and fuel debris configurations as a function of the fuel mass per unit length of the DFC. For the intact assemblies, the 15x15H assembly class was chosen (see Subsection 6.4.9.1). Table 6.4.11 lists the highest maximum  $k_{\text{eff}}$  for the various configurations. All maximum  $k_{\text{eff}}$  values are below the 0.95 regulatory limit.

#### 6.4.9.4 Results for Trojan MPC-24E and MPC-24EF

For the Trojan MPC-24E/EF, bare fuel rod arrays with arrays sizes between 11x11 and 23x23 were analyzed as damaged fuel/fuel debris, with a pellet diameter corresponding to the 17x17B assembly class. The highest maximum  $k_{\text{eff}}$  value is shown in Table 6.1.6, and is below the 0.95 regulatory limit. The realistic damaged fuel assembly configurations in the DFC, such as assemblies with missing rods, were not analyzed in the Trojan MPC-24E/EF since the evaluations for the generic MPC-24E/EF demonstrate that these conditions are bounded by the fuel debris model using bare fuel pellets.

#### 6.4.10 Non-fuel Hardware in PWR Fuel Assemblies

Non-fuel hardware such as Thimble Plugs (TPs), Burnable Poison Rod Assemblies (BPRAs), Rod Cluster Control Assemblies (RCCAs) and similar devices are permitted for storage with the PWR fuel assemblies in the Trojan MC-24E/EF. Non-fuel hardware is inserted in the guide tubes of the assemblies. For pure water, the reactivity of any PWR assembly with inserts is bounded by (i.e. lower than) the reactivity of the same assembly without the insert. This is due to the fact that the insert reduces the amount of moderator in the assembly, while the amount of fissile material remains unchanged.

Therefore, from a criticality safety perspective, non-fuel hardware inserted into PWR assemblies are acceptable for all allowable PWR types, and, depending on the assembly class, can increase the safety margin.

#### 6.4.11 Reactivity Effect of Potential Fixed Neutron Absorber Damage

During the manufacturing process of the fuel baskets, it is possible that minor damage to fixed neutron absorber panels occurs during welding operations. Criticality calculations have been performed for all basket types to determine whether this condition could have an effect on the reactivity of the system. Since the potential fixed neutron absorber damage is typically the result of welding operations, the damage would occur in a narrow area along the edge of the panel, and would only be present in a few panels within each basket. However, in order to maximize the potential reactivity effect of the damage in the calculations, it is assumed that the damage occurs in an area with a diameter of 1 inch at the center of the fixed neutron absorber panel, and that this condition exists in every panel in the basket. It is further assumed that the fixed neutron absorber in this area is completely replaced by water, while in reality only a relocation of the fixed neutron absorber would occur, since the fixed neutron absorber is completely covered by the sheathing. Calculations performed under these assumption demonstrate that the conservatively modeled fixed neutron absorber damage has a negligible effect on the reactivity, i.e. the difference to the condition without the damage is less than 2 standard deviations. For example, for the MPC-24 and MPC-24E, the change in reactivity is +0.0006 and -0.0004, respectively, for a standard deviation between 0.0004 and 0.0005. In the MPC-24E for Trojan, a specific potential damage was identified that is not bounded by the generic approach described above. To demonstrate that this condition is acceptable, a specific calculation was performed assuming a damage of 5 square-inches in a specific location in up to 8 fixed neutron absorber panels in the basket, and was found to have again a negligible effect on reactivity. In summary, these calculations demonstrate that fixed neutron absorber damage bounded by the configurations assumed in the analyses is acceptable and does not affect the reactivity of the HI-STAR System.

#### 6.4.12 Fixed Neutron Absorber Material

The MPCs in the HI-STAR 100 System can be manufactured with one of two possible neutron absorber materials: Boral or Metamic. Both materials are made of aluminum and  $B_4C$  powder. Boral has an inner core consisting of  $B_4C$  and aluminum between two outer layers consisting of aluminum only. This configuration is explicitly modeled in the criticality evaluation and shown in Figures 6.3.1 through 6.3.3 for each basket. Metamic is a single layer material with the same overall thickness and the same credited  $^{10}B$  loading (in  $g/cm^2$ ) for each basket. The majority of the criticality evaluations documented in this chapter are performed using Boral as the fixed neutron absorber. For a selected number of bounding cases, analyses are also performed using Metamic instead of Boral. The results for these cases are listed in Table 6.4.19, together with the corresponding result using Boral and the difference between the two materials for each case. Individual cases show small differences for the two materials. However, the differences are mostly below two times the standard deviation (the standard deviation is about 0.0008 for all cases in Table 6.4.19), indicating that the results are statistically equivalent. Furthermore, the average difference is well below two standard deviations, and all cases are below the regulatory limit of 0.95. The calculations therefore demonstrate that the two fixed neutron absorber materials are identical from a criticality perspective. All results obtained for Boral are therefore directly applicable to Metamic and no further evaluations using Metamic are required.

#### 6.4.13 Reactivity Effect of Manufacturing Variations

For additional flexibility in manufacturing neutron absorber panels, the following condition for the poison panels is evaluated to demonstrate that this condition is acceptable and does not lead to an increase in reactivity. The condition is:

- A poison panel might show a reduced width in a small section along the length, while the average width is equal to or larger than the required minimum. To conservatively model this condition, it is assumed that all panels have a width reduction below the minimum by 1/32 inch over a length of 12 inches at the axial center of the active length. The width of the remainder of the panel is increased slightly to maintain the minimum width on average for a panel length of 156 inches.

The results for this case are listed in Table 6.4.20, together with the corresponding results for the design basis, i.e. with the minimum panels width, and the reactivity difference for each case is shown. The differences are either below two times the standard deviation (the standard deviation is between 0.0004 and 0.0008 for all cases in Table 6.4.20), or the conditions result in a reduction in reactivity. Furthermore, the average difference is well below two standard deviations, and all cases are below the regulatory limit of 0.95. The calculations therefore demonstrate that the condition stated above have a negligible effect on reactivity and is therefore acceptable.

Table 6.4.1

MAXIMUM REACTIVITIES WITH REDUCED WATER DENSITIES FOR CASK  
ARRAYS<sup>†</sup> WITH MPC-24 AND MPC-68

Case Number	Water Density		MCNP4a Results					
	Internal	External	MPC-24 (17x17A01 @ 4.0%)			MPC-68 (8x8C04 @ 4.2%)		
			Max. $k_{\text{eff}}^{\dagger\dagger}$	1 $\sigma$	EALF (eV)	Max. $k_{\text{eff}}$	1 $\sigma$	EALF (eV)
1	100%	single cask	0.9368	0.0008	0.2131	0.9348	0.0007	0.2915
2	100%	100%	0.9354	0.0009	0.2136	0.9339	0.0005	0.2922
3	100%	70%	0.9362	0.0008	0.2139	0.9339	0.0006	0.2921
4	100%	50%	0.9352	0.0008	0.2144	0.9347	0.0004	0.2924
5	100%	20%	0.9372	0.0008	0.2138	0.9338	0.0005	0.2921
6	100%	10%	0.9380	0.0009	0.2140	0.9336	0.0005	0.2920
7	100%	5%	0.9351	0.0008	0.2142	0.9333	0.0006	0.2936
8	100%	0%	0.9342	0.0008	0.2136	0.9338	0.0005	0.2922
9	70%	0%	0.8337	0.0007	0.4115	0.8488	0.0004	0.6064
10	50%	0%	0.7426	0.0008	0.8958	0.7631	0.0004	1.4515
11	20%	0%	0.5606	0.0007	15.444	0.5797	0.0006	26.5
12	10%	0%	0.4834	0.0005	160.28	0.5139	0.0003	241
13	5%	0%	0.4432	0.0004	1133.9	0.4763	0.0003	1770
14	10%	100%	0.4793	0.0005	171.79	0.4946	0.0003	342

<sup>†</sup> For an infinite square array of casks with 60 cm spacing between cask surfaces.

<sup>††</sup> Maximum  $k_{\text{eff}}$  includes the bias, uncertainties, and calculational statistics, evaluated for the worst case combination of manufacturing tolerances.

Table 6.4.2

REACTIVITY EFFECTS OF SPACING AND WATER MODERATOR DENSITY FOR  
SQUARE ARRAYS OF MPC-24 CASKS  
(17x17A01 @ 4.0% E)

Cask-to-Cask External Spacing (cm)					
External Moderator Density (%)	2	10	20	40	60
5	0.9352	0.9389	0.9356	0.9345	0.9351
10	0.9366	0.9353	0.9338	0.9357	0.9380
20	0.9368	0.9371	0.9359	0.9366	0.9372
50	0.9363	0.9363	0.9371	0.9352	0.9352
100	0.9355	0.9369	0.9354	0.9354	0.9354

Note:

1. All values are maximum  $k_{\text{eff}}$  which include the bias, uncertainties, and calculational statistics, evaluated for the worst case combination of manufacturing tolerances.
2. The standard deviation ( $\sigma$ ) of the calculations ranges between 0.0007 and 0.0010.

Table 6.4.3

REACTIVITY EFFECTS OF SPACING AND WATER MODERATOR DENSITY FOR  
HEXAGONAL (TRIANGULAR-PITCHED) ARRAYS OF MPC-24 CASKS  
(17x17A01 @ 4.0% E)

External Moderator Density (%)	Cask-to-Cask External Spacing (cm)				
	2	10	20	40	60
5	0.9358	0.9365	0.9369	0.9354	0.9354
10	0.9363	0.9372	0.9351	0.9368	0.9372
20	0.9354	0.9357	0.9345	0.9358	0.9381
50	0.9347	0.9361	0.9371	0.9365	0.9370
100	0.9373	0.9381	0.9354	0.9354	0.9354

Note:

1. All values are maximum  $k_{\text{eff}}$  which include the bias, uncertainties, and calculational statistics, evaluated for the worst case combination of manufacturing tolerances.
2. The standard deviation ( $\sigma$ ) of the calculations ranges between 0.0007 and 0.0009.

Table 6.4.4

REACTIVITY EFFECTS OF SPACING AND EXTERNAL MODERATOR DENSITY FOR  
 HEXAGONAL (TRIANGULAR-PITCHED) ARRAYS OF MPC-24 CASKS (17x17A01 @  
 4.0% E) INTERNALLY FLOODED WITH WATER OF 10% FULL DENSITY

Cask-to-Cask External Spacing (cm)					
External Moderator Density (%)	2	10	20	40	60
10	0.4818	0.4808	0.4798	0.4795	0.4789
100	0.4798	0.4788	0.4781	0.4793	0.4793

Note:

1. All values are maximum  $k_{\text{eff}}$  which include the bias, uncertainties, and calculational statistics, evaluated for the worst case combination of manufacturing tolerances.
2. The standard deviation ( $\sigma$ ) of the calculations ranges between 0.0004 and 0.0005.



Table 6.4.5

CALCULATIONS FOR HEXAGONAL (TRIANGULAR-PITCHED) ARRAYS OF  
TOUCHING CASKS WITH MPC-24 AND MPC-68

MPC-24 (17x17A01 @ 4.0% ENRICHMENT)		
Internal Moderation (%)	External Moderation (%)	Maximum $k_{\text{eff}}$
0	0	0.3910
0	100	0.3767
100	0	0.9366
100	100	0.9341
MPC-68 (8x8C04 @ 4.2% ENRICHMENT)		
Internal Moderation (%)	External Moderation (%)	Maximum $k_{\text{eff}}$
0	0	0.4036
0	100	0.3716
100	0	0.9351
100	100	0.9340

Note:

1. All values are maximum  $k_{\text{eff}}$  which include bias, uncertainties, and calculational statistics, evaluated for the worst case combination of manufacturing tolerances.
2. The standard deviation ( $\sigma$ ) of the calculations ranges between 0.0007 and 0.0008 for 100% internal moderation, and between 0.0002 and 0.0003 for 0% internal moderation.

Table 6.4.6

## REACTIVITY EFFECTS OF PARTIAL CASK FLOODING FOR MPC-24 AND MPC-68

MPC-24 (17x17A01 @ 4.0% ENRICHMENT)			
Flooded Condition (% Full)	Vertical Orientation	Flooded Condition (% Full)	Horizontal Orientation
25	0.9157	25	0.8766
50	0.9305	50	0.9240
75	0.9330	75	0.9329
100	0.9368	100	0.9368
MPC-68 (8x8C04 @ 4.2% ENRICHMENT)			
Flooded Condition (% Full)	Vertical Orientation	Flooded Condition (% Full)	Horizontal Orientation
25	0.9132	23.5	0.8586
50	0.9307	50	0.9088
75	0.9312	76.5	0.9275
100	0.9348	100	0.9348

## Notes:

1. All values are maximum  $k_{\text{eff}}$  which include bias, uncertainties, and calculational statistics, evaluated for the worst case combination of manufacturing tolerances.
2. The standard deviation ( $\sigma$ ) of the calculations ranges between 0.0007 and 0.0010.

Table 6.4.7

REACTIVITY EFFECT OF FLOODING THE PELLET-TO-CLAD GAP FOR MPC-24 AND  
MPC-68

Pellet-to-Clad Condition	MPC-24 17x17A01 4.0% Enrichment	MPC-68 8x8C04 4.2% Enrichment
dry	0.9295	0.9279
flooded	0.9368	0.9348

Notes:

1. All values are maximum  $k_{\text{eff}}$  which includes bias, uncertainties, and calculational statistics, evaluated for the worst case combination of manufacturing tolerances.
2. The standard deviation ( $\sigma$ ) of the calculations ranges between 0.0007 and 0.0010.

Table 6.4.8

MAXIMUM  $k_{\text{eff}}$  VALUES<sup>†</sup> IN THE DAMAGED FUEL CONTAINER

Condition	MCNP4a Results					
	DFC Dimensions: ID 4.93” THK. 0.12”			DFC Dimensions: ID 4.81” THK. 0.11”		
	Max. <sup>†</sup> $k_{\text{eff}}$	1 $\sigma$	EALF (eV)	Max. <sup>††</sup> $k_{\text{eff}}$	1 $\sigma$	EALF (eV)
<u>6x6 Fuel Assembly</u>						
6x6 Intact Fuel	0.7086	0.0007	0.3474	0.7016	0.0006	0.3521
w/32 Rods Standing	0.7183	0.0008	0.2570	0.7117	0.0007	0.2593
w/28 Rods Standing	0.7315	0.0007	0.1887	0.7241	0.0006	0.1909
w/24 Rods Standing	0.7086	0.0007	0.1568	0.7010	0.0008	0.1601
w/18 Rods Standing	0.6524	0.0006	0.1277	0.6453	0.0007	0.1288
Collapsed to 8x8 array	0.7845	0.0007	1.1550	0.7857	0.0007	1.1162
Dispersed Powder	0.7628	0.0007	0.0926	0.7440	0.0007	0.0902
<u>7x7 Fuel Assembly</u>						
7x7 Intact Fuel	0.7463	0.0007	0.2492	0.7393	0.0006	0.2504
w/41 Rods Standing	0.7529	0.0007	0.1733	0.7481	0.0007	0.1735
w/36 Rods Standing	0.7487	0.0007	0.1389	0.7444	0.0006	0.1406
w/25 Rods Standing	0.6718	0.0007	0.1070	0.6644	0.0007	0.1082

<sup>†</sup> These calculations were performed with a planar-average enrichment of 3.0% and a  $^{10}\text{B}$  loading of  $0.0067 \text{ g/cm}^2$ , which is 75% of a minimum  $^{10}\text{B}$  loading of  $0.0089 \text{ g/cm}^2$ . The minimum  $^{10}\text{B}$  loading in the MPC-68F is  $0.010 \text{ g/cm}^2$ . Therefore, the listed maximum  $k_{\text{eff}}$  values are conservative.

<sup>††</sup> Maximum  $k_{\text{eff}}$  includes bias, uncertainties, and calculational statistics, evaluated for the worst case combination of manufacturing tolerances.

Table 6.4.9

DELETED

Table 6.4.10

## REACTIVITY EFFECT OF PREFERENTIAL FLOODING OF THE DFCs

DFC Configuration	Preferential Flooding	Fully Flooded
MPC-68 or MPC-68F with 68 DFCs (Assembly Classes 6x6A/B/C, 7x7A and 8x8A)	0.6560	0.7857
MPC-24E or MPC-24EF with 4 DFCs (Bounding All PWR Assembly Classes)	0.7895	0.9480

Notes:

1. All values are maximum  $k_{\text{eff}}$  which includes bias, uncertainties, and calculational statistics, evaluated for the worst case combination of manufacturing tolerances.

Table 6.4.11

MAXIMUM  $k_{\text{eff}}$  VALUES IN THE GENERIC PWR DAMAGED FUEL CONTAINER FOR A  
MAXIMUM INITIAL ENRICHMENT OF 4.0 wt%  $^{235}\text{U}$ .

Model Configuration inside the DFC	Maximum $k_{\text{eff}}$
Intact Assemblies (2 assemblies analyzed)	0.9340
Assemblies with missing rods (4 configurations analyzed)	0.9350
Collapsed Assemblies (6 configurations analyzed)	0.9360
Regular Arrays of Bare Fuel Rods (36 configurations analyzed)	0.9480

Notes:

1. All values are maximum  $k_{\text{eff}}$  which includes bias, uncertainties, and calculational statistics, evaluated for the worst case combination of manufacturing tolerances.
2. The standard deviation ( $\sigma$ ) of the calculations ranges between 0.0007 and 0.0010.

Table 6.4.12  
SUMMARY OF THE CRITICALITY RESULTS FOR THE MOST REACTIVE ASSEMBLY FROM  
THE MOST REACTIVE ASSEMBLY CLASS IN EACH MPC  
TO DEMONSTRATE COMPLIANCE WITH 10CFR71.55 AND 10CFR71.59

MPC-24, Assembly Class 15x15F, 4.1 wt% <sup>235</sup> U					
Configuration	% Internal Moderation	% External Moderation	Max. ‡ k <sub>eff</sub>	1 σ	EALF (eV)
Single Package, unreflected	100%	0%	0.9410	0.0007	0.2998
Single Package, fully reflected	100%	100%	0.9397	0.0008	0.3016
Containment, fully reflected	100%	100%	0.9397	0.0008	0.3006
Infinite Array of Damaged Packages	100%	100%	0.9436	0.0009	0.2998
Infinite Array of Undamaged Packages	0%	0%	0.3950	0.0004	82612.0
MPC-68, Assembly Class 9x9E/F, 4.0 wt% <sup>235</sup> U					
Configuration	% Internal Moderation	% External Moderation	Max. k <sub>eff</sub>	1 σ	EALF (eV)
Single Package, unreflected	100%	0%	0.9486	0.0008	0.2095
Single Package, fully reflected	100%	100%	0.9470	0.0008	0.2079
Containment, fully reflected	100%	100%	0.9461	0.0007	0.2092
Infinite Array of Damaged Packages	100%	100%	0.9468	0.0008	0.2106
Infinite Array of Undamaged Packages	0%	0%	0.3808	0.0003	85218.0
MPC-68F, Assembly Class 6x6C, 2.7 wt% <sup>235</sup> U					
Configuration	% Internal Moderation	% External Moderation	Max. k <sub>eff</sub>	1 σ	EALF (eV)
Single Package, unreflected	100%	0%	0.8021	0.0007	0.2139
Single Package, fully reflected	100%	100%	0.8033	0.0008	0.2142
Containment, fully reflected	100%	100%	0.8033	0.0008	0.2138
Infinite Array of Damaged Packages	100%	100%	0.8026	0.0008	0.2142
Infinite Array of Undamaged Packages	0%	0%	0.3034	0.0002	99463.0

---

‡ The maximum k<sub>eff</sub> is equal to the sum of the calculated k<sub>eff</sub>, two standard deviations, the code bias, and the uncertainty in the code bias.

---



Table 6.4.12 (continued)  
SUMMARY OF THE CRITICALITY RESULTS FOR THE MOST REACTIVE ASSEMBLY FROM  
THE MOST REACTIVE ASSEMBLY CLASS IN EACH MPC  
TO DEMONSTRATE COMPLIANCE WITH 10CFR71.55 AND 10CFR71.59

MPC-24E/EF, Assembly Class 15x15F, 4.5 wt% <sup>235</sup> U					
Configuration	% Internal Moderation	% External Moderation	Max. ‡ k <sub>eff</sub>	1 σ	EALF (eV)
Single Package, unreflected	100%	0%	0.9495	0.0008	0.3351
Single Package, fully reflected	100%	100%	0.9485	0.0008	0.3313
Containment, fully reflected	100%	100%	0.9486	0.0008	0.3362
Infinite Array of Damaged Packages	100%	100%	0.9495	0.0008	0.3335
Infinite Array of Undamaged Packages	0%	0%	0.4026	0.0004	87546.0
MPC-24E/EF TROJAN, Trojan Intact and Damaged Fuel, 3.7 wt% <sup>235</sup> U					
Configuration	% Internal Moderation	% External Moderation	Max. k <sub>eff</sub>	1 σ	EALF (eV)
Single Package, unreflected	100%	0%	0.9377	0.0008	n/c†
Single Package, fully reflected	100%	100%	0.9366	0.0008	n/c
Containment, fully reflected	100%	100%	0.9377	0.0008	n/c
Infinite Array of Damaged Packages	100%	100%	0.9383	0.0007	n/c
Infinite Array of Undamaged Packages	0%	0%	0.3518	0.0003	n/c
MPC-32, Assembly Class 15x15F and 17x17B					
Configuration	% Internal Moderation	% External Moderation	Max. k <sub>eff</sub>	1 σ	EALF (eV)
Single Package, unreflected	100%	0%	0.9450	0.0002	0.3849
Single Package, fully reflected	100%	100%	0.9448	0.0002	0.4782
Containment, fully reflected	100%	100%	0.9450	0.0003	0.4784
Infinite Array of Damaged Packages	100%	100%	0.9452	0.0002	0.3863
Infinite Array of Undamaged Packages	0%	0%	0.4420	0.0001	33652

‡ The maximum k<sub>eff</sub> is equal to the sum of the calculated k<sub>eff</sub>, two standard deviations, the code bias, and the uncertainty in the code bias.

† n/c = not calculated

Table 6.4.13

## RESULTS FOR EACH ASSEMBLY CLASS IN THE MPC-24

Fuel Assembly Class	Maximum Allowable Enrichment (wt% $^{235}\text{U}$ )	Max. $\dagger$ $k_{\text{eff}}$	1 $\sigma$	EALF (eV)
14x14A	4.6	0.9296	0.0008	0.2093
14x14B	4.6	0.9228	0.0008	0.2675
14x14C	4.6	0.9307	0.0008	0.3001
14x14D	4.0	0.8507	0.0008	0.3308
14x14E	5.0	0.7627	0.0007	0.3607
15x15A	4.1	0.9227	0.0007	0.2708
15x15B	4.1	0.9388	0.0009	0.2626
15x15C	4.1	0.9361	0.0009	0.2385
15x15D	4.1	0.9367	0.0008	0.2802
15x15E	4.1	0.9392	0.0008	0.2908
15x15F	4.1	0.9410	0.0007	0.2998
15x15G	4.0	0.8907	0.0008	0.3456
15x15H	3.8	0.9337	0.0009	0.2349
16x16A	4.6	0.9287	0.0008	0.2704
17x17A	4.0	0.9368	0.0008	0.2131
17x17B	4.0	0.9355	0.0008	0.2659
17x17C	4.0	0.9349	0.0009	0.2677

---

$\dagger$  The term "maximum  $k_{\text{eff}}$ " as used here, and elsewhere in this document, means the highest possible k-effective, including bias, uncertainties, and calculational statistics, evaluated for the worst case combination of manufacturing tolerances.

---

Table 6.4.14

## RESULTS FOR EACH ASSEMBLY CLASS IN THE MPC-68

Fuel Assembly Class	Maximum Allowable Enrichment (wt% $^{235}\text{U}$ )	Max. $^{\dagger}$ $k_{\text{eff}}$	1 $\sigma$	EALF (eV)
7x7B	4.2	0.9386	0.0007	0.3983
8x8B	4.2	0.9416	0.0007	0.3293
8x8C	4.2	0.9425	0.0007	0.3081
8x8D	4.2	0.9403	0.0006	0.2778
8x8E	4.2	0.9312	0.0008	0.2831
8x8F	4.0	0.9459	0.0007	0.2361
9x9A	4.2	0.9417	0.0008	0.2236
9x9B	4.2	0.9436	0.0008	0.2506
9x9C	4.2	0.9395	0.0008	0.2698
9x9D	4.2	0.9394	0.0009	0.2625
9x9E	4.0	0.9486	0.0008	0.2095
9x9F	4.0	0.9486	0.0008	0.2095
9x9G	4.2	0.9383	0.0008	0.2292
10x10A	4.2	0.9457	0.0008	0.2212
10x10B	4.2	0.9436	0.0007	0.2366
10x10C	4.2	0.9433	0.0007	0.2416
10x10D	4.0	0.9376	0.0008	0.3355
10x10E	4.0	0.9185	0.0007	0.2936

---

$^{\dagger}$  The term "maximum  $k_{\text{eff}}$ " as used here, and elsewhere in this document, means the highest possible k-effective, including bias, uncertainties, and calculational statistics, evaluated for the worst case combination of manufacturing tolerances.

---

Table 6.4.15

## RESULTS FOR EACH ASSEMBLY CLASS IN THE MPC-68F

Fuel Assembly Class	Maximum Allowable Enrichment (wt% $^{235}\text{U}$ )	Max.† $k_{\text{eff}}$	1 $\sigma$	EALF (eV)
6x6A	2.7††	0.7888	0.0007	0.2310
6x6B†††	2.7	0.7824	0.0006	0.2184
6x6C	2.7	0.8021	0.0007	0.2139
7x7A	2.7	0.7974	0.0008	0.2015
8x8A	2.7	0.7697	0.0007	0.2158

---

† The term "maximum  $k_{\text{eff}}$ " as used here, and elsewhere in this document, means the highest possible k-effective, including bias, uncertainties, and calculational statistics, evaluated for the worst case combination of manufacturing tolerances.

†† These calculations were performed for 3.0% planar-average enrichment; however, the authorized contents are limited to a maximum planar-average enrichment of 2.7%. Therefore, the listed maximum  $k_{\text{eff}}$  values are conservative.

††† Assemblies in this class contain both MOX and  $\text{UO}_2$  pins. The composition of the MOX fuel pins is given in Table 6.3.4. The maximum allowable planar-average enrichment for the MOX pins is given in the specification of authorized contents, Chapter 1.

---

Table 6.4.16

## RESULTS FOR EACH ASSEMBLY CLASS IN THE MPC-24E/EF

Fuel Assembly Class	Maximum Allowable Enrichment (wt% $^{235}\text{U}$ )	Max. $\dagger$ $k_{\text{eff}}$	1 $\sigma$	EALF (eV)
14x14A	5.0	0.9380	0.0008	0.2277
14x14B	5.0	0.9312	0.0008	0.2927
14x14C	5.0	0.9365	0.0008	0.3318
14x14D	5.0	0.8875	0.0009	0.4026
14x14E	5.0	0.7651	0.0007	0.3644
15x15A	4.5	0.9336	0.0008	0.2879
15x15B	4.5	0.9487	0.0009	0.3002
15x15C	4.5	0.9462	0.0008	0.2631
15x15D	4.5	0.9445	0.0008	0.3375
15x15E	4.5	0.9471	0.0008	0.3242
15x15F	4.5	0.9495	0.0008	0.3351
15x15G	4.5	0.9062	0.0008	0.3883
15x15H	4.2	0.9455	0.0009	0.2663
16x16A	5.0	0.9358	0.0008	0.3150
17x17A	4.4	0.9447	0.0007	0.2374
17x17B	4.4	0.9438	0.0008	0.2951
17x17C	4.4	0.9433	0.0008	0.2932

---

$\dagger$  The term "maximum  $k_{\text{eff}}$ " as used here, and elsewhere in this document, means the highest possible k-effective, including bias, uncertainties, and calculational statistics, evaluated for the worst case combination of manufacturing tolerances.

---

Table 6.4.17

## RESULTS FOR THE MPC-24E/EF TROJAN

Fuel Assembly Class	Maximum Allowable Enrichment (wt% $^{235}\text{U}$ )	Content	Max.† $k_{\text{eff}}$	1 $\sigma$	EALF (eV)
17x17B	3.7	Intact Fuel	0.9187	0.0009	not calculated
17x17B	3.7	Intact Fuel, Damaged Fuel and Fuel Debris	0.9377	0.0008	not calculated

---

† The term "maximum  $k_{\text{eff}}$ " as used here, and elsewhere in this document, means the highest possible k-effective, including bias, uncertainties, and calculational statistics, evaluated for the worst case combination of manufacturing tolerances.

---

Table 6.4.18

RESULTS FOR THE MPC-24E/EF TROJAN USING A FUEL FRAGMENT MODEL FOR  
DAMAGED FUEL AND FUEL DEBRIS

Fuel Cube OD (Inches)	Maximum $k_{\text{eff}}$			
	Fuel Volume / Water Volume			
	0.2	0.4	0.6	0.8
1	0.9098	0.9223	0.9260	0.9204
0.5	0.9156	0.9310	0.9273	0.9168
0.2	0.9254	0.9320	0.9216	0.9137
0.1	0.9253	0.9274	0.9183	0.9135
0.05	0.9224	0.9228	0.9168	0.9126
0.02	0.9183	0.9213	0.9140	0.9122

Table 6.4.19

COMPARISON OF MAXIMUM  $k_{\text{eff}}$  VALUES FOR DIFFERENT FIXED NEUTRON  
ABSORBER MATERIALS

CASE	Maximum $k_{\text{eff}}$		Reactivity Difference
	BORAL	METAMIC	
MPC-68	0.9486	0.9470	-0.0016
MPC-68F with 68 DFCs	0.8021	0.8019	-0.0002
MPC-24	0.9410	0.9425	+0.0015
MPC-24E, Intact Assemblies	0.9495	0.9494	-0.0001
MPC-24E, with 4 DFCs	0.9480	0.9471	-0.0009
Average Difference			-0.0003



Table 6.4.20

COMPARISON OF MAXIMUM  $k_{\text{eff}}$  VALUES FOR DIFFERENT FIXED NEUTRON  
ABSORBER CONDITIONS

CASE	Maximum $k_{\text{eff}}$		Reactivity Difference
	DESIGN BASIS (SINGLE PART PANEL AND MINIMUM WIDTH)	PANELS WITH WIDTH REDUCTION	
MPC-68	0.9486	0.9464	-0.0022
MPC-68F with 68 DFCs	0.8021	0.8023	+0.0002
MPC-24	0.9410	0.9411	+0.0001
MPC-24E, Intact Assemblies	0.9495	0.9494	-0.0001
MPC-24E, with 4 DFCs	0.9480	0.9470	-0.0010
Average Difference			-0.0006

FIGURES 6.4.1 THROUGH 6.4.12: [PROPRIETARY INFORMATION WITHHELD PER  
10CFR2.390]

## 6.5 CRITICALITY BENCHMARK EXPERIMENTS

Benchmark calculations have been made on selected critical experiments, chosen, insofar as possible, to bound the range of variables in the cask designs. The most important parameters are (1) the enrichment, (2) the water-gap size (MPC-24) or cell spacing (MPC-68), and (3) the  $^{10}\text{B}$  loading of the neutron absorber panels. Other parameters, within the normal range of cask and fuel designs, have a smaller effect, but are also included. No significant trends were evident in the benchmark calculations or the derived bias. Detailed benchmark calculations are presented in Appendix 6.A.

The benchmark calculations were performed with the same computer codes and cross-section data, described in Section 6.4, that were used to calculate the  $k_{\text{eff}}$  values for the cask. Further, all calculations were performed on the same computer hardware, specifically, personal computers using the pentium processor.

Additional benchmark calculations performed for the burnup methodology for the MPC-32 are presented in Appendix 6.C and Appendix 6.E.

## 6.6 REGULATORY COMPLIANCE

This chapter documents the criticality evaluation of the HI-STAR 100 System for the packaging and transportation of radioactive materials (spent nuclear fuel). This evaluation demonstrates that the HI-STAR 100 System is in full compliance with the criticality safety requirements of 10CFR71.

The criticality design is based on favorable geometry, fixed neutron poisons (Boral), and an administrative limit on the maximum allowable enrichment and the minimum allowable burnup in the MPC-32. The HI-STAR 100 System design structures and components important to criticality safety are described in sufficient detail in this chapter to identify the package accurately and provide a sufficient basis for the evaluation of the package, including the maximum allowable enrichments and minimum allowable burnups.

The HI-STAR 100 System is designed to be subcritical under both normal and hypothetical accident conditions of transport. The evaluations presented in the chapter address the criticality safety requirements of 10CFR71 and demonstrate that a single HI-STAR 100 System remains subcritical under the most reactive normal and hypothetical accident conditions of transport and that the most reactive infinite array of HI-STAR 100 Systems is subcritical under both normal and hypothetical accident conditions of transport. This corresponds to a transport index of zero (0) and demonstrates compliance with 10CFR71 criticality requirements.

Therefore, it is concluded that the criticality design features for the HI-STAR 100 System are in compliance with 10CFR71 and that the applicable design and acceptance criteria have been satisfied. This criticality evaluation provides reasonable assurance that the HI-STAR 100 System will allow safe transport of spent fuel.

## 6.7

REFERENCES

- [6.1.1] U.S. Code of Federal Regulations, “Packaging and Transportation of Radioactive Materials,” Title 10, Part 71.
- [6.1.2] NUREG-1617, Standard Review Plan for Transportation Packages for Spent Nuclear Fuel, USNRC, Washington, D.C., March 2000.
- [6.1.3] USNRC Standard Review Plan, NUREG-0800, Section 9.1.2, Spent Fuel Storage, Rev. 2 - July 1981.
- [6.1.4] J.F. Briesmeister, Ed., “MCNP - A General Monte Carlo N-Particle Transport Code, Version 4A,” Los Alamos National Laboratory, LA-12625-M (1993).
- [6.1.5] L.M. Petrie and N.F. Landers, “KENOVa - An Improved Monte Carlo Criticality Program with Supergrouping,” Volume 2, Section F11 from “SCALE: A Modular System for Performing Standardized Computer Analysis for Licensing Evaluation,” NUREG/CR-0200, Rev. 4, January 1990.
- [6.1.6] N.M. Greene, L.M. Petrie and R.M. Westfall, “NITAWL-II: Scale System Module For Performing Resonance Shielding and Working Library Production,” Volume 1, Section F1 from “SCALE: A Modular System for Performing Standardized Computer Analysis for Licensing Evaluation,” NUREG/CR-0200, Rev. 4, January 1990.
- [6.1.7] J.R. Knight, “SUPERDAN: Computer Programs for Calculating the Dancoff Factor of Spheres, Cylinders, and Slabs,” Oak Ridge National Laboratory, ORNL/NUREG/CSD/TM-2, March 1978, with correction published in “Proceedings of Seminar on SCALE-4,” Saclay, France, 1991.
- [6.1.8] M.G. Natrella, Experimental Statistics, National Bureau of Standards, Handbook 91, August 1963.
- [6.1.9] Deleted
- [6.1.10] “CASMO-4 Methodology”, Studsvik/SOA-95/2, Rev. 0, 1995.

- [6.1.11] “CASMO-4 A Fuel Assembly Burnup Program, Users Manual,” SSP-01/400, Rev. 1, Studsvik Scandpower, Inc., 2001.
- [6.1.12] “CASMO-4 Benchmark Against Critical Experiments”, Studsvik/SOA-94/13, Studsvik of America, 1995.
- [6.1.13] “QA Validation Manual for Computer Code CELLDAN,” Holtec International Report HI-90577.
- [6.3.1] A. Ahlin, M. Edenius, and H. Haggblom, “CASMO - A Fuel Assembly Burnup Program,” AE-RF-76-4158, Studsvik report.
- [6.3.2] A. Ahlin and M. Edenius, “CASMO - A Fast Transport Theory Depletion Code for LWR Analysis,” *Trans. Am. Nucl. Soc.*, 26, 604 (1977).
- [6.3.3] “CASMO-3 A Fuel Assembly Burnup Program, Users Manual,” Studsvik/NFA-87/7, Studsvik Energitechnik AB, November 1986.
- [6.3.4] M. Edenius and A. Ahlin, “CASMO-3: New Features, Benchmarking, and Advanced Applications,” *Nucl. Sci. Eng.*, 100, 342-351, (1988).
- [6.4.1] “SCALE 4.3: A Modular System for Performing Standardized Computer Analysis for Licensing Evaluations,” NUREG-CR-0200, Rev. 5, Oak Ridge National Laboratory (1995).
- [6.4.2] J.M. Cano, R. Caro, and J.M Martinez-Val, “Supercriticality Through Optimum Moderation in Nuclear Fuel Storage,” *Nucl. Technol.*, 48, 251-260, (1980).

## **APPENDIX 6.A: BENCHMARK CALCULATIONS**

**PROPRIETARY APPENDIX WITHHELD PER 10CFR2.390**

## APPENDIX 6.B: DISTRIBUTED ENRICHMENTS IN BWR FUEL

Fuel assemblies used in BWRs utilize fuel rods of varying enrichments as a means of controlling power peaking during in-core operation. For calculations involving BWR assemblies, the use of a uniform (planar-average) enrichment, as opposed to the distributed enrichments normally used in BWR fuel, produces conservative results. Calculations have been performed to confirm that this statement remains valid in the geometry of the MPC-68. These calculations are based on fuel assembly designs currently in use and two hypothetical distributions, all intended to illustrate that calculations with uniform average enrichments are conservative.

The average enrichment is calculated as the linear average of the various fuel rod enrichments, i.e.,

$$\bar{E} = \frac{1}{n} \sum_{i=1}^n E_i,$$

where  $E_i$  is the enrichment in each of the  $n$  rods, and  $\bar{E}$  is the assembly average enrichment. This parameter conservatively characterizes the fuel assembly and is readily available for specific fuel assemblies in determining the acceptability of the assembly for placement in the MPC-68 cask.

The criticality calculations for average and distributed enrichment cases are compared in Table 6.B.1 to illustrate and confirm the conservatism inherent in using average enrichments. With two exceptions, the cases analyzed represent realistic designs currently in use and encompass fuel with different ratios of maximum pin enrichment to average assembly enrichment. The two exceptions are hypothetical cases intended to extend the models to higher enrichments and to demonstrate that using the average enrichment remains conservative.

Table 6.B.1 shows that, in all cases, the averaged enrichment yields conservative values of reactivity relative to distributed enrichments for both the actual fuel designs and the hypothetical higher enrichment cases. Thus, it is concluded that uniform average enrichments will always yield higher (more conservative) values for reactivity than the corresponding distributed enrichments.<sup>†</sup>

---

†

This conclusion implicitly assumes the higher enrichment fuel rods are located internal to the assembly (as in BWR fuel), and the lower enriched rods are on the outside.



Table 6.B.1

**COMPARISON CALCULATIONS FOR BWR FUEL WITH AVERAGE AND  
DISTRIBUTED ENRICHMENTS**

<b>Case</b>	<b>Average %E</b>	<b>Peak Rod E%</b>	<b>Calculated <math>k_{eff}</math></b>	
			<b>Average E</b>	<b>Distributed E</b>
8x8C04	3.01	3.80	0.8549	0.8429
8x8C04	3.934	4.9	0.9128	0.9029
8x8D05	3.42	3.95	0.8790	0.8708
8x8D05	3.78	4.40	0.9030	0.8974
8x8D05	3.90	4.90	0.9062	0.9042
9x9B01	4.34	4.71	0.9347	0.9285
9x9D01	3.35	4.34	0.8793	0.8583
Hypothetical #1 (48 outer rods of 3.967%E, 14 inner rods of 5.0%)	4.20	5.00	0.9289	0.9151
Hypothetical #2 (48 outer rods of 4.354%E, 14 inner rods of 5.0%)	4.50	5.00	0.9422	0.9384

**Appendix 6.C**  
**PROPRIETARY APPENDIX WITHHELD PER 10CFR2.390**

## **APPENDIX 6.D**

### **PROPRIETARY APPENDIX WITHHELD PER 10CFR2.390**

## **Appendix 6.E**

**PROPRIETARY APPENDIX WITHHELD PER 10CFR2.390**

## SUPPLEMENT 6.I

### CRITICALITY EVALUATION OF **THE HI-STAR HB PACKAGE WITH MPC-HB**

#### 6.I.0 INTRODUCTION

This supplement is focused on providing criticality evaluations for fuel from the Humboldt Bay Power Plant (HBPP) in the HI-STAR HB. The evaluation presented herein supplements those evaluations contained in the main body of Chapter 6 of this SAR, and information in the main body of Chapter 6 is not repeated in this supplement. To aid the reader, the sections in this supplement are numbered in the same fashion as the corresponding sections in the main body of this chapter, i.e., Sections 6.I.1 through 6.I.6 correspond to Sections 6.1 through 6.6. Tables and figures in this supplement are labeled sequentially. The results of the evaluations in this supplement demonstrate that, for the designated fuel assembly classes and basket configurations, an infinite number of HI-STAR 100 Systems remain subcritical with a margin of subcriticality greater than  $0.05\Delta k$ . This corresponds to a Criticality Safety Index (CSI) of zero (0) and demonstrates compliance with 10CFR71 criticality requirements for normal and hypothetical accident conditions of transport.

#### 6.I.1 DISCUSSION AND RESULTS

Fuel from the HBPP is qualified in the main body of Chapter 6 of this SAR for transport in the HI-STAR 100 using the MPC-68 and MPC-68F. The assembly classes corresponding to this fuel are 6x6C and 7x7A. However, subsequent to these analyses, an additional basket design was developed for the HBPP fuel. Taking advantage of the smaller physical size of these assemblies, the capacity of the basket was increased to 80 assemblies while maintaining the same outer MPC diameter. The designated name of this MPC version is MPC-HB. Section 6.I.3 of this supplement provides the relevant details for this design. The MPC-HB is placed into the HI-STAR HB overpack, which is a shorter version of the HI-STAR 100 overpack. Also, revised assembly classes, designated 6x6D and 7x7C, are used in this supplement for the calculations with the MPC-HB. Finally, the number of cell locations for damaged fuel is increased to up to 40 per basket for the MPC-HB, compared to only 16 in the MPC-68. This is necessary since it is possible that a larger number of HBPP assemblies need to be loaded as damaged fuel.

The principal calculational results from this supplement, which address the following conditions:

- A single package, under the conditions of 10 CFR 71.55(b), (d), and (e);
- An array of undamaged packages, under the conditions of 10 CFR 71.59(a)(1); and
- An array of damaged packages, under the conditions of 10 CFR 71.59(a)(2)

are summarized in Table 6.I.1 for MPCs-HB and for the most reactive configuration and fuel

---

HOLTEC INTERNATIONAL COPYRIGHTED MATERIAL

condition. Results are shown for both intact or undamaged assemblies only, and the bounding condition for intact or undamaged and damaged fuel (see Section 6.I.4.1 for a discussion on undamaged assemblies). The results demonstrate that the HI-STAR 100 System is in full compliance with 10CFR71 (71.55(b), (d), and (e) and 71.59(a)(1) and (a)(2)). The calculations for package arrays are performed for infinite arrays of HI-STAR 100 Systems under flooded conditions. Therefore, the CSI is zero (0). In addition, the table shows the result for an unreflected, internally flooded cask for each MPC. This configuration is used in many calculations and studies throughout this chapter, and is shown to yield results that are statistically equivalent to the results for the corresponding reflected package.

## 6.I.2 SPENT FUEL LOADING

The evaluations in Section 6.2 of the main body of Chapter 6 demonstrate that the bounding fuel dimensions consist of maximum active fuel length, maximum fuel pellet diameter, minimum cladding outside diameter (OD), maximum cladding inside diameter (ID), minimum guide tube/water rod thickness, and maximum channel thickness. A detailed review of the HBPP fuel information indicated that not all assemblies were bounded by the specification of the assembly classes 6x6C and 7x7A defined in Section 6.2. Therefore, expanded assembly classes, designated 6x6D and 7x7C, are used in this supplement for the calculations with the MPC-HB. The characteristics of these assembly classes are provided in Table 6.I.2.

## 6.I.3 MODEL SPECIFICATION

### 6.I.3.1 Calculational model

Figure 6.I.1 shows a representative horizontal cross section of the MPC-HB cells used in the calculations, and Figure 6.I.2 illustrates the basket configuration used. Based on the evaluations performed for the MPC-68 described in Section 6.3 of the main body of Chapter 6, the calculations use the minimum cell pitch and cell ID, and nominal cell wall thickness. The same techniques and the same level of detail are used in the calculational models as described in the main body of this chapter. Although the neutron absorber panels are 88 inches in length, which is much longer than the active fuel length (maximum of 80 inches), they are assumed equal to the active fuel length in the calculations.

### 6.I.3.2 Regional Densities

The densities and material compositions unique to the calculations in the MPC-HB are for the fuel and for the neutron absorber. These are listed in Table 6.I.3. All other compositions are the same as listed in Section 6.3 of the main body of this chapter. Note that the calculations conservatively take credit for only 75% of the minimum B-10 areal density of the neutron absorber, which is less than the maximum value of 90% supported by the tests and qualifications prescribed in Chapter 8.

---

HOLTEC INTERNATIONAL COPYRIGHTED MATERIAL

## 6.I.4 CRITICALITY CALCULATIONS

### 6.I.4.1 Intact and Undamaged Assemblies

#### Intact Assemblies

Results for calculation with intact assemblies of assembly class 6x6D and 7x7C are summarized in Table 6.I.4. The following conditions are evaluated:

- Standard: Corresponds to assemblies located in the center of each cell, without DFCs
- Assemblies in DFCs: It might be beneficial to place not only damaged, but also intact assemblies into DFCs.
- Potential Poison Plate Damage: This condition is consistent with the condition evaluated in Section 6.4.11 of the main body of this chapter, assuming a 1 inch diameter at the center of each poison plate is replaced by water.
- Eccentric positioning: All assemblies are placed closest to the basket center

The results demonstrate that the assembly class 6x6D, with eccentric positioning and assumed poison plate damage is the bounding condition for intact assemblies.

#### Undamaged Assemblies

Fuel inspection for HB fuel is limited to visual inspection, focusing predominantly on the rods on the periphery of the fuel assemblies. Assemblies with defects are considered damaged, and need to be placed into DFCs. The modeling of those assemblies is discussed in detail in the following subsection. However, even if no defects are detected in the inspection, some defects could exist in the inner rods of the assemblies that are not easily visible in the inspection. This means that even if no defects are detected, the assemblies may not be intact. This condition could later result in rod-breakage, which could potentially result in local relocation of fuel, creating areas with larger or smaller fuel amounts in the assembly. Note that any lateral relocation would be limited by the outer row of intact rods, and axial relocation would be limited by the grid spacers. To ensure such assemblies are qualified for loading without DFCs, additional calculations were performed where potential defects in those assemblies are modeled. The assemblies qualified this way are considered undamaged in respect to the criticality function of the cask, but not intact. In these models, the fuel rods on the periphery of the assembly remain in its original location, whereas inside the assembly various arrays of fuel rods are assumed. The array size is varied between a 3x3 array and a 7x7 array, which conservatively represents various rod damages, including axial relocation of fuel within the assembly. For each array size, two different rod pitch values are analyzed, one which spaces the rods evenly within the bounds of the peripheral rods, and one with an enlarged pitch where the outer rods of the array are closer to the peripheral rods

---

HOLTEC INTERNATIONAL COPYRIGHTED MATERIAL

of the assembly. The higher of the two results is then used, which is typically that for the enlarged pitch. This variation in pitch is the reason that the undamaged 6x6 assembly with a 4x4 array of rods inside the peripheral rods has a higher  $k_{\text{eff}}$  than the corresponding intact assembly, despite the fact that the number of fuel rods is the same. To maximize any reactivity effect of these conditions, they are simultaneously assumed to be present in all assemblies in the basket, and along the entire active length. In the model for damaged fuel (see Section 6.I.4.2 below) it is conservatively assumed that all cladding has disappeared. This is not a credible condition for the defects in the interior rods of the assemblies, since there is no path for the cladding to get out of the interior of the assemblies. The various arrays used to represent the result of defects in the interior of the assembly are therefore modeled as cladless rods. Results of the analyses are shown in Table 6.I.4, and indicate a slight increase in reactivity for both assembly types compared to the intact condition. The maximum  $k_{\text{eff}}$  is determined for a 4x4 and 5x5 array within the fuel assembly for the 6x6 and 7x7 assemblies, respectively. As for intact fuel, the 6x6 assembly presents the higher  $k_{\text{eff}}$  value.

The condition with assembly class 6x6D, undamaged fuel, eccentric positioning, and assumed poison plate damage is therefore used for the calculations demonstrating compliance with the regulatory requirements shown in Table 6.I.1 for intact and undamaged fuel, except for the condition of the single unreflected package, which was analyzed without the assumed poison damage.

#### 6.I.4.2 Damaged Assemblies

To conservatively model conditions of damaged fuel and fuel debris, the same approach is used as in Section 6.4.9 of the main body of this chapter, i.e., the fuel is represented by arrays of bare fuel rods in the DFC. Both the fuel rod diameter of the 6x6D fuel and 7x7C fuel is analyzed. A total of 6 different array sizes are analyzed for each condition. Additionally, two different DFC patterns are evaluated. The first pattern allows damaged fuel/fuel debris in DFCs in the 28 peripheral cells of the basket only. This first configuration is shown in Figure 6.I.3. For the second configuration, a checkerboard array of cells with intact and damaged fuel is analyzed, resulting in a total of 40 cells qualified for damaged fuel and fuel debris. This second configuration is shown in Figure 6.I.4. The calculations are performed in several steps, where in each step some of the principal parameters are varied such that the  $k_{\text{eff}}$  value is maximized. In all cases, the intact or undamaged assemblies are assumed to be assembly class 6x6D, which is bounding as shown in the previous subsection. For the damaged fuel and fuel debris in the DFCs, it is assumed that the fuel is present along the entire length of the DFC, including the areas that are not covered by the poison in the basket. Results for the two patterns, two pellet diameters, and various array sizes are listed in Table 6.I.5 for damaged and intact fuel. The results show that the bounding condition exists for the checkerboard array with the larger pellet ID, and a 7x7 array of bare rods. For this condition, further calculations were performed with assumed poison plate damage and eccentric positioning, as for intact fuel in the previous subsection. These results are listed in Table 6.I.6. As for the intact assemblies, the eccentric position results in a higher reactivity. The assumed poison plate damage shows a slight reduction in reactivity, however, the difference is still within two standard variations, indicating that the results are

---

HOLTEC INTERNATIONAL COPYRIGHTED MATERIAL



statistically identical. Nevertheless, the condition with eccentric positioning and assumed poison plate damage is used as the bounding condition. Finally, calculations are performed with undamaged instead of intact assemblies, varying the array size inside those assemblies (see previous subsection). The bounding condition corresponds again to a 4x4 array to represent the inner area of the undamaged assembly, as shown in Table 6.I.7. The overall bounding condition is therefore characterizes as follows:

• DFC Configuration	40 DFC
• Damaged Fuel Representation	7x7 rod array, 0.488" OD
• Remaining Assemblies	6x6D, undamaged
• Undamaged Configuration	4x4 clad rod array inside peripheral rods, Increased rod pitch
• DFC and assembly position	Eccentric
• Poison Plate Damage	yes

This condition is then used to perform the calculations demonstrating compliance with the regulatory requirements shown in Table 6.I.1, except for the condition of the single unreflected package, which was analyzed without the assumed poison damage.

Two HBPP assemblies contain one fuel rod with an enrichment of 5.5 wt%  $^{235}\text{U}$ . At least one of these two assemblies is considered damaged. These assemblies have a planar average enrichment of less than 2.6 wt%  $^{235}\text{U}$ . For damaged fuel and fuel debris it is assumed that the fuel can relocate freely within the DFC. However, even if it would be conservatively assumed that the entire amount of fuel from one of these rods would accumulate in one area in the DFC, this area would be rather small. For example, the bounding configuration for damaged fuel consists of a 7x7 array of bare fuel rods. Under this configuration, a single rod with an active length of 80 inches would only occupy an axial length of  $80 \text{ inches} / 7 \times 7 = 1.63 \text{ inches}$ . Such a small section, which would only be present in a few DFCs in the basket, would have a negligible effect on reactivity. Further, it needs to be recognized that the damaged fuel and fuel debris model is a non-credible configuration (bare fuel rods in optimum moderation) chosen to conservatively bound any realistic fuel configuration by a significant margin, and that the average enrichment of the assemblies with the high enriched rods is below the enrichment used in the analysis. Therefore, the presence of the highly enriched rods is considered to be bounded by the damaged fuel model, and no specific calculations are necessary for the assemblies with these rods.

#### 6.I.4.3 Test for Optimum Moderation at Lower Water Densities

Section 6.4 demonstrates that no optimum moderation exists in the MPC basket, i.e. that the maximum reactivity corresponds to the fully flooded conditions. To confirm this for the MPC-HB, additional calculations were performed with reduced water densities, for a bounding case with intact assemblies and intact and damaged assemblies for a single fully reflected package. The intact assembly in all cases is from array class 6x6D. The results are presented in Table 6.I.8, and show that reducing the water density results in a monotonic reduction of the reactivity.

---

HOLTEC INTERNATIONAL COPYRIGHTED MATERIAL

Optimum moderation at lower water densities does therefore not exist, and the fully flooded condition is bounding.

#### 6.I.5 CRITICALITY BENCHMARKS

Fuel design, fuel conditions, basket design and moderation conditions are bounded by the corresponding conditions in the main body of Chapter 6. The benchmark calculations in the main body are therefore directly applicable to the calculations performed in this supplement.

#### 6.I.6 REGULATORY COMPLIANCE

In summary, the evaluation presented in this supplement demonstrates that the HI-STAR HB System with fuel of the assembly classes 6x6D and 7x7C in the MPC-HB is in full compliance with the criticality requirements of 10CFR71.

---

HOLTEC INTERNATIONAL COPYRIGHTED MATERIAL

HI-STAR SAR  
REPORT HI-951251

6.I-6

Rev. 16

Table 6.I.1

SUMMARY OF THE CRITICALITY RESULTS FOR THE MOST REACTIVE ASSEMBLY FROM  
THE ASSEMBLY CLASSES 6x6D AND 7x7C IN THE MPC-HB  
TO DEMONSTRATE COMPLIANCE WITH 10CFR71.55 AND 10CFR71.59

<b>MPC-HB, 2.6 wt% <sup>235</sup>U, all Intact or Undamaged Assemblies</b>				
Configuration	% Internal Moderation	% External Moderation	Applicable Requirement	Maximum $k_{eff}$
Single Package, unreflected	100%	0%	n/a	0.8464
Single Package, fully reflected	100%	100%	10CFR71.55 (b), (d), and (e)	0.8480
Containment, fully reflected	100%	100%		0.8472
Infinite Array of Damaged Packages	100%	100%	10CFR71.59 (a)(2)	0.8477
Infinite Array of Undamaged Packages	0%	0%	10CFR71.59 (a)(1)	0.3790
<b>MPC-HB, , 2.6 wt% <sup>235</sup>U, Intact or Undamaged and Damaged Assemblies</b>				
Configuration	% Internal Moderation	% External Moderation	Applicable Requirement	Maximum $k_{eff}$
Single Package, unreflected	100%	0%	n/a	0.9018
Single Package, fully reflected	100%	100%	10CFR71.55 (b), (d), and (e)	0.9017
Containment, fully reflected	100%	100%		<b>0.9026</b>
Infinite Array of Damaged Packages	100%	100%	10CFR71.59 (a)(2)	0.9022
Infinite Array of Undamaged Packages	0%	0%	10CFR71.59 (a)(1)	0.3858

---

HOLTEC INTERNATIONAL COPYRIGHTED MATERIAL

Table 6.I.2  
BWR FUEL CHARACTERISTICS AND ASSEMBLY CLASS DEFINITIONS FOR HBPP FUEL  
(all dimensions are in inches)

Fuel Assembly Designation	Clad Material	Pitch	Number of Fuel Rods	Cladding OD	Cladding Thickness	Pellet Diameter	Active Fuel Length	Number of Water Rods	Water Rod OD	Water Rod ID	Channel Thickness	Channel ID
6x6D Assembly Class												
6x6D01	Zr	0.740	36	0.5585	0.02675	0.4880	80	0	n/a	n/a	0.060	4.542
7x7C Assembly Class												
7x7C01	Zr	0.631	49	0.4860	0.0300	0.4110	80	0	n/a	n/a	0.060	4.542

---

HOLTEC INTERNATIONAL COPYRIGHTED MATERIAL

Table 6.I.3

[PROPRIETARY INFORMATION WITHHELD PER 10CFR2.390]

---

HOLTEC INTERNATIONAL COPYRIGHTED MATERIAL

HI-STAR SAR  
REPORT HI-951251

6.I-9

Rev. 16

Table 6.I.4

MAXIMUM  $k_{\text{eff}}$  VALUES FOR ASSEMBLY CLASSES 6x6D AND 7x7C IN THE MPC-HB  
FOR INTACT AND UNDAMAGED FUEL WITH AN AVERAGE ENRICHMENT OF 2.6  
wt%  $^{235}\text{U}$ .

Assembly Class	Configuration	Maximum $k_{\text{eff}}$
6x6D	Intact, Standard	0.8318
7x7C	Intact, Standard	0.8237
6x6D	Intact Assemblies in DFCs	0.8069
6x6D	Intact, Potential Poison Plate Damage	0.8335
6x6D	Intact, Eccentric Fuel Positioning	0.8401
6x6D	Undamaged, Eccentric Fuel Positioning	<b>0.8464</b>
7x7C	Undamaged	0.8333
7x7C	Undamaged, Eccentric Fuel Positioning	0.8400

---

HOLTEC INTERNATIONAL COPYRIGHTED MATERIAL

Table 6.I.5

MAXIMUM  $k_{\text{eff}}$  VALUES FOR THE MPC-HB WITH INTACT FUEL AND DAMAGED FUEL/FUEL DEBRIS WITH AN AVERAGE ENRICHMENT OF 2.6 wt%  $^{235}\text{U}$

	Maximum $k_{\text{eff}}$			
DFC Pattern	Basket Periphery (28 DFCs)		Checkerboard (40 DFCs)	
Pellet Diameter	0.411"	0.488"	0.411"	0.488"
DFC Rod Array				
5x5	n/c <sup>†</sup>	0.8307	n/c	0.8092
6x6	0.8324	0.8389	0.8234	0.8682
7x7	0.8383	0.8444	0.8684	<b>0.8906</b>
8x8	0.8433	0.8422	0.8875	0.8846
9x9	0.8449	0.8372	0.8875	0.8602
10x10	0.8400	0.8331	0.8742	0.8343
11x11	0.8352	n/c	0.8512	n/c

---

<sup>†</sup> n/c = not calculated

---

HOLTEC INTERNATIONAL COPYRIGHTED MATERIAL

Table 6.I.6

MAXIMUM  $k_{\text{eff}}$  VALUES FOR THE MPC-HB WITH INTACT FUEL AND DAMAGED FUEL/FUEL DEBRIS WITH AN AVERAGE ENRICHMENT OF 2.6 wt%  $^{235}\text{U}$

Configuration	Maximum $k_{\text{eff}}$
Standard	0.8906
Potential Poison Plate Damage	0.8896
Eccentric Fuel Positioning	<b>0.8981</b>

---

HOLTEC INTERNATIONAL COPYRIGHTED MATERIAL



Table 6.I.7

MAXIMUM  $k_{\text{eff}}$  VALUES FOR THE MPC-HB WITH UNDAMAGED FUEL AND DAMAGED FUEL/FUEL DEBRIS WITH AN AVERAGE ENRICHMENT OF 2.6 wt%  $^{235}\text{U}$

Rod Array inside undamaged assemblies	Maximum $k_{\text{eff}}$	
	Fuel and DFCs Centered in Basket Cells	Eccentric positioning of Fuel and DFCs
3x3	0.8784	0.8849
4x4	0.8938	<b>0.9018</b>
5x5	0.8786	0.8874
6x6	0.8601	0.8671

---

HOLTEC INTERNATIONAL COPYRIGHTED MATERIAL

Table 6.I.8  
 MAXIMUM  $k_{\text{eff}}$  VALUES  
 WITH REDUCED WATER DENSITY IN THE MPC.

<b>Water Density (% of Full Density)</b>	<b>Maximum <math>k_{\text{eff}}</math>, all intact assemblies</b>	<b>Maximum <math>k_{\text{eff}}</math>, intact and damaged assemblies</b>
100 (Reference)	0.8410	0.9003
98	0.8385	0.8997
95	0.8380	0.8951
90	0.8304	0.8857
80	0.8127	0.8717
70	0.7963	0.8513
50	0.7444	0.8113
30	0.6549	0.7870
10	0.5045	0.5832
5	0.4470	0.4782

---

HOLTEC INTERNATIONAL COPYRIGHTED MATERIAL

Figures 6.I.1 through 6.I.4: PROPRIETARY INFORMATION WITHHELD PER 10CFR2.390

**SUPPLEMENT 6.II****CRITICALITY EVALUATION OF THE HI-STAR HB PACKAGE WITH GWC-HB****6.II.0 INTRODUCTION**

The HI-STAR GTCC HB Package is designed to serve as a transportation cask for radioactive waste material. The total weight of the fissile material to be transferred in the HI-STAR GTCC HB Package no more than 19 grams per package. According to 10 CFR 71.15 (c)(1), if every gram of fissile material contains at least 2000 grams of solid nonfissile material and there is no more than 180 grams of fissile material distributed within 360 kg of contiguous nonfissile material then the fissile material is exempt from the fissile material package standards of 10 CFR 71.55 and 71.59. Therefore, a specific criticality evaluation for the HI-STAR GTCC HB Package containing the current radioactive material is not required.

---

HOLTEC INTERNATIONAL COPYRIGHTED MATERIALHI-STAR SAR  
REPORT HI-951251

6.II-1

Rev. 16

## SUPPLEMENT 6.III

### CRITICALITY EVALAUTION OF THE HI-STAR 100 PACKAGE WITH DIABLO CANYON MPC-32 AND BURNUP CREDIT

#### 6.III.0 INTRODUCTION

This supplement is focused on providing criticality evaluations with burnup credit for fuel from the Diablo Canyon Power Plant (DCPP) in the HI-STAR 100 with MPC-32. The evaluation presented herein supplements the evaluations contained in Appendix 6.C. Effort is made to not repeat generic evaluations presented in Appendix 6.C.

The evaluation presented in this supplement are performed to support the transport of DCPD specific fuel in the HI-STAR 100 with MPC-32 using burnup credit following the same methodology in Appendix 6.C. The reason a separate supplement is required for DCPD is that the results of the generic burnup credit evaluations presented in Appendix 6.C of this SAR are overly conservative with respect to the DCPD site fuel and therefore site specific burnup credit evaluations are required. The generic burnup credit evaluations presented in Appendix 6.C were performed in a very conservative manner such that the results would bound as many fuel designs and reactor sites as possible. The expectation that site specific evaluations would need to be performed requires that an appropriate site specific methodology to be developed. This supplement documents the site specific methodology for the DCPD, yet it is noted that the methodology is also applicable to other sites.

#### 6.III.1 DISCUSSION AND RESULTS

The evaluation of the DCPD specific fuel assemblies is performed consistent with the methodology presented in Appendix 6.C with additional enhancements. The following is a summary of the DCPD specific evaluations:

- Appendix 6.C burnup credit methodology is applied.
- Spent fuel loading curves are developed for Configuration A only (see Section 6.III.2.1).
- Spent fuel loading curves are developed for fuel assembly class 17x17A, subclass 17x17B06 (bounds all 17x17B fuel classes) and subclass 17x17B01 (see Section 6.III.2.2).
- Depletion calculations are performed using DCPD site specific core operating parameters (COP) (see Section 6.III.2.3).
- For the three fuel assembly classes and subclasses (17x17A, 17x17B06 and 17x17B01), loading curves are developed using the generic axial burnup profiles (see Appendix 6.E) and DCPD site specific axial burnup profiles (see Section 6.III.2.4).
- An evaluation is performed of the DCPD site specific spent fuel characteristics (initial enrichment and burnup by fuel assembly class) against the results of the evaluations in this supplement (see Figures 6.III.1 through 6.III.3).

---

HOLTEC INTERNATIONAL COPYRIGHTED MATERIAL

- In some instances, a fuel assembly may not be initially bounded by the enrichment versus burnup curves and therefore additional evaluations are performed to accept these fuel assemblies for qualification (see Section 6.III.2.5).

The results of the evaluations are presented Section 6.III.4 and those results demonstrate that, for the designated fuel assembly classes and basket configuration, an infinite number of HI-STAR 100 Systems with MPC-32 remain subcritical with a margin of subcriticality greater than  $0.05\Delta k$ . This corresponds to a Criticality Safety Index (CSI) of zero (0) and demonstrates compliance with 10CFR71 criticality requirements for normal and hypothetical accident conditions of transport.

### 6.III.2 SPENT FUEL LOADING

Burnup credit is necessary to store the DCPD PWR assemblies in the MPC-32, i.e. a required minimum average assembly burnup is specified as a function of the assembly initial enrichment. The maximum initial enrichment is 5.0 wt%  $^{235}\text{U}$ . The burnup credit methodology is the same as presented in Appendix 6.C, i.e. updated to ISG-8 Revision 3. Furthermore, for the purpose of this supplement for DCPD specific parameters, the burnup credit methodology considers DCPD specific core operating parameters, fuel assembly dimensions and axial burnup profiles. These parameters are further discussed in the following sections.

#### 6.III.2.1 DCPD Cask Loading Configuration

The DCPD operating history demonstrates that the site reactors are not normally operated with control rods inserted. Note that during normal plant operation various tests are performed that require the insertion and withdrawal of controls at full power. The insertion and withdrawal of control rods for testing during full power operations is not considered operation with control rods inserted. Note that any reactivity effect of full power insertion and withdrawal of control rods for testing at full power is well bounded by operation with the bounding fuel inserts and burnable poisons for the entire operating history of the fuel assembly considered for all fuel in Configuration A (see Appendix 6.C). Further, it is not possible to insert control rods into a fuel assembly that has fuel inserts, thus, any fuel assembly that experiences the insertion and withdrawal of control rods for testing at full power is well bounded by a fuel assembly with fuel inserts over the entire life of the fuel assembly. Therefore, the DCPD site specific calculations consider Configuration A only. The bounding fuel inserts from Appendix 6.E remain bounding for the DCPD specific fuel and are considered in the Configuration A depletion calculations without additional modification.

#### 6.III.2.2 DCPD Bounding Fuel Dimensions

The evaluations in Section 6.2 of the main body of Chapter 6 demonstrate that the bounding fuel dimensions consist of maximum active fuel length, maximum fuel pellet diameter, minimum cladding outside diameter (OD), maximum cladding inside diameter (ID) and minimum guide tube thickness. The results of those evaluations remain applicable for the DCPD specific calculations and are not repeated. Note that although the DCPD fuel is shorter (i.e. has an active

---

HOLTEC INTERNATIONAL COPYRIGHTED MATERIAL

length of 144 inches), the evaluation of the DCPD conservatively models the active length to be 150 inches consistent with the evaluations in Chapter 6.

A detailed review of the DCPD fuel information indicates that the DCPD VANTAGE 5 fuel assemblies are bounded by the 17x17A class and the DCPD LOPAR fuel assemblies are bounded by the 17x17B01 and 17x17B02 fuel subclasses (the 17x17B01 and 17x17B02 are essentially identical). See Table 6.III.1. DCPD specific evaluations are performed using the 17x17A fuel class (which bounds the DCPD VANTAGE 5 fuel assemblies), the 17x17B01 fuel subclass which bounds the DCPD specific LOPAR fuel assemblies and the 17x17B fuel subclass (which bounds all the DCPD fuel assemblies). These three sets of curves are evaluated to provide flexibility.

### 6.III.2.3 DCPD Core Operating Parameters

Core operating parameters are discussed in detail in Appendix 6.C. For the purpose of performing DCPD site specific evaluations, the COP considered in Appendix 6.C were revised to be consistent with the DCPD site specific parameters.

#### 6.III.2.3.1 Moderator Temperature

In Appendix 6.C the COP were evaluated in a generic manner so that they could be applicable to many different fuel designs and sites. The approach essentially used a 35% correction factor to bound the upper limit of operating moderator temperatures. The approach taken in this supplement uses core exit thermocouple data from Unit 1 and Unit 2 Cycle 19. These two cycles are representative of operating cycles at the DCPD because the DCPD operates historically at a constant thermal power. The core exit thermocouple cycle daily values were averaged over the entire cycle so that the maximum cycle average core exit thermal couple value was determined and used in the CASMO-5 depletion calculations. The COP considered in the DCPD specific calculations are presented in Table 6.III.2.

#### 6.III.2.3.2 Soluble Boron

The DCPD site specific soluble boron evaluation was performed using DCPD Unit 1 and 2 historical cycle boron let down curves. The value selected bounds the historical maximum average value for both Unit 1 and Unit 2. The COP considered in the DCPD specific calculations are presented in Table 6.III.2.

### 6.III.2.4 DCPD Axial Burnup Profiles

Axial burnup profiles are discussed in detail in Appendix 6.C and the generic profile from Appendix 6.C is used. Additionally, for the DCPD site specific evaluation, new site specific bounding profiles were also developed. The axial burnup profiles from 1764 fuel assemblies were evaluated. From the full data set, 673 profiles have four nodes and 1091 profiles have six nodes. The four node data set is applicable to the enrichment range from 2.0 wt% to 4.0 wt% <sup>235</sup>U and the six node data set is applicable to the enrichment range from 3.5 to 5.0 wt% <sup>235</sup>U.

---

HOLTEC INTERNATIONAL COPYRIGHTED MATERIAL

Previous studies have shown that axial burnup profiles with smaller numbers of nodes is acceptable [6.III.1]. The two DCPD site specific axial burnup profiles were developed in a conservative manner by finding the minimum value for each node over all nodes in the data set and not renormalizing the resulting profile. Note that these two profiles are not burnup dependent and therefore as burnup increases they are overly conservative. Additionally, the four node profile is very conservative since the end nodes are 12 inches long and have a very low relative burnup. Additionally, due to the shorter length of the DCPD specific fuel, the two large nodes in the center of the axial burnup profiles were extended by 3 inches; this has no impact on results because reactivity is dominated by the top node. For fuel within the enrichment range 3.5 to 4.0 wt%  $^{235}\text{U}$  the fuel is evaluated using both profiles due to the overlap in enrichment range applicability. The DCPD site specific axial burnup profiles are presented in Table 6.III.3.

#### 6.III.2.5 Fuel Temperature and Specific Power

In Appendix 6.C bounding values for the fuel temperature and specific power were developed to cover the full range of values from many plants. The data that was used as the basis for those values included DCPD site specific values for fuel temperature and core thermal power. The DCPD site specific values from that data set have been used here and are presented in Table 6.III.2.

### 6.III.3 MODEL SPECIFICATION

The HI-STAR 100 system is described in detail in Section 6.3. The discussion presented in Section 6.3 is directly applicable to the DCPD specific fuel and are not repeated here. The evaluations performed in this supplement for the DCPD specific fuel is consistent with the description in Section 6.3 with the following exceptions:

- The burnup credit methodology uses MCNP5 and CASMO-5 as discussed in Appendix 6.C.
- The CASMO-5 depletion calculations are performed with DCPD specific COP as discussed in Section 6.III.2.3.
- The MCNP5 calculations are performed with DCPD specific axial burnup profiles (see Section 6.III.2.4) in addition to the generic profiles (Appendix 6.C).

### 6.III.4 CRITICALITY CALCULATIONS

The criticality calculations are consistent with the description in Appendix 6.C. Where applicable, DCPD specific parameters have been considered as discussed in Section 6.III.2. The basket designs are intended to safely accommodate each DCPD fuel assembly type for Configuration A, the required burnups are then matched by a third-order polynomial fit as a function of enrichment. The resulting equations are listed in Table 6.III.4, and shown graphically in Figures 6.III.1, 6.III.2 and 6.III.3. The calculations were based on the assumption that the HI-STAR 100 System was fully flooded with water. In all cases, the calculations include bias and calculational uncertainties, as well as the reactivity effects of manufacturing tolerances,

---

HOLTEC INTERNATIONAL COPYRIGHTED MATERIAL



determined by assuming the worst case geometry. All these calculations were performed for a single package, internally flooded, and no external reflection. To satisfy the requirements of 10CFR71.55 and 10CFR71.59, additional calculations were performed. For these calculations, the 17x17A assembly is at 5 wt%  $^{235}\text{U}$ . This represents the case with the highest or close-to-highest reactivity. The results are listed in Table 6.III.5, and are below the regulatory limit of 0.95 in all cases.

Loading curve confirmatory calculations are presented in Table 6.III.6.

#### 6.III.4.1 Approach for Evaluation of Non-Bounded Fuel Assemblies

The DCPD site spent fuel inventory was characterized according to fuel assembly class, initial enrichment and discharge burnup. Five fuel assemblies that did not meet the requirements in Table 6.III.2 were further evaluated to demonstrate acceptability for transport in the HI-STAR 100. For each fuel assembly, additional evaluations were performed with the fuel assembly specific axial burnup profiles (see Table 6.III.7). Each of the five fuel assemblies were the DCPD LOPAR fuel design and therefore the 17x17B06 fuel subclass fuel parameters were used. The results of the calculations are presented in Table 6.III.7.

It should be noted that the evaluations in this supplement consider the entire cask to have the same enrichment and burnup combination. This approach is very conservative because actual casks have a variety of enrichment and burnup combinations, and as has been shown in the results presented in this supplement, the vast majority of the actual fuel stored in the casks has a reactivity substantially less than the reactivity at the loading curves.

Therefore, the following approach for qualification of the fuel in casks that is supported by the evaluations in this supplement that may be used independently or all together are:

- A single fuel assembly enrichment and burnup for all fuel in the cask or actual fuel assembly initial enrichments and burnups for every fuel assembly in the cask,
- Bounding fuel assembly class fuel assembly parameters or actual fuel assembly parameters,
- Generic fuel assembly axial burnup profiles or actual fuel assembly axial burnup profiles,
- Generic COP or site specific COP.

#### 6.III.5 REFERENCES

- [6.III.1] ORNL/TM-12973, “Sensitivity and Parametric Evaluations of Significant Aspects of Burnup Credit for PWR Spent Fuel Packages”, May 1996.

---

HOLTEC INTERNATIONAL COPYRIGHTED MATERIAL

Table 6.III.1

## Comparison of DCPD Fuel with Fuel Assembly Classes

(all dimensions are in inches)

264 fuel rods, 25 guide tubes, pitch=0.4960, Zr clad						
Comparison of DCPD Fuel to Fuel Assembly Class 17x17A Variations						
Fuel Assembly Designation	cladding OD	cladding ID	cladding thickness	pellet OD	fuel length	guide tube thickness
17x17A01	0.3600	0.3150	0.0225	0.3088	150	0.0160
17x17A02	0.3600	0.3100	0.0250	0.3030	150	0.0160
Dimensions Listed for Authorized Contents	0.3600 (min.)	0.3150 (max.)		0.3088 (max.)	150 (max.)	0.0160 (min.)
DCPD VANTAGE 5	0.3600	0.3150	0.0225	0.3088	144	0.0160
DCPD VANTAGE 5 bounding dimensions (17x17A01)	0.3600	0.3150	0.0225	0.3088	150	0.0160
Comparison of DCPD Fuel to Fuel Assembly Class 17x17B Variations						
17x17B01	0.3740	0.3290	0.0225	0.3225	150	0.0160
17x17B02	0.3740	0.3290	0.0225	0.3225	150	0.0160
17x17B03	0.3760	0.3280	0.0240	0.3215	150	0.0160
17x17B04	0.3720	0.3310	0.0205	0.3232	150	0.0140
17x17B05	0.3740	0.3260	0.0240	0.3195	150	0.0160
17x17B06	0.3720	0.3310	0.0205	0.3232	150	0.0140
Dimensions Listed for Authorized Contents	0.372 (min.)	0.3310 (max.)		0.3232 (max.)	150 (max.)	0.0140 (min.)
DCPD LOPAR	0.3740	0.3290	0.0225	0.3225	144	0.0160
DCPD LOPAR bounding dimensions (17x17B01)	0.3740	0.3290	0.0225	0.3225	150	0.0140 <sup>†</sup>

<sup>†</sup> This value remains unchanged from the 17X17B class bounding value.

Note: The shaded parameters are incorporated into the CoC by reference.

HOLTEC INTERNATIONAL COPYRIGHTED MATERIAL

Table 6.III.2

## DCPP Site Specific Core Operating Parameters

Parameter	Specific Power (MW/MTU)	Moderator Temperature (K)	Fuel Temperature (K)	Soluble Boron (ppm)
Diablo Canyon MPC-32	59.24	594	1122	900

---

HOLTEC INTERNATIONAL COPYRIGHTED MATERIAL

Table 6.III.3

## DCPP Site Specific Bounding Axial Burnup Profiles

4 Node Profile		6 Node Profile	
Node Size (inches)	Relative Nodal Burnup	Node Size (inches)	Relative Nodal Burnup
12 (bot)	0.791658	6 (bot)	0.185630
60	1.047715	6	0.821972
60	1.053847	60	1.003812
12	0.880056	60	1.035024
		6	0.850799
		6	0.186602

---

HOLTEC INTERNATIONAL COPYRIGHTED MATERIAL

Table 6.III.4

[PROPRIETARY INFORMATION WITHHELD PER 10CFR2.390]

---

HOLTEC INTERNATIONAL COPYRIGHTED MATERIAL

HI-STAR SAR  
REPORT HI-951251

6.III-9

Rev. 16

Table 6.III.5

Results of the 10CFR71.55 and 10CFR71.59 Calculations

Configuration	% Internal Moderation	% External Moderation	Max. $k_{\text{eff}}$	1 $\sigma$	EALF (eV)
17x17A, 5.0 wt% $^{235}\text{U}$ , 44.60 GWD/MTU, Configuration A					
Single Package, unreflected	100%	0%	0.9459	0.0002	0.3067
Single Package, fully reflected	100%	100%	0.9461	0.0003	0.3066
Containment, fully reflected	100%	100%	0.9458	0.0003	0.3066
Infinite Array of Damaged Packages	100%	100%	0.9460	0.0002	0.3064
Infinite Array of Undamaged Packages	0%	0%	0.4075	0.0001	32742

HOLTEC INTERNATIONAL COPYRIGHTED MATERIAL

HI-STAR SAR  
REPORT HI-951251

6.III-10

Rev. 16

Table 6.III.6

## Loading Curve Confirmatory Calculations

Assembly Subclass	wt% $^{235}\text{U}$	Profile	GWD/MTU	Max. $k_{\text{eff}}$
17x17B06	2.0	uniform	5.74	0.9451
		Generic (Appendix 6.E)		0.9452
	3.5	uniform	30.36	0.9188
		Generic (Appendix 6.E)		0.9453
	5.0	uniform	46.86	0.9251
		Generic (Appendix 6.E)		0.9455

---

HOLTEC INTERNATIONAL COPYRIGHTED MATERIAL

Table 6.III.7

## Fuel Assembly Specific Initial Enrichment, Burnup and Axial Burnup Profiles

Fuel Assembly	Assembly 1 (ID F18)	Assembly 2 (ID FH03)	Assembly 3 (ID FH01)	Assembly 4 (ID V82H)	Assembly 5 (ID V61H)
Enrichment (wt% $^{235}\text{U}$ )	3.808	4.201	4.203	4.402	4.413
Burnup (GWD/MTU)	30.92	35.61	36.50	39.00	39.39
Fuel Assembly Specific Axial Burnup Profile	0.240153	0.197841	0.200483	0.242293	0.238014
	0.918585	0.871467	0.858344	0.949787	0.941190
	1.072945	1.080849	1.079979	1.058576	1.055174
	1.096829	1.109648	1.112191	1.098220	1.101208
	0.947678	0.921722	0.912766	1.013694	1.034100
	0.230899	0.196366	0.196952	0.246861	0.250932
$k_{\text{calc}}$	0.9047	0.9133	0.9113	0.9050	0.9050
sigma	0.0003	0.0002	0.0003	0.0003	0.0003
$k_{\text{calc}}$	0.9883	0.9954	0.9916	0.9954	0.9952
sigma	0.0002	0.0003	0.0003	0.0003	0.0003
Max. $k_{\text{eff}}$	0.9321	0.9403	0.9386	0.9325	0.9325

---

HOLTEC INTERNATIONAL COPYRIGHTED MATERIAL



Figure 6.III.1  
[PROPRIETARY INFORMATION WITHHELD PER 10CFR2.390]

---

HOLTEC INTERNATIONAL COPYRIGHTED MATERIAL

HI-STAR SAR  
REPORT HI-951251

6.III-13

Rev. 16

Figure 6.III.2  
[PROPRIETARY INFORMATION WITHHELD PER 10CFR2.390]

---

HOLTEC INTERNATIONAL COPYRIGHTED MATERIAL

HI-STAR SAR  
REPORT HI-951251

6.III-14

Rev. 16

Figure 6.III.3  
[PROPRIETARY INFORMATION WITHHELD PER 10CFR2.390]

---

HOLTEC INTERNATIONAL COPYRIGHTED MATERIAL

HI-STAR SAR  
REPORT HI-951251

6.III-15

Rev. 16

## CHAPTER 7: OPERATING PROCEDURES

### 7.0 INTRODUCTION

This chapter provides the high level description of the essential elements necessary to prepare the system for shipment and to ensure that its performance under normal and accident conditions will be as described in the system evaluation. The information described in the chapter contains the minimum requirements that will ensure that the HI-STAR 100 System is operated in a safe and reliable manner consistent with the evaluation in the SAR. Holtec will use the information presented in this chapter along with their knowledge of the technical basis of the system design described in chapters 2 through 6 to develop more detailed generic procedures for the HI-STAR 100 System. Equipment specific operating details such as valve manipulation and onsite transporter operation will be provided to users based on the specific equipment selected and the configuration of the site. Licensees will utilize the information provided in this chapter, (understanding that it provides the essential operation elements that must be included in the detailed operating procedures), the conditions of the Certificate of Compliance (CoC), equipment-specific operating instructions, and plant working procedures and apply them to develop the site-specific written loading, unloading, and handling procedures to ensure that the system is operated in accordance with the system CoC and all applicable government regulatory requirements.

The operations described in this chapter assume that the fuel will be loaded into, or unloaded from, an MPC while in the HI-STAR overpack submerged in a spent fuel pool. Because the HI-STAR is a dual-use cask certified for use as a dry storage cask under 10 CFR 72, the descriptions below include the steps required to transport the cask after a period of storage. The chapter also provides a description of the essential elements necessary to transfer a Holtec MPC from a dry storage system into the HI-STAR system for transportation.

It is the cask user's responsibility to develop the site-specific operating procedures in accordance with the system CoC, the information presented in this chapter, and applicable regulatory requirements. Users will be required to develop or modify existing programs and procedures to account for the transport operation of the HI-STAR 100 System. Written procedures are required and will be developed or modified to account for such things as nondestructive examination (NDE) of the MPC welds, handling and storage of items and components identified as important to safety, heavy load handling, specialized instrument calibration, special nuclear material accountability, fuel handling procedures, training, equipment and process qualifications. Users shall implement controls to ensure that the lifted weights do not exceed the HI-STAR 100 lifting trunnion design limit. Users shall implement controls to monitor the time limit from the removal of the HI-STAR 100 from the spent fuel pool to the commencement of MPC draining to prevent boiling. Users shall also implement controls to ensure that the HI-STAR 100 overpack cannot be subjected to a fire in excess of design limits during loading operations.

Control of system operation shall be performed in accordance with the licensee's Quality Assurance (QA) program to ensure critical steps are not overlooked and that the MPC and

overpack, as applicable, have been confirmed to meet all requirements of the Part 71 CoC before being released for shipment.

Table 7.1.2 and Figure 7.1.1 provide the HI-STAR 100 System bolt torque and sequencing requirements, respectively. Fuel assembly selection and verification shall be performed by the licensee in accordance with written, approved procedures that ensure that only SNF assemblies authorized in the CoC are loaded into the HI-STAR 100 System. Fuel handling, including the handling of fuel assemblies in the Damaged Fuel Container (DFC) shall be performed in accordance with written site-specific procedures. Damaged fuel and fuel debris, as defined in the CoC, shall be loaded in DFCs.

ALARA notes and warnings are included to alert users to radiological issues. Actions identified with these notes and warnings are not mandatory and shall be implemented based on a determination by radiation protection.

Supplementary guidance for each of the sections in Chapter 7 that are specific to operations for the HI-STAR HB, the HI-STAR HB GTCC Package with GWC-HB, and the HI-STAR 100 Package with the Diablo Canyon MPC-32 are found in Supplements 7.I, 7.II and 7.III, respectively.

## 7.1 PROCEDURE FOR LOADING AND PREPARATION FOR TRANSPORT OF THE HI-STAR 100 SYSTEM

### 7.1.1 Overview of HI-STAR Loading Operations

The MPC loading operations described herein are for HI-STAR 100 systems prepared for "load-and-go" directly into transportation under 10CFR71. HI-STAR 100 systems that are loaded and stored on an ISFSI site must be prepared in accordance with the applicable Part 72 HI-STAR FSAR or HI-STORM FSAR license and respective Certificate of Compliance (CoC). Any HI-STAR overpack and/or MPC deployed at an ISFSI must be confirmed to meet all conditions of the 10CFR71 CoC prior to shipment. The dryness criteria under the Part 72 CoC shall be considered acceptable for use in transport under Part 71 [7.1.2], [7.1.6].

The HI-STAR 100 System (HI-STAR) is used to load and transport spent nuclear fuel (SNF). The essential elements required to prepare the HI-STAR for fuel loading, to load the fuel, to ready the system for transport, and to ship the HI-STAR are described below.

**Note:**

When loading MPCs requiring soluble boron, the boron concentration of the water shall be checked before and during operations with fuel and water in the MPC.

### 7.1.2 Preparation of HI-STAR for Loading

1. If the HI-STAR overpack has previously been used to transport SNF, the HI-STAR overpack is received and the personnel barrier, if attached, is removed. The security seals, if used, are inspected to verify there was no tampering and that they match the corresponding shipping documents.
2. The HI-STAR is visually receipt inspected to verify that there are no outward visual indications of impaired physical condition except for superficial marks and dents. Any road dirt is washed off and any foreign material is removed.
3. Radiological surveys are performed in accordance with 49CFR173.443 [7.1.3] and 10CFR20.1906 [7.1.4]. Any issues are identified to site management. The overpack is decontaminated as directed by site radiation protection. Appropriate notifications are made as detailed in the surveillance requirements.
4. The impact limiters, if attached, are removed and a second visual inspection to verify that there are no outward visual indications of impaired physical condition is performed.
5. The HI-STAR overpack is upended and the neutron shield relief devices are inspected to confirm that they are installed, intact, and not covered by tape or any other covering.

### 7.1.3 Loading of Contents into HI-STAR

#### 7.1.3.1 Loading of SNF into HI-STAR from a Spent Fuel Pool

1. Position the HI-STAR in the MPC loading area. For MPC-32 canisters, verify spent fuel pool for boron concentration requirements in accordance with Table 1.2.27. Testing must be completed within four hours prior to loading and every 48 hours after. Two independent measurements shall be taken to ensure that the requirement of 10 CFR 72.124(a) is met.
2. An empty MPC is upended and prepared for loading. The MPC is subjected to receipt inspection (inspected for cleanliness and outward visual indications of impaired physical condition except for superficial marks and dents). Road dirt/debris and any foreign material are removed from the MPC prior to placement in the spent fuel pool. Verification is made to ensure that the appropriate fuel spacers, as necessary, are used to position the active fuel zone within the neutron absorber plates of the MPC, and limit axial movement of the fuel assemblies in the MPC cavity. The empty MPC is raised and inserted into the HI-STAR overpack while being careful not to damage the HI-STAR sealing surface. The MPC is inspected to ensure that the neutron absorber panel sheathing is present and there are no signs of potential damage to the neutron absorber.
3. The annulus is filled with clean (uncontaminated) water and the annulus seal is installed in the annulus between the MPC and the HI-STAR overpack.

<b>ALARA Note:</b>
<p>A bottom protective cover may be attached to the cask bottom or placed in the designated preparation area or spent fuel pool. This will help prevent embedding contaminated particles in the cask bottom surface and ease the decontamination effort. Waterproof tape placed over empty bolt holes, and bolt plugs may also reduce the time required for decontamination. Wetting the components that enter the spent fuel pool may reduce the amount of decontamination work to be performed later.</p>

- |   |
|---|
| <b>ALARA Note:</b>  |
| <p>A bottom protective cover may be attached to the cask bottom or placed in the designated preparation area or spent fuel pool. This will help prevent embedding contaminated particles in the cask bottom surface and ease the decontamination effort. Waterproof tape placed over empty bolt holes, and bolt plugs may also reduce the time required for decontamination. Wetting the components that enter the spent fuel pool may reduce the amount of decontamination work to be performed later.</p> |
4. The MPC is filled with either spent fuel pool water or clean water and the HI-STAR is raised and lowered into the spent fuel pool for fuel loading. For MPC-32 canisters, refer to Table 1.2.27 for boron concentration requirements.
  5. Prior to loading the fuel into the MPC, the user identifies the fuel to be loaded. The loading plan for partially loaded MPCs shall meet the requirements of Table 7.1.1. A pre-loading verification is made to assure that damaged fuel and fuel debris will be placed in damaged fuel containers and that the DFCs will occupy authorized locations in the MPC. The fuel is independently verified to see that it meets the conditions of the CoC. The pre-selected assemblies are loaded into the MPC using DFCs as required, and a visual verification of the assembly identification is performed.

6. While still underwater, a thickly shielded lid (the MPC lid) is positioned over the pool surface and the drain line is installed. The MPC lid drain line is guided into its receiver and the MPC lid is installed. The upper surface of the MPC lid will seat approximately flush with the top edge of the MPC shell when properly installed. The lid may be removed and the drain line replaced should it be damaged during installation of the MPC lid. The user performs a site-specific Time-to-Boil analysis. This determines a time limit that ensures water in the MPC will not boil prior to the start of the draining operations. If it appears that the Time-to-Boil limit will be exceeded prior to draining the MPC, the user shall take appropriate action to prevent water from boiling.

<b>ALARA Note:</b>
Activated debris may have settled on flat surfaces of the cask during fuel loading. Cask surfaces suspected of carrying activated debris should be kept under water until a preliminary dose rate scan clears the cask for removal.

- |   |
|---|
| Activated debris may have settled on flat surfaces of the cask during fuel loading. Cask surfaces suspected of carrying activated debris should be kept under water until a preliminary dose rate scan clears the cask for removal. |
|---|
7. The lift attachment engages the HI-STAR overpack lifting trunnions to lift the HI-STAR overpack and loaded MPC close to the spent fuel pool surface. **Radiation dose readings are taken and the cask top surfaces are decontaminated as directed by radiation protection.**
  8. The HI-STAR is removed from the spent fuel pool. If a lid retention system is being used, it is installed to secure the MPC lid for the transfer to the cask preparation area. The lift attachment and HI-STAR overpack are sprayed with clean water to help remove contamination as they are removed from the spent fuel pool.
  9. The HI-STAR overpack is placed in the designated preparation area and the lift attachment and lid retention system, as applicable, are removed.
  10. The top surfaces of the MPC lid, upper accessible regions of the MPC external shell and the upper flange of the HI-STAR overpack are decontaminated.

<b>ALARA Note:</b>
The water in the HI-STAR 100 overpack-to-MPC annulus provides personnel shielding. The level should be checked periodically and refilled accordingly. Pocket trunnions, if present and not used are plugged to reduce radiation levels around the lower region of the overpack.

- |   |
|---|
| The water in the HI-STAR 100 overpack-to-MPC annulus provides personnel shielding. The level should be checked periodically and refilled accordingly. Pocket trunnions, if present and not used are plugged to reduce radiation levels around the lower region of the overpack. |
|---|
11. The temporary shield ring, if used, is installed. The annulus seal is removed, and an annulus shield is installed. The temporary shield ring provides additional personnel shielding around the top of the HI-STAR overpack during MPC closure operations. The annulus shield also provides additional personnel shielding at the top of the annulus and prevents small items from being dropped into the annulus.



12. Dose rates are measured at the MPC lid and around the HI-STAR overpack to establish appropriate radiological control.

**ALARA Warning:**

Personnel should remain clear of the drain lines any time water is being pumped or purged from the cask. Assembly crud, suspended in the water, may create a radiation hazard to workers. Dose rates will rise as water is drained from the cask. Continuous dose rate monitoring is recommended.

13. The MPC water level and water level in the annulus are lowered slightly. Appropriate monitoring for combustible gas shall be performed prior to, and during MPC lid welding operations. The space below the MPC lid shall be vented/exhausted or purged with inert gas prior to, and during MPC lid welding operations to provide additional assurance that flammable gas concentrations will not develop in this space. Purging is the recommended method to mitigate flammable gas accumulation.

**ALARA Warning:**

The use of manual welding should be minimized and only used when deemed advantageous from an ALARA perspective. If manual welding is elected, it should only be performed under conditions consistent with ALARA principals (e.g., utilizing temporary shielding).

14. The MPC lid is seal welded using an automated welding system, by manual welding, or a combination of both. Visual examinations are performed on the tack welds. Liquid penetrant (PT) examinations are performed on the root and final passes. A volumetric examination is performed on the MPC welds using the ultrasonic method to ensure that the completed weld is satisfactory. As an alternative to volumetric examination of the MPC lid-to-shell weld, a multi-layer PT may be performed including intermediate examinations after approximately every three-eighth inch of weld depth. Any unsatisfactory indications are repaired in accordance with the code requirements [7.1.1].
15. At the appropriate time in the sequence of activities, based on the type of test performed (hydrostatic or pneumatic), an ASME pressure test of the MPC enclosure vessel is performed in accordance with the requirements of Section III, Subsection NB, Article NB-6000 and applicable sub-articles [7.1.1]. Any non-satisfactory conditions require the user to determine the cause of the leak and make repairs as necessary to achieve a successful result.

**ALARA Note:**

Dose rates will rise as water is drained from the MPC. Continuous dose rate monitoring is recommended.

16. The MPC water is displaced from the MPC and the water is drained from the annulus area.
17. The Forced Helium Dehydration (FHD) is connected to the MPC and is used to remove moisture from the MPC. To ensure that the MPC cavity is suitably dry either the temperature or the dew point of the helium exiting the FHD demister shall be less than or equal to 22.9 °F for no less than 30 minutes.
18. The MPC helium backfill is adjusted to the pressure equivalent of greater than 0 psig and less than 44.8 psig at a reference temperature of 70 degrees Fahrenheit.
19. Cover plates are installed and seal welded over the MPC vent and drain ports and PT examinations are performed on the root (for multi-pass welds) and final passes. Any unsatisfactory indications are repaired in accordance with the code requirements.
20. The MPC closure ring is placed on the MPC.
21. The closure ring is aligned, tacked in place, and seal welded. Tack welds are visually examined and PT examinations are performed on the root (for multi-pass welds) and final welds.
22. The annulus shield and the temporary shield ring (if used) are removed.

#### 7.1.3.2 Not Used

#### 7.1.3.3 Loading a Loaded and Sealed MPC into HI-STAR Overpack

1. After the HI-STAR overpack has been prepared in accordance with Section 7.1.2 above, it is placed in the MPC transfer location and is fitted with a mating device to interface with the transfer cask.
2. The transfer cask with loaded MPC is brought to the MPC transfer location and placed atop the HI-STAR overpack and mating device.
3. The mating device is used to open the bottom of the transfer cask and the MPC is lowered into the HI-STAR overpack.
4. **If required, the MPC spacer is installed.**
5. The transfer cask and mating device are removed from the HI-STAR.

#### 7.1.4 Closure of HI-STAR

1. The MPC lid and accessible areas at the top of the MPC shell are smeared for removable contamination. Decontamination of the MPC lid and accessible areas at the top of the MPC may be performed at any time prior to closure of the HI-STAR overpack.
2. The sealing surfaces for the HI-STAR overpack are inspected for signs of damage. Any damage that would prevent a seal is remedied, any old seals are discarded, new seals are inserted for the closure plate, and the closure plate is installed with the bolts torqued in accordance with requirements in Table 7.1.2 and the order prescribed in Figure 7.1.1.
3. The HI-STAR overpack annulus is dried by evacuating to a pressure of less than or equal to 3 torr. The overpack annulus shall be considered dry when it can hold a stable pressure of less than or equal to 3 torr for at least 30 minutes.
4. The HI-STAR overpack is then backfilled with helium gas to a pressure of greater than or equal to 10 psig and less than or equal to 14 psig.
5. Any old seals are removed from the HI-STAR overpack vent and drain plugs and the plugs are installed with new seals and torqued in accordance with Table 7.1.2.
6. All HI-STAR overpack containment boundary seals, (i.e.; closure plate, vent and drain ports), are leak tested to assure they will provide long-term retention of the annulus helium. All HI-STAR overpack containment boundary seals shall be leak tested in accordance with ANSI N14.5 [7.1.5] and shall demonstrate compliance with the leakage rate acceptance criterion in SAR Section 4.1. Unacceptable leakage rates will require repair and re-testing of the seals. The leak test shall be performed within the 12-month period prior to each shipment. The leak test shall also be performed to confirm seal integrity of an affected containment boundary closure following de-tensioning of one or more overpack lid bolts, or of the drain or vent port plug(s);
7. The HI-STAR 100 overpack vent and drain port cover plates are installed.
8. The HI-STAR 100 overpack is surveyed for removable contamination per 49CFR173.443 [7.1.3]. If necessary, the overpack is further decontaminated to meet the surveillance requirements.

#### 7.1.5 Preparation of HI-STAR for Transport

1. Verify the HI-STAR has been leak tested within the past 12 months and no overpack lid bolts and vent and drain port plugs have been de-tensioned. If not, the HI-STAR is leak tested in accordance with Step 6 of Section 7.1.4 above.
2. The relief devices on the neutron shield vessel are verified that they have been replaced within the past 5 years. If not, the relief devices are replaced.

**ALARA Warning:**

Dose rates around the unshielded bottom end of the cask may be higher than other locations around the cask. After the cask is downended on the transport frame, the bottom impact limiter should be installed promptly. Personnel should remain clear and exercise other appropriate ALARA controls when working around the bottom end of the cask.

3. Buttress plate is installed and the HI-STAR overpack is moved to the transport location. The HI-STAR is down-ended and placed on the transport vehicle. Pocket trunnions, if present, are plugged.
4. HI-STAR is visually inspected for signs of impaired condition.
5. Contamination surveys are performed on the HI-STAR per 49CFR173.443 [7.1.3]. If necessary, the overpack is further decontaminated to meet the surveillance requirements.
6. The impact limiters are installed on the HI-STAR and the bolts are torqued in accordance with Table 7.1.2.
7. The tie-down system is installed and a security seal, one per impact limiter is installed and the seal numbers are recorded in the shipping documents.
8. Final radiation surveys of the package surfaces per 10CFR71.47 [7.1.4] and 49CFR173.443 [7.1.3] are performed and recorded in the shipping documents.
9. The personnel barrier is installed.
10. The assembled package is given a final inspection to verify that all conditions for transport have been met (inspection steps may be performed in any order):
  - a. Verify that required radiation survey results are properly documented on the shipping documentation.
  - b. Perform a HI-STAR overpack surface temperature check. The accessible surfaces of the HI-STAR Package (impact limiters and personnel barrier) shall not exceed the Exclusive Use temperature limits of 49CFR173.442 [7.1.3].
  - c. Verify that all required leakage testing has been performed, the acceptance criteria have been met, and the results have been documented on the shipping documentation.
  - d. Verify that the receiver has been notified of the impending shipment and that the receiver has the appropriate procedures and equipment available to safely receive and handle the HI-STAR (10CFR20.1906(e)) [7.1.4].

- e. Verify that the carrier has the written instructions and a list of appropriate contacts for notification of accidents or delays.
- f. Verify that the carrier has written instructions that the shipment is to be Exclusive Use in accordance with 49CFR173.441 [7.1.3].
- g. Verify that route approvals and notification to appropriate agencies have been completed.
- h. Verify that the appropriate labels have been applied in accordance with 49CFR172.403 [7.1.3].
- i. Verify that the appropriate placards have been applied in accordance with 49CFR172.500 [7.1.3].
- j. Verify that all required information is recorded on the shipping documentation.

11. Following the above checks, the HI-STAR 100 System is released for transport.

Table 7.1.1  
HI-STAR 100 SYSTEM PARTIAL MPC LOADING REQUIREMENTS

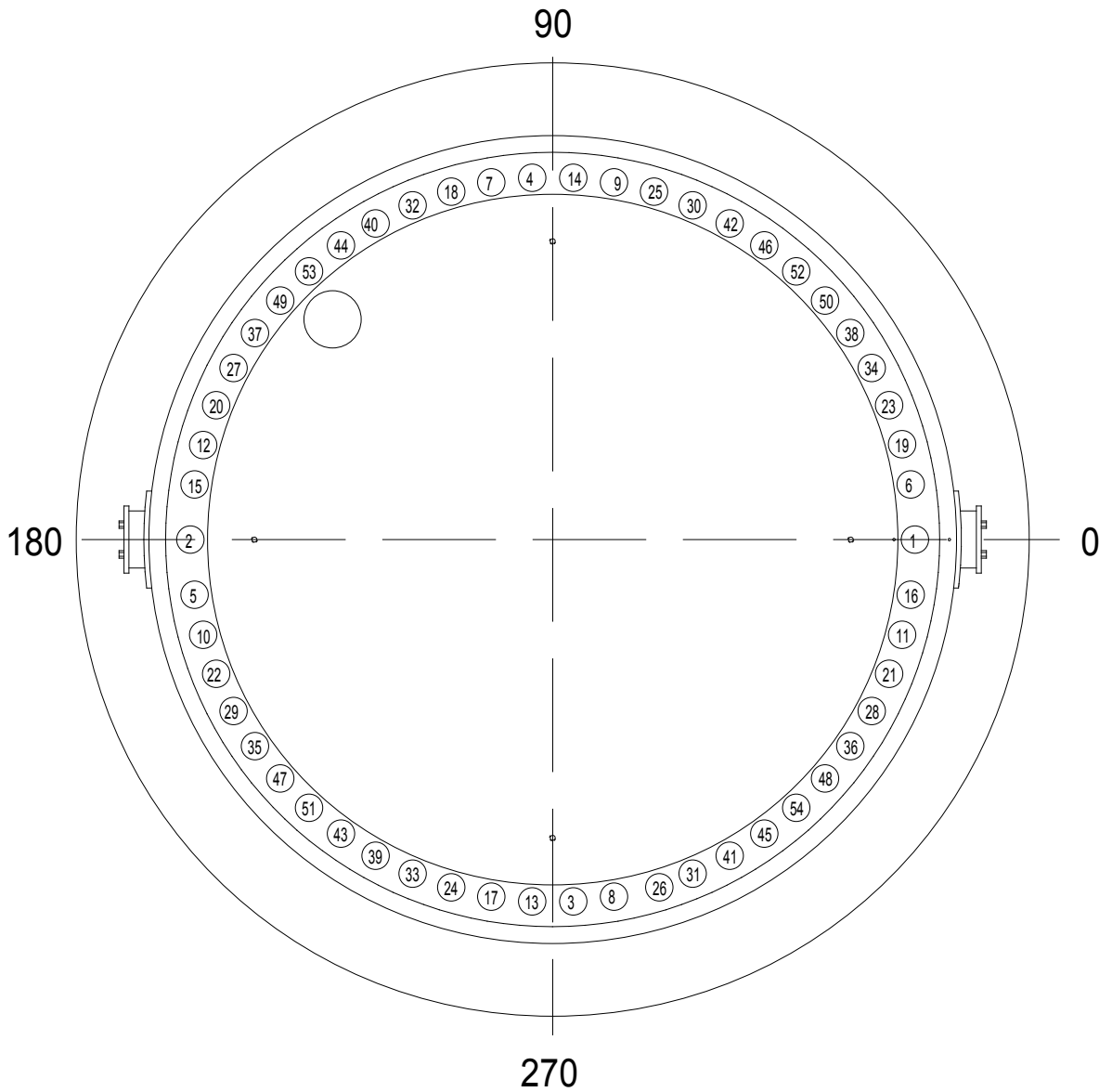
MPC Type	Min. # Cells Loaded	Load Balancing Instructions
MPC-24	12	To preserve the CG of the loaded MPC as near as practical to the centerline, the loading plan shall distribute the fuel assemblies so that in the loaded configuration the MPC is reasonably balanced.
MPC-32	16	
MPC-68	34	

Table 7.1.2  
HI-STAR 100 SYSTEM TORQUE REQUIREMENTS

Fastener	Torque (ft-lbs)	Pattern
Overpack Closure Plate Bolts <sup>†</sup> , <sup>††</sup>	First Pass – Hand Tight Second Pass – Wrench Tight Third Pass – 860 +25/-25 Fourth Pass – 1725 +50/-50 Final Pass - 2000 +250/-0	See Figure 7.1.1
Overpack Vent and Drain Port Plugs	31+5/-5	None
Closure Plate Test Port Plug	31+5/-5	None
Top Impact Limiter Attachment Bolt	256+10/-0	None
Bottom Impact Limiter Attachment Bolt	1500+45/-0	None

<sup>†</sup> Detorquing shall be performed by turning the bolts counter-clockwise in 1/3 turn +/- 30 degrees increments per pass according to Figure 7.1.1 for three passes. The bolts may then be removed.

<sup>††</sup> Bolts shall be cleaned and inspected for damage or excessive wear (replaced if necessary) and coated with a light layer of Fel-Pro Chemical Products, N-5000, Nuclear Grade Lubricant (or equivalent).



**Figure 7.1.1; HI-STAR Closure Plate Bolt Torquing Pattern**



## 7.2 PROCEDURE FOR UNLOADING THE HI-STAR 100 SYSTEM

The essential elements required to prepare the system for fuel unloading, to cool the stored fuel assemblies in the MPC, to flood the MPC cavity, to remove the lid welds, to unload the spent fuel assemblies, and to recover the HI-STAR 100 overpack and empty MPC are described below.

**Note:**

When unloading MPCs requiring soluble boron, the boron concentration of the water shall be checked before and during operations with fuel and water in the MPC.

### 7.2.1 Receipt of Package from Carrier

1. The HI-STAR 100 overpack is received from the carrier and inspected to verify that there are no outward visual indications of impaired physical conditions except for superficial marks and dents. Any road dirt is washed off and any foreign material is removed.
2. The personnel barrier is removed and the security seals are inspected to verify there was no evidence of tampering and that they match the corresponding shipping documents. Any discrepancies are identified to the site management and appropriate authorities.

**ALARA Warning:**

Dose rates around the unshielded bottom end of the HI-STAR 100 cask may be higher than other locations around the cask. After the impact limiter is removed, the cask should be upended promptly. Personnel should remain clear of the bottom of the unshielded cask and exercise other appropriate ALARA controls.

3. The impact limiters are removed.
4. The HI-STAR is visually inspected to verify there are no outward visual indications of impaired physical conditions except for superficial marks and dents, the neutron shield relief devices are inspected to confirm that they are installed, intact, and not covered, and radiation survey and removable contamination survey are performed per 49CFR173.443 [7.1.3]. Any issues are identified to site management and the overpack is decontaminated as directed by site radiation protection. Note that portions of the inspections, surveys, and decontamination activities described here-in may be performed prior to removal of the impact limiters.
5. The HI-STAR 100 overpack is upended and returned to the fuel building or other unloading area.

6. The buttress plate is removed and the HI-STAR 100 overpack is placed in the designated preparation area. Removal of the buttress plate may be performed prior to placing the HI-STAR in the designated preparation area.

## 7.2.2 Removal of Contents

1. The HI-STAR 100 overpack vent port cover plate is removed and a gas sample is drawn from the HI-STAR 100 overpack annulus to determine the condition of the MPC confinement boundary.
2. The annulus is depressurized in accordance with Radiation Protection directions and the HI-STAR 100 overpack closure plate is removed.
3. The annulus is filled with clean water and an annulus shield is installed to protect the annulus from debris produced from the lid removal process.
4. The MPC closure ring above the vent and drain ports and the vent and drain port cover plates are core-drilled and removed to access the vent and drain ports.

<b>ALARA Warning:</b>
Gas sampling is performed to assess the condition of the fuel cladding. If a leak is discovered in the fuel cladding, the user's Radiation Control organization may require special actions to vent the cask cavity.

5. A temporary attachment is connected to the vent port to open the vent port and collect a gas sample from inside the MPC. A gas sample analysis is performed to assess the condition of the fuel assembly cladding.
6. The MPC is cooled as necessary to reduce the MPC internal temperature. This allows water flooding without thermally shocking the fuel assemblies or over-pressurizing the MPC from the formation of steam. The MPC is then filled with water. **For MPC-32 canisters, refer to Table 1.2.27 for boron concentration requirements.**
7. Appropriate monitoring for combustible gas shall be performed prior to, and during MPC lid-to-shell weld removal operations. The space below the MPC lid shall be vented/exhausted or purged with inert gas prior to, and during MPC lid cutting operations to provide additional assurance that flammable gas concentrations will not develop in this space. Purging is the recommended method to mitigate flammable gas accumulation.
8. The MPC lid to MPC shell weld is removed using an automated weld removal system or other suitable equipment. The weld removal equipment is removed with the MPC lid left in place.
9. The top surfaces of the HI-STAR 100 overpack and MPC are cleared of metal shavings.

10. The annulus shield is removed and if necessary, the annulus is re-filled with clean water and an annulus seal is installed.
11. The MPC lid is rigged to the lift equipment and the lift attachment is engaged to the HI-STAR 100 overpack lifting trunnions.

<b>ALARA Note:</b>
Wetting the components that enter the spent fuel pool may reduce the amount of decontamination work to be performed later.

12. The HI-STAR 100 overpack is placed in the spent fuel pool or other appropriate unloading area and the MPC lid is removed. For MPC-32 canisters, verify spent fuel pool for boron concentration requirements in accordance with Table 1.2.27. Testing must be completed within four hours prior to unloading and every 48 hours after. Two independent measurements shall be taken to ensure that the requirement of 10 CFR 72.124(a) is met.
13. All fuel assemblies are returned to the spent fuel storage racks and the MPC fuel cells are vacuumed to remove any assembly debris and crud.
14. The fuel cells are inspected for any remaining items and these are removed as appropriate.

<b>ALARA Warning:</b>
Activated debris may have settled on flat surfaces of the cask during fuel unloading. Surfaces suspected of carrying activated debris should be kept under water until a preliminary dose rate scan clears the cask for removal. To reduce contamination of the cask, the surfaces of the cask and lift yoke should be kept wet until decontamination can begin.

15. The HI-STAR 100 overpack and MPC are returned to the designated preparation area where any water in the MPC is pumped back into the spent fuel pool, liquid radwaste system or other approved location as necessary.
16. The annulus water is drained and the MPC and overpack are decontaminated as directed by radiation protection.

### 7.3 PREPARATION OF AN EMPTY PACKAGE FOR TRANSPORT

The essential elements for preparing an empty package (previously used) for transport are similar to those required for transporting the loaded package with several exceptions. A survey for removable contamination is performed to verify that the removable contamination on the internal and external surfaces of the HI-STAR 100 overpack are ALARA and that the limits of 49CFR173.428 [7.1.3] and 10CFR71.87(i) [7.1.4] are met. At the user's discretion, impact limiters are installed and the personnel barrier is installed and locked. The installation of the impact limiters and personnel barrier are described in this Section. These steps may be omitted.

1. The Seal Surface Protector is removed from the HI-STAR 100 overpack if necessary.
2. HI-STAR 100 Overpack is surveyed for contamination and verified to be empty and contain less than 15 gm U-235 in accordance with 49CFR173.453(b) [7.1.3].
3. The closure plate is installed on the HI-STAR 100 overpack and the bolts are torqued in accordance with requirements in Table 7.1.2 and the order prescribed in Figure 7.1.1.
4. The vent and drain port cover plates are installed if necessary.
5. The HI-STAR 100 overpack is downended and positioned on the transport equipment.
6. A final inspection of the HI-STAR 100 overpack is performed and includes the following:
  - A final survey for removable contamination on the accessible external surfaces of the HI-STAR 100 overpack in accordance with 49CFR173.443(a) [7.1.3]. If necessary, the overpack is further decontaminated to meet the surveillance requirements.
  - A radiation survey of the HI-STAR 100 overpack to confirm that the radiation levels on any external surface of the overpack do not exceed the levels required by 49CFR173.421(b) [7.1.3]. Any issues are identified to site management and the overpack is decontaminated as directed by site radiation protection.
  - A visual inspection of the HI-STAR 100 overpack to verify that there are no outward visual indications of impaired physical condition except for superficial marks and dents and that the package is securely closed in accordance with 49CFR173.428(b) [7.1.3].
  - Verification is made that the HI-STAR 100 overpack neutron shield relief devices are installed, intact, and are not covered by tape or other covering.
7. If desired, the impact limiters are installed and the impact limiter bolts are torqued in accordance with requirements in Table 7.1.2.

8. A security seal is installed either on the closure plate or on both impact limiters, if installed. The security seal number(s) is (are) recorded on the shipping documentation.
9. Final radiation surveys of the package surfaces are performed per 10CFR71.47 [7.1.4], and 49CFR173.428(a) [7.1.3].
10. If desired, the personnel barrier and personnel barrier locks are installed and the personnel barrier keys are transferred to the carrier.
11. A final check to ensure that the package is ready for release is performed and includes the following checks:
  - Verification that the receiver has been notified of the impending shipment.
  - Verification that any labels previously applied in conformance with Subpart E of 49CFR172 [7.1.3] have been removed, obliterated, or covered and the "Empty" label prescribed in 49CFR172.450 [7.1.3] is affixed to the packaging in accordance with 49CFR173.428(e) [7.1.3].
  - Verification that all required information is recorded on the shipping documentation.
12. The HI-STAR 100 System is then released for transport.

#### 7.4 PROCEDURE FOR PREPARING THE HI-STAR 100 OVERPACK FOR TRANSPORT FOLLOWING A PERIOD OF STORAGE

The operations for preparing the loaded HI-STAR 100 Overpack for transport following a period of storage (in excess of one year from the date of completion of HI-STAR 100 overpack mechanical seal leakage testing) are identical to the cask loading and preparation for transport described in Section 7.1.2.

## 7.5 REFERENCE

- [7.1.1] American Society of Mechanical Engineers "Boiler and Pressure Vessel Code". 1995 Edition with 1996 and 1997 Addenda.
- [7.1.2] Holtec International Report HI-2012610, HI-STAR 100 System Final Safety Analysis Report.
- [7.1.3] U.S. Code of Federal Regulations, "Shippers – General Requirements for Shipments and Packages," Part 49, "Transportation."
- [7.1.4] U.S. Code of Federal Regulations, "Standards for Protection Against Radiation", Part 10, "Energy."
- [7.1.5] American National Standards Institute, Institute for Nuclear Materials Management, "American National Standard for Radioactive Materials – Leakage Tests on Packages for Shipment," ANSI N14.5-1997.
- [7.1.6] Holtec International Report HI-2002444, Final Safety Analysis Report for the HI-STORM 100 Cask System

**SUPPLEMENT 7.I****OPERATING PROCEDURES OF THE HI-STAR HB PACKAGE WITH MPC-HB****7.I.0 INTRODUCTION**

This chapter outlines the procedures for loading, preparation for shipment, unloading, and preparation for empty cask shipment of the HI-STAR HB System where it differs from the HI-STAR 100 System in accordance with 10CFR71 [7.0.1].

**7.I.1 PROCEDURE FOR LOADING AND PREPARATION FOR TRANSPORT OF THE HI-STAR HB SYSTEM****7.I.1.3 Loading of Contents into HI-STAR HB****7.I.1.3.1 Loading of SNF into HI-STAR HB from a Spent Fuel Pool**

Steps 1 through 17 as well as 19 through 22 are equivalent to HI-STAR 100 in Section 7.1.3.1. The following is an exception for HI-STAR HB:

18. The helium backfill is adjusted to the pressure equivalent of  $\geq 0$  psig and  $\leq 48.8$  psig at a reference temperature of 70 degrees Fahrenheit.

Table 7.1.1 is modified for HI-STAR HB as follows:

Table 7.I.1  
HI-STAR HB SYSTEM PARTIAL MPC LOADING REQUIREMENTS

<b>MPC Type</b>	<b>Min. # Cells Loaded</b>	<b>Load Balancing Instructions</b>
MPC-HB	48	To preserve the CG of the loaded MPC as near as practical to the centerline, the loading plan shall distribute the fuel assemblies so that in the loaded configuration the MPC is reasonably balanced.



## SUPPLEMENT 7.II

### OPERATING PROCEDURES OF THE HI-STAR HB GTCC PACKAGE WITH GWC-HB

This chapter outlines the procedures for loading, preparation for shipment, unloading, and preparation for empty cask shipment for the HI-STAR HB GTCC Package with GWC-HB configuration of the HI-STAR 100 System where it differs from the HI-STAR 100 System in accordance with 10CFR71 [7.0.1].

#### 7.II.0 INTRODUCTION

This chapter outlines the procedures for loading, preparation for shipment, unloading, and preparation for empty cask shipment of the HI-STAR HB GTCC System where it differs from the HI-STAR 100 System in accordance with 10CFR71 [7.0.1].

The operations described in this chapter assume that the waste will be loaded into, or unloaded from, an MPC while in the HI-STAR overpack submerged in a spent fuel pool. Because the HI-STAR is a dual-use cask certified for use as a dry storage cask under 10 CFR 72, the descriptions below include the steps required to transport the cask after a period of storage. The chapter also provides a description of the essential elements necessary to transfer a Holtec MPC from a dry storage system into the HI-STAR system for transportation.

#### 7.II.1 PROCEDURE FOR LOADING AND PREPARATION FOR TRANSPORT OF THE HI-STAR HB SYSTEM

##### 7.II.1.1 Overview of HI-STAR Loading Operations

The loading operations described herein are for HI-STAR HB GTCC systems prepared for "load-and-go" directly into transportation under 10CFR71. HI-STAR 100 systems that are loaded and stored on an ISFSI site must be prepared in accordance with the applicable Part 72 HI-STAR FSAR or HI-STORM FSAR license and respective Certificate of Compliance (CoC). Any HI-STAR overpack and/or GWC deployed at an ISFSI must be confirmed to meet all conditions of the 10CFR71 CoC prior to shipment. The dryness criteria under the Part 72 CoC shall be considered acceptable for use in transport under Part 71 [7.1.2], [7.1.6].

The HI-STAR 100 System (HI-STAR) is used to load and transport Greater Than Class C (GTCC) waste in the GTCC Waste Container (GWC). The essential elements required to prepare the HI-STAR for GTCC waste loading, to load the GTCC waste, to ready the system for transport, and to ship the HI-STAR are described below.

### 7.II.1.2 Preparation of HI-STAR for Loading

All steps except those identified below are equivalent to HI-STAR 100 in Section 7.1.2. The following are exceptions for HI-STAR HB GTCC cask:

1. The HI-STAR overpack is received and the security seals, if used, are inspected to verify there was no tampering and that they match the corresponding shipping documents.
5. The HI-STAR overpack is upended.

### 7.II.1.3 Loading of Contents into HI-STAR HB GTCC

#### 7.II.1.3.1 Loading of GTCC Waste into HI-STAR HB from a Spent Fuel Pool

All steps except those identified below are equivalent to HI-STAR 100 in Section 7.1.3.1. The following are exceptions for HI-STAR HB GTCC cask:

1. Position the HI-STAR in the MPC loading area.
2. An empty MPC is upended and prepared for loading. The MPC is subjected to receipt inspection (inspected for cleanliness and outward visual indications of impaired physical condition except for superficial marks and dents). Road dirt/debris and any foreign material are removed from the MPC prior to placement in the spent fuel pool. The empty MPC is raised and inserted into the HI-STAR overpack while being careful not to damage the HI-STAR sealing surface.
5. Prior to loading the MPC, the user identifies the waste material to be loaded, including dunnage if required, in accordance with Table 1.II.1.
6. While still underwater, a thickly shielded lid (the MPC lid) is positioned over the pool surface and the drain line is installed. The MPC lid drain line is guided into its receiver and the MPC lid is installed. The upper surface of the MPC lid will seat approximately flush with the top edge of the MPC shell when properly installed. The lid may be removed and the drain line replaced should it be damaged during installation of the MPC lid.
18. The MPC helium backfill is adjusted to the pressure equivalent of greater than 10 psig and less than 15 psig at a reference temperature of 70 degrees Fahrenheit.

### 7.II.1.4 Closure of HI-STAR

All steps except those identified below are equivalent to HI-STAR 100 in Section 7.1.4. The following are exceptions for HI-STAR HB GTCC cask:

2. The mating surfaces for the HI-STAR overpack are inspected for signs of damage. The closure plate is installed with the bolts torqued in accordance with requirements in Table 7.II.1.2 and the order prescribed in Figure 7.1.1.
3. Not used.
4. Not used.
5. Not used.
6. Not used.

#### 7.II.1.5 Preparation of HI-STAR for Transport

All steps except those identified below are equivalent to HI-STAR 100 in Section 7.1.5. The following are exceptions for HI-STAR HB GTCC cask:

1. Not used.
2. Not used.
9. Not used.

### 7.II.2 PROCEDURE FOR UNLOADING THE HI-STAR HB SYSTEM

The essential elements required to prepare the system for unloading, to flood the MPC cavity, to remove the lid welds, to unload the GTCC waste, and to recover the HI-STAR 100 overpack and empty MPC are described below.

#### 7.II.2.1 Receipt of Package from Carrier

All steps except those identified below are equivalent to HI-STAR 100 in Section 7.2.1. The following are exceptions for HI-STAR HB GTCC cask:

2. The security seals are inspected to verify there was no evidence of tampering and that they match the corresponding shipping documents. Any discrepancies are identified to the site management and appropriate authorities.
4. The HI-STAR is visually inspected to verify there are no outward visual indications of impaired physical conditions except for superficial marks and dents and radiation survey and removable contamination survey are performed per 49CFR173.443 [7.1.3]. Any issues are identified to site management and the overpack is decontaminated as

directed by site radiation protection. Note that portions of the inspections, surveys, and decontamination activities described here-in may be performed prior to removal of the impact limiters.

#### 7.II.2.2 Removal of Contents

All steps except those identified below are equivalent to HI-STAR 100 in Section 7.2.2. The following are exceptions for HI-STAR HB GTCC cask:

1. Not used.
5. Not used.
6. Not used.
13. GTCC waste is removed to appropriate storage locations.
14. Not used.

Table 7.II.1.2  
HI-STAR HB GTCC SYSTEM TORQUE REQUIREMENTS

Fastener	Torque (ft-lbs)	Pattern
Overpack Closure Plate Bolts	First Pass – Hand Tight Second Pass – Wrench Tight Third Pass – 700 +50/-50 Fourth Pass – 1400 +100/-100 Final Pass - 2000 +250/-0	See Figure 7.1.1
Overpack Vent and Drain Port Plugs	431+5/-5	None
Top Impact Limiter Attachment Bolt	256+10/-0	None
Bottom Impact Limiter Attachment Bolt	1500+45/-0	None

Table 7.II.1.1

NOT USED
----------

## SUPPLEMENT 7.III

### OPERATING PROCEDURES OF THE HI-STAR 100 PACKAGE WITH DIABLO CANYON MPC-32

This chapter outlines the procedures for loading, preparation for shipment, unloading, and preparation for empty cask shipment for the HI-STAR 100 with Diablo Canyon MPC-32 configuration of the HI-STAR 100 System where it differs from the HI-STAR 100 System in accordance with 10CFR71 [7.0.1].

#### 7.III.1.3.1 Loading of SNF into HI-STAR from a Spent Fuel Pool

All steps except those identified below are equivalent to HI-STAR 100 in Section 7.1.3.1. The following are exceptions for HI-STAR 100 with Diablo Canyon MPC-32 cask:

1. Position the HI-STAR in the MPC loading area. Verify spent fuel pool for boron concentration requirements in accordance with Table 1.III.2. Testing must be completed within four hours prior to loading and every 48 hours after. Two independent measurements shall be taken to ensure that the requirement of 10 CFR 72.124(a) is met.
4. The MPC is filled with either spent fuel pool water or clean water and the HI-STAR is raised and lowered into the spent fuel pool for fuel loading. Refer to Table 1.III.2 for boron concentration requirements.

#### 7.III.2.2 Loading of SNF into HI-STAR from a Spent Fuel Pool

All steps except those identified below are equivalent to HI-STAR 100 in Section 7.2.2. The following are exceptions for HI-STAR 100 with Diablo Canyon MPC-32 cask:

6. The MPC is cooled as necessary to reduce the MPC internal temperature. This allows water flooding without thermally shocking the fuel assemblies or over-pressurizing the MPC from the formation of steam. The MPC is then filled with water. Refer to Table 1.III.2 for boron concentration requirements.
12. The HI-STAR 100 overpack is placed in the spent fuel pool or other appropriate unloading area and the MPC lid is removed. Verify spent fuel pool for boron concentration requirements in accordance with Table 1.III.2. Testing must be completed within four hours prior to unloading and every 48 hours after. Two independent measurements shall be taken to ensure that the requirement of 10 CFR 72.124(a) is met.

## CHAPTER 8: ACCEPTANCE TESTS AND MAINTENANCE PROGRAM

### 8.0 INTRODUCTION

This chapter identifies the acceptance tests and maintenance program to be conducted on the HI-STAR 100 Package to verify that the structures, systems, and components (SSCs) classified as important to safety have been fabricated, assembled, inspected, tested, accepted, and maintained in accordance with the requirements set forth in this Safety Analysis Report (SAR), the applicable regulatory requirements, and the Certificate of Compliance (CoC). The acceptance criteria and maintenance program described in this chapter fully comply with the requirements of 10CFR Part 71 **Subpart G** [8.0.1].

## 8.1 ACCEPTANCE TESTS

This section provides the workmanship inspections and acceptance tests to be performed on the HI-STAR 100 Package prior to or during use. These inspections and tests provide assurance that the HI-STAR 100 Package has been fabricated, assembled, inspected, tested, and accepted for use and loading under the conditions specified in this SAR and the CoC issued by the NRC in accordance with the requirements of 10CFR Part 71.

### 8.1.1 Visual Inspections and Measurements

The HI-STAR 100 Package shall be assembled in accordance with the drawing package referenced in the CoC. Dimensional tolerances that define the limits on the dimensions critical to the licensing basis analysis are included in these drawings. Fabrication drawings provide additional dimensional tolerances necessary to ensure fit-up of parts as well as compliance with the design conditions. A fabrication sampling plan shall be made and controls shall be exercised to ensure that the packaging conforms to the dimensions and tolerances specified on the licensing and fabrication drawings. These dimensions are subject to independent confirmation and documentation in accordance with the Holtec QA program approved in NRC Docket No. 71-0784.

The following shall be verified as part of visual inspections and measurements:

- Visual inspections and measurements shall be made to ensure that the packaging effectiveness is not significantly reduced. Any *important-to-safety* component found to be under the minimum thickness requirement shall be repaired or replaced as required.
- The packaging shall be inspected for cleanliness and proper preparation for shipping in accordance with written and approved procedures.
- The packaging shall be visually inspected to ensure it is conspicuously and durably marked with the proper markings/labels in accordance with 10CFR71.85(c).
- Visual inspections shall be made to verify that neutron absorber panels are present on the basket cell walls as required by the basket design.

### 8.1.2 Weld Examinations

The examination of HI-STAR 100 Package welds shall be performed in accordance with the drawing package referenced in the CoC and applicable codes and standards in Table 8.1.4, including alternatives as specified in Table 8.1.5. Weld examinations and repairs shall be performed as specified below. All code weld inspections shall be performed in accordance with written and approved procedures by personnel qualified in accordance with SNT-TC-1A [8.1.2]. All required inspections, examinations, and tests shall become part of the final quality documentation package.



The following specific weld requirements shall be followed in order to verify fabrication in accordance with the drawings.

1. Cask containment boundary welds including any attachment welds (and temporary welds to the containment boundary) shall be examined in accordance with ASME Code Section V, with acceptance criteria per ASME Code Section III, Subsection NB, Article NB-5300. Examinations, Visual (VT), Radiographic (RT), and Liquid Penetrant (PT) or Magnetic Particle (MT), apply to these welds as defined by the code. These welds shall be repaired in accordance with the requirements of the ASME Code Section III, Article NB-4450 and examined after repair in the same manner as the original weld. Weld overlays for cask sealing surfaces shall be VT and PT examined to insure that a leakage path between the containment space and the outside environment that may violate the specified cask leak tightness criterion is detected and eliminated. Although ASME Code Section III, Subsection NB does not require visual examination of welds, the welds will be visually examined to ensure conformance with the fabrication drawings (e.g. proper geometry, workmanship etc.).
2. Code welds in the cask, impact limiter, and MPC spacer (excluding those listed above) shall be examined in accordance with ASME Code Section V, with acceptance criteria per ASME Code Section III, Subsection NF, Article NF-5300. These welds shall be repaired in accordance with ASME Code Section III, Article NF-4450 and examined after repair in the same manner as the original weld. These weld requirements are not applicable to NITS welds (e.g. seal welds) on the cask, impact limiters and MPC Spacer.
3. Code welds in the MPC enclosure vessel and fuel basket shall be examined in accordance with ASME Code Section V, with acceptance criteria per ASME Code Section III, Subsection NB, NF, and NG (Articles NB-5300, NF-5300 and NG-5300) as applicable. Examinations, Visual (VT), Radiographic (RT), and Liquid Penetrant (PT) or Magnetic Particle (MT), apply to these welds as defined by the code. These welds shall be repaired in accordance with the requirements of the ASME Code Section III, Articles NB-4450, NF-4450, and NG-4450, as applicable, and examined after repair in the same manner as the original weld. Although ASME Code Section III, Subsection NB does not require visual examination of welds, the welds will be visually examined to ensure conformance with the fabrication drawings (e.g. proper geometry, workmanship etc.). These weld requirements are not applicable to welds identified as NITS on the drawing package.
4. The MPC lid-to-shell weld shall be examined by either volumetric examination using ultrasonic methods or by using a progressive multi-layer liquid penetrant (PT) examination during welding. The multi-layer PT must, at a minimum, include the root and final weld layers and one intermediate PT after each approximately 3/8 inch weld depth has been completed.
5. Non-code welds shall be examined and repaired in accordance with written and approved procedures. The drawing package referenced in the CoC may require visual examination.

### 8.1.3 Structural and Pressure Tests

The HI-STAR 100 system containment boundary shall be examined and tested using pressure testing, ultrasonic testing, MT and/or PT, as applicable, to verify that it is free of cracks, pinholes, uncontrolled voids or other defects that could significantly reduce the effectiveness of the packaging.

#### 8.1.3.1 Lifting Trunnions

Two trunnions (located near the top of the HI-STAR overpack) are provided for vertical lifting and handling of the **loaded or empty cask**. The trunnions shall be inspected and tested in accordance with ANSI N14.6 [8.1.3].

The **top** trunnions shall be tested **in accordance with ANSI N14.6** at 300% of the maximum design (service) lifting load. **Load tests may be performed in excess of the test loads specified above provided an engineering evaluation is performed to ensure trunnions or other cask components will not be damaged by the load test.** The load shall be applied for a minimum of 10 minutes to the pair of lifting trunnions. The accessible parts of the **top** trunnions (**the cantilevered portion outside the cask**), and the local cask areas shall then be visually examined to verify no deformation, distortion, or cracking has occurred. Any evidence of deformation (**other than minor localized surface deformation due to contact pressure between lifting device/load test device and top trunnion**), distortion or cracking of the trunnion or adjacent cask areas shall require replacement of the trunnion and/or repair of the cask.

Following any replacements and/or repair, the load testing shall be re-performed and the components re-examined in accordance with the original procedure and acceptance criteria. Testing shall be performed in accordance with written and approved procedures. Certified material test reports verifying trunnion material mechanical properties meet ASME Code Section II requirements **shall be provided**. Test results shall be documented and shall become part of the final quality documentation package.

#### 8.1.3.2 Pressure Testing

##### 8.1.3.2.1 HI-STAR 100 Containment Boundary

**Pressure testing of the HI-STAR 100 cask containment boundary (cavity space) shall be performed in accordance with ASME Section III, Subsection NB, NB-6000 at a test pressure of not less than 150% of cask cavity maximum normal operating pressure per 10CFR71.85(b) or at a test pressure of 125% of the cask cavity design internal pressure; whichever is greater. All pressure testing shall be performed in accordance with written and approved procedures. The written and approved test procedure shall clearly define the test equipment arrangement. Pressure testing may be performed using a single temporary test seal on the lid.**

Test results shall be documented and shall become part of the final quality documentation package.

#### 8.1.3.2.2 MPC Pressure Boundary

Pressure testing of the MPC pressure boundary shall be performed in accordance with the requirements of the ASME Code Section III, Subsection NB, Article NB-6000, applicable sub-articles, and the code alternatives listed in Table 8.1.5 when field welding of the MPC lid-to-shell weld is completed. If hydrostatic testing is used, the MPC shall be pressure tested to 125% of design pressure. If pneumatic testing is used, the MPC shall be pressure tested to 120% of the design pressure. **All pressure testing shall be performed in accordance with written and approved procedures. The written and approved test procedure shall clearly define the test equipment arrangement.**

Test results shall be documented and shall become part of the final quality documentation package.

#### 8.1.3.3 Pneumatic Testing of the Neutron Shield Enclosure Vessel

A pneumatic pressure test of the neutron shield enclosure vessel shall be performed following final closure welding of the enclosure shell returns and enclosure panels. The pneumatic test pressure shall be **125%** of the relief device set pressure. The test shall be performed in accordance with approved written procedures. **Welds repair and examination after repair shall be performed in the same manner as the original weld.**

Test results shall be documented and shall become part of the final quality documentation package.

#### 8.1.4 Leakage Tests

**Leakage rate tests on the HI-STAR 100 cask containment system shall be performed per written and approved procedures in accordance with the requirements of Chapter 7 and the requirements of ANSI N14.5, 1997 [8.1.4]. Tables 8.1.1 and 8.1.2 specify the allowable leakage rate and test sensitivity in terms of helium leak tightness as well as components to be tested for fabrication, pre-shipment, periodic and maintenance leakage rate tests.**

**In case of an unsatisfactory leakage rate, weld repair, seal surface repair/polishing and/or seal change and retest shall be performed until the test acceptance criterion is satisfied.**

**Leakage rate test results shall become part of the final quality documentation package.**

#### 8.1.5 Component and Material Tests

##### 8.1.5.1 Seals

**Cask closure seals are specified in the drawing package referenced in the CoC to provide a high degree of assurance of leak tightness under normal and accident conditions of transport. Seal tests under the most severe package service conditions including performance at pressure under**

high and low temperatures will not challenge the capabilities of these seals and thus are not required.

#### 8.1.5.2 Impact Testing

To provide protection against brittle fracture under cold conditions, fracture toughness test criteria of cask ferritic components, including containment boundary welds, are specified in Table 8.1.6 and Table 8.1.7. Code alternatives listed in Table 8.1.5 may apply.

Test results shall become part of the final quality documentation package.

#### 8.1.5.3 Impact Limiter Crush Material Testing

Verification of the crush strength of the transport impact limiter crush material is accomplished by performance of a crush test of sample blocks. The verification tests may be performed by Holtec, the crush material supplier, or third party testing facility in accordance with approved procedures.

The certified test results shall be retained by Holtec International as archive record for each batch of impact limiter crush material manufactured and used. Test results shall be documented and shall become part of the final quality documentation package.

#### 8.1.5.4 Neutron Shielding Material

Manufacturing of Holtite neutron shielding material shall be conducted according to approved written procedures that shall ensure mix ratios and mixing methods are controlled in order to achieve proper material composition and distribution, and that emplacement is properly controlled. Each manufactured lot of Holtite neutron shield material shall be tested to verify that boron carbide content, hydrogen concentration (areal density) and bulk material density meet the requirements specified in Table 8.1.8. A manufactured lot is defined as the total amount of material used to make any number of mixed batches comprised of constituent ingredients from the same lot/batch identification numbers supplied by the constituent manufacturer. Testing shall be performed in accordance with written and approved procedures.

Holtec International shall maintain samples of each manufactured lot of neutron shielding material. Test results for each manufactured lot of neutron shield material shall become part of the final quality documentation package.

#### 8.1.5.5 Neutron Absorber Material

Each plate of neutron absorber shall be visually inspected for damage such as scratches, cracks, burrs, peeled cladding, foreign material embedded in the surfaces, voids, delamination, and surface finish.

8.1.5.5.1 Boral (75% Credit)

After manufacturing, a statistical sample of each lot of neutron absorber shall be tested using wet chemistry and/or neutron attenuation testing to verify minimum  $^{10}\text{B}$  content (areal density) in samples taken from the ends of the panel. The minimum  $^{10}\text{B}$  loading of the neutron absorber panels for each MPC model is provided in Table 8.1.3. Any panel in which  $^{10}\text{B}$  loading is less than the minimum allowed shall be rejected. Testing shall be performed using written and approved procedures. Results shall be documented and become part of the cask quality records documentation package.

8.1.5.5.2 METAMIC® (90% Credit)

NUREG/CR-5661 identifies the main reason for a penalty in the neutron absorber B-10 density as the potential of neutron streaming due to non-uniformities in the neutron absorber, and recommends comprehensive acceptance tests to verify the presence and uniformity of the neutron absorber for credits more than 75%. Since a 90% credit is taken for METAMIC®, the following criteria must be satisfied:

- The boron carbide powder used in the manufacturing of METAMIC® must have small particle sizes to preclude neutron streaming.
- The  $^{10}\text{B}$  areal density must comply with the limits of Table 8.1.3A.
- The  $\text{B}_4\text{C}$  powder must be uniformly dispersed locally, i.e. must not show any particle agglomeration. This precludes neutron streaming.
- The  $\text{B}_4\text{C}$  powder must be uniformly dispersed macroscopically, i.e. must have a consistent concentration throughout the entire neutron absorber panel.
- The  $\text{B}_4\text{C}$  content in the finished METAMIC® panel must comply with the limits of Table 8.1.3B.

To ensure that the above requirements are met the following tests shall be performed:

- All lots of boron carbide powder are analyzed to meet particle size distribution requirements.
- The following qualification testing shall be performed on the first production run<sup>1</sup> of METAMIC® panels for the MPCs in order to validate the acceptability and consistency of the manufacturing process and verify the acceptability of the METAMIC® panels for neutron absorbing capabilities:

<sup>1</sup> The requirement for qualification testing of the first production run of METAMIC® panels has been fulfilled and records are maintained by Holtec International. The results of the qualification testing demonstrated that the manufacturing process produces METAMIC® panels which meet or exceed the requirements for criticality control.

- 1) The boron carbide powder weight percent shall be verified by testing a sample from forty different mixed batches. (A mixed batch is defined as a single mixture of aluminum powder and boron carbide powder used to make one or more billets. Each billet will produce several panels.) The samples shall be drawn from the mixing containers after mixing operations have been completed. Testing shall be performed using the wet chemistry method.
  - 2) The  $^{10}\text{B}$  areal density shall be verified by testing a sample from one panel from each of forty different mixed batches. The samples shall be drawn from areas contiguous to the manufactured panels of METAMIC® and shall be tested using the wet chemistry method. Alternatively, or in addition to the wet chemistry tests, neutron attenuation tests on the samples may be performed to quantify the actual  $^{10}\text{B}$  areal density.
  - 3) To verify the local uniformity of the boron particle dispersal, neutron attenuation measurements of random test coupons shall be performed. These test coupons may come from the production run or from pre-production trial runs.
  - 4) To verify the macroscopic uniformity of the boron particle distribution, test samples shall be taken from the sides of one panel from five different mixed batches before the panels are cut to their final sizes. The sample locations shall be chosen to be representative of the final product. Wet chemistry or neutron attenuation shall be performed on each of the samples.
- During production runs, testing of mixed batches shall be performed on a statistical basis to verify the correct boron carbide weight percent is being mixed.
  - During production runs, samples from random METAMIC® panels taken from areas contiguous to the manufactured panels shall be tested via wet chemistry and/or neutron attenuation testing to verify the  $^{10}\text{B}$  areal density. This test shall be performed to verify the continued acceptability of the manufacturing process.

The measurements of B<sub>4</sub>C particle size,  $^{10}\text{B}$  isotopic assay, uniformity of B<sub>4</sub>C distribution and  $^{10}\text{B}$  areal density shall be made using written and approved procedures. Results shall be documented.

#### 8.1.6 Gamma Shielding

The gamma shielding (steel) in the construction of the HI-STAR 100 package is dimensionally inspected to assure compliance with the applicable drawings referenced in the CoC and as required in Subsection 8.1.1.

#### 8.1.7 Thermal Tests

The first fabricated HI-STAR 100 overpack was tested to confirm its heat transfer capability. The test was performed and documented in Holtec Document DOC-5014-03 [8.1.7]. The tests

have shown that the HI-STAR 100 system is within acceptable limits and future thermal testing is no longer required.

**Table 8.1.1**  
**Containment System Performance Specifications**

<b>Design Attribute</b>	<b>Design Rating</b>
Leakage Rate Acceptance Criterion	$2.15 \times 10^{-6}$ ref-cm <sup>3</sup> /s air
Leakage Rate Test Sensitivity	$1.075 \times 10^{-6}$ ref-cm <sup>3</sup> /s air (½ of the leakage rate acceptance criterion per ANSI N14.5-1997)

Note: For helium as the tracer gas, the Leakage Rate Acceptance Criterion and Test Sensitivity are multiplied by a factor of 2.



**Table 8.1.2**  
**Leakage Rate Tests For HI-STAR 100 Containment System**

Leakage Test	System Tested	Components Tested	Type of Leakage Rate Test (from ANSI N14.5-1997, App. A)	Allowable Leakage Rate
Fabrication Leakage Rate Test	HI-STAR 100 Cask	<ul style="list-style-type: none"> <li>• Containment Shell</li> <li>• Containment Bottom Forging</li> <li>• Containment Top Forging</li> <li>• Closure Lid</li> <li>• Closure Lid Port Cover Plate</li> <li>• Containment Shell Welds</li> <li>• Containment Shell to Containment Bottom Forging Weld</li> <li>• Containment Shell to Containment Top Forging Weld</li> </ul>	A.5.3	Table 8.1.1
		<ul style="list-style-type: none"> <li>• Closure Lid Inner Seal</li> <li>• Closure Lid Port Plug Seal</li> <li>• Drain Port Plug Seal</li> </ul>	A.5.4	Table 8.1.1
Pre-Shipment Leakage Rate Test	HI-STAR 100 Cask	<ul style="list-style-type: none"> <li>• Closure Lid Inner Seal</li> <li>• Closure Lid Port Plug Seal</li> <li>• Drain Port Plug Seal</li> </ul>	A.5.4	Table 8.1.1
Maintenance Leakage Rate Test	HI-STAR 100 Cask	<ul style="list-style-type: none"> <li>• Containment Shell</li> <li>• Containment Bottom Forging</li> <li>• Containment Top Forging</li> <li>• Closure Lid</li> <li>• Closure Lid Port Cover Plate</li> <li>• Containment Shell Welds</li> <li>• Containment Shell to Containment Bottom Forging Weld</li> <li>• Containment Shell to Containment Top Forging Weld</li> </ul>	A.5.3	Table 8.1.1
		<ul style="list-style-type: none"> <li>• Closure Lid Inner Seal</li> <li>• Closure Lid Port Plug Seal</li> <li>• Drain Port Plug Seal</li> </ul>	A.5.4	Table 8.1.1
Periodic Leakage Rate Test	HI-STAR 100 Cask	<ul style="list-style-type: none"> <li>• Closure Lid Inner Seal</li> <li>• Closure Lid Port Plug Seal</li> <li>• Drain Port Plug Seal</li> </ul>	A.5.4	Table 8.1.1

Note 1: For a Leakage Rate Acceptance Criterion performed to “Leak-tight as defined by ANSI N14.5” [8.1.4], the summation of individual component leakage rates of the containment boundary of a package is not required.

**Table 8.1.3A Neutron Absorber B-10 Content**

Neutron Absorber Type	Minimum $^{10}\text{B}$ loading ( $\text{g}/\text{cm}^2$ )	
	PWRs	BWRs
Boral neutron absorber	0.0267 (MPC-24) 0.0372 (MPC-24E/EF) 0.0372 (MPC-32)	0.0372 (MPC-68) 0.01 (MPC-68F)
Metamic neutron absorber	0.0267 (MPC-24) 0.0372 (MPC-24E/EF) 0.0310 (MPC-32)	0.0310 (MPC-68)

**Table 8.1.3B METAMIC<sup>®</sup> B<sub>4</sub>C Content**

Finished METAMIC Panel B <sub>4</sub> C Content
$\leq 33$ wt. %

**Table 8.1.4 (Sheet 1 of 2): Applicability of ASME Code Boiler & Pressure Vessel Code and Other Standards**

<b>Component ID</b>	<b>Material Procurement</b>	<b>Design Code</b>	<b>Stress and Deformation Analysis Criteria</b>	<b>Welding (Fabrication and Qualifications)</b>	<b>Inspection</b>	<b>Testing</b>
Cask Containment System (pressure vessel except closure seals)	ASME Code Section III Subsection NB-2000	ASME Code Section III Subsection NB-3000	ASME Code Section III Subsection NB-3200	ASME Code Section III Subsection NB-4000 and Chapter 8 of this SAR	ASME Code Section III Subsection NB-5000 and Chapter 8 of this SAR	ASME Code Section III Subsection NB-6000 and Chapter 8 of this SAR
Cask Dose Blocker Steel Components (Intermediate Shells)	ASME Code Section II Subsection NF	Non-Code	Section III, Subsection NF, NF-3300	Non-Code	Section V	Chapter 8 of this SAR
MPC Helium Retention Boundary	ASME Code Section III Subsection NB-2000	ASME Code Section III Subsection NB-3200	ASME Code Section III Subsection NB-3000	ASME Code Section III Subsection NB-4000	ASME Code Section III Subsection NB-5000	ASME Code Section III Subsection NB-6000
Cask Top Lifting Trunnions	ASME Code Section II	ANSI N14.6 and RG 3.61	ANSI N14.6 and RG 3.61	Not Applicable	Chapter 8 of this SAR	Chapter 8 of this SAR
Cask Neutron Shielding Material	Holtec Manufacturing Manual	Holtec Qualification Sourcebook	Not Applicable	Not Applicable	Holtec Manufacturing Manual	Chapter 8 of this SAR
MPC Fuel Basket	Section II; and Section III, Subsection NG, NG-2000 for core support structures (NG-1121)	Section III, Subsection NG, NG-3300 and NG-3200 for core support structures (NG-1121)	Section III, Subsection NG, NG-3300 and NG-3200 for core support structures (NG-1121)	Section III, Subsection NG, NG-4000 for core support structures (NG-1121)	Section III, Subsection NG, NG-5000 and Section V for core support structures (NG-1121)	Chapter 8 of this SAR
Cask Dose Blocker Steel Components (radial channels, outer enclosure)	ASME Code Section II	See licensing drawing package for specific applicability	No yielding under NCT and no significant loss of dose blocker steel under HAC	ASME Code Section IX (as clarified by the licensing drawing package)	ASME Code Section V	Chapter 8 of this SAR

**Table 8.1.4 (Sheet 2 of 2): Applicability of ASME Code Boiler & Pressure Vessel Code and Other Standards**

Impact Limiter Backbone Components	ASME Code Section II	See licensing drawing package for specific applicability	No rupture and no deformation leading to loss of function	ASME Code Section IX (as clarified by the licensing drawing package)	ASME Code Section V	Chapter 8 of this SAR
MPC Basket Supports (Angled Plates)	Section II, and Section III, Subsection NG, NG-2000 for internal structures (NG-1122)	Section III, Subsection NG, NG-3300 and NG-3200 for internal structures (NG-1122)	Section III, Subsection NG, NG-3300 and NG-3200 for internal structures (NG-1122)	Section III, Subsection NG, NG-4000 for internal structures (NG-1122) and Chapter 8 of this SAR	Section III, Subsection NG, NG-5000 and Section V for internal structures (NG-1122) and Chapter 8 of this SAR	Chapter 8 of this SAR
Damaged Fuel Container	Section II, and Section III, Subsection NG, NG-2000	Section III, Subsection NG, NG-3300 and NG-3200	Section III, Subsection NG, NG-3300 and NG-3200	Section III, Subsection NG, NG-4000	Section III, Subsection NG, NG-5000 and Section V	Chapter 8 of this SAR
MPC Spacer (Shell Type, e.g. Trojan)	Section II, and Section III, Subsection NF	Section III, Subsection NF, NF-3200	Section III, Subsection NF, NF-3200	Section III, Subsection NF, NF-4000	Section III, Subsection NF, NF-5360 and Section V	Chapter 8 of this SAR
MPC Spacer (Shim Type, e.g. generic design)	Section II	Non-code	Non-code	Section III, Subsection NF, NF-4000 or AWS D1.1	Section III, Subsection NF, NF-5360 or AWS D1.1	Chapter 8 of this SAR

**Notes**

1. The Holtec Manufacturing Manual contains detailed instructions for manufacturing of the subassemblies and the complete component in accordance with the applicable Codes and Standards. The Holtec Manufacturing Manual is a compilation of procedures, travelers, weld maps, specifications, standards, Metamic Manufacturing Manual and other documents as applicable, to ensure the manufacturing of the components are in full accord with the design conditions of the CoC. The latest issues of the manufacturing manual(s) are maintained in the company's network under Holtec's configuration control system.

**Table 8.1.5 (12 Sheets Total): ASME Code Requirements and Alternatives for the HI-STAR 100**

<b>Component</b>	<b>Reference ASME Code Section/Article</b>	<b>Code Requirement</b>	<b>Alternative, Justification &amp; Compensatory Measures</b>
MPC, MPC basket assembly, and HI-STAR overpack steel structure.	Subsection NCA	General Requirements. Requires preparation of a Design Specification, Design Report, Overpressure Protection Report, Certification of Construction Report, Data Report, and other administrative controls for an ASME Code stamped vessel.	<p>Because the MPC and overpack are not ASME Code stamped vessels, none of the specifications, reports, certificates, or other general requirements specified by NCA are required. In lieu of a Design Specification and Design Report, the HI-STAR SAR includes the design criteria, service conditions, and load combinations for the design and operation of the HI-STAR 100 System as well as the results of the stress analyses to demonstrate that applicable Code stress limits are met. Additionally, the fabricator is not required to have an ASME-certified QA program. All important-to-safety activities are governed by the NRC-approved Holtec QA program.</p> <p>Because the cask components are not certified to the Code, the terms “Certificate Holder” and “Inspector” are not germane to the manufacturing of NRC-certified cask components. To eliminate ambiguity, the responsibilities assigned to the Certificate Holder in the various articles of Subsections NB, NG, and NF of the Code, as applicable, shall be interpreted to apply to the NRC Certificate of Compliance (CoC) holder (and by extension, to the component fabricator) if the requirement must be fulfilled. The Code term “Inspector” means the QA/QC personnel of the CoC holder and its vendors assigned to oversee and inspect the manufacturing process.</p>
MPC	NB-1100	Statement of requirements for Code stamping of components.	MPC vessel is designed and will be fabricated in accordance with ASME Code, Section III, Subsection NB to the maximum practical extent, but Code stamping is not required.

<b>Component</b>	<b>Reference ASME Code Section/Article</b>	<b>Code Requirement</b>	<b>Alternative, Justification &amp; Compensatory Measures</b>
MPC	NB-2000	Requires materials to be supplied by ASME-approved material supplier.	Materials will be supplied by Holtec approved suppliers with Certified Material Test Reports (CMTRs) in accordance with NB-2000 requirements.
MPC basket supports and lift lugs	NB-1130	<p>NB-1132.2(d) requires that the first connecting weld of a nonpressure-retaining structural attachment to a component shall be considered part of the component unless the weld is more than <math>2t</math> from the pressure-retaining portion of the component, where <math>t</math> is the nominal thickness of the pressure-retaining material.</p> <p>NB-1132.2(e) requires that the first connecting weld of a welded nonstructural attachment to a component shall conform to NB-4430 if the connecting weld is within <math>2t</math> from the pressure-retaining portion of the component.</p>	The MPC basket supports (nonpressure-retaining structural attachments) and lift lugs (nonstructural attachments used exclusively for lifting an empty MPC) are welded to the inside of the pressure-retaining MPC shell, but are not designed in accordance with Subsection NB. The basket supports and associated attachment welds are designed to satisfy the stress limits of Subsection NG and the lift lugs and associated attachment welds are designed to satisfy the stress limits of Subsection NF, as a minimum. These attachments and their welds are shown by analysis to meet the respective stress limits for their service conditions. Likewise, non-structural items, such as shield plugs, spacers, etc. if used, can be attached to pressure-retaining parts in the same manner.
MPC, MPC basket assembly, and HI-STAR overpack steel structure.	NB-3100 NG-3100 NF-3100	Provides requirements for determining design loading conditions, such as pressure, temperature, and mechanical loads.	These requirements are not applicable. The HI-STAR SAR, serving as the Design Specification, establishes the service conditions and load combinations for the storage system.

Component	Reference ASME Code Section/Article	Code Requirement	Alternative, Justification & Compensatory Measures
MPC	NB-3350	NB-3352.3 requires, for Category C joints, that the minimum dimensions of the welds and throat thickness shall be as shown in Figure NB-4243-1.	<p>The MPC shell-to-baseplate weld joint design (designated Category C) may not include a reinforcing fillet weld or a bevel in the MPC baseplate, which makes it different than any of the representative configurations depicted in Figure NB-4243-1. The transverse thickness of this weld is equal to the thickness of the adjoining shell (1/2 inch). The weld is designed as a full penetration weld that receives VT and RT or UT, as well as final surface PT examinations. Because the MPC shell design thickness is considerably larger than the minimum thickness required by the Code, a reinforcing fillet weld that would intrude into the MPC cavity space is not included. Not including this fillet weld provides for a higher quality radiographic examination of the full penetration weld.</p> <p>From the standpoint of stress analysis, the fillet weld serves to reduce the local bending stress (secondary stress) produced by the gross structural discontinuity defined by the flat plate/shell junction. In the MPC design, the shell and baseplate thicknesses are well beyond that required to meet their respective membrane stress intensity limits.</p>
MPC, MPC basket assembly, and HI-STAR overpack steel structure	NB-4120 NG-4120 NF-4120	NB-4121.2, NG-4121.2, and NF-4121.2 provide requirements for repetition of tensile or impact tests for material subjected to heat treatment during fabrication or installation.	In-shop operations of short duration that apply heat to a component, such as plasma cutting of plate stock, welding, machining, coating, and pouring of Holtite are not, unless explicitly stated by the Code, defined as heat treatment operations.

Component	Reference ASME Code Section/Article	Code Requirement	Alternative, Justification & Compensatory Measures
MPC Enclosure Vessel	NB-4122	Implies that with the exception of studs, bolts, nuts and heat exchanger tubes, CMTRs must be traceable to a specific piece of material in a component.	MPCs are built in lots. Material traceability on raw materials to a heat number and corresponding CMTR is maintained by Holtec through markings on the raw material. Where material is cut or processed, markings are transferred accordingly to assure traceability. As materials are assembled into the lot of MPCs being manufactured, documentation is maintained to identify the heat numbers of materials being used for that item in the multiple MPCs being manufactured under that lot. A specific item within a specific MPC will have a number of heat numbers identified as possibly being used for the item in that particular MPC of which one or more of those heat numbers (and corresponding CMTRs) will have actually been used. All of the heat numbers identified will comply with the requirements for the particular item.
MPC and HI-STAR overpack steel structure	NB-4220 NF-4220	Requires certain forming tolerances to be met for cylindrical, conical, or spherical shells of a vessel.	The cylindricity measurements on the rolled shells are not specifically recorded in the shop travelers, as would be the case for a Code-stamped pressure vessel. Rather, the requirements on inter-component clearances (such as the MPC-to-overpack) are guaranteed through fixture-controlled manufacturing. The fabrication specification and shop procedures ensure that all dimensional design objectives, including inter-component annular clearances are satisfied. The dimensions required to be met in fabrication are chosen to meet the functional requirements of the dry storage components. Thus, although the post-forming Code cylindricity requirements are not evaluated for compliance directly, they are indirectly satisfied (actually exceeded) in the final manufactured components.
MPC Lid and Closure Ring Welds	NB-4243	Full penetration welds required for Category C Joints (flat head to main shell per NB-3352.3)	MPC lid and closure ring are not full penetration welds. They are welded independently to provide a redundant seal.



<b>Component</b>	<b>Reference ASME Code Section/Article</b>	<b>Code Requirement</b>	<b>Alternative, Justification &amp; Compensatory Measures</b>
MPC Lid-to-Shell Weld	NB-5230	Radiographic (RT) or ultrasonic (UT) examination required.	Only UT or multi-layer liquid penetrant (PT) examination is permitted. If PT alone is used, at a minimum, it will include the root and final weld layers and each approximately 3/8 inch of weld depth.
MPC Closure Ring, Vent and Drain Cover Plate Welds	NB-5230	Radiographic (RT) or ultrasonic (UT) examination required.	Root (if more than one weld pass is required) and final liquid penetrant examination to be performed in accordance with NB-5245. The closure ring provides independent redundant closure for vent and drain cover plates.

<b>Component</b>	<b>Reference ASME Code Section/Article</b>	<b>Code Requirement</b>	<b>Alternative, Justification &amp; Compensatory Measures</b>
MPC Enclosure Vessel and Lid	NB-6111	All completed pressure retaining systems shall be pressure tested.	The MPC vessel is seal welded in the field following fuel assembly loading. The MPC vessel shall then be pressure tested as defined in Chapter 8. Accessibility for leakage inspections precludes a Code compliant pressure test. All MPC vessel welds (except closure ring and vent/drain cover plate) are inspected by volumetric examination, except that the MPC lid-to-shell weld shall be verified by volumetric or multi-layer PT examination. If PT alone is used, at a minimum, it must include the root and final layers and each approximately 3/8 inch of weld depth. For either UT or PT, the maximum undetectable flaw size must be demonstrated to be less than the critical flaw size. The critical flaw size must be determined in accordance with ASME Section XI methods. The critical flaw size shall not cause the primary stress limits of NB-3000 to be exceeded. The inspection results, including relevant findings (indications) shall be made a permanent part of the user's records by video, photographic, or other means which provide an equivalent retrievable record of weld integrity. The video or photographic records should be taken during the final interpretation period described in ASME Section V, Article 6, T-676. The vent/drain cover plate welds are confirmed by liquid penetrant examination and the closure ring weld is confirmed by liquid penetrant examination. The inspection of the weld must be performed by qualified personnel and shall meet the acceptance requirements of ASME Code Section III, NB-5350 for PT or NB-5332 for UT.
MPC Enclosure Vessel	NB-7000	Vessels are required to have overpressure protection.	No overpressure protection is provided. The function of MPC vessel is as a helium retention boundary. MPC vessel is designed to withstand maximum internal pressure considering 100% fuel rod failure and maximum accident temperatures.

<b>Component</b>	<b>Reference ASME Code Section/Article</b>	<b>Code Requirement</b>	<b>Alternative, Justification &amp; Compensatory Measures</b>
MPC Enclosure Vessel	NB-8000	States requirements for nameplates, stamping and reports per NCA-8000.	HI-STAR 100 System to be marked and identified in accordance with 10CFR71 and 10CFR72 requirements. Code stamping is not required. QA data package to be in accordance with Holtec approved QA program.
Overpack Containment Boundary	NB-1100	Statement of requirements for Code stamping of components.	Overpack containment boundary is designed, and will be fabricated in accordance with ASME Code, Section III, Subsection NB to the maximum practical extent, but Code stamping is not required.
Overpack Containment Boundary	NB-2000	Requires materials to be supplied by ASME-approved material supplier.	Materials will be supplied by Holtec approved suppliers with CMTRs per NB-2000.
Overpack Containment Boundary	NB-7000	Vessels are required to have overpressure protection.	No overpressure protection is provided. Function of overpack vessel is as a radionuclide containment boundary under normal and hypothetical accident conditions. Overpack vessel is designed to withstand maximum internal pressure and maximum accident temperatures.
Overpack Containment Boundary	NB-8000	States requirements for nameplates, stamping and reports per NCA-8000.	HI-STAR 100 System to be marked and identified in accordance with 10CFR71 and 10CFR72 requirements. Code stamping is not required. QA data package to be in accordance with Holtec's approved QA program.
MPC Basket Assembly	NG-2000	Requires materials to be supplied by ASME-approved material supplier.	Materials will be supplied by Holtec approved supplier with CMTRs in accordance with NG-2000 requirements.

<b>Component</b>	<b>Reference ASME Code Section/Article</b>	<b>Code Requirement</b>	<b>Alternative, Justification &amp; Compensatory Measures</b>
MPC Basket Assembly	NG-4420	NG-4427(a) allows a fillet weld in any single continuous weld to be less than the specified fillet weld dimension by not more than 1/16 inch, provided that the total undersize portion of the weld does not exceed 10 percent of the length of the weld. Individual undersize weld portions shall not exceed 2 inches in length.	<p>Modify the Code requirement (intended for core support structures) with the following text prepared to accord with the geometry and stress analysis imperatives for the fuel basket: For the longitudinal MPC basket fillet welds, the following criteria apply: 1) The specified fillet weld throat dimension must be maintained over at least 92 percent of the total weld length. All regions of undersized weld must be less than 3 inches long and separated from each other by at least 9 inches. 2) Areas of undercuts and porosity beyond that allowed by the applicable ASME Code shall not exceed 1/2 inch in weld length. The total length of undercut and porosity over any 1-foot length shall not exceed 2 inches. 3) The total weld length in which items (1) and (2) apply shall not exceed a total of 10 percent of the overall weld length. The limited access of the MPC basket panel longitudinal fillet welds makes it difficult to perform effective repairs of these welds and creates the potential for causing additional damage to the basket assembly (e.g., to the neutron absorber and its sheathing) if repairs are attempted. The acceptance criteria provided in the foregoing have been established to comport with the objectives of the basket design and preserve the margins demonstrated in the supporting stress analysis.</p> <p>From the structural standpoint, the weld acceptance criteria are established to ensure that any departure from the ideal, continuous fillet weld seam would not alter the primary bending stresses on which the design of the fuel baskets is predicated. Stated differently, the permitted weld discontinuities are limited in size to ensure that they remain classifiable as local stress elevators ("peak stress", F, in the ASME Code for which specific stress intensity limits do not apply).</p>
MPC Basket Assembly	NG-8000	States requirements for nameplates, stamping and reports per NCA-8000.	The HI-STAR 100 System will be marked and identified in accordance with 10CFR71 and 10CFR72 requirements. No Code stamping is required. The MPC basket data package will be in conformance with Holtec's QA program.

<b>Component</b>	<b>Reference ASME Code Section/Article</b>	<b>Code Requirement</b>	<b>Alternative, Justification &amp; Compensatory Measures</b>
Overpack Intermediate Shells and Containment Boundary	NB-4622	All welds, including repair welds, shall be post-weld heat treated (PWHT).	PWHT of intermediate shell-to-top flange and intermediate shell-to-bottom plate welds do not require PWHT. These welds attach non-pressure retaining parts to pressure retaining parts. The pressure retaining parts are > 7 inches thick. Localized PWHT will cause material away from the weld to experience elevated temperatures which will have an adverse effect on the material properties.
Overpack Containment Boundary	NB-5120	Perform radiographic examination after post-weld heat treatment (PWHT).	Radiography of the helium retention boundary welds after PWHT is not required. All welds (including repairs) will have passed radiographic examination prior to PWHT of the entire containment boundary. Confirmatory radiographic examination after PWHT is not necessary because PWHT is not known to introduce new weld defects in nickel steels.
Overpack Intermediate Shells	NF-2000	Requires materials to be supplied by ASME-approved material supplier.	Materials will be supplied by Holtec approved supplier with CMTRs in accordance with NF-2000 requirements.

<b>Component</b>	<b>Reference ASME Code Section/Article</b>	<b>Code Requirement</b>	<b>Alternative, Justification &amp; Compensatory Measures</b>
Overpack Containment Boundary	NB-2330	Establish TNDT and test base metal, heat affected zone and weld metal at TNDT + 60°F.	<p>Rather than testing to establish the RTNDT as defined in paragraph NB-2331, the guidance from Reg Guide 7.11 [8.1.4] is used for materials less than 4 inches thick and Reg Guide 7.12 &amp; NUREG/CR 3826 are used for materials from greater than 4 up to 12 inches thick. Table 8.1.7 summarizes the specific impact testing requirements for the Containment Boundary components per Reg. Guides 7.11 endorsement of NUREG 1815, Reg. Guide 7.12 and NUREG/CR-3826 as applicable.</p> <p>All containment welds on the HI-STAR 190 will be involving the shell and have a nominal thickness of 50mm (2 inches). Therefore the TNDT for the containment welds will be the same as the TNDT for the containment shell as reflected in Table 8.1.7. Drop test to determine TNDT for containment weld is not required.</p>

<b>Component</b>	<b>Reference ASME Code Section/Article</b>	<b>Code Requirement</b>	<b>Alternative, Justification &amp; Compensatory Measures</b>
Overpack Containment Boundary	NF-3320 NF-4720	NF-3324.6 and NF-4720 provide requirements for bolting.	<p>These Code requirements are applicable to linear structures wherein bolted joints carry axial, shear, as well as rotational (torsional) loads. The overpack bolted connections in the structural load path are qualified by design based on the design loadings defined in the SAR. Bolted joints in these components see no shear or torsional loads under normal storage conditions. Larger clearances between bolts and holes may be necessary to ensure shear interfaces located elsewhere in the structure engage prior to the bolts experiencing shear loadings (which occur only during side impact scenarios).</p> <p>Bolted joints that are subject to shear loads in accident conditions are qualified by appropriate stress analysis. Larger bolt-to-hole clearances help ensure more efficient operations in making these bolted connections, thereby minimizing time spent by operations personnel in a radiation area. Additionally, larger bolt-to-hole clearances allow interchangeability of the lids from one particular fabricated cask to another.</p>

<b>Component</b>	<b>Reference ASME Code Section/Article</b>	<b>Code Requirement</b>	<b>Alternative, Justification &amp; Compensatory Measures</b>
MPC-68 Serial #1021-023, 036, 037 Closure Rings	NB-2531	Requires UT inspection of plate.	The sole deviation of the 3/8" thick austenitic stainless steel material used for the MPC closure ring is the omission of a straight beam UT inspection as required by NB-2531. The ASME Code required straight beam inspection for vessels because the predominant indication in plates is laminations. Straight beam inspection cannot detect indications perpendicular to the surface of the plate. With respect to maintaining confinement, an indication perpendicular to the surface of the plate is the most critical. Laminations in the plate parallel to the surface of the plate cannot cause leakage through the plate. Therefore, the straight beam UT inspection does not add any value for detecting a defect in the thin closure ring with respect to its confinement function.



**Table 8.1.6: Fracture Toughness Test Criteria: Cask Containment System  
(Sheet 1 of 2)**

Item	Material	Thickness in. (mm)	Qualification to LST of -29°C (-20°F) (Note 2)		Qualification to LST of -40°C (-40°F) (Note 2)	
			Charpy V-Notch Temperature	Drop Test Temperature (Note 1)	Charpy V-Notch Temperature	Drop Test Temperature (Note 1)
Weld Metal for NB Welds	As required	NA	$T_{NDT} \leq -102.5^{\circ}\text{F}$ (-74.7°C) with testing and acceptance criteria per ASME Section III, Subsection NB, Article NB-2430 and Article NB-2330	$T_{NDT} \leq -102.5^{\circ}\text{F}$ (-74.7°C) based on containment shell thickness	$T_{NDT} \leq -122.5^{\circ}\text{F}$ (-85.8°C) with testing and acceptance criteria per ASME Section III, Subsection NB, Article NB-2430 and Article NB-2330	$T_{NDT} \leq -122.5^{\circ}\text{F}$ (-85.8°C) based on containment shell thickness
Containment Shell	SA-203 E/ SA-350 LF3	2.5 (64)	$T_{NDT} \leq -102.5^{\circ}\text{F}$ (-74.7°C) with testing and acceptance criteria per ASME Section III, Subsection NB, Article NB-2330	$T_{NDT} \leq -102.5^{\circ}\text{F}$ (-74.7°C) per R.G. 7.11	$T_{NDT} \leq -122.5^{\circ}\text{F}$ (-85.8°C) with testing and acceptance criteria per ASME Section III, Subsection NB, Article NB-2330	$T_{NDT} \leq -122.5^{\circ}\text{F}$ (-85.8°C) per R.G. 7.11
Containment Closure Flange	SA-350 LF3	8.75 (222)	$T_{NDT} \leq -136^{\circ}\text{F}$ (-93.3°C) with testing and acceptance criteria per ASME Section III, Subsection NB, Article NB-2330	$T_{NDT} \leq -136^{\circ}\text{F}$ (-93.3°C) per R.G. 7.12.	$T_{NDT} \leq -113^{\circ}\text{F}$ (-80.6°C) with testing and acceptance criteria per ASME Section III, Subsection NB, Article NB-2330	$T_{NDT} \leq -113^{\circ}\text{F}$ (-80.6°C) per fracture initiation criteria developed in the NUREG-CR-3826 (Notes 3 and 4)
Containment Baseplate	SA-203 E/ SA-350 LF3	6 (151)	$T_{NDT} \leq -129^{\circ}\text{F}$ (-89.4°C) with testing and acceptance criteria per ASME Section III, Subsection NB, Article NB-2330	$T_{NDT} \leq -129^{\circ}\text{F}$ (-89.4°C) per R.G. 7.12.	$T_{NDT} \leq -97^{\circ}\text{F}$ (-71.7°C) with testing and acceptance criteria per ASME Section III, Subsection NB, Article NB-2330	$T_{NDT} \leq -97^{\circ}\text{F}$ (-71.7°C) per fracture initiation criteria developed in the NUREG-CR-3826 (Notes 3 and 4)

**Table 8.1.6: Fracture Toughness Test Criteria: Cask Containment System  
(Sheet 2 of 2)**

Item	Material	Thickness mm (in.)	Qualification to LST of -29°C (-20°F) (Note 2)		Qualification to LST of -40°C (-40°F) (Note 2)	
			Charpy V-Notch Temperature	Drop Test Temperature (Note 1)	Charpy V-Notch Temperature	Drop Test Temperature (Note 1)
Closure Lid	SA-203 E/ SA-350 LF3	6 (151)	T <sub>NDT</sub> ≤ -129°F (-89.4°C) with testing and acceptance criteria per ASME Section III, Subsection NB, Article NB-2330	T <sub>NDT</sub> ≤ -129°F (-89.4°C) per R.G 7.12.	T <sub>NDT</sub> ≤ -97°F (-71.7°C) with testing and acceptance criteria per ASME Section III, Subsection NB, Article NB-2330	T <sub>NDT</sub> ≤ -97°F (-71.7°C) per fracture initiation criteria developed in the NUREG-CR-3826 (Notes 3 and 4)

## Notes:

1. Materials to be tested in accordance with ASTM E208-87a.
2. Per Reg. Guide 7.8 [2.1.4], the LST which applies to impactive loads is -29°C (-20°F). The cask may be qualified to either to an LST of either -29°C (-20°F) or -40°C (-40°F).
3. Component to undergo 100% volumetric examination to confirm absence of flaws which exceed the critical values as defined in NUREG/CR-3826 Table 3. 100% volumetric re-examination is required for cask components qualified per NUREG/CR-3826 following cask operations which result in impactive or impulsive loadings in excess of those defined in the normal conditions of transport.
4. In lieu of qualification per NUREG/CR-3826, qualification per R.G. 7.12 may be applied.

**Table 8.1.7: Fracture Toughness Test Criteria: HI-STAR 100 Cask Dose Blocker Steel Parts**

<b>Item</b>	<b>Material</b>	<b>Charpy V-Notch Test Temperature</b>	<b>Remarks</b>
Intermediate Shells (1 inch) (Note 1)	SA516 Grade 70	Test at -40°C (-40°F)	Charpy energy is 18 ft.-lb. (average of 3 specimens and minimum of 13 ft.-lb. for any single specimen)
Intermediate Shells (1 1/4 inch) (Note 1)	SA516 Grade 70	Test at -40°C (-40°F)	Charpy energy is 21 ft.-lb. (average of 3 specimens and minimum of 16 ft.-lb. for any single specimen)
Cask Port Cover Plates (1 1/2 inch) (Notes 1 and 2)	SA203E or SA350-LF3	Test at -40°C (-40°F)	Charpy energy is 23 ft.-lb. (average of 3 specimens and minimum of 18 ft.-lb. for any single specimen)

**Notes:**

1. SA-516 Gr. 70 plate may be normalized.
2. Components may be exempt from impact testing as allowed by NF-2311 [8.1.1].

**Table 8.1.8: Properties of Neutron Shield Material (Holtite-A) for Shielding Function**

Property	Property Value
Nominal Bulk Density (g/cm <sup>3</sup> )	1.68
Minimum Hydrogen Density, (g/cm <sup>3</sup> )	0.096
Nominal Boron Carbide Content, (wt%)	1

Note: The Holtec Manufacturing Manual contains detailed instructions for manufacturing of Holtite-A including the control of variation (i.e. tolerances) of nominal properties listed in this table. Hydrogen density is the characteristic with greatest influence over the shielding performance of Holtite-A and is therefore specified as a minimum value.

## 8.2 MAINTENANCE PROGRAM

An ongoing maintenance program for the HI-STAR 100 Cask, impact limiter and MPC will be prepared and issued to each user prior to delivery and first use of the HI-STAR 100 Package as a part of its O&M Manual. This document shall delineate the detailed inspections, testing, and parts replacement necessary to ensure continued radiological safety, proper handling, and containment performance of the HI-STAR 100 Package in accordance with 10CFR71 regulations, conditions in the Certificate of Compliance (CoC), and the design requirements and criteria contained in this Safety Analysis Report (SAR).

The HI-STAR 100 Package is totally passive by design. There are no active components or systems required to assure the continued performance of its safety functions. As a result, only minimal maintenance will be required over its lifetime, and this maintenance would primarily result from weathering effects, and pre- and post-usage requirements for transportation. Typical of such maintenance would be the reapplication of corrosion inhibiting materials on accessible external surfaces, and seal replacement and leak testing following seal replacement. Such maintenance requires methods and procedures are no more demanding than those currently in use at nuclear power plants.

The maintenance program schedule for the HI-STAR 100 Package is provided in Table 8.2.1.

### 8.2.1 Structural and Pressure Tests

No periodic structural or pressure tests on the packaging following the initial acceptance tests are required to verify continuing performance.

### 8.2.2 Leakage Tests

A pre-shipment leakage rate test of cask containment seals is performed per Subsection 8.1.4 following loading of the HI-STAR 100 Overpack. This pre-shipment leakage rate test is valid for 1 year. If the pre-shipment leakage rate test expires, a periodic leakage rate test of the containment seals must be performed prior to transport. This periodic leakage rate test is valid for 1 year.

Maintenance leakage rate testing shall be performed prior to returning a cask to service following maintenance, repair (such as a weld repair), or replacement of containment system components (such closure lid or port cover plate). Only that portion of the containment system that is affected by the maintenance, repair or component replacement needs to be leak tested. Leakage rate tests on the cask containment system shall be performed per written and approved procedures in accordance with the requirements of ANSI N14.5.

Table 8.1.1 specifies the allowable leakage rate and test sensitivity in terms of helium leak tightness. Table 8.1.2 specifies the components subject to testing for fabrication, pre-shipment, periodic and maintenance leakage rate tests.

### 8.2.3 Component and Material Tests

#### 8.2.3.1 Relief Devices

The **neutron shield** relief devices on the overpack shall be visually inspected **for damage or indications of excessive corrosion** prior to each use of the HI-STAR 100 Package. If the inspection determines an unacceptable condition, the **neutron shield** relief devices shall be replaced. The **neutron shield** relief devices shall be replaced **periodically while the cask is in service if recommended by the manufacturer's O&M manual.**

#### 8.2.3.2 Shielding Materials

Periodic verification of the neutron shield integrity shall be performed within 5 years prior to each shipment. The periodic verification shall be performed by radiation measurements with either loaded contents or a check source. Measurements shall be taken at three cross sectional planes through the radial shield and at four points along each plane's circumference. The average measurement results from each sectional plane shall be compared to calculated values to assess the continued effectiveness of the neutron shield. The calculated values shall be representative of the loaded contents (i.e., fuel type, enrichment, burnup, cooling time, etc...) or the particular check source used for the measurements.

#### 8.2.3.3 Packaging Surfaces

Accessible external surfaces of the cask and impact limiters shall be visually inspected for damage prior to each fuel loading to ensure that the packaging effectiveness is not significantly reduced. Visual inspections of the cask and impact limiters shall be performed for external surface coating and component damage including surface denting, surface penetrations, weld cracking, chipped or missing coating. Where necessary, cask coatings shall be reapplied. Damage shall be evaluated for impact on packaging safety and shall be repaired or replaced accordingly. Wear and tear from normal use will not impact cask safety. Repairs or replacement in accordance with written and approved procedures, as set down in the O&M manual, shall be required if unacceptable conditions are identified.

Prior to installation or replacement of a closure seal, the cask sealing surface shall be cleaned and visually inspected for scratches, pitting or roughness, and affected surface areas shall be polished smooth or repaired as necessary in accordance with written and approved procedures.

#### 8.2.3.4 Packaging Fasteners

Cask closure fasteners and impact limiter fasteners shall be visually inspected for damage such as excessive wear, galling, or indentations on the threaded surfaces prior to installation. The severity of thread damage shall be evaluated per standard industry practice. Damaged fasteners shall be replaced accordingly. Damaged internal threads may be repaired per standard industry practice (e.g. threaded inserts). Any repair shall be evaluated to ensure ASME Code stress limits applicable to bolted closure joints are met. Any required material or manufacturing process testing would also be performed in accordance with the original applicable code.

Bolting of the closure lid and port cover plate, shall be replaced as guided by fatigue analysis per the provisions of ASME Code Section III. The maintenance program in Table 8.2.1 provides a bolt change out schedule to insure that the cumulative damage factor accumulated by a bolt shall be less than 1.0 with sufficient margin. One bolting cycle is the complete sequence of torquing and removal of bolts.

Containment Top Flange internal threads for closure bolts have a maximum service life limit based on bolting cycles as determined by fatigue analysis per the provisions of Section III of the ASME Code. The bolting cycles specified in Table 8.2.1 shall not be exceeded. One bolting cycle is the complete sequence of torquing and removal of bolts.

#### 8.2.3.5 Cask Trunnions

Cask trunnions shall be inspected prior to each fuel loading. The accessible parts of the trunnions (areas outside the cask), and the local cask areas shall be visually examined to verify no deformation, distortion, or cracking has occurred. Any evidence of deformation (other than minor localized surface deformation due to contact pressure between lifting device and trunnion), distortion or cracking of the trunnion or adjacent cask areas shall require repair or replacement of the trunnion and/or repair of the cask. Following any replacements and/or repair, the load testing shall be re-performed and the components re-examined in accordance with the original procedure and acceptance criteria.

#### 8.2.3.6 Closure Seals

The HI-STAR 100 Packaging is equipped with metallic containment closure seals on containment closure joints to ensure leak tightness. The closure seals are shipped from the factory pre-inspected and carefully packaged. Once installed and compressed, the seals should not be disturbed by removal of closure fasteners. Removal of closure fasteners requires replacement of closure seals and performance of a Maintenance Leakage Rate Test for closure seals classified as containment boundary seals. Closure seals are specified for long-term use and do not require additional maintenance.

#### 8.2.4 Thermal Tests

For each package, a periodic thermal performance test shall be performed within 5 years prior to each shipment, to demonstrate that the thermal capabilities of the cask remain within its design basis.

#### 8.2.5 Miscellaneous Tests

No additional tests are required for the HI-STAR 180D Packaging, packaging components, or packaging materials.

Table 8.2.1

## MAINTENANCE AND INSPECTION PROGRAM SCHEDULE

Task	Frequency
Cask and impact limiter visual inspection (See Paragraph 8.2.3.3)	Prior to each fuel loading
Cask closure fasteners/bolts visual inspection (See Paragraph 8.2.3.4)	Prior to installation and prior to each transport
Cask trunnion visual inspection (See Paragraph 8.2.3.5)	Prior to each fuel loading
Impact limiter and impact limiters fasteners visual inspection (See Paragraph 8.2.3.3 and 8.2.3.4)	Prior to installation and/or prior to transport
Neutron shield relief device visual inspection (See Paragraph 8.2.3.1)	Prior to transport
Pre-shipment leakage rate test of cask containment system seals (See Subsection 8.1.4)	Following each fuel loading and/or prior to transport
Periodic leakage rate test of cask containment system seals (See Subsection 8.2.2)	Prior to off-site transport if period from last test exceeds 1 year
Maintenance Leakage Rate Test of Cask containment boundary (See Subsection 8.2.2)	Following maintenance, repair or replacement of containment system components (optional for seal replacement)
Seal replacement for Closure Lid, Port Cover Plate, and/or Port Plug (See Paragraph 8.2.3.6)	Following removal of closure bolting or port plug, if seal found to be damaged or does not meet the maintenance leakage rate test or pre-shipment test OR if required based on seal design life limitations
Bolt replacement ( <i>Service Life</i> ) for Closure Lid (See Paragraph 8.2.3.4)	Every 166 bolting cycles (assumes 20 years at 8 cycles per year) – SB637-N07718
Containment Top Forging internal closure bolt thread <i>Service Life</i> (See Paragraph 8.2.3.4)	3950 bolting cycles
Neutron shield relief device replacement (See Paragraph 8.2.3.1)	As required by the manufacturer's O&M manual
Thermal Test (See Subsection 8.2.4)	Within 5 years prior to each shipment
Shielding Test (See Paragraph 8.2.3.2)	Within 5 years prior to each shipment



### 8.3 REFERENCES

The following generic industry and Holtec produced references may have been consulted in the preparation of this document. Where specifically cited, the identifier is listed in the SAR text or table. Active Holtec Calculation Packages or Technical Reports, which are the repository of all relevant licensing and design basis calculations, are annotated as “latest revision”. Submittal of the latest revision of such Calculation Packages to the USNRC and other regulatory authorities during the course of regulatory reviews is managed under the company’s Configuration Control system.

- [8.0.1] U.S. Code of Federal Regulations, Title 10, "Energy", Part 71, "Packaging and Transportation of Radioactive Materials.”
- [8.1.1] American Society of Mechanical Engineers, "Boiler and Pressure Vessel Code," Sections II, III, V, IX, and XI, 1995 Edition with 1996 and 1997 Addenda.
- [8.1.2] American Society for Nondestructive Testing, "Personnel Qualification and Certification in Nondestructive Testing," Recommended Practice No. SNT-TC-1A, December 1992.
- [8.1.3] American National Standards Institute, Institute for Nuclear Materials Management, "American National Standard for Radioactive Materials - Special Lifting Devices for Shipping Containers Weighing 10,000 Pounds (4500 kilograms) or More", ANSI N14.6, September 1993.
- [8.1.4] American National Standards Institute, Institute for Nuclear Materials Management, "American National Standard for Radioactive Materials Leakage Tests on Packages for Shipment", ANSI N14.5, 1997.
- [8.1.5] U.S. Nuclear Regulatory Commission, "Fracture Toughness Criteria of Base Material for Ferritic Steel Shipping Cask Containment Vessels with a Maximum Wall Thickness of 4 Inches (0.1m)," Regulatory Guide 7.11, June 1991.
- [8.1.6] U.S. Nuclear Regulatory Commission, "Fracture Toughness Criteria of Base Material for Ferritic Steel Shipping Cask Containment Vessels with a Wall Thickness Greater than 4 Inches (0.1m) But Not Exceeding 12 Inches (0.3m)," Regulatory Guide 7.12, June 1991.
- [8.1.7] Holtec International Document DOC-5014-03, “Acceptance Testing of First HI-STAR Overpack (Thermal and He Leak Tests)”, September 2006.

## **SUPPLEMENT 8.I**

### **ACCEPTANCE TEST AND MAINTENANCE PROGRAM OF THE HI-STAR HB PACKAGE WITH MPC-HB**

The main body of this chapter remains fully applicable for the HI-STAR HB configuration of the HI-STAR 100 System.

## SUPPLEMENT 8.II

### ACCEPTANCE TEST AND MAINTENANCE PROGRAM OF THE HI-STAR HB GTCC PACKAGE WITH GWC-HB

The main body of this chapter remains fully applicable (except as specified/clarified below) for the configuration of the HI-STAR HB GTCC Package with GWC-HB specified in the “II” Supplements in this SAR.

#### 8.II.1.2      Weld Examination

HI-STAR HB GTCC and GWC weld examinations shall be performed in accordance with the drawing package referenced in the CoC and applicable codes and standards in Table 8.II.1, including alternatives as specified in Table 8.1.5<sup>1</sup>. Weld examinations and repairs shall be performed as specified below. All code weld inspections shall be performed in accordance with written and approved procedures by personnel qualified in accordance with SNT-TC-1A [8.1.2]. All required inspections, examinations, and tests shall become part of the final quality documentation package.

The following specific weld requirements shall be followed in order to verify fabrication in accordance with the drawings.

1. Cask body welds (top flange, bottom plate and inner shell welds) including any attachment welds and temporary welds shall be examined in accordance with ASME Code Section V, with acceptance criteria per ASME Code Section III, Subsection NB, Article NB-5300. Examinations, Visual (VT), Radiographic (RT), and Liquid Penetrant (PT) or Magnetic Particle (MT), apply to these welds as defined by the code. These welds shall be repaired in accordance with the requirements of the ASME Code Section III, Article NB-4450 and examined after repair in the same manner as the original weld. Although ASME Code Section III, Subsection NB does not require visual examination of welds, the welds will be visually examined to ensure conformance with the fabrication drawings (e.g. proper geometry, workmanship etc.).
2. Code welds in the cask and impact limiter (excluding those listed above) shall be examined in accordance with ASME Code Section V, with acceptance criteria per ASME Code Section III, Subsection NF, Article NF-5300. These welds shall be repaired in accordance with ASME Code Section III, Article NF-4450 and examined after repair in the same manner as the original weld. These weld requirements are not applicable to NITS welds (e.g. seal welds) on the cask, impact limiters and MPC Spacer.

---

<sup>1</sup> Code alternatives to Subsection NB and NG as applied to the MPC EV and MPC fuel basket respectively also apply as code alternatives to Subsection ND as applied to the GWC and GWC primary waste basket where code equivalency exists.

3. GWC enclosure vessel (code containment welds) shall be examined in accordance with ASME Code Section V, with acceptance criteria per ASME Code Section III, Subsection ND (Article ND-5300). Examinations, Visual (VT), Radiographic (RT), and Liquid Penetrant (PT) or Magnetic Particle (MT), apply to these welds as defined by the code and the drawing package referenced in the CoC. These welds shall be repaired in accordance with the requirements of the ASME Code Section III, Articles ND-4450, as applicable, and examined after repair in the same manner as the original weld. The welds will be visually examined to ensure conformance with the fabrication drawings (e.g. proper geometry, workmanship etc.). These weld requirements are not applicable to welds identified as NITS on the drawing package.
4. Code welds in the GWC primary waste basket shall be examined in accordance with ASME Code Section V (for core support structures, ND-1121), with acceptance criteria per ASME Code Section III, Subsection ND (Article ND-5300). These welds shall be repaired in accordance with the requirements of the ASME Code Section III, Article ND-4450, and examined after repair in the same manner as the original weld. The welds will be visually examined to ensure conformance with the fabrication drawings (e.g. proper geometry, workmanship etc.). These weld requirements are not applicable to welds identified as NITS on the drawing package.
4. The GWC lid-to-shell weld shall be examined by either volumetric examination using ultrasonic methods or by using a progressive multi-layer liquid penetrant (PT) examination during welding. The multi-layer PT must, at a minimum, include the root and final weld layers and one intermediate PT after each approximately 3/8 inch weld depth has been completed.
5. Non-code welds (such as intermediate shell welds and secondary waste basket welds) shall be examined and repaired in accordance with written and approved procedures. The drawing package referenced in the CoC may require visual examination.

#### 8.II.1.3 Structural and Pressure Tests

The GWC-HB containment boundary shall be examined and tested using pressure testing, ultrasonic testing, MT and/or PT, as applicable, to verify that it is free of cracks, pinholes, uncontrolled voids or other defects that could significantly reduce the effectiveness of the packaging. The HI-STAR GTCC HB cask does not provide a containment function; nevertheless, similar examinations and tests (except for pressure testing) verify that it is free of cracks, uncontrolled voids or other defects that could significantly reduce the effectiveness of the packaging.

#### 8.II.1.3.2 Pressure Testing

##### 8.II.1.3.2.1 HI-STAR GTCC HB Body

Pressure testing of the HI-STAR GTCC HB body is not applicable.

##### 8.II.1.3.2.2 GWC Containment Boundary

Pressure testing of the GWC enclosure vessel containment boundary shall be performed in accordance with the ASME Code Section III, Subsection ND, Article ND-6000 at a test pressure of not less than 150% of cask cavity maximum normal operating pressure per 10CFR71.85(b) or at a test pressure of 125% of the GWC design internal pressure; whichever is greater. All pressure testing shall be performed in accordance with written and approved procedures.

Test results shall be documented and shall become part of the final quality documentation package.

##### 8.II.1.3.3 Pneumatic Testing of the Neutron Shield Enclosure Vessel

The HI-STAR GTCC HB package does not feature a neutron shield enclosure vessel.

#### 8.II.1.4 Leakage Testing

Leakage rate tests on the GWC containment system shall be performed per written and approved procedures in accordance with the requirements of Chapter 7. Tables 8.II.2. and 8.II.3 specify the allowable leakage rate and test sensitivity as well as components to be tested for fabrication, pre-shipment, periodic and maintenance leakage rate tests as applicable.

The GWC lid-to-shell weld shall have an indicated leakage rate not exceeding the leakage rate acceptance criterion reported in Table 8.II.2. The leakage rate acceptance criterion is met in a practical manner by the visual examination for water leakage per ASME Code Section III, Subsection ND, Article ND-6000 (hydrostatic test code requirements) to verify a water-tight closure. A verification of a water-tight closure confirms the required leaktightness is met.

In case of an unsatisfactory leakage rate, weld repair, seal surface repair/polishing and/or seal change and retest shall be performed until the test acceptance criterion is satisfied.

Test results shall be documented and shall become part of the final quality documentation package.

#### 8.II.1.5 Component and Material Tests

##### 8.II.1.5.1 Seals

The HI-STAR GTCC HB package does not feature a containment seals or other seals.

##### 8.II.1.5.3 Impact Limiter Crush Material Testing

To provide protection against brittle fracture under cold conditions, fracture toughness test criteria of cask ferritic components, including welds, are specified in Table 8.II.4. Code alternatives listed in Table 8.1.5 may apply. Fracture toughness testing for other cask dose blocker steel parts are not required.

Test results shall become part of the final quality documentation package.

##### 8.II.1.5.4 Neutron Shielding Material

The HI-STAR GTCC HB package does not feature neutron shielding material.

##### 8.II.1.5.5 Neutron Absorber Material

The HI-STAR GTCC HB package does not feature neutron absorber material.

#### 8.II.1.7 Thermal Tests

Additional testing is not applicable.

##### 8.II.2.2 Leakage Tests

Additional testing is not applicable.

#### 8.II.2.3 Component and Material Tests

##### 8.II.2.3.1 Relief Devices

The HI-STAR GTCC HB package does not feature relief devices.

##### 8.II.2.3.2 Shielding Materials

Additional testing is not applicable.

##### 8.II.2.3.6 Closure Seals

The HI-STAR GTCC HB package does not feature closure seals.

#### 8.II.2.4      Thermal Tests

Additional testing is not applicable.

#### 8.II.2.5      Miscellaneous Tests

Additional testing is not applicable.

**Table 8.II.1 (Sheet 1 of 2): Applicability of ASME Code Boiler & Pressure Vessel Code and Other Standards**

<b>Component ID</b>	<b>Material Procurement</b>	<b>Design Code</b>	<b>Stress and Deformation Analysis Criteria</b>	<b>Welding (Fabrication and Qualifications)</b>	<b>Inspection</b>	<b>Testing</b>
Cask Body (Bottom Plate, Inner Shell, Top Flange, Closure Lid, Closure Lid Bolts)	ASME Code Section III Subsection NB-2000	ASME Code Section III Subsection NB-3000	ASME Code Section III Subsection NB-3200	ASME Code Section III Subsection NB-4000 and Chapter 8 of this SAR	ASME Code Section III Subsection NB-5000 and Chapter 8 of this SAR	ASME Code Section III Subsection NB-6000 and Chapter 8 of this SAR
Cask Dose Blocker Steel Components (Intermediate Shells)	ASME Code Section II Subsection NF	Non-Code	Section III, Subsection NF, NF-3300	Non-Code	Section V	Chapter 8 of this SAR
GWC Containment Boundary	ASME Code Section III Subsection NB-2000	ASME Code Section III Subsection NB-3200	ASME Code Section III Subsection NB-3000	ASME Code Section III Subsection NB-4000 and Chapter 8 of this SAR	ASME Code Section III Subsection NB-5000 and Chapter 8 of this SAR	ASME Code Section III Subsection NB-6000 and Chapter 8 of this SAR
Cask Top Lifting Trunnions	ASME Code Section II	ANSI N14.6 and RG 3.61	ANSI N14.6 and RG 3.61	Not Applicable	Chapter 8 of this SAR	Chapter 8 of this SAR
GWC Primary Waste Basket	Section II; and Section III, Subsection ND, ND-2000 for core support structures (ND-1121)	Section III, Subsection ND, NG-3300 and ND-3200 for core support structures (ND-1121)	Section III, Subsection ND, NG-3300 and ND-3200 for core support structures (ND-1121)	Section III, Subsection ND, ND-4000 for core support structures (ND-1121)	Section III, Subsection ND, ND-5000 and Section V for core support structures (ND-1121)	Chapter 8 of this SAR
Cask Dose Blocker Steel Components (radial channels, outer enclosure)	ASME Code Section II	See licensing drawing package for specific applicability	No yielding under NCT and no significant loss of dose blocker steel under HAC	ASME Code Section IX (as clarified by the licensing drawing package)	ASME Code Section V	Chapter 8 of this SAR



**Table 8.II.1 (Sheet 2 of 2): Applicability of ASME Code Boiler & Pressure Vessel Code and Other Standards**

GWC Secondary Waste Basket	ASME Code Section II	Non-Code	Non-Code	Non-Code	Section V for core support structures (NG-1121) and Chapter 8 of this SAR	Chapter 8 of this SAR
Impact Limiter Backbone Components	ASME Code Section II	See licensing drawing package for specific applicability	No rupture and no deformation leading to loss of function	ASME Code Section IX (as clarified by the licensing drawing package)	ASME Code Section V	Chapter 8 of this SAR

## Notes

1. The Holtec Manufacturing Manual contains detailed instructions for manufacturing of the subassemblies and the complete component in accordance with the applicable Codes and Standards. The Holtec Manufacturing Manual is a compilation of procedures, travelers, weld maps, specifications, standards, Metamic Manufacturing Manual and other documents as applicable, to ensure the manufacturing of the components are in full accord with the design conditions of the CoC. The latest issues of the manufacturing manual(s) are maintained in the company's network under Holtec's configuration control system.

**Table 8.II.2**  
**Containment System Performance Specifications**

<b>Design Feature</b>	<b>Design Attribute</b>	<b>Design Rating</b>
GWC Closure Lid-To-Shell Weld	Leakage Rate Acceptance Criterion	$1 \times 10^{-2}$ ref-cm <sup>3</sup> /s air
	Leakage Rate Test Sensitivity	ASME Code Pressure Test
GWC Enclosure Vessel (Not including Closure Lid)	Leakage Rate Acceptance Criterion	$1.25 \times 10^{-6}$ ref-cm <sup>3</sup> /s air
	Leakage Rate Test Sensitivity	$0.625 \times 10^{-6}$ ref-cm <sup>3</sup> /s air (½ of the leakage rate acceptance criterion per ANSI N14.5-1997)

Note: For helium as the tracer gas, the Leakage Rate Acceptance Criterion and Test Sensitivity are multiplied by a factor of 2.

**Table 8.II.3**  
**Leakage Rate Tests For GWC-HB Containment System**

Leakage Test	System Tested	Components Tested	Type of Leakage Rate Test (from ANSI N14.5-1997, App. A)	Allowable Leakage Rate
Fabrication Leakage Rate Test	GWC	<ul style="list-style-type: none"> <li>• Shell</li> <li>• Baseplate</li> <li>• Shell Welds</li> <li>• Shell to Baseplate Weld</li> </ul>	A.5.3	Table 8.II.2
Pre-Shipment Leakage Rate Test	GWC'	Closure Lid to Shell Welds	N/A (ASME Code Pressure Test)	Table 8.II.2
Maintenance Leakage Rate Test	GWC'	N/A	N/A	N/A
Periodic Leakage Rate Test	GWC'	N/A	N/A	N/A

**Table 8.II.4: Fracture Toughness Test Criteria: Cask Containment System  
(Sheet 1 of 2)**

Item	Material	Thickness in. (mm)	Qualification to LST of -29°C (-20°F) (Note 2)		Qualification to LST of -40°C (-40°F) (Note 2)	
			Charpy V-Notch Temperature	Drop Test Temperature (Note 1)	Charpy V-Notch Temperature	Drop Test Temperature (Note 1)
Weld Metal for NB Welds	As required	NA	As required by ASME Section III, Subsection NB, Article NB-2430 and Article NB-2330 Max test temperature - 40 °F (-40°C)	As required by ASME Section III, Subsection NB, Article NB-2430 and Article NB-2330 $T_{NDT} \leq -70^{\circ}\text{F}$ (-56.7°C)	$T_{NDT} \leq -122.5^{\circ}\text{F}$ (-85.8°C) with testing and acceptance criteria per ASME Section III, Subsection NB, Article NB-2430 and Article NB-2330	$T_{NDT} \leq -122.5^{\circ}\text{F}$ (-85.8°C) based on containment shell thickness
Containment Shell	SA-203 E/ SA-350 LF3	2.5 (64)	$T_{NDT} \leq -102.5^{\circ}\text{F}$ (-74.7°C) with testing and acceptance criteria per ASME Section III, Subsection NB, Article NB-2330	$T_{NDT} \leq -102.5^{\circ}\text{F}$ (-74.7°C) per R.G. 7.11	$T_{NDT} \leq -122.5^{\circ}\text{F}$ (-85.8°C) with testing and acceptance criteria per ASME Section III, Subsection NB, Article NB-2330	$T_{NDT} \leq -122.5^{\circ}\text{F}$ (-85.8°C) per R.G. 7.11
Containment Closure Flange	SA-350 LF3	8.75 (222)	$T_{NDT} \leq -136^{\circ}\text{F}$ (-93.3°C) with testing and acceptance criteria per ASME Section III, Subsection NB, Article NB-2330	$T_{NDT} \leq -136^{\circ}\text{F}$ (-93.3°C) per R.G. 7.12.	$T_{NDT} \leq -113^{\circ}\text{F}$ (-80.6°C) with testing and acceptance criteria per ASME Section III, Subsection NB, Article NB-2330	$T_{NDT} \leq -113^{\circ}\text{F}$ (-80.6°C) per fracture initiation criteria developed in the NUREG-CR-3826 (Notes 3 and 4)

**Table 8.1.6: Fracture Toughness Test Criteria: Cask Containment System  
(Sheet 2 of 2)**

Item	Material	Thickness mm (in.)	Qualification to LST of -29°C (-20°F) (Note 2)		Qualification to LST of -40°C (-40°F) (Note 2)	
			Charpy V-Notch Temperature	Drop Test Temperature (Note 1)	Charpy V-Notch Temperature	Drop Test Temperature (Note 1)
Containment Baseplate	SA-203 E/ SA-350 LF3	6 (151)	$T_{NDT} \leq -129^{\circ}\text{F}$ (-89.4°C) with testing and acceptance criteria per ASME Section III, Subsection NB, Article NB-2330	$T_{NDT} \leq -129^{\circ}\text{F}$ (-89.4°C) per R.G 7.12.	$T_{NDT} \leq -97^{\circ}\text{F}$ (-71.7°C) with testing and acceptance criteria per ASME Section III, Subsection NB, Article NB-2330	$T_{NDT} \leq -97^{\circ}\text{F}$ (-71.7°C) per fracture initiation criteria developed in the NUREG-CR-3826 (Notes 3 and 4)

## Notes:

1. Materials to be tested in accordance with ASTM E208-87a.
2. Per Reg. Guide 7.8 [2.1.4], the LST which applies to impactive loads is -29°C (-20°F). The cask may be qualified to either to an LST of either -29°C (-20°F) or -40°C (-40°F).
3. Component to undergo 100% volumetric examination to confirm absence of flaws which exceed the critical values as defined in NUREG/CR-3826 Table 3. 100% volumetric re-examination is required for cask components qualified per NUREG/CR-3826 following cask operations which result in impactive or impulsive loadings in excess of those defined in the normal conditions of transport.
4. In lieu of qualification per NUREG/CR-3826, qualification per R.G. 7.12 may be applied.

## **SUPPLEMENT 8.III**

### **ACCEPTANCE TEST AND MAINTENANCE PROGRAM OF THE HI-STAR 100 PACKAGE WITH DIABLO CANYON MPC-32**

The main body of this chapter remains fully applicable for the HI-STAR 100 with Diablo Canyon MPC-32 configuration of the HI-STAR 100 System.